

## Friday, 21 April 2017

[Go to top](#)

---

## Saturday, 22 April 2017

[Go to top](#)

### Weekend Course

## Physics for Physicists

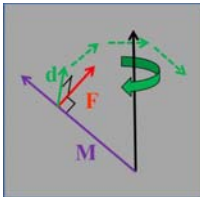
*Organizers:* Herbert Köstler, Dipl.-Phys. & N. Jon Shah, Ph.D.

Room 313BC                      Saturday 8:15 - 12:15                      *Moderators:* Adrienne Campbell-Washburn & Armin Nagel

---

8:15

### MRI: the Classical Description



The NMR (Nuclear Magnetic Resonance) signal can be described classically by considering the motion of the net magnetisation (the vector sum of magnetic moments of individual nuclei). By considering individual isochromats – i.e. subsets of the spins that are behaving identically– we can visualise how the received signal will decay away due to  $T_1$ ,  $T_2$  and  $T_2^*$  relaxation. By additionally considering the effects of magnetic field gradients, we can determine the spatial location of the signal, producing images. All these effects can be described by the Bloch equations, which give complete classical description of the behaviour of magnetisation.

Gareth Barker

---

8:45

### Signal & Noise in MRI

The signal-to-noise ratio (SNR) is a fundamental measure of quality and performance in MRI, most frequently used as a metric for comparing and optimizing imaging sequences, MR hardware (e.g., RF coils), or to assess and process new imaging and reconstruction techniques. Clinically, signal and noise considerations are important for image assessment such as in reliable lesion characterization, or in the context of accurate parameter fitting (relaxometry). This presentation will review the basic principles relevant to SNR, sources of noise, basic noise statistics, multi-channel noise, measurement of SNR and contrast-to-noise ratio, and factors influencing SNR.

Claudia Hillenbrand

---

9:15 Spatial Encoding (k-Space, MRI as a Linear & Shift-Invariant System, PSF, MTF)

Michael Steckner

---

9:45 Break & Meet the Teachers

---

10:15 MRI: a Systems Overview

The “big three” sections of an MR scanner are well known; Magnet, Gradient system, and RF system, and probably should have a fourth: Patient comfort and user experience components. We start with a review of these components, current limitations, and directions under investigation and continue to interaction between them needed to harmonize operation.

Lawrence Wald

---

10:45 Bloch Equations & Typical MRI Contrast

This presentation will provide an overview of the typical forms of the Bloch Equations, the physical mechanisms of relaxation phenomena as well as the basis of typical MRI contrasts.

Tobias Wech

---

11:15 Pulse Sequence Check: Reality vs. Ideal

The effect of any pulse sequence on the magnetization in an object can be predicted very accurately using the Bloch equation. A general algebraic inversion of the Bloch equation is not possible and thus, the full set of object and system properties and parameters cannot be derived from measurement data directly. Using a few assumptions and neglecting possible deviations, the results of a given pulse sequence can be calculated and the spatial encoding can be inverted to reconstruct an image. But what if these assumptions are wrong?

Oliver Speck

---

11:45 Basic MR Safety (Magnetic Fields, Peripheral Nerve Stimulation, etc)



Magnetic resonance techniques are considered to be not harmful. The three electromagnetic fields used for MR - static magnetic field, switched gradient fields, and radio frequency field - interact with human tissue, but also with other materials exposed to these fields. The physical interactions with human tissue do not cause irreversible physiological effects, as long as certain limits are not exceeded. Concerning foreign material (e.g. implants), the physical effects of the applied fields may cause severe hazards for patients, staff, and material, if MR examinations are not performed properly.  
Harald Kugel

---

12:15      Lunch & Meet the Teachers

---

## Weekend Course

# Introduction to fMRI: Task & Resting State fMRI Methods/Analysis

Organizers: Jay J. Pillai, M.D. & Joshua S. Shimony, M.D., Ph.D.

Room 312      Saturday 8:15 - 12:15      Moderators: Jay Pillai & Benedikt Poser

---

8:15      BOLD Data Acquisition Considerations

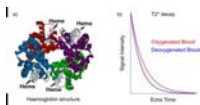
Through a series of complex processes, under the umbrella term of neurovascular coupling, neuronal activity ultimately manifests as a signal change in an MR image via the blood-oxygenation level dependent (BOLD) contrast. Functional MRI (fMRI) capitalises on this contrast mechanism to infer neuronal activity from BOLD contrast variation in a time series, typically acquired while the participant engages in a task. This approach has proved valuable in furthering our understanding of the working of the human brain. Here, issues pertinent to acquiring data with sufficiently high sensitivity to detect such changes are considered, e.g. susceptibility effects, physiological noise and approaches facilitating high spatio-temporal resolution.

Martina Callaghan

---

8:45

BOLD Signal/Physiology



Functional MRI has become a standard technique for exploring brain function, however this imaging modality is not a direct measure of neural activity. This course introduces the source of Blood Oxygenation Level Dependent (BOLD) contrast and the physiological mechanisms that drive the haemodynamic response to neural activity. The limitations and challenges of using blood as a surrogate for brain function are discussed, particularly in cohorts with differing cerebrovascular physiology. Potential solutions involving additional imaging modalities and complementary MRI contrast mechanisms may enable accurate understanding of the neuro-vascular processes underlying BOLD fMRI.

Molly Bright

---

9:15

### General Linear Model Analysis of Task Based fMRI Data

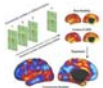
The general linear model (GLM) is one of the most commonly utilized statistical platform that is currently used in analyzing task-based fMRI data. In this talk we will introduce the general over view and basic concepts of GLM and how it is used in this very specific application of clinical neuroimaging. We will briefly review the history of introduction of GLM into the fMRI community and later use some examples to demonstrate the utility in analyzing fMRI data. In the end we will discuss some of its limitations.

Feroze Mohamed

---

9:45

### Introduction to Resting State Functional Connectivity



Steven Stufflebeam

---

10:15

### Break & Meet the Teachers

---

10:45

### Data Driven & Exploratory Analyses

Independent component analysis (ICA) has grown to be a widely used and continually developing staple for analyzing fMRI functional connectivity data. In this paper we discuss some key observations and assumptions regarding ICA and also key new applications of ICA to brain imaging data.

Vince Calhoun

---

11:15

### Dynamic Functional Connectivity



Dynamic functional connectivity (DFC) is the study of time-varying changes in functional interactions between brain regions. This talk will describe DFC methods along with the challenges involved in such analyses. We will also highlight results demonstrating associations between DFC and independently acquired measures of behavior, physiology, and neural activity, and will discuss the potential for DFC features to serve as clinical biomarkers.

Catie Chang

---

11:45 [Network Analysis](#)

This talk provides an introduction to network analysis of functional MRI, with an emphasis on the use of graph theory for understanding distinct aspects of brain organisation and dynamics.

Alex Fornito

---

12:15 [Adjournment & Meet the Teachers](#)

---

## Weekend Course

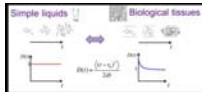
# Diffusion MRI: Principles & Applications

Organizers: Daniel C. Alexander, Ph.D. & Stephan E. Maier, M.D., Ph.D.

Room 311                      Saturday 8:15 - 11:45    Moderators: Daniel Alexander & Stephan Maier

---

8:15 [Introduction to Diffusion MRI](#)



This lecture will cover the basics of diffusion MRI. We will explore how diffusion in biological tissue serves as an in vivo microscope through its measurement with MRI by varying both diffusion gradient and the diffusion time  $t$ , the time over which the molecules diffuse. The concepts of q-space imaging, diffusion tensor imaging (DTI) and diffusion kurtosis imaging (DKI) will be covered, as well as other higher order diffusion methods (biophysical models versus representations). In addition, we will illustrate how varying the diffusion time  $t$  provides complimentary information about microstructural length scales.

Els Fieremans

---

8:45 [Diffusion Modeling and Microstructure Probing](#)

This lecture presents the key concepts behind modelling diffusion MRI signal. Specifically, it focuses on various techniques that go beyond the standard diffusion tensor model, and aim to provide biomarkers which can be related to tissue microstructure.

Andrada lanuş

---

9:15 [Tracking Fiber Structures](#)

Diffusion MRI tractography enables unprecedented visualization of the trajectory of white matter pathways in vivo. This course will introduce the fundamental principles of tracking fiber structures in diffusion MRI data, and will provide an overview of different tractography methods. Participants will learn about the current capabilities and limitations of tractography techniques for investigating white matter anatomy. Clinical applications of tractography will be presented and challenges of using tractography findings for clinical decision support will be discussed.

Sonia Pujol

---

9:45 [Break & Meet the Teachers](#)

---

10:15 [Neuro Applications of Diffusion MRI](#)

Michael Zeineh

---

10:45 [Body Applications of Diffusion MRI](#)

This presentation will review the added value of DWI in the body, particularly in the oncology patients.

Bachir Taouli

---

11:15 [Application of Diffusion MRI in Animal Models](#)

This lecture will provide a brief overview of technical considerations involved in diffusion MRI of small animals on preclinical scanners. Applications of diffusion MRI to examine neuroanatomy and brain development in small animals will be covered. We will examine the relations between metrics derived using different diffusion models and acquisition schemes and white matter pathological changes in animal models of injury and disease. In addition, emerging applications of diffusion MRI methods for characterization of brain tissue microstructure in animal models will be explored.

11:45

Adjournment & Meet the Teachers

---

## Weekend Course

# Introduction into Magnetic Resonance Spectroscopy

Organizers: Anke Henning, Ph.D. & Roland Kreis, Ph.D.

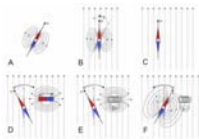
Room 314

Saturday 8:15 - 12:05 Moderators: Thomas Ernst & Harald Möller

---

8:15

Basic Principles of MRS (Chemical Shift, J-coupling, Spectral Resolution, Field Strength Effects)



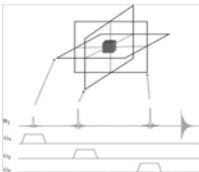
The basic principles of NMR are discussed based on classical concepts like compass needles, bar magnets, precession and electromagnetic induction. More advanced topics such as chemical shift, scalar coupling, T1 and T2 relaxation and basic MR sequences are also covered.

Robin de Graaf

---

8:40

Localization (Sequences: semiLASER, PRESS, STEAM, Chemical Shift Displacement)



Accurate localization is key for MR spectra quality and metabolites quantification. Metabolites low concentration and multiple frequencies pose more challenges in-vivo MRS than MRI, due to B0 inhomogeneity, insufficient B1, chemical shift displacement, and artifacts from lipids. Volume selection methods based on overlapping slices improves MRS quality by limiting the region of interest to areas where B0 and B1 can be better controlled. Spatial coverage can be improved by more modern approaches where arbitrary volumes can be shaped with parallel transmit, multiple volumes disentangled by parallel imaged, and different contributions to the MRS signal can be modeled in the reconstruction

Ovidiu Andronesi

---

9:05

Water & Lipid Suppression - VAPOR, WET, OVS, IR, Novel Approaches (MC, Crushers)

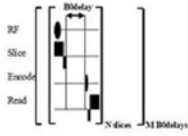
In this presentation, the need for water and lipid suppression, as well as the most widely used approaches to achieve this are explained.

Vincent Boer

---

9:30

Pre-Scan Adjustments (B0 Shimming, F0, PO, Water Suppression)



The pre-scan adjustments, while nearly invisible to many practitioners, are very important for the successful acquisition of many spectroscopic and imaging sequences. In this talk, approaches and constructs specific to B0 and B1 optimization are discussed with examples of methods and results.

Jullie Pan

9:55 Break & Meet the Teachers

10:25 MRSI (Basic Sequences & Acceleration)

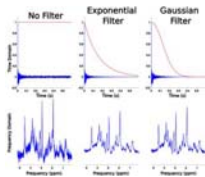
Ulrike Dydak

10:50 Editing, 2D & UHF - Detection a Comprehensive Neurochemical Profile

While the vast majority of MRS applications focus on the strong resonances of NAA, Cr, Cho and sometimes mIns and Glu+Gln, resonances from at least 15 neurochemicals, i.e., a comprehensive neurochemical profile are present in the spectrum. For detecting the small, weakly represented neurochemical resonances that underlie the typically detected large resonances such as NAA, Cr, Cho and mIns, options are: 1) to de-convolve all of the signals that are present or 2) to edit, i.e., to set the signal of interest apart (at least partially) from the others. Of course, there are advantages and disadvantages to each approach.

Melissa Terpstra

11:15 Postprocessing & Quality Assurance



In-vivo MRS data is unavoidably degraded by experimental imperfections such as subject motion, scanner drift, and eddy currents. Spectral preprocessing improves spectral quality and quantification reliability, and is an indispensable part of any in-vivo MRS experiment. MRS preprocessing is usually organized as a sequence, or 'pipeline' of individual processing routines, each designed to address a specific issue with the data. This talk covers some of the most common experimental issues affecting MRS data, and the processing routines and pipelines that can address these issues.

Jamie Near

11:40 Spectral Fitting & Absolute Quantification

MRS quantification is complicated due to the metabolic resonance overlap and complex line shapes. The modern methods for the spectral fitting increasingly relies on the linear combination (LC) modeling algorithms. The absolute quantification can be carried out using internal or external concentration references. The challenges remain in the following areas: the generation of the accurate prior knowledge, creating proper model/constraints for data fitting algorithms and choice of more robust concentration references.

Lana Kaiser

---

12:05      [Adjournment & Meet the Teachers](#)

---

## Weekend Course

# Cardiovascular MRI: Vascular

*Organizers:* James C. Carr, M.D. & Winfred A. Willinek, M.D.

Room 316A      Saturday 8:15 - 11:45      *Moderators:* Darren Lum & Jeffrey Maki

---

8:15      [Overview of CE & NCMRA Methods](#)

Principles of Contrast enhanced and non contrast enhanced MRA will be reviewed, as well as their clinical application.

Ruth Lim

---

8:35      [Flow Imaging Techniques](#)

Michael Hope

---

8:55      [Contrast Agents](#)

This lecture will deal with conventional Gd-based contrast agents. In particular the molecular basis of the paramagnetic enhancement as well as Gd-complexes stability will be addressed.

Daniela Delli Castelli

---

9:15      [Break & Meet the Teachers](#)

---

9:30      [Imaging Techniques: Current & Future](#)



Atherosclerosis, a systemic disease affecting large and medium sized arterial vessel walls is a leading cause of mortality in the world. MRI is quickly becoming the imaging modality of choice for visualizing atherosclerosis in the vessel wall. Atherosclerosis is evaluated in vivo by multi-contrast dark blood turbo spin echo imaging to evaluate plaque burden and composition. DCE- MRI can be used to evaluate plaque permeability. Recently, quantitative MR imaging in the form of T1 and T2 mapping of the vessel wall and on evaluating 4D flow, shear stress and circumferential strain in the arterial tree have become popular.

Venkatesh Mani

---

9:50

### Intracranial Atherosclerosis MR Imaging

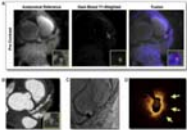
- Intracranial artery atherosclerosis (ICAS) is one of the major causes of ischemic stroke.
- MR vessel wall imaging techniques have been proposed and optimized dedicated for characterizing ICAS.
- High risk ICAS features, such as T1-hyperintense, positive remodeling, and contrast-enhancement, can be accurately identified by ICAS MR imaging.

Xihai Zhao

---

10:10

### Coronary, Aorta & Peripheral Vessel Wall MR Imaging



Magnetic resonance (MR) has emerged as a leading noninvasive imaging modality for assessing the wall disease beyond revealing luminal stenosis. Continued technical innovations are being proposed for MR atherosclerosis imaging, particularly vessel wall imaging, at coronary, aorta and peripheral vascular beds. Detailed knowledge about these techniques would foster adoption of MR as an effective imaging tool in future research and clinical practice. The present lecture will focus on technical developments in MR vessel wall imaging of these arteries.

Zhaoyang Fan

---

10:30

### Break & Meet the Teachers

---

10:45

### Supra-Aortic & Intracranial Vascular Disease

We will review the current recommended imaging parameters to achieve consistent high-quality head/neck contrast-enhanced MRA at both 1.5T and 3.0T. Discuss the utilization of clinical MPRAGE and 3D FSE T1W sequences to detect intraplaque hemorrhage and possibly necrotic core at the carotid bifurcation. Review how this additional vessel wall imaging affords better risk stratification of future stroke than carotid stenosis measurements. Discuss the rapidly evolving intracranial vessel wall imaging (IC VWI) techniques which are currently obtained with works-in-progress investigational sequences. Early implement has documented the potential added value of IC VWI to identify specific etiologies of proximal intracranial arterial narrowing.

J. Kevin DeMarco

---

11:05

### Chest & Abdominal

This presentation will discuss the following:

1. Sequences used for MRA chest & abdomen
2. Clinical applications for MRA chest
3. Clinical applications for MRA abdomen

Christopher Francois

---

11:25

### Peripheral Vascular Disease

Upon completion of this course, the attendee will be able to: Identify the appropriate technique for peripheral MRA depending on the available hardware and the clinical question and condition of the patient. Differentiate between different contrast agents and their specific characteristics. Chose between different contrast agent application schemes depending on the technique used and the clinical question. Compare the pros and cons of contrast-enhanced and non contrast-enhanced techniques for peripheral MRA.

Harald Kramer

---

11:45

### Adjournment & Meet the Teachers

---

## Weekend Course

# Brain Cancer: from Diagnosis to Treatment

*Organizers:* Kristine Glunde, Ph.D. & Natalie J. Serkova, Ph.D.

Room 316BC

Saturday 8:15 - 12:05 *Moderators:* Kristine Glunde & Natalie Serkova

---

8:15 [Introduction to Brain Cancer Imaging \(incl. RANO Criteria\)](#)

This presentation provides an introduction to brain cancer and major treatment options. An overview of current imaging methods is given, including approaches to diagnosis, characterisation and response assessment. The major MR methods available are briefly described, as an introduction to the following more detailed presentations on specific MR imaging Methods. Current approaches to objective imaging based response assessment are discussed.

Martin Leach

---

8:40 [Conventional Imaging: T1, T2 Bright Signal](#)

Noriko Salamon

---

9:05 [From Brain Tumor Angiogenesis to MRI Biomarker](#)

The devastating consequence of a brain tumor on a patient's quality of life and survival has sparked a widespread search for novel therapeutic approaches (e.g. antiangiogenic therapies) to arrest cancer progression. This in turn has galvanized the development of new biomarkers capable of assessing the efficacy of such drugs in vivo. This lecture will provide an overview of how, why and which MRI-derived biomarkers are ideally suited for assessing the angiogenic status of brain tumors, noninvasively and safely in patients. Specifically, this lecture will introduce core concepts about the blood vessels of brain tumors, their role in disease progression, and how one can image them with certain MRI contrast mechanisms, in the preclinical and clinical setting.

Arvind Pathak

---

9:30 [Diffusion & Perfusion Imaging Protocols for Gliomas](#)

We have much to gain by greater incorporation of advanced physiologic MRI methods such as diffusion MRI (DWI) and dynamic susceptibility contrast perfusion MRI (DSC-pMRI) methods into the treatment management protocols for patients with glioma. To motivate greater use this course will describe how these methods can be used at several critical junctures in the management of patients with glioma. Current questions and limitations, both scientific and technical, will also be discussed.

Kathleen Schmainda

---

9:55 [Break & Meet the Teachers](#)

---

10:25 [How Helpful is Neurochemical Characterization](#)



Carolyn Mountford

---

10:50 [MRI for Surgical Planning/Intraoperative MRI](#)

Usefulness of intraoperative MRI for glioma surgery, Akira Matsumura et al.  
Akira Matsumura

---

11:15 [Integrated Amide Proton Transfer Imaging in the Assessment of Pre- & Post-treatment Gliomas](#)

Ji Eun Park

---

11:40 [Radiogenomics in Neurooncology](#)

Olivier Gevaert

---

12:05 [Adjournment & Meet the Teachers](#)

---

## Weekend Course

# Frontiers in Neuroscience: Preclinical MRI-X

*Organizers:* Guoying Liu, Ph.D. & Ed X. Wu, Ph.D.

Room 315

Saturday 8:15 - 12:15 *Moderators:* Albrecht Stroh & Ed Wu

---

8:15 [Preclinical Neural MRI for Basic Neuroscience](#)

Anatomical and functional MRI, complemented by optical imaging methods and electrophysiology, have been at the forefront of unraveling the anatomical and functional organization of the brain. In this talk, we aim to show that high resolution anatomical MRI of the brain can be obtained with remarkable cytoarchitectonic detail, while fMRI can be used to study various sensory systems. Complementary to MRI/fMRI, optical microscopy enables the simultaneous recording of neuronal activity from thousands of neurons with single cell spatial resolution. When combined together, the practical advantages of multi-modal neuroimaging techniques make preclinical imaging an invaluable avenue in neuroscience research.

Afonso Silva

---

8:40 [Optogenetic fMRI Overview](#)

Jin Hyung Lee

---

9:05 [Optogenetic fMRI Application: Dissecting Brain Networks & Properties](#)

Understanding how individual cells and complex brain networks interact in both time and space has been one of the grand challenges in the 21st century. In 2010, Lee et. al. have demonstrated that optogenetic fMRI (ofMRI) within the living mammalian brain reveals BOLD signals in downstream targets distant from the stimulation site, indicating that this approach can be used to map the global effects of controlling a local cell-type specific neuronal population. Since then, multiple studies have utilized ofMRI to dissect brain networks and properties. In this session, technical considerations in the application of ofMRI will be examined. Studies dissecting brain networks and properties using ofMRI will be reviewed. The opportunities and challenges will be discussed.

Russell Chan

---

9:30 [Deep Brain Stimulation & Chemogenetic fMRI](#)

**Electrical deep brain stimulation** and **chemogenetics** are increasingly used with simultaneous fMRI. This lecture will introduce both techniques, discuss the strengths/weaknesses, and make suggestions to pilot studies.

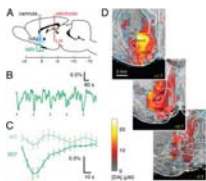
Yen-Yu Ian Shih

---

9:55 [Break & Meet the Teachers](#)

---

10:25 [Molecular fMRI: Imaging Probes for Brain Functions & Circuits](#)



A new experimental approach termed “molecular fMRI” aims to provide direct, minimally-invasive measures of neural function based on the application of molecular probes detectable in time-resolved MRI experiments. In this talk, we discuss the design and application of suitable probes for molecular fMRI, including their initial deployment for imaging several types of signaling molecules in the living brain. By improving the technology with more sensitive contrast agents and better brain delivery strategies, it will be possible to measure and map an expanding array of neurophysiological processes in animals and ultimately in humans.

Alan Jasanoff

---

10:50 [Origins of BOLD - Neuroscience Perspectives](#)

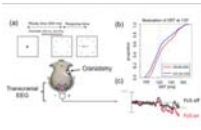
Our ability to study human brain is limited by the necessity to use noninvasive technologies. This is in contrast to animal models where a detailed view of cellular-level brain function has become available due to recent advances in microscopic optical imaging and genetics. Thus, a central challenge facing neuroscience today is leveraging these mechanistic insights from animal studies to accurately draw physiological inferences from noninvasive signals in humans. On the essential path towards this goal is the development of a detailed “bottom-up” forward model bridging neuronal activity at the level of cell-type-specific populations to noninvasive imaging signals.

Anna Devor

---

11:15

[Ultrasound Neuromodulation with MRI for Brain Circuitry in Non-Human Primates](#)



In this presentation, I will discuss ongoing work where we are using ultrasound in conjunction with fMRI to modulate and subsequently image brain circuits in non-human primates.

Charles Caskey

---

11:40

[Concurrent TMS with Neuroimaging - Human Applications](#)

Amit Etkin

---

12:05

[Adjournment & Meet the Teachers](#)

---

## Weekend Course

# MR Systems Engineering

*Organizers:* Gregor Adriany, Ph.D. , Mary P. McDougall, Ph.D. & Graham C. Wiggins, D.Phil.

Room 313A

Saturday 8:30 - 12:00

*Moderators:* Priti Balchandani & James Bankson

---

8:30

[MR Systems Overview](#)

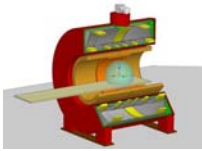
This educational talk is designed to provide a broad overview of the functions and interactions of the subsystems of a modern clinical MRI scanner and explain various design constraints originating from engineering and physiological limitations.

Seung-Kyun Lee

---

9:00

### Magnets: Design, Manufacturing, Installation, Present & Future Technology



The field of an MRI magnet is generated by a circulating current through a sectioned superconducting coil, kept at its operating temperature by a refrigerated cryostat. Active shielding coils confine the stray field to a small volume near the magnet. This presentation covers various aspects of design and operation of these magnets.

Johan Overweg

---

9:30

### Shimming: Superconducting & Passive Shims; Higher Order Shims, Shim Arrays & Dynamic Shimming

Shimming denotes the technical procedure to improve the homogeneity of the magnetic field in the MRI system. This presentation will give an overview about why the magnetic field is inhomogeneous at all, and what the consequence is. Passive and superconducting shims as technical means to improve the shim in every MRI system are described. Practical information on when shimming is needed, and what the operator can do to optimize the shim of their MRI system will be given as well. Moreover, latest developments like high-order shim systems, shim arrays and dynamic shimming will be presented.

Laura Schreiber

---

10:00

### Break & Meet the Teachers

---

10:30

### Gradient Coil Design Considerations, Manufacturing & Limitations

This presentation will describe the parameters that characterise the performance of the gradient coils which are used to generate magnetic fields that vary linearly with position in MRI. The methods for designing cylindrical gradient coils, including the incorporation of active magnetic screening, will then be described, along with boundary element methods that can be used to design coils on any surface. The important elements of coil fabrication will also be considered.

Richard Bowtell

---

11:00

### Gradient Drivers: Amplifier Considerations, Power, Tuning, & Cooling

Blaine Chronik

---

11:30

### Eddy Currents & Interactions: Calibration, Compensation, & Pre-Emphasis



The native accuracy of gradient and shim systems is too low in order to drive MRI sequences. To avoid corresponding image artefacts the gradient chains are feed-backed, pre-distorted and post-corrected based on accurate characterizations or direct measurements of the field evolution in the scanner. In this talk, the underlying principles of the encountered distortions and frequently applied correction methods will be discussed.

David Brunner

---

12:00 [Break & Meet the Teachers](#)

---

## Other

# March for Science Special Session

Plenary Hall                      Saturday 12:00 - 13:00 *(no CME credit)*

---

0:00

---

## Weekend Course

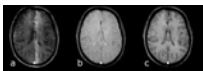
# Physics for Physicists

*Organizers:* Herbert Köstler, Dipl.-Phys. & N. Jon Shah, Ph.D.

Room 313BC                      Saturday 13:15 - 16:45                      *Moderators:* Ana-Maria Oros-Peusquens & Michael Steckner

---

13:15 [Sequences & Simulations](#)

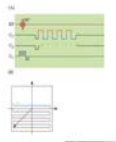


This presentation will provide an overview of the main gradient echo based (gradient spoiled, RF spoiled and balanced steady state free precession) and conventional/fast spin echo based pulse sequences and will illustrate some methods by which their behaviour can be simulated.

Martin Graves

---

13:45 [EPI Acquisition Strategies](#)



The presentation provides a summary of echo planar imaging (EPI) acquisition techniques with descriptions of methods used to shorten the acquisition interval to improve imaging performance ( resolution, SNR, distortion, and/or coverage)

14:15 EPI Artifacts & Correction Methods

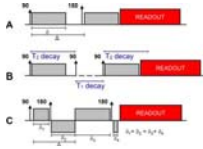
Maxim Zaitsev

---

14:45 Break & Meet the Teachers

---

15:15 Diffusion Weighted Imaging & Applications



Diffusion-weighted imaging (DWI) makes use of molecular water motion to probe tissue microstructure. This lecture will focus on the basic principles of DWI acquisition. After introducing the most commonly used diffusion modules, the main acquisition challenges will be discussed. Typical acquisition approaches will be presented, including single-shot and multi-shot sequences. Examples of frequent DWI image artefacts will be shown, and some of the approaches available for minimizing or correcting for their effect will be presented. The main applications of DWI to brain and body imaging will also be presented, focusing on stroke and lesion characterization.

Rita Nunes

---

15:45 Diffusion Tensor Imaging & Applications

This presentation will touch upon the following aspects: general properties of diffusion, acquisition methods, the diffusion tensor model and diffusion indices, correlations of these indices with other MRI parameters and histology-derived quantities, data sampling strategies, validation strategies, limitations of DTI and applications

Ana-Maria Oros-Peusquens

---

16:15 q-Space: What is it?

Diffusion MRI can provide useful information on microstructures that are much smaller than the imaging voxel sizes. This presentation will start from the original idea by Callaghan and Cory and Garroway showing that the diffusion NMR signal is the Fourier transformation of the displacement probability function, followed by examples of MRI experiments to infer microstructural properties of biological tissues. The basic concepts of q-space and propagator based methods will be discussed.

Qiuyun Fan

---

---

**Weekend Course**

# MR Systems Engineering

Organizers: Gregor Adriany, Ph.D. , Mary P. McDougall, Ph.D. & Graham C. Wiggins, D.Phil.

Room 313A

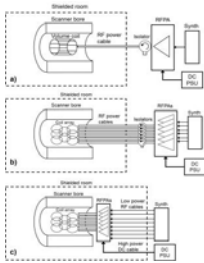
Saturday 13:15 - 16:45

Moderators: Priti Balchandani & James Bankson

---

13:15

RF Transmit: Power Delivery, Decoupling, & Duty Cycle

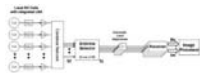


The RF transmit chain is one of several “black box” systems in the MRI scanner. The implementation of the RF transmit chain has remained fairly consistent since the earliest clinical MRI scanners. The advent of parallel transmission (pTX) provides a compelling opportunity to rethink not only the design of the RF power amplifiers (RFPAs) and coils, but of the entire MRI scanner. In this lecture we will review fundamental RFPA concepts such as linearity and efficiency. We will then explore advanced topics relating to pTX, including control, decoupling, local amplifiers, and switchmode amplifiers.

Michael Twieg

13:45

RF Receivers: Signal Detection Chain, Digitization, System Noise Figures - from MRI Signal to Bits



This presentation is designed to give an overview of the building blocks of an MRI receive RF chain, starting with the local MRI coil going all the way to the image processor.

Arne Reykowski

14:15

Controlling the MR Subsystems: Pulse Sequence Control, Waveform Generation & Real-Time Control

Lecture for scientists and clinicians interested in learning more details about the core software structure and control systems of an MRI machine.

Juan Santos

14:45

Multi-Modality Imaging in an MRI Scanner: Simultaneous Imaging & Therapy - Making the Systems Compatible

Although envisioned since the late 1980s, hybrid PET/MR systems only became commercially available in the last few years and more than a decade later than hybrid PET/CT. This is explained by the technological challenges originating from the combination of these two very different imaging modalities. Manifold interferences between the two modalities (in terms of B0, Gradient, RF, Temperature, Photon Attenuation, Space Constraints, Workflow, ...) needed to be identified, understood and solved.

Florian Wiesinger

---

15:15 Break & Meet the Teachers

---

15:45 Basic MR Safety: SAR to Temperature, Power Deposition/Monitoring, Effects of RF Coils & Field Strength

This lecture will cover basic safety issues related to MRI, focusing on power deposition and radio-frequency heating in the patients. Specific absorption rate (SAR) and its relation to temperature will be discussed. Various methods to simulate, predict, control and mitigate SAR and temperature will be introduced. Finally, the effects of RF coil geometry, field strength/frequency will be explained.

Yigitcan Eryaman

---

16:15 Peripheral Nerve Stimulation, Implants & Devices: Safe Use & Considerations for MRI

Simone Winkler

---

16:45 Adjournment & Meet the Teachers

---

## Weekend Course

# The Basics of Perfusion & Permeability Imaging

Organizers: Linda Knutsson, Ph.D. & Steven Sourbron, Ph.D.

Room 312 Saturday 13:15 - 16:45 Moderators: Thomas Okell & Ashley Stokes

---

13:15 The Physiology of Perfusion & Permeability

Symbol	Definition	Unit
$\rho$	Density of blood flow per unit volume of tissue	$\text{g cm}^{-3}$
$\mu$	Permeability coefficient for a given contrast agent	$\text{min}^{-1}$
$\lambda$	Permeability-surface product for a given contrast agent	$\text{min}^{-1}$
$\lambda_{\text{eff}}$	Effective permeability-surface product	$\text{min}^{-1}$
$\lambda_{\text{eff}}^{\text{rel}}$	Relative effective permeability-surface product	
$\lambda_{\text{eff}}^{\text{rel}}(\text{rel})$	Relative effective permeability-surface product (relative to a reference)	
$\lambda_{\text{eff}}^{\text{rel}}(\text{rel})$	Relative effective permeability-surface product (relative to a reference)	
$\lambda_{\text{eff}}^{\text{rel}}(\text{rel})$	Relative effective permeability-surface product (relative to a reference)	
$\lambda_{\text{eff}}^{\text{rel}}(\text{rel})$	Relative effective permeability-surface product (relative to a reference)	



This presentation will describe the mechanisms of microcirculation within the capillary network, as well as the microvascular parameters.

This knowledge is useful to understand dynamic contrast enhanced MRI (DCE-MRI), design acquisition protocols and analyze the data.

Charles Cuenod

---

13:45 [Tracer-Kinetic Analysis](#)

This seminar is intended to provide a broad overview of tracer kinetic modeling. While the basic underlying concepts are quite simple, there are innumerable details which bear close consideration when electing to utilize these methods to characterize the physiologic properties of various tissues in vivo. Multiple steps are involved in optimization of data acquisition and modeling, all of which must be appropriately adapted to the underlying unknowns. Participants should come away from this seminar with an understanding of these steps and a grasp of what considerations arise in planning and executing tracer kinetic studies.

Matthias Schabel

---

14:15 [Break & Meet the Teachers](#)

---

14:30 [Contrast Agent Methods: Data Acquisition & Image Reconstruction](#)

This lecture presents the main data acquisition and image reconstruction techniques for DCE-MRI and DSC-MRI, and discusses strengths, limitations and opportunities.

Ricardo Otazo

---

15:00 [Contrast Agent Methods - Post -Processing](#)

Post-processing methods for dynamic contrast agent acquisitions offer an improved understanding of the underlying tissue. Post-processing methods encompass a number of image processing and pharmacokinetic modeling techniques that lead to the estimation of physiologically relevant semi-quantitative and quantitative parameters from the acquired dynamic set of images. Some of the post-processing methods are broadly applicable to several clinical applications that include cardiovascular, tumor, and kidney imaging.

Ganesh Adluru

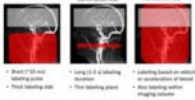
---

15:30 [Break & Meet the Teachers](#)

---

15:45

### ASL - Data Acquisition



This talk will outline the basic principles of arterial spin labelling (ASL) data acquisition. The different labeling approaches are compared, the compromise in post labeling delay duration is discussed, why background suppression pulses improve the ASL-signal stability is explained, readout options are described, acquisition parameters are explored and examples of both basic and advanced ASL-techniques are shown.

Sophie Schmid

---

16:15

### ASL- Post-Processing

This educational talk will cover common ASL post-processing steps. The talk includes (1) pre-processing of image data, (2) from general to basic models for perfusion quantification, (3) partial volume correction, and (4) advanced perfusion quantification. Focus will be put on the pre-processing and basic perfusion quantification.

André Ahlgren

---

16:45

### Adjournment & Meet the Teachers

---

## Weekend Course

# Connectivity: Structure & Function

*Organizers:* Jennifer A. McNab, Ph.D. & Joshua S. Shimony, M.D., Ph.D.

Room 311

Saturday 13:15 - 17:45

*Moderators:* Andrada Ianus & Elizabeth Meyerand

---

13:15

### Connectomics Primer

In this talk I will outline basic approaches for charting the organisation of functional connectivity and introduce novel tools and techniques that enable characterisation of functional connectors in terms gradual change in connectivity profiles. I will provide examples of how these techniques can be used in clinical and cognitive neuroscience research.

Christian Beckmann

---

13:45

### Measuring Connectivity with RSfMRI

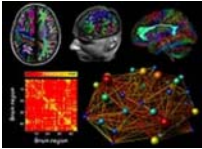
Connectivity in resting-state fMRI can be evaluated through a variety of different methods. These include methods for static functional connectivity, such as seed-correlation, spatial independent component analysis, and graph theoretical approaches. In addition, dynamic functional connectivity can be assessed using methods such as sliding window correlation, time-frequency analysis, co-activation patterns and temporal independence component analysis.

Mark Chiew

---

14:15

### Measuring Connectivity with Diffusion MRI



I will present the pipeline that is used for computing estimates of structural brain connectivity as obtained with diffusion tractography. Several methodological considerations will be discussed.

Alexander Leemans

---

14:45

### What Correlates with Your Connectome?

Since the introduction of functional and structural connectivity approaches, MRI has been used to assess age-related differences on a brain network level. A systems-level or network approach of brain structure and function provides an intuitive framework for understanding a complex dynamic system. In this talk I will discuss previous research that used MRI to study the effect of aging on brain networks in vivo, through functional connectivity measures derived from resting-state functional MRI and structural connectivity measures derived from diffusion MRI.

Jessica Damoiseaux

---

15:15

### Break & Meet the Teachers

---

15:45

### RSfMRI - correlation with optical imaging in neonates

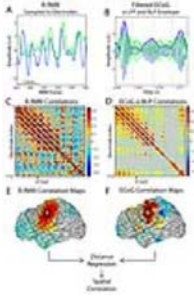
Diffuse optical imaging (DOI) is a portable imaging modality that provides the ability to perform early and continuous monitoring of brain function. Its portability overcomes many of the technical and logistical challenges of performing MRI investigations in hospitalized patients. While standard DOI systems suffer from low spatial resolution and lack of brain specificity, new developments in hardware and software have overcome many of these technical limitations. In this talk, I will introduce novel DOI techniques developed for bedside mapping of resting-state functional connectivity in neonates and adults and present multi-modal comparisons with functional MRI maps obtained in the same subjects.

Silvina Ferradal

---

16:15

### FMRI - Ecog Correlates



This talk will focus on recent developments in studying the electrophysiologic basis of functional MRI correlations. We will examine methods to measure the spatial correspondence between electrophysiologic band-limited power (BLP) and fMRI correlation patterns in human subjects. We will then discuss the available evidence that correlated, spontaneous activity of the brain exhibits frequency specificity, and outline a hypothesis that the spectral structure of task responses is reflected in the hierarchical organization of RSNs.

Carl Hacker

---

16:45

### Diffusion - Histology Correlates

MRI parcellation and connectivity is widely used in neuroscience, however their validation have been challenging. In this talk, several validation methods will be discussed, such as histology, polarized light imaging and optical coherence tomography.

Caroline Magnain

---

17:15

### Diffusion - Electrophysiology Correlates

The majority of fMRI studies use T2 or T2\* weighted scans. Studies have shown that diffusion MRI scans can detect activation. However, the exact biophysical mechanism remains unclear. We will explore the physiology of neuronal activation, the BOLD response, fMRI and diffusion MRI, and how to disentangle the BOLD response and microstructure changes.

Bernard Siow

---

17:45

### Adjournment & Meet the Teachers

---

## Weekend Course

# Novel & Mature MRI Contrast Agents

Organizers: Ichio Aoki, Ph.D. & Guanshu Liu, Ph.D.

Room 314

Saturday 13:15 - 17:15 Moderators: Ichio Aoki & Kevin Bennett

---

13:15

### Chemistry of MRI Tracer

Silvio Aime

---

13:45

### Nanoparticulate Agents for Imaging in Diabetes

Diabetes is a devastating disease hallmarked by high levels of blood glucose (hyperglycemia). While blood glucose measurement is considered a standard procedure for diabetic patients, it does not reflect a true status of functional beta cells and cannot be used for disease monitoring and evaluating the therapeutic response. The development of strategies for the noninvasive assessment of molecular events associated with diabetes constitutes an important healthcare priority. This presentation will focus on the development of imaging agents and techniques that could provide real time non-invasive data of biological parameters and their functions as they relate to diabetes progression and treatment.

Anna Moore

---

14:15

### Hyperpolarized MRI & MRS Tracers



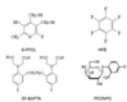
MRI relies on detecting signals in the radiofrequency range that are related to very small energy transitions of the detected molecules. While this is a blessing with regard to the harmless character of MRI, it imposes a serious problem in terms of the low sensitivity caused by almost vanishing spin polarization at ambient temperature. Increasing the sensitivity through special preparation of the spin system prior to the encoding and detection is therefore a powerful approach. The achieved hyperpolarization has enabled various applications for molecular and cellular imaging. This tutorial will summarize aspects of polarization methods, probe design and signal encoding.

Leif Schröder

---

14:45

### Beyond Proton MRI: <sup>19</sup>F MRI & More



<sup>19</sup>F NMR offers exceptional insights for diverse physiological and pharmaceutical investigations. High sensitivity and lack of interfering background signal in the body have enabled the observation of exogenously administered agents and their metabolites. <sup>19</sup>F exhibits a large chemical shift range, which is exquisitely sensitive to the microenvironment. In addition to chemical shift, relaxation processes ( $R_1$  and  $R_2$ ), and chemical exchange may be tailored to be responsive to a parameter of interest such as  $pO_2$ , pH, metal ion concentrations, transgene/enzyme activity or hypoxia. I will review <sup>19</sup>F NMR/MRI as a foundation for diverse applications and recent innovations.

Ralph Mason

---

15:15

### Break & Meet the Teachers

---

15:45

### MRI Biosensors

The role of MRI contrast agents is evolving, from enhancing tissue contrast to sensing physiological changes. New generation of MRI biosensors can detect and respond to biomarkers such as small molecules, metabolites, metal ions, proteins, enzymes or pH. The major hurdles in translating these biosensors from bench to bedside are their insufficient sensitivity and specificity in vivo. Various biosensors have addressed these issues in specific biomedical applications. In this talk, we will discuss the frontier MRI biosensor designs for imaging biomarkers in vivo, such as using nanomaterials and MRI contrast mechanisms to improve the sensitivity and specificity, and their features to overcome barriers in biomedical applications.

Kannie WY Chan

---

16:15 [Current Clinical Applications & Future Translation Potential](#)

Zahi Adel Fayad

---

16:45 [Dual-Mode Cellular Imaging for Immunotherapy & Cancer Vaccine Development](#)

Using magnetoGVAX and MRI for serially monitoring the afferent arm of the immune response (DCs), and bioluminescent imaging (BLI) for monitoring the efferent arm (T cells), one can apply dual-mode imaging to better understand the time course of antigen capture, lymph node delivery, and clonal T cell expansion. Depending on the timing of administration, immunoadjuvants either reduce or enhance antigen capture and delivery to the lymph nodes. The lack of antigen delivery to lymph nodes can be consistent with the lack of T cell BLI signal in the lymph nodes. In those cases, a massive extranodal T cell proliferation occurs in the liver and spleen. These types of studies can show how dual-mode imaging can be used to evaluate and optimize combinatorial cancer vaccines.

Jeff Bulte

---

17:15 [Adjournment & Meet the Teachers](#)

---

## Weekend Course

# Cardiac MRI: Function, Perfusion & Viability

*Organizers:* Reza Nezafat, Ph.D., Sonia Nelles-Vallespin, Ph.D. & Winfred A. Willinek, M.D.

Room 316A                      Saturday 13:15 - 17:25 *Moderators:* Andrew Scott & Behzad Sharif

---

13:15 [Clinical Needs & Applications: Evaluation of Cardiac Function](#)

13:35 [State of the Art: Acquisition & Processing](#)

Cardiovascular MRI provides detailed information about the health status of the heart and the progression of disease. This talk will give course participants an overview of current methods used to evaluate cardiac performance on a global and regional level. Particular focus will be on strengths and weakness of methods to quantify myocardial strain, and atlas based methods for quantifying cardiac remodelling as z-scores.

Alistair Young

---

13:55 [Future Perspectives: Acquisition & Processing](#)

Mehdi Hedjazi Moghari

---

14:15 [Clinical Needs: Ischemic Heart Disease](#)

Cardiovascular magnetic resonance (CMR) has become an established non-invasive imaging modality for the diagnosis of ischemic heart disease (IHD) and contributes important information for therapeutic decisions regarding revascularization. For the identification of ischemia, CMR provides two methods, which are routinely used in clinical practice. Ischemia can be visualized either as regional hypoperfusion when using CMR-perfusion imaging during vasodilator induced hyperaemia, or as impaired regional wall motion under dobutamine stress CMR. CMR has proven its robustness, diagnostic performance and prognostic value in patients with IHD in several multicenter trials.

Alexander Gotschy

---

14:35 [Quantitative Myocardial Perfusion](#)



Quantification of myocardial blood flow (MBF, in the unit of ml/min/g) is more objective to assess myocardial micro-circulation under rest and pharmaceutical or exercise stress condition and capture global flow reduction. Although perfusion quantification has been studied for the past 20 years, it is still not clear how to build a practical quantitative myocardial perfusion workflow. This syllabus reviews key components of such system and emphasizes on motion correction, intensity to Gd concentration conversion and Gd kinetics modelling. With recent developments more focusing on the automation and completeness of entire workflow, including fully automated processing and motion correction, the quantitative perfusion is becoming clinically practical.

Michael Hansen

---

14:55      [Dobutamine Stress MRI](#)

Connie Tsao

---

15:15      [Break & Meet the Teachers](#)

---

15:45      [Clinical Needs & Applications: Myocardial Tissue Relaxometry](#)

This lecture will discuss the clinical needs and applications of myocardial relaxometry. We will discuss the need to develop relaxometry imaging biomarkers which are sensitive, specific, predictive and robust. These criteria will need to be fulfilled to make clinical decisions in individual patients. We will also discuss current and emerging clinical applications of myocardial relaxometry.

Michael Salerno

---

16:05      [Myocardial T1 Imaging Techniques](#)

Sebastien Roujol

---

16:25      [Myocardial T2 & T2\\* & T1 Rho Mapping Techniques](#)

MRI measures of signal decay without refocusing, with intermittent refocusing and with continuous refocusing reflected by time constants  $T2^*$ ,  $T2$ , and  $T1\rho$  can yield important clinical information in myocardial pathophysiology.  $T2^*$  is used to characterize iron overload, although specificity is reduced by susceptibility effects. By incorporating refocusing of static inhomogeneity effects,  $T2$  yields more specific characterization of signal changes associated with changes in blood oxygenation reflecting ischemia and changes in water mobility reflecting inflammation. Decreasing refocusing interval reduces dephasing due to diffusion through gradients and chemical exchange effects and has been used to increase  $T1\rho$  contrast between healthy and infarcted myocardium.

Graham Wright

---

16:45      [Clinical Needs & Applications](#)

The following presentation will outline the clinical needs and applications for the use of CMR for cardiac function, perfusion and viability in clinical cardiology.

Raymond Chan

---

17:05      [State of the Art: Viability Sequences](#)



This talk will be presenting recent advances in late gadolinium enhancement (LGE) cardiac imaging which can overcome limitations of the standard protocol based on inversion recovery segmented 2D acquisition. The advanced approaches to be discussed will include single-shot imaging with motion corrected averaging, single-breath-hold 3D imaging, free-breathing isotropic 3D imaging with respiratory, and techniques to improve scar-blood contrast and scar-fat contrast.

Taehoon Shin

---

17:25 [Adjournment & Meet the Teachers](#)

---

## Weekend Course

# Imaging Biomarkers of Brain Disorders

Organizers: Kelvin O. Lim, M.D. & Kei Yamada, M.D.

Room 316BC      Saturday 13:15 - 17:15 *Moderators:* Kelvin Lim & Kei Yamada

---

13:15 [Diffusion as a Biomarker for Brain Disease](#)

This session focuses on and tries to appraise diffusion MRI (dMRI)-derived imaging biomarkers (dMRI-IB) for brain disease. To categorize dMRI-IB: 1) confirm the definition of IB; 2) proceed through dMRI-derived measures and applications; 3) introduce the possible candidate of dMRI-IB; and 4) discuss about barriers that dMRI-IB candidates should overcome. In addition, this session will address following issues: 1) why only limited dMRI measures can be considered for IB? 2) what is the problem for dMRI-IB candidates to become true IB? 3) what can we do for creating new IB?

Koji Sakai

---

13:45 [fMRI as a Biomarker for Brain Disease](#)

In this talk I will discuss current progress and challenges in the use of brain imaging for single subject prediction.

Vince Calhoun

---

14:15 [MRS as a Biomarker for Brain Disease](#)

Carolyn Mountford

---

14:45 Panel Discussion

---

15:00 Break & Meet the Teachers

---

15:30 State of the Art - Depression

Major depressive disorder is a serious public health problem, representing a leading cause of worldwide disability, and a major contributor to suicide. While treatments exist to address this problem, they are not always efficacious, highlighting the need for more research to better understand the neural circuitry underlying depression and its treatment. In the past 2 decades, human neuroimaging research has made great strides in providing information about which neural circuits are implicated in depression. In this talk we will review some of the major contributions to this body of knowledge including research using structural neuroimaging, positron emission tomography, and functional magnetic resonance imaging. We will also discuss the smaller but emerging literature using these tools in the context of clinical trials to begin to understand predictors and mechanisms of treatment response in patients with depression. While there have been great strides forward in understanding the neural circuitry underlying depression, much work still remains before this knowledge can be applied in the clinic. Heterogeneity in the findings across studies may reflect heterogeneity of MDD itself, where individuals that fall under the same diagnosis may have different neural circuitry signatures. Advanced methods that are designed to better understand these differences across subjects could provide the traction needed to develop personalized treatment approaches.

Kathryn Cullen

---

16:00 State of the Art - Epilepsy

Epilepsy is a broad syndrome that results in societal, economic and medical burdens. Identification and development of MRI based biomarkers that are predictive of epileptogenesis are urgently needed. We describe the development of one such biomarker for febrile seizures. Once definitive biomarker imaging approaches have been validated, therapeutic interventions can then be investigated.

Andre Obenaus

---

16:30 State of the Art - Parkinson's Disease

The major role of the imaging used to be ruling out other disorders which present the symptoms of Parkinsonism. However, there are several imaging method which can visualize the abnormality in the Parkinson's disease including neuromelanin image, diffusion images or susceptibility weighted imaging. This lecture will discuss on the recently developed imaging method for Parkinson's disease or related disorders.

Toshiaki Taoka

---

17:00 [Panel Discussion](#)

---

17:15 [Adjournment & Meet the Teachers](#)

---

## Weekend Course

# Quantitative Susceptibility Mapping & Electrical Properties of Tissues

*Organizers:* Dong-Hyun Kim, Ph.D., Chunlei Liu, Ph.D. & Peter van Zijl, Ph.D.

Room 315                      Saturday 13:15 - 17:15 *Moderators:* Dong-Hyun Kim & Sina Straub

---

13:15 [Interaction of Electromagnetic Fields with Tissue](#)

The interaction of electro-magnetic fields with tissues is mediated by Maxwell Equations and inherently related to the existing dielectric and magnetic tissue properties.

In this presentation we will cover some of the aspects known regarding: the physical mechanisms behind of magnetic susceptibility; the conductivity and electric permittivity at the frequencies of interest in MRI (MHz in the case of the resonating radio-frequency waves, and KHz in the case of the switching of encoding gradients).

The way these interactions influence not only the images acquired in MRI but also the comfort of subjects will be addressed.

José Marques

---

13:35 [Principle of QSM: Physics & Contrast Mechanism](#)

The principles of obtaining the physical quantity of magnetic susceptibility using MRI are being presented. Quantitative Susceptibility Mapping (QSM) reflects tissue susceptibility using the MR phase information acquired using a gradient echo sequence. To obtain susceptibility maps several steps are required in the reconstruction, including (i) phase measurement, (ii) field map estimation, (iii) background field removal, and (iv) susceptibility map calculation by solving the inverse problem. Examples and challenges of QSM are presented and discussed.

Markus Barth

---

13:55



### Principle of Electrical Properties Mapping

This study gives an overview of the principles of Electrical Properties Tomography. The aim is to introduce researchers new to EPT in the basic EPT reconstruction principles, EPT artifacts and new directions.

It reviews Helmholtz based reconstruction, B1+ phase and transceive phase, boundary errors of EPT, forward vs inversion based EPT reconstruction and the synergy of EPT at high fields.

Cornelis van den Berg

---

14:15

### Break & Meet the Teachers

---

14:30

### Application of QSM in the Brain: Neurovasculature

Clinical application of QSM in pediatric brain will be discussed including its clinical role for evaluating normal and abnormal cerebral neurovasculature, vascular malformations, and hemorrhagic conditions through various clinical scenarios. In addition, plural contrast imaging feasible with 3D GRE multi-echo imaging will be addressed and its potential role in assessing various types of pediatric brain pathology. Use of Ferumoyxtol as a nanoparticle vascular agent to augment neurovascular diagnostic evaluation will be addressed through clinical examples. Finally, pitfalls and artifacts associated with QSM and T2\* imaging will be discussed.

Kristen Yeom

---

14:50

### Application of QSM in the Brain: Neurodegenerative

Iron measured by MRI in vivo would contribute to searching for iron-related biomarkers in neurodegenerative diseases, like Parkinson's disease.

Here, we would like to briefly introduce the technological development of MRI in assessing brain iron, discuss the nigral iron as a potential marker for PD in both clinical and prodromal stages, further put insight into other influences of regional iron on PD symptoms.

Minming Zhang

---

15:10

### Application of QSM in the Body

The brain has long been a major focus for QSM, while applications of QSM outside the brain have occurred more recently. This course deals with both the technical aspects specific to QSM of the body and some of its clinical applications.

15:30

### Application of Electrical Properties Mapping



The contrast in electrical properties (EP's) between regions of interest (ROI's) is typically limited to less than 30%; within-subject and between-subject variability is also on the order of 30%. The SNR of reconstructed EP's depends on the reconstruction method used; for Laplacian-based EP reconstruction, SNR depends on field strength, absolute value of EP's and  $(ROI\_size)^{3.5}$ . At 3T and 7T, some applications for which relatively large ROI EP's are sought have promising results using standard EP reconstruction. In order for EP mapping to become a reality at spatial resolutions useful for clinical diagnosis, more advanced reconstruction methodologies are likely needed.

Ileana Hancu

---

15:50

### Break & Meet the Teachers

---

16:05

### Review of Algorithms of QSM

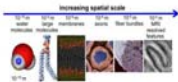
Quantitative susceptibility mapping aims to solve the magnetic dipolar inverse problem to reconstruct tissue magnetic susceptibility distributions from single- or multi-echo GRE phase data. Being an ill-conditioned inverse problem, computation of magnetic susceptibility is challenging and requires conditioning. Several approaches to solve this problem exist, including threshold-based masking or kernel modification, utilizing data redundancy achieved by multiple MRI measurements with different orientations of the object, or applying regularization techniques that incorporate prior information about the spatial distribution of susceptibility. Several of these approaches will be reviewed in this lecture.

Jürgen Reichenbach

---

16:25

### Microstructural Effect on Susceptibility

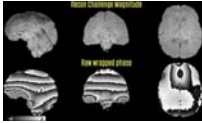


High field studies have brought to light not only that the composition of tissues affects MRI susceptibility contrast, but also that a tissue's sub-voxel structure at scales all the way down to the molecular level plays an important role as well. In this overview, various ways will be discussed by which sub-voxel structure can affect magnetic susceptibility contrast, and the extraction of quantitative magnetic susceptibility values. In addition, opportunities study the microstructural aspects of brain tissue with susceptibility weighted MRI will be reviewed, with an emphasis for inferring the orientation of fiber bundles in white matter and the relative size of the myelin water compartment.

Jeff Duyn

---

16:45



## QSM Software Demo

This demo focuses on the processing pipeline of the 2016 QSM Reconstruction Challenge. The aims of the Challenge were (i) to test the ability of QSM algorithms to recover the underlying susceptibility from phase data, and (ii) to provide a dataset that would help benchmark existing and future techniques. The demo begins with raw phase data and applies unwrapping, background removal, transmit phase mitigation, and finishes with fast dipole inversion techniques: TKD and Closed-Form L2-regularization. This replicates the pipeline through which the benchmark susceptibility maps were computed for the Challenge, and can serve as a starting point in future studies.

Berkin Bilgic

16:45

## QSM Software Demo

We have developed robust QSM software for both clinicians and researchers. For clinicians interested in using QSM in their daily practices, we present an automated QSM workflow that can be implemented across major MRI manufacturers at both 1.5 and 3T. QSM is automatically reconstructed and available for viewing at the end of each patient MRI session. For researchers interested in further developing QSM algorithms, we present MATLAB tools and source codes for the core Bayesian QSM algorithm, along with implementation for nonlinear field estimation, field unwrapping and background field removal. A GUI tool is provided and demonstrated.

Zhe Liu

16:45



## QSM Software Demo

Quantitative susceptibility mapping (QSM) and susceptibility tensor imaging (STI) are two recently developed imaging methods for quantifying tissue's magnetic property. Magnetic susceptibility offers a new contrast for high-resolution anatomical imaging; it further provides important information on tissue's chemical composition, especially myelin and iron, and white matter microstructures of the brain. However, processing QSM and STI still requires advanced technical expertise. The growing application and wider acceptance of this new technique has generated a need for a comprehensive software package that can easily perform all these analysis. Here, we have developed such a tool named "STI Suite". This software is based on our previous works. In this Matlab-based software package, we have implemented the essential algorithms for phase processing, QSM, STI, and related analysis tools. To facilitate the dissemination and evaluation of these methods, we make STI Suite freely available at <http://people.duke.edu/~cl160/> for non-commercial academic use. STI Suite contains both Matlab command-line functions and graphical user interfaces (GUIs) for phase processing, QSM, STI, and related visualization and ROI analysis tools.

Hongjiang Wei

---

17:15

Adjournment & Meet the Teachers

---

## Other

### Newbie Reception

Hilton Hawaiian Village    Saturday 19:00 - 21:00 *(no CME credit)*  
Great Lawn

---

## Sunday, 23 April 2017

Go to top

## Other

### ISMIRM Fun Run 2017

Sunday 5:00 - 7:30                      *(no CME credit)*

---

## Weekend Course

### IVIM & Cerebrovascular Reserve

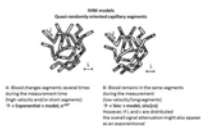
*Organizers:* Hanzhang Lu, Ph.D. & Stephan E. Maier, M.D.,Ph.D.

Room 311                      Sunday 8:15 - 11:45    *Moderators:* Hanzhang Lu & Stephan Maier

---

8:15

[Introduction to IVIM](#)



Intravoxel Incoherent Motion (IVIM) refers to translational movements which within a given voxel and during the measurement time present a distribution of speeds in orientation and/or amplitude. The IVIM concept has been used to estimate perfusion in tissues as blood flow in randomly oriented capillaries mimics a pseudo-diffusion process. IVIM-based perfusion MRI, which does not require contrast agents, has gained momentum recently, especially in the field oncology. In this introduction the basic principles, models, technical requirements and limitations inherent to IVIM-based perfusion MRI, as well as new, non-perfusion applications of IVIM MRI, such as virtual MR Elastography will be outlined.

Denis Le Bihan

---

8:45

### IVIM in the Body

Intravoxel incoherent motion (IVIM), which decomposes diffusion-weighted MRI signals in to microcirculation and microstructural components, has seen tremendous application throughout the body. This presentation will review the major trends, findings, and challenges of this surge of activity.

Eric Sigmund

---

9:15

### IVIM in the Brain

The lecture targets physicists, engineers and physicians with an interest in advanced brain perfusion imaging with intravoxel incoherent motion.

Christian Federau

---

9:45

### Break & Meet the Teachers

---

10:15



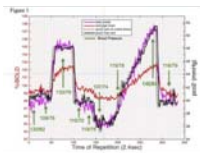
### Introduction To Cerebrovascular Reserve & Its Measurements

Cerebrovascular reserve is a marker of the brain's ability to compensate for a decreased perfusion pressure which would otherwise lead to a decreased cerebral blood flow with consequently ischemic events. In this lecture we will describe the concept of cerebrovascular reserve, we will briefly go through the different MRI methods to evaluate the cerebrovascular reserve and we will describe the challenges available to assess the cerebrovascular reserve.

Jill De Vis

---

10:45



### MRI Measurement of Cerebrovascular Reactivity: Clinical Implementation

The interest in translating MRI mapping of cerebrovascular reactivity (CVR) for the clinical assessment of hemodynamic insufficiency secondary to cerebrovascular disease is increasing. This presentation will focus on the current issues and potential solutions facing widespread dissemination of this methodology. Issues regarding the flow stimulus, flow sensitive pulse sequences, data analysis, and clinically relevant detection thresholds will be presented.

David Mikulis

---

11:15

### Applications of Cerebrovascular Reserve: Vascular Disease, Tumor, fMRI, Etc.



Measuring the brain perfusion responsive to the external vasodilators, termed cerebrovascular reactivity (CVR), is a useful tool towards better understanding of brain pathophysiological conditions, such as arterial stenosis, brain tumor, dementia, and traumatic brain injury. Moreover, CVR evaluation could serve as a novel approach to normalize the BOLD fMRI signal and quantify neural activity evoked by stimulation in calibrated fMRI as well, paving the way for neuroscience research.

Shin-Lei Peng

---

11:45 [Adjournment & Meet the Teachers](#)

---

## Weekend Course

# Body MRI: Optimize Your Clinical Practice: Approach to Setting Up a Body MRI Practice

*Organizers:* Kathryn Fowler, M.D., Kartik Jhaveri, M.D., F.R.C.P.C., Lorenzo Mannelli, M.D., Ph.D. & Edwin J.R. van Beek, M.D., Ph.D., M.Ed., FRCR

Room 315      Sunday 8:15 - 9:45      *Moderators:* Vikas Gulani & Darren Lum

---

8:15 [An Update on Pulse Sequences & Hardware for Body MRI](#)

This presentation will provide an update on pulse sequences and hardware for body MRI. This presentation is by no means a complete overview of the new hardware and pulse sequence development; due to the time constraints, this talk will highlight a few important developments pertinent to body MRI.

Shahid Hussain, MD, PhD, FACR

---

8:45 [Contrast Agents & Their Applications](#)

This educational talk provides a broad overview of gadolinium based contrast agents (GBCA) for MRI with a focus on the types of gadolinium chelators, toxicity concerns with a focus on nephrogenic systemic fibrosis (NSF), as well as potential applications for specific GBCA. Although numerous MRI contrast agents have been developed, this talk will focus on those that are clinically available to inform radiologists of potential clinical applications for GBCA.

Joseph Ippolito

---

9:15 [Non-Contrast Enhanced MR Imaging of the Body](#)

Contrast is widely used in body MRI, but is it always necessary? This presentation will review clinical scenarios and protocols where contrast may not be required.

Ruth Lim

---

9:45

Break & Meet the Teachers

---

## Weekend Course

# Multiparametric Imaging in Cancer - How & Why

Organizers: Gregory J. Metzger, Ph.D. & Natalie J. Serkova, Ph.D.

Room 314

Sunday 8:15 - 12:05

Moderators: Gregory Metzger & Natalie Serkova

---

8:15

## Quantitative Multiparametric Imaging in Oncology

Modality	Quantitative Parameter	Biophysical Basis	Applications
MR	ADC	Water molecule diffusion	Staging, treatment response
MR	Perfusion (DSC, ASL)	Microvascular blood flow	Staging, treatment response
MR	MR Spectroscopy	Metabolic profile	Staging, treatment response
MR	MR Elastography	Tissue stiffness	Staging, treatment response
MR	MR Fingerprinting	Multi-parametric tissue characterization	Staging, treatment response

This course will introduce the different imaging modalities that are used in (clinical) oncology research. This lecture gives a brief overview of these imaging techniques and the quantitative information that can be derived from it. Combining information from different modalities can aid in answering typical questions related to oncology.

### Learning goals

At the end of this lecture you will know:

- What different MR modalities are being used in oncology research (and clinic).
- What their quantitative endpoint is.
- What other imaging modalities such as PET and optical imaging have to offer for oncology (research) and what their quantitative endpoint is.
- How information of different modalities can be combined in research and clinical questions.

Jannie Wijnen

---

8:40

What Is the Ground Truth - Calibration & Standards

MR-based quantitative imaging biomarkers (QIBs) can provide anatomic and functional measures critical to the successful delivery of precision medicine by informing treatment selection, providing early non-invasive assessment of treatment response, and providing post-treatment surveillance. There are significant barriers, however, to successful implementation of such measures across imaging systems, centers, and time, including the need for phantoms (physical and digital) and standards. This presentation will provide examples of MR-based QIBs, describe key challenges to their disseminated implementation, and provide examples of approaches that a variety of agencies and organizations are taking to address those challenges.

Edward Jackson

---

9:05 [Parameters Derived from Diffusion Weighted Imaging](#)

John Gore

---

9:30 [Dynamic Contrast Enhanced \(DCE\) Imaging - Heuristic Versus Quantitative](#)

This lecture discusses the heuristic and quantitative methods for DCE-MRI data analysis, the clinical applications of both approaches in cancer imaging, the major factors that cause variabilities in the estimated heuristic metrics and quantitative pharmacokinetic parameters, and the need for standardization of data acquisition and analysis to improve reproducibility and repeatability and for consensus/guideline on whether heuristic or quantitative data analysis is the best-practice approach for a particular cancer imaging problem or topic.

Wei Huang

---

9:55 [Break & Meet the Teachers](#)

---

10:25 [Other Methods: DSC, BOLD, ASL, MRS](#)

This course will present a high level overview of the “other” MRI methods (dT1, DSC, BOLD, ASL, MRS) that have been used for the assessment of cancer, with a focus on their utility in brain tumors. The specific emphasis will be on quantification, which is becoming increasingly necessary to detect and track changes over time with the goal of optimal response assessment.

Kathleen Schmainda

---

10:50 [Feature Extraction & Radiomics](#)

Radiomics is defined as: "conversion of digital medical images into mineable high-dimensional data... motivated by the concept that biomedical images contain information that reflects underlying pathophysiology and that these relationships can be revealed via quantitative image analyses". Radiomic features are comprised of imaging biomarkers (IB) Some key questions must be answered at an early stage: "Does the IB fulfill an unmet clinical need?"; "Does data exist to evaluate the IB and if not can it be obtained?". At an early stage, technical validation including assessment of precision through repeatability and reproducibility must be determined. Furthermore, biologic and clinical validation must also be performed. Cost effectiveness must also be considered. The paradigm and consideration in radiomics research will be reviewed.

Masoom Haider

---

11:15 [Quantitative Multi-Modal PET/MR Imaging in Oncology](#)

PET and MR are two imaging modalities that complement each other, and by combining the two, both the anatomical depiction of MRI, and the high molecular sensitivity of PET can be exploited. With truly integrated PET/MR systems, PET and MR images can be acquired simultaneously in one imaging session, saving time and securing minimal need for registration between images. Within oncology, PET/MR could be a viable option in cancers where MR is the preferred imaging modality and where PET/CT currently has a limited role in the clinic.

Kirsten Selnæs

---

11:40 [Panel Discussion](#)

---

12:05 [Adjournment & Meet the Teachers](#)

---

## Weekend Course

# Translational Musculoskeletal Imaging: from Qualitative to Quantitative

*Organizers:* Jenny T. Bencardino, M.D., Eric Y. Chang, M.D., Christine Chung, M.D. & Philip Robinson, M.D.

Room 316A

Sunday 8:15 - 12:15

*Moderators:* Neal Bangerter & Catherine Roberts

---

8:15 [MR Imaging Around Metal: Technical Aspects](#)

Orthopedic implants cause significant artifact in MRI. Here, we will make a classification of these artifacts. Then approaches to minimize the susceptibility related artifacts are described, such as the use of "wide band" sequences, view angle tilting and multi-spectral imaging methods.

Clemens Bos

---

8:50



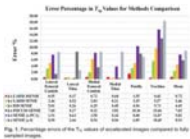
### MR Imaging Around Metal: Clinical Applications

Metal implants are now commonplace in modern medicine. MRI evaluation of symptomatic patients with orthopedic hardware used to be severely limited by susceptibility artifact. However, recent advances in metal suppression techniques allow improved imaging around metal, making MRI effective for evaluation of patients with symptomatic implants, even at higher magnetic field strengths. This lecture will cover some of the common clinical applications of metal suppression MRI, particularly with respect to total hip and knee arthroplasties, and will also demonstrate the utility of metal suppression with respect to other implants and in the evaluation of patients with spinal hardware.

Kathryn Stevens

---

9:25



### Acceleration Methods: Technical Aspects

MR quantitative imaging have been shown to be promising markers for detecting early degeneration and predicting disease progression in musculoskeletal (MSK) imaging due to its relatively independence of scanners/protocols. However, the long acquisition time and associated low resolution quantitative imaging have impeded their wide applications in clinical trials and practice. Recently compressed sensing and parallel imaging based acceleration methods have shown promise to address these challenges such that the quantitative imaging can be translated into clinical practice. Despite the extensive studies in other applications such as brain imaging, MR quantitative imaging in MSK has been overlooked. This course will teach some acceleration methods combining compressed sensing and parallel imaging and show their applications in MSK imaging.

Leslie Ying

---

10:00

### Acceleration Methods: Clinical Applications

Multiple different methods are now available which can be used to accelerate musculoskeletal MRI and improve the efficiency of MRI protocols for evaluating musculoskeletal diseases without compromising image quality or diagnostic performance. These methods including the use of highly efficient spiral and radial k-space trajectories, 3T scanners, parallel imaging acceleration, isotropic resolution imaging, compressed sensing k-space under-sampling, and T2 shuffling.

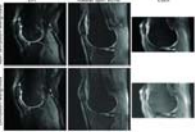
Richard Kijowski

---

10:35 Break & Meet the Teachers

---

11:05 MSK Applications of Diffusion Weighted Imaging: Technical Aspects



The objective of this talk is to present a hands-on on the acquisition and processing of diffusion-weighted imaging tailored to MSK applications. In this presentation we will

explain how diffusion is measured and which is the meaning of the experimental parameters;

- discuss the different acquisition strategies for diffusion-weighted imaging; and learn how to optimize a diffusion protocol for a given

Jose Raya

---

11:40 MSK Applications of Diffusion Weighted Imaging: Clinical Applications

Won Hee Jee

---

12:15 Break & Meet the Teachers

---

## Weekend Course

# Traumatic Brain Imaging: Whom, How, When

*Organizers:* Alex L. MacKay, D.Phil. & Andre Obenaus, Ph.D.

Room 312                      Sunday 8:15 - 12:15                      *Moderators:* Tim Duong & Andre Obenaus

---

8:15 MRI in Current Clinical Practice for TBI

Esther Yuh

---

8:45 Animal Models for MRI in TBI

TBI is devastating yet currently without a cure. Investigators are seeking therapeutic strategies through the preclinical animal model to elucidate changes occurring after brain injury and identify potential neuroprotective therapies for brain-injured patients. The choice of animal model depends on the research goal and underlying objectives. This lecture will introduce the animal models of TBI commonly used for MRI study and explain their biomechanical, pathological and neurological differences in characteristics. Recent advances of MRI in probing the pathophysiology responses in experimental TBI will also be reviewed.

Tsang-Wei Tu

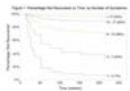
---

9:15 [Advances in White Matter Imaging](#)

Sumit Niogi

---

9:45 [Neurovascular Consequences of Traumatic Brain Injury](#)



Blood flow dysregulation is known to occur immediately after traumatic brain injury. Since neurovascular coupling is an essential component for maintaining the health of the neurovascular unit, impairment of this important regulatory mechanism can have significant implications on recovery from injury and may therefore be involved in the persistence of symptoms after injury. The ability to map dysregulation of blood flow using BOLD MRI cerebrovascular reactivity mapping offers the ability to investigate blood flow control providing a method to further understanding the relationship between post-injury blood flow derangements and recovery from injury.

David Mikulis

---

10:15 [Break & Meet the Teachers](#)

---

10:45 [Brain inflammation in Trauma – MRI, MRS & New Radioligands](#)

Both early and chronic inflammation are therapeutic targets in brain trauma. New PET radioligands allow targeting of several key components of the CNS inflammation. This talk will review the emerging PET tracers for neuroinflammation, and consider them in the context of experimental traumatic brain injury, temporal disease progression, and available MRI and MRS approaches.

Riikka Immonen

---

11:15 [Large Scale Clinical Studies in TBI](#)

11:45 [Controversies in TBI](#)

Enduring neuroimaging controversies exist in the study of traumatic brain injury (TBI) especially related to mild TBI (mTBI). The presentation begins with a brief historical overview of various definitional statements as to what constitutes a TBI, especially involving “concussion.” Although various lesion quantification methods have become standard, when to scan post-injury and what to quantify remain part of the debate. Individual differences and the heterogeneity of the injury complicate and may mask effects at the individual level. With advanced neuroimaging techniques, controversies remain as to acquisition, post-processing and study design questions and what outcome metrics should be examined.

Erin Bigler

---

12:15 [Adjournment & Meet the Teachers](#)

---

## Weekend Course

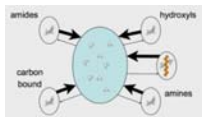
# CEST Imaging

Organizers: Guoying Liu, Ph.D. & Peter van Zijl, Ph.D.

Room 316BC      Sunday 8:15 - 11:45      Moderators: Guanshu Liu & Ravinder Reddy

---

8:15 [CEST, Basic Principles, Contributions To Z-Spectrum](#)

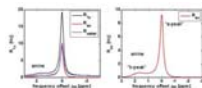


The purpose of this lecture is to introduce the ideas underlying 1) exchange effects in MRI, and CEST in particular; 2) the contributions to CEST contrast; 3) CEST comparisons to spectroscopy; and 4) current issues in CEST research related to pulse sequence design, imaging metrics, and solute specificity.

Daniel Gochberg

---

8:35 [CEST Theory, Exchange, T1p, T2 Relationship](#)



Analytical solutions provide sound insight in the Bloch-McConnell equations that underlie every exchange-weighted contrast, be it CEST, T1p or T2. In this lecture we show that for all experiment affecting the water magnetization, a single eigenvalue solution is able to describe all these experiments. This knowledge forms the basis for interpretation of the outcomes of different exchange-weighted contrasts as well as quantification of exchange.

Moritz Zaiss



---

8:55 [Pulsed Exchange Transfer Technologies](#)

Creative applications of pulse techniques can provide a way to increase detectability and specificity of CEST contrast. In this presentation, we will discuss the advantages and limitations of several pulsed CEST techniques including pulsed saturation, chemical exchange rotation transfer (CERT), frequency labeled exchange (FLEX), and variable delay multi-pulse (VDMP) methods.

Xiang Xu

---

9:15 [Break & Meet the Teachers](#)

---

9:30 [Designing ParaCEST Agents \(BASIC, Responsive\)](#)

This presentation will review Paramagnetic Chemical Exchange Saturation Transfer (ParaCEST) MRI contrast agents. These agents should be thoroughly characterized with regard to their dependence on saturation time, saturation power, concentration, pH and temperature. Responsive ParaCEST agents can detect or measure enzyme activity, metabolites, metal ions, pH, redox state, temperature, and light. Some ParaCEST agents can also exhibit T2-Exchange relaxation. The intermediate exchange rate of a T2ex agent does not affect the T1 relaxivity of the agent. Therefore, the T2/T1 ratio of a T2ex agent can be employed to detect a biomarker.

Marty Pagel

---

9:50 [LipoCEST, Basic Principles & Applications](#)

Daniela Delli Castelli

---

10:10 [DiaCEST Probes \(Reporter Genes, Ion Detection, pH Etc\)](#)

In light of the recent demand for new tools that will allow better investigation of complex biological processes, a new field has evolved at the interfaces of synthetic chemistry, molecular engineering, and cellular imaging. Label-free molecular probes based on diaCEST agents for molecular and cellular imaging applications provide the scientific community with unprecedented versatility to monitor wide range of biological events in health and disease. Although diaCEST molecular sensors should be further developed, their performances marks the dawn of a new scientific era for molecular and cellular MRI

Amnom Bar-Shir

---

10:30 [Break & Meet the Teachers](#)

---

10:45

[APT-Weighted MRI of Cancer & Ischemia](#)

Amide proton transfer-weighted (APT<sub>w</sub>) imaging, a variant of the CEST-based molecular MRI technique, is based on the chemical exchange between free bulk water protons and the amide protons (-NH) of mobile proteins and peptides. Theoretically, the APT<sub>w</sub>-MRI signal relies mainly on the mobile amide proton concentration and amide proton exchange rate which are related to tissue pH. Therefore, APT<sub>w</sub>-MRI has the potential to detect brain tumors (where many proteins are overexpressed) and ischemic strokes (where pH drop). Early pre-clinical and clinical data suggest that APT<sub>w</sub> imaging has unique features by which to detect and characterize brain tumors and strokes.

Hye-Young Heo

---

11:05

[Other Endogenous CEST Studies: GagCEST, GluCEST, Cr, etc.](#)

The aim of this presentation will be to give the MRI practitioner a good overview of the methods used in CEST and MT imaging, the current state of the art, and to outline the opportunities and limitations of the methods with respect to particular applications.

Alexej Jerschow

---

11:25

[GlycoCEST, GlucoCEST, pH Agents, Translation to Humans](#)

CEST is a powerful technique to measure metabolites and other molecules in small concentration through indirect exchange of its labile protons by saturation transfer. In this presentation, a review of its use to indirectly assess metabolic processes is presented, based on amide proton transfer imaging, as well as GlucoCEST and GlycoCEST.

Xavier Golay

---

11:45

[Adjournment & Meet the Teachers](#)

---

## Weekend Course

# RF Engineering: Coils

*Organizers:* Gregor Adriany, Ph.D. , Mary P. McDougall, Ph.D. & Graham C. Wiggins, D.Phil.

Room 313A

Sunday 8:30 - 12:00

*Moderators:* Ryan Brown & Hiroyuki Fujita

---

8:30

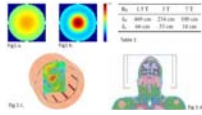
[Basics of Transmission Lines & Power Transfer](#)



Fundamentals of transmission lines and power transfer are presented to help in the understanding, design, implementation and performance evaluation of MRI hardware.  
Natalia Gudino

---

9:00



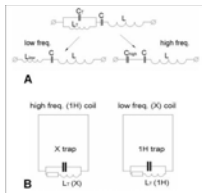
### Volume & Surface Coils

RF coils (antennas) for MRI are designed to generate a RF magnetic field inside the patient. Large body volume coils are optimized for the generation of a homogeneous RF magnetic field. Local surface coils are designed to provide high signal to noise ratio. Different designs and related physical aspects are discussed.

Christoph Leussler

---

9:30



### Multi-Tuned Coils

X-nuclei ( $^{13}\text{C}$ ,  $^{31}\text{P}$ ,  $^{19}\text{F}$  etc) MRI and spectroscopy are of great interest since these methods provide a non-invasive technique to study in-vivo metabolite changes due to various diseases. To provide anatomical landmarks for interpretation of X-nuclei spectroscopic data,  $^1\text{H}$  anatomical images are required. To eliminate uncertainties associated with repositioning the patient, the RF coil must also resonate at the  $^1\text{H}$  frequency. This technique is called double-tuning (DT) of the RF coils. The choice of DT design is determined by the requirements of a specific application. Various methods of constructing DT RF surface coils, volume coils, and phased arrays are discussed.

Nikolai Avdievich

---

10:00

### Break & Meet the Teachers

---

10:30

### Receive Arrays & Circuitry

Boris Keil

---

11:00



### Transmit Arrays & Circuitry

As the main magnetic field strength increases, the corresponding RF wavelength is shortened. This leads to pronounced wave effects in the transmit field, causing inhomogeneous excitation. Multi-channel arrays provide additional degrees of freedom to mitigate such effects and to manipulate (or to tailor) RF transmission. Roughly these can be divided in 3 types, namely local arrays, remote circumferential arrays and travelling wave arrays. Examples of these arrays are presented in this educational talk.

Stephan Orzada

---

11:30

RF Modelling



Mikhail Kozlov

---

12:00

Break & Meet the Teachers

---

## Weekend Course

# Image Acquisition & Reconstruction

Organizers: Edward V.R. DiBella, Ph.D. & Neville D. Gai, Ph.D.

Room 313BC

Sunday 8:30 - 12:00

Moderators: Mariya Doneva & Neville Gai

---

8:30

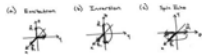
MR Basics (Refresher) Recap of Physics of RF & k-Space Acquisition.

Daniel Herzka

---

9:00

Excitation & Parallel Transmission

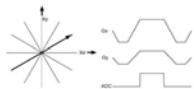


William Grissom

---

9:30

Cartesian & Non-Cartesian Sampling Schemes - Advantages & Disadvantages



This educational talk will cover the advantages and disadvantages of Cartesian and non-Cartesian sampling techniques. Cartesian, radial, and spiral k-space scanning methods will be compared with respect to scan efficiency, hardware considerations, off-resonance effects, motion sensitivity, and scan acceleration.

Craig Meyer

---

10:00

Break & Meet the Teachers

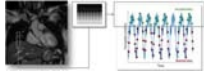
---

10:30

Motion Sensitization: PC Imaging etc

Motion sensitization techniques are used in various applications, such as flow imaging, black blood imaging, bright blood imaging, etc. Technical differences in motion/flow sensitization methods are discussed in this presentation.

11:00



### Motion Compensation: Pulse Sequence & Reconstruction Strategies

Over the past decade Magnetic Resonance Imaging (MRI) has become an increasingly important non-invasive tool in risk assessment and treatment monitoring of cardiovascular disease. However, despite ongoing progress and developments in MR acquisition and reconstruction technology, physiological motion remains a major problem in many cardiovascular MRI applications. Since MR acquisition is slow compared to physiological motion, the extensive cardiac and respiratory induced motion of the heart during the acquisition period can degrade image quality by introducing ghosting and blurring like motion artifacts. Several cardiac and respiratory motion compensation techniques have been proposed over the last two decades to overcome this problem. These techniques are based on minimizing or correcting the motion during the acquisition. This part of the Image Acquisition & Reconstruction Course at ISMRM 2017 will include an overview of some of these methods, discussing their strengths and limitations.

René Botnar

---

11:30

### Reduced FOV, Reference Scans, Gradient Pre-Emphasis

This lecture focuses on three pulse sequence strategies to increase spatial resolution, accelerate acquisition, and improve image quality while reducing artifacts. First, strategies for reducing the field-of-view (FOV) are described using examples of spatial saturation, multi-dimensional RF excitation, and selective RF refocusing. Second, reference scans are presented for measuring errors in k-space and enabling various phase corrections in echo-train pulse sequences. Third, gradient pre-emphasis is discussed as an effective method to reduce the adverse effects caused by eddy currents in a variety of pulse sequences. Although these three topics may appear isolated, together they reflect a central theme of how to improve image quality and/or speed while avoiding artifacts.

Xiaohong Joe Zhou

---

12:00

### Lunch & Meet the Teachers

---

## Weekend Course

# Body MRI: Optimize Your Clinical Practice: Focal Liver Lesions

*Organizers:* Kathryn Fowler, M.D., Kartik Jhaveri, M.D., F.R.C.P.C., Lorenzo Mannelli, M.D., Ph.D. & Edwin J.R. van Beek, M.D., Ph.D., M.Ed., FRCR

**10:15**      [MRI of Focal Lesions in the Non-Cirrhotic Liver](#)

The differential diagnosis of focal hepatic lesions in the non-cirrhotic liver is broad. MRI plays a crucial role in the non-invasive histologic characterization of these lesions and the decision making for patient management. In this talk we will present a simple, practical approach to focal hepatic lesions, review the MRI findings in the most common focal lesions in the non-cirrhotic liver, and discuss some of the pitfalls in image interpretation.

Ivan Pedrosa

---

**10:45**      [MRI in the Cirrhotic liver](#)

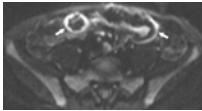
MRI in the cirrhotic liver has important roles in the standard care of cirrhotic patients. Recent advance in MRI also offers functional information which can serve as MR-based biomarker to predict patients' outcome.

Utaroh Motosugi

---

**Weekend Course****Body MRI: Optimize Your Clinical Practice: GI**

*Organizers:* Kathryn Fowler, M.D., Kartik Jhaveri, M.D., F.R.C.P.C., Lorenzo Mannelli, M.D., Ph.D. & Edwin J.R. van Beek, M.D., Ph.D., M.Ed., FRCR

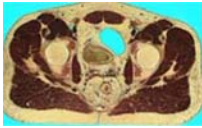
**11:15**      [MR Enterography](#)

*Magnetic resonance (MR) enterography* is a robust alternative to modalities utilizing ionizing radiation in evaluating small bowel and surrounding structures in children and adults. Technical advances enabling rapid relatively motion-insensitive MR sequences and protocol modifications adapted to patients' ages and morbidities will be detailed. Image optimization improves diagnostic capabilities, further enhanced by systematic review. Image interpretation, from detection and characterization to quantification of disease burden in inflammatory bowel disease (IBD) - and increasingly other bowel disorders - will be discussed. The expanding role *MR enterographic* findings play as imaging biomarkers in the management of IBD will also be considered.

Mary-Louise Greer

---

**11:45**      [Rectal CA Staging](#)



This lecture will cover the basic information needed to properly perform and interpret baseline MRI for rectal cancer staging. It includes recommended techniques and parameters by the ESGAR 2012/2016 guidelines. It illustrates how to interpret T- and N-staging as well as proper assessment of the CRM and of EMVI. It discusses geographic differences in treatment around the world and also introduces staging of low rectal cancer involving the anal sphincter apparatus.

Marc Gollub

---

12:15

Lunch & Meet the Teachers

---

## Weekend Course

# Image Acquisition & Reconstruction

Organizers: Edward V.R. DiBella, Ph.D. & Neville D. Gai, Ph.D.

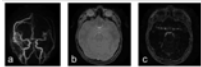
Room 313BC

Sunday 13:15 - 16:45 Moderators: Edward DiBella & Claudia Prieto

---

13:15

Sparsity & Compressed Sensing



Incomplete data sampling is an attractive approach to accelerate MRI but it requires prior knowledge-driven image reconstruction. Sparsity is a powerful concept that allows linking many different types of prior knowledge to the mathematical apparatus adopted in MR image reconstruction. Compressed sensing theory establishes conditions for optimal use of sparse representations for high quality MR image reconstruction from undersampled data. In this talk, we will cover the aforementioned concepts of advanced image reconstruction and demonstrate real examples of accelerated structural and dynamic MRI. We will also discuss both theoretical requirements of compressed sensing and essential aspects of its practical implementation.

Alexey Samsonov

---

13:45

MR Fingerprinting

Quantitative MR measurements are essential to assess complex changes in the brain and monitor treatment outcomes. Although full quantitative multi-parametric acquisition has long been the goal of research in MR, the conventional methods typically provide information on a single parameter at a time, thus requiring significant scan time. The purpose of Magnetic Resonance Fingerprinting (MRF) is to introduce a new framework to data acquisition and post-processing that permits the simultaneous quantification of multiple tissue properties in a time efficient manner.

Dan Ma

---

14:15      [Dictionary & Model-Based Methods](#)

This lecture explains the principles of model-based reconstruction methods and their linearization using dictionaries for MR parameter mapping.

Mariya Doneva

---

14:45      [Break & Meet the Teachers](#)

---

15:15      [Simultaneous Multi-Slice Methods](#)

Steen Moeller

---

15:45      [Motion Compensated Reconstruction](#)

Sajan Goud Lingala

---

16:15      [MRI & Manifolds](#)

Novel image and patch manifold models that can exploit the non-linear and non-local redundancies in a dynamic dataset will be introduced. Specifically, the collection of images/patches in the dataset is assumed to be on a smooth manifold. I will introduce novel iterative algorithms to exploit the structure of the data. The use of these algorithms enables implicit motion compensation and motion resolution, and hence is a good alternative to current strategies that perform these operations explicitly.

Mathews Jacob

---

16:45      [Adjournment & Meet the Teachers](#)

---

## Weekend Course

# Recent Advances in Diffusion, Perfusion & fMRI

*Organizers:* Daniel C. Alexander, Ph.D., Fernando Calamante, Ph.D., Benedikt A. Poser, Ph.D., Joshua S. Shimony, M.D., Ph.D. & Steven P. Sourbron, Ph.D.

Room 311

Sunday 13:15 - 16:45

*Moderators:* Joshua Shimony & Steven Sourbron

---





15:30 Break & Meet the Teachers

---

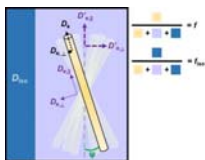
15:45 Acquisition: Novel Gradient Waveforms

Most diffusion MRI is today performed with the so-called pulsed gradient spin echo (PGSE) method, which encodes for diffusion using two gradient pulses. This method is sensitive to cellularity of tumours, orientation of white matter tracts, and microstructure features such as axon density and cell sizes. However, the PGSE method is fundamentally limited in several ways. This talk will pinpoint these limitations and show how novel gradient waveforms can overcome them.

Markus Nilsson

---

16:15 Analysis: Tissue & Signal Models



The diffusion signal provides unique, but indirect information about tissue microstructure. In this course, we will examine two main avenues for diffusion analysis: signal representations and tissue models. The former render the signal behavior without any assumptions about the tissue structure and thus produce sensitive but unspecific metrics (e.g. fractional anisotropy from DTI). For models, a theoretical expression of the diffusion signal in a given geometry (assumed to describe the tissue well) is fit to the data and characteristic parameters of the geometry are extracted. This approach should yield more specific metrics but is also more challenging to implement correctly.

Ileana Jelescu

---

16:45 Adjournment & Meet the Teachers

---

## Weekend Course

# Body MRI: Optimize Your Clinical Practice: Pelvis & GU

Organizers: Kathryn Fowler, M.D., Kartik Jhaveri, M.D., F.R.C.P.C., Lorenzo Mannelli, M.D., Ph.D. & Edwin J.R. van Beek, M.D., Ph.D., M.Ed., FRCR

Room 315

Sunday 13:15 - 16:15

Moderators: Jurgen Fütterer & Valeria Panebianco

---

13:15 Female Pelvis - Uterus

MRI plays an important role in accurate classification, treatment selection and planning of suspected uterine anomalies as well as evaluation of other benign uterine conditions such as leiomyomas and adenomyosis. It plays a crucial role in surgical planning of patients with endometrial cancer by accurately predicting depth of myometrial invasion, cervical stroma invasion and lymph node involvement. In young patients with low grade endometrial cancer who wish to preserve fertility, MRI is used to exclude myometrial invasion prior to hormonal therapy. MRI is valuable in distinguishing cervical from endometrial origin of uterine cancer in cases of biopsy proven adenocarcinoma.

Evis Sala

---

13:45

### Adnexal Masses

The superior soft tissue contrast of MRI aids characterisation of adnexal masses. T2-W contrast is the mainstay of diagnosis. Enhancement of T1-W images with gadolinium chelate is helpful in refining diagnosis. Examinations are optimized by scanning after the patient has emptied her bladder and intramuscular antiperistaltic agents have been administered. Classification into benign and malignant pathology is crucial for deciding on type of surgical management. In addition, recognition of disseminated malignant disease determines whether or not neoadjuvant chemotherapy is warranted prior to surgical debulking.

Nandita deSouza

---

14:15

### Fetal MRI

Fetal Body MRI requires different contrasts to adequately visualize the organs at different stages of maturation. A profound knowledge of often complex pathologies that may involve more than one organ, and that may be diagnosed prenatally, is necessary for a tailored management of these pregnancies. Among all extra-CNS indications assessment of the fetal lungs has become the most important one, allowing an accurate prediction of the respiratory state of the newborn.

Daniela Prayer

---

14:45

### Break & Meet the Teachers

---

15:15

### Renal



This clinically oriented talk will review the Renal Mass MRI technique/scanning protocols at NYU, review the basics in renal mass lesion subtyping and pitfalls in the characterization of renal lesions and the clinical impact therein.

Nicole Hindman

---

15:45

Prostate

This session discusses opportunities to take full advantage of current multiparametric prostate MRI to guide individual management in multiple clinical scenarios that affect prostate cancer patients.

Hebert Alberto Vargas

---

16:15

Adjournment & Meet the Teachers

---

## Weekend Course

# MRI, MRS & Molecular Imaging to Diagnose Disease & Assess Treatment

Organizers: Carolyn E. Mountford, D.Phil. & Bruce R. Rosen, M.D., Ph.D.

Room 314

Sunday 13:15 - 16:15

Moderators: In-Young Choi & Brenda Bartnik Olson

---

13:15

Deregulation, Disease & Damage Recorded by MRS

This presentation will enable you to describe the current state of magnetic resonance spectroscopy in the detection of pathology; understand the drawbacks and problems associated with the use of MRS; and understand how MRS could be further improved to allow better diagnostic and research utility.

Caroline Rae

---

13:45

Imaging Applications of Ferumoxytol for MRI: Focusing on the Vasculature & Inflammation



Ferumoxytol is an ultrasmall, paramagnetic iron oxide and also a novel magnetic resonance imaging (MRI) contrast agent. With its unique features (long plasma half-life and delayed intracellular uptake) ferumoxytol may play a crucial role in the MR imaging in the future. We have completed over 700 MRI studies with ferumoxytol in our institution, primarily for CNS imaging. In this presentation we go through the general properties and the specific opportunities of ferumoxytol-enhanced MRI in and outside the brain.

Edward Neuwelt

---

14:15

Molecular Imaging of In Vivo Gene Expression & Intracellular Messengers

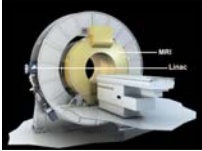
We cover the use MRI molecular imaging  
Zahi Adel Fayad

---

14:45 [Break & Meet the Teachers](#)

---

15:15 [MR-Guided Radiotherapy](#)



Online MRI guidance is the new disruptive technology for radiotherapy that will facilitate online and real-time adaptive treatments. An overview of the current hybrid MRI-guided treatment machines will be given. The MRI-Linac, which combines a 1.5T closed bore system with a modern 7MV linear accelerator will be described. Its clinical introduction is highlighted and the potential for future treatments and research is outlined.

Rob Tijssen

---

15:45 [Imaging of Non-Proton Nuclei: Methodology & Applications in Clinical Research](#)

In this presentation I will give an brief overview of X-nuclei MRI/MRS, of its challenges and potential clinical applications. I will mainly focus on  $^{23}\text{Na}$  MRI and  $^{31}\text{P}$  MRS/MRI as examples of potentially useful non-proton imaging methods that could give interesting new metabolic information in vivo in a non-invasive and quantitative manner.

Guillaume Madelin

---

16:15 [Adjournment & Meet the Teachers](#)

---

## Weekend Course

# Translational Musculoskeletal Imaging: From Qualitative to Quantitative

*Organizers:* Jenny T. Bencardino, M.D., Eric Y. Chang, M.D., Christine Chung, M.D. & Philip Robinson, M.D.

Room 316A

Sunday 13:15 - 16:05

*Moderators:* Neal Bangerter & Catherine Roberts

---

13:15 [Quantitative MR Imaging: Technical Aspects](#)

Quantitative MRI in musculoskeletal tissues is challenging. Our technical ability to accurately measure and reliably interpret MRI parameters in musculoskeletal tissues can be influenced by the complexity of our specimens (human patient, animals, ex vivo specimen), instrumentation, experimental details, and data-analysis. This talk examines a number of these issues and their impact on the robustness of quantitative MRI, using the examples mainly from articular cartilage and its degradation process that leads to osteoarthritis. A brief comparison between articular cartilage and other musculoskeletal tissues (tendon, nasal cartilage, meniscus, and bone) will also be given.

Yang Xia

---

13:50 [Quantitative MR Imaging: Clinical Applications](#)

Quantitative techniques such T2/T2\* imaging, sodium MRI and gagCEST help to analyze the composition of the connective tissues

Results from quantitative techniques provide additional information and predictive markers for MSK structures and have the potential for the development of imaging biomarkers.

Siegfried Trattnig

---

14:25 [Break & Meet the Teachers](#)

---

14:55 [MR Spectroscopy: Technical Aspects](#)

Chemical shift encoding techniques can quantify chemical species content and investigate metabolic changes in physiological and diseased conditions of multiple musculoskeletal tissues, including skeletal muscle, bone marrow, intervertebral disc, cartilage and bone. The present lecture aims to provide an overview of the most important technical aspects when applying chemical shift encoding techniques, including single-voxel magnetic resonance spectroscopy, chemical shift imaging and chemical shift encoding-based water-fat separation techniques, for targeting lipids, creatine, macromolecules, choline and phosphorous metabolites in musculoskeletal tissues.

Dimitrios Karampinos

---

15:30 [MR Spectroscopy: Clinical Applications](#)

MR spectroscopy is able to quantify intramyocellular lipids, intrahepatic lipids, and marrow adipose tissue in several clinical conditions.

Miriam Bredella

---

## Weekend Course

# Neurovascular MRI: from Micro to Macro

Organizers: Christopher P. Hess, M.D., Ph.D. & Daniel M. Mandell, M.D., Ph.D.

Room 312

Sunday 13:15 - 16:40

Moderators: Kevin DeMarco & Christopher Hess

13:15

## Intracranial Vessel Wall Imaging

Mahmud Mossa-Basha

13:40

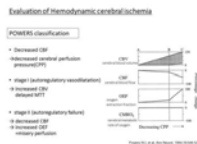
## Blood Flow Imaging

MR imaging is the only effective modality for imaging hemodynamic conditions in the intracranial vasculature. The use of these methods for evaluating healthy and diseased vessels will be discussed.

David Saloner

14:05

## Cerebrovascular Reserve Imaging

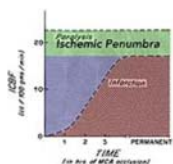


To understand the hemodynamic changes due to a decrease in cerebral perfusion pressure (CPP), and evaluation of cerebrovascular reserve (CVR) capacity in patients with cerebrovascular disease (CVD) is important to determine the risk of future ischemic events and in the selection and planning of the therapeutic interventions. 3 approaches (positron emission tomography, single photon emission computed tomography and MRI) can be used in the evaluation of CVR. We will present the basic concept to measure CVR in patients with CVD combined by nuclear medicine imaging and introduce the possibility of MRI application in measuring CVR.

Naomi Morita

14:30

## Penumbra Imaging



In acute stroke imaging, the “penumbra” usually refers to brain tissue that is considered to be at risk for infarction. Identification of the penumbra is consistently a focus of active imaging research, particularly in the development of strategies for selecting patients for intravenous thrombolysis and mechanical thrombectomy. Penumbra imaging approaches usually employ perfusion imaging, which provides a variety of complementary measurements of cerebral hemodynamics at the microvascular level. This talk will explore the relationship of penumbra imaging to fundamental principles of cerebrovascular physiology, addressing both currently implemented penumbra imaging techniques, and potential novel applications of perfusion imaging in stroke care.

William Copen

---

14:55 [Break & Meet the Teachers](#)

---

15:25 [Venous Imaging](#)

With increasing use of high field scanners and high resolution imaging protocols such as susceptibility-weighted imaging that can be used to visualize fine venous structures, understanding of the structure of fine venous anatomy has become important. Deep medullary veins drain into subependymal veins with four convergence zones and show parallel distribution patterns adjacent to the body or inferior horn and a radial pattern in the frontal horn or trigon of the lateral ventricle. Some disorders are related to deep medullary veins.

Toshiaki Taoka

---

15:50 [Neurovascular Case Review](#)

Michele Johnson

---

16:15 [Identifying & Characterizing Arteriovenous Shunting Lesions with Arterial Spin Labeling](#)

Greg Zaharchuk

---

16:40 [Adjournment & Meet the Teachers](#)

---

**Weekend Course**



# Biostatistics for Imaging Studies

Organizers: Dwight G. Nishimura, Ph.D.

Room 316BC

Sunday 13:15 - 16:45

Moderators: Priti Balchandani & Dwight Nishimura

---

## 13:15 [Designing Studies of Diagnostic Imaging](#)

The short-course is broken down into three sections:

First Hour: Foundations of Imaging Studies

Second Hour: Statistical Methods in Imaging Studies

Third Hour: Advanced Methods

Nancy Obuchowski

---

## 13:45 [Basic Concepts in Calculations of Sample Size & Statistical Power](#)

The Overview of Biostatistical Data Analysis Methods is comprised of the following 3 parts:

- Part 1: Basic concepts in calculations of sample size and statistical power
- Part 2: ROC Analysis in diagnostic medicine
- Part 3: Statistical prognostic/predictive modelling of quantitative imaging biomarkers (QIBs)

Todd Alonzo

---

## 14:15 [Break & Meet the Teachers](#)

---

## 14:30 [Part 1 of Assessing Quantitative Imaging Biomarkers \(QIBs\)](#)

---

## 14:55 [Part 1 of ROC Analysis in Diagnostic Medicine](#)

---

## 15:20 [Break & Meet the Teachers](#)

---

## 15:35 [Part 2 of ROC Analysis: Multi-Reader ROC & Other Advanced ROC Methods](#)

---

15:55

Part 2 of Assessing QIBs: Statistical Prognostic/Predictive Modeling of QIBs

---

16:15

Adjournment & Meet the Teachers

---

## Weekend Course

# RF Engineering: Coils

Organizers: Gregor Adriany, Ph.D. , Mary P. McDougall, Ph.D. & Graham C. Wiggins, D.Phil.

Room 313A

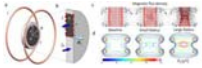
Sunday 14:00 - 16:15

Moderators: Ryan Brown & Hiroyuki Fujita

---

14:00

Dielectric Materials & Resonators



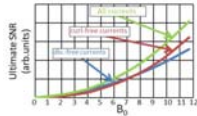
This talk will review and explain the dielectric effects in MRI using simple examples. Its applications in enhancing RF field using ultrahigh dielectric constant materials at 1.5T, 3T and 7T will be presented.

Qing Yang

---

14:30

UHF Coil & Array Design



Karthik Lakshmanan

---

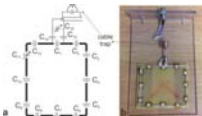
15:00

Break & Meet the Teachers

---

15:30

Construction of Rx Arrays



We aim to present a step-by-step method to construct a transmit array. The measurements will be demonstrated using an 8-channel transmit array. We will then extend this method to the development of a dual-row transmit array. Construction and characterisation of a receive coil element and combining a transmit and receive array is also included.

Shajan Gunamony

---

16:15

Adjournment & Meet the Teachers

---

## Plenary Session

# Lauterbur Lecture

Plenary Hall

Sunday 17:00 - 18:15

---

17:00      [Opening Remarks - Society Awards](#)

---

17:30      [Lauterbur Lecture: MRI as a Window into Cardiac Function](#)

Paul Lauterbur not only invented the basic concept of MRI, he also pioneered many of its extensions and applications, including to cardiovascular imaging. My research career has focused in part on exploring some of the ways in which the unique capabilities of MRI to reveal motion can be used to study cardiac function. While this area has still had limited clinical impact, due to persistent technical limitations, there is ongoing progress in overcoming them, with promising prospects for the future of MRI for characterizing cardiac function.

Leon Axel

---

---

## Other

# Opening Reception

Exhibition Hall

Sunday 18:30 - 20:00    *(no CME credit)*

---

---

## Monday, 24 April 2017

[Go to top](#)

## Sunrise Session

# Cardiovascular MR: "More is Better": LV Structure & Mechanics

*Organizers:* Daniel K. Sodickson, M.D., Ph.D., Bernd J. Wintersperger, M.D. & Sonia Nelles-Vallespin, Ph.D.

Room 310

Monday 7:00 - 7:50

*Moderators:* Daniel Ennis & David Sosnovik

---

7:00      [Cardiac Diffusion](#)  
Martijn Froeling

---

7:25      [Cardiac Mechanics](#)  
Daniel Auger

---

7:50      [Adjournment & Meet the Teachers](#)

---

### **Sunrise Session**

## **Bleeding Edge of Brain Techniques: Fingerprinting & Hyperpolarized C13**

*Organizers:* Fernando E. Boada, Ph.D. & Christopher P. Hess, M.D., Ph.D.

Room 311      Monday 7:00 - 7:50      *Moderators:* Fernando Boada & Christopher Hess

---

7:00      [Hyperpolarized 13C: New Kind on the Block](#)  
Myriam Chaumeil

---

7:25      [Brain MR Fingerprinting: Brain MR for the Masses?](#)  
Timothy Shepherd

---

7:50      [Adjournment & Meet the Teachers](#)

---

### **Sunrise Session**

## **Contrast Mechanisms in MSK Imaging**

*Organizers:* Jenny T. Bencardino, M.D., Eric Y. Chang, M.D., Christine Chung, M.D. & Philip Robinson, M.D.

Room 312      Monday 7:00 - 7:50      *Moderators:* Graeme Bydder & Ives Levesque

---

7:00      [Magnetization Transfer: Applications in MSK imaging](#)  
Ives Levesque

---

7:25      [Fat Water Separation: Applications in MSK imaging](#)  
Johan Berglund

---

7:50      [Adjournment & Meet the Teachers](#)

---

---

### **Sunrise Session**

## Magnetic Resonance Elastography: Overview & Technology

*Organizers:* Guoying Liu, Ph.D. & Joshua D. Trzasko, Ph.D.

Room 313A      Monday 7:00 - 7:50      *Moderators:* Curtis Johnson & Joshua Trzasko

---

7:00      [Overview & History](#)  
Richard Ehman

---

7:25      [MRE Technology](#)  
Ingolf Sack

---

7:50      [Adjournment & Meet the Teachers](#)

---

---

### **Sunrise Session**

## Individualized Brain MRI: Building a Neurosurgical Planning Toolbox

*Organizers:* Christopher P. Hess, M.D., Ph.D.

Room 313BC      Monday 7:00 - 7:50      *Moderators:* Jeffrey Berman & Manabu Kinoshita

---

7:00      [Fiber Tractography for Practical Neurosurgical Application](#)  
Shawna Farquharson

---

7:25      [Functional MRI for Practical Neurosurgical Application](#)  
Vivek Prabhakaran

---

7:50      [Adjournment & Meet the Teachers](#)

---

---

## Sunrise Session

# MR-Guided Focused Ultrasound in the Brain

Organizers: Edward V.R. DiBella, Ph.D. & Dennis L. Parker, Ph.D.

Room 314                      Monday 7:00 - 7:50                      Moderators: Kim Butts Pauly & Dennis Parker

---

7:00                      [MR-Guided Focused Ultrasound in the Brain - Description, Overview & Method](#)  
John Snell

---

7:25                      [MR-Guided Focused Ultrasound in the Brain - Clinical Potential & Relevance](#)  
Pejman Ghanouni

---

7:50                      [Adjournment & Meet the Teachers](#)

---

---

## Sunrise Session

# It Doesn't Have to Be That Way: Extreme Fields & Gradients

Organizers: Michael S. Hansen, Ph.D. & Joshua D. Trzasko, Ph.D.

Room 315                      Monday 7:00 - 7:50                      Moderators: Michael Hansen & Shengzhen Tao

---

7:00                      [Extreme Fields](#)  
Thomas Witzel

---

7:25                      [Gradients](#)  
Gigi Galiana

---

7:50                      [Adjournment & Meet the Teachers](#)

---

---

## Sunrise Session

# fMRI: Best Practices & Cautionary Tales: Acquisition & Pathology

Organizers: Hanzhang Lu, Ph.D. & Karla Miller, Ph.D.

Room 316A                      Monday 7:00 - 7:50                      Moderators: Hanzhang Lu & Victoria Morgan

---

7:00                      Acquisition Issues  
Benedikt Poser

---

7:25                      Pathological Issue (e.g. Metal Implants, Neurovascular Decoupling)  
Jay Pillai

---

7:50                      Adjournment & Meet the Teachers

---

### Sunrise Session

## PI-RADS: Yes or No

Organizers: Kathryn Fowler, M.D., Kartik Jhaveri, M.D., F.R.C.P.C., Lorenzo Mannelli, M.D., Ph.D. & Edwin J.R. van Beek, M.D., Ph.D., M.Ed., FRCR

Room 320                      Monday 7:00 - 7:50                      Moderators: Kathryn Fowler & Hebert Vargas

---

7:00                      PI-RADS: YES!  
Sadhna Verma

---

7:25                      PI-RADS: NO!  
Pieter De Visschere

---

7:50                      Adjournment & Meet the Teachers

---

### Traditional Poster: Acquisition, Reconstruction & Analysis

Exhibition Hall 1272-1296                      Monday 8:15 - 10:15                      (no CME credit)

---

### Electronic Poster: Cardiovascular

Exhibition Hall                      Monday 8:15 - 9:15                      (no CME credit)

---

### Electronic Poster: Body: Breast, Chest, Abdomen, Pelvis

Exhibition Hall                      Monday 8:15 - 9:15                      (no CME credit)

---

## Study Groups

### Hyperpolarization Methods & Equipment Study Group

Room 323ABC      Monday 8:15 - 10:15      *(no CME credit)*

---

## Study Groups

### Psychiatric MR Spectroscopy & Imaging Study Group

Room 317AB      Monday 8:15 - 10:15      *(no CME credit)*

---

## Educational Course

### ISMIRM-SMRT Joint Forum: Assessing Implant Safety: in the Clinic Now & as the Field Strength Rises

*Organizers:* Amanda Golsch, MBA, R.T. (R)(MR) & Karla L. Miller, Ph.D.

Room 311      Monday 8:15 - 10:15      *Moderators:* Amanda Golsch & Maureen Hood

---

8:15      [Introduction to MRI Safety](#)  
Vera Kimbrell

---

8:45      [Evaluation of MRI Issues for Implants & Devices](#)  
Frank G Shellock, Ph.D., FACR, FACC, FISMRM<sup>1</sup>

<sup>1</sup>*Radiology and Medicine, University of Southern California, Playa Del Rey, CA, United States*

---

9:15      [Implant Safety at Ultra-High Field](#)  
Stuart Clare<sup>1</sup> and Jon Campbell<sup>1</sup>

<sup>1</sup>*FMRIB Centre, University of Oxford, Oxford, United Kingdom*

[As the field strength rises to 7 Tesla and above, this talk will assess the risks of scanning patients with implants and surgeries at ultra-high-field and review what more needs to be done.](#)

---



9:45

## Building an MRI Safety Program

Bernd Ittermann<sup>1</sup>

<sup>1</sup>Physikalisch-Technische Bundesanstalt (PTB), Berlin, Germany

Certain organizational roles are frequently encountered in the MRI safety context: the MR Director (MRD), the MR Safety Officer (MRSO) and the MR Safety Expert (MRSE). It is attempted to describe their respective responsibilities and how these relate to each other. In addition, a set of minimum requirements shall be identified, an MR operator in a research setting should fulfill before scanning human subjects.

10:15

## Adjournment & Meet the Teachers

### Power Pitch

## Pitch: Interventional/Safety/Engineering

Power Pitch

Theater A -

Exhibition Hall

Monday 8:15 -  
9:15

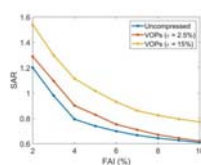
Moderators: Caroline Jordan

(no CME credit)

1



8:15



## Overcoming Limitations of Virtual Observation Points in pTx using IMPULSE

Mihir Pendse<sup>1</sup> and Brian K Rutt<sup>1</sup>

<sup>1</sup>Stanford University, Stanford, CA, United States

2

8:15



## Optical-based probe for real time assessment of RF electrical field during MRI exam

Isabelle Saniour<sup>1</sup>, Gwenaël Gaborit<sup>2,3</sup>, Lionel Duvaillaret<sup>3</sup>, Anne-Laure Perrier<sup>2</sup>, and Olivier Beuf<sup>1</sup>

<sup>1</sup>Univ. Lyon, CREATIS ; CNRS UMR 5220 ; INSERM U1206 ; INSA-Lyon ; UJM-Saint-Etienne ; Université Lyon1, Villeurbanne, France,

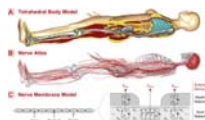
<sup>2</sup>Univ. Savoie-Mont-Blanc, IMEP-LAHC, Le Bourget-du-Lac, France,

<sup>3</sup>Kapteos, Sainte-Hélène-du-Lac, France

3



8:15



### Modeling of Peripheral Nervous Stimulation Thresholds in Realistic Body Models

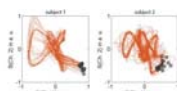
Mathias Davids<sup>1,2</sup>, Bastien Guérin<sup>2,3</sup>, Lothar R Schad<sup>1</sup>, and Lawrence L Wald<sup>2,3,4</sup>

<sup>1</sup>Computer Assisted Clinical Medicine, Heidelberg University, Mannheim, Germany, <sup>2</sup>Martinos Center for Biomedical Imaging, Massachusetts General Hospital, Charlestown, MA, United States, <sup>3</sup>Harvard Medical School, Boston, MA, United States, <sup>4</sup>Harvard-MIT Division of Health Sciences Technology, Cambridge, United States

4



8:15



### Cardiac Synchronization at Ultra-High Field Using a 3-Lead ECG Trigger Device

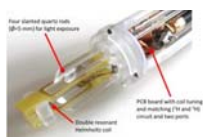
Daniel Stüb<sup>1</sup>, Juergen Roessler<sup>2</sup>, Kieran O'Brien<sup>3</sup>, Je Yen Su<sup>1</sup>, Christian Hamilton-Craig<sup>4</sup>, and Markus Barth<sup>1</sup>

<sup>1</sup>The Centre for Advanced Imaging, The University of Queensland, Brisbane, Australia, <sup>2</sup>Siemens Healthcare GmbH, Erlangen, Germany, <sup>3</sup>Siemens Healthcare Pty Ltd, Brisbane, Australia, <sup>4</sup>Richard Slaughter Centre of Excellence in CVMRI, The Prince Charles Hospital, Brisbane, Australia

5



8:15



### A Combined 7 Tesla MRI/NMR Probe Head for Photochemical Applications.

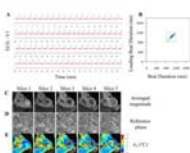
Jens Groebner<sup>1</sup>, Gernot Heitmann<sup>1</sup>, Marcel Dommaschk<sup>1</sup>, Lukas M. Huber<sup>2</sup>, Eduard Stadler<sup>3</sup>, Reiner Umathum<sup>4</sup>, Frank D. Sönnichsen<sup>1</sup>, and Rainer Herges<sup>1</sup>

<sup>1</sup>Otto Diels Institute for Organic Chemistry, Kiel University, Kiel, Germany, <sup>2</sup>Molecular Imaging North Competence Center, University Medical Center Schleswig-Holstein, Kiel, Germany, <sup>3</sup>Institute of Physical and Theoretical Chemistry, Graz University of Technology, Graz, Austria, <sup>4</sup>Medical Physics in Radiology, German Cancer Research Center, Heidelberg, Germany

6



8:15



### Evaluation of cardiac magnetic resonance thermometry in patients

Valery Ozenne<sup>1</sup>, Solenn Toupin<sup>1,2</sup>, Pierre Bour<sup>1</sup>, Baudouin Denis de Senneville<sup>3</sup>, Alexis Vaussy<sup>2</sup>, Matthieu Lepetit-Coiffé<sup>2</sup>, Pierre Jaïs<sup>4</sup>, Hubert Cochet<sup>4</sup>, and Bruno Quesson<sup>1</sup>

<sup>1</sup>Electrophysiology and Heart Modeling Institute, Bordeaux, France, <sup>2</sup>Siemens Healthcare, Paris, France, <sup>3</sup>Mathematical Institute of Bordeaux, Bordeaux, France, <sup>4</sup>Department of Cardiac Electrophysiology, Hôpital Cardiologique de Haut-Lévêque, Bordeaux, France

7

8:15



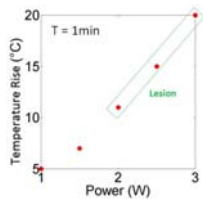
**MRI-monitored Anterior Cervical Discectomy and Fusion (ACDF) surgery: Observation of intra-procedural nerve decompression during surgery**

Ehud J Schmidt<sup>1</sup>, Daniel F Kacher<sup>1</sup>, Wei Wang<sup>1</sup>, Mitchel B Harris<sup>2</sup>, Thomas C Lee<sup>1</sup>, Ravi Seethamraju<sup>3</sup>, Clare M Tempany<sup>1</sup>, and Jay Zampini<sup>2</sup>

<sup>1</sup>Radiology, Brigham and Womens Hospital, Boston, MA, United States, <sup>2</sup>Orthopedic Surgery, Brigham and Womens Hospital, Boston, MA, United States, <sup>3</sup>MRI, Siemens Healthcare, Boston, MA, United States

8

8:15



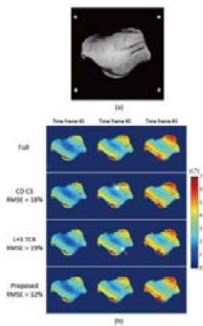
**Water diffusivity changes in the brain following exposure to low levels of focused ultrasound energy**

Sijia Guo<sup>1</sup>, Jiachen Zhuo<sup>1</sup>, Xin Lu<sup>1</sup>, Su Xu<sup>1</sup>, and Rao Gullapalli<sup>1</sup>

<sup>1</sup>Department of Diagnostic Radiology & Nuclear Medicine, University of Maryland School of Medicine, Baltimore, MD, United States

9

8:15



**Low Rank plus Sparse Compressed Sensing Reconstruction for PRF Temperature Imaging**

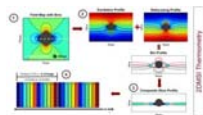
Zhipeng Cao<sup>1,2</sup>, Sumeeth V. Jonathan<sup>2,3</sup>, and William A. Grissom<sup>1,2</sup>

<sup>1</sup>Biomedical Engineering, Vanderbilt University, Nashville, TN, United States, <sup>2</sup>Institute of Imaging Science, Vanderbilt University, Nashville, TN, United States, <sup>3</sup>Radiology, Vanderbilt University, Nashville, TN, United States

10



8:15



**2D Multi-Spectral Thermometry for Monitoring Focused-Ultrasound Sonications Near Metallic Hardware**

Hans Weber<sup>1</sup>, Pejman Ghanouni<sup>1</sup>, Aurea Pascal-Tenorio<sup>2</sup>, Kim Butts Pauly<sup>1</sup>, and Brian A. Hargreaves<sup>1</sup>

<sup>1</sup>Radiology, Stanford University, Stanford, CA, United States,  
<sup>2</sup>Comparative Medicine, Stanford University, Stanford, CA, United States

---

11

8:15



[Toward individualized specific absorption rates: Building a surface-based human head model](#)

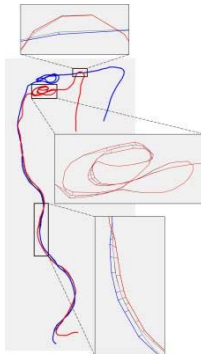
Mikhail Kozlov<sup>1</sup>, Benjamin Kalloch<sup>1,2</sup>, Pierre-Louis Bazin<sup>1</sup>, Mario Hlawitschka<sup>2</sup>, Nikolaus Weiskopf<sup>1</sup>, and Harald E Möller<sup>1</sup>

<sup>1</sup>Max Planck Institute for Human Cognitive and Brain Sciences, Leipzig, Germany, <sup>2</sup>Leipzig University of Applied Science, Leipzig, Germany

---

12

8:15



[Patient specific modeling of deep brain stimulation patients for MRI safety studies](#)

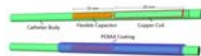
Bastien Guerin<sup>1,2</sup>, Peter Serano<sup>3,4</sup>, Maria I Iacono<sup>3</sup>, Todd Herrington<sup>2,5</sup>, Alik Widge<sup>2,6</sup>, Darin Dougherty<sup>2,6</sup>, Giorgio Bonmassar<sup>1,2</sup>, Leonardo M Angelone<sup>3</sup>, and Lawrence Wald<sup>1,2</sup>

<sup>1</sup>Radiology, Massachusetts General Hospital, Charlestown, MA, United States, <sup>2</sup>Harvard Medical School, Boston, MA, United States, <sup>3</sup>Division of Biomedical Physics, OSEL, CDRH, US Food and Drug Administration, Silver Spring, MD, United States, <sup>4</sup>Mechanical Engineering, University of Maryland, College Park, MD, United States, <sup>5</sup>Neurology, Massachusetts General Hospital, MA, United States, <sup>6</sup>Psychiatry, Massachusetts General Hospital, MA, United States

---

13

8:15



[Interventional Magnetic Resonance Imaging Guided Carotid Embolectomy using a Novel MRI-Conditional Resonant Catheter: Demonstration of Preclinical Feasibility](#)

Jeffrey K. Yang<sup>1</sup>, Andre Cote<sup>1</sup>, Caroline D. Jordan<sup>1</sup>, Aaron Losey<sup>1</sup>, David McCoy<sup>1</sup>, Andrew Chu<sup>2</sup>, Jay F. Yu<sup>1</sup>, Teri Moore<sup>1</sup>, Carol Stillson<sup>1</sup>, Fabio Settecase<sup>1</sup>, Matthew D. Alexander<sup>1</sup>, Andrew Nicholson<sup>1</sup>, Mariam Aboian<sup>1</sup>, Daniel L. Cooke<sup>1</sup>, Maythem Saeed<sup>1</sup>, Dave Barry<sup>2</sup>, Alastair J. Martin<sup>1</sup>, Mark W. Wilson<sup>1</sup>, and Steven W. Hetts<sup>1</sup>

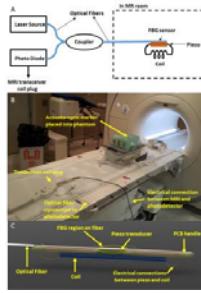
<sup>1</sup>Department of Radiology and Biomedical Imaging, UCSF, San Francisco, CA, United States, <sup>2</sup>Penumbra Inc, Alameda, CA, United States

---

14

8:15

[Acousto-optic Based Active MRI Marker for Interventional MRI Devices](#)



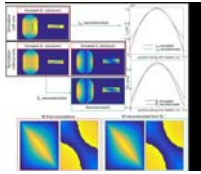
Yusuf Samet Yaras<sup>1</sup>, Sarp Satir<sup>1</sup>, Cagla Ozsoy<sup>2</sup>, Rajiv Ramasawmy<sup>3</sup>, Adrienne E Campbell-Washburn<sup>3</sup>, Anthony Faranesh<sup>3</sup>, Robert Lederman<sup>3</sup>, Ozgur Kocaturk<sup>2</sup>, and Levent Degertekin<sup>1</sup>

<sup>1</sup>G.W. Woodruff School of Mechanical Engineering, Georgia Institute of Technology, Atlanta, GA, United States, <sup>2</sup>Institute of Biomedical Engineering, Bogazici University, Istanbul, Turkey, <sup>3</sup>Division of Intramural Research, National Heart Lung and Blood Institute, National Institutes of Health, Bethesda, MD, United States

15

8:15

[MRI based RF safety characterization of implants using the implant response matrix: a simulation study.](#)



Janot P. Tokaya<sup>1</sup>, Alexander J.E. Raaijmakers<sup>2,3</sup>, Peter R. Luijten<sup>2</sup>, and Cornelis A.T. van den Berg<sup>1</sup>

<sup>1</sup>Radiotherapy, UMC Utrecht, Utrecht, Netherlands, <sup>2</sup>Radiology, UMC Utrecht, Utrecht, Netherlands, <sup>3</sup>Biomedical Image Analysis, Eindhoven University of Technology, Netherlands

## Power Pitch

### Pitch: 7T Neuroimaging

Power Pitch

Theater B -

Exhibition Hall

Monday 8:15 - 9:15 *Moderators: Penny Gowland & Janine Lupo*

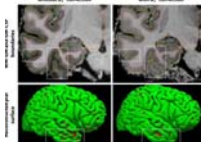
*(no CME credit)*

16



8:15

[The effects of B1+ correction of MP2RAGE on estimating cortical thickness and T1 at 7T](#)



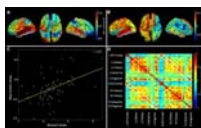
Roy Haast<sup>1</sup>, Dimo Ivanov<sup>1</sup>, Elia Formisano<sup>1</sup>, and Kâmil Uludağ<sup>1</sup>

<sup>1</sup>Department of Cognitive Neuroscience, Maastricht University, Maastricht, Netherlands

17

8:15

[The relationship between cortical myeloarchitecture and functional connectivity in the human brain](#)

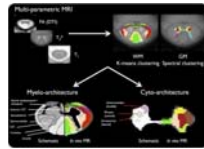


Olivier E. Mougin<sup>1</sup>, Benjamin A.E. Hunt<sup>1</sup>, Prejaas K. Tewarie<sup>1</sup>, Nicolas Geades<sup>1</sup>, Peter G. Morris<sup>1</sup>, Matthew J. Brookes<sup>1</sup>, and Penny A. Gowland<sup>1</sup>

18



8:15



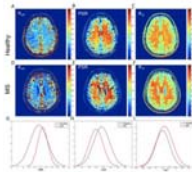
### Towards in vivo spinal cord cyto- and myelo-architecture deciphering using multi-modal MRI parcellation at 7T

Manuel Taso<sup>1,2,3</sup>, Aurélien Massire<sup>1,2,3</sup>, Pierre Besson<sup>1,2</sup>, Arnaud Le Troter<sup>1,2</sup>, Maxime Guye<sup>1,2</sup>, Jean-Philippe Ranjeva<sup>1,2,3</sup>, and Virginie Callot<sup>1,2,3</sup>

*<sup>1</sup>CRMBM, Aix-Marseille Univ, CNRS, Marseille, France, <sup>2</sup>Pôle d'imagerie médicale, Hôpital de la Timone, CEMEREM, AP-HM, Marseille, France, <sup>3</sup>Lab-Spine international associate laboratory, Marseille/Montréal, France*

19

8:15



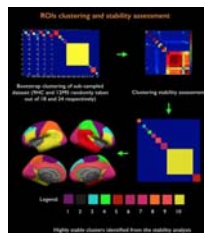
### 7T Quantitative Magnetization Transfer (qMT) of Cortical Gray Matter in Multiple Sclerosis Correlates with Cognitive Disability

Lydia McKeithan<sup>1,2</sup>, Bailey D. Lyttle<sup>2,3</sup>, Bailey A. Box<sup>2,3</sup>, Kristin P. O'Grady<sup>2,3</sup>, Richard D. Dortch<sup>1,2,3</sup>, Benjamin N. Conrad<sup>2</sup>, and Seth A. Smith<sup>1,2,3,4</sup>

*<sup>1</sup>Department of Biomedical Engineering, Vanderbilt University, Nashville, TN, United States, <sup>2</sup>Vanderbilt University Institute of Imaging Science, Vanderbilt University Medical Center, Nashville, TN, <sup>3</sup>Department of Radiology and Radiological Sciences, Vanderbilt University Medical Center, Nashville, TN, <sup>4</sup>Department of Ophthalmology, Vanderbilt University Medical Center, Nashville, TN*

20

8:15



### Changes in structural network connectivity in early-stage multiple sclerosis are associated with cortical demyelination

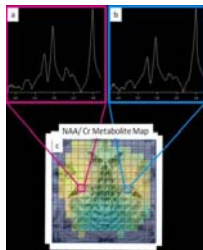
Atef Badji<sup>1,2</sup>, Gabriel Mangeat<sup>1,3</sup>, Russell Ouellette<sup>3,4</sup>, Constantina Andrada Treaba<sup>3,4</sup>, Tobias Granberg<sup>3,4,5</sup>, Elena Herranz<sup>3,4</sup>, Celine Louapre<sup>3,4</sup>, Nikola Stikov<sup>1,6</sup>, Jacob Sloane<sup>4,7</sup>, Pierre Bellec<sup>2</sup>, Caterina Mainero<sup>3,4</sup>, and Julien Cohen-Adad<sup>1,2</sup>

*<sup>1</sup>NeuroPoly Lab, Institute of Biomedical Engineering, Polytechnique Montreal, Montreal, QC, Canada, <sup>2</sup>Functional Neuroimaging Unit, CRIUGM, Université de Montréal, Montreal, QC, Canada, <sup>3</sup>Athinoula A. Martinos Center for Biomedical Imaging, MGH, <sup>4</sup>Harvard Medical School, <sup>5</sup>Department of Clinical Science, Intervention and Technology, Karolinska Institutet, <sup>6</sup>Montreal Health Institute, <sup>7</sup>Beth Israel Deaconess Medical Center*



21

8:15



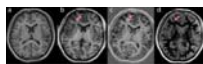
### 3D magnetic resonance spectroscopic imaging at 7 Tesla of patients with medically refractory focal epilepsy with non-lesional or inconclusive clinical MRIs: First Results

Rebecca Emily Feldman<sup>1</sup>, Madeline Cara Fields<sup>2</sup>, Bradley Neil Delman<sup>3</sup>, Lara Vanessa Marcuse<sup>4</sup>, and Priti Balchandani<sup>1</sup>

<sup>1</sup>Translational and Molecular Imaging Institute, Icahn School of Medicine at Mount Sinai, New York, NY, United States, <sup>2</sup>Department of Neurology, Mount Sinai Hospital, New York, NY, United States, <sup>3</sup>Radiology, Icahn School of Medicine at Mount Sinai, New York, NY, United States, <sup>4</sup>Department of Neurology, Mount Sinai Hospital

22

8:15



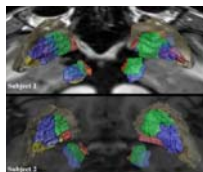
### The value of 7T in the clinical evaluation of epileptic patients with focal cortical dysplasia

Kaibao Sun<sup>1,2</sup>, Xueyuan Wang<sup>3</sup>, Zhongwei Chen<sup>1,2</sup>, Chang Liu<sup>3</sup>, Jianfei Cui<sup>4</sup>, Zhentao Zuo<sup>1</sup>, Rong Xue<sup>1,2</sup>, Yan Zhuo<sup>1</sup>, Lin Chen<sup>1,2</sup>, Shuli Liang<sup>4</sup>, Tao Yu<sup>3</sup>, and Bo Wang<sup>1</sup>

<sup>1</sup>State Key Laboratory of Brain and Cognitive Science, Beijing MRI Center for Brain Research, Institute of Biophysics, Chinese Academy of Sciences, Beijing, People's Republic of China, <sup>2</sup>University of Chinese Academy of Sciences, Beijing, People's Republic of China, <sup>3</sup>Xunanwu Hospital Capital Medical University, Beijing, People's Republic of China, <sup>4</sup>Chinese PLA general hospital, Beijing, People's Republic of China

23

8:15



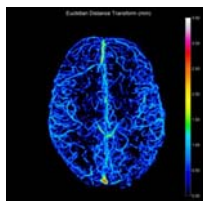
### Individualized Tractography-Based Parcellation of the Globus Pallidus Pars Interna using 7T MRI in patients with Parkinson's Disease Prior to DBS Surgery

Rémi Patriat<sup>1</sup>, Yuval Duchin<sup>1</sup>, Christophe Lenglet<sup>1</sup>, Joshua Aman<sup>2</sup>, Scott Cooper<sup>2</sup>, Jerrold Vitek<sup>2</sup>, and Noam Harel<sup>1</sup>

<sup>1</sup>CMRR / Radiology, University of Minnesota, Minneapolis, MN, United States, <sup>2</sup>Neurology, University of Minnesota, Minneapolis, MN, United States

24

8:15



### Assessment of cerebral vascular abnormalities in Huntington's Disease at 7Tesla

Richard J Dury<sup>1</sup>, Sarah L Mason<sup>2</sup>, Francesca Cicchetti<sup>3</sup>, Janelle Drouin-Ouellet<sup>2</sup>, Roger A Barker<sup>2</sup>, Penny A Gowland<sup>1</sup>, and Susan T Francis<sup>1</sup>

<sup>1</sup>Sir Peter Mansfield Imaging Centre, University of Nottingham, Nottingham, United Kingdom, <sup>2</sup>John van Geest Centre for Brain Repair, University of Cambridge, Cambridge, United Kingdom, <sup>3</sup>Département de Psychiatrie & Neurosciences, Université Laval, QC, Canada

25

8:15



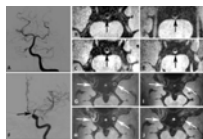
**7T TOF-MRA Shows Different Patterns of Perforating Artery in Patients with Intracranial Atherosclerosis Disease (ICAD) and Cerebral Autosomal-Dominant Arteriopathy with Subcortical Infarcts and Leukoencephalopathy (CADASIL)**

Qingle Kong<sup>1,2</sup>, Qi Yang<sup>3,4</sup>, Zhaoyang Fan<sup>3</sup>, Xianchang Zhang<sup>1,2</sup>, Yun Yuan<sup>5</sup>, Xiaojing Fang<sup>5</sup>, Jing An<sup>6</sup>, Yan Zhuo<sup>1</sup>, and Zihao Zhang<sup>1</sup>

<sup>1</sup>State Key Laboratory of Brain and Cognitive Science, Beijing MR Center for Brain Research, Institute of Biophysics, Chinese Academy of Sciences, Beijing, People's Republic of China, <sup>2</sup>University of Chinese Academy of Sciences, Beijing, People's Republic of China, <sup>3</sup>Biomedical Imaging Research Institute, Cedars-Sinai Medical Center, Los Angeles, CA, United States, <sup>4</sup>Xuanwu Hospital, Beijing, People's Republic of China, <sup>5</sup>Department of Neurology, Peking University First Hospital, Beijing, People's Republic of China, <sup>6</sup>Siemens Shenzhen Magnetic Resonance Ltd., Shenzhen, People's Republic of China

26

8:15



**Intracranial vessel wall imaging in suspected cerebral vasculitis: evaluation of diagnostic value and treatment effects using 3T and 7T MRI**

Nikki Dieleman<sup>1</sup>, Anja G. van der Kolk<sup>1</sup>, Catharina J.M. Frijns<sup>2</sup>, Anita A. Hartevelde<sup>1</sup>, Jaco J.M. Zwanenburg<sup>1</sup>, Hugo J. Kuijff<sup>3</sup>, Arjen Lindenholz<sup>1</sup>, L. Jaap Kappelle<sup>2</sup>, Peter R. Luijten<sup>1</sup>, and Jeroen Hendrikse<sup>1</sup>

<sup>1</sup>Radiology, University Medical Center Utrecht, Utrecht, Netherlands, <sup>2</sup>Neurology, University Medical Center Utrecht, Utrecht, Netherlands, <sup>3</sup>Images Science Institute, University Medical Center Utrecht, Utrecht, Netherlands

27

8:15



**Detection of intracranial vessel wall lesions using 7T MRI: patients with posterior circulation ischemia versus healthy controls**

Anita A. Hartevelde<sup>1</sup>, Anja G. van der Kolk<sup>1</sup>, H. Bart van der Worp<sup>2</sup>, Nikki Dieleman<sup>1</sup>, Peter R. Luijten<sup>1</sup>, Jaco J.M. Zwanenburg<sup>1</sup>, and Jeroen Hendrikse<sup>1</sup>





<sup>1</sup>Radiology, University Medical Center Utrecht, Utrecht, Netherlands,  
<sup>2</sup>Neurology and Neurosurgery, University Medical Center Utrecht,  
Utrecht, Netherlands

28

8:15

Metabolic differences between asymptomatic C9orf72 carriers and non-carriers assessed by brain 7T MRSI.



Henk-Jan Westeneng<sup>1</sup>, Carrie Wismans<sup>1</sup>, Abram D. Niter<sup>1</sup>, Renée Walhout<sup>1</sup>, Peter R. Luijten<sup>2</sup>, Jannie P. Wijnen<sup>2</sup>, and Leonard H. van den Berg<sup>1</sup>

<sup>1</sup>Department of Neurology, Brain Center Rudolf Magnus, University Medical Center Utrecht, Utrecht, Netherlands, <sup>2</sup>Department of Radiology, University Medical Center Utrecht, Utrecht, Netherlands

29

8:15

GABA and glutamate in children with Tourette Syndrome: a 7T 1H-MRS study



	TS		Controls			
	n	Mean (SD)	n	Mean (SD)	p	%
GABA	10	1.2 (0.4)	10	1.2 (0.4)	0.99	100
GLU	10	2.1 (0.6)	10	2.1 (0.6)	0.99	100
GLN	10	1.8 (0.5)	10	1.8 (0.5)	0.99	100
GLX	10	1.5 (0.4)	10	1.5 (0.4)	0.99	100
GLY	10	1.2 (0.3)	10	1.2 (0.3)	0.99	100
GLA	10	1.0 (0.2)	10	1.0 (0.2)	0.99	100
GLB	10	1.0 (0.2)	10	1.0 (0.2)	0.99	100
GLC	10	1.0 (0.2)	10	1.0 (0.2)	0.99	100
GLD	10	1.0 (0.2)	10	1.0 (0.2)	0.99	100
GLE	10	1.0 (0.2)	10	1.0 (0.2)	0.99	100
GLF	10	1.0 (0.2)	10	1.0 (0.2)	0.99	100
GLG	10	1.0 (0.2)	10	1.0 (0.2)	0.99	100
GLH	10	1.0 (0.2)	10	1.0 (0.2)	0.99	100
GLI	10	1.0 (0.2)	10	1.0 (0.2)	0.99	100
GLJ	10	1.0 (0.2)	10	1.0 (0.2)	0.99	100
GLK	10	1.0 (0.2)	10	1.0 (0.2)	0.99	100
GLL	10	1.0 (0.2)	10	1.0 (0.2)	0.99	100
GLM	10	1.0 (0.2)	10	1.0 (0.2)	0.99	100
GLN	10	1.0 (0.2)	10	1.0 (0.2)	0.99	100
GLO	10	1.0 (0.2)	10	1.0 (0.2)	0.99	100
GLP	10	1.0 (0.2)	10	1.0 (0.2)	0.99	100
GLQ	10	1.0 (0.2)	10	1.0 (0.2)	0.99	100
GLR	10	1.0 (0.2)	10	1.0 (0.2)	0.99	100
GLS	10	1.0 (0.2)	10	1.0 (0.2)	0.99	100
GLT	10	1.0 (0.2)	10	1.0 (0.2)	0.99	100
GLU	10	1.0 (0.2)	10	1.0 (0.2)	0.99	100
GLV	10	1.0 (0.2)	10	1.0 (0.2)	0.99	100
GLW	10	1.0 (0.2)	10	1.0 (0.2)	0.99	100
GLX	10	1.0 (0.2)	10	1.0 (0.2)	0.99	100
GLY	10	1.0 (0.2)	10	1.0 (0.2)	0.99	100
GLZ	10	1.0 (0.2)	10	1.0 (0.2)	0.99	100
GLAA	10	1.0 (0.2)	10	1.0 (0.2)	0.99	100
GLAB	10	1.0 (0.2)	10	1.0 (0.2)	0.99	100
GLAC	10	1.0 (0.2)	10	1.0 (0.2)	0.99	100
GLAD	10	1.0 (0.2)	10	1.0 (0.2)	0.99	100
GLAE	10	1.0 (0.2)	10	1.0 (0.2)	0.99	100
GLAF	10	1.0 (0.2)	10	1.0 (0.2)	0.99	100
GLAG	10	1.0 (0.2)	10	1.0 (0.2)	0.99	100
GLAH	10	1.0 (0.2)	10	1.0 (0.2)	0.99	100
GLAI	10	1.0 (0.2)	10	1.0 (0.2)	0.99	100
GLAJ	10	1.0 (0.2)	10	1.0 (0.2)	0.99	100
GLAK	10	1.0 (0.2)	10	1.0 (0.2)	0.99	100
GLAL	10	1.0 (0.2)	10	1.0 (0.2)	0.99	100
GLAM	10	1.0 (0.2)	10	1.0 (0.2)	0.99	100
GLAN	10	1.0 (0.2)	10	1.0 (0.2)	0.99	100
GLAO	10	1.0 (0.2)	10	1.0 (0.2)	0.99	100
GLAP	10	1.0 (0.2)	10	1.0 (0.2)	0.99	100
GLAQ	10	1.0 (0.2)	10	1.0 (0.2)	0.99	100
GLAR	10	1.0 (0.2)	10	1.0 (0.2)	0.99	100
GLAS	10	1.0 (0.2)	10	1.0 (0.2)	0.99	100
GLAT	10	1.0 (0.2)	10	1.0 (0.2)	0.99	100
GLAU	10	1.0 (0.2)	10	1.0 (0.2)	0.99	100
GLAV	10	1.0 (0.2)	10	1.0 (0.2)	0.99	100
GLAW	10	1.0 (0.2)	10	1.0 (0.2)	0.99	100
GLAX	10	1.0 (0.2)	10	1.0 (0.2)	0.99	100
GLAY	10	1.0 (0.2)	10	1.0 (0.2)	0.99	100
GLAZ	10	1.0 (0.2)	10	1.0 (0.2)	0.99	100
GLAA	10	1.0 (0.2)	10	1.0 (0.2)	0.99	100
GLAB	10	1.0 (0.2)	10	1.0 (0.2)	0.99	100
GLAC	10	1.0 (0.2)	10	1.0 (0.2)	0.99	100
GLAD	10	1.0 (0.2)	10	1.0 (0.2)	0.99	100
GLAE	10	1.0 (0.2)	10	1.0 (0.2)	0.99	100
GLAF	10	1.0 (0.2)	10	1.0 (0.2)	0.99	100
GLAG	10	1.0 (0.2)	10	1.0 (0.2)	0.99	100
GLAH	10	1.0 (0.2)	10	1.0 (0.2)	0.99	100
GLAI	10	1.0 (0.2)	10	1.0 (0.2)	0.99	100
GLAJ	10	1.0 (0.2)	10	1.0 (0.2)	0.99	100
GLAK	10	1.0 (0.2)	10	1.0 (0.2)	0.99	100
GLAL	10	1.0 (0.2)	10	1.0 (0.2)	0.99	100
GLAM	10	1.0 (0.2)	10	1.0 (0.2)	0.99	100
GLAN	10	1.0 (0.2)	10	1.0 (0.2)	0.99	100
GLAO	10	1.0 (0.2)	10	1.0 (0.2)	0.99	100
GLAP	10	1.0 (0.2)	10	1.0 (0.2)	0.99	100
GLAQ	10	1.0 (0.2)	10	1.0 (0.2)	0.99	100
GLAR	10	1.0 (0.2)	10	1.0 (0.2)	0.99	100
GLAS	10	1.0 (0.2)	10	1.0 (0.2)	0.99	100
GLAT	10	1.0 (0.2)	10	1.0 (0.2)	0.99	100
GLAU	10	1.0 (0.2)	10	1.0 (0.2)	0.99	100
GLAV	10	1.0 (0.2)	10	1.0 (0.2)	0.99	100
GLAW	10	1.0 (0.2)	10	1.0 (0.2)	0.99	100
GLAX	10	1.0 (0.2)	10	1.0 (0.2)	0.99	100
GLAY	10	1.0 (0.2)	10	1.0 (0.2)	0.99	100
GLAZ	10	1.0 (0.2)	10	1.0 (0.2)	0.99	100

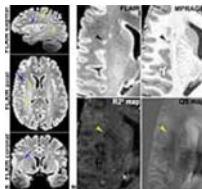
Nicolaas AJ Puts<sup>1,2</sup>, Richard AE Edden<sup>1,2</sup>, Matthew Ryan<sup>3</sup>, E Mark Mahone<sup>3,4</sup>, and Harvey S Singer<sup>5</sup>

<sup>1</sup>Russell H. Morgan Department of Radiology and Radiological Science, The Johns Hopkins University, Baltimore, MD, United States, <sup>2</sup>FM Kirby Research Center for Functional Brain Imaging, Kennedy Krieger Institute, Baltimore, MD, United States, <sup>3</sup>Department of Neuropsychology, Kennedy Krieger Institute, Baltimore, MD, United States, <sup>4</sup>Department of Psychiatry and Behavioral Sciences, The Johns Hopkins University, Baltimore, MD, United States, <sup>5</sup>Department of Neurology, The Johns Hopkins University, Baltimore, MD, United States

30

8:15

Multi-Parametric MRI at 7 T Enables Differentiation of MS and Age-Related White Matter Lesions



Zahra Hosseini<sup>1,2</sup>, David A. Rudko<sup>3</sup>, Jacob A. Matusinec<sup>4</sup>, Marcelo kremenchutzky<sup>5</sup>, Ravi Menon<sup>2,6</sup>, and Maria Drangova<sup>1,6,7</sup>

<sup>1</sup>Biomedical Engineering Graduate Program, University of Western Ontario, London, ON, Canada, <sup>2</sup>Imaging Research Laboratories, Robarts Research Institute, London, ON, Canada, <sup>3</sup>Montreal Neurological Hospital and Institute, McGill University, Montreal, QC, Canada, <sup>4</sup>Medicine, Schulich School of Medicine & Dentistry, University of Western Ontario, London, ON, Canada, <sup>5</sup>Department of Clinical Neurological Sciences, Schulich School of Medicine & Dentistry, University of Western Ontario, London, ON, Canada, <sup>6</sup>Department of Medical Biophysics, University of Western Ontario, London, ON, Canada, <sup>7</sup>Imaging Research Laboratories, Robarts Research Institute

---

Oral

## Young Investigator Awards

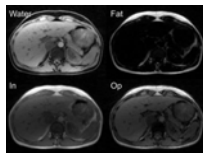
Room 310

Monday 8:15 - 10:15 Moderators: Elizabeth Hecht & Houchun Hu

---

31

8:15



Free-breathing volumetric fat/water separation by combining radial sampling, compressed sensing, and parallel imaging

Thomas Benkert<sup>1,2</sup>, Li Feng<sup>1,2</sup>, Daniel K. Sodickson<sup>1,2</sup>, Hersh Chandarana<sup>1,2</sup>, and Kai Tobias Block<sup>1,2</sup>

<sup>1</sup>Radiology, NYU School of Medicine, New York, NY, United States, <sup>2</sup>Bernard and Irene Schwartz Center for Biomedical Imaging, Department of Radiology, NYU School of Medicine, New York, NY, United States

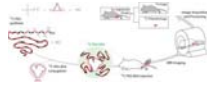
Fat-suppressed T1-weighted gradient-echo imaging is commonly used for abdominal MR examination. However, image quality can be compromised by inhomogeneous fat suppression and imperfect breath-holding. To overcome both limitations, we describe a novel technique for free-breathing fat/water separation (Dixon-RAVE).

Motion-robust acquisition is achieved by using radial sampling. A model-based reconstruction, which incorporates compressed sensing, parallel imaging, and fat deblurring, is used to obtain fat and water maps. Two extensions are described that enable motion-resolved fat/water separation (XD-Dixon-RAVE) and dynamic contrast-enhanced fat/water separation (DCE-Dixon-RAVE). The technique is demonstrated for various clinical applications, including free-breathing liver and breast exams in volunteers and patients.

---

32

8:35



### Direct Quantitative <sup>13</sup>C-Filtered <sup>1</sup>H Magnetic Resonance Imaging of PEGylated Biomacromolecules In Vivo

Rohan D. A. Alvares<sup>1</sup>, Justin Y. Lau<sup>2,3</sup>, Peter M. Macdonald<sup>1</sup>, Charles H. Cunningham<sup>2,3</sup>, and R. Scott Prosser<sup>1,4</sup>

<sup>1</sup>Department of Chemistry, University of Toronto, Toronto, ON, Canada,

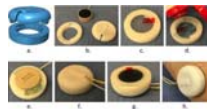
<sup>2</sup>Department of Medical Biophysics, University of Toronto, Toronto, ON, Canada, <sup>3</sup>Sunnybrook Research Institute, Toronto, ON, Canada,

<sup>4</sup>Department of Biochemistry, University of Toronto, Toronto, ON, Canada

We demonstrate a new platform technology in which macromolecular constituents, such as proteins and drug delivery systems, are observed directly and quantitatively in vivo using <sup>1</sup>H MRI of <sup>13</sup>C-labeled polyethylene glycol (<sup>13</sup>C-PEG) tags. The 28 kDa <sup>13</sup>C-PEG tags are non-immunogenic, and each bears approximately 2500 spectroscopically equivalent <sup>1</sup>H nuclei appearing at a single resonance position. By filtering the <sup>1</sup>H PEG signal through the directly coupled <sup>13</sup>C nuclei, background water and fat signals are largely eliminated. We demonstrate the approach by monitoring in real-time the distribution of <sup>13</sup>C-PEG and <sup>13</sup>C-pegylated albumin injected into the hind leg of a mouse.

33

8:55



### Hybrid MRI-ultrasound acquisitions, and scannerless real-time imaging

Frank Preiswerk<sup>1</sup>, Matthew Toews<sup>2</sup>, Cheng-Chieh Cheng<sup>1</sup>, Jr-yuan George Chiou<sup>1</sup>, Chang-Sheng Mei<sup>3</sup>, Lena F. Schaefer<sup>1</sup>, W. Scott Hoge<sup>1</sup>, Benjamin M. Schwartz<sup>4</sup>, Lawrence P. Panych<sup>1</sup>, and Bruno Madore<sup>1</sup>

<sup>1</sup>Department of Radiology, Brigham and Women's Hospital, Harvard

Medical School, Boston, MA, United States, <sup>2</sup>The Laboratory for Imagery, Vision and Artificial Intelligence, École de Technologie

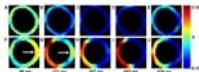
Supérieure, Montréal, QC, Canada, <sup>3</sup>Department of Physics, Soochow University, Taipei, Taiwan, <sup>4</sup>Google Inc, New York, NY, United States

The goal of this project was to combine MRI, ultrasound (US) and computer science methodologies toward generating MRI at high frame rates, inside and even outside the bore. A small US transducer, fixed to the abdomen, collected signals during MRI. Based on these signals and correlations with MRI, a machine-learning algorithm created synthetic MR images at up to 100 frames per second. In one particular implementation volunteers were taken out of the MRI bore with US sensor still in place, and MR images were generated on the basis of ultrasound signal and learned correlations alone, in a 'scannerless' manner.

---

34

9:15



Imaging Left-ventricular Mechanical Activation in Heart Failure Patients using Cine DENSE MRI: Validation and Implications for Cardiac Resynchronization Therapy

Daniel Auger<sup>1</sup>, Kenneth C. Bilchick<sup>2</sup>, Jorge A. Gonzalez<sup>2</sup>, Sophia X. Cui<sup>1</sup>, Jeffrey W. Holmes<sup>1,2</sup>, Christopher M. Kramer<sup>2,3</sup>, Michael Salerno<sup>1,2</sup>, and Frederick H. Epstein<sup>1,3</sup>

<sup>1</sup>Department of Biomedical Engineering, University of Virginia Health System, Charlottesville, VA, United States,

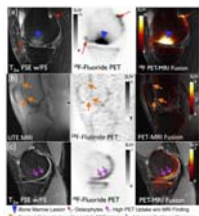
<sup>2</sup>Medicine/Cardiology/Electrophysiology, University of Virginia Health System, Charlottesville, VA, United States, <sup>3</sup>Radiology/Medical Imaging, University of Virginia Health System, Charlottesville, VA, United States

This study developed methods for imaging left-ventricular (LV) mechanical activation, with application to identifying optimal LV pacing sites for cardiac resynchronization therapy (CRT). Cine displacement encoding with stimulated echoes (DENSE) was used for strain imaging, and mechanical activation time was defined as the time of onset of circumferential shortening (TOS). Active contours were applied to strain data to automatically compute TOS. Results showed a strong correlation between TOS and electrical activation time, heterogeneity of the location of latest activation, and a significant association between TOS at the LV pacing site and CRT response. These methods may enable improved CRT implementation.

---

35

9:35



PET/MR Imaging of Metabolic Bone Activity in Osteoarthritis

Feliks Kogan<sup>1</sup>, Audrey Fan<sup>1</sup>, Emily McWalter<sup>2</sup>, Uchechukwuka Monu<sup>1</sup>, Edwin Oei<sup>3</sup>, Andrew Quon<sup>1</sup>, and Garry Gold<sup>1,4,5</sup>

<sup>1</sup>Radiology, Stanford University, Stanford, CA, United States,

<sup>2</sup>Department of Mechanical Engineering, University of Saskatchewan, Saskatoon, SK, Canada, <sup>3</sup>Department of Radiology & Nuclear Medicine, Erasmus MC, University Medical Center, Rotterdam, Netherlands, <sup>4</sup>Department of Bioengineering, Stanford University, Stanford, CA, United States, <sup>5</sup>Department of Orthopaedic Surgery, Stanford University, San Francisco, CA, United States

Osteoarthritis (OA) is a leading cause of disability, resulting in reduced quality of life, at tremendous societal cost. New hybrid PET/MR systems allow for simultaneous, sensitive, and quantitative assessments of early bone activity in OA with PET, which can be correlated with high-resolution quantitative MR methods of soft tissues to study the pathogenesis of OA. We demonstrate promising initial results of simultaneous PET/MR hybrid imaging of knee OA. Results suggest that PET/MR may detect metabolic abnormalities in subchondral bone, which appear normal on MRI. These advancements will allow us to detect and track early and reversible changes in OA.

36

9:55

In vivo (2018)	8T (PCMR)		8T (PCMR)	
	Mean (standard deviation)	Median (interquartile range)	Mean (standard deviation)	Median (interquartile range)
Peak CSF Velocity	Mean (standard deviation)	1.14 ± 0.07 cm/s	2.26 ± 0.75 cm/s	
	Min (standard deviation)	-1.02 ± 0.08 cm/s	-2.28 ± 0.58 cm/s	
Peak CSF Velocity (respiration only)	Mean (standard deviation)	0.58 ± 0.45 cm/s	0.84 ± 0.45 cm/s	
	Min (standard deviation)	-0.48 ± 0.27 cm/s	-0.55 ± 0.38 cm/s	
Peak CSF Velocity (cardiac-only)	Mean (standard deviation)	0.97 ± 0.20 cm/s	1.27 ± 0.20 cm/s	
	Min (standard deviation)	-0.97 ± 0.20 cm/s	-1.54 ± 0.28 cm/s	
Estimated Respiration	Respiration	0.10 ± 0.11 Hz	0.11 ± 0.09 Hz	
	Cardiac	1.17 ± 0.10 Hz	1.18 ± 0.11 Hz	
Phase-velo (2D)		0.14 ± 0.26	0.40 ± 0.47	

### Quantifying the Influence of Respiration and Cardiac Pulsations on the Cerebrospinal Fluid Dynamics using Real-Time Phase-Contrast MRI

Selda Yildiz<sup>1</sup>, Suraj Thyagaraj<sup>2</sup>, Ning Jin<sup>3</sup>, Xiadong Zhong<sup>4</sup>, Soroush Heidari Pahlavian<sup>2</sup>, Bryn Martin<sup>5</sup>, Francis Loth<sup>2</sup>, John Oshinski<sup>6</sup>, and Karim G. Sabra<sup>1</sup>

<sup>1</sup>Woodruff School of Mechanical Engineering, Georgia Institute of Technology, Atlanta, GA, United States, <sup>2</sup>Department of Mechanical Engineering, Conquer Chiari Research Center, The University of Akron, Akron, OH, United States, <sup>3</sup>MR R&D Collaborations, Siemens Healthcare, Columbus, OH, United States, <sup>4</sup>MR R&D Collaborations, Siemens Healthcare, Atlanta, GA, United States, <sup>5</sup>Department of Biological Engineering, The University of Idaho, Moscow, ID, United States, <sup>6</sup>Department of Radiology & Imaging Sciences and Biomedical Engineering, Emory University, Atlanta, GA, United States

Cerebrospinal fluid (CSF) flow undergoes periodic pulsatile motion driven by cardiac and the respiratory forces. Invasive studies using spinal taps as well as non-invasive studies using phase contrast MRI (PCMRI) sequences have well documented the cardiac-driven CSF flow. PCMRI, however, often uses a conventional cine-phase contrast technique gated to the cardiac cycle, and thus cannot measure the effects of respiration or other non-cardiac transient events such as coughing. Examining these effects requires the ability to perform real-time MRI measurements of continuous CSF flow along the spine and cranial cavity, and determine accurate instantaneous CSF flow velocity values.

Oral

# Myocardial Tissue Relaxometry

Room 312

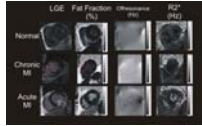
Monday 8:15 - 10:15 Moderators: Jihye Jang & Graham Wright

---

37

8:15

## Joint Native Myocardial Fat Fraction, Off-Resonance and $R2^*/T2^*$ Mapping in Ischemic Cardiomyopathies



James W Goldfarb<sup>1</sup>, Usama Hasan<sup>1</sup>, and Jie J Cao<sup>1</sup>

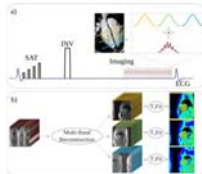
<sup>1</sup>St Francis Hospital, Roslyn, NY, United States

Myocardial fat content,  $R2^*/T2^*$  and off-resonance frequency can be measured with high resolution using a native MR water-fat separation imaging technique applied to multiple gradient echo images. Significant differences in myocardial fat fraction were found consistent with fatty metaplasia in a subset of chronic myocardial infarction patients. Off-resonance and  $T2^*$  changes consistent with intramyocardial hemorrhage were observed in a subset of acute myocardial infarction patients.

38

8:27

## Simultaneous Multi-Slice Imaging For Whole Heart Myocardial $T_1$ Mapping In A Single Breath-Hold



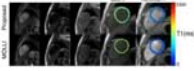
Sebastian Weingärtner<sup>1,2,3</sup>, Steen Moeller<sup>2</sup>, Kâmil Uğurbil<sup>2</sup>, Chetan Shenoy<sup>4</sup>, and Mehmet Akçakaya<sup>1,2</sup>

<sup>1</sup>Electrical and Computer Engineering, University of Minnesota, Minneapolis, MN, United States, <sup>2</sup>Center for Magnetic Resonance Research, University of Minnesota, Minneapolis, MN, United States, <sup>3</sup>Computer Assisted Clinical Medicine, Heidelberg University, Mannheim, Germany, <sup>4</sup>Department of Cardiology, University of Minnesota, Minneapolis, MN, United States

Myocardial  $T_1$ -mapping bears promise for evaluation of numerous cardiomyopathies, but requires multiple breath-hold scans with conventional techniques. In this study we explored the acceleration potential of multi-band imaging for myocardial SAPHIRE  $T_1$ -mapping with 3-slice coverage in a single breath-hold. Three linear methods for slice and in-plane unaliasing were evaluated. Phantom studies confirmed the accuracy of the proposed  $T_1$ -mapping method, and in-vivo evaluation has shown reliable image quality with 3-fold acceleration at the cost of 1.3 to 1.7-fold increased in-vivo variability. Smaller loss in-vivo precision was achieved using regularized methods, for the trade-off against increased inter-slice leakage.

---



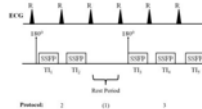


### Free-Breathing, Non-ECG-Gated, Continuous Myocardial T<sub>1</sub> Mapping and ECV Quantification with Multitasking

Jaime L. Shaw<sup>1,2</sup>, Anthony Christodoulou<sup>1,3</sup>, Behzad Sharif<sup>1</sup>, and Debiao Li<sup>1,2</sup>

<sup>1</sup>Biomedical Imaging Research Institute, Cedars-Sinai Medical Center, Los Angeles, CA, United States, <sup>2</sup>Department of Bioengineering, UCLA, Los Angeles, CA, United States, <sup>3</sup>Heart Institute, Cedars-Sinai Medical Center, Los Angeles, CA

Currently used T<sub>1</sub> mapping techniques utilize both ECG gating and breath-holds/navigators with low imaging efficiency and/or respiratory motion artifacts. We removed the need for ECG gating and respiratory monitoring with Cardiac MR Multitasking, a continuous acquisition technique using a low-rank tensor (LRT) imaging framework. The aim of this work is to validate a free-breathing, non-ECG-gated native T<sub>1</sub> mapping and ECV quantification method in healthy subjects against standard MOLLI T<sub>1</sub> mapping.

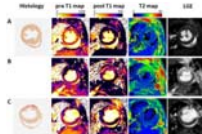


### Optimized Single Pre/Post Contrast Protocol for MOLLI T<sub>1</sub> Mapping with Inversion Group (IG) Fitting

Marshall Sussman<sup>1,2</sup>, Luigia D'Errico<sup>1</sup>, and Bernd Juergen Wintersperger<sup>1,2</sup>

<sup>1</sup>Medical Imaging, University Health Network, Toronto, ON, Canada, <sup>2</sup>Medical Imaging, University of Toronto, Toronto, ON, Canada

A major focus in cardiac research is the assessment of myocardial pathology using quantitative T<sub>1</sub> mapping. A number of sequences are being investigated for this task. One candidate is MOLLI. It provides superior precision to other cardiac T<sub>1</sub> mapping techniques. However, its precision is dependent on heart rate and range of T<sub>1</sub> values present. Current attempts at optimizing precision are somewhat impractical, as they utilize separate MOLLI protocols for different heart rates, and for pre/post contrast imaging. This study identifies a single MOLLI protocol optimal for precision over a broad range of heart rates and pre/post contrast T<sub>1</sub> values.



### Early Gradual Assessment of Tissue Injury and Functional Outcome after Myocardial Infarction by Cardiovascular Magnetic Resonance T<sub>1</sub> Mapping

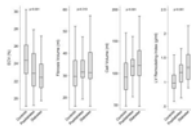
Sebastian Maximilian Haberkorn<sup>1,2</sup>, Christoph Jacoby<sup>1</sup>, Jürgen Schrader<sup>2,3</sup>, Malte Kelm<sup>1,3</sup>, and Uli Flögel<sup>2,3</sup>

<sup>1</sup>Department of Cardiology, University Hospital Duesseldorf, Duesseldorf, Germany, <sup>2</sup>Department of Molecular Cardiology, Heinrich-Heine University Duesseldorf, Duesseldorf, Germany, <sup>3</sup>Cardiovascular Research Institute Duesseldorf, Heinrich-Heine University, Duesseldorf, Germany

The value of CMR to distinguish between the severity of ischemic injuries after myocardial (MI) has yet to be established. Here, we quantified local tissue injuries and their correlation with functional outcome in two different experimental models of MI including native and post-contrast T1 maps, T2 maps and LGE. Only native T1 maps enabled in the acute phase after MI the detection of substantial differences in myocardial tissue texture between the two models, where neither of the other measures was indicative. In conclusion, native T1 mapping enables a gradual assessment of myocardial injury and holds predictive potential for the functional outcome.

42

9:15



Multiparametric Characterization of Myocardial Tissue by Contrast-Enhanced Cardiac Magnetic Resonance Imaging in Subjects with Prediabetes, Diabetes and Controls from a Western General Population – Results of the KORA-MRI-Study

Corinna Christina Storz<sup>1</sup>, Holger Hetterich<sup>2</sup>, Roberto Lorbeer<sup>2</sup>, Sigrid Auweter<sup>2</sup>, Wolfgang Rathmann<sup>3</sup>, Christopher L Schlett<sup>4</sup>, Annette Peters<sup>5,6,7</sup>, Konstantin Nikolaou<sup>8,7</sup>, Fabian Bamberg<sup>8</sup>, and Jeanette Schulz-Menger<sup>9,10</sup>

<sup>1</sup>Radiology, University Hospital Tuebingen, Tuebingen, Germany, <sup>2</sup>Clinical Radiology, Ludwig-Maximilians-University Munich, Germany, <sup>3</sup>Biometry and Epidemiology, German Diabetes Center Duesseldorf, Germany, <sup>4</sup>Diagnostic and Interventional Radiology, University Hospital Heidelberg, Germany, <sup>5</sup>Epidemiology II, Helmholtz Zentrum Munich, German Research Center for Environmental Health, Neuherberg, Germany, <sup>6</sup>Cardiovascular Prevention, Ludwig-Maximilians University Munich, Munich, Germany, <sup>7</sup>German Center for Cardiovascular Disease Research (DZHK e.V.) Munich, Munich, Germany, <sup>8</sup>Diagnostic and Interventional Radiology, University Hospital Tuebingen, Tuebingen, Germany, <sup>9</sup>Cardiology, Charité, Experimental and Clinical Research Center and HELIOS-Clinics Berlin-Buc, Germany, <sup>10</sup>German Center for Cardiovascular Disease Research (DZHK e. V.) Partnersite Berlin, Germany



Cardiac magnetic resonance imaging (CMR) allows for detailed characterization of the myocardium, which may be beneficial in assessing cardiomyopathy in the setting of hyperglycemic states. We performed a comprehensive CMR protocol in subjects with prediabetes, diabetes and controls and preserved left ventricular (LV) ejection fraction (EF) in a western population-based sample. Subjects with prediabetes and diabetes had an increased LV-remodeling-index as well as higher estimates of cell volume compared with controls, while extracellular volume, as a parameter of diffuse myocardial fibrosis (MF), was decreased. This may highlight the role for hypertrophy in the pathogenesis of diabetic cardiomyopathy in this western population.

43



9:27

Group	Age (years)	Sex	Diabetes	EF (%)	LVMI (g/m <sup>2</sup> )	ECV (%)	Cell Volume (g/m <sup>2</sup> )	MF (g/m <sup>2</sup> )
Controls	58.2 ± 12.1	M: 15, F: 15	0	58.2 ± 12.1	102.5 ± 15.2	23.5 ± 3.2	1.2 ± 0.2	0.8 ± 0.1
Prediabetes	59.1 ± 11.8	M: 12, F: 12	0	59.1 ± 11.8	115.2 ± 18.5	22.8 ± 2.8	1.5 ± 0.3	0.7 ± 0.1
Diabetes	60.3 ± 13.5	M: 10, F: 10	1	60.3 ± 13.5	128.7 ± 22.1	21.5 ± 2.5	1.8 ± 0.4	0.6 ± 0.1

### Comprehensive Cardiac Structure-Function MRI in Heart Transplant Recipients: Influence of Acute Cardiac Allograft Rejection

Ryan Dolan<sup>1</sup>, Amir Rahsepar<sup>1</sup>, Julie Blaisdell<sup>1</sup>, Kenichiro Suwa<sup>1</sup>, Allen Anderson<sup>2</sup>, Kambiz Ghafourian<sup>2</sup>, Esther Vorovich<sup>2</sup>, Jonathan Rich<sup>2</sup>, Jane Wilcox<sup>2</sup>, Clyde Yancy<sup>2</sup>, Jeremy Collins<sup>1</sup>, James Carr<sup>1</sup>, and Michael Markl<sup>1</sup>

<sup>1</sup>Radiology, Northwestern University, Chicago, IL, United States,

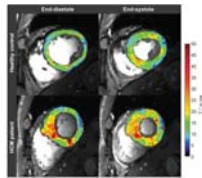
<sup>2</sup>Cardiology, Northwestern University, Chicago, IL, United States

Cardiac MRI provides a comprehensive structure-function evaluation of the heart with increasingly strong evidence of its ability to detect acute cardiac allograft rejection following heart transplant. In this large cohort of transplant recipients, quantitative T2 and ECV were significantly elevated during episodes of biopsy-proven rejection compared to baseline.

44



9:39



### Myocardial T2\* Changes Periodically across the Cardiac Cycle and is Prolonged in Hypertrophic Cardiomyopathy: A 7.0 Tesla MRI Patient Study

Till Huelnhagen<sup>1</sup>, Fabian Hezel<sup>1</sup>, Teresa Serradas Duarte<sup>1</sup>, Min-Chi Ku<sup>1</sup>, Bert Flemming<sup>2</sup>, Erdmann Seeliger<sup>2</sup>, Marcel Prothmann<sup>3</sup>, Jeanette Schulz-Menger<sup>3</sup>, and Thoralf Niendorf<sup>1,4,5</sup>

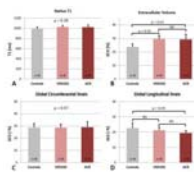
<sup>1</sup>Berlin Ultrahigh Field Facility (B.U.F.F.), Max Delbrück Center for Molecular Medicine in the Helmholtz Association(MDC), Berlin, Germany, <sup>2</sup>Institute for Physiology, Charité University Medicine, Berlin, Germany, <sup>3</sup>Working Group on Cardiovascular Magnetic Resonance, Experimental and Clinical Research Center, a joint cooperation between the Charité Medical Faculty and the Max Delbrück Center for Molecular Medicine in the Helmholtz Association, Berlin, Germany, <sup>4</sup>Experimental and Clinical Research Center, a joint cooperation between the, Charité Medical Faculty and the Max Delbrück Center for Molecular Medicine in the Helmholtz Association, Berlin, Germany, <sup>5</sup>DZHK (German Centre for Cardiovascular Research), partner site Berlin, Berlin, Germany

Ultrahigh field MR (UHF-MR) enables temporally resolved myocardial  $T_2^*$  mapping which benefits probing the myocardium at different physiological states. Myocardial BOLD contrast or  $T_2^*$  are commonly regarded as surrogates for myocardial tissue oxygenation, but the factors influencing  $T_2^*$  are manifold including cardiac macromorphology. Meaningful interpretation of myocardial  $T_2^*$  could be beneficial for understanding cardiac (patho)physiology in vivo, but requires careful identification of influential factors and their contributions to  $T_2^*$ . To this end, this study examines the relationship between myocardial  $T_2^*$  and myocardial wall thickness and investigates its capability to distinguish between healthy myocardium and myocardium affected by hypertrophic cardiomyopathy (HCM).

45



9:51



Myocardial extracellular volume expansion precedes functional myocardial alterations during the evolution of systemic sclerosis

Alexander Gotschy<sup>1,2</sup>, Constantin von Deuster<sup>1</sup>, Christian Stoeck<sup>1</sup>, Valeriy Vishnevskiy<sup>1</sup>, Lukas Wissmann<sup>1</sup>, Kerem Can Tezcan<sup>1</sup>, Markus Niemann<sup>3</sup>, Suzanna Jordan<sup>4</sup>, Britta Maurer<sup>4</sup>, Sebastian Kozerke<sup>1</sup>, Oliver Distler<sup>4</sup>, and Robert Manka<sup>2</sup>

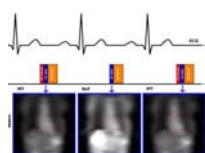
<sup>1</sup>Institute for Biomedical Engineering, University & ETH Zurich, Zurich, Switzerland, <sup>2</sup>Department of Cardiology, University Hospital Zurich, Zurich, Switzerland, <sup>3</sup>Faculty Mechanical and Medical Engineering, Furtwangen University, Schwenningen, Germany, <sup>4</sup>Department of Rheumatology, University Hospital Zurich, Zurich, Switzerland

Myocardial involvement is common in patients with systemic sclerosis and is known to cause myocardial fibrosis and subtle ventricular dysfunction. Both can be characterized by novel CMR methods like native T1-mapping, ECV quantification or LV deformation imaging. However, the temporal onset of myocardial fibrosis and functional impairment during the progression of the disease is still unknown. Therefore, we investigated the presence of subclinical functional and fibrotic myocardial involvement in patients with very early diagnosis of systemic sclerosis and found that the expansion of ECV can be detected before LV functional impairment, assessed by CMR feature tracking, can be observed.

46



10:03



Non-contrast free breathing and motion corrected 3D whole heart quantitative magnetization transfer imaging for assessment of myocardial fibrosis

Karina Lopez<sup>1</sup>, Radhouene Neji<sup>1,2</sup>, Rahul Mukherjee<sup>1</sup>, John Whitaker<sup>1</sup>, Reza Razavi<sup>1</sup>, Camila Muñoz<sup>1</sup>, Claudia Prieto<sup>1</sup>, Sebastien Roujol<sup>1</sup>, and Rene Botnar<sup>1</sup>

*<sup>1</sup>Division of Imaging Sciences and Biomedical Engineering, King's College London, London, United Kingdom, <sup>2</sup>MR Research Collaborations, Siemens Healthcare Limited, Frimley, United Kingdom*

We have developed a contrast-free free-breathing motion corrected (100% scan efficiency) 3D whole heart imaging technique for measurement of myocardial magnetization transfer ratio (MTR) maps. The sequence is based on the interleaved acquisition of MT weighted and non-MT weighted datasets and beat-to-beat rigid motion correction using 2D image navigators. Initial results in 4 healthy volunteers have shown good image quality, enabling the visualisation of the coronary arteries and MTR maps of healthy myocardium (MTR=41±7.2%). This approach promises higher sensitivity for measuring changes in macromolecule content associated with myocardial fibrosis than previous studies, justifying further investigation in a patient cohort.

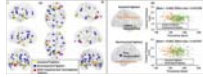
Oral

## White Matter & Connectivity in TBI

Room 313A

Monday 8:15 - 10:15

Moderators: Andre Obenaus & Sheng-Kwei Song

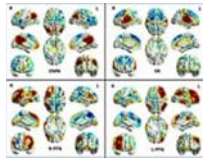


### Disrupted topological brain organizations in large-scale cortical networks between impaired and nonimpaired active fighters

Virendra Mishra<sup>1</sup>, Sarah Banks<sup>1</sup>, Charles Bernick<sup>1</sup>, and Dietmar Cordes<sup>1</sup>

<sup>1</sup>*Cleveland Clinic Lou Ruvo Center for Brain Health, Las Vegas, NV, United States*

Several MRI studies have shown structural differences in athletes with repetitive head trauma. However, whether coordinated variation exists in brain morphology of cognitively impaired-fighters is still unknown. Using graph-theoretical methods on inter-regional cortical thickness of impaired and nonimpaired fighters, we found alteration in the coordination of the large-scale structural brain-networks of impaired-fighters. The cortical thickness of regions identified as hubs showed a negative association with processing speed in impaired-fighters. Future studies will evaluate the role of network properties in predicting cognitive impairment in active fighters. Our study opens new avenues to understand impact of repetitive head trauma on brain organization.



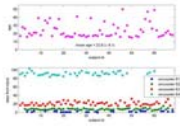
### Connectivity Domain Analysis of Mild Traumatic Brain Injury: A Multi-center Study to Extract Robust Imaging Biomarkers

Armin Irajji<sup>1</sup>, Jiachen Zhuo<sup>2</sup>, Natalie M. Wiseman<sup>3</sup>, Ali-Reza Mohammadi-Nejad<sup>4</sup>, Rao Gullapalli<sup>2</sup>, Zhifeng Kou<sup>1,5</sup>, and E. Mark Haacke<sup>1,5</sup>

<sup>1</sup>*Department of Biomedical Engineering, Wayne State University, Detroit, MI, United States*, <sup>2</sup>*Diagnostic Radiology and Nuclear Medicine, University of Maryland*, <sup>3</sup>*Department of Psychiatry and Behavioral Neurosciences, Wayne State University, Detroit, MI, United States*, <sup>4</sup>*Henry Ford Health System*, <sup>5</sup>*Department of Radiology, Wayne State University*

Identification of biomarkers for mild traumatic brain injury (mTBI) diagnosis and outcome prediction is challenging due to the heterogeneity of mTBI patients. Multi-center studies help to alleviate this, but functional MRI data can be difficult to combine across sites. Here, we applied our recent connectivity domain (CD) framework and identified predictive features of mTBI diagnosis and one-month outcome. Despite high heterogeneity of predictors between and within sites, classification accuracy did not suffer due to combination of datasets. Further multi-center analyses may benefit from use of the CD for generation of classification and outcome prediction models.

### Diffusion Kurtosis Imaging in mild TBI patients – a Longitudinal Study



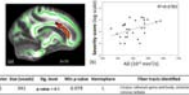
Jonathan I Sperl<sup>1</sup>, Xia Li<sup>2</sup>, Chitresh Bhushan<sup>2</sup>, Asha Singanamalli<sup>2</sup>, Ek T Tan<sup>2</sup>, Sumit N Niogi<sup>3</sup>, A. John Tsiouris<sup>3</sup>, Teena Shetty<sup>4</sup>, Pratik Mukherjee<sup>5</sup>, Joseph C Masdeu<sup>6</sup>, and Luca Marinelli<sup>2</sup>

<sup>1</sup>GE Global Research, Garching, Germany, <sup>2</sup>GE Global Research, Niskayuna, NY, United States, <sup>3</sup>Weill Cornell Medical Center, New York City, NY, United States, <sup>4</sup>Hospital for Special Surgery, New York City, NY, United States, <sup>5</sup>University of California, San Francisco, CA, United States, <sup>6</sup>Houston Methodist, Houston, TX, United States

Diffusion Kurtosis Imaging (DKI) allows for studying microscopic changes in human brain tissue. In traumatic brain injury (TBI), this may include axonal stretching, shearing, or swelling. Particularly in mild TBI cases, effects can be subtle and standard imaging modalities fail. We study DKI in 68 mild TBI patients with normal structural imaging in a series of four exams over a 90-day period. Using tract-based spatial statistics (TBSS) we observed increased kurtosis five to ten days post-injury followed by decreased kurtosis three months later. Diffusion tensor metrics such as fractional anisotropy in this study lack the sensitivity to track microstructural changes.

50

8:51



Acute white matter abnormalities in sport-related concussion: A DTI study

Sourajit Mitra Mustafi<sup>1,2</sup>, Jaroslaw Harezlak<sup>1,3</sup>, Kevin M Koch<sup>1,4</sup>, Andrew S Nencka<sup>1,4</sup>, Timothy B Meier<sup>1,4</sup>, Andrew J Saykin<sup>1,2</sup>, Micheal McCrea<sup>1,4</sup>, Thomas W McAllister<sup>1,5</sup>, and Yu-Chien Wu<sup>1,2</sup>

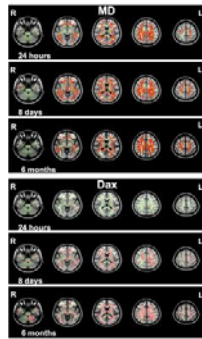
<sup>1</sup>Concussion Assessment, Research and Education (CARE) Consortium, Indianapolis, IN, United States, <sup>2</sup>Department of Radiology and Imaging Sciences, Indiana University, Indianapolis, IN, United States, <sup>3</sup>Department of Biostatistics, Indiana University, <sup>4</sup>The Medical College of Wisconsin, <sup>5</sup>Department of Psychiatry, Indiana University

In the present study, we use diffusion tensor imaging (DTI) to detect acute white matter alterations in football players after sport-related concussion. DTI scans were performed on 30 male football players who had acute concussion (24-48 hours post-injury). Another 28 matched contact-sport players were recruited as controls. Mean diffusivity (MD) increased significantly in concussive group compared to the contact-control group. Long fibers including corpus callosum, corona radiata, and longitudinal fasciculus were more vulnerable than the rest of the brain white matter. Within the concussed group, axial diffusivity (AD) demonstrated positive correlation with symptom severity indicating potential axonal changes/damage.

---

51

9:03



### Long Term Changes in White Matter Following Sport-Related Concussion Measured by Diffusion Kurtosis Tensor Imaging: 6 months follow up

L. Tugan Muftuler<sup>1</sup>, Daniel V. Olson<sup>2</sup>, Melissa A. Lancaster<sup>3</sup>, and Michael A. McCrea<sup>1</sup>

<sup>1</sup>Department of Neurosurgery, Medical College of Wisconsin, Milwaukee, WI, United States, <sup>2</sup>Department of Biophysics, Medical College of Wisconsin, Milwaukee, WI, United States, <sup>3</sup>Department of Psychiatry, Medical College of Wisconsin, Milwaukee, WI, United States

We investigated chronic white matter changes in high school and collegiate football players with history of sport-related concussion using diffusion kurtosis tensor imaging. Results demonstrated that the symptoms normalized after one week but, mean diffusivity remained significantly low in concussed football players. These findings have implications for determination of recovery following concussion.

---

52



9:15



### Diffusion Tensor Imaging Reveals Persistent Effects on White Matter Microstructure in High School Football Players with History of Sports-Related Concussion

Ikbeom Jang<sup>1</sup>, Yukai Zou<sup>2</sup>, Eric A Nauman<sup>2,3,4</sup>, and Thomas M Talavage<sup>1,2</sup>

<sup>1</sup>Electrical and Computer Engineering, Purdue University, West Lafayette, IN, United States, <sup>2</sup>Biomedical Engineering, Purdue University, <sup>3</sup>Mechanical Engineering, Purdue University, <sup>4</sup>Basic Medical Sciences, Purdue University

Diffusion Tensor Imaging has been considered a promising and sensitive imaging technology to detect subtle changes in white matter for people with mild traumatic brain injury. Although many studies have examined the immediate and near-term brain changes associated with sports-related concussions, the potential long-term consequences have been less-frequently investigated. In this study, a retrospective analysis was conducted on a subset of the Purdue Neurotrauma Group database to characterize the relationship between history of concussion and white matter diffusion properties.

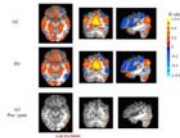
---

53

9:27

### Alterations in Brain Functional Connectivity and Global Cerebral Blood Flow in Collegiate Football Athletes over a Single Football Season





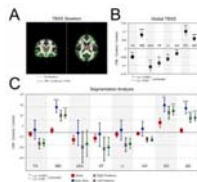
David C Zhu<sup>1</sup>, Peter Seidenberg<sup>2</sup>, Tim Bream<sup>2</sup>, Alexa Walter<sup>2</sup>, Xiaoxiao Bai<sup>2</sup>, Brian Johnson<sup>3</sup>, Hans Breiter<sup>4</sup>, Thomas M Talavage<sup>5</sup>, and Semyon Slobounov<sup>2</sup>

<sup>1</sup>Michigan State University, East Lansing, MI, United States, <sup>2</sup>Penn State University, University Park, PA, United States, <sup>3</sup>Philips Healthcare, <sup>4</sup>Northwestern University, Chicago, IL, United States, <sup>5</sup>Purdue University, West Lafayette, IN, United States

There has been growing concern over sports-related brain injuries and their long-term effects. However, the cumulative effect on the brain of sub-concussive hits is still poorly understood. Eighteen male collegiate student football athletes completed multi-modal MRI scans before and after a football season. We found significant changes of functional connectivity to the default-mode network, along with significant increase of cerebral blood flow both globally and at the postcentral gyrus. These changes point to the need for further investigation of the long-term development of brain networks in the presence of sub-concussive hits, and the potential relationship with brain vascular modification.

54

9:39



Combined DTI-derived metrics capture acute structural alterations in sports-related mild TBI (mTBI)

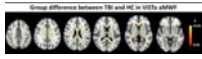
Arun Venkataraman<sup>1</sup>, Samuel B Tomlinson<sup>2</sup>, Steven Meyers<sup>3</sup>, Jeffrey J Bazarian<sup>4</sup>, and Jianhui Zhong<sup>5</sup>

<sup>1</sup>School of Medicine and Dentistry, University of Rochester, Rochester, NY, United States, <sup>2</sup>School of Medicine and Dentistry, University of Rochester, <sup>3</sup>Radiology, University of Rochester, <sup>4</sup>Neurology and Public Health, University of Rochester Medical Center, <sup>5</sup>Center for Brain Imaging, University of Rochester

Traumatic brain injury (TBI) is a source of considerable cost to society. Measures have been taken to increase awareness of possible injury, with safety precautions following suit. Despite this vigilance, the possibility of underdiagnosis is a reality. In this abstract, we seek to explain DTI-derived metrics and their application in the clinical setting. Tract based spatial statistics (TBSS), brain segmentation, and network analysis were applied to TBI and healthy cohorts to derive metrics that could aid in the diagnosis of mild TBI (mTBI), and provide a mechanism for quantification of severity and risk stratification.

9:51

Evaluation of Myelin Damage in Diffuse Traumatic Brain Injury using ViSTa-MWI



Joon Yul Choi<sup>1</sup>, Ji-Won Baek<sup>1</sup>, Jongho Lee<sup>1</sup>, and Junghoon Kim<sup>2,3</sup>

<sup>1</sup>Department of Electrical and Computer Engineering, Seoul National University, Seoul, Korea, Republic of, <sup>2</sup>CUNY School of Medicine, The City College of New York, New York, NY, United States, <sup>3</sup>Moss Rehabilitation Research Institute, Elkins Park, PA, United States

This study investigated myelin damage in subacute moderate to severe TBI using ViSTa-MWI. The results showed widespread reductions of MWF in patients, consistent with pathology involving diffuse axonal injury. Furthermore, the extent of myelin damage was strongly correlated with measures of injury severity and cognitive impairment, demonstrating its clinical relevance.

10:03

White matter changes and correlations with cognitive functions in semi-acute mild traumatic brain injury (mTBI): A hybrid diffusion imaging study

Sourajit Mitra Mustafi<sup>1</sup>, Chandana Kodiweera<sup>2</sup>, Jaroslaw Harezlak<sup>3</sup>, Laura A Flashman<sup>4</sup>, Thomas W McAllister<sup>5</sup>, and Yu-Chien Wu<sup>1</sup>

<sup>1</sup>Department of Radiology and Imaging Sciences, Indiana University School of Medicine, Indianapolis, IN, United States, <sup>2</sup>Department of Psychological and Brain Sciences, Dartmouth College, Lebanon, NH, United States, <sup>3</sup>Department of Biostatistics, Indiana University, Indianapolis, IN, United States, <sup>4</sup>Department of Psychiatry, Dartmouth Hitchcock Medical Center and New Hampshire Hospital, Lebanon, NH, United States, <sup>5</sup>Department of Psychiatry, Indiana University School of Medicine, Indianapolis, IN, United States

In the present study, we used multi-shell Hybrid Diffusion Imaging (HYDI) to study changes in white matter after mild traumatic brain injury (mTBI). From HYDI data, an array of diffusion metrics was computed including diffusion tensor imaging (DTI), neurite orientation distribution and density (NODDI), and return-to-origin ( $P_0$ ) of the q-space analysis. We study between group differences in diffusion metrics and within-group correlations with outcomes of cognitive functions. In addition, we tested the group effects (i.e., interaction or moderation) on the correlations between diffusion metrics and cognitive functions.

Oral

Tractography & Fiber Modeling



57



8:15



### A novel anatomy-based constrained global tractography

Achille Teillac<sup>1,2</sup>, Fabrice Poupon<sup>3</sup>, Jean-François Mangin<sup>3,4</sup>, and Cyril Poupon<sup>1,2</sup>

<sup>1</sup>Université Paris-Saclay, Orsay, France,

<sup>2</sup>CEA/DRF/I2BM/NeuroSpin/UNIRS, Gif-sur-Yvette, France,

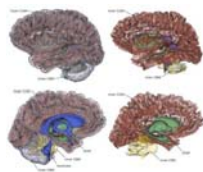
<sup>3</sup>CEA/DRF/I2BM/NeuroSpin/UNATI, Gif-sur-Yvette, France, <sup>4</sup><http://cati-neuroimaging.com/>, Orsay, France

Diffusion magnetic resonance imaging is still the unique tool capable of probe the structure of the brain connectivity in vivo. Although some great advances have been made in the past decade, reconstructed tractograms often lack of anatomically accuracy. The introduction of anatomical priors has become a promise land to tackle this issue, so in this work, we propose a general spin-glass-based global tractography framework constrained by anatomical priors to better represent the sharp turns of fibers entering a gyrus and connecting to the pial surface.

58



8:27

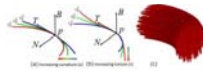


### Mesh-based anatomically-constrained tractography for effective tracking termination and structural connectome construction

Chun-Hung Yeh<sup>1</sup>, Robert Elton Smith<sup>1</sup>, Thijs Dhollander<sup>1</sup>, and Alan Connolly<sup>1,2</sup>

<sup>1</sup>The Florey Institute of Neuroscience and Mental Health, Melbourne, Australia, <sup>2</sup>The Florey Department of Neuroscience, University of Melbourne, Melbourne, Australia

This study introduces a novel diffusion MRI streamlines tractography framework called mesh-based anatomically-constrained tractography (MACT) that incorporates high-resolution surface models of various brain tissues as more accurate anatomical constraints in the fibre-tracking process. By detecting intersections between streamlines and tissue surfaces, MACT can effectively provide meaningful track terminations and inter-areal connections by associating streamlines with the structural labels of the intersected surfaces. This therefore minimises uncertainties caused by heuristic mechanisms of assigning streamlines to labelled structures in common image-based approaches. Methods that investigate the tractogram-based structural connectivity should benefit from the improved connectome reconstruction using the proposed technique.



## Topography preserving tractography for mapping human brain pathways

Dogu Baran Aydogan<sup>1</sup> and Yonggang Shi<sup>1</sup>

<sup>1</sup>Stevens Neuroimaging and Informatics Institute, University of Southern California, Los Angeles, CA, United States

Topographical organization is an integral property of brain's neural pathways. In this work we propose a novel approach to quantify the topographic preservation of fiber bundles obtained using dMRI based tractography. For that we used the well known organization of the somatosensory pathway. In our study we compared the tractograms obtained using our recently developed tractography algorithm with MRtrix's iFOD1 and iFOD2 probabilistic techniques. We believe topographical organization is critical to take into consideration for tractography research for both validation purposes as well as for developing better performing tractography algorithms.

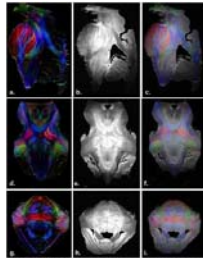


Figure 1. From left to right: Color-coded diffusion-weighted anatomical maps, and fibers of anatomical and color-coded directions maps in a sagittal (left), coronal (middle), and axial (right) view of the brainstem at 100µm isotropic.

## Characterization of the brainstem connectivity and its microstructure using diffusion MR microscopy at ultra-high field (UHF) with strong gradients

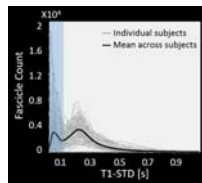
Justine Beaujoin<sup>1,2,3</sup>, Christophe Destrieux<sup>4</sup>, Jérémy Bernard<sup>1,3</sup>, Fabrice Poupon<sup>5</sup>, Jean-François Mangin<sup>2,3,6,7</sup>, and Cyril Poupon<sup>1,2,3,7</sup>

<sup>1</sup>UNIRS, CEA/I2BM/NeuroSpin, Gif-sur-Yvette, France, <sup>2</sup>Université Paris-Saclay, Orsay, France, <sup>3</sup>FLI / Noeud Paris-Sud, Orsay, France, <sup>4</sup>Laboratoire d'Anatomie, Faculté de Médecine/CHRU, Tours, France, <sup>5</sup>UNATI, CEA/I2BM/Neurospin, France, <sup>6</sup>CEA NeuroSpin / UNATI, Gif-sur-Yvette, France, <sup>7</sup><http://cati-neuroimaging.com/>, Gif-sur-Yvette, France

The brainstem is a crossroad of the major motor and sensitive pathways but its structure is challenging to image. In this work, we demonstrate that ultra-high field(11.7T) / ultra-high gradients(780mT/m) diffusion-weighted MRI and diffusion MRI microscopy enable to map not only its finer structures, but also its fine connectivity revealed by HARDI-based tractography with the mapping of the structural connectivity of the locus ceruleus. We also assessed the enhanced contrast brought by diffusion multicompartamental models such as NODDI that reveals the microstructure of the brainstem structures, thus allowing to go a step forward in the understanding of its anatomo-functional organization.

## Microstructure-Informed Tractography of the Human Optic Radiation In Vivo

61



Roey Schurr<sup>1</sup>, Yiran Duan<sup>2</sup>, Anthony M. Norcia<sup>2</sup>, Shumpei Ogawa<sup>3,4</sup>, Jason D. Yeatman<sup>5</sup>, and Aviv Mezer<sup>1</sup>

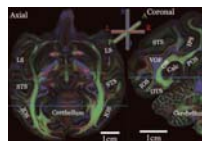
<sup>1</sup>Edmond and Lily Safra Center for Brain Sciences, Hebrew University of Jerusalem, Jerusalem, Israel, <sup>2</sup>Department of Psychology, Stanford University, CA, United States, <sup>3</sup>Department of Ophthalmology, Atsugi City Hospital, Kanagawa, Japan, <sup>4</sup>Department of Ophthalmology, The Jikei University School of Medicine, Tokyo, Japan, <sup>5</sup>Department of Speech & Hearing Sciences, University of Washington, Seattle, WA, United States

Accurate identification of the Optic Radiations (OR) in vivo has great clinical significance in pre-surgical planning. Yet traditional tractography algorithms based on diffusion MRI often fail to recover the full extent of the OR. Post-mortem histology studies show that the OR has a consistent signature of high myelination compared to adjacent white matter tracts. We therefore propose to use quantitative T1-mapping, which is sensitive to myelin, to eliminate candidate fascicles with highly variable T1 profiles. We introduce a fully automatic novel framework that integrates diffusion MRI with T1-mapping, and use it to reconstruct the OR in 62 healthy subjects.

62



9:15



Using diffusion MRI and tractography to identify macaque vertical occipital fasciculus

Hiromasa Takemura<sup>1,2</sup>, Franco Pestilli<sup>3</sup>, Kevin S Weiner<sup>4</sup>, Georgios A Keliris<sup>5,6</sup>, Sofia M Landi<sup>7</sup>, Julia Sliwa<sup>7</sup>, Frank Q Ye<sup>8</sup>, Michael A Barnett<sup>4</sup>, David A Leopold<sup>8</sup>, Winrich A Freiwald<sup>7</sup>, Nikos K Logothetis<sup>5</sup>, and Brian A Wandell<sup>4</sup>

<sup>1</sup>Center for Information and Neural Networks (CiNet), National Institute of Information and Communications Technology, Suita-shi, Japan, <sup>2</sup>Graduate School of Frontier Biosciences, Osaka University, Suita-shi, Japan, <sup>3</sup>Department of Psychological and Brain Sciences, Indiana University, Bloomington, IN, United States, <sup>4</sup>Department of Psychology, Stanford University, Stanford, CA, United States, <sup>5</sup>Max Planck Institute for Biological Cybernetics, Tübingen, Germany, <sup>6</sup>Department of Biomedical Science, University of Antwerp, Antwerp, Belgium, <sup>7</sup>The Rockefeller University, New York, NY, United States, <sup>8</sup>Neurophysiology Imaging Facility, National Institute of Mental Health, National Institute of Neurological Disorders and Stroke, National Eye Institute, National Institutes of Health, Bethesda, MD, United States

We evaluated the ability of diffusion MRI-based tractography to identify macaque vertical occipital fasciculus (VOF), an important but little-studied white-matter tract connecting dorsal and ventral visual cortex. We analyzed four macaque diffusion MRI datasets with different resolution. The high-resolution post-mortem dataset reliably detects the macaque VOF, in a consistent manner with previous invasive anatomical studies. Lower resolution in vivo data showed qualitatively consistent results, but the estimated tract endpoints are restricted to sulcus. Taken together, our results demonstrate that the need for high-resolution diffusion MRI to identify certain critical white matter tracts.



Table 1. Diffusion MRI datasets and algorithms for comparison

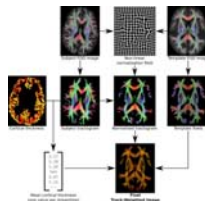
Diffusion MRI dataset	Main subject			
	Resolution	Post-mortem	In vivo	In vivo
VOF post-mortem dataset	0.5 mm	0.5 mm	0.5 mm	0.5 mm
VOF in vivo dataset	1.5 mm	1.5 mm	1.5 mm	1.5 mm
VOF in vivo dataset	3.0 mm	3.0 mm	3.0 mm	3.0 mm
VOF in vivo dataset	6.0 mm	6.0 mm	6.0 mm	6.0 mm
VOF in vivo dataset	12.0 mm	12.0 mm	12.0 mm	12.0 mm
VOF in vivo dataset	24.0 mm	24.0 mm	24.0 mm	24.0 mm
VOF in vivo dataset	48.0 mm	48.0 mm	48.0 mm	48.0 mm
VOF in vivo dataset	96.0 mm	96.0 mm	96.0 mm	96.0 mm
VOF in vivo dataset	192.0 mm	192.0 mm	192.0 mm	192.0 mm
VOF in vivo dataset	384.0 mm	384.0 mm	384.0 mm	384.0 mm
VOF in vivo dataset	768.0 mm	768.0 mm	768.0 mm	768.0 mm
VOF in vivo dataset	1536.0 mm	1536.0 mm	1536.0 mm	1536.0 mm
VOF in vivo dataset	3072.0 mm	3072.0 mm	3072.0 mm	3072.0 mm
VOF in vivo dataset	6144.0 mm	6144.0 mm	6144.0 mm	6144.0 mm
VOF in vivo dataset	12288.0 mm	12288.0 mm	12288.0 mm	12288.0 mm
VOF in vivo dataset	24576.0 mm	24576.0 mm	24576.0 mm	24576.0 mm
VOF in vivo dataset	49152.0 mm	49152.0 mm	49152.0 mm	49152.0 mm
VOF in vivo dataset	98304.0 mm	98304.0 mm	98304.0 mm	98304.0 mm
VOF in vivo dataset	196608.0 mm	196608.0 mm	196608.0 mm	196608.0 mm
VOF in vivo dataset	393216.0 mm	393216.0 mm	393216.0 mm	393216.0 mm
VOF in vivo dataset	786432.0 mm	786432.0 mm	786432.0 mm	786432.0 mm
VOF in vivo dataset	1572864.0 mm	1572864.0 mm	1572864.0 mm	1572864.0 mm
VOF in vivo dataset	3145728.0 mm	3145728.0 mm	3145728.0 mm	3145728.0 mm
VOF in vivo dataset	6291456.0 mm	6291456.0 mm	6291456.0 mm	6291456.0 mm
VOF in vivo dataset	12582912.0 mm	12582912.0 mm	12582912.0 mm	12582912.0 mm
VOF in vivo dataset	25165824.0 mm	25165824.0 mm	25165824.0 mm	25165824.0 mm
VOF in vivo dataset	50331648.0 mm	50331648.0 mm	50331648.0 mm	50331648.0 mm
VOF in vivo dataset	100663296.0 mm	100663296.0 mm	100663296.0 mm	100663296.0 mm
VOF in vivo dataset	201326592.0 mm	201326592.0 mm	201326592.0 mm	201326592.0 mm
VOF in vivo dataset	402653184.0 mm	402653184.0 mm	402653184.0 mm	402653184.0 mm
VOF in vivo dataset	805306368.0 mm	805306368.0 mm	805306368.0 mm	805306368.0 mm
VOF in vivo dataset	1610612736.0 mm	1610612736.0 mm	1610612736.0 mm	1610612736.0 mm
VOF in vivo dataset	3221225472.0 mm	3221225472.0 mm	3221225472.0 mm	3221225472.0 mm
VOF in vivo dataset	6442450944.0 mm	6442450944.0 mm	6442450944.0 mm	6442450944.0 mm
VOF in vivo dataset	12884901888.0 mm	12884901888.0 mm	12884901888.0 mm	12884901888.0 mm
VOF in vivo dataset	25769803776.0 mm	25769803776.0 mm	25769803776.0 mm	25769803776.0 mm
VOF in vivo dataset	51539607552.0 mm	51539607552.0 mm	51539607552.0 mm	51539607552.0 mm
VOF in vivo dataset	103079215104.0 mm	103079215104.0 mm	103079215104.0 mm	103079215104.0 mm
VOF in vivo dataset	206158430208.0 mm	206158430208.0 mm	206158430208.0 mm	206158430208.0 mm
VOF in vivo dataset	412316860416.0 mm	412316860416.0 mm	412316860416.0 mm	412316860416.0 mm
VOF in vivo dataset	824633720832.0 mm	824633720832.0 mm	824633720832.0 mm	824633720832.0 mm
VOF in vivo dataset	1649267441664.0 mm	1649267441664.0 mm	1649267441664.0 mm	1649267441664.0 mm
VOF in vivo dataset	3298534883328.0 mm	3298534883328.0 mm	3298534883328.0 mm	3298534883328.0 mm
VOF in vivo dataset	6597069766656.0 mm	6597069766656.0 mm	6597069766656.0 mm	6597069766656.0 mm
VOF in vivo dataset	13194139533312.0 mm	13194139533312.0 mm	13194139533312.0 mm	13194139533312.0 mm
VOF in vivo dataset	26388279066624.0 mm	26388279066624.0 mm	26388279066624.0 mm	26388279066624.0 mm
VOF in vivo dataset	52776558133248.0 mm	52776558133248.0 mm	52776558133248.0 mm	52776558133248.0 mm
VOF in vivo dataset	105553116266496.0 mm	105553116266496.0 mm	105553116266496.0 mm	105553116266496.0 mm
VOF in vivo dataset	211106232532992.0 mm	211106232532992.0 mm	211106232532992.0 mm	211106232532992.0 mm
VOF in vivo dataset	422212465065984.0 mm	422212465065984.0 mm	422212465065984.0 mm	422212465065984.0 mm
VOF in vivo dataset	844424930131968.0 mm	844424930131968.0 mm	844424930131968.0 mm	844424930131968.0 mm
VOF in vivo dataset	1688849860263936.0 mm	1688849860263936.0 mm	1688849860263936.0 mm	1688849860263936.0 mm
VOF in vivo dataset	3377699720527872.0 mm	3377699720527872.0 mm	3377699720527872.0 mm	3377699720527872.0 mm
VOF in vivo dataset	6755399441055744.0 mm	6755399441055744.0 mm	6755399441055744.0 mm	6755399441055744.0 mm
VOF in vivo dataset	13510798882111488.0 mm	13510798882111488.0 mm	13510798882111488.0 mm	13510798882111488.0 mm
VOF in vivo dataset	27021597764222976.0 mm	27021597764222976.0 mm	27021597764222976.0 mm	27021597764222976.0 mm
VOF in vivo dataset	54043195528445952.0 mm	54043195528445952.0 mm	54043195528445952.0 mm	54043195528445952.0 mm
VOF in vivo dataset	108086391056891904.0 mm	108086391056891904.0 mm	108086391056891904.0 mm	108086391056891904.0 mm
VOF in vivo dataset	216172782113783808.0 mm	216172782113783808.0 mm	216172782113783808.0 mm	216172782113783808.0 mm
VOF in vivo dataset	432345564227567616.0 mm	432345564227567616.0 mm	432345564227567616.0 mm	432345564227567616.0 mm
VOF in vivo dataset	864691128455135232.0 mm	864691128455135232.0 mm	864691128455135232.0 mm	864691128455135232.0 mm
VOF in vivo dataset	1729382256910270464.0 mm	1729382256910270464.0 mm	1729382256910270464.0 mm	1729382256910270464.0 mm
VOF in vivo dataset	3458764513820540928.0 mm	3458764513820540928.0 mm	3458764513820540928.0 mm	3458764513820540928.0 mm
VOF in vivo dataset	6917529027641081856.0 mm	6917529027641081856.0 mm	6917529027641081856.0 mm	6917529027641081856.0 mm
VOF in vivo dataset	13835058055282163136.0 mm	13835058055282163136.0 mm	13835058055282163136.0 mm	13835058055282163136.0 mm
VOF in vivo dataset	27670116110564326272.0 mm	27670116110564326272.0 mm	27670116110564326272.0 mm	27670116110564326272.0 mm
VOF in vivo dataset	55340232221128652544.0 mm	55340232221128652544.0 mm	55340232221128652544.0 mm	55340232221128652544.0 mm
VOF in vivo dataset	110680464442257305088.0 mm	110680464442257305088.0 mm	110680464442257305088.0 mm	110680464442257305088.0 mm
VOF in vivo dataset	221360928884514610176.0 mm	221360928884514610176.0 mm	221360928884514610176.0 mm	221360928884514610176.0 mm
VOF in vivo dataset	442721857769029220352.0 mm	442721857769029220352.0 mm	442721857769029220352.0 mm	442721857769029220352.0 mm
VOF in vivo dataset	885443715538058440704.0 mm	885443715538058440704.0 mm	885443715538058440704.0 mm	885443715538058440704.0 mm
VOF in vivo dataset	1770887431076116881408.0 mm	1770887431076116881408.0 mm	1770887431076116881408.0 mm	1770887431076116881408.0 mm
VOF in vivo dataset	3541774862152233762816.0 mm	3541774862152233762816.0 mm	3541774862152233762816.0 mm	3541774862152233762816.0 mm
VOF in vivo dataset	7083549724304467525632.0 mm	7083549724304467525632.0 mm	7083549724304467525632.0 mm	7083549724304467525632.0 mm
VOF in vivo dataset	14167099448608935101264.0 mm	14167099448608935101264.0 mm	14167099448608935101264.0 mm	14167099448608935101264.0 mm
VOF in vivo dataset	28334198897217870202528.0 mm	28334198897217870202528.0 mm	28334198897217870202528.0 mm	28334198897217870202528.0 mm
VOF in vivo dataset	56668397794435740405056.0 mm	56668397794435740405056.0 mm	56668397794435740405056.0 mm	56668397794435740405056.0 mm
VOF in vivo dataset	113336795588871481610112.0 mm	113336795588871481610112.0 mm	113336795588871481610112.0 mm	113336795588871481610112.0 mm
VOF in vivo dataset	226673591177742963220224.0 mm	226673591177742963220224.0 mm	226673591177742963220224.0 mm	226673591177742963220224.0 mm
VOF in vivo dataset	453347182355485926440448.0 mm	453347182355485926440448.0 mm	453347182355485926440448.0 mm	453347182355485926440448.0 mm
VOF in vivo dataset	906694364710971851880896.0 mm	906694364710971851880896.0 mm	906694364710971851880896.0 mm	906694364710971851880896.0 mm
VOF in vivo dataset	1813388729421943703761792.0 mm	1813388729421943703761792.0 mm	1813388729421943703761792.0 mm	1813388729421943703761792.0 mm
VOF in vivo dataset	3626777458843887407523584.0 mm	3626777458843887407523584.0 mm	3626777458843887407523584.0 mm	3626777458843887407523584.0 mm
VOF in vivo dataset	7253554917687774815047168.0 mm	7253554917687774815047168.0 mm	7253554917687774815047168.0 mm	7253554917687774815047168.0 mm
VOF in vivo dataset	14507109835375549630094336.0 mm	14507109835375549630094336.0 mm	14507109835375549630094336.0 mm	14507109835375549630094336.0 mm
VOF in vivo dataset	29014219670751099260188672.0 mm	29014219670751099260188672.0 mm	29014219670751099260188672.0 mm	29014219670751099260188672.0 mm
VOF in vivo dataset	58028439341502198520377344.0 mm	58028439341502198520377344.0 mm	58028439341502198520377344.0 mm	58028439341502198520377344.0 mm
VOF in vivo dataset	116056878683004397040754688.0 mm	116056878683004397040754688.0 mm	116056878683004397040754688.0 mm	116056878683004397040754688.0 mm
VOF in vivo dataset	232113757366008794081513776.0 mm	232113757366008794081513776.0 mm	232113757366008794081513776.0 mm	232113757366008794081513776.0 mm
VOF in vivo dataset	464227514732017588162827552.0 mm	464227514732017588162827552.0 mm	464227514732017588162827552.0 mm	464227514732017588162827552.0 mm
VOF in vivo dataset	92845502946403517632565504.0 mm	92845502946403517632565504.0 mm	92845502946403517632565504.0 mm	92845502946403517632565504.0 mm
VOF in vivo dataset	185691005892807035265131008.0 mm	185691005892807035265131008.0 mm	185691005892807035265131008.0 mm	185691005892807035265131008.0 mm
VOF in vivo dataset	371382011785614070530262016.0 mm	371382011785614070530262016.0 mm	371382011785614070530262016.0 mm	371382011785614070530262016.0 mm
VOF in vivo dataset	742764023571228141066054032.0 mm	742764023571228141066054032.0 mm	742764023571228141066054032.0 mm	742764023571228141066054032.0 mm
VOF in vivo dataset	1485528047142562821332108064.0 mm	1485528047142562821332108064.0 mm	1485528047142562821332108064.0 mm	1485528047142562821332108064.0 mm
VOF in vivo dataset	2971056094285125642664216128.0 mm	2971056094285125642664216128.0 mm	2971056094285125642664216128.0 mm	2971056094285125642664216128.0 mm
VOF in vivo dataset	5942112188570251284528432256.0 mm	5942112188570251284528432256.0 mm	5942112188570251284528432256.0 mm	5942112188570251284528432256.0 mm
VOF in vivo dataset	1188422437714050257056864512.0 mm	1188422437714050257056864512.0 mm	1188422437714050257056864512.0 mm	1188422437714050257056864512.0 mm
VOF in vivo dataset	2376844875428100514113729024.0 mm	2376844875428100514113729024.0 mm	2376844875428100514113729024.0 mm	2376844875428100514113729024.0 mm
VOF in vivo dataset	4753689750856201022827458048.0 mm	4753689750856201022827458048.0 mm	4753689750856201022827458048.0 mm	4753689750856201022827458048.0 mm
VOF in vivo dataset	9507379501712402045654916096.0 mm	9507379501712402045654916096.0 mm	9507379501712402045654916096.0 mm	9507379501712402045654916096.0 mm
VOF in vivo dataset	19014759003424804091309832192.0 mm	19014759003424804091309832192.0 mm	19014759003424804091309832192.0 mm	19014759003424804091309832192.0 mm
VOF in vivo dataset	38029518006849608182619664384.0 mm	38029518006849608182619664384.0 mm	38029518006849608182619664384.0 mm	38029518006849608182619664384.0 mm

Multi-shell, multi-tissue (MSMT) constrained spherical deconvolution (CSD) allows precise white matter tract reconstructions in healthy brains. However, its implications for connectivity mapping in multiple sclerosis (MS) are unknown. Here we compare MSMT-CSD versus single-shell single-tissue (SSST)-CSD algorithms over different clinically-feasible diffusion-weighted protocols regarding their ability to reconstruct connectivity metrics that distinguish patients with a first inflammatory-demyelinating episode (n=19) from controls (n=12). Methodical analysis of data from time- and directionality-matched protocols showed that a greater angular resolution improves results and is preferable to choosing multi-tissue-CSD algorithms. Given similar angular resolution, all algorithms perform similarly, producing highly reproducible brain connectivity metrics.

64



9:39



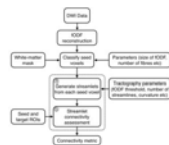
**Toward interrogating relationships between grey and white matter measures using Fixel Track-Weighted Imaging and Fixel-Based Analysis**  
 Robert E Smith<sup>1</sup>, David Raffelt<sup>1</sup>, David N Vaughan<sup>1,2</sup>, Fernando Calamante<sup>1,3</sup>, and Alan Connelly<sup>1,3</sup>

<sup>1</sup>The Florey Institute of Neuroscience and Mental Health, Heidelberg, Australia, <sup>2</sup>Department of Neurology, Austin Health, Melbourne, Australia, <sup>3</sup>Department of Medicine (AH/NH), The University of Melbourne, Australia

Neuroimaging studies assessing white and grey matter are most typically performed as independent analyses. The relationships between white and grey matter abnormalities are therefore poorly understood. We present a novel framework for interrogating relationships between quantitative measures derived from grey matter analysis, and diffusion MRI-based, fibre-specific white matter measures.

65

9:51



**Streamlet Tractography**  
 Matthew George Liptrot<sup>1,2</sup>, Sune Darkner<sup>1</sup>, Aasa Feragen<sup>1</sup>, and Francois Lauze<sup>1</sup>

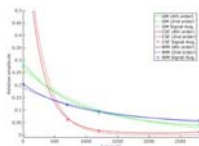
<sup>1</sup>Department of Computer Science, University of Copenhagen, Copenhagen, Denmark, <sup>2</sup>Department of Applied Mathematics and Computer Science, Technical University of Denmark, Lyngby, Denmark

Streamlet tractography is a novel approach that aims to combine the benefits of both streamline and global tractography approaches. In contrast to requiring individual streamlines to successfully propagate from seed to target regions to register as a connection, here short streamlines - streamlets - are initially generated from each white-matter voxel, and then seed-to-target connectivity is assessed by evaluating connectivity between these streamlets. In this way, streamlet generation can adapt to the local environment, whilst seed-to-target connectivity is assessed at the global level. Furthermore, the proposed framework permits the inclusion of previous results and alternative data sources.

66



10:03



Spherical Deconvolution of Non-Spherically Sampled Diffusion MRI Data  
Jan Morez<sup>1</sup>, Jan Sijbers<sup>1</sup>, and Ben Jeurissen<sup>1</sup>

<sup>1</sup>Vision Lab, Dept. of Physics, University of Antwerp, Antwerp, Belgium

Multi-tissue spherical deconvolution of multi-shell diffusion MRI data allows for simultaneous estimation of the white matter fiber orientation distribution function and the apparent densities of cerebrospinal fluid and grey matter. Current spherical deconvolution approaches require that the q-space samples are distributed across shells. Here we propose a new algorithm that allows one to perform spherical deconvolution on data obtained with non-spherical sampling schemes. The algorithm is demonstrated on real data with both spherical and cartesian sampling schemes.

Oral

## Relaxation Methods

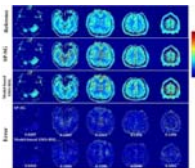
Room 314

Monday 8:15 - 10:15

Moderators: Charles Springer, Jr. & Pinar Özbay

67

8:15



Accelerated MR Parameter Mapping Exploiting Model-Based Simultaneous Multi-Slice Reconstruction with Hankel Subspace Learning: Application to T1 Quantification

Sugil Kim<sup>1,2</sup>, Suhyung Park<sup>2</sup>, and Jaeseok Park<sup>2</sup>



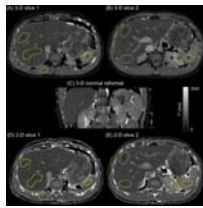
<sup>1</sup>Department of Brain and Cognitive Engineering, Korea University, Seoul, Korea, Republic of, <sup>2</sup>Biomedical Imaging and Engineering Lab, Department of Biomedical Engineering, Sungkyunkwan University, Suwon, Korea, Republic of

MR parameter mapping has been potentially of great value in diagnosing pathological diseases, but is difficult to be translated to clinical applications due to prohibitively long imaging time. It was recently shown in [1-4] that simultaneous multi-slice (SMS) imaging is highly efficient in reducing imaging time while well maintaining SNR. In this work, we propose a novel, model-based SMS reconstruction approach with Hankel subspace learning (Model-based SMS-HSL) for highly accelerated MR parameter mapping under the hypothesis that the null space in the spatial dimension, which filters out slices of no interest, is time-invariant in the parameter dimension while the dimension of temporal basis, which is found from signal evolution models, is limited.

---

68

8:27



### Single Breath-hold Abdominal T<sub>1</sub> Mapping using 3-D Cartesian Sampling and Spatiotemporally Constrained Reconstruction

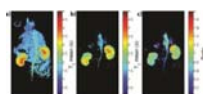
Felix Lugauer<sup>1</sup>, Jens Wetzl<sup>1</sup>, Christoph Forman<sup>2</sup>, Manuel Schneider<sup>1</sup>, Berthold Kiefer<sup>2</sup>, Dominik Nickel<sup>2</sup>, and Andreas Maier<sup>1</sup>

<sup>1</sup>Pattern Recognition Lab, Department of Computer Science, Friedrich-Alexander-Universität Erlangen-Nürnberg, Erlangen, Germany, <sup>2</sup>MR Applications Predevelopment, Siemens Healthcare GmbH, Erlangen, Germany

Volumetric T<sub>1</sub> mapping in the abdomen is desirable for whole liver assessment of hepatic diseases. In case of breath-hold imaging, accurate but time-consuming methods that sample the relaxation curve (IR or Look-Locker) are restricted to few slices only. To address these limitations, sparse Cartesian sampling with spatiotemporal incoherence is utilized to render 3-D Look-Locker within a single breath-hold possible. We demonstrate feasibility in both phantom and in-vivo measurements. The proposed method shows high agreement with a 2-D reference acquisition and enables an accurate mapping for a wide T<sub>1</sub> range, including very low values due to its high temporal resolution.

---

8:39



### Accelerating High Resolution Hyperpolarized <sup>13</sup>C T<sub>2</sub> Mapping Using a Local Low Rank plus Sparse Reconstruction

Eugene Milshteyn<sup>1,2</sup>, Galen D. Reed<sup>3</sup>, Cornelius von Morze<sup>1</sup>, Zihan Zhu<sup>1,2</sup>, Jeremy W. Gordon<sup>1</sup>, and Daniel B. Vigneron<sup>1,2</sup>

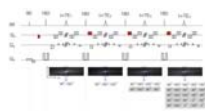


<sup>1</sup>Radiology and Biomedical Imaging, UCSF, San Francisco, CA, United States, <sup>2</sup>UC Berkeley-UCSF Graduate Program in Bioengineering, UCSF and University of California, Berkeley, San Francisco, CA, United States, <sup>3</sup>HeartVista Inc., Los Altos, CA, United States

Hyperpolarized <sup>13</sup>C probe development has allowed *in vivo* monitoring of different physiological processes relating to various diseases, including cancer and diabetes. Each new probe is typically characterized with polarization and T<sub>1</sub> measurements, but T<sub>2</sub> is also an important parameter for optimal sequence design, including progressive flip angle schemes. To improve the spatiotemporal resolution of T<sub>2</sub> mapping sequences and subsequent multi-exponential analysis, this project investigated using a local low rank plus sparse reconstruction for 2-fold acceleration of *in vivo* T<sub>2</sub> mapping with the bSSFP sequence.



8:51



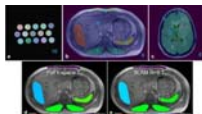
Ultrafast T2 mapping using echo-split GRASE acquisition and parametric POCSMUSE reconstruction

Mei-Lan Chu<sup>1,2</sup>, Hing-Chiu Chang<sup>3</sup>, Koichi Oshio<sup>4</sup>, and Nan-kuei Chen<sup>1,2</sup>

<sup>1</sup>Department of Biomedical Engineering, University of Arizona, Tucson, AZ, United States, <sup>2</sup>Brain Imaging and Analysis Center, Duke University Medical Center, Durham, NC, United States, <sup>3</sup>Department of Diagnostic Radiology, The University of Hong Kong, Hong Kong, <sup>4</sup>Department of Diagnostic Radiology, Keio University School of Medicine, Japan

Our novel ultrafast T2 mapping framework, which uniquely integrates echo-split GRASE acquisition and parametric POCSMUSE reconstruction, has the following major advantages. First, parametric T2 map and high-quality multi-contrast images can be derived from a single set of single-shot GRASE data, with inherently low susceptibility to motion artifacts. Second, contamination of stimulated and other high order echoes is minimized in the echo-split GRASE scans. Third, T2 relaxation times can be accurately measured by the parametric POCSMUSE algorithm, which incorporates multiplexed parallel MR reconstruction and multi-echo-pathway signal modeling into a unified procedure.

9:03



Ultrafast compartmental relaxation time mapping with linear algebraic modeling

Yi Zhang<sup>1</sup>, Xiaoyang Liu<sup>1,2</sup>, Jinyuan Zhou<sup>1,3</sup>, and Paul A. Bottomley<sup>1</sup>

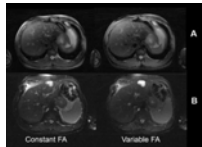


<sup>1</sup>Division of MR Research, Department of Radiology, Johns Hopkins University, Baltimore, MD, United States, <sup>2</sup>Department of Electrical and Computer Engineering, Baltimore, MD, United States, <sup>3</sup>F. M. Kirby Research Center for Functional Brain Imaging, Kennedy Krieger Institute, Baltimore, MD, United States

Image contrast afforded by tissue longitudinal ( $T_1$ ) and transverse ( $T_2$ ) relaxation times is central to the success of modern MRI. Here, a recently-proposed 'spectroscopy with linear algebraic modeling' (SLAM) method is adapted to dramatically accelerate relaxation time imaging at 3 Tesla in phantoms, the abdomens of six volunteers and in six brain tumor patients. SLAM is validated by omitting up to 15/16<sup>ths</sup> (94%) of the data acquired retroactively from inversion recovery and multi-echo spin-echo sequences, and proactively applied to accelerate abdominal and brain tumor  $T_1$  and  $T_2$  measurements by up to 16-fold in humans.

72

9:15



### Variable Flip Angle Radial Turbo Spin Echo Technique for Abdominal T2 Mapping

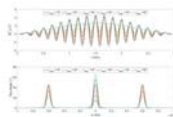
Mahesh Bharath Keerthivasan<sup>1</sup>, Manojkumar Saranathan<sup>2</sup>, Jean-Philippe Galons<sup>2</sup>, Diego R Martin<sup>2</sup>, Ali Bilgin<sup>1,2</sup>, and Maria Altbach<sup>2</sup>

<sup>1</sup>Electrical and Computer Engineering, University of Arizona, Tucson, AZ, United States, <sup>2</sup>Medical Imaging, University of Arizona, Tucson, AZ, United States

The estimation of T2 relaxation times within lesions can provide a quantitative method of classifying abdominal neoplasms. Accelerated T2 mapping approaches have been proposed using the Radial TSE (RADTSE) sequence, where high resolution images at multiple TEs are reconstructed from data acquired in a single breath hold. However, the slice coverage for TSE based breath-held imaging is SAR restricted, motivating the need to reduce the refocusing flip angle. We present a variable refocusing flip angle RADTSE sequence designed to optimize the signal evolution for T2 mapping in the abdomen with reduced SAR, thereby increasing the slice coverage.

73

9:27



### Robust VFA relaxometry by Continuous Saturation of Magnetization Transfer (CSMT) effects with Non-selective Multi-Band pulses.

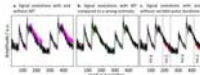
Rui Pedro A. G. Teixeira<sup>1,2</sup>, Anthony N. Price<sup>1,2</sup>, Ana A. Baburamani<sup>1</sup>, Shaihan J. Malik<sup>1</sup>, and Joseph V. Hajnal<sup>1,2</sup>

*<sup>1</sup>Imaging Sciences and Biomedical Engineering, King's College London, London, United Kingdom, <sup>2</sup>Centre for the Developing Brain, King's College London, London, United Kingdom*

Variable Flip Angle (VFA) relaxometry methods have recently been shown to be sensitive to magnetization transfer (MT) induced bias. Common description of this effect relies on a two-pool model (restricted macromolecular pool & visible free water pool). Current practice to restrict influence of MT consists in stretching of RF pulse durations in order to minimize/counter-balance the effect of macromolecular exchange for different flip angle measurements. This work proposes to minimize the estimation bias by using constant saturation MT pulses that simultaneously excite the free-water pool and saturate the restricted-pool creating constant RF-saturation conditions independently of the flip angle (FA) applied.

74

9:39



### Mitigating the Effect of Magnetization Transfer in Magnetic Resonance Fingerprinting

Tom Hilbert<sup>1,2,3</sup>, Tobias Kober<sup>1,2,3</sup>, Tiejun Zhao<sup>4</sup>, Tobias Kai Block<sup>5,6</sup>, Zidan Yu<sup>5,6</sup>, Jean-Philippe Thiran<sup>3</sup>, Gunnar Krueger<sup>2,3,7</sup>, Daniel K Sodickson<sup>5,6</sup>, and Martijn Cloos<sup>5,6</sup>

*<sup>1</sup>Advanced Clinical Imaging Technology, Siemens Healthcare AG, Lausanne, Switzerland, <sup>2</sup>Department of Radiology, University Hospital (CHUV), Lausanne, Switzerland, <sup>3</sup>LTS5, École Polytechnique Fédérale de Lausanne, Lausanne, Switzerland, <sup>4</sup>Siemens Medical Solution USA, Pittsburgh, PA, United States, <sup>5</sup>New York University School of Medicine, Bernard and Irene Schwartz Center for Biomedical Imaging, Department of Radiology, New York, NY, United States, <sup>6</sup>Center for Advanced Imaging Innovation and Research (CAI2R), Department of Radiology, New York University School of Medicine, New York, NY, United States, <sup>7</sup>Siemens Medical Solutions USA, Inc., Boston, MA, United States*

Magnetic Resonance Fingerprinting (MRF) is a powerful technique for the quantification of relaxation parameters, and ideally provides correct estimates independent from the sequence used. In this work, we show that the quantification can be influenced by the pulse duration or, equivalently, the pulse bandwidth. This behavior, which we hypothesize to be related to magnetization transfer (MT) effects, is shown for the PnP-MRF sequence. We propose a first approach to encode MT effects in the MRF sequence and to model MT effects in the reconstruction, showing that this mitigates the bias in the resulting relaxation estimates.

---

75

9:51



Clinically viable FAST-T2 based whole brain myelin water content mapping: T1 validation and initial MS lesion study

Thanh D. Nguyen<sup>1</sup>, Yihao Yao<sup>1</sup>, Pascal Spincemaille<sup>1</sup>, Eric Morris<sup>2</sup>, Susan A. Gauthier<sup>2</sup>, and Yi Wang<sup>1</sup>

<sup>1</sup>Radiology, Weill Cornell Medical College, New York, NY, United States,

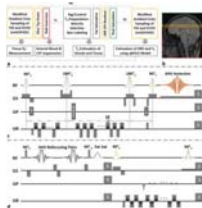
<sup>2</sup>Neurology, Weill Cornell Medical College, New York, NY, United States

The objectives of this study were to validate the accuracy of FAST-T1 mapping required for myelin water content (MWC) mapping, and to demonstrate the feasibility of fast MWC mapping in MS patients. FAST-T1 provides whole brain T1 map in 3 min, which was in excellent agreement with that obtained with the reference IR-FSE method. MWC mapping in 20 MS patients showed a consistent increase in water content in MS lesions (10.7% on average), accompanied by 62.8% increase in T1 and 44.6% decrease in MWC when compared to the contralateral NAWM.

---

76

10:03



Quantitative BOLD With Interleaved Acquisitions for Estimation of Extravascular  $R_2'$  and Intravascular  $R_2$  With Phase-Sensitive CSF Suppression

Hyunyeol Lee<sup>1</sup>, Cheng Li<sup>1</sup>, Erin K. Englund<sup>1</sup>, and Felix W. Wehrli<sup>1</sup>

<sup>1</sup>Radiology, University of Pennsylvania, Philadelphia, PA, United States

In the qBOLD technique, the accuracy of local deoxygenated blood volume and hemoglobin oxygen saturation ( $Y_v$ ) maps is potentially degraded due to high coupling of the two parameters in the model. As an alternative, the QUIXOTIC method measures local  $Y_v$  by selectively capturing venular spins via  $T_2$ -prepared velocity-selective-spin-labeling. However, CSF signals, if not suppressed, may impair accuracy of venular blood  $T_2$  estimation. In this work, extravascular  $R_2'$  and intravascular  $R_2$  mapping methods are interleaved to reduce estimation uncertainty in the qBOLD model while the accuracy of preliminary venular  $T_2$  estimates from the latter is further enhanced via phase-sensitive CSF suppression.

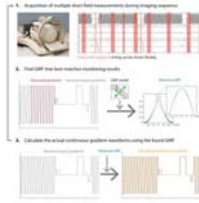
---

Oral

## System Imperfections: Measurement & Correction

77

8:15

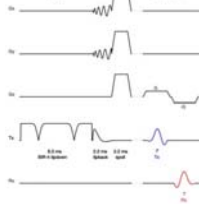
**Model-based Gradient Impulse Response Harvesting**Bertram Jakob Wilm<sup>1</sup>, Benjamin Emanuel Dietrich<sup>1</sup>, Jonas Reber<sup>1</sup>,  
Johanna Vannesjo<sup>2</sup>, Alen Mujkanovic<sup>1</sup>, and Klaas Paul Pruessmann<sup>1</sup>

<sup>1</sup>Institute for Biomedical Engineering, University of Zurich and ETH Zurich, Zurich, Switzerland, <sup>2</sup>FMRIB Centre, University of Oxford, Oxford, United Kingdom

Concurrent field monitoring is currently limited to observation times in the order of 100 ms. However, for many purposes it is desirable to determine field dynamics continuously without interruption. To address this need we propose model-based gradient impulse response function (GIRF) harvesting, where GIRFs are continuously updated during the MR experiment. From the harvested GRIFs and the known input to the gradient chains, continuous gradients are obtained. The model-based approach allows to robustly determine continuous gradient fields with high precision. The method is demonstrated by stabilizing a gradient-demanding EPI scan.

78

8:27

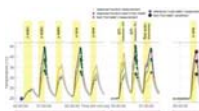
**Measurement of Small-Tip RF Pulses using Gradient Reversal**Vanessa Landes<sup>1</sup> and Krishna Nayak<sup>1</sup>

<sup>1</sup>University of Southern California, Los Angeles, CA, United States

We present a simple pulse sequence for measuring RF pulses in the small-tip regime. In a uniform phantom, results matched closely (<4% difference) with a pick-up RF coil over a broad range of RF pulse parameters, with one outlier (6.1% difference). In non-uniform phantoms and in-vivo, this method combined with an outer-volume suppression (OVS) pre-pulse produced accurate (<3% difference) measurements compared to a pick-up RF coil. Speed and lack of additional hardware could make the proposed method ideal for RF pre-distortion correction.

79

8:39

**Thermal Variation and Temperature-Based Prediction of Gradient Response**Benjamin Emanuel Dietrich<sup>1</sup>, Jennifer Nussbaum<sup>1</sup>, Bertram Jakob Wilm<sup>1</sup>,  
Jonas Reber<sup>1</sup>, and Klaas Paul Pruessmann<sup>1</sup>

<sup>1</sup>Institute for Biomedical Engineering, University of Zurich and ETH Zurich, Zurich, Switzerland

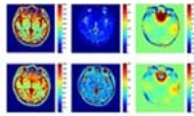


Under the assumption that a gradient system is linear and time-invariant (LTI), accurate gradient field waveforms can be predicted by gradient response functions. However, time-invariance can be violated due to heating of system components. Temperature sensors can be used to assess heating of the gradient coils. To assess the predictability of gradient response function based on temperature measurements, the temperature dependence of gradient response functions is analyzed using an NMR probe based field camera and optically connected temperature sensors. From this data a prediction model is generated and tested for its application in image reconstruction.

---

80

8:51



Effects of RF pulse profile and within-slice phase dispersion on accuracy of MR fingerprinting with balanced SSFP readout

Su-Chin Chiu<sup>1</sup>, Te-Ming Lin<sup>2</sup>, Jyh-Miin Lin<sup>3,4</sup>, Hsiao-Wen Chung<sup>5</sup>, Cheng-Wen Ko<sup>6</sup>, Martin Büchert<sup>7</sup>, and Michael Bock<sup>7</sup>

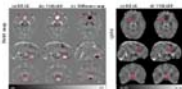
*<sup>1</sup>National Taiwan University, Taipei, Taiwan, <sup>2</sup>Radiology, Veterans General Hospital, Taipei, Taiwan, <sup>3</sup>Graduate Institute of Biomedical Electronics and Bioinformatics, National Taiwan University, Taipei, Taiwan, <sup>4</sup>Radiology, University of Cambridge, Cambridge, United Kingdom, <sup>5</sup>Electrical Engineering, National Taiwan University, Taipei, Taiwan, <sup>6</sup>Computer Science and Engineering, National Sun Yat-Sen University, Kaohsiung, Taiwan, <sup>7</sup>Radiology, University Medical Center Freiburg, Freiburg, Germany*

To investigate the effects of within-slice phase dispersion and RF pulse profile on quantitative relaxation mapping using MR fingerprinting with balanced steady-state free precession readout, simulations based on Bloch equations were performed assuming uniform distributions of off-resonance frequency (widths from 0, 1.0, to 2.0 Hz) and imperfect slice profiles of sinc-shaped RF pulses without and with side lobes. Results showed that slight within-slice phase dispersion by 1 to 2 Hz resulted in prominent T2 under-estimations, particularly at large T2 values. Slice profile imperfection led to under-estimations of T1, which became greater as regional off-resonance frequencies increased.

---

81

9:03



A New Background Field Removal Method Using Region Adaptive Kernel for Human Brain MRI

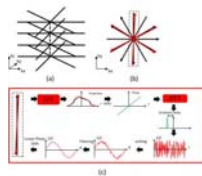
Jinsheng Fang<sup>1</sup>, Lijun Bao<sup>1</sup>, and Zhong Chen<sup>1</sup>

*<sup>1</sup>Department of Electronic Science, Xiamen University, Xiamen, People's Republic of China*

we propose a new background field removal method by using region adaptive kernel (REAK) based on local energy distribution. Experimental results on simulation data and in vivo human data demonstrated that our method has good performance on suppressing the susceptibility artifacts caused by large susceptibility variations, such as over boundary regions of brain skull, venous vessels and paranasal sinuses. This can facilitate the susceptibility map reconstruction and achieve more accurate QSM approximate to the results of COSMOS, which is helpful for the QSM technique and its application in the clinical medicine.

82

9:15



Influence of the gradient delay correction on self-navigated motion resolved reconstruction with golden angle stack-of-stars acquisition  
Xucheng Zhu<sup>1</sup>, Mariya Doneva<sup>2</sup>, Peder E.Z. Larson<sup>1,3</sup>, and Michael Lustig<sup>1,4</sup>

<sup>1</sup>Bioengineering, UC Berkeley-UCSF Graduate Program in Bioengineering, San Francisco, CA, United States, <sup>2</sup>Philips Research Europe, Hamburg, Germany, <sup>3</sup>Department of Radiology and Biomedical Imaging, University of California, San Francisco, San Francisco, CA, United States, <sup>4</sup>Department of Electrical Engineering and Computer Sciences, UC Berkeley, Berkeley, CA, United States

Gradient delay often leads to misalignment of k-space data, which induces artifacts on reconstructed images. As many self-gated motion correction methods largely depend on central k-space data, misalignment might affect motion state estimation and reconstruction. In order to acquire robust motion states and improve motion resolved reconstruction, we propose a workflow incorporating gradient delay correction, robust motion extraction, and motion resolved reconstruction. We tested our method on in vivo volunteer data, and demonstrate the improvement over a reconstruction that does not account for these delays.

83

9:27

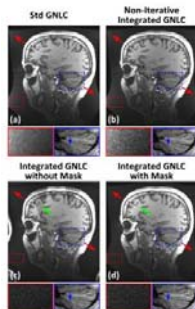


Image Reconstruction with Integrated Gradient-Nonlinearity Correction and Constrained Spatial Support

Shengzhen Tao<sup>1</sup>, Joshua D Trzasko<sup>1</sup>, Paul T Weavers<sup>1</sup>, Yunhong Shu<sup>1</sup>, John Huston III<sup>1</sup>, Erin M Gray<sup>1</sup>, and Matt A Bernstein<sup>1</sup>

<sup>1</sup>Radiology, Mayo Clinic, Rochester, MN, United States

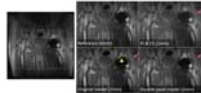


Due to engineering limitations, the spatial-encoding gradient fields in MRI are not exactly linear across the entire field-of-view. If not properly accounted for during reconstruction, the gradient-nonlinearity (GNL) causes image distortion and artificial signal intensity change. Conventionally, the GNL effects are corrected after image reconstruction using image-domain interpolation, followed by intensity correction using the Jacobian-determinant of the distortion field. Images corrected using this method can suffer from noise amplification at regions with strong GNL distortion. Here, we develop a model-based reconstruction method with integrated GNL correction and constrained spatial support, and demonstrate reduced noise amplification effect using this method.

84



9:39



### Accelerated Imaging of Metallic Implants Using a Double-Peak-Model Constraint

Xinwei Shi<sup>1,2</sup>, Evan Levine<sup>1,2</sup>, Hans Weber<sup>1</sup>, and Brian A. Hargreaves<sup>1,2</sup>

<sup>1</sup>Radiology, Stanford University, Stanford, CA, United States, <sup>2</sup>Electrical Engineering, Stanford University, Stanford, CA, United States

Multi-Spectral Imaging (MSI) enables MRI near metallic implants, but suffers from prolonged scan times. Model-based reconstruction accelerates MSI by enforcing a signal model along the spectral dimension to reduce the number of unknowns in image reconstruction. The previous signal model assumes that spins in one voxel have the same off-resonance frequency, which tends to fail where the off-resonance field changes rapidly. Here we propose a more flexible MSI signal model that allows multiple frequencies within a voxel, and demonstrate improvements with both simulated and in-vivo data. 3x net additional acceleration above partial-Fourier and parallel-imaging alone (20x in total) was achieved.

85



9:51

Method	SNR	Time (s)	Acceleration
Partial-Fourier	~1.0	~100	~1.5x
Parallel-imaging	~1.0	~100	~1.5x
Proposed	~1.0	~30	~3.0x

### Absolute MR Thermometry from Multi-Echo GRE with $B_0$ -Correction

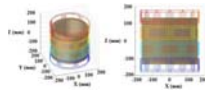
Patrick C McDaniel<sup>1</sup>, Mark Spatz<sup>1</sup>, Bastien Guérin<sup>2,3</sup>, Patricia Ellen Grant<sup>4,5</sup>, Lawrence L Wald<sup>2,3,6</sup>, and Elfar Adalsteinsson<sup>1,6</sup>

<sup>1</sup>Electrical Engineering and Computer Science, Massachusetts Institute of Technology, Cambridge, MA, United States, <sup>2</sup>Athinoula A Martinos Center for Biomedical Imaging, Massachusetts General Hospital, Charlestown, MA, United States, <sup>3</sup>Radiology, Harvard Medical School, Boston, MA, United States, <sup>4</sup>Radiology, Boston Children's Hospital, Boston, MA, United States, <sup>5</sup>Pediatrics, Boston Children's Hospital, Boston, MA, United States, <sup>6</sup>Institute for Medical Engineering and Science, Massachusetts Institute of Technology, Cambridge, MA, United States

MR thermometry offers the potential to obtain absolute and relative temperature measurements on a voxelwise basis, but is affected by  $B_0$  offsets. Since precise ( $<1^\circ\text{C}$ ) temperature measurements are important for simulation validation in phantom experiments, and since realistic phantoms and models have regions of high  $\Delta B_0$ , there is a need for accurate,  $B_0$ -robust temperature mapping methods. In this work, we propose such a method using a multi-TE GRE acquisition and validate it in phantom experiments.

86

10:03



### Uniform Spatiotemporal Excitation Despite Extreme $B_0$ Inhomogeneity Using Dynamically-Driven Multi-Coil Arrays

Mohan Lal Jayatilake<sup>1</sup>, Christoph Juchem<sup>2</sup>, Michael Mullen<sup>3</sup>, Lance DelaBarre<sup>3</sup>, Gregor Adriany<sup>4</sup>, Robin de Graaf<sup>5</sup>, and Michael Garwood<sup>3</sup>

<sup>1</sup>Center for Magnetic Resonance Research, University of Minnesota, Minnesota, MN, United States, <sup>2</sup>Departments of Biomedical Engineering and Radiology, Columbia University in the City of New York, NY, United States, <sup>3</sup>Center for Magnetic Resonance Research, University of Minnesota, MN, United States, <sup>4</sup>Center for Magnetic Resonance Research, University of Minnesota, Minnesota, United States, <sup>5</sup>Department of Radiology and Biomedical Imaging, Yale University School of Medicine, NY, United States



Developments of new imaging strategies that tolerate extreme  $B_0$  inhomogeneity can reduce size and cost of MRI magnets; but with conventional MRI methods, a highly uniform  $B_0$  is still required to obtain high quality images. Previously we demonstrated spatiotemporal excitation of spins in the presence of large  $B_0$  inhomogeneity when driving a multi-coil array with the dynamic multi-coil technique known as DYNAMITE. In that work, tolerance to  $B_0$  inhomogeneity began to degrade when the frequency variation exceeded  $\pm 40$  kHz, which is insufficient for imaging with a small magnet. Here we present a technique to substantially extend the range of  $B_0$  inhomogeneity tolerance of this approach when using RF pulses based on the principle of offset-independent adiabaticity (OIA).

---

## Oral

### Mostly Muscle

Room 316A

Monday 8:15 - 10:15

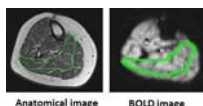
Moderators: Steven Baete & David Bluemke

---

87

8:15

Increased muscle BOLD following exercise training in older adults



Jill M Slade<sup>1</sup>, Anne Tonson<sup>2</sup>, David Hurley<sup>1</sup>, Mitchell Rozman<sup>1</sup>, George S Abela<sup>3</sup>, and Ronald A. Meyer<sup>2</sup>

<sup>1</sup>Radiology, Michigan State University, East Lansing, MI, United States, <sup>2</sup>Physiology, Michigan State University, <sup>3</sup>Medicine, Michigan State University

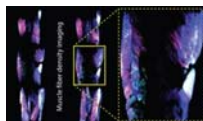
Functional MRI (BOLD) of skeletal muscle was used to evaluate changes in microvascular function before and after aerobic exercise training in older adults. Peak BOLD responses increased by  $\sim 30\%$  after exercise training, supporting the use and sensitivity of BOLD MRI to assess changes in microvascular function.

---

88

8:27

Improved Muscle Microstructure Analysis with Diffusion Weighted Imaging and Advanced Tissue Modeling



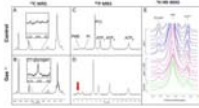
Nagesh Adluru<sup>1</sup>, Richard Kijowski<sup>2</sup>, and Fang Liu<sup>2</sup>

<sup>1</sup>Waisman Center, University of Wisconsin-Madison, Madison, WI, United States, <sup>2</sup>Radiology, University of Wisconsin-Madison

Studies on musculoskeletal systems can benefit by quantitative mapping of the tissue microstructure. Parameters from traditional diffusion tensor imaging (DTI) may serve as bio-markers for assessing muscle fiber health. While these parameters are sensitive to changes of muscle fiber orientation, length and tension, they are non-specific to the changes of microstructure and microcomposition of muscle fibers. In this study, we proposed to use multi-shell diffusion weighted imaging acquisition with advanced diffusion and micro tissue modeling to improve in-vivo muscle fiber analysis and demonstrated the feasibility of applying these methods on in-vivo human thigh muscle imaging.

89

8:39



### **<sup>13</sup>C/<sup>31</sup>P MRS biomarkers of disease progression and response to gene therapy in a mouse model of Pompe disease**

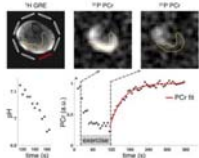
Celine Baligand<sup>1</sup>, Gary A. Todd<sup>2</sup>, Brittany Lee-McMullen<sup>3</sup>, Ravneet S. Vohra<sup>4</sup>, Barry J. Byrne<sup>2</sup>, Darin J. Falk<sup>2</sup>, and Glenn A. Walter<sup>5</sup>

*<sup>1</sup>Department of Radiology, Leiden University Medical Center, C.J. Gorter Center for High-field MRI, Leiden, Netherlands, <sup>2</sup>Department of Pediatrics, University of Florida, Gainesville, FL, United States, <sup>3</sup>Department of Genetics, Stanford School of Medicine, Stanford, CA, United States, <sup>4</sup>Department of Radiology, University of Washington, Seattle, WA, United States, <sup>5</sup>Department of Physiology and Functional Genomics, University of Florida, Gainesville, FL, United States*

With the emergence of rAAV-based gene therapy clinical trials in patients with glycogen storage disorders such as Pompe disease, there is a pressing need for early and non-invasive markers to assess treatment efficacy. While <sup>13</sup>C-MRS has been used for detection of glycogen in muscle, its clinical implementation remains limited, due to its low natural abundance and inherent low sensitivity. <sup>31</sup>P-MRS has higher sensitivity and can probe intermediates of glucose/glycogen metabolism. We sought to identify new biomarkers of Pompe disease progression in muscle using <sup>13</sup>C/<sup>31</sup>P-MRS and <sup>1</sup>H-HR-MAS in the mouse model of the disease, and tested their sensitivity to rAAV therapy.

90

8:51



### **Dynamic PCr and pH imaging of the human lower leg muscle during exercise at 3T**

Oleksandr Khagai<sup>1</sup>, Guillaume Madelin<sup>1,2</sup>, Ryan Brown<sup>1,2</sup>, and Prodromos Parasoglou<sup>1,2</sup>



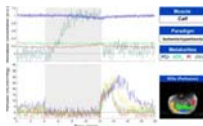
<sup>1</sup>Bernard and Irene Schwartz Center for Biomedical Imaging, Department of Radiology, New York University School of Medicine, New York, NY, United States, <sup>2</sup>Center for Advanced Imaging Innovation and Research (CAI2R), Department of Radiology, New York University School of Medicine, New York, NY, United States

Dynamic phosphorous MRSI is an established non-invasive method for studying muscle metabolism. It allows quantification of the post-exercise phosphocreatine resynthesis rate, which provides insights into various physiological and pathological conditions. Due to low SNR, <sup>31</sup>P imaging experiments are typically limited by long acquisition times relative to the metabolic recovery. We developed an imaging method to measure localized phosphocreatine resynthesis and pH changes in muscles of the lower leg following exercise at 3T with a high temporal resolution of 6 s required for an accurate estimation of quantitative phosphocreatine recovery rates.

---

91

9:03



Dynamic interleaved NMR measurements of perfusion, deoxymyoglobin and phosphorylated metabolites during ischemic and exercise paradigms in the calf and thigh muscles

Alfredo Liubomir Lopez Kolkovsky<sup>1,2</sup>, Benjamin Marty<sup>1,2</sup>, Bertrand Coppa<sup>1,2</sup>, Eric Giacomini<sup>1</sup>, and Pierre G Carlier<sup>1,2</sup>

<sup>1</sup>NMR Laboratory, Institute of Myology, Paris, France, <sup>2</sup>CEA, DRF, I2BM, MIRCen, Paris, France

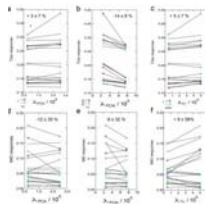
NMR allows to investigate multiple aspects of physiological parameters like regional perfusion, blood and tissue oxygenation, intracellular pH or high-energy phosphate metabolism. In the past, interleaved multi-parametric multi-nuclear dynamic NMR imaging and spectroscopy of skeletal muscle was developed on prototype scanners. Here we developed an interleaved pulse sequence combining NMR acquisitions of a perfusion image, <sup>1</sup>H deoxy-myoglobin and <sup>31</sup>P spectra on a clinical system without any hardware modifications from the customer. We successfully evaluated this sequence in the ischemic calf muscle and exercising quadriceps muscle. Nevertheless, using a surface coil for pulsed-ASL measurements remains a limitation at this time.

---

92

9:15

Dynamic Diffusion Tensor Imaging in Normal and Compartment Syndrome Calf Muscle with MEDITI



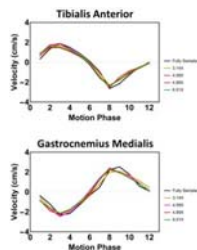
Eric Edward Sigmund<sup>1,2</sup>, Steven Hubert Baete<sup>1,2</sup>, Karan Patel<sup>1,3</sup>, Di Wang<sup>1,3</sup>, Ricardo Otazo<sup>1,2</sup>, Prodromos Parasoglou<sup>1,2</sup>, and Jenny Bencardino<sup>1</sup>

<sup>1</sup>Radiology, NYU Langone Medical Center, New York, NY, United States, <sup>2</sup>Center for Advanced Imaging and Innovation (CAIR), New York, NY, United States, <sup>3</sup>NYU Tandon School of Engineering

We describe measurement of skeletal muscle kinematics with a multiple echo diffusion tensor imaging (MEDITI) in clinical scanners. This approach allows characterization of the microstructural dynamics in healthy and diseased muscle. Combining the accelerated MEDITI directional encoding with a radial k-space trajectory and compressed sensing reconstruction allows spatially resolved DTI with a continuous temporal resolution of 16 s. Using an MR-compatible ergometer, post-exercise recovery of DTI metrics in calf muscle were quantified in a pilot cohort of 2 volunteers and 4 subjects with chronic exertional compartment syndrome (CECS). Results indicate anisotropic exercise response and recovery with kinetics differing from relaxation contrast.

93

9:27

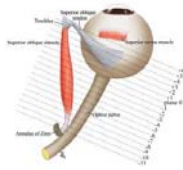


Compressed Sensing accelerated time-resolved 3D phase contrast MRI of the lower leg muscles during active dorsi- and plantarflexion

Lukas M. Gottwald<sup>1</sup>, Valentina Mazzoli<sup>1,2,3</sup>, Eva S. Peper<sup>1</sup>, Qinwei Zhang<sup>1</sup>, Bram F. Coolen<sup>4</sup>, Pim van Ooij<sup>1</sup>, Gustav J. Strijkers<sup>4</sup>, and Aart J. Nederveen<sup>1</sup>

<sup>1</sup>Department of Radiology, Academic Medical Center, Amsterdam, Netherlands, <sup>2</sup>Department of Biomedical Engineering, Eindhoven University of Technology, Eindhoven, Netherlands, <sup>3</sup>Orthopaedic Research Lab, Radboud UMCN, Nijmegen, Netherlands, <sup>4</sup>Department of Biomedical Engineering & Physics, Academic Medical Center, Amsterdam, Netherlands

Time-resolved 3D phase-contrast MRI can be applied to quantify muscle contraction. 3D coverage with sufficient spatiotemporal resolution ( $\sim 3 \times 3 \times 5 \text{ mm}^3$ , 160ms) can only be achieved by interleaved acquisitions during many repetitions of a motion task, resulting in long scan times (>10min). In this study we have developed an accelerated protocol, using k-space undersampling and compressed-sensing reconstruction, which was applied on the lower leg of 4 volunteers performing a foot plantar-dorsal flexion motion task. Muscle velocities during the motion cycle of fully-sampled and accelerated protocols were compared. Acceleration was successful up to 6.4X with comparable velocities, which confirmed the benefit of this approach.



## Magnetic Resonance Imaging of the Functional Anatomy of the Oblique Muscles in Patients with Primary Oblique Overaction

Qianwen Gong<sup>1,2</sup>, Longqian Liu<sup>1,3</sup>, and Miroslaw Janowski<sup>2,4</sup>

<sup>1</sup>Department of Optometry and Visual Science, West China Hospital, Sichuan University, Chengdu, People's Republic of China, <sup>2</sup>Department of Radiology and Radiological Science, Johns Hopkins University School of Medicine, Baltimore, MD, United States, <sup>3</sup>Department of Ophthalmology, West China Hospital, Sichuan University, Chengdu, People's Republic of China, <sup>4</sup>NeuroRepair Department, Mossakowski Medical Research Centre PAS, Warsaw, Poland

The cause of primary eye movement abnormality is unknown. The functional MRI of superior and inferior oblique muscles was instrumental to investigate the cause of overaction. We have shown similar size of superior oblique muscle in patients and controls in the resting state, while the MRI performed during gazes revealed differences in the contractility, what suggests the abnormal innervation as a cause of primary superior oblique muscles. In contrast, the inferior oblique muscle was larger in resting state, without a difference in contractility what indicates the hypertrophy as a basis for primary inferior oblique muscle overaction.

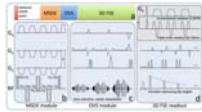


## An MRI-based assessment of the correlation between cerebral white matter changes, muscle structure, and muscle function in myotonic dystrophy

Daniel Thedens<sup>1</sup>, Cheryl Smith<sup>2</sup>, Peg Nopoulos<sup>3</sup>, Richard Shields<sup>4</sup>, and Laurie Gutmann<sup>2</sup>

<sup>1</sup>Radiology, University of Iowa, Iowa City, IA, United States, <sup>2</sup>Neurology, University of Iowa, Iowa City, IA, United States, <sup>3</sup>Psychiatry, University of Iowa, Iowa City, IA, United States, <sup>4</sup>Physical Therapy and Rehabilitation Science, University of Iowa, Iowa City, IA, United States

The purpose of this work was to study subjects with myotonic dystrophy (DM1) utilizing MRI to assess correlations between global cerebral white matter abnormalities, muscle structure, and muscle function. MRI-based measures of white matter (fractional anisotropy), muscle structure (volume, fat fraction, T2 mapping) along with muscle function testing demonstrated several significant correlations. The combination of neuroimaging and muscle structure assessment with MRI holds considerable promise towards elucidating the relationships between CNS abnormalities and neuromuscular dysfunction.



### A Flexible Technique for Flow-Sensitive Fat-Suppressed High-Resolution Peripheral Nerve Imaging

Valentina Taviani<sup>1</sup>, Miyoshi Mitsuharu<sup>2</sup>, Kang Wang<sup>3</sup>, Kevin King<sup>4</sup>, Suchandrima Banerjee<sup>1</sup>, Sandip Biswal<sup>5</sup>, Shreyas Vasanawala<sup>5</sup>, Daehyun Yoon<sup>5</sup>, and Robert Peters<sup>4</sup>

<sup>1</sup>Global MR Applications & Workflow, GE Healthcare, Menlo Park, CA, United States, <sup>2</sup>Global MR Applications & Workflow, GE Healthcare Japan, Hino, Japan, <sup>3</sup>Global MR Applications & Workflow, GE Healthcare, Madison, WI, United States, <sup>4</sup>Global MR Applications & Workflow, GE Healthcare, Waukesha, WI, United States, <sup>5</sup>Department of Radiology, Stanford University, Stanford, CA, United States

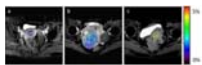
We developed a flow-sensitive 3D fast spin echo pulse sequence with Dixon-based water-fat separation and compressed sensing for robust and efficient peripheral nerve imaging. Outer volume suppression allows shorter scan times by limiting spatial encoding of the FOV to the anatomy of interest without aliasing concerns. In addition, it improves the performance of spectrally-selective fat suppression methods, that can be advantageous for very high resolution imaging but are typically hampered by B0 inhomogeneity, by allowing shimming over smaller regions. Preliminary data showed good delineation of peripheral nerves in different anatomies, with adequate resolution and clinically feasible acquisition times.

## Oral

## Female Pelvis, Fetal & Placental Imaging

Room 320

Monday 8:15 - 10:15 Moderators: Gabriele Masselli & Evis Sala



### Amide proton transfer magnetic resonance imaging of uterine endometrial cancer: Association with histologic grade

Yukihisa Takayama<sup>1</sup>, Akihiro Nishie<sup>2</sup>, Osamu Togao<sup>2</sup>, Yoshiki Asayama<sup>2</sup>, Kousei Ishigami<sup>2</sup>, Yasuhiro Ushijima<sup>2</sup>, Daisuke Okamoto<sup>2</sup>, Nobuhiro Fujita<sup>2</sup>, Kenzo Sonoda<sup>3</sup>, Jochen Keupp<sup>4</sup>, and Hiroshi Honda<sup>2</sup>

<sup>1</sup>Department of Radiology Informatics and Network, Kyushu University, Fukuoka, Japan, <sup>2</sup>Department of Clinical Radiology, Kyushu University, <sup>3</sup>Department of Gynecology & Obstetrics, Kyushu University, <sup>4</sup>Philips Research



The histologic grade of endometrioid adenocarcinoma (EMCA) is one of the important factors in choosing a treatment plan. Currently, needle biopsy or surgical resection is necessary to diagnose the histological grade; a less invasive procedure is strongly desired. In this study, we evaluated the utility of amide proton transfer (APT) imaging in estimating the histologic grade of EMCA. APT signal intensities (SIs) of EMCA increased in accordance with the progression of histologic grade. APT SIs of high-grade EMCA were significantly higher than those of low-grade EMCA. APT imaging has potential as a biomarker for histologic grade of EMCA.

98

8:27

The prognostic power of early and late phase DCE-MRI parameters in locally advanced cervix cancer.

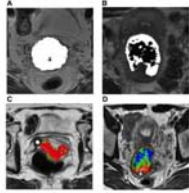


Figure 1

Kjersti Vassmo Lund<sup>1,2</sup>, Trude Golimo Simonsen<sup>2</sup>, Gunnar B. Kristensen<sup>3,4,5</sup>, and Einar K. Rofstad<sup>2</sup>

<sup>1</sup>Dept of Radiology and Nuclear Medicine, Oslo University Hospital, Oslo, Norway, <sup>2</sup>Dept. of Radiation Biology, Institute of cancer Research, Oslo University Hospital, Oslo, Norway, <sup>3</sup>Dept. of Gynecological Cancer, Oslo University Hospital, Oslo, Norway, <sup>4</sup>Institute for Cancer Genetics and Informatics, Oslo University Hospital, Oslo, Norway, <sup>5</sup>Institute for Clinical Medicine, University of Oslo, Oslo, Norway

DCE-MRI can provide prognostic information on locally advanced cervix carcinomas. Most studies have emphasis on the early phase of the Signal Intensity Time Curve (SITC). The purpose of this study was to explore the prognostic value of the late phase of the SITC and to reveal any added value to that of parameters from the early phase. Both the early phase parameter LETV and the late phase parameter TVIS was associated with overall survival. The association was independent of clinical factors like tumor volume, FIGO stage and lymph node status. TVIS did not provide any added prognostic value to LETV.

99

8:39

Histogram analysis of intravoxel incoherent motion MRI in predicting chemoradiotherapy response in cervical cancer

Jose Angelo Udal Perucho<sup>1</sup>, Elaine Yuen Phin Lee<sup>1</sup>, Wing Chi Lawrence Chan<sup>2</sup>, Nanjie Gong<sup>3</sup>, and Queenie Chan<sup>4</sup>

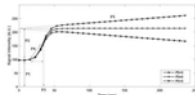
<sup>1</sup>Department of Diagnostic Radiology, The University of Hong Kong, Hong Kong, Hong Kong, <sup>2</sup>Department of Health Technology and Informatics, The Hong Kong Polytechnic University, Hong Kong, <sup>3</sup>University of California, Berkeley, CA, United States, <sup>4</sup>Philips Healthcare, Hong Kong, Hong Kong

Histogram analysis of intravoxel incoherent motion (IVIM) diffusion-weighted MRI (DWI) could be a promising quantitative approach in predicting tumour response to chemoradiotherapy (CRT) in cervical cancer. We retrospectively studied twenty-five patients with cervical cancer who had paired IVIM MRI examinations before and at week-4 of treatment. We observed that histogram skewness of true diffusion coefficient (D) prior to treatment and that a large increase in the 90th percentile of D following CRT were predictive of better CRT response.

---

100

8:51



### A One-Step Biomarker Quantification Methodology for DCE-MRI of Complex Ovarian Masses: Capturing Kinetic Pattern from Early to Late Enhancement

Anahita Fathi Kazerooni<sup>1,2</sup>, Mahnaz Nabil<sup>3</sup>, Hamidreza Haghighat Khah<sup>4</sup>, and Hamidreza Saligeh Rad<sup>1,2</sup>

<sup>1</sup>Quantitative MR Imaging and Spectroscopy Group, Research Center for Molecular and Cellular Imaging, Tehran University of Medical Sciences, Tehran, Iran, <sup>2</sup>Department of Medical Physics and Biomedical Engineering, Tehran University of Medical Sciences, Tehran, Iran, <sup>3</sup>Department of Mathematics, Islamic Azad University, Qazvin Branch, Qazvin, Iran, <sup>4</sup>Department of Diagnostic Imaging, Shohada-e-Tajrish Hospital, Shahid Beheshti University of Medical Sciences, Tehran, Iran

Accurate characterization of sonographically-indeterminate ovarian masses before surgery is crucial for proper disease management. While DCE-MRI has emerged as a problem-solving technique, accurate parameter estimations from semi-quantitative or PK analysis are dependent on multiple steps, including proper protocol design, motion reduction, selection of physiology-based PK model and AIF, which discourages development and reliability of computer-aided diagnostic procedures. Here, we aimed to develop a one-step pre-processing and quantification classification scheme based on a five-parameter Sigmoid model, capturing early- to late-enhancement kinetics, including washout as a previously overlooked parameter for ovarian masses, to generate accurate differentiation of complex ovarian masses.

---





### Ex vivo MRI evaluation of vulvar cancer to predict resection margins in fresh wide local excision specimens: a pilot study

Jan Heidkamp<sup>1</sup>, Petra Zusterzeel<sup>2</sup>, Andor Veltien<sup>1</sup>, Arie Maat<sup>3</sup>, Ilse Van Engen-Van Grunsven<sup>3</sup>, and Jurgen Fütterer<sup>1</sup>

<sup>1</sup>Radiology and Nuclear Medicine, Radboud university medical center, Nijmegen, Netherlands, <sup>2</sup>Obstetrics and Gynaecology, Radboud university medical center, Nijmegen, Netherlands, <sup>3</sup>Pathology, Radboud university medical center, Nijmegen, Netherlands

Currently there's no accurate and topical peroperative information available on the margin status of wide local resection specimens containing vulvar cancer. In this pilot study we performed a qualitative image evaluation of ex vivo 7T MR images acquired of fresh specimens of the vulva containing vulvar cancer using different MRI sequences. High resolution T2 weighted images obtained the highest score for image quality, visibility of the tumor, and visibility of the transition between the epidermis and the resection surface.

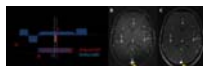


### Assessment of uterine artery hemodynamics in normal pregnancy with 4D Flow MRI

Eileen Hwuang<sup>1</sup>, Marta Vidorreta<sup>1</sup>, Nadav Schwartz<sup>1</sup>, John A Detre<sup>1</sup>, Daniel Licht<sup>2</sup>, and Walter RT Witschey<sup>1</sup>

<sup>1</sup>University of Pennsylvania, Philadelphia, PA, United States, <sup>2</sup>Children's Hospital of Philadelphia, Philadelphia, PA, United States

*In vivo* imaging of uterine artery blood flow during remodeling is potentially valuable in assessing placental function during pregnancy. We present 4D flow MRI of the uterine arteries, demonstrating inter- and intrasubject heterogeneity in vessel anatomy and hemodynamics. This high spatial resolution, multi-location approach potentially addresses the limitations of Doppler ultrasound in quantifying pulsatility and resistance indices as clinical biomarkers of placental health.



### In-utero non-contrast MR angiography of the fetal vasculature using a double-echo radial sampling scheme

Uday Krishnamurthy<sup>1,2</sup>, Brijesh K Yadav<sup>1</sup>, Pavan K Jella<sup>2</sup>, Swati Mody<sup>2</sup>, Edgar Hernandez-Andrade<sup>3,4</sup>, FeiFei Qu<sup>2</sup>, Anabela Trifan<sup>2</sup>, Ewart M Haacke<sup>1,2</sup>, Sonia S Hassan<sup>3,4</sup>, Roberto Romero<sup>4</sup>, and Jaladhar Neelavalli<sup>1,2</sup>

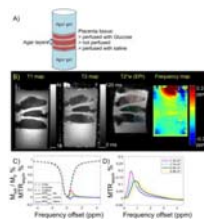
<sup>1</sup>Biomedical Engineering, Wayne State University, Detroit, MI, United States, <sup>2</sup>Radiology, Wayne State University, Detroit, MI, United States, <sup>3</sup>Obstetrics and Gynecology, Wayne State University, Detroit, MI, United States, <sup>4</sup>Perinatology Research Branch, NICHD/NIH/DHHS, Detroit, MI, United States

To show that the isotropic gradient delay issue can be addressed by a simple shift of the readout-window . We also report the use of a fully flow-compensated, readout-shifted 2D radial gradient echo sequence to perform non-contrast MRA of the human fetus in-utero

104



9:39



### Feasibility of glucose CEST in the human placenta

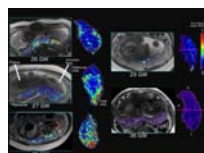
Jie Luo<sup>1</sup>, Yang Ji<sup>2,3</sup>, Esra Abaci Turk<sup>1</sup>, Iris Y Zhou<sup>2</sup>, Drucilla J. Roberts<sup>4</sup>, Patricia Ellen Grant<sup>1</sup>, and Phillip Zhe Sun<sup>2</sup>

<sup>1</sup>Fetal-neonatal Neuroimaging and Developmental Science Center, Boston Children's Hospital, Harvard Medical School, Boston, MA, United States, <sup>2</sup>Athinoula A. Martinos Center for Biomedical Imaging, Department of Radiology, Massachusetts General Hospital and Harvard Medical School, MA, United States, <sup>3</sup>Center for Biomedical Engineering, Department of Electronic Science and Technology, University of Science and Technology of China, People's Republic of China, <sup>4</sup>Pathology, Massachusetts General Hospital and Harvard Medical School, MA, United States

Placental glucose transfer is essential to sustain fetal development, yet there has been no report attempting to measure glucose transport across the human placenta with MRI-based approaches. Emerging glucose chemical exchange saturation transfer (glucoCEST) imaging is uniquely sensitive to glucose, which has been explored in tumor imaging. Herein, we have demonstrated glucoCEST MRI is a valid tool to monitor glucose perfusion in *ex vivo* human placenta, laying the groundwork for *in vivo* glucoCEST in human placenta.

105

9:51



### Parametric Mapping of Oxygen Activity in Human Placenta across Gestation using in utero BOLD imaging

Vidya Rajagopalan<sup>1,2</sup>, Vince Schmithorst, Julie Coloigner, Jessica Wisnowski, Matthew Borzage, Hollie Lai, Skorn Ponrartana, Ashok Panigrahy, and Stefan Bluml

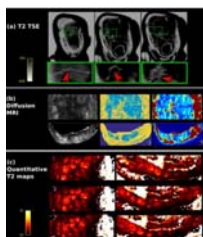
<sup>1</sup>Children's Hospital Los Angeles, Los Angeles, CA, United States, <sup>2</sup>Rudi Schulte Research Institute

We present here, for the first time, parametric maps of oxygen activity in normal human placenta using in utero functional MR imaging. Our method highlights anatomical and gestational age dependent patterns in placental activity. These maps can be used to gain insight into normative placental function and identifying insufficient or abnormal placental functioning at various points in gestation.

106

10:03

### [An exploration of quantitative physiological multi-modal in-vivo imaging of the human placenta](#)



Jana Hutter<sup>1,2</sup>, Paddy J Slator<sup>3</sup>, Jonathan O'Muircheartaigh<sup>4</sup>, Rui P Azeredo Gomes Teixeira<sup>1</sup>, Anthony N Price<sup>1</sup>, Ana Dos Santos Gomes<sup>4</sup>, Laura McCabe<sup>4</sup>, Sophie Arulkumaran<sup>4</sup>, Mary Rutherford<sup>4</sup>, and Joseph V Hajnal<sup>1</sup>

<sup>1</sup>Biomedical Engineering Department, King's College London, London, United Kingdom, <sup>2</sup>Centre for the Developing Brain, London, United Kingdom, <sup>3</sup>Centre for Medical Image Computing, University College London, London, United Kingdom, <sup>4</sup>Centre for the Developing Brain, King's College London, London, United Kingdom

The crucial role of the placenta in successful pregnancies is the transfer of oxygen within functional units – cotyledons. However, current screening falls short of visualizing this in-vivo. This study explores a multi-modal in-vivo MRI acquisition able to visualize and depict a range of spatial and temporal processes and the underlying micro-structure. Diffusion characteristics such as Mean Diffusivity and fractional anisotropy, quantitative T2\* maps, temporal characteristics and the depiction of vasculature allow insights and can be applied to a range of research questions.

## Combined Educational & Scientific Session

# Combining fMRI with Advanced Neurotechniques

Room 316BC

Monday 8:15 - 10:15

Moderators: Yihong Yang & Xin Yu

8:15

### [Overview of Cutting Edge Neurotechniques](#)

Anna Devor<sup>1,2</sup>

<sup>1</sup>Neurosciences and Radiology, UCSD, La Jolla, CA, United States,

<sup>2</sup>MGH/Harvard, Charlestown, MA, United States

The BRAIN Initiative targets a wide range of tools for sensing, tagging, and manipulation of multiple electrical, molecular/chemical, and connectivity parameters in the working brain. Combining these tools with fMRI measurements may accelerate our progress towards understanding the brain function in health and disease, open new avenues to guide the development of treatments, and build a stronger physiological foundation for human noninvasive imaging.

---

8:45 Challenges of Combining fMRI with other Neurotechniques  
Albrecht Stroh<sup>1</sup>

<sup>1</sup>*Johannes Gutenberg-University Mainz, Mainz, Germany*

107

9:15 Chemo-fMRI: a DREADD-based approach to unravel the brainwide substrates of neuromodulation



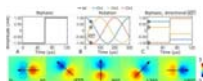
Andrea Giorgi<sup>1,2</sup>, Giacomo Maddaloni<sup>1</sup>, Alberto Galbusera<sup>2</sup>, Sara Migliarini<sup>1</sup>, Marta Gritti<sup>3</sup>, Raffaella Tonini<sup>3</sup>, Massimo Pasqualetti<sup>1,2</sup>, and Alessandro Gozzi<sup>2</sup>

<sup>1</sup>*Biology Department, University of Pisa, Pisa, Italy*, <sup>2</sup>*Functional Neuroimaging Laboratory, Center for Neuroscience and Cognitive Systems, Istituto Italiano di Tecnologia, Rovereto, Italy*, <sup>3</sup>*Neuroscience and Brain Technologies Department, Istituto Italiano di Tecnologia, Genova, Italy*

Notable examples of the combined use of optogenetics and fMRI (i.e. “opto-fMRI”) have been recently published, revealing the possibility to map the brainwide substrates modulated by focal neuronal population. However, opto-fMRI is complicated by the use of invasive cranial implants, and the need to control the insidious contribution of heat-induced hemodynamic-responses. Here we show that “chemo-fMRI”, e.g. the combined use of DREADD-based chemogenetics and fMRI, permits to overcome these limitations, by enabling non invasive brainwide mapping of tonically-stimulated neuromodulatory systems. Chemo-fMRI mapping of serotonin-producing neurons is described as an illustrative example of the power of this novel investigational approach.

---

9:27 Detecting orientation selective deep brain stimulation using BOLD fMRI



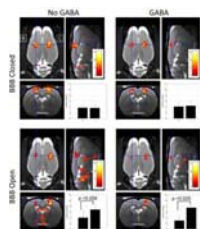


Lauri J Lehto<sup>1</sup>, Julia P Slopsema<sup>2</sup>, Matthew D Johnson<sup>2</sup>, Artem Shatillo<sup>3</sup>, Benjamin A Teplitzky<sup>2</sup>, Lynn Utecht<sup>1</sup>, Gregor Adriany<sup>1</sup>, Silvia Mangia<sup>1</sup>, Alejandra Sierra<sup>3</sup>, Walter C Low<sup>4</sup>, Olli Gröhn<sup>1,3</sup>, and Shalom Michaeli<sup>1</sup>

<sup>1</sup>Center for Magnetic Resonance Research, University of Minnesota, Minneapolis, MN, United States, <sup>2</sup>Department of Biomedical Engineering, University of Minnesota, Minneapolis, MN, United States, <sup>3</sup>A. I. Virtanen Institute for Molecular Sciences, University of Eastern Finland, Kuopio, Finland, <sup>4</sup>Department of Neurosurgery, University of Minnesota, Minneapolis, MN, United States

Spatial selectivity is of high importance for Deep Brain Stimulation (DBS). Here we used BOLD fMRI to demonstrate for the first time that axon-orientation selective stimulation can be achieved in the rat's corpus callosum by steering the stimulus phase of the independently driven channels in a tripolar DBS electrode. Pronounced angular dependence of the BOLD fMRI on the orientation of electric field gradient was detected. As expected based on simulations, the maximal (or minimal) BOLD response was observed when the induced dipole field was parallel (or perpendicular) to the axonal tract, respectively.

9:39



Functional MRI evaluation of a novel approach to neuromodulation: Targeted delivery of GABA via focused ultrasound-mediated disruption of the blood-brain barrier

Nick Todd<sup>1</sup>, Tao Sun<sup>1</sup>, Yongzhi Zhang<sup>1</sup>, Chanikarn Power<sup>1</sup>, Chanikarn Power<sup>1</sup>, Michael Arcaro<sup>2</sup>, Sam Patz<sup>1</sup>, Margaret Livingstone<sup>2</sup>, and Nathan McDannold<sup>1</sup>

<sup>1</sup>Brigham and Women's Hospital, Boston, MA, United States,

<sup>2</sup>Department of Neurobiology, Harvard Medical School, Boston, MA, United States

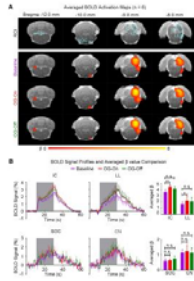
Here we present a novel approach to non-invasive neuromodulation that affects neuronal activity by delivering neurotransmitter chemicals to targeted areas of the brain. This is achieved by using focused ultrasound to transiently open the blood-brain barrier in a targeted brain region such that a systemically injected neuroactive chemical such as GABA or glutamate will leak out of the vessels and into the brain parenchyma only at the intended site. We demonstrate the proof of concept in a rodent model by delivering GABA to the somatosensory cortex to suppress activation from hindpaw stimulation.



9:51

### Optogenetically-evoked somatosensory inputs enhance sound processing in the auditory system

Celia M. Dong<sup>1,2</sup>, Alex T.L. Leong<sup>1,2</sup>, Russell W. Chan<sup>1,2</sup>, Xunda Wang<sup>1,2</sup>, and Ed X. Wu<sup>1,2</sup>



<sup>1</sup>Laboratory of Biomedical Imaging and Signal Processing, The University of Hong Kong, Hong Kong, Hong Kong, <sup>2</sup>Department of Electrical and Electronic Engineering, The University of Hong Kong, Hong Kong, Hong Kong

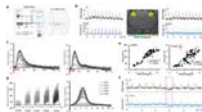
Brain-wide cross-modal interactions are important for building an accurate perception of the external world. Yet, whether and how somatosensory inputs influence the auditory processing remains unclear. Our recent study showed that low frequency optogenetic stimulation of somatosensory thalamus induced activation in auditory cortex (AC), but did not explore the functional effects on auditory system. This study investigated whether propagation of low frequency inputs from somatosensory system influences auditory processing. The results demonstrated that low frequency long-range propagation from somatosensory system enhanced auditory responses in most auditory structures, including lateral lemniscus, inferior colliculus, medial geniculate body and AC.



10:03

### Simultaneous fMRI with GCaMP6-mediated neuronal and astrocytic calcium signal recording

Maosen Wang<sup>1,2</sup>, Yi He<sup>1,2</sup>, and Xin Yu<sup>1</sup>



<sup>1</sup>High Field Magnetic Resonance Department, Max Planck Institute for Biological Cybernetics, Tuebingen, Germany, <sup>2</sup>Graduate Training Centre of Neuroscience, International Max Planck Research School, University of Tuebingen, Tuebingen, Germany

Neurovascular coupling is the basis of the BOLD fMRI, however, the mechanisms of the neurovascular coupling remains elusive. By simultaneous cell-type specific  $\text{Ca}^{2+}$  recording with BOLD fMRI, it allowed us to study the cellular specific coupling events through the neuron-glia-vessel network. This work showed neuronal  $\text{Ca}^{2+}$  and evoked astrocytic  $\text{Ca}^{2+}$  signal were positively correlated to the fMRI signal, but an intrinsic astrocytic  $\text{Ca}^{2+}$  signal was negatively correlated to the fMRI signal in the cortex. It indicated a novel neuron-glia-vascular coupling event mediated through the intrinsic astrocytic calcium signal (details mechanistic study in another abstract: ID 4475).

## Plenary Session

# Gadolinium Deposition

Organizers: Peter Caravan, Ph.D. & Winfried Willinek, M.D.

Plenary Hall

Monday 10:45 - 12:15

---

10:45      [Gadolinium Safety & Deposition: Past, Present, & Future](#)  
Michael F Tweedle<sup>1</sup>

*<sup>1</sup>Radiology, Ohio State University, Columbus, OH, United States*

---

11:15      [Gd Safety & Deposition: Impact on Practice, European Perspective](#)  
Harriet Thöny

---

11:45      [How Does Gd Enter the Brain, When the BBB is Intact?](#)  
Shinji Naganawa

---

12:15      [Adjournment & Meet the Teachers](#)

---

## Other

# Gold Corporate Symposium: Siemens Healthineers

Plenary Hall

Monday 12:15 - 13:45    *(no CME credit)*

---

## Traditional Poster: YIA

Exhibition Hall 31-36    Monday 13:45 - 15:45    *(no CME credit)*

---

## Electronic Poster: Diffusion

Exhibition Hall          Monday 13:45 - 14:45    *(no CME credit)*

---

## Electronic Poster: Body: Breast, Chest, Abdomen, Pelvis

Exhibition Hall          Monday 13:45 - 14:45    *(no CME credit)*

---

## Study Groups



# MR Safety & High Field Study Groups

Room 323ABC

Monday 13:45 - 15:45 (no CME credit)

---

## Study Groups

### Cardiac MR Study Group

Room 317AB

Monday 13:45 - 15:45 (no CME credit)

---

## Educational Course

### Advanced Imaging of Pain

Organizers: Jenny T. Bencardino, M.D., Eric Y. Chang, M.D., Christine Chung, M.D. & Philip Robinson, M.D.

Room 316A

Monday 13:45 - 15:45 Moderators: Emily McWalter & Edwin Oei

---

13:45

[Update on MRI Imaging of Low Back Pain](#)

Lawrence Neil Tanenbaum<sup>1</sup>

<sup>1</sup>*Imaging, Radnet, New York, NY, United States*

DWI is a powerful addition to the arsenal of MR imaging techniques for the detection of bone marrow tumor dissemination, improving sensitivity to involvement in a variety of tumor types (2). DWI increases confidence in monitoring treatment response and assisting in the differentiation of treatment related changes from tumor. Distinguishing between benign and malignant etiologies of vertebral fracture with MRI is problematic, particularly if only one vertebra is affected. The value of DWI in discriminating between osteoporotic and metastatic vertebral fractures is controversial and by consensus insufficiently reliable (4-6). DWI is useful for differentiation of degenerative and infectious endplate abnormalities (7-9). Symptomatic degenerative vertebral endplate signal changes (Modic type 1) can be difficult to differentiate from acute spondylodiscitis using conventional MRI techniques. Several studies have shown that DWI adds value in differentiating degenerative and infectious endplate abnormalities. The role of MRS in identifying the painful disc and PET MR in localizing back pain will be discussed

14:15

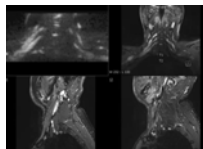
[MR Imaging of Brachial Plexus](#)

Kimberly Katz Amrami<sup>1</sup>

---



14:45



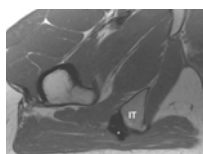
### Current Concepts on MR Neurography

Gustav Andreisek

MR Neurography has stepped out from being an emerging technique into clinical routine. This lecture will review current concepts on MR neurography and will provide an impression on how it may be used on a day-to-day basis.

---

15:15



### MR US Fusion Guided Intervention for Pain Syndromes

Christopher Burke

Ultrasound (US) systems equipped with position sensors can acquire three-dimensional spatial data allowing registration with previously acquired magnetic resonance (MR) imaging for fused real-time sonographic imaging. Co-registration and fusion of alignment involves sequential algorithmic transformations minimizing the error between the output and target image. An electromagnetic field generator is used to track transducer orientation to simultaneously map real-time US with corresponding anatomy on pre-acquired MR. The potential utility of this technology in the treatment of various pain syndromes in particular certain joint, tendon and perineural therapies will be described.

---

15:45

Adjournment & Meet the Teachers

---

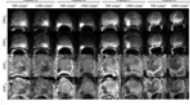
## Power Pitch

### Pitch: Body MRI Quantitative

Power Pitch  
Theater A - Monday 13:45 - *Moderators:* Edwin VanBeek & Patrick Bolan (no CME credit)  
Exhibition Hall 14:45

---

112 13:45 Accelerated Segmented Diffusion-Weighted Prostate Imaging for Higher Resolution, Higher Geometric Fidelity, and Multi-b Perfusion Quantification



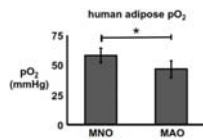
Pelin Aksit Ciris<sup>1</sup>, Jr-yuan George Chiou<sup>2</sup>, Daniel Glazer<sup>2</sup>, Shelley Hualei Zhang<sup>2</sup>, Tzu-Cheng Chao<sup>3</sup>, Bruno Madore<sup>2</sup>, and Stephan Ernst Maier<sup>2,4</sup>

<sup>1</sup>Department of Biomedical Engineering, Akdeniz University, Antalya, Turkey, <sup>2</sup>Department of Radiology, Brigham and Women's Hospital, Harvard Medical School, Boston, MA, United States, <sup>3</sup>Department of Computer Science, National Cheng Kung University, Tainan City, Taiwan, <sup>4</sup>University of Gothenburg, Gothenburg, Sweden

113



13:45



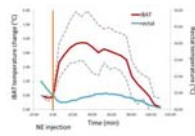
Towards validation and non-invasive interrogation of the hypoxia-driven insulin resistance hypothesis

Scott Charles Beeman<sup>1</sup>, Gordon Smith<sup>2</sup>, Joel Richard Garbow<sup>1</sup>, and Joseph JH Ackerman<sup>1,3</sup>

<sup>1</sup>Mallinckrodt Institute of Radiology, Washington University in St. Louis, St. Louis, MO, United States, <sup>2</sup>Department of Medicine, Washington University in St. Louis, St. Louis, MO, United States, <sup>3</sup>Department of Chemistry, Washington University in St. Louis

114

13:45



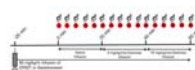
Measuring temperature in brown adipose tissue using the proton chemical shift

Clemens Diwok<sup>1</sup>, Renate Schreiber<sup>1</sup>, and Rudolf Zechner<sup>1</sup>

<sup>1</sup>Institute of Molecular Biosciences, University of Graz, Graz, Austria

115

13:45



Development of a Noninvasive Beta Cell Functional Assay Using a Novel Zinc-Sensitive MRI Contrast Agent in Non-Human Primates

Catherine D. G. Hines<sup>1</sup>, Veronica Clavijo-Jordan<sup>2,3</sup>, Liza T Gantert<sup>1</sup>, Stacey Conarello<sup>4</sup>, Christian Preihs<sup>2,5</sup>, Sarah Chirayil<sup>2</sup>, Rachel Ortiga<sup>4</sup>, Shu-An Lin<sup>1</sup>, Michael Klimas<sup>6</sup>, A. Dean Sherry<sup>2,3,5,7</sup>, and Jeff Evelhoch<sup>6</sup>

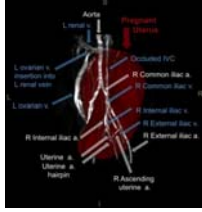
<sup>1</sup>Translational Imaging Biomarkers, Merck Research Laboratories, West Point, PA, United States, <sup>2</sup>Advanced Imaging Research Center, The University of Texas Southwestern Medical Center, Dallas, TX, United States, <sup>3</sup>Radiology, The University of Texas Southwestern Medical Center, Dallas, TX, United States, <sup>4</sup>Pharmacology, Merck Research Laboratories, West Point, PA, United States, <sup>5</sup>VitalQuan, LLC, Dallas, TX, United States, <sup>6</sup>Translational Biomarkers, Merck Research Laboratories, West Point, PA, United States, <sup>7</sup>Chemistry, The University of Texas at Dallas, Richardson, United States

116

13:45

### Feasibility of Estimating Placental Oxygen Metabolism in Pregnant Women \$\$\$in\$\$\$ \$\$\$vivo\$\$\$\$: Initial Experience

Ana E Rodríguez-Soto<sup>1</sup>, Michael C Langham<sup>1</sup>, Nadav Schwartz<sup>2</sup>, and Felix W Wehrli<sup>1</sup>



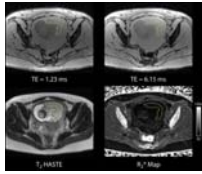
<sup>1</sup>Department of Radiology, University of Pennsylvania, Philadelphia, PA, United States, <sup>2</sup>Department of Obstetrics and Gynecology, Division of Maternal-Fetal Medicine, University of Pennsylvania, Philadelphia, PA, United States

117

13:45

### Free-breathing R2\* Characterization of the Placenta During Normal Early Gestation Using a Multiecho 3D Stack-of-Radial Technique

Tess Armstrong<sup>1,2</sup>, Dapeng Liu<sup>1</sup>, Thomas Martin<sup>1,2</sup>, Alto Stemmer<sup>3</sup>, Yutaka Natsuaki<sup>4</sup>, Sherin U. Devaskar<sup>5</sup>, Carla Janzen<sup>6</sup>, Teresa Chanlaw<sup>5</sup>, Rinat Masamed<sup>1</sup>, Daniel Margolis<sup>7</sup>, Kyunghyun Sung<sup>1,2</sup>, and Holden H. Wu<sup>1,2</sup>



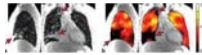
<sup>1</sup>Radiological Sciences, University of California Los Angeles, Los Angeles, CA, United States, <sup>2</sup>Physics and Biology in Medicine, University of California Los Angeles, Los Angeles, CA, United States, <sup>3</sup>Siemens Healthcare GmbH, Erlangen, Germany, <sup>4</sup>Siemens Healthcare, Los Angeles, CA, United States, <sup>5</sup>Pediatrics, David Geffen School of Medicine at UCLA, Los Angeles, CA, United States, <sup>6</sup>Obstetrics and Gynecology, David Geffen School of Medicine at UCLA, Los Angeles, CA, United States, <sup>7</sup>Radiology, Weill Cornell Medical College, New York, NY, United States

118

13:45

### Respiratory \$\$\$alpha\$\$\$-mapping of cystic fibrosis at 1.5T

Orso Pusterla<sup>1,2</sup>, Grzegorz Bauman<sup>1,2</sup>, Sylvia Nyilas<sup>3</sup>, Philipp Madörin<sup>1</sup>, Bernd Jung<sup>4</sup>, Michael Ith<sup>4</sup>, Enno Stranzinger<sup>4</sup>, Urs Frey<sup>5</sup>, Philipp Latzin<sup>3</sup>, and Oliver Bieri<sup>1,2</sup>



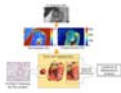
<sup>1</sup>Department of Radiology, Division of Radiological Physics, University of Basel Hospital, Basel, Switzerland, <sup>2</sup>Department of Biomedical Engineering, University of Basel, Basel, Switzerland, <sup>3</sup>Division of Respiratory Medicine, Department of Pediatrics, University Children's Hospital of Bern, Bern, Switzerland, <sup>4</sup>University Institute for Diagnostic, Interventional and Pediatric Radiology, Bern University Hospital, Bern, Switzerland, <sup>5</sup>Department of Pediatric Pneumology, University Children's Hospital Basel, Basel, Switzerland

119

13:45

### 5D MRI for late enhancement dynamics in lung fibrosis





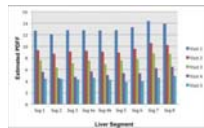
Yue Zhang<sup>1</sup>, Durga Udayakumar<sup>1</sup>, Ling Cai<sup>2</sup>, Zeping Hu<sup>2</sup>, Payal Kapur<sup>3</sup>, Eun-Young Kho<sup>2</sup>, Andrea Pavia-Jiménez<sup>4</sup>, Michael Fulkerson<sup>1</sup>, Alberto DiazdeLeon<sup>1</sup>, Qing Yuan<sup>1</sup>, Ivan E Dimitrov<sup>5</sup>, Takeshi Yokoo<sup>1</sup>, Jin Ye<sup>6</sup>, Matthew Mitsche<sup>6</sup>, Hyeonwoo Kim<sup>6</sup>, Jeffrey McDonald<sup>6</sup>, Yin Xi<sup>1</sup>, Ananth J Madhuranthakam<sup>1</sup>, Robert E Lenkinski<sup>1</sup>, Jeffrey A Cadeddu<sup>7</sup>, Vitaly Margulis<sup>7</sup>, James Brugarolas<sup>8</sup>, Ralph J Deberardinis<sup>2</sup>, and Ivan Pedrosa<sup>1</sup>

<sup>1</sup>Radiology, UT Southwestern Medical Center, Dallas, TX, United States, <sup>2</sup>Children's Medical Center Research Institute, UT Southwestern Medical Center, Dallas, TX, United States, <sup>3</sup>Pathology, UT Southwestern Medical Center, Dallas, TX, United States, <sup>4</sup>Internal Medicine, UT Southwestern Medical Center, Dallas, TX, United States, <sup>5</sup>Philips Medical Systems, Cleveland, OH, United States, <sup>6</sup>Molecular Genetics, UT Southwestern Medical Center, Dallas, TX, United States, <sup>7</sup>Urology, UT Southwestern Medical Center, Dallas, TX, United States, <sup>8</sup>Internal Medicine & Kidney Cancer Program, UT Southwestern Medical Center, Dallas, TX, United States

123

13:45

### Liver Fat Reduction Following Bariatric Weight Loss Surgery is Greater in the Right Lobe of the Liver



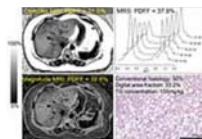
Soudabeh Fazeli Dehkordy<sup>1</sup>, Tanya Wolfson<sup>2</sup>, Cheng William Hong<sup>1</sup>, Alexandra Schlein<sup>1</sup>, Yesenia Covarrubias<sup>1</sup>, Jennifer Cui<sup>1</sup>, Ethan Z Sy<sup>1</sup>, Adrija Mamidipalli<sup>1</sup>, Gavin Hamilton<sup>1</sup>, Scott B Reeder<sup>3</sup>, and Claude B Sirlin<sup>1</sup>

<sup>1</sup>Liver Imaging Group, Department of Radiology, University of California San Diego, San Diego, CA, United States, <sup>2</sup>Computational and Applied Statistics Laboratory, University of California San Diego, San Diego, CA, United States, <sup>3</sup>Department of Radiology, Medical Physics, Biomedical Engineering, Medicine, and Emergency Medicine, University of Wisconsin Madison, Madison, WI, United States

124

13:45

### In Vivo Biochemical and Histological Validation of Proton Density Fat Fraction as a Quantitative Biomarker of Hepatic Steatosis



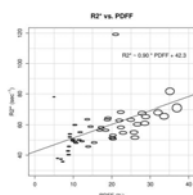
Scott B Reeder<sup>1,2,3,4,5</sup>, Curtis N Wiens<sup>1</sup>, Nathan Artz<sup>1,6</sup>, Jeffrey B Schwimmer<sup>7</sup>, Rashmi Agni<sup>8</sup>, Rao Watson<sup>8</sup>, Tanya Wolfson<sup>9</sup>, Anthony Gamst<sup>10</sup>, Guilherme Campos<sup>11,12</sup>, Santiago Horgan<sup>13</sup>, Luke Funk<sup>12</sup>, Garth Jacobsen<sup>13</sup>, Jacob Greenberg<sup>12</sup>, Alexandra Schlein<sup>14</sup>, Yesenia Covarrubias<sup>14</sup>, Jonathan C Hooker<sup>14</sup>, Michael S Middleton<sup>14</sup>, Gavin Hamilton<sup>14</sup>, Benjamin Ratliff<sup>1,3</sup>, Alan B McMillan<sup>1</sup>, Diego Hernando<sup>1,2</sup>, and Claude B Sirlin<sup>14</sup>

<sup>1</sup>Radiology, University of Wisconsin, Madison, WI, United States, <sup>2</sup>Medical Physics, University of Wisconsin, Madison, WI, <sup>3</sup>Biomedical Engineering, University of Wisconsin, Madison, WI, United States, <sup>4</sup>Medicine, University of Wisconsin, Madison, WI, United States, <sup>5</sup>Emergency Medicine, University of Wisconsin, Madison, WI, United States, <sup>6</sup>Diagnostic Imaging, St. Jude Children's Research Hospital, <sup>7</sup>Pediatrics, University of California, San Diego, <sup>8</sup>Pathology, University of Wisconsin, <sup>9</sup>San Diego Super Computer Center, University of California, San Diego, <sup>10</sup>Mathematics, University of California, San Diego, <sup>11</sup>Surgery, Virginia Commonwealth University, Richmond, VA, United States, <sup>12</sup>Surgery, University of Wisconsin, Madison, WI, <sup>13</sup>Surgery, University of California, San Diego, San Diego, CA, United States, <sup>14</sup>Radiology, University of California, San Diego

125



13:45



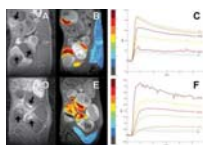
### Hepatic MRI-PDFF is positively correlated with R2\* across a range of fat spectral models

Cheng William Hong<sup>1</sup>, Adrija Mamidipalli<sup>1</sup>, Jonathan C Hooker<sup>1</sup>, Gavin Hamilton<sup>1</sup>, Tanya Wolfson<sup>2</sup>, Soudabeh Fazeli Dehkordy<sup>1</sup>, Michael S Middleton<sup>1</sup>, Scott B Reeder<sup>3</sup>, Rohit Loomba<sup>4</sup>, and Claude B Sirlin<sup>1</sup>

<sup>1</sup>Liver Imaging Group, Department of Radiology, University of California, San Diego, San Diego, CA, United States, <sup>2</sup>Computational and Applied Statistics Laboratory, University of California, San Diego, San Diego, CA, United States, <sup>3</sup>Departments of Radiology, Medical Physics, Biomedical Engineering, Medicine, and Emergency Medicine, University of Wisconsin, Madison, Madison, WI, United States, <sup>4</sup>NAFLD Research Center, Division of Gastroenterology, Department of Medicine, University of California, San Diego, San Diego, CA, United States

126

13:45



### Anatomical and functional deficits of the placenta identified by MRI in a rat model of preeclampsia

Emily Alexandria Waters<sup>1</sup>, Pamela Monahan<sup>2</sup>, Chad R Haney<sup>1</sup>, Michael Kevin Fritsch<sup>3</sup>, Thomas J Meade<sup>4</sup>, and Kelly E Mayo<sup>2</sup>

<sup>1</sup>Center for Advanced Molecular Imaging, Northwestern University, Evanston, IL, United States, <sup>2</sup>Molecular Biosciences, Northwestern University, Evanston, IL, United States, <sup>3</sup>Pathology, Northwestern University Feinberg School of Medicine, Chicago, IL, United States, <sup>4</sup>Chemistry, Molecular Biosciences, and Neurobiology, Northwestern University, Evanston, IL, United States



## Power Pitch

# Pitch: Highlights of Multiparametric Acquisition & Reconstruction

Power Pitch  
Theater B -  
Exhibition Hall

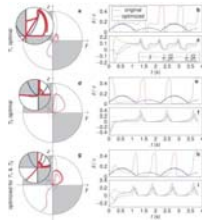
Monday 13:45 - *Moderators: Martijn Cloos & Mariya Doneva* (no CME credit)  
14:45

---

127



13:45



### Relaxation in Polar Coordinates: Analysis and Optimization of MR-Fingerprinting

Jakob Assländer<sup>1,2</sup>, Daniel K Sodickson<sup>1,2</sup>, Riccardo Lattanzi<sup>1,2</sup>, and Martijn A Cloos<sup>1,2</sup>

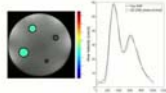
<sup>1</sup>Dept. of Radiology - Bernard and Irene Schwartz Center for Biomedical Imaging, New York University School of Medicine, New York, NY, United States, <sup>2</sup>Dept. of Radiology - Center for Advanced Imaging Innovation and Research, New York University School of Medicine, New York, NY, United States

---

128



13:45



### Quantification of Flow by Magnetic Resonance Fingerprinting

Sebastian Flassbeck<sup>1</sup>, Simon Schmidt<sup>1</sup>, Mathies Breithaupt<sup>1,2</sup>, Peter Bachert<sup>1</sup>, Mark E. Ladd<sup>1</sup>, and Sebastian Schmitter<sup>1,3</sup>

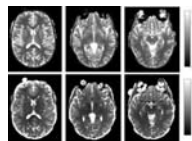
<sup>1</sup>Medical Physics in Radiology, German Cancer Research Center (DKFZ), Heidelberg, Germany, <sup>2</sup>Institute for Forensic Medicine and Traffic Medicine, Germany, <sup>3</sup>Physikalisch-Technische Bundesanstalt (PTB), Braunschweig and Berlin, Germany

---

129



13:45



### Applications of Low Rank Modeling to Fast 3D Magnetic Resonance Fingerprinting (MRF)

Dan Ma<sup>1</sup>, Eric Y. Pierre<sup>2</sup>, Debra McGivney<sup>1</sup>, Bhairav Mehta<sup>1</sup>, Yong Chen<sup>1</sup>, Yun Jiang<sup>1</sup>, and Mark Griswold<sup>1</sup>

<sup>1</sup>Radiology, Case Western Reserve University, Cleveland, OH, United States, <sup>2</sup>The Florey Institute of Neuroscience and Mental Health, Melbourne, Australia

---

130

13:45

### Magnetic Resonance Fingerprint Compression with Multiple Channel Transmission

Riccardo Lattanzi<sup>1,2</sup>, Bei Zhang<sup>1</sup>, Florian Knoll<sup>1</sup>, Jakob Assländer<sup>1</sup>, and Martijn Cloos<sup>1</sup>

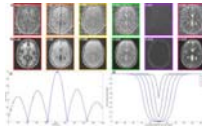




135

13:45

### Accelerated Magnetic Resonance Fingerprinting using Soft-weighted key-Hole (MRF-SOHO)



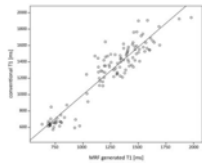
Gastao Cruz<sup>1</sup>, Andreia S. Gaspar<sup>1</sup>, Tom Bruijnen<sup>2</sup>, René Botnar<sup>1</sup>, and Claudia Prieto<sup>1</sup>

<sup>1</sup>Division of Imaging Sciences and Biomedical Engineering, King's College London, London, United Kingdom, <sup>2</sup>Center for image sciences, University Medical Center Utrecht, Utrecht, Netherlands

136

13:45

### Magnetic Resonance Fingerprinting - Evaluation of Brain Gliomas in Comparison to a Conventional Advanced Tumor Protocol - Preliminary Study



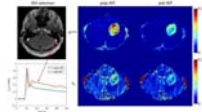
Siegfried Trattnig<sup>1,2</sup>, Wolfgang Bogner<sup>1</sup>, Bernhard Strasser<sup>1</sup>, Peter Bär<sup>1</sup>, Simone Kitzer<sup>1</sup>, Pavol Szomolanyi<sup>1</sup>, Matthias Nittka<sup>3</sup>, Wolfgang Marik<sup>4</sup>, Martin Zalaudek<sup>1</sup>, Markus Schreiner<sup>1</sup>, and Elisabeth Springer<sup>1</sup>

<sup>1</sup>Department of Biomedical Imaging and Image-guided Therapy, Medical University of Vienna, High Field MR Center, Vienna, Austria, <sup>2</sup>Christian Doppler Laboratory for Clinical Molecular MR Imaging, Vienna, Austria, <sup>3</sup>Siemens Healthineers, Erlangen, Germany, <sup>4</sup>Department of Biomedical Imaging and Image-guided Therapy, Medical University of Vienna, Vienna, Austria

137

13:45

### Joint estimation of arterial input function and tracer kinetic parameters from under-sampled DCE-MRI



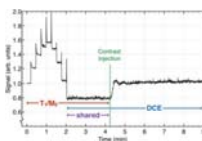
Yi Guo<sup>1</sup>, Sajan Goud Lingala<sup>1</sup>, R Marc Lebel<sup>2</sup>, and Krishna S Nayak<sup>1</sup>

<sup>1</sup>Electrical Engineering, University of Southern California, Los Angeles, CA, United States, <sup>2</sup>GE Healthcare, Calgary, AB, Canada

138

13:45

### Highly accelerated DCE imaging with integrated T1 mapping



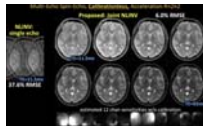
R Marc Lebel<sup>1,2,3</sup>, Yi Guo<sup>4</sup>, Sajan Goud Lingala<sup>4</sup>, Richard Frayne<sup>2,3</sup>, and Krishna S Nayak<sup>4</sup>

<sup>1</sup>GE Healthcare, Calgary, AB, Canada, <sup>2</sup>Radiology, University of Calgary, Calgary, AB, Canada, <sup>3</sup>Seaman Family Centre, Calgary, AB, Canada, <sup>4</sup>Electrical Engineering, University of Southern California, Los Angeles, CA, United States

139

13:45

### Calibrationless Parallel Imaging in Multi Echo/Contrast Data



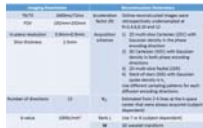
Berkin Bilgic<sup>1</sup>, Bo Zhao<sup>1</sup>, Itthi Chatnuntawech<sup>2</sup>, Lawrence L Wald<sup>1</sup>, and Kawin Setsompop<sup>1</sup>

<sup>1</sup>Martinos Center for Biomedical Imaging, Charlestown, MA, United States, <sup>2</sup>National Nanotechnology Center, Pathum Thani, Thailand

140

13:45

**Accelerated Cardiac Diffusion Tensor Imaging Using a Joint Low-Rank and Sparsity Constraint**



Sen Ma<sup>1,2</sup>, Christopher Nguyen<sup>1</sup>, Anthony Christodoulou<sup>1,3</sup>, Daniel Luthringer<sup>4</sup>, Jon Kobashigawa<sup>3</sup>, and Debiao Li<sup>1,2</sup>

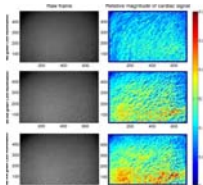
<sup>1</sup>Biomedical Imaging Research Institute, Cedars-Sinai Medical Center, Los Angeles, CA, United States, <sup>2</sup>Department of Bioengineering, University of California, Los Angeles, Los Angeles, CA, United States, <sup>3</sup>Heart Institute, Cedars-Sinai Medical Center, Los Angeles, CA, United States, <sup>4</sup>Department of Pathology, Cedars-Sinai Medical Center, Los Angeles, CA, United States

141



13:45

**An open-source hardware and software system for video-gated MRI**



Nicolai Spicher<sup>1</sup>, Stephan Orzada<sup>2</sup>, Stefan Maderwald<sup>2</sup>, Markus Kukuk<sup>1</sup>, and Mark E Ladd<sup>2,3</sup>

<sup>1</sup>University of Applied Sciences and Arts Dortmund, Dortmund, Germany, <sup>2</sup>Erwin L. Hahn Institute for Magnetic Resonance Imaging, University Duisburg-Essen, Essen, Germany, <sup>3</sup>Division of Medical Physics in Radiology, German Cancer Research Center, Heidelberg, Germany

Oral

**Cerebrovascular Disease: Intracranial & Extracranial**

Room 310

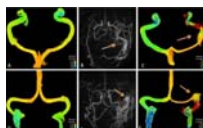
Monday 13:45 - 15:45 Moderators: Ian Marshall & Danny Wang

142



13:45

**4D Flow MRI for Assessment of Venous Pressure in Dural Arteriovenous Fistulas**



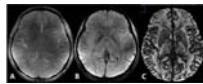
Leonardo A Rivera Rivera<sup>1</sup>, Zachary Clark<sup>2</sup>, Kevin M Johnson<sup>1,2</sup>, Patrick Turski<sup>1,2</sup>, and Oliver Wieben<sup>1,2</sup>

<sup>1</sup>Dept. of Medical Physics, University of Wisconsin-Madison, MADISON, WI, United States, <sup>2</sup>Dept. of Radiology, University of Wisconsin-Madison, Madison, WI, United States

Dural arteriovenous fistulas (DAVFs) are vascular malformations that can present aggressively. Venous hypertension is the pathophysiologic mechanism thought to be responsible for aggressive presentation. 4D flow MRI has demonstrated success generating pressure maps from velocity data in vessels. In this work we measure relative pressure in the dural sinuses in DAVFs patients using 4D flow MRI. Results support the hypothesis that DAVFs result in venous hypertension which may be the mechanism ultimately leading to aggressive presentation. 4D flow MRI allows blood flow directionality assessment along the dural sinuses, which helps to detect retrograde flow and classify the severity of DAVFs.

143

13:57



Enhanced detection of cerebral arterial system with USPIO-enhanced MRI

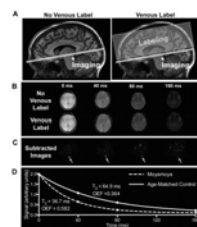
Yulin Ge<sup>1</sup>, Jean-Christophe Brisset<sup>2</sup>, Saifeng Liu<sup>3</sup>, and E. Mark Haacke<sup>3</sup>

<sup>1</sup>Radiology, New York University School of Medicine, New York, NY, United States, <sup>2</sup>Radiology, New York University School of Medicine, <sup>3</sup>Wayne State University

Although small arterial system plays a key role in delivering oxygen and glucose to brain tissue, the in vivo detection is still challenging. Using a low dose of ultra-small-superparamagnetic-iron-oxide (USPIO) contrast agent, it will induce susceptibility contrast in the arterial blood, which enhances the small arteries visibility on susceptibility weighted imaging. This study has demonstrated its feasibility in human brain. Such technique has potential to unveil underlying microvascular abnormalities in neurovascular diseases that cannot be done in vivo with any other conventional method in use today.

144

14:09



T2-relaxation-under-spin-tagging (TRUST) and Arterial Spin Labeling MRI elucidate discrepant hemo-metabolic mechanisms underlying elevated oxygen extraction fraction (OEF) in moyamoya and sickle cell anemia (SCA) patients

Jennifer M Watchmaker<sup>1</sup>, Meher R Juttukonda<sup>1</sup>, Larry T Davis<sup>1</sup>, Allison O Scott<sup>1</sup>, Carlos C Faraco<sup>1</sup>, Melissa C Gindville<sup>2</sup>, Lori C Jordan<sup>2</sup>, Petrice M Cogswell<sup>1</sup>, Angela L Jefferson<sup>3</sup>, Howard S Kirshner<sup>4</sup>, and Manus J Donahue<sup>1,4,5</sup>

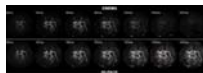
<sup>1</sup>Radiology & Radiological Sciences, Vanderbilt University Medical Center, Nashville, TN, United States, <sup>2</sup>Department of Pediatrics, Division of Pediatric Neurology, Vanderbilt University Medical Center, <sup>3</sup>Vanderbilt Memory & Alzheimer's Center, Vanderbilt University Medical Center, Nashville, TN, <sup>4</sup>Department of Neurology, Vanderbilt University Medical Center, <sup>5</sup>Department of Psychiatry, Vanderbilt University Medical Center

T<sub>2</sub>-relaxation-under-spin-tagging (TRUST-MRI) was performed in patients with intracranial stenosis due to moyamoya for determination of whole-brain oxygen extraction fraction (OEF). Elevated OEF was observed in this group compared to controls. In <sup>15</sup>O PET studies in individuals with intracranial stenosis, it has been shown that OEF increases regionally when cerebral blood volume (CBV) is inadequate to maintain cerebral blood flow (CBF) over a normal range, and importantly that regionally elevated OEF and CBV may be prognostic for recurrent stroke risk. This work has motivated the development and application of TRUST-MRI for use in patients with intracranial stenosis at risk for stroke.

---

145

14:21



4D MR Angiography with Pseudo-Continuous Arterial Spin Labelling Combined with CENTRA-Keyhole (4D-PACK): Visualization of Distal Cerebral Arteries in Moyamoya Disease

Osamu Togao<sup>1</sup>, Akio Hiwatashi<sup>1</sup>, Makoto Obara<sup>2</sup>, Koji Yamashita<sup>1</sup>, Ryotaro Kamei<sup>1</sup>, and Hiroshi Honda<sup>1</sup>

<sup>1</sup>Clinical Radiology, Graduate School of Medical Sciences, Kyushu University, Fukuoka, Japan, <sup>2</sup>Philips Electronics Japan, Tokyo, Japan

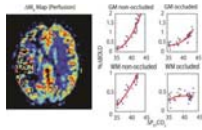
In the present study, we demonstrated the clinical utility of 4D-MR angiography with pCASL combined with CENTRA-keyhole (4D-PACK) in Moyamoya disease by comparing with a well-established pulsed ASL-based 4D-MRA called contrast inherent inflow enhanced multi-phase angiography (CINEMA). 4D-PACK provided higher CNRs than CINEMA in distal MCA branches in later phases indicating that 4D-PACK enables better visualizations of distal cerebral arteries supplied by collateral vessels during a long transit time. This could be due to higher flow signal obtained with pCASL and less saturation effect after labeling. 4D-PACK can be a non-invasive clinical tool in assessing hemodynamics in Moyamoya disease.

---

146

14:33

Probing the BOLD-CVR response to progressive hypercapnia in patients with uni-lateral carotid artery occlusions



Alex Bhogal<sup>1</sup>, Jeroen C.W. Siero<sup>1,2</sup>, Hans Hoogduin<sup>1</sup>, Peter R Luijten<sup>1</sup>, Jeroen Hendrikse<sup>3</sup>, and Jill B De Vis<sup>4</sup>

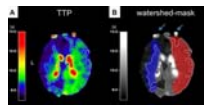
<sup>1</sup>Radiology, University Medical Center Utrecht, Utrecht, Netherlands, <sup>2</sup>Spinoza Center for Neuroimaging, Amsterdam, Netherlands, <sup>3</sup>Radiology, University Medical Center Utrecht, Netherlands, <sup>4</sup>University Medical Center Utrecht, Netherlands

We examine the BOLD-CVR response to a progressively increasing vascular stimulus between individuals with carotid artery occlusions and healthy, age/gender-matched controls. Using this paradigm, we aim to understand finer-scale interactions between impaired versus healthy cerebral hemispheres at different vascular stimulus magnitudes.

147



14:45



Analysis of cerebrovascular watershed areas in patients with high-grade carotid artery stenosis using DSC-based time-to-peak maps

Vanessa Griese<sup>1</sup>, Stephan Kaczmarz<sup>1</sup>, Anne Kluge<sup>1,2</sup>, Kim van de Ven<sup>3</sup>, Michael Helle<sup>4</sup>, Hendrik Kooijman-Kurfuerst<sup>4</sup>, Claus Zimmer<sup>1</sup>, Christian Sorg<sup>1,5</sup>, Jens Göttler<sup>1</sup>, and Christine Preibisch<sup>1,5,6</sup>

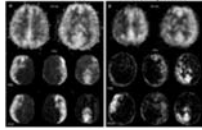
<sup>1</sup>Neuroradiology, Technical University of Munich, Munich, Germany, <sup>2</sup>Radiooncology and Radiotherapy, Charité Berlin, Berlin, Germany, <sup>3</sup>Philips Healthcare, Best, Netherlands, <sup>4</sup>Philips Research, Hamburg, Germany, <sup>5</sup>TUM Neuroimaging Center (TUM-NIC), Technical University of Munich, Munich, Germany, <sup>6</sup>Neurology, Technical University of Munich, Munich, Germany

Internal carotid artery stenosis (ICAS) is one of the leading causes for thromboembolic and hemodynamic cerebral infarction. Here, we present data from an ongoing clinical MRI-study in patients with asymptomatic, high-grade ICAS and healthy controls. Our major aim was to establish a method to delineate individual watershed areas in patients and controls using MRI-based dynamic susceptibility contrast (DSC) time-to-peak (TTP) maps, also including the anatomical information of magnetic resonance angiography (MRA) to define individual vascular territories. Watershed areas were enlarged and shifted in many of the vascular territories of stenosed carotid arteries, being verified by ss-pCASL in a subgroup.

148

14:57

Effective collateral circulation may related with better perfusion restoration after carotid endarterectomy (CEA): a pilot territory ASL (tASL) study



Tian-ye Lin<sup>1</sup>, Yue-lei Lv<sup>1</sup>, Zhi-chao Lai<sup>2</sup>, Hui You<sup>1</sup>, Bo Hou<sup>1</sup>, Bing Wu<sup>3</sup>, Jian-xun Qu<sup>3</sup>, Chang-wei Liu<sup>2</sup>, and Feng Feng<sup>1</sup>

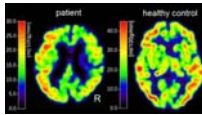
<sup>1</sup>Radiology, Peking Union Medical College Hospital, Beijing, People's Republic of China, <sup>2</sup>Vascular surgery, Peking Union Medical College Hospital, Beijing, People's Republic of China, <sup>3</sup>GE Healthcare, MR Research China, Beijing, Beijing, People's Republic of China

Flow territories normalization was observed in patients underwent carotid endarterectomy (CEA). To investigate whether collateral flow associated with the redistribution of blood we performed 3D ASL and tASL on 25 patients prior to (PRE) and after (POST) surgery. Collateral flow was read as the presence of arterial transit artifact (ATA) on 3D ASL images. Alteration of flow territories was determined by comparing the PRE and POST tASL images. Our study demonstrated that good collateral compensation shown in ASL was associated with normalization of tASL flow territories after CEA.

---

149

15:09



One-sided hypoperfusion is associated with contralateral attention deficits in asymptomatic high-grade carotid stenosis patients.

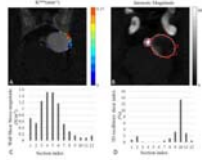
Jens Goettler<sup>1</sup>, Stephan Kaczmarz<sup>1</sup>, Rachel Nuttall<sup>1</sup>, Vanessa Griese<sup>1</sup>, Hendrik Kooijman<sup>2</sup>, Michael Helle<sup>2</sup>, Kim van de Ven<sup>3</sup>, Claus Zimmer<sup>1</sup>, Kathrin Finke<sup>4</sup>, Christian Sorg<sup>1</sup>, and Christine Preibisch<sup>1</sup>

<sup>1</sup>Department of Neuroradiology, Technische Universität München, Munich, Germany, <sup>2</sup>Philips Healthcare, Hamburg, Germany, <sup>3</sup>Philips Healthcare, Best, Netherlands, <sup>4</sup>Neuro-cognitive Psychology Unit, Department Psychologie, Ludwig-Maximilians-Universität, Munich, Germany

Patients with clinically asymptomatic, high-grade internal carotid artery stenosis (ICAS) often show cognitive impairments, such as memory dysfunction and attention deficits. However, it is still unclear whether these symptoms are caused by potentially reversible cerebral hypoperfusion or rather by a general unchangeable vascular damage. Here, 17 patients with one-sided high-grade, asymptomatic ICAS and 26 age-matched healthy controls underwent an MRI scan, including pCASL to assess brain perfusion, and a computer-based visual attention test. Patients show distinct unilateral cerebral hypoperfusion being significantly associated with contralateral attention deficits. Data indicate that chronic cerebral hypoperfusion in high-grade ICAS impairs cognitive function.

---



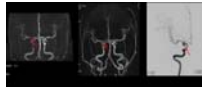


### Saccular intracranial aneurysm wall permeability and shear stress distribution: a further insight into rupture pathogenesis

Xian Liu<sup>1</sup>, Yu Chen<sup>1</sup>, Haikun Qi<sup>1</sup>, Peng Liu<sup>2</sup>, Yunduo Li<sup>1</sup>, Xiaole Wang<sup>1</sup>, Le He<sup>1</sup>, Qiang Zhang<sup>1</sup>, Zhensen Chen<sup>1</sup>, Rui Li<sup>1</sup>, Youxiang Li<sup>2</sup>, Chun Yuan<sup>3</sup>, and Huijun Chen<sup>1</sup>

<sup>1</sup>Center for Biomedical Imaging Research, Department of Biomedical Engineering, School of Medicine, Tsinghua University, Beijing, People's Republic of China, <sup>2</sup>Department of Interventional Neuroradiology, Beijing Neurosurgical Institute and Beijing Tiantan Hospital, Capital Medical University, Beijing, People's Republic of China, <sup>3</sup>Department of Radiology, University of Washington, Seattle, WA, United States

The purpose of this study is to explore the relationship between aneurysm wall permeability and the hemodynamic conditions of intracranial aneurysm (IA). The results showed that hot spot of IA wall permeability was spatially related with significantly lower wall shear stress magnitude and higher oscillatory shear index, which suggests the pathology of IA might be an interaction of both factors, and IA wall permeability could be a potential method for IA rupture risk assessment.



### Investigation of zero TE ASL MRA in the follow-up after endovascular treatment of intracranial aneurysm at 1.5T

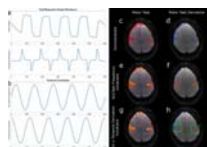
yan song<sup>1</sup>, Peng Qi, Juan Huang, Sheng Jiao, Tan Guo, Min Chen, Daming Wang, Jing Zhang, Bing Wu, and Zhe lin Luo

<sup>1</sup>Beijing Hospital, Beijing, People's Republic of China

It is necessary to follow up the intracranial aneurysms treated with coil or/and stent for recanalization or remnant. TOF MRA, though performed well, is susceptible to metallic artifact and flow artifact. ASL MRA with zero TE acquisition has potential advantages. The purpose of this study was to evaluate the performance of ASL MRA by comparing with TOF MRA, using DSA as gold standard. It was demonstrated that ASL MRA featured significantly better consistency with DSA for aneurysm remnant diagnosis and led to superior image quality in the presence of intra-stent lumen as compared to TOF at 1.5T.

152

13:45



### Accelerated rank-constrained fMRI data reconstruction informed by external temporal measures

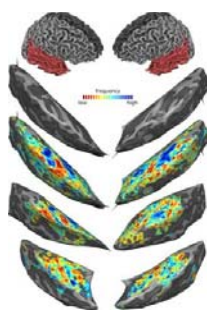
Mark Chiew<sup>1</sup>, Nadine N Graedel<sup>1</sup>, Jostein Holmgren<sup>2</sup>, Dean Fido<sup>1</sup>, Catherine E Warnaby<sup>1</sup>, and Karla L Miller<sup>1</sup>

<sup>1</sup>FMRIB Centre, University of Oxford, Oxford, United Kingdom, <sup>2</sup>Institute of Psychology, University of Oslo

Reconstruction of highly under-sampled fMRI data using low-rank constraints can suffer from loss of fidelity at high acceleration factors, or when signals are relatively weak. We introduce a method for improving reconstruction fidelity using external constraints, i.e., informative signals that are not data-derived. We show that this improves fMRI reconstruction quality in a number of conditions, including detecting subtle latency shifts between brain regions, and improving resting state network characterization using simultaneously acquired EEG information. We further show that this approach works with noisy or approximate constraints, and the derived benefit is commensurate with the information content they provide.

153

13:57



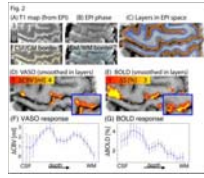
### Submillimeter 9.4 T fMRI of the human auditory cortex with tones, ripples, and real life sounds

Valentin G. Kemper<sup>1</sup>, Elia Formisano<sup>1</sup>, Sudhir Ramanna<sup>2</sup>, Essa Yacoub<sup>2</sup>, and Federico De Martino<sup>1,2</sup>

<sup>1</sup>Cognitive Neuroscience, Maastricht University, Maastricht, Netherlands, <sup>2</sup>Center for Magnetic Resonance Research, University of Minnesota, MN, United States

This study demonstrates auditory human fMRI conducted at 9.4T field strength and submillimeter resolution for the first time. Tonotopic maps were measured robustly and reliably. Further, cortical regions with preference for natural sound categories were delineated. We generated ripple control sounds that closely match low level acoustical properties of natural sounds in four natural sound categories, such that the original category is not recognizable. We show that, in areas preferring speech sounds over other natural sounds, ripple control sounds of speech elicit stronger responses than ripple control sounds of non-speech. This indicates tuning to the low-level acoustical properties of speech.



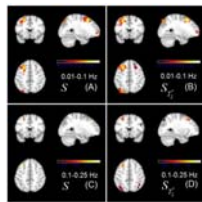


### Ultra-high resolution blood volume fMRI and BOLD fMRI in humans at 9.4 T: Capabilities and Challenges

Laurentius Huber<sup>1</sup>, Desmond H Y Tse<sup>2</sup>, Kashyap Sriranga<sup>2</sup>, Christopher Wiggins<sup>3</sup>, Kâmil Uludağ<sup>2</sup>, Peter A Bandettini<sup>1</sup>, Benedikt A Poser<sup>2</sup>, and Dimo Ivanov<sup>2</sup>

<sup>1</sup>SFIM, NIMH, Bethesda, MD, United States, <sup>2</sup>MBIC, Maastricht University, Netherlands, <sup>3</sup>Scannexus, Maastricht, Netherlands

fMRI at ultra-high field strengths of 9.4 T allows functional imaging with submillimeter spatial resolutions. CBV sensitive VASO-fMRI has been suggested to be weighted towards locally specific microvasculature changes close to neural activity changes. Hence, we sought to combine the high physiological specificity of CBV-fMRI with the high signal-to-noise ratio of 9.4 T imaging. In our experiments, we could identify and discuss numerous technical challenges of CBV-fMRI at 9.4 T regarding constraints of RF fields and VASO contrast generation. With the application of advanced imaging methods, we show promising functional results with clearly visible cortical depth-dependent activity patterns.



### Revealing the high frequency brain networks with multiband multi-echo fMRI data

Wenchao Yang<sup>1</sup>, Burak Akin<sup>1</sup>, Fei Wang<sup>1</sup>, Jürgen Hennig<sup>1</sup>, and Pierre LeVan<sup>1</sup>

<sup>1</sup>Dept. of Radiology · Medical Physics, University Medical Center Freiburg, Freiburg, Germany

The high frequency networks are hard to be observed with standard fMRI data. Those networks were submerged in the non-BOLD signal and could not be observed with standard fMRI methods. In this work, Multiband Multi-echo (MBME) sequence is used to sample brain fluctuations in high frequency (TR=0.75). By using acquired 8 echoes, T2\* and I0 (initial intensity) values are calculated and fluctuations in the brain were separated into BOLD and non-BOLD. Results showed that there is an improved detection in several high frequency networks like LECN, dDMN, Language and high Visual networks by using the separated BOLD signal.



### Empirical Mode Decomposition and Frequency Characteristics of the Default Mode Network on Group fMRI Resting-State Data

Dietmar Cordes<sup>1,2</sup>, Muhammad Kaleem<sup>3</sup>, Xiaowei Zhuang<sup>1</sup>, Karthik Sreenivasan<sup>1</sup>, Zhengshi Yang<sup>1</sup>, and Virendra Mishra<sup>1</sup>

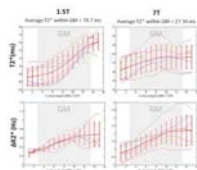
<sup>1</sup>Cleveland Clinic Lou Ruvo Center for Brain Health, LAS VEGAS, NV, United States, <sup>2</sup>University of Colorado Boulder, Boulder, CO, United States, <sup>3</sup>University of Management & Technology, Lahore, Pakistan

In this project, high-frequency contributions to functional connectivity of the Default Mode Network (DMN) are studied. Rather than relying on user-defined frequency bands, Empirical Mode Decomposition (EMD) is used to decompose the natural occurring frequency bands of the DMN. The novelty of our approach lies in the data-adaptive and user-independent decomposition of fMRI data using EMD, and identification of a resting-state network based on the frequency characteristics of intrinsic modes in the data, instead of using wavelet- or windowed-Fourier-transform methods. Results are shown for multiband MB8 resting-state data of a group of 22 healthy subjects.

157

14:45

An in vivo study of BOLD laminar responses as a function of echo time and magnetic field



Irati Markuerkiaga<sup>1</sup>, Lauren J Bains<sup>1</sup>, Jose P Marques<sup>1</sup>, and David G Norris<sup>1,2</sup>

<sup>1</sup>Donders Centre for Cognitive Neuroimaging, Nijmegen, Netherlands,

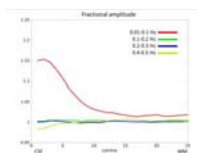
<sup>2</sup>Erwin L. Hahn Institute for Magnetic Resonance Imaging, Essen, Germany

In this study we evaluate the echo time of laminar BOLD responses of the human primary visual cortex at 1.5 and 7T. It is often assumed that lower magnetic field strengths are increasingly biased towards the signal arising from larger veins located towards the pial surface. In this study (performed with an isotropic resolution of 0.75mm) we found similar shaped laminar profiles at 1.5 and 7T.

158

14:57

Frequency signature of cortical laminar fMRI



Maria Guidi<sup>1</sup>, Irati Markuerkiaga<sup>2</sup>, Lauren Bains<sup>2</sup>, Laurentius Huber<sup>3</sup>, Harald E. Möller<sup>1</sup>, and David G. Norris<sup>2</sup>

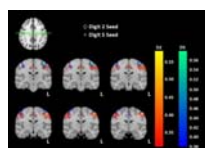
<sup>1</sup>Max Planck Institute for Human Cognitive and Brain Sciences, Leipzig, Germany, <sup>2</sup>Donders Centre for Cognitive Neuroimaging, Nijmegen, Netherlands, <sup>3</sup>NIMH, Bethesda, MD, United States

The nature of spontaneous oscillations in the blood oxygenation level dependent (BOLD) response is in the focus of current research. For resting-state network studies, the low-frequency band (0.01-0.1 Hz) is usually taken to be relevant for neuronal activity. However, this statement is based on low-resolution functional data, where the effect of the draining vasculature cannot always be characterized. This study investigates the distribution of the amplitude of resting-state BOLD fluctuations using a sub-millimeter resolution and shows that the low-frequency band is dominating at all cortical depths, but most of its power is located at the pial surface.

159



15:09



### Topographic Mapping of Resting State fMRI Data

Eleanor Barratt<sup>1</sup>, Michael Asghar<sup>1</sup>, Matthew Brookes<sup>1</sup>, and Susan Francis<sup>1</sup>

<sup>1</sup>*School of Physics, University of Nottingham, Nottingham, United Kingdom*

Task-based fMRI can provide robust somatotopic mapping of digits of the hand. Resting state fMRI (rs-fMRI) provides the ability to parcellate brain areas based on their connectivity. Here, we use simultaneous multislice to acquire high spatial resolution fMRI resting state data with a short TR to determine whether we can topographically map connectivity within the sensorimotor cortex. Seed based locations of the index finger (Digit 2) and little finger (Digit 5) are defined from somatotopic travelling wave and finger tapping tasks, and used to demonstrate significant topographic mapping in rs-fMRI data.

160

15:21



### Tonotopic mapping in the in vivo mouse via high resolution fMRI

Guilherme Blazquez Freches<sup>1</sup>, Cristina Chavarrias<sup>1</sup>, and Noam Shemesh<sup>1</sup>

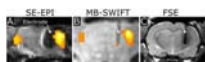
<sup>1</sup>*Champalimaud Neuroscience Programme, Champalimaud Centre for the Unknown, Lisbon, Portugal*

The rodent auditory system has been a popular research subject for electrophysiological studies for its complexity, fine tuning and adaptability. More recently, some studies on auditory Functional Magnetic Resonance Imaging (fMRI) in rats have surfaced, aiming to unravel this system's intricacies by capturing whole brain activity noninvasively. Auditory mapping in the mouse could be highly valuable given its importance vis-à-vis transgenic models and optogenetics. This study provides the first tonotopic mapping in the in vivo mouse via high resolution fMRI. We demonstrate robust activation in the auditory pathway, and specific tonotopy in several prominent regions along the pathway.

---

161

15:33



### MB-SWIFT functional MRI during deep brain stimulation in rats

Lauri Juhani Lehto<sup>1</sup>, Djaudat Idiyatullin<sup>1</sup>, Jinjin Zhang<sup>1</sup>, Lynn Utecht<sup>1</sup>, Gregor Adriany<sup>1</sup>, Michael Garwood<sup>1</sup>, Olli Gröhn<sup>1,2</sup>, Shalom Michaeli<sup>1</sup>, and Silvia Mangia<sup>1</sup>

<sup>1</sup>Center for Magnetic Resonance Research, University of Minnesota, Minneapolis, MN, United States, <sup>2</sup>A. I. Virtanen Institute for Molecular Sciences, University of Eastern Finland, Kuopio, Finland

Commercial electrodes used for Deep Brain Stimulation (DBS) cause severe artefacts in conventional echo based MRI. Here we show near artefact free functional MRI during DBS in rats using Multi-Band SWEEP Imaging with Fourier Transformation (MB-SWIFT) which allows acquisition at virtually zero-TE. MB-SWIFT showed strong responses in the somatosensory cortex while stimulating the ventromedial. The amplitude and extent of activation recorded with MB-SWIFT were similar with SE-EPI, although activation was flip angle dependent reflecting the possible influence of blood inflow. MB-SWIFT is a promising modality for fMRI in the presence of DBS leads or other severe susceptibility differences.

---

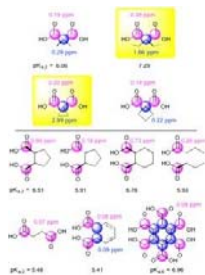
Oral

## Hyperpolarized <sup>13</sup>C Magnetic Resonance Imaging & Spectroscopy

Room 312

Monday 13:45 - 15:45 Moderators: Angus Lau & Rolf Schulte

---

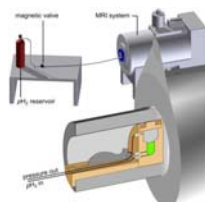


### Chemical Shift Imaging of pH with Hyperpolarized [2- $^{13}\text{C}$ ,D $_{10}$ ] Diethylmalonic Acid

David Korenchan<sup>1,2</sup>, Celine Taglang<sup>1</sup>, Cornelius von Morze<sup>1</sup>, Joseph Blecha<sup>1</sup>, Jeremy Gordon<sup>1</sup>, Peder Larson<sup>1,2</sup>, Henry VanBrocklin<sup>1</sup>, John Kurhanewicz<sup>1,2</sup>, David Wilson<sup>1</sup>, and Robert Flavell<sup>1</sup>

<sup>1</sup>Radiology and Biomedical Imaging, University of California, San Francisco, San Francisco, CA, United States, <sup>2</sup>Bioengineering, University of California, Berkeley, Berkeley, CA, United States

Imaging tumoral pH may aid in characterizing aggressiveness, metastasis, and therapeutic response. The study of hyperpolarized (HP)  $^{13}\text{C}$  chemical shift-based probes addresses some of the limitations of previously reported ratiometric methods, including HP  $^{13}\text{C}$  bicarbonate. We report the development of HP [2- $^{13}\text{C}$ ,D $_{10}$ ] diethylmalonic acid as a pH imaging agent, which exhibits a significant  $^{13}\text{C}$  chemical shift difference over the physiologic pH range. We demonstrate that this compound can be copolarized with *tert*-butanol to accurately measure pH in phantom studies. Furthermore, this HP compound showed high *in vivo* SNR in a murine model of prostate cancer.

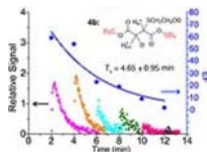


### Long-lasting, liquid-state $^{13}\text{C}$ hyperpolarization > 20 % generated in an MRI system within seconds enables fast $^{13}\text{C}$ imaging

Andreas Benjamin Schmidt<sup>1</sup>, Stephan Berner<sup>1</sup>, Waldemar Schimpf<sup>1</sup>, Christoph Müller<sup>1</sup>, Thomas Lickert<sup>2</sup>, Niels Schwaderlapp<sup>1</sup>, Stephan Knecht<sup>1</sup>, Jason Skinner<sup>1</sup>, Anna Dost<sup>1</sup>, Philipp Rovedo<sup>1</sup>, Jürgen Hennig<sup>1</sup>, Dominik von Elverfeldt<sup>1</sup>, and Jan-Bernd Hövener<sup>1,3</sup>

<sup>1</sup>University Medical Center Freiburg, Freiburg, Germany, <sup>2</sup>Fraunhofer Institute for Solar Energy Systems (ISE), Freiburg, Germany, <sup>3</sup>German Consortium for Cancer Research (DKTK), Heidelberg, Germany

Current methods for the production of hyperpolarized  $^{13}\text{C}$ -tracers require a dedicated, complex and costly polarizer device. Here we present, for the first time,  $^{13}\text{C}$ -hyperpolarization > 20% and *ex-vivo*  $^{13}\text{C}$ -MRI without an external polarizer, but by using the hardware of an MRI system instead: a simple, low-cost ( $\approx 1000\text{€}$ ) setup was built and high-field spin-order-transfer sequences were exploited to transfer the spin-order of parahydrogen to  $^{13}\text{C}$ ; the implementation on any multinuclear MRI system appears feasible. The tracer is produced near the application site and subsequent  $^{13}\text{C}$ -MRI is possible without transfer of the sample, at a fraction of the cost and complexity of external polarizers.

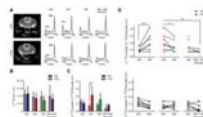


### Hyperpolarized Nuclear Spin Singlets. Opportunities for Polarization Storage. What Limits Their Lifetimes?

Alexej Jerschow<sup>1</sup>, Yuning Zhang<sup>1</sup>, Xueyou Duan<sup>1</sup>, Vladimir Sychrovsky<sup>2</sup>, and James Canary<sup>1</sup>

<sup>1</sup>New York University, New York, NY, United States, <sup>2</sup>Institute of Organic Chemistry and Biochemistry, Czech Academy of Sciences, Prague, Czech Republic

Hyperpolarization techniques have offered the prospect of higher sensitivity and fast imaging, as well as tracking of metabolism in real-time. Nuclear spin singlet states allow the storage of polarization for an extended period of time. Here we present results on the limiting factors for nuclear singlet state lifetimes, and methods by which they can be determined in organic molecules, which is important for designing appropriate contrast agents, or hyperpolarization techniques that track metabolites.



### Metabolic imaging of neuroinflammation in the cuprizone mouse model for Multiple Sclerosis using hyperpolarized [1-<sup>13</sup>C] pyruvate

Caroline Guglielmetti<sup>1,2,3</sup>, Chloe Najac<sup>2</sup>, Annemie Van der Linden<sup>3</sup>, Sabrina Ronen<sup>2,4</sup>, and Myriam Chaumeil<sup>1,2</sup>

<sup>1</sup>Department of Physical Therapy and Rehabilitation Science, University of California San Francisco, San Francisco, CA, United States, <sup>2</sup>Surbeck Laboratory of Advanced Imaging, Department of Radiology and Biomedical Imaging, University of California San Francisco, San Francisco, CA, United States, <sup>3</sup>Bio-Imaging Lab, Department Pharmaceutical, Veterinary and Biomedical Sciences, University of Antwerp, Antwerp, Belgium, <sup>4</sup>Surbeck Laboratory of Advanced Imaging, Department of Radiology and Biomedical Imaging, San Francisco, CA, United States

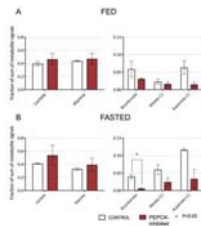
Our study demonstrates that metabolic imaging of hyperpolarized [1-<sup>13</sup>C] pyruvate can detect increased hyperpolarized lactate production *in vivo* in highly inflammatory white matter lesions in a preclinical model of Multiple Sclerosis. Increased lactate production was associated with the presence of pro-inflammatory macrophages upregulating pyruvate dehydrogenase kinase 1, as well as regional inhibition of pyruvate dehydrogenase, providing a likely mechanism for a decrease subsequent flux of pyruvate towards the Krebs cycle. Our study demonstrates that metabolic imaging of hyperpolarized [1-<sup>13</sup>C] pyruvate has high potential for *in-vivo* detection and monitoring of neuroinflammation levels during demyelination and remyelination.



14:33

### Effects of 3-MPA on *in vivo* hepatic metabolism of hyperpolarized [1-<sup>13</sup>C] pyruvate

Emine Can<sup>1</sup>, Hikari A.I. Yoshihara<sup>1,2</sup>, Jessica A.M. Bastiaansen<sup>1,2</sup>, Rolf Gruetter<sup>3,4</sup>, and Arnaud Comment<sup>1</sup>



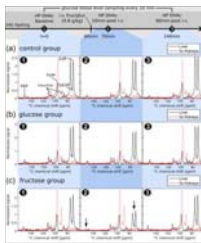
<sup>1</sup>Institute of Physics, Ecole Polytechnique Fédérale de Lausanne, Lausanne, Switzerland, <sup>2</sup>Division of Cardiology, University Hospital Lausanne (CHUV), Lausanne, Switzerland, <sup>3</sup>Laboratory for Functional and Metabolic Imaging, Ecole Polytechnique Fédérale de Lausanne, Lausanne, Switzerland, <sup>4</sup>Department of Radiology, University of Lausanne (UNIL), Lausanne, Switzerland

Ex vivo and *in vivo* studies on liver metabolism using hyperpolarized [1-<sup>13</sup>C]pyruvate report do not agree on whether hyperpolarized bicarbonate metabolite production results from pyruvate oxidation or gluconeogenesis. This study tested the ability of hyperpolarized [1-<sup>13</sup>C] pyruvate to probe gluconeogenesis in the liver of intact rats. While conversion to hyperpolarized bicarbonate was detected in the liver of fasted rats, treatment with the phosphoenolpyruvate carboxykinase inhibitor 3-mercaptopicolinic acid resulted in 7-fold lower levels. This result supports the notion that hepatic gluconeogenic metabolism can indeed be directly probed *in vivo* with hyperpolarized pyruvate.

14:45

### [2-<sup>13</sup>C]dihydroxyacetone as a real-time, *in vivo* sensor of acute hepatic and renal metabolic response after a fructose and glucose challenge

Irene Marco-Rius<sup>1</sup>, Cornelius Von Morze<sup>1</sup>, Renuka Sriram<sup>1</sup>, Peng Cao<sup>1</sup>, Gene-Yuan Chang<sup>2</sup>, Eugene Milshteyn<sup>1</sup>, Robert A. Bok<sup>1</sup>, Michael A. Ohliger<sup>1</sup>, David Pearce<sup>2</sup>, John Kurhanewicz<sup>1</sup>, Peder E. Z. Larson<sup>1</sup>, Dan B. Vigneron<sup>1</sup>, and Matthew Merritt<sup>3</sup>

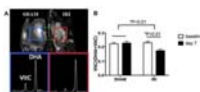


<sup>1</sup>Department of Radiology and Biomedical Imaging, University of California San Francisco, San Francisco, CA, United States, <sup>2</sup>Department of Medicine, Division of Nephrology, University of California San Francisco, San Francisco, CA, United States, <sup>3</sup>Department of Biochemistry and Molecular Biology, University of Florida, Gainesville, FL, United States

Hyperpolarized [2-<sup>13</sup>C]dihydroxyacetone was used to investigate the hepatic and renal metabolic response to acute intravenous administration of glucose or fructose in rats in vivo. <sup>13</sup>C-MR spectra were acquired before, 10 minutes and 80 minutes after the carbohydrate solution delivery. Changes in the metabolic products phosphoenolpyruvate (PEP) and glycerol 3-phosphate (G3P) were detected after fructose injection, while no metabolic perturbation was detected after the glucose injection. The observed effects possibly include ATP depletion and changes in the unlabelled pool sizes of glycolytic intermediates.

168

14:57



### Hyperpolarized <sup>13</sup>C Magnetic Resonance Evaluation of Renal Ischemia Reperfusion Injury in a Murine Model

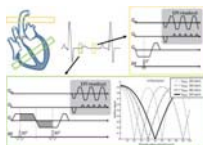
Celine Baligand<sup>1</sup>, Hecong Qin<sup>2</sup>, Aisha True-Yasaki<sup>2</sup>, Jeremy W. Gordon<sup>2</sup>, Cornelius VonMorze<sup>2</sup>, Justin DeLos Santos<sup>2</sup>, Joy P. Walker<sup>3</sup>, David M. Wilson<sup>2</sup>, Robert L. Raffai<sup>3</sup>, John Kurhanewicz<sup>2</sup>, David H. Lovett<sup>4</sup>, and Zhen J. Wang<sup>2</sup>

<sup>1</sup>Department of Radiology, Leiden University Medical Center, C.J. Gorter Center for High-field MRI, Leiden, Netherlands, <sup>2</sup>Department of Radiology and Biomedical Imaging, University of California San Francisco, San Francisco, CA, United States, <sup>3</sup>Department of Surgery, University of California San Francisco, San Francisco, CA, United States, <sup>4</sup>Department of Medicine, University of California San Francisco, San Francisco, CA, United States

Persistent oxidative stress and mitochondrial dysfunction have been implicated across diverse forms of acute kidney injury and in the transition to chronic kidney disease. We show that HP <sup>13</sup>C metabolic MR can be used to noninvasively assess the altered renal redox capacity and mitochondrial PDH activity following ischemic reperfusion injury. Such an imaging approach can potentially enhance the prediction and monitoring of progressive kidney injury.

169

15:09



### Towards Quantitative Cardiac First-Pass Perfusion Imaging using Hyperpolarized [<sup>13</sup>]-Urea

Maximilian Fuetterer<sup>1</sup>, Julia Busch<sup>1</sup>, Sophie M. Peereboom<sup>1</sup>, Lukas Wissmann<sup>1</sup>, Constantin von Deuster<sup>1</sup>, Nikola Cesarovic<sup>2</sup>, Miriam Lipiski<sup>2</sup>, Christian T. Stoeck<sup>1</sup>, and Sebastian Kozerke<sup>1</sup>

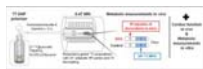


<sup>1</sup>Institute for Biomedical Engineering, University and ETH Zurich, Zurich, Switzerland, <sup>2</sup>Division of Surgical Research, University Hospital Zurich, Zurich, Switzerland

Hyperpolarized [<sup>13</sup>C] urea perfusion imaging using velocity-selective excitation is qualitatively and semi-quantitatively compared with clinically used [<sup>1</sup>H] Gadolinium first-pass perfusion imaging in healthy pigs. Higher contrast-to-noise ratios and comparable sensitivity for semi-quantitative perfusion measures over myocardial sectors can be achieved with [<sup>13</sup>C] urea. Arterial input sampling in the ascending aorta using a second imaging slice with conventional excitation is proposed. Feasibility of accurate absolute myocardial blood flow quantification using [<sup>13</sup>C] urea is demonstrated.

170

15:21



Measurement of metabolic changes in acute doxorubicin-induced cardiotoxicity in mice using hyperpolarized [<sup>1-13</sup>C]pyruvate

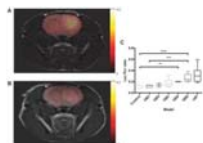
David Martin<sup>1</sup>, Hikari Ai Yoshihara<sup>1,2</sup>, Emine Can<sup>2</sup>, Roger Hullin<sup>1</sup>, and Jessica AM Bastiaansen<sup>3</sup>

<sup>1</sup>Division of Cardiology, University Hospital Lausanne (CHUV) and University of Lausanne (UNIL), Lausanne, Switzerland, <sup>2</sup>Institute of Physics, Swiss Federal Institute of Technology (EPFL), Lausanne, Switzerland, <sup>3</sup>Department of Radiology, Hospital Lausanne (CHUV) and University of Lausanne (UNIL), Lausanne, Switzerland

Chemotherapy cocktails containing doxorubicin produce irreversible cardiotoxic side effects that may progress to heart failure, which can only be avoided through dose limitation of the chemotherapeutic agents. Increasing evidence suggest that cardiac dysfunction caused by doxorubicin is triggered by an energetic deficit and alterations in mitochondrial metabolism. We quantified metabolic changes in vivo in a mouse model of acute doxorubicin-induced cardiotoxicity using hyperpolarized <sup>13</sup>C MRS.

171

15:33



Imaging c-Myc: Identification of metabolic phenotypes using MRSI of hyperpolarised [<sup>1-13</sup>C]pyruvate to [<sup>1-13</sup>C]lactate flux in glioblastoma patient-derived orthotopic xenografts.

Richard Mair<sup>1,2</sup>, Alan Wright<sup>1</sup>, Colin Watts<sup>2</sup>, and Kevin Brindle<sup>1</sup>

<sup>1</sup>CRUK Cambridge Institute, University of Cambridge, Cambridge, United Kingdom, <sup>2</sup>Division of Neurosurgery, Cambridge University Hospitals NHS Trust, Cambridge, United Kingdom

Heterogeneity at both a genomic and phenotypic level is extant within glioblastoma. We hypothesised that imaging of the flux from hyperpolarised [1-13C]pyruvate to [1-13C]lactate may inform upon this heterogeneity. We used patient derived orthotopic xenograft cohorts to identify differential lactate labelling and have related this to both glycolytic enzyme and c-Myc expression.

---

Oral

## Diffusion Acquisition & Reconstruction

Room 313A

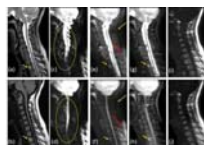
Monday 13:45 - 15:45 *Moderators:* Berkin Bilgic & Stefan Skare

---

172



13:45



Diffusion Weighted Imaging using a Dixon based Single Shot Turbo Spin Echo

Xinzeng Wang<sup>1</sup>, Holger Eggers<sup>2</sup>, Marco C. Pinho<sup>1,3</sup>, Ivan Pedrosa<sup>1,3</sup>, Robert E. Lenkinski<sup>1,3</sup>, and Ananth J. Madhuranthakam<sup>1,3</sup>

<sup>1</sup>Radiology, UT Southwestern Medical Center, Dallas, TX, United States, <sup>2</sup>Philips Research, Hamburg, Germany, <sup>3</sup>Advanced Imaging Research Center, UT Southwestern Medical Center, Dallas, TX, United States

Diffusion weighted imaging using single-shot turbo spin-echo (DWI-SShTSE) is increasingly used due to its robustness to geometric distortions, but often suffers from incomplete fat suppression at 3T using spectrally-selective fat suppression methods (SPIR/SPAIR etc.) in challenging areas with large field inhomogeneities. STIR can improve the fat suppression but at the expense of reduced SNR. In this work, we developed a multi-echo Dixon DWI-SShTSE sequence with shared field map between lower and higher b-values for uniform fat suppression without using image navigator and increasing scan times. We also demonstrated its robustness to the phase variations due to diffusion gradients.

---

173



13:57



Kt-dSTEAM: high resolution diffusion-weighted imaging of the ex vivo human brain using B1+ homogenized STEAM at 9.4T

Francisco J. Fritz<sup>1</sup>, Desmond H Y Tse<sup>1</sup>, Shubarthi Sengupta<sup>1</sup>, Tim K. Loderhose<sup>1</sup>, Bram Kraaijeveld<sup>1</sup>, Svenja Caspers<sup>2</sup>, Benedikt A. Poser<sup>1</sup>, and Alard Roebroeck<sup>1</sup>

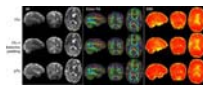
<sup>1</sup>Cognitive Neuroscience Department, Maastricht University, Maastricht, Netherlands, <sup>2</sup>Institut für Neurowissenschaften und Medizin (INM-1), Forschungszentrum Jülich, Jülich, Germany

The investigation of entire human brains post mortem with diffusion MRI is an important research tool. However, the achievable resolutions and contrast are limited by gradient performance, RF-field inhomogeneity and strongly reduced  $T_2$  and diffusivity. Here, a diffusion-weighted STEAM sequence was modified to enable the use of  $k_T$ -points  $B_1+$  homogenization and 3D segmented EPI readout. The resulting  $k_T$ -dSTEAM sequence allows for high resolution (1000 $\mu$ m, 500 $\mu$ m and 400 $\mu$ m isotropic) diffusion-weighted imaging the entire human brain with homogenous contrast at 9.4T.

---

174

14:09



High resolution whole brain diffusion MRI at 7 Tesla using RF parallel transmission

Xiaoping Wu<sup>1</sup>, Edward J. Auerbach<sup>1</sup>, An T. Vu<sup>2</sup>, Steen Moeller<sup>1</sup>, Christophe Lenglet<sup>1</sup>, Sebastian Schmitter<sup>1,3</sup>, Pierre-Francois Van de Moortele<sup>1</sup>, Essa Yacoub<sup>1</sup>, and Kamil Ugurbil<sup>1</sup>

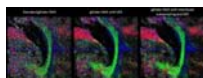
<sup>1</sup>Radiology, Medical School, University of Minnesota, Minneapolis, MN, United States, <sup>2</sup>Center for Imaging of Neurodegenerative Diseases, VA Healthcare System, San Francisco, CA, United States, <sup>3</sup>Physikalisch-Technische Bundesanstalt, Berlin, Germany

A major component of the Human Connectome Project (HCP) in the WU-Minn consortium is multiband (MB)-accelerated whole-brain diffusion MRI (dMRI) at both 3T and 7T. Although having some advantages over 3T dMRI in inferring connectivity, the 7T acquisition suffers from RF nonuniformity and is limited to MB2 acceleration because of SAR. Here, we demonstrate the utility of RF parallel transmission (pTx) for 7T HCP-type dMRI with ~1-mm isotropic resolution. Our results demonstrate that pTx can significantly improve RF uniformity across the entire brain and enable higher slice acceleration relative to single transmit configurations, thereby holding great potential for acquiring high quality, high resolution and high efficiency dMRI data.

---

175

14:21



Fast high-resolution diffusion MRI using gSlider-SMS, interlaced subsampling, and SNR-enhancing joint reconstruction

Justin P. Haldar<sup>1</sup> and Kawin Setsompop<sup>2</sup>

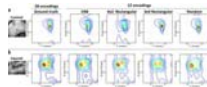
<sup>1</sup>Electrical Engineering, University of Southern California, Los Angeles, CA, United States, <sup>2</sup>A. A. Martinos Center for Biomedical Imaging, Department of Radiology, Massachusetts General Hospital, Charlestown, MA, United States

We describe a new approach that enables in vivo whole brain diffusion MRI with simultaneously high spatial resolution (660  $\mu\text{m}$  isotropic voxels) and high angular diffusion encoding resolution (64 orientations at  $b=1500 \text{ s/mm}^2$  and 4  $b=0 \text{ s/mm}^2$  images) in only 15 minutes. This is achieved by combining the gSlider-SMS acquisition strategy with constrained image reconstruction techniques that enable denoising (exploiting the fact that the diffusion images are smooth with correlated edge locations) and interlaced data subsampling (achieved by exploiting the same correlated edge constraints used for denoising, as well as through the use of q-space smoothness constraints).

176



14:33



Faster Diffusion-Relaxation Correlation Spectroscopic Imaging (DR-CSI) using Optimized Experiment Design

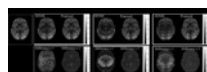
Daeun Kim<sup>1</sup> and Justin P. Haldar<sup>1</sup>

<sup>1</sup>Electrical Engineering, University of Southern California, Los Angeles, CA, United States

We propose a new experiment design method to accelerate the recent novel diffusion-relaxation correlation spectroscopic imaging (DR-CSI) experiment. DR-CSI acquires imaging data across a range of different b-value and echo time combinations. This enables new insights into tissue microstructure, but the contrast encoding can be slow. Our experiment design approach selects a small subset of the most informative observations to acquire using results from estimation theory. We demonstrate with ex vivo mouse spinal cord MR data that the new experiment design approach enables DR-CSI to be accelerated by a factor of more than 2 without a substantial loss in quality.

177

14:45



Accelerated k-q diffusion MRI reconstruction using Gaussian processes

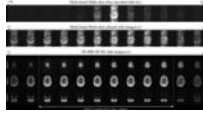
Wenchuan Wu<sup>1</sup>, Peter J Koopmans<sup>2</sup>, Jesper Andersson<sup>2</sup>, and Karla L Miller<sup>2</sup>

<sup>1</sup>FMRIB, University of Oxford, Oxford, United Kingdom, <sup>2</sup>FMRIB, University of Oxford

Diffusion MRI commonly acquires multiple diffusion volumes (directions), which shares plentiful common features. In this work, we propose integrating Gaussian Processes into image reconstruction to utilize the shared information between diffusion volumes to reduce image artefacts associated with parallel imaging.

178

14:57



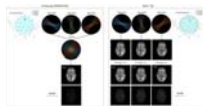
[3D Multi-Band, Multi-Slab, and Multi-Shot High-Resolution Diffusion MRI](#)  
Iain P Bruce<sup>1</sup>, Hing-Chiu Chang<sup>2</sup>, Nan-Kuei Chen<sup>1,3</sup>, and Allen W Song<sup>1</sup>

<sup>1</sup>*Brain Imaging and Analysis Center, Duke University Medical Center, Durham, NC, United States*, <sup>2</sup>*Department of Diagnostic Radiology, University of Hong Kong*, <sup>3</sup>*Biomedical Engineering, University of Arizona, Tuscan, AZ, United States*

When diffusion MRI data is acquired with 3D multi-slab and/or multi-shot imaging techniques, scan times are often lengthy and phase variations between the acquired shots and/or slice-encoding planes of 3D slabs introduce severe motion artifacts in slice images. To accelerate the acquisition of high spatial resolution diffusion MRI volumes with high SNR and fidelity, we outline a 3D image reconstruction model that simultaneously accounts for both in-plane and through-plane motion artifacts in 3D multi-band, multi-slab and multi-shot diffusion data. Diffusion data acquired and reconstructed in this fashion can be acquired at sub-millimeter spatial resolution with high SNR in ~1-2min.

179

15:09



[Improving angular resolution in multi-shot turbo spin-echo diffusion imaging using rotating single-shot acquisition \(RoSA\)](#)

Qiuting Wen<sup>1</sup>, Mark Graham<sup>2</sup>, Ivana Drobnjak<sup>2</sup>, Hui Zhang<sup>2</sup>, and Yu-Chien Wu<sup>1</sup>

<sup>1</sup>*Indiana University, Indianapolis, IN, United States*, <sup>2</sup>*University of College London*

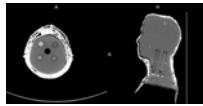
The rotating single-shot acquisition (RoSA) technique is proposed to accelerate multi-shot diffusion imaging acquisitions by acquiring one shot per diffusion direction. The RoSA approach utilizes similarity existing in diffusion-weighted contrast for image reconstruction. It has been successfully implemented with echo planar imaging (EPI). In this study, we use the RoSA approach to improve turbo spin-echo (TSE) based multi-shot sequences. In particular, we will demonstrate that with the same acquisition time, RoSA increases the diffusion angular sampling resolution by 3-fold compared to a TurboProp sequence.



---

180

15:21



Combination of integrated dynamic shimming and readout-segmented echo planar imaging for diffusion-weighted MRI of the head and neck region at 3 Tesla.

Sven Stephan Walter<sup>1</sup>, Alto Stemmer<sup>2</sup>, Berthold Kiefer<sup>2</sup>, Konstantin Nikolaou<sup>1</sup>, Petros Martirosian<sup>3</sup>, Mike Notohamiprodo<sup>1</sup>, and Sergios Gatidis<sup>1</sup>

*<sup>1</sup>Department of Radiology, University Hospital Tuebingen, Tuebingen, Germany, <sup>2</sup>Siemens Healthineers, Erlangen, Germany, <sup>3</sup>Department of Experimental Radiology, University Hospital Tuebingen, Tuebingen, Germany*

The purpose of this study was to evaluate possible improvements in EPI-based DWI of the head/neck at 3 Tesla using a combination of readout-segmented EPI and dynamic shimming. We assessed ADC quantification in an anthropomorphic phantom and evaluated the presence of geometric distortions, signal losses, ghosting artifacts, and overall image quality in both, phantom and in-vivo data from 10 volunteers. We found that combining integrated shimming with readout-segmented EPI significantly improves images quality of EPI based DWI of the head/neck at 3 Tesla compared to the single techniques alone or conventional single-shot EPI.

---

181

15:33



	EN-CODE	TRSE	TRSE
TE (ms)	120	120	120
SNR	1.0	1.0	1.0
Distortion (mm)	0.5	1.0	1.0

Reduced Distortion in Diffusion Tensor MRI with Eddy Current Nulled Convex Optimized Diffusion Encoding (EN-CODE)

Eric Aliotta<sup>1,2</sup>, Kevin Moulin<sup>1</sup>, and Daniel B. Ennis<sup>1,2</sup>

*<sup>1</sup>Department of Radiological Sciences, University of California, Los Angeles, CA, United States, <sup>2</sup>Biomedical Physics IDP, University of California, Los Angeles, CA, United States*

Eddy currents distort images and confound diffusion tensor reconstruction. In this work, convex optimized diffusion encoding (CODE) was extended to include an eddy current nulling term (EN-CODE) to achieve minimum TE diffusion tensor imaging (DTI) without eddy current distortions. EN-CODE was evaluated in simulations and through imaging in phantoms and healthy subjects. EN-CODE achieves distortion reduction on par with the existing twice refocused spin echo (TRSE) technique with a substantially shorter TE.

# Neuro Morphometry & Quantitative Analysis

Room 313BC

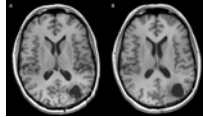
Monday 13:45 - 15:45

Moderators: Konstantinos Arfanakis & Elizabeth Meyerand

---

182

13:45



## Quality Assurance of Neuro-MRI within Multicenter Clinical Trials

Preethi Subramanian<sup>1</sup>, David P Poon<sup>1</sup>, Shivangi N Vora<sup>1</sup>, Sydney A Cearlock<sup>1</sup>, Xiangyu Yang<sup>1</sup>, Jun Zhang<sup>1</sup>, and Michael V Knopp<sup>1</sup>

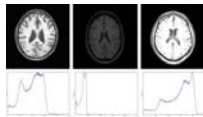
<sup>1</sup>Wright Center of Innovation in Biomedical Imaging, The Ohio State University, Columbus, OH, United States

Volumetric analysis and quantification especially of dynamic MR sequences is increasingly invaluable for assessing treatment response and time to progression in the majority of clinical trials focusing on neuro-oncology. These innovative therapeutic trials rely heavily on consistent image acquisitions even in multi-center Phase 2/3 trials. We have developed a highly structured DICOM tag based, parameter driven, semi-automated QC approach that readily enables visualization of acquisition inconsistencies using a heat-mapping spectrum. As the imaging core laboratory for several NCI-NCTN clinical trials, we expanded the QC methodology to also enable constructive feedback education / training to help improve the quality of Neuro-MRI submissions.

---

183

13:57



## Brain MR image intensity normalization in the presence of pathology

Hugo J Kuijf<sup>1</sup>, Mariëlle JA Jansen<sup>1</sup>, Mirjam I Geerlings<sup>2</sup>, and Max A Viergever<sup>1</sup>

<sup>1</sup>Image Sciences Institute, University Medical Center Utrecht, Utrecht, Netherlands, <sup>2</sup>Department of Epidemiology, University Medical Center Utrecht, Utrecht, Netherlands

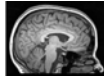
Brain MR image intensities do not have a fixed tissue-specific value. Especially in longitudinal studies, where a subjects' anatomy might change, pathology can arise, scanner software and hardware may be replaced, the resulting image intensities can differ widely. This thwarts subsequent post-processing or image analysis. Various image intensity normalization techniques exist, but are often evaluated on healthy subjects. In this work, we evaluate six normalization techniques on 25 image-pairs (five year interval) of subjects with brain pathology. Traditional methods (e.g. Gaussian and Z-Score) are clearly affected by the presence of pathology and perform less than more recent techniques.



---

184

14:09



**Novel Design of a 3D-Printed Anthropomorphic Brain Phantom for Segmentation Validation in Magnetic Resonance Imaging**

Anna Altermatt<sup>1,2</sup>, Francesco Santini<sup>1,3</sup>, Xeni Deligianni<sup>1,3</sup>, Stefano Magon<sup>2,4</sup>, Philippe Cattin<sup>1</sup>, Jens Wuerfel<sup>1,2</sup>, and Laura Gaetano<sup>2,4</sup>

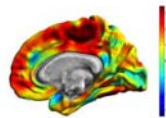
*<sup>1</sup>Department of Biomedical Engineering, University Basel, Basel, Switzerland, <sup>2</sup>Medical Image Analysis Center (MIAC) AG, Basel, Switzerland, <sup>3</sup>Department of Radiology, University Hospital Basel, Basel, Switzerland, <sup>4</sup>Department of Neurology, University Hospital Basel, Basel, Switzerland*

Precise brain phantoms are important for evaluating the quality of segmentation tools for brain MRI. Here we suggested the construction of a 3D physical brain phantom as gold standard to validate the performance of those tools. Folding patterns of grey and white matter compartments were replicated using 3D-printed models from a real structural brain scan. T1 and T2 intensities of these brain regions in a 3 Tesla MRI were mimicked by a 0.6% agar mixture containing the appropriate concentrations of the paramagnetic compounds Ferumoxide and Manganese chloride. With its 3D-printed brain-like design, the phantom showed to be a promising alternative to existing methods for MRI segmentation validation.

---

185

14:21



**Traffic-Related Air Pollution Associated with Reduced Cortical Thickness and Altered White Matter Organization in a Longitudinally Studied, Pediatric Cohort**

Kim M Cecil<sup>1</sup>, Travis Beckwith<sup>1</sup>, Mekibib Altaye<sup>2</sup>, Rachel Severs<sup>2</sup>, Christopher Wolfe<sup>2</sup>, Zana Percy<sup>3</sup>, Thomas Maloney<sup>1</sup>, Kimberly Yolton<sup>2</sup>, Grace LeMasters<sup>3</sup>, and Patrick Ryan<sup>2</sup>

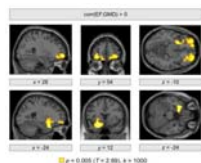
*<sup>1</sup>Radiology/Imaging Research Center, Cincinnati Children's Hospital Medical Center, Cincinnati, OH, United States, <sup>2</sup>Cincinnati Children's Hospital Medical Center, Cincinnati, OH, United States, <sup>3</sup>University of Cincinnati College of Medicine, Cincinnati, OH, United States*



Traffic-related air pollution (TRAP) is strongly associated with adverse cardiopulmonary health effects. Evidence suggests the developing brain may also be a target organ for particulate matter due to translocation either from the respiratory system or through the olfactory nerve. Using a pediatric cohort, we tested the hypothesis that exposure to TRAP during critical windows of brain development is significantly associated with changes in brain structure and organization. Children with high exposure levels at time of birth were associated with reductions in brain volume, cortical thickness, and diffusion abnormalities in white matter at 12 years compared with children at low exposure.

186

14:33



### Investigating structural brain change with heart failure using voxel-based morphometry

Karsten Mueller<sup>1</sup>, Friederike Thiel<sup>1</sup>, Andrej Teren<sup>2,3</sup>, Frank Beutner<sup>2,3</sup>, Stefan Frisch<sup>4</sup>, Joachim Thiery<sup>3,5</sup>, Harald E. Möller<sup>1</sup>, Arno Villringer<sup>1,3,6</sup>, and Matthias L. Schroeter<sup>1,3,6</sup>

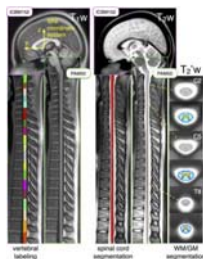
<sup>1</sup>Max Planck Institute for Human Cognitive and Brain Sciences, Leipzig, Germany, <sup>2</sup>Herzzentrum Leipzig, Leipzig, Germany, <sup>3</sup>Leipzig Research Center for Civilization Diseases (LIFE), Leipzig, Germany, <sup>4</sup>Department of Neurology, Center of Neurology and Neurosurgery, University Hospital Frankfurt, Frankfurt, Germany, <sup>5</sup>Institute of Laboratory Medicine, University Hospital Leipzig, Leipzig, Germany, <sup>6</sup>Clinic for Cognitive Neurology, University Hospital Leipzig, Leipzig, Germany

Heart failure is a multifactorial disease including a reduced pump efficiency leading to an insufficient oxygen supply for all body organs. However, the consequence of heart failure to brain structure is an important issue that needs further investigation. We used structural MRI with voxel-based morphometry to investigate a relationship between gray matter density and heart failure using ejection fraction and N-terminal prohormone of brain natriuretic peptide as markers for disease severity. These markers were found to be associated with decreased gray matter density in orbitofrontal and hippocampal brain regions indicating local gray matter abnormalities in these regions with heart failure.

14:45

### PAM50: Multimodal template of the brainstem and spinal cord compatible with the ICBM152 space

Benjamin De Leener<sup>1</sup>, Vladimir Fonov<sup>2</sup>, D. Louis Collins<sup>2</sup>, Virginie Callot<sup>3,4</sup>, Nikola Stikov<sup>1,5</sup>, and Julien Cohen-Adad<sup>1,6</sup>

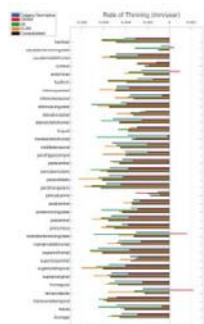


<sup>1</sup>NeuroPoly Lab, Institute of Biomedical Engineering, Polytechnique Montreal, Montreal, QC, Canada, <sup>2</sup>Montreal Neurological Institute, McGill University, Montreal, QC, Canada, <sup>3</sup>Aix-Marseille Univ, CNRS, CRMBM UMR 7339, Marseille, France, <sup>4</sup>CEMEREM, Hopital de la Timone, Pôle d'imagerie médicale, AP-HM, Marseille, France, <sup>5</sup>Montreal Heart Institute, Montreal, QC, Canada, <sup>6</sup>Functional Neuroimaging Unit, CRIUGM, Université de Montréal, Montreal, QC, Canada

Template-based analysis of multi-parametric MRI data of the spinal cord sets the foundation for multi-center studies with minimum bias, thereby helping the discovery of new biomarkers of spinal-related diseases. In this study, we introduce a spinal cord MRI template, the PAM50, which is anatomically compatible with the ICBM152 brain template and uses the same coordinate system. The fusion of the PAM50 and ICBM152 templates facilitates group studies and multi-center studies of combined brain and spinal cord MRI and also allows the use of existing atlases of the brainstem compatible with the ICBM template.



14:57



### Consistency of Inter-Database Cortical Thinning with Age

M. Ethan MacDonald<sup>1</sup>, Rebecca J. Williams<sup>1</sup>, Nils D Forkert<sup>1</sup>, Avery J.L. Berman<sup>1,2</sup>, Cheryl M McCreary<sup>1,3</sup>, Richard Frayne<sup>1,3</sup>, and Bruce Pike<sup>1</sup>

<sup>1</sup>Departments of Radiology and Clinical Neurosciences, University of Calgary, Calgary, AB, Canada, <sup>2</sup>Department of Biomedical Engineering, McGill University, Montreal, QC, Canada, <sup>3</sup>Seaman Family MR Research Centre, Foothills Medical Centre, AB, Canada

This work investigates cerebral cortical thinning as a function of age, and how this relationship varies between four healthy subject databases, with a consolidated 1,382 subjects. Cortical thickness measurements of each subject were computed for 68 regions. Linear regression was used to determine the thinning rate for each region in each database as well as for the consolidated database. ANCOVA tests were run to test the effect of database. Correlation matrices were used to test the intra-relationship of locations between databases. Statistically significant correlations were found with age and differences were found between databases in all regions.

15:09

	Gray matter	White matter	CSF	Brain	ICV
PNI	0.14%	0.11%	0.09%	0.10%	0.10%
HCP	0.10%	0.10%	0.10%	0.10%	0.10%
CAT12	0.10%	0.10%	0.10%	0.10%	0.10%

### A test-retest analysis of brain volume measurement techniques

Hugo J Kuijf<sup>1</sup>, Geert Jan Biessels<sup>2</sup>, Max A Viergever<sup>1</sup>, and Jaco JM Zwanenburg<sup>3</sup>

<sup>1</sup>Image Sciences Institute, University Medical Center Utrecht, Utrecht, Netherlands, <sup>2</sup>Department of Neurology, University Medical Center Utrecht, Utrecht, Netherlands, <sup>3</sup>Department of Radiology, University Medical Center Utrecht, Utrecht, Netherlands

Brain volume measurements should both be accurate and precise. Accuracy of brain segmentation techniques is well studied. With the availability of test-retest datasets, precision (low coefficient of variation (COV)) can be investigated. In this work, we studied the COV of the FSL, SPM, and CAT12 software packages on 120 3T brain MR images of three subjects (40 images each) and compare it to previous results of FreeSurfer on this dataset. CAT12 performs best on total gray matter, white matter, and brain volume; whereas FSL has the lowest COV for CSF. COV values should be considered when studying brain volume change.

190

15:21



### Altered grey matter volume in patients with type 2 diabetes mellitus

Jia Liu<sup>1</sup>, Taiyuan Liu<sup>2</sup>, Wenhui Wang<sup>2</sup>, Lun Ma<sup>2</sup>, Xiaoyue Ma<sup>2</sup>, Shaojie Shi<sup>2</sup>, and Meiyun Wang<sup>2</sup>

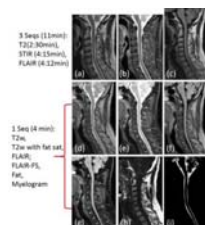
<sup>1</sup>Department of Radiology, Union Hospital of Tongji Medical College, Huazhong University of Science and Technology, Wuhan, People's Republic of China, <sup>2</sup>Department of Radiology, Henan Provincial People's Hospital & the People's Hospital of Zhengzhou University, Zhengzhou, People's Republic of China

Our meta-analysis indicates that patients with T2DM have significantly and robustly reduced grey matter, mainly in the cortical-striatal-limbic networks. The meta-regression results suggest that T2DM patients with longer illness duration may have smaller grey matter volume in the right MTG. Our finding supports the notion that T2DM could lead to subtle diabetic brain structural changes, which may be correlated with cognitive impairment in T2DM patients.

191



15:33



### Volumetric T2-weighted and FLAIR Imaging of Spine with Uniform Fat Suppression in a Single Acquisition

Xinzeng Wang<sup>1</sup>, Joshua S. Greer<sup>1,2</sup>, Marco C. Pinho<sup>1,3</sup>, Robert E. Lenkinski<sup>1,3</sup>, and Ananth J. Madhuranthakam<sup>1,3</sup>

<sup>1</sup>Radiology, UT Southwestern Medical Center, Dallas, TX, United States, <sup>2</sup>Bioengineering, UT Dallas, Dallas, TX, United States, <sup>3</sup>Advanced Imaging Research Center, UT Southwestern Medical Center, Dallas, TX, United States

2D T2-weighted turbo spin-echo (T2w-TSE), fluid attenuated inversion recovery (FLAIR) with and without fat suppression are widely used in the clinical brain and spine protocols to improve diagnosis. However, FLAIR suffers from low SNR and long scan times. In this work, we developed a dual-acquisition 3D TSE sequence combined with dual-echo Dixon based approach to generate T2-weighted and FLAIR images of the spine with and without fat suppression in a single acquisition using the similar acquisition time as 2D FLAIR. Uniform fat/water separation was achieved using a shared-field-map and complex subtraction was used to generate FLAIR-like images without artifacts.

---

Oral

## CEST: New Solutions & Old Problems

Room 314

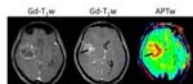
Monday 13:45 - 15:45 Moderators: Kejia Cai & Mark Pagel

---

192



13:45



[Amide proton transfer-weighted MRI signal as a surrogate biomarker to assess MGMT promoter methylation status in glioblastoma](#)

Shanshan Jiang<sup>1,2</sup>, Xianlong Wang<sup>2</sup>, Yu Wang<sup>3</sup>, Hao Yu<sup>2</sup>, Tianyu Zou<sup>2</sup>, Yongxing Du<sup>2</sup>, Charles Eberhart<sup>4</sup>, Maria Adelita Vizcaino Villalobos<sup>4</sup>, Yi Zhang<sup>1</sup>, Hye-Young Heo<sup>1</sup>, Peter Van Zijl<sup>1</sup>, Zhibo Wen<sup>2</sup>, and Jinyuan Zhou<sup>1</sup>

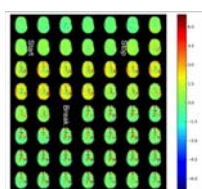
<sup>1</sup>Department of Radiology, Johns Hopkins University School of Medicine, Baltimore, MD, United States, <sup>2</sup>Department of Radiology, Southern Medical University, Zhujiang Hospital, Guangzhou, People's Republic of China, <sup>3</sup>Department of Pathology, Southern Medical University, Zhujiang Hospital, Guangzhou, People's Republic of China, <sup>4</sup>Department of Pathology, Johns Hopkins University School of Medicine, Baltimore, MD, United States

We explored the feasibility of using the APTW signal intensity as a surrogate biomarker to identify the methylation status of MGMT promoter in glioblastoma (GBM). Eighteen patients with newly diagnosed GBM were recruited and scanned. Results showed that the APTW signal intensities were significantly higher in the unmethylated MGMT promoter group than in the methylated MGMT promoter group. The area under the ROC curve (AUC) for APTW to differentiate these two GBM groups was 0.857. Preoperative APTW imaging may assist in predicting the MGMT promoter methylation status in patients with GBM.

193



13:57



### Dynamic Glucose Enhanced Imaging at 3T: First Human Data

Xiang Xu<sup>1,2</sup>, Akansha Sehgal<sup>1,2</sup>, Nirbhay N. Yadav<sup>1,2</sup>, Linda Knutsson<sup>1,3</sup>, John Laterra<sup>4</sup>, Martin Pomper<sup>1</sup>, Hailey Rosenthal<sup>1</sup>, and Peter C.M. van Zijl<sup>1,2</sup>

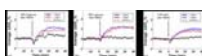
<sup>1</sup>Russell H. Morgan Department of Radiology and Radiological Science, Johns Hopkins University, Baltimore, MD, United States, <sup>2</sup>F. M. Kirby Research Center for Functional Brain Imaging, Kennedy Krieger Institute, Baltimore, MD, United States, <sup>3</sup>Department of Medical Radiation Physics, Lund University, Lund, Sweden, <sup>4</sup>Department of Neurology, Johns Hopkins University, Baltimore, MD, United States

Recently, it has been demonstrated that D-glucose has potential as an MRI contrast agent at 7T for imaging dynamic changes upon glucose infusion in brain tumors using chemical exchange saturation transfer (CEST) MRI. Here we show first data for the possibility of translating such technique to 3T using pseudo-continuous wave saturation and extend the method to acquire a 3D volume (10 slices) for better brain coverage. We present dynamic glucose-enhanced (DGE) data from healthy volunteers and a brain tumor patient with a low grade glioma showing the feasibility of glucose enhanced imaging at clinical field strength.

194



14:09



### Effect of Osmolality on Dynamic Glucose Enhanced(DGE) MRI

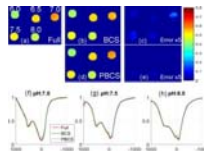
Wonmin Choi<sup>1,2</sup>, Julius Juhyun Chung<sup>1,3</sup>, Tao Jin<sup>4</sup>, and Seong-Gi Kim<sup>1,2,3</sup>

<sup>1</sup>Center for Neuroscience Imaging Research, Institute for Basic Science (IBS), Suwon, Korea, Republic of, <sup>2</sup>Department of Biomedical Engineering Sungkyunkwan University (SKKU), Suwon, Korea, Republic of, <sup>3</sup>Samsung Advanced Institute for Health Sciences and Technology, Sungkyunkwan University, Seoul, Korea, Republic of, <sup>4</sup>Department of Radiology, University of Pittsburgh, Pittsburgh, PA, United States

Dynamic glucose enhanced(DGE) MRI has shown promise in glucose metabolism studies. In recent studies, a hypertonic dextrose solution was used for reliable detection of glucose in the brain. However, the effects of the hypertonic solution on DGE signal have not been verified yet. This study aimed to investigate the signal contributions from non-glucose related components. We used hypertonic D-, L-glucose, and NaCl solution to identify osmolality effects. Our data show an osmotic shift of water between the extravascular and intravascular space, induced by administering D-glucose(50%), can highly affect the DGE signal but negligible contributions were observed from the intravascular space.

195

14:21



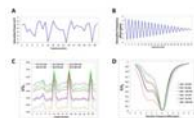
**Accelerated CEST Imaging with Parallel Blind Compressed Sensing**  
Huajun She<sup>1</sup>, Bian Li<sup>1</sup>, Joshua S. Greer<sup>1,2</sup>, Jochen Keupp<sup>3</sup>, Ananth Madhuranthakam<sup>1,4</sup>, Ivan E. Dimitrov<sup>1,5</sup>, Robert Lenkinski<sup>1,4</sup>, and Elena Vinogradov<sup>1,4</sup>

<sup>1</sup>Radiology, UT Southwestern Medical Center, Dallas, TX, United States, <sup>2</sup>Bioengineering, UT Dallas, Dallas, TX, United States, <sup>3</sup>Philips Research, Hamburg, Germany, <sup>4</sup>Advanced Imaging Research Center, UT Southwestern Medical Center, Dallas, TX, United States, <sup>5</sup>Philips Healthcare, Gainesville, FL, United States

This work investigates accelerating CEST imaging using parallel blind compressed sensing (BCS). BCS method assumes a few functions are enough to represent the dynamic behavior. In CEST imaging, the Z-spectrum performs similar in the same compartment, which is suitable for BCS reconstruction. The traditional BCS method does not consider the coil sensitivity, which is complementary sparse information with spatial-temporal dictionary. The proposed method addresses the coil sensitivity information and the sparsity prior information in CEST and further improves the BCS method, demonstrating a better estimation of the CEST effect for both phantom and in vivo brain data.

196

14:33



**Quantitative Chemical Exchange Saturation Transfer (CEST) Imaging with Magnetic Resonance Fingerprinting (MRF)**

Shuning Huang<sup>1</sup>, Ouri Cohen<sup>1,2</sup>, Michael T. McMahon<sup>3,4</sup>, Young R. Kim<sup>1,2</sup>, Matthew S. Rosen<sup>1,2,5</sup>, and Christian T. Farrar<sup>1,2</sup>

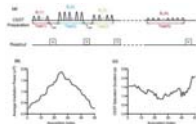


<sup>1</sup>Athinoula A. Martinos Center for Biomedical Imaging, Department of Radiology, Massachusetts General Hospital, Charlestown, MA, United States, <sup>2</sup>Radiology, Harvard Medical School, Boston, MA, United States, <sup>3</sup>The Russel H. Morgan Department of Radiology and Radiological Science, The Johns Hopkins University, Baltimore, MD, United States, <sup>4</sup>F.M. Kirby Research Center for Functional Brain Imaging, Kennedy Krieger Institute, Baltimore, MD, United States, <sup>5</sup>Department of Physics, Harvard University, Cambridge, MA, United States

CEST MRI suffers from several limitations including long image acquisition times and the qualitative nature of the CEST contrast. Clinical translation of CEST MRI would benefit greatly from the development of quantitative and rapid CEST methods. Here we build on the recently developed Magnetic Resonance Fingerprinting (MRF) technique and report the first use of a fast CEST fingerprinting method for generating quantitative exchange rate and exchangeable proton concentration maps of L-Arginine phantoms and a permanent MCAO rat stroke model.

197

14:45



### CEST Fingerprinting: A Novel Approach for Exchange Rate Quantification

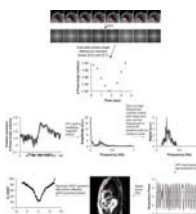
Zhengwei Zhou<sup>1,2</sup>, Pei Han<sup>3</sup>, and Debiao Li<sup>1,2</sup>

<sup>1</sup>Biomedical Imaging Research Institute, Cedars-Sinai Medical Center, Los Angeles, CA, United States, <sup>2</sup>Department of Bioengineering, University of California, Los Angeles, Los Angeles, CA, United States, <sup>3</sup>Department of Engineering Physics, Tsinghua University, Beijing, People's Republic of China

In this work, we developed a CEST fingerprinting technique for exchange rate quantification. This method utilizes CEST saturation with varying  $B_1$  amplitudes and durations to create uniqueness of signal evolution for different exchange rates. The acquired signal was matched to a predefined dictionary. Preliminary studies were performed in phantoms to show the feasibility.

198

14:57



### Measuring APT contrast in the lung using CEST FT-phase MRI and a retrospective gating technique

Kyle M. Jones<sup>1</sup>, Carol A. Steum<sup>2</sup>, Charles C. Hsu<sup>3</sup>, Phillip H. Kuo<sup>2</sup>, Mark D. Pagel<sup>2</sup>, and Edward A. Randtke<sup>2</sup>

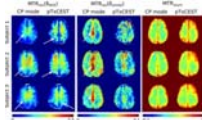
<sup>1</sup>Biomedical Engineering, University of Arizona, Tucson, AZ, United States, <sup>2</sup>Medical Imaging, University of Arizona, Tucson, AZ, United States, <sup>3</sup>Medicine, University of Arizona, Tucson, AZ, United States

We have developed a CEST FT-phase MRI method that can measure endogenous Amide Proton Transfer (APT) contrast in lung tumors and other tissues that are affected by lung motion. The method monitors the breathing cycle based on the relative phase angle between adjacent pixels, and selects a subset of images during the quiescent period between breaths. The resulting  $MTR_{asym}$  contrast of an oscillating egg white phantom, volunteers, and patients with lung tumors showed that CEST FT-phase MRI produced more precise quantitative assessments of APT.

199



15:09



### B1+ inhomogeneity mitigation in CEST using parallel transmission: pTxCEST

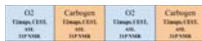
Nuno André da Silva<sup>1</sup>, Desmond H. Y. Tse<sup>2</sup>, Benedikt A Poser<sup>2</sup>, and N Jon Shah<sup>1,3,4</sup>

<sup>1</sup>Institute of Neuroscience and Medicine - 4, Forschungszentrum Jülich, Jülich, Germany, <sup>2</sup>Faculty of Psychology and Neuroscience, Maastricht University, Maastricht, Netherlands, <sup>3</sup>Department of Neurology, Faculty of Medicine, RWTH Aachen University, JARA, Aachen, Germany, <sup>4</sup>Department of Electrical and Computer Systems Engineering, and Monash Biomedical Imaging, School of Psychological Sciences, Monash University, Melbourne, Australia

To demonstrate the benefits from the increased spectral bandwidth at ultra-high field (UHF) by using parallel transmission (pTx) to mitigate flip-angle inhomogeneity in chemical exchange saturation transfer (CEST) imaging. A pTx basis pulse is homogenised by magnitude least-squares (MLS) optimisation and expanded to form a frequency-selective saturation pulse for CEST. The pTx saturation pulse was validated by both Bloch-McConnell simulation and in vivo imaging at 7T. Improved homogeneity in contrasts and relaxation-compensated CEST metrics were observed in our in vivo data when the pTx saturation pulse was used instead of the standard CP-mode Gaussian pulse.

200

15:21



### Understanding concomitant effects between CEST and ASL contrast.

Francisco Torrealdea<sup>1,2</sup>, Marilena Rega<sup>3</sup>, Mohamed Tachrount<sup>1</sup>, Magdalena Sokolska<sup>4</sup>, and Xavier Golay<sup>1</sup>



<sup>1</sup>Institute of Neurology, UCL, London, United Kingdom, <sup>2</sup>Centre for Medical Imaging, University College London, London, United Kingdom, <sup>3</sup>Institute of Nuclear Medicine, UCLH, London, United Kingdom, <sup>4</sup>Medical Physics and Biomedical Engineering, UCLH, London

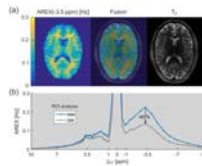
This study aims to assess the relationship between brain perfusion and CEST measurements. For this purpose, an oxygen-carbogen challenge experiment was designed in order to compare CEST measurements of the rat brain in low and high perfusion conditions.

Comparison of the CEST with CBF measurement show strong correlation ( $p < 0.005$  with Spearman  $Rho = 0.976$ ). From the results of the study it is notable that blood perfusion is a strong modulator of the observed CEST signal in the rat brain.

---

201

15:33



### CEST Signals of Lipids

Steffen Goerke<sup>1</sup>, Moritz Zaiss<sup>1,2</sup>, Dario Longo<sup>3</sup>, Francesca Garello<sup>4</sup>, Enza Di Gregorio<sup>4</sup>, Johannes Breitling<sup>1</sup>, Mark E Ladd<sup>1</sup>, and Peter Bachert<sup>1</sup>

<sup>1</sup>Division of Medical Physics in Radiology, German Cancer Research Center (DKFZ), Heidelberg, Germany, <sup>2</sup>Department of High-field Magnetic Resonance, Max-Planck-Institute for Biological Cybernetics, Tübingen, Germany, <sup>3</sup>Institute of Biostructure and Bioimaging, Consiglio Nazionale delle Ricerche (CNR), Turin, Italy, <sup>4</sup>Department of Molecular Biotechnology and Health Sciences, University of Turin, Turin, Italy

In this study, lipids were identified to be an important contributor to the upfield chemical exchange saturation transfer (CEST) signals of brain tissue. This finding can explain the pronounced CEST image contrast between gray and white matter observed in healthy volunteers.

---

Oral

## New Perspectives in DSC & DCE

Room 316BC

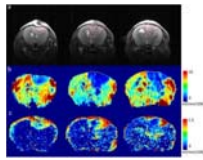
Monday 13:45 - 15:45 Moderators: David Buckley & Joel Garbow

202

13:45

### D2O Perfusion MRI of Brain Tumor on a Mouse Model: A Preliminary Study

Pei-Lun Yu<sup>1</sup>, Sheng-Min Huang<sup>1</sup>, Cheng-He Li<sup>1</sup>, Sheng-Yan Wu<sup>1</sup>, Chi-Shiun Chiang<sup>1</sup>, Kung-Chu Ho<sup>2</sup>, and Fu-Nien Wang<sup>1</sup>



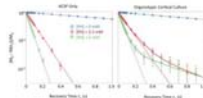
<sup>1</sup>Department of Biomedical Engineering and Environmental Sciences, National Tsing Hua University, Hsinchu, Taiwan, <sup>2</sup>Nuclear Medicine, Chang Gung Memorial Hospital, Taoyuan, Taiwan

Recently, deuterium oxide (D<sub>2</sub>O) has been proposed as an alternative contrast agent on rodent brain perfusion by monitoring the attenuation of <sup>1</sup>H signal. Since D<sub>2</sub>O is a highly diffusible contrast agent, the revealed information of Gd chelates and D<sub>2</sub>O are different. In this study, we aimed to re-investigate the perfusion information carried by D<sub>2</sub>O with advanced spatial resolution. We speculated that D<sub>2</sub>O slowly diffused into tumor area and continuously exchanged with tissue water until a balanced concentration. Inside the tumor region, the heterogeneity shown by D<sub>2</sub>O and Gd-DTPA are somewhat different.

203



13:57



Measuring transmembrane water exchange in rat brain cortical cells in normal and pathological conditions

Ruiliang Bai<sup>1</sup>, Charles S. Springer, Jr.<sup>2</sup>, Dietmar Plenz<sup>3</sup>, and Peter Basser<sup>1</sup>

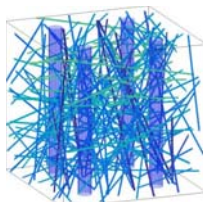
<sup>1</sup>Section on Quantitative Imaging and Tissue Sciences, DIBGI, NICHD, National Institutes of Health, Bethesda, MD, United States, <sup>2</sup>Advanced Imaging Research Center, Oregon Health & Science University, Portland, OR, United States, <sup>3</sup>Section on Critical Brain Dynamics, LSN, NIMH, National Institutes of Health, Bethesda, MD, United States

Knowledge of transmembrane water exchange kinetics is invaluable for the correct interpretation of many MRI experiments, e.g., DCE-MRI, diffusion MRI, etc. Here we quantitatively studied the transmembrane water exchange in organotypic cultures from rat brain cortex with an MR relaxation contrast agent. In normal states, we determined the equilibrium cellular water efflux rate constant [ $k_{io}$ ] is  $2.15 (\pm 1.28) \text{ s}^{-1}$  at  $34 (\pm 1) \text{ }^\circ\text{C}$ . In the likely cell-swollen state induced by Ouabain perfusion, we, for the first time, quantitatively measured a global increase of the intracellular volume fraction ( $\sim 104\%$ ) together and a large decrease of  $k_{io}$  ( $\sim 64\%$ ).

204



14:09



Anisotropic cerebral vascular architecture causes orientation dependency in cerebral blood flow and volume measured with spin echo dynamic susceptibility contrast magnetic resonance imaging

Jonathan Doucette<sup>1,2</sup>, Luxi Wei<sup>1,3</sup>, Christian Kames<sup>1,2</sup>, Eneidino Hernández-Torres<sup>1,4</sup>, Rasmus Aamand<sup>5</sup>, Torben E. Lund<sup>5</sup>, Brian Hansen<sup>5</sup>, and Alexander Rauscher<sup>1,4</sup>

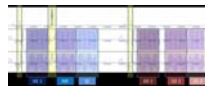
<sup>1</sup>UBC MRI Research Centre, University of British Columbia, Vancouver, BC, Canada, <sup>2</sup>Engineering Physics, University of British Columbia, Vancouver, BC, Canada, <sup>3</sup>Department of Physics and Astronomy, University of British Columbia, Vancouver, BC, Canada, <sup>4</sup>Pediatrics, University of British Columbia, Vancouver, BC, Canada, <sup>5</sup>Center of Functionally Integrative Neuroscience (CFIN) and MINDLab, Department of Clinical Medicine, Aarhus University, Aarhus, Denmark

Cerebral white matter tissue perfusion measured with gradient echo dynamic susceptibility contrast (DSC) imaging exhibits a strong dependency on the angle between white matter fibres and the main magnetic field. Here, we investigate how spin echo DSC depends on the orientation of white matter and explain orientation effects by a model of diffusion within a magnetically inhomogeneous environment created by a vascular bed with isotropic and anisotropic components. We found that the change in  $R_2^*$  value for the SE DSC is 20% larger in WM fibres perpendicular to  $B_0$  than for those parallel, compared with 100% larger in GRE DSC.

205



14:21



### Simultaneous-multi-slice and Alternating Multi-echo Measurement Sequence (SAME) for Perfusion Imaging

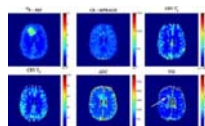
Elias Kellner<sup>1</sup>, Marco Reiser<sup>1</sup>, Benedikt A Poser<sup>2</sup>, Irina Mader<sup>3</sup>, Valerij G Kiselev<sup>1</sup>, and Michel Herbst<sup>1</sup>

<sup>1</sup>Department of Radiology, University Medical Center Freiburg, Freiburg, Germany, <sup>2</sup>Department of Cognitive Neuroscience, Maastricht Brain Imaging Centre (MBIC), Maastricht University, <sup>3</sup>Department of Neuroradiology, University Medical Center Freiburg, Freiburg, Germany

In this work, we combine simultaneous multi-slice acquisition with a multi-echo readout, dedicated to dynamic susceptibility-contrast perfusion imaging (DSC). With this approach, multiple spin and gradient echo images can be obtained at short repetition times to determine both T2 and T1 effects of contrast agent in a robust and stable manner.

206

14:33



### Full Brain Vasculature Analysis using Gradient/Spin-Echo Multi-band EPIK: Tumour Evaluation with MR-PET

Nuno André da Silva<sup>1</sup>, N Jon Shah<sup>1,2,3</sup>, Rute Lopes<sup>1,4</sup>, Ezequiel Farrher<sup>1</sup>, and Seong Dae Yun<sup>1</sup>

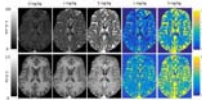
<sup>1</sup>Institute of Neuroscience and Medicine - 4, Forschungszentrum Jülich, Jülich, Germany, <sup>2</sup>Department of Neurology, Faculty of Medicine, RWTH Aachen University, JARA, Aachen, Germany, <sup>3</sup>Department of Electrical and Computer Systems Engineering, and Monash Biomedical Imaging, School of Psychological Sciences, Monash University, Melbourne, Australia, <sup>4</sup>Institute of Biomedical Engineering and Biophysics, Science Faculty of University of Lisbon, Lisbon, Portugal

Perfusion weighted imaging (PWI) using dynamic susceptibility contrast (DSC) imaging is a widely used technique in tumour imaging. The use of multi-echo DSC, gradient and spin echo (GESE), allows one to obtain vasculature information. However, trade-off between number of echoes, spatial resolution and brain coverage is required. In this work, the use of EPI with keyhole (EPIK) combined with multi-band is proposed to obtain a whole brain multi-echo GESE-DSC in clinically relevant acquisition times. The method was applied in a cohort of brain tumour patients in a MR-PET scanner enabling localisation of the tumour based on metabolic information from PET.

---

207

14:45



Comparison of Ferumoxytol based Cerebral Blood Volume estimates using Multi-Echo T2\* and Ultrashort Echo Time T1 Imaging

Leonardo Rivera Rivera<sup>1</sup>, Tilman Schubert<sup>2</sup>, Patrick A Turski<sup>2</sup>, and Kevin M Johnson<sup>1</sup>

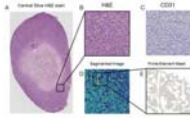
<sup>1</sup>Dept. of Medical Physics, University of Wisconsin-Madison, Madison, WI, United States, <sup>2</sup>Dept. of Radiology, University of Wisconsin-Madison, Madison, WI, United States

Intracranial vascularity is modified in a wide array of diseases including cancer, various forms of dementia, and stroke. Steady state imaging with Ferumoxytol provides unique opportunities to estimate cerebral blood volume (CBV). In this work, we investigate the correlation between relaxometry changes measured utilizing ultrashort echo time variable flip angle (UTE-VFA) R1 and a multi-echo R2\* approaches. Initial results from 8 healthy volunteers shows a high degree of correlation of R1 with R2\* measures and improved performance in and around vessels. This, and opportunities to probe disease induced disagreements, suggests potential value in combined R1 and R2\* measures.

---

14:57

The effects of intra-voxel contrast agent diffusion on the analysis of DCE-MRI data in realistic tissue domains

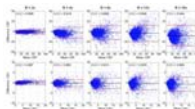


Ryan Thomas Woodall<sup>1</sup>, Stephanie L Barnes<sup>1</sup>, Anna G Sorace<sup>2</sup>, David A Hormuth II<sup>1</sup>, C Chad Quarles<sup>3</sup>, and Thomas E Yankeelov<sup>1</sup>

<sup>1</sup>Biomedical Engineering, The University of Texas at Austin, Austin, TX, United States, <sup>2</sup>Dell Medical School, The University of Texas at Austin, TX, United States, <sup>3</sup>Barrow Neurological Institute, AZ, United States

Standard compartmental models for quantitative dynamic contrast enhanced MRI (DCE-MRI) typically assume active delivery of contrast agent that is instantaneously distributed within the extravascular extracellular space within each imaging voxel. The goal of this study is to determine the error accumulated in the estimated pharmacokinetic parameters when these assumptions are not satisfied. Using finite element methods to model contrast agent arrival and diffusion throughout realistic tissue domains (obtained from histological stains of tissue sections from a murine cancer model), it was rigorously determined that parameterization error is highest in regions of low vascularity, and lowest in well-perfused regions.

15:09



A Robust Reconstruction Method for Quantitative Perfusion MRI: Application to Brain Dynamic Susceptibility Contrast (DSC) Imaging  
Cagdas Ulas<sup>1,2</sup>, Pedro A. Gomez<sup>1,2</sup>, Jonathan I. Sperl<sup>2</sup>, Christine Preibisch<sup>3</sup>, Marion I. Menzel<sup>2</sup>, Axel Haase<sup>4</sup>, and Bjoern H. Menze<sup>1</sup>

<sup>1</sup>Department of Computer Science, Technische Universität München, Munich, Germany, <sup>2</sup>GE Global Research, Munich, Germany, <sup>3</sup>Department of Neuroradiology, Technische Universität München, Munich, Germany, <sup>4</sup>Zentralinstitut für Medizintechnik, Technische Universität München, Munich, Germany

We propose a robust reconstruction model for dynamic perfusion magnetic resonance imaging (MRI) from undersampled k-space data. Our method is based on a joint penalization of the pixel-wise incoherence on temporal differences and patch-wise dissimilarities between spatio-temporal neighborhoods of perfusion image series. We evaluate our method on dynamic susceptibility contrast (DSC)–MRI brain perfusion datasets and demonstrate that the proposed reconstruction model can achieve up to 8-fold acceleration by yielding improved spatial reconstructions and providing highly accurate matching of perfusion time-intensity curves, thus leading to more precise quantification of clinically relevant perfusion parameters over two existing reconstruction methods.

210



15:21

Parameter	Value
Flipangle prescans (°)	5; 13; 20
Flipangle dynamics (°)	15
TR (ms)	5.9
Echo times (ms)	1.80; 4.0
Acquisition time (s)	3.9
No. dynamics	25
Parallel imaging	SENSE 2.5
Number of slices	25
Slice thickness (mm)	3.0
Voxel size (mm)	1.25x1.25
Acquisition matrix	168x168
FOV (mm)	420x420

### Automated renal motion correction using fat-images derived from Dixon reconstruction of DCE MRI

Anneloes de Boer<sup>1</sup>, Tim Leiner<sup>1</sup>, and Nico van den Berg<sup>1</sup>

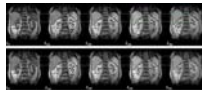
<sup>1</sup>University Medical Center Utrecht, Utrecht, Netherlands

In renal dynamic contrast enhanced (DCE) MRI respiratory motion of the kidneys necessitates registration of the dynamics. Since image contrast varies during contrast agent passage, automatic registration is challenging. We show that on Dixon-derived fat-images this contrast change is virtually absent. Therefore, we propose to perform automated image registration using fat-images and apply the resulting transformation to the water-images. We applied this method to DCE data of 10 patients and show its superiority over a conventional registration approach. Pharmacokinetic fits to a two-compartment model yielded realistic values for renal perfusion and filtration.

211



15:33



### Motion correction for 3D free-breathing renal DCE-MRI using tracer kinetic model-driven registration

Dimitra Flouri<sup>1,2</sup>, Daniel Lesnic<sup>2</sup>, Constantina Chrysochou<sup>3</sup>, Philip Kalra<sup>3</sup>, and Steven P Sourbron<sup>1</sup>

<sup>1</sup>Division of Biomedical Imaging, University of Leeds, Leeds, United Kingdom, <sup>2</sup>Department of Applied Mathematics, University of Leeds, Leeds, United Kingdom, <sup>3</sup>University of Manchester, Salford, United Kingdom

Tracer-kinetic model driven motion-correction is a highly effective strategy for 2D free-breathing DCE-MRI. In this study we address the challenge of translation to 3D by improving computational efficiency and evaluating performance in the presence of ghosting artefacts. Results in 8 patient cases show that the optimised algorithm is feasible in realistic computation times and effectively removes between-frame breathing motion despite significant within-frame artefacts. Quantitative evaluation against reference measurements shows a reduction of the bias, but precision is limited by within-frame artefacts and will require an integrated motion-correction and image reconstruction strategy.

Oral

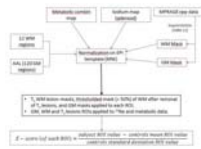
MS: Cutting Edge Methods



212



13:45



### Metabolic counterparts of sodium accumulation in Multiple Sclerosis: A whole brain 1H-MRSI and 23Na-MRI study

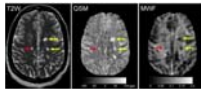
Maxime Donadieu<sup>1,2,3</sup>, Adil Maarouf<sup>1,4</sup>, Yann Le Fur<sup>1,4</sup>, Soraya Gherib<sup>1,4</sup>, Elisabeth Soulier<sup>1,4</sup>, Lauriane Pini<sup>1,4</sup>, Stanislas Rapacchi<sup>1,4</sup>, Sylviane Confort-Gouny<sup>1,4</sup>, Maxime Guye<sup>1,4</sup>, Jean Pelletier<sup>5</sup>, Bertrand Audoin<sup>5</sup>, Wafaa Zaaraoui<sup>1,4</sup>, and Jean-Philippe Ranjeva<sup>1,4</sup>

<sup>1</sup>Aix-Marseille University, CNRS, CRMBM UMR 7339, Medical School of Marseille, Marseille, France, Metropolitan, <sup>2</sup>AP-HM, CHU Timone, Department of Imaging, CEMEREM, Marseille, France, <sup>3</sup>Siemens Healthineers, Saint-Denis, France, Metropolitan, <sup>4</sup>AP-HM, CHU Timone, Department of Imaging, CEMEREM, Marseille, France, Metropolitan, <sup>5</sup>AP-HM, CHU Timone, Department of Neurology, Marseille, France, Metropolitan

To determine the metabolic counterparts of cerebral total sodium accumulations in patients with Multiple Sclerosis, we acquired fast 3D-<sup>1</sup>H-EPSI and Density-adapted 3D-UTE <sup>23</sup>Na MRI at 3 Tesla covering the whole brain in 21 patients and 20 volunteers. Patients showed increased <sup>23</sup>Na and decreased NAA, Glx and Cho levels. Stepwise analyses highlights association of <sup>23</sup>Na accumulations with i) decreased NAA and Glx levels and increased Cho levels within GM, ii) with decreased NAA and increased Cho levels within NAWM and T<sub>2</sub> lesion compartments. Clinical status of patients assessed by MSFC was correlated to GM and NAWM <sup>23</sup>Na, NAA and Glx levels.

213

13:57



### MS lesions demonstrating a QSM hyperintense-rim have more myelin loss compared to those without a QSM hyperintense-rim

Yihao Yao<sup>1</sup>, Thanh D. Nguyen<sup>2</sup>, Sneha Pandya<sup>2</sup>, Sandra Hurtado Rúa<sup>3</sup>, Amy Kuceyeski<sup>4</sup>, Yi Wang<sup>2,5</sup>, and Susan A. Gauthier<sup>6</sup>

<sup>1</sup>Department of Radiology, Tongji Hospital, Tongji Medical College, Huazhong University of Science & T, Wuhan, People's Republic of China, <sup>2</sup>Department of Radiology, Weill Cornell Medical College, New York, NY, United States, <sup>3</sup>Department of Mathematics, Cleveland State University, Cleveland, OH, <sup>4</sup>Department of Radiology, Weill Cornell Medicine Feil Family Brain and Mind Research Institute, New York, NY, United States, <sup>5</sup>Biomedical Engineering, Cornell University, Ithaca, NY, United States, <sup>6</sup>Department of Neurology, Weill Cornell Medical College, New York, NY, United States

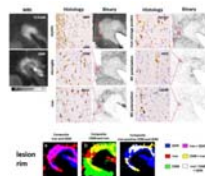


Iron causes proinflammatory activation of microglia near the rim of white matter MS lesion. This is chronic inflammation with associated myelin tissue damage. We propose to use quantitative susceptibility mapping (QSM) to assess chronic inflammation, as hyperintense rim on QSM can be unequivocally interpreted as iron. We use myelin water fraction (MWF) to measure myelin. We have found that MS lesions with hyperintense rims on QSM have lower MWF and higher susceptibility compared to lesions without hyperintense rims on QSM ( $p < 0.01$ ). Hyperintense rim on QSM may provide a biomarker for tissue injury due to iron associated chronic inflammation.

214



14:09



### Combining QSM and MWF in multiple sclerosis: a marker for the inflammatory state of MS lesions?

Carsten Stueber<sup>1,2</sup>, Alexey Dimov<sup>1</sup>, Kofi Deh<sup>1</sup>, Thanh Nguyen<sup>1</sup>, Yi Wang<sup>1</sup>, and David Pitt<sup>2</sup>

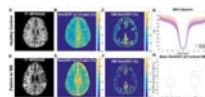
<sup>1</sup>Weill Cornell Medicine, New York, NY, United States, <sup>2</sup>Yale University, New Haven, CT, United States

Multiple sclerosis (MS) is a demyelinating disease of the central nervous system. In particular, excess iron is considered to play an essential role in lesion activity. In this study, we combine iron-reflecting quantitative susceptibility mapping (QSM) and myelin water fraction (MWF) with histology in post-mortem tissue. Our results show that elevated iron concentrations at the lesion rim reflect pro-inflammatory microglial activity, suggesting to use QSM to determine levels of lesion inflammation and MWF for detecting ongoing demyelination.

215



14:21



### Glutamate-Sensitive CEST in Cortical Gray Matter: Application to Cognitive Impairment in Multiple Sclerosis

Kristin P. O'Grady<sup>1,2</sup>, Adrienne N. Dula<sup>3,4,5</sup>, Bailey D. Lyttle<sup>1,2</sup>, Benjamin N. Conrad<sup>2</sup>, Bailey A. Box<sup>1,2</sup>, Siddharama Pawate<sup>6</sup>, Francesca R. Bagnato<sup>6</sup>, and Seth A. Smith<sup>1,2,7</sup>

<sup>1</sup>Department of Radiology and Radiological Sciences, Vanderbilt University Medical Center, Nashville, TN, United States, <sup>2</sup>Vanderbilt University Institute of Imaging Science, Vanderbilt University Medical Center, Nashville, TN, United States, <sup>3</sup>Stroke Institute, Seton Dell Medical School, Austin, TX, United States, <sup>4</sup>Department of Neurology, Seton Dell Medical School, Austin, TX, United States, <sup>5</sup>Department of Neuroscience, University of Texas, Austin, TX, United States, <sup>6</sup>Department of Neurology, Vanderbilt University, Nashville, TN, United States, <sup>7</sup>Department of Biomedical Engineering, Vanderbilt University, Nashville, TN, United States

Altered glutamate regulation in gray matter (GM) has been implicated in the pathogenesis of cognitive impairment in multiple sclerosis (MS), but such pathology in GM is subtle and difficult to detect using conventional MRI techniques. In this work, we apply a quantitative, glutamate-sensitive chemical exchange saturation transfer (GluCEST) MRI technique at 7.0T to gain new insights into molecular changes underlying GM pathology and their relationship to cognitive impairment in MS. We found significant differences in cortical GM GluCEST contrast between healthy controls and patients with MS, and in some cortical regions, GluCEST contrast correlates significantly with measures of cognitive impairment.

216

14:33

Using myelin water and diffusion basis spectrum imaging to differentiate demyelination, inflammation, oedema and axonal damage in subjects with multiple sclerosis



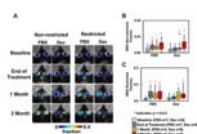
Irene Margaret Vavasour<sup>1</sup>, Peng Sun<sup>2</sup>, Shannon H Kolind<sup>1,3</sup>, David KB Li<sup>1</sup>, Alex L MacKay<sup>1,4</sup>, Sheng-Kwei Song<sup>2</sup>, Robert Carruthers<sup>3</sup>, and Anthony L Traboulsee<sup>3</sup>

<sup>1</sup>Radiology, University of British Columbia, Vancouver, BC, Canada, <sup>2</sup>Radiology, Washington University, St. Louis, MO, United States, <sup>3</sup>Medicine (Neurology), University of British Columbia, Vancouver, BC, Canada, <sup>4</sup>Physics and Astronomy, University of British Columbia, Vancouver, BC, Canada

This study compared myelin water fraction (MWF), intra/extracellular water geometric mean  $T_2$  (ieGMT<sub>2</sub>) and diffusion basis spectrum imaging (DBSI)-derived measures in multiple sclerosis (MS) lesions and normal appearing white matter. 14 MS subjects were scanned with 48-echo  $T_2$  relaxation and DBSI sequences. Significant correlations were found for MWF vs radial diffusivity, MWF vs fiber fraction, and ieGMT<sub>2</sub> vs restricted fraction. Lesions showed changes consistent with decreased myelin and axons. Enhancing lesions also showed increased oedema. By quantitatively distinguishing and tracking inflammation, axon and myelin injury, DBSI and myelin water imaging can inform us of the pathological processes involved in MS.

217

14:45



### Corticosteroid Treatment Fails to Prevent Long-term Axonal Loss Assessed by Diffusion Basis Spectrum Imaging

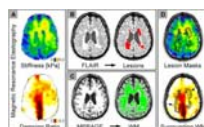
Tsen-Hsuan (Abby) Lin<sup>1</sup>, Jie Zhan<sup>2</sup>, Chunyu Song<sup>3</sup>, Michael Wallendorf<sup>4</sup>, Peng Sun<sup>1</sup>, Anne H Cross<sup>5,6</sup>, and Sheng-Kwei Song<sup>1,3,6</sup>

<sup>1</sup>Radiology, Washington University School of Medicine, St. Louis, MO, United States, <sup>2</sup>Radiology, The First Affiliated Hospital of Nanchang University, Jiangxi, People's Republic of China, <sup>3</sup>Biomedical Engineering, Washington University in St. Louis, St. Louis, MO, United States, <sup>4</sup>Biostatistics, Washington University School of Medicine, St. Louis, United States, <sup>5</sup>Neurology, Washington University School of Medicine, St. Louis, MO, United States, <sup>6</sup>The Hope Center for Neurological Disorders, Washington University School of Medicine, St. Louis, MO, United States

Glucocorticoids are commonly used to treat acute optic neuritis. Herein, we employed longitudinal diffusion basis spectrum imaging (DBSI) to examine and compare optic nerve integrity in EAE with PBS or Dexamethasone treatment. Our results indicate that anti-inflammatory treatment with corticosteroids alone is not sufficient to prevent eventual axonal loss in mice, and may have relevance for treatment of MS exacerbations with corticosteroids. DBSI could serve as an outcome measure to monitor longitudinal disease progression and to help stratify treatments.

218

14:57



### Multiple sclerosis lesions are softer than surrounding white matter: An MR elastography study

Curtis L Johnson<sup>1</sup>, Christian A Thompson<sup>1</sup>, Brian M Sandroff<sup>2</sup>, Thomas A Edwards<sup>3</sup>, Elizabeth A Hubbard<sup>3</sup>, Rachel E Klaren<sup>3</sup>, Hillary Schwarb<sup>4</sup>, Bradley P Sutton<sup>4</sup>, Lara A Pilutti<sup>5</sup>, and Robert W Motl<sup>6</sup>

<sup>1</sup>Department of Biomedical Engineering, University of Delaware, Newark, DE, United States, <sup>2</sup>Kessler Foundation, East Hanover, NJ, United States, <sup>3</sup>Department of Kinesiology and Community Health, University of Illinois at Urbana-Champaign, Urbana, IL, United States, <sup>4</sup>Beckman Institute for Advanced Science and Technology, University of Illinois at Urbana-Champaign, Urbana, IL, United States, <sup>5</sup>Interdisciplinary School of Health Sciences, University of Ottawa, Ottawa, ON, Canada, <sup>6</sup>Department of Physical Therapy, University of Alabama at Birmingham, Birmingham, AL, United States

Mechanical properties of the brain measured with magnetic resonance elastography (MRE) have proven sensitive to tissue health in neurological conditions, including multiple sclerosis (MS). In this study, we use high-resolution MRE to examine the mechanical properties of focal lesions in subjects with MS to determine if they exhibit viscoelastic signatures that differ from surrounding white matter. In a sample of fourteen subjects, we found that lesions are significantly softer than surrounding white matter. This finding suggests MRE is sensitive to tissue disruption localized to focal lesions, and may provide novel measures of tissue health in the assessment of MS.

219

15:09

Number of subjects	Age (years)	Sex	EDSS	MS subtype
14	38.1 ± 10.1	10 F, 4 M	2.5 ± 0.8	10 RRMS, 4 SPMS
10	37.1 ± 10.1	7 F, 3 M	2.5 ± 0.8	10 RRMS
4	40.0 ± 10.0	3 F, 1 M	2.5 ± 0.8	4 SPMS

### Investigation of outer and inner cerebellar MTR abnormalities in different MS clinical subtypes

Rebecca Sara Samson<sup>1</sup>, Manuel J Cardoso<sup>2,3</sup>, Nils Muhlert<sup>1,4</sup>, Varun Sethi<sup>1,5</sup>, Özgür Yaldizli<sup>1,6</sup>, Maria A Ron<sup>1</sup>, Ferran Prados<sup>1,2</sup>, Sebastian Ourselin<sup>2,3</sup>, David H Miller<sup>1,7</sup>, Claudia A M Gandini Wheeler-Kingshott<sup>1,8,9</sup>, and Declan T Chard<sup>1,7</sup>

<sup>1</sup>UCL Institute of Neurology, Queen Square MS Centre, University College London, London, United Kingdom, <sup>2</sup>Translational Imaging Group, Centre for Medical Image Computing, Department of Medical Physics and Biomedical Engineering, University College London, London, United Kingdom, <sup>3</sup>Dementia Research Centre, Department of Neurodegenerative Diseases, UCL Institute of Neurology, University College London, London, United Kingdom, <sup>4</sup>Division of Neuroscience and Experimental Psychology, University of Manchester, Manchester, United Kingdom, <sup>5</sup>Department of Neurology, Nottingham University Hospitals, Nottingham, United Kingdom, <sup>6</sup>Department of Neurology, University Hospital Basel, Basel, Switzerland, <sup>7</sup>National Institute for Health Research (NIHR) University College London Hospitals Biomedical Research Centre, United Kingdom, <sup>8</sup>Department of Brain and Behavioural Sciences, University of Pavia, Pavia, Italy, <sup>9</sup>Brain MRI 3T Center, C. Mondino National Neurological Institute, Pavia, Italy

Histopathology has demonstrated extensive grey matter (GM) damage in MS, and an association with meningeal inflammatory factors has previously been suggested. We applied a method to subdivide the cerebellar GM (CGM) into inner and outer regions, and investigated for magnetization transfer ratio (CGM-MTR) abnormalities in MS subtypes compared to healthy controls (HC). Outer was lower than inner CGM-MTR in all groups including HC. Outer and inner CGM-MTR reductions were observed in progressive MS subtypes. Stronger correlations of outer than inner CGM-MTR with clinical scores were observed, suggesting that outer CGM-MTR may reflect more clinically relevant pathology, particularly in progressive MS.

220

15:21

### High Spatial Resolution Mapping of Trans-Capillary Water Exchange in Progressive Multiple Sclerosis

Group	n	Mean Age (SD), yrs	Age Range (yrs)
HC			
Female	7	53.3 (11.7)	34-64
Male	7	46.4 (12.2)	34-64
SPMS			
Female	10	57.7 (7.2)	43-64
Male	6	54.5 (11.5)	35-65

Ian Tagge<sup>1</sup>, Manoj Sammi<sup>1</sup>, Rebecca Spain<sup>2</sup>, Dennis Bourdette<sup>2</sup>, Randy West<sup>2</sup>, John Grinstead<sup>1,3</sup>, Katherine Powers<sup>1</sup>, Xin Li<sup>1</sup>, Charles Springer<sup>1</sup>, and William Rooney<sup>1</sup>

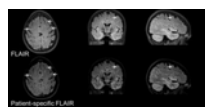
<sup>1</sup>Advanced Imaging Research Center, Oregon Health & Science University, Portland, OR, United States, <sup>2</sup>Neurology, Oregon Health & Science University, Portland, OR, United States, <sup>3</sup>Siemens Medical Solutions, Portland, OR

DCE-MRI data were acquired from 14 healthy control (HC) and 16 secondary progressive multiple sclerosis subjects on a 7T MRI instrument to investigate difference in brain blood vessel properties. The Shutter-Speed Paradigm was used to map blood volume fraction and trans-capillary water exchange kinetics. Our findings suggest abnormalities in brain blood vessel properties suggestive of impaired metabolism in secondary progressive MS.

221

15:33

### Improving white matter lesion conspicuity in multiple sclerosis using patient-specific optimization of 3D FLAIR



Refaat E Gabr<sup>1</sup>, Amol S Pednekar<sup>2</sup>, Koushik A Govindarajan<sup>1</sup>, Xiaojun Sun<sup>1</sup>, Roy F Riascos<sup>1</sup>, María G Ramirez<sup>1</sup>, Khader M Hasan<sup>1</sup>, John A Lincoln<sup>3</sup>, Flavia M Nelson<sup>3</sup>, Jerry S Wolinsky<sup>3</sup>, and Ponnada A Narayana<sup>1</sup>

<sup>1</sup>Diagnostic and Interventional Imaging, University of Texas Health Science Center at Houston, Houston, TX, United States, <sup>2</sup>Philips Healthcare, Cleveland, OH, United States, <sup>3</sup>Neurology, University of Texas Health Science Center at Houston, Houston, TX, United States

Fluid-attenuated inversion recovery (FLAIR) imaging is widely used in multiple sclerosis (MS) scan protocols for its good lesion to tissue contrast. Optimization of 3D FLAIR acquisition parameters for the individual patient could further improve lesion conspicuity. In this work, tissue contrast between lesions and white matter for 3D FLAIR was optimized in the same scan session based on fast measurement of the relaxation times and proton density. Results on 16 MS patients show ~30% improved lesion contrast with the patient-specific acquisition parameters compared to the fixed-parameter 3D FLAIR sequence.

---

---

## Combined Educational & Scientific Session

### Studying the Value of MRI

Organizers: Vikas Gulani, M.D., Ph.D. & James G. Pipe, Ph.D.

Room 315                      Monday 13:45 - 15:45    *Moderators: Vikas Gulani & James Pipe*

---

13:45

Studying Value in MRI: A US Perspective

Yoshimi Anzai<sup>1</sup>

<sup>1</sup>*University of Utah Health*

The current healthcare transformation provides a perfect opportunity for the entire MR community to deliberate the value of MRI. It is essential to understand what each stakeholder wants or needs from MR or information obtained from MRI. A focused MR protocol with shorter scan time, reduced costs and accurate, timely, and actionable diagnosis are just a few examples. The challenges provide strong motivation and incentives for us to make strategies for developing high-value MRI. By doing so, imaging will become the value center, not the cost center, for the health system and patient care spectrum.

13:49

Studying Value in MRI: A South Korean Perspective

Jeong Min Lee<sup>1</sup>

<sup>1</sup>*Seoul National University Hospital*

In summary, MR allows a high detection and characterization rate in the abdomen, without ionizing radiation. Also, abbreviated noncontract MRI protocol can be used for screening several abdominal diseases. To further increase the value of MRI, the additional effort for increasing compliance of patients for MR examination by incorporating free breathing sequences or shortening examination time, and increasing awareness of its superiority to CT in imaging many of the abdominal organs would be necessary.

---

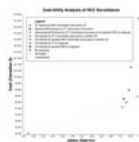
13:53

Opening Remarks

---

222

13:57



Cost-Utility Analysis of Ultrasound, Computed Tomography, Abbreviated and Standard MRI for Hepatocellular Carcinoma Surveillance

An Tang<sup>1,2</sup>, Boyan Fan<sup>1</sup>, Joshua Bérubé<sup>1</sup>, Milena Cerny<sup>1</sup>, Damien Olivé<sup>1</sup>, Jeanne-Marie Giard<sup>3</sup>, Luigi Lepanto<sup>1,4</sup>, and Jean Lachaine<sup>5</sup>

*<sup>1</sup>Radiology, University of Montreal, Montreal, QC, Canada, <sup>2</sup>Centre de recherche du Centre hospitalier de l'Université de Montréal (CRCHUM), Montreal, QC, Canada, <sup>3</sup>Gastroenterology and Hepatology, University of Montreal, Montreal, QC, Canada, <sup>4</sup>Health Technology Assessment Unit, <sup>5</sup>Faculty of Pharmacy and Pharmacoeconomics, University of Montreal, Montreal*

Current clinical practice guidelines recommend ultrasound (US) every 6 months for surveillance of hepatocellular carcinoma (HCC) in at-risk patients. Despite higher sensitivity, there is uncertainty regarding the role of MRI for HCC surveillance, whether as an add-on or replacement test. Our results indicate that surveillance with standard MRI followed by CT if technically inconclusive provided the highest level of effectiveness. However, CT followed by MRI was more cost-effective than alternative surveillance strategies using a threshold of \$50,000 per QALY gained. Further, lower cost of abbreviated MRI will be required to be used as a first-line imaging technique for surveillance.

---

223

14:01



Optimizing MRI for Focal Liver Lesions: Are All Our Sequences Really Necessary?

Sara Dastmalchian<sup>1</sup>, Nicholas Fulton<sup>2,3</sup>, Majid Chalian<sup>2,3</sup>, Ozden Kilinc<sup>1</sup>, Mark Griswold<sup>4</sup>, Vikas Gulani<sup>2,3</sup>, and Karin Herrmann<sup>2,3</sup>



<sup>1</sup>Department of Radiology, Case Western Reserve University, Department of Radiology, Cleveland, OH, United States, <sup>2</sup>Department of Radiology, University hospitals Cleveland medical center, Cleveland, OH, United States, <sup>3</sup>University Hospitals Cleveland Medical Center, Cleveland, OH, United States, <sup>4</sup>Case Western University

In this proof-of-concept study, our aim was to determine an optimal minimum number of MRI sequences which allow confident characterization of liver lesions into benign versus malignant categories with reasonable accuracy. We hypothesized that an abbreviated liver MRI protocol including single shot T2-weighted, pre and dynamic post-contrast T1-weighted images has the potential to reduce overall scan time and throughput. If this can be performed without significant loss in diagnostic accuracy it may improve efficacy and be beneficial to current practice.

224

14:05

Image set	Standard	Abbreviated	Per Patient %	Per Patient %
Standard set	Standard set	Standard set	100%	100%
Abbreviated set	Standard set	Abbreviated set	100%	100%
Standard set	Abbreviated set	Standard set	100%	100%
Abbreviated set	Abbreviated set	Abbreviated set	100%	100%

Short 15-min surveillance-protocol multiphasic contrast enhanced MRI for hepatocellular carcinoma detection in cirrhosis

Takeshi Yokoo<sup>1</sup>, Gaurav Khatri<sup>1</sup>, Lakshmi Ananthakrishnan<sup>1</sup>, David Fetzer<sup>1</sup>, Yin Xi<sup>1</sup>, and Ivan Pedrosa<sup>1</sup>

<sup>1</sup>Radiology, UT Southwestern Medical Center, Dallas, TX, United States

Patient with cirrhosis are at increased risk of developing hepatocellular carcinoma (HCC) and routine surveillance imaging is recommended every 6 months. While MRI has high sensitivity for HCC detection, its routine use is controversial due to its long exam time, high cost, and limited access. In this prospective study, we demonstrated that a short 15-min surveillance MRI has similar HCC detection performance as the standard 45-min diagnostic MRI in patients with cirrhosis. Therefore, a short surveillance MRI may allow for a more efficient and cost-effective alternative to the current standard-of-care MRI for HCC surveillance.

225

14:09

	Standard	Abbreviated	Standard	Abbreviated
Sensitivity	88.8%	87.5%	87.5%	87.5%
Specificity	88.8%	100%	87.5%	100%
PPV	88.8%	87.5%	87.5%	87.5%
NPV	88.8%	87.5%	87.5%	87.5%
Accuracy	88.8%	87.5%	87.5%	87.5%

Diagnostic performance of an abbreviated gadoxetic acid enhanced-MRI (AMRI) vs. ultrasound for detection of small HCC: pilot study.

Cecilia Besa<sup>1</sup>, Sara Lewis<sup>1</sup>, Mathilde Wagner<sup>1,2</sup>, Yujin Hoshida<sup>3</sup>, Ruth Carlos<sup>4</sup>, Claude B Sirlin<sup>5</sup>, and Bachir Taouli<sup>1</sup>

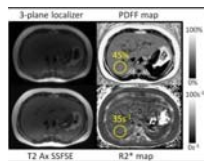
<sup>1</sup>Translational and Molecular Imaging Institute, Icahn School of Medicine at Mount Sinai, New York, NY, United States, <sup>2</sup>Radiology, Groupe Hospitalier Pitié Salpêtrière, Paris, France, <sup>3</sup>Department of Medicine/Division of Liver Diseases, Icahn School of Medicine at Mount Sinai, New York, NY, United States, <sup>4</sup>Radiology, Division of Abdominal Radiology, University of Michigan Health System, Ann Arbor, MI, United States, <sup>5</sup>Liver Imaging Group, Department of Radiology, University of California, San Diego, CA, United States

In this study, we aim to test the diagnostic value of an abbreviated MRI (AMRI) using gadoxetic acid (with patient injected outside the MRI room) compared to ultrasound (US) for hepatocellular carcinoma (HCC) detection in a population of patients with small HCC and controls. This study demonstrates that AMRI using T1WI obtained at the hepatobiliary phase (T1w-HBP), diffusion weighted imaging (DWI) and T2WI has superior diagnostic performance for HCC detection compared to US. This could serve as the basis for a future study assessing AMRI for HCC screening/surveillance in patients with cirrhosis.

---

226

14:13



Demonstrating the Clinical Feasibility of a Rapid Non-Contrast MRI Protocol for Detection and Quantification of Hepatic Steatosis and Iron Overload

B. Dustin Pooler<sup>1</sup> and Scott B. Reeder<sup>1</sup>

<sup>1</sup>University of Wisconsin, Madison, WI, United States

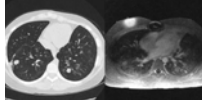
Many clinical scenarios necessitate evaluation for hepatic steatosis or iron overload without indication for a complicated MR exam. Emerging confounder-corrected chemical shift encoded MRI (CSE-MRI) techniques can provide simultaneous estimation of liver proton density fat fraction (PDFF) and R2\* as biomarkers of steatosis and iron overload, respectively. We have developed a highly focused CSE-MRI protocol which obtains these metrics in approximately 5 minutes of table time. Our initial clinical experience has shown this protocol to be feasible for evaluation of patients ranging from pediatric to geriatric, with clinically significant disease detected in a large fraction of patients scanned to date.

---

14:17

Discussion

---

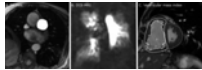


Contrast-enhanced Ultrashort Echo Time (UTE) MR of the chest to evaluate for metastatic nodules in pediatric patients with malignancy undergoing abdomen MR staging and surveillance: a high-value alternative or adjunct to CT

Anshul Haldipur<sup>1</sup>, Evan James Zucker<sup>1</sup>, Joseph Y. Cheng<sup>1</sup>, and Shreyas S. Vasanaawala<sup>1</sup>

<sup>1</sup>Radiology, Stanford University, Stanford, CA, United States

Ultrashort Echo Time (UTE) MRI of the chest can be optimized for detection of metastatic lung nodules. In pediatric patients with a history of abdominal malignancies undergoing routine re-staging contrast-enhanced MRI exams, clinically significant metastatic lung nodules are detectable which, if diagnosed, could obviate or decrease the frequency of subsequent separate CT scans of the chest. Though cost of a chest CT is lower than an MRI, it is substantially more than the incremental cost of adding an additional sequence during already-scheduled MR Abdomen exams. Additionally, ionizing radiation is avoided, alleviating concerns about cumulative exposure following multiple serial follow-up examinations.

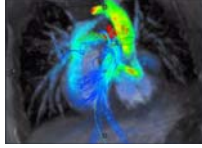


The use of MRI in the diagnosis of Chronic Thromboembolic Pulmonary Hypertension

Christopher S Johns<sup>1</sup>, Andy J Swift<sup>1,2</sup>, Jens Vogel-Claussen<sup>3</sup>, David G Kiely<sup>4</sup>, and Jim M Wild<sup>1</sup>

<sup>1</sup>Academic Radiology, The University of Sheffield, Sheffield, United Kingdom, <sup>2</sup>Insigneo, Institute of In-Vivo Medicine, <sup>3</sup>Medizinische Hochschule Hannover, Germany, <sup>4</sup>Pulmonary Vascular Disease Unit, Sheffield Teaching Hospitals, United Kingdom

As surgical pulmonary endarterectomy significantly improves survival in patients with chronic thrombo-embolic pulmonary hypertension it is important to correctly identify patients. Using cardiopulmonary MRI it is possible to screen for the presence of chronic thrombo-emboli in all cases who can tolerate MRI, reducing the requirement for SPECT (and therefore patient radiation exposure). The same scan can also predict the presence of pulmonary hypertension, and due to a high specificity we can reduce the reliance upon an invasive test (right heart catheterisation) by around 50%.

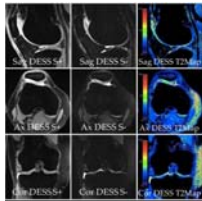


### Combined 3D Cine/4D Flow Accelerated Cardiac Imaging with Cloud Computing. Toward Streamlined and Fast Comprehensive Cardiac MRI Exam

Haonan Wang<sup>1</sup>, Peng Lai<sup>2</sup>, Piero Ghedin<sup>1</sup>, Shreyas S Vasanawala<sup>3</sup>, Anja C.S Brau<sup>2</sup>, and El-Sayed Ibrahim<sup>1</sup>

<sup>1</sup>GE Healthcare, Waukesha, WI, United States, <sup>2</sup>GE Healthcare, Menlo Park, CA, United States, <sup>3</sup>Radiology, Stanford University, CA, United States

Currently, cine MRI is the gold standard for evaluating cardiac function. Nevertheless, in today's practice, slices need to be acquired at different oblique, and 12-16 short-axis slices needs to be acquired for sufficient ventricular coverage. The same limits apply to hemodynamics-related assessment of valvular and vascular performance, for which multiple 2D oblique flow measurements need to be acquired. In this abstract, we present a combined 3D Cine/4D Flow accelerated cardiac imaging technique with cloud computing, which significantly reduces the scan and processing time, reduces the scan's complexity, alleviates misregistration problems, and increases productivity.



### 5 Minute Comprehensive Knee MRI with 3D Double-Echo Steady-State (DESS)

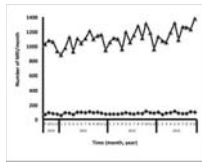
Akshay S Chaudhari<sup>1</sup>, Bragi Sveinsson<sup>1</sup>, Jeff P Wood<sup>1</sup>, Dushyant S Thakur<sup>1</sup>, Kathryn J Stevens<sup>1</sup>, Chris F Beaulieu<sup>1</sup>, Marcus T Alley<sup>1</sup>, Curtis Abercrombie<sup>1</sup>, Garry E Gold<sup>1</sup>, and Brian A Hargreaves<sup>1</sup>

<sup>1</sup>Radiology, Stanford University, Stanford, CA, United States

Knee MRI is performed commonly in the US for assessing acute injuries as well as degenerative diseases. However, current knee MRI protocols can require 25-30 minutes or more and cost approximately \$1.1billion/year. In such instances, a short knee protocol could lower costs while increasing patient throughput, comfort, and access to care. In this study, we show that a five-minute double-echo steady-state (DESS) scan, with automatic T<sub>2</sub> maps and fluid-nulled images, offers high efficacy and diagnostic utility compared to the standard knee protocol. These results suggest that a five-minute DESS scan could be used for comprehensive MRI of the knee.

### Targeted Rapid Knee MRI Exam using T2 Shuffling





Elaine Lui<sup>1</sup>, David Wang<sup>1</sup>, Nawaf Yassi<sup>2</sup>, Bruce Campbell<sup>2</sup>, and Patricia Desmond<sup>1</sup>

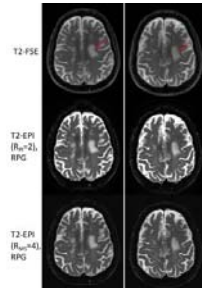
<sup>1</sup>Radiology, Royal Melbourne Hospital, University of Melbourne, Melbourne, Australia, <sup>2</sup>Neurology, Royal Melbourne Hospital, University of Melbourne, Melbourne, Australia

Stroke is an emergency. Although MRI is the imaging gold standard for the ischemic “core” in the hyperacute setting, MRI must be “quick” to remain relevant in the management pathway of this common disease. A “quick diffusion weighted imaging”(qDWI) protocol for acute stroke consisting of a single DWI sequence was implemented at our institution. qDWI reduced scan time by 84% compared to our conventional “Stroke” protocol, was 96.5% diagnostic, and with 90% not requiring further MRI. There was also a statistically significant quicker referral to scan time compared to the conventional “Stroke” MRIs.

234

14:53

### High-Resolution, Echo Planar Imaging on a Compact MRI Scanner: Applications in Stroke and Neuroimaging



Ek T Tan<sup>1</sup>, Paul T Weavers<sup>2</sup>, Erin M Gray<sup>2</sup>, Christopher J Hardy<sup>1</sup>, John F Schenck<sup>1</sup>, Matt A Bernstein<sup>2</sup>, Yunhong Shu<sup>2</sup>, Thomas KF Foo<sup>1</sup>, and John Huston<sup>2</sup>

<sup>1</sup>GE Global Research, Niskayuna, NY, United States, <sup>2</sup>Radiology, Mayo Clinic, Rochester, MN, United States

Rapid (six minutes and under) neuroimaging protocols can improve patient throughput and scanner utilization, especially when accelerated using the relatively fast EPI readout. However, susceptibility-related image distortion in EPI has limited its useful spatial resolution (2-2.5mm) conventional, whole-body 3T MRI. A 3.5-fold faster slew-rate head-only gradient on a novel low-cryogen compact 3T scanner can provide an effective platform for twofold-faster EPI that achieves higher spatial resolution (1mm). The utility of rapid (under one minute) single- and multi-shot T2-weighted EPI on the compact 3T is evaluated and compared to routine T2-FSE imaging in patients with brain tumors and stroke.

235

14:57

### Accelerating multi-contrast imaging in neuro-exam with sharable information

Example of proposed acceleration to multi-contrast neuro-imaging protocol

Sequence	Resolution	Time (min)	Contrast
ax T1 Brain	ax 0.5	3.0	ax
ax T2 FSE	ax 0.5	2.0	ax
ax T2 FSE	ax 0.5	2.0	ax
ax DWI	ax 0.5	0.5	ax
ax DWI	ax 0.5	0.5	ax

Enhao Gong<sup>1</sup>, John Pauly<sup>1</sup>, and Greg Zaharchuk<sup>2</sup>

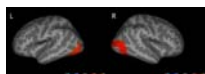
<sup>1</sup>Electrical Engineering, Stanford University, Stanford, CA, United States,  
<sup>2</sup>Radiology, Stanford University, Stanford, CA, United States

Neurological disorders results in great clinical challenges and high societal burdens. Currently multi-contrast MRI exams are frequently used for diagnosis because of the various tissue contrasts provides complementary diagnosis information to distinguish normal tissue from pathology. However, the cost of acquiring these multiple sequences is extensive scanning time, which significantly increases both the diagnosis cost and patients' discomfort. Here we proposed a new approach to accelerate multi-contrast imaging by using Parallel Imaging, Compressed Sensing and sharable information. We validated the new approach with experiments on both patients and healthy subjects. We demonstrate that we can reduce the multi-contrast MRI scanning time significantly while preserving the diagnostic information.

---

236

15:01



Prediction of treatment response using baseline structural and functional MRI in first-episode antipsychotic-naive schizophrenia

Su Lui<sup>1</sup>, Lu Liu<sup>2</sup>, Yuan Xiao<sup>2</sup>, Bo Tao<sup>2</sup>, Biqu Tang<sup>2</sup>, and Qiyong Gong<sup>2</sup>

<sup>1</sup>west china hospital of sichuan university, chengdu, People's Republic of China, <sup>2</sup>west china hospital of sichuan university

Finding imaging biomarkers which could predict the treatment response is quite important to help the selection of therapy and save health resource.

---

15:05

Discussion

---

15:09

Closing Remarks

---

### Traditional Poster: Musculoskeletal

Exhibition Hall 1532-  
1562

Monday 16:15 - 18:15 (no CME credit)

---

### Electronic Poster: Molecular Imaging

Exhibition Hall

Monday 16:15 - 17:15 (no CME credit)

---



## Electronic Poster: Contrast Mechanisms

Exhibition Hall                      Monday 16:15 - 17:15    *(no CME credit)*

---

### Study Groups

## MR Engineering Study Group

Room 323ABC                      Monday 16:15 - 18:15    *(no CME credit)*

---

### Study Groups

## Hyperpolarized Media MR Study Group

Room 317AB                      Monday 16:15 - 18:15    *(no CME credit)*

---

### Educational Course

## MR Physics & Techniques for Clinicians

*Organizers:* Marcus T. Alley, Ph.D. & Bernd Jung, Ph.D.

Room 316BC                      Monday 16:15 - 18:15    *Moderators:* Marcus Alley & Oliver Wieben

---

16:15                      [Spin Gymnastics 1 & 2](#)  
Walter Kucharczyk

[This is non-mathematical overview of how MRI signals are generated, received, and encoded to form magnetic resonance images.](#)

---

17:35                      [Image quality](#)  
Rafael O'Halloran<sup>1</sup>

<sup>1</sup>*Radiology, Icahn School of Medicine at Mount Sinai, New York, NY, United States*

[We will take a graphical approach to explore key concepts of image quality and discuss how sequence parameters affect image quality using the idea of k-space. Using cartoons and images we will demonstrate how resolution, field-of-view, and SNR can be understood in terms of k-space coverage and sampling. The implications on image quality will be discussed and demonstrated with example images.](#)

---

**Educational Course****Multiple Sclerosis: State of the Field in 2017**

Organizers: Alex L. MacKay, D.Phil.

Room 315                      Monday 16:15 - 18:15    Moderators: Alex MacKay & Rebecca Samson

---

16:15

**Pathology of Multiple Sclerosis**Bruce D. Trapp<sup>1</sup>

*<sup>1</sup>Cleveland Clinic Foundation, Cleveland, OH, United States*

We describe postmortem characteristics of individuals with multiple sclerosis that have spinal cord demyelination, cortical demyelination, and an absence of cerebral white matter demyelination. Despite the paucity of cerebral white matter demyelination, cortical neuronal loss, cortical atrophy, and cerebral white matter MRI abnormalities were similar to those found in multiple sclerosis brains with abundant cerebral white matter demyelination. We identify myelinated axonal swellings as the pathological correlate of the focal white matter MRI abnormalities and establish that degeneration of cortical neurons and cerebral white matter demyelination can be independent events in individuals with “myelocortical multiple sclerosis.”

---

16:45

**Role of MR in MS Diagnosis & Management**Yukio Miki<sup>1</sup>

*<sup>1</sup>Osaka City University, Japan*

MR imaging has been established as the most important tool for diagnosing multiple sclerosis (MS). In addition, this modality is increasingly being used to monitor disease activity, disease progression and therapeutic effects, and is therefore now recognized as an “imaging biomarker” for MS. Furthermore, MR imaging is also useful for diagnosing the side effects of pharmacotherapies. This lecture focuses on the role of MR imaging in the diagnosis and management in MS.

---

17:15

**Role of MR in MS Clinical Trials**

Anthony Traboulsee<sup>1</sup>

<sup>1</sup>Neurology, University of British Columbia, Vancouver, BC, Canada

---

17:45 [Advanced MR Techniques for Characterization of MS Pathology in Brain & Spine](#)

Claudia Gandini Wheeler-Kingshott<sup>1</sup>

<sup>1</sup>Queen Square MS Centre, UCL Institute of Neurology, University College London, London, United Kingdom

In this teaching talk I will present how MRI can be used for investigating multiple sclerosis using advanced methods in the brain and spine. Two distinct approaches are focusing on investigating microstructural characteristics or network-based damage. Overall, the message will be that MRI is offering a widespread diversity of methods for assessing the multi-facet aspects of MS pathology.

---

18:15 [Adjournment & Meet the Teachers](#)

---

## Educational Course

### Pelvic MR Imaging

Organizers: Kathryn Fowler, M.D., Kartik Jhaveri, M.D., F.R.C.P.C., Lorenzo Mannelli, M.D., Ph.D. & Edwin J.R. van Beek, M.D., Ph.D., M.Ed., FRCR

Room 316A      Monday 16:15 - 18:15      Moderators: Yuliya Lakhman & Gabriele Masselli

---

16:15 [Gynecologic MRI: Prognostication, Treatment Planning & Treatment Response](#)

Kaori Togashi<sup>1</sup> and Aki Kido<sup>1</sup>

<sup>1</sup>Department of Radiology, Kyoto University, Kyoto, Japan

The lecture will include the clinical usages of recent MR techniques for the assessment of gynecologic cancer patients.

---

16:45

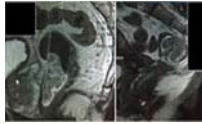
## Prostate MRI Image Interpretation

Jurgen Futterer<sup>1</sup>

<sup>1</sup>Radboudumc

---

17:15



## Rectal Cancer-Shifting Paradigms-Predicting Complete Pathologic Response & Facilitating Non-Operative Management

Marc Gollub

This lecture will illustrate and teach the important concepts regarding post treatment assessment of rectal cancer after chemo-radiotherapy. Limitations, a key evolving concept will be stressed. T2, DWI and DCE will be included. At least 2 suggested systems for post treatment evaluation will be illustrated with discussion of their relative merits: mrTRG grading system and DWI + endoscopy systems. In particular, the growing trend towards Watch and Wait, AKA, non-operative management or organ sparing approaches will be discussed.

---

17:45

## MR Urography

Bobby Kalb

Recent advances in sequence design and image processing have allowed for the simultaneous acquisition of dynamic perfusion imaging data (necessary for modelling of quantitative renal function) and also high-quality anatomic images of the renal and urothelial system (necessary for tumor diagnostics). A streamlined protocol allows for a more comprehensive evaluation of patient with diseases of the renal and urothelial system, optimizing management decisions through non-invasive diagnostics.

---

18:15

## Adjournment & Meet the Teachers

---

### Power Pitch

Pitch: Cutting Edge fMRI

237



16:15



**Cortical depth-dependent fMRI: heterogeneity across tasks, across participants, across days and along the cortical ribbon**

Laurentius Huber<sup>1</sup>, Daniel A Handwerker<sup>1</sup>, Andrew Hall<sup>1</sup>, David C Jangraw<sup>2</sup>, Javier Gonzalez-Castillo<sup>1</sup>, Maria Guidi<sup>3</sup>, Dimo Ivanov<sup>4</sup>, Benedikt A Poser<sup>4</sup>, and Peter A Bandettini<sup>1</sup>

<sup>1</sup>SFIM, NIMH, Bethesda, MD, United States, <sup>2</sup>NIMH, United States, <sup>3</sup>Max Planck Institute for human cognitive and Brain science, Leipzig, Germany, <sup>4</sup>MBIC, Maastricht University, Netherlands

238

16:15



**Simultaneous GCaMP6 based fiber photometry and fMRI in rats**

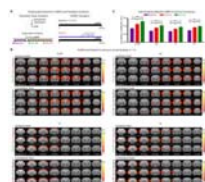
Zhifeng Liang<sup>1,2</sup>, Yuncong Ma<sup>2</sup>, and Nanyin Zhang<sup>2</sup>

<sup>1</sup>Institute of Neuroscience, Chinese Academy of Sciences, Shanghai, People's Republic of China, <sup>2</sup>Department of Biomedical Engineering, Pennsylvania State University, PA, United States

239



16:15



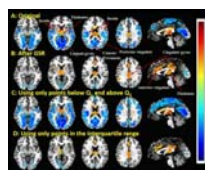
**Optogenetic resting-state fMRI reveals thalamic modulation of long-range sensory networks**

Alex T. L. Leong<sup>1,2</sup>, Xunda Wang<sup>1,2</sup>, Russell W. Chan<sup>1,2</sup>, Leon C. Ho<sup>1,2</sup>, Yongrong Qiu<sup>1,2</sup>, Celia M. Dong<sup>1,2</sup>, and Ed X. Wu<sup>1,2</sup>

<sup>1</sup>Laboratory of Biomedical Imaging and Signal Processing, The University of Hong Kong, Hong Kong, Hong Kong, <sup>2</sup>Department of Electrical and Electronic Engineering, The University of Hong Kong, Hong Kong, Hong Kong

240

16:15



**Global signal regression alters the correlation between resting-state BOLD fluctuations and EEG vigilance measures**

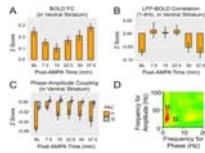
Maryam Falahpour<sup>1</sup>, Alican Nalci<sup>1</sup>, Chi Wah Wong<sup>1</sup>, and Thomas Liu<sup>1</sup>

<sup>1</sup>Center for functional MRI, University of California San Diego, San Diego, CA, United States

241

16:15

**What is the neurophysiological bases of resting state functional connectivity?**



Hanbing Lu<sup>1</sup>, Saul Jaime<sup>2</sup>, Elliot A Stein<sup>1</sup>, Jose E Cavazos<sup>2</sup>, and Yihong Yang<sup>1</sup>

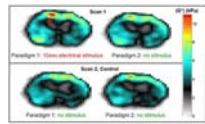
<sup>1</sup>National Institute on Drug Abuse, NIH, Baltimore, MD, United States,

<sup>2</sup>University of Texas Health Science Center at San Antonio, TX, United States

242

16:15

Functional Neuroimaging in the Brain using Magnetic Resonance Elastography



Samuel Patz<sup>1,2</sup>, Navid Nazari<sup>3</sup>, Paul E. Barbone<sup>4</sup>, Ben Fabry<sup>5</sup>, Dan Fovargue<sup>6</sup>, David Nordsletten<sup>6</sup>, and Ralph Sinkus<sup>6</sup>

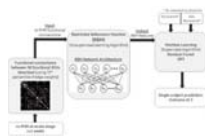
<sup>1</sup>Radiology, Brigham & Women's Hospital, Boston, MA, United States,

<sup>2</sup>Harvard Medical School, Boston, MA, United States, <sup>3</sup>Biomedical Engineering, Boston University, Boston, MA, United States, <sup>4</sup>Mechanical Engineering, Boston University, Boston, MA, United States, <sup>5</sup>Physics, University of Erlangen-Nuremberg, Erlangen, Germany, <sup>6</sup>Biomedical Engineering, Kings College London, London, United Kingdom

243

16:15

Fully Automated Learning based Method for resting state fMRI Connectomics Analysis



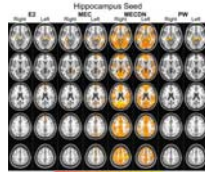
Arathi Sreekumari<sup>1</sup>, Radhika Madhavan<sup>1</sup>, Rakesh Mullick<sup>1</sup>, Teena Shetty<sup>2</sup>, Pratik Mukherjee<sup>3</sup>, Joseph Masdeu<sup>4</sup>, Luca Marinelli<sup>5</sup>, and Suresh Emmanuel Joel<sup>1</sup>

<sup>1</sup>GE Global Research, Bangalore, India, <sup>2</sup>Hospital for Special Surgery, New York, NY, United States, <sup>3</sup>University of California, San Francisco, San Francisco, CA, United States, <sup>4</sup>Houston Methodist, Houston, TX, Houston, TX, United States, <sup>5</sup>GE Global Research, Niskayuna, NY, United States

244

16:15

A Multiband Multi-Echo Simultaneous ASL/BOLD Acquisition for Resting State Functional Connectivity



Alexander D. Cohen<sup>1</sup>, Andrew S. Nencka<sup>1</sup>, and Yang Wang<sup>1</sup>

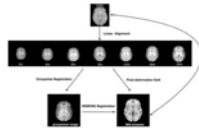
<sup>1</sup>Radiology, Medical College of Wisconsin, Milwaukee, WI, United States

245

16:15

The first two years of whole brain functional development can be separated into three distinct time periods

Weiyang Yin<sup>1</sup> and Weili Lin<sup>2</sup>

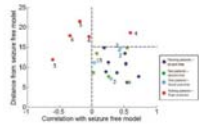


<sup>1</sup>Department of Biomedical Engineering and Biomedical Research Imaging Center, University of North Carolina at Chapel Hill, Chapel Hill, NC, United States, <sup>2</sup>Department of Radiology and Biomedical Research Imaging Center, University of North Carolina at Chapel Hill, Chapel Hill, NC, United States

246

16:15

**MRI Connectivity Predictors of Post-Surgical Seizure Outcome in Temporal Lobe Epilepsy**



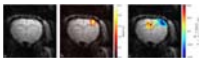
Victoria L Morgan<sup>1</sup>, Dario J Englot<sup>2</sup>, Adam W Anderson<sup>3</sup>, Bennett A Landman<sup>4</sup>, Ahmet Cakir<sup>4</sup>, Baxter P Rogers<sup>1</sup>, and Bassel Abou-Khalil<sup>5</sup>

<sup>1</sup>Institute of Imaging Science, Vanderbilt University, Nashville, TN, United States, <sup>2</sup>Neurosurgery, Vanderbilt University, Nashville, TN, United States, <sup>3</sup>Biomedical Engineering, Vanderbilt University, Nashville, TN, United States, <sup>4</sup>Electrical Engineering and Computer Science, Vanderbilt University, Nashville, TN, United States, <sup>5</sup>Neurology, Vanderbilt University, Nashville, TN, United States

247

16:15

**CEST fMRI at ultra-high magnetic field**



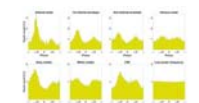
Tangi Roussel<sup>1</sup>, Lucio Frydman<sup>2</sup>, Denis Le Bihan<sup>1</sup>, and Luisa Ciobanu<sup>1</sup>

<sup>1</sup>NeuroSpin, Commissariat à l'Energie Atomique et aux Energies Alternatives, Gif-sur-Yvette, France, <sup>2</sup>Department of Chemical Physics, Weizmann Institute of Science, Rehovot, Israel

248

16:15

**EPI-signal fluctuations at the cardiac frequency: A tissue-specific quantification of inflow, displacement and potential oxygenation effects over the cardiac cycle.**



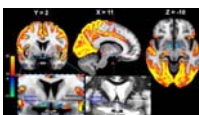
Olivia Viessmann<sup>1</sup> and Peter Jezzard<sup>1</sup>

<sup>1</sup>FMRIB Centre, Nuffield Department of Clinical Neurosciences, Oxford University, Oxford, United Kingdom

249

16:15

**The global resting-state fMRI signal is associated with opposite changes at subcortical structures regulating arousal.**



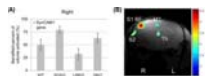
Xiao Liu<sup>1,2</sup>, Jacco A de Zwart<sup>2</sup>, David A Leopold<sup>3</sup>, and Jeff H Duyn<sup>2</sup>



<sup>1</sup>Biomedical Engineering, Pennsylvania State University, University Park, PA, United States, <sup>2</sup>National Institute of Neurological Disorders and Stroke, National Institutes of Health, Bethesda, MD, United States, <sup>3</sup>National Institute of Mental Health, National Institutes of Health, MD, United States

250

16:15



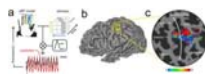
### Functional connectivity is globally altered by schizophrenia-linked genes

Garth J Thompson<sup>1,2</sup>, Karen Perez De Arce<sup>3</sup>, Basavaraju G Sanganahalli<sup>1,2,4</sup>, Stephen M Strittmatter<sup>5</sup>, Thomas Biederer<sup>3</sup>, and Fahmeed Hyder<sup>1,2,4,6</sup>

<sup>1</sup>Radiology and Biomedical Imaging, Yale University, New Haven, CT, United States, <sup>2</sup>Magnetic Resonance Research Center (MRRC), Yale University, New Haven, CT, United States, <sup>3</sup>Neuroscience, Tufts University School of Medicine, Boston, MA, United States, <sup>4</sup>Quantitative Neuroscience with Magnetic Resonance (QNMR) Core Center, Yale University, New Haven, CT, United States, <sup>5</sup>Cellular Neuroscience, Neurodegeneration, and Repair Program, and Departments of Neurology and Neurobiology, Yale University School of Medicine, New Haven, CT, United States, <sup>6</sup>Biomedical Engineering, Yale University, New Haven, CT, United States

251

16:15



### Population Receptive Field Mapping of Human Somatosensory Cortex at 7 T

Michael Asghar<sup>1</sup>, Rosa Sanchez-Panchuelo<sup>1</sup>, Denis Schluppeck<sup>2</sup>, and Susan Francis<sup>1</sup>

<sup>1</sup>SPMIC, School of Physics, University of Nottingham, Nottingham, United Kingdom, <sup>2</sup>School of Psychology, University of Nottingham, Nottingham, United Kingdom

## Power Pitch

## Pitch: Quantitation, Prediction & Machine Learning in the Brain

Power Pitch  
Theater B - Monday 16:15 Moderators: Konstantinos Arfanakis  
Exhibition Hall - 17:15 & Justin Haldar (no CME credit)

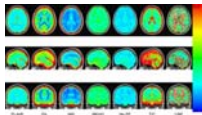
Machine Learning Based Diagnosis of Early Parkinson's Disease using QSM



Seon Lee<sup>1</sup>, Joon Yul Choi<sup>2</sup>, Jeehun Kim<sup>2</sup>, Sun Won Park<sup>3</sup>, and Jongho Lee<sup>2</sup>

<sup>1</sup>Department of Mechanical and Aerospace Engineering, Seoul National University, Seoul, Korea, Republic of, <sup>2</sup>Department of Electrical and Computer Engineering, Seoul National University, Seoul, Korea, Republic of, <sup>3</sup>Department of Radiology, Seoul National University Boramae Medical Center, Seoul, Korea, Republic of

Reproducibility of advanced MR metrics in a multi-site, multi-vendor study of mild traumatic brain injury



Andrew Scott Nencka<sup>1</sup>, Timothy Meier<sup>2</sup>, Yang Wang<sup>1</sup>, Yu-Chien Wu<sup>3</sup>, Brad Swearingen<sup>2</sup>, Robin Karr<sup>1</sup>, Melissa Koschnitzke<sup>2</sup>, Andy Saykin<sup>3</sup>, Michael McCrea<sup>2</sup>, and Kevin M Koch<sup>1</sup>

<sup>1</sup>Radiology, Medical College of Wisconsin, Milwaukee, WI, United States, <sup>2</sup>Neurosurgery, Medical College of Wisconsin, Milwaukee, WI, United States, <sup>3</sup>Radiology and Imaging Services, Indiana University, Indianapolis, IN

Characteristic Changes of Volume and Shape of Subcortical Structures in Obsessive-Compulsive Disorder

Table 1. Descriptive and Statistical Data of Patients with Obsessive-Compulsive Disorder (OCD) and Healthy Controls (HC)

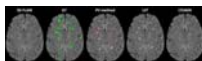
	OCD	HC	P-value
Age, mean (SD), years	38.22(10.01)	38.22(10.01)	0.91
Sex, male (SD), years	37.45(10.11)	38.92(10.01)	0.78
Female, mean (SD), years	38.99(9.91)	38.22(10.01)	0.88
Site, in the study	47(96.0)	97(96.0)	0.90
Education, mean (SD), years	14.92(1.0)	-	-
HC	13.82(1.0)	-	-
Stria	14.92(1.0)	-	0.427
CGM (Caudate, mean (SD), years	5.55(1.0)	-	-
HC	5.48(1.0)	-	-
Stria	5.55(1.0)	-	0.897
MDL (caudate, mean (SD)	34.45(1.0)	-	-
HC	34.45(1.0)	-	-
Stria	34.45(1.0)	-	0.108
MDL (putamen, mean (SD)	14.44(1.0)	-	-
HC	14.44(1.0)	-	-
Stria	14.44(1.0)	-	0.507
MDL (putamen, mean (SD)	8.99(1.0)	-	-
HC	8.99(1.0)	-	-
Stria	8.99(1.0)	-	0.109
MDL (putamen, mean (SD)	8.99(1.0)	-	-
HC	8.99(1.0)	-	-
Stria	8.99(1.0)	-	0.827
MDL (putamen, mean (SD)	8.99(1.0)	-	-
HC	8.99(1.0)	-	-
Stria	8.99(1.0)	-	0.827

p-value indicates a t-test between groups for OCD group.

Lianqing Zhang<sup>1</sup>, Xinyu Hu<sup>1</sup>, Ming Zhou<sup>1</sup>, Lu Lu<sup>1</sup>, Xiaoxiao Hu<sup>1</sup>, and Xiaoqi Huang<sup>1</sup>

<sup>1</sup>Radiology Department, Huaxi MR Research Center (HMRR), West China Hospital of Sichuan University, Chengdu, People's Republic of China

PARTIAL VOLUME ESTIMATION IN MULTIPLE SCLEROSIS LESION SEGMENTATION



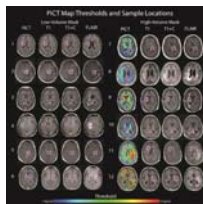
Mário João Fartaria<sup>1,2,3</sup>, Alexandra Şorega<sup>4</sup>, Tobias Kober<sup>1,2,3</sup>, Gunnar Krueger<sup>5</sup>, Cristina Granziera<sup>6,7</sup>, Alexis Roche<sup>1,2,3</sup>, and Meritxell Bach Cuadra<sup>2,3,8</sup>

<sup>1</sup>Advanced Clinical Imaging Technology, Siemens Healthcare AG, Lausanne, Switzerland, <sup>2</sup>Department of Radiology, Centre Hospitalier Universitaire Vaudois (CHUV) and University of Lausanne (UNIL), Lausanne, Switzerland, <sup>3</sup>Signal Processing Laboratory (LTS 5), Ecole Polytechnique Fédérale de Lausanne (EPFL), Lausanne, Switzerland, <sup>4</sup>Department of Radiology, Valais Hospital, Sion, Switzerland, <sup>5</sup>Siemens Medical Solutions USA, Boston, MA, United States, <sup>6</sup>Martinos Center for Biomedical Imaging, Massachusetts General Hospital and Harvard Medical School, Boston, MA, United States, <sup>7</sup>Department of Clinical Neurosciences, Centre Hospitalier Universitaire Vaudois (CHUV) and University of Lausanne (UNIL), Lausanne, Switzerland, <sup>8</sup>Medical Image Analysis Laboratory (MIAL), Centre d'Imagerie BioMédicale (CIBM), Lausanne, Switzerland

---

256

16:15



[Predictive cytological topography highlights regions of pathologically confirmed non-enhancing hypercellular tumor in glioblastoma patients](#)

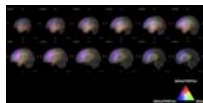
Sarah L Hurrell<sup>1</sup>, Elizabeth Cochran<sup>2</sup>, Sean D McGarry<sup>1</sup>, Amy L Kaczmarowski<sup>1</sup>, Jennifer Connelly<sup>3</sup>, Wade Mueller<sup>4</sup>, Scott D Rand<sup>1</sup>, Kathleen M Schmainda<sup>1</sup>, and Peter S LaViolette<sup>1</sup>

<sup>1</sup>Radiology, Medical College of Wisconsin, Milwaukee, WI, United States, <sup>2</sup>Pathology, Medical College of Wisconsin, Milwaukee, WI, United States, <sup>3</sup>Neurology, Medical College of Wisconsin, Milwaukee, WI, United States, <sup>4</sup>Neurosurgery, Medical College of Wisconsin, Milwaukee, WI, United States

---

257

16:15



[Radiogenomics of 201 WHO grade 2 and 3 gliomas](#)

Manabu Kinoshita<sup>1,2</sup>, Hideyuki Arita<sup>2</sup>, Masamishi Takahashi<sup>3</sup>, Yoshitaka Narita<sup>3</sup>, Yuzo Terakawa<sup>2</sup>, Naohiro Tsuyuguchi<sup>2</sup>, Yoshiko Okita<sup>2</sup>, Masahiro Nonaka<sup>2</sup>, Shusuke Moriuchi<sup>2</sup>, Junya Fukai<sup>2</sup>, Shuichi Izumoto<sup>2</sup>, Kenichi Ishibashi<sup>2</sup>, Yoshinori Kodama<sup>2</sup>, Kanji Mori<sup>2</sup>, Koichi Ichimura<sup>3</sup>, and Yonehiro Kanemura<sup>2,4</sup>

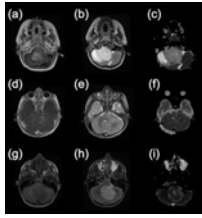
<sup>1</sup>Neurosurgery, Osaka Medical Center for Cancer and Cardiovascular Diseases, Osaka, Japan, <sup>2</sup>Kansai Molecular Diagnosis Network for CNS Tumors, Osaka, Japan, <sup>3</sup>National Cancer Center Hospital, Japan, <sup>4</sup>Osaka National Hospital, Osaka, Japan

---

258

16:15

[Classification of Pediatric Brain Tumours using Apparent Diffusion Coefficient – a Multi-Centre Study](#)



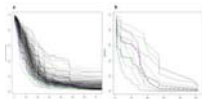
Jan Novak<sup>1,2</sup>, Niloufar Zarinabad<sup>1,2</sup>, Theodoros N Arvanitis<sup>3</sup>, Lesley MacPherson<sup>4</sup>, Daniel Rodriguez<sup>5,6</sup>, Richard Grundy<sup>6</sup>, Dorothee Auer<sup>7,8</sup>, Tim Jaspan<sup>6</sup>, Shivaram Avula<sup>9</sup>, Laurence Abernethy<sup>9</sup>, Patrick Hales<sup>10</sup>, Ramneek Kaur<sup>10</sup>, Darren Hargrave<sup>11</sup>, Dipayan Mitra<sup>12</sup>, Simon Bailey<sup>13</sup>, Nigel Davies<sup>14</sup>, Christopher Clark<sup>10</sup>, and Andrew Peet<sup>2,15</sup>

<sup>1</sup>*Institute of Cancer and Genomic Sciences, University of Birmingham, Birmingham, United Kingdom*, <sup>2</sup>*Oncology, Birmingham Children's Hospital, Birmingham, United Kingdom*, <sup>3</sup>*Institute of Digital Healthcare, University of Warwick, Coventry, United Kingdom*, <sup>4</sup>*Radiology, Birmingham Children's Hospital, Birmingham, United Kingdom*, <sup>5</sup>*Division of Clinical Neuroscience, University of Nottingham, Nottingham, United Kingdom*, <sup>6</sup>*The Children's Brain Tumour Research Centre, University of Nottingham, Nottingham, United Kingdom*, <sup>7</sup>*Sir Peter Mansfield Imaging Centre, University of Nottingham, Nottingham, United Kingdom*, <sup>8</sup>*Department of Neuroradiology, Nottingham University Hospital Trusts, Nottingham, United Kingdom*, <sup>9</sup>*Radiology, Alder Hey Children's NHF Foundation Trust, Liverpool, United Kingdom*, <sup>10</sup>*Developmental Imaging and Biophysics Section, University College London, London, United Kingdom*, <sup>11</sup>*Haematology and Oncology Department, Great Ormond Street Children's Hospital, London, United Kingdom*, <sup>12</sup>*The Newcastle upon Tyne Hospitals NHS Foundation Trust, Newcastle, United Kingdom*, <sup>13</sup>*Sir James Spence Institute of Child Health, Royal Victoria Infirmary, Newcastle upon Tyne, United Kingdom*, <sup>14</sup>*Radiation Protection Services, University Hospitals Birmingham NHS Foundation Trust, Birmingham, United Kingdom*, <sup>15</sup>*Institute of Cancer and Genomic Sciences, University of Birmingham, BIRMINGHAM, United Kingdom*

---

259

16:15



### Exploiting radiogenomics data for personalised prediction of glioblastoma

Paul Blakeley<sup>1,2</sup>, Chia-Feng Lu<sup>2,3,4</sup>, Fei-Ting Hsu<sup>2,5</sup>, Li-Chun Hsieh<sup>2,5</sup>, Yu-Chieh Jill Kao<sup>2,3</sup>, Huai-Lu Chen<sup>1,2</sup>, Ping-Huei Tsai<sup>2,3,5</sup>, Hua-Shan Liu<sup>2,6</sup>, Gilbert Aaron Lee<sup>1,2</sup>, and Cheng-Yu Chen<sup>2,3,5</sup>

<sup>1</sup>*Department of Medical Research, Taipei Medical University Hospital, Taipei, Taiwan*, <sup>2</sup>*Translational Imaging Research Center, College of Medicine, Taipei Medical University, Taipei, Taiwan*, <sup>3</sup>*Department of Radiology, School of Medicine, College of Medicine, Taipei Medical University, Taipei, Taiwan*, <sup>4</sup>*Department of Biomedical Imaging and Radiological Sciences, National Yang-Ming University, Taipei, Taiwan*, <sup>5</sup>*Department of Medical Imaging, Taipei Medical University Hospital, Taipei, Taiwan*, <sup>6</sup>*School of Biomedical Engineering, College of Biomedical Engineering, Taipei Medical University, Taipei, Taiwan*

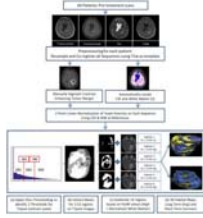
---

260

16:15

### Multiparameter MRI Predictors of Extreme Survival in Glioblastoma Multiforme

Natarajan Raghunand<sup>1</sup>, Olya Stringfield<sup>2</sup>, John Arrington<sup>3</sup>, and Robert A Gatenby<sup>3</sup>



<sup>1</sup>Cancer Imaging & Metabolism, Moffitt Cancer Center, Tampa, FL, United States, <sup>2</sup>IRAT Shared Service, Moffitt Cancer Center, Tampa, FL, United States, <sup>3</sup>Diagnostic Imaging & Interventional Radiology, Moffitt Cancer Center, Tampa, FL, United States

261

16:15

### Multi-Site Concordance of DSC-MRI Analysis for Brain Tumors: Results of a NCI Quantitative Imaging Network DSC-MRI Collaborative Project

Kathleen M Schmainda<sup>1</sup>, Melissa A Prah<sup>1</sup>, Scott D Rand<sup>2</sup>, Mark Muzi<sup>3</sup>, Swati D Rane<sup>3</sup>, Xiao Da<sup>4</sup>, Yi-Fen Yen<sup>5</sup>, Jayashree Kalpathy-Cramer<sup>5</sup>, Thomas L Chenevert<sup>6</sup>, Dariya Malyarenko<sup>6</sup>, Benjamin Hoff<sup>6</sup>, Brian Ross<sup>6</sup>, Yue Cao<sup>7</sup>, Madhava P Aryal<sup>7</sup>, Bradley Erickson<sup>8</sup>, Panagiotis Korfiatis<sup>8</sup>, Laura Bell<sup>9</sup>, Leland Hu<sup>10</sup>, and Christopher Chad Quarles<sup>9</sup>

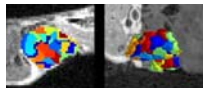
<sup>1</sup>Radiology, Medical College of Wisconsin, Milwaukee, WI, United States, <sup>2</sup>Radiology, Medical College of Wisconsin, WI, United States, <sup>3</sup>Radiology, University of Washington, WA, United States, <sup>4</sup>Radiology, Massachusetts General Hospital, MA, United States, <sup>5</sup>Radiology, Massachusetts General Hospital, Charlestown, MA, United States, <sup>6</sup>Radiology, University of Michigan, Ann Arbor, MI, United States, <sup>7</sup>Radiation Oncology, University of Michigan, Ann Arbor, MI, United States, <sup>8</sup>Mayo Clinic, MN, United States, <sup>9</sup>Barrow Neurological Institute, Phoenix, AZ, United States, <sup>10</sup>Radiology, Mayo Clinic, Phoenix, AZ, United States

262

16:15

### Perfusion-supervoxels for DCE-MRI based tumor subregion assessment

Benjamin John Irving<sup>1</sup>, Jolanta Mirecka<sup>1</sup>, Ana L Gomes<sup>2</sup>, Danny Allen<sup>2</sup>, Paul Kinchesh<sup>2</sup>, Veerle Kersemans<sup>2</sup>, Stuart Gilchrist<sup>2</sup>, Sean Smart<sup>2</sup>, Julia A Schnabel<sup>3</sup>, Sir J Michael Brady<sup>2</sup>, and Michael Chappell<sup>1</sup>

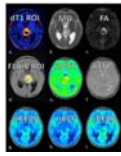


<sup>1</sup>Institute of Biomedical Engineering, University of Oxford, Oxford, United Kingdom, <sup>2</sup>Department of Oncology, University of Oxford, Oxford, United Kingdom, <sup>3</sup>Division of Imaging Sciences and Biomedical Engineering, King's College London, London, United Kingdom

263

16:15

### A New Combined Perfusion and Diffusion MRI Biomarker to Distinguish Pediatric High-Grade Glioma from Pilocytic Astrocytoma



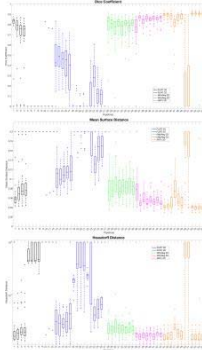
Kathleen M Schmainda<sup>1</sup>, Melissa A Prah<sup>1</sup>, Jose A Palomares<sup>1</sup>, Mohit Maheshwari<sup>1</sup>, Sean Lew<sup>2</sup>, and Teresa Kelly<sup>1</sup>

<sup>1</sup>Radiology, Medical College of Wisconsin, Milwaukee, WI, United States, <sup>2</sup>Neurosurgery, Medical College of Wisconsin, Milwaukee, WI, United States

264

16:15

[A ranking of pipelines for optimal co-registration of anatomical and diffusion weighted images of the cervical spinal cord](#)



Stephanie Alley<sup>1</sup>, Francesco Grussu<sup>1</sup>, Marios C. Yiannakas<sup>1</sup>, Hugh Kearney<sup>1</sup>, Olga Ciccarelli<sup>1</sup>, Ferran Prados<sup>1,2</sup>, Sébastien Ourselin<sup>2</sup>, and Claudia AM Gandini Wheeler-Kingshott<sup>1,3,4</sup>

<sup>1</sup>UCL Institute of Neurology, Queen Square MS Centre, University College London, London, United Kingdom, <sup>2</sup>Translational Imaging Group, Centre for Medical Image Computing, Department of Medical Physics and Biomedical Engineering, University College London, London, United Kingdom, <sup>3</sup>Department of Brain and Behavioural Sciences, University of Pavia, Pavia, Italy, <sup>4</sup>Brain MRI 3T Mondino Research Center, C. Mondino National Neurological Institute, Pavia, Italy

265

16:15

[Deep-Neural-Network based image diagnosis: comparing various image preprocessing strategies to achieve higher accuracy and understanding of the decision](#)



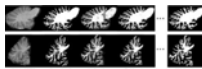
Yasuhiko Tachibana<sup>1</sup>, Takayuki Obata<sup>1</sup>, Jeff Kershaw<sup>1</sup>, Yoko Ikoma<sup>1</sup>, Tokuhiko Omatsu<sup>1</sup>, Riwa Kishimoto<sup>1</sup>, and Tatsuya Higashi<sup>2</sup>

<sup>1</sup>Applied MRI Research, Department of Molecular Imaging and Theranostics, National Institute of Radiological Sciences, Chiba, Japan, <sup>2</sup>Department of Molecular Imaging and Theranostics, National Institute of Radiological Sciences, Chiba, Japan

266

16:15

[Cerebellum Tissue Segmentation with Ensemble Sparse Learning](#)



Jiawei Chen<sup>1</sup>, Li Wang<sup>1</sup>, and Dinggang Shen<sup>1</sup>

<sup>1</sup>Department of Radiology and BRIC, University of North Carolina at Chapel Hill, Chapel Hill, NC, United States

Oral



# Stroke & Vessel Wall Imaging

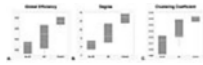
Room 310

Monday 16:15 - 18:15 Moderators: Linda Knutsson & William Copen

---

267

16:15



## Alterations in brain structural connectivity in comatose cardiac arrest patients

Ona Wu<sup>1</sup>, Eric S. Rosenthal<sup>2</sup>, Gaston Cudemus-Deseda<sup>3</sup>, Brian L. Edlow<sup>2</sup>, Marjorie Villien<sup>1</sup>, Brittany B. Mills<sup>2</sup>, Joseph T. Giacino<sup>4</sup>, James L. Januzzi<sup>5</sup>, Ming Ming Ning<sup>2</sup>, W. Taylor Kimberly<sup>2</sup>, William A. Copen<sup>6</sup>, Pamela W. Schaefer<sup>6</sup>, and David M. Greer<sup>7</sup>

<sup>1</sup>Athinoula A. Martinos Center for Biomedical Imaging, Massachusetts General Hospital, Charlestown, MA, United States, <sup>2</sup>Department of Neurology, Massachusetts General Hospital, Boston, MA, United States, <sup>3</sup>Department of Cardiac Anesthesiology and Critical Care Medicine, Massachusetts General Hospital, Boston, MA, United States, <sup>4</sup>Department of Physical Medicine and Rehabilitation, Spaulding Rehabilitation Hospital, Charlestown, MA, United States, <sup>5</sup>Department of Medicine, Cardiology Division, Massachusetts General Hospital, Boston, MA, United States, <sup>6</sup>Department of Radiology, Massachusetts General Hospital, Boston, MA, United States, <sup>7</sup>Department of Neurology, Yale School of Medicine, New Haven, CT, United States

Cardiac arrest patients in coma after restoration of spontaneous circulation were prospectively studied to determine whether variability in structural connectivity can discriminate patients likely to recover consciousness from those who will not. Compared to healthy controls, cardiac arrest patients overall had significantly lower values in the following structural connectivity parameters: global efficiency, clustering coefficient, and degree. Cardiac arrest patients who failed to recover alertness had a significantly lower global clustering coefficient compared to patients who woke up. Alterations in structural connectivity may play an important role in predicting recovery and guiding patient management decisions in comatose cardiac arrest patients.

268

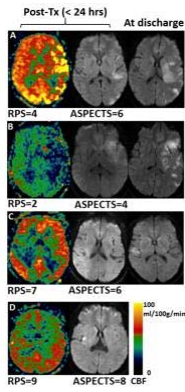
16:27



## ASPECTS Based Reperfusion Status on Arterial Spin Labeling Is Associated with Clinical Outcome in Acute Ischemic Stroke Patients

Samantha J. Ma<sup>1</sup>, Songlin Yu<sup>2</sup>, David Liebeskind<sup>3</sup>, Dandan Yu<sup>4</sup>, Ning Li<sup>5</sup>, Xingfeng Shao<sup>1</sup>, Jeffrey Saver<sup>6</sup>, Noriko Salamon<sup>7</sup>, and Danny JJ Wang<sup>1</sup>



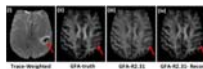


<sup>1</sup>Neurology, University of Southern California, Los Angeles, CA, United States, <sup>2</sup>Neurosurgery, Beijing Tiantan Hospital, Capital Medical University, Beijing, People's Republic of China, <sup>3</sup>Neurovascular Imaging Research Core and Department of Neurology, UCLA, Los Angeles, CA, United States, <sup>4</sup>Neuro-Intensive Care Unit, Neurology, Beijing Tiantan Hospital, Capital Medical University, Beijing, People's Republic of China, <sup>5</sup>Biomathematics, UCLA, Los Angeles, CA, United States, <sup>6</sup>Neurology, UCLA, Los Angeles, CA, United States, <sup>7</sup>Radiology, UCLA, Los Angeles, CA, United States

An automatic scoring system for assessing reperfusion status based on arterial spin labeled (ASL) perfusion MRI was developed and evaluated for acute ischemic stroke patients who received thrombolysis and/or endovascular treatment. Reperfusion injury is considered to have the same detrimental effects as non-reperfusion, and we applied the ASPECTS model to address the existence of heterogeneity of hypo- and hyper-perfusion despite vessel recanalization. Our newly devised reperfusion scoring system is highly associated with patient functional outcome and provides a useful tool to complement other clinical methods for managing corresponding strategies after treatment.

269

16:39

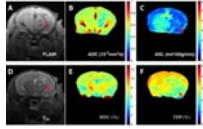


Estimation of microstructure measures in stroke subjects with a rapid DSI acquisition

Ganesh Adluru<sup>1</sup>, Kyler Hodgson<sup>2</sup>, Jennifer Majersik<sup>3</sup>, Lorie Richards<sup>4</sup>, and Edward DiBella<sup>1,2</sup>

<sup>1</sup>Radiology and Imaging Sciences, University of Utah, Salt lake city, UT, United States, <sup>2</sup>Bioengineering, University of Utah, Salt lake city, UT, United States, <sup>3</sup>Neurology, University of Utah, Salt Lake City, UT, United States, <sup>4</sup>Occupational Therapy, University of Utah, Salt Lake City, UT, United States

Diffusion spectrum imaging (DSI) is a promising tool for estimation of white-matter fiber structure. DSI also allows for model-based estimation of several microstructure measures. However, the long data acquisition time associated with DSI limits its application in stroke patients. Here we combine a simultaneous multi-slice acquisition with an undersampled q-space acquisition and dictionary reconstruction to accelerate DSI. The two complementary acceleration schemes allow for a rapid 5.5 minute DSI acquisition in stroke subjects. We used generalized fractional anisotropy and microstructure measures computed from the NODDI model to evaluate the rapid DSI framework in stroke patients.

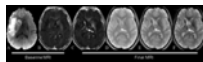


### Highly sensitive pH mapping during ischemia using Total Fast-exchanging Protons (TFP) imaging

Jiadi Xu<sup>1</sup>, Kathryn Schunke<sup>1,2</sup>, Lin Chen<sup>1,3</sup>, Xiang Xu<sup>1</sup>, Yuguo Li<sup>1</sup>, Guanshu Liu<sup>1</sup>, Shuhui Cai<sup>3</sup>, Raymond C Koehler<sup>2</sup>, Jiangyang Zhang<sup>4</sup>, Peter C. M. van Zijl<sup>1</sup>, and Nauder Faraday<sup>2</sup>

<sup>1</sup>kirby Center / Radiology Department, Kennedy Krieger Institute / Johns Hopkins University, Baltimore, MD, United States, <sup>2</sup>Department of Anesthesiology/Critical Care Medicines, Johns Hopkins University School of Medicine, Baltimore, MD, United States, <sup>3</sup>Department of Electronic Science, Xiamen University, Xiamen, People's Republic of China, <sup>4</sup>Bernard and Irene Schwartz Center for Biomedical Imaging, New York University School of Medicine, New York, NY, United States

Ischemia in a mouse stroke model was assessed by pH mapping using the on-resonance variable-delay multi-pulse (onVDMP) CEST scheme. In the method, an on-resonance binomial pulse train is applied at the water resonance to achieve high labeling efficiency for fast-exchanging protons. Since the CEST signal intensity for the total fast-exchanging protons is far greater than that of amide protons, high detection sensitivity is expected. The final stroke region determined by the method was verified by histologic analysis.



### In-vivo Detection of Remote Neurodegeneration within Thalamic Nuclei after Stroke Using Iron Quantification with R2\* Mapping

Grégory Kuchcinski<sup>1</sup>, Fanny Munsch<sup>2</sup>, Renaud Lopes<sup>1</sup>, Jason Su<sup>3</sup>, Antoine Bigourdan<sup>2</sup>, Brian K. Rutt<sup>3</sup>, Vincent Dousset<sup>2</sup>, Igor Sibon<sup>4</sup>, and Thomas Tourdias<sup>2</sup>

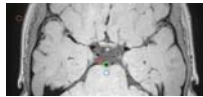
<sup>1</sup>Neuroradiology, Univ. Lille, CHU Lille, Lille, France, <sup>2</sup>Neuroimagerie diagnostique et thérapeutique, Université de Bordeaux, CHU de Bordeaux, France, <sup>3</sup>Richard M. Lucas Center for Imaging Radiology Department, Stanford University, United States, <sup>4</sup>Unité neurovasculaire, Université de Bordeaux, CHU de Bordeaux, France

In stroke patients, remote thalamic alterations including iron deposition have been reported and attributed to the disruption of cortico-thalamic projections. Nevertheless, secondary thalamic degeneration has never been quantified so far in humans at the nucleus scale and its clinical impact is unknown. By using R2\* mapping, we demonstrated (i) that iron accumulates with a focal distribution especially within the medio-dorsal nucleus and the pulvinar, (ii) that such focal thalamic iron accumulation is strongly linked to the initial stroke location, consistent with the known connectivity between thalamic nuclei and cortico-subcortical areas and (iii) is significantly impacting specific cognitive and emotional functions.

272



17:15



### Evaluation of CSF Suppression Techniques for Intracranial Vessel Wall Imaging

Petrice M. Cogswell<sup>1</sup>, Jeroen C.W. Siero<sup>2,3</sup>, Guillaume Gilbert<sup>4</sup>, Taylor Davis<sup>1</sup>, Allison O. Scott<sup>1</sup>, Katie Lants<sup>1</sup>, Helen B. Mahany<sup>1</sup>, Jennifer M. Watchmaker<sup>1</sup>, Jeroen Hendrikse<sup>2</sup>, and Manus J. Donahue<sup>1</sup>

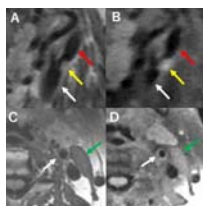
<sup>1</sup>Vanderbilt University Medical Center, Nashville, TN, United States, <sup>2</sup>Radiology, University Medical Center Utrecht, Netherlands, <sup>3</sup>Spinoza Center for Neuroimaging, Amsterdam, Netherlands, <sup>4</sup>MR Clinical Science, Philips Healthcare Canada, Markham, Canada

This work compares vessel wall SNR and CSF suppression from multiple approaches to determine optimal imaging parameters for intracranial VWI at the clinically-available field strength of 3T. T1-weighted TSE acquisition using variable refocusing angle pulse-train and DANTE preparation provides for blood and CSF suppression while maintaining adequate vessel wall SNR. The use of a variable refocusing pulse train with sweep of 40-120° provides improved performance compared to a sweep of 50-120°. Variation of the DANTE flip angle showed that a flip angle of 8° provides good CSF suppression with minimal SNR loss compared to flip angles of 10 and 12°.

273



17:27



### Visualization of Carotid Plaque: T1-SPACE vs. Compressed Sensing T1-SPACE

Sachi Okuchi<sup>1</sup>, Yasutaka Fushimi<sup>1</sup>, Tomohisa Okada<sup>2</sup>, Akira Yamamoto<sup>1</sup>, Tsutomu Okada<sup>1</sup>, Takayuki Yamamoto<sup>1</sup>, Katsutoshi Murata<sup>3</sup>, Yuta Urushibata<sup>3</sup>, and Kaori Togashi<sup>1</sup>

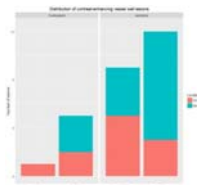
<sup>1</sup>Department of Diagnostic Imaging and Nuclear Medicine, Graduate School of Medicine, Kyoto University, Kyoto, Japan, <sup>2</sup>Human Brain Research Center, Graduate School of Medicine, Kyoto University, Kyoto, Japan, <sup>3</sup>Siemens Japan K.K., Tokyo, Japan

Compressed sensing (CS) algorithm has been brought into MRI. CS realizes iterative reconstruction of images from incoherently under-sampled data, which leads to shorter acquisition time. A 3D T1-weighted fast spin echo (T1-FSE) scan has been often used for plaque imaging. We compared visualization of carotid plaque and internal carotid artery (ICA) between 3D T1-FSE imaging with SPACE and with a prototype CS SPACE. In the result, CS-T1-SPACE revealed an equivalent visualization compared with T1-SPACE in evaluation of carotid plaque and ICA. CS-T1-SPACE would be useful for the visualization of carotid plaque and ICA.

274



17:39



High-resolution MR vessel wall imaging after intra-arterial treatment for acute ischemic stroke

Arjen Lindenholz<sup>1</sup>, Irene C van der Schaaf<sup>1</sup>, Anita A Harteveld<sup>1</sup>, Bart H van der Worp<sup>2</sup>, Anja G Van der Kolk<sup>1</sup>, and Jeroen Hendrikse<sup>1</sup>

<sup>1</sup>Radiology, UMC Utrecht, Utrecht, Netherlands, <sup>2</sup>Neurology and Neurosurgery, UMC Utrecht, Utrecht, Netherlands

Intra-arterial treatment (IAT) may damage the arterial vessel wall, which might lead to recurrent thrombosis and distal embolism. In this study the intracranial vessel wall was evaluated in patients with acute ischemic stroke after IAT using high-resolution vessel wall MRI. Thirteen patients underwent both 3T and 7T pre- and postcontrast vessel wall MRI to detect contrast-enhancing lesions. Significantly more enhancing vessel wall lesions and concentric enhancing lesions ipsilateral to IAT were found compared to the contralateral side. The higher number of concentric enhancing lesions ipsilateral to the IAT may be related to the presence of the thrombus and the performed IAT.

275

17:51

Parameter	3T (n=13)	7T (n=13)	P-value
Concentric	10	5	0.03
Eccentric	15	10	0.15
Total	25	15	0.01

Determinants of Symptomatic Intracranial Atherosclerotic Plaque Enhancement on 3D DANTE T1-SPACE Vessel Wall MRI and Relationship to Recurrent Stroke or TIA

Adam de Havenon<sup>1</sup>, Nabeel Chauhan<sup>1</sup>, Seong-Eun Kim<sup>2</sup>, J. Rock Hadley<sup>2</sup>, Ka-Ho Wong<sup>1</sup>, David Tirschwell<sup>3</sup>, Jennifer J. Majersik<sup>1</sup>, Dennis Parker<sup>2</sup>, and J. Scott McNally<sup>2</sup>

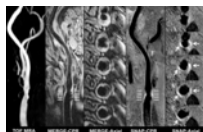
<sup>1</sup>Neurology, University of Utah, Salt Lake City, UT, United States,  
<sup>2</sup>Radiology, University of Utah, Salt Lake City, UT, United States,  
<sup>3</sup>Neurology, University of Washington, Seattle, WA, United States

Intracranial atherosclerotic enhancement on vessel wall MRI is associated with symptomatic plaque, but there is insufficient data on the clinical characteristics associated with atherosclerotic enhancement on T1-weighted vessel wall MRI sequences or the relationship between atherosclerotic enhancement and recurrent stroke or TIA. Our study demonstrates that intracranial atherosclerotic plaque enhancement detected on 3T vessel wall MRI with 3D DANTE T1-SPACE accurately predicts a high risk of early stroke or TIA recurrence, with a potentially modifiable risk factor: elevated serum hemoglobin A1c.

276



18:03



Characteristics of Morphology, Compositions and Distribution of Carotid Artery Atherosclerotic Plaques in Asymptomatic Elderly Population: A Three-Dimensional, Multicontrast Magnetic Resonance Vessel Wall Imaging Study

Ying Cai<sup>1</sup>, Le He<sup>2</sup>, Chun Yuan<sup>2,3</sup>, Huijun Chen<sup>2</sup>, Qiang Zhang<sup>2</sup>, Rui Li<sup>2</sup>, Cheng Li<sup>4</sup>, and Xihai Zhao<sup>2</sup>

<sup>1</sup>Department of Radiology, Yangzhou First People's Hospital, Yangzhou, People's Republic of China, <sup>2</sup>Center for Biomedical Imaging Research, Department of Biomedical Engineering, Tsinghua University, Beijing, People's Republic of China, <sup>3</sup>Department of Radiology, University of Washington, Seattle, United States, <sup>4</sup>Department of Radiology, Zhongda Hospital, Medical School of Southeast University, Nanjing, People's Republic of China

This study investigated the morphology, compositions and distribution of carotid artery atherosclerotic plaques in asymptomatic elderly population using 3D multicontrast MR vessel wall imaging. The atherosclerotic plaques were found to be prevalent (62.1%) and more than 12% subjects had high risk plaques (HRP) in this study population. Among carotid arteries without luminal stenosis, the prevalence of plaque and HRP was 43.2% and 8.3%, respectively. Benefiting from the 3D vessel wall imaging with large longitudinal coverage, near 14% of subjects had plaques in either distal ICA or proximal CCA segment which cannot be captured by traditional 2D vessel wall imaging.

# Microstructure

Room 311

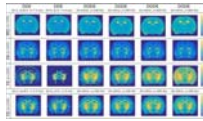
Monday 16:15 - 18:15 Moderators: Susie Huang & Itamar Ronen

---

277



16:15



Time dependence of microscopic anisotropy in the mouse brain measured with double oscillating diffusion encoding (DODE) MRI

Andrada Ianus<sup>1,2</sup>, Sune N. Jespersen<sup>3,4</sup>, Daniel C. Alexander<sup>2</sup>, Ivana Drobnjak<sup>2</sup>, and Noam Shemesh<sup>1</sup>

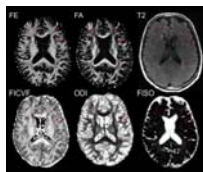
*<sup>1</sup>Champalimaud Neuroscience Programme, Champalimaud Centre for the Unknown, Lisbon, Portugal, <sup>2</sup>Centre for Medical Image Computing, Department of Computer Science, University College London, London, United Kingdom, <sup>3</sup>Center of Functionally Integrative Neuroscience (CFIN) and MINDLab, Clinical Institute, Aarhus University, Aarhus, Denmark, <sup>4</sup>Department of Physics and Astronomy, Aarhus University, Aarhus, Denmark*

Time dependence of microscopic anisotropy measured with diffusion MRI can reveal the cellular eccentricity at different lengths scales, which is an important step towards the goal of non-invasive characterization of tissue microstructure. Diffusion sequences which vary the gradient orientation within one measurement can probe microscopic anisotropy, regardless of the macroscopic tissue configuration. Here we employ the newly proposed Double Oscillating Diffusion Encoding (DODE) sequences, consisting of two independent trains of oscillating gradients which can have different orientations, in order to measure the time dependence of microscopic anisotropy in the mouse brain.

---

278

16:27



Comparison of Double Diffusion Encoding and NODDI

Grant Kaijuin Yang<sup>1,2</sup>, Qiyuan Tian<sup>1,2</sup>, Christoph Leuze<sup>2</sup>, and Jennifer McNab<sup>2</sup>

*<sup>1</sup>Electrical Engineering, Stanford University, Stanford, CA, United States, <sup>2</sup>Radiology, Stanford University, Stanford, CA, United States*

In this study, we compare fractional eccentricity (FE) measured by double diffusion encoding (DDE) to NODDI estimates of neurite density and orientation distribution in six normal subjects and one subject with benign T2 hyperintensities. The results of the comparison support the hypothesis that FE is independent of fiber orientation and correlates strongly with intracellular volume fraction.

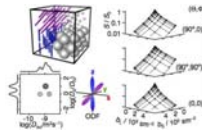
---

279

16:39

Diffusion tensor distribution imaging





Daniel Topgaard<sup>1</sup>

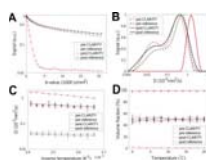
<sup>1</sup>Department of Chemistry, Lund University, Lund, Sweden

Diffusion MRI is an excellent method for detecting subtle changes of brain microstructure, but rarely gives unambiguous information about whether the observations originate from variations in cell density, size, shape, orientation, or any combination thereof. Capitalizing on our recent pulse sequences with data acquisition as a function of both the spherical and the conventional linear components of the diffusion encoding tensor **b**, we here introduce and demonstrate a method to quantify the composition of a heterogeneous voxel as a multidimensional distribution of diffusion tensors where the information about size, shape, and orientation is cleanly separated in the respective dimensions of the distribution. When transferred to a neuroimaging context, our method will allow for unconstrained estimation of fiber bundle orientation distributions and radial and axial diffusivities, as well as fractions of extracellular water and cerebrospinal fluid.

280



16:51



Validation of the two-pool diffusion model in post-mortem white matter using the CLARITY method

Jakob Georgi<sup>1</sup>, Markus Morawski<sup>2</sup>, Carsten Jäger<sup>1,2</sup>, and Harald E. Möller<sup>1</sup>

<sup>1</sup>Max-Planck-Institute for Human Cognitive and Brain Sciences, Leipzig, Germany, <sup>2</sup>Paul-Flechsig-Institute for Brain Research, Leipzig, Germany

Water diffusion in tissues is known to be non-Gaussian. Moreover, two different water regimes have been found in brain tissue and assigned to a bulk-like compartment and water in contact with macromolecules. Here, we investigate the influence of membranes in post-mortem white matter, which are assumed to be responsible for the second pool observed in MR-diffusion measurements. Using a newly developed CLARITY method, which removes lipids from brain tissue while keeping the brain structure intact, we found that the slow compartment vanished while the mobility of the fast pool increased, which directly demonstrates the influence of membranes on water dynamics.

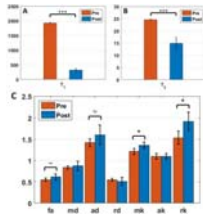
281

17:03

Intra- and extra-axonal axial diffusivities in the white matter: which one is faster?

Ileana Ozana Jelescu<sup>1</sup>, Nicolas Kunz<sup>1</sup>, Analina Raquel Da Silva<sup>1</sup>, and Rolf Gruetter<sup>1</sup>



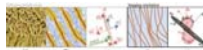


<sup>1</sup>Centre d'Imagerie Biomédicale, Ecole Polytechnique Fédérale de Lausanne, Lausanne, Switzerland

The typical two-compartment model of diffusion in the white matter is associated with two plausible solutions, the choice between which relies on whether intra-axonal or extra-axonal axial diffusivity is faster. Here we use an intracerebroventricular perfusion of gadolinium in the rat brain to suppress the extra-cellular signal. Diffusion measurements before and after perfusion show a mild increase in axial diffusivity post-perfusion, which suggests intra-axonal diffusivity is higher than extra-axonal axial diffusivity. This can help solve the current indetermination in parameter estimation and allow diffusion models to regain their claimed specificity.

282

17:15



Universal power-law scaling of water diffusion in human brain defines what we see with diffusion MRI

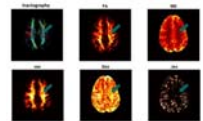
Jelle Veraart<sup>1</sup>, Els Fieremans<sup>1</sup>, and Dmitry S Novikov<sup>1</sup>

<sup>1</sup>Center for Biomedical Imaging, New York University School of Medicine, New York City, NY, United States

Here we identify a universal power-law scaling behavior of the diffusion MRI signal on a clinical scanner. This specific functional form provides a defining signature of water confined within narrow *sticks* establishing that exchange between intra- and extra-axonal water is not relevant, and the fraction of fully restricted water is negligible in the clinically accessible regime. The observed scaling for the first time *in vivo* validates the key ingredient specific to the microstructural models of MRI signal from neuronal tissue and enables the *in vivo* quantification of intra-axonal properties.

283

17:27



Multi-compartment microscopic diffusion imaging with oscillating gradients: simulation validation and application in multiple sclerosis patients

Hua Li<sup>1,2</sup>, Enrico Kaden<sup>3</sup>, Daniel C. Alexander<sup>3</sup>, John C. Gore<sup>1,2</sup>, Bagnato R. Francesca<sup>1,2,4</sup>, and Junzhong Xu<sup>1,2</sup>

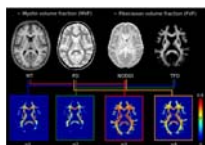
<sup>1</sup>Institute of Imaging Science, Vanderbilt University, Nashville, TN, United States, <sup>2</sup>Department of Radiology and Radiological Sciences, Vanderbilt University, Nashville, TN, United States, <sup>3</sup>Centre for Medical Image Computing, University College London, United Kingdom, <sup>4</sup>Neuroimmunology Division/Neuroimaging Unit, Department of Neurology, Vanderbilt University, Nashville, TN, United States

Microscopic diffusion imaging using spherical mean technique (SMT) and oscillating gradient spin echo (OGSE) was applied in multiple sclerosis patients, along with computer simulation validation. The results suggested that there are significant decreases of axon volume fraction in multiple sclerosis patients compared with contralateral normal tissue.

---

284

17:39



Comparing in vivo MR g-ratio mapping methods: accuracy and precision at the group level

Isabel Ellerbrock<sup>1</sup> and Siawoosh Mohammadi<sup>1,2,3</sup>

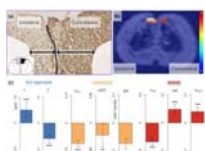
*<sup>1</sup>Department of Systems Neuroscience, Medical Center Hamburg-Eppendorf, Hamburg, Germany, <sup>2</sup>UCL Institute of Neurology, University College London, London, United Kingdom, <sup>3</sup>Department of Neurophysics, Max Planck Institute for Human Cognitive and Brain Sciences, Leipzig, Germany*

The g-ratio, the ratio between the inner and outer diameter of a myelinated axon, is of great neuroscientific interest because it is a relative measure of axonal myelination and functionally linked to conduction velocity. In vivo g-ratio mapping has been recently suggested using a flexible biophysical model that relates the microscopic g-ratio, only accessible by histology, to MRI biomarkers for the myelin and fiber compartment. This study investigates the question which MRI biomarker is optimal for MR g-ratio mapping concerning precision (determined by scan-rescan reproducibility) and accuracy (assessed by comparability to previous in vivo and the ex vivo results).

---

285

17:51



Microstructure imaging from a dictionary of Monte Carlo signals: assessment on a rat model of Wallerian degeneration

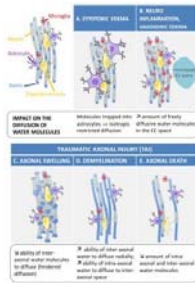
Gaëtan Rensonnet<sup>1</sup>, Benoît Scherrer<sup>2</sup>, Simon K. Warfield<sup>2</sup>, Benoît Macq<sup>1</sup>, and Maxime Taquet<sup>1,2</sup>

*<sup>1</sup>ICTEAM, Université catholique de Louvain, Louvain-la-Neuve, Belgium, <sup>2</sup>Computational Radiology Laboratory, Boston Children's Hospital, Harvard Medical School, Boston, MA, United States*

We estimate microstructural features of the nervous tissues from diffusion-weighted MRI by using sparse optimization techniques on a dictionary of pre-computed Monte Carlo signals, which more faithfully describe the complex diffusion process in the extra-axonal space of the white matter. The method is validated on synthetic data including single and crossing fibers and on an in vivo rat spinal cord model of Wallerian degeneration. We obtain in vivo microstructural estimates that can be directly related to histological evidence whereas the traditional closed-form formula models DIAMOND and NODDI yield results that are more challenging to interpret physically.

286

18:03



Diffusion compartment imaging reveals microstructural injuries in a mouse model of mild traumatic brain injury

Benoit Scherrer<sup>1</sup>, Jianhua Qiu<sup>2</sup>, Jumana Hashim<sup>2</sup>, Onur Afacan<sup>1</sup>, Yaotang Wu<sup>1</sup>, Michael Marcotrigiano<sup>1</sup>, Simon K Warfield<sup>1</sup>, and Rebekah Mannix<sup>2</sup>

<sup>1</sup>Department of Radiology, Boston Children's Hospital, Harvard Medical School, Boston, MA, United States, <sup>2</sup>Division of Emergency Medicine, Boston Children's Hospital, Harvard Medical School, Boston, MA, United States

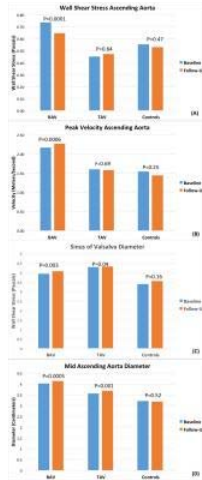
Although about 30% of patients with mild traumatic brain injury (mTBI) suffer prolonged symptoms after injury<sup>1</sup>, conventional anatomic magnetic resonance imaging (MRI) has not proven useful in diagnosing or predicting outcomes after mTBI. In this work we evaluated a novel technique, diffusion compartment imaging (DCI), with a mouse model of mTBI that enables study of mTBI under controlled conditions. We compared DCI and diffusion tensor imaging (DTI) changes to histopathological observations in two injury conditions (with and without persistent functional deficits). Our results suggest that, unlike DTI, DCI detects specific evidence of traumatic axonal injury. Moreover, DCI detects changes only in mice with persistent functional deficits.

Oral

## Velocity & Flow Imaging: Clinical Research

Room 312

Monday 16:15 - 18:15 Moderators: Jeremy Collins & Tino Ebbers



### Multi-year 4D flow MRI Follow-Up Study of Bicuspid and Tricuspid Aortic Valve patients and Association between Wall Shear Stress and Aortic Diametric Growth

Ozair Rahman<sup>1</sup>, Alex Barker<sup>2</sup>, Carmen Blanken<sup>2</sup>, Emilie Bollache<sup>2</sup>, Michael Rose<sup>3</sup>, Pim Van Ooij<sup>2</sup>, Jeremy Collins<sup>2</sup>, James Carr<sup>2</sup>, Chris Malaisrie<sup>4</sup>, Patrick McCarthy<sup>4</sup>, and Michael Markl<sup>2</sup>

<sup>1</sup>Radiology, Northwestern University, Chicago, IL, United States,

<sup>2</sup>Radiology, Northwestern University, <sup>3</sup>Radiology, Ann & Robert H. Lurie Children's Hospital of Chicago, <sup>4</sup>Cardiac Surgery, Northwestern University

Patients with Bicuspid Aortic Valve (BAV) are at increased risk of developing aortopathy compared to Tricuspid Aortic Valve (TAV) patients. However, there is limited data presenting the development of pathophysiologic changes taking place over multi year time period. Our study attempts to quantify the changes that take place from baseline and follow-up scans to help us better understand this process.



### 3D Linear Regression Analysis Reveals Relationships of 4D flow MRI-derived Aortic Dimensions with Age, Gender and Wall Shear Stress in Patients with Aortopathy

Pim van Ooij<sup>1,2</sup>, Jeremy D. Collins<sup>2</sup>, Paul W. M. Fedak<sup>3,4</sup>, Aart J. Nederveen<sup>1</sup>, James C Carr<sup>2</sup>, Michael Markl<sup>2,5</sup>, and Alex J. Barker<sup>2</sup>

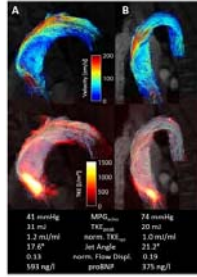
<sup>1</sup>Radiology, Academic Medical Center, Amsterdam, Netherlands,

<sup>2</sup>Radiology, Northwestern University, Chicago, IL, United States,

<sup>3</sup>Division of Surgery-Cardiac Surgery, Northwestern University, Chicago, IL, <sup>4</sup>Cardiac Sciences, University of Calgary, Calgary, Canada,

<sup>5</sup>Biomedical Engineering, Northwestern University, Chicago, IL, United States

In two groups of patients with bicuspid valves (BAV) and with tricuspid valves with dilated aortas (TAV), 3D correlation coefficient  $r$  maps were created to investigate linear relationships between 3D aortic diameter maps and 3D wall shear stress maps (WSS), with age and gender as co-variables. The dependence of diameter on gender was higher for TAV, whereas the dependence of diameter on age was higher for BAV patients. With the addition of WSS to the model,  $r$  increased slightly for both groups. In general,  $r$  was significantly higher for TAV: BAV mediated aortopathy is suspected to have genetic associations.

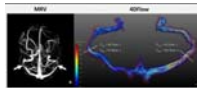


### Multiparametric Assessment of Patients with Aortic Stenosis using Multipoint 4D Flow MRI - Correlation with Cardiac Biomarkers

Alexander Gotschy<sup>1,2</sup>, Christian Binter<sup>1</sup>, Robert Manka<sup>2</sup>, and Sebastian Kozerke<sup>1</sup>

<sup>1</sup>Institute for Biomedical Engineering, University & ETH Zurich, Zurich, Switzerland, <sup>2</sup>Department of Cardiology, University Hospital Zurich, Zurich, Switzerland

Various flow characteristics, such as Turbulent Kinetic Energy (TKE), flow displacement or jet angle, derived from 4D Flow MRI, have been used to investigate the hemodynamic effects of aortic stenosis (AS). However, the predictive value of these flow parameters is still unknown. Therefore, we investigated the correlation between multiple flow parameters and cardiac biomarkers which are known to provide prognostic information on the progression and outcome of AS. Our results revealed that MRI-based TKE and peak velocity significantly correlate with NT-proBNP, implying potential relevance of these imaging parameter for future risk stratification of AS patients.

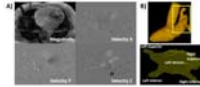


### Blood flow characterization in sigmoid-sinus using 4D-Flow MR among patients with pulsatile tinnitus

Yunduo Li<sup>1</sup>, Le He<sup>1</sup>, Xiangyu Cao<sup>2</sup>, Xianling Wang<sup>3</sup>, Shubin Chen<sup>4</sup>, Huijun Chen<sup>1</sup>, Rui Li<sup>1</sup>, and Chun Yuan<sup>1,5</sup>

<sup>1</sup>Center for Biomedical Imaging Research, Department of Biomedical Engineering, School of Medicine, Tsinghua University, Beijing, People's Republic of China, <sup>2</sup>Neurosurgery department of the general hospital of PLA, Beijing, People's Republic of China, <sup>3</sup>Xuanwu Hospital, Capital Medical University, Beijing, People's Republic of China, <sup>4</sup>Department of Otolaryngology Head and Neck Surgery, Beijing Tongren Hospital, Capital Medical University, Beijing, People's Republic of China, <sup>5</sup>Department of Radiology, University of Washington, Seattle, United States

Pulsatile tinnitus (PT) is suspected to be associated with abnormal hemodynamics in sigmoid-sinus. In this study, we used 4D-Flow MRI to characterize blood flow in sigmoid-sinus among patients with pulsatile tinnitus and demonstrated that high blood velocity in sigmoid-sinus might be an authentic marker of PT. This study may provide more information for diagnosis and treatment of pulsatile tinnitus, especially for patients with PT of venous origin.

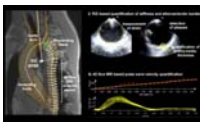


#### 4-Dimensional Phase-Contrast Magnetic Resonance Imaging of Left Atrial Stasis in Patients with Paroxysmal Atrial Fibrillation: A Comparative Study of Patients Pre- and Post-Ablation

Julio Garcia<sup>1</sup>, Michael S Bristow<sup>2,3</sup>, Carmen Lydell<sup>3,4</sup>, Andrew G Howarth<sup>2,3</sup>, Bobby Heydari<sup>2,3</sup>, Frank S Prato<sup>5</sup>, Maria Drangova<sup>5</sup>, Rebecca Thornhill<sup>6</sup>, Pablo Nery<sup>7</sup>, Stephen Wilton<sup>3</sup>, Allan Skanes<sup>8</sup>, and James White<sup>2,3</sup>

<sup>1</sup>Department of Cardiac Sciences - Stephenson Cardiac Imaging Centre, University of Calgary, Calgary, AB, Canada, <sup>2</sup>Department of Medicine, University of Calgary, Calgary, AB, Canada, <sup>3</sup>Stephenson Cardiac Imaging Centre, Libin Cardiovascular Institute of Alberta, Calgary, AB, Canada, <sup>4</sup>Diagnostic Imaging, University of Calgary, Calgary, AB, Canada, <sup>5</sup>Medical Imaging, University of Western Ontario, London, ON, Canada, <sup>6</sup>Diagnostic Imaging, The Ottawa Hospital, Ottawa, ON, Canada, <sup>7</sup>Electrophysiology, University of Ottawa, Ottawa, ON, Canada, <sup>8</sup>Department of Medicine, University of Western Ontario, London, ON, Canada

This study may be of interest for clinicians and clinical researchers who study atrial diseases. This study demonstrates that 4D flow-derived LA 3D stasis is clinically feasible and it may be useful for characterize differences between pre- and post-ablation patients.



#### 4D flow MRI based quantification of regional stiffness in the thoracic aorta in stroke patients compared to transesophageal echocardiography

Thomas Wehrum<sup>1</sup>, Felix Günther<sup>2</sup>, Anja Hennemuth<sup>3</sup>, Johann Drexl<sup>3</sup>, Hanieh Mirzaee<sup>3</sup>, and Andreas Harloff<sup>1</sup>

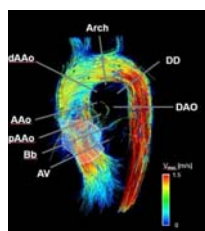
<sup>1</sup>Department of Neurology and Neurophysiology, University Medical Center Freiburg, Freiburg, Germany, <sup>2</sup>Department of Cardiology and Angiology, University Medical Center Freiburg, Freiburg, Germany, <sup>3</sup>Fraunhofer MEVIS, Bremen, Germany



Our purpose was to quantify regional stiffness in the aorta in stroke patients using 4D flow MRI based pulse-wave-velocity quantification in comparison with stiffness quantification using parameters based on transesophageal echocardiography (TEE). MRI and TEE based stiffness parameters were highly correlated and increased stiffness as measured using 4D flow MRI and TEE was associated with presence of atherosclerosis. Accordingly, we were able to predict the presence of atherosclerotic lesions with high sensitivity and specificity using both, 4D flow MRI and TEE. Hence, especially non-invasive 4D flow MRI can be used in future longitudinal studies investigating early development of atherosclerotic lesions.

293

17:27



Increased aortic wall shear stress and wall shear stress gradient in patients with an anatomically shaped sinus prosthesis using 4D Flow MRI

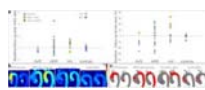
Victoria Schultz<sup>1</sup>, Thekla Oechtering<sup>1</sup>, Malte Sieren<sup>1</sup>, Michael Scharfschwerdt<sup>2</sup>, Anja Hennemuth<sup>3</sup>, Markus Hüllebrand<sup>3</sup>, Hans-Hinrich Sievers<sup>2</sup>, Jörg Barkhausen<sup>1</sup>, and Alex Frydrychowicz<sup>1</sup>

<sup>1</sup>Clinic for Radiology and Nuclear Medicine, University Hospital Schleswig-Holstein, Lübeck, Germany, <sup>2</sup>Department of Cardiac and Cardiothoracic Vascular Surgery, University Hospital Schleswig-Holstein, Lübeck, Germany, <sup>3</sup>Mevis, Fraunhofer, Bremen, Germany

Patients with anatomically shaped sinus prosthesis have been shown to have near physiological hemodynamics in the aortic bulb but altered flow characteristics distal to the prosthesis. The aim of this study was to compare the aortic wall shear of 12 patients with sinus prosthesis with 12 age-matched volunteers using 4D flow sensitive MRI. The wall shear stress analysis in 8 analysis planes revealed a tendency towards decreased WSS in the region of the prosthesis and increased WSS values distal to the prosthesis. Interestingly, the WSS gradient per plane and segmental WSS distal to the prosthesis were increased throughout the patients.

294

17:39



Post-surgical changes in aortic wall shear stress patterns in patients with aortopathy: a follow-up 4D flow MRI study

Emilie Bollache<sup>1</sup>, Paul W.M. Fedak<sup>2,3</sup>, Pim van Ooij<sup>4</sup>, Ozair Rahman<sup>1</sup>, Alex Hong<sup>1</sup>, Eric J. Keller<sup>1</sup>, S Chris Malaisrie<sup>3</sup>, Patrick M. McCarthy<sup>3</sup>, James C. Carr<sup>1</sup>, Jeremy D. Collins<sup>1</sup>, Michael Markl<sup>1,5</sup>, and Alex J. Barker<sup>1</sup>



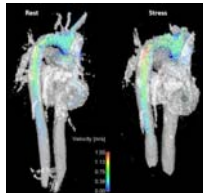
<sup>1</sup>Department of Radiology, Northwestern University, Chicago, IL, United States, <sup>2</sup>Department of Cardiac Sciences, University of Calgary, Calgary, AB, Canada, <sup>3</sup>Division of Surgery-Cardiac Surgery, Northwestern University, Chicago, IL, United States, <sup>4</sup>Department of Radiology, Academic Medical Center, Amsterdam, Netherlands, <sup>5</sup>Department of Biomedical Engineering, Northwestern University, Chicago, IL, United States

Our purpose was to follow up post-surgical changes in peak wall shear stress (WSS) and extent of at-risk tissue using 4D flow MRI in 34 aortopathy patients. Highly variable changes between pre- and post-surgery were found according to the intervention or replaced aortic valve type, while WSS patterns were unchanged in 20 other patients who did not undergo surgery. The reproducible 4D flow MRI WSS indices should be studied in larger cohorts and compared with patient outcome to potentially detect risk of future events in aortopathy patients, while optimizing the extent of resected aortic tissue.

295



17:51



4D Flow MRI during Exercise in Prematurely Born Adults and Children

Jacob Macdonald<sup>1</sup>, Arij Beshish<sup>2</sup>, Kristin Haraldsdottir<sup>2</sup>, Marlowe Eldridge<sup>2</sup>, Oliver Wieben<sup>1,3</sup>, and Christopher J Francois<sup>3</sup>

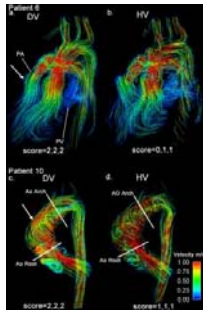
<sup>1</sup>Medical Physics, University of Wisconsin - Madison, Madison, WI, United States, <sup>2</sup>Pediatrics, University of Wisconsin - Madison, Madison, WI, United States, <sup>3</sup>Radiology, University of Wisconsin - Madison, Madison, WI, United States

Preterm birth can result in impaired development of lung airways and vasculature, but the long term implications are unclear. With this in mind, we performed 4D flow imaging in the aorta and pulmonary artery during exercise at 70% maximal power in both children and adults who had been born prematurely to identify any differences in flow characteristics relative to healthy controls. Although no statistically significant differences were identified between our groups, some preterm cohorts showed increased cardiac output and mean velocity. The significance of these trends should become apparent as we continue to recruit subjects and increase our statistical power.

296

18:03

k-t Accelerated Dual-Venc 4D flow MRI for Improved Flow Visualization in Pediatric Patients with Congenital Heart Disease



Liliana Ma<sup>1,2</sup>, Michael Rose<sup>3</sup>, Ozair Rahman<sup>1</sup>, Kelly Jarvis<sup>1,2</sup>, Joshua Robinson<sup>1,3</sup>, Cynthia Rigsby<sup>1,3,4,5</sup>, Michael Markl<sup>1,2,3,4,5</sup>, and Susanne Schnell<sup>1</sup>

<sup>1</sup>Department of Radiology, Northwestern University, Feinberg School of Medicine, Chicago, IL, United States, <sup>2</sup>Department of Biomedical Engineering, Northwestern University, Chicago, IL, United States, <sup>3</sup>Department of Medical Imaging, Ann & Robert H. Lurie Children's Hospital of Chicago, Chicago, IL, United States, <sup>4</sup>Department of Pediatrics, Northwestern University, Feinberg School of Medicine, Chicago, IL, United States, <sup>5</sup>Division of Cardiology, Ann & Robert H. Lurie Children's Hospital of Chicago, Chicago, IL, United States

This study explores the potential of using dual-velocity encoding 4D flow MRI for in-vivo assessment of complex blood flow patterns in patients with diverse presentations of congenital heart disease.

## Oral

### Motion Correction: All Brain

Room 313A      Monday 16:15 - 18:15    Moderators: Jacco de Zwart & Emine Saritas

297

16:15



#### Prediction of Motion Induced Image Degradation Using a Markerless Motion Tracker

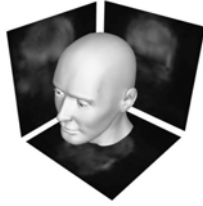
Rasmus Munch Olsen<sup>1</sup>, Helle Hjorth Johannesen<sup>2</sup>, Otto Mølby Henriksen<sup>2</sup>, Lisbeth Marner<sup>2</sup>, and Oline Vinter Olesen<sup>1,2,3</sup>

<sup>1</sup>DTU Compute, Technical University of Denmark, Lyngby, Denmark, <sup>2</sup>Department of Clinical Physiology, Nuclear Medicine & PET, Rigshospitalet, Copenhagen University Hospital, Copenhagen, Denmark, <sup>3</sup>TraInnovations, Ballerup, Denmark

In this work a markerless motion tracker, TCL2, is used to predict image quality in 3D T1 weighted MPRAGE MRI brain scans. An experienced radiologist scored the image quality for 172 scans as being usable or not usable, i.e. if a repeated scan was required. Based on five motion parameters, a classification algorithm was trained and an accuracy for identifying not usable images of 95.9% was obtained with a sensitivity of 91.7% and specificity of 96.3%. This work shows the feasibility of the markerless motion tracker for predicting image quality with a high accuracy.

298

16:27



Towards a prospective motion correction for the clinic: increasing the accuracy and robustness of collapsed FatNav

Enrico Avventi<sup>1,2</sup>, Henric Ryden<sup>1</sup>, Ola Norbeck<sup>1,2</sup>, and Stefan Skare<sup>1,2</sup>

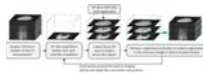
<sup>1</sup>Neuroradiology, Karolinska University Hospital, Stockholm, Sweden,

<sup>2</sup>Karolinska Institutet, Stockholm, Sweden

Collapsed FatNav is a navigator for prospective motion correction which samples the signal from the fat around the skull collapsed along three orthogonal directions with consecutive EPI readouts. The six rigid body motion parameters can be obtained by performing a 2D/3D projection-based registration. In this work we have greatly improved collapsed FatNav's accuracy and precision. Additionally, by combining with PROPELLER's retrospective correction, we can obtain image quality typical of images acquired without motion.

299

16:39



A Novel Approach to Prospective Motion Correction Using Multi-Slice-to-Volume Registration

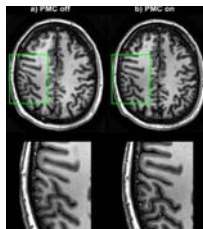
Daniel Christopher Hoinkiss<sup>1</sup> and David Andrew Porter<sup>1</sup>

<sup>1</sup>MR Physics, Fraunhofer MEVIS, Bremen, Germany

This study introduces a novel 2D-EPI-navigated prospective motion correction technique to correct for in-plane and through-plane motion that establishes a flexible steady-state during the measurement. It utilizes a rigid-body multi-slice-to-volume registration using three parallel and well-separated EPI slices. The technique was evaluated using a well-defined motion protocol with translations up to 13mm and rotations up to 9°, which was executed by a volunteer. Results show a substantial reduction of motion parameters to below  $\pm 0.5\text{mm}/\pm 0.5^\circ$  and an increase in overall image quality in comparison to a no-motion scan. The navigator acquisition scheme can be adapted for use with a range of multi-shot 2D sequences to allow EPI navigators to be acquired with limited effect on the overall scan time or the contrast-to-noise ratio.

300

16:51



Active-marker motion detection with real-time field tracking in the laboratory frame

Alexander Aranovitch<sup>1</sup>, Maximilian Haeberlin<sup>1</sup>, Simon Gross<sup>1</sup>, Benjamin Dietrich<sup>1</sup>, Lars Kasper<sup>1</sup>, Bertram Wilm<sup>1,2</sup>, David Otto Brunner<sup>1</sup>, Thomas Schmid<sup>1</sup>, and Klaas Pruessmann<sup>1</sup>

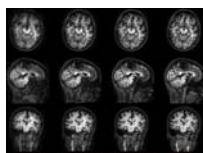
*<sup>1</sup>Institute for Biomedical Engineering, ETH Zurich and University of Zurich, Zurich, Switzerland, <sup>2</sup>Skope Magnetic Resonance Technologies, Zurich, Switzerland*

We introduce a technique to track NMR markers without a prior calibration measurement. This significantly improves the ease of implementation of field probe based prospective motion correction (PMC). We propose to use rigidly mounted NMR field probes in the laboratory frame to perform concurrent field measurements, which are used for real-time tracking of head-mounted field probes. The proposed method achieves very good tracking performance and is demonstrated in-vivo with PMC of high-resolution brain scans.

---

301

17:03



Motion correction in volumetric brain imaging based on DISORDER: Distributed and Incoherent Sample Orders for Reconstruction Disentanglement using Encoding Redundancy

Lucilio Cordero-Grande<sup>1</sup>, Giulio Ferrazzi<sup>1</sup>, Rui Pedro AG Teixeira<sup>1</sup>, Hassan Shahzad<sup>2</sup>, Anthony N Price<sup>1</sup>, and Joseph V Hajnal<sup>1</sup>

*<sup>1</sup>Division of Imaging Sciences and Biomedical Engineering, King's College London, London, United Kingdom, <sup>2</sup>Electrical Engineering Department, COMSATS Institute of Information Technology, Islamabad, Pakistan*

The DISORDER framework for motion tolerant reconstruction in parallel volumetric brain imaging synergistically combines distributed and incoherent sample orders with a joint retrospective motion estimation and reconstruction technique based on encoding redundancy provided by coil arrays. DISORDER is fully data-based, does not make use of external sensors or acquisition of navigators, does not require data rejection, and can be applied to different sampling schemes and imaging modalities. In-vivo application of DISORDER has shown robustness against extreme and continuous motion in low resolution images and moderate and continuous motion in standard and high resolution images as well as slightly improved contrast properties in high resolution motion images without deliberate motion.

---

302

17:15

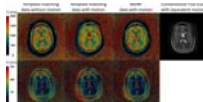


Image Reconstruction Algorithm for Motion Insensitive Magnetic Resonance Fingerprinting (MRF)

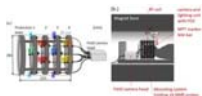
Bhairav Bipin Mehta<sup>1</sup>, Dan Ma<sup>1</sup>, Simone Coppo<sup>1</sup>, and Mark Alan Griswold<sup>1</sup>

*<sup>1</sup>Radiology, Case western reserve university, Cleveland, OH, United States*

Motion is one of the biggest challenges in clinical MRI. The recently introduced Magnetic Resonance Fingerprinting (MRF) has been shown to be less sensitive to motion. However, it is still susceptible to patient motion primarily occurring in the early stages of the acquisition. In this study, we propose a novel reconstruction algorithm for MRF, which decrease the motion sensitivity of MRF. The evaluation of the algorithm was performed using simulated head tilt and nodding motion, and with prospectively motion corrupted data from healthy volunteers.

303

17:27



Relating external magnetic field changes to head movement using motion and field cameras

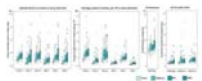
Laura I. Bischoff<sup>1</sup>, James A. Smith<sup>1</sup>, Olivier E. Mougin<sup>1</sup>, Glyn S. Spencer<sup>1</sup>, Kingkarn Aphiwatthanasumet<sup>1</sup>, Penny A. Gowland<sup>1</sup>, and Richard W. Bowtell<sup>1</sup>

*<sup>1</sup>Physics and Astronomy, University of Nottingham, Nottingham, United Kingdom*

The effect of head movement in high-field MRI is assessed by measuring changes in the spatial pattern of magnetic field perturbation, generated outside the head, using a set of 16 NMR probes fixed into a specially constructed coil mount. Information from the field probes was combined with head position measurements provided by an optical tracking system and quantitative relations between field and position changes were characterised. By relating the field probe and optical tracking measurements, acquired in a training-phase, it was possible to predict head movements based solely on measured magnetic field changes made in subsequent recordings.

304

17:39



On the impact of real-time motion and B0 correction during 3D-MRSI measurements in Parkinson's, Mild Cognitive Impairment and young/elderly controls

Eva Heckova<sup>1</sup>, Michal Považan<sup>1,2</sup>, Bernhard Strasser<sup>1</sup>, Petra Hnilicova<sup>3</sup>, Ovidiu C Andronesi<sup>4</sup>, Andre van der Kouwe<sup>4</sup>, Jozef Ukropec<sup>5</sup>, Siegfried Trattnig<sup>1,2</sup>, and Wolfgang Bogner<sup>1,2</sup>

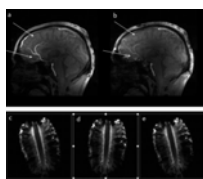
<sup>1</sup>High Field MR Centre, Medical University of Vienna, Vienna, Austria, <sup>2</sup>Christian Doppler Laboratory for Clinical Molecular MR Imaging, Vienna, Austria, <sup>3</sup>Biomedical Center Martin, Division of Neurosciences, Jessenius Faculty of Medicine in Martin, Comenius University in Bratislava, Martin, Slovakia, <sup>4</sup>Martinos Center for Biomedical Imaging, Massachusetts General Hospital, Harvard Medical School, Boston, MA, United States, <sup>5</sup>Institute of Experimental Endocrinology, Biomedical Research Center, Slovak Academy of Sciences, Bratislava, Slovakia

Presence of motion during MRSI acquisition and scanner instabilities affect the localization accuracy of the measurement and consequential quality of the data. We determined the extent of inter-acquisition head movement, frequency and B0 shim changes during approximately 20 min MEGA-edited MRSI scan with integrated vNav in 4 different groups of subject, with significantly larger amount of head motion in Parkinson's patients, Mild Cognitive Impairment and elderly controls comparing to young healthy volunteers. With real-time motion, B0 correction and reacquisition we obtained satisfactory data quality in all groups of subjects, which makes it a valuable tool for spectral quality accuracy.

---

305

17:51



AMoCo, a software package for prospective motion correction

Ali Aghaeifar<sup>1,2</sup>, Martin Eschelbach<sup>1</sup>, Jonas Bause<sup>1</sup>, Axel Thielscher<sup>1</sup>, and Klaus Scheffler<sup>1,3</sup>

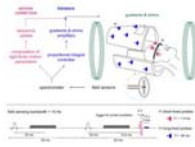
<sup>1</sup>Max Planck Institute for Biological Cybernetics, Tübingen, Germany, <sup>2</sup>IMPRS for Cognitive and Systems Neuroscience, University of Tübingen, Tübingen, Germany, <sup>3</sup>Department of Biomedical Magnetic Resonance, University of Tübingen, Tübingen, Germany

Long scan time makes MRI prone to subject motion which can result in image artifacts. Here we introduce a library for advanced motion correction (AMoCo) for Siemens platforms which can be embedded in any sequence and enables connecting to any tracking device. The library is programmed in a modular way that allows user to customize the correction procedure. The library is integrated with EPI, GRE, and FLASH sequences and tested with various tracking devices.

---

18:03

Simultaneous prospective motion correction and feedback field control: T2\* weighted imaging at high field



Laetitia Vionnet<sup>1</sup>, Alexander Aranovitch<sup>1</sup>, Yolanda Duerst<sup>1</sup>, Maximilian Haeberlin<sup>1</sup>, Benjamin Emanuel Dietrich<sup>1</sup>, Simon Gross<sup>1</sup>, Lars Kasper<sup>1,2</sup>, Thomas Schmid<sup>1</sup>, and Klaas Paul Pruessmann<sup>1</sup>

<sup>1</sup>ITET, IBT, UZH & ETHZ, Zurich, Switzerland, <sup>2</sup>TNU, UZH & ETHZ, Zurich, Switzerland

T2\* weighted imaging, which is particularly relevant in studying dementia, is prompt to artefacts caused by subject-induced field fluctuation and head motion. Solutions have been proposed to tackle each of these issues separately. In this work we propose to address the two issues concurrently with feedback field control and marker-based prospective motion correction based on gradient-tones. We demonstrate the effectiveness of the combination in the scenario of limb motion.

## Oral

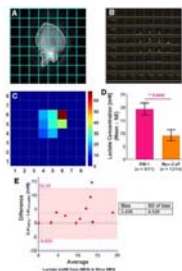
# Preclinical Tumor Microenvironment Imaging

Room 313BC

Monday 16:15 - 18:15 *Moderators:* Kristine Glunde & Eugene Kim

307

16:15



## Imaging of the Tumor Type-specific Microenvironment in Preclinical Cancer Models of Varying Malignancy

Ellen Ackerstaff<sup>1</sup>, Natalia Kruchevsky<sup>1</sup>, Ekaterina Moroz<sup>1</sup>, H. Carl LeKaye<sup>1</sup>, Kristen L. Zakian<sup>1</sup>, SoHyun Han<sup>2</sup>, HyungJoon Cho<sup>2</sup>, Radka S. Stoyanova<sup>3</sup>, Nirilanto Ramamonjisoa<sup>1</sup>, Inna S. Serganova<sup>1</sup>, Ronald G. Blasberg<sup>1</sup>, and Jason A. Koutcher<sup>1</sup>

<sup>1</sup>Memorial Sloan-Kettering Cancer Center, New York, NY, United States, <sup>2</sup>Ulsan National Institute of Science and Technology, Ulsan, Korea, Republic of, <sup>3</sup>Miller School of Medicine, University of Miami, Miami, FL, United States

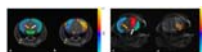


An abnormal tumor microenvironment characterized by hypoxia, low extracellular pH (pHe), vascular abnormalities, and high tumor lactate has been associated with aggressive, treatment-resistant tumors. Using tumor models of different origin and malignancy, and focusing on prostate cancer, we investigated the relationship of lactate metabolism and vascularity, and, in selected models, localized pHe. We found differences in whole-tumor lactate concentrations between tumor models and successfully mapped lactate concentrations. Vascular blood flow and permeability varied significantly between tumor models in well-vascularized areas, while being similar across all models in hypoxic areas, emphasizing a need for spatial characterization of the tumor microenvironment.

308



16:27



### Brain Tumors Disrupt the Resting-State Connectome

Darian Hadjiabadi<sup>1</sup>, Leland Pung<sup>1</sup>, Jiangyang Zhang<sup>2</sup>, BD Ward<sup>3</sup>, Woo-Taek Lim<sup>1</sup>, Meghana Kalavar<sup>2</sup>, Nitish V Thakor<sup>1</sup>, Bharat B Biswal<sup>4</sup>, and Arvind P Pathak<sup>1,2,5</sup>

<sup>1</sup>Department of Biomedical Engineering, Johns Hopkins University, Baltimore, MD, United States, <sup>2</sup>Russell H. Morgan Department of Radiology and Radiological Science, Johns Hopkins University School of Medicine, Baltimore, MD, United States, <sup>3</sup>Department of Biophysics, The Medical College of Wisconsin, Milwaukee, WI, United States, <sup>4</sup>Department of Biomedical Engineering, New Jersey Institute of Technology, Newark, NJ, United States, <sup>5</sup>Sidney Kimmel Comprehensive Cancer Center, Johns Hopkins University School of Medicine, Baltimore, MD, United States

Resting-state functional MRI (rsfMRI) has become indispensable for mapping the changes in 'connectivity' between brain regions in a range of diseases including brain tumors. However, the complex interplay between abnormal brain tumor vasculature, tumor blood flow, and cancer cell-induced neurovascular uncoupling can confound the interpretation of resting-state connectivity in patients. Therefore, in this preclinical study we quantified brain tumor-induced changes on resting-state connectivity relative to that in healthy brains, followed by histological validation. RsfMRI revealed that brain tumors alter the resting-state connectome, and histology confirmed that this was largely due to cancer cell-induced disruption of the neurovascular unit.

16:39

Multiparametric MR for assessment of tissue characteristics of small intestine neuroendocrine tumour evaluated by histological correlations



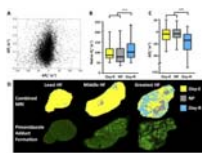
Author	Department	Address
Mikael Montelius <sup>1</sup>	Department of Radiation Physics	University of Gothenburg, Gothenburg, Sweden
Oscar Gustafsson <sup>1</sup>	Department of Radiation Physics	University of Gothenburg, Gothenburg, Sweden
Johan Spetz <sup>1</sup>	Department of Radiation Physics	University of Gothenburg, Gothenburg, Sweden
Ola Nilsson <sup>2</sup>	Department of Pathology	University of Gothenburg, Gothenburg, Sweden
Eva Forssell-Aronsson <sup>1</sup>	Department of Radiation Physics	University of Gothenburg, Gothenburg, Sweden
Maria Ljungberg <sup>1</sup>	Department of Radiation Physics	University of Gothenburg, Gothenburg, Sweden

Mikael Montelius<sup>1</sup>, Oscar Gustafsson<sup>1</sup>, Johan Spetz<sup>1</sup>, Ola Nilsson<sup>2</sup>, Eva Forssell-Aronsson<sup>1</sup>, and Maria Ljungberg<sup>1</sup>

<sup>1</sup>Department of Radiation Physics, University of Gothenburg, Gothenburg, Sweden, <sup>2</sup>Department of Pathology, University of Gothenburg, Gothenburg, Sweden

This study investigates the relations between MR derived, quantitative parameters reflecting perfusion, diffusion and relaxation, and histological indices reflecting apoptosis, proliferation, vascularity and fibrosis. We show that important biological characteristics of tumour tissue can be probed by multiparametric MRI.

16:51



Understanding the relationship between  $R_2^*$  and  $R_1$  MRI biomarkers of hypoxia: insights from 786-0 renal cancer xenografts and patients with renal carcinoma

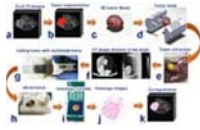
Ross A Little<sup>1</sup>, Yann Jamin<sup>2</sup>, Jessica KR Boulton<sup>2</sup>, Josephine H Naish<sup>1</sup>, Yvonne Watson<sup>1</sup>, Susan Cheung<sup>1</sup>, Huiqi Lu<sup>1</sup>, Damien J McHugh<sup>1</sup>, Geoff JM Parker<sup>1,3</sup>, Joely Irlam<sup>4</sup>, Catherine ML West<sup>4</sup>, John C Waterton<sup>1</sup>, Simon P Robinson<sup>2</sup>, and James PB O'Connor<sup>4,5</sup>

<sup>1</sup>Centre for Imaging Sciences, University of Manchester, Manchester, United Kingdom, <sup>2</sup>Division of Radiotherapy and Imaging, The Institute of Cancer Research, London, United Kingdom, <sup>3</sup>Bioxydyn Ltd, Manchester, United Kingdom, <sup>4</sup>Institute of Cancer Sciences, University of Manchester, Manchester, United Kingdom, <sup>5</sup>Department of Radiology, The Christie NHS Foundation Trust, Manchester, United Kingdom

Quantification of tumour  $R_2^*$  and oxygen-induced  $\Delta R_2^*$  and  $\Delta R_1$  are being investigated as potential biomarkers of tumour hypoxia, but their relationship is complex and not well understood. Here, we used a validated  $R_1$  biomarker (oxygen refractory fraction, termed "Oxy-R") to segment tumours into hypoxic and non-hypoxic sub-regions. This revealed a clear relationship between hypoxic status and native  $R_2^*$  and hyperoxia-induced  $\Delta R_2^*$ . Preclinical findings were replicated in clinical data from patients with renal carcinoma. These data highlight the importance of heterogeneity-based analysis of tumours and provide further validation of Oxy-R as a biomarker of tumour hypoxia.

17:03

Co-registration of multi-parametric MRI and histology to study breast cancer Habitats in a preclinical model.



William Dominguez-Viqueira<sup>1</sup>, Bruna V Jardim-Perassi<sup>1,2</sup>, Mikalai Budzevich<sup>1</sup>, Epifanio Ruiz<sup>1</sup>, Suning Huang<sup>1</sup>, Pedro M Enriquez-Navas<sup>1</sup>, Jan Poleszczuk<sup>3</sup>, Debora A.P.C. Zuccari<sup>2</sup>, Robert J Gillies<sup>1</sup>, and Gary V Martinez<sup>1</sup>

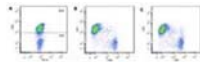
*<sup>1</sup>Department of Cancer Imaging and Metabolism, Moffitt Cancer Center, Tampa, FL, United States, <sup>2</sup>Faculdade de Medicina de Sao Jose do Rio Preto, Sao Jose do Rio Preto, Brazil, <sup>3</sup>Nalecz Institute of Biocybernetics and Biomedical Engineering, Warsaw, Poland*

Different tumor micro-environments or habitats are discernible by MRI. In order to study these, a co-registration framework was developed using 3D-printed tumor-molds created from in-vivo MRI images of five mice with implanted breast cancer tumors. The results of automated 3D-alignment of MRI images and histology slices are promising and encourage further experiments using the presented workflow. Tumor habitats clustering from multi-parametric MRI images showed encouraging results with similarities to the hypoxic pattern observed by immunohistochemistry. This work will help understanding MRI habitats to monitor cancer evolution as a means to aid treatment decisions in the future.

312



17:15



Fluorine-19 NMR cytometry to quantify human transgenic CAR T cell biodistribution in murine studies of glioblastoma immunotherapy  
Fanny Chapelin<sup>1</sup>, Hideho Okada<sup>2</sup>, and Eric T Ahrens<sup>3</sup>

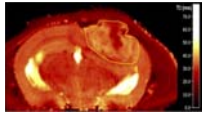
*<sup>1</sup>Bioengineering, University of California San Diego, La Jolla, CA, United States, <sup>2</sup>Neurological surgery, University of California San Francisco, San Francisco, CA, United States, <sup>3</sup>Radiology, University of California San Diego, La Jolla, CA, United States*

Technologies to quantify the biodistribution of emerging immunotherapeutic cell therapies against cancer can accelerate the timeline to evaluate potential candidates. In this study, we describe the use of in 'NMR cytometry' to assay immunotherapeutic cell biodistribution in a mouse model of sub-cutaneous glioblastoma (U87) treated with chimeric antigen receptor (CAR) T-cells. We examine CAR T cell <sup>19</sup>F labeling efficiency, phenotype and biodistribution with <sup>19</sup>F NMR at day 2 and 7 post infusion to elucidate T-cell tumor homing, survival, and tissue distribution.

313

17:27

Correlated quantitative assessment of glioblastoma-angiogenesis by T2-mapping and in vivo multiphoton microscopy



Artur Hahn<sup>1</sup>, Ke Zhang<sup>2</sup>, Gergely Solecki<sup>3,4</sup>, Michael O. Breckwoldt<sup>1,5</sup>, Lukas R. Buschle<sup>1,6</sup>, Sabine Heiland<sup>1</sup>, Christian H. Ziener<sup>1,6</sup>, Martin Bendszus<sup>1</sup>, Frank Winkler<sup>3,7</sup>, and Felix T. Kurz<sup>1</sup>

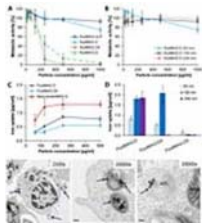
<sup>1</sup>Neuroradiology, University Hospital Heidelberg, Heidelberg, Germany, <sup>2</sup>German Cancer Research Center (DKFZ), Heidelberg, Germany, <sup>3</sup>Neurology Clinic and National Center for Tumor Diseases, University Hospital Heidelberg, Heidelberg, Germany, <sup>4</sup>Clinical Cooperation Unit Neurooncology, German Cancer Consortium (DKTK), Heidelberg, Germany, <sup>5</sup>Clinical Cooperation Unit Neuroimmunology and Brain Tumor Immunology, German Cancer Research Center (DKFZ), Heidelberg, Germany, <sup>6</sup>E010 Radiology, German Cancer Research Center (DKFZ), Heidelberg, Germany, <sup>7</sup>Neurooncology (G370), German Cancer Research Center, Heidelberg, Germany

Microvasculatures in healthy cortical tissue, in untreated and in antiangiogenically treated glioblastoma multiforme are compared in a mouse model. From T2-maps, the information entropy is determined for each tissue type. In addition, capillaries are directly imaged through in vivo multiphoton microscopy to obtain sets of microvascular parameters. The T2-entropy is lowest in healthy tissue and significantly higher in glioblastoma, with a moderate decrease in treated tumors. Several vascular characteristics correlate with the T2-entropy. The correlations provide insight into the influence of microvasculature on MR-dephasing.

314



17:39



In vivo tracking of iron oxide labeled T-cells infiltrating preclinical tumor models

Johannes Riegler<sup>1</sup>, Vincent Javinal<sup>2</sup>, Maj Hedehus<sup>1</sup>, Mike Reichelt<sup>3</sup>, Meredith Sagolla<sup>3</sup>, Jill Schartner<sup>2</sup>, Franklin Peal<sup>4</sup>, and Richard A.D. Carano<sup>1</sup>

<sup>1</sup>Biomedical Imaging, Genentech, South San Francisco, CA, United States, <sup>2</sup>In vivo Pharmacology, Genentech, South San Francisco, CA, United States, <sup>3</sup>Center for Advanced Light Microscopy, Genentech, South San Francisco, CA, United States, <sup>4</sup>Pathology, Genentech, South San Francisco, CA, United States

The discovery of immune checkpoint pathways such as CTLA4 and PD1/PDL1, which control T-cell activation and activity, has fuelled interest in their modulation to achieve sustained anti-tumor immunity. This requires sufficient T-cell infiltration and activity in tumors. However, these processes are incompletely understood, in part due to the terminal nature of current analysis techniques. We therefore optimized labeling of activated T-cells with iron oxide nanoparticles, transferred labeled T-cells into tumor bearing hosts and performed serial MRI. Although, hypointense spots could be detected in the tumor rim following T-cell transfer, quantification is complicated by vascular abnormality induced susceptibility changes.

315

17:51

### Magnetisation Transfer MRI Facilitates Non-Invasive Identification of Fibrosis in Chemically-Induced Rat Mammary Carcinomas Imaged on a 1.5T Clinical Platform

Jessica KR Boulton<sup>1</sup>, Neil P Jerome<sup>1</sup>, Matthew R Orton<sup>1</sup>, James d'Arcy<sup>1</sup>, Martin O Leach<sup>1</sup>, Dow-Mu Koh<sup>1,2</sup>, David J Collins<sup>1</sup>, and Simon P Robinson<sup>1</sup>

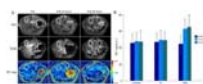
<sup>1</sup>CRUK Cancer Imaging Centre, Division of Radiotherapy and Imaging, The Institute of Cancer Research, London, United Kingdom,

<sup>2</sup>Department of Radiology, Royal Marsden NHS Foundation Trust, London, United Kingdom

Intratumoural fibrosis is associated with poor prognosis in breast cancer patients. Non-invasive detection of such fibrosis may contribute to the provision of personalised treatment regimens. Multi-parametric MRI, using a clinical MRI scanner and incorporating endogenous contrast mechanisms, was performed on MNU-induced rat mammary carcinomas to identify parameters sensitive to the detection and quantification of fibrosis. Magnetisation transfer MRI derived parameters correlated with percentage picrosirius red staining, which detects collagen I/III, major components of fibrosis, in this heterogeneous tumour cohort. These results strongly support the inclusion of magnetisation transfer in clinical MR breast imaging protocols.

316

18:03



### MRI Tracking and Quantitative Analyzing Natural Killer Cell Infusion for Hepatocellular Carcinoma Treatment in a Rodent Model

Zhanliang Su<sup>1,2</sup>, Xifu wang<sup>2,3</sup>, Linfeng Zheng<sup>2,3</sup>, Tianchu Lyu<sup>2</sup>, Matteo Figini<sup>2</sup>, Guohong Han<sup>4</sup>, Daniel Procissi<sup>2</sup>, Lei Qin<sup>5</sup>, Bin Zhang<sup>5</sup>, Jeremy Shi Zhang<sup>2</sup>, Wei Xing<sup>6</sup>, Yihe Yang<sup>2</sup>, Kejiang Wang<sup>1</sup>, Shixin Wang<sup>1</sup>, Vahid Yaghmai<sup>2,7</sup>, Andrew Christian Larson<sup>2,7</sup>, and Zhuoli Zhang<sup>2,7</sup>

<sup>1</sup>Department of Radiology, Tianjin Xiqing Hospital, Tianjin, People's Republic of China, <sup>2</sup>Department of Radiology, Feinberg School of Medicine, Northwestern University, Chicago, IL, United States, <sup>3</sup>Department of Radiology, Shanghai General Hospital, Shanghai Jiaotong University, Shanghai, People's Republic of China, <sup>4</sup>Department of Liver Disease and Digestive Interventional Radiology, Xijing Hospital, Xi'an, United States, <sup>5</sup>Department of Medicine, Division of Hematology/Oncology, Feinberg School of Medicine, Northwestern University, Chicago, IL, United States, <sup>6</sup>Department of Radiology, Affiliated Third Hospital of Suzhou University, Changzhou, People's Republic of China, <sup>7</sup>Robert H. Lurie Comprehensive Cancer Center

This paper presents the first evidence that transcatheter IHA NK cell local delivery for HCC adoptive transfer immunotherapy in a rat model.

We use a clinically feasible method by combining FDA-approved drugs heparin, protamine and ferumoxytol to compound HPF nanocomplexes for magnetic NK cell labeling so that their biodistribution can be visualized and quantized *in vivo* with MRI.

We demonstrated: a) transcatheter IHA NK cell infusion improved their homing efficacy to target tumors; b) quantitative analysis result of serial MRI monitoring of NK cell migrate to target tumors could serve as a key early biomarker for predicting longitudinal response.

---

## Oral

## Pancreatobiliary

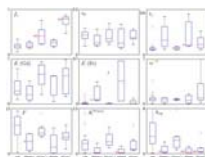
Room 320

Monday 16:15 - 18:15 Moderators: Sooah Kim & Bachir Taouli

---

317

16:15



### Physiologically-constrained Multiagent DCE-MRI for Pancreatic Cancer Imaging

Matthias C Schabel<sup>1,2</sup>, Erin Gilbert<sup>3</sup>, Alexander Guimaraes<sup>4</sup>, and Cory Wyatt<sup>1</sup>

<sup>1</sup>Advanced Imaging Research Center, Oregon Health & Science University, Portland, OR, United States, <sup>2</sup>Utah Center for Advanced Imaging Research, University of Utah, Salt Lake City, UT, United States, <sup>3</sup>Surgery, Oregon Health & Science University, Portland, OR, United States, <sup>4</sup>Radiology, Oregon Health & Science University, Portland, OR, United States



Physiologically-constrained multiagent pharmacokinetic modeling in pancreas using sequential injections of gadoteridol and ferumoxytol reveals differences between healthy pancreas in high-risk patients and both IPMN and pancreatic ductal adenocarcinoma.

---

318

16:27



### Improved Characterization of Contrast Uptake in Human Pancreatic Cancer

Douglas Arthur Charles Kelley<sup>1</sup>, Benjamin Yeh<sup>2</sup>, Michael Ohliger<sup>2</sup>, Eric Collisson<sup>2</sup>, and Zhen Wang<sup>2</sup>

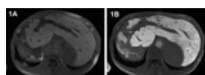
<sup>1</sup>Radiology and Biomedical Imaging, GE Healthcare and UCSF, Larkspur, CA, United States, <sup>2</sup>Radiology and Biomedical Imaging, UCSF

We present an improved method for quantifying contrast agent uptake in highly desmoplastic pancreatic tumors in human patients. The new method separates the T1 and T2\* effects of the Gadolinium-based contrast agent; uses fast acquisition and non-rigid registration to minimize motion effects; and two point Dixon imaging to separate the water component on a pixel by pixel basis.

---

319

16:39



### Prognostic value of hepatobiliary phase MRI in patients with primary sclerosing cholangitis – Assessment of clinical outcome and evaluation of surrogate parameters

Jennifer Schulze<sup>1</sup>, Henrike Lenzen<sup>2</sup>, Jan Hinrichs<sup>1</sup>, Michael Manns<sup>2</sup>, Frank Wacker<sup>1</sup>, and Kristina Imeen Ringe<sup>1</sup>

<sup>1</sup>Department of Diagnostic and Interventional Radiology, Hannover Medical School, Hannover, Germany, <sup>2</sup>Department of Gastroenterology, Hepatology and Endocrinology, Hannover Medical School, Hannover, Germany

In this prospective study we assessed the prognostic value of hepatobiliary phase (HBP) MRI in patients with primary sclerosing cholangitis (PSC). Relative enhancement (RE) in the HBP after gadoxetate disodium injection correlated significantly with clinical scores (MELD, Mayo Risk) established to estimate survival in patients with chronic liver disease and PSC. More importantly, a significant correlation with previously suggested surrogate parameters for clinical outcome as well as with solid clinical endpoints (development of tumor, liver transplantation, death) at follow-up could be observed. These promising results attest HBP MRI in patients with PSC a potential prognostic role and warrant further long-term evaluation.



320

16:51

### Early screening of pancreatic iron overload in thalassemia major with MRI T2\*

Patient	
TM (µm)	11 865 063.3 05.00
Age(y)	7808.802
Number of slices(S)	3465.051248.00000 00.13000
MF(mm)	23218.292
Subvolume(slices,S)	18.301800.000
Initial transverse(s)	9.818.81.346
Duration transverse(s)	7807.292
Initial sagittal(s)	78.77249.0000.208.00
Initial coronal(s)	1.1213.3100.20.000
Duration Axial(s)	6.8515.5805.5.546
Regular spheric(slices,S)	7303.792
Cardiac T2*(ms)	20.16451.5703.23.40.846
User T2*(ms)	2.7862.7500.73.18.602
Automatic T2*(ms)	10.00205.6702.00.40.846
TM (µm)	3.0060.0103.70.7.960
Tuning glucose level(slices,S)	0.0163.5613.40.18.770
Image (s)	24.78243.9800.000
Amplitude(s)	38.77623.3700.1410

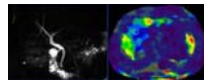
Jingwen Huang<sup>1</sup>, Qihua Yang<sup>1</sup>, Jinglian Zhong<sup>1</sup>, Xiaodong Chen<sup>2</sup>, Ziliang Cheng<sup>1</sup>, Taihui Yu<sup>1</sup>, Yun Su<sup>1</sup>, and Bilong Liang<sup>1</sup>

<sup>1</sup>Sun Yat-sen Memorial Hospital, Guangzhou, People's Republic of China, <sup>2</sup>Guangdong Medical College, People's Republic of China

Diabetes Mellitus is a serious complication of thalassemia major. Intensive chelation therapy in the early stage may avoid diabetes. So we aimed to determine the optimal timing age of pancreatic iron screening with MRI T2\* technique. Early pancreatic hemosiderin was found in thalassemia major, with the youngest one of 5.3 years old. Early dysfunction of pancreatic exocrine and endocrine glands was found in thalassemia major, with the youngest one of 5.5 years old. Therefore, we suggest age of 5 to 6 years old as the optimal initial age for pancreatic T2\* scanning.

321

17:03



### The Development And Prognostication Of Magnetic Resonance Elastography Thresholds In Primary Sclerosing Cholangitis

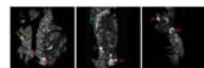
Kartik Jhaveri<sup>1</sup>, Hooman Hosseini-Nik, Nima Sadoughi, Harry Janssen, Jordan Feld, Sandra Fischer, Ravi Menezes, and Angela Cheung

<sup>1</sup>UHN, University of Toronto, Toronto, ON, Canada

Primary sclerosing cholangitis (PSC) is a chronic, progressive, cholestatic liver disease which causes bile duct structuring and eventually causes liver cirrhosis requiring liver transplantation. Due to heterogeneity of liver fibrosis distribution and lack of optimal method to assess disease severity accurate disease stratification is challenging. Magnetic resonance elastography (MRE) has shown very good results for quantification of hepatic fibrosis. MRE may provide a unique means of stratification and prognostication in PSC with its ability to assess a larger volume of hepatic tissue compared to biopsy or transient elastography(VCTE) and this what we explored in this prospective study.

322

17:15



### Diffusion imaging detects differences in disease trajectory between two mouse models of pancreatic cancer

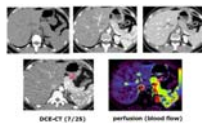
Palamadai Nilakantan Venkatasubramanian<sup>1</sup>, Matthew Smith<sup>2</sup>, Jesse Yan<sup>2</sup>, Brian Hallis<sup>2</sup>, Emman Mascarinas<sup>3</sup>, Andrew Diaz<sup>3</sup>, Brian DeCant<sup>3</sup>, Ron McKinney<sup>3</sup>, Paul J Grippo<sup>3</sup>, and Alice M Wyrwicz<sup>1</sup>

<sup>1</sup>Radiology, NorthShore University HealthSystem, Evanston, IL, United States, <sup>2</sup>NorthShore University HealthSystem, Evanston, IL, United States, <sup>3</sup>Medicine, University of Illinois at Chicago

Multiparametric MR microimaging detected differences in pancreatic microstructure between two mouse models of pancreatic cancer, EL-KRASG12D (EK) and p48-Cre/LSL-Kras (KC) mice, that overexpress mutant KRas via different mechanisms. MR signatures characteristic of acinar-ductal metaplasia, fibrosis, cystic neoplasms and precancerous lesions revealed different trajectories of disease development between the two genetically engineered mice.

323

17:27



Insulinoma localization with cross-sectional imaging: head-to-head comparison of contrast-enhanced CT, volume perfusion CT and multi-parametric MR

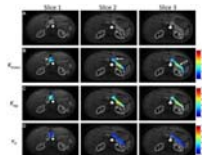
Liang Zhu<sup>1</sup>, Zhao-yong Sun<sup>1</sup>, Hua-dan Xue<sup>1</sup>, Tian-yi Qian<sup>2</sup>, and Zheng-yu Jin<sup>1</sup>

<sup>1</sup>Radiology, Peking Union Medical College Hospital, Beijing, People's Republic of China, <sup>2</sup>MR collaborations NE Asia, Siemens Healthcare, Beijing, People's Republic of China

This study aims to compare insulinoma localization with CECT, VPCT and multi-parametric MR (mp-MR) at 3T in the same patients, in a prospective manner. CECT, VPCT and mp-MR were performed in patients with suspected insulinomas. The presence/absence of tumor within the pancreatic head, neck, body and tail region was evaluated with 5-scale confidence levels. ROC analysis was performed. Surgical pathology served as reference standard. We found that VPCT and mp-MR showed improved diagnostic performance for insulinoma localization, compared to CECT. Both modalities could serve as problem-solving tools in difficult cases. mp-MR has the potential to replace CECT as the first-line examination.

324

17:39



3D Pancreatic Perfusion MRI using Through-Time Spiral GRAPPA Acceleration

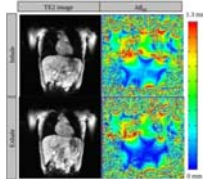
Yong Chen<sup>1</sup>, Shivani Pahwa<sup>1</sup>, Mark Griswold<sup>1</sup>, Nicole Seiberlich<sup>2</sup>, and Vikas Gulani<sup>1</sup>

<sup>1</sup>Radiology, Case Western Reserve University, Cleveland, OH, United States, <sup>2</sup>Biomedical Engineering, Case Western Reserve University

In this study, free-breathing 3D pancreatic perfusion quantification was achieved using a rapid non-Cartesian parallel imaging technique. The method was applied to 11 asymptomatic subjects and the values are in good agreement with literature values. Significant differences in both  $K_{trans}$  and  $K_{ep}$  were noticed between different locations in the pancreas, but no significant difference was found in the volume of distribution ( $V_e$ ).

325

17:51



Geometric distortion due to  $B_0$  inhomogeneity in liver MR imaging under inhalation and exhalation breath-hold

Oi Lei Wong<sup>1</sup>, Jing Yuan<sup>1</sup>, Yihang Zhou<sup>1</sup>, Siu Ki Yu<sup>1</sup>, and Kin Yin Cheung<sup>1</sup>

<sup>1</sup>Medical Physics and Research Department, Hong Kong Sanatorium & Hospital, Hong Kong, Hong Kong

Geometric accuracy is critical for radiotherapy and is one major concern in the application of MRI in radiotherapy. Since the geometric distortion and  $B_0$  inhomogeneity are related, we aim to evaluate the geometric distortion due to  $\Delta B_0$  variation at inhalation and exhalation breath-hold. Based on our results, larger geometric distortion was noted during inhalation than exhalation.

326

18:03



Simultaneous Iron and Fat Quantification Using an Auto Regressive Moving Average Model at 1.5T and 3T

Aaryani Tipirneni-Sajja<sup>1</sup>, Axel J. Krafft<sup>2</sup>, Brian Taylor<sup>3</sup>, Ralf B. Loeffler<sup>1</sup>, Ruitian Song<sup>1</sup>, Nathan Artz<sup>1</sup>, Jane S. Hankins<sup>4</sup>, and Claudia M. Hillenbrand<sup>1</sup>

<sup>1</sup>Diagnostic Imaging, St. Jude Children's Research Hospital, Memphis, TN, United States, <sup>2</sup>Radiology – Medical Physics, Medical Center – University of Freiburg, Freiburg, Germany, <sup>3</sup>Imaging Physics, The University of Texas MD Anderson Cancer Center, TX, United States, <sup>4</sup>Hematology, St. Jude Children's Research Hospital, Memphis, TN, United States

A major confounder of hepatic iron assessment by R2\*-MRI is fat (e.g. steatosis) which introduces signal modulations. In this study, we systematically evaluate two signal modeling techniques, an autoregressive moving average (ARMA) model and the method provided by the ISMRM Fat-Water Toolbox for simultaneous iron and fat quantification in phantoms and in vivo. Preliminary data suggest that ARMA and Toolbox can be used for iron and fat quantification at 1.5T and 3T. In severe iron-overload cases, both, ARMA and the Toolbox might produce inaccurate FF results, however in vivo ARMA seemed to provide a more robust liver R2\* quantification.

---

---

## Combined Educational & Scientific Session

# Metabolomics & Metabolic Fluxes

Organizers: Jürgen K. Hennig, Ph.D., Roland Kreis, Ph.D. & Peter van Zijl, Ph.D.

Room 314                      Monday 16:15 - 18:15    Moderators: John Griffiths & Arend Heerschap

---

16:15                      [Metabolomic, tissue](#)  
Peter Vermathen<sup>1</sup>

*<sup>1</sup>Department of Clinical Research, Inselspital, University of Bern, Switzerland*

Metabolomics denotes the comprehensive and simultaneous systematic profiling of metabolite levels through the study of biofluids and tissues. As such metabolomics is now considered an integral part of systems biology. Besides Mass Spectrometry, NMR Spectroscopy is the main analytical technique for simultaneous assessment of metabolites in biological fluids and tissues.

---

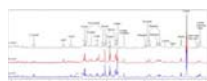
16:45                      [13C Metabolic Fluxes, not Hyperpolarized](#)  
Douglas L. Rothman<sup>1</sup>

*<sup>1</sup>Yale University*

An introduction to the use of  $^{13}\text{C}$  and  $^1\text{H}$ - $^{13}\text{C}$  MRS to measure metabolic fluxes in pre clinical models and clinical research studies will be presented. The presentation will have the following sections: 1. introduction to  $^{13}\text{C}$  MRS 2. use of  $^{13}\text{C}$  MRS to measure metabolite labeling 3. calculations of metabolic fluxes from metabolite labeling curves 4. applications to study metabolism in health and disease 5. application to study therapy. The main goals are to provide the audience with basic knowledge of how to perform and interpret  $^{13}\text{C}$  MRS measurements of metabolic fluxes and their potential for use in clinical research.

327

17:15



### NMR-based metabolomics and metabolic pathway networks from patient-matched colorectal cancers, adjacent non-cancerous tissues and fecal extracts

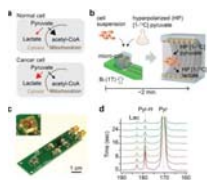
Yan Lin<sup>1</sup>, Changchun Ma<sup>2</sup>, Zhening Wang<sup>1</sup>, Jiahao Liang<sup>1</sup>, Yao Huang<sup>1</sup>, and Renhua Wu<sup>1</sup>

<sup>1</sup>Radiology department, Second Affiliated Hospital, Shantou University Medical College, Shantou City, People's Republic of China, <sup>2</sup>Department of Radiation Oncology, Cancer Hospital, Shantou University Medical College, Guangdong Province, China, People's Republic of China

This study aimed to profile paralleled metabolites of CRC tissues and adjacent non-cancerous tissues alongside pre- and post-operative stools from the same patients, to investigate how fecal metabolomic phenotypes correlate with the tumor tissue especially in a molecular pathology context. Our patient-matched cohort revealed a few overlapping discriminatory metabolites between the CRC and stool metabolomes, indicating the networks for metabolic pathway aberrations across both matrices. The altered metabolites potentially involved in the disruption of normal bacterial ecology, malabsorption of nutrients, increased glycolysis, TCA cycle and glutaminolysis, implying a Warburg effect for cell energy production required for rapid proliferation

328

17:27



### Hyperpolarized Micro-NMR for Metabolic Flux Analysis in Cancer Stem Cells and Rapid Assessment of Therapeutic Response

Sangmoo Jeong<sup>1</sup>, Roozbeh Eskandari<sup>1</sup>, Sun Mi Park<sup>2</sup>, Ralph Weissleder<sup>3,4</sup>, Michael G. Kharas<sup>2,5</sup>, Hakho Lee<sup>3,4</sup>, and Kayvan R. Keshari<sup>1,5</sup>



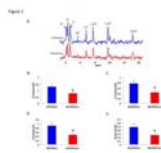
<sup>1</sup>Department of Radiology/Molecular Pharmacology Program, Memorial Sloan Kettering Cancer Center, New York, NY, United States, <sup>2</sup>Center for Cell Engineering/Molecular Pharmacology Program, Memorial Sloan Kettering Cancer Center, New York, NY, United States, <sup>3</sup>Center for Systems Biology, Massachusetts General Hospital, Boston, MA, United States, <sup>4</sup>Department of Radiology, Harvard Medical School, Boston, MA, United States, <sup>5</sup>Weill Cornell Medical College, New York, NY, United States

Aberrant metabolic features of cancer cells are closely related to tumorigenesis and therapeutic response. Here, we report a sensitive magnetic resonance sensing platform, capable of analyzing metabolic fluxes in mass-limited samples. Termed hyperpolarized micromagnetic resonance spectrometer (HMRS), this platform achieved to characterize the metabolic flux in cancer stem cells in real-time and assess therapeutic responses much earlier than any changes in cell viability. This will become a versatile platform for rapid and sensitive exploration of metabolic dynamics in cancer.

---

329

17:39



IDH1 mutation down-regulates choline and ethanolamine metabolism in gliomas

Pavithra Viswanath<sup>1</sup>, Jose Luis Izquierdo-Garcia<sup>1</sup>, Joanna J Phillips<sup>2</sup>, Russell O Pieper<sup>2</sup>, and Sabrina M Ronen<sup>1</sup>

<sup>1</sup>Radiology and Biomedical Imaging, University of California San Francisco, San Francisco, CA, United States, <sup>2</sup>Neurological Surgery, University of California San Francisco, San Francisco, CA, United States

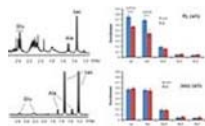
Aberrant choline and ethanolamine metabolism with elevated phosphocholine (PC) and phosphoethanolamine (PE) levels has emerged as a hallmark of cancer. Interestingly, PC and PE levels are reduced in gliomas with the isocitrate dehydrogenase 1 (IDH1) mutation relative to wild-type tumors. Here, we investigated the mechanism behind the reduction in PC and PE levels in genetically-engineered cells and tumor xenografts. Our results indicate that mutant IDH1 gliomas down-regulate the activities of choline kinase and ethanolamine kinase, the enzymes involved in PC and PE synthesis. Reduced PC and PE levels constitute unique metabolic biomarkers and potential therapeutic opportunities in mutant IDH1 gliomas.

---

330

17:51

<sup>13</sup>C NMR metabolic flux analysis of mantle cell lymphoma cells to Bruton tyrosine kinase inhibitors



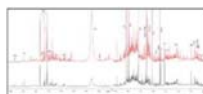
Seung-Cheol Lee<sup>1</sup>, Alex Shestov<sup>1</sup>, Stephen Pickup<sup>1</sup>, Jeff Roman<sup>1</sup>,  
Mariusz Wasik<sup>2</sup>, and Jerry Glickson<sup>1</sup>

<sup>1</sup>Department of Radiology, University of Pennsylvania, Philadelphia, PA, United States, <sup>2</sup>Department of Pathology and Laboratory Medicine, University of Pennsylvania, Philadelphia, PA, United States

We analyzed various metabolic fluxes of mantle cell lymphoma cells upon Bruton tyrosine kinase signaling inhibitors using <sup>13</sup>C NMR and a bonded cumomer modeling method and identified <sup>1</sup>H NMR biomarkers translatable to clinic.

331

18:03



Identification of potential biomarkers for Parkinson's disease by <sup>1</sup>H NMR spectroscopy

Senthil Kumaran<sup>1</sup>, Sadhana Kumari<sup>1</sup>, Vinay Goyal<sup>2</sup>, SN Dwivedi<sup>3</sup>, Achal Srivastava<sup>2</sup>, and Naranamangalam R Jagannathan<sup>1</sup>

<sup>1</sup>Department of NMR and MRI Facility, All India Institute of Medical Sciences, New Delhi, India, <sup>2</sup>Department of Neurology, All India Institute of Medical Sciences, New Delhi, India, <sup>3</sup>Department of Biostatistics, All India Institute of Medical Sciences, New Delhi, India

We studied the metabolic profile of urine samples of patients with Parkinson's disease (PD) and healthy controls (HC) using 700 MHz NMR spectrometer (Varian, M/s Agilent Technologies, USA). The data were processed using Vnmrj (version:2.3A) and binning data estimated using MestReNova software (version :10.0, Mestrelab Research, Spain). PLS-DA multivariate analysis was carried out using MetaboAnalyst (ver.3.0), a web-based metabolomics data processing tool to evaluate significance of metabolites in PD with respect to HC. We observed elevated levels of lactate, tryptophan, glycine and reduced levels of citrate, leucine, isoleucine (t-test, p<0.05), suggestive of several metabolic abnormalities, as mitochondrial dysfunction and reduced bioenergetics efficiency in PD patients.

Other

## Special Session: Manuscript Reviewing for JMRI

Room 314      Monday 18:30 - 19:15      Moderators: Mark Schweitzer      (no CME credit)



---

Tuesday, 25 April 2017

Go to top

**Sunrise Session**

## Cardiovascular MR: "More is Better": Tissue Characterization

*Organizers:* Daniel K. Sodickson, M.D., Ph.D., Bernd J. Wintersperger, M.D. & Sonia NIELLES-VALLESPIN, Ph.D.

**Room 310**                      **Tuesday 7:00 - 7:50**                      *Moderators:* Pedro Ferreira & Christian Stoeck

---

7:00                      [MR Relaxometry in the Heart](#)  
Matthew Robson

---

7:25                      [MR Fingerprinting](#)  
Nicole Seiberlich

---

7:50                      [Adjournment & Meet the Teachers](#)

---

**Sunrise Session**

## UTE & ZTE Imaging Techniques & Applications

*Organizers:* Jenny T. Bencardino, M.D., Eric Y. Chang, M.D., Christine Chung, M.D. & Philip Robinson, M.D.

**Room 312**                      **Tuesday 7:00 - 7:50**                      *Moderators:* Eric Chang & Florian Wiesinger

---

7:00                      [UTE & ZTE Imaging Techniques](#)  
Florian Wiesinger

---

7:25                      [Clinical Applications of UTE/ZTE](#)  
Richard Hodgson

---

7:50                      [Adjournment & Meet the Teachers](#)

---

**Sunrise Session**

# Bleeding Edge of Brain Techniques: Beyond Conventional MRI

*Organizers:* Fernando E. Boada, Ph.D. & Christopher P. Hess, M.D., Ph.D.

Room 311

Tuesday 7:00 - 7:50

*Moderators:* Fernando Boada & Christopher Hess

---

7:00

[Sodium MRI in the Clinic: What You Can Learn from a 10 Min Scan](#)

Armin Nagel

---

7:25

[Conventional MRI: What We are Missing](#)

Keith Thulborn

---

7:50

[Adjournment & Meet the Teachers](#)

---

## Sunrise Session

# Magnetic Resonance Elastography: Brain & Breast

*Organizers:* Guoying Liu, Ph.D. & Joshua D. Trzasko, Ph.D.

Room 313A

Tuesday 7:00 - 7:50

*Moderators:* Curtis Johnson & Joshua Trzasko

---

7:00

[Brain](#)

Lynne Bilston

---

7:25

[MR-Elastography of the Breast](#)

Ralph Sinkus

---

7:50

[Adjournment & Meet the Teachers](#)

---

## Sunrise Session

# Low Field MR: Systems & Applications

*Organizers:* Jie Luo, Ph.D., Thomas W. Okell, Ph.D., Signe Johanna Vannesjö, Ph.D., Puneet Bagga, Ph.D., Mary P. McDougall, Ph.D.

Room 313BC

Tuesday 7:00 - 7:50

*Moderators:* Fraser Robb & Jason Stockmann

---

7:00 Low Field MR - System Design & Imaging Aspects  
Clarissa Cooley

---

7:25 Magnetic Particle Imaging  
Emine Saritas

---

7:50 Adjournment & Meet the Teachers

---

### Sunrise Session

## It Doesn't Have to Be That Way: Non-Traditional Acquisition

*Organizers:* Michael S. Hansen, Ph.D. & Joshua D. Trzasko, Ph.D.

Room 315 Tuesday 7:00 - 7:50 *Moderators:* Michael Hansen & Sebastian Kozerke

---

7:00 RF  
David Brunner

---

7:25 Data  
Dong Liang

---

7:50 Adjournment & Meet the Teachers

---

### Sunrise Session

## fMRI: Best Practices & Cautionary Tales: Analysis & Resting-State Indices

*Organizers:* Hanzhang Lu, Ph.D. & Karla Miller, Ph.D.

Room 316A Tuesday 7:00 - 7:50 *Moderators:* Molly Bright & Hanzhang Lu

---

7:00 Analysis Issues  
James Pekar

---

7:25      Resting-State fMRI: Which Index is Really Useful?  
Sheila Keilholz

---

7:50      Adjournment & Meet the Teachers

---

### Sunrise Session

## Assessing Response to Immunotherapy

*Organizers:* Linda Moy, M.D. & Valeria Panebianco, M.D.

Room 314      Tuesday 7:00 - 7:50      *Moderators:* Carolyn Mountford & Linda Moy

---

7:00      Brain Gliomas: Imaging Response to Immunotherapy  
Alberto Bizzi

---

7:25      Investigation & Evaluation of Immunotherapies with Molecular Imaging  
Kimberly Brewer

---

7:50      Adjournment & Meet the Teachers

---

### Sunrise Session

## Addressing Clinical Challenges in the Body with MRI

*Organizers:* Kathryn Fowler, M.D., Kartik Jhaveri, M.D., F.R.C.P.C., Lorenzo Mannelli, M.D., Ph.D. & Edwin J.R. van Beek, M.D., Ph.D., M.Ed., FRCR

Room 320      Tuesday 7:00 - 7:50      *Moderators:* Utaroh Motosugi & Mi-Suk Park

---

7:00      Cholangiopathies  
Jeong-Min Lee

---

7:25      Pancreas  
Richard (Kinh Gian) Do

---

7:50      Adjournment & Meet the Teachers

---

---

## Traditional Poster: fMRI

Exhibition Hall 1623-1656      Tuesday 8:15 - 10:15    *(no CME credit)*

---

## Electronic Poster: Acquisition, Reconstruction & Analysis

Exhibition Hall      Tuesday 8:15 - 9:15    *(no CME credit)*

---

## Study Groups

### MR of Cancer Study Group

Room 323ABC      Tuesday 8:15 - 10:15    *(no CME credit)*

---

---

## Study Groups

### Diffusion Study Group

Room 317AB      Tuesday 8:15 - 10:15    *(no CME credit)*

---

---

## Educational Course

### Being Vendor Agnostic

*Organizers:* Michael S. Hansen, Ph.D. & Joshua D. Trzasko, Ph.D.

Room 314      Tuesday 8:15 - 10:15    *Moderators:* Michael Hansen & Joshua Trzasko

---

8:15



#### Sequences

Maxim Zaitsev

On the example of PulSeq, an open-source platform independent sequence programming framework, we consider advantages of the hardware-abstraction in pulse sequence programming as well as the associated challenges.

---

8:45

#### Reconstruction & Raw Data

Nicholas Zwart

This session will highlight some of the open source software resources available to the MR community. There will also be some tips on what steps an MR developer can take to keep their code open and dogma free.

---

9:15

### Image Analysis

Anastasia Yendiki<sup>1</sup>

<sup>1</sup>*Athinoula A. Martinos Center for Biomedical Imaging, Harvard Medical School and Massachusetts General Hospital*

Combining MRI data collected at multiple sites allows researchers to achieve the large sample sizes required to detect subtle disease effects, although at the expense of increased inhomogeneity in the data due to differences in acquisition hardware and software. This presentation will address what is known about the reproducibility of biomarkers derived from structural, functional, and diffusion MRI data across scanners from different vendors, as well as image analysis strategies that have been proposed to mitigate the effects of scanner-related differences.

---

9:45

### Panel Discussion

---

10:15

### Adjournment & Meet the Teachers

---

## Educational Course

# MR Physics & Techniques for Clinicians

Organizers: Marcus T. Alley, Ph.D. & Bernd Jung, Ph.D.

Room 316BC

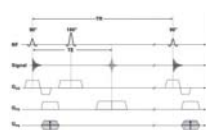
Tuesday 8:15 - 10:15 Moderators: Michael Ith & Oliver Wieben

---

8:15

### Spin Echo Imaging

Valentina Taviani<sup>1</sup>



<sup>1</sup>*MR Applications & Workflow, GE Healthcare, Menlo Park, United States*

The spin echo pulse sequence is one of the most important pulse sequences in MRI. Fast spin echo imaging is routinely used due to its robustness to susceptibility variations and local field inhomogeneities, as well as for its ability to produce excellent T1, T2 and PD images. The aim of this lecture is to describe the basic physical principles governing spin echo imaging and to illustrate the effect of key imaging parameters, such as TE, TR and ETL (echo train length) on image contrast.

9:15 Gradient Echo Imaging  
Armin M. Nagel<sup>1</sup>

<sup>1</sup>*Institute of Radiology, University Hospital Erlangen, Erlangen, Germany*

Magnetic resonance imaging (MRI) techniques can usually be classified into spin-echo (SE) and gradient-echo (GRE) pulse sequences. In this presentation, the basic physical principles of GRE imaging, as well as different mechanisms to generate image contrast will be explained. Differences between SE and GRE MRI will be discussed. Additionally, the influence of different pulse sequence parameters (e.g. echo time, repetition time, flip angle; as well as spoiling techniques and preparation pulses) on the image contrast will be covered. Clinical applications of GRE imaging techniques will be shown exemplarily.

10:15 Adjournment & Meet the Teachers

### Power Pitch

## Pitch: Best of Cardiovascular MR: Hemodynamics & Atherosclerosis

Power Pitch  
Theater A - Exhibition Hall  
Tuesday 8:15 - 9:15  
*Moderators: Alex Barker & Michael Hope*  
*(no CME credit)*

332 8:15 Utilizing Quantitative Measurements of Carotid Intraplaque Hemorrhage can Improve on Presence Alone in Classifying Patients with and without Acute Cerebral Infarcts  
Li Dong<sup>1</sup>, Zhaoqi Zhang<sup>1</sup>, Wei Yu<sup>1</sup>, Sheng Wang<sup>2</sup>, Qiang Shen<sup>1</sup>, and Chun Yuan<sup>3</sup>

		Brain MRI	
		Yes	No
AMI	Yes	8	8
	No	8	11



<sup>1</sup>Department of Radiology, Beijing Anzhen Hospital, Capital Medical University, Beijing, People's Republic of China, <sup>2</sup>Department of Vascular disease, Beijing Anzhen Hospital, Capital Medical University, Beijing, People's Republic of China, <sup>3</sup>Department of Radiology, University of Washington, Seattle, WA, United States

333

8:15



### Whole-Brain Vessel Wall MR Imaging Using Inversion-Recovery Prepared SPACE: Reproducibility and Accuracy of Intracranial Artery Morphology

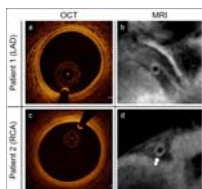
Na Zhang<sup>1,2</sup>, Fan Zhang<sup>1</sup>, Zixin Deng<sup>1</sup>, Qi Yang<sup>1</sup>, Xiaoming Bi<sup>3</sup>, Debiao Li<sup>1</sup>, Xin Liu<sup>2</sup>, and Zhaoyang Fan<sup>1</sup>

<sup>1</sup>Biomedical Imaging Research Institute, Cedars Sinai Medical Center, Los Angeles, CA, United States, <sup>2</sup>Shenzhen Institutes of Advanced Technology, Chinese Academy of Sciences, Shenzhen, People's Republic of China, <sup>3</sup>Siemens Healthcare

334



8:15



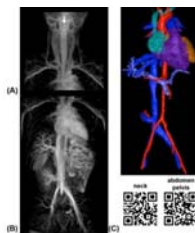
### A Preliminary Report on Time-Resolved Coronary Vessel Wall MRI in Heart Transplant Recipients

Giulia Ginami<sup>1,2</sup>, Jerome Yerly<sup>1,3</sup>, Jessica AM Bastiaansen<sup>1</sup>, Ruud B van Heeswijk<sup>1</sup>, Nathalie Lauriers<sup>4</sup>, Juan F Iglesias<sup>5</sup>, Sophie Degrauwe<sup>5</sup>, Andrea Zuffi<sup>5</sup>, Roger Hullin<sup>5</sup>, and Matthias Stuber<sup>1,3</sup>

<sup>1</sup>Department of Radiology, University Hospital (CHUV) and University of Lausanne (UNIL), Lausanne, Switzerland, <sup>2</sup>Division of Imaging Sciences and Biomedical Engineering, King's College London, London, United Kingdom, <sup>3</sup>Centre for Biomedical Imaging (CIBM), Lausanne, Switzerland, <sup>4</sup>Department of Radiology, University Hospital (CHUV) of Lausanne, Lausanne, Switzerland, <sup>5</sup>Service de Cardiologie, University Hospital (CHUV) of Lausanne, Lausanne, Switzerland

335

8:15



### Non-Gadolinium-Contrast Relaxation-Enhanced MR Angiography in Children with an Inversion Recovery and T2-Prepared 3D mDIXON Gradient-Echo Technique: Preliminary Experience

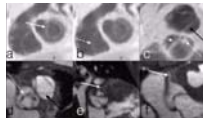
Amber L. Pokorney<sup>1</sup>, Jonathan M. Chia<sup>2</sup>, Dianna ME Bardo<sup>1</sup>, Mittun Patel<sup>1</sup>, Smita S. Bailey<sup>1</sup>, Scott Jorgensen<sup>1</sup>, Deepa Biyyam<sup>1</sup>, Scott Willard<sup>1</sup>, Jeffrey H. Miller<sup>1</sup>, Houchun Harry Hu<sup>1</sup>, and Masami Yoneyama<sup>3</sup>

<sup>1</sup>Radiology, Phoenix Children's Hospital, Phoenix, AZ, United States, <sup>2</sup>Philips HealthTech, Dallas, TX, United States, <sup>3</sup>Philips Electronics, Tokyo, Japan

---

336

8:15



**Ultra-High Spatiotemporal Resolution 4D Flow for Valve and Coronary Arterial Delineation**

Shreyas S. Vasanawala<sup>1</sup>, Furhawn Shah<sup>1</sup>, Marcus T. Alley<sup>1</sup>, and Joseph Y. Cheng<sup>1</sup>

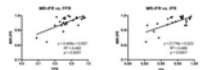
<sup>1</sup>Department of Radiology, Stanford University, Stanford, CA, United States

---

337



8:15



**Noninvasive Functional Evaluation of Coronary Stenosis Using MR Instantaneous wave-Free Ratio (MR-iFR): Pilot patient study using invasive fractional flow reserve as a reference**

Zixin Deng<sup>1,2</sup>, Sang-Eun Lee<sup>3</sup>, Zhaoyang Fan<sup>1</sup>, Christopher Nguyen<sup>1</sup>, Yibin Xie<sup>1</sup>, Jianing Pang<sup>1</sup>, Xiaoming Bi<sup>4</sup>, Qi Yang<sup>1</sup>, Byoung-Wook Choi<sup>5</sup>, Jung-Sun Kim<sup>3</sup>, Daniel Berman<sup>1</sup>, Hyuk-Jae Chang<sup>3</sup>, and Debiao Li<sup>1</sup>

<sup>1</sup>Biomedical Imaging Research Institute, Cedars-Sinai Medical Center, Los Angeles, CA, United States, <sup>2</sup>Bioengineering, University of California, Los Angeles, Los Angeles, CA, United States, <sup>3</sup>Cardiology, Severance Cardiovascular Hospital, <sup>4</sup>Siemens Healthcare R&D, <sup>5</sup>Radiology, Severance Cardiovascular Hospital

---

338

8:15



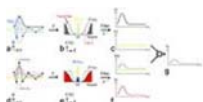
**Analysis of 4D flow hemodynamics parameters in BAV patients using a finite element method**

Julio Sotelo<sup>1,2</sup>, Lydia Dux-Santoy<sup>3</sup>, Andrea Guala<sup>3</sup>, Jose Rodríguez-Palomares<sup>3</sup>, Arturo Evangelista<sup>3</sup>, Daniel Hurtado<sup>4</sup>, and Sergio Uribe<sup>5</sup>

<sup>1</sup>Biomedical Imaging Center, Pontificia Universidad Católica de Chile, Santiago, Chile, <sup>2</sup>Department of Electrical Engineering, Pontificia Universidad Católica de Chile, Santiago, Chile, <sup>3</sup>Department of Cardiology, Hospital Universitari Vall d'Hebron. Vall d'Hebron Institut de Recerca (VHIR). Universitat Autònoma de Barcelona., Barcelona, Spain, <sup>4</sup>Department of Structural and Geotechnical Engineering, Pontificia Universidad Católica de Chile, Santiago, Chile, <sup>5</sup>Department of Radiology, School of Medicine, Pontificia Universidad Católica de Chile, Santiago, Chile

---

8:15



**Phase-Contrast MRI with Hybrid One- and Two-sided Flow-Encoding and Velocity SPectrum SepAration (HOTSPA)**

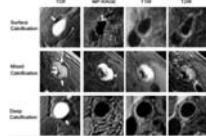
Da Wang<sup>1,2</sup>, Jiaxin Shao<sup>1</sup>, Daniel B. Ennis<sup>1,2,3</sup>, and Peng Hu<sup>1,2</sup>



<sup>1</sup>Department of Radiological Sciences, David Geffen School of Medicine, University of California, Los Angeles, Los Angeles, CA, United States, <sup>2</sup>Biomedical Physics Interdepartmental Graduate Program, University of California, Los Angeles, Los Angeles, CA, United States, <sup>3</sup>Department of Bioengineering, University of California, Los Angeles, Los Angeles, CA, United States



8:15



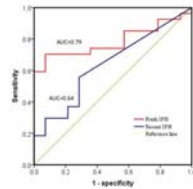
### Association between Carotid Atherosclerotic Plaque Calcification and Intraplaque Hemorrhage: A High Resolution Magnetic Resonance Imaging Study

Shuo Chen<sup>1</sup>, Ruolan Lin<sup>2</sup>, Gaifen Liu<sup>3</sup>, Rui Li<sup>1</sup>, Yunjing Xue<sup>2</sup>, and Xihai Zhao<sup>1</sup>

<sup>1</sup>Center for Biomedical Imaging Research, Department of Biomedical Engineering, School of Medicine, Tsinghua University, Beijing, People's Republic of China, <sup>2</sup>Department of Radiology, Fujian Union Hospital, People's Republic of China, <sup>3</sup>Department of Neurology, Beijing Tiantan Hospital, Capital Medical University, People's Republic of China



8:15

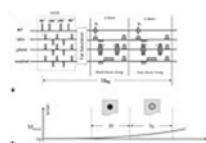


### Association between Age of Intraplaque Hemorrhage and Fibrous Cap Rupture in Carotid Artery Atherosclerosis: A High Resolution Magnetic Resonance Imaging Study

Yuanyuan Cui<sup>1</sup>, Xihai Zhao<sup>2</sup>, Huiyu Qiao<sup>2</sup>, Dongxiang Xu<sup>3</sup>, Mingming Lu<sup>1</sup>, Xiaoyi Chen<sup>2,4</sup>, Lu Ma<sup>1</sup>, and Jianming Cai<sup>1</sup>

<sup>1</sup>Department of Radiology, The General Hospital of People's Liberation Army (301 hospital), Beijing, People's Republic of China, <sup>2</sup>Center for Biomedical Imaging Research, Department of Biomedical Engineering, Tsinghua University, Beijing, People's Republic of China, <sup>3</sup>Department of Radiology, University of Washington, Seattle, United States, <sup>4</sup>Beijing Institute for Brain Disorders, Capital Medical University, Beijing, People's Republic of China

8:15



### Compressed Sensing based Simultaneous Black- and Gray-blood Carotid Vessel Wall MR Imaging

Bo Li<sup>1,2</sup>, Hao Li<sup>3</sup>, Guofu Huang<sup>1</sup>, Xia Qian<sup>1</sup>, Wei Wang<sup>1</sup>, and Li Dong<sup>4</sup>

<sup>1</sup>Center Laboratory, The First Hospital of Nanchang City, Nanchang, People's Republic of China, <sup>2</sup>Department of Radiology, The Third Affiliated Hospital of Nanchang University, Nanchang, People's Republic of China, <sup>3</sup>Department of Radiology, University of Cambridge, Cambridge, United Kingdom, <sup>4</sup>Department of Radiology, Beijing Anzhen Hospital, Beijing, People's Republic of China

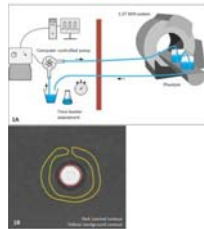
---

343

8:15

Comparison of acceleration algorithms in whole-heart 4D flow MRI for aortic and mitral valve flow assessment

Jos Westenberg<sup>1</sup>, Pankaj Garg<sup>2</sup>, Pieter van den Boogaard<sup>1</sup>, and Sven Plein<sup>2</sup>



<sup>1</sup>Radiology, Leiden University Medical Center, Leiden, Netherlands, <sup>2</sup>University of Leeds, Leeds, United Kingdom

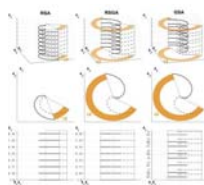
---

344

8:15

Golden Step, Golden Angle, Spiral-Cartesian Imaging for Flexible Gated Three-dimensional Angiography

Grzegorz Tomasz Kowalik<sup>1</sup>, Jennifer Anne Steeden<sup>1</sup>, David Atkinson<sup>2</sup>, Kristian Mortensen<sup>3</sup>, and Vivek Muthurangu<sup>1,3</sup>



<sup>1</sup>Institute of Cardiovascular Science, University College London, London, United Kingdom, <sup>2</sup>Centre for Medical Imaging, Division of Medicine, University College London, London, United Kingdom, <sup>3</sup>Great Ormond Street Hospital for Children, London, United Kingdom

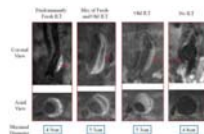
---

345

8:15

Distribution of Intraluminal Thrombus Composition in Abdominal Aortic Aneurysms by Diameter: a High Resolution MRI study

Chengcheng Zhu<sup>1</sup>, Bing Tian<sup>2</sup>, Joseph Leach<sup>1</sup>, Qi Liu<sup>2</sup>, Jianping Lu<sup>2</sup>, David Saloner<sup>1</sup>, and Michael D Hope<sup>1</sup>



<sup>1</sup>Radiology, University of California, San Francisco, San Francisco, CA, United States, <sup>2</sup>Radiology, Changhai Hospital, Shanghai, People's Republic of China

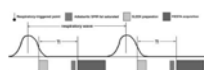
---

346

8:15

Evaluation of Portal Vein System in patients after liver transplantation by Unenhanced MR Angiography Using Spatial Labeling with Multiple Inversion Pulses Sequence and by CT portography

hao tang<sup>1</sup>, daoyu hu, xiaoyan meng, zi wang, zhen li, and yanchun wang



## Power Pitch

# Pitch: Brain Physiology: Flow, Oxygen, Metabolism

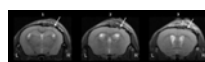
Power Pitch  
Theater B - Tuesday 8:15 - Moderators: Molly Bright & (no CME credit)  
Exhibition Hall 9:15 Hanzhang Lu

---

347



8:15



### Long-term Cerebrovascular Dysfunction Following Repeated Mild Traumatic Brain Injury

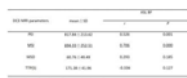
Conner Adams<sup>1,2</sup>, Margaret Koletar<sup>1</sup>, Tina L. Beckett<sup>1</sup>, Lindsay Cahill<sup>3</sup>, Lydiane Hirschler<sup>4,5,6</sup>, Jan M. Warnking<sup>4,6</sup>, Emmanuel L. Barbier<sup>4,6</sup>, JoAnne McLaurin<sup>1,7</sup>, John G. Sled<sup>2,3</sup>, and Bojana Stefanovic<sup>1,2</sup>

*<sup>1</sup>Sunnybrook Research Institute, Toronto, ON, Canada, <sup>2</sup>Medical Biophysics, University of Toronto, Toronto, ON, Canada, <sup>3</sup>Mouse Imaging Centre, The Hospital For Sick Children, Toronto, ON, Canada, <sup>4</sup>Grenoble Institut des Neurosciences, Université Grenoble Alpes, Grenoble, France, <sup>5</sup>Bruker Biospin MRI, Ettlingen, Germany, <sup>6</sup>Inserm, U1216, Grenoble, France, <sup>7</sup>Laboratory Medicine and Pathobiology, University of Toronto, Toronto, ON, Canada*

---

348

8:15



100	100	100	100
100	100	100	100
100	100	100	100
100	100	100	100

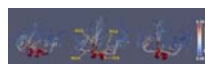
### Comparative Study of 3D Arterial Spin Labeling and dynamic contrast-enhanced MRI of Nasopharyngeal Carcinoma perfusion imaging

Bohan Xiao<sup>1</sup>, Zhaoxiang Ye<sup>1</sup>, Peiguo Wang<sup>1</sup>, Ying Liu<sup>1</sup>, Yingyu Zhao<sup>1</sup>, and Dandan Zheng<sup>2</sup>

*<sup>1</sup>Key Laboratory of Cancer Prevention and Therapy, Department of Radiology, Tianjin Medical University Cancer Institute & Hospital, Tianjin, People's Republic of China, <sup>2</sup>MR Research China, GE Healthcare, Beijing, People's Republic of China*

---

8:15



### Non-contrast vascular compliance mapping using time-resolved VASO CBV imaging

Yang Li<sup>1,2</sup>, Deng Mao<sup>1,2</sup>, Jay J. Pillai<sup>1</sup>, and Hanzhang Lu<sup>1</sup>

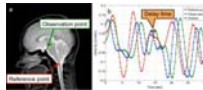


<sup>1</sup>Department of Radiology, Johns Hopkins University School of Medicine, Baltimore, MD, United States, <sup>2</sup>Graduate School of Biomedical Sciences, UT Southwestern Medical Center, Dallas, TX, United States

350



8:15



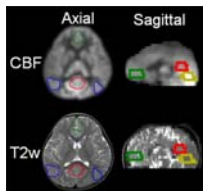
Propagation Patterns of Cardiac-driven and Respiratory-driven Cerebrospinal Fluid Velocity Waves Characterized by Correlation Mapping in Conjunction with Asynchronous 2-Dimensional Phase Contrast Technique

Satoshi Yatsushiro<sup>1</sup>, Saeko Sunohara<sup>2</sup>, Mitsunori Matsumae<sup>3</sup>, and Kagayaki Kuroda<sup>1,2</sup>

<sup>1</sup>Graduate School of Science and Technology, Tokai University, Hiratsuka, Kanagawa, Japan, <sup>2</sup>Graduate School of Engineering, Tokai University, Hiratsuka, Kanagawa, Japan, <sup>3</sup>Department of Neurosurgery, Tokai University School of Medicine, Isehara, Kanagawa, Japan

351

8:15



Regionally differentiated cerebral blood flow increases during infancy measured with pCASL MRI

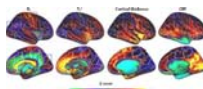
Qinlin Yu<sup>1,2,3,4</sup>, Huiying Kang<sup>1,5</sup>, Minhui Ouyang<sup>1,2</sup>, Yun Peng<sup>5</sup>, Fang Fang<sup>3,4</sup>, and Hao Huang<sup>1,2</sup>

<sup>1</sup>Department of Radiology, Children's Hospital of Philadelphia, Philadelphia, PA, United States, <sup>2</sup>Department of Radiology, Perelman School of Medicine, University of Pennsylvania, Philadelphia, PA, United States, <sup>3</sup>School of Psychological and Cognitive Sciences, Peking University, Beijing, People's Republic of China, <sup>4</sup>Peking-Tsinghua Center for Life Science, Peking University, Beijing, People's Republic of China, <sup>5</sup>Department of Radiology, Beijing Children's Hospital, Capital Medical University, Beijing, People's Republic of China

352



8:15



Cerebral blood flow as a marker for cortical parcellation

Roy Haast<sup>1</sup>, Dimo Ivanov<sup>1</sup>, Elia Formisano<sup>1</sup>, and Kâmil Uludağ<sup>1</sup>

<sup>1</sup>Department of Cognitive Neuroscience, Maastricht University, Maastricht, Netherlands



353



8:15



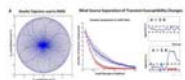
### Changes in cerebral blood flow and default mode network connectivity following mTBI observed with pulsed arterial spin labeling

Natalie M. Wiseman<sup>1</sup>, Armin Iraj<sup>2</sup>, E. Mark Haacke<sup>2,3</sup>, and Zhifeng Kou<sup>2,3</sup>

<sup>1</sup>Department of Psychiatry and Behavioral Neurosciences, Wayne State University, Detroit, MI, United States, <sup>2</sup>Department of Biomedical Engineering, Wayne State University, Detroit, MI, United States, <sup>3</sup>Department of Radiology, Wayne State University, Detroit, MI, United States

354

8:15



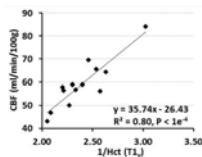
### A Novel Approach to Measuring Cerebral Oxygen Extraction Fraction and Vascular Reserve Using MRI

Charles Cantrell<sup>1</sup>, Yong Jeong<sup>2</sup>, Kevin Midlash<sup>3</sup>, Parmede Vakil<sup>2</sup>, Sameer Ansari<sup>2</sup>, and Timothy J Carroll<sup>3</sup>

<sup>1</sup>Northwestern University, Chicago, IL, United States, <sup>2</sup>Northwestern University, <sup>3</sup>University of Chicago

355

8:15



### Measurements of Oxygen Delivery and Consumption Using Hematocrit Derived from Blood T1 Quantification

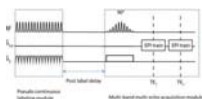
Feng Xu<sup>1,2,3</sup>, Wenbo Li<sup>1,2</sup>, Peiying Liu<sup>1,2</sup>, Hanzhang Lu<sup>1,2</sup>, John J. Strouse<sup>4</sup>, James J Pekar<sup>1,2</sup>, Peter C.M. van Zijl<sup>1,2</sup>, and Qin Qin<sup>1,2</sup>

<sup>1</sup>F.M. Kirby Center for Functional Brain Imaging, Kennedy Krieger Institute, Baltimore, MD, United States, <sup>2</sup>The Russell H. Morgan Department of Radiology and Radiology Science, Johns Hopkins University, Baltimore, MD, United States, <sup>3</sup>Developing Brain Research Laboratory, Children's National Medical Center, Washington DC, DC, United States, <sup>4</sup>Department of Medicine, Duke University, Durham, NC, United States

356



8:15



### Simultaneous cerebral blood flow and bold oxygen level dependent signal assessments using multi-band multi-echo pseudo-continuous arterial spin labeling (M2-PCASL)

Shiyang Chen<sup>1</sup>, Junjie Wu<sup>2</sup>, Kyle Pate<sup>2</sup>, Xiaodong Zhong<sup>2,3</sup>, Bruce Crosson<sup>2,4</sup>, and Deqiang Qiu<sup>2</sup>

<sup>1</sup>Georgia Institute of Technology, Atlanta, GA, United States, <sup>2</sup>Department of Radiology and Imaging Sciences, Emory University, Atlanta, GA, United States, <sup>3</sup>MR R&D Collaborations, Siemens Healthcare, Atlanta, GA, United States, <sup>4</sup>Department of Neurology, Emory University, Atlanta, GA, United States



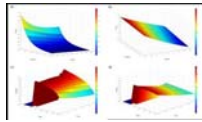
---

357

8:15

Measuring Blood Oxygenation and Hematocrit with a Combined T2 and T1 Approach: Initial Experience in Humans

Thomas Christen<sup>1</sup>, Jia Guo<sup>1</sup>, Wendy Wei Ni<sup>1</sup>, Michael Moseley<sup>1</sup>, and Greg Zaharchuk<sup>1</sup>



<sup>1</sup>Radiology, Stanford University, Palo Alto, CA, United States

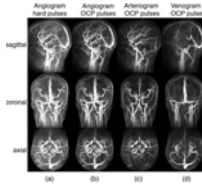
---

358

8:15

Whole-Brain Arteriography and Venography Using an Improved Velocity-Selective Saturation (VSS) Pulse Trains

Wenbo Li<sup>1,2</sup>, Feng Xu<sup>1,2,3</sup>, Jing Liu<sup>1,4</sup>, Michael Schär<sup>1</sup>, Taehoon Shin<sup>5</sup>, Peter van Zijl<sup>1,2</sup>, Ye Qiao<sup>1</sup>, Bruce Wasserman<sup>1</sup>, and Qin Qin<sup>1,2</sup>



<sup>1</sup>Department of Radiology, Johns Hopkins University School of Medicine, Baltimore, MD, United States, <sup>2</sup>F.M. Kirby Research Center for Functional Brain Imaging, Kennedy Krieger Institute, Baltimore, MD, United States, <sup>3</sup>Developing Brain Research Lab, Children's National Medical Center, Washington, DC, United States, <sup>4</sup>Department of Radiology, People's Hospital, Guangzhou, People's Republic of China, <sup>5</sup>Department of Diagnostic Radiology and Nuclear Medicine, University of Maryland, Baltimore, MD, United States

---

359

8:15

Simultaneous acquisition of oxygen extraction fraction and cerebral blood flow during brain activation

Yayan Yin<sup>1</sup>, Yaoyu Zhang<sup>1</sup>, Yang Fan<sup>2</sup>, Bing Wu<sup>2</sup>, and Jia-Hong Gao<sup>1</sup>



<sup>1</sup>Center for MRI Research, Peking University, Beijing, People's Republic of China, <sup>2</sup>MR Research China, GE Healthcare, Beijing, People's Republic of China

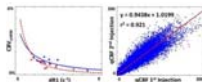
---

360

8:15

A Method for Quantitative Cerebrovascular Reserve

Yong Ik Jeong<sup>1</sup>, Charles G Cantrell<sup>1</sup>, Kevin Midlash<sup>2</sup>, Renee Qian, Parmede Vakili<sup>3</sup>, Sameer A Ansari<sup>3</sup>, Gregory Christoforidis<sup>2</sup>, and Timothy J Carroll<sup>2</sup>



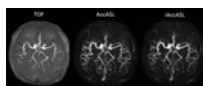
<sup>1</sup>Northwestern University, Evanston, IL, United States, <sup>2</sup>University of Chicago, <sup>3</sup>Northwestern University

---

361

8:15

Robust Visualization of MCA Main Trunk by Improved Acceleration-Selective Arterial Spin Labeling (iAccASL) for Intracranial MR Angiography



Yuta Akamine<sup>1</sup>, Makoto Obara<sup>1</sup>, Osamu Togao<sup>2</sup>, Shuhei Shibukawa<sup>3</sup>, Masami Yoneyama<sup>1</sup>, Tomoyuki Okuaki<sup>4</sup>, and Marc Van Cauteren<sup>4</sup>

<sup>1</sup>Philips Electronics Japan, Shinagawa, Tokyo, Japan, <sup>2</sup>Department of Clinical Radiology, Graduate School of Medical Science, Kyushu University, Fukuoka, Japan, <sup>3</sup>Department of Radiology, Tokai University Hospital, Japan, <sup>4</sup>Asia Pacific, Philips Healthcare, Shinagawa, Tokyo, Japan

---

Oral

## Liver Quantitation

Room 310

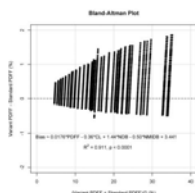
Tuesday 8:15 - 10:15

Moderators: Sachin Jambawalikar & Eric Sigmund

362



8:15

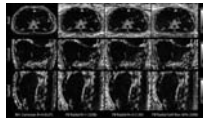


Robust agreement between MRI and MRS hepatic proton density fat fraction despite biologically plausible variability in fat spectra in patients with nonalcoholic steatohepatitis

Cheng William Hong<sup>1</sup>, Adrija Mamidipalli<sup>1</sup>, Jonathan C Hooker<sup>1</sup>, Gavin Hamilton<sup>1</sup>, Tanya Wolfson<sup>2</sup>, Soudabeh Fazeli Dehkordy<sup>1</sup>, Scott B Reeder<sup>3</sup>, Rohit Loomba<sup>4</sup>, and Claude B Sirlin<sup>1</sup>

<sup>1</sup>Liver Imaging Group, Department of Radiology, University of California, San Diego, San Diego, CA, United States, <sup>2</sup>Computational and Applied Statistics Laboratory, University of California, San Diego, San Diego, CA, United States, <sup>3</sup>Departments of Radiology, Medical Physics, Biomedical Engineering, Medicine, and Emergency Medicine, University of Wisconsin, Madison, Madison, WI, United States, <sup>4</sup>NAFLD Research Center, Division of Gastroenterology, Department of Medicine, University of California, San Diego, San Diego, CA, United States

MRI- and MRS-based proton density fat fraction (PDFFF) techniques require accurate modeling of the multi-peak spectrum of triglycerides (TG) in order to achieve accurate hepatic fat quantification. However, variations in TG spectrum may lead to quantification variability. We performed a secondary analysis of adults with biopsy-confirmed nonalcoholic steatohepatitis undergoing confounder-corrected chemical-shift-encoded 3T MRI and MRS, and calculated variant PDFFF values using a range of biologically plausible spectral models. Within the range of fat fractions seen in the liver, PDFFF estimation using MRI and MRS was robust to variability in the TG spectrum. Greater bias was seen when the baseline fat fraction was higher, but remained low.



### Free-breathing Fat Quantification in the Liver Using a Multiecho 3D Stack-of-Radial Technique: Investigation of Motion Compensation and Quantification Accuracy

Tess Armstrong<sup>1,2</sup>, Thomas Martin<sup>1,2</sup>, Alto Stemmer<sup>3</sup>, Xinzhou Li<sup>1,4</sup>, Yutaka Natsuaki<sup>5</sup>, Kyunghyun Sung<sup>1,2</sup>, and Holden H. Wu<sup>1,2</sup>

<sup>1</sup>Radiological Sciences, University of California Los Angeles, Los Angeles, CA, United States, <sup>2</sup>Physics and Biology in Medicine, University of California Los Angeles, Los Angeles, CA, United States, <sup>3</sup>Siemens Healthcare GmbH, Erlangen, Germany, <sup>4</sup>Bioengineering, University of California Los Angeles, Los Angeles, CA, United States, <sup>5</sup>Siemens Healthcare, Los Angeles, CA, United States

Multiecho Cartesian MRI methods can non-invasively quantify liver fat, but are susceptible to motion artifacts and limited by breath-hold (BH) imaging. We have developed a new free-breathing (FB) liver fat quantification technique using 3D stack-of-radial imaging (Radial). In this work, we further investigate motion compensation and quantification accuracy for FB Radial. In n=11 healthy volunteers, FB Radial fat quantification demonstrated significant correlation ( $\rho > 0.9876$ ) and low mean difference ( $< -1.19\%$ ) compared to BH Cartesian and BH single-voxel spectroscopy. FB Radial can potentially achieve accurate whole-liver fat quantification with either a fast 1-2 minute scan or a 3-minute self-navigated scan.



### Linearity, Bias, and Precision of Proton-Density Fat Fraction for Liver Fat Quantification: A Meta-Analysis

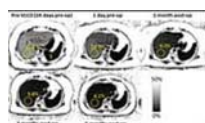
Ali Pirasteh<sup>1</sup>, Mustafa Bashir<sup>2</sup>, Scott B Reeder<sup>3</sup>, Claude B Sirlin<sup>4</sup>, An Tang<sup>5</sup>, Guido M Kukuk<sup>6</sup>, Jens-Peter Kuhn<sup>7</sup>, Holger Hetterich<sup>8</sup>, Ji Soo Song<sup>9</sup>, and Takeshi Yokoo<sup>1</sup>

<sup>1</sup>Radiology, University of Texas Southwestern Medical Center, Dallas, TX, United States, <sup>2</sup>Radiology, Center for Advanced Magnetic Resonance Development, Duke University Medical Center, Durham, NC, United States, <sup>3</sup>Radiology, Medical Physics, Biomedical Engineering, Medicine, and Emergency Medicine, University of Wisconsin, Madison, WI, United States, <sup>4</sup>Liver Imaging Group, Radiology, University of California San Diego, San Diego, CA, United States, <sup>5</sup>Radiology, University of Montréal, Montréal, QC, Canada, <sup>6</sup>Radiology, University of Bonn, Bonn, Germany, <sup>7</sup>University Greifswald, Greifswald, Germany, <sup>8</sup>Ludwig-Maximilian University Hospital, Munich, Germany, <sup>9</sup>Chonbuk National University Medical School and Hospital, Jeonju, Korea, Republic of

Proton-density fat fraction (PDFFF) is a quantitative imaging biomarker (QIB) of hepatic triglyceride concentration and steatosis. Liver PDFFF can be measured noninvasively using magnetic resonance imaging (MRI) or spectroscopy (MRS). Various MRI-based PDFFF methods have been validated in single-center studies at 1.5T or 3T field strength using a specific reconstruction algorithm on a single vendor platform. However, its technical performance as a QIB is unknown in a multi-center, multi-vendor setting. In this meta-analysis of previously published data from multiple studies, we demonstrated excellent linearity, negligible bias, and high repeatability/reproducibility of MRI-PDFFF across different field strengths, vendors, and reconstruction algorithms.

365

8:51



### Monitoring Resolution of Fatty Liver Disease with MRI following Bariatric Surgery: A Prospective, Multi-center Study

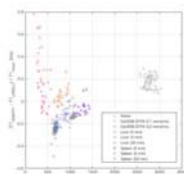
B. Dustin Pooler<sup>1</sup>, Curtis Wiens<sup>1</sup>, Alan McMillan<sup>1</sup>, Nathan Artz<sup>2</sup>, Alexandra Schlein<sup>3</sup>, Yesenia Covarrubias<sup>3</sup>, Jonathan Hooker<sup>3</sup>, Jeffrey Schwimmer<sup>3</sup>, Luke Funk<sup>1</sup>, Guilherme Campos<sup>4</sup>, Jacob Greenberg<sup>1</sup>, Garth Jacobsen<sup>3</sup>, Santiago Horgan<sup>3</sup>, Claude B. Sirlin<sup>3</sup>, and Scott B. Reeder<sup>1</sup>

<sup>1</sup>University of Wisconsin, Madison, WI, United States, <sup>2</sup>St. Jude Children's Research Hospital, Memphis, TN, <sup>3</sup>University of California-San Diego, San Diego, CA, <sup>4</sup>Virginia Commonwealth University, Richmond, VA

The temporal resolution of fatty liver disease following bariatric surgery is poorly understood. We used a validated chemical shift encoded MRI (CSE-MRI) method to measure liver proton density fat fraction (PDFFF) as a biomarker of liver fat. We followed a cohort of 50 obese adults undergoing bariatric surgery with pre-operative very low calorie diet (VLCD) and conclude that average liver PDFFF normalizes to <5% by 6 months following bariatric surgery. Normalization of liver fat is seen in 79% of patients who lower body mass index (BMI) by  $\geq 10$  mg/k<sup>2</sup> and 83% of patients who lose  $\geq 30$  kg.

366

9:03



### A paradoxical systemic bias in Gd-EOB-DTPA-enhanced T1 relaxometry of the liver: a comparison of SMART1Map and MOLLI.

Akira Yamada<sup>1</sup>, Sachie Fujita<sup>1</sup>, Yoshihiro Kitoh<sup>2</sup>, Yasuo Adachi<sup>2</sup>, Hayato Hayashibara<sup>2</sup>, Aya Shiobara<sup>2</sup>, Atsushi Nozaki<sup>3</sup>, Yuji Iwadate<sup>3</sup>, Glenn S Slavin<sup>4</sup>, Yasunari Fujinaga<sup>1</sup>, and Masumi Kadoya<sup>1</sup>

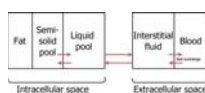
<sup>1</sup>Department of Radiology, Shinshu Univ. School of Medicine, Matsumoto, Japan, <sup>2</sup>Department of Radiology, Shinshu Univ. Hospital, Matsumoto, Japan, <sup>3</sup>GE Healthcare Japan, Japan, <sup>4</sup>GE Healthcare, United States

SMART<sub>1</sub>Map (saturation method using adaptive recovery times for cardiac T1 mapping) is a new single-point T1 mapping technique that directly measures true T1 unlike look-locker approaches. The feasibility of Gd-EOB-DTPA-enhanced T1 relaxometry of the liver using SMART<sub>1</sub>Map was evaluated comparing with modified look-locker inversion recovery (MOLLI). A significant paradoxical systemic bias was observed between and within SMART<sub>1</sub>Map and MOLLI in Gd-EOB-DTPA-administrated liver, although SMART<sub>1</sub>Map may be more reproducible than MOLLI in the rest of conditions. Careful consideration should be given to the effect of the paradoxical systemic bias in the evaluation of liver function using Gd-EOB-DTPA-enhanced T1 relaxometry.

367



9:15



Determining the T1 of the water in the liver by modelling the effects of fat, iron and off-resonance frequencies on MOLLI T1 measurements

Ferenc Emil Mozes<sup>1</sup>, Elizabeth Mary Tunnicliffe<sup>1</sup>, Thomas Marjot<sup>2</sup>, Christina Kim Levick<sup>1,3</sup>, Michael Pavlides<sup>1,3</sup>, and Matthew David Robson<sup>1</sup>

<sup>1</sup>University of Oxford Centre for Magnetic Resonance Research, University of Oxford, Oxford, United Kingdom, <sup>2</sup>Oxford Centre for Diabetes, Endocrinology and Metabolism, University of Oxford, Oxford, United Kingdom, <sup>3</sup>Translational Gastroenterology Unit, University of Oxford, Oxford, United Kingdom

The frequency dependence of balanced steady-state free precession signals causes significant alterations in modified Look-Locker inversion recovery T1 measurements of livers with fat accumulation, leading to either under- or over-estimation of liver T1 values. This is further to the already-known influence of iron. The present study shows a possibility to correct for these effects, yielding a T1 measurement that represents the T1 of the water component independent of the fat and is tested both in phantoms and human participants.

368

9:27

Bayesian prediction for insufficient liver enhancement in gadoxetic acid-enhanced hepatobiliary phase imaging

Yuki Mori<sup>1</sup>, Utaroh Motosugi<sup>1</sup>, Tatsuya Shimizu<sup>1</sup>, Shintaro Ichikawa<sup>1</sup>, and Hiroshi Onishi<sup>1</sup>

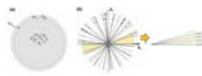


<sup>1</sup>Department of Radiology, University of Yamanashi, Chuo, Japan

Insufficient liver enhancement due to decreased liver function is a major limitation in gadoxetic acid-enhanced hepatobiliary phase imaging (HBP). Recent research shows that insufficient liver enhancement is associated with liver function tests including total bilirubin level, Child-Pugh classifications, indocyanine green tests, and liver stiffness measured by MR elastography. However, none of these tests have been practically used for determining the patients with insufficient liver enhancement before MR imaging. We used univariate tests and logistic regression to determine predictive factors and performed cross validation to reveal utility of Bayesian method for predicting patients with insufficient liver enhancement in gadoxetic acid-enhanced HBP.

369

9:39



Flexible and Efficient 2D Radial TSE T<sub>2</sub> Mapping with Tiered Echo Sharing and with “Pseudo” Golden Angle Ratio Reordering

Yutaka Natsuaki<sup>1</sup>, Mahesh Bharath Keerthisavan<sup>2</sup>, Ali Bilgin<sup>2,3</sup>, Bradley D Bolster<sup>4</sup>, Kevin J Johnson<sup>5</sup>, Xiaoming Bi<sup>1</sup>, Gerhard Laub<sup>6</sup>, and Maria I Altbach<sup>7</sup>

<sup>1</sup>Siemens Healthcare, Los Angeles, CA, United States, <sup>2</sup>Electrical and Computer Engineering, University of Arizona, Tucson, AZ, United States, <sup>3</sup>Biomedical Engineering, University of Arizona, Tucson, AZ, United States, <sup>4</sup>Siemens Healthcare, Salt Lake City, UT, United States, <sup>5</sup>Siemens Healthcare, Tucson, AZ, United States, <sup>6</sup>Siemens Healthcare, San Francisco, CA, <sup>7</sup>Medical Imaging, University of Arizona, Tucson, AZ, United States

There has been recent increased interest in quantitative T<sub>2</sub> mapping for accurate diagnosis of many pathological disorders. 2D radial TSE with tiered echo sharing and bit-reverse view ordering acquires TE data for T<sub>2</sub> mapping in an efficient and motion robust fashion, but imposes limits on the choice of Echo Train Length (ETL). The current work introduces a novel view ordering algorithm with “pseudo” Golden Angle ratio (pGA) that removes restrictions in the ETL. With this algorithm, the scan time of 2D radial TSE is reduced (by 18% in this study) without a compromise in image quality or in T<sub>2</sub> mapping accuracy.

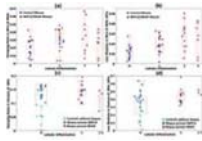
370

9:51

Assessment of Nonalcoholic Fatty Liver Disease (NAFLD) Activity Score (NAS) with MR Elastography (MRE)

Meng Yin<sup>1</sup>, Alina M. Allen<sup>2</sup>, Kevin J. Glaser<sup>1</sup>, Sudhakar K. Venkatesh<sup>1</sup>, Taofic Mounajjed<sup>3</sup>, Vijay Shah<sup>2</sup>, and Richard L. Ehman<sup>1</sup>



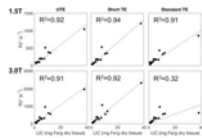


<sup>1</sup>Radiology, Mayo Clinic, Rochester, MN, United States,  
<sup>2</sup>Gastroenterology and Hepatology, Mayo Clinic, Rochester, MN, United States,  
<sup>3</sup>Anatomic Pathology, Mayo Clinic, Rochester, MN, United States

To investigate the utility of a hepatic imaging protocol “hepatogram”, which includes multi-parametric MR Elastography (MRE) and fat fraction assessment, in predicting nonalcoholic fatty liver disease (NAFLD) activity score (NAS: 0-8). In both preclinical and clinical subjects with histology-proven NAFLD, generalized linear models of liver stiffness, damping ratio and fat fraction successfully distinguished each NAS score with excellent accuracy (AUROC>0.89 for all). Misclassifications in distinguishing steatohepatitis (NAS≥3) from NAFLD (NAS<3) was only 2/64 mice and 3/51 human subjects. Our findings indicate the hepatogram imaging protocol can predict NAS score and may be useful to monitor NAFLD disease progression and regression.

371

10:03



Accuracy and Reproducibility of Iron Quantification using Ultra-Short TE Imaging at 1.5T and 3.0T

Curtis N Wiens<sup>1</sup>, Ante Zhu<sup>1,2</sup>, Kevin M Johnson<sup>1,3</sup>, Scott B Reeder<sup>1,2,3,4,5</sup>, and Diego Hernando<sup>1,3</sup>

<sup>1</sup>Radiology, University of Wisconsin, Madison, WI, United States,  
<sup>2</sup>Biomedical Engineering, University of Wisconsin, Madison, WI, United States,  
<sup>3</sup>Medical Physics, University of Wisconsin, Madison, WI, United States,  
<sup>4</sup>Medicine, University of Wisconsin, Madison, WI, United States,  
<sup>5</sup>Emergency Medicine, University of Wisconsin, Madison, WI, United States

This work examined the accuracy and reproducibility of ultra-short TE (UTE) R2\* mapping in patients with liver iron overload. Fifteen subjects with known or suspected liver iron overload were scanned at 1.5T and 3.0T using a radial UTE, two Cartesian multi-echo, gradient-echo acquisitions, and an R2-based (FerriScan) reference acquisition. UTE R2\* measurements demonstrated excellent reproducibility across field strengths (with expected linear increase with field strength) and high correlation with liver iron concentration. Cartesian approaches offered excellent reproducibility for R2\*<1000s<sup>-1</sup>. However R2\*>1000s<sup>-1</sup>, neither Cartesian approach were reproducible across field strength, suggesting that the range of R2\* had been surpassed.



# The Matrix: Collagen Function & Microstructure

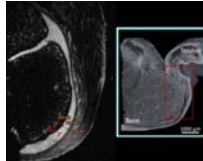
Room 311

Tuesday 8:15 - 10:15 *Moderators: Ashley Williams & Martijn Froeling*

---

372

8:15



## 7T Diffusion Tensor Imaging of High Mechanical Stress Achilles Tendon-to-Bone Interface

Simone Angela Winkler<sup>1</sup>, Lara Kuntz<sup>1,2</sup>, Christoph Leuze<sup>1</sup>, Hossein Nejadnik<sup>1</sup>, Laura J Pisani<sup>1</sup>, and Heike Daldrup-Link<sup>1</sup>

<sup>1</sup>*Dept of Radiology, Stanford University, Stanford, CA, United States,*  
<sup>2</sup>*Clinics of Orthopedics and Chair of Cellular Biophysics, Technische Universitaet Muenchen, Munich, Germany*

We present imaging analysis using MRI of the Achilles tendon-to-bone interface (“enthesis”) to investigate on the four distinct zones responsible for mechanical force transfer. Conventional T1- and T2-weighted imaging in humans yields very low MR signal. We therefore present T1-weighted FLASH 3D imaging at ultra high-field (7T), using a porcine sample from a minipig leg. We were able to identify the four zones (fibrous connective tissue, uncalcified fibrocartilage, calcified fibrocartilage, and bone) in both T1 and diffusion tensor imaging (DTI).

---

373

8:27



## 3D UTE-T2\* analysis of diseased Achilles tendons and the correlation with clinical score

Yang Qiao<sup>1</sup>, Hong-Yue Tao<sup>1</sup>, Yi-Wen Hu<sup>1</sup>, Jianxun Qu<sup>2</sup>, Kui Ma<sup>3</sup>, Zi-Ying Wu<sup>3</sup>, and Shuang Chen<sup>1</sup>

<sup>1</sup>*Department of Radiology, Fudan University Affiliated Huashan Hospital, Shanghai, People's Republic of China,* <sup>2</sup>*MR Research China, GE Healthcare, Shanghai, People's Republic of China,* <sup>3</sup>*Department of Sports Medicine, Fudan University Affiliated Huashan Hospital, Shanghai, People's Republic of China*

This study used 3D UTE-T2\*, a novel quantitative technique with potential short-T2\* relaxations to investigate T2\* value in diseased Achilles tendon(AT) and correlation between T2\* value and AOFAS, ATRS scores. Fifteen patients with AT disease and ten healthy controls matched sex, age, BMI were included. The results showed T2\* values of insertion(INS), middle(MID), muscle-tendon junction(MTJ) and bulk region of AT in patients were statistically higher than healthy controls and negatively correlated with AOFAS, ATRS scores, which suggests UTE-T2\* may be a promising marker for the detection of matrix changes in AT and give a precise guidance to clinical outcome.

---

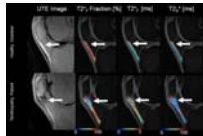


### Difference Image Ultra-Short Echo Time T2\* Mapping Using a 3D Cones Trajectory

Amin Nazaran<sup>1,2</sup>, Grayson Tarbox<sup>3</sup>, Randy Hartley<sup>4</sup>, and Neal Bangerter<sup>4,5</sup>

<sup>1</sup>Electrical Engineering, Brigham Young University, Provo, UT, United States, <sup>2</sup>University of California San Diego, San Diego, CA, United States, <sup>3</sup>Brigham Young University, Provo, UT, United States, <sup>4</sup>Electrical Engineering, Brigham Young University, <sup>5</sup>Radiology, University of Utah

This study introduces a methodology for detecting subtle variations in tissues with very rapid T2\* decay through a difference image ultra-short T2\* mapping technique using a 3D cones k-space trajectory. The new method is demonstrated in both a normal and surgically repaired Achilles tendon. The resulting UTE images were differenced and T2\* values were calculated using a mono-exponential least squares fit on a voxel by voxel basis. The ultrashort T2\* maps yield very consistent short T2\* values in healthy tendon of 0.3 – 0.5 ms, while notable variations and elevations of T2\* values are observed in the surgically repaired tendon.



### Bi-Component Ultra-short Echo-Time T2\* Analysis in Patients with Patellar Tendinopathy

Fang Liu<sup>1</sup>, John Wilson<sup>2</sup>, and Richard Kijowski<sup>1</sup>

<sup>1</sup>Department of Radiology, University of Wisconsin-Madison, Madison, WI, United States, <sup>2</sup>Department of Orthopedics, University of Wisconsin-Madison, Madison, WI

A bi-component ultra-short echo-time (UTE) T2\* mapping sequence was performed on the knees of 10 patients with patellar tendinopathy and 10 healthy volunteers at 3T. The fraction of the fast relaxing water component (FF) and the T2 relaxation times of the fast relaxing (T2\*F,) and slow relaxing (T2\*S) water components of patellar tendon were measured. Patients with patellar tendinopathy had significantly lower FF (P=0.007), significantly higher T2\*F (P=0.014), and similar T2\*S (P=0.10) of patellar tendon when compared to healthy volunteers. Our results suggest that bi-component UTE T2\* analysis can detect early compositional and microstructural changes in degenerative tendon.

### Rotator Cuff Tendon Assessment Using Magic-Angle Insensitive 3D Ultrashort Echo Time Cones Magnetization Transfer (UTE-Cones-MT) Imaging and Modeling

Yanchun Zhu<sup>1</sup>, Yajun Ma<sup>1</sup>, Jiang Du<sup>1</sup>, and Eric Y Chang<sup>1,2</sup>



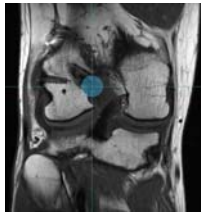
*<sup>1</sup>Department of Radiology, University of California, San Diego, La Jolla, CA, United States, <sup>2</sup>Radiology Service, VA San Diego Healthcare System, San Diego, CA, United States*

The rotator cuff tendon (RCT) is the primary dynamic stabilizer of the glenohumeral joint. However magic angle effect decrease the sensitivity of MRI in assessment of RCT. The purpose of our study is to utilize the 3D ultrashort echo time Cones sequence with magnetization transfer preparation (UTE-Cones-MT) and two-pool quantitative MT modeling to assess the RCT.

---

377

9:15



### Diffusion Tensor Imaging of the Anterior Cruciate Ligament Graft

Pieter Van Dyck<sup>1</sup>, Eline De Smet<sup>1</sup>, Martijn Froeling<sup>2</sup>, Peter Verdonk<sup>3</sup>, Michaël Torfs<sup>1</sup>, Pim Pullens<sup>1</sup>, Jan Sijbers<sup>4</sup>, Paul M Parizel<sup>1</sup>, and Ben Jeurissen<sup>4</sup>

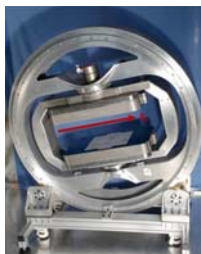
*<sup>1</sup>Dept. of Radiology, University Hospital Antwerp, Edegem, Belgium, <sup>2</sup>Dept. of Radiology, University Medical Center Utrecht, Netherlands, <sup>3</sup>Dept. of Orthopedics, Monica Orthopedic Research (MoRe) Foundation, Monica Hospital, Belgium, <sup>4</sup>Vision Lab, Dept. of Physics, University of Antwerp, Belgium*

Anterior cruciate ligament (ACL) reconstruction using a tendon graft remains the standard of care for ACL injuries. Postoperatively, the graft undergoes a biologic transition from tendinous to ligamentous in appearance. Despite substantial research efforts, little is known about the human ACL graft ligamentization process. Much of the current knowledge on graft ligamentization have been derived from biopsy studies. However, biopsies are invasive and suffer from sampling error. Our study demonstrates the feasibility and reliability of diffusion tensor imaging (DTI) for visualization and quantification of the ACL graft and supports its potential to serve as a biomarker to assess graft maturity.

---

378

9:27



### Advances in Angle Sensitive MRI: Towards in vivo analysis of collagen fibre tracts in the Anterior Cruciate Ligament

Karyn E Chappell<sup>1</sup>, Quentin Herreros<sup>2</sup>, Donald W McRobbie<sup>3</sup>, and Djordje Brujic<sup>4</sup>

<sup>1</sup>*Surgery and Cancer, Imperial College London, London, United Kingdom,* <sup>2</sup>*Institut de Physique Nucléaire de Lyon, Lyon, France,* <sup>3</sup>*Medical Physics & Radiation Safety, Flinders Medical Centre, Adelaide, Australia,* <sup>4</sup>*Mechanical Engineering, Imperial College London, London, United Kingdom*

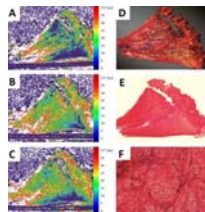
There is great interest in collagen MR imaging due to its non-invasive nature. To be able to detect early structural changes in collagen the main magnetic field must move around the patient.

A new rotatable MR system enabling *in vivo* Angle Sensitive MRI was designed and its prototype has been built. Key elements of the new method are: optimisation of scanning directions, collagen orientation distribution computation and fibre tract reconstruction.

We have proved that nine scans in optimal directions achieve satisfactory accuracy. Previous Angle Sensitive MRI times are almost halved whilst analysis time is shortened by more than 100 times.

379

9:39



#### Collagen fiber to magnetic field angle dependence in human meniscus – a preliminary T2\* MR-microscopy study at 7T

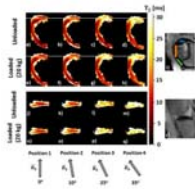
Benedikt Hager<sup>1,2</sup>, Sonja Walzer<sup>3</sup>, Vladimir Juras<sup>1,4</sup>, Martin Zalaudek<sup>1</sup>, Xeni Deligianni<sup>5</sup>, Oliver Bieri<sup>5</sup>, Andreas Berg<sup>6</sup>, Joachim Friske<sup>1</sup>, Markus Schreiner<sup>3</sup>, Reinhard Windhager<sup>3</sup>, and Siegfried Trattnig<sup>1,2</sup>

<sup>1</sup>*High Field MR Centre, Department of Biomedical Imaging and Image-guided Therapy, Medical University of Vienna, Vienna, Austria,* <sup>2</sup>*Christian Doppler Laboratory for Clinical Molecular MR Imaging, Vienna, Austria,* <sup>3</sup>*Department of Orthopaedic Surgery, Medical University of Vienna, Vienna, Austria,* <sup>4</sup>*Department of Imaging Methods, Institute of Measurement Science, Slovak Academy of Sciences, Bratislava, Slovakia,* <sup>5</sup>*Department of Radiology, Division of Radiological Physics, University of Basel Hospital, Basel, Switzerland,* <sup>6</sup>*Center for Medical Physics and Biomedical Engineering, Medical University of Vienna, Vienna, Austria*

We evaluated the fiber-to-field dependence of a meniscal specimen using T2\* mapping on high-field 7T MRI in combination with an MR microimaging insert and validated the results with histology. We found that, different structures of the meniscus behave very differently with orientation to the magnetic field. For example, short T2/T2\* tendon-like structure located in the external circumference showed strongest T2\* dependence reflecting the anisotropic nature of these structures and consequential incomplete averaging of dipolar coupling. The results shown here are the first MR Microscopy evaluations of the orientational dependence of T2\* relaxation in human meniscus.

380

9:51



The magic angle effect can (partially) explain load-induced increases in meniscal T2 and T1 $\rho$

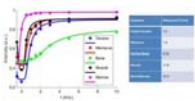
Valentina Mazzoli<sup>1,2,3</sup>, Danny Tsui<sup>2</sup>, Larry de Graaf<sup>2</sup>, Klaas Nicolay<sup>2</sup>, Andre M Sprengers<sup>3</sup>, Dennis Janssen<sup>3</sup>, Nico Verdonschot<sup>3</sup>, Aart J Nederveen<sup>1</sup>, and Gustav J Strijkers<sup>4</sup>

<sup>1</sup>Department of Radiology, Academic Medical Center, Amsterdam, Netherlands, <sup>2</sup>Biomedical NMR, Department of Biomedical Engineering, Eindhoven University of Technology, Eindhoven, Netherlands, <sup>3</sup>Orthopaedic Research Lab, Radboud UMC, Nijmegen, Netherlands, <sup>4</sup>Biomedical Engineering and Physics, Academic Medical Center, Amsterdam, Netherlands

Often, knee injury and disorders are caused by or lead to abnormal biomechanical loading patterns in the knee joint menisci. Quantitative information on in vivo loading patterns is therefore in high demand to evaluate therapy and prevent further damage. T<sub>1 $\rho$</sub>  and T<sub>2</sub> in meniscus were shown to increase upon application of compressive load, although the mechanisms leading to changes remain unclear. In this work we apply compressive load on the meniscus of volunteers and one cadaver and show that compression-induced internal fiber reorganization may manifest as the magic angle effect, which may be responsible for load-induced T<sub>2</sub> and T<sub>1 $\rho$</sub>  increases.

381

10:03



Quantitative Off Resonance Saturation 3D UTE Imaging

Michael Carl<sup>1</sup>, Yajun Ma<sup>2</sup>, and Jiang Du<sup>2</sup>

<sup>1</sup>GE Healthcare, San Diego, CA, United States, <sup>2</sup>UCSD, CA, United States

Off-resonance saturation (ORS) is a tool which can be used in UTE magnetic resonance imaging to selectively reduce short  $T_2$  signals. Here we develop a simple quantitative theoretical model. The theoretical equations can be used to determine the ORS sequence parameters such as  $f_{\text{off}}$  and  $\theta_{\text{ORS}}$  to maximize short  $T_2$  contrast.

Oral

## Novel Pulse Sequences

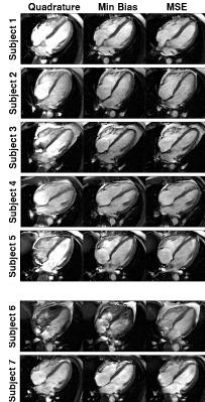
Room 312

Tuesday 8:15 - 10:15 Moderators: Priti Balchandani & Klaus Scheffler

382



8:15



**Extended RF shimming: Sequence level parallel transmission optimization applied to steady state free precession MRI of the heart**

Arian Beqiri<sup>1</sup>, Anthony N Price<sup>1,2</sup>, Joseph V Hajnal<sup>1,2</sup>, and Shaihan J Malik<sup>1</sup>

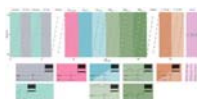
<sup>1</sup>Biomedical Engineering and imaging Sciences, King's College London, London, United Kingdom, <sup>2</sup>Centre for the Developing Brain, King's College London, London, United Kingdom

**Balanced steady-state free precession (bSSFP) cardiac MRI benefits greatly from reduced repetition time (TR). Minimum TR is often limited by specific absorption rate (SAR) and hardware constraints. RF shimming can be used with parallel transmission (PTx) to work within such constraints, but direct minimization of TR is not straightforward since the constraints themselves vary as TR is reduced.**

**We present an extended RF shimming framework in which PTx degrees of freedom are simultaneously optimised with pulse sequence properties. The result is minimum TR bSSFP sequences that operate at the SAR limits and within hardware constraints for 3T cardiac MRI.**

383

8:27



**Multi-Contrast EPI for use as a Neuro MR Scout and Screening**

Mathias Engström<sup>1</sup>, Enrico Avventi<sup>2,3</sup>, Ola Norbeck<sup>2,3</sup>, Henric Rydén<sup>2,3</sup>, and Stefan Skare<sup>2,3</sup>



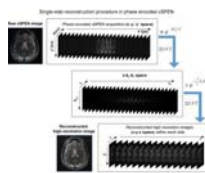
<sup>1</sup>Applied Science Laboratory, GE Healthcare, Uppsala, Sweden, <sup>2</sup>Dept. of Neuroradiology, Karolinska University Hospital, Stockholm, Sweden, <sup>3</sup>Dept. of Clinical Neuroscience, Karolinska Institutet, Stockholm, Sweden

This work describes a new sub-minute EPI-based sequence that produce T2\*, T2, T2-FLAIR, T1-FLAIR, DWI, and ADC images as well as a 3-plane localizer as an alternative to the conventional scout, enabling a clinical screening at the beginning of the exam.

384



8:39



High resolution imaging by phase encoded xSPEN MRI

Zhiyong Zhang<sup>1</sup>, Michael Lustig<sup>2</sup>, and Lucio Frydman<sup>1</sup>

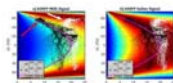
<sup>1</sup>Department of Chemical Physics, Weizmann Institute of Science, Rehovot, Israel, <sup>2</sup>Department of Electrical Engineering and Computer Sciences, University of California, Berkeley, CA, United States

We have recently introduced cross-term SPatiotemporal ENcoding (xSPEN), a technique with exceptional resilience to field heterogeneities. Like other single-shot methods, however, xSPEN's resolution and SNR are intrinsically limited. This study explores a multi-scan, phase-encoded extension of xSPEN, which improves sensitivity while increasing resolution along both the phase-encoded and the slice-selection dimensions simultaneously. This reflects xSPEN's unusual kernel whereby a y-axis can be sampled by a z-gradient and *viceversa*. Furthermore, as each phase-encoded xSPEN scan provides an entire 2D image, each low-resolution xSPEN scan in the set may be used to correct motions leading to very high definition 3D MRI capabilities.

385



8:51



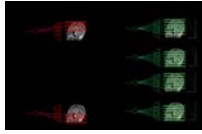
Improved signal uniformity for balanced steady-state free precession by employing Direct Signal Control parallel transmission

Francesco Padormo<sup>1</sup> and Priti Balchandani<sup>1</sup>

<sup>1</sup>Translational and Molecular Imaging Institute, Icahn School of Medicine at Mount Sinai, New York, NY, United States

We present a method to minimize signal intensity variations observed when performing balanced steady state free precession imaging in non-uniform  $B_0$  and  $B_1+$  fields. This is achieved by harnessing parallel transmission, with RF shims calculated in order to produce the most uniform signal for the desired tissues given measured  $B_0$  and  $B_1+$  field maps.





### Faster than Multiband ... Advanced Pseudo Fourier Imaging's (API) response to the current state of the art

Nishant Zachariah<sup>1</sup>, Jason Langley<sup>2</sup>, Justin Romberg<sup>1</sup>, and Xiaoping P. Hu<sup>3</sup>

<sup>1</sup>Department of Electrical and Computer Engineering, Georgia Institute of Technology, Atlanta, GA, United States, <sup>2</sup>Center for Advanced Neuroimaging, University of California at Riverside, CA, United States, <sup>3</sup>Department of Bioengineering, University of California at Riverside, CA, United States

Multiband (MB) imaging is limited in its acceleration factor by the high correlation that exists between receiver coils. In this work, we present a novel technique, **A**dvanced **P**seudo **F**ourier **I**maging (API) which achieves parallel excitation beyond that which is currently possible using multiband imaging. In doing so, API forms a generic framework for seamless transition from 2D to 3D imaging. Unlike MB, API is less sensitive to the RF excitation profile in its slice reconstruction by virtue of the introduced phase variations. We demonstrate the viability of API through 1D simulations and 3D head phantom data acquired at 3T.

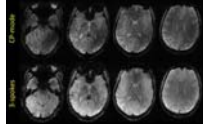


### Whole Brain Inversion Recovery Diffusion Weighted Imaging Using Slice-Shuffled Acquisition

Hua Wu<sup>1</sup>, Qiyuan Tian<sup>2,3</sup>, Christian Poetter<sup>1</sup>, Kangrong Zhu<sup>2</sup>, Matthew J Middione<sup>4</sup>, Adam B Kerr<sup>2</sup>, Jennifer A McNab<sup>3</sup>, and Robert F Dougherty<sup>1</sup>

<sup>1</sup>Center for Cognitive and Neurobiological Imaging, Stanford University, Stanford, CA, United States, <sup>2</sup>Department of Electrical Engineering, Stanford University, Stanford, CA, United States, <sup>3</sup>Department of Radiology, Stanford University, Stanford, CA, United States, <sup>4</sup>Applied Sciences Laboratory West, GE Healthcare, Menlo Park, CA, United States

Combined acquisition of diffusion weighted MRI and T1 relaxation allows us to extract information about the microstructures of human brain on a sub-voxel level. We design an inversion recovery pulse sequence with diffusion weighting using the slice-shuffled technique to accelerate the T1 measurement and demonstrate whole brain scans acquired in under 20 minutes. We show potential applications of the sequence in differentiating the T1 relaxation of compartments with different diffusion properties within a voxel .

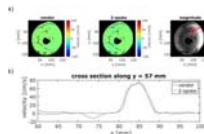


### Whole-brain multi-slice multi-spoke parallel transmit RF pulse design in the large flip angle regime at 7 Tesla

Vincent Gras<sup>1</sup>, Alexandre Vignaud<sup>1</sup>, Alexis Amadon<sup>1</sup>, Franck Mauconduit<sup>2</sup>, Denis Le Bihan<sup>1</sup>, and Nicolas Boulant<sup>1</sup>

<sup>1</sup>UNIRS, CEA/DRF/I2BM/Neurospin, Gif-sur-Yvette, France, <sup>2</sup>Siemens Healthcare, Saint Denis, France

At ultra-high field, transmit RF field inhomogeneity mitigation methods exploiting parallel transmission and multi-spoke pulses are readily applicable for brain imaging with small flip angle (FA) protocols. The extension to large FAs yet appears more challenging due to the inherent computationally extensive calculations. Dealing now with multi-slice applications, where specific absorption rate (SAR) issues often come into play, a SAR-aware slice-specific pulse design algorithm can improve significantly the output. This work thus presents a large FA slice-specific multi-spoke pulse design approach enforcing explicitly SAR constraints and, to reduce computations, where the spin dynamics is approximated with Average Hamiltonian Theory.

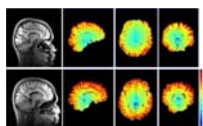


### Velocity Encoded and Compensated Multi-Spoke RF Pulses for Flow Quantification at Ultra-High Fields

Simon Schmidt<sup>1</sup>, Sebastian Flassbeck<sup>1</sup>, Mathies Breithaupt<sup>1,2</sup>, Peter Bachert<sup>1</sup>, Mark E. Ladd<sup>1</sup>, and Sebastian Schmitter<sup>1,3</sup>

<sup>1</sup>Medical Physics in Radiology, German Cancer Research Center (DKFZ), Heidelberg, Germany, <sup>2</sup>Institute for Forensic Medicine and Traffic Medicine, University Hospital Heidelberg, Heidelberg, Germany, <sup>3</sup>Physikalisch-Technische Bundesanstalt (PTB), Braunschweig and Berlin, Germany

In this work we present and demonstrate a novel technique to generate multi-spoke RF excitation with arbitrary zeroth and first gradient moments, allowing for clean flow imaging without errors. The RF pulses are demonstrated in flow phantoms and in-vivo at 7 Tesla, paving the road for 4D flow imaging using pTX spoke excitation.



### A single-channel universal SPINS pulse for calibration-free homogeneous excitation without PTX

Ronald Mooiweer<sup>1,2</sup>, Joseph V Hajnal<sup>1</sup>, and Shaihan J Malik<sup>1</sup>

<sup>1</sup>Imaging Sciences and Biomedical Engineering, King's College London, London, United Kingdom, <sup>2</sup>UMC Utrecht, Utrecht, Netherlands

A universal single-channel pulse was created that improves excitation homogeneity at 3T, for low flip angles. This method does not require subject specific calibration nor a PTX system, thus making it widely applicable. Though even better homogeneity could be achieved through the use of PTX or subject-specific pulse design, in our study the universal single-channel pulse always outperformed the quadrature mode excitation. This could be used to create more uniform contrast in MP-RAGE imaging.

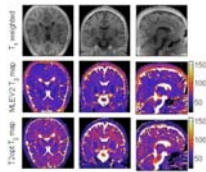
391

10:03

Optimal control B1-robust T2 preparation

Martin A Janich<sup>1</sup>, Ana Beatriz Solana Sánchez<sup>1</sup>, and Florian Wiesinger<sup>1</sup>

<sup>1</sup>GE Global Research, Munich, Germany



T<sub>2</sub> is an important MR imaging contrast, including visualizing edema, myocarditis, separating coronary lumen from myocardium, as well as cerebrospinal fluid from gray and white matter. For diagnostic accuracy, it is important to achieve uniform T<sub>2</sub>-weighting throughout the imaging field-of-view. This is often not achievable because of non-uniform B<sub>1</sub>, especially at ultra-high magnetic field. This limitation was overcome by numerical optimization of a T<sub>2</sub> preparation module. The optimal control T<sub>2</sub> preparation pulse achieved good T<sub>2</sub> contrast despite ±40% B<sub>1</sub> variation and was scalable to achieve different T<sub>2</sub> weighting times. Evaluation was done with Zero-TE imaging in the human brain at 3T.

Oral

From Aging Brain to Alzheimer's Disease

Room 313A

Tuesday 8:15 - 10:15 Moderators: Eric Achten & Masaaki Hori

392

8:15

Age-related neuropathologies associated with white matter hyperintensities burden: a study of a community cohort of older adults.

Nabil Alqam<sup>1</sup>, Arnold Evia<sup>1</sup>, Luis Filipe Campos Cardoso<sup>1</sup>, Lucas Fagundes Lopes<sup>1</sup>, Diego Vieira Pereira<sup>1</sup>, Julie A. Schneider<sup>2,3,4</sup>, Sue E. Leurgans<sup>2,3</sup>, David A. Bennett<sup>2,3</sup>, and Konstantinos Arfanakis<sup>1,2,5</sup>

Characteristics	Total
n	613
Age at death, years (SD)	90 (7)
Males, n (%)	160 (27%)
Education, years (SD)	10 (6)
Median time between last evaluation and death, years	0.81
Antemortem clinical diagnosis, n (%)	169 (27%)
- No cognitive impairment	164 (27%)
- Mild cognitive impairment	184 (30%)
- Dementia	265 (43%)
Global cognition score, mean (SD)	-1.0 (1.2)
Episodic memory score, mean (SD)	-1.2 (1.4)
Semantic memory score, mean (SD)	-1.2 (1.7)
Working memory score, mean (SD)	-0.8 (1.1)
Perceptual speed score, mean (SD)	-1.2 (1.2)
Visuospatial ability score, mean (SD)	-0.8 (1.2)
Mini-mental State Examination (MMSE), mean (SD)	25.1 (9.5)
Mini-mental State Examination (MMSE), median	24
Right hemisphere, n (%)	288 (47%)
Phantom interval to Reeler, hours (SD)	8.8 (8.3)

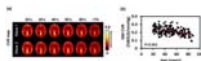
*<sup>1</sup>Department of Biomedical Engineering, Illinois Institute of Technology, Chicago, IL, United States, <sup>2</sup>Rush Alzheimer's Disease Center, Rush University Medical Center, Chicago, IL, United States, <sup>3</sup>Department of Neurological Sciences, Rush University Medical Center, Chicago, IL, United States, <sup>4</sup>Department of Pathology, Rush University Medical Center, Chicago, IL, United States, <sup>5</sup>Department of Diagnostic Radiology, Rush University Medical Center, Chicago, IL, United States*

White matter hyperintensities (WMH) are lesions commonly observed in the brain of older adults, and have been associated with lower cognitive function, lower motor performance, and increased risk of dementia. The purpose of this work was to investigate the neuropathologic correlates of WMH burden by combining ex-vivo MRI and pathology on a large community cohort of older adults.

---

393

8:27



Age-related changes in cerebrovascular reactivity and their relationship to cognition and vascular risk: A four-year longitudinal study

Shin-Lei Peng<sup>1,2</sup>, Xi Chen<sup>3</sup>, Yang Li<sup>1</sup>, Karen M Rodrigue<sup>3</sup>, Denise C Park<sup>3</sup>, and Hanzhang Lu<sup>1</sup>

*<sup>1</sup>Department of Radiology, Johns Hopkins University School of Medicine, Baltimore, MD, United States, <sup>2</sup>Department of Biomedical Imaging and Radiological Science, China Medical University, <sup>3</sup>Center for Vital Longevity, School of Behavioral and Brain Sciences, University of Texas at Dallas*

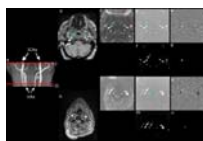
Although cerebrovascular factors are the cause of cognitive impairment, the vascular decline in aging have not been characterized. In this work, we present four-year longitudinal cerebrovascular reactivity (CVR) data measured in 116 individuals. Our data revealed temporal lobe showed the fastest CVR decline and middle age manifested the fastest CVR decline. Vascular risk of hypertension results in a lower CVR when compared to normal and well-controlled subjects. Individuals with poorer general cognitive status, as indexed by a low mini-mental-state-exam (MMSE), had a lower CVR compared to participants with higher MMSE scores. These findings help elucidate age-related decline in brain hemodynamics.

---

394

8:39

Cerebral Arteries Hemodynamics in Alzheimer's Disease Assessed by Phase-Contrast Velocity Mapping



Reyes García de Eulate<sup>1</sup>, Irene Goñi<sup>2</sup>, Alvaro Galiano<sup>1</sup>, Marta Vidorreta<sup>3</sup>, Miriam Recio<sup>4</sup>, Mario Riverol<sup>4</sup>, Jose Luis Zubieta<sup>1</sup>, and María Fernández-Seara<sup>1,2</sup>

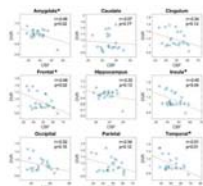
<sup>1</sup>Radiology, University of Navarra Hospital, Pamplona, Spain, <sup>2</sup>Biomedical Engineering, TECNUN, University of Navarra, San Sebastian, Spain, <sup>3</sup>Center for Functional Neuroimaging, University of Pennsylvania, Philadelphia, United States, <sup>4</sup>Neurology, University of Navarra Hospital, Pamplona, Spain

Vascular disease increases the risk of Alzheimer's disease. The assessment of vascular dysfunction in subjects at risk for AD has the potential to contribute to the disease early diagnosis and management. In this work, the phase-contrast velocity mapping MRI technique was used to evaluate cerebral hemodynamics in patients with cognitive dysfunction and healthy controls. Results showed significant differences in hemodynamic parameters (velocity and flow) across groups with lower mean values in the AD and MCI groups compared to the CO group. PC-MRI can be used to assess hypoperfusion in an early stage of AD.

---

395

8:51



Association of cerebral blood flow and amyloid burden in autosomal dominant Alzheimer's disease

Lirong Yan<sup>1</sup>, Collin Liu<sup>2</sup>, Koon-Pong Wong<sup>3</sup>, Sung-Cheng Huang<sup>3</sup>, John Ringman<sup>2</sup>, and Danny JJ Wang<sup>1</sup>

<sup>1</sup>Stevens Neuroimaging and Informatics Institute, University of Southern California, Los Angeles, CA, United States, <sup>2</sup>Neurology, University of Southern California, Los Angeles, CA, United States, <sup>3</sup>University of California Los Angeles, United States

The purpose of this study was to investigate the association of cerebral blood flow alternation with cerebral amyloid deposition in autosomal dominant Alzheimer's disease. Cross-subject negative correlation between cerebral blood flow and amyloid deposition was observed, indicating brain regions with high amyloid deposition may be associated with hypoperfusion. Our finding suggests cerebral hypoperfusion may contribute to the onset and progression of AD.

---

396

9:03

Association of vascular risk factors with cerebral metabolic rate

Kevin King<sup>1</sup>, Min Sheng<sup>2</sup>, Peiying Liu<sup>3</sup>, Christopher Maroules<sup>4</sup>, Craig Rubin<sup>5</sup>, Ron Peshock<sup>6</sup>, Roderick McColl<sup>7</sup>, and Hanzhang Lu<sup>8</sup>

Female	36 (51%)
Diabetic	8 (11%)
Hypertriglyceridemic	16 (23%)
Low HDL	18 (26%)
Hypertension Medication	40 (57%)
Systolic blood pressure (mmHg)	132.2 ± 14.2
Diastolic blood pressure (mmHg)	77.8 ± 7.5
CBF (ml/100g/min)	60.3 ± 12.6
OEF (%)	34.8 ± 6.3
CMRO <sub>2</sub> (μmol/100g/min)	166.4 ± 32.5

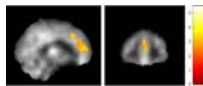
Values represent n and % of cohort or mean and standard deviation.

<sup>1</sup>Huntington Medical Research Institutes, Pasadena, CA, United States, <sup>2</sup>Advanced Imaging Research Center, UT Southwestern Medical Center, Dallas, TX, United States, <sup>3</sup>Radiology, Johns Hopkins University School of Medicine, Baltimore, MD, <sup>4</sup>Radiology, UT Southwestern Medical Center, Dallas, TX, <sup>5</sup>Geriatrics, UT Southwestern Medical Center, Dallas, TX, United States, <sup>6</sup>Radiology, Internal Medicine, UT Southwestern Medical Center, Dallas, TX, United States, <sup>7</sup>Radiology, UT Southwestern Medical Center, Dallas, TX, United States, <sup>8</sup>Radiology, Johns Hopkins University School of Medicine, Baltimore, MD, United States

Vascular risk factors that confer a susceptibility for dementia are thought to result in silent brain changes decades before disease onset. We hypothesized that vascular risk factors would be associated decreased Cerebral Metabolic Rate of Oxygen consumption (CMRO<sub>2</sub>). CMRO<sub>2</sub> was derived from Arterial Spin Labelling cerebral blood flow (CBF) and oxygen extraction fraction (OEF) from TRUST MRI in this IRB approved study with informed consent on 70 participants. In stepwise linear regression higher diastolic blood pressure was correlated with decreased CMRO<sub>2</sub> but was not associated with CBF, suggesting mechanisms other than insufficient blood flow underlie the association with metabolic rate.

397

9:15



One-year aerobic exercise increases regional cerebral blood flow in anterior cingulate cortex: a blinded, randomized trial in patients with amnesic Mild Cognitive Impairment

Binu P. Thomas<sup>1</sup>, Takashi Tarumi<sup>2</sup>, Min Sheng<sup>1</sup>, Benjamin Y. Tseng<sup>2</sup>, Kyle Womack<sup>3</sup>, Munro C. Cullum<sup>4</sup>, Rong Zhang<sup>2,5</sup>, and Hanzhang Lu<sup>1,6</sup>

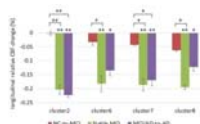
<sup>1</sup>Advanced Imaging Research Center, UT Southwestern Medical Center, Dallas, TX, United States, <sup>2</sup>Institute for Exercise and Environmental Medicine, Texas Health Presbyterian Hospital, Dallas, TX, United States, <sup>3</sup>Department of Neurology and Neurotherapeutic, UT Southwestern Medical Center, Dallas, TX, United States, <sup>4</sup>Department of Psychiatry, UT Southwestern Medical Center, Dallas, TX, United States, <sup>5</sup>Department of Internal Medicine, UT Southwestern Medical Center, Dallas, TX, United States, <sup>6</sup>Department of Radiology & Radiological Science, Johns Hopkins University School of Medicine, Baltimore, MD, United States



Amnesic mild cognitive impairment (MCI) represents the early stage of Alzheimer's disease (AD). Much research has focused on preventing the inevitable decline of MCI to AD. Aerobic exercise is considered a viable choice, and is shown to improve cognitive function in MCI. We focus on understanding the mechanisms that lead to this improvement. Pseudo-continuous-arterial-spin-labeling (PCASL) was used to assess resting cerebral blood flow (CBF) in two MCI groups. One group performed aerobic exercise, while another non-aerobic stretching. CBF was measured before and after training. CBF increase in the anterior-cingulate-cortex (ACC) was the proven mechanism that improves cognitive function in MCI.

398

9:27



Cross-sectional and Longitudinal Cerebral Blood Flow Changes in the Progression from Normal Cognition to Alzheimer's Disease Measured with Continuous Arterial Spin Labeling (CASL)

Wenna Duan<sup>1</sup>, H. Michael Gach<sup>2</sup>, Arvind Balachandrasekaran<sup>3</sup>, Parshant Sehrawat<sup>1</sup>, Ashish B. Bhumkar<sup>1</sup>, Paresh B. Boraste<sup>1</sup>, James T. Becker<sup>4</sup>, Oscar L. Lopez<sup>5</sup>, and Weiying Dai<sup>1</sup>

<sup>1</sup>Department of Computer Science, Binghamton University (SUNY), Binghamton, NY, United States, <sup>2</sup>Department of Radiation Oncology, Washington University, Saint Louis, St. Louis, MO, United States, <sup>3</sup>Department of Electrical and Computer Engineering, University of Iowa, Iowa City, IA, United States, <sup>4</sup>Department of Psychology, University of Pittsburgh, Pittsburgh, PA, United States, <sup>5</sup>Department of Psychiatry and Neurology, University of Pittsburgh, Pittsburgh, PA, United States

Cross-sectional and longitudinal analysis of cerebral blood flow (CBF) versus cognitive status were performed in an elderly cohort. Voxel-based ANOVA was used to test the CBF difference between normal control (NC), mild cognitive impairment (MCI) and Alzheimer's Disease (AD) groups at the baseline. Eight significant clusters were found between groups. The longitudinal CBF change in each cluster was compared across 4 longitudinal groups (stable NC, NC-to-MCI, stable MCI, and MCI/AD-to-AD) using a multiple linear regression model. The results indicated that CBF rises in AD-related regions of the brain during MCI and then drops dramatically in advanced MCI or early AD.

9:39

Effects of transactive response DNA-binding protein 43 (TDP43) pathology on amygdala volume and shape, in a community cohort of older adults





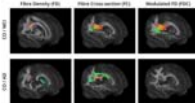
Characteristics	Total
N	462
Age at death, years (SD)	76.2
Male, n (%)	18 (21%)
Education, years (SD)	14.2
Median time between last evaluation and death, years	0.75
Autopsy-confirmed diagnosis, n (%)	
- No cognitive impairment	17 (21%)
- Mild cognitive impairment	61 (23%)
- Dementia	189 (28%)
Global cognition scores, mean (SD)	-1.1 (1.2)
Episodic memory scores, mean (SD)	-1.0 (1.4)
Semantic memory scores, mean (SD)	-1.0 (1.4)
Working memory scores, mean (SD)	-0.9 (1.3)
Perceptual speed scores, mean (SD)	-0.8 (1.4)
Visuospatial ability scores, mean (SD)	-1.1 (1.2)
Mini-mental state Examination (MMSE) scores (SD)	19.2 (3.4)
Right hemisphere, n (%)	221 (28%)
Postmortem status of the specimen, mean (SD)	0.7 (0.7)

Nazanin Makkinejad<sup>1</sup>, Junxiao Yu<sup>1</sup>, Aikaterini Kotrotsou<sup>1</sup>, Arnold M. Evia<sup>1</sup>, Julie A. Schneider<sup>2,3,4</sup>, Sue E. Leurgans<sup>2,3</sup>, David A. Bennett<sup>2,3</sup>, and Konstantinos Arfanakis<sup>1,2,5</sup>

<sup>1</sup>Department of Biomedical Engineering, Illinois Institute of Technology, Chicago, IL, United States, <sup>2</sup>Rush Alzheimer's Disease Center, Rush University Medical Center, Chicago, IL, United States, <sup>3</sup>Department of Neurological Sciences, Rush University Medical Center, Chicago, IL, United States, <sup>4</sup>Department of Pathology, Rush University Medical Center, Chicago, IL, United States, <sup>5</sup>Department of Diagnostic Radiology, Rush University Medical Center, Chicago, IL, United States

TDP43 pathology is now recognized as a common and deleterious neuropathology of the aging brain. TDP43 pathology typically originates in the amygdala, which is, however, commonly affected by other age-related neurodegenerative pathologies. The purpose of this work was to investigate the effects of TDP43 pathology on the volume and shape of the amygdala in a large community cohort of older adults.

9:51



Fixel-based analysis of Alzheimer's Disease using multi-tissue constrained spherical deconvolution of multi-shell diffusion MRI

Diana L. Giraldo<sup>1,2</sup>, Hanne Struyfs<sup>3</sup>, David A. Raffelt<sup>4</sup>, Paul M. Parizel<sup>5</sup>, Sebastiaan Engelborghs<sup>3,6</sup>, Eduardo Romero<sup>2</sup>, Jan Sijbers<sup>1</sup>, and Ben Jeurissen<sup>1</sup>

<sup>1</sup>Vision Lab, Department of Physics, University of Antwerp, Antwerp, Belgium, <sup>2</sup>Computer Imaging and Medical Applications Laboratory, Universidad Nacional de Colombia, Bogota, Colombia, <sup>3</sup>Reference Center for Biological Markers of Dementia (BIODEM), University of Antwerp, Antwerp, Belgium, <sup>4</sup>Florey Institute of Neuroscience and Mental Health, Melbourne, Australia, <sup>5</sup>Department of Radiology, University of Antwerp, Antwerp, Belgium, <sup>6</sup>Department of Neurology and Memory Clinic, Hospital Network Antwerp (ZNA) Middelheim and Hoge Beuken, Antwerp, Belgium

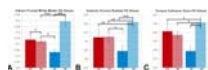
In this study, we used multi-shell, multi-tissue constrained spherical deconvolution to investigate group differences in white matter between control subjects, patients with mild cognitive impairment (MCI) due to Alzheimer's Disease (AD) and patients with dementia due to AD. Using the recently proposed fixel-based analysis approach, we distinguish between different fibre populations within a single voxel and characterize them with 3 measures: fibre density, fibre cross-section and the product of these two. We found significant decreases of these metrics in MCI and AD patients compared to healthy controls.

---

401

10:03

### HFE Mutations Alter White Matter Diffusion and Relaxation Parametrics in Alzheimer's Disease



Mark D Meadowcroft<sup>1,2</sup>, Jianli D. Wang<sup>2</sup>, Carson J Purnell<sup>1</sup>, Paul J Eslinger<sup>3</sup>, James R Connor<sup>1</sup>, and Qing X Yang<sup>2</sup>

<sup>1</sup>Neurosurgery, The Pennsylvania State University - College of Medicine, Hershey, PA, United States, <sup>2</sup>Radiology, The Pennsylvania State University - College of Medicine, Hershey, PA, United States, <sup>3</sup>Neurology, The Pennsylvania State University - College of Medicine, Hershey, PA, United States

This work demonstrates that HFE mutations in cognitively normal compared to wild-type subjects lead to differences in diffusion and relaxation parametrics, such that HFE mutation carrier parametrics converge towards AD subjects. Furthermore, HFE mutations appeared to be preservative against white matter integrity loss in AD patients. Iron-loading HFE mutations appear to preserve relaxation and diffusion neuroimaging biomarkers in AD patients, but adversely affect cognitively normal subjects.

---

Oral

## Late-Breaking Abstracts: Machine Learning

Room 313BC

Tuesday 8:15 - 10:15 Moderators: Tim Leiner & Reza Nezafat

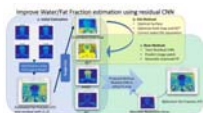
---

5657

8:15

### Improved Multi-echo Water-fat Separation Using Deep Learning

Enhao Gong<sup>1</sup>, Greg Zaharchuk<sup>2</sup>, and John Pauly<sup>1</sup>



<sup>1</sup>Electrical Engineering, Stanford University, Stanford, CA, United States,

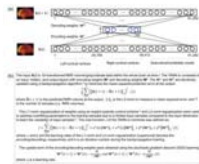
<sup>2</sup>Radiology, Stanford University, Stanford, CA, United States



Multi-echo water/fat separation may fail on cases due to noise, inaccurate estimation of water/fat signal and inhomogeneous  $B_0$  field. Here we developed novel data-driven method to improve water/fat separation using Deep Learning. A Residual-Convolutional-Neural-Network model was trained on image patches of multi-contrast information (from initial estimation of water/fat signal,  $R2^*$  map and field map), to generate better estimation of Fat-Fraction (FF) image patches and entire FF image. The proposed approach was validated and demonstrated improvement from existing methods on ISMRM datasets with variable anatomies. This method can handle flexible echo times in acquisition and is efficient and effective.

5658

8:27



Temporal-autoencoding neural network revealed the underlying functional dynamics of fMRI data: Evaluation using the Human Connectome Project data

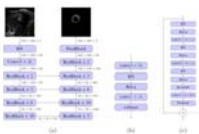
Jong-Hwan Lee<sup>1,2</sup>, Eric C. Wong<sup>3</sup>, and Peter Bandettini<sup>2</sup>

<sup>1</sup>Department of Brain and Cognitive Engineering, Korea University, Seoul, Korea, Republic of, <sup>2</sup>Section on Functional Imaging Methods, Laboratory of Brain and Cognition, National Institute of Mental Health, National Institutes of Health, Bethesda, MD, United States, <sup>3</sup>Department of Radiology, University of California, San Diego, La Jolla, CA, United States

We proposed a novel approach based on a temporal autoencoding neural network (TANN) model to predict the fMRI volume in the next time point or repetition time (TR) based on the fMRI volume in the present TR. Using motor task data from the Human Connectome Project, our TANN model revealed the human motor cortex dynamics. The highly task-specific foot, hand, and tongue networks within the motor-related areas were clearly identified from the TANN weight features and the task-associated networks across the frontal, parietal, temporal, and visual areas were also clearly parcellated without any task information.

5659

8:39



Fully Automated Left Ventricle Scar Quantification with Deep Learning

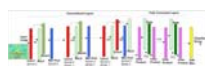
Johannes Rausch<sup>1</sup>, Bjoern Menze<sup>1</sup>, Raymond H Chan<sup>2</sup>, Jihye Jang<sup>1,3</sup>, Evan Appelbaum<sup>3</sup>, and Reza Nezafat<sup>3</sup>

<sup>1</sup>Technical University of Munich, Munich, Germany, <sup>2</sup>Toronto General Hospital, University Health Network, Toronto, Canada, <sup>3</sup>Department of Medicine, Beth Israel Deaconess Medical Center and Harvard Medical School, Boston, MA, United States

We present a fully automated approach for quantification of left ventricle scar in Late Gadolinium Enhancement (LGE) cardiac MR (CMR), using a residual neural network. LGE images were acquired in 1075 patients with known hypertrophic cardiomyopathy in a multi-center clinical trial. Scar segmentation was performed in all patients by a CMR-trained cardiologist. For training, we use a two-phase procedure, using cropped and full-sized images consecutively. We train different models using sigmoid cross-entropy loss and Dice loss and measure average LV segmentation Dice scores of  $0.77 \pm 0.10$  and  $0.70 \pm 0.12$  and estimated scar percentage mismatches of 3.59% and 3.00%, respectively.

5660

8:51



### Predicting Osteoarthritis Radiographic Incidence by Coupling Quantitative Compositional MRI and Deep Learning

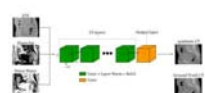
Valentina Padoia<sup>1</sup>, Jan Neumann<sup>1</sup>, Ursula Heilmeyer<sup>1</sup>, Jenny Haefeli<sup>1</sup>, Adam R Ferguson<sup>1</sup>, Thomas Link<sup>1</sup>, and Sharmila Majumdar<sup>1</sup>

<sup>1</sup>University of California, San Francisco, San Francisco, CA, United States

In this study quantitative compositional MRI and deep learning were coupled to discover latent feature representations, non-linear aggregation among elementary features able to characterize relaxation maps for Osteoarthritis diagnosis and progression prediction. 1,348 subjects from the Osteoarthritis Initiative (OAI) public dataset were considered.  $T_2$  relaxation map were automatically analyzed to build a 2D feature map used to train a convolutional neural network for the classification of subjects in OA, control and progression groups. The proposed method was able to detect OA subjects with 95.2% accuracy, and to detect controls subjects that demonstrated OA signs 4 years later with 80.7% accuracy.

5661

9:03



### Direct Pseudo-CT Image Synthesis Using Deep Learning for Pelvis PET/MR Attenuation Correction

Andrew Palmera Leynes<sup>1</sup>, Jaewon Yang<sup>2</sup>, Dattesh D Shanbhag<sup>3</sup>, Sandeep S Kaushik<sup>3</sup>, Florian Wiesinger<sup>4</sup>, Youngho Seo<sup>2</sup>, Thomas Armstrong Hope<sup>2</sup>, and Peder Larson<sup>1</sup>

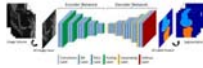
<sup>1</sup>Radiology and Biomedical Imaging, University of California San Francisco, San Francisco, CA, United States, <sup>2</sup>University of California San Francisco, San Francisco, CA, United States, <sup>3</sup>GE Global Research, Bangalore, India, <sup>4</sup>GE Global Research, Munich, Germany

A deep learning model with fully-convolutional networks was used to directly synthesize pseudo-CT images from MR images. The pseudo-CT images were used for MR-based attenuation correction (MRAC) of PET reconstruction in PET/MRI. The effects of the MRAC on high-uptake volumes are evaluated quantitatively. We demonstrate that the deep learning-based MRAC significantly improves PET uptake quantification.

5662



9:15



### Deep Convolutional Auto-Encoder and 3D Deformable Approach for Tissue Segmentation in Magnetic Resonance Imaging

Fang Liu<sup>1</sup>, Zhaoye Zhou<sup>2</sup>, Hyungseok Jang<sup>1</sup>, Alan McMillan<sup>1</sup>, and Richard Kijowski<sup>1</sup>

<sup>1</sup>Department of Radiology, University of Wisconsin-Madison, Madison, WI, United States, <sup>2</sup>Department of Biomedical Engineering, University of Minnesota, Minneapolis, MN, United States

A fully-automated segmentation pipeline was built by combining a deep Convolutional Auto-Encoder (CAE) network and 3D simplex deformable modeling. The CAE was applied as the core of the segmentation method to perform high resolution pixel-wise multi-class tissue classification. The 3D simplex deformable modeling refined output from CAE to preserve the overall shape and maintain a desirable smooth surface for structure. The fully-automated segmentation method was tested using a publicly available knee joint image dataset to compare with currently used state-of-the-art segmentation methods. The fully-automated method was also evaluated on morphological MR images with different tissue contrasts and image training datasets.

5663



9:27



### Improving the PI+CS Reconstruction for Highly Undersampled Multi-contrast MRI using Local Deep Network

Enhao Gong<sup>1</sup>, Greg Zaharchuk<sup>2</sup>, and John Pauly<sup>1</sup>

<sup>1</sup>Electrical Engineering, Stanford University, Stanford, CA, United States, <sup>2</sup>Radiology, Stanford University, Stanford, CA, United States

A typical clinical MR protocol includes multiple scans with different contrasts for complementary diagnostic information. Various methods have been proposed to specifically accelerate multi-contrast scans by using more complicated sparsity regularization in PI+CS.

Here we proposed a Non-iterative Deep-Learning approach to further improve existing methods for highly undersampled multi-contrast MRI reconstruction.

This method uses a Sequential+Joint+Local scheme, which takes fast PI+CS reconstruction as the initial input, uses a Deep-Network on local patches, and efficiently generates a better reconstruction for different contrasts with reduced noise and artifacts.

Experiments demonstrate the proposed method has superior performance compared with existing PI+CS methods.

5664

9:39

Functional Connectome Features				
Model	Accuracy	Sensitivity	Specificity	
Conventional	85.9%	88.2%	90.2%	
Proposed	87.0%	87.7%	89.0%	

Structural Connectome Features				
Model	Accuracy	Sensitivity	Specificity	
Conventional	88.1%	85.8%	90.0%	
Proposed	78.1%	76.9%	80.0%	

Integrated Functional and Structural Connectome Features				
Model	Accuracy	Sensitivity	Specificity	
Conventional	78.9%	84.6%	70.0%	
Proposed	81.3%	82.8%	80.0%	

## An Artificial Neural Network Framework for Early Prediction of Cognitive Deficits in Very Preterm Infants

Lili He<sup>1,2</sup>, Hailong Li<sup>1,2</sup>, Weihong Yuan<sup>1</sup>, and Nehal A. Parikh<sup>1,2</sup>

<sup>1</sup>*Pediatric Neuroimaging Research Consortium, Cincinnati Children's Hospital Medical Center, Cincinnati, OH, United States*, <sup>2</sup>*Perinatal Institute, Cincinnati Children's Hospital Medical Center, Cincinnati, OH, United States*

Annually, approximately 22,000 very preterm infants (i.e.  $\leq 32$  weeks gestational age) in the United States develop cognitive deficits. Infant brains are highly malleable, making it especially important to identify those at highest risk as early as possible to allow effective early interventions. Research supports the notion that cognitive deficits may result from a disturbance/breakdown in the connectome. We propose to develop a robust artificial neural network framework that can analyze integrated structural and functional brain connectome data obtained at term corrected age to predict long-term cognitive outcomes in very preterm infants.

5665

9:51

	Median [min, max]
Age	69 [18, 92]
Time, onset to MRI	128 [15, 525]
Admission NIHSS	8 [1, 26]
Follow-up FLAIR volume (ml)	4.8 [0, 211.1]
DWI volume (ml)	4.0 [0, 173.7]
TTP volume (ml)	42.3 [0, 369.4]
Follow up FLAIR time (days)	32 [18, 47] <sup>1,2</sup>

## Deep learning: Utilizing the potential in data bases to predict individual outcome in acute stroke

Anne Nielsen<sup>1,2</sup>, Kim Mouridsen<sup>1</sup>, Mikkel Bo Hansen<sup>1</sup>, and Jens Kjærgaard Boldsen<sup>1</sup>

<sup>1</sup>Center of Functionally Integrative Neuroscience and MINDLab, Institute of Clinical Medicine, Aarhus University, Aarhus C, Denmark, <sup>2</sup>Combat Stroke, Aarhus C, Denmark

Acute ischemic stroke is a major disease and one of the leading causes of adult death and disability. Brain tissue infarcts permanently within hours after onset and rapid reperfusion treatment is therefore of utmost importance. Current methods to predict the tissue outcome are too simplistic. In this project a more advanced approach using deep neural networks to utilize the information from previous patient developments was established and compared to current state-of-the-art. The predictions from the deep neural networks were showed to be superior to the state-of-the-art method improving prediction accuracy and hence leading to better decision support.

---

5666

10:03



### Cardiovascular Event Prediction by Machine Learning: The Multi-Ethnic Study of Atherosclerosis

Bharath Ambale Venkatesh<sup>1</sup>, Xiaoying Yang<sup>2</sup>, Colin Wu<sup>3</sup>, W. Gregory Hundley<sup>4</sup>, Antoinette S Gomes<sup>5</sup>, Eliseo Guallar<sup>6</sup>, David A Bluemke<sup>3</sup>, and Joao A C Lima<sup>6</sup>

<sup>1</sup>Radiology, Johns Hopkins University, Baltimore, MD, United States,

<sup>2</sup>George Washington University, Washington DC, DC, United States,

<sup>3</sup>National Institutes of Health, Bethesda, MD, United States, <sup>4</sup>Wake Forest University Health Sciences, Winston-Salem, NC, United States,

<sup>5</sup>UCLA School of Medicine, Los Angeles, CA, United States, <sup>6</sup>Johns Hopkins University, Baltimore, MD, United States

Event prediction has been the cornerstone of cardiovascular epidemiology and have allowed us to characterize sub-clinical disease processes and target key risk factors for modification. Epidemiological studies used to derive such predictive models frequently contain hundreds of variables from multiple tests. Random survival forests may be an effective machine learning strategy for incident event prediction in large populations with large phenotypic datasets. These methods do not require a priori assumptions regarding causality and may thus be suitable to defining the role of novel biomarkers and tests (such as imaging, biomarker panels, ECG, etc) for cardiovascular disease prediction. We explore the role of MRI in the prediction of incident heart failure and all-cause death.

---

---



Oral

## Functional & Diffusion MRS

Room 316A

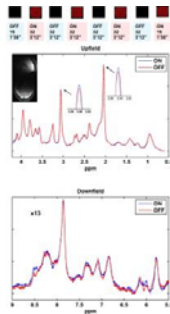
Tuesday 8:15 - 10:15

Moderators: Malgorzata Marjanska & Itamar Ronen

402



8:15



### Functional Magnetic Resonance Spectroscopy (fMRS) using metabolite cycled semi-LASER at 9.4T: a pilot study

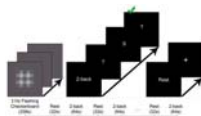
Ioannis-Angelos Giapitzakis<sup>1,2</sup>, Nikolai Avdievitch<sup>1</sup>, Saipavitra Murali Manohar<sup>1</sup>, Nicole Fichtner<sup>3,4</sup>, Roland Kreis<sup>3</sup>, and Anke Henning<sup>1,5</sup>

<sup>1</sup>High Field Magnetic Resonance, Max Planck Institute for Biological Cybernetics, Tuebingen, Germany, <sup>2</sup>Graduate School of Neural and Behavioural Sciences, Tuebingen, Germany, <sup>3</sup>Departments of Radiology and Clinical Research, University Bern, Bern, Switzerland, <sup>4</sup>Institute for Biomedical Engineering, UZH and ETH Zurich, Zurich, Switzerland, <sup>5</sup>Institute of Physics, Ernst-Moritz-Arndt University Greifswald, Greifswald, Germany

The purpose of this work is to explore the potentials of fMRS under a visual stimulation at 9.4T using a metabolite cycled (MC) semi-LASER sequence. The MC technique allows for simultaneous acquisition of water and metabolite spectra enabling the synchronous investigation of dynamic alternations of BOLD signal and metabolite levels. Correlation of FWHM<sub>Cr</sub> and FWHM<sub>NAA</sub> with SNR<sub>water</sub> is demonstrated. The influence of misaligned subtraction is evaluated and the requirement of linewidth, frequency and phase-correction is highlighted. Finally, all previously reported alterations of upfield metabolites are confirmed and for first time also potential difference of downfield metabolites are observed.

403

8:27



### Glutamate modulation during working memory task performance: A functional proton magnetic resonance spectroscopy study in healthy adult volunteers

Eric Andrew Woodcock<sup>1</sup>, Chaitali Anand<sup>1</sup>, Jonathan Lynn<sup>1</sup>, Dalal Khatib<sup>1</sup>, and Jeffrey A Stanley<sup>1</sup>

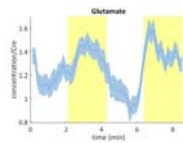
<sup>1</sup>Psychiatry and Behavioral Neurosciences, Wayne State University School of Medicine, Detroit, MI, United States

Glutamate is involved in excitatory neurotransmission and oxidative metabolism. *In vivo* glutamate measurements at task-relevant temporal resolution are possible using functional proton magnetic resonance spectroscopy. The present study quantified glutamate levels in the dorsolateral prefrontal cortex during working memory task performance and interspersed periods of rest. Results demonstrated that our approach was feasible and quantification of glutamate levels was reliable at 32s temporal resolution. Statistical analyses demonstrated that glutamate levels were elevated during working memory task performance (relative to rest), consistent with our hypotheses. Elevated glutamate levels during task performance likely reflect increased oxidative metabolism due to excitatory neurotransmission.

404



8:39



Dynamic changes of glutamate detected by functional MR spectroscopy in human visual cortex in regions with positive and negative BOLD response

Miguel Martínez-Maestro<sup>1</sup>, Christian Labadie<sup>2</sup>, Ioannis Angelos Giapitzakis<sup>3</sup>, and Harald E. Möller<sup>1</sup>

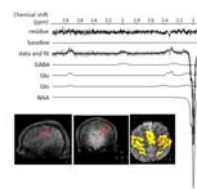
<sup>1</sup>Max Planck Institute for Human Cognitive and Brain Sciences, Leipzig, Germany, <sup>2</sup>Berlin Center for Advanced Neuroimaging, Charité Universitätsmedizin, Berlin, Germany, <sup>3</sup>Max Planck Institute for Biological Cybernetics, Tuebingen, Germany

Dynamic changes of metabolite concentrations have been presented in human visual cortex in response to stimulus that induce a positive BOLD response (PBR). The present study compares the metabolic profile of the positive and the negative bold response (NBR). The application of different fMRS block designs showed a significant increase in Glutamate (+7.3%) during the PBR stimulation paradigm in agreement with previous studies and a decrease (-6.6%) during the NBR, which provides new information about its underlying mechanisms.

405



8:51



Activation induced changes in GABA: functional MRS at 7T with MEGA-SLASER

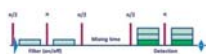
Chen Chen<sup>1</sup>, Hilmar P. Sigurdsson<sup>2</sup>, Sophia E. Pépés<sup>2</sup>, Dorothee P. Auer<sup>3</sup>, Penny A. Gowland<sup>1</sup>, Paul S. Morgan<sup>3</sup>, and Stephen R. Jackson<sup>2</sup>

<sup>1</sup>Sir Peter Mansfield Imaging Centre, University of Nottingham, Nottingham, United Kingdom, <sup>2</sup>School of Psychology, University of Nottingham, Nottingham, United Kingdom, <sup>3</sup>School of Medicine, University of Nottingham, Nottingham, United Kingdom

To investigate changes in GABA levels in human motor cortex in response to the hand clenching task, the macromolecule-corrected MEGA-sLASER sequence was used in functional MRS (fMRS) experiments conducted at 7T. During motor activation, the total creatine (tCr) signal remained stable, while a significant transient increase in GABA/tCr ( $20\% \pm 11\%$ ) was observed. The measured increase in Glx/tCr ( $12\% \pm 6\%$ ) was higher but consistent with changes reported for Glutamate. With consistent editing performance for GABA detection and the advantage of visually identifying GABA peaks in spectra, this spectral editing approach showed its potential for future fMRS studies of GABA.

406

9:03



Detection of Changes in the Creatine Kinase Cycle Rate in the Human Visual Cortex During Visual Stimulation with Filter Exchange 1H MR Spectroscopy (FEXSY) at 7T

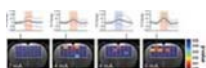
Casper Wolf<sup>1</sup>, Andrew Webb<sup>2</sup>, and Itamar Ronen<sup>2</sup>

<sup>1</sup>Vrije Universiteit, Amsterdam, Netherlands, <sup>2</sup>Radiology, Leiden University Medical Center, Leiden, Netherlands

We selectively monitored the Cr/PCr exchange rate during visual stimulation using filter exchange spectroscopy (FEXSY), a pulse sequence sensitized to exchange between two pools with different diffusion coefficients. A significant difference was observed between the filtered and non-filtered D(tCr) during rest, and vanished during stimulation, indicating an increase in the rate of creation of a fast-diffusing species in the tCr complex during stimulation. This suggests an increased production of Cr from PCr resulting from increased metabolic demand, or an increase in “free” vs. enzyme-bound tCr. The non-filtered ADC of NAA significantly increased during activation, suggesting microstructural change during activation.

407

9:15



Dynamics of lactate levels measured by functional proton magnetic resonance imaging in the rat somatosensory cortex upon increasing electrical hindpaw stimuli.

Aline Seuwen<sup>1</sup>, Aileen Schroeter<sup>1</sup>, and Markus Rudin<sup>1,2</sup>

<sup>1</sup>Institute for Biomedical Engineering, University & ETH Zürich, Zürich, Switzerland, <sup>2</sup>Institute of Pharmacology and Toxicology, University of Zurich



MRSI in mice reveals changes in glutamate and lactate levels in somatosensory brain areas elicited by electric hindpaw stimulation. Using increasing stimulus amplitudes, lactate signals consistently decreased with increasing stimulus strength. This surprising result might reflect accelerated lactate clearance triggered by a generalized CBF increase in response to hindpaw stimulation, previously observed in this species. In contrast to mice, Lac levels in the contralateral somatosensory cortex of rats significantly increased with stimulus amplitude reflecting increased glycolytic activity and no obvious indication of increased lactate clearance. Despite the difference in Lac responses, similar Glu responses have been observed in both species.

408

9:27



Apparent diffusion coefficients of the five major metabolites in the human brain at 3 T

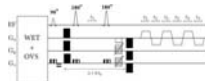
Dinesh K Deelchand<sup>1</sup>, Edward J Auerbach<sup>1</sup>, and Malgorzata Marjańska<sup>1</sup>

<sup>1</sup>CMRR, University of Minnesota, Minneapolis, MN, United States

The goal of this study was to measure the apparent diffusion coefficients (ADC) of five main metabolites in the human brain at 3 T using PRESS and STEAM sequences where measurement biases due to cross-terms were avoided by using positive and negative diffusion gradient polarity. This study shows that comparable trace/3 ADC values for total *N*-acetyl aspartate, total creatine, total choline, glutamate and *myo*-inositol can be successfully measured with both acquisition methods on a clinical scanner with STEAM providing slightly better quantification precision for *J*-coupled metabolites.

409

9:39



Diffusion-Weighted Echo Planar J-resolved Spectroscopic Imaging

Manoj K Sarma<sup>1</sup>, Zohaib Iqbal<sup>1</sup>, Andres Saucedo<sup>1</sup>, Paul M Macey<sup>2</sup>, and M. Albert Thomas<sup>1</sup>

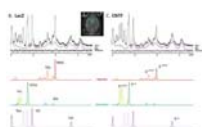
<sup>1</sup>Radiological Sciences, UCLA School of Medicine, Los Angeles, CA, United States, <sup>2</sup>School of Nursing, UCLA School of Medicine, Los Angeles, CA, United States

Diffusion weighted spectroscopy enables investigation of brain intracellular microstructure in-vivo. Here we implemented a novel technique called diffusion-weighted echo-planar J-resolved spectroscopic imaging (DW-EPJRESI) which is capable of giving information about metabolite diffusivity beyond NAA, Cr and Cho in multiple brain locations simultaneously. The technique was evaluated in a brain phantom and four healthy volunteers. Highly reproducible diffusion-weighted metabolite maps were obtained. The ADC values were in good agreement with previous reported values. Further optimization of the DW-EPJRESI sequence will become more practical for clinical use.

410



9:51



Probing alterations of cellular metabolism and structure in CNTF-induced mouse model of astrocytic activation using in vivo MRS and diffusion-weighted MRS

Clemence Ligneul<sup>1</sup>, Marco Palombo<sup>1</sup>, Edwin Hernandez Gazon<sup>1</sup>, Martine Guillermier<sup>1</sup>, Sueva Bernier<sup>1</sup>, Kelly Ceyzeriat<sup>1</sup>, Laurene Abjean<sup>1</sup>, Julien Flament<sup>1,2</sup>, Carole Escartin<sup>1</sup>, and Julien Valette<sup>1</sup>

<sup>1</sup>Molecular Imaging Research Center (MIRCent), Commissariat à l'Energie Atomique (CEA), Fontenay aux Roses, France, <sup>2</sup>UMS 27, INSERM, Fontenay aux Roses, France

In this work we use in vivo MRS and diffusion-weighted MRS (DW MRS) on a model of astrocytic activation induced by the ciliary neurotrophic factor (CNTF) in mice striatum. We observe a massive metabolic remodeling in CNTF mice in comparison with control mice. We demonstrate the intrinsic potential of DW MRS to detect alterations in cellular structure by measuring substantial variations in diffusion properties of astrocytic and neuronal metabolites. Modeling suggests significantly larger astrocytic processes, consistently with astrocytic hypertrophy as observed by microscopy in the context of activation.

411

10:03



Comparison diffusion behavior of metabolites in brains of congenital portal systemic shunt and healthy mice in vivo at 14.1T

Masoumeh Dehghani<sup>1</sup>, Nicolas Kunz<sup>2</sup>, Rolf Gruetter<sup>1,2,3</sup>, and Hongxia Lei<sup>2,3</sup>

<sup>1</sup>Laboratory of Functional and Metabolic Imaging (LIFMET), Ecole Polytechnique Fédérale de Lausanne, Lausanne, Switzerland, <sup>2</sup>Center for Biomedical Imaging (CIBM), Ecole Polytechnique Fédérale de Lausanne, Lausanne, Switzerland, <sup>3</sup>Department of Radiology, University of Geneva, Geneva, Switzerland

The aim of this study was to determine whether diffusion behavior of metabolites in the congenital portal systemic shunt (PSS) mouse brain is different from ones of the healthy controls *in vivo*, combining large diffusion weighting and <sup>1</sup>H MRS methods. The diffusion behavior of most investigated metabolites except taurine was in excellent agreement with those in control mouse brain. The reduced diffusivities of taurine in PSS mice compared to control ones may be due to possible cellular redistribution of taurine in response to some osmotic perturbations in PSS mice *in vivo*, however, it needs to be further explored.

---

## Oral

### MS: Spinal Cord

Room 320

Tuesday 8:15 - 10:15 Moderators: Nivedita Agarwal & Gary Miller

---

412

8:15



#### SPINAL CORD SODIUM AND AXONAL LOSS IN MULTIPLE SCLEROSIS

Bhavana Shantilal Solanky<sup>1</sup>, Ferran Prados<sup>2</sup>, Carmen Tur<sup>1</sup>, Sebastien Ourselin<sup>2</sup>, Xavier Golay<sup>3</sup>, Olga Ciccarelli<sup>1</sup>, and Claudia A M Gandini Wheeler-Kingshott<sup>1,4,5</sup>

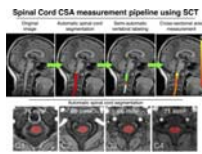
<sup>1</sup>UCL Institute of Neurology, Queen Square MS Centre, University College London, London, United Kingdom, <sup>2</sup>Translational Imaging Group, Centre for Medical Image Computing, Department of Medical Physics and Biomedical Engineering, University College London, London, United Kingdom, <sup>3</sup>UCL Institute of Neurology, University College London, London, United Kingdom, <sup>4</sup>Department of Brain and Behavioural Sciences, University of Pavia, Pavia, Italy, <sup>5</sup>Brain MRI 3T Mondino Research Center, C. Mondino National Neurological Institute, Pavia, Italy

Increased sodium concentration in the normal appearing brain of multiple sclerosis (MS) patients has recently been reported, which may be a consequence of axonal loss or an accumulation of intracellular sodium. Here we investigated spinal cord total sodium concentrations in MS patients and healthy controls. Spinal cord atrophy, as a result of axonal loss, often presents in MS, therefore we also tested for the association of sodium with SC area. We found increased total sodium levels in the SC, but no correlation with the decrease in SC cross sectional area in the MS cohort.

413



8:27



Repeatability and reproducibility of spinal cord atrophy measurements in a multiple sclerosis population using the Spinal Cord Toolbox

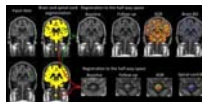
Benjamin De Leener<sup>1</sup>, Tobias Granberg<sup>2,3</sup>, Katharina Fink<sup>4,5</sup>, Nikola Stikov<sup>1,6</sup>, and Julien Cohen-Adad<sup>1,7</sup>

<sup>1</sup>NeuroPoly Lab, Institute of Biomedical Engineering, Polytechnique Montreal, Montreal, QC, Canada, <sup>2</sup>Department of Clinical Science, Intervention and Technology, Karolinska Institutet, Stockholm, Sweden, <sup>3</sup>Department of Radiology, Karolinska University Hospital, Stockholm, Sweden, <sup>4</sup>Department of Clinical Neuroscience, Karolinska Institutet, Stockholm, Sweden, <sup>5</sup>Department of Neurology, Karolinska University Hospital, Stockholm, Sweden, <sup>6</sup>Montreal Heart Institute, Montreal, QC, Canada, <sup>7</sup>Functional Neuroimaging Unit, CRIUGM, Université de Montréal, Montreal, QC, Canada

Spinal cord atrophy is a major determinant of physical disability in multiple sclerosis (MS) and other diseases with neurodegeneration. The upper spinal cord cross-sectional area (CSA) is therefore a clinically important measurement reflecting global spinal cord atrophy. New image analysis software enable semi- and fully-automatic quantification of spinal cord atrophy. This study characterizes the repeatability and reproducibility of semi-automatic CSA measurements of the spinal cord in healthy subjects and in patients with multiple sclerosis, using the Spinal Cord Toolbox (SCT). Results demonstrated the high repeatability and reproducibility of CSA measures using SCT in both healthy persons and in MS.

414

8:39



Boundary shift integral to compute brain and cervical spinal cord longitudinal volume changes using the same 3DT1w volumetric scans in multiple sclerosis



Ferran Prados<sup>1,2</sup>, Özgür Yaldizli<sup>3</sup>, Manuel Jorge Cardoso<sup>1</sup>, Marios C Yiannakas<sup>2</sup>, Francesco Grussu<sup>2</sup>, Esther Ruberte<sup>4</sup>, Jens Wuerfel<sup>4</sup>, Frederik Barkhof<sup>1,2,5</sup>, Claudia AM Gandini Wheeler-Kignshott<sup>2,6,7</sup>, and Sebastien Ourselin<sup>1</sup>

<sup>1</sup>*Translational Imaging Group, CMIC, Dep. of Medical Physics and Biomedical Engineering, University College London, London, United Kingdom,* <sup>2</sup>*UCL Institute of Neurology, Queen Square MS Centre, University College London, London, United Kingdom,* <sup>3</sup>*Department of Neurology, University Hospital Basel, Switzerland,* <sup>4</sup>*Medical Image Analysis Center Basel, Switzerland,* <sup>5</sup>*Radiology & Nuclear Medicine, VU University Medical Centre, Netherlands,* <sup>6</sup>*Department of Brain and Behavioural Sciences, University of Pavia, Italy,* <sup>7</sup>*Brain MRI 3T Mondino Research Center, C. Mondino National Neurological Institute, Italy*

Brain atrophy is considered to be the net accumulative irreversible disease burden as the ultimate consequence of different pathological processes found in the multiple sclerosis brain. A recent cross-sectional study demonstrated the possibility to assess atrophy of the spinal cord using 3DT1w brain volumetric scans. However, to date, no unified technique has been presented to longitudinally assess brain and spinal cord atrophy using the same MRI acquisition. Here we present a proof-of-concept data from a pipeline that uses the boundary shift integral to compute both brain and cervical spinal cord atrophy rates using the same 3DT1w brain volumetric scans.

---

415

8:51



Improved Visualization of the Spinal Cord Lesions in Multiple Sclerosis using MP2RAGE at 3T

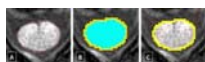
Jennifer A. Lefevre<sup>1,2</sup>, Sunil Patil<sup>3</sup>, Gunnar Krueger<sup>4</sup>, Tobias Kober<sup>5,6,7</sup>, Stéphane Lehericy<sup>2</sup>, Daniel S. Reich<sup>1</sup>, and Govind Nair<sup>1</sup>

<sup>1</sup>*TNS/NIB/NINDS, National Institutes of Health, Bethesda, MD, United States,* <sup>2</sup>*CENIR, UPMC-Inserm U1127, CNRS 7225, Institut Cerveau Moelle, Paris, France,* <sup>3</sup>*HC NAM USA DI MR COLLAB, Siemens Medical Solutions, Bethesda, MD, United States,* <sup>4</sup>*HC NAM USA DI MR COLLAB, Siemens Medical Solutions, Boston, MA, United States,* <sup>5</sup>*Advanced Clinical Imaging Technology, Siemens Healthcare AG, Lausanne, Switzerland,* <sup>6</sup>*Department of Radiology, Centre Hospitalier Universitaire Vaudois, Lausanne, Switzerland,* <sup>7</sup>*Signal Processing Laboratory (LTS 5), Ecole Polytechnique Fédérale de Lausanne, Lausanne, Switzerland*

Spinal cord lesions are known to be prevalent and contribute to disability in multiple sclerosis (MS). We explored the use of the MP2RAGE sequence for better delineation of spinal cord lesions in a clinical setting, and compared it with standard sequences used in MS. A more accurate measurement of lesion load and better visualization of the lesion location within the spinal cord can help improving MS diagnosis and may be developed to an imaging biomarker of disease burden.

416

9:03



Outer spinal cord rim visualization using magnetization-prepared 3D T1w TFE at 3T: Application to multiple sclerosis.

Marios C Yiannakas<sup>1</sup>, Torben Schneider<sup>2</sup>, Matthew Clemence<sup>2</sup>, James Fairney<sup>3</sup>, Ferran Prados<sup>1,4</sup>, Hugh Kearney<sup>1</sup>, Sebastien Ourselin<sup>4</sup>, David H Miller<sup>1,5</sup>, and Claudia AM Gandini Wheeler-Kingshott<sup>1,6,7</sup>

<sup>1</sup>UCL Institute of Neurology, Queen Square MS Centre, University College London, London, United Kingdom, <sup>2</sup>Philips Healthcare, Guildford, United Kingdom, <sup>3</sup>Medical Physics and Biomedical Engineering, University College London, London, United Kingdom, <sup>4</sup>Translational Imaging Group, CMIC, Dep. of Medical Physics and Biomedical Engineering, University College London, London, United Kingdom, <sup>5</sup>UCL-UCLH NIHR Biomedical Research Centre, London, United Kingdom, <sup>6</sup>Department of Brain and Behavioural Sciences, University of Pavia, Pavia, Italy, <sup>7</sup>Brain MRI 3T Mondino Research Center, C. Mondino National Neurological Institute, Pavia, Italy

Neuropathological studies in multiple sclerosis (MS) have suggested that meningeal inflammation in the brain and spinal cord (SC) may be associated with disease progression. However, the use of structural imaging protocols to depict meningeal tissues has not been reported. Herein, we investigate the feasibility of obtaining sufficiently high image contrast to resolve the SC rim that we speculate corresponds to the SC pia mater (SCPM) using the magnetization-prepared 3D T1w TFE sequence. Preliminary results show that it is possible to resolve SCPM, and that significant differences in signal intensity values within SCPM exist between healthy controls and people with MS.

417

9:15



On the Relationship between Tissue Damage in Cervical Spinal Cord and Brain in Multiple Sclerosis.

Biao Xiang<sup>1</sup>, Jie Wen<sup>2</sup>, Amber Salter<sup>3</sup>, Anne H. Cross<sup>3</sup>, and Dmitriy A. Yablonskiy<sup>2</sup>

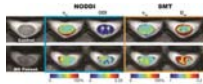
<sup>1</sup>Department of Chemistry, Washington University in St. Louis, Saint Louis, MO, United States, <sup>2</sup>Department of Radiology, Washington University in St. Louis, St. Louis, MO, United States, <sup>3</sup>Department of Neurology, Washington University in St. Louis, St. Louis, MO, United States

We examined quantitative relationships between tissue damage in the cervical spinal cord (characterized by cross-sectional area (CSA)) and cortical gray matter (GM) (characterized by thickness and tissue specific  $R2^*$  values) in multiple sclerosis (MS) patients, and determined relative contributions of these to neurologic disability. We found correlations between CSA and GM  $R2^*$  values and thickness of several cortical regions. Compared with cortical  $R2^*$  and thickness, cervical spinal cord CSA correlated better with neurological impairment status. CSA, thickness and age-corrected  $R2^*$  values all differentiated MS subjects from healthy Controls. CSA and GM thickness could further distinguish MS clinical subtypes.

---

418

9:27



#### Investigation of Advanced Diffusion Models in the Spinal Cord: Comparison of NODDI and SMT in MS Patients

Samantha By<sup>1,2</sup>, Junzhong Xu<sup>2,3</sup>, Bailey Box<sup>2</sup>, and Seth A. Smith<sup>1,2,3</sup>

<sup>1</sup>Biomedical Engineering, Vanderbilt University, Nashville, TN, United States, <sup>2</sup>Vanderbilt University Institute of Imaging Science, Vanderbilt University Medical Center, Nashville, TN, United States, <sup>3</sup>Radiology and Radiological Sciences, Vanderbilt University Medical Center, Nashville, TN, United States

NODDI and Spherical Mean Technique (SMT) are multi-compartmental diffusion models that have demonstrated promise in the brain, but have never been applied to the in vivo spinal cord in multiple sclerosis (MS) patients. These models estimate axonal volume fractions, which can be indicative of microstructural integrity. We apply NODDI and SMT in healthy controls and MS patients to evaluate feasibility of both models in the human spinal cord. Results indicate that NODDI ( $p=0.004$ ) and SMT ( $p=0.030$ ) can characterize disparity in axonal volume fraction in MS patients, suggesting potential utility of advanced diffusion models in the spinal cord.

---

419

9:39

#### Column-specific demyelination in Spinal Cord Normal Appearing White Matter occurring in Multiple Sclerosis: A preliminary study using inhomogeneous Magnetization Transfer and DTI

Author	Henitsoa RASOANANDRIANINA, Bertrand AUDOIN, Olivier GIRARD, Guillaume DUHAMEL, Sarah DEMORTIERE, Maxime GUYE, Jean-Philippe RANJEVA, Jean PELLETIER, and Virginie CALLOT
Title	
Abstract	
Keywords	
DOI	
URL	
Notes	

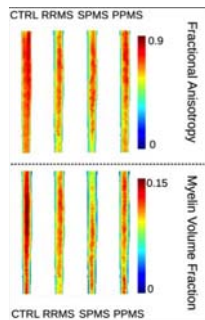
Henitsoa RASOANANDRIANINA<sup>1,2,3</sup>, Bertrand AUDOIN<sup>1,4</sup>, Olivier GIRARD<sup>1,2</sup>, Guillaume DUHAMEL<sup>1,2</sup>, Sarah DEMORTIERE<sup>4</sup>, Maxime GUYE<sup>1,2</sup>, Jean-Philippe RANJEVA<sup>1,2</sup>, Jean PELLETIER<sup>1,4</sup>, and Virginie CALLOT<sup>1,2,3</sup>

<sup>1</sup>Aix Marseille Univ, CNRS, CRMBM, Marseille, France, <sup>2</sup>AP-HM, Pôle d'Imagerie Médicale, Hopital de La Timone, CEMEREM, Marseille, France, <sup>3</sup>iLab-Spine International Associated Laboratory, Marseille, France, <sup>4</sup>Aix Marseille Univ, APHM, Hopital de La Timone, Pôle de Neurosciences Cliniques, Service de Neurologie, Marseille, France

This preliminary study investigates the added value of the inhomogeneous Magnetization Transfer (ihMT) technique when studying Spinal Cord (SC) tissue demyelination occurring in Multiple Sclerosis (MS). DTI and MT/ihMT data collected in 9 MS patients, analyzed in specific normal appearing white matter regions, indicated significant demyelination in corticospinal and posterior sensory tracts as compared to age-matched healthy controls, with a very high sensitivity of ihMTR that appears very promising for further objective therapeutic evaluation or topographic quantification of progressive SC demyelination.

420

9:51

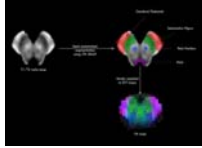


### Comparative Myelin Imaging and Multi-Shot Diffusion Tensor Imaging in Multiple Sclerosis Cervical Spinal Cord

Hagen H Kitzler<sup>1</sup>, Hannes Wahl<sup>1</sup>, Gesine Pach<sup>1</sup>, Judith C Eisele<sup>2</sup>, Katja Thomas<sup>2</sup>, Sean Deoni<sup>3</sup>, Tjalf Ziemssen<sup>2</sup>, and Jennifer Linn<sup>1</sup>

<sup>1</sup>Neuroradiology, Technische Universität Dresden, Dresden, Germany, <sup>2</sup>Neurology, Technische Universität Dresden, Dresden, Germany, <sup>3</sup>Pediatric Radiology Research, Children's Hospital, Colorado, University of Colorado Medical School, Boulder, CO, United States

Spinal cord myelin imaging holds potential to quantify cervical spinal cord tissue myelin loss, and hence, the subtle spinal burden of demyelinating diseases, invisible for conventional magnetic resonance imaging. We present the approach of combined spinal 3D double-inversion recovery imaging with diffusion tensor imaging and myelin sensitive multicomponent driven equilibrium single pulse observation of T1 and T2, with subsequent normal spine space registration and group comparison in different multiple sclerosis courses. Whereas no significant differences were found between the different disease courses using fractional anisotropy, relapsing-remitting and primary-progressive multiple sclerosis were discriminated based on differences in relative cord myelin content.



### DTI abnormalities in the midbrain in pediatric-onset multiple sclerosis.

Ritobrato Datta<sup>1,2</sup>, Sophia Ly<sup>3</sup>, Christine Till<sup>4</sup>, Elisea De Somma<sup>4</sup>, Nadine Akbar<sup>5</sup>, Sudipto Dolui<sup>6</sup>, Douglas L. Arnold<sup>7</sup>, Sridar Narayanan<sup>8</sup>, and Brenda L. Banwell<sup>1</sup>

<sup>1</sup>Neurology, The Children's Hospital of Philadelphia, Philadelphia, PA, United States, <sup>2</sup>Neurology, University of Pennsylvania, Philadelphia, PA, United States, <sup>3</sup>Biology, University of Pennsylvania, Philadelphia, PA, United States, <sup>4</sup>Psychology, York University, Toronto, ON, Canada, <sup>5</sup>Hospital for Sick Children, Toronto, ON, Canada, <sup>6</sup>Radiology, University of Pennsylvania, Philadelphia, PA, United States, <sup>7</sup>Montreal Neurological Institute, McGill University, Montreal, QC, Canada, <sup>8</sup>Neurology and Neurosurgery, Montreal Neurological Institute, McGill University, Montreal, QC, Canada

Pediatric-onset MS (POMS) is characterized by a high frequency of brainstem lesions early in the disease. It is unknown whether normal-appearing tissue in this region is involved at this early time point. Using diffusion tensor imaging (DTI) at 3T, we evaluated fractional anisotropy (FA) changes in midbrain substructures in POMS patients and age- and sex-matched healthy controls. Mean FA of midbrain was significantly reduced in the MS group, a difference that remained significant even after removing any focal midbrain lesions. Our results indicate a widespread disruption in the midbrain that exceeds lesional tissue disruption alone.

## Combined Educational & Scientific Session

### 4D Flow MRI: Moving to Clinical Practice

Organizers: Harald Kramer, M.D.

Room 315      Tuesday 8:15 - 10:15      Moderators: Harald Kramer & Sergio Uribe

8:15

4D Flow MRI: Technical

tino ebbers<sup>1</sup>

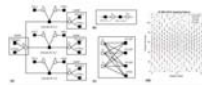
<sup>1</sup>linkoping university

Four-dimensional flow magnetic resonance imaging (4D flow MRI) enables comprehensive access to time-varying and multidirectional blood flow through the cavities of the heart and great vessels. This presentation aims to assist understanding of acquisition and analysis methods of 4D flow MRI with a focus on the heart and greater vessels. Different visualization strategies and computation of derived flow parameters, as wall shear stress, pressure difference, turbulent kinetic energy, and intracardiac flow components, are discussed.

422



8:45



### A Bayesian Approach to Enable Single Breath-Hold 4D Flow MRI

Adam Rich<sup>1</sup>, Lee C. Potter<sup>1,2</sup>, Ning Jin<sup>3</sup>, Yingmin Liu<sup>2</sup>, Orlando P. Simonetti<sup>2,4,5</sup>, and Rizwan Ahmad<sup>1,2</sup>

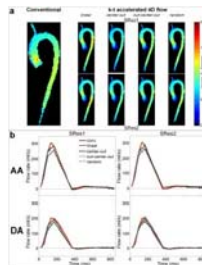
<sup>1</sup>Electrical and Computer Engineering, The Ohio State University, Columbus, OH, United States, <sup>2</sup>Dorothy M. Davis Heart and Lung Research Institute, The Ohio State University, Columbus, OH, United States, <sup>3</sup>Siemens Medical Solutions, Columbus, OH, United States, <sup>4</sup>Department of Radiology, Columbus, OH, United States, <sup>5</sup>Division of Cardiovascular Medicine Department of Internal Medicine, Columbus, OH, United States

PC-MRI based 4D flow imaging is a powerful tool to quantify hemodynamics within the heart and the great vessels. We develop a Bayesian technique to greatly accelerate 4D flow image acquisition. Our technique exploits the rich structure in 4D flow images within a joint reconstruction algorithm. We validate the technique using retrospectively accelerated flow phantom data and prospectively accelerated, single breath-hold in vivo data. In the flow phantom, stroke volume differed by  $\leq 9\%$  for  $R \leq 28$  when compared to fully sampled data. The high acceleration provided by the Bayesian approach could allow for clinical application of single breath-hold 4D flow imaging.

423



9:00



### k-t accelerated aortic 4D flow MRI in under 2 minutes: feasibility and impact of resolution, k-space sampling patterns, and respiratory navigator gating on hemodynamic measurements

Emilie Bollache<sup>1</sup>, Alex J. Barker<sup>1</sup>, Jeremy D. Collins<sup>1</sup>, Pim van Ooij<sup>2</sup>, Rouzbeh Ahmadian<sup>1</sup>, Alex Powell<sup>1</sup>, James C. Carr<sup>1</sup>, Julia Geiger<sup>1</sup>, and Michael Markl<sup>1,3</sup>

<sup>1</sup>Department of Radiology, Northwestern University, Chicago, IL, United States, <sup>2</sup>Department of Radiology, Academic Medical Center, Amsterdam, Netherlands, <sup>3</sup>Department of Biomedical Engineering, Northwestern University, Chicago, IL, United States

Our objective was to assess the performance of eight highly k-t accelerated non-gated free-breathing aortic 4D flow MRI measurements acquired in under 2 minutes (PEAK GRAPPA R=5; TRes=67.2ms; four  $k_y$ - $k_z$ -space Cartesian fillings: linear, center-out, out-center-out, random; two spatial resolutions= $3.5 \times 2.3 \times 2.6 \text{mm}^3$ ,  $4.5 \times 2.3 \times 2.6 \text{mm}^3$ ), both *in vitro* and in 10 healthy volunteers. Despite lower image quality, the significantly shorter k-t accelerated datasets provided aortic hemodynamic indices in agreement with conventional respiratory-gated 4D flow measurements. Differences were non-significant when using linear and out-center-out k-space samplings (absolute differences  $\leq 22\%$ ). In conclusion, aortic 4D flow MRI in under 2 minutes is feasible with moderate underestimation of flow indices.

---

9:15

#### 4D Flow: Clinical

Ann Bolger<sup>1,2</sup>

<sup>1</sup>Medicine, University of California, San Francisco, San Francisco, CA, United States, <sup>2</sup>Linköping University, Linköping, Sweden

Four dimensional flow visualization and quantification using phase contrast MRI has expanded the functional assessment of intracardiac and vascular blood flow in health as well as many forms of common disease. The impacts of chamber remodeling, endothelial disruption, material property changes related to infarction, atherosclerosis, or inflammation may all influence site-specific and global flow, and provide clues to their presence and severity. Further, the tolerance for variability in load, heart rate and rhythm may also be predicted by flow-based measures at baseline. Definition of the range of normal flow across the gender and age spectrum is critical to utilizing 4D flow methods in clinical applications.

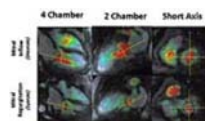
---

424

9:45

#### Reproducibility and Accuracy of 4D Flow Valve Tracking for Assessment of Mitral Regurgitation

Kanae Mukai<sup>1</sup>, Purvi Parwani<sup>1</sup>, and Michael D Hope<sup>2</sup>





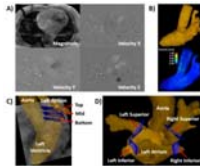
<sup>1</sup>Cardiology, UCSF, San Francisco, CA, United States, <sup>2</sup>Department of Radiology and Biomedical Imaging, UCSF, San Francisco, CA, United States

Quantification of mitral regurgitation (MR) is challenging to accurately perform with echocardiography.<sup>1</sup> Recent data suggest that MRI is more accurate than echocardiography, but the conventional approach used requires the combination of data from two different types of MRI sequences.<sup>2</sup> This study investigated the direct measurement of mitral regurgitation with 4D Flow using a valve tracking approach. We used both mitral annulus tracking and mitral flow jet tracking, and compared measurements to the conventional MRI approach for calculating mitral regurgitation. Flow jet but not annulus tracking demonstrated good reproducibility of measurement and correlation with the conventional MRI approach.

425



10:00



#### Exploration for Novel Markers of Left Atrial Disease and Thrombo-embolic Risk in Patients with Paroxysmal Atrial Fibrillation Using 4D Flow MRI

Julio Garcia<sup>1,2</sup>, Michael S Bristow<sup>2,3</sup>, Carmen Lydell<sup>2,4</sup>, Andrew G Howarth<sup>2,3</sup>, Bobby Heydari<sup>2,3</sup>, Frank S Prato<sup>5</sup>, Maria Drangova<sup>5</sup>, Rebecca Thornhill<sup>6</sup>, Pablo Nery<sup>7</sup>, Stephen Wilton<sup>2</sup>, Allan Skanes<sup>8</sup>, and James White<sup>2,3</sup>

<sup>1</sup>Department of Cardiac Sciences, University of Calgary, Calgary, AB, Canada, <sup>2</sup>Stephenson Cardiac Imaging Centre, Libin Cardiovascular Institute of Alberta, Calgary, AB, Canada, <sup>3</sup>Department of Medicine, University of Calgary, Calgary, AB, Canada, <sup>4</sup>Diagnostic Imaging, University of Calgary, Calgary, AB, Canada, <sup>5</sup>Medical Imaging, University of Western Ontario, London, ON, Canada, <sup>6</sup>Diagnostic Imaging, The Ottawa Hospital, Ottawa, ON, Canada, <sup>7</sup>Electrophysiology, University of Ottawa, Ottawa, ON, Canada, <sup>8</sup>Department of Medicine, University of Western Ontario, London, ON, Canada

This study may be of interest for clinicians and clinical researchers who study or measure left atrial blood flow. This pilot study demonstrates that: 1) 4D flow imaging of LA inflow and vortex formation is clinically feasible, 2) Significant differences in LA flow can be identified in patients with paroxysmal AF versus healthy controls; 3) Asymmetry of pulmonary vein inflow was observed in this population and may be contributory to (or as a result of) alterations in LA vortical flow, and 4) Vortical flow is fractionated in patients with a history of paroxysmal AF. These early observations seed interest for LA 4D flow as a marker of early or established left atrial disease and may provide value for the prediction of thrombo-embolic events.

---

---

## Plenary Session

### NIBIB New Horizons Lecture

Plenary Hall

Tuesday 10:45 - 11:15

---

10:45

[NIBIB New Horizons Lecture](#)

Nicole Seiberlich<sup>1</sup>

<sup>1</sup>Case Western Reserve University

---

---

## Plenary Session

### Dynamic Real Time Imaging

Organizers: Michael S. Hansen, Ph.D. & Joshua D. Trzasko, Ph.D.

Plenary Hall

Tuesday 11:15 - 12:15

---

11:15

[Real-Time MRI Technology](#)

Jennifer Anne Steeden<sup>1</sup>

<sup>1</sup>Centre for Cardiovascular Imaging, University College London, London, United Kingdom

---

---

11:45

[Diagnostic Real-Time MRI](#)

Krishna Nayak

---

---

12:15      [Interventional Image Guidance](#)  
Reza Razavi

---

12:45      [Adjournment & Meet the Teachers](#)

---

---

**Other**

## Gold Corporate Symposium: GE Healthcare

Plenary Hall      Tuesday 12:15 - 13:45 *(no CME credit)*

---

**Other**

## Gold Corporate Symposium: Philips Healthcare

Plenary Hall      Tuesday 12:15 - 13:45 *(no CME credit)*

---

**Traditional Poster: Diffusion**

Exhibition Hall 1730-  
1776      Tuesday 13:45 - 15:45 *(no CME credit)*

---

**Electronic Poster: Neuro**

Exhibition Hall      Tuesday 13:45 - 14:45 *(no CME credit)*

---

**Study Groups**

## MR in Drug Research Study Group

Room 323ABC      Tuesday 13:45 - 15:45 *(no CME credit)*

---

**Study Groups**

## MR Elastography Study Group

Room 317AB      Tuesday 13:45 - 15:45 *(no CME credit)*

---

## Educational Course

# Susceptibility Imaging as a New Window on Disease, Iron & Hypoxia

Organizers: Jeff F. Dunn, Ph.D. & Linda Moy, M.D.

Room 316A      Tuesday 13:45 - 15:45    Moderators: Hongfu Sun & Alan Wilman

---

13:45      [Using Desoxyhemoglobin & Susceptibility as a Contrast Agent in Cancer](#)  
Gregory Karczmar

---

14:15      [Abdominal Cancer](#)  
Bachir Taouli<sup>1</sup>

<sup>1</sup>Mount Sinai

In this lecture, we will review the current susceptibility imaging methods used for indirectly assessing tumor hypoxia in abdominal cancers, in preclinical and clinical applications. We will review the scientific evidence, potential applications and limitations of BOLD/TOLD imaging.

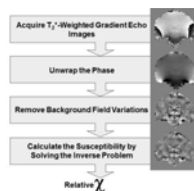
---

14:45      [Cell Tracking & Molecular Contrast](#)  
Paula Foster

This lecture will discuss the use of iron based contrast agents for cellular and molecular MRI. The mechanisms of contrast, detection limits, limitations and advances will be described.

---

15:15      [Susceptibility Mapping in Brain Diseases: Iron, Myelin & More](#)  
Karin Shmueli



Tissue magnetic susceptibility can be calculated from gradient-echo phase images using quantitative susceptibility mapping (QSM). Several clinical applications of QSM are emerging based on its sensitivity to tissue iron, myelin and deoxyhaemoglobin content. These include visualising iron in deep-brain structures in Parkinson's disease and other dementias, evaluating microbleed burden and haemorrhages and distinguishing these from calcifications. QSM also allows quantification of venous oxygenation with functional QSM now able to detect brain activity. QSM reveals demyelination: changes in both myelin and iron content drive QSM differences in Multiple Sclerosis which may be associated with inflammation, perhaps due to iron in microglia/macrophages.

15:45

Adjournment & Meet the Teachers

## Power Pitch

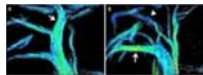
### Pitch: Liver

Power Pitch  
 Theater A - Tuesday 13:45 - Moderators: Richard (Kinh Gian)  
 Exhibition Hall 14:45 Do & Yu-Chien Wu (no CME credit)

426

13:45

Relationship between hepatic blood flow and segmental liver hypertrophy after portal vein embolization using 4D flow MRI



Tilman Schubert<sup>1</sup>, Kevin Johnson<sup>2</sup>, Alejandro Roldan Alzate<sup>1</sup>, and Scott Reeder<sup>1,2</sup>

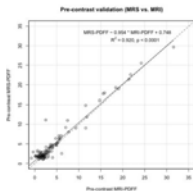
<sup>1</sup>Radiology, UW Wisconsin Madison, Madison, WI, United States,

<sup>2</sup>Medical Physics, UW Wisconsin Madison, Madison, WI, United States

427

13:45

Proton Density Fat Fraction Estimation Accuracy of High-Flip-Angle, Contrast-Enhanced, Magnitude-Based Multi-Gradient-Echo MR Imaging at 3T



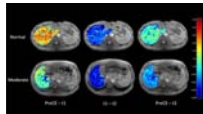
Ethan Z Sy<sup>1</sup>, Cheng William Hong<sup>1</sup>, Soudabeh Fazeli Dehkordy<sup>1</sup>, Charlie C Park<sup>1</sup>, Alexandra Schlein<sup>1</sup>, Jonathan C Hooker<sup>1</sup>, Jennifer Cui<sup>1</sup>, Gavin Hamilton<sup>1</sup>, and Claude B Sirlin<sup>1</sup>

<sup>1</sup>University of California, San Diego, San Diego, CA, United States

---

428

13:45



Assessment of liver function using an uptake ratio based on multiple-time points hepatocyte mapping

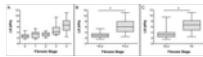
Tomoyuki Okuaki<sup>1</sup>, Kosuke Morita<sup>2</sup>, Tomohiro Namimoto<sup>3</sup>, Morikatsu Yoshida<sup>3</sup>, Shinya Shiraishi<sup>3</sup>, Yasuyuki Yamashita<sup>3</sup>, and Marc Van Cauteren<sup>1</sup>

<sup>1</sup>MR Clinical Science, Philips Healthtech, Tokyo, Japan, <sup>2</sup>Department of Central Radiology, Kumamoto University Hospital, Kumamoto, Japan, <sup>3</sup>Department of Diagnostic Radiology, Faculty of Life Sciences, Kumamoto University, Kumamoto, Japan

---

429

13:45



Detection of Advanced Liver Fibrosis and Cirrhosis using MR elastography compared to liver surface nodularity measurement, EOB-DTPA uptake and blood tests

Cecilia Besa<sup>1</sup>, Mathilde Wagner<sup>1,2</sup>, Grace Lo<sup>1</sup>, Sonja Gordic<sup>1</sup>, Manjil Chatterji<sup>1</sup>, Ashley Stueck<sup>3</sup>, James Babb<sup>4</sup>, Andrew Smith<sup>5</sup>, and Bachir Taouli<sup>1</sup>

<sup>1</sup>Translational and Molecular Imaging Institute, Icahn School of Medicine at Mount Sinai, New York, NY, United States, <sup>2</sup>Radiology, Groupe Hospitalier Pitié Salpêtrière, Paris, France, <sup>3</sup>Pathology, Icahn School of Medicine at Mount Sinai, New York, NY, United States, <sup>4</sup>Radiology, New York University Langone Medical Center, New York, United States, <sup>5</sup>Radiology, University of Mississippi Medical Center, Jackson, MS, United States

---

430

13:45

Diagnostic performance of LI-RADS major features, ancillary features, and categories on MRI for diagnosis of hepatocellular carcinoma

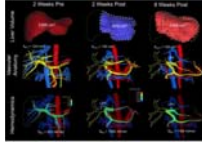
Milena Cerny<sup>1</sup>, Catherine Bergeron<sup>1</sup>, Jean-Sébastien Billiard<sup>1</sup>, Jessica Murphy-Lavallée<sup>1</sup>, Damien Olivieri<sup>1</sup>, Joshua Bérubé<sup>1</sup>, Boyan Fan<sup>1</sup>, Hélène Castel<sup>2</sup>, Simon Turcotte<sup>3</sup>, Pierre Perrault<sup>1</sup>, and An Tang<sup>1,4</sup>

<sup>1</sup>Department of Radiology, Centre hospitalier de l'Université de Montréal (CHUM), MONTREAL, QC, Canada, <sup>2</sup>Department of Gastroenterology and Hepatology, Centre hospitalier de l'Université de Montréal (CHUM), MONTREAL, QC, Canada, <sup>3</sup>Department of Surgery, Centre hospitalier de l'Université de Montréal (CHUM), MONTREAL, QC, Canada, <sup>4</sup>Centre de recherche du Centre hospitalier de l'Université de Montréal (CRCHUM), MONTREAL, QC, Canada

---

431

13:45



### Longitudinal Characterization of Liver Regeneration and Portal Hemodynamics in Living Donor Liver Transplant

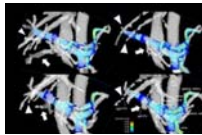
Alejandro Roldán-Alzate<sup>1,2,3</sup>, David R Rutkowski<sup>2</sup>, Luis A Fernandez<sup>4</sup>, and Scott B Reeder<sup>1,3,5,6</sup>

<sup>1</sup>Radiology, University of Wisconsin, Madison, WI, United States,

<sup>2</sup>Mechanical Engineering, University of Wisconsin, Madison, WI, United States, <sup>3</sup>Biomedical Engineering, University of Wisconsin, Madison, WI, United States, <sup>4</sup>Surgery, University of Wisconsin, Madison, WI, United States, <sup>5</sup>Medical Physics, University of Wisconsin, Madison, United States, <sup>6</sup>Medicine, University of Wisconsin, Madison, United States

432

13:45



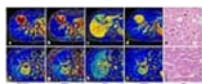
### 4D flow MRI of Liver Hemodynamics: Influence of Velocity Encoding, Different Field Strength and Contrast Application on Visualization and Quantification of blood flow

Zoran Stankovic<sup>1</sup>, Bernd Jung<sup>1</sup>, Alan Arthur Peters<sup>1</sup>, Jelena Surla<sup>2</sup>, Edouard Semaan<sup>2</sup>, Michael Ith<sup>1</sup>, Johannes Heverhagen<sup>1</sup>, Michael Markl<sup>2</sup>, and Jeremy D. Collins<sup>2</sup>

<sup>1</sup>DIPR, Inselspital, University Hospital Bern, University of Bern, Bern, Switzerland, <sup>2</sup>Radiology, Northwestern University, Chicago, IL, United States

433

13:45



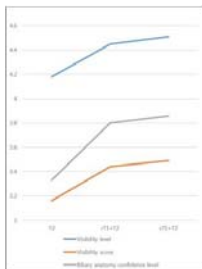
### Quantitative Free-Breathing Dynamic Contrast-enhanced MRI in Hepatocellular Carcinoma Using Gd-EOB-DTPA : Correlations With Ki67 Proliferation Status and Histological Grades

Jie Chen<sup>1</sup>, Chenyang Chen<sup>1</sup>, Chunchao Xia<sup>2</sup>, and Bin Song<sup>2</sup>

<sup>1</sup>West China Medical School of Sichuan University, Chengdu, People's Republic of China, <sup>2</sup>Departmento of Radiology, West China Hospital of Sichuan University, Chengdu, People's Republic of China

434

13:45



### The value of high resolution gadoexetic acid-enhanced MR cholangiography for evaluating biliary anatomy of living liver donor: comparison with T2 weighted (T2W) MR cholangiography and conventional gadoxetic acid enhanced MR cholangiography

Hyo-Jin Kang<sup>1</sup>, Jeong Min Lee<sup>1</sup>, Jeong Hee Yoon<sup>1</sup>, Won Chang<sup>1</sup>, Ijin Joo<sup>1</sup>, and Joon Koo Han<sup>1</sup>

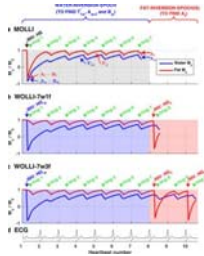
<sup>1</sup>Radiology, Seoul National University Hospital, Seoul, Korea, Republic of



435

13:45

Water-Only Look-Locker Inversion recovery (WOLLI) T<sub>1</sub> mapping



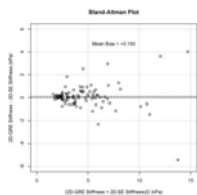
Liam D. Garrison<sup>1</sup>, Christina Levick<sup>1,2</sup>, Michael Pavlides<sup>1,2</sup>, Tom Marjot<sup>3</sup>, Ferenc Mozes<sup>1</sup>, Leanne Hodson<sup>3</sup>, Stefan Neubauer<sup>1</sup>, Matthew Robson<sup>1</sup>, and Christopher T. Rodgers<sup>1</sup>

<sup>1</sup>OCMR, RDM Cardiovascular Medicine, University of Oxford, Oxford, United Kingdom, <sup>2</sup>Translational Gastroenterology Unit, Nuffield Department of Medicine, University of Oxford, Oxford, United Kingdom, <sup>3</sup>Oxford Centre for Diabetes, Endocrinology and Metabolism (OCDEM), Radcliffe Department of Medicine, University of Oxford, United Kingdom

436

13:45

Region-of-interest size of hepatic 2D MR elastography decreases with increasing R2\* for gradient-echo but not spin-echo techniques



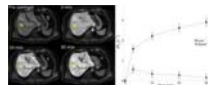
Cheng William Hong<sup>1</sup>, Adrija Mamidipalli<sup>1</sup>, Ethan Z Sy<sup>1</sup>, Jonathan C Hooker<sup>1</sup>, Calvin Andrew Tran<sup>1</sup>, Tanya Wolfson<sup>2</sup>, Soudabeh Fazeli Dehkordy<sup>1</sup>, Scott B Reeder<sup>3</sup>, Rohit Loomba<sup>4</sup>, and Claude B Sirlin<sup>1</sup>

<sup>1</sup>Liver Imaging Group, Department of Radiology, University of California, San Diego, San Diego, CA, United States, <sup>2</sup>Computational and Applied Statistics Laboratory, University of California, San Diego, San Diego, CA, United States, <sup>3</sup>Departments of Radiology, Medical Physics, Biomedical Engineering, Medicine, and Emergency Medicine, University of Wisconsin, Madison, Madison, WI, United States, <sup>4</sup>NAFLD Research Center, Division of Gastroenterology, Department of Medicine, University of California, San Diego, San Diego, CA, United States

437

13:45

Estimating Liver Function in Chronic Liver Disease Patients Using DCE-MRI and Whole-Body Pharmacokinetic Modeling



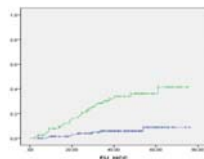
Markus Karlsson<sup>1,2</sup>, Mikael F Forsgren<sup>1,2</sup>, Olof Dahlqvist-Leinhard<sup>1,2</sup>, Nils Dahlström<sup>1,2</sup>, Bengt Norén<sup>2</sup>, Mattias Ekstedt<sup>1</sup>, Stergios Kechagias<sup>1</sup>, Gunnar Cedersund<sup>3</sup>, and Peter Lundberg<sup>1,2</sup>

<sup>1</sup>Department of Health and Medicine, Linköping University, Linköping, Sweden, <sup>2</sup>Center for Medical Image Science and Visualisation, Linköping University, Linköping, Sweden, <sup>3</sup>Department of Biomedical Engineering, Linköping University, Linköping, Sweden

438

13:45

Prognostic Role of Liver Stiffness Measurement Using Magnetic Resonance Elastography in Patients with Compensated Chronic Liver Disease



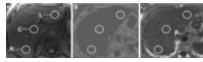
Dong Ho Lee<sup>1</sup> and Jeong Min Lee<sup>2</sup>

<sup>1</sup>Radiology, Seoul National University Hospital, Seoul, Korea, Republic of, <sup>2</sup>Korea, Republic of

---

439

13:45



[Epidemiology and spatial heterogeneity of hepatic fat and iron deposition: an MRI-based analysis](#)

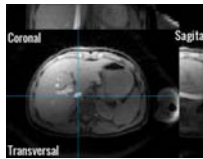
Daniel R Ludwig<sup>1</sup>, Tyler J Fraum<sup>1</sup>, Scott Kilian<sup>2</sup>, and Kathryn J Fowler<sup>1</sup>

<sup>1</sup>Mallinckrodt Institute of Radiology, Washington University School of Medicine, St Louis, MO, United States, <sup>2</sup>Southern Illinois University School of Medicine

---

440

13:45



[Free breathing T2\\* mapping of the Liver using a compressed sensing reconstruction](#)

Paul de Heer<sup>1</sup>, Oliver J Gurney-Champion<sup>1</sup>, Jurgen H. Runge<sup>1,2</sup>, Remy Klaassen<sup>3</sup>, Jasper Schoormans<sup>1</sup>, Bram F. Coolen<sup>4</sup>, Hanneke W.M. van Laarhoven<sup>3</sup>, Gustav J. Strijkers<sup>4</sup>, Jaap Stoker<sup>1</sup>, and Aart J. Nederveen<sup>1</sup>

<sup>1</sup>Radiology, AMC, Amsterdam, Netherlands, <sup>2</sup>Division of Imaging Sciences and Biomedical Engineering, King's College London, London, United Kingdom, <sup>3</sup>Medical Oncology, AMC, Amsterdam, Netherlands, <sup>4</sup>Biomedical Engineering & Physics, AMC, Amsterdam, Netherlands

---

## Power Pitch

### Pitch: Reconstruction Highlights

Power Pitch

Theater B -

Exhibition Hall

Tuesday 13:45 - Moderators: Anthony

14:45

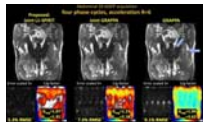
Christodoulou & Rebecca Ramb

(no CME credit)

---

441

13:45



[Joint Reconstruction of Phase-Cycled Balanced SSFP with Constrained Parallel Imaging](#)

Berkin Bilgic<sup>1</sup>, Thomas Witzel<sup>1</sup>, Himanshu Bhat<sup>2</sup>, Lawrence L Wald<sup>1</sup>, and Kawin Setsompop<sup>1</sup>

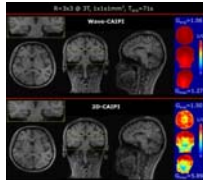
<sup>1</sup>Martinos Center for Biomedical Imaging, Charlestown, MA, United States, <sup>2</sup>Siemens Medical Solutions, Charlestown, MA, United States

---

13:45

[Wave-CAIPI for Highly Accelerated MP-RAGE Imaging](#)

442



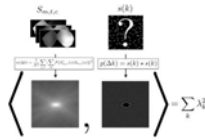
Daniel Polak<sup>1,2</sup>, Kawin Setsompop<sup>1,3,4</sup>, Stephen F. Cauley<sup>1,3</sup>, Borjan A. Gagoski<sup>3,5</sup>, Himanshu Batt<sup>6</sup>, Florian Maier<sup>2</sup>, Lawrence L. Wald<sup>1,3,4</sup>, and Berkin Bilgic<sup>1,3</sup>

<sup>1</sup>Massachusetts General Hospital, Boston, MA, United States, <sup>2</sup>German Cancer Research Center, Heidelberg, Germany, <sup>3</sup>Harvard Medical School, Boston, MA, United States, <sup>4</sup>Harvard-MIT Health Sciences and Technology, Boston, MA, United States, <sup>5</sup>Boston Children's Hospital, Boston, MA, United States, <sup>6</sup>Siemens Medical Solutions Inc, Malvern, PA, United States

443



13:45



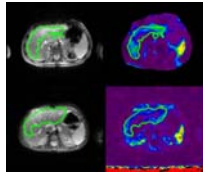
### Differential Domain Analysis for 3D Cartesian Sampling

Evan Levine<sup>1,2</sup> and Brian Hargreaves<sup>2</sup>

<sup>1</sup>Electrical Engineering, Stanford University, Stanford, CA, United States, <sup>2</sup>Radiology, Stanford University, Stanford, CA, United States

444

13:45



### Comparison of 2D and 3D MR Liver Elastography in 600 Patients

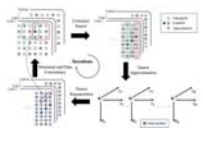
Bogdan Dzyubak<sup>1</sup>, Kevin J. Glaser<sup>1</sup>, Sudhakar K. Venkatesh<sup>1</sup>, and Richard L. Ehman<sup>1</sup>

<sup>1</sup>Radiology, Mayo Clinic, Rochester, MN, United States

445



13:45



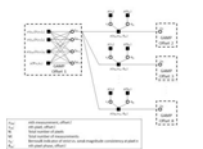
### Calibrationless Parallel Imaging Reconstruction Using Hankel Tensor Completion (HTC)

Yilong Liu<sup>1,2</sup>, Jun Cao<sup>1,2</sup>, Mengye Lyu<sup>1,2</sup>, and Ed X. Wu<sup>1,2</sup>

<sup>1</sup>Laboratory of Biomedical Imaging and Signal Processing, The University of Hong Kong, Hong Kong, People's Republic of China, <sup>2</sup>Department of Electrical and Electronic Engineering, The University of Hong Kong, Hong Kong, People's Republic of China

446

13:45



### Highly Accelerated Magnetic Resonance Elastography via Bayesian Modeling

Christopher Ebersole<sup>1,2</sup>, Rizwan Ahmad<sup>1</sup>, Adam Rich<sup>1</sup>, Lee C. Potter<sup>1</sup>, and Arunark Kolipaka<sup>2</sup>

<sup>1</sup>Electrical and Computer Engineering, The Ohio State University, Columbus, OH, United States, <sup>2</sup>Radiology, The Ohio State University Wexner Medical Center, Columbus, OH, United States

447



13:45



**RACE-GRASP: Respiratory-weighted and Aortic Contrast Enhancement-guided GRASP MRI**

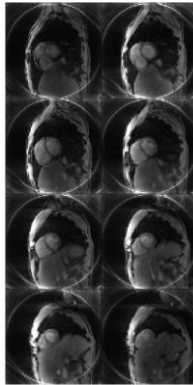
Li Feng<sup>1</sup>, Krishna Shanbhogue<sup>1</sup>, Daniel K Sodickson<sup>1</sup>, Hersh Chandarana<sup>1</sup>, and Ricardo Otazo<sup>1</sup>

<sup>1</sup>Center for Advanced Imaging Innovation and Research (CAI2R), New York University School of Medicine, New York, NY, United States

448



13:45



**Real-time 3D cardiac MRI using through-time radial GRAPPA and GPU-enabled reconstruction pipelines in the Gadgetron framework**

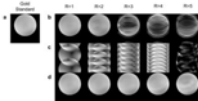
Dominique Franson<sup>1</sup>, James Ahad<sup>2</sup>, Jesse Hamilton<sup>1</sup>, Wei-Ching Lo<sup>1</sup>, Yun Jiang<sup>1</sup>, Yong Chen<sup>3</sup>, and Nicole Seiberlich<sup>1,3</sup>

<sup>1</sup>Biomedical Engineering, Case Western Reserve University, Cleveland, OH, United States, <sup>2</sup>School of Medicine, Case Western Reserve University, Cleveland, OH, <sup>3</sup>Radiology, University Hospitals, Cleveland, OH

449



13:45



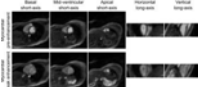
**Navigator-free EPI ghost correction using low-rank matrix modeling: Theoretical insights and practical improvements**

Rodrigo A. Lobos<sup>1</sup>, Tae Hyung Kim<sup>1</sup>, W. Scott Hoge<sup>2,3</sup>, and Justin P. Haldar<sup>1</sup>

<sup>1</sup>Electrical Engineering, University of Southern California, Los Angeles, CA, United States, <sup>2</sup>Radiology, Brigham and Women's Hospital, Boston, MA, United States, <sup>3</sup>Radiology, Harvard Medical School, Boston, MA, United States

450

13:45



**Non-ECG First-Pass Myocardial Perfusion T1 Mapping with Low-Rank Tensor Cardiovascular MR Multitasking**

Anthony G. Christodoulou<sup>1,2</sup>, Jaime L. Shaw<sup>1,3</sup>, Xiaoming Bi<sup>4</sup>, Behzad Sharif<sup>1,5</sup>, and Debiao Li<sup>1,3</sup>

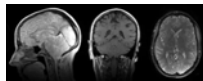
<sup>1</sup>Biomedical Imaging Research Institute, Cedars-Sinai Medical Center, Los Angeles, CA, United States, <sup>2</sup>Cedars-Sinai Heart Institute, Cedars-Sinai Medical Center, Los Angeles, CA, United States, <sup>3</sup>Department of Bioengineering, University of California, Los Angeles, Los Angeles, CA, United States, <sup>4</sup>Siemens Healthcare, Los Angeles, CA, United States, <sup>5</sup>Department of Biomedical Sciences, Cedars-Sinai Medical Center, Los Angeles, CA, United States

---

451



13:45



### T1-T2 Shuffling: Multi-Contrast 3D Fast Spin-Echo with T1 and T2 Sensitivity

Jonathan I Tamir<sup>1</sup>, Valentina Taviani<sup>2</sup>, Shreyas S Vasawala<sup>3</sup>, and Michael Lustig<sup>1</sup>

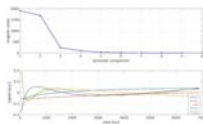
<sup>1</sup>Electrical Engineering and Computer Sciences, University of California, Berkeley, Berkeley, CA, United States, <sup>2</sup>MR Applications and Workflow, GE Healthcare, Menlo Park, CA, United States, <sup>3</sup>Radiology, Stanford University, CA, United States

---

452



13:45



### Simultaneous T1/T2 measurements in combination with PCA-SENSE reconstruction (T1\* shuffling) and multicomponent analysis

Julian Pfister<sup>1</sup>, Martin Blaimer<sup>1</sup>, Peter M. Jakob<sup>2</sup>, and Felix A. Breuer<sup>1</sup>

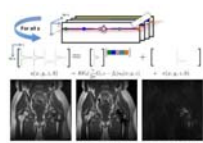
<sup>1</sup>Magnetic Resonance and X-ray Imaging, Fraunhofer Development Center X-ray Technology (EZRT), Würzburg, Germany, <sup>2</sup>Experimental Physics 5, University of Würzburg, Würzburg, Germany

---

453



13:45



### Accelerated 3D Multispectral MRI with Robust Principal Component Analysis for Separation of On and Off-resonance Signals

Evan Levine<sup>1,2</sup>, Kathryn Stevens<sup>2</sup>, and Brian Hargreaves<sup>2</sup>

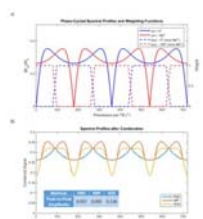
<sup>1</sup>Electrical Engineering, Stanford University, Stanford, CA, United States, <sup>2</sup>Radiology, Stanford University, Stanford, CA, United States

---

454



13:45



### Field Map Combination Method for Multiple-Acquisition bSSFP

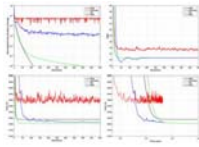
Anjali Datta<sup>1</sup> and Dwight G Nishimura<sup>1</sup>

<sup>1</sup>Electrical Engineering, Stanford University, Stanford, CA, United States

455

13:45

### Stochastic Primal-Dual Optimization for Locally Low-Rank MRI Reconstruction: A Stable Alternative to Cycle Spinning

Joshua D. Trzasko<sup>1</sup><sup>1</sup>Radiology, Mayo Clinic, Rochester, MN, United States

Oral

## fMRI: Mechanisms & Physiology

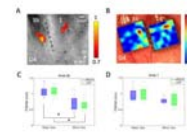
Room 310

Tuesday 13:45 - 15:45 Moderators: Nicholas Blockley &amp; Xiaoping Hu

456

13:45

### Comparable intrinsic spatial profiles of BOLD signals and local field potentials after stimulation and in resting-state within primary somatosensory cortex

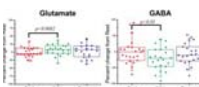
Zhaoyue Shi<sup>1</sup>, Ruiqi Wu<sup>1</sup>, Pai-Feng Yang<sup>1</sup>, Feng Wang<sup>1</sup>, Tung-Lin Wu<sup>1</sup>, Arabinda Mishra<sup>1</sup>, Li Min Chen<sup>1</sup>, and John Gore<sup>1</sup><sup>1</sup>Vanderbilt University Institute of Imaging Science, Nashville, TN, United States

We directly compared the spatial extents of stimulated activations and the profiles of inter-voxel resting-state correlations between high resolution BOLD data at 9.4T and local field potentials (LFPs) using 98-channel microelectrode arrays, in functionally distinct somatosensory areas 3b and 1 in monkeys. We found the point spread functions of BOLD and LFP responses were comparable (~1mm) in the stimulus condition, and were more spatially constrained than correlations at rest. Our results showed spatial agreement of resting-state functional connectivity between BOLD and LFP and demonstrated that BOLD responses were as focal as underlying electrical activity.

457

13:57

### Primary neurotransmitter variations upon forepaw stimulation revealed by functional Magnetic Resonance Spectroscopy in the rat

Tal Shemesh<sup>1</sup> and Noam Shemesh<sup>1</sup><sup>1</sup>Champlimaud Neuroscience Programme, Champlimaud Centre for the Unknown, Lisbon, Portugal

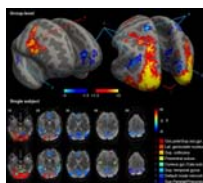


Functional Magnetic Resonance Spectroscopy (fMRS) could potentially provide much information on neurotransmitters, and hence, could shed light into excitation / inhibition imbalances. However, it was scarcely used, in particular in rodents, presumably due to low SNR. Here, we used a cryoprobe at 9.4T to record fMRS spectra in the rat in just a few minutes. SNR>50 was documented for the N-acetylaspartate resonance. We show statistically significant increases in Glutamate and decrease in GABA upon forepaw stimulation. Our results are suggestive of differential relaxation between vesicular and synaptic neurotransmitter pools, and are promising for more detailed investigations, e.g., using optogenetics.

458



14:09



Mapping and characterization of positive and negative BOLD responses to visual stimulation in multiple regions across the brain at 7T

João Jorge<sup>1</sup>, Patrícia Figueiredo<sup>2</sup>, Wietske van der Zwaag<sup>3</sup>, and Rolf Gruetter<sup>1,4</sup>

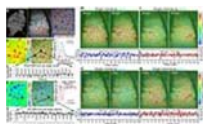
<sup>1</sup>Laboratory for Functional and Metabolic Imaging, École Polytechnique Fédérale de Lausanne, Lausanne, Switzerland, <sup>2</sup>ISR-Lisboa/LARSyS and Department of Bioengineering, Instituto Superior Técnico, Universidade de Lisboa, Lisbon, Portugal, <sup>3</sup>Spinoza Centre for Neuroimaging, Amsterdam, Netherlands, <sup>4</sup>Department of Radiology, University of Lausanne and University of Geneva, Lausanne, Switzerland

Negative BOLD responses (NBRs) have been associated with changes in neuronal activity, but are challenging to detect due to a lower contrast-to-noise ratio compared to positive BOLD responses (PBRs). In this work, the high sensitivity available at 7T was explored with accelerated fMRI acquisition, vein segmentation and ICA denoising techniques, to map PBRs and NBRs to visual stimulation in various brain regions beyond the visual cortex. Multiple regions with significant PBRs and NBRs could be detected, and their dependence on stimulus duration was found to differ significantly across regions, suggesting the presence of dynamic, stimulus-dependent interactions across the brain.

459



14:21



Mapping the task-related and resting-state vascular dynamic network connectivity in rats and humans

Yi He<sup>1,2</sup>, Rolf Pohmann<sup>1</sup>, Klaus Scheffler<sup>1</sup>, David Kleinfeld<sup>3</sup>, Bruce Rosen<sup>4</sup>, and Xin Yu<sup>1</sup>



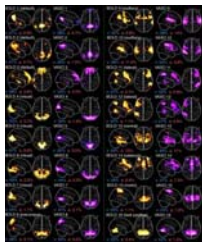
<sup>1</sup>High-field Magnetic Resonance, Max Planck Institute for Biological Cybernetics, Tuebingen, Germany, <sup>2</sup>Graduate Training Centre of Neuroscience, International Max Planck Research School, University of Tuebingen, Tuebingen, Germany, <sup>3</sup>Department of Physics/Section on Neurobiology, University of California at San Diego, La Jolla, CA, United States, <sup>4</sup>MGH/MIT/HMS Athinoula A. Martinos Center for Biomedical Imaging, MGH, Harvard Medical School, Charlestown, MA, United States

We have previously shown that hemodynamic signals can be directly detected from individual arterioles and venules penetrating the cortex. Here, the temporal correlation patterns of the vessel-specific hemodynamic signal are characterized in both rodent and human brains. At the resting state, the blood-oxygen-level-dependent (BOLD) signal from venules and the cerebral blood volume (CBV) signal from arterioles show large-scale vessel-specific correlation patterns in rats under anesthesia. Similarly, in awake human subjects, the BOLD hemodynamic signal correlated at the sulcus veins (3T), as well as at a few intra-cortical veins detected at 9.4T, showing vessel-specific activity and connectivity patterns with slow-frequency oscillation up to 0.1Hz.

460



14:33



Simultaneous multi-slice whole-brain VASO-BOLD, ToF, and SWI at 3T to investigate the vascular contributions in resting-state networks

Michaël Bernier<sup>1</sup>, Guillaume Gilbert<sup>2</sup>, Stephen C Cunnane<sup>3,4,5</sup>, and Kevin Whittingstall<sup>6</sup>

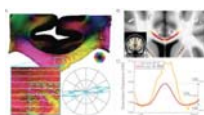
<sup>1</sup>Nuclear medicine and radiobiology, Université de Sherbrooke, Sherbrooke, QC, Canada, <sup>2</sup>MR Clinical Science, Philips Healthcare Canada, Markham, ON, Canada, <sup>3</sup>Research center of aging, CSSS-IUGS, Sherbrooke, QC, Canada, <sup>4</sup>Department of Pharmacology and Physiology, Université de Sherbrooke, Sherbrooke, QC, Canada, <sup>5</sup>Department of Medecine, Université de Sherbrooke, Sherbrooke, QC, Canada, <sup>6</sup>Diagnostic radiology, Université de Sherbrooke, Sherbrooke, QC, Canada

The structural nature of BOLD and CBV fluctuations during resting-state remains unclear. To address this, we first developed a simultaneous multi-slice VASO-BOLD EPI sequence at 3T and isolated resting-state VASO- and BOLD- based networks. We then performed ToF and SWI to quantify the arterial and venous contributions in each network. Overall, both BOLD and VASO showed similar networks which were spatially localized near large veins. Also, similar proportions of vasculature were observed throughout all networks. These results suggest that simultaneous BOLD-CBV acquisitions are feasible at 3T and that their resting state networks are spatially and structurally similar.

---

461

14:45



Fibre orientation dispersion in the corpus callosum relates to interhemispheric functional connectivity

Jeroen Mollink<sup>1,2</sup>, Saad Jbabdi<sup>1</sup>, Stephen M Smith<sup>1</sup>, Fidel Alfaro-Almagro<sup>1</sup>, Michiel Kleinnijenhuis<sup>1</sup>, Anne-Marie van Cappellen van Walsum<sup>2</sup>, and Karla Loreen Miller<sup>1</sup>

<sup>1</sup>FMRIB centre, University of Oxford, Oxford, United Kingdom,

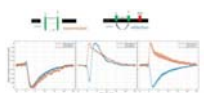
<sup>2</sup>Department of Anatomy, Donders Institute for Brain, Cognition and Behaviour, Radboud University Medical Centre, Nijmegen, Netherlands

Fibre orientation dispersion was previously demonstrated to be higher at the center compared to lateral aspects of the corpus callosum (CC) using microscopy data and diffusion MRI data. We hypothesize that this pattern of dispersion in the CC relates to the degree of heterotopic connections in the brain. In a large cohort of 4903 subjects from the Biobank UK, resting-state functional MRI and diffusion MRI data were compared against each other to find associations between fibre dispersion and functional interhemispheric connectivity

---

462

14:57



Parallel processes of neuro-vascular and neuro-cellular coupling

Wen-Ju Pan<sup>1</sup>, Jacob Billings<sup>1</sup>, Maysam Nezafati<sup>1</sup>, Waqas Majeed<sup>1</sup>, and Shella Keilholz<sup>1</sup>

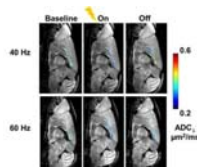
<sup>1</sup>Emory University/Georgia Institute of Technology, Atlanta, GA, United States

Neural activity leads to cellular swelling along with the hemodynamic response from the vasculature. The latter process is the basis for the BOLD signal detected with fMRI; the former may underlie the changes observed with diffusion-weighted fMRI. Optical intrinsic signals can detect neuro-vascular activity (typically observed in in vivo studies of reflectance) and neuro-cellular swelling (observed mostly by transmittance in brain slices). We designed a novel miniature probe for in vivo transmittance studies in the rat brain and examined neuro-cellular coupling and neuro-vascular coupling in vivo to better understand the basis of the MRI techniques.

463



15:09



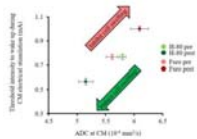
Functional response of corpus callosum to electrical stimulation of S1 cortex in mice

Tsen-Hsuan (Abby) Lin<sup>1</sup>, Willaim M Spees<sup>1,2</sup>, Michael Wallendorf<sup>3</sup>, Yen-Yu Ian Shih<sup>4</sup>, Anne H Cross<sup>2,5</sup>, and Sheng-Kwei Song<sup>1,2,6</sup>

<sup>1</sup>Radiology, Washington University School of Medicine, St. Louis, MO, United States, <sup>2</sup>The Hope Center for Neurological Disorders, Washington University School of Medicine, St. Louis, MO, United States, <sup>3</sup>Biostatistics, Washington University School of Medicine, St. Louis, United States, <sup>4</sup>Neurology, The University of North Carolina in Chapel Hill, NC, United States, <sup>5</sup>Neurology, Washington University School of Medicine, St. Louis, MO, United States, <sup>6</sup>Biomedical Engineering, Washington University in St. Louis, St. Louis, MO, United States

The corpus callosum (CC) is the major pathway for interhemispheric communication and a primary target of white-matter neurodegenerative diseases. Diffusion MRI is widely used to assess white-matter structural alternations in diseases. In addition to morphological changes, we previously demonstrated the feasibility to assess white matter function using diffusion MRI. We observed a 27% perpendicular apparent diffusion coefficient ( $\text{ADC}_{\perp}$ ) decrease in normal mouse optic nerve during visual stimulation. In the current study, we implanted MR-compatible tungsten wires at primary somatosensory cortex and observed 15 – 21%  $\text{ADC}_{\perp}$  decrease in CC, suggesting diffusion MRI can be applied to study function at this site.

15:21



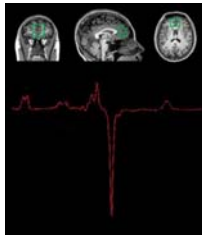
Relationship between cell swelling, functional neuronal status and water diffusion in the rat brain

Yoshifumi Abe<sup>1</sup>, Tomokazu Tsurugizawa<sup>1</sup>, and Denis Le Bihan<sup>1</sup>

<sup>1</sup>NeuroSpin, CEA, Gif-sur-Yvette, France



Diffusion fMRI (DfMRI) allows to monitor brain function without BOLD vascular confounding effects. Infusion in the rat brain thalamus central median nucleus (CM) of a cell swelling inducer/blocker resulted in ADC changes confirming DfMRI sensitivity to local cell size status. ADC changes closely reflected local functional neuronal status, as evidenced from LFP recordings and electrical current thresholds required to wake-up the animals. They were also observed in remote locations connected with CM. Those results support that neural swelling is an important mechanism underlying DfMRI, and that cell size variations in neuronal networks are an important feature associated with their activity.



Deactivation responses induced by acupuncture are associated with changes in GABA concentrations: a BOLD fMRI and MEGA-PRESS 1H-MRS Study

Jiliang Fang<sup>1</sup>, Yuanyuan Chen<sup>1</sup>, Yanping Zhao<sup>1</sup>, Guiyong Liu<sup>1</sup>, Xiaoling Wang<sup>1</sup>, Feng Feng<sup>2</sup>, Bo Hou<sup>2</sup>, Bingzhen Lei<sup>3</sup>, Xiaojiao Li<sup>1</sup>, Ahn Sinyeob<sup>4</sup>, and Tianyi Qian<sup>5</sup>

<sup>1</sup>Guang An Men Hospital, China Academy of Chinese Medical Sciences, Beijing, People's Republic of China, <sup>2</sup>Peking Union Hospital, Peking Union Medical University, Beijing, People's Republic of China, <sup>3</sup>Beijing Institute of Technology, Beijing, People's Republic of China, <sup>4</sup>Siemens Healthcare, MR Collaboration, CA, United States, <sup>5</sup>Siemens Healthcare, MR Collaboration NE Asia, Beijing, People's Republic of China

This study investigated the neurological mechanism that mediates the deactivation of the medial prefrontal cortex induced by acupuncture. Gamma-aminobutyric acid (GABA) concentrations before and immediately after acupuncture stimulation in healthy volunteers were assessed with MEGA-PRESS 1H-MRS. We found that GABA concentrations in the medial prefrontal cortex decreased significantly after acupuncture stimulation compared with control stimulation with Von Frey sensory. Analysis of the task-functional magnetic resonance image (fMRI) acquired during acupuncture showed deactivation in the same area. These results demonstrated that the decreased blood oxygenation level dependent (BOLD) response induced by acupuncture was associated with inhibitory effects.

# Microstructure (Non-Diffusion)

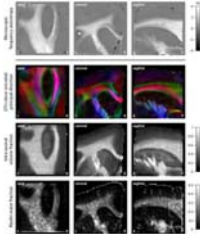
Room 311

Tuesday 13:45 - 15:45 *Moderators: Guillaume Duhamel & Samuel Hurley*

---

466

13:45



## Microscopic susceptibility anisotropy mapping

Enrico Kaden<sup>1</sup>, Irina Y. Barskaya<sup>2</sup>, Nathaniel D. Kelm<sup>2</sup>, Kathryn L. West<sup>2</sup>, Mark D. Does<sup>2</sup>, and Daniel C. Alexander<sup>1</sup>

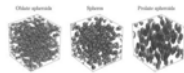
<sup>1</sup>Centre for Medical Image Computing, Department of Computer Science, University College London, London, United Kingdom, <sup>2</sup>Institute of Imaging Science, Vanderbilt University, Nashville, TN, United States

The gradient-echo signal in brain white matter does not only depend on microscopic tissue features such as myelination, but also on the axon orientation distribution with respect to the external magnetic field. Therefore, to map microscopic susceptibility, we need to factor out the confounding effects of fibre crossings and orientation dispersion. This work adapts the Spherical Mean Technique (SMT), recently introduced in diffusion MRI, to estimate the microscopic susceptibility anisotropy in directionally heterogeneous tissue. Moreover, we show that, in combination with diffusion measurements, the proposed technique may be viable in the clinic.

---

467

13:57



## Larmor frequency shift in anisotropic heterogeneous media

Alexander Ruh<sup>1,2</sup> and Valerij G. Kiselev<sup>1,2</sup>

<sup>1</sup>Dept. of Radiology, Medical Physics, Medical Center - University of Freiburg, Freiburg, Germany, <sup>2</sup>Faculty of Medicine, University of Freiburg, Freiburg, Germany

The question about the precise value of the proton Larmor frequency in neuronal tissues is a major topic in current research. In this study we present a comprehensive answer for spins moving in magnetically heterogeneous media formed by impermeable susceptibility inclusions. We obtain an analytic result for the mean Larmor frequency in the limit of fast diffusing spins in the space external to the inclusions. This mean frequency explicitly depends on the correlation function of the inclusion. For anisotropic media this results in a nonzero frequency shift, which is confirmed by Monte Carlo simulations.

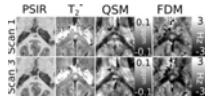
---

468

14:09

Frequency difference mapping as a marker of microstructural integrity of white matter in multiple sclerosis at 7T





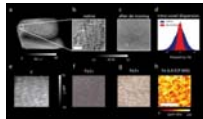
Matthew Cronin<sup>1</sup>, Nicholas Geades<sup>2</sup>, Olivier Mougin<sup>2</sup>, Kingkarn Aphiwatthanasumet<sup>2</sup>, Nikos Evangelou<sup>2</sup>, Penny Gowland<sup>2</sup>, and Richard Bowtell<sup>2</sup>

<sup>1</sup>University of California, Berkeley, CA, United States, <sup>2</sup>Sir Peter Mansfield Imaging Centre, University of Nottingham, Nottingham, United Kingdom

Frequency difference maps derived from GRE phase data have been shown to generate orientation-dependent contrast in white matter tracts in the brain due to signal compartmentalization in myelinated nerve fibers. Here, we investigate the use of frequency difference mapping (FDM) as a marker of white matter integrity; comparing FDM with PSIR; T2\*-weighted magnitude; and quantitative susceptibility mapping (QSM) images of focal white matter lesions in patients with multiple sclerosis. FDM shows clear contrast between these lesions and the surrounding white matter, suggesting that it has potential as a means of quantitatively identifying changes in white matter integrity in vivo.

469

14:21



More Than Simply Iron: How the Mesoscopic and Cellular Distribution of Iron Impacts the MR Contrast

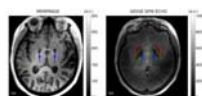
Evgeniya P. Kirilina<sup>1,2</sup>, Katja Reimann<sup>3</sup>, Isabel Weigelt<sup>3</sup>, Thomas Arendt<sup>3</sup>, Andreas Deistung<sup>4,5</sup>, Jürgen R. Reichenbach<sup>4</sup>, Steffen Jankuhn<sup>6</sup>, Larissa Müller<sup>7</sup>, Norbert Jakobowski<sup>7</sup>, Markus Morawski<sup>3</sup>, and Nikolaus Weiskopf<sup>1</sup>

<sup>1</sup>Neurophysics, Max Planck Institute for Human Cognitive and Brain Sciences, Leipzig, Germany, <sup>2</sup>Center for Cognitive Neuroscience Berlin, Free University Berlin, Berlin, Germany, <sup>3</sup>Paul-Flechsig-Institute for Brain Research, Leipzig, Germany, <sup>4</sup>Medical Physics Group, Institute of Diagnostic and Interventional Radiology, Jena University Hospital – Friedrich Schiller University Jena, Jena, Germany, <sup>5</sup>Section of Experimental Neurology, Department of Neurology, Essen University Hospital, <sup>6</sup>Department of Solid State Physics, Faculty of Physics and Earth Sciences Leipzig University, Leipzig, <sup>7</sup>Bundesanstalt für Materialforschung und –prüfung BAM, Berlin, Germany

Iron is an important source of MRI contrast in the brain. Herein, we investigated the influence of the cellular and subcellular iron distribution on the iron-induced MR contrast. Quantitative MRI on post mortem brain samples was combined with quantitative iron mapping and numerical simulations of local field distributions. We show that iron is heterogeneously distributed in both grey and white matter as well as in subcortical nuclei and different scales of heterogeneity play a role for MR contrast in these regions. Our results provide an important step towards quantitative understanding of iron induced MR-contrast and its microstructural underpinnings.

470

14:33



Calcification and iron deposition in basal ganglia structures: reversible and irreversible transverse relaxation rates at 7T

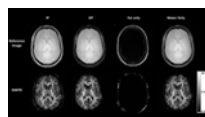
Mukund Balasubramanian<sup>1,2</sup>, Robert V. Mulkern<sup>1,2</sup>, and Jonathan R. Polimeni<sup>2,3,4</sup>

*<sup>1</sup>Department of Radiology, Boston Children's Hospital, Boston, MA, United States, <sup>2</sup>Harvard Medical School, Boston, MA, United States, <sup>3</sup>Athinoula A. Martinos Center for Biomedical Imaging, Department of Radiology, Massachusetts General Hospital, Charlestown, MA, United States, <sup>4</sup>Harvard-MIT Division of Health Sciences and Technology, Massachusetts Institute of Technology, Cambridge, MA, United States*

Gradient-Echo Sampling of the Spin Echo (GESSE) data were acquired at 7T in 16 volunteers (ages: 23-87 years). In globus pallidus and putamen, the reversible and irreversible transverse relaxation rates derived from this data varied with age in a manner largely consistent with prior postmortem studies of iron concentration. The exception to this was when calcifications appeared to be present, leading to outliers in the reversible (but not irreversible) relaxation rates. Our results suggest that consideration of both reversible and irreversible transverse relaxation rates may reveal valuable information about tissue microstructure and may complement measurements based primarily on phase contrast.

471

14:45



Combining inhomogenous Magnetization Transfer (ihMT) with multi-point Dixon (mDixon) for myelin imaging with efficient fat suppression

Ece Ercan<sup>1</sup>, Ivan E Dimitrov<sup>2,3</sup>, Gopal Varma<sup>4</sup>, Xinzeng Wang<sup>1</sup>, Marco Pinho<sup>1,2</sup>, Ananth J Madhuranthakam<sup>1,2</sup>, Robert E Lenkinski<sup>1,2</sup>, and Elena Vinogradov<sup>1,2</sup>

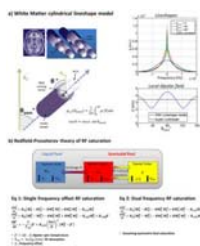


<sup>1</sup>Radiology, University of Texas Southwestern Medical Center, Dallas, TX, United States, <sup>2</sup>Advanced Imaging Research Center, University of Texas Southwestern Medical Center, Dallas, TX, United States, <sup>3</sup>Philips Healthcare, Gainesville, FL, United States, <sup>4</sup>Radiology, Division of MR Research, Beth Israel Deaconess Medical Center, Harvard Medical School, Boston, MA, United States

Inhomogeneous magnetization transfer (ihMT) imaging is a novel enhanced magnetization transfer technique which has recently been applied in human brain and spinal cord. Spinal cord applications of ihMT can especially benefit from a robust fat suppression to help with reducing of the strong fat signal from the large voxel size used by this method. Here we introduce a pulsed ihMT-prepared 3D SPGR sequence with multi-echo Dixon acquisition for a robust fat suppression of the ihMT images. The ihMT multi-echo Dixon method is shown to provide an excellent fat and water separation without a compromise of the observable ihMT effect.

472

14:57



### Anisotropy of inhomogeneous Magnetization Transfer (ihMT) in White Matter

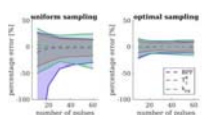
Olivier M. Girard<sup>1</sup>, Valentin H. Prevost<sup>1</sup>, Samira Mchinda<sup>1</sup>, Gopal Varma<sup>2</sup>, David C. Alsop<sup>2</sup>, and Guillaume Duhamel<sup>1</sup>

<sup>1</sup>Aix Marseille Univ, CNRS, CRMBM, Marseille, France, <sup>2</sup>Division of MR Research, Beth Israel Deaconess Medical Center, Harvard Medical School, Boston, MA, United States

Inhomogeneous magnetization transfer (ihMT) is a new endogenous contrast mechanism that has been proposed for imaging myelinated tissues. The dipolar interaction underlying the ihMT effect is intrinsically anisotropic, exhibiting the well-known  $(3\cos^2\theta - 1)$  angle dependency. Here we report experimental evidence of the anisotropy of ihMT in white matter and we derive a realistic theoretical model combining the angular dependency of the myelin lineshape and dipolar-order RF saturation theory.

473

15:09



### Optimal framework for quantitative magnetization transfer imaging of small structures

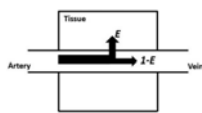
Marco Battiston<sup>1</sup>, Francesco Grussu<sup>1</sup>, Andrada Ianus<sup>2,3</sup>, Torben Schneider<sup>4</sup>, Ferran Prados<sup>1,5</sup>, James Fairney<sup>6</sup>, Sebastien Ourselin<sup>5</sup>, Daniel C Alexander<sup>2</sup>, Mara Cercignani<sup>7</sup>, Claudia A M Gandini Wheeler-Kingshott<sup>1,8,9</sup>, and Rebecca S Samson<sup>1</sup>

<sup>1</sup>*UCL Institute of Neurology, Queen Square MS Centre, UCL, London, United Kingdom,* <sup>2</sup>*Centre for Medical Image Computing, Department of Computer Science, UCL, London, United Kingdom,* <sup>3</sup>*Champalimaud Neuroscience Programme, Champalimaud Centre for the Unknown, Lisbon, Portugal,* <sup>4</sup>*Philips Healthcare, Guilford, United Kingdom,* <sup>5</sup>*Translational Imaging Group, Centre for Medical Image Computing, Department of Medical Physics and Biomedical Engineering, UCL, London, United Kingdom,* <sup>6</sup>*Department of Medical Physics and Bioengineering, UCL, London, United Kingdom,* <sup>7</sup>*CISC, Brighton & Sussex Medical School, Brighton, United Kingdom,* <sup>8</sup>*Department of Brain and Behavioural Sciences, University of Pavia, Pavia, Italy,* <sup>9</sup>*Brain MRI 3T Mondino Research Center, C. Mondino National Neurological Institute, Pavia, Italy*

Quantitative Magnetization Transfer (qMT) Imaging allows quantification of parameters describing the macromolecular component of tissues, potentially specific for myelin in the central nervous system. To date, applications of qMT in small structures (e.g. the spinal cord) have been hampered by prohibitively long acquisition. We present a framework for robust qMT examinations in small structures. It consists of: a dedicated MT-weighted sequence for reduced field-of-view imaging, explicit modelling of the non-steady state signal, and optimal definition of the sampling scheme. Superiority of the framework compared to a conventional qMT protocol is demonstrated in the healthy spinal cord and in the brainstem.

474

15:21



Towards a non-contrast assessment of blood-brain-barrier permeability  
Zixuan Lin<sup>1</sup>, Yang Li<sup>2</sup>, Pan Su<sup>2</sup>, Jay J. Pillai<sup>2</sup>, Matthias van Osch<sup>3</sup>, and Hanzhang Lu<sup>2</sup>

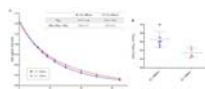
<sup>1</sup>*Department of Biomedical Engineering, Johns Hopkins University, Baltimore, MD, United States,* <sup>2</sup>*The Russell H. Morgan Department of Radiology and Radiological Science, Johns Hopkins University, Baltimore, MD, United States,* <sup>3</sup>*C.J. Gorter Center for high field MRI, Radiology, Leiden University Medical Center, Leiden, Netherlands*

Blood-brain-barrier (BBB) permeability has been shown to be disrupted in many diseases. Current study proposes a non-invasive method to measure the extraction fraction and BBB permeability of water. Studies were performed to provide proof-of-principle and a new sequence was developed to improve efficiency. These methods provided consistent results with previous literature. CO<sub>2</sub> effect on permeability was explored and increased measurement sensitivity was demonstrated.

475

15:33

### Non-invasive Assessment of Vascular Water Permeability in the Mouse Brain using multi-TE ASL



Yolanda Ohene <sup>1</sup>, Ian F Harrison <sup>1</sup>, Payam Nahavandi <sup>1</sup>, Ozama Ismail <sup>1</sup>, David Thomas <sup>2</sup>, Mark Lythgoe <sup>1</sup>, and Jack Wells <sup>1</sup>

<sup>1</sup>*UCL Centre for Advanced Biomedical Imaging, Division of Medicine, University College London, London, United Kingdom,* <sup>2</sup>*Leonard Wolfson Experimental Neurology Centre, UCL Institute of Neurology, London, United Kingdom*

We apply a multi-TE ASL technique in the mouse brain, to separate intravascular and extravascular components of the ASL signal, as a non-invasive assessment of vascular permeability. Methodological development enabled the technique to reliably capture ASL signal compartmentation in the mouse brain, despite inherently low SNR. We report a significant decrease in intravascular fraction of the ASL signal from 0.66 ( $\pm$  0.17) to 0.35 ( $\pm$  0.10) as inflow time increases from 1000ms to 1500ms. This technique can be applied to transgenic mouse models of neurodegeneration, and a kinetic model can extract vascular permeability parameters from the ASL signal distribution.

## Oral

## MR Safety

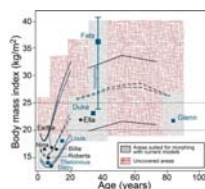
Room 312

Tuesday 13:45 - 15:45 *Moderators:* Michael Steckner & Douglas Kelley

476

13:45

### Morphing and Posing of Computational Anatomical Models: Enhanced Patient-Specific MRI RF Exposure Prediction



Manuel Murbach<sup>1</sup>, Bryn A. Lloyd<sup>1</sup>, Esra Neufeld<sup>1</sup>, Wolfgang Kainz<sup>2</sup>, and Niels Kuster<sup>1,3</sup>

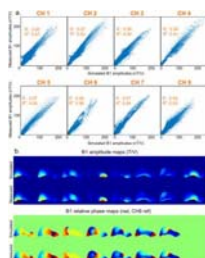
<sup>1</sup>*ITIS Foundation, Zurich, Switzerland,* <sup>2</sup>*US Food and Drug Administration (FDA), Silver Spring, MD, United States,* <sup>3</sup>*ETH Zurich, Zurich, Switzerland*

The current MRI safety standards for exposure to radiofrequency fields are conservative and intended to protect the entire patient population. Limits set on whole-body average specific absorption rate take the patient's weight into consideration, which allows robust, but only very rudimentary patient-specific exposure estimation. The introduction of combined morphing and posing in computational anatomical human models will enable further improvements in the accuracy of *in silico* local exposure estimation. In this study, we developed refined morphing techniques and explored the benefits for estimating personalized radiofrequency absorption, which could substantially reduce the safety margins necessary for conservative assessment of radiofrequency exposure.

477



13:57



An 8Tx/8Rx coil validation workflow toward Virtual Observation Points-based parallel transmission cervical spinal cord *in vivo* imaging at 7T  
Aurélien Massire<sup>1,2,3</sup>, Andreas K. Bitz<sup>4</sup>, Nicolas Boulant<sup>5</sup>, Dorothee Schüller<sup>6</sup>, Tobias Wichmann<sup>6</sup>, Thomas Troalen<sup>7</sup>, Jean-Philippe Ranjeva<sup>1,2,3</sup>, and Virginie Callot<sup>1,2,3</sup>

<sup>1</sup>Aix-Marseille Université, CNRS, CRMBM UMR 7339, Marseille, France, Marseille, France, <sup>2</sup>AP-HM, Hôpital de la Timone, Pôle d'imagerie médicale, CEMEREM, Marseille, France, <sup>3</sup>iLab-Spine - Laboratoire international associé - Imagerie et Biomécanique du rachis, France/Canada, <sup>4</sup>Medical Physics in Radiology, German Cancer Research Center (DKFZ), Heidelberg, Germany, <sup>5</sup>UNIRS, NeuroSpin, CEA/DSV/I2BM, Gif-sur-Yvette, France, <sup>6</sup>RAPID Biomedical GmbH, Rimpfing, Germany, <sup>7</sup>Siemens Healthineers, Saint-Denis, France

Parallel transmission is a cutting-edge asset to tackle RF field inhomogeneity or to realize inner volume selection for cervical spinal cord imaging at 7T. To perform VOP-based pTx *in vivo* exams with a dedicated 8Tx/8Rx coil the following workflow is proposed: 1) starting from electromagnetic simulations on generic human body models, Q-matrices sets were compressed with the VOP method. 2) B<sub>1</sub><sup>+</sup> mapping was performed on a phantom with known properties to validate these electromagnetic simulations by deriving calibration matrices, and initialize error propagations and further related safety margins. 3) MR thermometry was also performed to cross-check obtained results.

478

14:09

Massively accelerated VOP compression for population-scale RF safety models  
Andre Kuehne<sup>1</sup>, Helmar Waiczies<sup>1</sup>, and Thoralf Niendorf<sup>2</sup>



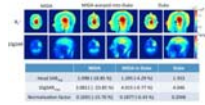
<sup>1</sup>MRI.TOOLS GmbH, Berlin, Germany, <sup>2</sup>Berlin Ultrahigh Field Facility (B.U.F.F.), Max Delbrück Center for Molecular Medicine, Germany

Generating high-accuracy VOP sets for safety assessment is hampered by long computation times. We present modifications to the generalized VOP algorithm, significantly increasing its compression capabilities and speed. The novel algorithm is validated and benchmarked on SAR and temperature matrices from nine different coil arrays.

479



14:21



### A personalised SAR model for subject-specific RF safety

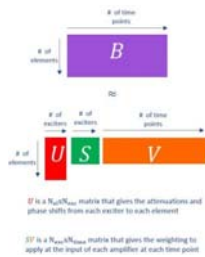
Hongbae Jeong<sup>1</sup>, Jesper Andersson<sup>1</sup>, Aaron Hess<sup>2</sup>, and Peter Jezzard<sup>1</sup>

<sup>1</sup>Nuffield Department of Clinical Neurosciences, FMRIB Centre, University of Oxford, Oxford, United Kingdom, <sup>2</sup>Department of Cardiovascular Medicine, Department of Cardiovascular Medicine, University of Oxford, Oxford, United Kingdom

In this study, we introduce a method to personalise SAR modelling by non-linear registration of a high-resolution reference voxel model into a target (subject-specific) head morphometry. We evaluate this by using two well characterised electromagnetic models, Duke and MIDA, by comparing MIDA-warped-into-Duke (MIKE), Duke and MIDA. Maps of 10g SAR across a range of B1+ shims were evaluated, showing improved agreement between the MIKE and Duke models, versus the native MIDA and Duke models. By employing personalised SAR models an increased confidence in EM simulation can be achieved.

480

14:33

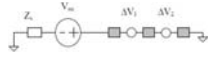


### SAR-aware parallel transmit channel compression

Mihir Pendse<sup>1</sup> and Brian K Rutt<sup>1</sup>

<sup>1</sup>Stanford University, Stanford, CA, United States

We describe a new approach for performing channel compression for pTx in cases where the number of elements in the transmit coil exceeds the number of exciters. Unlike previous methods for channel compression, the current approach takes local SAR information into account and seeks to minimize SAR while obtaining a uniform flip angle distribution. We demonstrate mitigation of local SAR hotspots with the current approach and show 30% reduction in peak local SAR compared to a SAR unaware approach.

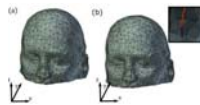


A Hybrid model for calculation of Radio Frequency heating at the electrodes of an implanted neuro-stimulator.

John Nyenhuis<sup>1</sup>, Krishna Singhal<sup>1</sup>, and Peter Single<sup>2</sup>

<sup>1</sup>Electrical and Computer Engineering, Purdue University, West Lafayette, IN, United States, <sup>2</sup>Saluda Medical, Artarmon NSW, Australia

We present an efficient computational method to calculate the temperature rise during MRI of tissue surrounding the electrodes of an active implanted lead. Inputs to the model are transmission line parameters as derived from electrical tests on the lead and the calculated tangential electric-field along the length of the lead during MRI. The method was validated by comparing measured and calculated temperature rises at the electrodes of a neurostimulation lead in a phantom test. The distribution of temperature rise in the tissues surrounding the electrode array was calculated for a whole body SAR of 2 W/kg. The maximum temperature rise was 5.4°C, which is expected to be safe, but more work would be required to assess uncertainty in this determination.

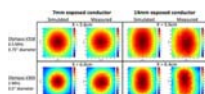


Low Heating B1 Mapping in Parallel Transmit for Deep Brain Stimulators

Clare McElcheran<sup>1</sup>, Laleh Golestanirad<sup>2</sup>, Maria Iacono<sup>3</sup>, Benson Yang<sup>4</sup>, Kevan Anderson<sup>5</sup>, Giorgio Bonmassar<sup>2</sup>, and Simon Graham<sup>4</sup>

<sup>1</sup>University of Toronto, Toronto, ON, Canada, <sup>2</sup>Massachusetts General Hospital, MA, United States, <sup>3</sup>US Food and Drug Administration, Silver Spring, MD, United States, <sup>4</sup>Sunnybrook Health Sciences Centre, ON, Canada, <sup>5</sup>Innovere Medical, ON, Canada

Deep brain stimulators and other elongated implants interact with the RF transmission fields used in MRI, potentially causing unsafe levels of localized tissue heating. It may be possible to suppress these heating effects using parallel RF transmission (pTx) methods, but a practical approach still remains to be implemented. Toward this goal, we present a method that combines intra-operative computed tomography (CT) data, electromagnetic simulations, and low-SAR B<sub>1</sub>-mapping to determine pTx input parameters for suppressing heating effects in DBS patients.



FDTD Simulation of Thermo-Acoustic Ultrasound for Detection of RF Tip Heating

Neerav Dixit<sup>1</sup>, Pascal Stang<sup>2</sup>, John Pauly<sup>1</sup>, and Greig Scott<sup>1</sup>





<sup>1</sup>Electrical Engineering, Stanford University, Stanford, CA, United States,

<sup>2</sup>Procyon Engineering, San Jose, CA, United States

Thermo-acoustic ultrasound uses the acoustic waves generated by thermoelastic expansion to detect peaks in local SAR and could be used to assess the risk of RF heating for patients with implanted or interventional devices. We developed simulations to characterize the generation and propagation of thermo-acoustic waves from device lead tips, and we validated the simulations with experimental results. The simulations provide insight into the properties of thermo-acoustic signals and can aid in the development of a thermo-acoustic ultrasound system for the assessment of RF safety.

15:21



Variation of RF heating around deep brain stimulation leads during 3.0 T MRI in fourteen patient-derived realistic lead models: The role of extracranial lead management

Laleh Golestanirad<sup>1</sup>, Julie Pilitsis<sup>2</sup>, Alastair Martin<sup>3</sup>, Paul Larson<sup>4</sup>, Boris Keil<sup>5</sup>, Giorgio Bonmassar<sup>6</sup>, and Lawrence L Wald<sup>7</sup>

<sup>1</sup>Radiology, Massachusetts General Hospital, Brookline, MA, United States, <sup>2</sup>Neurosurgery, Albany Medical Center, <sup>3</sup>Radiology, UCSF School of Medicine, <sup>4</sup>Neurological Surgery, University of California San Francisco, <sup>5</sup>Life Science Engineering, Institute of Medical Physics and Radiation Protection, Mittelhessen University of Applied Sciences (THM), <sup>6</sup>Radiology, Massachusetts General Hospital, <sup>7</sup>Massachusetts General Hospital, Charlestown, MA, United States

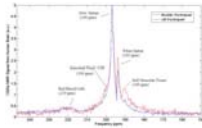
Post-operative MRI of patients with deep brain stimulation (DBS) implants is useful to assess complications and diagnose comorbidities. More than one third of medical centers, however, do not perform MRI on this patient population due to safety risks. Almost nothing is known about the variation and extent of RF heating of DBS leads during MRI at higher fields (>1.5 T) in a real patient population. Here we report the results of SAR calculations around DBS leads in a cohort of fourteen realistic DBS lead geometries. We also present preliminary results of applying an intra-operative lead management technique to reduce SAR during 3.0 T MRI.

15:33

Specific Absorption Rate, dB/dt, and Device Parameters Following MRI of Patients with Implanted Cardiac Devices







Tao Li<sup>1</sup>, Francis T. Hane<sup>1,2</sup>, Jane M. Lawrence-Dewar<sup>2</sup>, Ayman Hassan<sup>3</sup>, Karl Granberg<sup>3</sup>, Raiili M. Pellizzari<sup>1</sup>, Jennifer A. Plata<sup>2</sup>, and Mitchell S. Albert<sup>1,2,4</sup>

<sup>1</sup>Department of Chemistry, Lakehead University, Thunder Bay, ON, Canada, <sup>2</sup>Thunder Bay Regional Health Research Institute, Thunder Bay, ON, Canada, <sup>3</sup>Thunder Bay Regional Health Sciences Centre, Thunder Bay, ON, Canada, <sup>4</sup>Northern Ontario School of Medicine, Thunder Bay, ON, Canada

In this work, we present the first hyperpolarized <sup>129</sup>Xe human brain MR spectra and human brain MR images from participants with Alzheimer's Disease. We found a marked difference in the wash-out of dissolved phase xenon from the brain between the two groups, likely resulting from impaired cerebral blood flow in the Alzheimer's Disease participants. By exploring this difference, we demonstrate the feasibility and sensitivity of hyperpolarized <sup>129</sup>Xe MRI in detecting changes in cerebral perfusion and evaluating this important physiological characteristic during an early stage of mild to moderate Alzheimer's Disease.

488



14:09

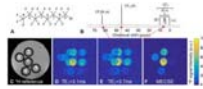


Direct ESTimation of <sup>17</sup>O MR ImageS (DIESIS) for CMRO<sub>2</sub> Quantification in the Human Brain with Partial Volume Correction

Dmitry Kurzhunov<sup>1</sup>, Robert Borowiak<sup>1,2,3</sup>, Marco Reiser<sup>1</sup>, Axel Joachim Krafft<sup>1</sup>, and Michael Bock<sup>1</sup>

<sup>1</sup>Dept. of Radiology, Medical Physics, Medical Center – University of Freiburg, Freiburg, Germany, <sup>2</sup>German Cancer Consortium (DKTK), Heidelberg, Germany, <sup>3</sup>German Cancer Research Center (DKFZ), Heidelberg, Germany

Direct <sup>17</sup>O-MRI enables quantification of cerebral metabolic rate of oxygen consumption (CMRO<sub>2</sub>). The low MR sensitivity of the <sup>17</sup>O nucleus prevents pixel-wise CMRO<sub>2</sub> quantification and the fast T<sub>2</sub>\*≈2ms decay leads to partial volume artifacts. In this work the DIESIS method is proposed, which performs a direct least squares estimation of the <sup>17</sup>O-MR signal in image regions (parcels) obtained from coregistered <sup>1</sup>H data. CMRO<sub>2</sub> values of 1.38-1.87 μmol/gtissue/min and 0.51-0.77 μmol/gtissue/min were found with DIESIS in gray and white matter consistent with rates from <sup>15</sup>O-PET studies. With DIESIS, CMRO<sub>2</sub> maps of high resolution can be reconstructed and partial volume artifacts can be reduced.

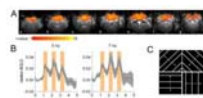


### Multi-echo chemical shift encoding (MECSE) for sensitive fluorine-19 MRI of complex spectra

Ruud B van Heeswijk<sup>1</sup>, Roberto Colotti<sup>1</sup>, Emeline Darçot<sup>1</sup>, Jean Delacoste<sup>1</sup>, Maxime Pellegrin<sup>2</sup>, Davide Piccini<sup>1,3</sup>, and Diego Hernando<sup>4,5</sup>

<sup>1</sup>Radiology, Lausanne University Hospital (CHUV), Lausanne, Switzerland, <sup>2</sup>Angiology, Lausanne University Hospital (CHUV), Lausanne, Switzerland, <sup>3</sup>Advanced Clinical Imaging Technology, Siemens Healthcare AG, Lausanne, Switzerland, <sup>4</sup>Radiology, University of Wisconsin-Madison, Madison, WI, United States, <sup>5</sup>Medical Physics, University of Wisconsin-Madison, Madison, WI, United States

Now that several clinical trials are underway, sensitive fluorine-19 MRI of biocompatible perfluorocarbons with complex MR spectra, such as perfluorooctyl bromide (PFOB), is seeing increased interest. We here therefore propose a novel multi-echo chemical shift encoding (MECSE) technique that accounts for all resonances in k-space and reconstructs a high-sensitivity image free of chemical-shift-displacement artifacts. MECSE was developed and characterized in a phantom study, compared to established techniques for imaging compounds with complex spectra, and preliminarily demonstrated in vivo.



### Coupling of the glutamate-glutamine cycle rate with both glial and neuronal oxidative metabolism in the visual cortex of the Tupaia belangeri

Sarah Sonnay<sup>1</sup>, Jordan Poirot<sup>2</sup>, Nathalie Just<sup>3</sup>, Anne-Catherine Clerc<sup>1</sup>, Rolf Gruetter<sup>1,4,5</sup>, Gregor Rainer<sup>2</sup>, and João M.N. Duarte<sup>1</sup>

<sup>1</sup>Laboratory of Functional and Metabolic Imaging (LIFMET), Ecole Polytechnique Fédérale de Lausanne (EPFL), Lausanne, Switzerland, <sup>2</sup>Department of Medicine, Visual Cognition Laboratory, University of Fribourg, Fribourg, Switzerland, <sup>3</sup>University Hospital Münster, Münster, Germany, <sup>4</sup>Department of Radiology, University de Lausanne, Lausanne, Switzerland, <sup>5</sup>Department of Radiology, University de Geneva, Geneva, Switzerland

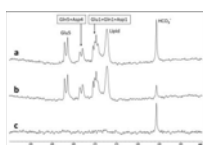
Cerebral function relies on cooperative interaction between neuronal and glial cells. While neuronal oxidative metabolism has been shown to be coupled to the glutamate-glutamine cycle that represents glutamatergic neurotransmission, it remains unclear whether similar coupling occurs for glial oxidative metabolism. We investigated cortical metabolism *in vivo* using  $^{13}\text{C}$  magnetic resonance spectroscopy (MRS) along with infusion of  $[1,6-^{13}\text{C}]$ glucose during continuous stimulation of the tree shrew visual cortex (V1). Data indicate that both neuronal and glial oxidative metabolism scale with the glutamate-glutamine cycle.

491

14:45

### Detection of Carbonic Anhydrase Activity in Human Brain in Vivo

Shizhe Li<sup>1</sup>, Li An<sup>1</sup>, Christopher Johnson<sup>1</sup>, Maria Ferraris Araneta<sup>1</sup>, and Jun Shen<sup>1</sup>



<sup>1</sup>National Institutes of Health, Bethesda, MD, United States

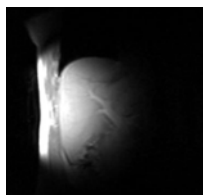
This study demonstrates the feasibility of detecting carbonic anhydrase activity in the human brain. A very large magnetization transfer effect on the bicarbonate signal was measured in healthy human subjects using  $^{13}\text{C}$  MRS upon saturation of carbon dioxide. Despite the large variations in blood glucose response to oral administration of  $^{13}\text{C}$ -labeled glucose the magnetization transfer effect was measured with high precision.

492

14:57

### MRS measurements of $[2-^{13}\text{C}]$ glycine conversion to glutathione in the liver: A new method of measuring hepatic oxidative stress defences in vivo

Stephen Bawden<sup>1,2</sup>, Bernard Lanz<sup>2</sup>, Mehri Kaviani<sup>2</sup>, Peter Morris<sup>2</sup>, Penny Gowland<sup>2</sup>, Peter Theilwall<sup>3,4</sup>, and Guruprasad P Aithal<sup>1</sup>



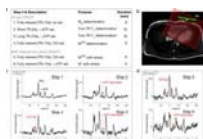
<sup>1</sup>NIHR Nottingham Digestive Diseases Unit, Nottingham University Hospitals, University of Nottingham, Nottingham, United Kingdom, <sup>2</sup>Sir Peter Mansfield Imaging Center, Physics and Astronomy, University of Nottingham, Nottingham, United Kingdom, <sup>3</sup>Newcastle Magnetic Resonance Center, Newcastle University, <sup>4</sup>Institute of Cellular Medicine, Newcastle University

With rising incidents of fatty liver disease and metabolic disorder there is a need for biomarkers that can assess progression to steatohepatitis and other forms of liver damage. Oxidative stress in the mitochondria may play a central role in disease progression, with glutathione acting as the main antioxidant. In this study we developed a method previously suggested to monitor hepatic glutathione production in vivo by administering oral [2-13C] labelled glycine and using  $^{13}\text{C}$  MRS to measure conversion to glutathione. Following optimization, we tested variability in 8 healthy volunteers over two visits.

493



15:09



### StreST: Myocardial Creatine Kinase Rate in Both Rest and Stress.

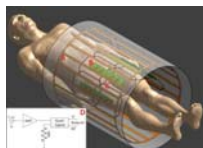
William T Clarke<sup>1</sup>, Jennifer J Rayner<sup>1</sup>, Betty Raman<sup>1</sup>, Stefan Neubauer<sup>1</sup>, Oliver J Rider<sup>1</sup>, and Christopher T Rodgers<sup>1</sup>

<sup>1</sup>OCMR, CV Med RDM, University of Oxford, Oxford, United Kingdom

A method for reduced time and stress myocardial creatine kinase measurements using 31P-MRS at 3T is presented. The new method is validated in healthy controls and demonstrated in 27 obese and heart-failure patients. In addition, the existing TRiST method is applied in 63 subjects for the first time on a Siemens platform.

494

15:21



### Multi-transmit proton MRI combined with high power body transmit and receive array for 7 Tesla phosphorus imaging

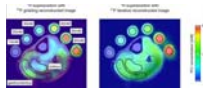
Mark Gosselink<sup>1</sup>, Dimitri Welting<sup>1</sup>, Tim Linnartz<sup>2</sup>, Ingmar Voogt<sup>1</sup>, Bart Steensma<sup>1</sup>, Lucian A.B. Purvis<sup>3</sup>, Christopher T. Rodgers<sup>3</sup>, Tijn van der Velden<sup>1</sup>, Wybe van der Kemp<sup>1</sup>, and Dennis W.J. Klomp<sup>1</sup>

<sup>1</sup>University Medical Center Utrecht, Utrecht, Netherlands, <sup>2</sup>MRCOils, Zaltbommel, Netherlands, <sup>3</sup>University of Oxford Centre for Clinical Magnetic Resonance Research (OCMR), Oxford, United Kingdom

We have integrated a body RF coil tuned at the 31P frequency outside the patient tube in a 7T MR system for homogeneous B1 transmit and combined it with a 8 channel 31P receive array for optimal sensitivity. Imaging and B0 shimming is done with radiative antennas integrated in the receiver setup. With this setup, large field of view imaging and broadband 31P MRSI with high SNR can be obtained.

15:33

Fast quantitative 31P MRI using prior information from 1H MRI



Kristian Rink<sup>1</sup>, Nicolas G.R. Behl<sup>1</sup>, Christine Gnahn<sup>1</sup>, Peter Bachert<sup>1</sup>, and Armin M. Nagel<sup>1,2</sup>

<sup>1</sup>German Cancer Research Center (DKFZ), Heidelberg, Germany,

<sup>2</sup>University Hospital Erlangen, Erlangen, Germany

Phosphorus-containing biomolecules play a crucial role in the energy metabolism of the human body. Compared to hydrogen, the *in vivo* phosphorus MR signal is four orders of magnitude lower. In this study, a conventional gridding reconstruction applied on the phosphocreatine signal of the human calf was compared to a constraint iterative approach, which uses prior knowledge from hydrogen MRI data. For both reconstructions, different acquisition times were tested and phosphocreatine concentrations in the gastrocnemius and soleus muscles were estimated.

## Oral

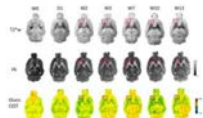
# Multimodal & Multiparametric Neuroimaging

Room 313BC

Tuesday 13:45 - 15:45 *Moderators:* Florian Knoll & Xiaohong Joe Zhou

496

13:45



## LONG TERM EFFECTS OF PULSED FOCUSED ULTRASOUND AND MICROBUBBLES DETECTED BY MULTIVARIATE IMAGING MODALITIES

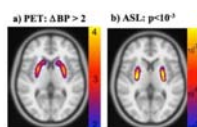
Zsofia I Kovacs<sup>1</sup>, Tsang-Wei Tu<sup>1</sup>, Georgios Z Papadakis<sup>1,2</sup>, William C Reid<sup>2</sup>, Dima A Hammoud<sup>2</sup>, and Joseph A Frank<sup>1,3</sup>

<sup>1</sup>Frank Laboratory, Radiology and Imaging Sciences, Clinical Center, National Institutes of Health, Bethesda, MD, United States, <sup>2</sup>Center for Infectious Disease Imaging (CIDI), Radiology and Imaging Sciences, National Institutes of Health, Bethesda, MD, United States, <sup>3</sup>National Institute of Biomedical Imaging and Bioengineering, National Institutes of Health, Bethesda, MD, United States

Blood brain barrier (BBB) opening by MR-guided pulsed Focused Ultrasound (pFUS) and microbubbles (MB) is a non-invasive treatment of various central nervous system diseases. However, the potential adverse effects of repeated pFUS+MB exposure have not been thoroughly elucidated and may limit clinical translation. To date MRI scans of repeated BBB opening by pFUS+MB have been achieved without hemorrhage, edema and behavioral changes in non-human primates (Arvanitis, et al. 2015; Downs, et al. 2015). By incorporating detailed multivariate imaging modalities we characterized the long term effects of single or repeated pFUS+MB in the rat brain.

497

13:57



### Function versus occupancy in the human brain: PET/fMRI during infusion of D2 antagonist

Tracy Barbour<sup>1,2</sup>, Christin Sander<sup>3,4</sup>, Daphne J. Holt<sup>1,5</sup>, and Joseph Mandeville<sup>3,4</sup>

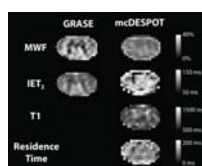
<sup>1</sup>Psychiatry, Massachusetts General Hospital and Athinoula A. Martinos Center for Biomedical Imaging, Boston, MA, United States, <sup>2</sup>Harvard Medical School, Boston, MA, United States, <sup>3</sup>Radiology, Massachusetts General Hospital and Athinoula A. Martinos Center for Biomedical Imaging, Boston, MA, United States, <sup>4</sup>Radiology, Harvard Medical School, Boston, MA, United States, <sup>5</sup>Psychiatry, Harvard Medical School, Boston, MA, United States

Simultaneous PET and fMRI were employed in healthy human subjects to investigate the dose-dependent relationship between drug occupancies of a D2-receptor antagonist and induced CBF responses measured by arterial spin labeling. Results indicate a super-linear relationship between CBF and occupancy, with a larger CBF response in putamen than in caudate at matched occupancies. These results inform dopaminergic neurophysiology, and the method may provide general utility for probing dopaminergic function in human subject cohorts.

498



14:09



### Myelin Water Imaging Using T2-Relaxation in the Spinal Cord; Comparison of Multi-echo GRASE and mcDESPT

Emil Ljungberg<sup>1</sup>, Irene Vavasour<sup>2</sup>, Alexander Rauscher<sup>3</sup>, Anthony Traboulsee<sup>1</sup>, Alex MacKay<sup>2,4</sup>, and Shannon Kolind<sup>1,2</sup>

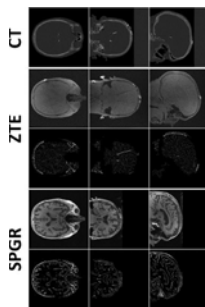


<sup>1</sup>Medicine, University of British Columbia, Vancouver, BC, Canada,  
<sup>2</sup>Radiology, University of British Columbia, Vancouver, BC, Canada,  
<sup>3</sup>Pediatrics, University of British Columbia, Vancouver, BC, Canada,  
<sup>4</sup>Physics and Astronomy, University of British Columbia, Vancouver, BC,  
Canada

There are currently several techniques for in vivo myelin water imaging using  $T_2$  relaxation. In this study we compare two clinically feasible myelin water imaging protocols for the cervical spinal cord: mcDESPOT and multi-echo GRASE. Myelin estimates from GRASE were consistently higher than mcDESPOT in white matter, but both techniques were able to differentiate between white and gray matter.  $T_1$  estimates from mcDESPOT also showed clear differences between white and gray matter. By combining GRASE and mcDESPOT, with total acquisition time less than 15 min, we can build a better picture of the tissue microstructure of the spinal cord.

499

14:21



#### Improved Localisation of DBS Electrodes using Pseudo-Positive Contrast from a Zero-Echo-Time Acquisition

Rolf F Schulte<sup>1</sup>, Jeffrey Ashe<sup>2</sup>, Sohan Ranjan<sup>3</sup>, Julia Prusik<sup>4</sup>, Julie Pilitsis<sup>4</sup>, Stanley Hayes<sup>5</sup>, Anne Menini<sup>1</sup>, Florian Wiesinger<sup>1</sup>, and Ileana Hancu<sup>2</sup>

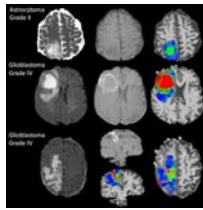
<sup>1</sup>GE Global Research, Munich, Germany, <sup>2</sup>GE Global Research, Niskayuna, NY, United States, <sup>3</sup>GE Global Research, Bangalore, India, <sup>4</sup>Albany Medical College, Albany, NY, United States, <sup>5</sup>Alliance Healthcare Radiology, Nathan Littauer, Gloversville, NY, United States

The goal of this work is to reduce artefact extent and improve localisation of deep-brain stimulation (DBS) electrodes with MRI. A Zero Echo-Time (ZTE) sequence was used for data acquisition in a phantom and a patient; the minimal signal voids around electrodes, the ZTE's natural proton-density weighting and low SAR/ $B_{1rms}$  make it ideal for imaging implants. A pseudo-positive contrast image was first generated by inverting ZTE image intensity values, fitting and subtracting the background signal; a centre of mass calculation and singular value decomposition were then employed for electrode detection. Similar-sized artefacts as in CT images and improved precision over standard T1-weighted imaging were demonstrated.

500

14:33

Tissue type mapping of gliomas using multimodal MRI



Felix Raschke<sup>1</sup>, Thomas Richard Barrick<sup>2</sup>, Guang Yang<sup>3</sup>, Timothy Lloyd Jones<sup>4</sup>, Xujiong Ye<sup>5</sup>, and Franklyn Arron Howe<sup>2</sup>

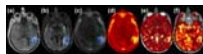
<sup>1</sup>Faculty of Medicine and University Hospital Carl Gustav Carus, OncoRay – National Center for Radiation Research in Oncology, Dresden, Germany, <sup>2</sup>Neurosciences Research Centre, St George's, University of London, London, United Kingdom, <sup>3</sup>National Heart and Lung Institute, London, United Kingdom, <sup>4</sup>Academic Neurosurgery Unit, St George's, University of London, London, United Kingdom, <sup>5</sup>Laboratory of Vision Engineering, School of Computer Science, University of Lincoln

1H MRSI can assess glioma infiltration margins and malignant invasion but technical limitations prevent widespread use. In this study we used 2D 1H MRSI to determine voxels of specific tumour tissue type from which we extracted multimodal MRI (M-MRI) image characteristics. Subsequently, we applied superpixel segmentation and Bayesian statistical analysis to M-MRI alone to derive nosologic tumor images of these same tissue types with whole brain coverage. We obtained 100% classification accuracy for overall glioma grade, and an average 0.77 Dice overlap coefficient with the manual segmentation volume. Such methodology could aid prognostic assessment, surgical treatment and radiotherapy dose planning.

---

501

14:45



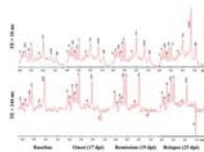
### Multimodal Imaging of Vascularity and Drug Delivery in GBM Patients Treated with Anti-angiogenesis Inhibitor

Yi-Fen Yen<sup>1</sup>, Jayashree Kalpathy-Cramer<sup>1</sup>, Ciprian Catana<sup>1</sup>, Xiao Da<sup>2</sup>, Yangming Ou<sup>1</sup>, Andrew L. Beers<sup>1</sup>, Jacob Hooker<sup>1</sup>, Bruce Rosen<sup>1</sup>, Tracy Batchelor<sup>3</sup>, and Elizabeth R. Gerstner<sup>3</sup>

<sup>1</sup>Athinoula A. Martinos Center for Biomedical Imaging, Massachusetts General Hospital, Charlestown, MA, United States, <sup>2</sup>Functional Neuroimaging Laboratory, Brigham and Women's Hospital, Boston, MA, United States, <sup>3</sup>Department of Neuro-oncology, Massachusetts General Hospital, Boston, MA, United States

Anti-angiogenic agents can decrease vessel permeability and perfusion, raising concerns that these agents may also decrease blood brain barrier penetration of concomitantly administered chemotherapy. Using MR-PET multimodal imaging, we found radiolabeled temozolomide correlated with permeability and perfusion in patients with recurrent GBM treated with bevacizumab. MR assessment of vascularity may be a surrogate marker for concomitant drug delivery.

---



Haemodynamic and metabolic MR biomarkers of disease progression in an animal model of relapsing-remitting multiple sclerosis

Mohamed Tachrount<sup>1</sup>, Andrew Davies<sup>1</sup>, Flavia Rosianu<sup>1</sup>, Roshni Desai<sup>1</sup>, David Thomas<sup>1</sup>, Kenneth Smith<sup>1</sup>, and Xavier Golay<sup>1</sup>

<sup>1</sup>Institute of Neurology, UCL, London, United Kingdom

Multiple sclerosis (MS) is a chronic inflammatory demyelinating and neurodegenerative disorder of unknown cause affecting the central nervous system. We have assessed haemodynamic and metabolic alterations within spinal cord during disease progression in an animal model (experimental autoimmune encephalomyelitis (EAE) by combining both arterial spin labelling (ASL) and MR Spectroscopy. We demonstrate for the first time that the neurological deficits are strongly correlated with impaired blood flow and reveal both reversible and irreversible simultaneous metabolic alterations.

Table 1: Significant differences between HIV+ and control volume and thickness measures

Brain region	HIV+ (MP)	Control (MP)	F	p
Right Thalamus	1075.17 (24.36)	1022.17 (24.51)	4.58	0.033
Midline Corpus Callosum	104.27 (2.86)	107.88 (2.46)	4.35	0.040
Left Corpus Callosum	103.00 (2.7)	105.00 (2.7)	4.35	0.040
Mid Corpus Callosum	103.00 (2.7)	105.00 (2.7)	4.35	0.040
Total Corpus Callosum	103.00 (2.7)	105.00 (2.7)	4.35	0.040
Total Hippocampus	17.00 (0.7)	17.00 (0.7)	5.81	0.019
Right Hippocampus	17.00 (0.7)	17.00 (0.7)	5.81	0.019
Left Hippocampus	17.00 (0.7)	17.00 (0.7)	5.81	0.019

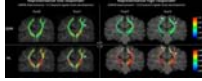
<sup>a</sup>Values adjusted for age and sex.

Multimodal MR investigation of brain and behavioral changes in patients with HIV-infections

Michael Albert Thomas<sup>1</sup>, Rajakumar Nagarajan<sup>2</sup>, Eric S Daar<sup>3</sup>, Santosh K Yadav<sup>4</sup>, Charles H Hinkin<sup>5</sup>, Manoj K Sarma<sup>6</sup>, Zohaib Iqbal<sup>1</sup>, Sathya Arumugam<sup>1</sup>, Mario Guerrero <sup>3</sup>, Mohammad Haris<sup>4</sup>, and Ebrahim Haroon<sup>7</sup>

<sup>1</sup>Radiological Sciences, UCLA Geffen School of Medicine, Los Angeles, CA, United States, <sup>2</sup>Radiological Science, UCLA Geffen School of Medicine, Los Angeles, CA, United States, <sup>3</sup>Medicine, Harbor-UCLA Medical Center, Torrance, CA, United States, <sup>4</sup>Research Branch, Sidra Medical and Research center, Doha, Qatar, <sup>5</sup>Psychiatry, UCLA Geffen School of Medicine, Los Angeles, CA, United States, <sup>6</sup>Radiological Sciences, UCLA Geffen School of Medicine, Los Angeles, CA, <sup>7</sup>Psychiatry, Emory University, Atlanta, GA, United States

Regional brain volumes and cortical thickness using 3D T1-weighted MP-RAGE and neurometabolites quantitated using 5D EP-JRESI MRSI were obtained from a group of HIV+ (n=16) and HIV-subjects (n=15). Compared to HIV- subjects, following findings were observed in HIV+: i) decreases in the volume of right thalamus, mid anterior corpus callosal region and cortex (right, left, combined), and ii) decreases in cortical thickness of superior parietal and inferior temporal regions. The cortical thickness and volumetric changes were predicted by (increased choline, decreased NAA and Glx). Right basal ganglia glutamate/glutamine ratios and HIV+ status together significantly predicted psychomotor slowing during neurocognitive testing.

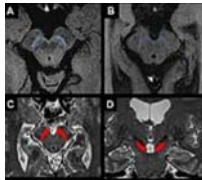


Combined tract-based analysis of diffusion fractional anisotropy and quantitative susceptibility mapping: a joint assessment of axonal and myelin microstructural changes in children with cerebral palsy

Lijia Zhang<sup>1</sup>, Lyon Wade Chen<sup>1</sup>, Susan Ellor<sup>1</sup>, Jessica Sun<sup>1</sup>, Joanne Kurtzberg<sup>1</sup>, and Allen Song<sup>1</sup>

<sup>1</sup>*Brain Imaging and Analysis Center, Durham, NC, United States*

In this report we developed a tract-based diffusion anisotropy and magnetic susceptibility analysis approach to jointly evaluate the potential mechanisms for axonal growth and myelin repair in children undergoing autologous cord blood stem cell therapy. Advancing from our prior findings that baseline brain connectivity is correlated with CP disease severity and that brain connectivity increase is correlated with functional motor improvement in CP patients, we provide further evidence that the increased brain connectivity may be the result of increased myelination of the affected neural pathways, in addition to the possibility of axonal regeneration.



Multimodal MRI biomarker study of substantia nigra damage in idiopathic REM sleep behavior disorder

Nadya Pyatigorskaya<sup>1,2,3</sup>, Rahul Gaurav<sup>2</sup>, Dario Arnaldi<sup>4</sup>, Smaranda Leu-Semenescu<sup>5</sup>, Lydia Yahia-Cherif<sup>2</sup>, Romain Valabregue<sup>2</sup>, Marie Vidailhet<sup>3,6</sup>, and Stephane Lehericy<sup>1,2,3</sup>

<sup>1</sup>*Neuroradiology department, APHP, Pitié Salpêtrière, Paris, France,* <sup>2</sup>*Centre de NeuroImagerie de Recherche – CENIR, ICM, ICM, Paris, France,* <sup>3</sup>*UPMC Univ Paris 06, UMR S 1127, CNRS UMR 7225, ICM, F-75013, Paris, France, Sorbonne universités, Paris, France,* <sup>4</sup>*Clinical Neurology, Dept. of Neuroscience, University of Genoa, Italy,* <sup>5</sup>*Service des pathologies du Sommeil, Hôpital Pitié-Salpêtrière, APHP, Pitié Salpêtrière, Paris, France,* <sup>6</sup>*Clinique des mouvements anormaux, Département des Maladies du Système Nerveux, APHP, Pitié Salpêtrière, Paris, France*

We quantified substantia nigra (SN) damage in idiopathic REM sleep behavior disorder (iRBD) patients using multimodal MRI biomarkers and determined biomarker efficacy. Nineteen patients with iRBD and 18 healthy volunteers underwent 3-Tesla MRI, including diffusion tensor imaging, neuromelanin (NM)-sensitive imaging and T2\* mapping. The volume and normalized signal intensity in NM-sensitive images, R2\* and diffusion tensor measures were quantified in the SN. Patients with iRBD showed reduced NM-sensitive volume and signal intensity and reduced fractional anisotropy versus controls in the SN. Combination of the three biomarkers had excellent diagnostic accuracy. These measures may represent valuable biomarkers for prodromal Parkinson's disease.

---

Oral

## Psychiatric Neuroimaging

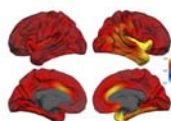
Room 314

Tuesday 13:45 - 15:45 *Moderators: Salil Soman & Meiyun Wang*

---

506

13:45

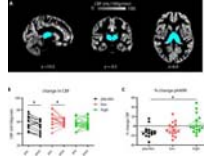


Structural brain changes after Electroconvulsive therapy are broadly distributed.

Leif Oltedal<sup>1,2</sup>, Ute Kessler<sup>3</sup>, Donald Hagler<sup>1</sup>, Vera Jane Erchinger<sup>2</sup>, Dominic Holland<sup>1</sup>, Ketil J Oedegaard<sup>2</sup>, and Anders M Dale<sup>1,4</sup>

*<sup>1</sup>Center for Multimodal Imaging and Genetics, University of California San Diego, San Diego, CA, United States, <sup>2</sup>Department of Clinical Medicine, University of Bergen, Bergen, Norway, <sup>3</sup>Division of Psychiatry, Haukeland University Hospital, Bergen, Norway, <sup>4</sup>Department of Radiology, University of California San Diego, CA, United States*

Major depression is the leading cause of disability in the world. Electroconvulsive therapy (ECT) which is used in major depression when other treatments are ineffective, has been shown to cause increased volume of multiple specific subcortical and cortical regions. A sample of 19 patients with T1-weighted 3D volumes acquired before and after ECT was analyzed by using nonlinear registration and unbiased methods for quantification of regional anatomical change (Quarc). The effect sizes of ECT-induced brain changes are large, and the changes are more broadly distributed than previously thought. The results suggest a global effect, probably modulated by the stimulation parameters.

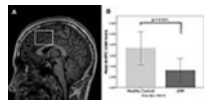


### Dose-dependent effects of citalopram on serotonergic function assessed with SPECT and pharmacological MRI

Anouk Schrantee<sup>1</sup>, Henk JMM Mutsaerts<sup>1,2</sup>, Jan Booij<sup>3</sup>, and Liesbeth Reneman<sup>1</sup>

<sup>1</sup>Department of Radiology, Academic Medical Center, University of Amsterdam, Amsterdam, Netherlands, <sup>2</sup>Sunnybrook Research Institute, University of Toronto, Toronto, Canada, <sup>3</sup>Department of Nuclear Medicine, Academic Medical Center, University of Amsterdam, Amsterdam, Netherlands

Serotonin transporter (SERT) imbalances are involved in the pathogenesis of a wide range of neuropsychiatric diseases, including depression. SERT blockers, like citalopram, decrease radioligand binding to the SERT in a dose-dependent manner, as measured with SPECT. In addition to replicating this finding, we show that pharmacological MRI (phMRI) can also detect differences in SERT occupancy with different oral doses of citalopram; higher citalopram plasma levels are associated with lower subsequent changes in the phMRI signal upon an intravenous citalopram challenge. This is important as this non-ionizing technique allows longitudinal assessment of the serotonin system.



### Relationship Between Prefrontal GABA Levels and Hippocampal Resting Activity in Subjects at Ultra High Risk of Psychosis: A Combined MRS-pCASL study

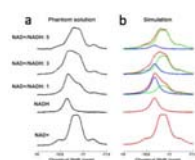
Gemma Modinos<sup>1</sup>, Fatma Simsek<sup>1</sup>, Jamie Horder<sup>1</sup>, Matthijs Bossong<sup>2</sup>, Carly Samson<sup>3</sup>, Matilda Azis<sup>1</sup>, Beverly Quinn<sup>4</sup>, Ilaria Bonoldi<sup>1</sup>, Paul Allen<sup>1,5</sup>, Philip McGuire<sup>1</sup>, and James Stone<sup>1</sup>

<sup>1</sup>Institute of Psychiatry, Psychology & Neuroscience, King's College London, London, United Kingdom, <sup>2</sup>University Medical Center Utrecht, Utrecht, Netherlands, <sup>3</sup>University of Surrey, Guildford, United Kingdom, <sup>4</sup>CAMEO, Cambridgeshire and Peterborough Mental Health Partnership NHS Trust, Cambridge, United Kingdom, <sup>5</sup>University of Roehampton, London, United Kingdom

Converging evidence from preclinical studies indicates that dysfunction of the gamma-aminobutyric acidergic (GABAergic) neurotransmitter system plays a major role in the pathophysiology of schizophrenia. Despite the improved methods and reliability of neuroimaging measurements, which have recently facilitated testing predictions from animal models in humans, the extent to which GABAergic neurotransmission is altered in patients with psychosis is less clear. Furthermore, although preclinical evidence suggests that decreased cortical interneuron function leads to hippocampal activity overdrive, no study has explicitly investigated the relationship between neurotransmission and neurophysiology in humans. Here we show that prefrontal GABA function is reduced in individuals at ultra high risk of developing psychosis and that this reduction is related to hippocampal (and nominally to prefrontal) resting activity. These findings shed light on the pathophysiology of vulnerability for schizophrenia by showing that alterations in GABAergic systems have downstream effects on hippocampus before the onset of psychosis.

509

14:33



#### “Brain Rust” in Schizophrenia Revealed by in vivo Redox (NAD<sup>+</sup>/NADH) Measurement

Fei Du<sup>1</sup>, Sang-Young Kim<sup>1</sup>, Bruce M. Cohen<sup>1</sup>, Xi Chen<sup>1</sup>, Scott Lukas<sup>1</sup>, Ann Shinn<sup>1</sup>, Cagri Yuksel<sup>1</sup>, Tao Li<sup>2</sup>, and Dost Ongur<sup>1</sup>

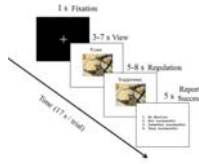
<sup>1</sup>McLean Hospital, Harvard Medical School, Belmont, MA, United States, <sup>2</sup>West China Hospital, Sichuan University, Chengdu, People's Republic of China

A growing body of evidence suggests that an “immuno-oxidative” pathway including redox dysregulation associated with oxidative stress, mitochondrial dysfunction, neuroinflammation, and cell-mediated immune response may contribute to disruptions in brain activity in schizophrenia (SZ). The aim of this study is to assess possible redox imbalance in SZ patients by using a novel in vivo <sup>31</sup>P-MRS technique to measure NAD<sup>+</sup> and NADH. Our results revealed a ~40% decrease of NAD<sup>+</sup>/NADH ratio compared to healthy individuals of similar age, indicating higher levels of oxidative stress in patients with schizophrenia. This work may lead to new strategies to protect the brain from oxidative stress and improve brain function in schizophrenia or the other brain disorders.

14:45

Effective Connectivity Network of Emotion Regulation in Soldiers with Trauma





D Rangaprakash<sup>1,2</sup>, Michael N Dretsch<sup>3,4</sup>, Thomas A Daniel<sup>5,6</sup>, Thomas S Denney<sup>1,5,7</sup>, Jeffrey S Katz<sup>1,5,7</sup>, and Gopikrishna Deshpande<sup>1,5,7</sup>

<sup>1</sup>AU MRI Research Center, Department of Electrical and Computer Engineering, Auburn University, Auburn, AL, United States, <sup>2</sup>Department of Psychiatry and Biobehavioral Sciences, University of California Los Angeles, Los Angeles, CA, United States, <sup>3</sup>Human Dimension Division, HQ TRADOC, Fort Eustis, Fort Eustis, VA, United States, <sup>4</sup>U.S. Army Aeromedical Research Laboratory, Fort Rucker, Fort Rucker, AL, United States, <sup>5</sup>Department of Psychology, Auburn University, Auburn, AL, United States, <sup>6</sup>Department of Psychology, Westfield State University, Westfield, MA, United States, <sup>7</sup>Alabama Advanced Imaging Consortium, Auburn University and University of Alabama Birmingham, Birmingham, AL, United States

Conscious regulation of emotions is essential for sound functioning of an individual, while its disruption leads to several severe symptoms observed in psychiatric disorders like posttraumatic stress disorder (PTSD) and mild-traumatic brain injury (mTBI). While the brain regions activated in emotion regulation have been elucidated in prior works, an understanding of the underlying network has been elusive. Employing an emotion regulation task, we discovered the network of emotion regulation in healthy soldiers, and dysregulation in soldiers with comorbid PTSD/mTBI (N=59). Our work is significant given that we present, for the first time, the evidence for the network of emotion regulation/dysregulation.

14:57



Investigating Brain Connectomic Alterations in PTSD and PCS using the Reproducibility of Independent Components obtained from Resting-State Functional MRI Data

Mohammed Syed<sup>1</sup>, D Rangaprakash<sup>2,3</sup>, Michael N Dretsch<sup>4,5</sup>, Thomas S Denney<sup>2,6,7</sup>, Jeffrey S Katz<sup>2,6,7</sup>, and Gopikrishna Deshpande<sup>2,6,7</sup>

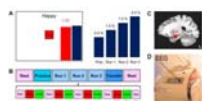
<sup>1</sup>Department of Computer Science and Software Engineering, Auburn University, Auburn, AL, United States, <sup>2</sup>AU MRI Research Center, Department of Electrical and Computer Engineering, Auburn University, Auburn, AL, United States, <sup>3</sup>Department of Psychiatry and Biobehavioral Sciences, University of California Los Angeles, Los Angeles, CA, United States, <sup>4</sup>Human Dimension Division, HQ TRADOC, Fort Eustis, Fort Eustis, VA, United States, <sup>5</sup>U.S. Army Aeromedical Research Laboratory, Fort Rucker, Fort Rucker, AL, United States, <sup>6</sup>Department of Psychology, Auburn University, Auburn, AL, United States, <sup>7</sup>Alabama Advanced Imaging Consortium, Auburn University and University of Alabama Birmingham, Birmingham, AL, United States

Posttraumatic stress disorder (PTSD) and Post-concussion syndrome (PCS) are heterogeneous neurological disorders where fMRI connectivity metrics derived from them may not be highly reproducible, leading to poor generalizability and consequently lower classification accuracies. We present a method that characterizes the reproducibility of networks using 'generalized Ranking and Averaging Independent Component Analysis by Reproducibility' (gRAICAR) algorithm followed by unsupervised clustering to discriminate between the groups based on functional brain networks that are most reproducible within PTSD, PCS, and healthy control groups separately. We identify dorsolateral prefrontal cortex, inferior parietal lobule, caudate and medial prefrontal cortex as regions within the most reproducible independent components.

---

512

15:09



Real-time fMRI Neurofeedback of the Amygdala Enhances Amygdala-orbitofrontal Connectivity and Lateralized EEG Coherence in Veterans with Combat-related PTSD

Vadim Zotev<sup>1</sup>, Raquel Phillips<sup>1</sup>, Masaya Misaki<sup>1</sup>, Chung Ki Wong<sup>1</sup>, Brent Wurfel<sup>1</sup>, Matthew Meyer<sup>1,2</sup>, Frank Krueger<sup>1,3</sup>, Matthew Feldner<sup>1,4</sup>, and Jerzy Bodurka<sup>1,5</sup>

<sup>1</sup>Laureate Institute for Brain Research, Tulsa, OK, United States,

<sup>2</sup>Laureate Psychiatric Clinic and Hospital, Tulsa, OK, United States,

<sup>3</sup>Neuroscience Dept., George Mason University, Fairfax, VA, United States,

<sup>4</sup>Dept. of Psychological Science, University of Arkansas,

Fayetteville, AR, United States, <sup>5</sup>College of Engineering, Stephenson

School of Biomedical Engineering, University of Oklahoma, Tulsa, OK, United States

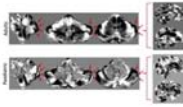
We have performed a study of emotion regulation training in veterans with combat-related PTSD using real-time fMRI neurofeedback (rtfMRI-nf) with simultaneous EEG. Eighteen PTSD patients learned to upregulate their left amygdala activity using rtfMRI-nf during a positive emotion induction task based on retrieval of happy autobiographical memories. Enhancement in the amygdala-orbitofrontal functional connectivity during the rtfMRI-nf task showed positive correlation with severity of PTSD symptoms. Enhancement in left-lateralized upper alpha EEG coherence also positively correlated with PTSD severity. These results suggest that the rtfMRI-nf of the amygdala has the potential to correct the functional connectivity deficiencies specific to PTSD.

---

513

15:21

The Cerebellum and Brainstem Together Increase Classification Accuracy for Autism Spectrum Disorder over the Whole Brain



Muriel M. K. Bruchhage<sup>1</sup>, Leon M. Aksman<sup>1</sup>, Andre F. Marquand<sup>2</sup>, MRC AIMS Consortium<sup>3</sup>, EU TACTICS Consortium<sup>4</sup>, Jan Buitelaar<sup>2</sup>, Declan Murphy<sup>5</sup>, and Steven C. R. Williams<sup>1</sup>

<sup>1</sup>Centre for Neuroimaging Sciences, Institute of Psychiatry, Psychology and Neuroscience, King's College London, London, United Kingdom,

<sup>2</sup>Department of Cognitive Neuroscience, Donders Institute for Brain, Cognition and Behaviour, Radboud University Medical Center,

Nijmegen, Netherlands, <sup>3</sup>Centre for Neuroimaging Sciences, Institute of Psychiatry, Psychology and Neuroscience, King's College London;

Cambridge University; Oxford University, London; Cambridge; Oxford, United Kingdom, <sup>4</sup>Radboud University Medical Center; King's College

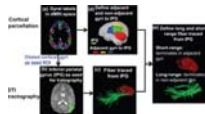
London; University Medical Center Utrecht; Central Institute of Mental Health Mannheim, Nijmegen; London; Utrecht; Mannheim, Netherlands,

<sup>5</sup>Sackler Institute of Translational Neuroimaging, Department of Forensics and Neurodevelopmental Sciences, Institute of Psychiatry, Psychology and Neuroscience, King's College London, London, United Kingdom

Autism spectrum disorder (ASD) has been linked to cerebellar and brainstem dysfunction and abnormal development, but it remains unclear whether these regional abnormalities can help classify the disorder. Performing machine learning based classification using Jacobian determinant based features on two independent male ASD cohorts (adult and paediatric) of different sizes and age range, we demonstrated a consistently higher classification accuracy by up to 15% using the cerebellum and brainstem as regions of interest classifiers over the whole brain. In both cohorts, classification was driven by regional differences in the posterior lateral cerebellum.

514

15:33



Atypical maturation of short-range fibers connecting higher-order brain regions in children with autism aged 2-7 years

Minhui Ouyang<sup>1</sup>, Jennifer Muller<sup>1</sup>, Hua Cheng<sup>2</sup>, Yun Peng<sup>2</sup>, J. Christopher Edgar<sup>1,3</sup>, Timothy P.L. Roberts<sup>1,3</sup>, and Hao Huang<sup>1,3</sup>

<sup>1</sup>Radiology, Children's Hospital of Philadelphia, Philadelphia, PA, United States, <sup>2</sup>Radiology, Beijing Children's Hospital, Capital Medical University, Beijing, People's Republic of China, <sup>3</sup>Radiology, Perelman School of Medicine, University of Pennsylvania, Philadelphia, PA, United States

A pattern of local or short-distance “over-connectivity” and long-range under-connectivity is frequently hypothesized in individuals with autism spectrum disorder (ASD). Little is known about the spatiotemporal characterization of structural short-distance connections in typically developing (TD) children or children with ASD. We hypothesized that altered trajectories of short-range association fibers (SAF) are not uniform across the brain regions, with abnormal maturation primarily observed in higher-order but not in primary sensory brain regions in children in ASD. Here, we quantified SAF with a novel index defined as normalized SAF (NSAF) based on diffusion MRI tractography, and characterized its trajectories across brain regions.

---

Oral

## Simultaneous Multi-Slice

Room 316BC

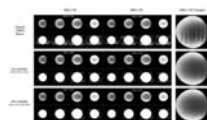
Tuesday 13:45 - 15:45 *Moderators:* Markus Barth & William Grissom

---

515



13:45



[Robust 2D Nyquist Ghost Correction for Simultaneous Multislice \(SMS\) EPI Using Phase Error Correction SENSE and Virtual Coil SAKE](#)

Mengye Lyu<sup>1,2</sup>, Markus Barth<sup>3</sup>, Victor B. Xie<sup>1,2,4</sup>, Yilong Liu<sup>1,2</sup>, Yanqiu Feng<sup>1,5</sup>, and Ed X. Wu<sup>1,2</sup>

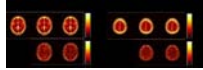
<sup>1</sup>Laboratory of Biomedical Imaging and Signal Processing, The University of Hong Kong, Hong Kong SAR, People's Republic of China, <sup>2</sup>Department of Electrical and Electronic Engineering, The University of Hong Kong, Hong Kong SAR, People's Republic of China, <sup>3</sup>Centre for Advanced Imaging, University of Queensland, Brisbane, Australia, <sup>4</sup>Toshiba Medical Systems (China), Beijing, People's Republic of China, <sup>5</sup>School of Biomedical Engineering, Southern Medical University, Guangzhou, People's Republic of China

Nyquist ghost is problematic in SMS EPI because the ghost is slice-dependent and can interfere with slice separation process. The inconsistency between positive and negative echoes can be represented by 2D phase error maps. This study presents a new and robust SENSE-based method. It estimates both phase error maps and coil sensitivities from one plain EPI based calibration scan, and then uses these maps for ghost-free SMS EPI reconstruction. Further, to improve coil sensitivity estimation, virtual coil SAKE is incorporated to reduce the high order Nyquist ghost in the calibration scan.

516



13:57



### A Maximum Likelihood Approach to Simultaneous Multislice Magnetic Resonance Fingerprinting

Bo Zhao<sup>1,2</sup>, Berkin Bilgic<sup>1,2</sup>, Jason Stockmann<sup>1,2</sup>, Lawrence L. Wald<sup>1,2</sup>, and Kawin Setsompop<sup>1,2</sup>

<sup>1</sup>Martinos Center for Biomedical Imaging, Chalestown, MA, United States, <sup>2</sup>Department of Radiology, Harvard Medical School, Boston, MA, United States

Magnetic resonance fingerprinting is an efficient quantitative MRI paradigm, which simultaneously acquires multiple MR tissue parameters. Recently, simultaneous multislice (SMS) acquisition has been used to further speed up MRF experiments. In this abstract, we present a maximum likelihood formulation to enable improved SMS-MRF reconstruction. We further describe an algorithm based on variable splitting, the alternating direction method of multipliers, and the variable projection method to solve the resulting nonlinear and nonconvex optimization problem. Representative results are shown to demonstrate that the proposed method enables more accurate MR tissue parameter maps compared to the recent SMS-MRF approach utilizing direct pattern matching.

517



14:09



### Simultaneous Multi Slice Imaging using Matrix Gradient Coils

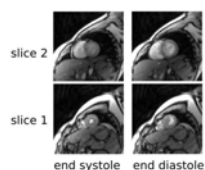
Sebastian Littin<sup>1</sup>, Kawin Setsompop<sup>2</sup>, Feng Jia<sup>1</sup>, Huijun Yu<sup>1</sup>, Stefan Kroboth<sup>1</sup>, and Maxim Zaitsev<sup>1</sup>

<sup>1</sup>Department of Radiology, Medical Physics, University Medical Center, Freiburg, Germany, <sup>2</sup>Athinoula A. Martinos Center for Biomedical Imaging, Department of Radiology, Massachusetts General Hospital, Charlestown, MA, United States

Novel SMS techniques become possible by applying specially designed spatial encoding magnetic fields (SEMs) during RF excitation or read out. Two new methods have been implemented using a matrix gradient coil.

518

14:21



### Simultaneous Multi-Slice Real-Time Imaging with Radial Multi-Band FLASH and Nonlinear Inverse Reconstruction

Sebastian Rosenzweig<sup>1,2</sup>, H. Christian M. Holme<sup>1,2</sup>, Robin N. Wilke<sup>1,2</sup>, and Martin Uecker<sup>1,2</sup>

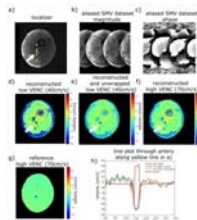
<sup>1</sup>Institut für Diagnostische und Interventionelle Radiologie Göttingen, University Medical Center Göttingen, Göttingen, Germany, <sup>2</sup>Partner site Göttingen, German Centre for Cardiovascular Research (DZHK), Göttingen, Germany

Simultaneous multi-slice (SMS) MRI allows for the acquisition of several slices at the same time. We propose a novel reconstruction technique for radial SMS MRI based on Regularized Nonlinear Inversion (NLINV). This method does not require a priori knowledge of the coil sensitivities. We present the simultaneous estimation of images and coil sensitivities of two slices of a phantom from 10-fold undersampled data. Image quality is analyzed for different sampling schemes and compared to single-slice acquisitions. Clinical relevance is demonstrated by in-vivo imaging of two slices of a human heart in real-time at a time-resolution of 30.8 ms per frame.

519



14:33



### Simultaneous Multi-VENC Imaging

Simon Schmidt<sup>1</sup>, Sebastian Flassbeck<sup>1</sup>, Mathies Breithaupt<sup>1,2</sup>, Mark E. Ladd<sup>1</sup>, and Sebastian Schmitter<sup>1,3</sup>

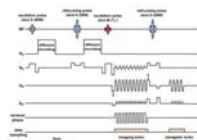
<sup>1</sup>Medical Physics in Radiology, German Cancer Research Center, Heidelberg, Germany, <sup>2</sup>Institute for Forensic Medicine and Traffic Medicine, University Hospital Heidelberg, Heidelberg, Germany, <sup>3</sup>Physikalisch-Technische Bundesanstalt (PTB), Braunschweig and Berlin, Germany

In this work we introduce and investigate the feasibility of "Simultaneous Multi-VENC" (SMV) imaging. This technique is inspired by "spokes" RF pulses used for parallel transmission and by Simultaneous-Multi-Slice (SMS) imaging. SMV enables encoding of a single 2D plane by two or more 2D phase images with different velocity sensitivities, allowing multiple encoding velocities (VENC). Only a single readout is used to acquire all VENC data, which are separated using a standard SMS slice-GRAPPA algorithm. The feasibility of SMV is demonstrated in a flow phantom and in-vivo for three spokes with two different VENC values.

520



14:45



### Simultaneous Multi-Contrast Imaging with Readout-Segmented EPI

Nora-Josefin Breutigam<sup>1</sup>, Robert Frost<sup>2</sup>, Klaus Eickel<sup>1,3</sup>, and David Porter<sup>1</sup>



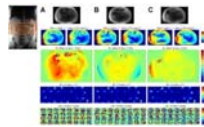
<sup>1</sup>MR Physics, Fraunhofer MEVIS, Bremen, Germany, <sup>2</sup>Athinoula A. Martinos Center for Biomedical Imaging, MA, United States, <sup>3</sup>mediri GmbH, Heidelberg, Germany

A new method is presented for acquiring multiple image contrasts simultaneously. The technique reduces patient examination times and facilitates accurate image registration between contrasts. This work focuses on a variant of the method, in which readout-segmented EPI (rs-EPI) is used to perform high-quality, navigator-corrected, diffusion-weighted imaging simultaneously with a T2\*-weighted acquisition. This combination of contrasts has clinical significance in acute stroke, providing a registered data set for assessing the infarct and possibility of associated hemorrhage. The proposed method modifies the contrast as a function of slice position and uses blipped CAIPIRINHA and slice-GRAPPA to separate the contrasts into individual images.

521



14:57



Fast multi-slice B1 and B0 mapping (B01TIAMO) for 32-channel pTx body MRI at 7 Tesla

Sascha Brunheim<sup>1,2</sup>, Sören Johst<sup>1</sup>, Stephan Orzada<sup>1</sup>, Jose P Marques<sup>3</sup>, Marcel Gratz<sup>1,2</sup>, Mark E Ladd<sup>1,4</sup>, and Harald H Quick<sup>1,2</sup>

<sup>1</sup>Erwin L. Hahn Institute for Magnetic Resonance Imaging, University Duisburg-Essen, Essen, Germany, <sup>2</sup>High Field and Hybrid MR Imaging, University Hospital Essen, Essen, Germany, <sup>3</sup>Donders Institute for Brain, Cognition and Behaviour, Radboud University Nijmegen, Nijmegen, Netherlands, <sup>4</sup>Medical Physics in Radiology, German Cancer Research Center (DKFZ), Heidelberg, Germany

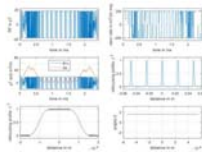
The aim of this work was to improve the recently developed B1TIAMO method at ultra-high magnetic field for a 32-channel body transceiver array by providing complete information about both the B0 and B1+ distribution within the human abdomen without movement artifacts by breathing. Therefore, a fast multi-slice version including two-echo B0 maps with time interleaved acquisition of modes (B01TIAMO) was introduced. Furthermore, B1+ phase calculation was improved by geometric-decomposition coil compression, resulting in accurate single-channel B1+ and B0 maps for three different slices within only 21s versus the 42s step-by-step measurement for a single slice with normal B1TIAMO.

522

15:09

Simultaneous multislice refocusing by time-optimal control





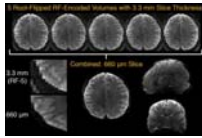
Armin Rund<sup>1,2</sup>, Christoph Stefan Aigner<sup>3</sup>, Karl Kunisch<sup>1</sup>, and Rudolf Stollberger<sup>2,3</sup>

<sup>1</sup>Institute for Mathematics and Scientific Computing, University of Graz, Graz, Austria, <sup>2</sup>BioTechMed Graz, Graz, Austria, <sup>3</sup>Institute of Medical Engineering, Graz University of Technology, Graz, Austria

We demonstrate the design of minimum duration SMS refocusing pulses and slice selective gradient shapes with specific hardware constraints such as peak B1, peak slew rate and peak amplitude of the slice gradient. The proposed bi-level time-optimal control method works with a detailed description of the slice profile accuracy by inequality constraints, and allows the use of fine spatial and temporal grids. The optimized results are validated on a 3T scanner with phantom and in vivo measurements demonstrating the practical realizability of the presented approach.

523

15:21



Minimum peak power root-flipped gSlider-SMS RF pulses for high-resolution in vivo diffusion imaging

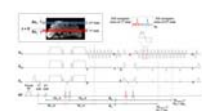
Jun Ma<sup>1</sup>, Thomas Witzel<sup>2</sup>, William A Grissom<sup>1</sup>, and Kawin Setsompop<sup>2</sup>

<sup>1</sup>Biomedical Engineering, Vanderbilt University, Nashville, TN, United States, <sup>2</sup>Athinoula A. Martinos Center for Biomedical Imaging, Massachusetts General Hospital, Charlestown, MA, United States

gSlider is an RF encoding method that increases SNR in high-resolution diffusion imaging, by repeatedly acquiring high-SNR thick-slab images with distinct through-slice RF phase encoding. The method is currently based on linear-phase RF pulses designed using the inverse scattering transform. However, the high peak power of the associated refocusing pulses requires VERSE to meet practical peak RF amplitude constraints. Here we show that the pulses can be equivalently designed using the SLR algorithm, and that the refocusing pulse can be further root-flipped to minimize its peak amplitude and obviate the use of VERSE, while preserving gSlider encoding and linear-phase spin echoes.

524

15:33



3D Multi-band Interleaved DW-EPI with 3D Phase Correction

Hing-Chiu Chang<sup>1</sup>, Edward S. Hui<sup>1,2</sup>, Xiaoxi Liu<sup>1</sup>, and Nan-kuei Chen<sup>3,4</sup>

<sup>1</sup>Department of Diagnostic Radiology, The University of Hong Kong, Hong Kong, Hong Kong, <sup>2</sup>The State Key Laboratory of Brain and Cognitive Sciences, The University of Hong Kong, Hong Kong, <sup>3</sup>Department of Biomedical Engineering, University of Arizona, Tucson, AZ, United States, <sup>4</sup>Brain Imaging and Analysis Center, Duke University Medical Center, Durham, NC, United States

The optimal SNR efficiency of 3D multi-slab multi-shot DWI acquisition can be enabled by using a TR range of 1-2s. However, due to the low feasible slab thickness, the multi-slab acquisition can only achieve limited brain coverage when using a short TR. In this study, we first develop a 3D multi-band (MB) iDW-EPI sequence with MB-EVI-based navigator to increase brain coverage when using optimal TR. Second, we extend 3D-MUSER algorithm, which is proposed in another study, to reconstruct 3D-MB-iDW-EPI data with 3D phase correction. Our preliminary result demonstrates the feasibility of 3D MB DWI with 3D phase correction.

Oral

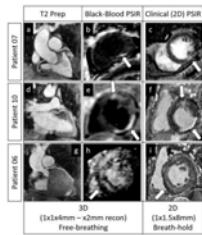
## Myocardial Viability & Perfusion

Room 320

Tuesday 13:45 - 15:45 Moderators: Ganesh Adluru & Leon Axel

525

13:45



3D Whole-Heart Phase Sensitive Inversion Recovery (PSIR) for Simultaneous Bright Blood Coronary Angiography and Black Blood Late Gadolinium Enhancement (LGE)

Giulia Ginami<sup>1</sup>, Radhouene Neji<sup>2</sup>, Tevfik Ismail<sup>1</sup>, Amedeo Chiribiri<sup>1</sup>, Rene Botnar<sup>1</sup>, and Claudia Prieto<sup>1</sup>

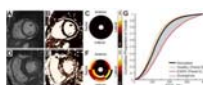
<sup>1</sup>Division of Imaging Sciences and Biomedical Engineering, King's College London, London, United Kingdom, <sup>2</sup>MR Research Collaborations, Siemens Healthcare Limited, Frimley, United Kingdom

This study introduces a free-breathing 3D whole-heart sequence with image-based navigation for post-contrast phase sensitive inversion recovery (PSIR) allowing for simultaneous bright-blood coronary angiography and black-blood late gadolinium enhancement (LGE) imaging. Such approach was successfully tested in a cohort of 10 patients with cardiovascular disease. Data acquisition was performed in free-breathing with 100% scan efficiency, thus allowing for predictable scan time. The proposed sequence allowed for LGE visualization with high volumetric coverage and improved contrast (black-blood dataset) while simultaneously providing sharp visualization of the coronary arteries and heart anatomy (bright-blood dataset).

526



13:57



### Magnetization Transfer-weighted Cardiac MRI in End Stage Renal Disease Quantifies Fibrosis and Identifies Biochemical Markers of Fibrosis without Gadolinium

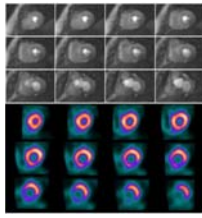
Tori Stromp<sup>1,2</sup>, Rebecca M Kidney<sup>2</sup>, Tyler J Spear<sup>2</sup>, Kristin N Andres<sup>3</sup>, Joshua C Kaine<sup>3</sup>, Steve W Leung<sup>4</sup>, and Moriel H Vandsburger<sup>1,2,5,6</sup>

<sup>1</sup>Physiology, University of Kentucky, Lexington, KY, United States, <sup>2</sup>Cardiovascular Research Center, University of Kentucky, Lexington, KY, United States, <sup>3</sup>College of Medicine, University of Kentucky, KY, United States, <sup>4</sup>Gill Heart Institute, University of Kentucky, KY, United States, <sup>5</sup>Biomedical Engineering, University of Kentucky, KY, United States, <sup>6</sup>Bioengineering, University of California Berkeley, Berkeley, CA

Cardiac fibrosis is prevalent in end stage renal disease (ESRD). Contraindication to late gadolinium enhancement (LGE) cardiac MRI (CMR) obstructs diagnosis, treatment selection, and potential therapeutic target identification. Currently, ventricular hypertrophy and function are used as surrogate measures of fibrosis and correlates of biomarkers. We used magnetization transfer (MT) weighted CMR to quantify fibrosis, comparing to structure, function, and blood biomarkers. We recapitulated prevalent fibrosis found previously by LGE. Results suggest hypertrophy or strains may be inappropriate fibrosis measures in ESRD. Extracellular matrix turnover markers, e.g. TIMPs, may represent more specific biomarkers of fibrosis and molecular targets for therapeutics development.

14:09

Free-breathing 3D whole-heart stress myocardial perfusion using compressed sensing

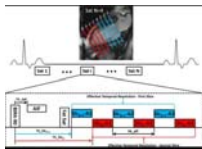


Merlin J Fair<sup>1,2</sup>, Eliana Reyes<sup>1</sup>, Peter D Gatehouse<sup>1,2</sup>, Ganesh Adluru<sup>3</sup>, Jason Mendes<sup>3</sup>, Ricardo Wage<sup>1</sup>, Edward VR DiBella<sup>3</sup>, and David N Firmin<sup>1,2</sup>

<sup>1</sup>CBRU, Royal Brompton Hospital, London, United Kingdom, <sup>2</sup>NHLI, Imperial College London, London, United Kingdom, <sup>3</sup>UCAIR, University of Utah, UT, United States

A consistent, reliable, 3D myocardial first-pass perfusion sequence is developed using a stack-of-stars design and tested at both stress and rest during free-breathing. A compressed sensing algorithm is used to compensate for the high undersampling rates, including a modified form with temporal pixel reordering designed to better cope with respiratory motion. Reconstructions were successful, despite large respiratory motion, in all cases. An example of a perfusion defect in a coronary artery disease patient is presented, with confirmation from recent SPECT myocardial perfusion scintigraphy.

14:21



#### Clinical Evaluation of Whole-Heart Quantitative Adenosine Stress CMR with Motion-compensated L1-SPIRIT

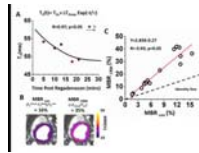
Michael Salerno<sup>1</sup>, Yang Yang<sup>1</sup>, Stephen McHugh<sup>1</sup>, Eric Holland<sup>1</sup>, Jonathan Pan<sup>2</sup>, Craig H Meyer<sup>2</sup>, Angela Taylor<sup>1</sup>, and Christopher M Kramer<sup>3</sup>

<sup>1</sup>Department of Medicine, University of Virginia, Charlottesville, VA, United States, <sup>2</sup>Department of Biomedical Engineering, University of Virginia, Charlottesville, VA, United States, <sup>3</sup>Department of Radiology and Medical Imaging, University of Virginia, Charlottesville, VA, United States

Adenosine stress CMR has potential advantages over competing modalities for diagnosing coronary artery disease (CAD) including the ability to quantify myocardial perfusion, however current CMR techniques have limited spatial coverage. We perform a clinical assessment of the diagnostic performance of whole-heart spiral perfusion imaging using motion compensated compressed sensing for detection of CAD and demonstrate good image quality, minimal motion artifacts, and high diagnostic accuracy for both visual and quantitative evaluation.

14:33

#### Coronary Relaxation Mapping for Multi-fold Amplification in Myocardial BOLD Sensitivity

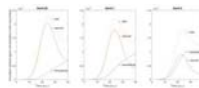


Hsin-Jung yang<sup>1</sup>, Damini Dey<sup>1</sup>, Behzad Sharif<sup>1</sup>, Jane Sykes<sup>2</sup>, John Butler<sup>2</sup>, Ivan Cokic<sup>1</sup>, Sotirios Tsaftaris<sup>3</sup>, Piotr Slomka<sup>1</sup>, Frank Prato<sup>2</sup>, and Rohan Dharmakumar<sup>1</sup>

<sup>1</sup>Cedars Sinai Medical Center, Los Angeles, CA, United States, <sup>2</sup>Lawson Health Research Institute, <sup>3</sup>IMT School for Advanced Studies Lucca

Over the past two decades cardiac BOLD MRI has seen major technical advances. However, its reliability for detecting ischemic heart disease remains poor. We hypothesized that the reliability of cardiac BOLD MRI can be improved by repeatedly acquiring BOLD images following regadenoson injection. We found that repeatedly acquired myocardial BOLD imaging following regadenoson administration can be used to significantly amplify the BOLD sensitivity and improve the reliability of myocardial BOLD MRI in health and disease.

14:45

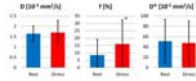


Quantification of Perfusion in Hypertrophic Cardiomyopathy using 3D Contrast Agent Flow Simulation

Leili Riazzy<sup>1</sup>, Marc Olbrich<sup>2</sup>, Tobias Schaeffter<sup>3</sup>, Simone Fritschi<sup>4,5</sup>, Thoralf Niendorf<sup>1</sup>, and Jeanette Schulz-Menger<sup>4,5</sup>

<sup>1</sup>Berlin Ultrahigh Field Facility (B.U.F.F.), Max-Delbrueck Center for Molecular Medicine, Berlin, Germany, <sup>2</sup>Technical University Berlin, Berlin, Germany, <sup>3</sup>Medical Physics and Metrological Information Technology, Physikalisch-Technische Bundesanstalt, Berlin, Germany, <sup>4</sup>Working Group on Cardiovascular Magnetic Resonance, Experimental and Clinical Research Center (ECRC), Berlin, Germany, <sup>5</sup>Department of Cardiology and Nephrology, HELIOS Klinikum Berlin Buch, Berlin, Germany

Hypertrophic Cardiomyopathy (HCM) is a common cause of sudden heart death in young adults. MRI is a powerful tool for the diagnosis and surveillance of this myocardial morphology as well as tissue injury. In clinical routine the assessment is mainly based on visual assessment or semi-quantification is increasingly used. Quantification of perfusion defect should be nowadays assessed with computational tools. We aim at quantifying differences in perfusion with a computational flow model that incorporates the vascular, as well as extracellular compartment, using the Damköhler Number  $Da$ . Areas of different perfusion in  $N=5$  patients with HCM were fitted in  $Da$  with model-derived curves with an overall error of 10.48%.



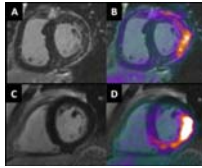
### Intravoxel Incoherent Motion Model in the Heart of Patients under Adenosine Induced Stress

Georg Spinner<sup>1</sup>, Constantin von Deuster<sup>1</sup>, Sabrina Oebel<sup>2</sup>, Christian Torben Stoeck<sup>1</sup>, Robert Manka<sup>2</sup>, and Sebastian Kozerke<sup>1</sup>

<sup>1</sup>Institute for Biomedical Engineering, ETH Zürich, Zürich, Switzerland,

<sup>2</sup>Cardiology, University Hospital Zürich

Intravoxel Incoherent Motion Imaging (IVIM) in the in vivo human heart has the potential of measuring myocardial perfusion without the need for contrast agents. In order to validate previous IVIM animal studies, patients were measured both during rest and under adenosine induced stress using a slice following second-order motion compensated diffusion weighted imaging sequence. The IVIM perfusion fraction is found to significantly increase during stress, which shows that IVIM imaging allows measuring a perfusion surrogate. This can hence be used for example to assess perfusion deficits in patients with ischemia.



### Combined Late Gadolinium Enhancement (LGE) and 18F-fluorodeoxyglucose (18F-FDG) Uptake in a Hybrid PET/MR System to Diagnose Active Cardiac Sarcoidosis

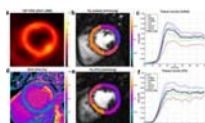
Philip M Robson<sup>1</sup>, Maria Giovanna Trivieri<sup>2</sup>, Ronan Abgral<sup>3</sup>, Marc R Dweck<sup>4</sup>, Nicolas A Karakatsanis<sup>1</sup>, Venkatesh Mani<sup>1</sup>, Maria M Padilla<sup>5</sup>, Marc M Miller<sup>6</sup>, Anarahda Lala<sup>6</sup>, Javier Sanz<sup>6</sup>, Jagat Narula<sup>6</sup>, Valentin Fuster<sup>6</sup>, Johanna Contreras<sup>6</sup>, Jason Kovacic<sup>6</sup>, and Zahi A Fayad<sup>1</sup>

<sup>1</sup>Translational and Molecular Imaging Institute, icahn school of medicine at mount sinai, New York, NY, United States, <sup>2</sup>icahn school of medicine at mount sinai, New York, NY, United States, <sup>3</sup>Department of Nuclear Medicine, European University of Brittany, <sup>4</sup>British Heart Foundation/University Centre for Cardiovascular Science, University of Edinburgh, <sup>5</sup>Division of Pulmonary, Critical Care and Sleep Medicine, icahn school of medicine at mount sinai, New York, NY, United States, <sup>6</sup>Cardiovascular Institute, icahn school of medicine at mount sinai, New York, NY, United States

Recent advances in hybrid Positron Emission Tomography (PET) Magnetic Resonance (MR) technology have enabled simultaneous imaging with both modalities. Sarcoidosis is a granulomatous disease that, when involving the heart has a poor prognosis. However, cardiac sarcoidosis has been shown to respond to immunosuppressive therapy. Currently, both late gadolinium enhancement (LGE)-MR and 18F-fluorodeoxyglucose (18F-FDG)-PET are used separately to evaluate the disease yet a clear diagnosis is not easily achieved. In this work, we investigate the potential improvement in evaluation with combined 18F-FDG-PET/MR imaging.

533

15:21



Microvascular tissue characterization with cardiac PET/MRI: Quantitative comparison of myocardial DCE-MRI perfusion flow with 18F-FDG viability PET and coronary angiography

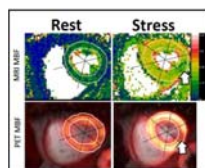
Karl P Kunze<sup>1</sup>, Teresa Vitadello<sup>2</sup>, Christoph Rischpler<sup>1</sup>, Markus Schwaiger<sup>1</sup>, and Stephan G Nekolla<sup>1</sup>

<sup>1</sup>Nuclear Medicine, TU Munich, Munich, Germany, <sup>2</sup>Cardiology, TU Munich, Munich, Germany

This cardiac multimodality study combines the use of metabolic 18F-FDG PET imaging with coronary angiography as well as DCE-MR perfusion imaging to investigate the relationship of myocardial metabolism and perfusion in chronic ischemia. A patient group with chronic total occlusion received exams pre- (PET/MRI+Angiography) as well as post- (MRI+Angiography) coronary intervention. Results showed a range of subtle to heavy resting perfusion deficits, with variable intra-patient relationships to metabolic deficits as indicated by 18F-FDG PET. Comparison of coronary angiography results with the corresponding quantitative perfusion analysis pre- and post-intervention suggest that resting perfusion is more sensitive to micro- than macrovascular coronary integrity.

534

15:33



Correlations and differences of myocardial blood flow with simultaneous measurements of MRI and PET

Masoud Edalati<sup>1</sup>, David Muccigrosso<sup>1</sup>, Richard Laforest<sup>1</sup>, Pamela K Woodard<sup>1</sup>, and Jie Zheng<sup>1</sup>

<sup>1</sup>Department of Radiology, Mallinckrodt Institute of Radiology, Washington University in St. Louis, Saint Louis, MO, United States



The presented study explores correlations and differences of myocardial blood flow measured with MRI and PET. We employed a post-processing method to estimate the arterial input function using gamma variate model. Rest/stress quantitative PET/MRI cardiac perfusion study were simultaneously performed on sixteen patients with myocardial ischemia. The results demonstrated the feasibility of the new AIF estimation method for the quantification of MBF by MRI without using special sequences or dual bolus injections of contrast media. Statistical analysis between PET and MRI data demonstrated good correlation with a linear trend and error ranges comparable to those previously reported in the literature.

---

---

## Combined Educational & Scientific Session

### Spinning Off Axis

Organizers: Jenny T. Bencardino, M.D., Emily McWalter, Ph.D, Edwin H.G. Oei, M.D., Ph.D., & Philip Robinson, M.D.

Room 315

Tuesday 13:45 - 15:45

Moderators: Christopher Burke & L. Tugan Muftuler

---

13:45

[Update on MRI Degenerative Disc Disease: Beyond Modic Changes](#)  
Jason F Talbott<sup>1</sup>

<sup>1</sup>Radiology, Zuckerberg San Francisco General Hospital, Novato, CA, United States

---

14:15

[What's new on Spine Imaging: Beyond Degenerative Disc Disease](#)  
Elisabeth Garwood<sup>1</sup>

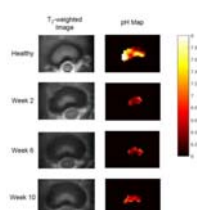
<sup>1</sup>New York

---

535



14:45



[pH Measurement of Intervertebral Disc in the Process of Disc Degeneration Using Quantitative Chemical Exchange Saturation Transfer \(qCEST\)](#)

Zhengwei Zhou<sup>1,2</sup>, Maxim Bez<sup>3</sup>, Wafa Tawackoli<sup>1,4,5</sup>, Dmitriy Sheyn<sup>4,5</sup>, Joseph C. Giaconi<sup>6</sup>, Zulma Gazit<sup>3,4,5,7</sup>, Gadi Pelled<sup>1,3,4,5</sup>, Dan Gazit<sup>1,3,4,5,7</sup>, and Debiao Li<sup>1,2</sup>

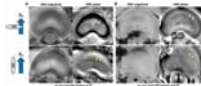
<sup>1</sup>Biomedical Imaging Research Institute, Cedars-Sinai Medical Center, Los Angeles, CA, United States, <sup>2</sup>Department of Bioengineering, University of California, Los Angeles, <sup>3</sup>Skeletal Biotech Laboratory, Hebrew University of Jerusalem, Israel, <sup>4</sup>BOG Regenerative Medicine Institute, Cedars-Sinai Medical Center, Los Angeles, CA, United States, <sup>5</sup>Department of Surgery, Cedars-Sinai Medical Center, Los Angeles, CA, United States, <sup>6</sup>Department of Imaging, Cedars-Sinai Medical Center, CA, United States, <sup>7</sup>Department of Orthopedics, Cedars-Sinai Medical Center, Los Angeles, CA, United States

Several hypotheses associate the pathogenesis of discogenic low back pain with low pH. In this study, we used qCEST MRI technique to monitor the pH changes of the intervertebral disc in the process of degeneration in porcine model. A significant pH drop was observed at 2 weeks following degeneration induction. This trend is correlated with the expression of pain markers. These results suggest that qCEST MRI has the potential to serve as a novel and non-invasive method for the diagnosis of discogenic pain.

536



14:57



### Feasibility study of intervertebral disc degeneration assessment using phase imaging

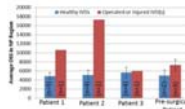
Yoonho Nam<sup>1</sup>, Joonsung Lee<sup>2</sup>, Eo-Jin Hwang<sup>1</sup>, and Joon-Yong Jung<sup>1</sup>

<sup>1</sup>Department of Radiology, Seoul St.Mary's Hospital, College of Medicine, The Catholic University of Korea, Seoul, Korea, Republic of, <sup>2</sup>Center for neuroscience imaging research, Institute for Basic Science, Suwon, Korea, Republic of

In this study, we hypothesized that a GRE phase can be a potential indicator of annulus fibrosus integrity, because of its high sensitivity to micro-structural tissue change. With this hypothesis, we investigate the feasibility of GRE phase in the assessment of intervertebral disc degeneration in the lumbar spine. Ex vivo animal disk samples and nine human subjects were scanned and the high-pass filtered phase images were evaluated. For both ex vivo and in vivo experiments, distinctive phase contrasts were observed in the annulus fibrosus of the normal intervertebral discs.

537

15:09



### Detection of Internal Tissue Disruptions within the Intervertebral Disc via Magnetic Resonance Elastography: A Feasibility Study

Benjamin A Walter<sup>1,2</sup>, Prasath Mageswaran<sup>1,3</sup>, Elizabeth Yu<sup>1,4</sup>, Safdar Khan<sup>1,4</sup>, William S Marras<sup>1,3</sup>, and Arunark Kolipaka<sup>1,5</sup>

<sup>1</sup>Spine Research Institute, The Ohio State University, Columbus, OH, United States, <sup>2</sup>Department of Biomedical Engineering, The Ohio State University, Columbus, OH, United States, <sup>3</sup>Department of Integrated Systems Engineering, The Ohio State University, Columbus, OH, United States, <sup>4</sup>Department of Orthopaedics, The Ohio State University Wexner Medical Center, Columbus, OH, United States, <sup>5</sup>Department of Radiology, The Ohio State University Wexner Medical Center, Columbus, OH, United States

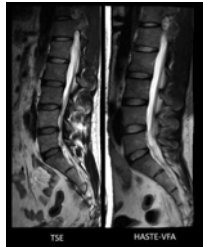
Magnetic resonance elastography (MRE) was used to non-invasively assess regions of internal tissue disruption within intervertebral discs (IVD) that were known to contain tissue damage. Internal tissue disruptions were assessed via measurements of wave continuity as they propagated throughout the IVD. Results demonstrated that injured IVD's had an elevated octahedral shear strain (OSS) compared to non-operated control IVDs and OSS maps allowed visualization of potential location of internal tissue disruptions. Overall, results of this study suggest that MRE may provide a non-invasive way of identifying internal tissue disruptions within the IVD.

---

538

15:21

### Clinical utility of a novel ultrafast T2 Weighted sequence for Spine Imaging



Mahesh Bharath Keerthivasan<sup>1</sup>, Ali Bilgin<sup>1,2</sup>, Diego R Martin<sup>2</sup>, Jennifer L Becker<sup>2</sup>, Maria Altbach<sup>2</sup>, and Manojkumar Saranathan<sup>2</sup>

<sup>1</sup>Electrical and Computer Engineering, University of Arizona, Tucson, AZ, United States, <sup>2</sup>Medical Imaging, University of Arizona, Tucson, AZ, United States

T2 weighted imaging of the spine is commonly performed using Turbo Spin Echo (TSE) sequences, resulting in long scan times and vulnerability to motion artifacts. While the single-shot sequences such as HASTE could be used for rapid screening, their use is limited by poor spatial resolution and SAR limitations. We investigated the use of a variable flip angle HASTE (HASTE-VFA) sequence for ultrafast motion robust T2 weighted spine imaging and compared its performance to T2 TSE in 13 patients.

---

539

15:33

### Feasibility of Synthetic MRI of the spine – fast and quantitative imaging

Maria Isabel Vargas<sup>1</sup>, Bénédicte MA Delattre<sup>1</sup>, José Manuel Baiao Boto<sup>1</sup>, Karl-Olof Lövblad<sup>1</sup>, and Sana Boudabbous<sup>1</sup>



<sup>1</sup>Geneva University Hospitals, Geneva, Switzerland

Synthetic MRI was already validated in some cerebral applications. We adapted it to evaluate the spine and showed that it produces, in general, good image quality and diagnostic confidence. Efforts will still have to be made to increase image quality in the dorso-lumbar spine. However, the non-negligible time saving and the ability to obtain quantitative measurements as well as to generate several contrasts with a single acquisition should secure an interesting and useful future for synthetic MRI in clinical routine.

---

### **Traditional Poster: Contrast Mechanisms**

Exhibition Hall 1877-1898      Tuesday 16:15 - 18:15 *(no CME credit)*

---

### **Electronic Poster: Engineering**

Exhibition Hall      Tuesday 16:15 - 17:15 *(no CME credit)*

---

### **Electronic Poster: General Cancer Imaging**

Exhibition Hall      Tuesday 16:15 - 17:15 *(no CME credit)*

---

### **Study Groups**

#### **MR Spectroscopy Study Group**

Room 323ABC      Tuesday 16:15 - 18:15 *(no CME credit)*

---

### **Study Groups**

#### **Pediatric MR Study Group**

Room 317AB      Tuesday 16:15 - 18:15 *(no CME credit)*

---

### **Educational Course**

#### **Liver MR Imaging: Quantitative Approaches to Liver Disease**

*Organizers:* Kathryn Fowler, M.D., Kartik Jhaveri, M.D., F.R.C.P.C., Lorenzo Mannelli, M.D., Ph.D. & Edwin J.R. van Beek,

Room 315

Tuesday 16:15 - 18:15

Moderators: Rebecca Rakow-Penner & Bachir Taouli

---

16:15

The Hepatologist's Perspective of MRI in the Management of Liver Diseases

Yuko Kono

Cirrhosis and hepatocellular carcinoma (HCC) are major health problems world-wide and in the United States. It is estimated 10 to 20 million American people have non-alcoholic steatohepatitis (NASH), which can lead to cirrhosis. HCC is the second cause of cancer death world-wide, and the fastest growing cause of cancer death in the United States. MRI can provide information such as fat quantification, iron quantification in the liver, as well as liver stiffness estimation by MR elastography. Early and accurate diagnosis of HCC is critical for improved outcome of this deadly disease. Non-invasive diagnosis of chronic liver diseases and HCC are indispensable in hepatology practice. Current epidemiology of liver disease and how MRI can help liver patients' management will be discussed.

---

16:45

Liver Fibrosis

Richard Ehman

This presentations reviews the rationale, principles, and practical application of MRI-based methods for diagnosing hepatic fibrosis. MR elastography is addressed in detail.

---

17:15

Iron Overload

Takeshi Yokoo

---

17:45

Hepatic Steatosis

Claude Sirlin<sup>1</sup>

<sup>1</sup>University of California, San Diego

---

18:15

Adjournment & Meet the Teachers

---

---

## Educational Course

# Sports Related Injuries

Organizers: Jenny T. Bencardino, M.D., Eric Y. Chang, M.D., Christine Chung, M.D. & Philip Robinson, M.D.

Room 316A                      Tuesday 16:15 - 18:15    Moderators: Hollis Potter & Ashley Williams

---

16:15                      [Gym Craze](#)  
Alice Ha<sup>1</sup>

<sup>1</sup>University of Washington

---

16:45                      [Racquet Sports](#)  
Gajan Rajeswaran

---

17:15                      [Soccer & Rugby](#)  
Mark Schweitzer

---

17:45                      [Track & Field](#)  
Catherine N. Petchprapa<sup>1</sup>

<sup>1</sup>New York University School of Medicine, New York, NY, United States

Recreational and competitive running is increasing in popularity worldwide and in all age groups, and running injuries are becoming more prevalent. Symptoms and clinical exam can be nonspecific and suggest a wide differential diagnosis. Imaging, especially MR, can help diagnose injury, determine the location, severity and extent of injury thereby providing prognostic information, exclude diagnoses, and help direct the type and timing of treatment, making it invaluable in the workup of the injured athlete. This session will help familiarize the participant of the common lower extremity injuries, relevant anatomy and pathogenesis of injury in track and field athletes and the MR imaging findings seen in these patients.

---

18:15                      [Adjournment & Meet the Teachers](#)

---

## Power Pitch

# Pitch: Best of Cardiovascular MR: Myocardial Tissue Characterization

Power Pitch  
Theater A - Tuesday 16:15 - Moderators: Fred Epstein & Tobias Wech  
Exhibition Hall 17:15 (no CME credit)

---

540

16:15

Three-dimensional holographic visualization of high-resolution myocardial scar on HoloLens



Jihye Jang<sup>1,2</sup>, Gifty Addae<sup>1</sup>, Warren Manning<sup>1,3</sup>, and Reza Nezafat<sup>1</sup>

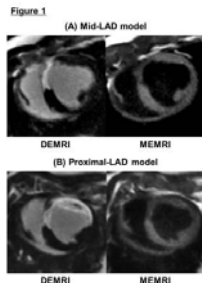
<sup>1</sup>Department of Medicine, Beth Israel Deaconess Medical Center and Harvard Medical School, Boston, MA, United States, <sup>2</sup>Department of Computer Science, Technical University of Munich, Munich, Germany, <sup>3</sup>Department of Radiology, Beth Israel Deaconess Medical Center and Harvard Medical School, Boston, MA, United States

---

541

16:15

Inducibility of ventricular arrhythmia correlates with the indices of myocardial viability using manganese enhanced MRI (MEMRI) in a porcine ischemia reperfusion model



Atsushi Tachibana<sup>1,2,3</sup>, Junaid Zaman<sup>1</sup>, Yuko Tada<sup>1</sup>, Michelle R. Santoso<sup>1</sup>, and Phillip C. Yang<sup>1</sup>

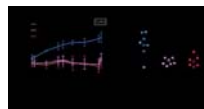
<sup>1</sup>Cardiovascular Medicine, Stanford University, Stanford, CA, United States, <sup>2</sup>Radiology, AIC Yaesu Clinic, Tokyo, Japan, <sup>3</sup>Graduate School of Human Health Sciences, Tokyo Metropolitan University, Tokyo, Japan

---

542

16:15

In Vivo Hyperpolarized MRS Study Showing Improved Cardiac Metabolism in Type 1 Diabetes with Daily L-Carnitine Treatment.



Dragana Savic<sup>1</sup>, Kerstin N. Timm, Vicky Ball, Lisa Heather, and Damian J. Tyler

<sup>1</sup>University of Oxford, Oxford, United Kingdom

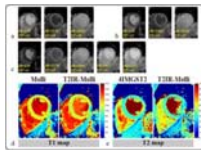
---

16:15

Integrated T2 preparation and Inversion Recovery pulse (T2IR) for combined myocardium T1 and T2 mapping

Rui Guo<sup>1</sup>, Zhensen Chen<sup>1</sup>, Jianwen Luo<sup>1</sup>, and Haiyan Ding<sup>1</sup>

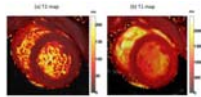




<sup>1</sup>Center for Biomedical Imaging Research, Department of Biomedical Engineering, School of Medicine, Tsinghua University, Beijing, People's Republic of China

16:15

### Non-contrast assessment of vasodilator response using native myocardial T1 and T2 mapping and Arterial Spin Labeled CMR

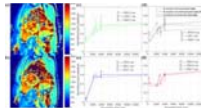


Nilesh R Ghugre<sup>1,2,3</sup>, Hung P Do<sup>4</sup>, Kenneth Chu<sup>3</sup>, Venkat Ramanan<sup>1</sup>, Krishna S Nayak<sup>5</sup>, and Graham A Wright<sup>1,2,3</sup>

<sup>1</sup>Physical Sciences Platform, Sunnybrook Research Institute, Toronto, ON, Canada, <sup>2</sup>Schulich Heart Program, Sunnybrook Research Institute, Toronto, ON, Canada, <sup>3</sup>Department of Medical Biophysics, University of Toronto, Toronto, ON, Canada, <sup>4</sup>Department of Physics and Astronomy, University of Southern California, Los Angeles, CA, United States, <sup>5</sup>Ming Hsieh Department of Electrical Engineering, University of Southern California, Los Angeles, CA, United States

16:15

### Dictionary-based Reconstruction for Free-Breathing Myocardial T<sub>1</sub> Mapping

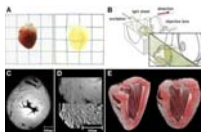


Jinkyu Kang<sup>1,2</sup>, Jihye Jang<sup>1</sup>, Vahid Tarokh<sup>2</sup>, and Reza Nezafat<sup>1</sup>

<sup>1</sup>Department of Medicine, Beth Israel Deaconess Medical Center and Harvard Medical School, Boston, MA, United States, <sup>2</sup>School of Engineering and Applied Science, Harvard University, Cambridge, MA, United States

16:15

### Validation of Cardiac Diffusion Tensor MRI using Transparent Tissue Preparation (CLARITY) with 3D Optical Microscopy



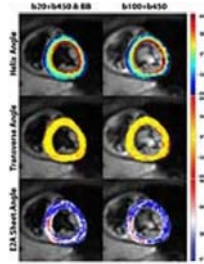
Christopher Nguyen<sup>1</sup>, Sang-Eun Lee<sup>2</sup>, Jongjin Yoon<sup>3</sup>, Hyuk-Jae Chang<sup>2</sup>, Sekeun Kim<sup>2</sup>, Chul Hoon Kim<sup>3</sup>, and Debiao Li<sup>1,4</sup>

<sup>1</sup>Biomedical Imaging Research Institute, Cedars-Sinai Medical Center, Los Angeles, CA, United States, <sup>2</sup>Division of Cardiology, Yonsei University College of Medicine, Seoul, Korea, Republic of, <sup>3</sup>Department of Pharmacology, Yonsei University College of Medicine, Seoul, Korea, Republic of, <sup>4</sup>Bioengineering, University of California Los Angeles, Los Angeles, CA, United States

547



16:15



### Free-breathing Black-blood Prepared Cardiac Diffusion Tensor Imaging

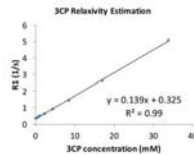
Constantin von Deuster<sup>1</sup>, Georg Spinner<sup>1</sup>, Robbert van Gorkum<sup>1</sup>, Christian T. Stoeck<sup>1</sup>, and Sebastian Kozerke<sup>1</sup>

<sup>1</sup>Institute for Biomedical Engineering, ETH and University Zurich, Zurich, Switzerland

548



16:15



### First-Pass Nitroxide-Enhanced MRI for Imaging Myocardial Perfusion without Gadolinium

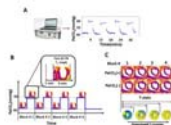
Sophia Xinyuan Cui<sup>1</sup> and Frederick H. Epstein<sup>1,2</sup>

<sup>1</sup>Biomedical Engineering, University of Virginia, Charlottesville, VA, United States, <sup>2</sup>Radiology, University of Virginia, Charlottesville, VA, United States

549



16:15



### Cardiac fMRI - A Novel Approach for Reliably Detecting Myocardial Oxygenation Changes with Precise Modulation of Arterial CO<sub>2</sub>

Hsin-Jung yang<sup>1</sup>, Ilkay Oksuz<sup>2</sup>, Michael Klein<sup>3</sup>, Olivia Sobczyk<sup>3</sup>, Damini Dey<sup>1</sup>, Jane Sykes<sup>4</sup>, John Butler<sup>4</sup>, Xiaoming Bi<sup>5</sup>, Behzad Sharif<sup>1</sup>, Ivan Cokic<sup>1</sup>, Debiao Li<sup>1</sup>, Piotr Slomka<sup>1</sup>, Frank S Prato<sup>4</sup>, Joseph Fisher<sup>3</sup>, Sotirios Tsaftaris<sup>2</sup>, and Rohan Dharmakumar<sup>1</sup>

<sup>1</sup>Cedars Sinai Medical Center, Los Angeles, CA, United States, <sup>2</sup>IMT School for Advanced Studies Lucca, <sup>3</sup>University of Toronto, <sup>4</sup>Lawson Health Research Institute, <sup>5</sup>Siemens Healthcare

550

16:15



### High-fat diet feeding in mice may partially protect the heart from pressure overload induced heart failure - a longitudinal study of cardiac metabolism and function

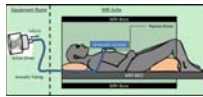
Emmy Manders<sup>1</sup>, Desiree Abdurrachim<sup>1</sup>, Miranda Nabben<sup>2</sup>, Klaas Nicolay<sup>1</sup>, and Jeanine J Prompers<sup>1,3</sup>

<sup>1</sup>Department of Biomedical Engineering, Biomedical NMR, Eindhoven University of Technology, Eindhoven, Netherlands, <sup>2</sup>Department of Genetics and Cell Biology, CARIM school for cardiovascular diseases, Maastricht University, Netherlands, <sup>3</sup>Department of Radiology, University Medical Center, Utrecht, Netherlands

16:15

### Cardiac Magnetic Resonance Elastography for Quantitative Assessment of Elevated Myocardial Stiffness in Cardiac Amyloidosis

551

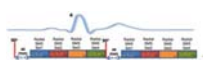


Arvin Arani<sup>1</sup>, Shivaram P. Arunachalam<sup>1</sup>, Ian CY Chang<sup>2</sup>, Francis Baffour<sup>1</sup>, Kevin J Glaser<sup>1</sup>, Joshua D Trzasko<sup>1</sup>, Kiaran McGee<sup>1</sup>, Armando Manduca<sup>1</sup>, Martha Grogan<sup>2</sup>, Angela Dispenzieri<sup>3,4</sup>, Richard L Ehman<sup>1</sup>, and Philip A Araoz<sup>1</sup>

<sup>1</sup>Radiology, Mayo Clinic, Rochester, MN, United States, <sup>2</sup>Cardiovascular Diseases, Mayo Clinic, Rochester, MN, United States, <sup>3</sup>Medicine: Division of Hematology, Mayo Clinic, Rochester, MN, United States, <sup>4</sup>Laboratory Medicine and Pathology, Mayo Clinic

552

16:15



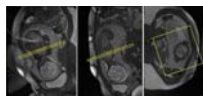
Ungated myocardial perfusion imaging with complete left ventricular coverage using radial simultaneous multi-slice imaging

Ganesh Adluru<sup>1</sup>, Jason Mendes<sup>1</sup>, Ye Tian<sup>1</sup>, Brent Wilson<sup>2</sup>, and Edward DiBella<sup>1</sup>

<sup>1</sup>Radiology and Imaging Sciences, University of Utah, Salt lake city, UT, United States, <sup>2</sup>Cardiology, University of Utah, Salt lake city, UT, United States

553

16:15



As Easy as Echo: Interactive Fetal Cardiac MR Imaging

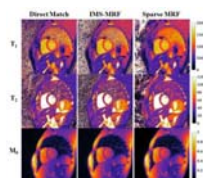
Davide Piccini<sup>1,2,3</sup>, Jérôme Yerly<sup>2,4</sup>, Jérôme Chaptinel<sup>2</sup>, Milan Prsa<sup>5</sup>, Yvan Mivelaz<sup>5</sup>, Leonor Alamo<sup>2</sup>, Yvan Vial<sup>6</sup>, Gregoire Berchier<sup>2</sup>, Chantal Rohner<sup>2</sup>, Peter Speier<sup>7</sup>, Tobias Kober<sup>1,2,3</sup>, and Matthias Stuber<sup>2,4</sup>

<sup>1</sup>Advanced Clinical Imaging Technology, Siemens Healthcare AG, Lausanne, Switzerland, <sup>2</sup>Department of Radiology, University Hospital (CHUV) and University of Lausanne (UNIL), Lausanne, Switzerland, <sup>3</sup>LTS5, École Polytechnique Fédérale de Lausanne (EPFL), Lausanne, Switzerland, <sup>4</sup>Center for Biomedical Imaging (CIBM), Lausanne, Switzerland, <sup>5</sup>Department of Pediatrics, University Hospital (CHUV) and University of Lausanne (UNIL), Lausanne, Switzerland, <sup>6</sup>Department of Gynecology-Obstetrics, University Hospital (CHUV) and University of Lausanne (UNIL), Lausanne, Switzerland, <sup>7</sup>Magnetic Resonance, Siemens Healthcare GmbH, Erlangen, Germany

554



16:15



Low Rank Compressed Sensing Reconstruction for More Precise Cardiac MRF Measurements

Jesse Ian Hamilton<sup>1</sup>, Yun Jiang<sup>1</sup>, Dan Ma<sup>2</sup>, Yong Chen<sup>2</sup>, Shivani Pawha<sup>2</sup>, Wei-Ching Lo<sup>1</sup>, Joshua Batesole<sup>2</sup>, Mark Griswold<sup>1,2</sup>, and Nicole Seiberlich<sup>1</sup>

<sup>1</sup>Biomedical Engineering, Case Western Reserve University, Cleveland, OH, United States, <sup>2</sup>Radiology, University Hospitals, Cleveland, OH, United States

---

## Power Pitch

# Pitch: New Molecular & Metabolic Imaging Approaches

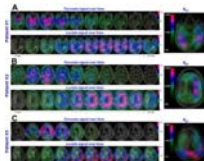
Power Pitch  
Theater B - Tuesday 16:15 - Moderators: Leo Cheng & Anke (no CME credit)  
Exhibition Hall 17:15 Henning

---

555

16:15

### Dynamic Hyperpolarized <sup>13</sup>C Metabolic Imaging of Patients with Brain Tumors



Ilwoo Park<sup>1</sup>, Peder EZ Larson<sup>1</sup>, Jeremy Gordon<sup>1</sup>, Lucas Carvajal<sup>1</sup>, Hsin-Yu Chen<sup>1</sup>, Mark VanCrieking<sup>1</sup>, Robert Bok<sup>1</sup>, Jason C Crane<sup>1</sup>, Adam Elkhalel<sup>1</sup>, Joanna Phillips<sup>2</sup>, James B Slater<sup>1</sup>, Marcus Ferrone<sup>3</sup>, John Kurhanewicz<sup>1</sup>, Dan Vigneron<sup>1</sup>, Susan Chang<sup>2</sup>, and Sarah J Nelson<sup>1</sup>

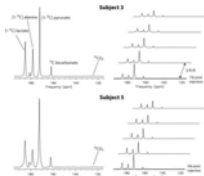
<sup>1</sup>Radiology and Biomedical Imaging, University of California San Francisco, San Francisco, CA, United States, <sup>2</sup>Neurological Surgery, University of California San Francisco, San Francisco, CA, United States, <sup>3</sup>Department of Clinical Pharmacy, University of California San Francisco, San Francisco, CA, United States

---

556

16:15

### Hyperpolarized <sup>13</sup>C MRS of the Human Heart



Albert P. Chen<sup>1</sup>, Justin Y.C. Lau<sup>2,3</sup>, Benjamin J. Geraghty<sup>2,3</sup>, William J. Perks<sup>4</sup>, Idan Roifman<sup>5</sup>, Graham A. Wright<sup>2,3,5</sup>, Kim A. Connelly<sup>6</sup>, and Charles H. Cunningham<sup>2,3</sup>

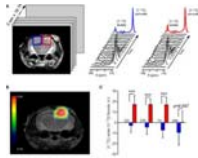
<sup>1</sup>GE Healthcare, Toronto, ON, Canada, <sup>2</sup>Physical Sciences, Sunnybrook Research Institute, Toronto, ON, Canada, <sup>3</sup>Medical Biophysics, University of Toronto, Toronto, ON, Canada, <sup>4</sup>Pharmacy, Sunnybrook Health Sciences Centre, Toronto, ON, Canada, <sup>5</sup>Schulich Heart Program, Sunnybrook Health Sciences Centre, Toronto, ON, Canada, <sup>6</sup>Cardiology, St. Michael's Hospital, Toronto, ON, Canada

---

557

16:15

### In vivo metabolic imaging of neuroinflammation following traumatic brain injury using hyperpolarized [1-<sup>13</sup>C] pyruvate



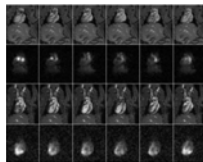
Caroline Guglielmetti<sup>1,2</sup>, Austin Chou<sup>1,2</sup>, Karen Krukowski<sup>1,2</sup>, Maria Serena Paladini<sup>1,2</sup>, Lara-Kirstie Riparip<sup>1,2</sup>, Susanna Rosi<sup>1,2,3</sup>, and Myriam Chaumeil<sup>2,4</sup>

<sup>1</sup>Brain and Spinal Injury Center, University of California San Francisco, San Francisco, CA, United States, <sup>2</sup>Department of Physical Therapy and Rehabilitation Science, University of California San Francisco, San Francisco, CA, United States, <sup>3</sup>Department of Neurological Surgery, University of California San Francisco, San Francisco, CA, United States, <sup>4</sup>Surbeck Laboratory of Advanced Imaging, Department of Radiology and Biomedical Imaging, University of California San Francisco, San Francisco, CA, United States

558

16:15

[Toward Dynamic 3D Cardiac Perfusion Imaging Using bSSFP and Hyperpolarized tert-Butanol](#)



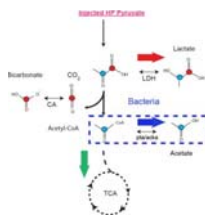
Timothy Pagliaro<sup>1</sup>, Gopal Varma<sup>1</sup>, Li Zhao<sup>1</sup>, David C Alsop<sup>1</sup>, and Aaron K Grant<sup>1</sup>

<sup>1</sup>Radiology, Beth Israel Deaconess Medical Center and Harvard Medical School, Boston, MA, United States

559

16:15

[Detection of Bacteria-specific metabolism using hyperpolarized <sup>13</sup>C pyruvate](#)



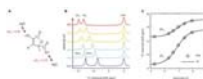
Renuka Sriram<sup>1</sup>, Jinny Sun<sup>1</sup>, Javier Villanueva-Meyer<sup>1</sup>, Justin DesLos Santos<sup>1</sup>, Christopher Mutch<sup>1</sup>, Oren Rosenberg<sup>2</sup>, Mark Van Criekinge<sup>1</sup>, John Kurhanewicz<sup>1</sup>, David Wilson<sup>1</sup>, and Michael Ohliger<sup>1</sup>

<sup>1</sup>Radiology and Biomedical Imaging, University of California San Francisco, San Francisco, CA, United States, <sup>2</sup>Department of Infectious Diseases, University of California San Francisco, San Francisco, CA, United States

560

16:15

[In vivo pH imaging using hyperpolarized <sup>13</sup>C-labelled zymonic acid](#)



Stephan Dewel<sup>1,2,3</sup>, Christian Hundshammer<sup>1,2</sup>, Malte Gersch<sup>4</sup>, Benedikt Feurerecker<sup>1</sup>, Axel Haase<sup>3</sup>, Steffen J Glaser<sup>2</sup>, Markus Schwaiger<sup>1</sup>, and Franz Schilling<sup>1</sup>

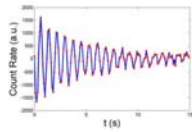
<sup>1</sup>Department of Nuclear Medicine, Technical University of Munich, Munich, Germany, <sup>2</sup>Department of Chemistry, Technical University of Munich, Garching, Germany, <sup>3</sup>Institute of Medical Engineering, Technical University of Munich, Garching, Germany, <sup>4</sup>Medical Research Council Laboratory of Molecular Biology, Cambridge, United Kingdom

561

16:15

### A new method for measuring $T_{\rho}$ of hyperpolarized radioactive isotopes using gamma rays

Yuan Zheng<sup>1,2</sup>, Gordon D. Cates<sup>1</sup>, William A. Tobias<sup>1</sup>, and G. Wilson Miller<sup>3</sup>



<sup>1</sup>Department of Physics, University of Virginia, Charlottesville, VA, United States, <sup>2</sup>UIH America, Houston, TX, United States, <sup>3</sup>Radiology and Medical Imaging, University of Virginia, Charlottesville, VA, United States

562

16:15

### Occupational Manganese Exposure: Reversibility of Increased GABA Levels and Brain Mn Accumulation

David A. Edmondson<sup>1</sup>, Ruoyun Ma<sup>1</sup>, Chien-Lin Yeh<sup>1</sup>, S. Elizabeth Zauber<sup>2</sup>, Sandy Snyder<sup>1</sup>, Eric Ward<sup>1</sup>, and Ulrike Dydak<sup>1</sup>



<sup>1</sup>School of Health Sciences, Purdue University, West Lafayette, IN, United States, <sup>2</sup>Department of Neurology, Indiana University School of Medicine, Indianapolis, IN, United States

563

16:15

### CM101: an optimized MR probe targeting type I collagen for detection of liver fibrosis

Christian T. Farrar<sup>1</sup>, Richard Kennan<sup>2</sup>, Eric Gale<sup>1</sup>, Ian Ramsay<sup>1,3</sup>, Ricard Masia<sup>4</sup>, Gunisha Arora<sup>5</sup>, Kailyn Looby<sup>5</sup>, Lan Wei<sup>5</sup>, Michelle Bunzel<sup>2</sup>, Chunlian Zhang<sup>2</sup>, Yonghua Zhu<sup>2</sup>, Taro Akiyama<sup>2</sup>, Michael Klimas<sup>2</sup>, Shirly Pinto<sup>2</sup>, Himashinie Diyabalanage<sup>3</sup>, Valerie Humblet<sup>3</sup>, Bryan C. Fuchs<sup>5</sup>, and Peter Caravan<sup>1</sup>



<sup>1</sup>Athinoula A. Martinos Center for Biomedical Imaging, Department of Radiology, Massachusetts General Hospital and Harvard Medical School, Charlestown, MA, United States, <sup>2</sup>Merck Research Laboratories, Kenilworth, NJ, United States, <sup>3</sup>Collagen Medical, Belmont, MA, United States, <sup>4</sup>Pathology, Massachusetts General Hospital, Boston, MA, <sup>5</sup>Surgical Oncology, Massachusetts General Hospital, Boston, MA, United States

564

16:15

### A High Throughput, MEMRI-Based Imaging Pipeline to Study Mouse Models of Sporadic Human Cancer

Harikrishna Rallapalli<sup>1,2</sup>, I-Li Tan<sup>3</sup>, Alexandre Wojcinski<sup>3</sup>, Alexandra L Joyner<sup>3</sup>, and Daniel H Turnbull<sup>1,2</sup>





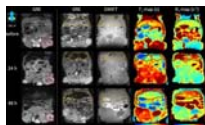
*<sup>1</sup>Kimmel Center for Biology and Medicine at the Skirball Institute of Biomolecular Medicine, New York University School of Medicine, New York, NY, United States, <sup>2</sup>Biomedical Imaging Graduate Program and Department of Radiology, New York University School of Medicine, New York, NY, United States, <sup>3</sup>Developmental Biology, Sloan Kettering Institute, New York, NY, United States*

---

565

16:15

**In vivo quantification of IONP-labeled PAR T-cells using positive contrast MRI**



Jinjin Zhang<sup>1</sup>, Sidath C Kumarapperuma<sup>2</sup>, Qi Shao<sup>3</sup>, Lakmal Kotelawala<sup>2</sup>, John C Bischof<sup>3</sup>, Carston R Wagner<sup>2</sup>, and Michael Garwood<sup>1</sup>

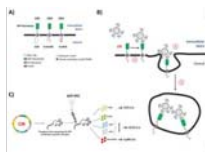
*<sup>1</sup>Center for Magnetic Resonance Research, Department of Radiology, University of Minnesota, Minneapolis, MN, United States, <sup>2</sup>Department of Medicinal Chemistry, University of Minnesota, Minneapolis, MN, United States, <sup>3</sup>Department of Mechanical Engineering, University of Minnesota, Minneapolis, MN, United States*

---

566

16:15

**A Unique 'Cargo Internalization Receptor (CIR)' System for In Vivo Tracking of Individual Cell Populations by 19F MRI**



Pascal Bouvain<sup>1</sup>, Paul Baran<sup>2</sup>, Tuba Güden-Silber<sup>1</sup>, Sebastian Temme<sup>1</sup>, Jens Moll<sup>2</sup>, Doreen Floss<sup>2</sup>, Christoph Grapentin<sup>3</sup>, Jürgen Scheller<sup>2</sup>, and Ulrich Flögel<sup>1</sup>

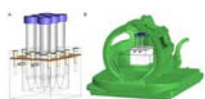
*<sup>1</sup>Molecular Cardiology, Heinrich-Heine University, Düsseldorf, Germany, <sup>2</sup>Biochemistry and Molecular Biology II, Heinrich-Heine University, Germany, <sup>3</sup>Pharmaceutical Technology and Biopharmacy, Albert-Ludwigs-University*

---

567

16:15

**Characterization of Gd-DOTA-APC, a novel cancer-targeting MRI contrast agent**



Christina Brunnquell<sup>1</sup>, Ray Zhang<sup>2</sup>, Benjamin Cox<sup>1,3</sup>, Anatoly Pinchuk<sup>2</sup>, Alan McMillan<sup>2</sup>, and Jamey Weichert<sup>2</sup>

*<sup>1</sup>Medical Physics, University of Wisconsin-Madison, Madison, WI, United States, <sup>2</sup>Radiology, University of Wisconsin-Madison, Madison, WI, United States, <sup>3</sup>Medical Engineering Group, Morgridge Institute for Research, Madison, WI, United States*

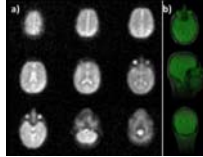
---



568



16:15



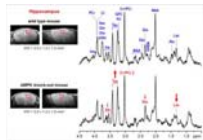
### CMRO<sub>2</sub> Quantification in Human Brain with Direct <sup>17</sup>O-MRI: Profile Likelihood Analysis for Optimization of Temporal Resolution

Dmitry Kurzhunov<sup>1</sup>, Robert Borowiak<sup>1,2,3</sup>, Ali Caglar Özen<sup>1</sup>, and Michael Bock<sup>1</sup>

<sup>1</sup>Dept. of Radiology, Medical Physics, Medical Center – University of Freiburg, Freiburg, Germany, <sup>2</sup>German Cancer Consortium (DKTK), Heidelberg, Germany, <sup>3</sup>German Cancer Research Center (DKFZ), Heidelberg, Germany

569

16:15



### Region-Specific Effects of AMP-Activated Protein Kinase on the Neurochemical Profiles of the Hippocampus and Midbrain in Mice

Ivan Tkac<sup>1</sup>, Biplab Dasgupta<sup>2</sup>, and Raghavendra Rao<sup>3</sup>

<sup>1</sup>Center for Magnetic Resonance Research, University of Minnesota, Minneapolis, MN, United States, <sup>2</sup>Division of Oncology, Cincinnati Children's Hospital Medical Center, Cincinnati, OH, United States, <sup>3</sup>Department of Pediatrics, Division of Neonatology, University of Minnesota, Minneapolis, MN, United States

## Oral

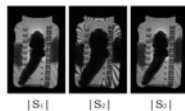
## Artifacts & Corrections

Room 310

Tuesday 16:15 - 18:15 Moderators: Brian Hargreaves &amp; Tolga Cukur

570

16:15



### A Fourier Approach to bSSFP Debanding with 3 Phase-Cycled Acquisitions

Qing-San Xiang<sup>1</sup>

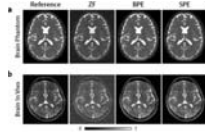
<sup>1</sup>Radiology, University of British Columbia, Vancouver, BC, Canada

The highly efficient balanced Steady-State Free Precession (bSSFP) sequence has many research and clinical applications. However, it has a peculiar sensitivity to magnetic field inhomogeneity, often resulting in artifacts seen as dark bands. Phase-cycling can generate multiple acquisitions in which the banding is spatially shifted, and subsequently reduced by various algorithms. With 4 acquisitions and an elliptical signal model, it is possible to eliminate the banding by solving the system geometrically, algebraically, or in a combined manner for improved SNR. This work reports a Fourier approach that can effectively reduce the banding using only 3 acquisitions.

571



16:27



### Parameter-Free Profile Encoding Reconstruction for Multiple-Acquisition bSSFP Imaging

Efe Ilicak<sup>1,2</sup> and Tolga Çukur<sup>1,2,3</sup>

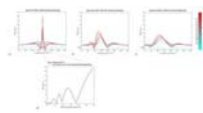
<sup>1</sup>Electrical and Electronics Engineering, Bilkent University, Ankara, Turkey, <sup>2</sup>National Magnetic Resonance Research Center (UMRAM), Bilkent University, Ankara, Turkey, <sup>3</sup>Graduate School of Engineering and Science, Bilkent University, Neuroscience Program, Ankara, Turkey

Several recent studies suggested accelerating multiple-acquisition balanced steady-state free precession acquisitions to suppress banding artifacts while maintaining scan efficiency. However, these approaches employ regularization terms, which require labor-intensive manual tuning of penalty weights. Here, we propose a parameter-free framework to select penalty weights adaptively for profile-encoding reconstructions. Results indicate the proposed method achieves equivalent image quality to conventional reconstructions, without an exhaustive manual tuning of penalty weights.

572



16:39



### Mitigation of bSSFP Flow Artifacts using Partial Dephasing

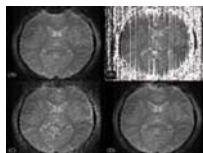
Anjali Datta<sup>1</sup>, Joseph Y Cheng<sup>2</sup>, Corey A Baron<sup>1</sup>, and Dwight G Nishimura<sup>1</sup>

<sup>1</sup>Electrical Engineering, Stanford University, Stanford, CA, United States, <sup>2</sup>Radiology, Stanford University, Stanford, CA, United States

We show that partial dephasing mitigates artifacts from through-plane flow near dark bands in balanced SSFP. A 30°-60° range in the phase accrual during a TR is created over the voxel by slightly unbalancing the slice-select rephaser. The effects of partial dephasing on the spectral profiles for various flow rates were simulated, and the simulations were validated in a flow phantom. By decreasing the strength and non-linearity of the signal's dependence on through-plane flow rate, partial dephasing mitigates the transient artifacts caused by pulsatile flow. In volunteer studies, it noticeably decreased artifacts in all of the phase-cycled cardiac cine datasets acquired.

573

16:51



### Correction of Susceptibility-Related Image Distortion Based on an Analytic Point-Spread Function

Franz Patzig<sup>1</sup>, Toralf Mildner<sup>1</sup>, and Harald Möller<sup>1</sup>

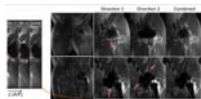
*<sup>1</sup>Max Planck Institute for Human Cognitive and Brain Sciences, Leipzig, Germany*

Geometric distortions caused by magnetic susceptibility variations in the underlying medium can severely corrupt the image. A novel correction method is proposed, which uses the prior knowledge of the analytic point spread function (PSF) of the used imaging sequence and a map of the underlying field inhomogeneities. From this input, a PSF operator can be devised and applied to correct the image by performing a deconvolution. Regularization techniques are used to improve and stabilize the outcome. A significant reduction in geometric distortions is demonstrated for human brain images as well as some advantages over existing correction methods.

574



17:03



### Pile-up and Ripple Artifact Correction Near Metallic Implants by Alternating Gradients

Xinwei Shi<sup>1,2</sup>, Brady Quist<sup>1,2</sup>, and Brian A. Hargreaves<sup>1,2</sup>

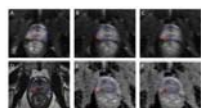
*<sup>1</sup>Radiology, Stanford University, Stanford, CA, United States, <sup>2</sup>Electrical Engineering, Stanford University, Stanford, CA, United States*

Multi-Spectral Imaging techniques have been shown to significantly reduce metal-induced artifacts. However, they often suffer from residual pile-up and ripple artifacts in the vicinity of metal, where the metal-induced off-resonance gradient “cancels” the frequency-encoding gradient. Fully phase-encoded methods can overcome the drawbacks of frequency encoding, but usually incur prohibitively long scan times. Here we address this limitation by combining two acquisitions with alternating-sign readout and slice-select gradients. We demonstrate with simulations, phantom and in-vivo scans that the proposed method can effectively suppress pile-up and ripple artifacts, and reduce the signal loss areas near the implants.

575



17:15



### Geometric Distortion Correction of Diffusion-Weighted MRI and its Effect on quantitative ADC analysis

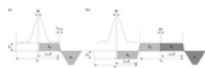
Gabriel Nketiah<sup>1</sup>, Kirsten M. Selnaes<sup>1,2</sup>, Elise Sandsmark<sup>1</sup>, Jose R. Teruel<sup>3</sup>, Tone F. Bathen<sup>1,2</sup>, and Mattijs Elschot<sup>1</sup>

<sup>1</sup>Department of Circulation and Medical Imaging, NTNU, Norwegian University of Science and Technology, Trondheim, Norway, <sup>2</sup>St. Olavs Hospital, Trondheim University Hospital, Trondheim, Norway, <sup>3</sup>Department of Radiology, University of California San Diego, CA, United States

Tissue water diffusion (ADC) quantification through diffusion-weighted imaging (DWI) currently plays an integral clinical role in prostate cancer. The echo-planar imaging technique employed in DWI is however prone to geometric distortion due to static magnetic field (B<sub>0</sub>) inhomogeneity. We investigated the effect of the correction of this distortion on the quantification of ADC values in the prostate. Our study showed that there is a significant association between the amount of distortion (mm) and the difference between ADC values before and after correction, which implies that correction for this could be necessary, especially for voxel-based quantitative analysis.

576

17:27



Estimating and eliminating excitation errors in bipolar gradient composite excitations caused by RF-gradient delay: example of bipolar spokes pulses in parallel transmission

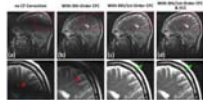
Desmond H Y Tse<sup>1</sup>, Christopher J Wiggins<sup>2</sup>, and Benedikt A Poser<sup>1</sup>

<sup>1</sup>Faculty of Psychology and Neuroscience, Maastricht University, Maastricht, Netherlands, <sup>2</sup>Scannexus BV, Maastricht, Netherlands

Parallel transmission of spokes pulses is a promising way of mitigating flip-angle inhomogeneity in 2D imaging at ultra-high-field MRI. Bipolar slice-selective gradient is often used to minimise the overall duration of these pulses, making them more resilient to off-resonance related artefacts, but they are prone to errors caused by RF-gradient timing mismatch. In this study, we present a mathematical description for the effect of such delay on bipolar-gradient composite excitations. We demonstrate the effect with both flip-angle maps and EPI images. Finally, we propose a navigator approach to estimate the delay and show two effective ways of eliminating these errors.

577

17:39



Effect of Concomitant Field in Fast Spin Echo Acquisition on an Asymmetric MRI Gradient System

Shengzhen Tao<sup>1</sup>, Paul T Weavers<sup>1</sup>, Joshua D Trzasko<sup>1</sup>, Yunhong Shu<sup>1</sup>, Erin M Gray<sup>1</sup>, John Huston III<sup>1</sup>, and Matt A Bernstein<sup>1</sup>

<sup>1</sup>Radiology, Mayo Clinic, Rochester, MN, United States

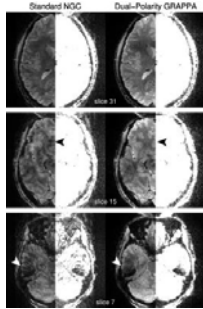


Fast-spin-echo (FSE) acquisitions are routinely used in clinical MRI, but can be affected by concomitant field (CF)-induced phase errors. The conventional whole-body MR gradient typically employs symmetric design. On such systems only CFs of 2nd-order spatial dependence are significant. These CFs can cause ghosting in large-FOV FSE acquisition, but are typically negligible over a brain scan volume. Recently, a high-performance, asymmetric gradient system was developed whose CF contains additional zeroth and first-order spatially-dependent fields. Here, we investigate the effect of CF in FSE on this system using extended-phase-graphs simulation, and demonstrate a real-time compensation for them.

578

17:51

Artifact Correction in Accelerated-Segmented EPI data via Dual-Polarity GRAPPA



W. Scott Hoge<sup>1,2</sup> and Jonathan R Polimeni<sup>3,4</sup>

<sup>1</sup>Radiology, Brigham and Women's Hospital, Boston, MA, United States, <sup>2</sup>Harvard Medical School, Boston, MA, United States, <sup>3</sup>Radiology, Massachusetts General Hospital, MA, United States, <sup>4</sup>Harvard Medical School, MA, United States

A method to reconstruct images from multiple EPI segments is presented. Leveraging the reconstruction framework from Dual-Polarity GRAPPA, data from each segment and readout polarity are modeled as sampled on separate grids. After phase-matching calibration data to each segment, a GRAPPA-like reconstruction kernel is generated. This parameterization ensures that differences in signal phase across all data polarities and segments can be captured in the reconstruction kernel. We present *in-vivo* images reconstructed using this approach from concurrently segmented and accelerated high-resolution gradient-echo and spin-echo data acquired at 7T.

579

18:03

Variable Projection SENSE for Reference-free EPI Nyquist Ghost Correction



Yue Zhang<sup>1,2,3</sup>, Mengye Lyu<sup>1,2</sup>, Yilong Liu<sup>1,2</sup>, Yifan Chen<sup>3</sup>, and Ed X. Wu<sup>1,2</sup>

<sup>1</sup>Laboratory of Biomedical Imaging and Signal Processing, The University of Hong Kong, Hong Kong SAR, People's Republic of China, <sup>2</sup>Department of Electrical and Electronic Engineering, The University of Hong Kong, Hong Kong SAR, People's Republic of China, <sup>3</sup>Department of Electrical and Electronic Engineering, Southern University of Science and Technology, Shenzhen, People's Republic of China

In this abstract, variable projection sensitivity encoding (VP-SENSE) method is proposed to correct phase error, which is the main cause of Nyquist ghost in EPI. In VP-SENSE, the unknown images are fully represented by a function of phase error and the least squares solution is sought regarding phase error only. Our results have indicated that this approach can robustly remove ghost without apparent SNR penalty. With prior phase error information as constraints, ghost level can be further reduced and the SNR loss can be further minimized through constrained variable projection approach (CVP-SENSE).

---

Oral

## Pushing the Envelope of fMRI Acquisition

Room 312

Tuesday 16:15 - 18:15 Moderators: Tony Stoecker & An Vu

---

580

16:15

3D-EPI-CAIPI and 2D-Multiband-EPI: which is best for fMRI at 3T?

Nadège Corbin<sup>1</sup>, Oliver Josephs<sup>1</sup>, and Martina F Callaghan<sup>1</sup>

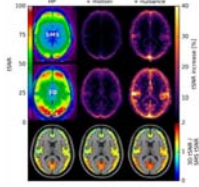


<sup>1</sup>Wellcome Trust Centre for Neuroimaging, UCL Institute of Neurology, London, United Kingdom

2D-MB-EPI and 3D-EPI-CAIPI acquisition schemes can be used to increase spatiotemporal resolution in fMRI. This study examined which approach is optimal at 3T, over a range of temporal and spatial resolutions, while maintaining extended brain coverage. 10 protocols were tested in vivo for each sequence spanning low and high spatial resolution and a range of through-plane acceleration factors. 3D-EPI-CAIPI outperforms 2D-MB-EPI at lower temporal resolutions, as long as physiological effects are corrected and the maximal CAIPIRINHA shift is used. The benefit is greater at higher spatial resolution. However, as the temporal resolution increases, by increasing the through-plane acceleration, 2D-MB-EPI becomes preferable.

---



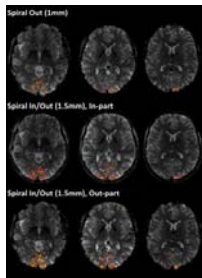


### The effect of motion and nuisance regression on resting-state fMRI using highly accelerated SMS- or 3D-EPI

Rüdiger Stirnberg<sup>1</sup>, Willem Huijbers<sup>2</sup>, Monique Breteler<sup>2</sup>, and Tony Stöcker<sup>1,3</sup>

<sup>1</sup>MR Physics, DZNE (Bonn), Bonn, Germany, <sup>2</sup>Population Health Sciences, DZNE (Bonn), Bonn, Germany, <sup>3</sup>Department of Physics and Astronomy, University of Bonn, Bonn, Germany

We compare the effects of motion and nuisance regression on highly accelerated resting-state fMRI of 10 subjects scanned at 3T using state-of-the-art simultaneous multi-slice EPI and segmented 3D-EPI with controlled aliasing. While both TR-matched protocols are per design fast enough to separate the cardiac frequency peak from BOLD signal, gray matter signal-to-noise ratio with the 3D-EPI protocol improves almost twice as much as compared to the SMS-EPI protocol. Template based rotation functional connectivity analysis on average shows greater statistical loadings for several known networks when using cleaned 3D-EPI data than when using cleaned SMS-EPI data.



### High-resolution Spiral fMRI at 7T

Lars Kasper<sup>1,2</sup>, Maria Engel<sup>1</sup>, Christoph Barmet<sup>1,3</sup>, Thomas Schmid<sup>1</sup>, Klaas Enno Stephan<sup>4,5,6</sup>, and Klaas Paul Pruessmann<sup>1</sup>

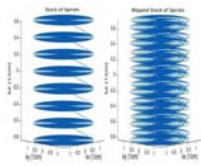
<sup>1</sup>Institute for Biomedical Engineering, ETH Zurich and University of Zurich, Zurich, Switzerland, <sup>2</sup>Translational Neuromodeling Unit, IBT, University of Zurich and ETH Zurich, Zurich, Switzerland, <sup>3</sup>Skope Magnetic Resonance Technologies, Zurich, Switzerland, <sup>4</sup>Translational Neuromodeling Unit, IBT, University of Zurich and ETH Zurich, Zurich, Switzerland, <sup>5</sup>Wellcome Trust Centre for Neuroimaging, University College London, London, United Kingdom, <sup>6</sup>Max Planck Institute for Metabolism Research, Cologne, Germany

High-resolution spiral fMRI acquisition at 7 Tesla is shown with excellent image quality and geometric veracity. Both, high-resolution spiral-out (1mm isotropic) and multi-echo spiral-in/out readouts (1.5mm) are acquired in a visual paradigm, performed by 2 subjects. The datasets are analyzed by SPM and activation patterns are shown overlaid over the actual fMRI datasets of almost structural imaging quality.

### Blipped Stack of Spirals for Fast Volumetric Functional MRI

V. Andrew Stenger<sup>1</sup> and Christoph Rettenmeier<sup>1</sup>



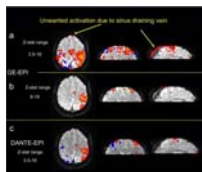


<sup>1</sup>University of Hawaii, Honolulu, HI, United States

This work presents a volumetric acquisition technique for fast fMRI using spirals and parallel imaging. Gradient blips were added along the readout of a stack of spirals sequence to produce a blipped stack of spirals for a more efficient sampling scheme. Phantom images and human fMRI experiments show that the method is capable of providing approximately a factor of two speed increase compared to a standard volumetric stack of spirals.

584

17:03



Localization of Neural Activity Using DANTE-Prepared Multi-slice EPI (DANTE-EPI) for BOLD Detection

Linqing Li<sup>1</sup>, Christine Law<sup>2</sup>, Karla Miller<sup>3</sup>, and Peter Jezzard<sup>3</sup>

<sup>1</sup>National Institute of Mental Health, National Institute of Health, Rockville, MD, United States, <sup>2</sup>Systems Neuroscience and Pain Lab, Stanford University, CA, United States, <sup>3</sup>Nuffield Department of Clinical Neurosciences, FMRIB Centre, University of Oxford, Oxford, United Kingdom

To assess whether DANTE-EPI (Delay Alternating with Nutation for Tailored Excitation) sequence for moving blood suppressed fMRI images can effectively reduce inflow effects and, physiological noise originating from intravascular blood signal, and spurious (false positive) functional activation resulting from draining vein effects. Results were compared with images from conventional gradient echo planar imaging (GE-EPI).

585

17:15

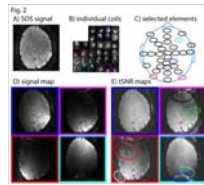


Silent, Multi-Echo T2\* Looping Star fMRI

Ana Beatriz Solana<sup>1</sup>, Anne Menini<sup>1</sup>, Brice Fernandez<sup>2</sup>, and Florian Wiesinger<sup>1</sup>

<sup>1</sup>GE Global Research, Munich, Germany, <sup>2</sup>GE Healthcare, Orsay, France

In this work, we propose a novel method for quiet, 3D, T2\* BOLD fMRI in form of multi-echo Looping Star. Its inaudible scanning offers unique potential for pediatric imaging, imaging auditory or speech paradigms, as well as for resting-state studies. In comparison to standard Gradient-Echo EPI, Looping Star demonstrated better tSNR and lower temporal drift. Motor activation and identification of resting state networks are demonstrated for single and combined echo processing.



### Simple approach to improve time series fMRI stability: STAbility-weighted Rf-coil Combination (STARC)

Laurentius Huber<sup>1</sup>, David Jangraw<sup>2</sup>, Sean Marrett<sup>2</sup>, and Peter A Bandettini<sup>3</sup>

<sup>1</sup>NIMH, Bethesda, MD, United States, <sup>2</sup>NIMH, United States, <sup>3</sup>SFIM, NIMH, Bethesda, MD, United States

Advanced EPI -especially at high resolutions- is often limited by signal instabilities arising from a variety of unwanted artifacts. These include: GRAPPA ghosts interference, Nyquist ghosts, phase offset interference patterns, and fat rings. The sources of these artifacts are all somewhat locally confined and are often differently pronounced in different elements of multi coil arrays. Here we propose a simple approach of STAbility-weighted Rf-coil Combination (STARC) that reduces the likelihood of those artifacts. It increases tSNR and fMRI sensitivity up to 50% without a loss in quantifiability, without loss in temporal resolution, and without loss in spatial resolution.



### Multi-channel fMRI Denoising Based on Tensor Decomposition

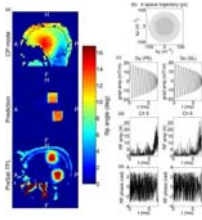
Jun Cao<sup>1,2</sup>, Yilong Liu<sup>1,2</sup>, Mengye Lyu<sup>1,2</sup>, Grantham K. Pang<sup>2</sup>, and Ed X. Wu<sup>1,2</sup>

<sup>1</sup>Laboratory of Biomedical Imaging and Signal Processing, The University of Hong Kong, Hong Kong, People's Republic of China, <sup>2</sup>Department of Electrical and Electronic Engineering, The University of Hong Kong, Hong Kong, People's Republic of China

Conventional fMRI analysis applies spatial Gaussian smoothing to increase SNR, which does not fully utilize multichannel information in fMRI, and often lead to smearing of fMRI images. In this work, we proposed to denoise multichannel fMRI data based on tensor decomposition. Specifically, fMRI data are treated as a 3rd-order tensor, and Canonical Polyadic Decomposition (CPD) is used to approximate fMRI data with sum of limited number of rank-1 terms. Results show its effectiveness in denoising block-design task-related fMRI data, leading to increased temporal SNR and sensitivity of activation detection without sacrificing spatial resolution.

### Dual region-selective spiral pTX excitation for digit mapping fMRI in motor cortex and cerebellum

Benedikt A Poser<sup>1</sup>, Amanda L Kaas<sup>1</sup>, Christopher J Wiggins<sup>2</sup>, Kâmil Uludağ<sup>1</sup>, and Desmond H Y Tse<sup>1</sup>



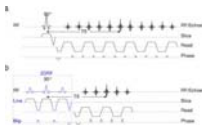
<sup>1</sup>Faculty of Psychology and Neuroscience, Maastricht University, Maastricht, Netherlands, <sup>2</sup>Scannexus BV, Maastricht, Netherlands

We demonstrate the use of 2D-selective excitation with parallel transmission to (a) simultaneously perform BOLD fMRI on two apart brain regions, and (b) benefit from high acceleration factors achievable with sparse volume excitation. Using 8ch pTX at 7T, we apply spatially selective pulses to excite the primary motor and sensory cortices, as well as cerebellum. tSNR measures confirm superior performance compared to whole-brain excitation at the same TR. A finger tapping task is used to elicit digit-specific activation, which is observed in primary cortex and cerebellum.

589

18:03

T2\*-Weighted Echo-Planar Imaging of the Spinal Cord: Full vs. Inner Fields-of-View



Jürgen Finsterbusch<sup>1</sup>

<sup>1</sup>Systems Neuroscience, University Medical Center Hamburg-Eppendorf, Hamburg, Germany

BOLD-based fMRI of the spinal cord is challenging because the high resolution required and the field inhomogeneities present promote geometric distortions in echo-planar imaging and T2\*-related signal losses which both hamper the image quality and the SNR. With inner-field-of-view imaging techniques, e.g. based on spatially 2D-selective RF excitations, the acquisition can be focussed to the spinal cord which allows to minimize geometric distortions. Furthermore, shorter echo time can be achieved resulting in a significantly increased SNR that may make fMRI feasible throughout the spinal cord.

Oral

## Preclinical Models of Neurologic Disease

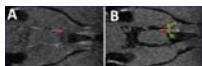
Room 313A

Tuesday 16:15 - 18:15 Moderators: Myriam Chaumeil & Afonso Silva

590

16:15

Investigation of the role of the venous system and the glymphatic system in brain waste clearance



Yimin shen<sup>1</sup>, Quan Jiang<sup>2</sup>, Guangliang Ding<sup>2</sup>, Nicholas Guys<sup>1</sup>, E. Mark Haacke<sup>1</sup>, and Jiani Hu\*<sup>1</sup>

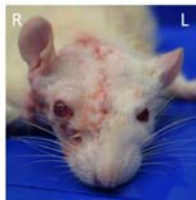
*<sup>1</sup>Department of Radiology, Wayne State University, Detroit, MI, United States, <sup>2</sup>Neurology, Henry Ford Health System, Detroit, MI, United States*

The recently discovered glymphatic system has become an exciting area of research because of its broad implications in both normal neurophysiological activities and neurological disorders. However, the exact relationship between the vascular system and the glymphatic system in terms of waste clearance for the brain is unclear. In addition to the glymphatic system, our preliminary MRI results suggest that the venous (but not the arterial) system also directly participates in waste removal. Fully elucidating the roles of the venous and glymphatic systems in waste removal from the brain is important for understanding the influence of waste clearance on neurological diseases.

591



16:27



#### Anterograde manganese transport in donor optic nerve following whole eye transplantation

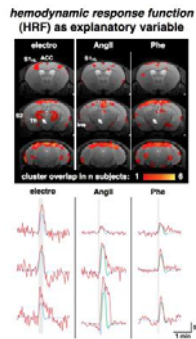
Yolandi van der Merwe<sup>1,2,3</sup>, Chiaki Komatsu<sup>4</sup>, Lin He<sup>4</sup>, Maxine R Miller<sup>3,4</sup>, Ian Rosner<sup>4</sup>, Huamin Tang<sup>4</sup>, Joel S. Schuman<sup>5</sup>, Jose-Alain Sahel<sup>3</sup>, Michael B. Steketee<sup>3</sup>, Kia M. Washington<sup>4</sup>, and Kevin C. Chan<sup>2,3</sup>

*<sup>1</sup>Department of Bioengineering, University of Pittsburgh, Pittsburgh, PA, United States, <sup>2</sup>Neuroimaging Laboratory, University of Pittsburgh, Pittsburgh, PA, United States, <sup>3</sup>Department of Ophthalmology, University of Pittsburgh, Pittsburgh, PA, United States, <sup>4</sup>Department of Surgery, University of Pittsburgh, Pittsburgh, PA, United States, <sup>5</sup>Department of Ophthalmology, New York University, New York, NY, United States*

Approximately 39 million people worldwide suffer from irreversible blindness. Our recently established whole eye transplant model (WET) gives the opportunity to provide an intact optical system that could restore lost vision. In this study we use manganese-enhanced MRI to examine the anterograde transport of the transplanted and recipient visual pathways following WET. Our results show comparable manganese enhancement between donor and naïve intraorbital optic nerves, suggesting the presence of anterograde manganese transport in the donor optic nerve. This in vivo imaging model system may allow future examinations of neuroregenerative approaches for connecting between the transplanted eye and the recipient's brain.

16:39

Detailing the Origin of BOLD fMRI in Mice: Somatosensory Stimulation versus Pharmacologically Induced Blood Pressure Alterations

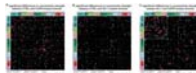


Henning Matthias Reimann<sup>1</sup>, Mihail Todiras<sup>2</sup>, Till Huelnhagen<sup>1</sup>, Michael Bader<sup>2</sup>, Andreas Pohlmann<sup>1</sup>, and Thoralf Niendorf<sup>1,3</sup>

<sup>1</sup>Berlin Ultrahigh Field Facility (B.U.F.F.), Max Delbrueck Center for Molecular Medicine (MDC), Berlin, Germany, <sup>2</sup>Max Delbrueck Center for Molecular Medicine (MDC), Berlin, Germany, <sup>3</sup>Experimental and Clinical Research Center (ECRC), a joint cooperation between the Charité Medical Faculty and the Max Delbrueck Center, Berlin, Germany

The combination of somatosensory fMRI (sfMRI) and mouse genomics holds great potential to unravel the underlying mechanisms of chronic pain. Transient stimuli were shown to induce unspecific BOLD patterns in mice. It is known that increases in *mean arterial blood pressure* (MABP) can mimic BOLD activations in rats. To detail the origin of the unspecific BOLD patterns evoked in the murine brain we performed sfMRI along with pharmacologically induced blood pressure alterations while monitoring MABP. We compared MABP changes, BOLD signals and BOLD patterns between the types of stimuli and observed confounding effects of MABP on murine BOLD fMRI.

16:51



Remodeling of resting state functional connectivity following thyromimetic induced remyelination in the mouse brain

Neele Saskia Hübner<sup>1</sup>, Annika Carolin Hammerschmitt<sup>1</sup>, Thiago Marques De Melo<sup>1,2</sup>, Thomas Bienert<sup>1</sup>, Jürgen Hennig<sup>1</sup>, Dominik von Elverfeldt<sup>1</sup>, and Laura Adela Harsan<sup>1,3,4</sup>

<sup>1</sup>Department of Radiology, Medical Physics, University Medical Center Freiburg, Freiburg, Germany, <sup>2</sup>Spemann Graduate School of Biology and Medicine, Albert-Ludwigs-University of Freiburg, Freiburg, Germany, <sup>3</sup>Laboratory of Engineering, Informatics and Imaging, University of Strasbourg, Strasbourg, France, <sup>4</sup>Department of Biophysics and Nuclear Medicine, University Hospital Strasbourg, Strasbourg, France

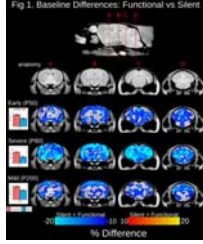
Characterization of the brain network architecture and its alterations in pathologies are essential for a better understanding of mechanisms of action in health and disease and paves the way for the development of targeted therapeutic strategies. In the field of demyelinating disorders, thyromimetic treatment provides a promising remyelinating strategy inducing oligodendrogenesis *in vitro*. We tested the potential of sobetirome (GC-1), a thyroid hormone analogue, to induce remyelination *in vivo* in the cuprizone demyelinated mouse model and we investigated its action on the resting state (rsfMRI) mouse brain functional connectivity.

594

17:03

### Genetic rescue of brain morphometry in a mouse model of neurodevelopmental disorder

Rylan Allemang-Grand<sup>1</sup>, Jacob Ellegood<sup>1</sup>, Leigh Spencer Noakes<sup>1</sup>, Brian J Nieman<sup>1</sup>, and Jason P Lerch<sup>1</sup>



<sup>1</sup>Neurosciences and Mental Health, SickKids Hospital, Toronto, ON, Canada

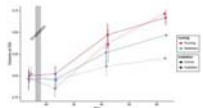
In this study, we scanned a mouse model of Rett syndrome before and after reactivation of *Mecp2*, the gene strongly implicated in the disorder. We found that reactivation of *Mecp2* at three different time points in adulthood lead to drastic growth of the neuroanatomy across many regions of the cortex, cerebellum and medulla. Our findings demonstrate that the developmental delayed brain retains an innate plasticity that can be recruited to restore neuroanatomical structure in adulthood.

595

17:15

### Can mice outrun the deleterious impacts of radiation to the brain?

Kamila U. Szulc<sup>1</sup>, Shannon Egan<sup>2</sup>, Elizabeth A. de Guzman<sup>2,3,4</sup>, Aidin Arbabi<sup>2,3,4</sup>, Donald J. Mabbott<sup>1,5</sup>, and Brian J. Nieman<sup>2,3,4</sup>



<sup>1</sup>Neurosciences and Mental Health, Hospital for Sick Children, Toronto, ON, Canada, <sup>2</sup>Mouse Imaging Centre, Hospital for Sick Children, Toronto, ON, Canada, <sup>3</sup>Ontario Institute for Cancer Research, Toronto, ON, Canada, <sup>4</sup>Department of Medical Biophysics, University of Toronto, Toronto, ON, Canada, <sup>5</sup>Department of Psychology, University of Toronto, Toronto, ON, Canada

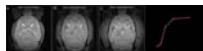
Pediatric cancer patients who receive cranial radiation therapy (CRT) exhibit cognitive deficits later in life. These deficits are often accompanied by brain structure abnormalities, especially prevalent in the white matter and hippocampus. The objective of this study was to explore the potential of physical exercise to mitigate some of the deleterious effects of CRT on the brain, using a mouse model and high-resolution MRI as a measure of brain structure. We found that irradiated mice housed in cages with access to running wheels showed a remarkable recovery of a number of CRT-induced brain volume deficits, most notably in the hippocampus.

596

17:27

### MRI visualization of brain-like tissue formation following implantation of neural precursors into in cerebrospinal fluid

Nikorn Pothayee<sup>1</sup>, Dragan Maric<sup>2</sup>, Kathryn Sharer<sup>1</sup>, Jung-Hwa Tao-Cheng<sup>3</sup>, Stephen Dodd<sup>1</sup>, Alec Calac<sup>1</sup>, James Pickel<sup>4</sup>, and Alan Koretsky<sup>1</sup>





*<sup>1</sup>Laboratory of Functional and Molecular Imaging, National Institute of Neurological Disorders and Stroke, National Institutes of Health, Bethesda, MD, United States, <sup>2</sup>Flow Cytometry Core Facility, National Institute of Neurological Disorders and Stroke, National Institutes of Health, Bethesda, MD, United States, <sup>3</sup>Electron Microscopy Facility, National Institute of Neurological Disorders and Stroke, National Institutes of Health, Bethesda, MD, United States, <sup>4</sup>Transgenic Core Facility, National Institute of Mental Health, National Institutes of Health, Bethesda, MD, United States*

Neural stem cell transplantation has been hailed as a promising approach for treatment of neurological diseases. While most in vivo studies have implanted cells into specific sites in brain tissue, little is known whether the cerebrospinal fluid (CSF) provides a permissive environment in cultivating tissue growth. Here, using MRI, we investigate whether early neural precursor cells could initiate a large-scale formation of new brain tissue in the CSF of adult rat.

---

597

17:39



Use of Pharmacological MRI (phMRI) to understand the mechanisms leading to convergent procognitive effects of 5-HT<sub>6</sub> serotonergic receptors agonist (EMD-386088) and antagonist (SB-271046).

Willy Gsell<sup>1</sup>, Rachel Asselot<sup>2</sup>, Nicolas Delcroix<sup>3</sup>, Uwe Himmelreich<sup>1</sup>, Valentine Bouet<sup>2</sup>, and François Dauphin<sup>2</sup>

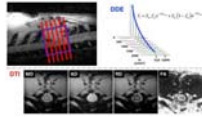
*<sup>1</sup>Biomedical MRI group, KU Leuven, Leuven, Belgium, <sup>2</sup>GMPc (Groupe Mémoire et Plasticité comportementale), University of Caen-Normandie, Caen, France, <sup>3</sup>CNRS UMS3408, GIP CYCERON, Caen, France*

Either blocking or activating 5HT<sub>6</sub> receptors (5-HT<sub>6</sub>R), respectively with antagonists or agonists, exert beneficial cognitive effects. Through phMRI, we demonstrated for the first time the similarities and discrepancies in the brain activation induced by an agonist and an antagonist of 5-HT<sub>6</sub>R. Both drugs similarly activate cortices and hippocampus. SB-271046 positively activates a network including the medio-dorsal raphe while EMD-386088 activates the rostral dorsal raphe. The different patterns of activation elicited in brain regions such as the habenula and the MG/DG nuclei (for SB-271046), or the amygdala and substantia nigra (for EMD-386088) supports different interactions with polysynaptic pathways.

---



17:51



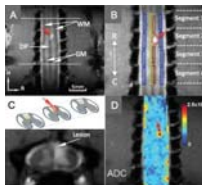
### Predicting Functional and Histological Outcomes in Spinal Cord Injury: Comparing Double Diffusion Encoding and Diffusion Tensor Imaging in the Rat

Nathan Skinner<sup>1,2</sup>, Shekar Kurpad<sup>3,4</sup>, Brian Schmit<sup>5</sup>, Natasha Beucher<sup>3</sup>, Kyle Stehlik<sup>3</sup>, L. Tugan Muftuler<sup>3</sup>, and Matthew Budde<sup>3</sup>

<sup>1</sup>*Biophysics Graduate Program, Medical College of Wisconsin, Milwaukee, WI, United States*, <sup>2</sup>*Medical Scientist Training Program, Medical College of Wisconsin, Milwaukee, WI, United States*, <sup>3</sup>*Neurosurgery, Medical College of Wisconsin, Milwaukee, WI, United States*, <sup>4</sup>*Clement J Zablocki Veterans Affairs Medical Center, Milwaukee, WI, United States*, <sup>5</sup>*Biomedical Engineering, Marquette University, Milwaukee, WI, United States*

Using a rat model of spinal cord injury (SCI), diffusion tensor imaging (DTI) is compared to double diffusion encoding (DDE) at the acute and chronic stages after injury. Acute DDE measurements show a strong relationship with chronic functional outcomes whereas DTI has poor prognostic sensitivity. On the other hand, during the chronic stage, DTI outperforms DDE as a marker of functional status. The differences reflect evolving pathologies that must be considered for the appropriate application and interpretation of DTI and DDE. The results also highlight the prognostic potential of DDE in acute SCI.

18:03



### Spinal DTI Parametric Changes Following Traumatic Injury in Monkeys

Arabinda Mishra<sup>1</sup>, Feng Wang<sup>1</sup>, Li Min Chen<sup>1</sup>, and John C Gore<sup>1</sup>

<sup>1</sup>*Radiology, Vanderbilt University Medical Center, Nashville, TN, United States*

The proposed DTI study aims at quantification of the effect of experimentally induced dorsal column lesion at upper cervical level (C4/5) in squirrel monkeys. Diffusion parametric changes based on the directionality, and mobility of water molecules in the cellular environment, characterizes the spinal cord. Change in diffusion parameters on specific white matter tracks above and below the SCI location were compared between the lesioned and normal side of the spinal cord. A systematic group analysis of the inter-ROI changes along the white matter pathways can therefore be used to correlate the loss and recovery of sensory/motor functions over time.

# Diffusion: Multi-Site & Validation

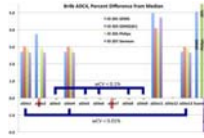
Room 313BC

Tuesday 16:15 - 18:15 Moderators: Kathryn Keenan & Ek Tan

---

600

16:15



## Multi-site Concordance of DWI Metrics: Results of the NCI Quantitative Imaging Network ADC Mapping Collaborative Project

David C Newitt<sup>1</sup>, Dariya Malyarenko<sup>2</sup>, Thomas L Chenevert<sup>2</sup>, C. Chad Quarles<sup>3</sup>, Laura Bell<sup>3</sup>, Andrey Fedorov<sup>4</sup>, Fiona Fennessy<sup>4</sup>, Michael A Jacobs<sup>5</sup>, Meiyappan Solaiyappan<sup>5</sup>, Stefanie Hectors<sup>6</sup>, Bachir Taouli<sup>6</sup>, Kathleen M Schmainda<sup>7</sup>, Melissa A Prah<sup>7</sup>, Yi-Fen Yen<sup>8</sup>, Jayashree Kalpathy-Cramer<sup>8</sup>, Erin Taber<sup>9</sup>, Christopher Kroenke<sup>9</sup>, Yue Cao<sup>10</sup>, Madhava Aryal<sup>11</sup>, Mark Muzi<sup>12</sup>, Paul Kinahan<sup>12</sup>, Thomas E Yankeelov<sup>13</sup>, Lori R Arlinghaus<sup>14</sup>, Michael A Boss<sup>15</sup>, Amita Shukla-Dave<sup>16</sup>, and Nola Hylton<sup>1</sup>

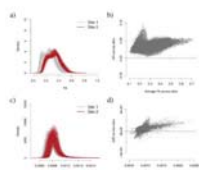
<sup>1</sup>Radiology and Biomedical Imaging, University of California, San Francisco, CA, United States, <sup>2</sup>Radiology, University of Michigan Health System, Ann Arbor, MI, United States, <sup>3</sup>Translational Bioimaging Group, Barrow Neurological Institute, Phoenix, AZ, United States, <sup>4</sup>Brigham and Womens Hospital, Boston, MA, United States, <sup>5</sup>Radiology and Radiological Science, Johns Hopkins University, Baltimore, MD, United States, <sup>6</sup>Translational and Molecular Imaging Institute, Icahn School of Medicine at Mount Sinai, New York, NY, United States, <sup>7</sup>Radiology and Biophysics, Medical College of Wisconsin, Milwaukee, WI, United States, <sup>8</sup>Martinos Center, Massachusetts General Hospital, Boston, MA, United States, <sup>9</sup>Oregon Health & Science University, Portland, OR, United States, <sup>10</sup>Radiation Oncology, Radiology, and Biomedical Engineering, University of Michigan, Ann Arbor, MI, United States, <sup>11</sup>Radiation Oncology, University of Michigan, Ann Arbor, MI, United States, <sup>12</sup>Radiology, Neurology & RadOnc, University of Washington, Seattle, WA, United States, <sup>13</sup>University of Texas, Austin, TX, United States, <sup>14</sup>Institute of Imaging Science, Vanderbilt University Medical Center, Nashville, TN, United States, <sup>15</sup>Applied Physics Division, National Institute of Standards and Technology, Boulder, CO, United States, <sup>16</sup>Medical Physics and Radiology, Memorial Sloan-Kettering Cancer Center, New York, NY, United States

Reproducibility of diffusion metrics is essential given the increasing role quantitative diffusion weighted imaging plays in diagnosis and treatment monitoring. Here we examined the variability in apparent diffusion coefficient (ADC) measures resulting from different post-processing software implementations utilized by researchers across the NCI Quantitative Imaging Network. Agreement between the majority of implementations was good; typical biases for *in vivo* ADC measures of 2-3%, and lower biases in phantom scans. Higher deviations (above 5%) detected among individual implementations and scanner-generated parametric maps highlighted inadequacies in meta-data and post-processing parameters that need to be addressed in multi-site study settings.

---

601

16:27



### Statistical harmonization of multi-site diffusion tensor imaging data with ComBat

Jean-Philippe Fortin<sup>1</sup>, Drew Parker<sup>2</sup>, Birkan Tunç<sup>2</sup>, Takanori Watanabe<sup>2</sup>, Mark A. Elliott<sup>2</sup>, Kosha Ruparel<sup>3</sup>, Ruben C. Gur<sup>3</sup>, Raquel E Gur<sup>3</sup>, Robert T. Schultz<sup>4</sup>, Russell T Shinohara<sup>1</sup>, and Ragini Verma<sup>2</sup>

<sup>1</sup>Department of Biostatistics and Epidemiology, University of Pennsylvania, Philadelphia, PA, United States, <sup>2</sup>Department of Radiology, University of Pennsylvania, Philadelphia, PA, United States, <sup>3</sup>Department of Psychiatry, University of Pennsylvania, Perelman School of Medicine, Philadelphia, PA, United States, <sup>4</sup>Center for Autism Research, Children's Hospital of Philadelphia, Philadelphia, PA, United States

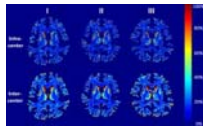
Diffusion tensor imaging (DTI) is a well-established magnetic resonance imaging technique to study microstructural changes in the white matter (WM). DTI images suffer from unwanted inter-scanner variability, which is problematic when combining datasets from different sites. In this work, we propose to use ComBat, a location-scale Empirical Bayes model largely used in genomics, to combine and harmonize multi-site DTI datasets. Using a study of 210 subjects with an age range of 8 to 18 years old from two imaging sites, we show that ComBat (1) removes unwanted variation associated with imaging site and (2) improves the power at detecting regions known to exhibit microstructural changes in this age range.

---

602

16:39

### Variability and Reproducibility of Multicenter Human Diffusion Measurements with Track-density Imaging Analysis



Qiqi Tong<sup>1</sup>, Ting Gong<sup>1</sup>, Peipeng Liang<sup>2</sup>, Tianyi Qian<sup>3</sup>, Xu Yan<sup>3</sup>, Yi Sun<sup>3</sup>, Chen Li<sup>1</sup>, Qiuping Ding<sup>1</sup>, Hongjian He<sup>1</sup>, Kuncheng Li<sup>2</sup>, and Jianhui Zhong<sup>1</sup>

<sup>1</sup>Center for Brain Imaging Science and Technology, Department of Biomedical Engineering, Zhejiang University, Hangzhou, People's Republic of China, <sup>2</sup>Department of Radiology, Xuanwu Hospital, Capital Medical University, Beijing, People's Republic of China, <sup>3</sup>MR Collaboration NE Asia, Siemens Healthcare, Shanghai, People's Republic of China

In a multicenter imaging study, it is vital to properly evaluate the variability of image quality among scanners. For diffusion imaging, estimations based on ADC and FA measurements with tensor models have previously been studied. However, such evaluation is not sufficient for studies with more diffusion directions like HARDI or DSI. This study uses track-density imaging to estimate the variability and reproducibility of multi-shell diffusion images from multicenter data acquired in the same subjects.

603

16:51

	Site 1	Site 2
No. participants	100	100
Number of sites	100	100
Number of subjects	100	100
Number of sessions	100	100
Number of scans	100	100
Number of volumes	100	100
Number of slices	100	100
Number of voxels	100	100
Number of tracks	100	100
Number of connections	100	100

### Normalization of inter-site Structural Connectivity Data for Regression analysis

Takanori Watanabe<sup>1</sup>, Birkan Tunc<sup>1</sup>, Drew Parker<sup>1</sup>, Jean-Philippe Fortin<sup>2</sup>, Mark A. Elliott<sup>1</sup>, Kosha Ruparel<sup>3</sup>, Ruben C. Gur<sup>3</sup>, Raquel E. Gur<sup>3</sup>, Robert Schultz<sup>4</sup>, Russell T. Shinohara<sup>2</sup>, and Ragini Verma<sup>1</sup>

<sup>1</sup>Department of Radiology, Perelman School of Medicine, University of Pennsylvania, Philadelphia, PA, United States, <sup>2</sup>Department of Biostatistics and Epidemiology, Perelman School of Medicine, University of Pennsylvania, <sup>3</sup>Department of Psychiatry, Perelman School of Medicine, University of Pennsylvania, <sup>4</sup>Center for Autism Research, Children's Hospital of Philadelphia

Diffusion tensor imaging (DTI) and tractography have revealed many critical insights about how the human brain is organized as a large-scale complex network. As multisite imaging studies are becoming increasingly popular within the neuroimaging field, it is imperative to develop methods that can correct for inter-site differences, facilitating the combination of data from multiple sites. In this study, we present a normalization scheme that will correct for site-specific differences in diffusion-based structural connectivity data, and demonstrate its efficacy through multivariate regression experiments using the normalized structural connectivity features to predict subject's age.

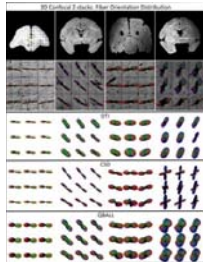


### MRI vs. X-ray scattering: comparative study of myelin distribution, fiber direction and white matter tracts in mouse brain

Marios Georgiadis<sup>1</sup>, Zirui Gao<sup>1</sup>, Dario Zingariello<sup>1</sup>, Valerio Zerbi<sup>2</sup>, Marianne Liebi<sup>3</sup>, Stefan Sommer<sup>1</sup>, Mark Augath<sup>1</sup>, Oliver Bunk<sup>3</sup>, Manuel Guizar-Sicairos<sup>3</sup>, Aileen Schroeter<sup>1</sup>, and Markus Rudin<sup>1</sup>

<sup>1</sup>Institute for Biomedical Engineering, ETH Zurich, Zurich, Switzerland, <sup>2</sup>Neural Control of Movement Lab, ETH Zurich, Zurich, Switzerland, <sup>3</sup>Paul Scherrer Institute, Switzerland

MRI is the method of choice for brain imaging. However, it uses indirect structural information to infer densities of molecules such as myelin, and water diffusion direction as a proxy for fiber direction. Small-angle X-ray scattering tensor tomography (SAXSTT) provides an alternative approach to assess myelin distribution and fiber direction using directly structural information related to the molecular structure of myelin sheath. We applied SAXSTT to mouse brain to validate and compare different MRI methods (MT, DWI). We found a high degree of similarity with MT macromolecule distribution, and also DWI-derived white matter tracts, but with significant region-specific differences.



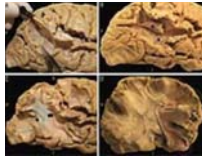
### Histological Validation of Orientation Dispersion and Fiber Orientation

Kurt Schilling<sup>1</sup>, Vaibhav Janve<sup>1</sup>, Yurui Gao<sup>1</sup>, Iwona Stepniewska<sup>2</sup>, Bennett A Landman<sup>1,3</sup>, and Adam W Anderson<sup>1</sup>

<sup>1</sup>Department of Biomedical Engineering, Vanderbilt University, Nashville, TN, United States, <sup>2</sup>Department of Psychology, Vanderbilt University, Nashville, TN, United States, <sup>3</sup>Department Electrical Engineering, Vanderbilt University, Nashville, TN, United States

In this study, using 3D confocal microscopy to extract histological fiber orientation distributions, we validate tract-specific measures of dispersion and orientation derived from high angular resolution diffusion imaging techniques. We find a correlation between histological and diffusion measures of dispersion in q-ball imaging and constrained spherical deconvolution. We also find that an increased dispersion leads to greater error in fiber orientation estimates, as well as the presence of false positive peaks in the diffusion profiles. Future work will validate these measures in more high angular resolution diffusion techniques and microstructural models.

### Topography of the acoustic radiation as revealed by ex-vivo fiber dissections and in-vivo diffusion-based tractography



Chiara Maffei<sup>1</sup>, Jorge Jovicich<sup>1</sup>, Alessandro De Benedictis<sup>2</sup>, Franco Chioffi<sup>3</sup>, and Silvio Sarubbo<sup>3</sup>

<sup>1</sup>*CIMeC Center for Mind/Brain Sciences, Trento University, Trento, Italy,*

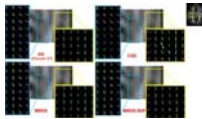
<sup>2</sup>*Division of Neurosurgery, Bambino Gesù Hospital, Rome, Italy,*

<sup>3</sup>*Structural and Functional Connectivity Lab, Div. of Neurosurgery,*

*“S. Chiara Hospital, Trento APSS, Italy*

The acoustic radiation (AR) is a compact bundle of fibers conveying auditory information from the thalamus to the cortex. Topographical knowledge of this bundle is scarce and its diffusion-based tractographic reconstruction remains hardly achievable, especially for commonly available MRI acquisition protocols. In this scenario, validation of tractography results is particularly important. In this study we used blunt dissection to precisely characterize AR topography and relationships with adjacent bundles. Being aware of the anatomical characteristics of the tract provides us with the underlying ground truth on which methodological decisions, aimed at overcoming the limits of the tractographic reconstruction, can be made.

17:39



Robust Estimation and In-vivo Validation of the Axon Bundle Diffusivity Profiles

Ricardo Coronado-Leija<sup>1</sup>, Alonso Ramirez-Manzanares<sup>1</sup>, and Jose Luis Marroquin<sup>1</sup>

<sup>1</sup>*Computer Science, Centro de Investigacion en Matematicas, Guanajuato, Mexico*

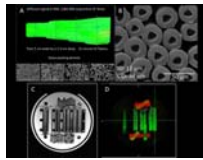
A stable, accurate and robust-to-noise general framework for the estimation of the intra-voxel axial and radial diffusivity parameters for diffusion-weighted magnetic resonance imaging is presented. The method estimates the diffusion profiles at multi-fiber voxels, improving the estimation of the intra-voxel geometry at challenging microstructure configurations. It naturally constrains the sparsity on the recovered solutions and exploits the spatial redundancy of the axon packs. A useful evaluation metric is proposed: it combines the information of the success rate of the number of bundles and their angular error. A new evaluation method for the in-vivo estimations on large datasets is also proposed.

17:51

Validation of axon diameter and density estimates by TractCaliber MRI in a biomimetic brain phantom

Susie Y Huang<sup>1</sup>, Qiuyun Fan<sup>1</sup>, Barbara Wichtmann<sup>2</sup>, Aapo Nummenmaa<sup>1</sup>, Walter Schneider<sup>3</sup>, and Lawrence L Wald<sup>1</sup>





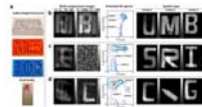
<sup>1</sup>Athinoula A. Martinos Center for Biomedical Imaging, Department of Radiology, Massachusetts General Hospital, Harvard Medical School, Charlestown, MA, United States, <sup>2</sup>Computer Assisted Clinical Medicine, Medical Faculty Mannheim, Heidelberg University, Mannheim, Germany, <sup>3</sup>Learning Research and Development Center, University of Pittsburgh, Pittsburgh, PA, United States

We validate axon diameter and density estimates using a novel biomimetic brain phantom that emulates the microstructural features of white matter, consisting of hollow textile axons (“taxons”) on the micron scale with distinct intra- and extra-axonal compartments and crossing regions. Diffusion data acquired over a range of gradient strengths, directions and diffusion times were fitted with the TractCaliber approach. Taxon volume fractions were accurately estimated, and the diameters were slightly overestimated in areas with less densely packed fibers. Such phantoms may be useful for testing microstructural models of the diffusion signal, and for scanner and protocol calibration.

---

609

18:03



#### Phantom Validation of Diffusion-Relaxation Correlation Spectroscopic Imaging (DR-CSI)

Daeun Kim<sup>1</sup>, Eamon K. Doyle<sup>2,3</sup>, Jessica L. Wisnowski<sup>4</sup>, and Justin P. Haldar<sup>1,2</sup>

<sup>1</sup>Electrical Engineering, University of Southern California, Los Angeles, CA, United States, <sup>2</sup>Biomedical Engineering, University of Southern California, Los Angeles, CA, United States, <sup>3</sup>Cardiology, Children's Hospital Los Angeles, Los Angeles, CA, United States, <sup>4</sup>Radiology, Children's Hospital Los Angeles, Los Angeles, CA, United States

Diffusion-relaxation correlation spectroscopic imaging (DR-CSI) is a novel multidimensional MR imaging approach that infers microscopic tissue compartments using simultaneous diffusion and relaxation information. The approach was previously demonstrated with biological data, although validation was not possible in the absence of a gold standard reference. In this work, we perform simulation and experimental studies, using a gold standard for validation. Specifically, we custom-built a multi-compartment diffusion-relaxation phantom with known characteristics, and performed extensive comparisons between DR-CSI and conventional multi-compartment estimation methods. Our results demonstrate that DR-CSI has good performance, enabled by the combination of multidimensional encoding and constrained spectroscopic image reconstruction.

---



---

Oral

## Parkinson's & ALS

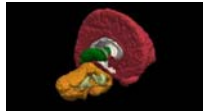
Room 314

Tuesday 16:15 - 18:15 Moderators: Geon-Ho Jahng & Toshiaki Taoka

---

610

16:15



Diffusion tensor and restriction spectrum imaging reflect different aspects of neurodegeneration in Parkinson's disease

Tuva Hope<sup>1</sup>, Per Selnes<sup>2</sup>, Irena Rektorová<sup>3</sup>, Zuzana Balážová<sup>3</sup>, Anders Dale<sup>4</sup>, Atle Bjørnerud<sup>1</sup>, and Tormod Fladby<sup>2</sup>

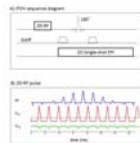
*<sup>1</sup>Oslo University Hospital, Oslo, Norway, <sup>2</sup>Akershus University Hospital, Lørenskog, Norway, <sup>3</sup>Central European Institute of Technology, Brno, Czech Republic, <sup>4</sup>University of California San Diego, La Jolla, CA, United States*

Diffusion measures within the brain are assumed to be associated with neuronal and glial structure and integrity. In this study, we compare how diffusion tensor imaging (DTI) and restriction spectrum imaging (RSI) detect micro-structural changes within brain regions associated with motor function in Parkinson's Disease.

---

611

16:27



Lateral Dependence of Brainstem Structural Abnormalities in Parkinson's Disease as Revealed by High-Resolution Non-Gaussian Diffusion MR Imaging

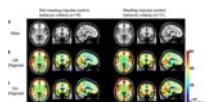
Zheng Zhong<sup>1,2</sup>, Douglas Merkitch<sup>3</sup>, Muge Karaman<sup>1</sup>, Yi Sui<sup>1</sup>, Jennifer Goldman<sup>3</sup>, and Xiaohong Joe Zhou<sup>1,4</sup>

*<sup>1</sup>Center for MR Research, University of Illinois at Chicago, Chicago, IL, United States, <sup>2</sup>Department of Bioengineering, University of Illinois at Chicago, Chicago, IL, United States, <sup>3</sup>Department of Neurological Sciences, Rush University Medical Center, Chicago, IL, United States, <sup>4</sup>Departments of Radiology, Neurosurgery and Bioengineering, University of Illinois at Chicago, Chicago, IL, United States*

Parkinson's disease (PD) is a neurodegenerative disorder characterized by progressive degeneration of dopaminergic neurons in the substantia nigra (SN). With the ability to reveal tissue microstructural changes, non-Gaussian diffusion models with high  $b$ -values can provide a wealth of information related to the neurodegenerative process and complement the conventional Gaussian diffusion model. Non-Gaussian diffusion imaging is typically performed with limited spatial resolution and subject to image distortion. In this study, we have combined a high-resolution, distortion-free diffusion sequence with a non-Gaussian diffusion model to analyze the lateral dependence of tissue abnormalities in the SN of PD patients compared to healthy controls.

612

16:39



Pharmacological arterial spin labeling reveals distinct mesocorticolimbic blood flow in Parkinson's disease patients with compulsive reward-driven behaviors

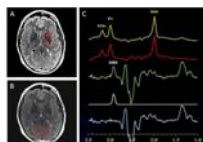
Daniel Claassen<sup>1</sup>, Adam Stark<sup>2</sup>, Charis Spears<sup>2</sup>, Kalen Petersen<sup>3</sup>, Scott Wylie<sup>2</sup>, Nelleke van Wouwe<sup>2</sup>, Robert Kessler<sup>4</sup>, David Zald<sup>5</sup>, and Manus J Donahue<sup>3</sup>

<sup>1</sup>Neurology, Vanderbilt University Medical Center, Nashville, TN, United States, <sup>2</sup>Neurology, Vanderbilt University Medical Center, <sup>3</sup>Radiology, Vanderbilt University Medical Center, <sup>4</sup>Radiology, University of Alabama at Birmingham, <sup>5</sup>Psychology, Vanderbilt University Medical Center

The overall goal of this work is to apply pharmacological arterial spin labeling (ASL) to investigate fundamental hypotheses regarding the role of dopamine agonist (DAgonist) therapy in patients with Parkinson's disease and impulse control behavior (ICB). Parkinson's disease patients ( $n=35$ ; age range=40-79 years; gender=23/12 males/females) receiving DAgonist therapy, with ( $n=17$ ) and without ( $n=18$ ) DAgonist-induced ICB were scanned at 3T using cerebral blood flow (CBF)-weighted pCASL MRI. Region-of-interest analyses revealed significantly increased bilateral ventral striatal ( $P<0.01$ ) CBF in patients with ICB in the On- DAgonist state; voxel-wise analysis of CBF confirmed widespread DAgonist-induced CBF increases in mesolimbic, mesocortical, and midbrain regions.

613

16:51



Striatal Glutathione Deficit in Parkinson's Disease Measured In Vivo with J-edited <sup>1</sup>H MRS Directly Implicates Oxidative Stress in Disorder Pathophysiology

Dikoma C. Shungu<sup>1</sup>, Xiangling Mao<sup>1</sup>, Nora Weiduschat<sup>1</sup>, Aneliya Hanineva<sup>2</sup>, Yize Zhao<sup>3</sup>, Halinder S. Mangat<sup>2</sup>, Guoxin Kang<sup>1</sup>, James Carter<sup>2</sup>, Natalie Hellmers<sup>2</sup>, and Claire Henchcliffe<sup>2</sup>

<sup>1</sup>Radiology, Weill Cornell Medicine, New York, NY, United States,

<sup>2</sup>Neurology and Neuroscience, Weill Cornell Medicine, New York, NY,

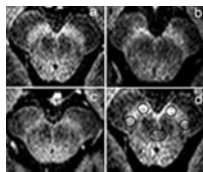
United States, <sup>3</sup>Healthcare Policy and Research, Weill Cornell Medicine, New York, NY, United States

*Postmortem* studies of Parkinson's disease (PD) brain have consistently reported deficits of nigrostriatal glutathione (GSH) – the most abundant antioxidant in living tissue – of up to 40% compared to normal brain, strongly implicating **oxidative stress** in the pathophysiology of PD. However, direct evidence corroborating a striatal GSH deficit in PD brain *in vivo* is currently lacking. Using J-edited <sup>1</sup>H MRS, this study measured striatal GSH *in vivo* in patients with PD and in matched control subjects, and found not only a 15% deficit of striatal GSH in PD that corroborated *postmortem* data, but also evidence of nigrostriatal neurodegeneration in the disorder.

614



17:03



### Subtypes Evaluation of Motor Dysfunction in Parkinson's Disease using Neuromelanin-sensitive Magnetic Resonance Imaging

Tao Gong<sup>1,2</sup>, Yuanyuan Xiang<sup>3</sup>, Guangbin Wang<sup>4</sup>, and Richard A.E. Edden<sup>2</sup>

<sup>1</sup>MRI, Shandong Medical Imaging Research Institute, Shandong

University, Jinan, People's Republic of China, <sup>2</sup>Russell H. Morgan

Department of Radiology and Radiological Science, The Johns Hopkins

University School of Medicine, Baltimore, MD, United States, <sup>3</sup>Shandong

University, Jinan, People's Republic of China, <sup>4</sup>MRI, Shandong Medical

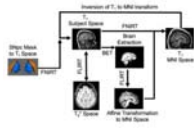
Imaging Research Institute

The aim of this study was to evaluate the differences in NM-MRI between PD motor subtypes. We compared the signal intensity contrast ratios in medial and lateral regions of the SNc using NM-MRI in TD, PIGD and controls. The results demonstrated more severe signal attenuation in the medial part of SNc in PIGD patients compared with TD group. And the medial part of SNc showed high power to discriminate the PD motor subtypes. NM-MRI affords us a valuable examination method to discriminate the PD motor subtypes, providing a new evidence for the neuropathological basis of differences between the two subtypes.

---

615

17:15



Reproducible detection of nigral iron deposition in Parkinson's disease: Validation in two cohorts

Jason Langley<sup>1</sup>, Naying He<sup>1,2</sup>, Daniel E Huddleston<sup>3</sup>, Fuhua Yan<sup>2</sup>, and Xiaoping Hu<sup>4</sup>

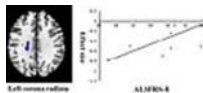
<sup>1</sup>Center for Advanced Neuroimaging, University of California Riverside, Riverside, CA, United States, <sup>2</sup>Department of Radiology, Ruijin Hospital, Shanghai Jiao Tong University, People's Republic of China, <sup>3</sup>Department of Neurology, Emory University, Atlanta, GA, United States, <sup>4</sup>Department of Bioengineering, University of California Riverside, Riverside, CA, United States

A characteristic of Parkinson's disease is neuronal loss in substantia nigra pars compacta (SNpc). In healthy subjects, SNpc contains a dense distribution of neuromelanin containing dopaminergic neurons and significant degeneration in SNpc has occurred at the time Parkinsonian symptom onset. Furthermore, extensive evidence suggests that iron deposition is related to neuronal loss and reduction of neuromelanin in SNpc. In this abstract, we examine the reproducibility of iron deposition in SNpc.

---

616

17:27



Altered white matter microarchitecture in amyotrophic lateral sclerosis : a voxel-based meta-analysis of diffusion tensor imaging

Guangxiang Chen<sup>1</sup>, Feifei Zhang<sup>1</sup>, Song Wang<sup>1</sup>, Xiaoqi Huang<sup>1</sup>, and Qiyong Gong<sup>1</sup>

<sup>1</sup>Huaxi MR Research Center (HMRRRC), Department of Radiology, West China Hospital, Sichuan University, Chengdu, People's Republic of China

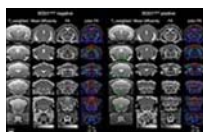
The results of recent diffusion tensor imaging (DTI) studies on amyotrophic lateral sclerosis (ALS) have been inconclusive and controversial. We performed a voxel-based meta-analysis to identify statistical consensus between published DTI studies for altered white matter (WM) microarchitecture in ALS. Our findings provides a thorough profile of WM microarchitecture alterations in ALS and further evidence that the neuronal degeneration is not limited to the corticospinal tract but also includes the extra-motor areas, supporting the view of ALS being a multisystem degenerative disorder involving WM.

---

617

17:39

Diffusion and T2 characterizations in hindbrain and spinal cord in SOD1 mouse model of ALS



Luke Xie<sup>1</sup>, Robert Brendza<sup>2</sup>, Maj Hedehus<sup>1</sup>, Sara Dominguez<sup>2</sup>, Oded Foreman<sup>3</sup>, Arundhati Sengupta Ghosh<sup>2</sup>, William J. Meilandt<sup>2</sup>, Gai Ayalon<sup>2</sup>, and Richard A. D. Carano<sup>1</sup>

<sup>1</sup>Biomedical Imaging, Genentech, South San Francisco, CA, United States, <sup>2</sup>Neuroscience, Genentech, South San Francisco, CA, United States, <sup>3</sup>Pathology, Genentech, South San Francisco, CA, United States

Amyotrophic lateral sclerosis (ALS) is a devastating neurological disease characterized by motor neuron loss and eventual paralysis and respiratory failure. The SOD1 transgenic mouse model exhibits many aspects of human ALS and is useful for evaluating treatment strategies. MRI of the nervous system can provide the critical insights to motor neuron and upper body functional deterioration in ALS. In this study, we applied T<sub>2</sub> and DTI to assess gray and white matter degeneration in the brain and cervical spine in a SOD1 mouse model.

---

618

17:51



Sodium accumulation in primary motor areas, an early feature of amyotrophic lateral sclerosis patients

Aude-Marie Grapperon<sup>1,2</sup>, Annie Verschueren<sup>2</sup>, Adil Maarouf<sup>1,3</sup>, Lauriane Pini<sup>1</sup>, Sylviane Confort-Gouny<sup>1</sup>, Jean-Philippe Ranjeva<sup>1</sup>, Maxime Guye<sup>1,3</sup>, Shahram Attarian<sup>2</sup>, and Wafaa Zaaraoui<sup>1</sup>

<sup>1</sup>Aix-Marseille Univ, CNRS, CRMBM, Marseille, France, <sup>2</sup>Aix-Marseille Univ, APHM, Hopital de la Timone, ALS department, Marseille, France, <sup>3</sup>Aix-Marseille Univ, APHM, Hopital de la Timone, CEMEREM, Marseille, France

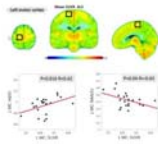
Amyotrophic lateral sclerosis (ALS) is a rapidly fatal neurodegenerative disease characterized by upper (in brain) and lower (in spine) motor neuron degeneration. As conventional MRI fails to show brain motor neurons impairment in ALS, advanced techniques are needed to improve the diagnosis and to monitor the progression of the disease. In this study, brain <sup>23</sup>Na MRI was applied in 15 ALS patients and 31 controls. A common pattern of sodium accumulation was found in patients in the primary motor areas while no atrophy was detected. The occurrence of sodium accumulation without atrophy probably reflects early neuronal injury in ALS.

---

619

18:03

Glial activation measured by [11C]-PBR28 PET correlates with 1H-MRS brain metabolites in amyotrophic lateral sclerosis



Eva-Maria Ratai<sup>1,2</sup>, Mohamad J Alshikho<sup>2,3</sup>, Nicole R. Zürcher<sup>1,2</sup>, Marco L. Loggia<sup>1</sup>, Paul Cernasov<sup>3</sup>, Jennifer Fish<sup>3</sup>, Raghav Seth<sup>1</sup>, Sabrina Paganoni<sup>2,3</sup>, Bruce R. Rosen<sup>1,2</sup>, Jacob M. Hooker<sup>1,2</sup>, and Nazem Atassi<sup>2,3</sup>

<sup>1</sup>Radiology, A. A. Martinos Center for Biomedical Imaging, Massachusetts General Hospital, Charlestown, MA, United States, <sup>2</sup>Harvard Medical School, <sup>3</sup>Neurology, Neurological Clinical Research Institute (NCRI), A. A. Martinos Center for Biomedical Imaging, Massachusetts General Hospital, Boston, MA, United States

The purpose of our study was to evaluate the relationship between glial activation assessed by [<sup>11</sup>C]-PBR28 positron emission tomography, and neuronal integrity and gliosis/neuroinflammation measured by magnetic resonance spectroscopy in people with amyotrophic lateral sclerosis (ALS). Glial activation measured by increased [<sup>11</sup>C]-PBR28 uptake correlated with increased levels of myo-Inositol/Creatine, a spectroscopic marker of gliosis/neuroinflammation in the brain stem and motor cortices. Furthermore, increased [<sup>11</sup>C]-PBR28 uptake correlated with neuronal damage measured by decreased N-acetylaspartate/Creatine levels. To our knowledge, this is the first study to evaluate the relationship between glial activation, measured by [<sup>11</sup>C]-PBR28 PET, and brain metabolites assessed by MRS.

## Oral

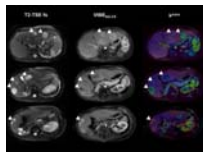
# Perfusion & Diffusion in Cancer

Room 316BC

Tuesday 16:15 - 18:15 *Moderators: Patrick Bolan & Ashley Stokes*

620

16:15



Feasibility and evaluation of free-breathing and self-gated cartesian-sampled T1-weighted 4D MRI with compressed sensing resulting in combined diagnostic image quality and perfusion analysis

Christer Ruff<sup>1</sup>, Jakob Weiss<sup>1</sup>, Ahmed Othman<sup>1</sup>, Petros Martirosian<sup>2</sup>, Marcel Dominik Nickel<sup>3</sup>, Robert Grimm<sup>3</sup>, Manuel Kolb<sup>1</sup>, Matthias Kündel<sup>1</sup>, Fabian Bamberg<sup>1</sup>, Konstantin Nikolaou<sup>1</sup>, and Mike Notohamiprodjo<sup>1</sup>

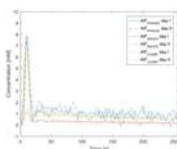
<sup>1</sup>Diagnostic and Interventional Radiology, University Hospital Tuebingen, Tuebingen, Germany, <sup>2</sup>Section on Experimental Radiology, University Hospital Tuebingen, <sup>3</sup>Siemens Healthcare, Erlangen, Germany

In clinical practice, a remaining challenge of dynamic contrast-enhanced (DCE)-MRI is to acquire a high spatio-temporal resolution without motion artifacts and diagnostic quality, despite acquisitions over several minutes. In particular, iterative reconstruction techniques have brought free-breathing acquisitions in clinical range. In this study, we proved feasibility and evaluated a prototype Cartesian-sampled fat-saturated T1-weighted 3D gradient-echo sequence with automated respiratory self-gating and compressed sensing reconstruction (VIBE<sub>SG-CS</sub>) for continuous dynamic contrast-enhanced (DCE) MRI and perfusion analysis including lesion detection of the liver using a Tofts model. VIBE<sub>SG-CS</sub> including perfusion analysis showed better motion robustness and similar lesion conspicuity compared to a standard morphology sequence (fat-saturated T2-TSE).

621



16:27



### Robust arterial input functions by fitting the complex DCE-MRI signal: a test-retest study in prostate cancer

Edzo M.E. Klawer<sup>1</sup>, Petra J. van Houdt<sup>1</sup>, Frank F.J. Simonis<sup>2</sup>, Cornelis A.T. van den Berg<sup>2</sup>, Floris J. Pos<sup>1</sup>, Stijn W.T.P. Heijmink<sup>3</sup>, and Uulke A. van der Heide<sup>1</sup>

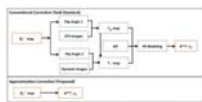
<sup>1</sup>Department of radiation oncology, The Netherlands Cancer Institute, Amsterdam, Netherlands, <sup>2</sup>Department of radiation oncology, Imaging Division, University Medical Center, Utrecht, Netherlands, <sup>3</sup>Department of radiology, The Netherlands Cancer Institute, Amsterdam, Netherlands

The arterial input function is still one of the main problems for quantitative DCE analysis. In this study, we show that the repeatability of individual AIFs improve by using the complex signal instead of magnitude or phase signal alone by using test-retest DCE-MRI data of prostate cancer. This will eventually result in an accurate quantitative DCE-MRI analysis by including patient inter and intra-variability.

622



16:39



### Evaluation of Approximation Method for B1+ Correction using Digital Reference Object in Prostate DCE-MRI

Xinran Zhong<sup>1,2</sup>, Holden Wu<sup>1,2</sup>, Krishna Nayak<sup>3</sup>, and Kyunghyun Sung<sup>1,2</sup>

<sup>1</sup>Department of Radiological Sciences, University of California, Los Angeles, Los Angeles, CA, United States, <sup>2</sup>Physics and Biology in Medicine IDP, University of California, Los Angeles, Los Angeles, CA, United States, <sup>3</sup>Department of Electrical Engineering, University of Southern California, Los Angeles, CA, United States

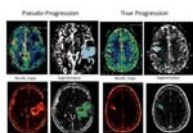


A digital reference object (DRO) for prostate dynamic contrast-enhanced MRI application is created by modifying DRO created by the RRSNA Quantitative Imaging Biomarkers Alliance (QIBA). Our previously proposed approximation  $B_1^+$  correction method for pharmacokinetic modeling was then tested on this DRO assuming  $B_1^+$  variation of 20%, considering practical considerations such as fitting method, arterial input function selection and noise level. The proposed approximation method introduced error is shown to be negligible compared to  $B_1^+$  introduced error and noise introduced error.

623



16:51



### Radiomic Texture Features from MR Perfusion images Predicts Pseudoprogression from True Progression in Glioblastoma Patients: A Multi-Institutional Study

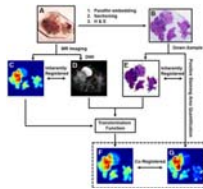
Aikaterini Kotrotsou<sup>1</sup>, Nabil A Elshafeey<sup>1</sup>, Srishti Abrol<sup>1</sup>, Dunia Giniebra Camejo<sup>2</sup>, Islam Hassan<sup>1</sup>, Ahmed Hassan<sup>1</sup>, Kamel El Salek<sup>1</sup>, Ahmed T Shaaban<sup>1</sup>, Samuel Bergamaschi<sup>3</sup>, Fanny E Moron<sup>4</sup>, Meng Law<sup>3</sup>, Pascal O Zinn<sup>5</sup>, and Rivka R Colen<sup>1,2</sup>

<sup>1</sup>Diagnostic Radiology, MD Anderson Cancer Center, Houston, TX, United States, <sup>2</sup>Cancer Systems Imaging, MD Anderson Cancer Center, Houston, TX, United States, <sup>3</sup>Neuroradiology, University of Southern California Keck Medical Center, Los Angeles, CA, United States, <sup>4</sup>Neuroradiology, Baylor College of Medicine, Houston, TX, United States, <sup>5</sup>Neurosurgery, Baylor College of Medicine, Houston, TX, United States

Response assessment criteria, such as RANO, struggle to distinguish between true progression and pseudoprogression. In this work we evaluated the performance of radiomic texture features extracted from MR perfusion images (Dynamic contrast enhancement (DCE) and Dynamic susceptibility contrast (DSC)) in discriminating true progression from pseudoprogression. Using a large multi-institutional cohort, we demonstrated that changes in texture features of perfusion maps (DCE and DSC) can be effective predictors of progressive disease. We present a noninvasive, complimentary method that is directly applicable in clinical setting and can assist physicians in diagnosis and therapy planning.

17:03

Quantitatively Differentiating Multiple Co-Existing Pathologies in High-Grade Glioma



Ze-Zhong Ye<sup>1</sup>, Richard Price<sup>2</sup>, Peng Sun<sup>3</sup>, Ajit George<sup>3</sup>, Chunyu Song<sup>4</sup>, Sonika Dahiya<sup>5</sup>, Albert Kim<sup>2,6,7</sup>, and Sheng-Kwei Song<sup>3,4,8</sup>

<sup>1</sup>Chemistry, Washington University, St. Louis, MO, United States,

<sup>2</sup>Neurological Surgery, Washington University, St. Louis, MO, United States,

<sup>3</sup>Radiology, Washington University, St. Louis, MO, United States,

<sup>4</sup>Biomedical Engineering, Washington University, St. Louis, MO, United States,

<sup>5</sup>Pathology and Immunology, Washington University, St. Louis, MO, United States,

<sup>6</sup>Neurology, Washington University, St. Louis, MO, United States,

<sup>7</sup>Developmental Biology, Washington University, St. Louis, MO, United States,

<sup>8</sup>Hope Center for Neurological Disorder, Washington University, St. Louis, MO, United States

We demonstrate diffusion MRI histology (D-Histo) is able to detect, differentiate and quantify various co-existing pathologies and structures including tumor, tumor infiltration, necrosis within human brain tumor specimen while conventional MRI and DTI fails. Quantitative maps of H&E and GFAP were generated and co-registered with D-Histo for voxel-wise correlative analysis. D-Histo-derived restricted-isotropic-diffusion fraction correlated with the area of hematoxylin and GFAP positive stain. D-Histo-derived hindered-isotropic-diffusion fraction successfully predicted the distribution of tumor necrosis corresponding with H & E. D-Histo is promising for brain tumor diagnosis, surgical planning, and treatment response monitoring.

17:15



Effects of AIF Quantification Variations on Shutter-Speed

Pharmacokinetic Modeling of Prostate DCE-MRI Data: A Multicenter Data Analysis Challenge, Part II

Wei Huang<sup>1</sup>, Yiyi Chen<sup>1</sup>, Andriy Fedorov<sup>2</sup>, Xia Li<sup>3</sup>, Guido Jajamovich<sup>4</sup>, Dariya Malyarenko<sup>5</sup>, Madhava Aryal<sup>5</sup>, Peter LaViolette<sup>6</sup>, Matthew Oborski<sup>7</sup>, Finbarr O'Sullivan<sup>8</sup>, Richard Abramson<sup>9</sup>, Kourosh Jafari-Khouzani<sup>10</sup>, Aneela Afzal<sup>1</sup>, Alina Tudorica<sup>1</sup>, Brendan Moloney<sup>1</sup>, Sandeep Gupta<sup>3</sup>, Cecilia Besa<sup>4</sup>, Jayashree Kalpathy-Cramer<sup>10</sup>, James Mountz<sup>7</sup>, Charles Laymon<sup>7</sup>, Mark Muzi<sup>11</sup>, Paul Kinahan<sup>11</sup>, Kathleen Schmainda<sup>6</sup>, Yue Cao<sup>5</sup>, Thomas Chenevert<sup>5</sup>, Bachir Taouli<sup>4</sup>, Thomas Yankeelov<sup>12</sup>, Fiona Fennessy<sup>2</sup>, and Xin Li<sup>1</sup>

<sup>1</sup>Oregon Health & Science University, Portland, OR, United States,

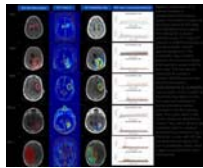
<sup>2</sup>Brigham and Women's Hospital, <sup>3</sup>GE Global Research, <sup>4</sup>Icahn School of Medicine at Mt Sinai, <sup>5</sup>University of Michigan, <sup>6</sup>Medical College of Wisconsin, <sup>7</sup>University of Pittsburgh, <sup>8</sup>University College, <sup>9</sup>Vanderbilt University, <sup>10</sup>Massachusetts General Hospital, <sup>11</sup>University of Washington, <sup>12</sup>The University of Texas at Austin

Prostate tumor DCE-MRI data sets from 11 patients were shared among nine institutions, which determined AIFs using site-specific methods. The managing center performed pharmacokinetic data analysis using the Shutter-Speed model and these AIFs, and their scaled variants obtained with the reference-tissue method. Among the estimated parameters,  $K^{trans}$  has the highest whereas  $\tau_i$  has the lowest variability due to AIF uncertainty. The use of reference-tissue-adjusted AIFs reduces parameter variations.  $k_{ep}$  and  $\tau_i$  are nearly insensitive to AIF scaling, suggesting that they may be robust imaging biomarkers in multicenter DCE-MRI trials where accurate and consistent AIF determination may be unattainable across sites.

---

626

17:27



[DCE time-series characterization with supervised deep learning: Alternative to PK model approaches](#)

Dattesh D Shanbhag<sup>1</sup>, Vivek Vaidya<sup>1</sup>, Uday Patil<sup>1</sup>, Sandeep N Gupta<sup>2</sup>, and Rakesh Mullick<sup>1</sup>

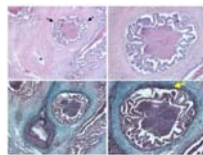
<sup>1</sup>GE Global Research, Bangalore, India, <sup>2</sup>GE Global Research, Niskayuna, NY, United States

We demonstrate feasibility of using a supervised deep learning method with DCE time-series data to obtain consistent numerical cutoff for tumor regions. DL based characterization is robust to fluctuations in DCE data due to protocol and patient physiology differences, which typically hinders such a classification with PK maps in clinical practice.

---

627

17:39



[MRI Detection of Extramural Venous Invasion in Rectal Cancer: Correlation with Histopathology Utilizing Elastin Stain](#)

Kartik Jhaveri<sup>1</sup>, Hooman Hosseini-Nik, Seng Thippavong, Naziheh Assarzaghan, Ravi Menezes, Erin Kennedy, and Richard Kirsch

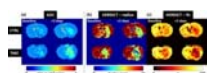
<sup>1</sup>UHN, University of Toronto, Toronto, ON, Canada

Extramural venous invasion (EMVI) in Rectal cancer is an independent predictor of local and distant recurrence, nodal disease and overall survival. Accurate preoperative EMVI detection has implications for treatment decisions. Previously, MRI has been evaluated for this purpose previously against histopathology with Hematoxylin-Eosin(HE) staining. Recently histopathology with Elastin stain has been recommended for EMVI detection given its 2-3-fold increase in accuracy and improved prognostication compared to HE stain. The diagnostic performance of MRI for EMVI detection compared to elastin stain based histopathology is unknown and in this study, we present our results to address this issue.

628



17:51



Quantifying microstructure changes in a mouse brain tumour model following Temozolomide therapy with VERDICT MRI

Thomas A Roberts<sup>1</sup>, Giulia Agliardi<sup>1</sup>, Ben Hipwell<sup>1</sup>, Angela D'Esposito<sup>1</sup>, Andrada Ianus<sup>2</sup>, James O Breen-Norris<sup>1</sup>, Valerie Taylor<sup>1</sup>, Mark F Lythgoe<sup>1</sup>, Bernard Siow<sup>1</sup>, Eleftheria Panagiotaki<sup>2</sup>, Daniel C Alexander<sup>2</sup>, and Simon Walker-Samuel<sup>1</sup>

*<sup>1</sup>Centre for Advanced Biomedical Imaging, University College London, London, United Kingdom, <sup>2</sup>Centre for Medical Image Computing, Department of Computer Science, University College London, London, United Kingdom*

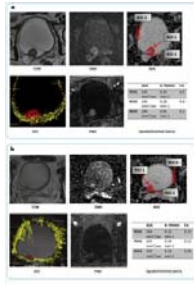
In this study, we use VERDICT (Vascular, Extracellular and Restricted Diffusion for Cytometry in Tumours) MRI to assess longitudinal changes in the microstructure of a mouse model of glioma (GL261), following treatment with Temozolomide, an alkylating chemotherapeutic agent. VERDICT estimates of cell radius and intracellular volume fraction decreased significantly at day-6 of therapy, relative to control animals, and in advance of changes in tumour volume and ADC. These changes were consistent with histological changes measured in the same tumours, and are likely to correspond to microstructural changes induced by apoptosis.

629

18:03

Optimization of mpMRI protocol in differentiating muscle-invasive from non-muscle invasive Bladder Cancer: is there room for Diffusion Tensor Imaging (DTI)?

Giovanni Barchetti<sup>1</sup>, Marcello Grompone<sup>1</sup>, Maurizio Del Monte<sup>1</sup>, Davide Carano<sup>1</sup>, Carlo Catalano<sup>1</sup>, and Valeria Panebianco<sup>1</sup>



*<sup>1</sup>Department of Radiological Sciences, Sapienza University of Rome, Rome, Italy*

Staging of BCa is critical, especially in differentiating non-invasive from muscle infiltrative lesions, as patient management strongly differs according to stage. Currently, patients with bladder lesions undergo two invasive procedures to diagnose and eventually treat the tumor if it is superficial. In this study we showed that mp-MRI has high capability for differentiating superficial from deep lesions, thanks also to DTI ability to directly visualize detrusor muscle layers. Mp-MRI could therefore be included systematically in the diagnostic evaluation of patients with suspicious bladder lesions in order to possibly avoid the first diagnostic cystoscopy once detrusor muscle invasion has been excluded.

Oral

## CV Innovations: New Methods & Image Processing

Room 320

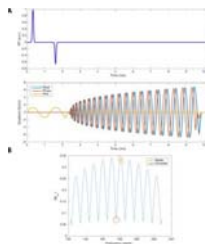
Tuesday 16:15 - 18:15

Moderators: Giulia Ginami & Sebastian Kozerke

630



16:15



[Hyperpolarized \[1,4-<sup>13</sup>C<sub>2</sub>\]Fumarate is a probe of necrosis in myocardial infarction](#)

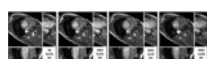
Jack Julian James Jenkins Miller<sup>1,2,3</sup>, Angus Zoen Lau<sup>1,4</sup>, Giles McMullen-Klein<sup>1</sup>, Andrew Lewis<sup>1</sup>, Vicky Ball<sup>1</sup>, Carolyn Carr<sup>1</sup>, Ferdia Gallagher<sup>5</sup>, Damian John Tyler<sup>1,2</sup>, and Marie Schroder<sup>6</sup>

*<sup>1</sup>Department of Physiology, Anatomy & Genetics, University of Oxford, Oxford, United Kingdom, <sup>2</sup>Oxford Centre for Clinical Magnetic Resonance Research, University of Oxford, Oxford, United Kingdom, <sup>3</sup>Department of Physics, University of Oxford, Oxford, United Kingdom, <sup>4</sup>Physical Sciences, Sunnybrook Research Institute, Toronto, ON, Canada, <sup>5</sup>Department of Radiology, University of Cambridge, Cambridge, United Kingdom, <sup>6</sup>MR Centret, Århus University Hospital, Skejby, Denmark*

Previous work has shown that hyperpolarized [1,4-<sup>13</sup>C<sub>2</sub>]fumarate is a probe of cellular necrosis. We demonstrate here that the ratio of cardiac hyperpolarized malate to fumarate is increased by a factor of  $\sim 82$  one day after cryoinduced myocardial infarction in rats, decreasing to an  $\sim 30$ -fold increase one week after injury. We additionally image this injury with a novel spiral multiband pulse sequence. Hyperpolarized fumarate therefore forms a sensitive probe of myocardial injury in vivo, and could form a clinical monitor of cellular damage and necrosis after infarction.

631

16:27



### Accelerated Cine Imaging of the Heart using Blipped Multiband SSFP

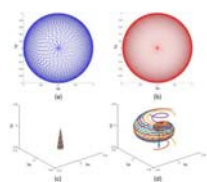
Anthony N Price<sup>1</sup>, Lucilio Cordero-Grande<sup>1</sup>, Shaihan J Malik<sup>1</sup>, and Joseph V Hajnal<sup>1</sup>

*<sup>1</sup>Division of Imaging Sciences and Biomedical Engineering, King's College London, London, United Kingdom*

Multiband accelerated cine SSFP of the heart is demonstrated using blipped gradients for controlled aliasing of simultaneous slices. The benefit of using this method over the more complex phase cycling RF multiband pulse sets is that the frequency response, and thus banding artefacts, remain unchanged. Here we demonstrate up to MB4 acceleration of full short-axis stacks, sufficient to cover the left ventricle within a single breath-hold.

632

16:39



### Improved Whole-Heart Coronary MR Angiography Using a 3D Cones Phyllotaxis Sequence

Mario O. Malavé<sup>1</sup>, Corey A. Baron<sup>1</sup>, Nii Okai Addy<sup>1</sup>, Joseph Y. Cheng<sup>2</sup>, Bob S. Hu<sup>1,3</sup>, Phillip C. Yang<sup>4</sup>, and Dwight G. Nishimura<sup>1</sup>

*<sup>1</sup>Electrical Engineering, Stanford University, Stanford, CA, United States,*

*<sup>2</sup>Radiology, Stanford University, Stanford, CA, United States,*

*<sup>3</sup>Cardiology, Palo Alto Medical Foundation, Palo Alto, CA, United States,*

*<sup>4</sup>Cardiovascular Medicine, Stanford University, Stanford, CA, United States*



We have developed a 3D cones alternating-TR steady state free precession (SSFP) sequence for whole-heart coronary MR angiography (CMRA). In this study, we compare motion artifacts and coronary image quality between a sequential-cones and phyllotaxis-cones sequence. Coronary image quality was analyzed using qualitative scores obtained through blinded reading by two board-certified cardiologists, and the IEPA vessel sharpness metric. The results of the study show that the phyllotaxis-cones acquisition can alleviate motion artifacts, improve qualitative image quality scores and increase coronary vessel sharpness.

---

633

16:51



### Automated Heartbeat Detection for Self-Gated Fetal Cardiac MRI

Robin Demesmaeker<sup>1</sup>, Tobias Kober<sup>1,2,3</sup>, Jérôme Yerly<sup>3,4</sup>, Jérôme Chaptinel<sup>3</sup>, Milan Prsa<sup>5</sup>, Yvan Mivelaz<sup>5</sup>, Leonor Alamo<sup>3</sup>, Yvan Vial<sup>6</sup>, Gregoire Berchier<sup>3</sup>, Chantal Rohner<sup>3</sup>, Matthias Stuber<sup>3,4</sup>, and Davide Piccini<sup>1,2,3</sup>

<sup>1</sup>Advanced Clinical Imaging Technology, Siemens Healthcare AG, Lausanne, Switzerland, <sup>2</sup>LTS5, École Polytechnique Fédérale de Lausanne (EPFL), Lausanne, Switzerland, <sup>3</sup>Department of Radiology, University Hospital (CHUV) and University of Lausanne (UNIL), Lausanne, Switzerland, <sup>4</sup>Center for Biomedical Imaging (CIBM), Lausanne, Switzerland, <sup>5</sup>Department of Pediatrics, University Hospital (CHUV) and University of Lausanne (UNIL), Lausanne, Switzerland, <sup>6</sup>Department of Gynecology-Obstetrics, University Hospital (CHUV) and University of Lausanne (UNIL), Lausanne, Switzerland

Fetal cardiac cine MRI requires an MRI-based cardiac gating signal since recording a fetal ECG is fraught with significant challenges. Existing approaches usually extract the signal from real-time image series and mandate semi-manual user interaction. However, these give often inconsistent results or suffer from reduced spatio-temporal resolution. We propose a novel algorithm which automatically localizes the fetal heart on real-time low-resolution images, and provides a precise frequency estimate of the cardiac motion signal that can be used for gating. We show that this automated method leads to images with equal or better quality than those obtained with the manual approach.

---

634

17:03

### Automated Left Ventricular Volumetric Quantitation from Short-axis CMR Images with Machine Learning using a Deep Convolutional Neural Network

James W Goldfarb<sup>1</sup>, Jie J Cao<sup>1</sup>, and Julian de Wit<sup>2</sup>





<sup>1</sup>St Francis Hospital, Roslyn, NY, United States, <sup>2</sup>DWS Systems, Hoek van Holland, Netherlands

Automatic segmentation of the LV bloodpool using deep learning with a convolutional neural network is a promising, accurate and efficient method for segmentation of cardiac MR images. Although there were a few cases with inaccurate results, "big fails", accuracy is high,  $R^2=0.93$  and ejection fraction error  $\sim 4\%$ . In the future it may provide a customizable, fast and accurate method for comprehensive evaluation of cardiac MR images.

635

17:15



### DeepVentricle: A Fully Convolutional Neural Network for Automating Functional Measurements in Cardiac MR

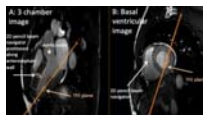
Hok Kan Lau<sup>1</sup>, Jesse Lieman-Sifry<sup>1</sup>, Matthieu Le<sup>1</sup>, Sean Sall<sup>1</sup>, John Axerio-Cilies<sup>1</sup>, Dominik Fleischmann<sup>2</sup>, Aya Kino<sup>3</sup>, Frandics Chan<sup>2</sup>, and Daniel Golden<sup>1</sup>

<sup>1</sup>Arterys, Inc, San Francisco, CA, United States, <sup>2</sup>General Radiology, Stanford University School of Medicine, Stanford, CA, <sup>3</sup>Radiology, Stanford University School of Medicine, Stanford, CA

We present DeepVentricle, an automated approach to ventricular segmentation in cardiac MR. DeepVentricle uses a fully convolutional neural network to simultaneously perform semantic segmentation of the left ventricle (LV) and right ventricle (RV) endocardium, and LV epicardium; segmentations are then used to estimate ejection fraction and myocardial mass. We show that the error rates of LV ejection fraction and mass are within the expected range of expert annotator inter-rater variation. This suggests that contours calculated using DeepVentricle could be useful on their own or as an initial estimate for clinicians as part of their semi-automated annotation workflow.

636

17:27



### Using transient intrinsic torsional shear wave propagation to measure Left Ventricular Myocardial stiffness with a 2D pencil beam navigator at 0.5ms temporal resolution: Initial results from phantom studies and volunteers

Jessica Webb<sup>1,2</sup>, Jurgen Runge<sup>1,3</sup>, Jordi Martorell<sup>4</sup>, Gerald Carr-White<sup>1,2</sup>, Reza Razavi<sup>1,2</sup>, David Nordsletten<sup>1</sup>, and Ralph Sinkus<sup>1</sup>

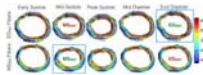
<sup>1</sup>Imaging Sciences & Biomedical Engineering, King's College London, London, United Kingdom, <sup>2</sup>Department of Cardiology, Guys and St Thomas' NHS Trust, London, United Kingdom, <sup>3</sup>Department of Radiology, Academic Medical Center, Amsterdam, Netherlands, <sup>4</sup>Department of Chemical Engineering, Universitat Ramon Llull, Barcelona, Spain

Heart Failure with preserved Ejection Fraction is common, associated with high morbidity and mortality, and is challenging to diagnose. We have developed a novel patient friendly non-invasive technique to quantify myocardial stiffness using transient MR Elastography. Aortic valve closure results in a shear wave propagating through the myocardium. The torsional wave propagation can be visualised using a 2D pencil beam navigator positioned along the myocardium, using four breath holds each 15 seconds. With a temporal resolution of 0.5ms this technique can be used in all patients in sinus rhythm. Increased myocardial stiffness results in increased speed of shear wave propagation.

---

637

17:39



#### Time Resolved In Vivo Myofiber Orientations from Combined Cardiac DENSE and cDTI

Patrick Magrath<sup>1,2</sup>, Luigi E. Perotti<sup>1,2</sup>, Eric Aliotta<sup>2,3</sup>, Ilya A. Verzhbinsky<sup>2</sup>, Kévin Moulin<sup>2</sup>, and Daniel B. Ennis<sup>1,2,3</sup>

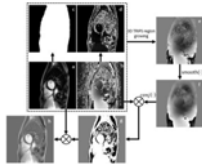
<sup>1</sup>Department of Bioengineering, University of California, Los Angeles, CA, United States, <sup>2</sup>Department of Radiological Sciences, University of California, Los Angeles, CA, United States, <sup>3</sup>Biomedical Physics IDP, University of California, Los Angeles, CA, United States

Resolving the dynamics of cardiac myofiber orientations with cDTI could have significant value in the assessment of cardiac disease. Unfortunately, cDTI measurements are not reliable at all cardiac phases and would require extremely long acquisitions. Fusing cDTI with time-resolved displacement maps from cine DENSE could enable evaluation of the dynamics of myofiber orientations using cDTI obtained at a single cardiac phase. The objective of this study was to generate dynamic myocardial fiber maps and validate the approach with dual-phase cDTI measurements.

---

17:51

#### 3D True Polarity Recovery with Independent Phase Estimation Using Multi-layer Stacks Based Region-Growing (3D-TRIPS)

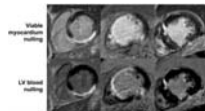


Haining Liu<sup>1</sup>, Gregory J Wilson<sup>2</sup>, Niranjana Balu<sup>2</sup>, Jeffery H Maki<sup>2</sup>, Martin L Gunn<sup>2</sup>, Hiroko Watase<sup>2</sup>, Daniel S Hippe<sup>2</sup>, and Chun Yuan<sup>2</sup>

<sup>1</sup>Department of Bioengineering, University of Washington, Seattle, WA, United States, <sup>2</sup>Department of Radiology, University of Washington, Seattle, WA, United States

3D whole heart phase sensitive late gadolinium enhanced (LGE) imaging can improve myocardial scar detection. Phase sensitive inversion recovery (PSIR) LGE is sub-optimal for clinical 3D application as it doubles the scan time with a fully sampled reference image. To address this, we develop 3D True Polarity Recovery with Independent Phase Estimation Using Multi-layer Stacks Based Region-Growing (3D-TRIPS) for direct reconstruction of 3D phase sensitive images without need for a separate reference scan. We demonstrate that 3D-TRIPS images shows good agreement and less artifacts compared with PSIR images. 3D-TRIPS will allow 3D-LGE imaging with half the scan time of PSIR.

18:03



Dark-Blood Late Gadolinium Enhanced MRI: A Novel Method without Additional Magnetization Preparation for Improved Myocardial Scar Detection

Robert J Holtackers<sup>1</sup>, Amedeo Chiribiri<sup>1</sup>, David M Higgins<sup>2</sup>, and Rene M Botnar<sup>1</sup>

<sup>1</sup>Division of Imaging Sciences and Biomedical Engineering, King's College London, London, United Kingdom, <sup>2</sup>Philips, Guildford, United Kingdom

Late gadolinium enhanced (LGE) MRI often suffers from poor scar-to-blood contrast when used for detection of endocardial scar due to the bright signal of adjacent blood. We report a method that significantly reduces left ventricular blood signal by setting a shorter inversion time in combination with a phase-sensitive inversion recovery (PSIR) sequence. Nulling the left ventricular blood signal with PSIR significantly increases scar-to-blood contrast since blood signal and scar signal no longer have similar signal levels. As no additional magnetization preparation is used, clinical application on current MR systems is readily available without the need for software modifications or additional training.

# Learning Image Reconstruction: Will Neural Networks Change Everything?

Organizers: Garry E. Gold, M.D., Daniel K. Sodickson, M.D., Ph.D.

Room 311

Tuesday 16:15 - 18:15 Moderators: Mehmet Akcakaya & Martin Uecker

---

16:15

[A Primer on AI: How Deep Learning is Changing Everything](#)

Krzysztof J. Geras<sup>1</sup>

<sup>1</sup>*New York University*

---

16:45

[Leveraging the Potential of Neural Networks for Image Reconstruction](#)

Florian Knoll<sup>1,2</sup>

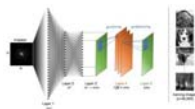
<sup>1</sup>*Radiology, NYU, New York, NY, United States*, <sup>2</sup>*CAI2R, NYU, New York, NY, United States*

This talk will provide an introduction to the use of machine learning and neural networks in the field of MR image reconstruction. We will use the example of reconstruction from undersampled data from accelerated acquisitions throughout the talk and will base our formulation on iterative reconstruction methods as used in compressed sensing (CS). We will formulate a network architecture based reconstruction that can be seen as a generalization of CS, and explain how we can learn an entire image reconstruction procedure. Using selected examples, we will discuss both advantages and challenges, covering topics like reconstruction time, design of the training procedure, error metrics and training efficiency and validation of image quality.

---

640

17:15



[Neural Network MR Image Reconstruction with AUTOMAP: Automated Transform by Manifold Approximation](#)

Bo Zhu<sup>1,2,3</sup>, Jeremiah Z. Liu<sup>1,4</sup>, Bruce R. Rosen<sup>1,2</sup>, and Matthew S. Rosen<sup>1,2,3</sup>

<sup>1</sup>*A.A. Martinos Center for Biomedical Imaging, Dept. of Radiology, Massachusetts General Hospital, Boston, MA, United States*, <sup>2</sup>*Harvard Medical School, Boston, MA, United States*, <sup>3</sup>*Dept. of Physics, Harvard University, Cambridge, MA, United States*, <sup>4</sup>*Department of Biostatistics, Harvard University, Boston, MA, United States*

It has been widely observed that real-world data presented in high dimensional space tend to lie along a nonlinear manifold with much lower dimensionality. The reduced dimensionality manifold captures intrinsic data properties such as sparsity in a transform domain. We describe here an automated neural network framework that exploits the universal function approximation of multilayer perceptron regression and the manifold learning properties demonstrated by autoencoders to enable a new robust generalized reconstruction methodology. We demonstrate this approach over a variety of MR image acquisition strategies, showing excellent immunity to noise and acquisition artifacts.

641



17:27



### Compressed sensing and Parallel MRI using deep residual learning

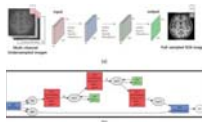
Dongwook Lee<sup>1</sup>, Jaejun Yoo<sup>1</sup>, and Jong Chul Ye<sup>1</sup>

*<sup>1</sup>Korea Advanced Institute of Science and Technology, Daejeon, Korea, Republic of*

A deep residual learning algorithm is proposed to reconstruct MR images from highly down-sampled k-space data. After formulating a compressed sensing problem as a residual regression problem, a deep convolutional neural network (CNN) was designed to learn the aliasing artifacts. The residual learning algorithm took only 30-40ms with significantly better reconstruction performance compared to GRAPPA and the state-of-the-art compressed sensing algorithm, ALOHA.

642

17:39



### 1D Partial Fourier Parallel MR imaging with deep convolutional neural network

Shanshan Wang<sup>1</sup>, Ningbo Huang<sup>1,2</sup>, Tao Zhao<sup>1,3</sup>, Yong Yang<sup>2</sup>, Leslie Ying<sup>4</sup>, and Dong Liang<sup>1</sup>

*<sup>1</sup>Paul C. Lauterbur Research Center for Biomedical Imaging, SIAT, Chinese Academy of Sciences, Shenzhen, People's Republic of China, <sup>2</sup>School of Computer Science and Technology, Changchun University of Science and Technology, Changchun, People's Republic of China, <sup>3</sup>College of Mining and Safety Engineering, Shandong University of Science and Technology, Qingdao, People's Republic of China, <sup>4</sup>Department of Biomedical Engineering and Department of Electrical Engineering, The State University of New York, NY, United States*

This paper develops a multi-coil SuperCNN network for 1D Partial Fourier Parallel MR imaging. With the utilization of enormous existing undersampled multi-channel images as inputs and their corresponding square root of sum-of-squares of images obtained from the fully sampled data as labels, the network is trained to identify the nonlinear mapping relationship and then performed as a predictor to reconstruct the online MR images. Experimental results on an in vivo dataset show that the proposed multi-coil SuperCNN is able to reconstruct more accurate MR images in less time compared to GRAPPA and SPIRiT from the same amount of undersampled data.

---

643

17:51



### A Deep Cascade of Convolutional Neural Networks for MR Image Reconstruction

Jo Schlemper<sup>1</sup>, Jose Caballero, Joseph V. Hajnal<sup>2</sup>, Anthony Price<sup>2</sup>, and Daniel Rueckert<sup>3</sup>

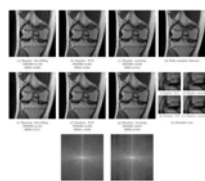
*<sup>1</sup>Department of Computing, Imperial College London, London, United Kingdom, <sup>2</sup>King's College London, <sup>3</sup>Imperial College London*

The acquisition of Magnetic Resonance Imaging (MRI) is inherently slow. Inspired by recent advances in deep learning, we propose a framework for reconstructing MRI images from undersampled data using a deep cascade of convolutional neural networks. We show, for Cartesian undersampling of 2D cardiac MR images, the proposed deep learning reconstruction method outperforms the state-of-the-art compressed sensing approaches, such as dictionary learning-based MRI (DLMRI) reconstruction, both in terms of reconstruction error, the perceptual quality and the reconstruction speed for 4-fold and 8-fold undersampling.

---

644

18:03



### On the Influence of Sampling Pattern Design on Deep Learning-Based MRI Reconstruction

Kerstin Hammernik<sup>1</sup>, Florian Knoll<sup>2,3</sup>, Daniel K Sodickson<sup>2,3</sup>, and Thomas Pock<sup>1,4</sup>

*<sup>1</sup>Institute of Computer Graphics and Vision, Graz University of Technology, Graz, Austria, <sup>2</sup>Center for Biomedical Imaging and Center for Advanced Imaging Innovation and Research (CAI2R), NYU School of Medicine, New York, NY, United States, <sup>3</sup>Department of Radiology, NYU School of Medicine, New York, NY, United States, <sup>4</sup>Safety & Security Department, AIT Austrian Institute of Technology GmbH, Vienna, Austria*

In this work, we address the question if variable density sampling of 2D Cartesian knee sequences can improve deep learning-based MRI reconstruction. Our results suggest that incoherent artifacts introduced by variable density sampling are beneficial to reconstruct highly accelerated sequences. Additionally, we show that our learning-based approach for regular sampling improves reconstruction results compared to classical compressed sensing methods with variable density sampling for our target application.

---

---

### **Electronic Poster: Ad Hoc**

Exhibition Hall                      Tuesday 17:15 - 18:15 *(no CME credit)*

---

### **Other**

## **Bronze Corporate Evening Symposium: Bracco**

Tuesday 18:30 - 20:30                      *(no CME credit)*

---

---

## **Wednesday, 26 April 2017**

[Go to top](#)

### **Sunrise Session**

## **Cardiovascular MR: "More is Better": More Speed**

*Organizers:* Sonia Nielles-Vallespin, Ph.D., Daniel K. Sodickson, M.D., Ph.D. & Bernd J. Wintersperger, M.D.

**Room 310                      Wednesday 7:00 - 7:50 *Moderators:* Giulia Ginami & Daniel Herzka**

---

7:00                      [Hardware & Software for Rapid Image Reconstruction](#)  
Adrienne Campbell-Washburn

---

7:25                      [Rapid Continuous Acquisition](#)  
Li Feng

---

7:50                      [Adjournment & Meet the Teachers](#)

---

---



## Sunrise Session

# Hyperpolarization & MR Applications

*Organizers:* Sebastian Kozerke, Ph.D. & Greig C. Scott, Ph.D.

Room 311                      Wednesday 7:00 - 7:50                      *Moderators:* James Bankson & Jessica Bastiaansen

---

7:00                      [Hyperpolarization - Description, Overview & Method](#)  
Peder Larson

---

7:25                      [Hyperpolarization - Clinical Potential & Relevance](#)  
Marie Schroeder

---

7:50                      [Adjournment & Meet the Teachers](#)

---

## Sunrise Session

# MR Imaging of Small Joints: Fingers & Toes

*Organizers:* Jenny T. Bencardino, M.D., Eric Y. Chang, M.D., Christine Chung, M.D. & Philip Robinson, M.D.

Room 312                      Wednesday 7:00 - 7:50                      *Moderators:* Kimberly Amrami & Edwin Oei

---

7:00                      [MR of Finger Injuries](#)  
Catherine Petchprapa

---

7:25                      [Turf Toe & Lesser Metatarsal Joints](#)  
Jana Crain

---

7:50                      [Adjournment & Meet the Teachers](#)

---

## Sunrise Session

# Gadolinium in MSK Imaging

*Organizers:* Jenny T. Bencardino, M.D., Eric Y. Chang, M.D., Christine Chung, M.D. & Philip Robinson, M.D.

Room 313A                      Wednesday 7:00 - 7:50 *Moderators: Jung-Ah Choi & Mark Schweitzer*

---

7:00                      [Gadolinium in MSK Imaging: Technical Aspects](#)  
Michael Tweedle

---

7:25                      [Contrast Enhanced MRI of the MSK System: How & When?](#)  
Jung-Ah Choi

---

7:50                      [Adjournment & Meet the Teachers](#)

---

### **Sunrise Session**

## **Individualized Brain MRI: Single-Subject Analysis**

*Organizers:* Christopher P. Hess, M.D., Ph.D.

Room 313BC                      Wednesday 7:00 - 7:50 *Moderators: Thijs Dhollander & Dan Wu*

---

7:00                      [Methods for Single Subject Brain Analysis](#)  
Duygu Tosun

---

7:25                      [Atlas-Based Analysis for Neuroimaging Informatics](#)  
Andreia Faria

---

7:50                      [Adjournment & Meet the Teachers](#)

---

### **Sunrise Session**

## **MRI Assessment in Monitoring Cancer Therapy**

*Organizers:* Linda Moy, M.D. & Valeria Panebianco, M.D.

Room 314                      Wednesday 7:00 - 7:50 *Moderators: Sungehon Gene Kim & Valeria Panebianco*

---

7:00                      [Multiparametric MRI for Tumor Therapy Response](#)  
Anwar Padhani

---

7:25 Sarcoma Imaging  
Laura Fayad

---

7:50 Adjournment & Meet the Teachers

---

### Sunrise Session

## It Doesn't Have to Be That Way: Information & Diagnosis

*Organizers:* Michael S. Hansen, Ph.D. & Joshua D. Trzasko, Ph.D.

Room 315 Wednesday 7:00 - 7:50 *Moderators:* Michael Hansen & Sebastian Kozerke

---

7:00 Artifact to Information using Structured Low Rank Matrix Completion  
Jong Chul Ye

---

7:25 Computer Assisted Diagnosis  
Alistair Young

---

7:50 Adjournment & Meet the Teachers

---

### Sunrise Session

## Dynamic Functional Connectivity MRI: Approaches & Mechanisms

*Organizers:* Hanzhang Lu, Ph.D. & Jay J. Pillai, M.D.

Room 316A Wednesday 7:00 - 7:50 *Moderators:* Peiying Liu & Jeroen Siero

---

7:00 Dynamic fcMRI: Approaches  
Xiao Liu

---

7:25 Dynamic fcMRI: Mechanisms & Applications  
Silvina Horovitz

---

7:50

Adjournment & Meet the Teachers

---

---

## Sunrise Session

# Clinical Applications of PET-MRI in Body Imaging

*Organizers:* Kathryn Fowler, M.D., Kartik Jhaveri, M.D., F.R.C.P.C., Lorenzo Mannelli, M.D., Ph.D. & Edwin J.R. van Beek, M.D., Ph.D., M.Ed., FRCR

Room 320

Wednesday 7:00 - 7:50

*Moderators:* Hersh Chandarana & Lorenzo Mannelli

---

7:00

Challenges-MRAC & Motion Correction

Alan McMillan

---

7:25

Current Clinical Applications & Novel Tracers, Future Directions

Thomas Hope

---

7:50

Adjournment & Meet the Teachers

---

---

## Traditional Poster: Body: Breast, Chest, Abdomen, Pelvis

Exhibition Hall 1990-  
2030

Wednesday 8:15 - 10:15 *(no CME credit)*

---

## Electronic Poster: Neuro

Exhibition Hall

Wednesday 8:15 - 9:15 *(no CME credit)*

---

## Study Groups

### Electro-Magnetic Tissue Properties (SWI) Study Group

Room 323ABC

Wednesday 8:15 - 10:15 *(no CME credit)*

---

---

## Study Groups

### Current Issues in Brain Function Study Group

**Educational Course**

# Prototype to Product: Pathways to Commercialization

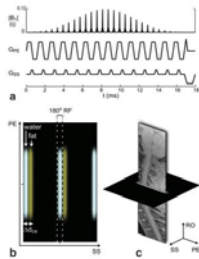
Organizers: Priti Balchandani, Ph.D. & Elena A. Kaye, Ph.D.

Room 315                      Wednesday 8:15 - 10:15                      Moderators: Rebecca Rakow-Penner & Matthew Robson

---

8:15                      [Historical Perspective](#)  
Manojkumar Saranathan

8:30                      [Case Study: FOCUS](#)  
Emine Ulku Saritas<sup>1,2,3</sup>



<sup>1</sup>Electrical & Electronics Engineering, Bilkent University, Ankara, Turkey, <sup>2</sup>National Magnetic Resonance Research Center (UMRAM), Bilkent University, Ankara, Turkey, <sup>3</sup>Neuroscience Program, Sabuncu Brain Research Center, Bilkent University, Ankara, Turkey

FOCUS is the product name for the technique that achieves reduced FOV imaging using a 2D spatially selective RF excitation. This technique provides increased image resolution while significantly reducing off-resonance induced artifacts for single-shot echo planar imaging (ssEPI) in diffusion weighted imaging (DWI). This presentation will cover the technical details and the product development stages of FOCUS.

8:45                      [Simultaneous Multislice](#)  
Kawin Setsompop

This talk outlines the path to commercialization of “Simultaneous MultiSlice EPI acquisition with blipped-CAIPI”; a technology that is now being used widely for diffusion, fMRI and perfusion imaging. Historical perspective, and key developments and insights important for the commercialization of this sequence will be described, along with key lessons learned.

9:00                      [Case Study: Skope](#)

9:15      Adoption & Commercialization of the Novel Techniques: Vendors' Perspective  
Anja Brau

---

9:15      Adoption & Commercialization of the Novel Techniques: Vendors' Perspective  
Holger Eggert<sup>1</sup>

*<sup>1</sup>Philips Research, Hamburg, Germany*

Numerous MR image acquisition and reconstruction methods are devised each year, notably by researchers in academia. Only a few of them can be commercialized by industry, a prerequisite for them to become available on many MR scanners and to have significant impact on clinical care. In this presentation, some of the main criteria applied in this selection process and some of the key steps involved in the subsequent development process are outlined. In addition, some subjective suggestions are made to researchers interested in improving the chances of success of their methods in this respect.

---

9:15      Adoption & Commercialization of the Novel Techniques: Vendors' Perspective  
Andreas Greiser<sup>1</sup>, Edgar Mueller<sup>1</sup>, and Lars Lauer<sup>1</sup>



*<sup>1</sup>Siemens Healthineers, Erlangen, Germany*

Siemens Healthineers is the MRI vendor with the largest market share in MR. Our main goal is to facilitate advances by providing a reliable platform for MR applications and research to generate added value to users and patients. Here we want to outline important criteria to leverage product integration of new methods and trends. Using prototypes, multi-center testing can be employed to validate new methods. Based on collaboration, a Works-in-Progress can be developed for wider validation and as input for productization. Siemens Healthineers just recently reemphasized its commitment to actively support 3<sup>rd</sup>-party integration as integral part of clinical solutions.

---

9:15 Adoption & Commercialization of the Novel Techniques: Vendors' Perspective  
Mitsue Miyazaki<sup>1</sup>

<sup>1</sup>Toshiba Medical Research Institution, IL, United States

The experience of commercializing a non-contrast MRA technique, named fresh blood imaging (FBI) into Toshiba product is introduced.

---

9:45 Panel Discussion

---

10:15 Adjournment & Meet the Teachers

---

## Educational Course

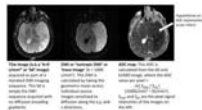
# MR Physics & Techniques for Clinicians

Organizers: Marcus T. Alley, Ph.D. & Bernd Jung, Ph.D.

Room 316BC Wednesday 8:15 - 10:15 Moderators: Marcus Alley & Daniel Gallichan

---

8:15 Diffusion & Perfusion Weighted Imaging



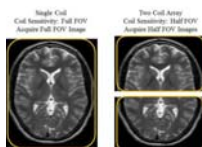
Samantha J Holdsworth<sup>1</sup>

<sup>1</sup>Lucas Center for Imaging, Department of Radiology, Stanford University, Stanford, CA, United States

This lecture is devoted to the basic technological aspects of diffusion-weighted imaging (DWI) and perfusion-weighted imaging (PWI), using neuroimaging applications as examples, and with the concepts explained with minimal use of equations.

---

8:55 Parallel Imaging



Katherine Wright<sup>1</sup>

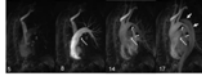
<sup>1</sup>Case Western Reserve University



This review of parallel imaging techniques will focus on learning basic principles and its clinical use. Specifically, we will discuss how data are accelerated, and the resulting aliasing artifacts that occur. We will explore how coil sensitivities and parallel imaging reconstruction methods can be used to reconstruct undersampled data. Lastly, we will review clinical applications of parallel imaging.

---

9:35



### MR Angiography

Oliver Wieben<sup>1</sup>

<sup>1</sup>*Depts. of Medical Physics & Radiology, University of Wisconsin-Madison, Madison, WI, United States*

Traditional clinical MR Angiography (MRA) provides volumetric datasets to characterize the vessel lumen. These MRA techniques can be generally separated into two categories: contrast-enhanced MRA, which requires the venous injection of a paramagnetic contrast agent in form of a Gadolinium (Gd) chelate and non-contrast-enhanced MRA (NCE MRA), which relies on signal properties of the blood or the motion of the blood to create signal differences between the blood pool and the surrounding tissues. The underlying contrast mechanisms of contrast-enhanced (CE MRA), time-of-flight, phase-contrast, and balanced steady state free precession (bSSFP) MRA will be discussed including recent developments in accelerated dynamic contrast-enhanced MRA (CE-MRA), the use of iron-based contrast agents, and velocity-encoded MRI.

---

10:15

Adjournment & Meet the Teachers

---

## Power Pitch

### Pitch: Marching on Musculoskeletal

Power Pitch  
Theater A -  
Exhibition Hall

Wednesday 8:15 - 9:15

Moderators: Hongyu An &  
Catalina Arteaga de Castro

(no CME credit)

---

645

8:15

Accelerated knee imaging using a deep learning based reconstruction



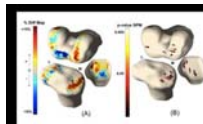
Florian Knoll<sup>1,2</sup>, Kerstin Hammernik<sup>3</sup>, Elisabeth Garwood<sup>1,2</sup>, Anna Hirschmann<sup>4</sup>, Leon Rybak<sup>1,2</sup>, Mary Bruno<sup>1,2</sup>, Tobias Block<sup>1,2</sup>, James Babb<sup>1,2</sup>, Thomas Pock<sup>3,5</sup>, Daniel K Sodickson<sup>1,2</sup>, and Michael P Recht<sup>1,2</sup>

<sup>1</sup>Radiology, NYU, New York, NY, United States, <sup>2</sup>CAI2R, NYU, New York, NY, United States, <sup>3</sup>Institute of Computer Graphics and Vision, Graz University of Technology, Graz, Austria, <sup>4</sup>Radiology, University Hospital Basel, Basel, Switzerland, <sup>5</sup>Austria Safety & Security Department, AIT Austrian Institute of Technology GmbH, Vienna, Austria

646

8:15

### Anterior Tibial Translation Following ACL Reconstruction is Associated with Postsurgical Cartilage Matrix Changes.



Alan K Li<sup>1</sup>, Valentina Padoia<sup>2</sup>, Keiko Amano<sup>2</sup>, Jonathan Ochoa<sup>2</sup>, Qi Li<sup>2</sup>, Benjamin Ma<sup>2</sup>, and Xiaojuan Li<sup>2</sup>

<sup>1</sup>University of California, Berkeley, Berkeley, CA, United States, <sup>2</sup>University of California, San Francisco, San Francisco, CA, United States

647

8:15

### Longitudinal characterization of deformation-induced skeletal muscle damage by T2-mapping, DWI and MRE



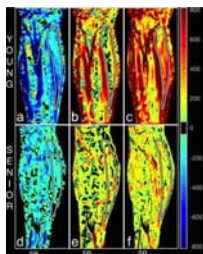
Jules L. Nelissen<sup>1,2</sup>, Willeke A. Traa<sup>3</sup>, Larry de Graaf<sup>1</sup>, Cees W. J. Oomens<sup>3</sup>, Jurgen H. Runge<sup>4,5</sup>, Ralph Sinkus<sup>4</sup>, Klaas Nicolay<sup>1</sup>, Aart J. Nederveen<sup>5</sup>, Martijn Froeling<sup>6</sup>, and Gustav J. Strijkers<sup>2</sup>

<sup>1</sup>Biomedical NMR, Eindhoven University of Technology, Eindhoven, Netherlands, <sup>2</sup>Preclinical and Translational MRI, Academic Medical Center, Amsterdam, Netherlands, <sup>3</sup>Biomechanics of Soft Tissues, Eindhoven University of Technology, Eindhoven, Netherlands, <sup>4</sup>Division of Imaging Sciences & Biomedical Engineering, King's College London, London, United Kingdom, <sup>5</sup>Radiology, Academic Medical Center, Amsterdam, Netherlands, <sup>6</sup>Department of Radiology, University Medical Center Utrecht, Utrecht, Netherlands

648

8:15

### Age Related Differences in Shear Strain in Medial Gastrocnemius: Implications for Lateral Transmission of Force



Vadim Malis<sup>1</sup>, Usha Sinha<sup>2</sup>, Robert Csapo<sup>3</sup>, and Shantanu Sinha<sup>3</sup>

<sup>1</sup>Physics, UC San Diego, San Diego, CA, United States, <sup>2</sup>Physics, San Diego State University, San Diego, CA, United States, <sup>3</sup>Radiology, UC San Diego, San Diego, CA, United States



649

8:15

Parameter	High-BW TSE	Compressed Sensing SEMAC
Orientation	axial	axial
Weighting	intermediate	intermediate
Repetition time (ms)	4120	3750
Echo time (ms)	26	26
Flip angle (deg)	10	10
Acquisition time (min)	-	-
Number of SEMAC slices	-	10
Echo train length	10	11
Receiver bandwidth (pixels/cm)	501	507
File width (bytes)	100	100
Field of view (cm)	170 x 170	170 x 170
Matrix	501 x 206	501 x 206
Pixel resolution (mm)	0.3 x 0.3	0.3 x 0.3
Slice thickness (mm)	3.0	3.0
Number of acquisitions	3	1
Number of interleaves	2	1
Number of slices	10	10
Acceleration factor	1	2
Parallel Imaging scaling method	uniform to posterior	uniform to posterior
Acquisition time	4:20:40	4:20:40

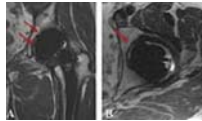
### Metal Artifact Reduction MRI for the Assessment of the Rotational Alignment Knee Arthroplasty Implants: Compressed Sensing SEMAC TSE versus High-Bandwidth TSE

Filippo Del Grande<sup>1,2</sup>, Benjamin Fritz<sup>3</sup>, Satri Stuelke<sup>4</sup>, Steven E Stern<sup>5</sup>, Susanne Bensler<sup>3</sup>, and Jan Fritz<sup>1</sup>

<sup>1</sup>Radiology, The Johns Hopkins University School of Medicine, Baltimore, MD, United States, <sup>2</sup>Radiology, Ospedale Regionale di Lugano, Lugano, Switzerland, <sup>3</sup>Radiology, Orthopedic University Hospital Balgrist, Zurich, Switzerland, <sup>4</sup>Radiology, The Johns Hopkins University School of Medicine, Baltimore, MD, <sup>5</sup>Queensland University of Technology

650

8:15



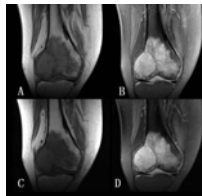
### Ability of MAVRIC MRI to Predict Component Loosening in Total Hip Arthroplasty

Alissa Jo Burge<sup>1</sup>, Gabrielle P Konin<sup>1</sup>, Jennifer Berkowitz<sup>1</sup>, Matthew Koff<sup>1</sup>, Douglas Padgett<sup>2</sup>, and Hollis Potter<sup>3</sup>

<sup>1</sup>Radiology and Imaging, Hospital for Special Surgery, New York, NY, United States, <sup>2</sup>Adult Reconstruction and Joint Replacement, Hospital for Special Surgery, New York, NY, United States, <sup>3</sup>Hospital for Special Surgery, New York, NY, United States

651

8:15



### Simultaneous multi-slice TSE for clinical MR Imaging of lesions in the knee

Xiaona Li<sup>1</sup>, Zhigang Peng<sup>1</sup>, Yi Sun<sup>2</sup>, Panli Zuo<sup>2</sup>, Dingxin Wang<sup>3</sup>, and Jianling Cui<sup>1</sup>

<sup>1</sup>Radiology, the Third Hospital of Henbei Medical University, Shijiazhuang, People's Republic of China, <sup>2</sup>MR Collaboration NE Asia, Siemens Healthcare, Shang Hai, People's Republic of China, <sup>3</sup>Siemens Medical Solutions USA, Inc., Minneapolis, MN, United States

652

8:15



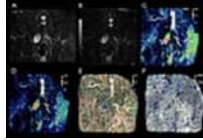
### Simultaneous T2 Relaxometry and Morphometry of Cartilage and Meniscus with Double-Echo in Steady-State in Five Minutes

Akshay S Chaudhari<sup>1</sup>, Marianne S Black<sup>1</sup>, Bragi Sveinsson<sup>1</sup>, Garry E Gold<sup>1</sup>, and Brian A Hargreaves<sup>1</sup>

<sup>1</sup>Radiology, Stanford University, Stanford, CA, United States

653

8:15



### Soft Tissue Tumors: Use of Intravoxel Incoherent Motion MR Imaging for Assessment of Diffusion and Perfusion for the Differentiation of Benign from Malignant Tumors

Haijun Wu<sup>1</sup> and Changhong Liang<sup>1</sup>

<sup>1</sup>Department of Radiology, Guangdong General Hospital, Guangdong Academy of Medical Sciences, Guangzhou, People's Republic of China

654

8:15

Parameter	Pre-TNF	Post-TNF
Mean T1ρ (ms)	120.5 ± 15.2	115.8 ± 14.1
Standard Deviation (ms)	18.3	17.5
Range (ms)	85 - 155	80 - 150
Median (ms)	110	105
Interquartile Range (ms)	95 - 125	90 - 120
Skewness	0.8	0.7
Kurtosis	3.2	3.1
Correlation Coefficient	0.95	0.92

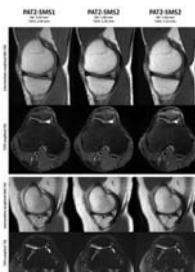
### 1-year Follow-Up of T1ρ for Assessing Radiocarpal Cartilage Matrix Changes after Anti-TNF treatment for Rheumatoid Arthritis: Preliminary Results

Eric Ku<sup>1</sup>, Valentina Pedita<sup>1</sup>, Matthew Tanaka<sup>1</sup>, Hyo Jin Choi<sup>1</sup>, Ursula Heilmeyer<sup>1</sup>, Andrew Burghardt<sup>1</sup>, Jonathan Graf<sup>2</sup>, John Imboden<sup>2</sup>, Thomas Link<sup>1</sup>, and Xiaojuan Li<sup>1</sup>

<sup>1</sup>Department of Radiology and Biomedical Imaging, UCSF, San Francisco, CA, United States, <sup>2</sup>Department of Medicine, UCSF, San Francisco, CA, United States

655

8:15



### Simultaneous Multi-Slice Accelerated High Resolution MRI of the Knee: Comparison with In-plane Parallel Imaging Acceleration

Jan Fritz<sup>1</sup>, Benjamin Fritz<sup>2</sup>, Jialu Zhang<sup>3,4</sup>, Dharmdev H Joshi<sup>1</sup>, Gaurav K Thawait<sup>1</sup>, Li Pan<sup>5</sup>, and Dingxin Wang<sup>3,5</sup>

<sup>1</sup>The Johns Hopkins University School of Medicine, Baltimore, MD, United States, <sup>2</sup>Orthopaedic University Hospital Balgrist, <sup>3</sup>University of Minnesota, <sup>4</sup>Zhejiang University, <sup>5</sup>Siemens Healthcare USA

656

8:15



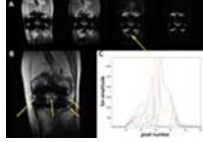
### New insights into the predilection sites of Juvenile Osteochondritis Dissecans using Quantitative Susceptibility Mapping

Jutta Ellermann<sup>1</sup>, Casey P Johnson<sup>2</sup>, Luning Wang<sup>3</sup>, Ferenc Toth<sup>4</sup>, Kevin Shea<sup>5</sup>, Cathy Carlson<sup>6</sup>, and Mikko J Nissi<sup>7,8</sup>

<sup>1</sup>Radiology, University of Minnesota, Minneapolis, MN, United States, <sup>2</sup>Radiology, CMRR, University of Minnesota, <sup>3</sup>University of Minnesota, <sup>4</sup>College of Veterinary Medicine, University of Minnesota, <sup>5</sup>St. Lukes Orthopaedics, Boise, ID, <sup>6</sup>College of Veterinary Medicine, University of Minnesota, St. Paul, MN, <sup>7</sup>Department of Applied Physics, University of Eastern Finland, <sup>8</sup>Diagnostic Imaging Center, Kuopio University Hospital, Kuopio, Finland

657

8:15



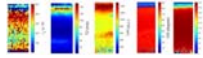
Pile up correction for 3D-Multi Spectral Imaging using Gaussian Spectral Modeling and Bin Expansion

S Sivaram Kaushik<sup>1</sup> and Kevin Koch<sup>2</sup>

<sup>1</sup>MR Applications and Workflow, GE Healthcare, Waukesha, WI, United States, <sup>2</sup>Radiology, Medical College of Wisconsin, Milwaukee, WI, United States

658

8:15



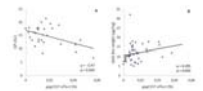
Correlation Time Mapping of Articular Cartilage: correlation with tissue composition and structure

Hassaan Elsayed<sup>1,2</sup>, Stefan Zbyn<sup>2</sup>, Mikko J Nissi<sup>3,4</sup>, Jari Rautiainen<sup>1,2,3,5</sup>, Matti Hanni<sup>1,2,5</sup>, and Miika T Nieminen<sup>1,2,5</sup>

<sup>1</sup>Medical Research Center, University of Oulu and Oulu University Hospital, Oulu, Finland, <sup>2</sup>Research Unit of Medical Imaging, Physics and Technology, University of Oulu, Oulu, Finland, <sup>3</sup>Department of Applied Physics, University of Eastern Finland, Kuopio, Finland, <sup>4</sup>Diagnostic Imaging Center, Kuopio University Hospital, Kuopio, Finland, <sup>5</sup>Department of Diagnostic Radiology, Oulu University Hospital, Oulu, Finland

659

8:15



Correlation of 7T gagCEST MRI with Electromechanical and Biochemical Properties of Femoral Articular Cartilage

Sander Brinkhof<sup>1</sup>, Razmara Nizak<sup>2</sup>, Sotcheadt Sim<sup>3</sup>, Vitaliy Khlebnikov<sup>1</sup>, Dennis Klomp<sup>1</sup>, and Daniel Saris<sup>2,4</sup>

<sup>1</sup>Radiology, University Medical Center Utrecht, Utrecht, Netherlands, <sup>2</sup>Orthopaedics, University Medical Center Utrecht, Utrecht, <sup>3</sup>Biomomentum Inc., Laval, QC, Canada, <sup>4</sup>MIRA Institute for Biomedical Technology and Technical Medicine, University of Twente, Enschede, Netherlands

**Power Pitch**

**Pitch: Cancer Imaging in the Body**

Power Pitch

Theater B -

Exhibition Hall

Wednesday 8:15

- 9:15

Moderators: Ruiliang Bai

(no CME credit)

660

8:15

### Interobserver Agreement and Diagnostic Performance of LI-RADS v2014 on contrast-enhanced MRI for non-HCC malignancies.

Observer	LI-RADS Category	Final Diagnosis
Observer 1	LI-RADS 4	LI-RADS 4
Observer 2	LI-RADS 4	LI-RADS 4
Observer 3	LI-RADS 4	LI-RADS 4
Observer 4	LI-RADS 4	LI-RADS 4
Observer 5	LI-RADS 4	LI-RADS 4
Observer 6	LI-RADS 4	LI-RADS 4
Observer 7	LI-RADS 4	LI-RADS 4
Observer 8	LI-RADS 4	LI-RADS 4
Observer 9	LI-RADS 4	LI-RADS 4
Observer 10	LI-RADS 4	LI-RADS 4

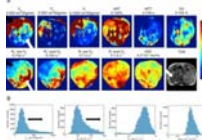
Nataly de Souza Maciel Rocha Horvat<sup>1</sup>, Ines Nikolovski<sup>1</sup>, Niamh Long<sup>1</sup>, Scott Gerst<sup>1</sup>, Jian Zheng<sup>1</sup>, Linda Ma Pak<sup>1</sup>, Junting Zheng<sup>1</sup>, Lorenzo Mannelli<sup>1</sup>, and Richard Kinh Gian Do<sup>1</sup>

<sup>1</sup>Memorial Sloan Kettering Cancer Center, NY, NY, United States

661

8:15

### Quantification of hepatocellular carcinoma tumor heterogeneity with multiparametric MRI



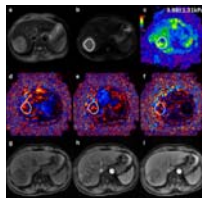
Stefanie Hectors<sup>1</sup>, Mathilde Wagner<sup>1</sup>, Octavia Bane<sup>1</sup>, Cecilia Besa<sup>1</sup>, Sara Lewis<sup>2</sup>, Romain Remark<sup>3</sup>, Nelson Chen<sup>1</sup>, M. Isabel Fiel<sup>4</sup>, Hongfa Zhu<sup>4</sup>, Sacha Gnjatic<sup>5</sup>, Miriam Merad<sup>3</sup>, Yujin Hoshida<sup>6</sup>, and Bachir Taouli<sup>1</sup>

<sup>1</sup>Translational and Molecular Imaging Institute, Icahn School of Medicine at Mount Sinai, New York, NY, United States, <sup>2</sup>Department of Radiology, Icahn School of Medicine at Mount Sinai, New York, NY, United States, <sup>3</sup>Immunology Institute, Icahn School of Medicine at Mount Sinai, New York, NY, United States, <sup>4</sup>Department of Pathology, Icahn School of Medicine at Mount Sinai, New York, NY, United States, <sup>5</sup>Oncological Science, Icahn School of Medicine at Mount Sinai, New York, NY, United States, <sup>6</sup>Department of Medicine/Division of Liver Diseases, Icahn School of Medicine at Mount Sinai, New York, NY, United States

662

8:15

### 3D MR Elastography in Prediction of Tumor Capsule Formation of Hepatocellular Carcinoma (HCC) in Patients with Hepatitis B Virus Infection



Jin Wang<sup>1</sup>, Hao Yang<sup>1</sup>, Yong Liu<sup>2</sup>, Jingbiao Chen<sup>1</sup>, Tianhui Zhang<sup>1</sup>, Kevin J. Glaser<sup>3</sup>, Xin Li<sup>4</sup>, Jun Chen<sup>3</sup>, Yao Zhang<sup>1</sup>, Qungang Shan<sup>1</sup>, Bingjun He<sup>1</sup>, Zhuang Kang<sup>1</sup>, Yin Meng<sup>3</sup>, Dzyubak Bogdan<sup>3</sup>, Venkatesh SK<sup>3</sup>, Ronghua Yan<sup>1</sup>, Xi Long<sup>1</sup>, and Richard L. Ehman<sup>3</sup>

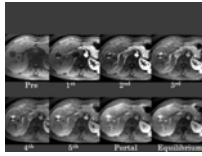
<sup>1</sup>Department of Radiology, the Third Affiliated Hospital, Sun Yat-sen University (SYSU), Guangzhou, People's Republic of China, <sup>2</sup>Department of Pathology, the Third Affiliated Hospital, Sun Yat-sen University (SYSU), Guangzhou, People's Republic of China, <sup>3</sup>Department of Radiology, Mayo Clinic, Rochester, United States, <sup>4</sup>GE Healthcare MR Research China, Guangzhou, People's Republic of China

663

8:15

### Dynamic Contrast Enhanced MR Imaging of Hepatopancreatobiliary lesions in Combined use of Parallel Imaging and Compressed Sensing



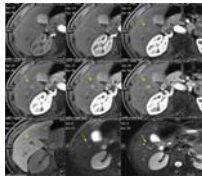


Takayuki Masui<sup>1</sup>, Motoyuki Katayama<sup>1</sup>, Yuji Iwadate<sup>2</sup>, Naoyuki Takei<sup>2</sup>, Kang Wang<sup>3</sup>, Kevin King<sup>4</sup>, Kei Tsukamoto<sup>1</sup>, Mitsuteru Tsuchiya<sup>1</sup>, Yuki Hayashi<sup>1</sup>, Masako Sasaki<sup>1</sup>, Takahiro Yamada<sup>1</sup>, Kenichi Mizuki<sup>1</sup>, Harumi Sakahara<sup>5</sup>, Koji Yoneyama<sup>1</sup>, and Yuki Takayanagi<sup>1</sup>

<sup>1</sup>Radiology, Seirei Hamamatsu General Hospital, Hamamatsu, Japan, <sup>2</sup>Global MR Applications and Workflow, GE Healthcare Japan, Hino, Japan, <sup>3</sup>Global MR Applications and Workflow, GE Healthcare, Madison, WI, United States, <sup>4</sup>Global MR Applications and Workflow, GE Healthcare, Waukesha, WI, United States, <sup>5</sup>Radiology, Hamamatsu University School of Medicine, Hamamatsu, Japan

664

8:15



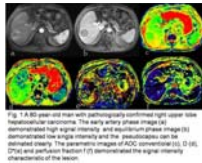
Detection and measurement of neuroendocrine tumors liver metastases using Gd-EOB-DTPA enhanced MRI: comparison between multiple arterial phases, hepatobiliary phase, and DWI

Jia Xu<sup>1</sup>, Xuan Wang<sup>1</sup>, Hua dan Xue<sup>1</sup>, Shi tian Wang<sup>1</sup>, Hui Liu<sup>2</sup>, and Zheng yu Jin<sup>1</sup>

<sup>1</sup>Department of Radiology, Peking Union Medical College Hospital, Beijing, People's Republic of China, <sup>2</sup>Siemens Ltd, Shanghai, People's Republic of China

665

8:15



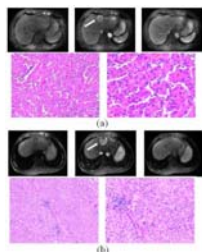
Integrated slice-specific shimming (iShim) intravoxel incoherent motion diffusion-weighted MR imaging in the liver: the value of differential diagnosis between benign and malignant hepatic tumors

Hongxia Wang<sup>1</sup>, Qingbo Li<sup>2</sup>, Bin Wang<sup>3</sup>, Qinglei Shi<sup>4</sup>, Yan Feng<sup>1</sup>, Xingyue Jiang<sup>1</sup>, and Peigong Zhang<sup>3</sup>

<sup>1</sup>Radiology Department, Binzhou Medical University Hospital, Binzhou, People's Republic of China, <sup>2</sup>Emergency Department, Binzhou People's Hospital, Binzhou, People's Republic of China, <sup>3</sup>Binzhou Medical University, Yantai, People's Republic of China, <sup>4</sup>MR Scientific NE Asia, Siemens Healthcare, Beijing, People's Republic of China

666

8:15



Quantitative texture feature to predict Microscopic portal vein invasion of Hepatocellular carcinoma with contrast-enhanced MR images

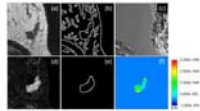
Wu Zhou<sup>1</sup>, Qiyao Wang<sup>1</sup>, Su Yao<sup>2</sup>, Guangyi Wang<sup>3</sup>, Zaiyi Liu<sup>3</sup>, Changhong Liang<sup>3</sup>, and Lijuan Zhang<sup>1</sup>



<sup>1</sup>Shenzhen Institutes of Advanced Technology, Chinese Academy of Sciences, Shenzhen, People's Republic of China, <sup>2</sup>Department of Pathology, Guangdong General Hospital, Guangdong Academy of Medical Sciences, <sup>3</sup>Department of Radiology, Guangdong General Hospital, Guangdong Academy of Medical Sciences

667

8:15



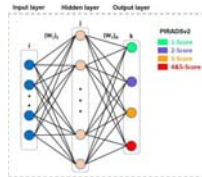
### Conductivity of different malignancy grades of invasive ductal carcinomas and fibroadenomas

Ulrich Katscher<sup>1</sup>, Mussa Gagiye<sup>1</sup>, Naoko Mori<sup>2</sup>, Keiko Tsuchiya<sup>3</sup>, Jochen Keupp<sup>1</sup>, and Hiroyuki Abe<sup>4</sup>

<sup>1</sup>Philips Research Europe, Hamburg, Germany, <sup>2</sup>Tohoku University, Sendai, Japan, <sup>3</sup>Shiga University, Hikone, Japan, <sup>4</sup>University of Chicago, IL, United States

668

8:15



### A computer aided diagnosis (CAD) scoring tool: prostate cancer risk evaluation with PI-RADS v2 Guidelines

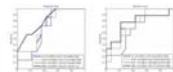
Lian Ding<sup>1</sup>, Ge Gao<sup>2</sup>, Yajing Zhang<sup>3</sup>, Chengyan Wang<sup>1</sup>, Jue Zhang<sup>1,4</sup>, Xiaoying Wang<sup>1,2</sup>, and Jing Fang<sup>1,4</sup>

<sup>1</sup>Academy for Advanced Interdisciplinary Studies, Peking University, Beijing, People's Republic of China, <sup>2</sup>Department of Radiology, Peking University Frist Hospital, Beijing, People's Republic of China, <sup>3</sup>Philips Healthcare, Suzhou, China, Beijing, People's Republic of China, <sup>4</sup>College of Engineering, Peking University, Beijing, People's Republic of China

669



8:15

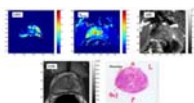


### Deep learning to improve prostate cancer diagnosis

Nikolaos Dikaios<sup>1</sup>, Edward W Johnston<sup>2</sup>, Harbir S Sidhu<sup>2</sup>, Mrishta B Appaya<sup>2</sup>, Alex Freeman<sup>3</sup>, Hashim U Ahmed<sup>4</sup>, and Shonit Punwani<sup>2</sup>

<sup>1</sup>Electrical Engineering, University of Surrey, Guildford, United Kingdom, <sup>2</sup>Centre for Medical Imaging, University College London, <sup>3</sup>Histopathology, University College London, <sup>4</sup>Surgery and Interventional Science, University College London

8:15

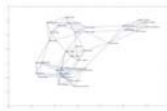


### Comparing the Diagnostic Accuracy of Luminal Water Imaging with Diffusion-Weighted and Dynamic Contrast-Enhanced MRI for Evaluation of Prostate Cancer.



Shirin Sabouri<sup>1</sup>, Silvia D Chang<sup>2,3,4</sup>, Richard Savdie<sup>2</sup>, Edward C Jones<sup>5</sup>, S. Larry Goldenberg<sup>2,3</sup>, Peter C Black<sup>2,3</sup>, and Piotr Kozlowski<sup>2,3,4,6</sup>

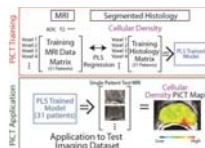
<sup>1</sup>Department of Physics and Astronomy, University of British Columbia, Vancouver, BC, Canada, <sup>2</sup>Department of Urologic Sciences, University of British Columbia, Vancouver, BC, Canada, <sup>3</sup>Vancouver Prostate Centre, Vancouver, BC, Canada, <sup>4</sup>Department of Radiology, University of British Columbia, Vancouver, BC, Canada, <sup>5</sup>Department of Pathology and Laboratory Medicine, University of British Columbia, Vancouver, BC, Canada, <sup>6</sup>UBC MRI Research Center, Vancouver, BC, Canada



### Novel Informatics Modeling of Magnetic Resonance Imaging Metrics for Characterizing Prostate Lesions with Pathology Correlation.

Katarzyna J. Macura<sup>1,2</sup>, Vishwa Parekh<sup>3</sup>, Seyed Saeid<sup>4</sup>, and Michael A. Jacobs<sup>1,2</sup>

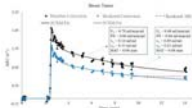
<sup>1</sup>The Russell H. Morgan Dept of Radiology and Radiological Science, The Johns Hopkins University School of Medicine, Baltimore, MD, United States, <sup>2</sup>Sidney Kimmel Comprehensive Cancer Center, The Johns Hopkins University School of Medicine, Baltimore, MD, United States, <sup>3</sup>Computer Science, The Johns Hopkins University, Baltimore, MD, United States, <sup>4</sup>Dept of Radiology, University of Minnesota, Minneapolis, United States



### Predictive Cytological Topography (PiCT): a Radiopathomics Approach to Mapping Prostate Cancer Cellularity

Amy Kaczmarowski<sup>1</sup>, Kenneth A Iczkowski<sup>2</sup>, Sarah L Hurrell<sup>1</sup>, Sean D McGarry<sup>1</sup>, Kenneth Jacobsohn<sup>3</sup>, William A Hall<sup>4</sup>, Mark Hohenwalter<sup>1</sup>, William See<sup>3</sup>, and Peter S LaViolette<sup>1</sup>

<sup>1</sup>Radiology, Medical College of Wisconsin, Milwaukee, WI, United States, <sup>2</sup>Pathology, Medical College of Wisconsin, Milwaukee, WI, United States, <sup>3</sup>Urology, Medical College of Wisconsin, Milwaukee, WI, United States, <sup>4</sup>Radiation Oncology, Medical College of Wisconsin, Milwaukee, WI, United States



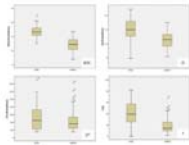
### Estimating breast tumor blood flow and blood volume using MRI: DCE vs IVIM

Leonidas Georgiou<sup>1</sup>, Nisha Sharma<sup>2</sup>, Daniel Wilson<sup>3</sup>, and David L Buckley<sup>1</sup>

*<sup>1</sup>Division of Biomedical Imaging, University of Leeds, Leeds, United Kingdom, <sup>2</sup>Department of Radiology, Leeds Teaching Hospital NHS Trust, <sup>3</sup>Department of Medical Physics and Engineering, Leeds Teaching Hospital NHS Trust*

674

8:15



**Discrimination of Malignant versus Benign Mediastinal Lymph Nodes Using Diffusion MRI with An IVIM Analysis**

Li-Ping Qi<sup>1,2</sup>, Wan-Pu Yan<sup>3</sup>, Ke-Neng Chen<sup>3</sup>, Zheng Zhong<sup>2,4</sup>, Kejia Cai<sup>2,5</sup>, Xiao-Ting Li<sup>1</sup>, Ying-Shi Sun<sup>1</sup>, and Xiaohong Joe Zhou<sup>2,6</sup>

*<sup>1</sup>Radiology, Peking University Cancer Hospital and Institute, Beijing, People's Republic of China, <sup>2</sup>Center for MR Research, University of Illinois at Chicago, Chicago, IL, United States, <sup>3</sup>Thoracic Surgery, Peking University Cancer Hospital and Institute, Beijing, People's Republic of China, <sup>4</sup>Bioengineering, University of Illinois at Chicago, Chicago, IL, United States, <sup>5</sup>Radiology and Bioengineering, University of Illinois at Chicago, Chicago, IL, United States, <sup>6</sup>Radiology, Neurosurgery, and Bioengineering, University of Illinois at Chicago, Chicago, IL, United States*

Oral

## Arterial Spin Labeling: Making it More Robust & Informative

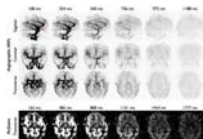
Room 310

Wednesday 8:15 -  
10:15

Moderators: Eric Achten & Linda Knutsson

675

8:15



**4D Combined Angiography and Perfusion using Radial Imaging and Arterial Spin Labeling**

Thomas W Okell<sup>1</sup>

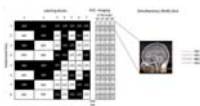
*<sup>1</sup>FMRIB Centre, Nuffield Department of Clinical Neurosciences, University of Oxford, Oxford, United Kingdom*

Complete assessment of blood flow to the brain requires both knowledge of blood flow through the large arteries and perfusion at the tissue level. However, separate acquisition of dynamic angiograms and perfusion maps is time-consuming. In this work a 4D implementation of the Combined Angiography and Perfusion using Radial Imaging and Arterial Spin Labeling (CAPRIA) sequence is presented, allowing the reconstruction of whole-brain dynamic angiograms and time-resolved perfusion maps from the same raw data set. In addition, a variable flip angle imaging scheme is shown to benefit the visualization of tissue perfusion without compromising angiographic image quality.

676



8:27



More and faster: multi-timepoint ASL at 150ms time-resolution with whole brain coverage by combining time-encoding, Look-Locker, Multi-Band and flip-angle sweep

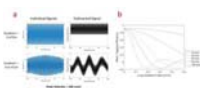
Merlijn C.E. van der Plas<sup>1</sup>, Wouter M. Teeuwisse<sup>1</sup>, Sophie Schmid<sup>1</sup>, and Matthias J. van Osch<sup>1</sup>

<sup>1</sup>C.J. Gorter Center for high field MRI, Department of Radiology, Leiden University Medical Center, Leiden, Netherlands

Multi-timepoint ASL can be acquired with several methods; however, most of these methods have some confounding aspects, such as loss of temporal resolution or limited brain coverage. We combine Hadamard-8 time-encoded-pCASL with Look-Locker readout (4 phases×150ms) for a high temporal resolution; moreover, multiband-factor 4 is used for a time efficient acquisition manner enabling whole brain coverage. This combination of techniques results in 25 PLDs for 16 slices, which provides information about the inflow of labeled blood and tissue perfusion. These images have a temporal resolution of 150ms, whereas inflow of label is measured at 75ms resolution.

677

8:39



Evaluation of Velocity Selective ASL Tagging Efficiency Utilizing Accelerated 3D Angiography

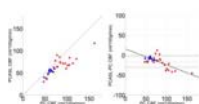
James H Holmes<sup>1</sup>, Tilman Schubert<sup>1</sup>, Prateek Sanan<sup>1</sup>, Patrick A Turski<sup>1</sup>, and Kevin M Johnson<sup>1,2</sup>

<sup>1</sup>Radiology, University of Wisconsin-Madison, Madison, WI, United States, <sup>2</sup>Medical Physics, University of Wisconsin-Madison, Madison, WI, United States

Velocity Selective Arterial Spin Labeling (VS-ASL) has been suggested as a possible solution for evaluating perfusion and MRA in complex geometries without well-defined labeling planes as well as in cases of slow or complex flow patterns. The goal of this work is to assess the spatial distribution of VS-ASL tagging efficiency utilizing MR angiography. Specifically, we identify and characterize errors introduced by susceptibility induced magnetic gradients. In controlled phantom experiments and human subjects tagging efficiency demonstrated dependence both on the magnitude of susceptibility shift and the velocity of vessels flowing through those regions.

678

8:51



### Pseudo Continuous Arterial Spin Labeling Quantification Considerations in Hyperemic Cerebral Blood Flow

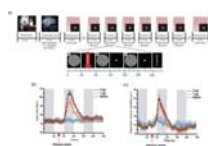
Adam Bush<sup>1</sup>, Thomas Coates<sup>2</sup>, and John Wood<sup>3</sup>

<sup>1</sup>Biomedical Engineering/ Cardiology, University of Southern California/ Children's Hospital Los Angeles, Los Angeles, CA, United States, <sup>2</sup>Hematology, Children's Hospital Los Angeles, Los Angeles, CA, United States, <sup>3</sup>Cardiology, University of Southern California/ Children's Hospital Los Angeles, Los Angeles, CA, United States

In this work we compare 2D phase contrast (PC) and pseudo continuous arterial spin labeling (PCASL) estimates in subjects with hyperemic cerebral blood flow. We found that B1 inefficiency dependent reductions in labeling efficiency and venous outflow of ASL tracer in PCASL leads to underestimation of PC CBF estimates.

679

9:03



### Cardiorespiratory noise correction improves the ASL signal

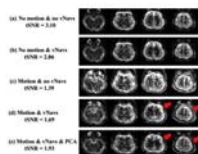
Mahlega S Hassanpour<sup>1</sup>, Qingfei Luo<sup>1</sup>, W. Kyle Simmons<sup>1,2</sup>, Justin S Feinstein<sup>1,2</sup>, Martin Paulus<sup>1</sup>, Wenming Luh<sup>3</sup>, Jerzy Bodurka<sup>1,4</sup>, and Sahib S Khalsa<sup>1,2</sup>

<sup>1</sup>Laureate Institute for Brain Research, Tulsa, OK, United States, <sup>2</sup>Oxley College of Health Sciences, University of Tulsa, <sup>3</sup>Cornell MRI Facility, Cornell University, <sup>4</sup>Stephenson School of Biomedical Engineering, University of Oklahoma

The use of ASL fMRI to study brain function is constrained by its low signal-to-noise ratio and large temporal signal variations. We evaluated the influence of cardiorespiratory activity on the amount of variance in resting state and task based ASL data via several different physiological noise models. We further tested the utility of physiological noise correction approaches by pharmacologically inducing cardiorespiratory fluctuations and evaluating for improvements in the ASL signal. We found that regressing out these non-neuronal, cardiorespiratory-related signal variations substantially improved the ASL signal, offering an important advance for quantitative studies of cognitive processes.

680

9:15



### Prospective motion correction for 3D GRASE pCASL with volumetric navigators

Xingfeng Shao<sup>1</sup>, M. Dylan Tisdall<sup>2</sup>, Danny JJ Wang<sup>1</sup>, and Andre Jan Willem van der Kouwe<sup>3,4</sup>

<sup>1</sup>Laboratory of FMRI Technology (LOFT), Mark & Mary Stevens Neuroimaging and Informatics Institute, Keck School of Medicine, University of Southern California, Los Angeles, CA, United States, <sup>2</sup>Radiology, Perelman School of Medicine, University of Pennsylvania, Philadelphia, PA, United States, <sup>3</sup>A. A. Martinos Center for Biomedical Imaging, Massachusetts General Hospital, Charlestown, MA, United States, <sup>4</sup>Radiology, Harvard Medical School, Boston, MA, United States

We propose a prospective motion correction approach for background suppressed (BS) segmented 3D GRASE pCASL using volumetric EPI-based navigators (vNavs), which causes minimal contrast change and no extra time. vNavs reduced motion artifacts effectively and increased temporal signal-to-noise ratio (t-SNR). Principle component analysis (PCA) is able to further reduce residual motion artifacts and restore the details of gyral structure in perfusion weighted images.

681

9:27



### A Calibrated Perfusion Phantom for Quality Assurance of Quantitative Arterial Spin Labelling.

Aaron Oliver-Taylor<sup>1</sup>, Miguel Gonçalves<sup>1</sup>, Thomas Hampshire<sup>1</sup>, Bradley Davis<sup>1</sup>, Pankaj Daga<sup>1</sup>, Laura Evans<sup>1</sup>, Alan Bainbridge<sup>2</sup>, Claudia Wheeler-Kingshott<sup>3</sup>, Magdalena Sokolska<sup>2</sup>, John Thornton<sup>4</sup>, Enrico De Vita<sup>4</sup>, and Xavier Golay<sup>1,3</sup>



<sup>1</sup>Gold Standard Phantoms Limited, London, United Kingdom, <sup>2</sup>Medical Physics and Biomedical Engineering, UCLH NHS Trust, London, United Kingdom, <sup>3</sup>Institute of Neurology, University College London, London, United Kingdom, <sup>4</sup>Lysolm Department of Neuroradiology, National Hospital for Neurology and Neurosurgery, London, United Kingdom

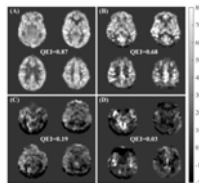
Arterial Spin Labelling shows great promise for perfusion measurements, however its clinical adoption is precluded by the lack of a standardised phantom to validate such measurements. A perfusion phantom specially designed and built for optimal use with clinical ASL sequences is presented, alongside characterisation results. Measurements of perfusion rate and arterial transit time were made using a multi-TI FAIR PASL sequence. Results indicate the phantom has good stability, high SNR and exhibits perfusion rates and arterial transit times that are comparable with human physiology.

682

9:39

### Automated Quality Evaluation Index for 2D ASL CBF Maps

Sudipto Dolui<sup>1,2</sup>, Ronald L. Wolf<sup>1</sup>, Seyed Ali Nabavizadeh<sup>1</sup>, David A. Wolk<sup>2</sup>, and John A. Detre<sup>1,2</sup>



<sup>1</sup>Department of Radiology, University of Pennsylvania, Philadelphia, PA, United States, <sup>2</sup>Department of Neurology, University of Pennsylvania, Philadelphia, PA, United States

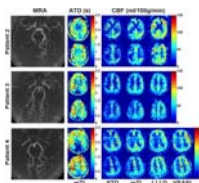
We propose an automated Quality Evaluation Index (QEI) for evaluating the quality of cerebral blood flow (CBF) maps obtained using arterial spin labeling (ASL). Agreement between the proposed QEI and human ratings was comparable to that between human ratings. Poor quality CBF maps as assessed by QEI significantly correlated with lower test-retest reliability of mean CBF in different regions of interest for elderly control subjects. The proposed QEI can potentially be used in large-scale studies to automatically identify and discard degraded data from analysis, thereby reducing human effort and potential user bias.

683

9:51

### Extreme ASL: Challenges and Solutions to Improve Perfusion Imaging in Patients with Markedly Prolonged Arterial Transit Delays

Jia Guo<sup>1</sup>, Audrey Fan<sup>1</sup>, Marc R. Lebel<sup>2</sup>, Samantha Holdsworth<sup>1</sup>, Ajit shankaranarayanan<sup>3</sup>, and Greg Zaharchuk<sup>1</sup>



<sup>1</sup>Radiology, Stanford University, Stanford, CA, United States, <sup>2</sup>GE Healthcare, Calgary, Canada, <sup>3</sup>GE Healthcare, Menlo Park, CA, United States



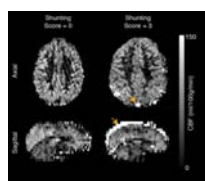


It is known that if labeling parameters are not properly adjusted in the presence of prolonged arterial transit delays (ATDs), perfusion may be underestimated using arterial spin labeling (ASL), yielding false negatives and possibly unnecessary interventions. In this study we evaluate the cases where the prolonged ATDs due to cerebrovascular disease posed challenges to perfusion quantification using ASL. Some possible solutions, which we term 'extreme ASL', were explored and discussed.

684



10:03



### Evidence of arteriovenous shunting in arterial spin labeling MRI in adults with sickle cell anemia

Meher R Juttukonda<sup>1</sup>, Manus J Donahue<sup>1</sup>, Melissa C Gindville<sup>2</sup>, Jeroen Hendrikse<sup>3</sup>, and Lori C Jordan<sup>2</sup>

<sup>1</sup>Radiology and Radiological Sciences, Vanderbilt University Medical Center, Nashville, TN, United States, <sup>2</sup>Pediatrics - Division of Pediatric Neurology, Vanderbilt University Medical Center, Nashville, TN, United States, <sup>3</sup>Radiology, University Medical Center Utrecht, Utrecht, Netherlands

High cervical arterial flow velocity may cause rapid erythrocyte transit through cerebral capillaries resulting in arteriovenous shunting, which may present as hyperintensities in pseudo-continuous arterial spin labeling (pCASL) MR difference images in draining veins. In an analysis of 36 adults with sickle cell anemia (SCA) and 11 age-matched controls, hyperintense superior sagittal sinus pCASL signal was present in 9% of controls and 61% of patients and correlated with elevated flow velocities. This shunting effect also trended with other markers of hemo-metabolic impairment in patients, such as elevated oxygen extraction fraction, elevated cerebral blood flow, and decreased blood hematocrit.

Oral

## Artificial Intelligence & Deep Learning

Room 311

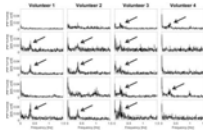
Wednesday 8:15 -  
10:15

Moderators: Daniel Alexander & Tim Leiner

8:15

Prediction of breathing related B0-field fluctuations via artificial neural networks trained on magnetic field monitoring data

685



Niklas Wehkamp<sup>1</sup>, Frederik Testud<sup>1,2</sup>, Patrick Hucker<sup>1</sup>, Stefan Kroboth<sup>1</sup>, Benjamin Richard Knowles<sup>1,3</sup>, Jürgen Henning<sup>1</sup>, and Maxim Zaitsev<sup>1</sup>

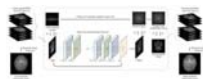
<sup>1</sup>Department of Radiology - Medical Physics, Medical Center – University of Freiburg, Freiburg, Germany, <sup>2</sup>Siemens Healthcare AB, Malmö, Sweden, <sup>3</sup>German Cancer Research Center, Heidelberg, Germany

The presented approach utilizes artificial neural networks trained on magnetic field monitoring data in order to predict respiration induced  $B_0$ -field fluctuations in the brain under the condition of normal breathing. From the predicted  $B_0$ -field fluctuations it is possible to distinguish the respiration induced resonance offset from the resonance offsets induced by other sources during the course of the experiment. This allows for the quantification of breathing related  $B_0$ -field fluctuations in the brain of normally breathing healthy volunteers. Furthermore it was observed that the  $B_0$ -field fluctuations resulting from normal respiration show individual spatial dynamics for every volunteer.

686



8:27



Deep Convolutional Neural Network for Acceleration of Magnetic Resonance Angiography (MRA)

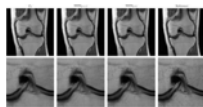
Yohan Jun<sup>1</sup>, Taejoon Eo<sup>1</sup>, Taeseong Kim<sup>1</sup>, Jinseong Jang<sup>1</sup>, and Dosik Hwang<sup>1</sup>

<sup>1</sup>Yonsei University, Seoul, Korea, Republic of

In this paper, we propose a deep CNN with skip connection for reconstruction of highly undersampled MRA images. According to the experiments, the proposed method could restore most of fine vessel structures manifested in full-sampled MRA images.

687

8:39



L2 or not L2: Impact of Loss Function Design for Deep Learning MRI Reconstruction

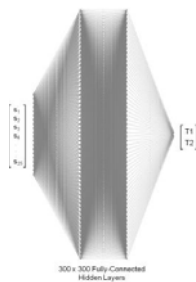
Kerstin Hammernik<sup>1</sup>, Florian Knoll<sup>2,3</sup>, Daniel K Sodickson<sup>2,3</sup>, and Thomas Pock<sup>1,4</sup>

<sup>1</sup>Institute of Computer Graphics and Vision, Graz University of Technology, Graz, Austria, <sup>2</sup>Center for Biomedical Imaging and Center for Advanced Imaging Innovation and Research (CAI2R), NYU School of Medicine, New York, NY, United States, <sup>3</sup>Department of Radiology, NYU School of Medicine, New York, NY, United States, <sup>4</sup>Safety & Security Department, AIT Austrian Institute of Technology GmbH, Vienna, Austria

Human radiologists gain experience from reading numerous MRI images to recognize pathologies and anatomical structures. To integrate this experience into deep learning approaches, two major components are required: We need both a suitable network architecture and a suitable loss function that measures the similarity between the reconstruction and the reference. In this work, we compare pixel-based and patch-based loss functions. We show that it is beneficial to consider other loss functions than the squared L2 norm to get a better representation of the human perceptual system and thus to preserve the texture in the tissue.

688

8:51



### Deep learning for fast MR Fingerprinting Reconstruction

Ouri Cohen<sup>1,2</sup>, Bo Zhu<sup>1,2</sup>, and Matthew S. Rosen<sup>1,3</sup>

<sup>1</sup>Athinoula A. Martinos Center, Charlestown, MA, United States,

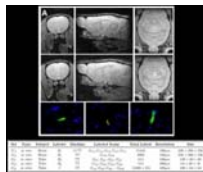
<sup>2</sup>Radiology, Massachusetts General Hospital, Boston, MA, United States,

<sup>3</sup>Physics, Harvard University, Cambridge, MA, United States

The exponential growth in the number of dictionary entries with increasing dictionary dimensions places a practical limit on the number of tissue parameters that may be simultaneously reconstructed. While a sparse sampling of some dimensions can mitigate the problem it also introduces significant errors into the reconstruction. In this work we demonstrate that Deep Learning methods can be used to train a compact neural network with sparse dictionaries without penalty on the reconstruction accuracy.

689

9:03



### Machine Learning for Intelligent Detection and Quantification of Transplanted Cells in MRI

Muhammad Jamal Afridi<sup>1</sup>, Arun Ross<sup>2</sup>, and Erik M Shapiro<sup>3</sup>

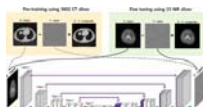
<sup>1</sup>Michigan State University, East Lansing, MI, United States, <sup>2</sup>Michigan State University, MI, United States, <sup>3</sup>Radiology, Michigan State University, MI, United States

Cell based therapy (CBT) is promising for treating a number of diseases. The ability to serially and non-invasively measure the number and determine the precise location of cells after delivery would aid both the research and development of CBT and also its clinical implementation. MRI-based cell tracking, employing magnetically labeled cells has been used for the past 20 years to enable detection of transplanted cells, achieving detection limits of individual cells, *in vivo*. These individual cells can be detected as dark spots in T2\* weighted MRI. Manual enumeration of these spots, and hence, counting cells, in an *in vivo* MRI is a tedious and highly time consuming task that is prone to inconsistency. Therefore, it becomes practically infeasible for an expert to conduct such manual enumeration for a very large scale analysis, consequentially affecting our ability to monitor CBT. To solve this challenge, we have designed a machine learning methodology for automatically quantifying transplanted cells in MRI in an accurate and efficient manner.

---

690

9:15



### Accelerated Projection Reconstruction MR imaging using Deep Residual Learning

Yo Seob Han<sup>1</sup>, Dongwook Lee<sup>1</sup>, JaeJun Yoo<sup>1</sup>, and Jong Chul Ye<sup>1</sup>

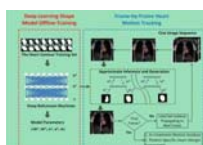
<sup>1</sup>KAIST, daejeon, Korea, Republic of

We propose a novel deep residual learning approach to reconstruct MR images from radial k-space data. We apply a transfer learning scheme that first pre-trains the network using large X-ray CT data set, and then performs a network fine-tuning using only a few MR data set. The proposed network clearly removes the streaking artifact better than other existing compressed sensing algorithm. Moreover, the computational speed is extremely faster than that of compressed sensing MRI.

---

691

9:27



### Deep Boltzmann Machines-Driven Method for In-treatment Heart Motion Tracking Using Cine MRI

Jian Wu<sup>1</sup>, Nalini Daniel<sup>1</sup>, Hilary Lashmett<sup>1</sup>, Thomas Mazur<sup>1</sup>, Michael Gach<sup>1</sup>, Laura Ochoa<sup>1</sup>, Imran Zoberi<sup>1</sup>, Su Ruan<sup>2</sup>, Mark Anastasio<sup>3</sup>, Sasa Mutic<sup>1</sup>, Maria Thomas<sup>1</sup>, and Hua Li<sup>1</sup>

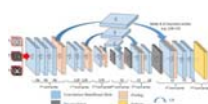
<sup>1</sup>Department of Radiation Oncology, Washington University in St. Louis, St. Louis, MO, United States, <sup>2</sup>Laboratoire LITIS, University of Rouen, France, <sup>3</sup>Department of Biomedical Engineering, Washington University in St. Louis, St. Louis, MO, United States

We developed a hierarchical deep learning shape model-driven method to automatically track the motion of the heart, a complex and highly deformable organ, on two-dimensional cine MRI images. The deep-learning shape model was trained based on a Deep Boltzmann Machine (DBM)<sup>1,2</sup> to characterize both global and local shape properties of the heart for accurate heart segmentation on each cine frame. Preliminary experimental results demonstrate the superior shape tracking performance of our proposed method versus two other methods. The tracking method is designed for heart motion pattern analysis during MRI-guided radiotherapy and the subsequent evaluation of potential heart toxicity from radiotherapy.

---

692

9:39



### Multi-modal Isointense Infant Brain Image Segmentation with Deep Learning based Methods

Dong Nie<sup>1,2</sup>, Li Wang<sup>1</sup>, Roger Trullo<sup>1</sup>, Ehsan Adeli<sup>1</sup>, Weili Lin<sup>1</sup>, and Dinggang Shen<sup>1</sup>

<sup>1</sup>Department of Radiology and BRIC, UNC-Chapel Hill, USA, Chapel Hill, NC, United States, <sup>2</sup>Department of Computer Science, UNC-Chapel Hill, USA, Chapel Hill, NC, United States

Accurate segmentation of infant brain images into different regions of interest is one of the most important fundamental steps in studying early brain development. In this paper, we propose a framework based on the recently well-received and prominent deep learning methods. Specifically, we propose a novel 3D multimodal fully convolutional network (FCN) architecture for segmentation of isointense phase brain MR images. Our proposed framework can model the brain tissue structures more accurately compared to the traditional methods. The conducted experiments show that our proposed 3D multimodal FCN model outperforms all previous methods by a large margin, in terms of segmentation accuracy.

---

693

9:51



### Fracture Risk Assessment using Deep Learning and Hip Microarchitecture MRI

Cem M Deniz<sup>1,2</sup>, Kyunghyun Cho<sup>3</sup>, Stephen Honig<sup>4</sup>, Kenneth A Egol<sup>5</sup>, Daniel K Sodickson<sup>1,2</sup>, and Gregory Chang<sup>6</sup>

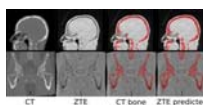
<sup>1</sup>Department of Radiology, Center for Advanced Imaging Innovation and Research (CAI2R) and Bernard and Irene Schwartz Center for Biomedical Imaging, New York University School of Medicine, New York, NY, United States, <sup>2</sup>The Sackler Institute of Graduate Biomedical Sciences, New York University School of Medicine, New York, NY, United States, <sup>3</sup>Courant Institute of Mathematical Sciences & Centre for Data Science, New York University, New York, NY, United States, <sup>4</sup>Osteoporosis Center, Hospital for Joint Diseases, NYU Langone Medical Center, New York, NY, United States, <sup>5</sup>Department of Orthopaedic Surgery, Hospital for Joint Diseases, NYU Langone Medical Center, New York, NY, United States, <sup>6</sup>Department of Radiology, Center for Musculoskeletal Care, New York University Langone Medical Center, New York, NY, United States

The identification of subjects with high risk of developing osteoporosis-related fracture remains challenging. In this project, we developed supervised convolutional neural networks for hip fracture risk identification using proximal femur MR microarchitecture images and patients' history of fragility fractures. We found that the proposed fracture risk assessment method provides superior discrimination of fragility fracture patients from controls compared to the current standard of care, DXA.

---

694

10:03



Deep Learning based pseudo-CT estimation using ZTE and Dixon MR images for PET attenuation correction

Sandeep Kaushik<sup>1</sup>, Dattesh Shanbhag<sup>1</sup>, Andrew Leynes<sup>2</sup>, Hariharan Ravishankar<sup>1</sup>, Jaewon Yang<sup>2</sup>, Peder Larson<sup>2</sup>, Thomas Hope<sup>2</sup>, and Florian Wiesinger<sup>3</sup>

<sup>1</sup>GE Global Research, Bangalore, India, <sup>2</sup>Department of Radiology and Biomedical Imaging, University of California, San Francisco, San Francisco, CA, United States, <sup>3</sup>GE Global Research, Garching b. Munchen, Germany

Simultaneous PET/MR is now being adapted for clinical studies. Earlier methods of PET/MR-AC have considered all bones as a single entity irrespective of their density. In this work, we demonstrate using ZTE and Dixon LAVA-Flex MRI data, and deep learning framework, a continuous density pseudo-CT (pCT) image which combines soft tissue pCT (from Dixon LAVA-Flex) with a continuous density bone pCT from ZTE.

---

---

# High-Resolution Brain Anatomy

Room 312

Wednesday 8:15 -  
10:15

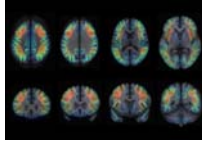
Moderators: Dimo Ivanov & Jennifer McNab

---

695



8:15



Interhemispheric differences of the U-shape fibre system in the human brain

Francisco De Santiago Requejo<sup>1</sup>, Pedro Luque-Laguna<sup>1</sup>, Ahmad Beyh<sup>1,2</sup>, Steven Williams<sup>1</sup>, Marco Catani<sup>1,2</sup>, and Flavio Dell'Acqua<sup>1,2</sup>

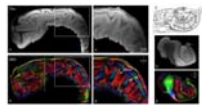
<sup>1</sup>Dept of Neuroimaging, King's College London, London, United Kingdom, <sup>2</sup>Dept of Forensic and Neurodevelopmental Sciences, King's College London, London, United Kingdom

The white matter of the human brain is mostly composed of myelinated axonal bundles connecting different brain regions. Within these tracts, U-shape fibres are short association connections that link adjacent gyri. Although they were first described by Meynert in the 19th century most of the mapping in the human brain has remained incomplete (Catani et al., 2012).

---

696

8:27



Laminar microstructure and subfield connectivity of the human hippocampus revealed with ultra-high field diffusion MRI at 11.7T

Manisha Aggarwal<sup>1</sup>, Priya Sathyanarayan<sup>2</sup>, and David W. Nauen<sup>3</sup>

<sup>1</sup>Department of Radiology, Johns Hopkins University, Baltimore, MD, United States, <sup>2</sup>Department of Biomedical Engineering, Johns Hopkins University, Baltimore, MD, United States, <sup>3</sup>Department of Pathology, Johns Hopkins University, Baltimore, MD, United States

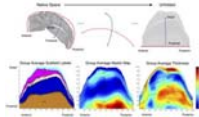
In this work, we demonstrate high-field (11.7T) 3D diffusion MRI (dMRI) of the fixed human hippocampal formation to investigate its internal organization. The results of this study show delineation of fine hippocampal microstructure and inner connectivity of the human hippocampal subfields based on HARDI. Further, we demonstrate 3D reconstruction of intra-hippocampal subfield connectivity, e.g. the trisynaptic hippocampal circuit, using fODF-based probabilistic tractography with combined high spatial and angular resolution, which has important future applications for mapping of pathology-induced changes in the hippocampus in Alzheimer's disease and related neurological disorders.

---



697

8:39



### Unfolded hippocampal coordinate system for quantitative mapping and subfield segmentation

Jordan DeKraker<sup>1</sup>, Kayla Ferko<sup>1</sup>, Jonathan Lau<sup>2</sup>, Stefan Köhler<sup>1</sup>, and Ali R. Khan<sup>2</sup>

<sup>1</sup>Brain and Mind Institute, Western University, London, ON, Canada,

<sup>2</sup>Robarts Research Institute, Western University, London, ON, Canada

This work presents a novel computational technique for unfolding the hippocampus, providing a smooth and consistent mapping from native 3D space to a common coordinate system that is intrinsically defined by hippocampal anatomy. This coordinate system allows for laminar-based sampling of quantitative volumetric data and a means to pool data across subjects without additional registration or warping. We demonstrate the value of this technique with data from a set of healthy young participants scanned at 7T, taking advantage of high-resolution isotropic imaging for visualizing intra-hippocampal features, and employ a single surgical patient case with histology for validation.

698

8:51



### Segmentation of the Human Nucleus Accumbens Using High-Resolution Diffusion Tractography

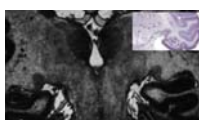
Samuel Cartmell<sup>1</sup>, Qiyuan Tian, Grant Yang, Christoph Leuze, Jennifer McNab, and Casey Harrison Halpern

<sup>1</sup>Stanford University, Palo Alto, CA, United States

Tractography-based parcellation of the Nucleus Accumbens (NAc) was performed using high-resolution diffusion data from the Human Connectome Project. Analysis of clustering indicated the NAc was best separated into 2 subregions, consistent with anatomical and histological studies of animals. Output of the procedure gave qualitatively similar results across subjects, producing clusters that tended to occupy the ventromedial and dorsolateral portions of the NAc. The ventromedial subregion demonstrated increased task fMRI activation and displayed preferential connections to known biased projection areas such as medial orbitofrontal cortex. Finally, qualitatively similar results were obtained by performing the clustering procedure on a separate, lower-quality dataset.

699

9:03



### Optimization of Lateral Geniculate Nucleus Volume Determination at 3T and 7T

Njoud Aldusary<sup>1,2</sup>, Lars Michels<sup>1</sup>, Birgit Keisker<sup>1</sup>, Michael Wyss<sup>3</sup>, Karen Huebel<sup>1</sup>, Arwa Baeshen<sup>1,2</sup>, David Otto Brunner<sup>3</sup>, Klaas Paul Pruessmann<sup>3</sup>, Klara Landau<sup>4</sup>, Spyridon Kollias<sup>1</sup>, and Marco Piccirelli<sup>1</sup>

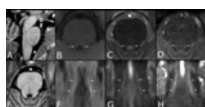
<sup>1</sup>Neuroradiology, University Hospital Zurich, Zurich, Switzerland, <sup>2</sup>King Abdulaziz University, Jedaah, Saudi Arabia, <sup>3</sup>Inst. for Biomed. Eng., University and ETH Zurich, Zurich, Switzerland, <sup>4</sup>Ophthalmology, University Hospital Zurich, Zurich, Switzerland

The clinical 2D PD scans and the research very high resolution 3D T1 scans used to determine the lateral geniculate nucleus (LGN) have high contrast respectively high resolution, but too low resolution respectively too long acquisition time. Nevertheless, volumetric and contrast quantification of the LGN and of other brain tissues might increase in clinical relevance. Therefore, we optimized the contrast of 3D T1 MPRAGE to obtain the best contrast with sufficient resolution to quantify volume and contrast of the LGN.

---

700

9:15



In vivo imaging of human Locus coeruleus at 3 and 7 Tesla

Nikos Priovoulos<sup>1</sup>, Heidi IL Jacobs<sup>1,2</sup>, Dimo Ivanov<sup>2</sup>, Kamil Uludag<sup>2</sup>, Frans Verhey<sup>1</sup>, and Benedikt A Poser<sup>2</sup>

<sup>1</sup>Faculty of Health and Medicine, Maastricht University, Maastricht, Netherlands, <sup>2</sup>Faculty of Physiology and Neuroscience, Maastricht University, Maastricht, Netherlands

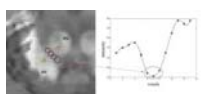
Structural and functional alterations of the Locus coeruleus (LC) are implicated in various neurological diseases, including Alzheimer's.

Current standard spin-echo based approaches to imaging the LC suffer from several limitations at 3T, including long acquisition time and highly anisotropic resolution. In this study, we have evaluated in healthy human subjects different MRI contrasts both at 3 and 7 Tesla to image LC. We show that visualization of the locus coeruleus is best achieved with magnetization transfer contrast at 7T superior to standard T1- and T2-weighted methods.

---

701

9:27



A seed point discontinuity-based level set method for accurate substantia nigra and red nucleus segmentation in QSM images

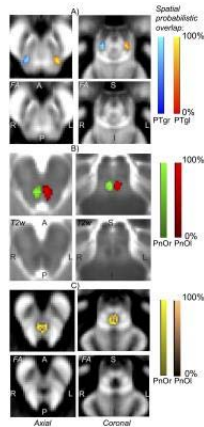
Tian Guo<sup>1</sup>, Binshi Bo<sup>1</sup>, Xinxin Zhao<sup>1</sup>, Xu Yan<sup>2</sup>, Yang Song<sup>1</sup>, Caixia Fu<sup>3</sup>, Dongya Huang<sup>4</sup>, Hedi An<sup>4</sup>, Nan Shen<sup>4</sup>, Yi Wang<sup>5</sup>, Jianqi Li<sup>1</sup>, and Guang Yang<sup>1</sup>

<sup>1</sup>Department of Physics, Shanghai Key Laboratory of Magnetic Resonance, East China Normal University, Shanghai, People's Republic of China, <sup>2</sup>MR Collaboration NE Asia, Siemens Healthcare, Shanghai, People's Republic of China, <sup>3</sup>Siemens Shenzhen Magnetic Resonance Ltd., Shenzhen, People's Republic of China, <sup>4</sup>Department of Neurology, East Hospital Affiliated to Tongji University, Shanghai, People's Republic of China, <sup>5</sup>Department of Radiology, Weill Medical College of Cornell University, New York, United States

Accurate segmentation of substantia nigra (SN) and red nucleus (RN) in quantitative susceptibility mapping (QSM) images has great clinical value in quantifying iron deposition and measuring disease severity. We propose a new segmentation algorithm which uses the discontinuity of seed points in different tissues as prior knowledge. Seed points in SN or RN can be obtained from standard atlas or specified manually. This prior was then incorporated into level set method to segment SN and RN. Experiments on in-vivo MR images showed that the proposed method achieved more accurate segmentation results than the atlas-based method and classic level-set method.

702

9:39



In vivo 7 Tesla probabilistic neuroimaging structural atlas of human pedunculotegmental, oral pontine reticular and paramedian-raphe nuclei

Marta Bianciardi<sup>1</sup>, Christian Strong<sup>2</sup>, Nicola Toschi<sup>1,3</sup>, Brian Edlow<sup>4</sup>, Bruce Fischl<sup>1</sup>, Emery N Brown<sup>5</sup>, Bruce R Rosen<sup>1</sup>, and Lawrence L Wald<sup>1</sup>

<sup>1</sup>Department of Radiology, A.A. Martinos Center for Biomedical Imaging, MGH and Harvard Medical School, Boston, MA, United States,

<sup>2</sup>Department of Neurosurgery, Brigham and Women's Hospital and Harvard Medical School, Boston, MA, United States, <sup>3</sup>Medical Physics Section, Department of Biomedicine and Prevention, Faculty of

Medicine, University of Rome "Tor Vergata", Rome, Italy, <sup>4</sup>Department of Neurology, A. A. Martinos Center for Biomedical Imaging, MGH and Harvard Medical School, Boston, MA, United States, <sup>5</sup>Department of

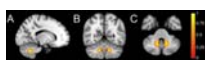
Anesthesia, Critical Care and Pain Medicine, MGH, Boston, MA, United States

States

Mesopontine-tegmental nuclei such as the pedunculotegmental, oral-pontine-reticular and paramedian-raphé nuclei modulate arousal and motor functions. Dysfunction of these nuclei is implicated in the pathogenesis of disorders of consciousness, sleep disorders, and neurodegenerative diseases. However, a stereotaxic probabilistic atlas of these nuclei in humans does not exist. We used segmentation of 1.1 mm-isotropic 7 Tesla diffusion-fractional-anisotropy and T2-weighted images to generate and validate an in vivo probabilistic neuroimaging structural atlas of these nuclei in MNI space. We constructed this atlas to aid the localization of these nuclei in conventional images in future research and clinical studies of arousal and motor functions.

703

9:51



### An Improved Probabilistic Atlas of the Dentate Nucleus Derived with QSM

Naying He<sup>1,2</sup>, Jason Langley<sup>3</sup>, Daniel E Huddleston<sup>4</sup>, Huawei Ling<sup>5</sup>, Hongmin Xu<sup>5</sup>, Chunlei Liu<sup>6</sup>, Yong Zhang<sup>7</sup>, Fuhua Yan<sup>8</sup>, and Xiaoping Hu<sup>9,10</sup>

<sup>1</sup>Radiology, Ruijin Hospital, Shanghai Jiao Tong University School of Medicine, Shanghai, People's Republic of China, <sup>2</sup>Center for Advanced Neuroimaging, University of California, Riverside, Riverside, CA, United States, <sup>3</sup>Center for Advanced Neuroimaging, University of California Riverside, Riverside, CA, United States, <sup>4</sup>the department of Neurology, Emory School of Medicine, Atlanta, GA, United States, <sup>5</sup>Radiology, Ruijin Hospital, Shanghai Jiao Tong University School of Medicine, <sup>6</sup>Electrical Engineering and Computer Sciences, University of California, Berkeley, CA, United States, <sup>7</sup>MR Research, GE Healthcare, Shanghai, People's Republic of China, <sup>8</sup>Radiology, Ruijin Hospital, Shanghai Jiao Tong University School of Medicine, Shanghai, People's Republic of China, <sup>9</sup>Center for Advanced Neuroimaging, University of California, Riverside, CA, United States, <sup>10</sup>Bioengineering, University of California, Riverside, Riverside, CA, United States

Prior dentate nucleus (DN) atlases were derived using T<sub>1</sub>-, T<sub>2</sub>\*- or susceptibility-weighted imaging. Accurate delineation of the DN boundary is difficult in these images. We present an atlas derived from quantitative susceptibility maps, which exhibit better contrast between DN and surrounding cerebellum tissue. An improved delineation of DN boundaries was achieved, resulting in increased maximum overlap in our DN atlas as compared to previously published results. We anticipate the atlas to be used in a variety of imaging applications ranging from functional imaging of DN to measuring DN iron deposition arising from disease.

---

704

10:03



Measurements of cardiac related pulsatile volumetric strain in grey and white matter brain tissue with high resolution DENSE at 7T

Ayodeji Adams<sup>1</sup>, Peter R Luijten<sup>1</sup>, and Jaco J.M Zwanenburg<sup>1</sup>

*<sup>1</sup>Department of Radiology, University Medical Center Utrecht, Utrecht, Netherlands*

The aim of this study was to investigate the cardiac induced volumetric strain differences between grey and white matter at 7T with DENSE in young, healthy volunteers, which may provide information on properties of the microvasculature. Increasing volumetric strain was seen in the systolic phase of the heart. The average strain in the grey matter was larger compared to white matter, but this was not significant. Measuring whole brain volumetric strain is feasible with DENSE at 7T, and has the potential to assess microvascular function (passive swelling over the cardiac cycle) in various brain areas.

---

Oral

## Brain Tumor Imaging

Room 313A

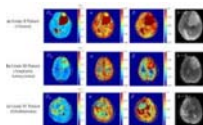
Wednesday 8:15 -  
10:15

Moderators: Janine Lupo & Tomohisa Okada

---

705

8:15



Towards Glioma Grading Using Non-Gaussian Diffusion Imaging with a Continuous-time Random Walk Model and A Quantile Histogram Analysis

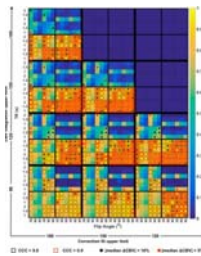
Muge Karaman<sup>1</sup>, Jiaxuan Zhang<sup>1,2</sup>, Zheng Zhong<sup>1,3</sup>, Kejia Cai<sup>1,4</sup>, Wenzhen Zhu<sup>2</sup>, and Xiaohong Joe Zhou<sup>5</sup>

*<sup>1</sup>Center for MR Research, University of Illinois at Chicago, Chicago, IL, United States, <sup>2</sup>Department of Radiology, Tongji Hospital, Tongji Medical College, Huazhong University of Science and Technology, People's Republic of China, <sup>3</sup>Department of Bioengineering, Chicago, IL, United States, <sup>4</sup>Department of Bioengineering, University of Illinois at Chicago, Chicago, IL, United States, <sup>5</sup>Departments of Radiology, Neurosurgery, and Bioengineering, University of Illinois at Chicago, IL, United States*

Gliomas are the most common primary tumors of the central nervous system. As surgical biopsy may not be always feasible, an accurate noninvasive glioma grading is highly desirable for planning treatments. Recently, a number of non-Gaussian diffusion models were developed to characterize the anomalous diffusion behavior of the complex biological tissue. Among these, the continuous-time random walk (CTRW) model showed a great potential to probe the tissue heterogeneity and complexity that is elevated with tumor progression. In this study, we show that the CTRW parameters are capable of differentiating glioma grades, beyond simply separating low-grade and high-grade as in many diffusion MR studies on gliomas.

706

8:27



Optimization of acquisition and analysis methods for clinical dynamic susceptibility contrast (DSC) MRI using a validated digital reference object

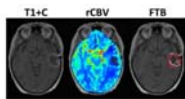
Natnael B Semmineh<sup>1</sup>, Ashley M Stokes<sup>1</sup>, Laura C Bell<sup>1</sup>, Jerrold L Boxerman<sup>2</sup>, C Chad Quarles<sup>1</sup>, and Natnael B Semmineh<sup>3</sup>

<sup>1</sup>Translational Bioimaging, Barrow Neurological Institute, Phoenix, AZ, United States, <sup>2</sup>Diagnostic Imaging, Rhode Island Hospital, Providence, RI, United States, <sup>3</sup>imaging research, Barrow Neurological Institute, Phoenix, AZ, United States

Brain tumor DSC-MRI studies can be confounded by T1 and T2\* effects that occur when the contrast agent extravasates. Traditionally a combination of contrast agent pre-loading and leakage correction techniques are used to minimize T1 leakage effects, but currently there is no consensus on the most robust dosing scheme. Using a validated DSC-MRI digital reference object we characterize the influence of pre-load dosing schemes, acquisition pulse parameters, and leakage correction methods on CBV accuracy. Our goal is to leverage this computational approach to identify the optimal combination of parameters for brain tumor CBV mapping.

707

8:39



MRI-perfusion derived fractional tumor burden (FTB) is predictive of overall and progression free survival in newly diagnosed glioblastoma following concomitant chemoradiotherapy

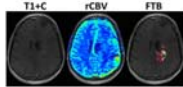
Melissa A Prah<sup>1</sup>, Jennifer M Connelly<sup>2</sup>, and Kathleen M Schmainda<sup>1,3</sup>

<sup>1</sup>Radiology, Medical College of Wisconsin, Milwaukee, WI, United States, <sup>2</sup>Neurology, Medical College of Wisconsin, Milwaukee, WI, United States, <sup>3</sup>Biophysics, Medical College of Wisconsin, Milwaukee, WI, United States

The phenomenon of pseudoprogression (PsP) on standard imaging can make response assessment difficult in patients with glioblastoma who have undergone standard chemoradiation treatment (CRT). PsP mimics tumor progression on standard imaging, yet is thought to represent a positive biological response to treatment. Recent efforts to define rCBV thresholds to distinguish tumor from treatment effect has enabled the creation of fractional tumor burden (FTB) maps. FTB maps quantify the percent of tumor within an enhancing lesion. This study shows that, within 4-months post-CRT, FTB is a better indicator of PFS and OS than median rCBV or methylation status alone.

708

8:51



MRI-perfusion derived Fractional Tumor Burden (FTB) stratifies survival in recurrent glioblastoma following treatment with bevacizumab

Melissa A Prah<sup>1</sup>, Jennifer M Connelly<sup>2</sup>, Scott D Rand<sup>1</sup>, and Kathleen M Schmainda<sup>1,3</sup>

<sup>1</sup>Radiology, Medical College of Wisconsin, Milwaukee, WI, United States, <sup>2</sup>Neurology, Medical College of Wisconsin, Milwaukee, WI, United States, <sup>3</sup>Biophysics, Medical College of Wisconsin, Milwaukee, WI, United States

Imaging response, in patients with recurrent glioblastoma (rGBM) who are treated with bevacizumab (which decreases vascular permeability), is often difficult to assess since decreased contrast agent uptake might falsely underestimate lesion size or biologic activity. Alternatively, relative cerebral blood volume (rCBV) has shown promise to identify true responders. Fractional tumor burden (FTB) maps, which are derived from rCBV, allow spatially quantifiable characterization of rGBM within lesion enhancement, and therefore may provide additional value to post-treatment response-assessment. This work demonstrates that patients with less than 75% FTB following treatment with bevacizumab have a clear progression-free and overall survival benefit.

709

9:03



Improvement in Diagnostic Accuracy and Reliability of Pharmacokinetic Parameters from DCE MR Imaging by using Arterial Input Function Obtained from DSC MR imaging: Differentiation of High Grade Glioma from Low Grade Glioma.



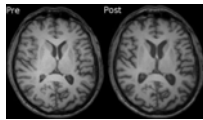
Sung-Hye You<sup>1</sup> and Seung Hong Choi<sup>1</sup>

<sup>1</sup>Department of Radiology, Seoul National University Hospital, Seoul, Korea, Republic of

The aim of this study was to compare two AIFs derived from DCE (AIF<sub>DCE</sub>) and DSC MR imaging (AIF<sub>DSC</sub>) in terms of the diagnostic accuracy and reliability of pharmacokinetic parameters from DCE MRI for differentiation of high grade from low grade glioma. This retrospective study included 70 patients with pathologically confirmed gliomas. In all of the patients, we performed preoperative DSC and DCE MRI, and two AIFs (AIF<sub>DSC</sub> and AIF<sub>DCE</sub>) were obtained from each image. Pharmacokinetic parameters ( $K_{trans}$ ,  $V_p$ , and  $V_e$ ) were processed. DCE MRI parameters obtained using AIF<sub>DSC</sub> showed better accuracy and reliability than those derived from AIF<sub>DCE</sub>.

710

9:15



Brain volume loss in glioblastoma patients following photon and proton radiochemotherapy

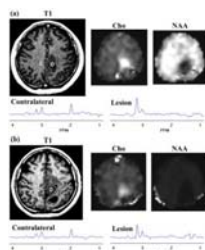
Jan Petr<sup>1</sup>, Frank Hofheinz<sup>1</sup>, Andreas Gommlich<sup>2,3,4</sup>, Felix Raschke<sup>2</sup>, Esther Troost<sup>2,3,5,6,7</sup>, Bettina Beuthien-Baumann<sup>1,8</sup>, Annetrin Seidlitz<sup>2,5,6,7</sup>, Ivan Platzek<sup>9</sup>, Michael Baumann<sup>2,3,5,6,7</sup>, Mechthild Krause<sup>2,3,5,6,7</sup>, and Jörg van den Hoff<sup>1,8</sup>

<sup>1</sup>PET center, Institute of Radiopharmaceutical Cancer Research, Helmholtz-Zentrum Dresden-Rossendorf, Dresden, Germany, <sup>2</sup>OncoRay – National Center for Radiation Research in Oncology, Faculty of Medicine and University Hospital Carl Gustav Carus, Dresden, Germany, <sup>3</sup>Institute of Radiooncology, Helmholtz-Zentrum Dresden-Rossendorf, Dresden, Germany, <sup>4</sup>NCT - National Center for Tumor Disease, Dresden, Germany, <sup>5</sup>Department of Radiation Oncology, Faculty of Medicine and University Hospital Carl Gustav Carus, Technical University Dresden, Dresden, Germany, <sup>6</sup>German Cancer Consortium (DKTK), Dresden, Germany, <sup>7</sup>German Cancer Research Center (DKFZ), Heidelberg, Germany, <sup>8</sup>Department of Nuclear Medicine, University Hospital Carl Gustav Carus, Technical University Dresden, Dresden, Germany, <sup>9</sup>Department of Radiology, University Hospital Carl Gustav Carus, Technical University Dresden, Dresden, Germany

Gray matter (GM) atrophy in healthy brain tissue following radiochemotherapy was shown in brain-tumor patients in several studies. Here, we aimed to study GM and white matter (WM) changes in glioblastoma patients undergoing photon (n=43) and proton (n=12) radiochemotherapy. In photon-therapy patients, a statistically significant decrease of both GM (~2%) and WM (1.3-2.3%) volume was found with a positive influence of the RT-dose on the GM volume loss. In proton-therapy patients, no significant changes in GM and WM volumes were observed after therapy. This indicates that the proton-therapy has the potential to reduce structural GM changes in healthy tissue.

711

9:27



Volumetric 3D analysis of high grade glioma at pre- and post-radiation therapy by magnetic resonance echo-planar spectroscopic imaging

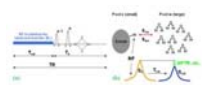
Yanqin Lin<sup>1</sup>, Doris Lin<sup>2</sup>, Karim Snoussi<sup>2</sup>, Anouk Marsman<sup>2</sup>, Andrew A. Maudsley<sup>3</sup>, Sulaiman Sheriff<sup>3</sup>, Katie Link<sup>2</sup>, Peter B. Barker<sup>2,4</sup>, and Lawrence Kleinberg<sup>5</sup>

<sup>1</sup>Department of Electronic Science, Xiamen University, Xiamen, People's Republic of China, <sup>2</sup>Department of Radiology and Radiological Science, Johns Hopkins University School of Medicine, Baltimore, MD, United States, <sup>3</sup>Department of Radiology, University of Miami, Miami, FL, United States, <sup>4</sup>F.M. Kirby Center for Functional Brain Imaging, Kennedy Krieger Institute, Baltimore, MD, United States, <sup>5</sup>Department of Radiation Oncology & Molecular Radiation Sciences, Sidney Kimmel Comprehensive Cancer Center, Johns Hopkins University School of Medicine, Baltimore, MD, United States

31 patients with high grade glioma were recruited at both pre- and post-radiation therapy. 3D EPSI was employed on a Siemens 1.5 T scanner. NAA and Cho in lesion are normalized to Cr at contralateral part. At pre-radiation, Cho/Cr at lesion is significantly higher than that in contralateral part ( $p = 0.003$ ). From pre- to post-radiation, Cho/Cr at lesion is significantly decreased ( $p < 0.007$ ). Elevated Cho level can be an indicator for residual glioma tumor after surgery. Cho/Cr ratio can be used to monitor the treatment response. EPSI technique can be a promising way to monitor treatment response.

712

9:39



Differentiating Recurrent Glioma from Treatment Effects Using Amide Proton Transfer-Weighted MRI

Shanshan Jiang<sup>1</sup>, Yi Zhang<sup>1</sup>, Hye-Young Heo<sup>1</sup>, Peter Van Zijl<sup>1,2</sup>, and Jinyuan Zhou<sup>1,2</sup>

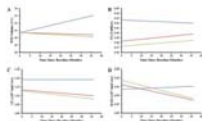
<sup>1</sup>Department of Radiology, Johns Hopkins University School of Medicine, Baltimore, MD, United States, <sup>2</sup>F.M. Kirby Research Center for Functional Brain Imaging, Kennedy Krieger Institute, Baltimore, MD, United States

We assess the feasibility and the value of amide proton transfer-weighted (APT<sub>w</sub>) MRI in identifying viable malignant glioma. 22 patients with suspected recurrent glioma following chemoradiation were scanned at 3T. A total of 64 stereotactic biopsy specimens were obtained from gadolinium-enhancing regions of interest with varying APT<sub>w</sub> signals, 47 of which were histopathologically assigned as recurrent tumor and 17 treatment effects. APT<sub>w</sub> MRI revealed different signal intensities in the biopsied sites showing recurrent tumor (hyperintense signal) or treatment effects (iso-intense to minimally hyperintense signal). APT<sub>w</sub> signal intensity identified recurrent tumor with 97.9% sensitivity and 88.2% specificity.

---

713

9:51



#### Disrupted Integrity of Frontal White Matter and Neurocognitive Correlates in Patients Treated for Pediatric Medulloblastoma

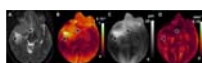
John O Glass<sup>1</sup>, Robert J Ogg<sup>1</sup>, Jung W Hyun<sup>2</sup>, Julie H Harreld<sup>1</sup>, Jane E Schreiber<sup>3</sup>, Yimei Li<sup>2</sup>, Amar J Gajjar<sup>4</sup>, and Wilburn E Reddick<sup>1</sup>

<sup>1</sup>Diagnostic Imaging, St. Jude Children's Research Hospital, Memphis, TN, United States, <sup>2</sup>Biostatistics, St. Jude Children's Research Hospital, Memphis, TN, United States, <sup>3</sup>Psychology, St. Jude Children's Research Hospital, Memphis, TN, United States, <sup>4</sup>Oncology, St. Jude Children's Research Hospital, Memphis, TN, United States

This study assessed the longitudinal white matter (WM) microstructure of 146 patients and 72 normal healthy age-similar controls. WM volume, fractional anisotropy (FA), and radial (RAD) and axial (AX) diffusivity trajectories were examined and correlated with neurocognitive performance at 36 months. After surgery but before any additional therapy, frontal WM volume in patients was similar to controls but FA was significantly reduced and was significantly correlated with neurocognitive performance three years later. Over the next three years, WM volume significantly decreased in patients and was significantly correlated with decreased Working Memory.

---

10:03



Improved prediction of meningioma-brain adhesion with normalized octahedral shear strain using slip interface imaging based on MR-elastography



Ziying Yin<sup>1</sup>, Joshua D Hughes<sup>2</sup>, Joshua D Trzasko<sup>1</sup>, Kevin J Glaser<sup>1</sup>, Armando Manduca<sup>3</sup>, Jamie J Van Gompel<sup>2</sup>, Michael J Link<sup>2</sup>, Anthony Romano<sup>4</sup>, Richard L Ehman<sup>1</sup>, and John Huston III<sup>1</sup>

<sup>1</sup>Radiology, Mayo Clinic, Rochester, MN, United States, <sup>2</sup>Neurosurgery, Mayo Clinic, MN, United States, <sup>3</sup>Physiology and Biomedical Engineering, Mayo Clinic, MN, United States, <sup>4</sup>Naval Research Laboratory, Code 7160, Washington, DC

Knowledge of meningioma-brain adhesion can be important to surgical outcome but has been reliably assessed only during surgery. Slip interface imaging (SII), a recently developed MR-elastography based technique, is capable of determining the degree of meningioma-brain adhesion preoperatively. In SII, a non-adherent meningioma demonstrates a hyper-intense octahedral shear strain (OSS) contour along the tumor-brain interface. In 25 meningiomas, an algorithm improved by normalizing OSS to the combined wave amplitude provided a more accurate prediction in the setting of peritumoral edema. Normalized OSS increased SII accuracy from 72% to 92%, and the kappa coefficient increased from 0.37 (fair) to 0.86 (good).

## Oral

### Gray Matter Diffusion Studies

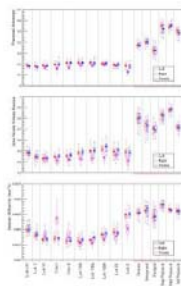
Room 313BC

Wednesday 8:15 -  
10:15

Moderators: Andrada Ianus & Michiel  
Kleinnijenhuis



8:15



#### Characterisation of cerebellar microstructure with two-compartment Spherical Mean Technique

Giovanni Savini<sup>1,2</sup>, Fulvia Palesi<sup>2,3</sup>, Gloria Castellazzi<sup>2,4</sup>, Letizia Casiraghi<sup>2,5</sup>, Francesco Grussu<sup>6</sup>, Alessandro Lascialfari<sup>1,3</sup>, Egidio D'Angelo<sup>2,5</sup>, and Claudia AM Gandini Wheeler-Kingshott<sup>5,6,7</sup>

<sup>1</sup>Department of Physics, University of Milan, Milan, Italy, <sup>2</sup>Brain Connectivity Center, C. Mondino National Neurological Institute, Pavia, Italy, <sup>3</sup>Department of Physics, University of Pavia, Pavia, Italy, <sup>4</sup>Department of Electrical, Computer and Biomedical Engineering, University of Pavia, Pavia, Italy, <sup>5</sup>Department of Brain and Behavioral Sciences, University of Pavia, Pavia, Italy, <sup>6</sup>Queen Square MS Centre, Department of Neuroinflammation, UCL Institute of Neurology, University College London, London, United Kingdom, <sup>7</sup>Brain MRI 3T Mondino Research Center, C. Mondino National Neurological Institute, Pavia, Italy

Cerebrum microstructure has been extensively investigated with diffusion-weighted MRI, but little attention has been dedicated to the microstructural characterisation of the cerebellum.

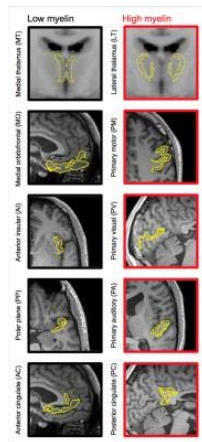
We considered an anatomical parcellation of the cerebellum and fitted a multi-compartment model to diffusion data exploiting the spherical mean technique, which provides parametric maps unconfounded by the underlying fibre orientation distribution. For each region we report average values for multi-compartment parameters (e.g. intra-neurite volume fraction and intrinsic diffusivity) and diffusion tensor metrics.

Multi-compartment metrics more specific to microstructure provide information complementary to diffusion tensor metrics in the cerebellum, thus giving new insights about microstructural correlations between regions.

716



8:27



Microscopic anisotropy in gray matter is evidence of myelinated axons but not dendrites? An in vivo study using diffusion MRI with variable shape of the b-tensor.

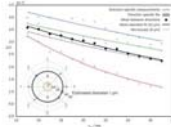
Björn Lampinen<sup>1</sup>, Filip Szczepankiewicz<sup>1</sup>, Mikael Novén<sup>2</sup>, Carl-Fredrik Westin<sup>3</sup>, Elisabet Englund<sup>4</sup>, Johan Mårtensson<sup>5</sup>, and Markus Nilsson<sup>6</sup>

<sup>1</sup>Clinical Sciences Lund, Medical Radiation Physics, Lund University, Lund, Sweden, <sup>2</sup>Centre for Languages and Literature, Lund University, Lund, Sweden, <sup>3</sup>Brigham and Women's Hospital, Harvard Medical School, Boston, MA, United States, <sup>4</sup>Clinical Sciences Lund, Oncology and Pathology, Lund University, Lund, Sweden, <sup>5</sup>Department of Psychology, Faculty of Social Science, Lund University, Lund, Sweden, <sup>6</sup>Clinical Sciences Lund, Radiology, Lund University, Lund, Sweden

Microscopic anisotropy was measured in vivo using a novel tensor-valued diffusion encoding approach. In gray matter, the microscopic anisotropy was generally low, but its variation corresponded well to known differences in myelination. We hypothesize that myelinated axons cause microscopic diffusion anisotropy but that the contribution from dendrites is negligible. This hypothesis is supported by comparisons with independent myelin assessments using T1W/T2W-ratios, T2-mapping, and myelin stains from histology. We also demonstrate that the "neurite density index" detected by NODDI is less sensitive to these changes, and why NODDI cannot map the neurite density accurately.

717

8:39



Pore size estimation using the mixing time dependence of a double diffusion encoding experiment: experimental validation on a clinical MR system

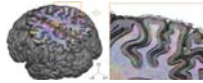
Vincent Methot<sup>1</sup>, Patricia Ulloa<sup>1</sup>, and Martin A. Koch<sup>1</sup>

<sup>1</sup>University of Luebeck, Luebeck, Germany

Diffusion MRI provides information about microstructure, but is limited in complex situations. Double diffusion encoding makes assessment of shape and size possible in these contexts. The time delay (mixing time) between diffusion encodings has not been studied closely outside of the short and long regimes. We present here an experimental study of the mixing time dependence. In spherical pores, the parallel-antiparallel signal difference can be approximately described as an exponential decay with a rate related to diameter. This decay was obtained on a clinical scanner in a water-in-oil emulsion.

718

8:51



Layer-specific analysis of cortical microstructure using in-vivo 7T diffusion MRI

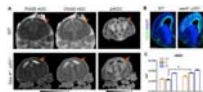
Omer Faruk Gülban<sup>1</sup>, Federico De Martino<sup>1</sup>, An Thanh Vu<sup>2</sup>, Kamil Ugurbil<sup>3</sup>, Essa Yacoub<sup>3</sup>, and Christophe Lenglet<sup>3</sup>

<sup>1</sup>Department of Cognitive Neuroscience, Maastricht University, Maastricht, Netherlands, <sup>2</sup>Center for Imaging of Neurodegenerative Diseases, Veterans Affairs Health Care System, San Francisco, CA, United States, <sup>3</sup>Center for Magnetic Resonance Research, University of Minnesota, Minneapolis, MN, United States

We present unique in-vivo human 7T diffusion MRI data and a dedicated layer-specific analysis pipeline. We leverage the high spatial and angular resolution of this dataset to improve cortical fiber orientation mapping (i.e. limit gyral bias and identify fiber crossings), and study axonal trajectories within the cortex across depths.

719

9:03



HARDI and oscillating gradient diffusion MRI reveal disrupted embryonic cortical microstructure

Dan Wu<sup>1</sup>, Wei Shao<sup>2,3</sup>, Songhai Shi<sup>2,3,4</sup>, and Jiangyang Zhang<sup>5</sup>



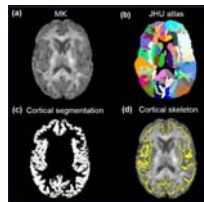
<sup>1</sup>Radiology, Johns Hopkins University School of Medicine, BALTIMORE, MD, United States, <sup>2</sup>BCMB Allied Graduate Program, Weill Cornell Graduate School of Medical Sciences, <sup>3</sup>Developmental Biology Program, Memorial Sloan Kettering Cancer Center, <sup>4</sup>Graduate Program in Neuroscience, Weill Cornell Graduate School of Medical Sciences, <sup>5</sup>Radiology, New York University School of Medicine, NY, United States

We investigated the capability of advanced diffusion MRI, including high-angular resolution diffusion MRI (HARDI) and oscillating gradient diffusion MRI, to characterize cortical microstructural organization in the embryonic mouse brains. HARDI-based tractography revealed reduced axons in the intermediate zone of the embryonic cortex in the *Sas-4<sup>-/-</sup>;p53<sup>-/-</sup>* mice compared to the wildtypes. The oscillating gradient diffusion MRI delineated a three-lamina structure in the cortex of the normal embryonic brain, reflecting the neuronal cell distributions during embryonic brain development, which was altered by mislocalized RGPs in extra-ventricular zone, resulting in diminished contrast in the mutant cortex.

---

720

9:15



Mapping of cerebral cortical microstructure characterized by non-Gaussian water diffusion in aging

Qinmu Peng<sup>1,2</sup>, King Kevin<sup>3,4</sup>, Minhui Ouyang<sup>1</sup>, Hanzhang Lu<sup>5</sup>, and Hao Huang<sup>1,2</sup>

<sup>1</sup>Department of Radiology, Children's Hospital of Philadelphia, Philadelphia, PA, United States, <sup>2</sup>Department of Radiology, Perelman School of Medicine, University of Pennsylvania, Philadelphia, PA, United States, <sup>3</sup>Department of Imaging, Huntington Medical Research Institutes, <sup>4</sup>Department of Radiology, University of Texas Southwestern Medical Center, <sup>5</sup>Department of Radiology, Johns Hopkins University

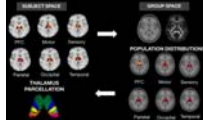
The cellular and molecular processes inside the cerebral cortex play a critical role in aging and neurodegenerative disorders. The microstructural changes associated to these cortical processes can be assessed with multi-shell diffusion MRI. Here, we aimed to accurately quantify the regional cortical microstructural changes of the aging brains. Multi-shell diffusion MRI was acquired to measure mean kurtosis (MK) derived from DKI at the center of the cerebral cortical layer for specific cortical regions. Significant MK decreases were found in the primary somatosensory regions, but not in prefrontal and visual regions, suggesting differentiated aging processes in different cortical regions.

---



721

9:27



### Improved tractography-based segmentation of the human thalamus

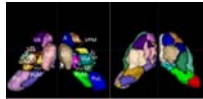
Carla Semedo<sup>1</sup>, M. Jorge Cardoso<sup>1</sup>, Sjoerd B. Vos<sup>1,2</sup>, Alex F. Mendelson<sup>1</sup>, Annemie Ribbens<sup>3</sup>, Dirk Smeets<sup>3</sup>, Jonathan D. Rohrer<sup>4</sup>, and Sebastien Ourselin<sup>1</sup>

<sup>1</sup>Translational Imaging Group, UCL, London, United Kingdom, <sup>2</sup>MRI Unit, Epilepsy Society, Chalfont St Peter, United Kingdom, <sup>3</sup>Icometrix, Leuven, Belgium, <sup>4</sup>Dementia Research Centre, UCL, London, United Kingdom

Accurate segmentation of the thalamus and its nuclei is a prerequisite for studying anatomical connectivity and its correlation to neurological diseases. The probabilistic tractography pipeline in FSL is commonly used for thalamus connectivity-based parcellation. However, dMRI data analysis and tractography are done in a mix of standard and subject spaces which can bias anatomical connectivity findings. Here, we presented a framework that improves thalamus parcellation by performing DW data processing and probabilistic tractography in the subject's native space, as well by generating population- connectivity priors. Higher segmentation accuracy was achieved with it when compared to FSL's available pipeline.

722

9:39



### Validation of DTI-based parcellation of the thalamus in the squirrel monkey

Yurui Gao<sup>1,2</sup>, Kurt G Schilling<sup>1</sup>, Iwona Stepniewska<sup>3</sup>, Landman A Bennett<sup>4</sup>, and Adam W Anderson<sup>5</sup>

<sup>1</sup>Biomedical Engineering, Vanderbilt University, Nashville, TN, United States, <sup>2</sup>Institute of Imaging Science, Vanderbilt University, Nashville, TN, United States, <sup>3</sup>Psychological Sciences, Vanderbilt University, <sup>4</sup>Electrical Engineering, Vanderbilt University, <sup>5</sup>Biomedical Engineering, Vanderbilt University

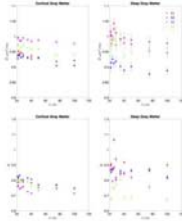
DTI has been used to noninvasively resolve major thalamic nuclei using an unsupervised clustering algorithm. However, rigorous validation of the method has not been studied. Here, we evaluated the method by comparing the parcellation results with histology in the same non-human primate. We found that some nuclei were clustered with larger differences from histology. That probably was because the diffusion properties of these nuclei were not coherent. In addition, the pipeline constructed in this study is also a framework to validate other approaches for thalamic nuclei parcellation.

723

9:51

### In vivo observation and interpretation of time dependent diffusion in human gray matter

Antonios Papaioannou<sup>1</sup>, Dmitry Novikov<sup>1</sup>, and Els Fieremans<sup>1</sup>



<sup>1</sup>Radiology, New York University School of Medicine, Center for Biomedical Imaging, New York, NY, United States

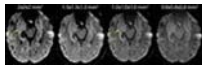
The temporal scaling of the diffusion coefficient and diffusional kurtosis may reveal the underlying microstructural features of the human brain. Here we demonstrate time-dependent diffusion coefficient and kurtosis in gray matter areas of the human brain in vivo. Our results suggest that the major contribution of time-dependence in gray matter originates from intra-neurite water with the main source of restrictions, e.g. dendrites and beads, being short-range disordered in their placement.

724

10:03

### High Resolution Diffusion Imaging of the Human Hippocampus

Sarah C Treit<sup>1</sup>, Trevor Steve<sup>1</sup>, Donald Gross<sup>1</sup>, and Christian Beaulieu<sup>1</sup>



<sup>1</sup>University of Alberta, Edmonton, Canada

Diffusion imaging of the human hippocampus is typically limited to low spatial resolution due to challenges with low signal-to-noise ratio. Here we demonstrate error in fractional anisotropy/mean diffusivity in high resolution diffusion imaging acquired with multiple gradient directions and 1 average, which is mitigated by acquiring fewer directions and multiple signal averages. Using this approach, 1x1x1 mm<sup>3</sup> diffusion data at 3T is shown to produce mean diffusion weighted images with excellent contrast within the hippocampus, acquired in a clinically feasible scan time of 6 minutes. High resolution diffusion imaging will impact the study of numerous disorders affecting the hippocampus.

## Oral

## Clinical & Translational Molecular/Metabolic Imaging

Room 316A

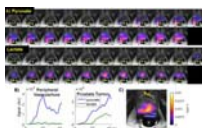
Wednesday 8:15 -  
10:15

Moderators: Kai-Hsiang Chuang & Ferdia  
Gallagher

725

8:15

### Phase II Clinical Hyperpolarized <sup>13</sup>C 3D-Dynamic Metabolic Imaging of Prostate Cancer using a B1-insensitive Variable Flip Angle Design



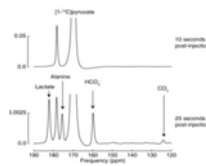
Hsin-Yu Chen<sup>1,2</sup>, Peder E.Z. Larson<sup>1,2</sup>, Jeremy W. Gordon<sup>1</sup>, Robert A. Bok<sup>1</sup>, Marcus Ferrone<sup>3</sup>, Mark van Criekinge<sup>1</sup>, Lucas Carvajal<sup>1</sup>, Rahul Aggarwal<sup>4</sup>, James B. Slater<sup>1</sup>, Ilwoo Park<sup>1</sup>, Eugene Milshteyn<sup>1,2</sup>, Sarah J. Nelson<sup>1,2</sup>, John Kurhanewicz<sup>1,2</sup>, and Daniel B. Vigneron<sup>1,2</sup>

<sup>1</sup>Department of Radiology and Biomedical Imaging, University of California, San Francisco, San Francisco, CA, United States, <sup>2</sup>UCSF/UC Berkeley Graduate Program in Bioengineering, University of California, San Francisco, San Francisco, CA, United States, <sup>3</sup>Department of Clinical Pharmacy, University of California, San Francisco, San Francisco, CA, United States, <sup>4</sup>School of Medicine, University of California, San Francisco, San Francisco, CA, United States

The 3D compressed-sensing echo-planar spectroscopic imaging (CS-EPSI) sequence has enabled 5-dimensional HP-<sup>13</sup>C imaging of human prostate cancer with full-prostate coverage and high spatial and temporal resolution. A new variable flip angle design substantially desensitizes the sequence to B<sub>1</sub> variations for improved quantitative analysis of pyruvate-to-lactate rate constant (k<sub>PL</sub>) measurements. Pre-clinical animal and clinical patient studies demonstrate that the resulting sequence enabled improved quantitative accuracy while maintaining excellent metabolite SNR.

726

8:27



Demonstrating the Randle Cycle In Vivo: Assessment of Physiological Alterations in Human Cardiac Metabolism Using Hyperpolarised <sup>13</sup>C MR Spectroscopy

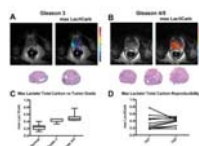
Damian Tyler<sup>1</sup>, Oliver Rider<sup>2</sup>, Michael Dodd<sup>1</sup>, Angus Lau<sup>3</sup>, Andrew Lewis<sup>2</sup>, Jack Miller<sup>1,4</sup>, Mark Peterzan<sup>2</sup>, Claire Trumper<sup>1</sup>, and Stefan Neubauer<sup>2</sup>

<sup>1</sup>Department of Physiology, Anatomy & Genetics, University of Oxford, Oxford, United Kingdom, <sup>2</sup>Radcliffe Department of Medicine, University of Oxford, Oxford, United Kingdom, <sup>3</sup>Physical Sciences, Sunnybrook Research Institute, Toronto, Canada, <sup>4</sup>Department of Physics, University of Oxford, Oxford, United Kingdom

The recent introduction of dissolution Dynamic Nuclear Polarization (DNP) has opened up a new window on *in vivo* metabolism and in this work we present the first demonstration that dissolution-DNP can observe physiological modulation of metabolism in the healthy human heart. The transition from the fasted to the fed state is shown to lead to an increase in flux through the key regulatory enzyme, pyruvate dehydrogenase, due to a metabolic switch away from fatty acid oxidation towards glucose oxidation. Such studies will provide the basis for future clinical studies exploring the metabolic alterations that occur in the diseased heart.

727

8:39



Utilizing hyperpolarized MRI in prostate cancer to assess metabolic dynamics and histopathologic grade

Kristin L Granlund<sup>1,2</sup>, Hebert A Vargas<sup>1</sup>, Serge K Lyashchenko<sup>3</sup>, Phillip J DeNoble<sup>3</sup>, Vincent Laudone<sup>4</sup>, James A Eastham<sup>4</sup>, Ramon A Sosa<sup>1</sup>, Matthew Kennedy<sup>1</sup>, Duane Nicholson<sup>1</sup>, YanWei W Guo<sup>1</sup>, Albert Chen<sup>5</sup>, James Tropp<sup>6</sup>, Hedvig Hricak<sup>1,2</sup>, and Kayvan R Keshari<sup>1,2</sup>

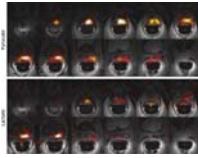
<sup>1</sup>Radiology, Memorial Sloan Kettering Cancer Center, New York, NY, United States, <sup>2</sup>Molecular Pharmacology, Memorial Sloan Kettering Cancer Center, New York, NY, United States, <sup>3</sup>Radiochemistry & Imaging Probes (RMIP) Core, Memorial Sloan Kettering Cancer Center, New York, NY, United States, <sup>4</sup>Surgery, Memorial Sloan Kettering Cancer Center, New York, NY, United States, <sup>5</sup>GE Healthcare, Toronto, ON, <sup>6</sup>Berkshire Magnetics, Berkeley, CA

A hallmark of prostate cancer is the reprogramming of prostate cancer metabolism which has been exploited for both <sup>31</sup>P and <sup>1</sup>H MRSI. In recent work, we and others have shown that hyperpolarized substrates can be used in living systems to measure changes in metabolic dynamics. Many studies have focused on the use of HP pyruvate in preclinical models, though the characterization of prostate cancer in man using HP MRI has been limited. In this work, we demonstrate the use of HP pyruvate MRI in prostate cancer patients. We assess the metabolic dynamics to the prostate of pyruvate as well as its conversion to lactate. Moreover we extend this analysis to the comparison of HP lactate to prostate cancer grade showing that not only does this approach have the potential to measure differences in grade it also can provide reproducible metabolic signatures across patients.

728

8:51

Human Hyperpolarized C-13 MRI Using a Novel Echo-Planar Imaging (EPI) Approach



Jeremy W Gordon<sup>1</sup>, Hsin-Yu Chen<sup>1</sup>, Peder EZ Larson<sup>1</sup>, Ilwoo Park<sup>1</sup>, Mark Van Criekinge<sup>1</sup>, Eugene Milshteyn<sup>1</sup>, Robert Bok<sup>1</sup>, Rahul Aggarwal<sup>2</sup>, Marcus Ferrone<sup>3</sup>, James B Slater<sup>1</sup>, John Kurhanewicz<sup>1</sup>, and Daniel B Vigneron<sup>1</sup>

<sup>1</sup>Radiology & Biomedical Imaging, UCSF, San Francisco, CA, United States, <sup>2</sup>Medicine, UCSF, San Francisco, CA, United States, <sup>3</sup>Clinical Pharmacy, UCSF, San Francisco, CA, United States

In this pilot study, we developed and applied a specialized symmetric EPI approach for the study of hyperpolarized [1-<sup>13</sup>C]pyruvate metabolism in the human prostate. We show that this approach can acquire ghost-free hyperpolarized [1-<sup>13</sup>C]pyruvate and [1-<sup>13</sup>C]lactate images with high spatiotemporal resolution in a clinical setting.

---

729

9:03



In Vivo Visualization of Orbital Immune Cell Infiltration During Early Development of Graves' Disease by 19F MRI

Ulrich Flögel<sup>1</sup>, Anja Eckstein<sup>2</sup>, and Utta Berchner-Pfannschmidt<sup>3</sup>

<sup>1</sup>Experimental Cardiovascular Imaging, Heinrich Heine University, Düsseldorf, Germany, <sup>2</sup>Ophthalmic Clinic, University Hospital Essen, <sup>3</sup>Molecular Ophthalmology, University Hospital Essen

Graves' disease is an antibody-mediated autoimmune condition of the thyroid gland, which is frequently associated with Graves' orbitopathy (GO), where inflammation of the orbit results in a detrimental remodeling of the orbital soft tissue. To investigate the molecular basis of GO and evaluate new therapeutic targets for treatment, we used a recently established mouse model of GO and analyzed the interplay of inflammation and adipogenesis using anatomical <sup>1</sup>H MRI and <sup>19</sup>F MRI for immune cell tracking. Hereby, the infiltration of immune cells could be identified as initial step leading to the remodeling of the orbital soft tissue in GO mice.

---

730

9:15



19F-perfluorocarbon-labeled human peripheral blood mononuclear cells can be detected in vivo using clinical MRI parameters in a therapeutic cell setting

Corby Fink<sup>1</sup>, Jeffrey Gaudet<sup>2</sup>, Matthew S Fox<sup>3</sup>, Shashank Bhatt<sup>4</sup>, Sowmya Viswanathan<sup>4</sup>, Michael Smith<sup>1</sup>, Joseph Chin<sup>5</sup>, Paula Foster<sup>2</sup>, and Gregory Dekaban<sup>1</sup>

<sup>1</sup>Microbiology and Immunology, Robarts Research Institute, London, ON, Canada, <sup>2</sup>Medical Biophysics, Robarts Research Institute, London, ON, Canada, <sup>3</sup>Medical Biophysics, Lawson Health Sciences Centre, London, ON, Canada, <sup>4</sup>Cell Therapy Program, Krembil Research Institute, Toronto, ON, Canada, <sup>5</sup>Urology, University of Western Ontario, London, ON, Canada

A major hurdle in advancing cell-based cancer vaccines is the inability to track where therapeutic cells migrate post-injection. We present the first study conducted in which primary Good Manufacturing Practice-grade <sup>19</sup>Fluorine (<sup>19</sup>F) labeled all peripheral blood mononuclear cell lineages (PBMC) and <sup>19</sup>F cellular MRI was used to track and quantify in vivo migration in a mouse model. Secondly, we present the highest sensitivity for <sup>19</sup>F detection reported in the literature and the first time a 1.2cm deep injection of <sup>19</sup>F-labeled PBMC using a small dual-tuned surface coil has been detected using a clinical scanner and MR protocol.

731



9:27



#### Molecular MR imaging of renal fibrogenesis in a mouse model

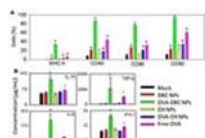
Philip Alan Waghorn<sup>1</sup>, Iris Chen<sup>1</sup>, Nicholas Rotile<sup>1</sup>, Chloe Jones<sup>1</sup>, Diego Ferreira<sup>1</sup>, Lan Wei<sup>2</sup>, Bryan Fuchs<sup>2</sup>, and Peter Caravan<sup>1</sup>

<sup>1</sup>A.A. Martinos Center for Biomedical Imaging, Charlestown, MA, United States, <sup>2</sup>Division of Surgery, Massachusetts General Hospital, Boston, MA, United States

The fibrotic deposition and remodeling of extracellular matrix (ECM) proteins to form cross-linked collagen and elastin fibers is a characteristic feature of chronic kidney disease (CKD). Critical to fiber formation is the presence of allysine, which facilitates fibril cross-linking through condensation reactions with neighboring allysine and lysine residues on collagen and elastin. We have developed a novel Gd-based MR probe, GdOA, designed to target allysine for non-invasive molecular imaging of active fibrogenesis in kidney disease, allowing the onset of fibrogenesis to be detected and provide a quantitative measure of the efficacy of future anti-fibrotic targeted therapies.

732

9:39



#### Chitin and dibutylchitin nanoparticles as imaging enabled vaccine nanocarriers

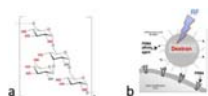
Barbara Blanco Fernandez<sup>1</sup>, Yasser A Aldhamen<sup>2</sup>, Shatadru Chakravarty<sup>1</sup>, Andrea Amalfitano<sup>2</sup>, and Erik M Shapiro<sup>1</sup>

<sup>1</sup>Radiology, Michigan State University, East Lansing, MI, United States,  
<sup>2</sup>Microbiology and Molecular Genetics, Michigan State University, East Lansing, MI, United States

We describe a strategy for fabricating chitin and dibutyrilchitin –an organo-soluble chitin derivative- nanoparticles (NPs) encapsulating a model antigen (ovalbumin) or iron oxide nanocrystals. The use of MRI enabled the determination of the cell migration of vaccinated cells, allowing the determination of the immunization efficiency in early stages. To form DBC, a reversible acylation of chitin was performed and NPs were fabricated using an emulsification/evaporation method, then chitin was regenerated by alkaline saponification. NPs had vaccine adjuvant properties and allowed the track of immune cells to lymph nodes, proving their utility as vaccine adjuvants and imaging agents.

733

9:51



CEST MRI of PSMA expression using natural dextran-based contrast agents

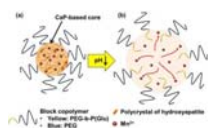
Guanshu Liu<sup>1,2</sup>, Sangeeta Ray Banerjee<sup>2</sup>, Xing Yang<sup>2</sup>, Nirbhay Yadav<sup>1</sup>, Ala Lisok<sup>2</sup>, Anna Jablonska<sup>2</sup>, Jiadi Xu<sup>1,2</sup>, Yuguo Li<sup>1,2</sup>, Martin Pomper<sup>2</sup>, and Peter van Zijl<sup>1,2</sup>

<sup>1</sup>F.M. Kirby Research Center for Functional Brain Imaging, Kennedy Krieger Institute, Baltimore, MD, United States, <sup>2</sup>The Russell H. Morgan Department of Radiology and Radiological Science, Johns Hopkins University, Baltimore, MD, United States

It is desirable to have non-invasive imaging methods able not only to render the expression and distribution of receptors, enzymes and other targets relevant to cancer, but also have a safety profile enabling use as a screening tool. We have developed an enzyme-targeted MR imaging approach that uses non-metallic, non-radioactive dextran as the imaging agent detected by CEST MRI. Our results indicate that imaging tumors expressing the prostate-specific membrane antigen (PSMA) could be accomplished using urea-conjugated dextran particles that could be detected in micromolar (per particle) concentration by MRI.

734

10:03



Detection of tumor hypoxic region using pH-activatable nanoparticles containing manganese contrast agent

Daisuke Kokuryo<sup>1,2</sup>, Peng Mi<sup>3,4,5</sup>, Horacio Cabral<sup>6</sup>, Tsuneo Saga<sup>1</sup>, Ichio Aoki<sup>1</sup>, Nouhiro Nishiyama<sup>3,4</sup>, and Kazunori Kataoka<sup>4,6,7</sup>



<sup>1</sup>Department of Molecular Imaging and Theranostics, National Institute for Radiological Sciences, National Institutes for Quantum and Radiological Science and Technology, Chiba, Japan, <sup>2</sup>Graduate School of System Informatics, Kobe University, Kobe, Japan, <sup>3</sup>Institute of Innovative Research, Tokyo Institute of Technology, Japan, <sup>4</sup>Innovation Center of Nanomedicine (iCONM), Kawasaki Institute of Industry Promotion, Kawasaki, Japan, <sup>5</sup>State Key Laboratory of Biotherapy and Cancer Center, Sichuan University, People's Republic of China, <sup>6</sup>Graduate School of Engineering, The University of Tokyo, Japan, <sup>7</sup>Graduate School of Medicine, The University of Tokyo, Japan

Assessing the environment inside a tumor would aid the development of an effective therapeutic strategy. Our group has recently developed a pH-activatable nanoparticle containing MR contrast agents, which is called MnCaP micelle. For an *in vivo* tumor model, a specific and strong enhancement of MR signal in the tumor was obtained after the administration. The enhanced area was agreed with the high lactate region found with <sup>1</sup>H-MRS and which corresponds to the hypoxic region inside tumor. We conclude that MnCaP micelle detects hypoxic regions in the tumor clearly and therefore it has potential to provide important information for tumor therapy.

---

## Oral

### MR-Guided Interventions

Room 320

Wednesday 8:15 -  
10:15

Moderators: Michael Bock & Reza Razavi

---

735

8:15



#### MRI-guided Needle Biopsy using Augmented Reality

Michael A. Lin<sup>1</sup>, Jung Hwa Bae<sup>1</sup>, Subashini Srinivasan<sup>2</sup>, Steffi L Perkins<sup>3</sup>, Christoph Leuze<sup>2</sup>, Brian Hargreaves<sup>2</sup>, Mark R Cutkosky<sup>4</sup>, and Bruce Daniel<sup>2</sup>

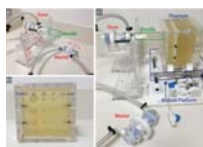
<sup>1</sup>Mechanical Engineering, Stanford University, Stanford, CA, United States, <sup>2</sup>Radiological Sciences, Stanford University, CA, United States, <sup>3</sup>Bioengineering, Stanford University, CA, United States, <sup>4</sup>Mechanical Engineering, Stanford University, CA, United States

We present an augmented reality system that integrates needle shape sensing technology and a visual tracking system to enable a more effective visualization of preoperative MR images during MR-guided needle biopsy procedure. It allows physicians to view 3D MR images of targets within the patient fused onto the patient anatomy as well as a virtual biopsy needle registered to the real needle. This provides what-you-see-is-what-you-get interaction even after the needle is inserted into the opaque body and can improve on current MR-guided needle biopsy by providing a faster tracking, and by enabling real-time interactive procedures based on pre-acquired scans, thus avoiding costly MRI scans.

---

736

8:27



### Real-Time MRI-Guided Targeted Needle Placement During Motion using Rolling-Diaphragm Hydrostatic Actuators

Samantha Mikael<sup>1,2</sup>, James Simonelli<sup>3</sup>, Yu-Hsiu Lee<sup>3</sup>, Xinzhou Li<sup>1,4</sup>, Yong Seok Lee<sup>1,5</sup>, David Lu<sup>1</sup>, Kyunghyun Sung<sup>1,2,4</sup>, Tsu-Chin Tsao<sup>3</sup>, and Holden H Wu<sup>1,2,4</sup>

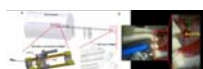
*<sup>1</sup>Radiological Sciences, University of California Los Angeles, Los Angeles, CA, United States, <sup>2</sup>Biomedical Physics, University of California Los Angeles, Los Angeles, CA, United States, <sup>3</sup>Mechanical and Aerospace Engineering, University of California Los Angeles, Los Angeles, CA, United States, <sup>4</sup>Bioengineering, University of California Los Angeles, Los Angeles, CA, United States, <sup>5</sup>Department of Radiology, Dongguk University Ilsan Hospital, Korea, Republic of*

In this work, we present a new version of our hydrostatically actuated system and investigate its accuracy and time efficiency for real-time MRI-guided targeted needle placement in a motion phantom. We show that actuator-assisted needle placement was able to reach the targets with greater accuracy and in less time than free-hand step-and-shoot placement for both static and simulated respiration motion. Our new rolling-diaphragm hydrostatic actuators can potentially enable physicians to remotely perform real-time MRI-guided interventions during motion.

---

737

8:39



### MRI-guided robotic arm (MgRA) to target deep brain nuclei in vivo

Yi Chen<sup>1,2</sup>, Jan Kevin Schlüsener<sup>1</sup>, and Xin Yu<sup>1</sup>

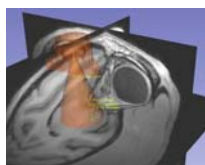
*<sup>1</sup>Research Group of Translational Neuroimaging and Neural Control, High-Field Magnetic Resonance, Max Planck Institute for Biological Cybernetics, Tuebingen, Germany, <sup>2</sup>Graduate School of Neural Information Processing, Tuebingen, Germany*



We develop a multiple degree-of-freedom robotic controlling system to target brain nuclei in the rat brain inside the high field (14.1T) MRI scanner. This MRI-compatible robot arm provides high targeting accuracy by using MRI images as a feedback to guide the brain intervention. Meanwhile, an MR-compatible camera-monitored insertion trajectory can be optimized through the controlling software in order to investigate the effectiveness, safety and feasibility of deep brain nuclei targeting for translational application.

738

8:51



### Targeted Delivery of Stem Cells to the Brain using Real Time Interventional MRI

Miles E. Olsen<sup>1</sup>, Scott C. Vermilyea<sup>2,3</sup>, Jianfeng Lu<sup>4</sup>, Ethan K. Brodsky<sup>1,5</sup>, Scott Guthrie<sup>2</sup>, Yunlong Tao<sup>4</sup>, Eva M. Fekete<sup>6</sup>, Marissa K. Riedel<sup>6</sup>, Kevin Brunner<sup>2</sup>, Carissa Boettcher<sup>2</sup>, Viktorya Bondarenko<sup>2</sup>, Andrew A. Alexander<sup>1,2,4,6</sup>, Soo Chun Zhang<sup>3,7</sup>, Marina E. Emborg<sup>1,2,3</sup>, and Walter F. Block<sup>1,8</sup>

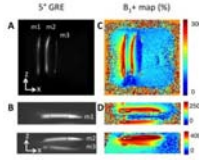
<sup>1</sup>Medical Physics, University of Wisconsin - Madison, Madison, WI, United States, <sup>2</sup>Preclinical Parkinson's Research Program, University of Wisconsin - Madison, Madison, WI, United States, <sup>3</sup>Neuroscience Training Program, University of Wisconsin - Madison, Madison, WI, United States, <sup>4</sup>Waisman Center, University of Wisconsin - Madison, Madison, WI, United States, <sup>5</sup>Radiology, University of Wisconsin - Madison, Madison, WI, United States, <sup>6</sup>Psychiatry, University of Wisconsin - Madison, Madison, WI, United States, <sup>7</sup>Neuroscience, University of Wisconsin - Madison, Madison, WI, United States, <sup>8</sup>Biomedical Engineering, University of Wisconsin - Madison, Madison, WI, United States

We present an intraoperative MRI protocol for stereotaxic surgery to precisely deliver induced pluripotent stem cells to targeted locations within the brain of a non-human primate model.

Previously, these surgeries were performed in stereotaxic operating rooms with no intraoperative imaging, or in a conventional MRI system without real-time guidance. Those environments complicate the goals of ensuring precise cannula tip placement before injection, and being able to perform the desired number of injections during the anesthesia window. Our platform enables surgeons to quickly achieve precise tip placement, and confirm via imaging that cells were deposited at the intended target.

### A Method for a Wireless Marker Using a Monopole Antenna for Endovascular Catheter Navigation

Caroline D. Jordan<sup>1</sup>, Steven W. Hetts<sup>1</sup>, and Xiaoliang Zhang<sup>1</sup>

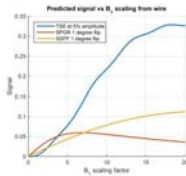


<sup>1</sup>Radiology and Biomedical Imaging, University of California San Francisco, San Francisco, CA, United States

Inductively coupled RF coils have been used as markers for MR guidance of endovascular catheters using lumped elements, and a monopole antenna could be used as a marker that is more compact and easy to build. We built three prototypes for 3T, acquired GRE sequences and  $B_1+$  maps in two orientations, and modeled electromagnetic fields using low and high permittivity dielectric coating on the monopole. Measured Q-factors were 7.6–11.7, scaled experimental  $B_1+$  of marker signal were 198–272%, and modeled electric fields were reduced. This work demonstrates feasibility of a monopole antenna as a wireless marker for interventional MRI.

### Tissue and device visualization using parallel transmission for interventional MRI

Felipe Godinez<sup>1</sup>, Joseph Hajnal<sup>1</sup>, Greig Scott<sup>2</sup>, Ronald Mooiweer<sup>1</sup>, Francesco Padormo<sup>3</sup>, and Shaihan Malik<sup>1</sup>

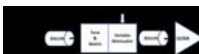


<sup>1</sup>Imaging and Biomedical Engineering, King's College London, London, United Kingdom, <sup>2</sup>Electrical Engineering, Stanford University, United States, <sup>3</sup>Translational and Molecular Imaging Institute, The Icahn School of Medicine at Mount Sinai, New York, NY, United States

It is demonstrated that parallel transmit (PTx) can be used to both safely visualise tissue (no heating even from high SAR sequences), and safely visualise a wire by direct coupling using low power MR sequences. A low power version of a TSE sequence was found to give the best depiction of the wire when using this method.

### Operator Controlled Illumination of Active Catheter Tips using a Variable Attenuator

Ali Caglar Özen<sup>1</sup>, Thomas Lottner<sup>1</sup>, Simon Reiss<sup>1</sup>, Axel Krafft<sup>1</sup>, Timo Heidt<sup>2</sup>, Constantin von zur Muhlen<sup>2</sup>, and Michael Bock<sup>1</sup>



<sup>1</sup>Department of Radiology, Medical Physics, Medical Center – University of Freiburg, Freiburg, Germany, <sup>2</sup>Department of Cardiology and Angiology, University Heart Center, Freiburg, Germany

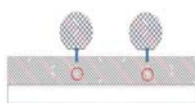


Accurate visualization of catheter tip is important in MR-guided interventional procedures, in particular in the coronary arteries where the tip orientation is essential to introduce the catheter into the target vessel. Active catheters generally provide a positive MR signal around the tracking coil at the tip. In this study, an operator-controlled variable attenuator is attached to an active catheter to enable rapid manual adjustment of the tip signal by the operator. The system was tested in an animal experiment at 3 T, and the active catheter was successfully introduced into the left coronary artery multiple times.

---

742

9:39



### AN MR-SAFE METAL-BRAIDED CATHETER DESIGN FOR INTERVENTIONAL CMR

Burcu Basar<sup>1</sup>, Korel Yildirim<sup>2</sup>, Robert J Lederman<sup>1</sup>, and Ozgur Kocaturk<sup>2</sup>

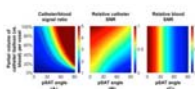
<sup>1</sup>Cardiovascular and Pulmonary Branch, Division of Intramural Research, National Heart Lung and Blood Institute, NIH, Bethesda, MD, United States, <sup>2</sup>Institute of Biomedical Engineering, Bogazici University, Istanbul, Turkey

Interventional cardiovascular magnetic resonance (iCMR) can enable radiation-free catheterization procedures. However, the lack of MR-safe devices limits clinical iCMR procedures. An MR-safe, metal-braided catheter that avoids RF-heating at 1.5 Tesla was prototyped. RF-heating of the device was eliminated by virtue of segmenting its metal components. RF-safety and mechanical integrity were confirmed through in vitro tests per ASTM standards. The proposed method could be an attractive technique to construct MR-safe metal-braided catheters for iCMR procedures.

---

743

9:51



### Passive Tracking Sequence with Positive Contrast using Partial Saturation for MR-guided Cardiac Catheterisation

Mari Nieves Velasco Forte<sup>1</sup>, Kuberan Pushparajah<sup>1</sup>, Nycholas Byrne<sup>2</sup>, Mazen Alhrishy<sup>1</sup>, Bram Ruijsink<sup>1</sup>, Israel Valverde<sup>1,3</sup>, Tobias Schaeffter<sup>1</sup>, Reza Razavi<sup>1</sup>, and Sébastien Roujol<sup>1</sup>

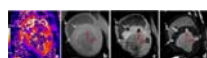
<sup>1</sup>Division of Imaging Sciences & Biomedical Engineering, King's College London, London, United Kingdom, <sup>2</sup>Medical Physics, King's College London, London, United Kingdom, <sup>3</sup>Cardiovascular Imaging, Institute of Biomedicine of Seville, Seville, Spain

Cardiac MRI-guided catheterization offers an alternative to conventional fluoroscopy. This technique has been used in congenital heart disease for diagnostic purposes using passive tracking methods, with either CO<sub>2</sub> or gadolinium filled balloon wedge catheters. The gadolinium filled balloon is easier to visualize. The sequence, real-time bSSFP, can be used with or without saturation prepulse, leading to either suppression of soft tissue signal or poor catheter visualization. We have developed a partial saturation pulse sequence providing high contrast between tissue, blood and balloon. After optimization in phantoms and volunteers, this sequence has shown excellent results during MR-guided catheterization in patients.

---

744

10:03



Dependence of T2\* Relaxation Time of Cardiac Cryo and RF Lesions on Time after Ablation: A New Approach to Non-contrast MRI of Cardiac Ablation Lesions

Eugene G. Kholmovski<sup>1,2</sup>, Sathya Vijayakumar<sup>1,2</sup>, and Nassir F. Marrouche<sup>2</sup>

*<sup>1</sup>UCAIR, Department of Radiology and Imaging Science, University of Utah, Salt Lake City, UT, United States, <sup>2</sup>CARMA Center, University of Utah, Salt Lake City, UT, United States*

RF and Cryo ablations are being increasingly used for treatment of cardiac arrhythmias. LGE-MRI is widely used for characterization of RF and Cryo lesions. However, LGE-MRI requires contrast injection. Recently proposed native T1w techniques are only useful for visualization of acute (< 3 days) RF lesions. T2\* relaxation time of RF and Cryo lesions significantly changes with time after ablation. T2\* time of ablated myocardium is considerably lower than T2\* time of normal myocardium after 1 week post-ablation. A native T2\*-weighted MRI technique which can be used to visualize both RF and Cryo lesions has been developed and validated in animal studies.

---

## Combined Educational & Scientific Session

# Demystifying Dielectrics & Understanding Reciprocity

Organizers: Gregor Adriany, Ph.D., Christoph Juchem, Ph.D., Mary P. McDougall, Ph.D. & Greig C. Scott, Ph.D.

Room 314

Wednesday 8:15 -  
10:15

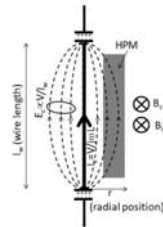
Moderators: Cornelis van den Berg & Lukas  
Winter

---

8:15

### Demystifying Dielectrics

Chris Collins<sup>1</sup>



<sup>1</sup>NYU Langone Medical Center

Historical and recent examples of materials having a high relative electric permittivity as used to enhance or even create the electromagnetic fields in MRI for improved performance will be reviewed with an eye to the physical mechanisms by which they can act to improve MRI performance.

8:45

### The Principle of Reciprocity

Cornelis A.T. van den Berg<sup>1</sup> and Rob Remis<sup>2</sup>

<sup>1</sup>Centre for Image Sciences, University Medical Center Utrecht, Netherlands, <sup>2</sup>Faculty Electrical Engineering, Mathematics and Computer Science, TU Delft, Delft, Netherlands

745



9:15

### Flexible and compact hybrid metasurfaces for enhanced ultra high field in vivo magnetic resonance imaging

Rita Schmidt<sup>1</sup>, Alexey Slobozhanyuk<sup>2,3</sup>, Pavel Belov<sup>2</sup>, and Andrew Webb<sup>1</sup>



<sup>1</sup>Radiology, Leiden University Medical Center, Leiden, Netherlands, <sup>2</sup>Nanophotonics and Metamaterials, ITMO University, St. Petersburg, Russian Federation, <sup>3</sup>Nonlinear Physics Center, Australian National University, ACT 2601, Australia

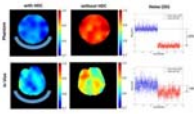
In previous research it has been shown that high permittivity material pads can be used for global and local RF shimming, as well as local SNR increase. Another recent approach is using metamaterials. In this study we designed a thin, compact and flexible metasurface which consists of metallic strips attached to 8mm thick pad made from a CaTiO<sub>3</sub> suspension in water. We show applications of the hybrid metasurface in an examination of the human brain at 7T, concentrating to produce a local increase in the SNR in the occipital cortex for imaging as well as for spectroscopy.

746

9:27

### Improving B1 Field Efficiency and Reducing noise for In Vivo 31P MRSI with Ultrahigh Dielectric Constant Material





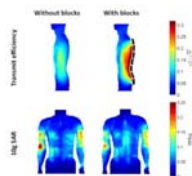
Byeong-Yeul Lee<sup>1</sup>, Xiao-Hong Zhu<sup>1</sup>, Sebastian Rupprecht<sup>2</sup>, Michalel T. Lanagan<sup>3</sup>, Qing X. Yang<sup>2</sup>, and Wei Chen<sup>1</sup>

<sup>1</sup>Center for Magnetic Resonance Research, Department of Radiology, University of Minnesota Medical School, Minneapolis, MN, United States, <sup>2</sup>Center for NMR Research, Department of Radiology, The Pennsylvania State College of Medicine, Hershey, PA, United States, <sup>3</sup>Department of Engineering Science and Mechanics, The Pennsylvania State College of Engineering, University Park, PA, United States

X-nuclei MRS for human application faces two challenges: high RF power requirement (thus, higher SAR) for achieving the same RF pulse flip angle due to a relatively lower gyromagnetic ratio, and limit of detection sensitivity (or SNR) even at high/ultrahigh field. In this work, we report that by incorporating ultra-high dielectric constant (uHDC) material into the RF head volume coil, huge RF transmit power reduction was observed in the regions near the uHDC pads for <sup>31</sup>P MRSI at 7T. Concomitantly, the B<sub>1</sub> efficiency for acquiring the spectra was increased about 100%. Strikingly, up to ~20% denoising effect was also observed with the uHDC material. Our results demonstrated that incorporating uHDC with RF coil can significantly boost SNR and reduce SAR in X-nuclei MRS applications; such improvements are beyond the gains obtainable at very high field strength magnet that has approached to its technologic limits.

747

9:39



Improved Image Quality and Decreased Power Deposition in the Spine at 3T using Extremely High Permittivity Materials

Kirsten Koolstra<sup>1</sup>, Peter Börnert<sup>2</sup>, Wyger Brink<sup>1</sup>, and Andrew Webb<sup>1</sup>

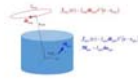
<sup>1</sup>Radiology, Leiden University Medical Center, Leiden, Netherlands, <sup>2</sup>Philips Research Hamburg, Germany

High field MR imaging of the spine suffers from a low transmit efficiency. The aim of this study is to improve the transmit profile of the 3T body coil in the spine region by using extremely high permittivity ceramics. This dielectric shimming approach with novel materials offers the opportunity to improve clinical spine image quality on MR systems that are not equipped with multi-transmit hardware. The developed approach is also compared with RF shimming in terms of image quality and power requirements.

748

9:51

Understanding Reciprocity  
Daniel K. Sodickson<sup>1,2</sup>



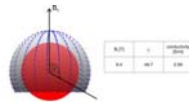
<sup>1</sup>Center for Advanced Imaging Innovation and Research (CAI2R) and Bernard and Irene Schwartz Center for Biomedical Imaging, Department of Radiology, New York University School of Medicine, New York, NY, United States, <sup>2</sup>Sackler Institute of Graduate Biomedical Sciences, New York University School of Medicine, New York, NY, United States

The principle of reciprocity, as it applies to magnetic resonance, is both remarkably powerful and regrettably easy to misconstrue. As evidence of this fact, each of us with an interest in the operation of radiofrequency coils need only recall the time we have spent trying to understand, in our guts, the difference between transmit and receive sensitivity patterns. As a respectful supplement to Dr. Hoult's seminal explications, we here provide a highly streamlined derivation, aimed at bolstering intuition, and offer a simple but fundamental mnemonic to keep your pluses and your minuses straight.

---

749

10:03



The ultimate intrinsic SNR in a spherical phantom with regard to an open-pole surface current distribution at 9.4T

Andreas Pfrommer<sup>1</sup> and Anke Henning<sup>1,2</sup>

<sup>1</sup>High-Field MR Center, Max Planck Institute for Biological Cybernetics, Tuebingen, Germany, <sup>2</sup>Institute of Physics, Ernst-Moritz-Arndt University Greifswald, Greifswald, Germany

RF coils for human head imaging need to provide access for the human neck and cannot be entirely closed. In this work, we investigate the ultimate intrinsic signal-to-noise ratio (UISNR) in a spherical phantom due to an open-pole surface current distribution, where the generic surface current patterns run on a spherical cap. The influence of the cap's opening angle  $\vartheta_0$  on UISNR, parallel imaging performance and on the contribution of curl-free and divergence-free current patterns to UISNR is studied.

---

Other

## Hands-On Workshop: GE Healthcare 1

Room 322AB

Wednesday 8:15 - 10:15 (no CME credit)

---

Other

# Hands-On Workshop: Philips Healthcare 1

Room 324

Wednesday 8:15 - 10:15 (no CME credit)

---

## Plenary Session

### Theranostic MRI in Precision Medicine

Organizers: Kristine Glunde, Ph.D. & Natalie J. Serkova, Ph.D.

Plenary Hall

Wednesday 10:45 - 11:45

---

10:45

[Magnetic Nanoparticle Theranostics for Brain Tumors](#)

Constantinos G. Hadjipanayis<sup>1</sup>

<sup>1</sup>*Neurosurgery, Icahn School of Medicine at Mount Sinai*

---

11:05

[Theranostic MRI in Oncology](#)

Zaver M Bhujwala<sup>1</sup>

<sup>1</sup>*Russell H. Morgan Department of Radiology and Radiological Science, Johns Hopkins Univ. School of Medicine, Baltimore, MD, United States*

---

11:25

[Theranostic MRI in Inflammation & Arthritis](#)

Thoralf Niendorf<sup>1</sup>, Jason Millward<sup>1</sup>, and Sonia Waiczies<sup>1</sup>

<sup>1</sup>*Berlin Ultrahigh Field Facility (B.U.F.F.), Max-Delbrueck Center for Molecular Medicine, Berlin, Germany*

---

## Oral

### Special Session: Scientific Highlights of the 25th Annual Meeting

Plenary Hall

Wednesday 11:45 -  
12:15

Moderators: Ileana Hancu & Valeria  
Panebianco

---

750

11:45

[Dynamic Diffusion MRI Signal Changes Accompany Electrical Activity in Myelinated Axons](#)



William M Spees<sup>1,2</sup>, Tsen-Hsuan Lin<sup>1</sup>, Peng Sun<sup>1</sup>, Sam E Gary<sup>1</sup>, and Sheng-Kwei Song<sup>1,2</sup>

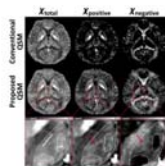
<sup>1</sup>Mallinckrodt Institute of Radiology, Washington University School of Medicine, St. Louis, MO, United States, <sup>2</sup>Hope Center for Neurological Disorders, Washington University School of Medicine, St. Louis, MO, United States

Because of its exceptionally robust nature, the *ex vivo* frog sciatic nerve has been the subject of numerous electrophysiology and MRI studies over the years. Here we report on diffusion MRI signal changes resulting from 50 and 100 Hz in-magnet electrical stimulation of perfused bullfrog sciatic nerves. The inexpensive perfusion system we have implemented allows for good long-term in-magnet stability and simultaneous MRI/electrophysiology studies. Decreases in water diffusivity and compound action potential conduction velocities accompany prolonged periods of repetitive electrical stimulation. Both of these changes are consistent with hypothesized microstructural alterations of the PNS myelin.

751



11:50



### Separating positive and negative susceptibility sources in QSM

Jingu Lee<sup>1</sup>, Yoonho Nam<sup>2</sup>, Joon Yul Choi<sup>1</sup>, Hyeonggeol Shin<sup>1</sup>, Taehyun Hwang<sup>1</sup>, and Jongho Lee<sup>1</sup>

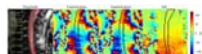
<sup>1</sup>Department of Electrical and Computer Engineering, Seoul National University, Seoul, Korea, Republic of, <sup>2</sup>Department of Radiology, Seoul St. Mary's Hospital, College of Medicine, The Catholic University of Korea, Seoul, Korea, Republic of

We proposed a new QSM algorithm that separates positive and negative susceptibility sources within a voxel by utilizing signal relaxation ( $R_2'$ ) for dipole inversion. The new method was tested in computer simulated phantoms and in-vivo data, and successfully separated positive and negative susceptibility sources.

752



11:55



### Spatiotemporal analysis of breathing-induced fields in the cervical spinal cord at 7T

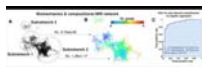
S. Johanna Vannesjo<sup>1</sup>, Karla L. Miller<sup>1</sup>, Stuart Clare<sup>1</sup>, and Irene Tracey<sup>1</sup>

<sup>1</sup>FMRIB centre, Nuffield Department of Clinical Neurosciences, University of Oxford, Oxford, United Kingdom

Time-varying  $B_0$  fields related to breathing is one major source of image artifacts in spinal cord imaging at ultra-high field. Here we aim to measure spatial and temporal characteristics of breathing-induced fields in the cervical spinal cord at 7T. We perform a principal component analysis on field measurements based on fast gradient-echo images acquired during free breathing. We observed field variations of about 30Hz at C7 during normal breathing. Furthermore, we observed that a single principal component explained over 90% of the field variance during normal and deep breathing.

753

12:00



### Using Machine Learning to study knee Osteoarthritis: the path towards OA Precision Medicine

Valentina Pedita<sup>1</sup>, Jenny Haefeli<sup>1</sup>, Kazuhito Morioka<sup>1</sup>, Hsiang-Ling Tang<sup>1</sup>, Lorenzo Nardo<sup>2</sup>, Richard B Swoza<sup>1</sup>, Adam R Ferguson<sup>1</sup>, and Sharmila Majumdar<sup>1</sup>

<sup>1</sup>University Of California, San Francisco, San Francisco, CA, United States, <sup>2</sup>Memorial Sloan Kettering Cancer Center, New York, New York, NY, United States

In this study we describe the analysis of a dataset including 178 subjects with and without Osteoarthritis using Topological data analysis (TDA), a machine-learning tool that involves projecting individual patients into the ‘syndromic space’ defined by all outcome variables simultaneously. Demographics, patient reported outcomes Kellgren-Lawrence grading, MRI WOMBS morphological grading, cartilage relaxation times, gait kinematics and kinetics during walking were simultaneously considered to define the data topology. TDA shows the presence of subgroups characterized by a strong biochemical signature, showing how this new technique could be used to extract insight from complex data, allowing for more personalized characterization of each individual.

754



12:05

Parameter	Mean	SD	Min	Max	Q1	Q3
Age	65.2	10.5	45	85	55	75
Sex (Male)	0.65	0.48	0	1	0	1
Height (cm)	175.5	7.5	160	190	170	180
Weight (kg)	80.5	15.5	60	110	70	90
BMI (kg/m²)	26.5	4.5	20	35	23	29
Heart Rate (b/min)	72	10	55	95	65	80
Blood Pressure (mmHg)	120/80	15/10	90/60	150/100	110/70	130/90
Cholesterol (mg/dL)	200	50	120	280	150	220
Glucose (mg/dL)	100	20	70	130	90	110
Hemoglobin (g/dL)	14.5	1.5	12	17	13.5	15.5
Hematocrit (%)	45	5	35	55	40	48
Platelets (10 <sup>9</sup> /L)	250	50	150	350	200	300
Prothrombin Time (sec)	12.5	1.5	10	15	11.5	13.5
Partial Thromboplastin Time (sec)	35	5	25	45	30	40
Fibrinogen (mg/dL)	350	50	250	450	300	400
D-Dimer (ng/mL)	0.5	0.2	0.1	1.0	0.3	0.7
Creatinine (mg/dL)	1.2	0.3	0.8	1.8	1.0	1.4
BUN (mg/dL)	20	5	12	28	18	22
Urea Nitrogen (mg/dL)	15	3	10	20	13	17
Serum Calcium (mg/dL)	10.0	0.2	9.0	11.0	9.8	10.2
Serum Phosphorus (mg/dL)	3.5	0.5	2.5	4.5	3.2	3.8
Serum Magnesium (mg/dL)	1.8	0.2	1.5	2.1	1.7	1.9
Serum Potassium (mEq/L)	4.0	0.3	3.5	4.5	3.8	4.2
Serum Sodium (mEq/L)	140	3	135	145	138	142
Serum Chloride (mEq/L)	105	3	100	110	102	108
Serum Bicarbonate (mEq/L)	24	2	20	28	22	26
Serum Lactate (mg/dL)	1.0	0.5	0.5	2.0	0.8	1.2
Serum Amylase (U/L)	40	10	20	60	30	50
Serum Lipase (U/L)	60	15	30	90	45	75
Serum Triglycerides (mg/dL)	150	50	80	220	100	180
Serum HDL Cholesterol (mg/dL)	50	15	30	70	40	60
Serum LDL Cholesterol (mg/dL)	130	40	80	180	100	150
Serum VLDL Cholesterol (mg/dL)	30	10	15	45	20	35
Serum Total Cholesterol (mg/dL)	210	60	120	280	160	230
Serum Apolipoprotein B (mg/dL)	100	30	60	140	70	120
Serum Apolipoprotein A (mg/dL)	150	40	100	200	120	180
Serum Apolipoprotein A2 (mg/dL)	30	10	15	45	20	35
Serum Apolipoprotein B48 (mg/dL)	10	5	5	15	8	12
Serum Apolipoprotein B100 (mg/dL)	90	25	50	125	60	108
Serum Apolipoprotein A1 (mg/dL)	140	35	90	175	100	165
Serum Apolipoprotein A2 (mg/dL)	25	8	10	35	15	25
Serum Apolipoprotein A3 (mg/dL)	5	2	2	8	3	6
Serum Apolipoprotein A4 (mg/dL)	1	0.5	0.5	2	0.5	1.5
Serum Apolipoprotein A5 (mg/dL)	0.5	0.2	0.2	1	0.3	0.7
Serum Apolipoprotein A6 (mg/dL)	0.2	0.1	0.1	0.5	0.1	0.3
Serum Apolipoprotein A7 (mg/dL)	0.1	0.05	0.05	0.2	0.05	0.15
Serum Apolipoprotein A8 (mg/dL)	0.05	0.02	0.02	0.1	0.02	0.08
Serum Apolipoprotein A9 (mg/dL)	0.02	0.01	0.01	0.05	0.01	0.03
Serum Apolipoprotein A10 (mg/dL)	0.01	0.005	0.005	0.02	0.005	0.015
Serum Apolipoprotein A11 (mg/dL)	0.005	0.002	0.002	0.01	0.002	0.008
Serum Apolipoprotein A12 (mg/dL)	0.002	0.001	0.001	0.005	0.001	0.003
Serum Apolipoprotein A13 (mg/dL)	0.001	0.0005	0.0005	0.002	0.0005	0.0015
Serum Apolipoprotein A14 (mg/dL)	0.0005	0.0002	0.0002	0.001	0.0002	0.0008
Serum Apolipoprotein A15 (mg/dL)	0.0002	0.0001	0.0001	0.0005	0.0001	0.0003
Serum Apolipoprotein A16 (mg/dL)	0.0001	0.00005	0.00005	0.0002	0.00005	0.00015
Serum Apolipoprotein A17 (mg/dL)	0.00005	0.00002	0.00002	0.0001	0.00002	0.00008
Serum Apolipoprotein A18 (mg/dL)	0.00002	0.00001	0.00001	0.00005	0.00001	0.00003
Serum Apolipoprotein A19 (mg/dL)	0.00001	0.000005	0.000005	0.00002	0.000005	0.000015
Serum Apolipoprotein A20 (mg/dL)	0.000005	0.000002	0.000002	0.00001	0.000002	0.000008
Serum Apolipoprotein A21 (mg/dL)	0.000002	0.000001	0.000001	0.000005	0.000001	0.000003
Serum Apolipoprotein A22 (mg/dL)	0.000001	0.0000005	0.0000005	0.000002	0.0000005	0.0000015
Serum Apolipoprotein A23 (mg/dL)	0.0000005	0.0000002	0.0000002	0.000001	0.0000002	0.0000008
Serum Apolipoprotein A24 (mg/dL)	0.0000002	0.0000001	0.0000001	0.0000005	0.0000001	0.0000003
Serum Apolipoprotein A25 (mg/dL)	0.0000001	0.00000005	0.00000005	0.0000002	0.00000005	0.00000015
Serum Apolipoprotein A26 (mg/dL)	0.00000005	0.00000002	0.00000002	0.0000001	0.00000002	0.00000008
Serum Apolipoprotein A27 (mg/dL)	0.00000002	0.00000001	0.00000001	0.00000005	0.00000001	0.00000003
Serum Apolipoprotein A28 (mg/dL)	0.00000001	0.000000005	0.000000005	0.00000002	0.000000005	0.000000015
Serum Apolipoprotein A29 (mg/dL)	0.000000005	0.000000002	0.000000002	0.00000001	0.000000002	0.000000008
Serum Apolipoprotein A30 (mg/dL)	0.000000002	0.000000001	0.000000001	0.000000005	0.000000001	0.000000003
Serum Apolipoprotein A31 (mg/dL)	0.000000001	0.0000000005	0.0000000005	0.000000002	0.0000000005	0.0000000015
Serum Apolipoprotein A32 (mg/dL)	0.0000000005	0.0000000002	0.0000000002	0.000000001	0.0000000002	0.0000000008
Serum Apolipoprotein A33 (mg/dL)	0.0000000002	0.0000000001	0.0000000001	0.0000000005	0.0000000001	0.0000000003
Serum Apolipoprotein A34 (mg/dL)	0.0000000001	0.00000000005	0.00000000005	0.0000000002	0.00000000005	0.00000000015
Serum Apolipoprotein A35 (mg/dL)	0.00000000005	0.00000000002	0.00000000002	0.0000000001	0.00000000002	0.00000000008
Serum Apolipoprotein A36 (mg/dL)	0.00000000002	0.00000000001	0.00000000001	0.00000000005	0.00000000001	0.00000000003
Serum Apolipoprotein A37 (mg/dL)	0.00000000001	0.000000000005	0.000000000005	0.00000000002	0.000000000005	0.000000000015
Serum Apolipoprotein A38 (mg/dL)	0.000000000005	0.000000000002	0.000000000002	0.00000000001	0.000000000002	0.000000000008
Serum Apolipoprotein A39 (mg/dL)	0.000000000002	0.000000000001	0.000000000001	0.000000000005	0.000000000001	0.000000000003
Serum Apolipoprotein A40 (mg/dL)	0.000000000001	0.0000000000005	0.0000000000005	0.000000000002	0.0000000000005	0.0000000000015
Serum Apolipoprotein A41 (mg/dL)	0.0000000000005	0.0000000000002	0.0000000000002	0.000000000001	0.0000000000002	0.0000000000008
Serum Apolipoprotein A42 (mg/dL)	0.0000000000002	0.0000000000001	0.0000000000001	0.0000000000005	0.0000000000001	0.0000000000003
Serum Apolipoprotein A43 (mg/dL)	0.0000000000001	0.00000000000005	0.00000000000005	0.0000000000002	0.00000000000005	0.00000000000015
Serum Apolipoprotein A44 (mg/dL)	0.00000000000005	0.00000000000002	0.00000000000002	0.0000000000001	0.00000000000002	0.00000000000008
Serum Apolipoprotein A45 (mg/dL)	0.00000000000002	0.00000000000001	0.00000000000001	0.00000000000005	0.00000000000001	0.00000000000003
Serum Apolipoprotein A46 (mg/dL)	0.00000000000001	0.000000000000005	0.000000000000005	0.00000000000002	0.000000000000005	0.000000000000015
Serum Apolipoprotein A47 (mg/dL)	0.000000000000005	0.000000000000002	0.000000000000002	0.00000000000001	0.000000000000002	0.000000000000008
Serum Apolipoprotein A48 (mg/dL)	0.000000000000002	0.000000000000001	0.000000000000001	0.000000000000005	0.000000000000001	0.000000000000003
Serum Apolipoprotein A49 (mg/dL)	0.000000000000001	0.0000000000000005	0.0000000000000005	0.000000000000002	0.0000000000000005	0.0000000000000015
Serum Apolipoprotein A50 (mg/dL)	0.0000000000000005	0.0000000000000002	0.0000000000000002	0.000000000000001	0.0000000000000002	0.0000000000000008
Serum Apolipoprotein A51 (mg/dL)	0.0000000000000002	0.0000000000000001	0.0000000000000001	0.0000000000000005	0.0000000000000001	0.0000000000000003
Serum Apolipoprotein A52 (mg/dL)	0.0000000000000001	0.00000000000000005	0.00000000000000005	0.0000000000000002	0.00000000000000005	0.00000000000000015
Serum Apolipoprotein A53 (mg/dL)	0.00000000000000005	0.00000000000000002	0.00000000000000002	0.0000000000000001	0.00000000000000002	0.00000000000000008
Serum Apolipoprotein A54 (mg/dL)	0.00000000000000002	0.00000000000000001	0.00000000000000001	0.00000000000000005	0.00000000000000001	0.00000000000000003
Serum Apolipoprotein A55 (mg/dL)	0.00000000000000001	0.000000000000000005	0.000000000000000005	0.00000000000000002	0.000000000000000005	0.000000000000000015
Serum Apolipoprotein A56 (mg/dL)	0.000000000000000005	0.000000000000000002	0.000000000000000002	0.00000000000000001	0.000000000000000002	0.000000000000000008
Serum Apolipoprotein A57 (mg/dL)	0.000000000000000002	0.000000000000000001	0.000000000000000001	0.000000000000000005	0.000000000000000001	0.000000000000000003
Serum Apolipoprotein A58 (mg/dL)	0.000000000000000001	0.0000000000000000005	0.0000000000000000005	0.000000000000000002	0.0000000000000000005	0.0000000000000000015
Serum Apolipoprotein A59 (mg/dL)	0.0000000000000000005	0.0000000000000000002	0.0000000000000000002	0.000000000000000001	0.0000000000000000002	0.0000000000000000008
Serum Apolipoprotein A60 (mg/dL)	0.0000000000000000002	0.0000000000000000001	0.0000000000000000001	0.0000000000000000005	0.0000000000000000001	0.0000000000000000003
Serum Apolipoprotein A61 (mg/dL)	0.0000000000000000001	0.00000000000000000005	0.00000000000000000005	0.0000000000000000002	0.00000000000000000005	0.00000000000000000015
Serum Apolipoprotein A62 (mg/dL)	0.00000000000000000005	0.00000000000000000002	0.00000000000000000002	0.00000000000000000001	0.00000000000000000002	0.00000000000000000008
Serum Apolipoprotein A63 (mg/dL)	0.00000000000000000002	0.00000000000000000001	0.00000000000000000001	0.00000000000000000005	0.00000000000000000001	0.00000000000000000003
Serum Apolipoprotein A64 (mg/dL)	0.00000000000000000001	0.000000000000000000005	0.000000000000000000005	0.00000000000000000002	0.000000000000000000005	0.000000000000000000015
Serum Apolipoprotein						

<sup>1</sup>Radiology, Academic Medical Center, Amsterdam, Netherlands,  
<sup>2</sup>Radiology, Northwestern University, Chicago, IL, United States,  
<sup>3</sup>Biomedical Engineering, Northwestern University, Chicago, IL, United States,  
<sup>4</sup>Division of Surgery-Cardiac Surgery, Northwestern University, Chicago, IL, United States, <sup>5</sup>Medicine-Cardiology, Feinberg School of Medicine, Northwestern University, Chicago, IL, United States, <sup>6</sup>Cardiac Sciences, University of Calgary, Calgary, Canada

4D flow MRI-derived 3D velocity and wall shear stress (WSS) maps in a large cohort of patients with aortopathy (n=515), stratified for valve morphology and stenosis severity, were compared with age-matched cohort-averaged maps of healthy controls (n=56) to yield maps of abnormally elevated hemodynamics. These maps were projected onto shared geometries and summed to map the incidence of abnormal velocity and WSS. Without stenosis, hemodynamics were significantly increased (Bonferroni corrected Mann-Whitney tests) in patients with bicuspid valves compared to patients with tricuspid valves. Incidence of elevated hemodynamics increased similarly for both cohorts (significant differences disappeared) with increasing stenosis severity.

---

---

### **Traditional Poster: Neuro**

Exhibition Hall 2165-2197      Wednesday 13:45 - 15:45      *(no CME credit)*

---

### **Electronic Poster: Cardiovascular**

Exhibition Hall      Wednesday 13:45 - 14:45      *(no CME credit)*

---

### **Electronic Poster: Body: Breast, Chest, Abdomen, Pelvis**

Exhibition Hall      Wednesday 13:45 - 14:45      *(no CME credit)*

---

### **Study Groups**

#### **Musculoskeletal MR Study Group**

Room 323ABC      Wednesday 13:45 - 15:45      *(no CME credit)*

---

---

## Study Groups

### Perfusion Study Group

Room 317AB      Wednesday 13:45 -      (no CME credit)  
15:45

---

## Educational Course

### Body MRS: How & Why?

Organizers: Anke Henning, Ph.D., Gregory J. Metzger, Ph.D. & Valeria Panebianco, M.D.

Room 315      Wednesday 13:45 -      Moderators: Gregory Metzger & Valeria  
15:45      Panebianco

---

13:45

#### Prostate Cancer: Proton & Beyond

Tom WJ Scheenen<sup>1</sup>

*<sup>1</sup>Radiology and Nuclear Medicine, Radboud university medical center, Nijmegen, Netherlands*

The use of proton spectroscopic imaging in prostate cancer at clinical field strengths of 1.5 and 3T will be discussed. Moreover, latest developments at 3T, as well as the possibilities of 7T are shown for proton as well as phosphorous spectroscopic imaging, culminating in the ultimate multi-parametric MRI examination...

---

14:15

#### Breast Cancer

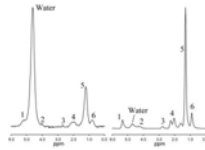
Uma Sharma

Magnetic resonance imaging (MRI) has high sensitivity for detection of breast cancer but low specificity. Qualitative and quantitative measurements of choline containing (tCho) compounds by MR spectroscopy have shown promise in diagnosis as well as in non-invasive therapeutic assessment of breast cancer. Diffusion weighted imaging (DWI) allows mapping of apparent diffusion coefficient (ADC) of tissues. The lower ADC value has been reported in malignant compared to benign disease. Use of these techniques in combination has been documented to increase the specificity of MRI. This talk highlights the role of MRS and DWI in breast cancer management.

---



14:45



## MRS in Hepatic Disease

Gavin Hamilton<sup>1</sup>

<sup>1</sup>*Department of Radiology, University of California, San Diego, La Jolla, CA, United States*

The <sup>1</sup>H MR spectrum of the liver is dominated by a water peak and peaks associated with fat. This talk will examine the technical challenges associated with MRS of fat and water in the liver and examine how to minimize or correct confounders associated with estimation of three tissue properties: Proton Density Fat Fraction, Liver Triglyceride Composition, and Liver Water and Fat Relaxation.

---

15:15

## Cardiac Spectroscopy

Christopher T. Rodgers<sup>1</sup>

<sup>1</sup>*University of Oxford*

Magnetic resonance spectroscopy (MRS)<sup>1-4</sup> is a method for non-invasively probing metabolism. The major nuclei studied by MRS methods in the heart include <sup>1</sup>H (for measures of fat fraction, creatine content, etc), <sup>31</sup>P (for measures of energy transport through the creatine-kinase system in the form of ATP, phosphocreatine, and their kinetics, and for determination of pH), <sup>13</sup>C (for stable-isotope tracer studies, and more recently with hyperpolarised pyruvate to study glycolysis), and more recently <sup>17</sup>O (to trace oxidative respiration) and other nuclei. This lecture provides an overview of the major methods of cardiac spectroscopy and their contributions to biomedicine.

---

15:45

Adjournment & Meet the Teachers

---

## Educational Course

### Junior Fellows Symposium: Machine Learning in Imaging

*Organizers:* Jakob Assländer, Ph.D., Steven H. Baete, Ph.D., Adrienne E. Campbell-Washburn, Ph.D., Thijs Dhollander, Ph.D. & Signe Johanna Vannesjö, Ph.D.

Room 313BC

Wednesday 13:45 -  
15:45

*Moderators:* Jakob Assländer & Steven Baete

---

13:45

### Machine Learning & Opportunities in MRI

Daniel Alexander<sup>1</sup>

<sup>1</sup>*UCL*

The talk will give an introduction to machine learning and explore opportunities to exploit the technology in MRI development and application.

---

14:15

### Insights into Learning-Based MRI Reconstruction

Kerstin Hammernik<sup>1</sup>

<sup>1</sup>*Institute of Computer Graphics and Vision, Graz University of Technology, Graz, Austria*

In this educational, we give an overview of the current developments in deep learning-based MRI reconstruction of undersampled k-space data. We show the advantages of deep learning-based approaches over compressed sensing approaches in terms of improved image quality and suppressed artifacts. We will also discuss several challenges that are encountered during learning covering the design of a training database, deep network architectures and image quality measures.

---

14:45

### Computer Aided Diagnosis

Dinggang Shen<sup>1</sup>

<sup>1</sup>*Department of Radiology and Biomedical Research Imaging Center (BRIC), UNC-Chapel Hill*

Deep learning is rapidly becoming the state of the art, leading to enhanced performance in various medical applications. In this talk, I will introduce the fundamentals of deep learning methods and their applications in computer-aided diagnosis for Alzheimer's Disease (AD), breast cancer, lung cancer, and brain tumors.

---

15:15

### Introduction by Discussion Leaders

Adrienne Campbell-Washburn<sup>1</sup>

<sup>1</sup>*National Heart, Lung, and Blood Institute, National Institutes of Health, MD*

A panel discussion regarding the role of machine learning in clinical MRI

---

15:15

[Introduction by Discussion Leaders](#)

Thijs Dhollander<sup>1</sup>

*<sup>1</sup>The Florey Institute of Neuroscience and Mental Health, Melbourne, Australia*

---

15:15

[Radiologist vs. Computer: Panel Discussion](#)

Vikas Gulani<sup>1</sup>

*<sup>1</sup>Radiology, Case Western Reserve University, Cleveland, United States*

---

15:15

[Radiologist vs. Computer: Panel Discussion](#)

Susie Y Huang<sup>1</sup>

*<sup>1</sup>Department of Radiology, Massachusetts General Hospital, Boston, MA, United States*

[Panel discussion on machine learning](#)

---

15:15

[Radiologist vs. Computer: Panel Discussion](#)

Tim Leiner

---

15:45

[Adjournment & Meet the Teachers](#)

---

## Power Pitch

### Pitch: RF Arrays & Systems

Power Pitch

Theater A -

Exhibition Hall

Wednesday 13:45  
- 14:45

Moderators: Joseph Risoli &  
Steven Wright

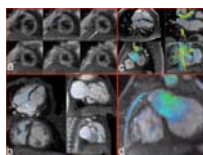
*(no CME credit)*

---

755

13:45

[Development and Clinical Implementation of Very Light Weight and Highly Flexible AIR Technology Arrays](#)



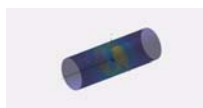
Shreyas S Vasanaawala<sup>1</sup>, Robert Stormont<sup>2</sup>, Scott Lindsay<sup>2</sup>, Thomas Grafendorfer<sup>2</sup>, Joseph Y Cheng<sup>1</sup>, John M Pauly<sup>3</sup>, Michael Lustig<sup>4</sup>, Greig Scott<sup>3</sup>, Jorge X Guzman<sup>2</sup>, Victor Taracila<sup>2</sup>, Daniel Chirayath<sup>2</sup>, and Fraser Robb<sup>2</sup>

<sup>1</sup>Radiology, Stanford University, Stanford, CA, United States, <sup>2</sup>GE Healthcare, <sup>3</sup>Electrical Engineering, Stanford University, <sup>4</sup>Electrical Engineering and Computer Science, UC Berkeley

---

756

13:45



[The Optimality Principle for MR signal excitation and reception: new physical insights into ideal RF coil design](#)

Daniel K. Sodickson<sup>1,2</sup>, Riccardo Lattanzi<sup>1,2</sup>, Manushka Vaidya<sup>1,2</sup>, Gang Chen<sup>1,2</sup>, Dmitry S. Novikov<sup>1,2</sup>, Christopher M. Collins<sup>1,2</sup>, and Graham C. Wiggins<sup>1,2</sup>

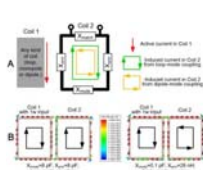
<sup>1</sup>Center for Advanced Imaging Innovation and Research (CAI2R) and Bernard and Irene Schwartz Center for Biomedical Imaging (CBI), Department of Radiology, New York University School of Medicine, New York, NY, United States, <sup>2</sup>Sackler Institute of Graduate Biomedical Sciences, New York University School of Medicine, New York, NY, United States

---

757



13:45



[Self-Decoupled RF Coils](#)

Xinqiang Yan<sup>1,2</sup>, John C. Gore<sup>1,2,3</sup>, and William A. Grissom<sup>1,2,3</sup>

<sup>1</sup>Institute of Imaging Science, Vanderbilt University, Nashville, TN, United States, <sup>2</sup>Department of Radiology and Radiological Sciences, Vanderbilt University, Nashville, TN, United States, <sup>3</sup>Department of Biomedical Engineering, Vanderbilt University, Nashville, TN, United States

---

758



13:45



[Optically Controlled Four-Channel Transceiver for 7T imaging with RF Monitoring Feedback](#)

Natalia Gudino<sup>1</sup>, Jacco A de Zwart<sup>1</sup>, Peter van Gelderen<sup>1</sup>, and Jeff H Duyn<sup>1</sup>

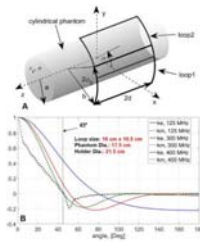
<sup>1</sup>Advanced MRI Section, LFMI, NINDS, National Institutes of Health, Bethesda, MD, United States

---

759

13:45

[Double-Row 16-element Tight-Fit Transceiver Phased Array with High Transmit Performance for Whole Human Brain Imaging at 9.4T.](#)



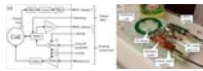
Nikolai I. Avdievich<sup>1</sup>, Ioannis A. Giapitzakis<sup>1</sup>, and Anke Henning<sup>1,2</sup>

<sup>1</sup>Max Planck Institute for Biological Cybernetics, Tübingen, Germany,

<sup>2</sup>Institute of Physics, Ernst-Moritz-Arndt University, Greifswald, Germany

760

13:45



[Compact iPRES coil assembly for Magnetic Resonance Fingerprinting](#)

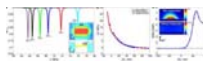
Michael Twieg<sup>1</sup>, Bhairav B Mehta<sup>2</sup>, Simone Coppo<sup>2</sup>, Haoqin Zhu<sup>3</sup>, Labros Petropoulos<sup>3</sup>, Hiroyuki Fujita<sup>3</sup>, and Mark A Griswold<sup>4</sup>

<sup>1</sup>Dept of Radiology, Case Western Reserve University, Cleveland Heights, OH, United States, <sup>2</sup>Dept of Radiology, Case Western Reserve University, Cleveland, OH, United States, <sup>3</sup>Quality Electrodynamics, Mayfield Village, OH, United States, <sup>4</sup>Dept of Radiology, Case Western Reserve University, OH, United States

761



13:45



[Wireless coil based on meta-technologies for MRI implementations](#)

Alena Shchelokova<sup>1</sup>, Alexey Slobozhanyuk<sup>1,2</sup>, Irina Melchakova<sup>1</sup>, Andrew Webb<sup>3</sup>, Yuri Kivshar<sup>1,2</sup>, and Pavel Belov<sup>1</sup>

<sup>1</sup>Department of Nanophotonics and Metamaterials, ITMO University, St.Petersburg, Russian Federation, <sup>2</sup>Nonlinear Physics Center, Research School of Physics and Engineering, Australian National University, Canberra, Australia, <sup>3</sup>Department of Radiology, Leiden University Medical Center, Leiden, Netherlands

762



13:45



[Development and performance evaluation of the second prototype of a RF-coil integrated PET insert for existing 3T MRI systems](#)

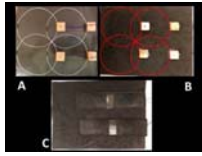
Md Shahadat Hossain Akram<sup>1</sup>, Fumihiko Nishikido<sup>1</sup>, Takayuki Obata<sup>1</sup>, Mikio Suga<sup>2</sup>, Eiji Yoshida<sup>1</sup>, Hedeaki Tashima<sup>1</sup>, Keiji Shimizu<sup>3</sup>, Masanori Fujiwara<sup>2</sup>, Akram Mohammadi<sup>1</sup>, and Taiga Yamaya<sup>1</sup>

<sup>1</sup>National Institute of Radiological Sciences, Chiba, Japan, <sup>2</sup>Chiba University, Chiba, Japan, <sup>3</sup>Hamamatsu Photonics K.K., Hamamatsu, Japan

763

13:45

[Characterization of a new ultra-flexible, low profile RF receive coil technology.](#)



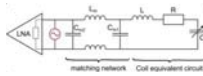
Philip Rossman<sup>1</sup>, Robert Stormont<sup>2</sup>, Scott Lindsay<sup>2</sup>, Fraser Robb<sup>2</sup>, Dennis Savitskij<sup>2</sup>, David Stanley<sup>2</sup>, John Huston<sup>1</sup>, Timothy Kaufmann<sup>1</sup>, and Kiaran McGee<sup>1</sup>

<sup>1</sup>Department of Radiology, Mayo Clinic, Rochester, MN, United States, <sup>2</sup>GE Healthcare, Waukesha, WI

---

764

13:45



[Resonance frequency detection of a stretchable RF receiver coil for MRI](#)

Andreas Mehmann<sup>1</sup>, Christian Vogt<sup>1</sup>, Benjamin Sporrer<sup>2</sup>, Matija Varga<sup>1</sup>, Qiuting Huang<sup>2</sup>, and Gerhard Troester<sup>1</sup>

<sup>1</sup>Electronics Laboratory, ETH Zurich, Zurich, Switzerland, <sup>2</sup>Integrated Systems Laboratory, ETH Zurich, Switzerland

---

765

13:45



[Mary had a little Lamb: Scanner-recorded speech during MRI without gradient-induced sound](#)

Jan Ole Pedersen<sup>1,2</sup>, Christian Hanson, Rong Xue<sup>3</sup>, and Lars G. Hanson<sup>1,2</sup>

<sup>1</sup>Danish Research Centre for Magnetic Resonance, Centre for Functional and Diagnostic Imaging and Research, Copenhagen University Hospital, Kgs Lyngby, Denmark, <sup>2</sup>Centre for Magnetic Resonance, DTU Elektro, Technical University of Denmark, Kgs Lyngby, Denmark, <sup>3</sup>State Key Laboratory of Brain and Cognitive Science, Research, Institute of Biophysics, Chinese Academy of Sciences

---

766

13:45



[Dielectric resonator antenna receive array at 7 Tesla using detunable ceramic resonators](#)

Thomas Ruytenberg<sup>1</sup> and Andrew Webb<sup>1</sup>

<sup>1</sup>Radiology, Leiden University Medical Center, Leiden, Netherlands

---

767

13:45



[Top-Hat Dipole RF Coil with Large Field of View for 7 T Brain MR Imaging](#)

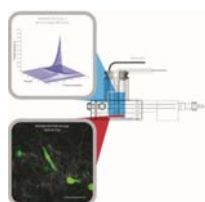
Chang-Hyun Oh<sup>1,2,3,4</sup>, Chulhyun Lee<sup>5</sup>, Suchit Kumar<sup>3</sup>, Jun-Sik Yoon<sup>1</sup>, Ha-Kyu Jeong<sup>6</sup>, Jeong-Hee Kim<sup>2</sup>, Young-Seung Jo<sup>1,5</sup>, Jong-Min kim<sup>1</sup>, Christian Bruns<sup>7</sup>, Tim Herrmann<sup>7</sup>, Johannes Bernarding<sup>7</sup>, and Zang-Hee Cho<sup>8</sup>

<sup>1</sup>Department of Electronics and Information Technology, Korea University, Seoul, Korea, Republic of, <sup>2</sup>Research Institute for Advanced Industrial Technology, Korea University, Sejong City, Korea, Republic of, <sup>3</sup>Department of Biomicrosystem Technology, Korea University, Seoul, Korea, Republic of, <sup>4</sup>ICT Convergence Technology for Health & Safety, Korea University, Sejong City, Korea, Republic of, <sup>5</sup>Korea Basic Science Institute, Cheongju, Chungcheongbuk-do, Korea, Republic of, <sup>6</sup>BIU Clinical Science MR, Philips Korea, Seoul, Korea, Republic of, <sup>7</sup>Department for Biometrics und Medical Informatics, Otto-von-Guericke University, Magdeburg, Germany, <sup>8</sup>Advanced Institutes of Convergence Technology, Seoul National University, Seoul, Korea, Republic of

768



13:45



**Bioreactor for in vitro optical fluorescence and magnetic resonance spectroscopy**

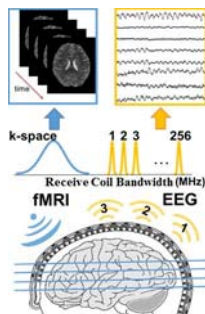
Benjamin L Cox<sup>1,2,3</sup>, Joseph M Szulczewski<sup>3,4</sup>, Kai D Ludwig<sup>1</sup>, Erin B Adamson<sup>1</sup>, Robert A Swader<sup>2</sup>, Sarah A Erickson-Bhatt<sup>2,3,4</sup>, Patricia J Keely<sup>4</sup>, Kevin W Eliceiri<sup>1,2,3,5</sup>, and Sean B Fain<sup>1,6</sup>

<sup>1</sup>Medical Physics, University of Wisconsin - Madison, Madison, WI, United States, <sup>2</sup>Medical Engineering, Morgridge Institute for Research, Madison, WI, United States, <sup>3</sup>Laboratory for Optical and Computational Instrumentation (LOCI), University of Wisconsin - Madison, Madison, WI, United States, <sup>4</sup>Cell and Regenerative Biology, University of Wisconsin - Madison, Madison, WI, United States, <sup>5</sup>Biomedical Engineering, University of Wisconsin - Madison, Madison, WI, United States, <sup>6</sup>Radiology, University of Wisconsin - Madison, Madison, WI, United States

769



13:45



**Multimodal Imaging: MR-Compatible, Gradient Artifact free, Wireless recording system integrated with MR-scanner for Simultaneous EEG and fMRI acquisition**

Ranajay Mandal<sup>1</sup>, Nishant Babaria<sup>2</sup>, Jiayue Cao<sup>1</sup>, and Zhongming Liu<sup>1,2</sup>

<sup>1</sup>Biomedical Engineering, Purdue University, West Lafayette, IN, United States, <sup>2</sup>Electrical and Computer Engineering, Purdue University, West Lafayette, IN, United States

770

13:45

**Sustainable RF-coil for Breast or Other Applications in Research and Development (SURFBOARD)**

Christopher John Wiggins<sup>1</sup> and Benedikt A Poser<sup>2</sup>





<sup>1</sup>Scannexus BV, Maastricht, Netherlands, <sup>2</sup>Faculty of Psychology and Neuroscience, Maastricht University, Maastricht, Netherlands

---

## Power Pitch

### Pitch: Post-Processing & Motion

Power Pitch  
Theater B -  
Exhibition Hall

Wednesday  
13:45 - 14:45

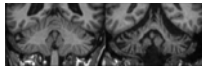
Moderators: Ricardo Otazo &  
Stefan Skare

(no CME credit)

---

771

13:45



[cBEaST: Cerebellar Brain Extraction based on Nonlocal Segmentation Technique – A comparison with state-of-the-art methods](#)

Daniel Güllmar<sup>1</sup>, Viktor Pfaffenrot<sup>2,3</sup>, Rossitza Draganova<sup>2</sup>, Xiang Feng<sup>1</sup>, Jürgen R Reichenbach<sup>1</sup>, Dagmar Timmann<sup>2</sup>, and Andreas Deistung<sup>1,2</sup>

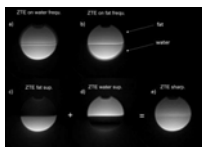
<sup>1</sup>Medical Physics Group, Institute for Diagnostic and Interventional Radiology, Jena University Hospital – Friedrich Schiller-University, Jena, Germany, <sup>2</sup>Section of Experimental Neurology, Department of Neurology, Essen University Hospital, Germany, <sup>3</sup>Erwin L. Hahn Institute for Magnetic Resonance Imaging, University Duisburg-Essen, Essen, Germany

---

772



13:45



[Signal-model-based water-fat separation in Zero Echo Time \(ZTE\) MRI](#)

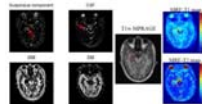
Romain Nicolas Froidevaux<sup>1</sup>, Markus Weiger<sup>1</sup>, Po-Jui LU<sup>2</sup>, and Klaas Paul Pruessmann<sup>1</sup>

<sup>1</sup>University and ETH Zurich, Zürich, Switzerland, <sup>2</sup>ETH Zurich, Zurich, Switzerland

---

773

13:45



[Suspicious Component Segmentation for Identifying Hippocampal Sclerosis Using Regularized Tissue-Fraction MR Fingerprinting](#)

Kang Wang<sup>1</sup>, Congyu Liao<sup>2</sup>, Xiaozhi Cao<sup>2</sup>, Zhixing Wang<sup>2</sup>, Dengchang Wu<sup>1</sup>, Hongjian He<sup>2</sup>, Qiuping Ding<sup>2</sup>, and Jianhui Zhong<sup>2</sup>

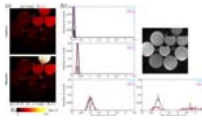
<sup>1</sup>Department of Neurology, The First Affiliated Hospital, School of Medicine, Zhejiang University, Hangzhou, People's Republic of China, <sup>2</sup>Center for Brain Imaging Science and Technology, Department of Biomedical Engineering, Zhejiang University, Hangzhou, People's Republic of China

---

774



13:45



Improved Short-T2\* Estimation with Bloch Equation-Modeled Concurrent Excitation and Relaxation

Ethan M Johnson<sup>1</sup>, Kim Butts Pauly<sup>2</sup>, and John M Pauly<sup>1</sup>

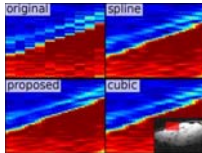
<sup>1</sup>Electrical Engineering, Stanford University, Stanford, CA, United States,

<sup>2</sup>Radiology, Stanford University, Stanford, CA, United States

---

775

13:45



Edge preserving upsampling of image resolution in MRI

Marco Reiser<sup>1</sup> and Elias Kellner<sup>1</sup>

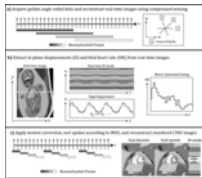
<sup>1</sup>Dep. of Radiology, Medical Physics, University Medical Center Freiburg, Freiburg, Germany

---

776



13:45



Motion-compensated reconstruction of fetal cardiac MRI using a golden-angle radial acquisition, retrospective gating, and compressed sensing

Christopher W. Roy<sup>1,2</sup>, Mike Seed<sup>3,4</sup>, and Christopher K. Macgowan<sup>1,2</sup>

<sup>1</sup>Medical Biophysics, University of Toronto, Toronto, ON, Canada,

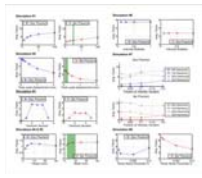
<sup>2</sup>Physiology and Experimental Medicine, Hospital for Sick Children, Toronto, ON, Canada, <sup>3</sup>Pediatric Cardiology, Hospital for Sick Children, Toronto, ON, Canada, <sup>4</sup>Pediatric and Diagnostic Imaging, University of Toronto, Toronto, ON, Canada

---

777



13:45



From Visualization to Quantification: Calibrating Motion Magnification by Amplified Magnetic Resonance Imaging

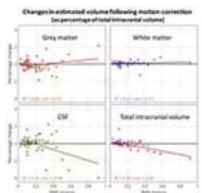
Wendy W Ni<sup>1</sup>, Maged Goubran<sup>1</sup>, Greg Zaharchuk<sup>1</sup>, Michael Moseley<sup>1</sup>, Kristen Yeom<sup>1</sup>, and Samantha Holdsworth<sup>1</sup>

<sup>1</sup>Radiology, Stanford University, Stanford, CA, United States

---

778

13:45



Assessing the effect of head-motion on tissue volume estimates

Daniel Gallichan<sup>1,2</sup>

<sup>1</sup>School of Engineering, Cardiff University, Cardiff, United Kingdom,

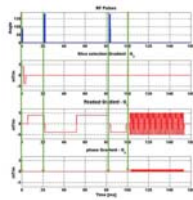
<sup>2</sup>EPFL- CIBM, Lausanne, Switzerland

---

779

13:45

Prospective motion correction on diffusion weighted imaging: improving data quality with four radio frequency and gradient pulses updates.



Danilo Maziero<sup>1</sup>, Michael Herbst<sup>2</sup>, and Thomas Ernst<sup>3</sup>

<sup>1</sup>University of Hawaii, Honolulu, HI, United States, <sup>2</sup>Department of Radiology, University Medical Center Freiburg, Freiburg, Germany,

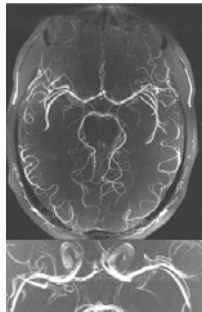
<sup>3</sup>Department of Medicine, John A. Burns School of Medicine, University of Hawaii, Honolulu, HI, United States

---

780



13:45



[Motion corrected high resolution time-of-flight angiography at 7T using Segmented FatNavs](#)

Frédéric Gretschi<sup>1</sup> and Daniel Gallichan<sup>2</sup>

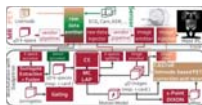
<sup>1</sup>EPFL, Lausanne, Switzerland, <sup>2</sup>School of Engineering, Cardiff, United Kingdom

---

781



13:45



[Motion correction on a human PET/MR scanner: Clinical feasibility of a motion correction system in patients – an update report](#)

Thomas Küstner<sup>1,2</sup>, Christian Würsli<sup>3</sup>, Martin Schwartz<sup>2,4</sup>, Hadi Fayad<sup>5</sup>, Thibaut Merlin<sup>5</sup>, Christopher Gilliam<sup>6</sup>, Thierry Blu<sup>6</sup>, Petros Martirosian<sup>4</sup>, Fritz Schick<sup>4</sup>, Bin Yang<sup>2</sup>, Holger Schmidt<sup>1</sup>, and Nina F Schwenzer<sup>1</sup>

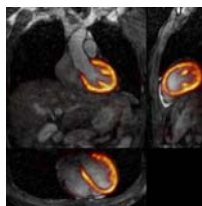
<sup>1</sup>Department of Radiology, University of Tuebingen, Tuebingen, Germany, <sup>2</sup>Institute of Signal Processing and System Theory, University of Stuttgart, Stuttgart, Germany, <sup>3</sup>University of Stanford, Palo Alto, CA, United States, <sup>4</sup>Section on Experimental Radiology, University of Tuebingen, Tuebingen, Germany, <sup>5</sup>LaTIM, INSERM, University of Bretagne, Brest, France, <sup>6</sup>Department of Electronic Engineering, Chinese University of Hong Kong, Hong Kong, Hong Kong

---

782



13:45



[Respiratory motion-corrected simultaneous cardiac PET and coronary MR angiography using a hybrid 3T PET-MR](#)

Camila Munoz<sup>1</sup>, Radhouene Neji<sup>1,2</sup>, Gastao Cruz<sup>1</sup>, Rene Botnar<sup>1</sup>, and Claudia Prieto<sup>1</sup>

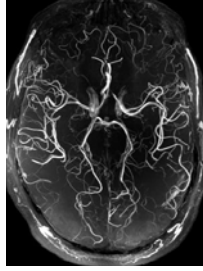
<sup>1</sup>Division of Imaging Sciences and Biomedical Engineering, King's College London, London, United Kingdom, <sup>2</sup>MR Research Collaborations, Siemens Healthcare, Frimley, United Kingdom

---

783



13:45



### Beyond the biological resolution limit: Prospectively motion corrected Time of Flight angiography at 7T

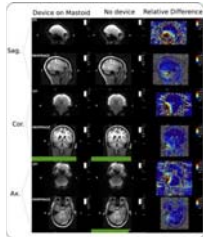
Hendrik Mattern<sup>1</sup>, Alessandro Sciarra<sup>1</sup>, Frank Godenschweger<sup>1</sup>, Daniel Stucht<sup>1</sup>, Falk Lüsebrink<sup>1</sup>, and Oliver Speck<sup>1,2,3,4</sup>

<sup>1</sup>BMMR, Otto-von-Guericke-University, Magdeburg, Germany, <sup>2</sup>German Center for Neurodegenerative Disease, Magdeburg, Germany, <sup>3</sup>Center for Behavioral Brain Sciences, Magdeburg, Germany, <sup>4</sup>Leibniz Institute for Neurobiology, Magdeburg, Germany

784



13:45



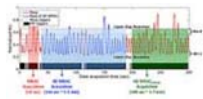
### Implementation of a 2.4 GHz wireless sensing platform for transmission of motion data from within a head coil at 3T.

Adam M.J. van Niekerk<sup>1</sup>, Andre J. W. van der Kouwe<sup>1,2,3</sup>, and Ernesta M. Meintjes<sup>1</sup>

<sup>1</sup>Division of Biomedical Engineering, Human Biology, University of Cape Town, Cape Town, South Africa, <sup>2</sup>Athinoula A. Martinos Center, Massachusetts General Hospital, Charlestown, MA, United States, <sup>3</sup>Radiology, Harvard Medical School, Boston, MA, United States

785

13:45



### Respiratory Phase-Matched MR-based Attenuation Correction (MRAC) for Four-Dimensional (4D) PET in PET/MRI: A Feasibility Study

Jaewon Yang<sup>1</sup>, Florian Wiesinger<sup>2</sup>, Anne Menini<sup>2</sup>, Jing Liu<sup>1</sup>, Thomas A. Hope<sup>1</sup>, Youngho Seo<sup>1</sup>, and Peder E. Z. Larson<sup>1</sup>

<sup>1</sup>Radiology and Biomedical Imaging, UCSF, San Francisco, CA, United States, <sup>2</sup>GE Global Research

## Oral

## Quantification of Microstructure

Room 311

Wednesday 13:45 -  
15:45

Moderators: Gareth Barker & Dan Wu

786

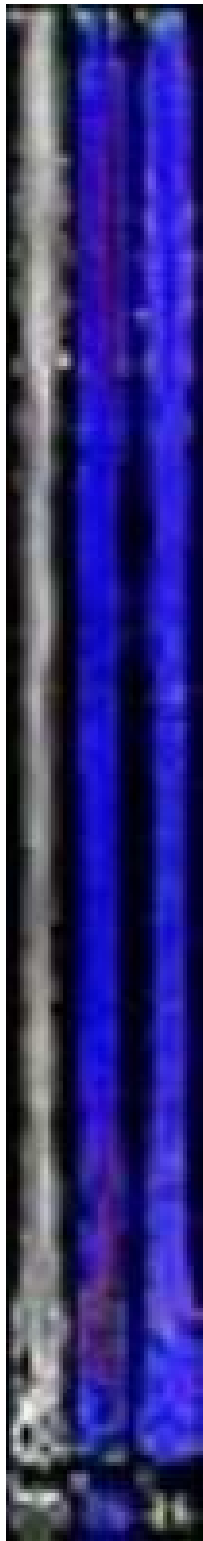


13:45

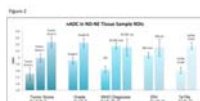
### Diffusion MRI of the entire postmortem human spinal cord at microscopic resolution

Evan Calabrese<sup>1</sup>, Gary Cofer<sup>1</sup>, Nandan Lad<sup>1</sup>, and G. Allan Johnson<sup>1</sup>

<sup>1</sup>Duke University, Durham, NC, United States



Diffusion MR imaging of the human spinal cord has become increasingly important in both clinical diagnostics, and research science.<sup>1</sup> As MRI methods improve, there is a need to understand the limits of diffusion MRI in the human spinal cord. Here, we present a microscopic resolution diffusion MRI dataset of the entire postmortem human spinal cord, generated from a multi-segment acquisition, using an automated image-processing pipeline. These data provide unique insights for spinal cord research, future diagnostic imaging applications, and for postmortem pathologic evaluation of spinal cord specimens.

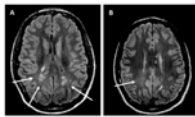


<sup>1</sup>University of California San Francisco, San Francisco, CA, United States

The relationship of diffusion imaging parameters with prognostic histological and molecular factors for patients with grade II and III gliomas is unclear, particularly for tumors that are non-enhancing on post-Gadolinium images. We investigated the relationship of ADC and FA values with histological tumor score, tumor grade, and molecular characteristics for non-enhancing (NE) vs contrast-enhancing (CE) and newly-diagnosed (ND) vs recurrent (REC) disease. In NE patients, histopathological and molecular characteristics associated with poorer clinical outcome were found to have higher ADC and lower FA. In CE patients, some characteristics associated with poorer outcome had lower ADC and higher FA.

788

14:09



Prevalence of diffusely abnormal white matter in individuals with clinically isolated syndromes suggestive of multiple sclerosis

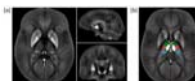
Cornelia Laule<sup>1,2,3</sup>, Jimmy Lee<sup>1</sup>, Guojun Zhao<sup>4,5</sup>, Rick White<sup>6</sup>, Irene M. Vavasour<sup>1</sup>, Andrew Riddehough<sup>4,5</sup>, Anthony L. Traboulsee<sup>4,5</sup>, Luanne Metz<sup>7</sup>, and David K.B. Li<sup>1,4,5</sup>

<sup>1</sup>Radiology, University of British Columbia, Vancouver, BC, Canada, <sup>2</sup>Pathology & Laboratory Medicine, University of British Columbia, Vancouver, BC, Canada, <sup>3</sup>International Collaboration on Repair Discoveries, University of British Columbia, Vancouver, BC, Canada, <sup>4</sup>Medicine (Neurology), University of British Columbia, Vancouver, BC, Canada, <sup>5</sup>MS/MRI Research Group, University of British Columbia, Vancouver, BC, Canada, <sup>6</sup>Statistics, University of British Columbia, Vancouver, BC, Canada, <sup>7</sup>Medicine, University of Calgary, Calgary, AB, Canada

Diffusely abnormal white matter (DAWM) is present in individuals with clinically isolated syndromes (CIS) suggestive of multiple sclerosis (MS) at a similar frequency as seen in definite MS. CIS subjects with DAWM showed reduced brain volume and greater lesion load, both of which are known to correlate with clinical disability and progression. DAWM may have prognostic importance in CIS so examining its impact on conversion to MS, future disability and progression is warranted.

789

14:21



Decreasing magnetic susceptibility (QSM) of thalamic nuclei in Multiple Sclerosis (MS) – the thalamus as a target of projected inflammation?



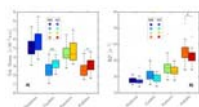
Ferdinand Schweser<sup>1,2</sup>, Ana Luiza Raffaini Duaete Martins<sup>1</sup>, Fuchun Lin<sup>1</sup>, Jesper Hagemeyer<sup>1</sup>, Jannis Hanspach<sup>1</sup>, Bianca Weinstock-Guttman<sup>3</sup>, Nicola Bertolino<sup>1</sup>, Dhaval Shah<sup>1</sup>, Niels P Bergsland<sup>1,4</sup>, Michael G Dwyer<sup>1</sup>, and Robert Zivadinov<sup>1,2</sup>

<sup>1</sup>Buffalo Neuroimaging Analysis Center, Department of Neurology, Jacobs School of Medicine and Biomedical Sciences, University at Buffalo, The State University of New York, Buffalo, NY, United States, <sup>2</sup>MRI Clinical and Translational Research Center, Jacobs School of Medicine and Biomedical Sciences, University at Buffalo, The State University of New York, Buffalo, NY, United States, <sup>3</sup>BairdMS Center, Department of Neurology, Jacobs School of Medicine and Biomedical Sciences, The State University of New York at Buffalo, Buffalo, NY, United States, <sup>4</sup>MR Research Laboratory, IRCCS, Don Gnocchi Foundation ONLUS, Milan, Italy

This work studied intra-thalamic magnetic susceptibility changes in 120 patients with clinically isolated syndrome (CIS), relapsing-remitting MS (RRMS), and secondary progressive MS (SPMS). We detected decreased magnetic susceptibility in several nuclear groups of the thalamus in MS patients compared to controls, indicative of decreased iron concentration.

790

14:33



Iron loss occurs in the deep gray matter of multiple sclerosis patients

Eneido Hernández-Torres<sup>1,2</sup>, Vanessa Wiggermann<sup>1,2,3</sup>, David K Li<sup>2,4,5</sup>, Lindsay Machan<sup>4</sup>, A Dessa Sadovnick<sup>5,6,7</sup>, Anthony Traboulsee<sup>5,6</sup>, Simon Hametner<sup>8</sup>, and Alexander Rauscher<sup>1,2</sup>

<sup>1</sup>Department of Pediatrics, Division of Neurology, University of British Columbia, Vancouver, Canada, <sup>2</sup>UBC MRI Research Centre, University of British Columbia, Vancouver, Canada, <sup>3</sup>Department of Physics and Astronomy, University of British Columbia, Vancouver, Canada, <sup>4</sup>Department of Radiology, University of British Columbia, Vancouver, Canada, <sup>5</sup>Department of Medicine, Division of Neurology, University of British Columbia, Vancouver, Canada, <sup>6</sup>Centre for Brain Health, University of British Columbia, Vancouver, Canada, <sup>7</sup>Department of Medical Genetics, University of British Columbia, Vancouver, Canada, <sup>8</sup>Department of Neuroimmunology, Center for Brain Research, Medical University of Vienna, Vienna, Austria



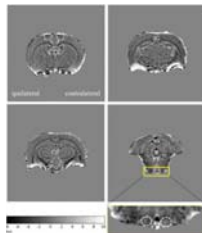
In this work, a new approach for looking at the “iron deposition” in deep gray matter is presented. We investigated iron deposition in the deep gray matter indirectly by measuring  $R2^*$ . In addition, we assessed the normalized volume of the structures of the DGM. We found a stronger association between increases in  $R2^*$  and volume reductions of the same DGM structures in the MS group compared with the control group. Finally, we corrected the  $R2^*$  measurements by the volume of the structures ( $R2^*_m$ ). The  $R2^*_m$  values were reduced in the MS group suggesting that iron accumulation is not a common feature of MS but on the contrary a redistribution/reduction of the iron takes place, which may be masked by structural atrophy.

791

14:45

Phase imaging of axonal integrity of cranial corticospinal tract in experimental spinal cord injury at 9.4T

Genxia He<sup>1,2</sup> and Junchao Qian<sup>1</sup>



<sup>1</sup>High Magnetic Field Lab of Chinese Academy of Sciences, Hefei, People's Republic of China, <sup>2</sup>Department of Neurology, Anhui Medical University, Hefei, People's Republic of China

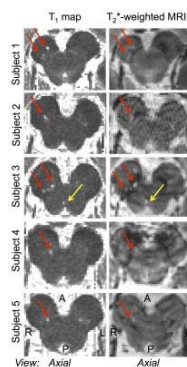
Spinal cord injury (SCI) leads to neuronal cell death, axonal damage and demyelination. Brain undergo anatomical changes following SCI. Recently MR phase imaging has shown promising application in visualizing demyelination. In this study we explored the possibility to investigate integrity of cranial corticospinal tract in SCI using phase imaging. Diffusion tensor imaging was also used to verify the axonal integrity. The results showed phase contrast decreased along with axial diffusivity did not significantly change in contralateral pyramid two weeks post-injury compared to pre-injury levels. Thus, phase imaging is a potential endogenous biomarker for brain axonal integrity after SCI.

792

14:57

7 Tesla imaging of microstructural brainstem changes in REM sleep behavior disorder

Marta Bianciardi<sup>1</sup>, Laura D Lewis<sup>1</sup>, Lawrence L Wald<sup>1</sup>, Bruce R Rosen<sup>1</sup>, and Aleksandar Videnovic<sup>2</sup>



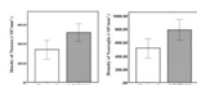
<sup>1</sup>Department of Radiology, A.A. Martinos Center for Biomedical Imaging, MGH and Harvard Medical School, Boston, MA, United States,

<sup>2</sup>Department of Neurology, MGH and Harvard Medical School, Boston, MA, United States

REM-sleep-behavior-disorder (RBD) is characterized by the absence of muscle-atonía during REM-sleep and is thought to be related to a dysfunction of brainstem-nuclei (Bn) of the arousal/motor networks. Yet, a precise identification of the Bn involved in vivo is still missing, thus limiting our understanding of this disease. Through multi-contrast high-spatial-resolution 7Tesla-MRI and a recently developed stereotaxic-Bn-atlas, we consistently detected across RBD-patients microstructural-changes in a subregion of the substantia nigra, consistent with pars reticulata, and in a peri-nigral area. Interestingly, these changes were compatible with the presence of lacunar infarcts, finding that differs from recent reports of nigral iron-accumulation in RBD.

793

15:09



### Detecting DISC1 Related Microstructural Abnormalities using Non-Gaussian Diffusion (DKI & NODDI) and QSM: with Histological Validation

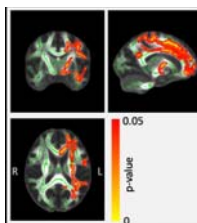
Nan-Jie Gong<sup>1,2</sup>, Russell Dibb<sup>3</sup>, Kyle Decker<sup>3</sup>, Mikhail Pletnikov<sup>4</sup>, Eric Benner<sup>3</sup>, and Chunlei Liu<sup>1,3</sup>

<sup>1</sup>Electrical Engineering and Computer Sciences, University of California Berkeley, Berkeley, CA, United States, <sup>2</sup>Brain Imaging and Analysis Center, Duke University School of Medicine, <sup>3</sup>Duke University School of Medicine, <sup>4</sup>Johns Hopkins University School of Medicine

Metrics provided by DKI could be used to detect microstructural changes. However, they bear no explicit neurobiological interpretations. In contrast, the biophysical model of NODDI could provide metrics sensitive to density of neuron. The magnetic susceptibility derived from QSM method can sever as a sensitive biomarker for quantifying density of cells including both neurons and neuroglia.

794

15:21



### A quantitative MRI study of APOE-dependent microstructural differences in young healthy volunteers using NODDI, qMT and g-ratio

Nicholas G Dowell<sup>1</sup>, Simon L Evans<sup>2</sup>, Sarah L King<sup>2</sup>, and Jennifer M Rusted<sup>2</sup>

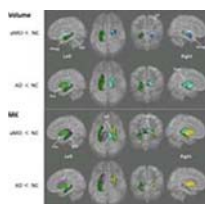
<sup>1</sup>CISC, BSMS, Brighton, United Kingdom, <sup>2</sup>Psychology, University of Sussex, Brighton, United Kingdom

We present the first NODDI, qMT and g-ratio study of microstructural differences between carriers and non-carriers of the APOE-e4 gene. This gene is a risk factor for the development of Alzheimer's Disease later in life. Our work shows that the more specific microstructural measures offered by the NODDI technique has revealed an increase in the non-tissue ( $V_{iso}$ ) component in the brain among APOE-e4 carriers. Importantly, the other NODDI parameters and g-ratio show no difference suggesting that although the tissue component among APOE-e4 carriers is reduced, there is no detectable difference to the underlying microstructure. This important finding has not been shown before, and supports the large body of evidence that shows young healthy APOE-e4 carriers are not disadvantaged across a number of cognitive domains and (in some tasks) out-perform their non-e4 peers.

---

795

15:33



### Spatial and Temporal Relationship between Microstructural and Morphological Abnormalities of Alzheimer's disease: Evidence in Cortical and Deep Gray Matter

Nan-Jie Gong<sup>1,2</sup>, Chun-Chung Chan<sup>3</sup>, Lam-Ming Leung<sup>3</sup>, Chun-Sing Wong<sup>4</sup>, Russell Dobb<sup>5</sup>, and Chunlei Liu<sup>5,6</sup>

<sup>1</sup>University of California Berkeley, Berkeley, CA, United States, <sup>2</sup>Brain Imaging and Analysis Center, Duke University School of Medicine, Durham, NC, United States, <sup>3</sup>United Christian Hospital, Hong Kong, <sup>4</sup>The University of Hong Kong, Hong Kong, <sup>5</sup>Duke University School of Medicine, <sup>6</sup>Electrical Engineering and Computer Sciences, University of California Berkeley, Berkeley, CA, United States

Non-Gaussian diffusion metrics such as MK from DKI can complement conventional MD and FA for detecting microstructural changes, especially in deep gray matter. This can potentially improve the efficacy of diffusion metrics for serving as diagnostic imaging biomarkers. We also provided evidence supporting the proposed notion that microstructural changes in cortical and deep gray matter predate macrostructural changes such as volume and cortical thickness.

---

Oral

## Vascular Imaging: Lumen, Vessel Wall & Function

Room 312

Wednesday 13:45 -  
15:45

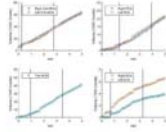
Moderators: René Botnar & Xihai Zhao

---

796



13:45



### Volumetric blood flow measurement with territorial segmentation of time-resolved contrast enhanced magnetic resonance angiography of the brain

Oren Geri<sup>1,2</sup>, Shelly I. Shiran<sup>3</sup>, Jonathan Roth<sup>4</sup>, Moran Artzi<sup>1</sup>, Liat Ben-Sira<sup>3</sup>, and Dafna Ben Bashat<sup>1,2,5</sup>

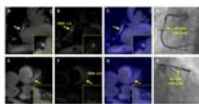
<sup>1</sup>Functional Brain Center, The Wohl Institute for Advanced Imaging, Tel Aviv Sourasky Medical Center, Tel Aviv, Israel, <sup>2</sup>Sagol School of Neuroscience, Tel Aviv University, Tel Aviv, Israel, <sup>3</sup>Department of Radiology, Tel Aviv Sourasky Medical Center, Tel Aviv, Israel, <sup>4</sup>Department of NeuroSurgery, Tel Aviv Sourasky Medical Center, Tel Aviv, Israel, <sup>5</sup>Sackler Faculty of Medicine, Tel Aviv University, Tel Aviv, Israel

We propose a method for territorial segmentation and volumetric flow rate (VFR) measurement based on time-resolved contrast enhanced MR-angiography. Eight territories: right/left internal carotid arteries; the two anterior cerebral arteries (combined); the right/left external carotid arteries; the right/left posterior cerebral arteries; and the vertebrobasilar territory, were segmented using an iterative region-growing algorithm based on the bolus-arrival-time with increased temporal resolution. VFR was measured based on the territorial volume as a function of time. Healthy subjects' VFR results were similar to literature values. The clinical potential of this method is demonstrated on one patient with Moyamoya before and after surgery.

797



13:57



### Coronary Plaque Hyper-Intensity on Dark-Blood T1-Weighted MRI Helps Identify Lesion-Specific Ischemia: Insights from the Comparison Study with Invasive Fractional Flow Reserve (FFR)

Yibin Xie<sup>1</sup>, Young-Jin Kim<sup>2</sup>, Sang-Eun Lee<sup>3</sup>, Jianing Pang<sup>4</sup>, Anthony Christodoulou<sup>1</sup>, Qi Yang<sup>1</sup>, Zixin Deng<sup>1</sup>, Daniel Berman<sup>5</sup>, Hyuk-Jae Chang<sup>3</sup>, and Debiao Li<sup>1</sup>

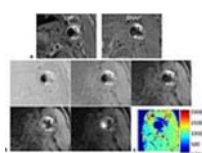
<sup>1</sup>Biomedical Imaging Research Institute, Cedars-Sinai Medical Center, Los Angeles, CA, United States, <sup>2</sup>Department of Radiology, Severance Hospital, Yonsei University College of Medicine, Seoul, Korea, Republic of, <sup>3</sup>Division of Cardiology, Severance Cardiovascular Hospital, Yonsei University College of Medicine, Seoul, Korea, Republic of, <sup>4</sup>Siemens Healthcare, Chicago, IL, United States, <sup>5</sup>Heart Institute, Cedars-Sinai Medical Center, Los Angeles, CA, United States

Coronary Atherosclerosis T1-weighted Characterization (CATCH) is an accelerated MR technique for detecting high-risk atherosclerotic lesions. However, the relationship between plaque signal and lesion-specific ischemia is still unclear. In this study we applied CATCH in a patient cohort undergoing invasive FFR and discovered the association between plaque hyper-intensity and hemodynamic functional significance. The results presented here support the potential clinical utility and added value of MR coronary plaque characterization as a “gate-keeper” for invasive and costly coronary procedures.

798



14:09



### Multi-contrast Acquisition in a Single Scan (MASS) for Three-dimensional Quantitative T1 Mapping of Carotid Atherosclerosis

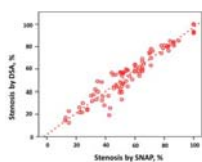
Haikun Qi<sup>1</sup>, Huiyu Qiao<sup>1</sup>, Shuo Chen<sup>1</sup>, Zechen Zhou<sup>2</sup>, Xinlei Pan<sup>1</sup>, Yishi Wang<sup>1</sup>, Chun Yuan<sup>1,3</sup>, and Huijun Chen<sup>1</sup>

<sup>1</sup>Center for Biomedical Imaging Research, School of Medicine, Tsinghua University, Beijing, People's Republic of China, <sup>2</sup>Philips Research China, Shanghai, People's Republic of China, <sup>3</sup>Department of Radiology, University of Washington School of Medicine, Seattle, WA, United States

Intra-plaque hemorrhage (IPH) is a dynamic process and change of the IPH MR signal was found to be correlated with plaque developments. So quantitative T1 mapping of plaque is essential to monitor plaque progression. In this study, we proposed an IR prepared 3D golden angle radial sampling sequence, enabling multiple T1 contrasts acquisition in a single scan (MASS) with application to carotid artery T1 mapping. The accuracy and feasibility of MASS was demonstrated in phantom studies and in vivo imaging experiments on healthy volunteers and carotid atherosclerosis patients. MASS may be a one-stop solution to carotid atherosclerotic plaque imaging.

799

14:21



### Assessment of Carotid Atherosclerotic Disease Using 3D Simultaneous Non-contrast Angiography and Intraplaque Hemorrhage (SNAP) imaging: Comparison with Digital Subtraction Angiography

Huilin Zhao<sup>1</sup>, Jianrong Xu<sup>1</sup>, Xiaosheng Liu<sup>1</sup>, Beibei Sun<sup>1</sup>, Weibo Chen<sup>2</sup>, Chun Yuan<sup>3</sup>, and Xihai Zhao<sup>4</sup>

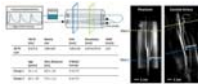
<sup>1</sup>Radiology, Renji Hospital, Shanghai Jiao Tong University School of Medicine, Shanghai, People's Republic of China, <sup>2</sup>MR Clinical Science, Philips Healthcare, Greater China, People's Republic of China, <sup>3</sup>University of Washington, WA, United States, <sup>4</sup>Center for Biomedical Imaging Research, Department of Biomedical Engineering, Tsinghua University, Beijing, People's Republic of China

3D fast Simultaneous Non-contrast Angiography and intraPlaque hemorrhage (SNAP) imaging was recently proposed as a technique for joint MRA and intraplaque hemorrhage (IPH) imaging. This study sought to determine the accuracy of this technique at quantifying carotid atherosclerosis disease compared to conventional intra-arterial digital subtraction angiography (DSA) in patients with at least 50% carotid stenosis. We found that 3D SNAP imaging had excellent agreement with DSA in measuring luminal stenosis and identification of ulceration in carotid arteries. Our findings suggest that, SNAP imaging might be a potential candidate technique for comprehensive evaluation of carotid high-risk atherosclerotic disease.

800



14:33



Measuring Local Pulse Wave Velocity in the Carotid Arteries using a Compressed Sensing reconstruction for high temporal resolution (4 ms) 2D PC CINE MRI

Eva S Peper<sup>1</sup>, Wouter V Potters<sup>2</sup>, Abdallah G Motaal<sup>3</sup>, Pim van Ooij<sup>1</sup>, Aart J Nederveen<sup>1</sup>, Gustav J Strijkers<sup>4</sup>, and Bram F Coolen<sup>4</sup>

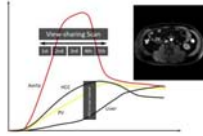
<sup>1</sup>Department of Radiology, Academic Medical Center, Amsterdam, Netherlands, <sup>2</sup>Neurologie en Klinische Neurofysiologie, Academic Medical Center, Amsterdam, Netherlands, <sup>3</sup>Imaging Clinical Applications and Platform, Philips Healthcare, Netherlands, <sup>4</sup>Department of Biomedical Engineering & Physics, Academic Medical Center, Amsterdam, Netherlands

Measuring PWV with MRI would provide a useful tool to measure arterial stiffness locally. However, the limitation of MRI for this implementation is temporal resolution. This study validates a technique to measure local PWV at up to only 5 cm of the carotid arteries using 2D PC CINE MRI data of a high temporal resolution compressed sensing (CS) reconstruction. The method is validated using a pulsatile flow phantom and two groups of 10 elderly and 10 younger healthy volunteers. A significant difference between age groups was found.







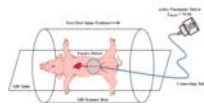


### Simultaneous acquisition of MR angiography and diagnostic images on contrast-enhanced view-sharing multi-arterial phases

Yoshifumi Noda<sup>1</sup>, Satoshi Goshima<sup>1</sup>, Kimihiro Kajita<sup>1</sup>, Hiroshi Kawada<sup>1</sup>, Nobuyuki Kawai<sup>1</sup>, Hiromi Koyasu<sup>1</sup>, Masayuki Matsuo<sup>1</sup>, Tomohiro Namimoto<sup>2</sup>, Norihiro Shinkawa<sup>3</sup>, Masataka Nakagawa<sup>2</sup>, Toshinori Hirai<sup>3</sup>, and Yasuyuki Yamashita<sup>2</sup>

<sup>1</sup>Department of Radiology, Gifu University, Gifu, Japan, <sup>2</sup>Department of Diagnostic Radiology, Faculty of Life Sciences, Kumamoto University, Japan, <sup>3</sup>Department of Radiology, Faculty of Medicine, University of Miyazaki, Japan

While magnetic resonance angiography (MRA) is clinically used to evaluate vascular anatomy, whereas it needs independent scan leading to a decreased throughput. We generated MRA using early phase images in the contrast-enhanced multi-arterial phase images with view-sharing technique. Aortic branches and anatomical anomalies were clearly visualized on MRA without significant differences in contrast effect and conspicuity regardless of contrast material with different r1 value (gadoterate meglumine and gadobutrol).



### In Vivo Magnetic Resonance Elastography of Abdominal Aortic Aneurysm in A Porcine Model

Huiming Dong MS<sup>1,2</sup>, Matthew Joseph BS<sup>3</sup>, Prateek Kalra MS<sup>1</sup>, Xiaokui Mo PhD<sup>4</sup>, Richard White MD<sup>1,5</sup>, Rizwan Ahmad<sup>6</sup>, and Arunark Kolipaka PhD<sup>1,2,5</sup>

<sup>1</sup>Department of Radiology, The Ohio State University Wexner Medical Center, Columbus, OH, United States, <sup>2</sup>Department of Biomedical Engineering, The Ohio State University, Columbus, OH, United States, <sup>3</sup>Dorothy M. Davis Heart and Lung Research Institute Interventional Cardiology Cath Core Lab, The Ohio State University Wexner Medical Center, Columbus, OH, United States, <sup>4</sup>Center for Biostatistics, The Ohio State University Wexner Medical Center, Columbus, OH, United States, <sup>5</sup>Department of Internal Medicine-Cardiology, The Ohio State University Wexner Medical Center, Columbus, OH, United States, <sup>6</sup>Department of Electrical and Computer Engineering, The Ohio State University, Columbus, OH, United States

Abdominal aortic aneurysm (AAA) can result in life-threatening aortic rupture. Although AAA diameter is utilized for assessing rupture risk clinically, it is a poor indicator of rupture potential. Aortic stiffness is an important biomechanical property that can provide critical information about the overall mechanical integrity of AAA and thus results in more accurate rupture risk evaluation. Therefore, the aim of this study is to utilize non-invasive in vivo MRE to estimate aortic stiffness in AAA-induced animal models, and compare it with the stiffness obtained from ex vivo mechanical testing as well as AAA diameters.

805

15:33

Parameter	Value	Unit
...	...	...
...	...	...
...	...	...

**Robust MR Lymphangiography using DARC-MRL: Evaluation of Venous Suppression and Strategies for More Efficient Clinical Examinations**  
 Jeffrey H Maki<sup>1</sup>, Beth A Ripley<sup>1,2</sup>, Neeraj Lalwani<sup>1</sup>, Noah Briller<sup>1</sup>, Peter C Neligan<sup>3</sup>, and Gregory J Wilson<sup>1</sup>

<sup>1</sup>Radiology, University of Washington, Seattle, WA, United States,  
<sup>2</sup>Diagnostic Services, Puget Sound VA HCS, Seattle, WA, United States,  
<sup>3</sup>Plastic Surgery, University of Washington, Seattle, WA, United States

Dual Agent Relaxation Contrast MR Lymphangiography (DARC-MRL) effectively eliminates venous enhancement through the up-front i.v. injection ferumoxytol (USPIO causing marked blood T2\* shortening) combined with obtaining MRL datasets at prolonged, precisely determined echo times. Echo time prolongation does cause an approximately 45% loss of lymphatic signal intensity, however with excellent lymphatic-to-tissue contrast, there was no clinically significant lymphatic signal loss. Data regarding the time course of lymphatic enhancement progression demonstrate most MRL enhancement can be fully captured in only two time points, allowing for a more efficient, faster examination. Multi-echo DARC offers to add further robustness and visualization capability.

**Oral**

## Pediatric Brain Development

Room 313A

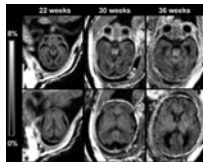
Wednesday 13:45 -  
15:45

*Moderators:* Petra Huppi & Jeff Neil

806

13:45

Quantitative assessment of the fetal brain myelination in vivo using fast macromolecular proton fraction mapping



Alexandra M. Korostyshevskaya<sup>1</sup>, Irina Yu. Prihod'ko<sup>1</sup>, Andrey A. Savelov<sup>2</sup>, and Vasily L. Yarnykh<sup>3,4</sup>

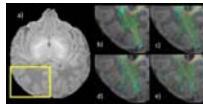
<sup>1</sup>Medical Diagnostics, International Tomography Center of the Siberian Branch of the Russian Academy of Sciences, Novosibirsk, Russian Federation, <sup>2</sup>International Tomography Center of the Siberian Branch of the Russian Academy of Sciences, Novosibirsk, Russian Federation, <sup>3</sup>Radiology, University of Washington, Seattle, WA, United States, <sup>4</sup>Tomsk State University, Tomsk, Russian Federation

Macromolecular proton fraction (MPF) is a biophysical parameter describing cross-relaxation and closely correlated with myelin content in neural tissues. This study presents the first evaluation of the fast MPF mapping method in prenatal clinical neuroimaging and suggests that MPF in the fetal brain structures is sensitive to the earliest stages of myelin development.

---

807

13:57



Anatomically constrained tractography and structural connectome of the neonatal brain

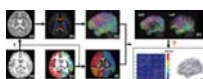
Manuel Blesa<sup>1</sup>, Ahmed Serag<sup>1</sup>, Devasuda Anblagan<sup>1,2</sup>, Emma J. Telford<sup>1</sup>, Sarah A. Sparrow<sup>1</sup>, Scott I. Semple<sup>3</sup>, Mark E. Bastin<sup>2</sup>, and James P. Boardman<sup>1,2</sup>

<sup>1</sup>MRC Centre for Reproductive Health, University of Edinburgh, Edinburgh, United Kingdom, <sup>2</sup>Centre for Clinical Brain Sciences, University of Edinburgh, Edinburgh, United Kingdom, <sup>3</sup>Clinical Research Imaging Centre, University of Edinburgh, Edinburgh, United Kingdom

The Anatomically-Constrained Tractography framework (ACT) is an advanced method to create tractography that relies on very accurate segmentation of the brain. To evaluate its role in tractography of the developing brain, we optimised the pipeline for neonatal data and compared against other methods (FA and WM seeding, with deterministic and probabilistic algorithms) used for the computation of neonatal structural connectivity. The results suggest that ACT with seeding at the GM / WM interface enhances anatomic accuracy of neonatal tractography, compared with other methods, and it has a significant impact on network measures.

---

14:09

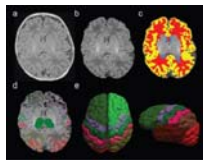


The short-range association fibers underlie brain network reconfiguration in typically and atypically developing children

Minhui Ouyang<sup>1</sup>, Jennifer Muller<sup>1</sup>, Hua Cheng<sup>2</sup>, Yun Peng<sup>2</sup>, J. Christopher Edgar<sup>1,3</sup>, John A. Detre<sup>3,4</sup>, Timothy P.L. Roberts<sup>1,3</sup>, and Hao Huang<sup>1,3</sup>

<sup>1</sup>Radiology, Children's Hospital of Philadelphia, Philadelphia, PA, United States, <sup>2</sup>Radiology, Beijing Children's Hospital, Capital Medical University, Beijing, People's Republic of China, <sup>3</sup>Radiology, Perelman School of Medicine, University of Pennsylvania, Philadelphia, PA, United States, <sup>4</sup>Neurology, Perelman School of Medicine, University of Pennsylvania, Philadelphia, PA, United States

Short-range association fibers (SAF) or U-fibers, connect adjacent gyri and constitute the majority of brain white matter. During development, SAF undergo dramatic changes in conjunction with brain network reconfiguration. How SAF reshape the brain network configuration during typical and atypical development is unknown. In this study, SAF was quantified with an index defined as normalized short-range association fibers (NSAF). We found that NSAF decreases were associated with increases in brain network efficiency in the typical developing brain from 2-7 years. Similar association were not observed in children with autism.



### Multimodal thalamocortical connectivity patterns in early brain development

Silvina Laura Ferradal<sup>1</sup>, Borjan Gagoski<sup>2</sup>, Camilo Jaimes Cobos<sup>3</sup>, Francesca Yi<sup>1</sup>, Clarissa Carruthers<sup>1</sup>, Catherine Vu<sup>1</sup>, Ryan Larsen<sup>4</sup>, Brad Sutton<sup>4</sup>, P. Ellen Grant<sup>1</sup>, and Lilla Zollei<sup>3</sup>

<sup>1</sup>Newborn Medicine, Boston Children's Hospital, Boston, MA, United States, <sup>2</sup>Radiology, Boston Children's Hospital, Boston, MA, United States, <sup>3</sup>Massachusetts General Hospital, Boston, MA, United States, <sup>4</sup>University of Illinois at Urbana-Champaign, Urbana, IL, United States

Understanding normal thalamocortical organization in early brain development has significant clinical relevance as it could provide early indicators of neurodevelopmental disorders which could originate from alterations in functional and structural brain maturation. Here we show structural and functional thalamocortical connectivity patterns derived from twenty healthy term infants scanned within the first weeks of life. Our results show that while there is a general good spatial agreement between both modalities, there are certain regions that exhibit different thalamocortical patterns. These discrepancies are possibly mediated by maturational processes such as axonal myelination and synaptogenesis.

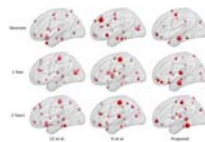


### Socioeconomic Status Influences Early Longitudinal Cortical and Subcortical Development

Justin Remer<sup>1</sup>, Douglas C Dean III<sup>2</sup>, and Sean C.L. Deoni<sup>1,3</sup>

<sup>1</sup>Advanced Baby Imaging Lab, Department of Engineering, Brown University, Providence, RI, United States, <sup>2</sup>Waisman Center, University of Wisconsin Madison, Madison, WI, United States, <sup>3</sup>Department of Pediatric Radiology, Children's Hospital Colorado, Aurora, CO, United States

Brain development may be influenced by socioeconomic status (SES), a marker of a family's income and parental education. SES differences may result in exposure to extra stress during critical periods of neurodevelopment. We performed the first longitudinal analysis of differential brain development in 70 healthy infants and young children (1 year to 6 years of age) stratified by familial SES using high resolution T1 MRI. We demonstrated that trajectories of subcortical and cortical maturation are significantly different between infants and children from low and high SES families over the first 6 years of life.



### Novel Functional Brain Development Patterns during Infancy Revealed through the Application of Functionally Derived Brain Parcellations

Feng Shi<sup>1</sup>, Andrew P Salzwedel<sup>1</sup>, Weili Lin<sup>2</sup>, John H Gilmore<sup>3</sup>, and Wei Gao<sup>1</sup>

<sup>1</sup>Biomedical Imaging Research Institute, Cedars Sinai Medical Center, Los Angeles, CA, United States, <sup>2</sup>Biomedical Research Imaging Center, University of North Carolina at Chapel Hill, Chapel Hill, NC, United States, <sup>3</sup>Department of Psychiatry, University of North Carolina at Chapel Hill, Chapel Hill, NC, United States

Signal heterogeneity within the predefined regions of interest (ROIs) may confound the functional connectivity estimation. In this study, we generate brain parcellations for neonate, 1-year, and 2-year-old infants, respectively, and use them to reveal potential novel functional developmental patterns. Our results show the progression of local functional specialization during early brain development. Moreover, different patterns of hub distributions are observed using different functional parcellation schemes suggesting the importance of selecting appropriate functionally-derived brain parcellations in characterizing infant whole brain connectivity pattern.

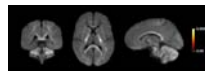


### Comparison of NODDI and WMTI microstructural parameters in typical development

Kirsten M. Lynch<sup>1</sup>, Farshid Seppehrband<sup>1</sup>, Arthur W. Toga<sup>1</sup>, and Kristi A. Clark<sup>1</sup>

*<sup>1</sup>Laboratory of Neuro Imaging, University of Southern California, Los Angeles, CA, United States*

Childhood and adolescence is an extended period of postnatal maturation characterized by dynamic changes in white matter microstructure. Multi-shell diffusion MRI (dMRI) models, such as neurite orientation dispersion and density imaging (NODDI) and white matter tract integrity (WMTI) provide an invaluable measure for the study of child development with tissue compartment estimates. NODDI and WMTI are based on similar frameworks, however they differ in several model assumptions. This study provides a comparison of NODDI and WMTI intra-axonal volume fraction model fittings in a cohort of children ages 0 -18 years in order to determine which model best reflects neurodevelopmental features.



### Pubertal contributions to white matter apparent fibre density in late childhood: a fixel-based analysis

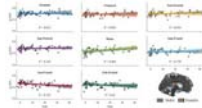
Sila Genc<sup>1,2</sup>, Marc Seal<sup>1,2</sup>, Thijs Dhollander<sup>3</sup>, Charles B Malpas<sup>2,4</sup>, Philip Hazell<sup>5</sup>, and Timothy J Silk<sup>1,2</sup>

*<sup>1</sup>Department of Paediatrics, The University of Melbourne, Melbourne, Australia, <sup>2</sup>Developmental Imaging, Murdoch Childrens Research Institute, Melbourne, Australia, <sup>3</sup>The Florey Institute of Neuroscience and Mental Health, Melbourne, Australia, <sup>4</sup>Department of Medical Education, The University of Melbourne, Melbourne, Australia, <sup>5</sup>Discipline of Psychiatry, The University of Sydney, Sydney, Australia*

Recent evidence supports the contribution of pubertal stage to local and global grey and white matter remodelling. Using fixel-based analyses, we show that pubertal children have greater apparent fibre density in the splenium of the corpus callosum compared with age-matched pre-pubertal children. This finding suggests that pubertal onset itself, rather than chronological age, drives the remodelling of white matter microstructure – which is an important consideration for assessing biological age. This is particularly important for studying paediatric and adolescent populations, as pubertal stage may be an important factor to consider in addition to chronological age.



15:21



In vivo measurement of g-ratio in the Corpus Callosum using the macromolecular tissue volume: evaluating changes as a function of Callosal subregions, age and sex.

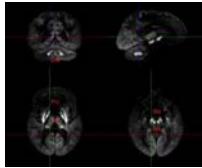
Shai Berman<sup>1</sup>, Jason Yeatman<sup>2</sup>, and Aviv Mezer<sup>1</sup>

<sup>1</sup>The Edmond and Lily Safra Center for Brain Science, The Hebrew University of Jerusalem, Jerusalem, Israel, <sup>2</sup>The Institute for Learning & Brain Sciences and the Department of Speech and Hearing Sciences, The University of Washington, Seattle, WA, USA.

Recent developments in quantitative and diffusion MRI, have made it possible to estimate the axonal g-ratio in human white-matter in-vivo. g-ratio is the ratio between the inner and outer radii of the myelin sheath wrapped around the axon. We suggest a simplified measurement of g-ratio incorporating proton density mapping, and implement it in the Corpus-Callosum of 100 subjects (ages 8-80). We find the g-ratio values agree with previously results. Furthermore, g-ratio values are stable over the lifespan and between the sexes. These results converge with theoretical evidence suggesting g-ratio has an optimal value for white-matter function.

815

15:33



Greater Relaxivity in Brain Regions Indicates Tissue Iron Deposition in Adolescence to Adulthood

Eric Thomas Peterson<sup>1</sup>, Dongjin Kwon<sup>1</sup>, Beatriz Luna<sup>2,3,4</sup>, Bart Larsen<sup>2</sup>, Devin Prouty<sup>1</sup>, Edith Vioni Sullivan<sup>5</sup>, and Adolf Pfefferbaum<sup>1</sup>

<sup>1</sup>Biosciences, SRI International, Menlo Park, CA, United States, <sup>2</sup>Psychology, University of Pittsburgh, Pittsburgh, PA, United States, <sup>3</sup>Center for the Neural Basis of Cognition, Pittsburgh, PA, United States, <sup>4</sup>Western Psychiatric Institute and Clinic, University of Pittsburgh Medical Center, Pittsburgh, PA, United States, <sup>5</sup>Psychiatry and Behavioral Sciences, Stanford University, Stanford, CA, United States

This study investigates non-heme iron deposition in the adolescent brain in specific iron-susceptible regions as a function of age, sex, body mass index, supratentorial brain volume, handedness, scanning site, and race. A large cohort of 531 healthy adolescents, ages 12 to 22 years, were scanned at five sites on GE and Siemens systems using standard DTI and fMRI pulse sequence. This study demonstrates that in bilateral pallidum, putamen, dentate nucleus, red nucleus, and substantia nigra, both  $T_2$  and  $T_2^*$  show age-related declines. These results suggest ferritin-encapsulated iron deposition in specific brain regions is associated with normal adolescent brain development.



---

Oral

## Renal Imaging: Structure & Function

Room 314

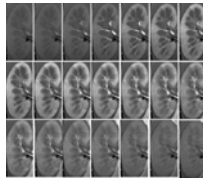
Wednesday 13:45 -  
15:45

Moderators: Siarhei Kharuzhyk & Diego Martin

---

816

13:45



[An MR compatible kidney perfusion system to assess kidney function and organ preservation.](#)

Abhishek Pandey<sup>1,2</sup>, Catherine Min<sup>3</sup>, Zhitao Li<sup>1,2</sup>, Kevin Johnson<sup>4</sup>, Leah Steyn<sup>3</sup>, William Purvis<sup>3</sup>, Robert C. Harland<sup>5</sup>, Klearchos K. Papas<sup>5</sup>, Puneet Sharma<sup>6</sup>, Diego R Martin<sup>1</sup>, Manojkumar Saranathan<sup>1</sup>, and Jean-Philippe Galons<sup>1</sup>

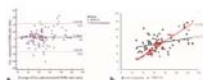
<sup>1</sup>Medical Imaging, University of Arizona, Tucson, AZ, United States, <sup>2</sup>Electrical and Computer Engineering, University of Arizona, Tucson, AZ, United States, <sup>3</sup>Physiological Sciences, University of Arizona, Tucson, AZ, United States, <sup>4</sup>Siemens Medical Solutions USA, Inc., United States, <sup>5</sup>Surgery, University of Arizona, Tucson, AZ, United States, <sup>6</sup>Radiology and Imaging Sciences, Emory University Hospital, Atlanta, GA, United States

[A MR-compatible kidney perfusion system is presented to assess the quality of kidney preservation schemes for transplantation. DCE-MRI is used to estimate and compare the glomerular filtration rate \(GRF\) in kidneys following a 24 hrs cold gaseous oxygen perfusion \(persufflation\) Vs a standard 24 hrs cold ischemic storage.](#)

---

817

13:57



[The comparative study of MR renography versus 99mTc-DTPA renal scintigraphy for determining split renal function of the transplanted kidney](#)

Jing Wang<sup>1</sup>, Yang Fan<sup>2</sup>, and Yudong Zhang<sup>3</sup>

<sup>1</sup>Center for Medical Device Evaluation, CFDA, Beijing, People's Republic of China, <sup>2</sup>MR Research China, GE Healthcare, Beijing, People's Republic of China, <sup>3</sup>Department of Radiology, the First Affiliated Hospital with Nanjing Medical University, Nanjing, People's Republic of China

The evaluation of split kidney function is of clinical significance for patients after renal transplantation. This study explored two available approaches, dynamic MR renography vs.  $^{99m}\text{Tc}$ -DTPA clearance, for determining split renal GFR in 57 transplanted patients. MR-based GFR was measured using an established Baumann-Rudin model, modified two-compartment and three-compartment model. MR results were compared with  $^{99m}\text{Tc}$ -DTPA, using 24-h creatinine clearance rate as a reference. MRR using a 2C model had significantly higher accuracy ( $r = 0.925$ ) than  $^{99m}\text{Tc}$ -DTPA clearance ( $r = 0.317$ ), thus could be a more promising way for evaluation of transplanted kidney function.

---

818

14:09



Initial experience with magnetic resonance elastography and acoustic radiation force impulse elastography in renal transplant patients

Paul Kennedy<sup>1</sup>, Octavia Bane<sup>1</sup>, Sonja Gordic<sup>1</sup>, Cecilia Besa<sup>1</sup>, Stefanie Hectors<sup>1</sup>, Mathilde Wagner<sup>1,2</sup>, Rafael Khaim<sup>3</sup>, Madhav Menon<sup>3</sup>, Vinay Nair<sup>3</sup>, Sara Lewis<sup>1</sup>, and Bachir Taouli<sup>1</sup>

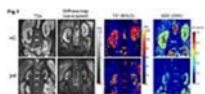
<sup>1</sup>Translational and Molecular Imaging Institute, Icahn School of Medicine at Mount Sinai, New York, NY, United States, <sup>2</sup>Radiology, Groupe Hospitalier Pitié Salpêtrière, Paris, France, <sup>3</sup>Recanati Miller Transplantation Institute, Icahn School of Medicine at Mount Sinai, New York, NY, United States

In this prospective study we compared renal transplant stiffness measured with MRE and ARFI ultrasound in 9 patients. Repeatability of both modalities was determined through test-retest imaging in 5 patients. MRE stiffness was significantly lower than ARFI stiffness as expected. MRE test-retest repeatability was excellent with mean coefficient of variation (CV) of 6%, while ARFI had CV of 30%. In addition, ARFI measurements exhibited a high inter-quartile range in the majority of cases suggesting inconsistency in the measurements. Our results suggest MRE is a more robust choice for renal transplant measurement compared to ARFI.

---

819

14:21



In vivo multifrequency MR elastography for the assessment of renal stiffness in patients with IgA nephropathy

Jing Guo<sup>1</sup>, Stephan Marticorena Garcia<sup>1</sup>, Michael Dürr<sup>2</sup>, Florian Dittmann<sup>1</sup>, Sebastian Hirsch<sup>1</sup>, Jürgen Braun<sup>3</sup>, and Ingolf Sack<sup>1</sup>

<sup>1</sup>Department of Radiology, Charité - Universitätsmedizin Berlin, Berlin, Germany, <sup>2</sup>Department of Nephrology, Charité - Universitätsmedizin Berlin, Berlin, Germany, <sup>3</sup>Department of Medical Informatics, Charité - Universitätsmedizin Berlin, Berlin, Germany

Renal stiffness was investigated using multifrequency MRE in healthy controls and patients with IgA nephropathy. Patients show a reduced renal stiffness as compared to healthy controls. DWI and BOLD imaging were also applied to the subjects. Both ADC and T2\* were linearly correlated with wave speed obtained from MRE. By mechanical vascular-solid tissue interactions, wave speed measurements by multifrequency MRE offer a quantitative measure for the noninvasive assessment renal function.

---

820

14:33



### Using Cardiorenal MRI to assess fluid balance

Chris Bradley<sup>1,2</sup>, Damian Bragg<sup>2</sup>, Eleanor F Cox<sup>1,2</sup>, Ahmed M El-Sharkawy<sup>2</sup>, Abeer H Chowdhury<sup>2</sup>, Dileep N Lobo<sup>2</sup>, and Susan T Francis<sup>1,2</sup>

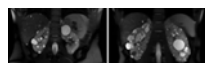
<sup>1</sup>Sir Peter Mansfield Imaging Centre, University of Nottingham, Nottingham, United Kingdom, <sup>2</sup>NIHR Nottingham Digestive Diseases Biomedical Research Unit, University of Nottingham, Nottingham, United Kingdom

We used quantitative MRI measurements to perform a randomised, double-blind crossover study on the effects of isovolumetric and isoeffective infusions of colloid versus crystalloid on structural and haemodynamic (ASL, ADC, flow, volume) changes in the kidney and cardiac output. No significant differences were observed between the blood expanding properties of the infusions, despite using a colloid infusion one-third the volume of the reference crystalloid infusion. We observed a trend of less oedema using an isoeffective volume of colloid. Repeated MRI measurements demonstrated low CoVs, allowing MRI to assess subtle changes in structure and haemodynamics for determining optimal perioperative infusions.

---

821

14:45



### Inter-rater Reliability and Translational Implications of MR-based Polycystic Kidney Volume Measurements by Stereology at Early and Late Stage Disease

Rebecca J. Lepping<sup>1</sup>, Rainer T. Karcher<sup>1</sup>, Paul Keselman<sup>1</sup>, Darren P. Wallace<sup>2</sup>, Alan Yu<sup>2</sup>, Laura E. Martin<sup>1,3</sup>, and William M. Brooks<sup>1,4</sup>

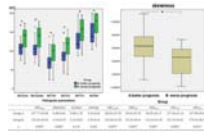
<sup>1</sup>Hoglund Brain Imaging Center, University of Kansas Medical Center, Kansas City, KS, United States, <sup>2</sup>Medicine-Nephrology, University of Kansas Medical Center, Kansas City, KS, United States, <sup>3</sup>Preventive Medicine and Public Health, University of Kansas Medical Center, Kansas City, KS, United States, <sup>4</sup>Neurology, University of Kansas Medical Center, Kansas City, KS, United States

Autosomal dominant polycystic kidney disease (ADPKD) is characterized by the presence of fluid-filled cysts that grow over time. Total kidney volume (TKV) is one of the main biomarkers of disease progression, and is estimated through the technique of stereology. We tested whether patients' kidney size impacted inter-rater reliability using the same stereology protocol. Stereology yielded excellent inter-rater reliability at both early and late stage disease, however, some pathology would still benefit from expert guidance in determining kidney tissue. This technique can easily be translated to animal models of ADPKD.

---

822

14:57



Quantitative Volumetric Histogram Analysis of Diffusion-weighted Magnetic Resonance Imaging: An Initial Experience of Solid Renal Cell Carcinoma with Different Prognosis

Anqin Li<sup>1</sup>, Zhen Li<sup>1</sup>, Haojie Li<sup>1</sup>, and Daoyu Hu<sup>1</sup>

<sup>1</sup>Department of Radiology, Tongji Hospital, Tongji Medical College, Huazhong University of Science and Technology, Wuhan, People's Republic of China

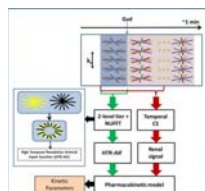
To evaluate the value of quantitative volumetric ADC histogram analysis for differentiation of clear cell RCC (ccRCC) from papillary RCC (pRCC) and chromophobe RCC (chRCC) which having different prognosis. Differences of ADC histogram parameters between better prognosis group and worse prognosis group were compared. There were significant differences on ADC<sub>mean</sub>, ADC<sub>median</sub>, ADC<sub>10%</sub>, ADC<sub>25%</sub>, ADC<sub>75%</sub>, ADC<sub>90%</sub> and skewness between these two different prognosis groups and the ADC<sub>10%</sub> showed the best diagnostic value. Therefore, quantitative volumetric ADC histogram analysis can be considered a useful and noninvasive method to help distinguish three subtypes renal cell carcinomas which having different prognosis.

---

15:09

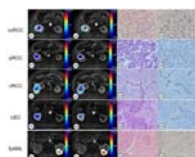
Glomerular filtration rate estimation in vivo using 3D radial MRI and a novel multiresolution reconstruction technique

Abhishek Pandey<sup>1,2</sup>, Jean-Philippe Galons<sup>1</sup>, Kevin Johnson<sup>3</sup>, Diego R Martin<sup>1</sup>, Maria I Altbach<sup>1</sup>, Ali Bilgin<sup>2,4</sup>, and Manojkumar Saranathan<sup>1,4</sup>



<sup>1</sup>Medical Imaging, University of Arizona, Tucson, AZ, United States, <sup>2</sup>Electrical and Computer Engineering, University of Arizona, Tucson, AZ, United States, <sup>3</sup>Siemens Medical Solutions USA, Inc., <sup>4</sup>Biomedical Engineering, University of Arizona, Tucson, AZ, United States

Dynamic contrast enhanced MRI can be used to obtain single-kidney GFR estimates but tradeoffs between spatial and temporal resolution lead to errors. We propose a novel reconstruction technique where AIFs are generated from images reconstructed with high temporal resolution while renal parenchyma signal is extracted from images reconstructed over a larger temporal window to generate images with high spatial resolution and improved image quality. We demonstrate the clinical validity of the method by estimating the GFR using our proposed method and compare it with serum creatinine based eGFR estimate.

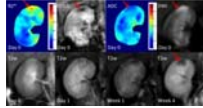


### Dynamic Contrast-enhanced MRI in Renal Tumors: Common Subtype Differentiation using Pharmacokinetics

Haiyi Wang<sup>1</sup>, Lu Ma<sup>1</sup>, Zihua Su<sup>2</sup>, Ning Huang<sup>2</sup>, Xiao Xu<sup>3</sup>, Zhipeng Sun<sup>4</sup>, Aitao Guo<sup>5</sup>, and Huiyi Ye<sup>1</sup>

<sup>1</sup>Department of Radiology, Chinese PLA General Hospital, Beijing, People's Republic of China, <sup>2</sup>Lift Science, Advanced Application Team, GE Healthcare China, Beijing, People's Republic of China, <sup>3</sup>Lift Science, Advanced Application Team, GE Healthcare China, Shanghai, People's Republic of China, <sup>4</sup>Department of Radiology, No.1 Hospital of Zhangjiakou, Zhangjiakou, People's Republic of China, <sup>5</sup>Department of Pathology, Chinese PLA General Hospital, Beijing, People's Republic of China

In this prospective study on pharmacokinetic parameters ( $K^{\text{trans}}$  &  $V_e$ ) of renal tumors, we enrolled the patients with five common subtypes of renal tumor - clear cell renal cell carcinoma (ccRCC), papillary renal cell carcinoma (pRCC), chromophobic renal cell carcinoma (cRCC), uroepithelial carcinoma (UEC), and fat poor angiomyolipoma (fpAML) to undergo DCE-MRI pharmacokinetic studies. Our results demonstrated that ccRCC, pRCC, cRCC, UEC and fpAML are pharmacokinetically different ( $K^{\text{trans}}$  &  $V_e$ ).  $K^{\text{trans}}$  could distinguish ccRCC from non-ccRCC (pRCC & cRCC) and differentiate fpAML with non-ccRCC with high specificity and sensitivity, which probably can facilitate the precise treatment of renal tumors in the future clinical practice.



### Comparison of BOLD-contrast imaging and DW imaging for early prediction of renal damage after microemboli-induced acute kidney injury in animal model

Chengyan Wang<sup>1</sup>, Hanjing Kong<sup>1</sup>, Fei Gao<sup>2</sup>, Wenjian Huang<sup>1</sup>, Lian Ding<sup>1</sup>, Rui Wang<sup>3</sup>, Li Jiang<sup>4</sup>, Yan Jia<sup>5</sup>, Hui Xu<sup>5</sup>, He Wang<sup>6</sup>, Xiaodong Zhang<sup>3</sup>, Li Yang<sup>5</sup>, Jue Zhang<sup>1,2</sup>, Xiaoying Wang<sup>1,3</sup>, and Jing Fang<sup>1,2</sup>

<sup>1</sup>Academy for Advanced Interdisciplinary Studies, Peking University, Beijing, People's Republic of China, <sup>2</sup>College of Engineering, Peking University, Beijing, People's Republic of China, <sup>3</sup>Department of Radiology, Peking University First Hospital, Beijing, People's Republic of China, <sup>4</sup>Philips Healthcare, Suzhou, People's Republic of China, <sup>5</sup>Renal Division, Peking University First Hospital, Beijing, People's Republic of China, <sup>6</sup>Institute of Science and Technology for Brain-Inspired Intelligence, Fudan University, Shanghai, People's Republic of China

Atheroembolic renal disease (AERD) is an important yet under-diagnosed kidney diseases associated with atherosclerosis. This study investigates the utility of BOLD and DWI in the assessment of microemboli-induced AKI, and compares the performances of both techniques for early prediction of renal damage. AKI was induced by injection of microspheres into the right kidney. The results indicate that both techniques can serve as reliable indicators to focal severe regional ischemia before renal damage occurs, while BOLD imaging seems to be more sensitive in early detection of moderate ischemia.

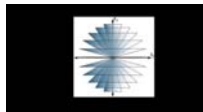
## Oral

### Thoracic MRI: Functional & Oncological Imaging of the Chest

Room 316A

Wednesday 13:45 -  
15:45

Moderators: David Bluemke & Jens Vogel-  
Claussen



### Free-Breathing Pediatric Chest MRI: Utility of Self-Navigated Golden-Angle Ordered Conical Ultrashort Echo Time (UTE) Acquisition

Evan James Zucker<sup>1</sup>, Joseph Yitan Cheng<sup>1</sup>, Anshul Haldipur<sup>1</sup>, Michael Carl<sup>2</sup>, and Shreyas S Vasanawala<sup>1</sup>

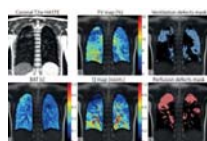
<sup>1</sup>Department of Radiology, Stanford University, Stanford, CA, United States, <sup>2</sup>Applied Science Laboratory, GE Healthcare, San Diego, CA

To assess feasibility of conical k-space trajectory free-breathing UTE chest MRI versus 4D flow and effects of 50% data subsampling and soft-gated motion correction, 32 consecutive children were recruited. Images scored by two blinded radiologists showed good to excellent delineation of all evaluated structures. UTE surpassed 4D flow for lungs and airways and was equivalent for pulmonary arteries. 50% subsampling mildly reduced but maintained diagnostic image quality, favoring its shorter scan time. Soft-gating slightly improved pulmonary artery delineation for one reader but overall degraded images, possibly due to noise from data subsampling, and suggesting motion-robustness of the conical golden-ordered trajectory.

---

827

13:57



Functional lung MRI using matrix pencil decomposition and N2 multiple-breath washout measurements in cystic fibrosis

Grzegorz Bauman<sup>1,2</sup>, Sylvia Nyilas<sup>3,4</sup>, Orso Pusterla<sup>1,2</sup>, Tanja Haas<sup>1</sup>, Michael Ith<sup>5</sup>, Bernd Jung<sup>5</sup>, Carmen Casaulta<sup>3</sup>, Gregor Sommer<sup>6</sup>, Enno Stranzinger<sup>5</sup>, Urs Frey<sup>4</sup>, Philipp Latzin<sup>3,4</sup>, and Oliver Bieri<sup>1,2</sup>

*<sup>1</sup>Division of Radiological Physics, Department of Radiology, University of Basel Hospital, Basel, Switzerland, <sup>2</sup>Department of Biomedical Engineering, University of Basel, Basel, Switzerland, <sup>3</sup>Division of Respiratory Medicine, Department of Pediatrics, University Children's Hospital of Bern, Bern, Switzerland, <sup>4</sup>Department of Pediatric Pneumology, University Children's Hospital Basel (UKBB), Basel, Switzerland, <sup>5</sup>University Institute for Diagnostic, Interventional and Pediatric Radiology, Inselspital, Bern University Hospital, Bern, Switzerland, <sup>6</sup>Department of Radiology, University of Basel Hospital, Basel, Switzerland*

This study examines a correlation between the functional lung MRI using matrix pencil decomposition and lung function tests in patients with cystic fibrosis. A strong correlation between the global ventilation inhomogeneity index (LCI) from multiple breath washout and ventilation/perfusion impairment in the lung determined by functional MRI is observed. The results of our study support the potential of functional MRI as a diagnostic tool in monitoring disease progression in cystic fibrosis.

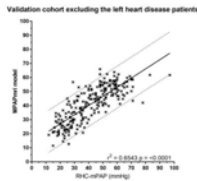
---

14:09

Cardiopulmonary MRI as a diagnostic tool in Pulmonary Hypertension

Christopher S Johns<sup>1</sup>, David G Kiely<sup>2</sup>, David A Capener<sup>1</sup>, Charlotte Hammerton<sup>1</sup>, Neil Hamilton<sup>2</sup>, Robin Condliffe<sup>2</sup>, Charlie Elliott<sup>2</sup>, Athanasios Charalampopoulos<sup>2</sup>, Jim M Wild<sup>1</sup>, and Andy J Swift<sup>1,3</sup>





<sup>1</sup>Academic Radiology, The University of Sheffield, Sheffield, United Kingdom, <sup>2</sup>Pulmonary Vascular Disease Unit, Sheffield Teaching Hospitals, United Kingdom, <sup>3</sup>Insigneo, Institute of In-Vivo Medicine

Pulmonary hypertension has a poor prognosis. Invasive right heart catheter measured mean pulmonary artery pressure (RHC-MPAP) is the gold standard for clinical diagnosis. Here we present a parametric model derived from cardio-pulmonary MRI for the prediction of pulmonary hypertension with a strong correlation with RHC-MPAP and a high diagnostic accuracy. In certain patients, right heart catheterisation may be avoided due to high specificity of this cardio-pulmonary MR model.



14:21



Assessment of cystic fibrosis disease using UTE imaging with XD-GRASP reconstruction: a comparison with CT

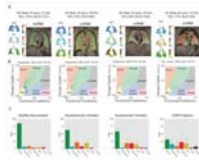
Jean Delacoste<sup>1</sup>, Catherine Beigelman<sup>1</sup>, Li Feng<sup>2</sup>, Jerome Yerly<sup>1,3</sup>, Davide Piccini<sup>1,4</sup>, Daniel K. Sodickson<sup>2</sup>, Ricardo Otazo<sup>2</sup>, Matthias Stuber<sup>1,3</sup>, and Alain Sauty<sup>5,6</sup>

<sup>1</sup>Department of Radiology, University Hospital (CHUV) and University of Lausanne (Unil), Lausanne, Switzerland, <sup>2</sup>Center for Advanced Imaging Innovation and Research (CAI2R), Department of Radiology, New York University School of Medicine, New York, NY, United States, <sup>3</sup>Center for Biomedical Imaging (CIBM), Lausanne, Switzerland, <sup>4</sup>Advanced Clinical Imaging Technology, Siemens Healthcare, Lausanne, Switzerland, <sup>5</sup>Adult CF multisites unit, Hospital of Morges, Morges, Switzerland, <sup>6</sup>Service of Pneumology, Department of Medicine, University Hospital (CHUV), Lausanne, Switzerland

Motion resolved reconstructions, using compressed sensing, of 3D ultra short echo time (UTE) acquisitions in cystic fibrosis patients were performed. The definition of the lung-liver interface was quantified and found to be significantly higher than that in motion corrupted reconstructions of the whole datasets. The Helbich-Bhalla score for cystic fibrosis was determined using both computed tomography (CT) and MRI data. Correlation between scores obtained with both modalities was good ( $p=0.77$ ) but consistency was moderate ( $ICC=0.62$ ). This was due to average MRI scores being lower by 15%, most likely because mosaic perfusion could not be assessed with MRI.

14:33

Multi-parametric Response Map Using Hyperpolarized Gas MR Imaging to Retain Regionality: Making Hyperpolarized Gas Imaging Great Again



Hooman Hamedani<sup>1</sup>, Yi Xin<sup>1</sup>, Stephen Kadlec<sup>1</sup>, Ian Duncan<sup>1</sup>, Sarmad Siddiqui<sup>1</sup>, Mehrdad Pourfathi<sup>1</sup>, Nicholas Drachman<sup>1</sup>, Kai Ruppert<sup>1</sup>, Joe Naji<sup>1</sup>, Maurizio Cereda<sup>2</sup>, and Rahim Rizi<sup>1</sup>

<sup>1</sup>Radiology, University of Pennsylvania, Philadelphia, PA, United States,

<sup>2</sup>Anesthesiology and Critical Care, University of Pennsylvania, Philadelphia, PA, United States

By establishing multi-parametric response map (mPRM) of Gas MRI, we suggested a multifaceted regional combination of the imaged mPRM that best explain lung function deterioration while had a meaningful representation of each subject lung function condition.

831

14:45



Using dynamic MRI to create moving boundary conditions for CFD: determining the causes of upper airway motion in sleep apnea

Alister Bates<sup>1,2</sup>, Andreas Schuh<sup>3</sup>, Brynne Williams<sup>2</sup>, Matthew Lanier<sup>2</sup>, Keith McConnell<sup>1</sup>, Wolfgang Loew<sup>2</sup>, Robert Fleck<sup>4</sup>, Jason Woods<sup>1,2</sup>, Charles Dumoulin<sup>2</sup>, and Raouf Amin<sup>1</sup>

<sup>1</sup>Division of Pulmonary Medicine, Cincinnati Children's Hospital, Cincinnati, OH, United States, <sup>2</sup>Imaging Research Center, Cincinnati Children's Hospital, Cincinnati, OH, United States, <sup>3</sup>Department of Computing, Imperial College London, London, United Kingdom, <sup>4</sup>Division of Radiology, Cincinnati Children's Hospital, Cincinnati, OH, United States

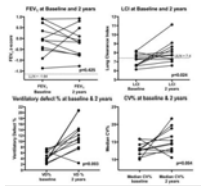
The upper airway consists of complex mobile structures such as the tongue, soft palate and larynx that make predicting surgical outcomes in obstructive sleep apnea difficult. Dynamic computational fluid simulations provide a method to assess the causes of airway deformation, but require information on the airway shape and motion. Combining MR imaging from three sequences provides this information in high spatiotemporal resolution. Simulations allow characterization of airway wall motion as either in the same or opposite direction as the force applied by the intraluminal airflow, which can be used to better understand the subject-specific mechanics of sleep apnea.

832

14:57

LONGITUDINAL MONITORING OF DISEASE PROGRESSION IN CHILDREN WITH MILD CYSTIC FIBROSIS USING HYPERPOLARISED GAS MRI AND LUNG CLEARANCE INDEX

Laurie Smith<sup>1,2</sup>, Paul J.C. Hughes<sup>1</sup>, Felix Horn<sup>1</sup>, Helen Marshall<sup>1</sup>, Graham Norquay<sup>1</sup>, Guilhem Collier<sup>1</sup>, David Hughes<sup>2</sup>, Chris Taylor<sup>2</sup>, Noreen West<sup>2</sup>, Ina Aldag<sup>2</sup>, Alex Horsley<sup>3</sup>, and Jim Wild<sup>1</sup>



<sup>1</sup>University of Sheffield, Sheffield, United Kingdom, <sup>2</sup>Sheffield Children's Hospital, Sheffield, United Kingdom, <sup>3</sup>Manchester Adult CF Centre, Manchester, United Kingdom

Hyperpolarised gas ventilation MRI is a sensitive method for evaluating disease progression in subjects with cystic fibrosis and normal spirometry. Ventilation defect % (VD%) increased in 10/11 subjects studied with a mean change of 201%. The MRI coefficient of variance (CV) of signal intensity was similarly sensitive to change. 10/11 subjects had increased lung clearance index (LCI) at 2-years but no subject had abnormal spirometry at either visit. The % change in LCI demonstrated strong correlations with the % change in CV outcomes. VD% and CV reflect different but complimentary aspects of lung disease that appear to track disease progression.

833

15:09



### 3D Radial UTE MRI outperforms 3D Cartesian conventional echo time MRI for evaluation of cystic fibrosis lung disease

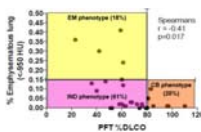
Scott K Nagle<sup>1</sup>, Christopher J Francois<sup>1</sup>, Madeline E Poranski<sup>1</sup>, Laura C Bell<sup>2</sup>, Kevin M Johnson<sup>3</sup>, and Sean B Fain<sup>3</sup>

<sup>1</sup>Radiology, University of Wisconsin, Madison, WI, United States, <sup>2</sup>Translational Bioimaging, Barrow Neurological Institute, <sup>3</sup>Medical Physics, University of Wisconsin

In this prospective cross-sectional study of 30 cystic fibrosis (CF) subjects, 3D radial ultrashort echo time (UTE) MRI significantly outperformed 3D Cartesian conventional echo time MRI when compared with reference standard computed tomography (CT), especially with respect to the depiction of air trapping. Short-term 1-2 week repeatability was comparable with CT. Since air trapping is considered one of the earliest signs of CF lung disease, and potentially reversible, the use of UTE MRI could significantly improve the utility of MRI as a biomarker for treatment effect in mild CF lung disease.

834

15:21



### A new COPD phenotype characterized by hyperpolarized xenon-129 MRI

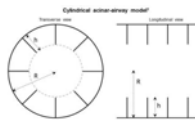
Kun Qing<sup>1</sup>, Sahar Mansoor<sup>1</sup>, John P. Mugler, III<sup>1</sup>, Talissa A. Altes<sup>2</sup>, Nicholas J. Tustison<sup>1</sup>, Kai Ruppert<sup>3</sup>, Jaime F. Mata<sup>1</sup>, G.Wilson Miller<sup>1</sup>, Iulian C. Ruset<sup>4</sup>, F.William Hersman<sup>4,5</sup>, Joanne M. Cassani<sup>2</sup>, and Yun Michael Shim<sup>1</sup>

<sup>1</sup>University of Virginia, Charlottesville, VA, United States, <sup>2</sup>University of Missouri School of Medicine, Columbia, MO, United States, <sup>3</sup>University of Pennsylvania, Philadelphia, PA, United States, <sup>4</sup>Xemed, LLC, Durham, NH, United States, <sup>5</sup>University of New Hampshire, Durham, NH, United States

Existing literature describes two distinctive phenotypes of chronic obstructive pulmonary disease (COPD): airway-predominant chronic bronchitis and alveolar-predominant emphysema. In this study, based on results from pulmonary function tests and computed tomography, we found a new mixed phenotype of COPD. This mixed phenotype showed minimal emphysematous tissue destruction, but low diffusion lung capacity (DLCO). Subsequent hyperpolarized xenon-129 MRI results indicated that gas exchange to the pulmonary blood in lungs for this mixed phenotype was significantly impaired as compared to controls and the classic COPD phenotypes.

835

15:33



#### Hyperpolarized <sup>3</sup>He gas MRI in infant lungs: investigating alveolar-airspace size with restricted gas diffusion

Nara S Higano<sup>1,2</sup>, Robert P Thomen<sup>2</sup>, James D Quirk<sup>3</sup>, Kenneth G Parks<sup>2</sup>, Heidie L Huyck<sup>4</sup>, Andrew D Hahn<sup>5</sup>, Sean B Fain<sup>5,6</sup>, Michael L Baker<sup>7</sup>, Gloria S Pryhuber<sup>4</sup>, and Jason C Woods<sup>1,2,8</sup>

<sup>1</sup>Physics, Washington University in St. Louis, St. Louis, MO, United States, <sup>2</sup>Center for Pulmonary Imaging Research, Cincinnati Children's Hospital Medical Center, Cincinnati, OH, United States, <sup>3</sup>Mallinckrodt Institute of Radiology, Washington University in St. Louis, St. Louis, MO, United States, <sup>4</sup>Pediatrics, University of Rochester Medical Center, Rochester, NY, United States, <sup>5</sup>Medical Physics, University of Wisconsin - Madison, Madison, WI, United States, <sup>6</sup>Radiology, University of Wisconsin - Madison, Madison, WI, United States, <sup>7</sup>Pathology, Cincinnati Children's Hospital Medical Center, Cincinnati, OH, United States, <sup>8</sup>Radiology, Cincinnati Children's Hospital Medical Center, Cincinnati, OH, United States

Acinar development in infant humans has not been extensively studied. Hyperpolarized gas diffusion MRI has been shown to relate directly to alveolar-airspace size in adults, pediatrics, canines, and mice. Using ex-vivo lungs from 7 healthy and 1 diseased infant humans, we investigated the relationship between  $^3\text{He}$  apparent diffusion coefficient (ADC) via mono-exponential decay, alveolar-duct radius via a restricted diffusion model originally developed for mice, and radius via histological measurement. While the mouse model is invalid in the infant diffusion regime, ADC measurements reflect changes in alveolar-airspace size. This method shows promise for longitudinal in-vivo acinar-airway monitoring in neonatal patients.

---

Oral

## Diffusion: Time-Dependence & Relaxation

Room 316BC

Wednesday 13:45 -  
15:45

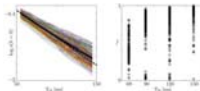
Moderators: Els Fieremans & Greg Stanisz

---

836



13:45



Quantifying neuronal microstructure integrity with TE dependent Diffusion Imaging (TEdDI)

Jelle Veraart<sup>1</sup>, Els Fieremans<sup>1</sup>, and Dmitry S. Novikov<sup>1</sup>

<sup>1</sup>Center for Biomedical Imaging, New York University School of Medicine, New York, NY, United States

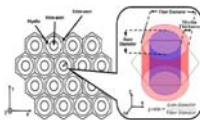
We resolve degeneracies in the estimation of parameters of white matter integrity by exploiting the observed echo time dependency of diffusion MRI signal in human brain white matter. Empirical results and statistical analyses reveal that adding compartment-specific  $T_2$  relaxation times to biophysical models of diffusion MRI improves the parameter estimation in terms of precision and accuracy.

---

837



13:57



A Novel Method for Assessing Myelination with TE dependence of DTI-derived Parameters

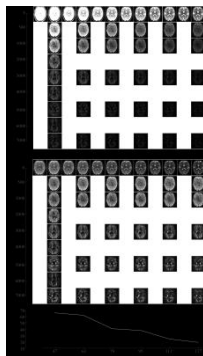
Mu Lin<sup>1</sup>, Qiuping Ding<sup>1</sup>, Xu Yan<sup>2</sup>, Thorsten Feiweier<sup>3</sup>, Hongjian He<sup>1</sup>, and Jianhui Zhong<sup>4</sup>

<sup>1</sup>Center for Brain Imaging Science and Technology, Zhejiang University, Hangzhou, Zhejiang, China, Hangzhou, People's Republic of China, <sup>2</sup>MR Collaboration NE Asia, Siemens Healthcare, Shanghai, China., <sup>3</sup>Siemens Healthcare GmbH, Erlangen, Germany., <sup>4</sup>Department of Imaging Sciences, University of Rochester, Rochester, NY, USA.

Myelin water is abundant in white matter but myelin signal is often ignored in diffusion models due to its short T2. There is however substantial water exchange between myelin and non-myelin water within typical diffusion times. Using Monte Carlo simulation and in-vivo measurement, we demonstrate that this water exchange might result in an echo-time (TE) dependence of DTI-derived parameters. As myelin water exchange increases with the thickness of myelin sheath, the TE dependence can be used to assess the degree of myelination.

838

14:09



Disentangling in two dimensions in the living human brain: Feasibility of relaxometry-diffusometry using ultra-strong gradients

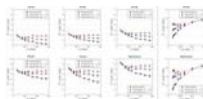
Chantal MW Tax<sup>1</sup>, Umesh S Rudrapatna<sup>1</sup>, Thomas Witzel<sup>2</sup>, and Derek K Jones<sup>1</sup>

<sup>1</sup>CUBRIC, Cardiff University, Cardiff, United Kingdom, <sup>2</sup>MGH/HST Martinos Center for Biomedical Imaging, Harvard Medical School, Boston, MA, United States

Combining multiple, complementary contrasts into one analysis will yield deeper understanding of white matter physiology than using diffusion MRI (dMRI) alone. Varying TE in a PGSE sequence would allow for the exploration of D-T2 spectra in tissue. However, typical hardware and time constraints render the acquisition of such diffusion/relaxation spectra in the living human impractical. In this work, we explore how 300 mT/m gradients of a Connectom scanner could help in further investigating 1) the reported TE dependency of DTI parameters and 2) D-T2 spectra in the living human brain.

839

14:21



T1-induced apparent time dependence of diffusion coefficient measured with stimulated echo due to exchange with myelin water

Hong-Hsi Lee<sup>1</sup>, Dmitry S. Novikov<sup>1</sup>, and Els Fieremans<sup>1</sup>

<sup>1</sup>Center for Biomedical Imaging, New York University, New York, NY, United States



For diffusion measurements, stimulated-echo acquisition mode (STEAM) has been widely used. To enhance sensitivity to microstructure, previous studies used STEAM to vary the diffusion time by changing the mixing time  $t_M$ . Here we show that varying  $t_M$  results in an “apparent” STEAM-measured diffusivity dependence on  $t_M$ , irrespective of genuine microstructure-specific time dependence. This effect is caused by  $T_1$ -relaxation and water exchange between myelin water and “free” water (intra- and extra-axonal water). We propose a modified Kärger model considering diffusion+ $T_1$ -relaxation+exchange, and demonstrate that exchange-induced  $t_M$ -dependence explains ~20-50% of the total diffusion time dependence, and should be considered while using STEAM.

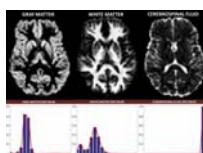
---

840

14:33

### Isotropic Diffusion Relaxometry Imaging (IDRI)

Alexandru Vlad Avram<sup>1</sup>, Joelle Sarlls<sup>2</sup>, Elizabeth Hutchinson<sup>3</sup>, and Peter Basser<sup>3</sup>



<sup>1</sup>NIBIB, National Institutes of Health, Bethesda, MD, United States,

<sup>2</sup>NINDS, National Institutes of Health, Bethesda, MD, United States,

<sup>3</sup>NICHD, National Institutes of Health, Bethesda, MD, United States

We describe a model-free method to quantify the spectrum of water mobilities in fixed and live brain tissues. We eliminate confounds caused by anisotropic diffusion in brain tissues by measuring orientationally-averaged diffusion weighted images over a large range of b-values. Spectra of orientationally-averaged water diffusivities show clear distinctions between white matter, gray matter and cerebrospinal fluid, and could provide new biologically-specific clinical markers for studying and diagnosing ischemic stroke, tumors, and neurodegenerative disorders and diseases, including inflammation.

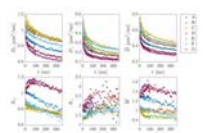
---

841

14:45

### Time Dependence Of White Matter Biomarkers From Axially Symmetric Diffusion Kurtosis Imaging

Jonas Lynge Olsen<sup>1</sup>, Brian Hansen<sup>2</sup>, Noam Shemesh<sup>3</sup>, and Sune Nørhøj Jespersen<sup>1,2</sup>



<sup>1</sup>Department of Physics and Astronomy, Aarhus University, Aarhus, Denmark, <sup>2</sup>CFIN/MINDLab at the Department of Clinical Medicine, Aarhus University, Aarhus, Denmark, <sup>3</sup>Champalimaud Neuroscience Programme, Champalimaud Centre for the Unknown, Lisbon, Portugal

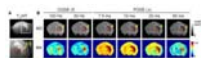


Using a recently developed PFG-based framework for fast diffusion kurtosis imaging we observe a strong time dependence of diffusion and kurtosis metrics in fixed spinal cord white matter from 6-350 ms. DKI metrics can be expressed in terms of intra- and extra axonal properties using white matter tract integrity (biexponential modelling), but a sign ambiguity results in two solutions of the inverse problem. The time dependence of the two solutions observed here help identify the correct solution, and allows comparing time-dependent compartment diffusivities with theory.

---

842

14:57



### Diffusion time dependence of kurtosis reveals microstructural changes after neonatal hypoxia-ischemia

Dan Wu<sup>1</sup>, Frances J Northington<sup>2</sup>, Els Fieremans<sup>3</sup>, Dmitry Novikov<sup>3</sup>, and Jiangyang Zhang<sup>3</sup>

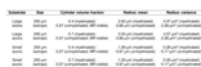
*<sup>1</sup>Radiology, Johns Hopkins University School of Medicine, Baltimore, MD, United States, <sup>2</sup>Pediatrics, Johns Hopkins University School of Medicine, Baltimore, MD, United States, <sup>3</sup>Radiology, New York University School of Medicine, NY, United States*

Apparent diffusion coefficient (ADC) and diffusion kurtosis are both sensitive markers to ischemic brain injury. We investigated the diffusion time ( $t_d$ )-dependency of ADC and kurtosis at nine  $t_d$ 's ranging from 2.5 to 60 ms in a mouse model of neonatal hypoxic-ischemic injury. In the hippocampus, ADCs showed a monotonous decrease with increasing  $t_d$ , whereas kurtosis reached its maximum at  $t_d$  of 5-10 ms and decreased for longer  $t_d$ 's. At the shortest  $t_d$  in this study, we found significant increased kurtosis in the edema region but no significant reduction in diffusivity, suggesting their different sensitivities to microstructural changes after ischemic injury.

---

843

15:09



### Origin of the time dependence of the diffusion-weighted signal in spinal cord white matter

Francesco Grussu<sup>1</sup>, Andrada Ianus<sup>2,3</sup>, Carmen Tur<sup>1</sup>, Ferran Prados<sup>1,4</sup>, Torben Schneider<sup>1,5</sup>, Sébastien Ourselin<sup>4</sup>, Ivana Drobnjak<sup>2</sup>, Hui Zhang<sup>2</sup>, Daniel C. Alexander<sup>2</sup>, and Claudia A. M. Gandini Wheeler-Kingshott<sup>1,6,7</sup>

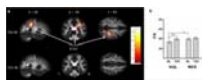
<sup>1</sup>UCL Institute of Neurology, Queen Square MS Centre, University College London, London, United Kingdom, <sup>2</sup>Centre for Medical Image Computing, Department of Computer Science, University College London, London, United Kingdom, <sup>3</sup>Champalimaud Centre for the Unknown, Champalimaud Foundation, Lisbon, Portugal, <sup>4</sup>Translational Imaging Group, Centre for Medical Image Computing, Department of Medical Physics and Biomedical Engineering, University College London, London, United Kingdom, <sup>5</sup>Philips UK, Guildford, Surrey, United Kingdom, <sup>6</sup>Department of Brain and Behavioural Sciences, University of Pavia, Pavia, Italy, <sup>7</sup>Brain MRI 3T Mondino Research Center, C. Mondino National Neurological Institute, Pavia, Italy

Time dependence of the brain white matter diffusion-weighted signal originates from both intra-axonal and extra-axonal spaces. Here, we investigate which of these contributions dominates in spinal cord white matter for clinically feasible acquisitions, to inform accurate model-based microstructural imaging. We analyse data from Monte Carlo simulations and from in vivo scans, and find that for diffusion times of 20-70 ms time dependence has mostly intra-axonal origin. Such a time dependence influences the estimation of axonal volume fraction and extra-axonal diffusivity, and highlights the importance of using long diffusion times to support stick-like models for axons in the spinal cord.

---

844

15:21



Sleep deprivation affects white matter integrity in cognitively vulnerable individuals

Hengyi Rao<sup>1</sup>, Sihua Xu<sup>1</sup>, Zhuo Fang<sup>1</sup>, Fan Yang<sup>1</sup>, Andrea Spaeth<sup>1</sup>, Namni Goel<sup>1</sup>, Mathias Basner<sup>1</sup>, Sumei Wang<sup>1</sup>, David F. Dinges<sup>1</sup>, and John A. Detre<sup>1</sup>

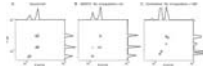
<sup>1</sup>University of Pennsylvania, Philadelphia, PA, United States

Using DTI, we examined the effects of one night of acute total sleep deprivation on fractional anisotropy (FA), an index reflecting the degree of anisotropic water diffusion in brain white matter. Sleep deprivation significantly increases FA in the right superior longitudinal fasciculus (SLF) in individuals who were cognitively vulnerable to sleep loss, while no FA changes were observed in cognitively resistant individuals. Vulnerable subjects also showed lower FA in the right SLF than resistant subjects at baseline before sleep loss, suggesting both trait- and state-dependent interactions between SLF microstructure and cognitive vulnerability to sleep deprivation.

---

845

15:33



### Clinically feasible relaxation-diffusion correlation MRI using MADCO

Dan Benjamini<sup>1</sup> and Peter J Basser<sup>1</sup>

<sup>1</sup>*Quantitative Imaging and Tissue Sciences, National Institutes of Health, Bethesda, MD, United States*

Even though the brain is microscopically heterogeneous, the majority of currently used quantitative MRI methods in brain research employ idealized models to describe specific structures. Multidimensional relaxation-diffusion correlation (REDCO) is an assumption-free method that measures how water is distributed within the tissue. REDCO had never been used in clinical applications because of the large amount of data it requires. Here we apply the concept of marginal distributions constrained optimization (MADCO) to REDCO-MRI experiments. Using this approach data requirements are vastly reduced, making REDCO-MRI a clinically feasible imaging technique to infer the underlying microstructure, number of compartments, and possibly their function.

## Oral

### Bones: Ultrastructure in Health & Disease

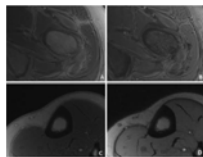
Room 320

Wednesday 13:45 -  
15:45

*Moderators: Richard Hodgson & Mary Kate Manhard*

846

13:45



### A preliminary application of Porosity Index measured by UTE MRI sequence in the femoral neck

Min Chen<sup>1</sup>, Huishu Yuan<sup>1</sup>, and Lizhi Xie<sup>2</sup>

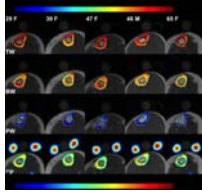
<sup>1</sup>*Radiology Department of Peking University Third H, Beijing, People's Republic of China*, <sup>2</sup>*GE Healthcare, MR Research China, BeiJing, People's Republic of China*

The current study aims to assess the feasibility of porosity index (PI) measurements derived from ultra-short echo time (UTE) MRI technology in the femoral neck and to further investigate its latent associations with age, gender, body mass index (BMI) and tibial PI. It was concluded that cortical PI measured by UTE MRI sequence can be applied in femoral neck and cannot be replaced by tibial measurement. Femoral neck and tibial PI were observed to correlate with age and BMI, which worth further study.

847



13:57



### Feasibility of bone mineral and water quantification *in vivo* by solid-state $^{31}\text{P}$ and $^1\text{H}$ MRI at 3T

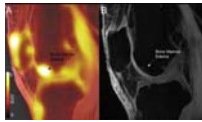
Xia Zhao<sup>1</sup>, Hee Kwon Song<sup>1</sup>, Alan C. Seifert<sup>1</sup>, Cheng Li<sup>1</sup>, and Felix W. Wehrli<sup>1</sup>

<sup>1</sup>University of Pennsylvania, Philadelphia, PA, United States

Surrogates for bone matrix density, pore volume fraction and mineral density can be studied with solid-state MRI. Here, we developed an *in vivo* MRI protocol to simultaneously quantify bone mineral  $^{31}\text{P}$  and bound and pore water on a 3 Tesla clinical MRI system with a dual-frequency extremity coil and 3D  $^1\text{H}$  UTE and  $^{31}\text{P}$  PETRA-ZTE pulse sequences. Measurements in the mid-tibia of 10 subjects yielded  $7.06 \pm 1.53 \text{ mol/L}$   $^{31}\text{P}$ , and  $13.99 \pm 1.26$  and  $10.39 \pm 0.80 \text{ mol/L}$   $\text{H}_2\text{O}$  for total and bound water, respectively, in good agreement with prior *ex vivo* data. The work suggests that both organic and inorganic phases of cortical bone can be quantitatively evaluated *in vivo* with a single, integrated protocol.

848

14:09



### Study Of The Associations Between $[^{18}\text{F}]\text{-NaF}$ PET Bone Remodeling, MRI Trabecular Bone Structure and Patient Reported Outcomes in subjects with Osteoarthritis

Valentina Pedita<sup>1</sup>, Rohit Curucundhi<sup>1</sup>, Dragana Savic<sup>2</sup>, Misung Han<sup>1</sup>, Youngho Seo<sup>1</sup>, Matthew D. Bucknor<sup>1</sup>, Benjamin L. Franc<sup>1</sup>, and Sharmila Majumdar<sup>1</sup>

<sup>1</sup>Radiology and Biomedical Imaging, University Of California, San Francisco, San Francisco, CA, United States, <sup>2</sup>Department of Physiology, Anatomy and Genetics, University of Oxford

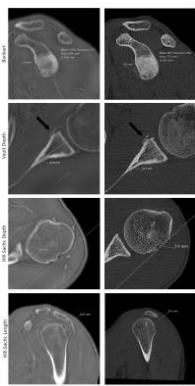
In Osteoarthritis (OA) degeneration of articular cartilage, are accompanied by changes in subchondral and trabecular bone. In this study we analyzed bone structure, cartilage degeneration and bone remodeling, quantified using simultaneous PET/MRI system in fourteen subjects with radiographic or symptomatic OA. The aim of this study was to evaluate these imaging biomarkers in association with patient reported outcomes for evaluating this technique as a tool for assessing OA. Our results showed associations between Standardized Uptake Values (SUV) and both level of pain measured by KOOS and cartilage degeneration measured using  $T_{1\rho}$  and  $T_2$  relaxation times.

849

14:21

### Zero Echo Time MRI: Osseous Shoulder Imaging

Ryan Breighner<sup>1</sup>, Yoshimi Endo<sup>1</sup>, Gabrielle Konin<sup>1</sup>, Lawrence Gulotta<sup>2</sup>, Matthew F. Koff<sup>1</sup>, and Hollis G. Potter<sup>1</sup>



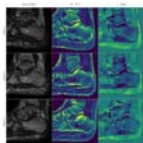
<sup>1</sup>Radiology and Imaging, Hospital for Special Surgery, New York, NY, United States, <sup>2</sup>Sports Medicine, Hospital for Special Surgery, New York, NY, United States

Routine MRI fails to provide direct visualization of bone due to the short tissue relaxation times and limited signal intensity. This study investigates the use of proton density zero echo time (ZTE) MRI for bone in the shoulder. Shoulder CT and ZTE images were acquired for 31 patients. Five measures of osseous defect and lesion sizes were compared between the two modalities. 'Fair' to 'excellent' intraobserver agreement was observed between CT and ZTE MRI. Zero Echo Time MRI may obviate the need for additional CT evaluation in some cases.

850



14:33



### Simultaneous R2\* and Quantitative Susceptibility Mapping of Trabecularized Yellow Bone Marrow: Initial Results in the Calcaneus

Maximilian Nikolaus Diefenbach<sup>1</sup>, Jakob Meineke<sup>2</sup>, Peter Foehr<sup>3</sup>, Stefan Ruschke<sup>1</sup>, Thomas Baum<sup>1</sup>, Jan S Kirschke<sup>4</sup>, Andreas Hock<sup>5</sup>, Hendrik Kooijman<sup>5</sup>, Ernst J Rummeny<sup>1</sup>, and Dimitrios C Karampinos<sup>1</sup>

<sup>1</sup>Department of Diagnostic and Interventional Radiology, Technical University of Munich, Munich, Germany, <sup>2</sup>Philips Research Laboratory, Hamburg, Germany, <sup>3</sup>Department of Orthopedics and Sport Orthopedics, Technical University of Munich, Munich, Germany, <sup>4</sup>Section of Neuroradiology, Technical University of Munich, Munich, Germany, <sup>5</sup>Philips Healthcare, Hamburg, Germany

R2\* mapping has been previously used to measure trabecular bone density by quantifying the magnetic field inhomogeneity effects induced by the susceptibility difference between trabecular bone and marrow. Quantitative susceptibility mapping (QSM) has been emerging in other body parts for measuring the field-independent magnetic susceptibility. Trabecular bone is in many locations embedded in yellow fatty marrow. Therefore, trabecular bone QSM requires to account for the presence of fat. The purpose of the present work is to develop a methodology for simultaneous R2\* mapping and QSM of trabecularized yellow bone marrow and apply the technique in the calcaneus of healthy volunteers.

14:45



### Proximal Femur Marrow Adipose Tissue Assessment Using 3T Multi-Parametric Chemical Shift Encoded MRI: Preliminary Results in Osteoporotic Patients

Dimitri MARTEL<sup>1</sup>, Gregory CHANG<sup>1</sup>, Mary BRUNO<sup>1</sup>, and Benjamin LEPORQ<sup>2</sup>

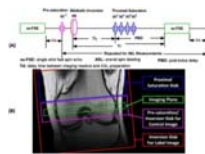


<sup>1</sup>Department of Radiology, New York University School of Medicine, Bernard and Irene Schwartz Center for Biomedical Imaging, New York City, NY, United States, <sup>2</sup>Université de Lyon; CREATIS CNRS UMR 5220, Inserm U1206, INSA-Lyon, UCBL Lyon 1, Villeurbanne, France

Recent assessment of osteoporosis by monovoxel magnetic resonance spectroscopy states interesting feature about subregional femoral marrow fat composition. In this study, we evaluate differences in bone marrow fat of the proximal femurs of controls and patients with OP using a novel quantitative multi-parametric MRI approach that provides information about fat content, fatty acid composition, transverse relaxation and internal magnetic susceptibility.

852

14:57



### Epiphyseal Bone Marrow Perfusion Imaging in the Distal Femur Using Arterial Spin Labeling: Feasibility and Challenges

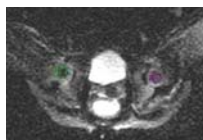
Xiufeng Li<sup>1</sup>, Casey P. Johnson<sup>1</sup>, and Jutta Ellermann<sup>1</sup>

<sup>1</sup>Radiology-CMRR, University of Minnesota, Minneapolis, MN, United States

Epiphyseal bone marrow perfusion of the distal femur is a valuable biomarker for knee diseases or injuries, such as anterior cruciate ligament tears and post-traumatic osteoarthritis. Bone marrow perfusion imaging is also of interest in the management of developmental knee diseases, such as osteochondritis dissecans, where the capacity to heal may be related to sufficient perfusion to the site of injury. ASL is well suited for monitoring of knee disease progression, assessment of therapy response, and use in pediatric populations. This study is to evaluate the feasibility and challenges of epiphyseal bone marrow ASL imaging in the distal femur.

853

15:09



### MRI quantification of diffusion and perfusion in epiphysis of femoral heads after close reduction of children with DDH by intravoxel incoherent movement

Xiang Hong Meng<sup>1</sup>, Zhi Wang<sup>1</sup>, Dan Dan Zheng<sup>2</sup>, Jian Ping Yang<sup>3</sup>, and Zhong Li Zhang<sup>3</sup>

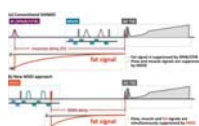
<sup>1</sup>Radiology, Tian Jin Hospital, Tian Jin, People's Republic of China, <sup>2</sup>MR Research China, GE Healthcare, People's Republic of China, <sup>3</sup>Pediatric Orthopedics, Tian Jin Hospital, Tian Jin, People's Republic of China



Developmental dysplasia of the hip (DDH) is a common disease of the development of hips. Some children with DDH need close reduction followed by immobilization in spica casting, but excessive hip abduction may lead to avascular necrosis of the epiphysis of femoral head. Therefore, this study would like to use IVIM method to help the pediatric orthopaedic doctors to know whether the blood supply of epiphysis of femoral heads is insufficiency or not in patients with DDH after close reduction.

854

15:21



Motion-Sensitized Driven-Inversion (MSDI) for improvement of diffusion-prepared MR neurography (SHINKEI) in the brachial plexus

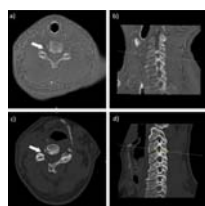
Masami Yoneyama<sup>1</sup>, Iain Ball<sup>2</sup>, Yasuhiro Goto<sup>3</sup>, Hitoshi Tadenuma<sup>3</sup>, Kayoko Abe<sup>4</sup>, Makoto Obara<sup>1</sup>, Tetsuo Ogino<sup>1</sup>, Tomoyuki Okuaki<sup>5</sup>, Michinobu Nagao<sup>4</sup>, and Marc Van Cauteren<sup>5</sup>

<sup>1</sup>Philips Electronics Japan, Tokyo, Japan, <sup>2</sup>Philips Electronics Australia, North Ryde, Australia, <sup>3</sup>Department of Radiological Services, Tokyo Women's Medical University Hospital, Tokyo, Japan, <sup>4</sup>Department of Diagnostic Imaging & Nuclear Medicine, Tokyo Women's Medical University Hospital, Tokyo, Japan, <sup>5</sup>Philips Healthcare AsiaPacific, Tokyo, Japan

Brachial plexus is anatomically complex and may be involved in a variety of pathologies that leads to significant morbidity. MR neurography, based on diffusion-prepared MR neurography (SHINKEI), plays a major role in the diagnostic work-up of plexus pathologies. To solve the problems that caused by the current fat suppression techniques (SPAIR and STIR) with SHINKEI, we developed motion-sensitized driven inversion (MSDI). MSDI could simultaneously suppress fat, flow and muscle signals using only one pre-pulse module. SHINKEI with MSDI provides uniform fat suppression in the brachial plexus, as in STIR, with no significant decrease in SNR compared to SPAIR.

855

15:33



Diagnostic Accuracy of Zero Echo Time Magnetic Resonance Imaging for Grading of Cervical Spine Neural Foraminal Stenosis

Darryl B. Sneag<sup>1</sup>, Parina H. Shah<sup>1</sup>, Ryan Breighner<sup>1</sup>, Yoshimi Endo<sup>1</sup>, Erin C. Argentieri<sup>1</sup>, and Matthew F. Koff<sup>1</sup>

<sup>1</sup>Department of Radiology and Imaging, Hospital for Special Surgery, New York, NY, United States



A challenge for orthopaedic radiologists is utilizing MRI to assess neuroforaminal (NF) stenosis of the cervical spine as cortical bone does not display with sufficient signal intensity. This study utilized zero echo time (ZTE) imaging to visualize the cervical spine and compare evaluation of NF stenosis to corresponding CT imaging. Substantial agreement was found between ZTE and CT ( $\kappa=0.71$ ). ZTE tended to underestimate stenotic grade in 25% of foramina, with a majority (66%) of differences within one grading level. Further development of ZTE and image processing may minimize the need for cervical spine CT in assessing NF stenosis.

## Combined Educational & Scientific Session

# CEST from Equations to Cells to Humans

Organizers: Guanshu Liu, Ph.D., Steven P. Sourbron, Ph.D., & Elena Vinogradov, Ph.D.

Room 310

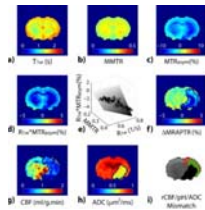
Wednesday 13:45 -  
15:45

Moderators: Feliks Kogan & Peter van Zijl

13:45

### Introduction to CEST & Quantification

Phillip Zhe Sun<sup>1</sup>



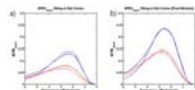
<sup>1</sup>Harvard University

CEST MRI has emerged as a sensitive contrast mechanism for several metabolites such as glucose, glycogen, creatine and glutamate, as well as tissue pH. It has promising applications in a host of disorders including acute stroke, epilepsy and tumor. As we make the transition from CEST-weighted MRI toward quantitative *in vivo* CEST imaging for improved characterization of the underlying physiology, it is helpful to review persistent progress in the field of CEST imaging from equations, cells, rodents and patients.

856

14:05

### Characterization of *in vivo* Chemical Exchange Parameters Using Chemical Exchange-Sensitive MRI at 9.4 T and 15.2 T



Julius Juhyun Chung<sup>1,2</sup>, Wonmin Choi<sup>1,3</sup>, Tao Jin<sup>4</sup>, Jung Hee Lee<sup>1,2,3,5</sup>, and Seong-Gi Kim<sup>1,2,3</sup>

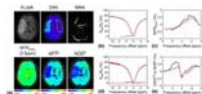
<sup>1</sup>Center for Neuroscience Imaging Research, Institute for Basic Science (IBS), Suwon, Korea, Republic of, <sup>2</sup>Samsung Advanced Institute for Health Sciences and Technology, SKKU, Seoul, Korea, Republic of, <sup>3</sup>Biomedical Engineering, Sungkyunkwan University, Suwon, Korea, Republic of, <sup>4</sup>Radiology, University of Pittsburgh, <sup>5</sup>Radiology, Sungkyunkwan University, Seoul, Korea, Republic of

Chemical-exchange sensitive imaging can prove to be complex particularly when imaging intermediate exchanges in-vivo where contrast comes from an amalgamation of different sources. We propose a method that utilizes Z-spectra data from multiple fields to determine apparent exchange parameters that characterize the exchange to which a particular saturation scheme is sensitive. Parameter determination in glutamate phantoms proved commensurate to utilizing an on-resonance dispersion measurement and in the rat brain cortex the  $k_{ex}$  was measured to be  $11,240 \text{ s}^{-1}$  antemortem and  $7070 \text{ s}^{-1}$  postmortem. This method is useful for determining exchange parameters relevant to complex systems when signal source is unclear.

857



14:15



Improving Amide Proton Transfer (APT) MRI Quantification in Acute Human Stroke Patients: Achieving More Pure APT Signals and Higher Detection Sensitivity

Hye-Young Heo<sup>1,2</sup>, Yi Zhang<sup>1</sup>, Tina Burton<sup>3</sup>, Shanshan Jiang<sup>1</sup>, Peter C.M. van Zijl<sup>1,2</sup>, Richard Leigh<sup>3</sup>, and Jinyuan Zhou<sup>1,2</sup>

<sup>1</sup>Russell H Morgan Department of Radiology and Radiological Science, Johns Hopkins University, Baltimore, MD, United States, <sup>2</sup>F.M. Kirby Research Center for Functional Brain Imaging, Kennedy Krieger Institute, Baltimore, MD, United States, <sup>3</sup>Stroke Diagnostics and Therapeutics Section, National Institute of Neurological Diseases and Stroke, National Institutes of Health, Bethesda, MD, United States

APT-weighted (APT<sub>w</sub>) imaging based on MTR asymmetry analysis has shown promise for identifying ischemic lesions, but suffers from low accuracy due to small APT<sub>w</sub> intensity changes. Quantitative APT, nuclear overhauser enhancement (NOE), perfusion and diffusion MRI were performed on acute stroke patients (n=30). The results showed that while APT<sub>w</sub> MRI for pH analysis based on  $MTR_{asym}$  analysis was confounded by upfield NOE effects, NOE-free APT-MRI contrast between normal and ischemic lesions was substantially increased, nearly 3 times larger than that based on  $MTR_{asym}$  analysis. Furthermore, noticeable NOE contrast was observed for lesions, explained in terms of a relayed-NOE transfer mechanism.

---

14:25

DIACEST Exogenous

Assaf A. Gilad<sup>1</sup>

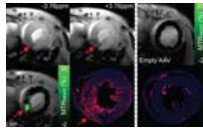
<sup>1</sup>*Johns Hopkins University*

We will review the principles for designing an optimal bioorganic probes that are based on the specific targets. In addition we will discuss how to design a genetically encoded probe for a specific scientific question.

---

858

14:45



Spatiotemporal quantification of reporter gene expression in the mouse heart using the Lysine Rich Protein and cardiac chemical exchange saturation transfer

Shelby Meier<sup>1</sup>, Jose Abisambra<sup>2</sup>, J Brandon<sup>3</sup>, Assaf Gilad<sup>4</sup>, and Moriel Vandsburger<sup>1,5</sup>

<sup>1</sup>*Physiology, University of Kentucky, Lexington, KY, United States,*

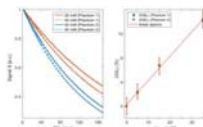
<sup>2</sup>*Physiology, University of Kentucky,* <sup>3</sup>*University of Kentucky,* <sup>4</sup>*Radiology and Radiological Sciences, Johns Hopkins University,* <sup>5</sup>*Bioengineering, U.C. Berkeley, Berkeley, CA, United States*

We utilized cardiac chemical exchange saturation transfer MRI and an artificial reporter gene, the Lysine Rich Protein (LRP), to image gene transfer in the mouse heart using 2 routes of viral vector administration.

---

859

14:55



T1ρ-weighted Dynamic Glucose Enhanced MRI

Patrick Schuenke<sup>1</sup>, Daniel Paech<sup>1</sup>, Christina Koehler<sup>1,2</sup>, Johannes Windschuh<sup>1</sup>, Peter Bachert<sup>1</sup>, Mark E. Ladd<sup>1</sup>, Heinz-Peter Schlemmer<sup>1</sup>, Alexander Radbruch<sup>1,2</sup>, and Moritz Zaiss<sup>3</sup>

<sup>1</sup>*German Cancer Research Center (DKFZ), Heidelberg, Germany,*

<sup>2</sup>*University Hospital Heidelberg, Heidelberg, Germany,* <sup>3</sup>*Max-Planck-Institute for Biological Cybernetics, Tuebingen, Germany*



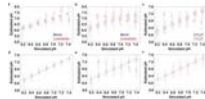


A correct preoperatively grading of glioma is always the most important issue in clinic. APT and IVIM imaging are designed to assess glioma on the level of cell and molecule. So, in this study we combined these two functional techniques hoping to explore their diagnostic performance in differentiating HGG from LGG.

---

861

15:35



### Clinical Translation of Tumor Acidosis Measurements with AcidoCEST MRI

Kyle M. Jones<sup>1</sup>, Edward A. Randtke<sup>2</sup>, Eriko Yoshimaru<sup>3</sup>, Christine M. Howison<sup>2</sup>, Pavani Chalasani<sup>4</sup>, Robert R Klein<sup>4</sup>, Setsuko K. Chambers<sup>3</sup>, Phillip H. Kuo<sup>2</sup>, and Mark D. Pagel<sup>2</sup>

<sup>1</sup>Biomedical Engineering, University of Arizona, Tucson, AZ, United States, <sup>2</sup>Medical Imaging, University of Arizona, Tucson, AZ, United States, <sup>3</sup>University of Arizona Cancer Center, University of Arizona, Tucson, AZ, United States, <sup>4</sup>Medicine, University of Arizona, Tucson, AZ, United States

We optimized acidoCEST MRI, a method that measures extracellular pH (pHe), and translated this method for clinical imaging. We fit CEST spectra with the Bloch equations modified to include the direct estimation of pH, and generated parametric maps of tumor pHe in the SKOV3 tumor model, a patient with high grade invasive ductal breast carcinoma, and a patient with metastatic ovarian cancer. AcidoCEST MRI successfully measured a pH 6.58 in a tumor of the patient with metastatic ovarian cancer. The primary breast tumor failed to accumulate sufficient agent to generate pHe measurements.

---

### Traditional Poster: Interventional MRI

Exhibition Hall 2585-2618      Wednesday 16:15 - 18:15      (no CME credit)

---

### Traditional Poster: MRI Safety

Exhibition Hall 2619-2653      Wednesday 16:15 - 18:15      (no CME credit)

---

### Traditional Poster: Engineering

Exhibition Hall 2654-2674      Wednesday 16:15 - 18:15      (no CME credit)

---

## Electronic Poster: Musculoskeletal

Exhibition Hall                      Wednesday 16:15 -  
17:15                                      *(no CME credit)*

---

## Electronic Poster: Acquisition, Reconstruction & Analysis

Exhibition Hall                      Wednesday 16:15 -  
17:15                                      *(no CME credit)*

---

## Study Groups

### White Matter Study Group

Room 323ABC                      Wednesday 16:15 -  
18:15                                      *(no CME credit)*

---

## Study Groups

### Detection & Correction of Motion in MRI & MRS Study Group

Room 317AB                      Wednesday 16:15 -  
18:15                                      *(no CME credit)*

---

## Educational Course

### Heart Failure & Arrhythmia

*Organizers:* Tim Leiner, M.D., Ph.D., Reza Nezafat, Ph.D. & Bernd J. Wintersperger, M.D.

Room 316A                      Wednesday 16:15 -  
18:15                                      *Moderators:* Jeremy Collins & Peng Hu

---

16:15                      [Clinical Needs of imaging in Heart Failure: Impact on Patient Management](#)

David Sosnovik<sup>1</sup>

<sup>1</sup>*Massachusetts General Hospital, Harvard Medical School*

[NA](#)

---

16:45                      [State of the art Imaging in Heart Failure: Cardiac MR in the Multi-Modality Environment](#)

Jeanette Schulz-Menger<sup>1</sup>

<sup>1</sup>University of Berlin, Berlin, Germany

---

17:15

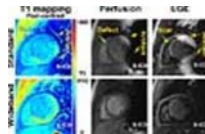
[The Challenging Role & Approaches to Cardiac MR in Arrhythmia](#)  
Dana Peters<sup>1</sup>

<sup>1</sup>Radiology and Biomedical Imaging, Yale University, New Haven, CT, United States

This material covers the basic and advanced approaches for preserving image quality in patients with arrhythmia, for cine, flow and late gadolinium enhancement techniques. Furthermore, it presents some advanced MRI methods for evaluating patients with arrhythmic disease, namely atrial fibrillation, ventricular arrhythmias, and arrhythmogenic right ventricular cardiomyopathy (ARVC).

---

17:45



[Cardiac Devices: Safety Aspects & Challenges in Cardiac MR](#)  
Daniel Kim

This lecture will describe some of the safety and image artifact issues related to performing MRI in patients with an implantable device (e.g., pacemaker, ICD, CRT).

---

18:15

[Adjournment & Meet the Teachers](#)

---

## Power Pitch

### Pitch: Diffusion: Outside the Brain

Power Pitch  
Theater A -  
Exhibition Hall

Wednesday 16:15  
- 17:15

Moderators: Seung-Kyun Lee &  
Jelle Veraart

(no CME credit)

---

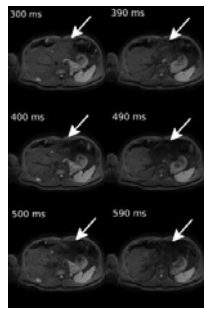
862

16:15

[Analysis of abdominal movement with Phase Optical Flow: Application to Diffusion imaging.](#)

Stephan Hahn<sup>1</sup>, Maxime Gérard<sup>1</sup>, Damien Dasnoy-Sumell<sup>1</sup>, Julie Absil<sup>2</sup>, Olivier Debeir<sup>1</sup>, and Thierry Metens<sup>2</sup>

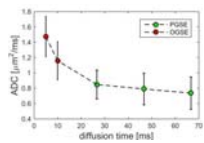




<sup>1</sup>Laboratories of Image, Signal processing and Acoustics, ULB, Brussels, Belgium, <sup>2</sup>MRI Clinics&Radiology, Hôpital Erasme, Brussels, Belgium

863

16:15



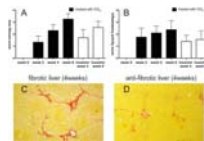
**In vivo imaging of mean cell size and density of human breast tumors**

Hua Li<sup>1,2</sup>, Lori R. Arlinghaus<sup>1,2</sup>, A. Bapsi Chakravarthy<sup>3</sup>, Vandana G. Abramson<sup>2</sup>, John C. Gore<sup>1,2</sup>, and Junzhong Xu<sup>1,2</sup>

<sup>1</sup>Institute of Imaging Science, Vanderbilt University, Nashville, TN, United States, <sup>2</sup>Department of Radiology and Radiological Sciences, Vanderbilt University, Nashville, TN, United States, <sup>3</sup>Department of Radiation Oncology, Vanderbilt University, Nashville, TN, United States

864

16:15



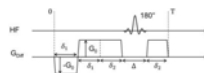
**Intravoxel incoherent motion MR imaging for staging liver fibrosis and monitoring anti-fibrotic response to losartan: an experimental study in rat model**

Caiyuan Zhang<sup>1</sup>, Yong Zhang<sup>2</sup>, and Dengbin Wang<sup>1</sup>

<sup>1</sup>Radiology, Xinhua Hospital, Shanghai Jiao Tong University School of Medicine, Shanghai, People's Republic of China, <sup>2</sup>MR Research China, GE Healthcare, Shanghai, China, Shanghai, People's Republic of China

865

16:15



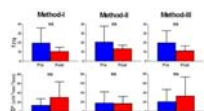
**Diffusion-weighted MRI and coherent flow in the kidney**

Andreas Max Weng<sup>1</sup>, Fabian Hilbert<sup>1</sup>, Henning Neubauer<sup>1</sup>, Simon Veldhoen<sup>1</sup>, Thorsten Alexander Bley<sup>1</sup>, and Herbert Köstler<sup>1</sup>

<sup>1</sup>Department of Diagnostic and Interventional Radiology, University Hospital of Würzburg, Würzburg, Germany

866

16:15



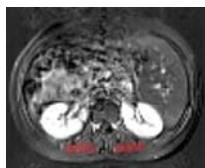
**An assessment of Intravoxel Incoherent Motion (IVIM) imaging in Detection of Acute Kidney Injury in Rodents**

Keisuke Ishimatsu<sup>1</sup>, Shanrong Zhang<sup>1</sup>, Koji Sagiyama<sup>1</sup>, Ming Chang Hu<sup>2</sup>, Orson W Moe<sup>2</sup>, and Masaya Takahashi<sup>1</sup>

<sup>1</sup>Advanced Imaging Research Center, UT Southwestern Medical Center, Dallas, TX, United States, <sup>2</sup>Department of Internal Medicine / Charles and Jane Pak Center of Mineral Metabolism and Clinical Research, UT Southwestern Medical Center, Dallas, TX, United States

867

16:15



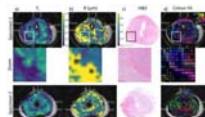
**Diffusion-Weighted MRI Identifies Viable Tissue in Wilms Tumour: Application for Subtype Analysis and Response to Chemotherapy**

Harriet Rogers<sup>1</sup>, Patrick Hales<sup>1</sup>, Kathy Pritchard-Jones<sup>2</sup>, and Christopher Clark<sup>1</sup>

<sup>1</sup>Developmental Imaging and Biophysics, Institute of Child Health, University College London, London, United Kingdom, <sup>2</sup>Developmental Biology and Cancer, Institute of Child Health, University College London, London, United Kingdom

868

16:15



**Validation of VERDICT MRI using fresh and fixed prostate specimens with aligned histological slices**

Colleen Bailey<sup>1</sup>, Roger M Bourne<sup>2</sup>, Bernard Siow<sup>3,4</sup>, Edward W Johnston<sup>5</sup>, Hayley Pye<sup>6,7</sup>, Susan Heavey<sup>6,7</sup>, Thomy Mertzani<sup>1</sup>, Hayley Whitaker<sup>6</sup>, Alexander Freeman<sup>8</sup>, Dominic Patel<sup>8</sup>, Greg Shaw<sup>6,7</sup>, Ashwin Sridhar<sup>6,7</sup>, Shonit Punwani<sup>5</sup>, David J Hawkes<sup>1</sup>, Daniel C Alexander<sup>1</sup>, and Eleftheria Panagiotaki<sup>1</sup>

<sup>1</sup>Centre for Medical Image Computing, University College London, London, United Kingdom, <sup>2</sup>Discipline of Medical Radiation Sciences, University of Sydney, Sydney, Australia, <sup>3</sup>Centre for Advanced Biomedical Imaging, University College London, London, United Kingdom, <sup>4</sup>Imaging, Francis Crick Institute, London, United Kingdom, <sup>5</sup>Centre for Medical Imaging, University College London, London, United Kingdom, <sup>6</sup>Division of Surgery and Interventional Science, University College London, London, United Kingdom, <sup>7</sup>Department of Urology, University College London Hospitals, London, United Kingdom, <sup>8</sup>Department of Research Pathology, University College London, London, United Kingdom

869

16:15

Region	Number of patients	Percentage of patients with viable tissue
Subtotal	10	100
Subtotal (n=10)	10	100
Subtotal (n=10)	10	100
Subtotal (n=10)	10	100
Subtotal (n=10)	10	100
Subtotal (n=10)	10	100
Subtotal (n=10)	10	100
Subtotal (n=10)	10	100
Subtotal (n=10)	10	100
Subtotal (n=10)	10	100

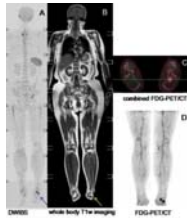
**Diffusion-weighted MRI in the evaluation of posttherapeutic residual masses in lymphoma**

Siarhei Kharuzhyk<sup>1</sup>, Edward Zhavrid<sup>2</sup>, and Nina Sachivko<sup>2</sup>

<sup>1</sup>Radiology, N.N. Alexandrov National Cancer Center, Minsk, Belarus,  
<sup>2</sup>Chemotherapy, N.N. Alexandrov National Cancer Center, Minsk,  
Belarus

870

16:15



The clinical evaluation of combining DWIBS with whole body T1w imaging for diagnosing bone marrow involvement in lymphoma patients: a comparison with PET/CT

Mengtian Sun<sup>1</sup>, Jingliang Cheng<sup>1</sup>, Yun Meng<sup>1</sup>, and Zhizheng Zhuo<sup>2</sup>

<sup>1</sup>The First Affiliated Hospital of Zhengzhou University, 1st, Zhengzhou, People's Republic of China, <sup>2</sup>Philips Healthcare, Beijing, People's Republic of China

871

16:15

A table with multiple columns and rows, likely representing quantitative data from the study. The columns include parameters such as 'b-value', 'ADC', 'IVIM-f', 'IVIM-s', and 'IVIM-D'. The rows represent different patient groups or conditions. The data is presented in a structured, tabular format.

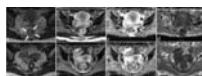
Intravoxel incoherent motion diffusion-weighted imaging for discriminating the pathological response to neoadjuvant chemoradiotherapy in locally advanced rectal cancer

Wen Lu<sup>1</sup>, Yu xiaoping<sup>1</sup>, and Zhang zhongping<sup>2</sup>

<sup>1</sup>Hunan Cancer Hospital, Chang sha, People's Republic of China, <sup>2</sup>GE Healthcare China, Beijing, People's Republic of China

872

16:15

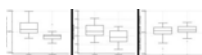


The value of diffusion kurtosis imaging in assessing pathological complete response to neoadjuvant chemoradiation therapy in rectal cancer: a comparison with conventional diffusion-weighted imaging  
Fei-Xiang Hu<sup>1</sup>, Tong Tong<sup>1</sup>, Wei Tang<sup>1</sup>, Yi-Qun Sun<sup>1</sup>, Dang Wang<sup>1</sup>, San-Jun Cai<sup>2</sup>, Zhen Zhang<sup>3</sup>, Grimm Robert<sup>4</sup>, Xu Yan<sup>5</sup>, Cai-xia Fu<sup>6</sup>, and Wei-Jun Peng<sup>1</sup>

<sup>1</sup>Radiology, Fudan University Shanghai Cancer Center, Shanghai, People's Republic of China, <sup>2</sup>Colorectal Surgery, Fudan University Shanghai Cancer Center, Shanghai, People's Republic of China, <sup>3</sup>Radiotherapy, Fudan University Shanghai Cancer Center, Shanghai, People's Republic of China, <sup>4</sup>MR Applications Predevelopment, Siemens Healthcare GmbH, Germany, <sup>5</sup>MR Collaboration NE Asia, Siemens Healthcare, People's Republic of China, <sup>6</sup>APPL, Siemens Shenzhen Magnetic Resonance Ltd., People's Republic of China

873

16:15



The application of whole lesion IVIM analysis using iZOOM DWI in the diagnosis of thyroid tumor

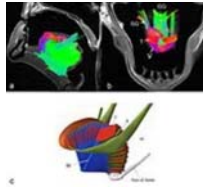
Yunlong Yue<sup>1</sup>, Lili Zuo<sup>1</sup>, Kaining Shi<sup>2</sup>, Lee Jiang<sup>3</sup>, Jinsong Guo<sup>1</sup>, and Yanfang Jin<sup>1</sup>

<sup>1</sup>Department of MR, Beijing Shijitan hospital of capital medical university, Beijing, People's Republic of China, <sup>2</sup>Philips Healthcare (China), Beijing, People's Republic of China, <sup>3</sup>Philips Healthcare (China), Suzhou, People's Republic of China

874

16:15

### Diffusion Spectrum Imaging Tractography of the Human Tongue



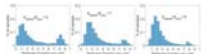
Nahla M H Elsaid<sup>1</sup>, Maureen Stone<sup>2</sup>, Steven Roys<sup>1</sup>, Rao P Gullapalli<sup>1</sup>, Jerry L Prince<sup>3</sup>, and Jiachen Zhuo<sup>1</sup>

<sup>1</sup>Diagnostic Radiology, University of Maryland School of Medicine, Baltimore, MD, United States, <sup>2</sup>Neural and Pain Sciences and Orthodontics, University of Maryland Dental School, Baltimore, MD, United States, <sup>3</sup>Electrical and Computer Engineering, Johns Hopkins University, Baltimore, MD, United States

875

16:15

### Acquisition at maximum blood velocity overcomes the problem of the ill-posedness of the IVIM model: a demonstration with renal diffusion MRI



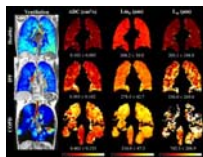
Bastien Milani<sup>1</sup>, Jean-Baptiste Ledoux<sup>2</sup>, and Menno Pruijm<sup>3</sup>

<sup>1</sup>Nephrology, CHUV, Lausanne, Switzerland, <sup>2</sup>Radiology, CHUV, <sup>3</sup>Nephrology, CHUV

876

16:15

### Comparison of in-vivo Lung Morphometry Models from 3D Multiple b-value <sup>3</sup>He Diffusion-Weighted MRI



Ho-Fung Chan<sup>1</sup>, Juan Parra-Robles<sup>1,2</sup>, Guilhem J Collier<sup>1</sup>, and Jim M Wild<sup>1</sup>

<sup>1</sup>Academic Unit of Radiology, University of Sheffield, Sheffield, United Kingdom, <sup>2</sup>Department of Bioengineering, Universidad Carlos III de Madrid, Madrid, Spain

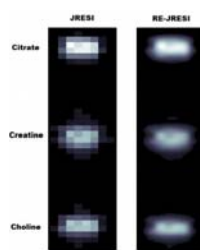
Power Pitch

Pitch: MRS/MRSI Applications

877



16:15



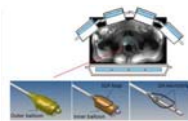
Resolution Enhanced accelerated Four Dimensional Echo Planar Spectroscopic Imaging: Application in Prostate Cancer

Zohaib Iqbal<sup>1</sup>, Brian L. Burns<sup>1</sup>, Rajakumar Nagarajan<sup>1</sup>, Robert E. Reiter<sup>2</sup>, Steven S. Raman<sup>1</sup>, and M. Albert Thomas<sup>1</sup>

<sup>1</sup>Radiological Sciences, University of California - Los Angeles, Los Angeles, CA, United States, <sup>2</sup>Urology, University of California - Los Angeles, Los Angeles, CA, United States

878

16:15



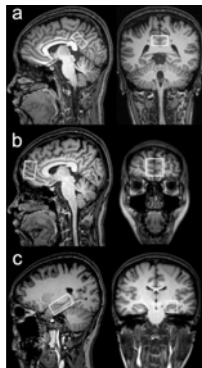
Initial results of combined 1H and 31P spectroscopic imaging of the prostate at 7 Tesla

Bart WJ Philips<sup>1</sup>, Mark van Uden<sup>1</sup>, and Tom WJ Scheenen<sup>1</sup>

<sup>1</sup>Radiology and Nuclear Medicine, Radboud University Medical Centre Nijmegen, Nijmegen, Netherlands

879

16:15



Reduced GABA levels correlate with cognitive impairment in relapsing-remitting multiple sclerosis

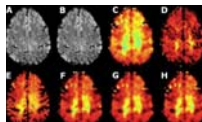
Guanmei Cao<sup>1</sup>, Bin Zhao<sup>1</sup>, Guangbin Wang<sup>1</sup>, Weibo Chen<sup>2</sup>, and Fei Gao<sup>1</sup>

<sup>1</sup>Shandong Medical Imaging Research Institute, Shandong University, Jinan, Shandong, People's Republic of China, <sup>2</sup>Philips Healthcare, Shanghai, China, People's Republic of China

880



16:15



Patch-based super-resolution of MRSI data in multiple sclerosis patients at 7 T

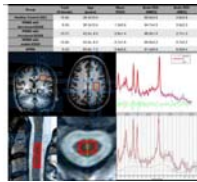
Saurabh Jain<sup>1</sup>, Gilbert Hangel<sup>2</sup>, Diana Sima<sup>1,3</sup>, Wolfgang Bogner<sup>2,4</sup>, Siegfried Trattnig<sup>2,4</sup>, Sabine Van Huffel<sup>3,5</sup>, Frederik Maes<sup>5,6</sup>, and Dirk Smeets<sup>1,7</sup>

<sup>1</sup>icometrix, R&D, Leuven, Belgium, <sup>2</sup>High Field MR Centre, Medical University of Vienna, Vienna, Austria, <sup>3</sup>Department of Electrical Engineering-ESAT, STADIUS Center for Dynamical Systems, Signal Processing and Data Analytics, KU Leuven, Leuven, Belgium, <sup>4</sup>Christian Doppler Laboratory for Clinical Molecular MR Imaging, Vienna, Austria, <sup>5</sup>Medical IT, iMinds, Leuven, Belgium, <sup>6</sup>Department of Electrical Engineering-ESAT, PSI Medical Image Computing, KU Leuven, Leuven, Belgium, <sup>7</sup>Biolmaging Lab, Universiteit Antwerpen, Antwerp, Belgium

881



16:15



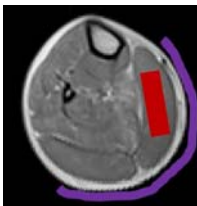
**Cervical spinal cord and brain MRS alterations in normal appearing white matter of multiple sclerosis (MS) patients at 3T**

Patrik Oliver Wyss<sup>1,2,3,4</sup>, Anke Henning<sup>1,2,5</sup>, Andreas Hock<sup>1,6</sup>, Andreas Lutterotti<sup>7</sup>, Roland Martin<sup>7</sup>, and Spyros Kollias<sup>4</sup>

<sup>1</sup>Institute for Biomedical Engineering, University and ETH Zurich, Zurich, Switzerland, <sup>2</sup>Max Planck Institute for Biological Cybernetics, Tuebingen, Germany, <sup>3</sup>Swiss Paraplegic Centre, Nottwil, Switzerland, <sup>4</sup>Institute of Neuroradiology, University Hospital Zurich, Zurich, Switzerland, <sup>5</sup>Institute of Physics, Ernst-Moritz-Arndt University Greifswald, Greifswald, Germany, <sup>6</sup>Department of Psychiatry, Psychotherapy and Psychosomatics Hospital of Psychiatry, University of Zurich, Zurich, Switzerland, <sup>7</sup>Neuroimmunology and Multiple Sclerosis Research, Department of Neurology, University Hospital and University Zurich, Zurich, Switzerland

882

16:15



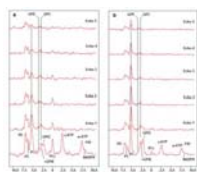
**<sup>1</sup>H-NMR of carnosine combined with <sup>31</sup>P-NMRS to better characterize skeletal muscle pH dysregulation in Duchenne muscular dystrophy**

Harmen Reyngoudt<sup>1,2</sup>, Suna Turk<sup>1,2</sup>, and Pierre G. Carlier<sup>1,2</sup>

<sup>1</sup>NMR Laboratory, Institute of Myology, Paris, France, <sup>2</sup>CEA, DRF, I<sup>2</sup>BM, MIRCen, Paris, France

883

16:15



**Apparent short transverse relaxation time of inorganic phosphate in breast cancer tissue at 7 tesla.**

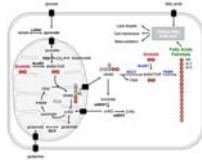
Wybe JM van der Kemp<sup>1</sup>, Tijn A van der Velden<sup>1</sup>, Alexander M Schmitz<sup>1</sup>, Kenneth G Gilhuijs<sup>1</sup>, Peter R Luijten<sup>1</sup>, Dennis WJ Klomp<sup>1</sup>, and Jannie P Wijnen<sup>1</sup>

<sup>1</sup>Department of Radiology, UMC Utrecht, Utrecht, Netherlands



884

16:15



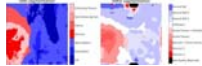
### Acetate metabolism towards fatty acids is down-regulated in IDH1 mutant glioma as shown by <sup>13</sup>C MRS

Chloé Najac<sup>1</sup>, Marina Radoul<sup>1</sup>, Pavithra Viswanath<sup>1</sup>, Myriam M Chaumeil<sup>1</sup>, and Sabrina M Ronen<sup>1</sup>

<sup>1</sup>Radiology and Biomedical Imaging, University of California San Francisco, San Francisco, CA, United States

885

16:15



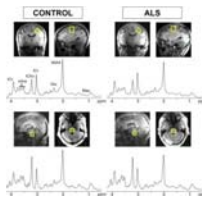
### Automatic tissue-type classification of <sup>1</sup>H-MRSI spectra in patients with glioblastoma

Nuno Pedrosa de Barros<sup>1</sup>, Raphael Meier<sup>2</sup>, Martin Pletscher<sup>1</sup>, Urspeter Knecht<sup>1</sup>, Mauricio Reyes<sup>2</sup>, Roland Wiest<sup>1</sup>, and Johannes Slotboom<sup>1</sup>

<sup>1</sup>SCAN / Neuroradiology, University Hospital Bern (Inselspital), Bern, Switzerland, <sup>2</sup>Institute for Surgical Technology & Biomechanics, University of Bern, Bern, Switzerland

886

16:15



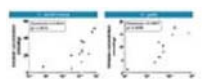
### High and Ultra-High Field Proton MR Spectroscopy in Early Amyotrophic Lateral Sclerosis

Ian Cheong<sup>1</sup>, Malgorzata Marjanska, Dinesh Deelchand, Lynn Eberly, David Walk, and Gulin Oz

<sup>1</sup>University of Minnesota Twin Cities, Minneapolis, MN, United States

887

16:15



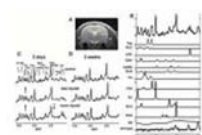
### Detection of in vivo biomarkers in fungal brain infection models and potential determination of cell viability.

Liesbeth Vanherp<sup>1</sup>, Amy Hillen<sup>1</sup>, Jennifer Poelmans<sup>1</sup>, Katrien Lagrou<sup>2</sup>, Greetje Vande Velde<sup>1</sup>, and Uwe Himmelreich<sup>1</sup>

<sup>1</sup>Imaging and Pathology, University of Leuven, Leuven, Belgium, <sup>2</sup>Laboratory of Clinical Bacteriology and Mycology, University of Leuven, Leuven, Belgium

888

16:15



### Metabolic variability in a brief status epilepticus model

Jullie W Pan<sup>1</sup>, Yijen Wu<sup>2</sup>, Patrice Pearce<sup>3</sup>, Nihal de Lanerolle<sup>4</sup>, and Kevin Kelly<sup>5</sup>

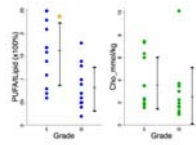
<sup>1</sup>MRRC, University of Pittsburgh, Pittsburgh, PA, United States, <sup>2</sup>Developmental Biology, Children's Hospital Pittsburgh, Pittsburgh, PA, <sup>3</sup>Neurology, University of Pittsburgh, Pittsburgh, PA, <sup>4</sup>Neurosurgery, Yale University, <sup>5</sup>Allegheny Singer Research Institute, Pittsburgh, PA



889



16:15



Polyunsaturated fatty acid (PUFA) is associated with tumour grading – An ex vivo study on whole breast tumours using multiple quantum coherence (MQC) MRS

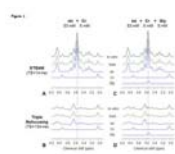
Sai Man Cheung<sup>1</sup>, Ehab Husain<sup>2,3</sup>, Yazan Masannat<sup>3,4</sup>, Klaus Wahle<sup>3,5</sup>, Steven D Heys<sup>3,4</sup>, and Jiabao He<sup>1</sup>

<sup>1</sup>Aberdeen Biomedical Imaging Centre, University of Aberdeen, Aberdeen, United Kingdom, <sup>2</sup>Pathology Department, Aberdeen Royal Infirmary, Aberdeen, United Kingdom, <sup>3</sup>School of Medicine, University of Aberdeen, Aberdeen, United Kingdom, <sup>4</sup>Breast Unit, Aberdeen Royal Infirmary, Aberdeen, United Kingdom, <sup>5</sup>Strathclyde Institute of Pharmacy and Biological Sciences, Glasgow, United Kingdom

890



16:15



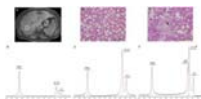
In-Vivo Regional detection of Gly in Human Brain: Implications in Glioma Patients at 3T

Vivek Tiwari<sup>1</sup>, Zhongxu An<sup>1</sup>, Sandeep Kumar Ganji<sup>1</sup>, and Changho Choi<sup>1</sup>

<sup>1</sup>Advanced Imaging Research Center, UT Southwestern Medical Center, Dallas, TX, United States

891

16:15



Differential diagnosis of Hepatic metabolites between non-alcoholic steatohepatitis and simple steatosis in humans and a murine model using a 1H MR spectroscopy study with long TE

Tae-Hoon Kim<sup>1</sup>, Hong Young Jun<sup>1</sup>, Chang-Won Jeong<sup>1</sup>, Jong-Hyun Ryu<sup>1</sup>, Kou Gyeom Kim<sup>1</sup>, and Kwon-Ha Yoon<sup>2</sup>

<sup>1</sup>Radiology, Imaging Science Research Center, Iksan, Korea, Republic of, <sup>2</sup>Radiology, Wonkwang University School of Medicine, Iksan, Korea, Republic of

## Oral

# Neuroimaging of High-Risk Pediatric Populations

Room 310

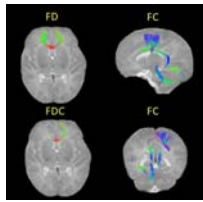
Wednesday 16:15 -  
18:15

Moderators: Chris Smyser & Duan Xu

892

16:15

Fixel-based morphometry detects alterations in specific fibres in association with preterm birth: a proof-of-concept study.



Manuel Blesa<sup>1</sup>, Ahmed Serag<sup>1</sup>, Devasuda Anblagan<sup>1,2</sup>, Emma J. Telford<sup>1</sup>, Sarah A. Sparrow<sup>1</sup>, Scott I. Semple<sup>3</sup>, Mark E. Bastin<sup>2</sup>, and James P. Boardman<sup>1,2</sup>

<sup>1</sup>MRC Centre for Reproductive Health, University of Edinburgh, Edinburgh, United Kingdom, <sup>2</sup>Centre for Clinical Brain Sciences, University of Edinburgh, Edinburgh, United Kingdom, <sup>3</sup>Clinical Research Imaging Centre, University of Edinburgh, Edinburgh, United Kingdom

Preterm birth is closely associated with diffuse white matter injury which contributes to long term neurocognitive impairment among survivors. Fixel-based analysis (FBA) is the study of specific fibre populations within a voxel; it provides measures of fibre bundle morphology by combining information about fibre density with structure. In this work, we applied FBA to neonatal dMRI data and provide proof-of-concept that fibre density and fibre bundle cross section may be useful measures for evaluating alterations to brain development associated with preterm birth.

893

16:27



Characterising white matter tracts of the limbic system and neurodevelopmental outcomes in children born very preterm

Claire E Kelly<sup>1</sup>, Peter J Anderson<sup>1,2</sup>, Jenny Pham<sup>1</sup>, Thanh Nguyen<sup>1</sup>, Malcolm Cooper<sup>1</sup>, Andrea L Murray<sup>1</sup>, Wai Yen Loh<sup>1,3,4</sup>, Joseph YM Yang<sup>5,6,7</sup>, Jeanie LY Cheong<sup>1,8,9</sup>, Lex W Doyle<sup>1,2,8,9</sup>, and Deanne K Thompson<sup>1,2,3</sup>

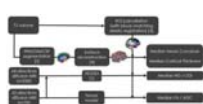
<sup>1</sup>Murdoch Childrens Research Institute, Melbourne, Australia, <sup>2</sup>Department of Paediatrics, The University of Melbourne, Melbourne, Australia, <sup>3</sup>Florey Institute of Neuroscience and Mental Health, Melbourne, Australia, <sup>4</sup>The Florey Department of Neuroscience and Mental Health, The University of Melbourne, Melbourne, Australia, <sup>5</sup>Department of Neurosurgery, The Royal Children's Hospital, Melbourne, Australia, <sup>6</sup>Neuroscience Research, Murdoch Childrens Research Institute, Melbourne, Australia, <sup>7</sup>Developmental Imaging, Murdoch Childrens Research Institute, Melbourne, Australia, <sup>8</sup>Neonatal services, Royal Women's Hospital, Melbourne, Australia, <sup>9</sup>Department of Obstetrics and Gynaecology, The University of Melbourne, Melbourne, Australia

Children born very preterm are at risk of having problems with memory, learning, behavioural and emotional functioning, which are key functions of the brain's limbic system. In 144 very preterm compared with 33 full-term 7-year-olds, altered microstructure, including axon density and orientation dispersion, and lower volume of limbic tracts were found, particularly for the fornix, cingulum and medial forebrain bundle. Associations were found between limbic tract microstructure and volume, particularly of the cingulum, uncinate fasciculus and anterior thalamic radiation, and memory, learning, behavioural and emotional functioning. This study improves knowledge of the contributing factors to poor neurodevelopmental outcomes in preterm children.

894



16:39



**Micro- and macro-structural development of the cortex in preterm infants**  
Dafnis Batalle<sup>1</sup>, Hui Zhang<sup>2</sup>, Jonathan O'Muircheartaigh<sup>1,3</sup>, Antonios Makropoulos<sup>4</sup>, Emer Hughes<sup>1</sup>, Madeleine Barnett<sup>1</sup>, Paul Aljabar<sup>1</sup>, Daniel C Alexander<sup>2</sup>, Joseph V Hajnal<sup>1</sup>, A David Edwards<sup>1</sup>, and Serena J Counsell<sup>1</sup>

*<sup>1</sup>Centre for the Developing Brain, Division of Imaging Sciences & Biomedical Engineering, King's College London, London, United Kingdom, <sup>2</sup>Centre for Medical Image Computing, Department of Computer Science, University College London, London, United Kingdom, <sup>3</sup>Department of Neuroimaging, Institute of Psychiatry, Psychology and Neuroscience, King's College London, London, United Kingdom, <sup>4</sup>Biomedical Image Analysis Group, Department of Computing, Imperial College London, London, United Kingdom*

We assessed micro and macrostructural cortical development in preterm infants using cortical curvature and thickness measures and neurite orientation and density imaging (NODDI). We studied two independent datasets of 64 and 42 neonates, and characterised the association between cortical features (median FA, MD, NDI, ODI, mean curvature and cortical thickness) and post-menstrual age (PMA) at MRI and gestational age at birth (degree of prematurity). We found a distinct pattern of development between the term (>37 weeks PMA) and preterm period (<37 weeks PMA), and different growth patterns between somatosensory and fronto-temporal areas.

16:51

**White matter diffusion properties at term equivalent age are associated with subsequent motor performance in infants born preterm**

### R CST



FA



MD



RD

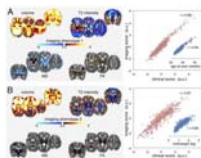


AD

Diliana Pecheva<sup>1</sup>, Hui Zhang<sup>2</sup>, Madeleine Barnett<sup>1</sup>, Andrew Chew<sup>1</sup>, Shona Falconer<sup>1</sup>, Mary Rutherford<sup>1</sup>, Nigel Kinnea<sup>3</sup>, Joseph V. Hajnal<sup>1</sup>, Daniel C. Alexander<sup>2</sup>, A. David Edwards<sup>1</sup>, and Serena J. Counsell<sup>1</sup>

<sup>1</sup>Centre for the Developing Brain, Division of Imaging Sciences & Biomedical Engineering, King's College London, London, United Kingdom, <sup>2</sup>Centre for Medical Image Computing, Department of Computer Science, University College London, London, United Kingdom, <sup>3</sup>Neonatal Unit, St Georges Hospital NHS Trust, London, United Kingdom

Preterm birth is associated with a high prevalence of neuro-motor impairment. We studied the relationship between motor function at two years and DTI measures in white matter (WM) fasciculi at term equivalent age using tract specific analysis in 109 preterm infants. Motor performance was significantly positively correlated with FA and negatively correlated with RD and MD in the corticospinal tract (CST) and corpus callosum (CC). DTI measures in other tracts were not related to motor function, suggesting a specific relationship between WM in the CST and CC and motor ability in this vulnerable group.



### Identifying cerebral endophenotypes with associated clinical risk factors in preterm neonates

Gareth Ball<sup>1,2</sup>, Paul Aljabar<sup>1</sup>, Shona Falconer<sup>1</sup>, Andrew T. M Chew<sup>1</sup>, Nicholas Harper<sup>1</sup>, Chiara Nosarti<sup>1</sup>, Mary A Rutherford<sup>1</sup>, Serena J Counsell<sup>1</sup>, and A. David Edwards<sup>1</sup>

<sup>1</sup>Centre for the Developing Brain, Division of Imaging Sciences and Bioengineering, King's College London, London, United Kingdom, <sup>2</sup>Developmental Imaging, Murdoch Children's Research Institute, Melbourne, Australia

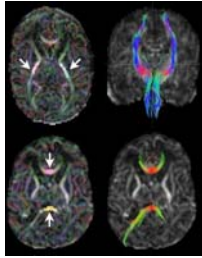
In this study, we combine multimodal neuroimaging and multivariate statistical analysis in a large cohort of preterm infants at term-equivalent age. We report a set of orthogonal imaging phenotypes associated with specific antenatal and postnatal factors that correlate with cognitive and motor outcomes at 2 years. We conclude that contemporaneous environmental factors including adverse intrauterine conditions and postnatal clinical management may prefigure the high incidence of neurocognitive impairment in preterm-born individuals via the cumulative expression of distinct diffuse injury patterns.

897

17:15

Thyroxine Treatment in Preterms with Grade III/IV Hemorrhage and Microstructural White Matter Assessment with Diffusion Tensor Imaging: A Pilot Study

Vincent Kyu Lee<sup>1,2</sup>, Ashok Panigrahy<sup>1,2</sup>, and Praveen Ballabh<sup>3,4</sup>



<sup>1</sup>Radiology, University of Pittsburgh, Pittsburgh, PA, United States,

<sup>2</sup>Radiology, Children's Hospital of Pittsburgh UPMC, Pittsburgh, PA, United States, <sup>3</sup>Pediatrics (Neonatology), Albert Einstein College of

Medicine, New York, NY, United States, <sup>4</sup>Neuroscience, Albert Einstein College of Medicine, New York, NY, United States

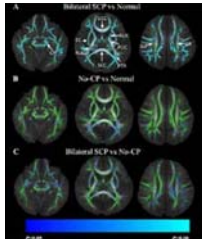
Intraventricular hemorrhage (IVH) in preterm infants is a complication that leads to neurodevelopmental delay and neurologic disorders. In this study we used diffusion tensor imaging (DTI) to analyze the myelination and structural integrity of white matter in preterms with and without T4 treatment using a manual uniform region of interest based analysis and semi-automated method of tractography. This small cohort pilot study of preterm subjects with Grade III-IV IVH demonstrated that thyroxine therapy may result in improved microstructural changes in certain tracts, and DTI maybe able to serve as neuroimaging biomarker for treatment efficacy in relation to thyroxine intervention.

898

17:27

DTI reveals crucial white matter lesions in bilateral spastic cerebral palsy in infants with non-cystic periventricular leukomalacia

Haoxiang Jiang<sup>1,2,3</sup>, Xianjun Li<sup>1,2</sup>, Chao Jin<sup>1</sup>, Miaomiao Wang<sup>1</sup>, Congcong Liu<sup>1</sup>, Kevin C. Chan<sup>4</sup>, and Jian Yang<sup>1,2</sup>

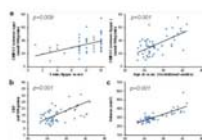


<sup>1</sup>Department of Diagnostic Radiology, The First Affiliated Hospital, Xi'an Jiaotong University, Xi'an, People's Republic of China, <sup>2</sup>Department of Biomedical Engineering, School of Life Science and Technology, Xi'an Jiaotong University, Xi'an, People's Republic of China, <sup>3</sup>Department of Diagnostic Radiology, Xi'an Children Hospital, Xi'an, People's Republic of China, <sup>4</sup>Departments of Ophthalmology and Bioengineering, University of Pittsburgh, PA, United States

Predicting cerebral palsy (CP) in infants with periventricular leukomalacia (PVL) is important for early treatment and rehabilitation. This study aimed to determine the crucial WM lesions in spastic CP (SCP) of non-cystic PVL infants using diffusion tensor imaging (DTI). Our results suggest that there was decreased FA in the corticospinal tract (CST) of bilateral SCP infants, but not in PVL infants without CP. Meanwhile, the posterior thalamic radiation, and the splenium of corpus callosum were damaged both in SCP and No-CP PVL infants. Therefore, Lower FA in the CST maybe a prerequisite and biomarker for identifying and predicting the outcome of SCP in infants with non-cystic PVL.

899

17:39



Brain metabolic rate, but not perfusion or brain volume, predicts clinical scores in newborns at risk for brain injury

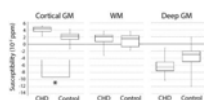
Peiyong Liu<sup>1</sup>, Ying Qi<sup>2</sup>, Zixuan Lin<sup>1</sup>, Kaining Shi<sup>3</sup>, Qiyong Guo<sup>2</sup>, Xiaoming Wang<sup>2</sup>, and Hanzhang Lu<sup>1</sup>

<sup>1</sup>Radiology, Johns Hopkins University School of Medicine, Baltimore, MD, United States, <sup>2</sup>Radiology, Shengjing hospital of China Medical University, Shenyang, People's Republic of China, <sup>3</sup>Imaging Systems Clinical Science, Philips Healthcare, Beijing, People's Republic of China

Hypoxic brain injury due to perinatal oxygen deprivation is one of the leading reasons of neonatal death and long-term disabilities. In this study, we evaluated the predictive values of cerebral blood flow (CBF), oxygen extraction fraction (OEF), cerebral oxygen metabolism (CMRO2), and brain volume as biomarkers in the assessment of hypoxic brain injuries in neonatal patients. Our results showed that among these biomarkers, only CMRO2 was significantly associated with Apgar score, which is the standard clinical score indicating the risks of prenatal and perinatal brain injuries. CBF and brain volume increase with age, but have no relationship with Apgar score.

900

17:51



Quantitative susceptibility mapping in the neonatal brain with congenital heart disease

Zungho Zun<sup>1,2,3</sup>, Kushal Kapse<sup>1</sup>, Gilbert Vezina<sup>1,3</sup>, Mary T Donofrio<sup>2,3,4</sup>, and Catherine Limperopoulos<sup>1,2,3</sup>



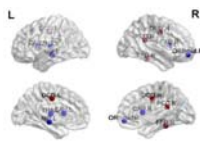
<sup>1</sup>Division of Diagnostic Imaging and Radiology, Children's National Medical Center, Washington, DC, United States, <sup>2</sup>Division of Fetal and Transitional Medicine, Children's National Medical Center, Washington, DC, United States, <sup>3</sup>Departments of Radiology and Pediatrics, George Washington University, Washington, DC, United States, <sup>4</sup>Division of Cardiology, Children's National Medical Center, Washington, DC, United States

Brain injury is a frequent complication in newborns with complex congenital heart disease (CHD) secondary to hemodynamic instability and increased risk for hypoxic-ischemic injury. In this study quantitative susceptibility mapping (QSM) was performed in newborns with complex CHD prior to open heart surgery and was compared to healthy control newborns. Mean susceptibility was significantly higher in the cortical gray matter of neonates with CHD versus controls suggesting reduced oxygenation in the cerebral vasculature in CHD preoperatively. QSM images also depicted less contrast in the CHD, which may be associated with delayed brain development. This is the first report to demonstrate the feasibility of neonatal QSM and susceptibility differences between CHD and controls.

---

901

18:03



Altered Functional Network Topology in Children with Complex Congenital Heart Disease is Associated with Reduced Regional Cerebral Perfusion and Cognitive Outcomes

Vincent Schmithorst<sup>1</sup>, Vince Lee<sup>1</sup>, Cecilia Lo<sup>2</sup>, and Ashok Panigrahy<sup>1</sup>

<sup>1</sup>Radiology, Children's Hospital of Pittsburgh of UPMC, Pittsburgh, PA, United States, <sup>2</sup>University of Pittsburgh

Pseudo-continuous ASL (pCASL) and resting-state BOLD data was obtained from a cohort of pre-adolescent patients with complex congenital heart disease (CHD) and healthy controls. CHD patients displayed altered functional network topology (network segregation) in posterior default mode, subcortical, and prefrontal regions, as well as decreased regional CBF in subcortical and anterior default mode regions. These alterations in functional topology and regional CBF were also associated with deficits in cognitive performance as measured by the NIH Toolbox (crystallized cognition). These results suggest regional alterations in neuronal-vascular coupling may underlie neurocognitive deficits in pre-adolescent CHD patients.

---

---



Oral

## Liver New Technique

Room 311

Wednesday 16:15 -  
18:15

Moderators: Shintaro Ichikawa & Riccardo  
Lattanzi

902



16:15



[Comprehensive T1-weighted dynamic liver MRI during free-breathing using fat/water separation, radial sampling, compressed sensing, parallel imaging, and motion-weighted reconstruction](#)

Thomas Benkert<sup>1,2</sup>, Li Feng<sup>1,2</sup>, Luke Gerges<sup>1,2</sup>, Krishna P Shanbhogue<sup>1,2</sup>, Chenchan Huang<sup>1,2</sup>, Daniel K Sodickson<sup>1,2</sup>, Hersh Chandarana<sup>1,2</sup>, and Kai Tobias Block<sup>1,2</sup>

<sup>1</sup>Center for Advanced Imaging Innovation and Research (CAI2R), Department of Radiology, New York University School of Medicine, New York, NY, United States, <sup>2</sup>Bernard and Irene Schwartz Center for Biomedical Imaging, Department of Radiology, New York University School of Medicine, New York, NY, United States

Conventional clinical liver MRI consists of several exams, including pre-contrast in-phase, opposed-phase, and fat-saturated scans as well as multiple scans with contrast-enhancement. For each of these acquisitions, accurate breath-holding is required to ensure diagnostic image quality.

Here, we demonstrate how this entire protocol can be replaced by using a single comprehensive exam, where only one dataset has to be acquired during free-breathing. All relevant images can be retrospectively generated with model-based fat/water separation, which incorporates compressed sensing and parallel imaging. This approach has the potential to improve clinical workflow and eliminate the risk for failed exams caused by imperfect breath-holding.

903

16:27

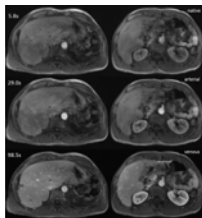


[Image quality assessment for free-breathing dynamic liver examination using a self-navigated Cartesian acquisition with iterative reconstruction](#)

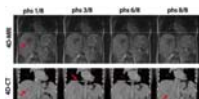
Benjamin Kaltenbach<sup>1</sup>, Dominik Nickel<sup>2</sup>, Ralph Strecker<sup>2</sup>, Andreas Bucher<sup>1</sup>, Thomas J. Vogl<sup>1</sup>, and Boris Bodelle<sup>1</sup>

<sup>1</sup>Goethe University Frankfurt, Frankfurt, Germany, <sup>2</sup>Siemens Healthcare GmbH, Erlangen, Germany

Free-breathing DCE-MRI of the liver is feasible using a Cartesian acquisition with self-navigation and hard-gated reconstruction in oncological patients. Compared to a standard BH-VIBE, image quality was rated marginally lower but with useful robustness regarding breathing artifacts. Therefore, the proposed sequence is a promising alternative in patients who cannot comply with breathing commands, like children or elderly patients.

904

16:39



Respiratory resolved, self-gated, 4-dimensional MRI using Rotating Cartesian K-Space (ROCK): technical validation and initial clinical experience on an MRI-guided radiation therapy system

Fei Han<sup>1</sup>, Ziwu Zhou<sup>1</sup>, Yu Gao<sup>1</sup>, Percy Lee<sup>2</sup>, Minsong Cao<sup>2</sup>, Daniel Low<sup>2</sup>, Ke Sheng<sup>2</sup>, Yingli Yang<sup>2</sup>, and Peng Hu<sup>1</sup>

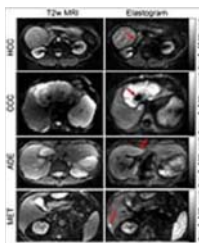
<sup>1</sup>Radiology, University of California, Los Angeles, CA, United States,

<sup>2</sup>Radiation Oncology, University of California, Los Angeles, CA, United States

Respiratory resolved 4D-MRI is used to quantify patient-specific respiratory motion to ensure optimal dose delivery in the radiation therapy of abdominal tumors. In this work, we developed a 4D-MRI technique using 3D k-space encoding, respiratory motion self-gating, and compressive sensing image reconstruction. The proposed 4D-MRI technique could provide high resolution, high quality, respiratory motion resolved 4D images with good soft-tissue contrast and are free of the “stitching” artifacts usually seen on 4D-CT, which is the current clinical standard. Results from motion phantom, healthy volunteers in a 1.5T diagnostic scanner and liver cancer patient in a 0.35T MRI-guided radiation therapy system demonstrated the feasibility of using the proposed 4D-MRI in radiation treatment planning.

905

16:51



High resolution multifrequency MR elastography of hepatic tumors for measurement of stiffness and mechanical heterogeneity

Mehrgan Shahryari<sup>1</sup>, Jing Guo<sup>1</sup>, Florian Dittmann<sup>1</sup>, Heiko Tzschätzsch<sup>1</sup>, Sebastian Hirsch<sup>1</sup>, Eric Barnhill<sup>1</sup>, Georg Böning<sup>1</sup>, Uli Fehrenbach<sup>1</sup>, Timm Denecke<sup>1</sup>, Jürgen Braun<sup>1</sup>, and Ingolf Sack<sup>1</sup>

<sup>1</sup>Charité - Universitätsmedizin Berlin, Berlin, Germany

High-resolution MRE of the liver based on multifrequency wave excitation and tomoelastography reconstruction is proposed for the mechanical characterization of hepatic tumors including stiffness and heterogeneity of the mechanical properties. We investigated 62 tumors in 43 patients and observed that high-grade tumors are stiffer than surrounding parenchyma, while low-grade hepatic adenoma had no altered stiffness. The intra-tumor heterogeneity of stiffness values was higher than in non-tumorous liver tissue. The proposed multifrequency MRE protocol could easily be integrated into the standard radiological workflow of our institution, thereby adding valuable information on tumor aggressiveness to standard clinical imaging markers.

906

17:03



Comparison of Spin-Echo Echoplanar Imaging and Gradient Recalled Echo Magnetic Resonance Elastography Pulse Sequences Among Patients with Hepatic Iron Overload at 3.0 T

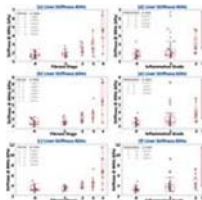
Ely R Felker<sup>1</sup>, Steven S Raman<sup>1</sup>, Bradley D Bolster<sup>2</sup>, Holden Wu<sup>1</sup>, Kyung Sung<sup>1</sup>, Stephan Kannengiesser<sup>2</sup>, Brenda J Brown<sup>1</sup>, and David S Lu<sup>1</sup>

<sup>1</sup>Radiology, UCLA, Los Angeles, CA, United States, <sup>2</sup>Siemens Healthcare

Most technical failures of GRE-based MR elastography are related to iron overload, especially at 3.0 T. SE-EPI-based MR elastography may be a useful alternative. 3.0 T GRE and SE-EPI MR elastography sequences were compared in 20 patients with iron overload (mean R2\* 114 sec<sup>-1</sup>) in terms of quantitative liver stiffness (LS) and image quality score (IQS), based on wave propagation and confidence mask coverage, as determined by two experienced radiologists. LS measurements were not significantly different between the two sequences. SE-EPI showed a trend toward higher confidence mask coverage and significantly higher IQS for both readers compared to GRE.

907

17:15



A New MR Elastography Parameter for Diagnosing Hepatic Fibrosis and Inflammation: Shear Attenuation

Meng Yin<sup>1</sup>, Jun Chen<sup>1</sup>, Kevin J. Glaser<sup>1</sup>, Jayant A. Talwalkar<sup>2</sup>, and Richard L. Ehman<sup>1</sup>

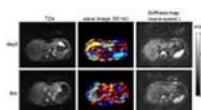
<sup>1</sup>Radiology, Mayo Clinic, Rochester, MN, United States,

<sup>2</sup>Gastroenterology and Hepatology, Mayo Clinic, Rochester, MN, United States

Liver attenuation was investigated in comparison to the well-established liver stiffness for detecting hepatic fibrosis in 108 patients with histology-proven chronic liver diseases. Both liver stiffness and attenuation successfully detected varying fibrosis and inflammation with equivalent accuracy. At 40 and 60Hz, both have excellent accuracy for distinguishing clinical significant fibrosis or inflammation from others; moderate accuracy were obtained in distinguishing mild abnormalities from patients without abnormalities. Steatosis extent had no significant effect on liver stiffness and attenuation measurements. Our findings indicate that shear attenuation has equivalent diagnostic performance to that of liver stiffness for detecting liver disease progression.

908

17:27



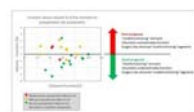
Treatment response of hepatic and renal stiffness in patients with chronic HCV infection monitored by multifrequency MR elastography  
Jing Guo<sup>1</sup>, Stephan Marticorena Garcia <sup>1</sup>, Florian Dittmann<sup>1</sup>, Thomas Fischer<sup>1</sup>, Jürgen Braun<sup>2</sup>, and Ingolf Sack<sup>1</sup>

<sup>1</sup>Department of Radiology, Charité - Universitätsmedizin Berlin, Berlin, Germany, <sup>2</sup>Department of Medical Informatics, Charité - Universitätsmedizin Berlin, Berlin, Germany

Multifrequency abdominal MRE was applied to monitor stiffness of the liver and kidney in renal transplant recipients with chronic HCV infection after antiviral therapy. Within a 6-months period after medication, hepatic stiffness was significantly reduced while renal stiffness in kidney transplants was not altered. Wave speed obtained by high-resolution multifrequency MRE can serve as a quantitative imaging maker to assess the treatment response and monitor abdominal organ stiffness longitudinally.

909

17:39



Dynamic Gadoxetate Enhanced MRI measurement of segmental liver function – A novel imaging biomarker for predicting Post-Hepatectomy Liver Failure

David Alexander Longbotham<sup>1</sup>, Daniel Wilson<sup>2</sup>, Ashley Guthrie<sup>3</sup>, Ernest Hidalgo<sup>1</sup>, Raj Prasad<sup>1</sup>, and Steven Sourbron<sup>4</sup>

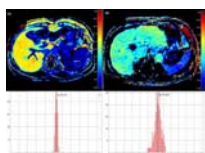
<sup>1</sup>Department of HPB and Transplantation Surgery, St James's University Hospital, Leeds, United Kingdom, <sup>2</sup>Department of Medical Physics, St James's University Hospital, Leeds, United Kingdom, <sup>3</sup>Department of Radiology, St James's University Hospital, Leeds, United Kingdom, <sup>4</sup>Division of Biomedical Imaging, University of Leeds, Leeds, United Kingdom

Current risk assessment for post-hepatectomy liver failure (PHLF) is based on the volume of the future liver remnant (FLR). This is inaccurate when liver function is inhomogeneously distributed. We investigated whether the function of the FLR measured with DCE-MRI improves outcome predictions in 28 patients who had curative resection for colorectal liver metastases. We found the difference in preoperative estimates of FLR function and volume predicted PHLF with a **sensitivity of 83% and specificity of 91%**, indicating that: (1) inhomogeneous distribution of function is a major risk factor for PHLF; (2) DCE-MRI can improve patient outcome by correcting for the bias caused by volumetry.

---

910

17:51



Liver function estimation using hepatocyte fraction map at gadoxetic acid enhanced liver MRI in patients with chronic liver disease

Jeong Hee Yoon<sup>1</sup>, Eunju Kim<sup>2</sup>, Tomoyuki Okuaki<sup>3</sup>, and Jeong Min Lee<sup>1</sup>

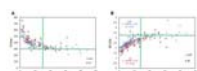
<sup>1</sup>Seoul National University Hospital, Seoul, Korea, Republic of, <sup>2</sup>Philips Healthcare Korea, <sup>3</sup>Philips Healthcare Japan

Hepatocyte fraction derived from gadoxetic acid enhanced liver MRI may provide quantitative surrogate marker of liver function for ICG R15 in patients with chronic liver disease.

---

911

18:03



Does T1 Mapping Provide Additional Information in the Context of Hepatic Iron Overload?

Aaryani Tipirneni-Sajja<sup>1</sup>, Eric M. Kercher<sup>1</sup>, Ralf B. Loeffler<sup>1</sup>, Ruitian Song<sup>1</sup>, Matthew D. Robson<sup>2</sup>, M. Beth McCarville<sup>1</sup>, Jane S. Hankins<sup>3</sup>, and Claudia M. Hillenbrand<sup>1</sup>

<sup>1</sup>Diagnostic Imaging, St. Jude Children's Research Hospital, Memphis, TN, United States, <sup>2</sup>Radcliffe Department of Medicine, University of Oxford, Oxford, United Kingdom, <sup>3</sup>Hematology, St. Jude Children's Research Hospital, Memphis, TN, United States

Hepatic iron content (HIC) is linearly correlated with R2\*. Currently, there is little data on in vivo human liver iron assessment via longitudinal relaxation T1 (or R1) although an animal study previously suggested linear association, too. This study investigates hepatic T1 quantification in a breathhold by using ShMOLLI. T1 and T2\* liver mapping were performed in 124 iron loaded patients. We found linear association between R1 and R2\*/HIC values for mild-moderate HIC at 1.5T and 3T. No association between T1 and T2\* was found for high HIC, which is most likely due to technical limits of ShMOLLI for short T2\*.

---

Oral

## Spinal Cord Injury & Myelopathy

Room 312

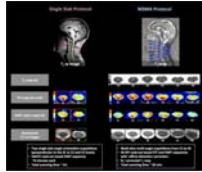
Wednesday 16:15 -  
18:15

Moderators: Gary Miller & Jason Talbott

---

912

16:15



Regional and structural integrity of the whole cervical spinal cord using 3D-T1 MP2RAGE and multi-slice multi angle DTI and ihMT sequences at 3T: preliminary investigations on age-related changes.

Henitsoa RASOANANDRIANINA<sup>1,2,3</sup>, Guillaume DUHAMEL<sup>1,2</sup>, Thorsten FEIWEIER<sup>4</sup>, Manuel TASO<sup>1,2,3</sup>, Aurélien MASSIRE<sup>1,2,3</sup>, Olivier GIRARD<sup>1,2</sup>, Maxime GUYE<sup>1,2</sup>, Jean-Philippe RANJEVA<sup>1,2</sup>, and Virginie CALLOT<sup>1,2,3</sup>

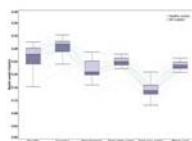
<sup>1</sup>Aix Marseille Univ, CNRS, CRMBM, Marseille, France, <sup>2</sup>AP-HM, Pôle d'Imagerie Médicale, Hopital de La Timone, CEMEREM, Marseille, France, <sup>3</sup>iLab-Spine International Associated Laboratory, Marseille, France, <sup>4</sup>Siemens Healthcare GmbH, Erlangen, Germany

In this study, we present a 3T multi-parametric MR protocol allowing structural and diffuse evaluation of the whole cervical spinal cord (SC), within a clinically acceptable scan-time. The MRI protocol includes high-resolution anatomical T2\*-weighted images allowing WM/GM atrophy evaluation, a MP2RAGE sequence allowing T1-mapping, a Multi-Slice Multi-Angle (MSMA) DTI sequence allowing evaluation of tissue structural organization and, last but not least, a MSMA inhomogeneous Magnetization transfer (ihMT) sequence allowing myelin-content evaluation in whole cervical SC. This protocol was combined with a template-based automated post-processing pipeline in a preliminary study investigating age- and region-related microstructural differences in specific regions along the cervical SC.

---

913

16:27



Quantitative measurement of myelin in distinct pathways of the spinal cord: Implications for assessing neuropathic pain after spinal cord injury  
Hanwen Liu<sup>1,2</sup>, Emil Ljungberg<sup>3</sup>, Erin MacMillan<sup>3</sup>, Laura Barlow<sup>4</sup>, Shannon Kolind<sup>3</sup>, John Kramer<sup>2,5</sup>, and Cornelia Laule<sup>2,6,7</sup>

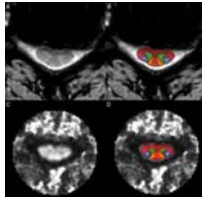
<sup>1</sup>Physics, University of British Columbia, Vancouver, BC, Canada, <sup>2</sup>International Collaboration on Repair Discoveries, Vancouver, BC, Canada, <sup>3</sup>Medicine, University of British Columbia, Vancouver, BC, Canada, <sup>4</sup>UBC Hospital, University of British Columbia, Vancouver, BC, Canada, <sup>5</sup>Kinesiology, University of British Columbia, Vancouver, BC, Canada, <sup>6</sup>Radiology, University of British Columbia, Vancouver, BC, Canada, <sup>7</sup>Pathology and Laboratory Medicine, University of British Columbia, BC, Canada

Neuropathic pain is common in people with spinal cord injury (SCI). To better understand the type and severity of damage in the spinal cord associated with neuropathic pain, we used myelin water imaging (MWI) combined with spinal cord toolbox to study myelin content in specific pathways of spinal cord for both healthy and SCI subjects. Results show that MWI can distinguish different pathways of spinal cord and reduced myelin content in some specific pathways is found in SCI subjects. Our findings suggest that MWI with pathway-based analysis is capable of examining the correlation between damage pattern and neuropathic pain.

---

914

16:39



#### Multi-Parametric Spinal Cord MRI Detects Subclinical Tissue Injury in Asymptomatic Cervical Spinal Cord Compression

Allan R. Martin<sup>1</sup>, Benjamin De Leener<sup>2</sup>, Julien Cohen-Adad<sup>2</sup>, David W. Cadotte<sup>3</sup>, Jefferson R. Wilson<sup>1</sup>, Lindsay Tetreault<sup>1,4</sup>, Aria Nouri<sup>1</sup>, Adrian Crawley<sup>5</sup>, David J. Mikulis<sup>5</sup>, Howard Ginsberg<sup>1</sup>, and Michael G. Fehlings<sup>1</sup>

<sup>1</sup>Neurosurgery, University of Toronto, Toronto, ON, Canada, <sup>2</sup>Electrical Engineering, École Polytechnique de Montréal, Montréal, QC, Canada, <sup>3</sup>Neurosurgery, University of Calgary, Calgary, AB, Canada, <sup>4</sup>Medicine, University College Cork, Cork, Ireland, <sup>5</sup>Medical Imaging, University of Toronto, Toronto, ON, Canada

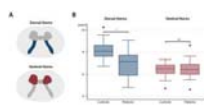


Degenerative cervical myelopathy (DCM) involves extrinsic spinal cord (SC) compression causing tissue injury and neurological dysfunction. Asymptomatic SC compression is much more common (8-26%), but it is unknown if tissue injury occurs in this group. Our multi-parametric MRI protocol previously identified 10 measures of tissue injury in DCM. Using these techniques, we demonstrate that asymptomatic SC compression subjects show a similar pattern of tissue injury, with 8/10 measures ( $p=0.05$ ) showing the same direction of changes and  $MTR_{\text{Rostral}}$  ( $p=0.002$ ),  $MTR_{\text{MCL}}$  ( $p=0.03$ ), and  $T_2^*w \text{ WM/GM}_{\text{Rostral}}$  ( $p=0.04$ ) showing significant univariate differences. A logistic regression model retaining 3 MRI measures shows 86% discrimination between compressed and uncompressed subjects.

915



16:51



Ventral and dorsal horn grey matter neurodegeneration remote from stenosis in cervical spondylotic myelopathy

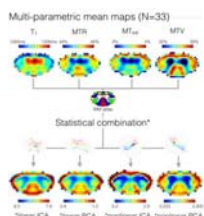
Patrick Grabher<sup>1</sup>, Siawoosh Mohammadi<sup>2</sup>, Gergely David<sup>1</sup>, and Patrick Freund<sup>1,3,4,5</sup>

<sup>1</sup>Spinal Cord Injury Center, University of Zurich, Zurich, Switzerland, <sup>2</sup>Department of Systems Neuroscience, University Medical Center Hamburg-Eppendorf, Hamburg, Germany, <sup>3</sup>Department of Neurophysics, Max Planck Institute for Human Cognitive and Brain Sciences, Leipzig, Germany, <sup>4</sup>Wellcome Trust Centre for Neuroimaging, UCL Institute of Neurology, London, United Kingdom, <sup>5</sup>Department of Brain Repair and rehabilitation, UCL Institute of Neurology, London, United Kingdom

Cervical spondylotic myelopathy (CSM) is the most frequent spinal cord disorder. Next to focal degeneration at the compression site, the rostral cervical white and grey matter undergo atrophic changes, the magnitude relating to clinical impairment. In this study, we assess above stenosis regional grey matter changes and demonstrate that next to bilateral dorsal horn atrophy, the normal appearing ventral horns show diffusivity changes which relate to white matter integrity loss.

916

17:03



Statistical combinations of T1, MTR, MTsat and Macromolecular Tissue Volume to improve myelin content estimation in the human spinal cord at 3T

Simon Lévy<sup>1</sup>, Ali Khatibi<sup>2,3,4,5</sup>, Gabriel Mangeat<sup>1</sup>, Jen-I Chen<sup>2,6</sup>, Kristina Martinu<sup>2</sup>, Pierre Rainville<sup>2,6</sup>, Nikola Stikov<sup>1,7</sup>, and Julien Cohen-Adad<sup>1,8</sup>

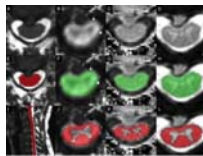
<sup>1</sup>NeuroPoly Lab, Institute of Biomedical Engineering, Polytechnique Montreal, Montreal, QC, Canada, <sup>2</sup>Centre de Recherche de l'Institut Universitaire de Gériatrie de Montréal (CRIUGM), Montreal, QC, Canada, <sup>3</sup>Psychology Department, Bilkent University, Ankara-06800, Turkey, <sup>4</sup>Interdisciplinary program in Neuroscience, Bilkent University, Ankara-06800, Turkey, <sup>5</sup>National Magnetic Resonance Research Center (UMRAM), Bilkent University, Ankara-06800, Turkey, <sup>6</sup>Department of Stomatology, Faculty of Dentistry, Université de Montréal, Montreal, QC, Canada, <sup>7</sup>Montreal Heart Institute, Montreal, QC, Canada, <sup>8</sup>Functional Neuroimaging Unit, Centre de Recherche de l'Institut Universitaire de Gériatrie de Montréal (CRIUGM), Montreal, QC, Canada

Several quantitative MRI metrics have been proposed to quantify myelin in the central nervous system but each of them includes confounding factors that impair their sensitivity and specificity. Because these factors are different across metrics, data driven approaches developed for blind source separation problems to extract the common component between recordings of the same sources seem appropriate. This study compares linear and nonlinear methods to combine myelin-sensitive metrics: T1, MTR, MTsat, MTV (1 – PD). The repeatability of the resulting combined metrics as well as their sensitivity to different microstructural features are tested. A higher sensitivity is achieved with linear combinations.

---

917

17:15



[Multi-Parametric Cervical Spinal Cord MRI Provides An Accurate Diagnostic Tool for Detecting Clinical Myelopathy](#)

Allan R. Martin<sup>1</sup>, Benjamin De Leener<sup>2</sup>, Julien Cohen-Adad<sup>2</sup>, David W. Cadotte<sup>3</sup>, Jefferson R. Wilson<sup>1</sup>, Lindsay Tetreault<sup>1,4</sup>, Stefan F. Lange<sup>1</sup>, Aria Nouri<sup>1</sup>, Adrian Crawley<sup>5</sup>, David J. Mikulis<sup>5</sup>, Howard Ginsberg<sup>1</sup>, and Michael G. Fehlings<sup>1</sup>

<sup>1</sup>Neurosurgery, University of Toronto, Toronto, ON, Canada, <sup>2</sup>Electrical Engineering, École Polytechnique de Montréal, Montréal, QC, Canada, <sup>3</sup>Neurosurgery, University of Calgary, Calgary, AB, Canada, <sup>4</sup>Medicine, University College Cork, Cork, Ireland, <sup>5</sup>Medical Imaging, University of Toronto, Toronto, ON, Canada

ddd

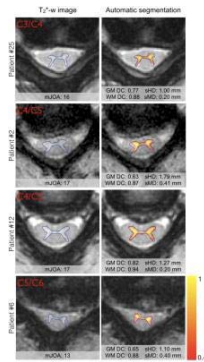
---

918

17:27

[Fully automatic segmentation of spinal cord gray matter on patients with degenerative cervical myelopathy](#)

Sara M. Dupont<sup>1</sup>, Allan R. Martin<sup>2,3</sup>, Nikola Stikov<sup>1,4</sup>, Michael G. Fehlings<sup>2,3</sup>, and Julien Cohen-Adad<sup>1,5</sup>

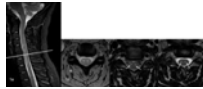


<sup>1</sup>NeuroPoly Lab, Institute of Biomedical Engineering, Polytechnique Montreal, Montreal, QC, Canada, <sup>2</sup>Division of Neurosurgery, Department of Surgery, University of Toronto, Toronto, ON, Canada, <sup>3</sup>Toronto Western Hospital, University Health Network, Toronto, ON, Canada, <sup>4</sup>Montreal Heart Institute, Montreal, QC, Canada, <sup>5</sup>Functional Neuroimaging Unit, CRIUGM, Université de Montréal, Montreal, QC, Canada

Degenerative cervical myelopathy (DCM) occurs when arthritic changes cause extrinsic spinal cord (SC) compression, inducing motor and sensory disabilities due to gray matter (GM) and white matter (WM) injury. GM segmentation of MR images can quantify atrophy of both GM and WM and may offer biomarkers to improve diagnosis, monitoring of disease progression, and prognosis. In this study, the GM of 33 DCM patients and 8 healthy subjects was automatically segmented using the method included in the Spinal Cord Toolbox (SCT). GM segmentation results were in good accordance with the underlying anatomy, demonstrating the feasibility of automatic GM segmentation in DCM patients exhibiting severe SC compression.

919

17:39



The use of 3D FSE in place of 2D T2-FSE, 2D T2\*-GRE in the diagnosis of cervical spinal non-neoplastic lesion

tianyong xu<sup>1</sup>, guang han<sup>2</sup>, songguo liu<sup>2</sup>, mingzhi pan<sup>3</sup>, yang li<sup>4</sup>, zhenyu zhou<sup>5</sup>, and bing wu<sup>5</sup>

<sup>1</sup>MR application, GE healthcare china, shanghai, People's Republic of China, <sup>2</sup>radiology, Chinese medicine hospital of Linyi, shandong, People's Republic of China, <sup>3</sup>radiology, the second affiliated hospital of Shandong university of traditional Chinese medicine, shandong, People's Republic of China, <sup>4</sup>radiology, the second hospital of Shandong university, shandong, People's Republic of China, <sup>5</sup>MR modality, GE healthcare china, beijing, People's Republic of China

Magnetic resonance imaging has been accepted as the predominant imaging tool for diagnosis of spinal disease, such as protrusion of intervertebral disc, tumor, inflammation, trauma [1]. T2 weighted imaging is commonly used for diagnosis in many medical centers, however 2D fast spin echo (FSE) image quality is often limited by several practical factors including low fat content, high susceptibility effect and vulnerability to motion and pulsation. T2\* weighted imaging is another popular choice [2]. Improved contrast may be obtained between gray matter and white matter of medulla. The drawback of T2\* imaging is the hyperintense gray matter signal may cause the small cervical spinal cord lesion to be overlooked. In this work, the use of 3D FSE is assessed and compared to 2D T2 and T2\* imaging, and hypothesized to overcome their shortcomings.

---

920

17:51

### Anthropomorphic Spinal Cord Phantom with Induced Field Inhomogeneity



Alan C Seifert<sup>1,2,3</sup>, Vaishali Patel<sup>1</sup>, Merin Grace<sup>1</sup>, Robin Li<sup>1</sup>, Mohammad Molla<sup>4</sup>, Joseph Borrello<sup>1,2,3</sup>, and Junqian Xu<sup>1,2,3,5</sup>

<sup>1</sup>Translational and Molecular Imaging Institute, Icahn School of Medicine at Mount Sinai, New York, NY, United States, <sup>2</sup>Department of Radiology, Icahn School of Medicine at Mount Sinai, New York, NY, United States, <sup>3</sup>Graduate School of Biomedical Sciences, Icahn School of Medicine at Mount Sinai, New York, NY, United States, <sup>4</sup>Department of Mechanical Engineering, The City College of New York, New York, NY, United States, <sup>5</sup>Department of Neuroscience, Icahn School of Medicine at Mount Sinai, New York, NY, United States

The human spinal cord exists in a particularly unfavorable magnetic field environment. Technical development of diffusion and functional MRI methods would be facilitated by a phantom to model spatially and temporally periodic field inhomogeneities. We have designed a phantom capable of simulating these specific field disturbances. The spinal canal was machined from acrylic, and the cord was cast of polyvinyl alcohol. The phantom was imaged using anatomical CT and MRI, and functional and diffusion EPI protocols. The phantom has relaxation and diffusion properties similar to the human cord, and air-filled vials create spatially periodic frequency shifts of -100 Hz.

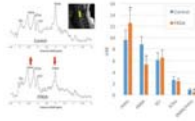
---

921

18:03

### Longitudinal MRS, MRI and DTI of the spinal cord in Friedreich's Ataxia

Pierre-Gilles Henry<sup>1</sup>, James M Joers<sup>1</sup>, Dinesh K Deelchand<sup>1</sup>, Diane Hutter<sup>1</sup>, Khalaf O Bushara<sup>1</sup>, Gülin Öz<sup>1</sup>, and Christophe Lenglet<sup>1</sup>



<sup>1</sup>Center for Magnetic Resonance Research, University of Minnesota, Minneapolis, MN, United States

We report the first longitudinal MRS, structural MRI, and diffusion MRI data in the cervical spinal cord of subjects with Friedreich's ataxia. We were able to detect significant changes in spinal cord area (-18%), tNAA/mlns ratio (-17%), fractional anisotropy (-11%) and mean diffusivity (+26%) in a group of 10 patients over 24 months. Our data suggest that MR of the spinal cord could be useful to assess the impact of potential treatments on neurodegeneration in upcoming clinical trials in FRDA.

Oral

## Structure & Function Imaging of the Heart

Room 313A      Wednesday 16:15 - 18:15      Moderators: Martijn Froeling & David Sosnovik

922

16:15



Quantification of Increased Myocardial Stiffness in Patients with Hypertrophic Cardiomyopathy Using 3D High Frequency Cardiac Magnetic Resonance Elastography

Shivaram Poigai Arunachalam<sup>1</sup>, Arvin Arani<sup>1</sup>, Ian Chang<sup>2</sup>, Yi Sui<sup>1</sup>, Phillip Rossman<sup>1</sup>, Kevin Glaser<sup>1</sup>, Joshua Trzasko<sup>1</sup>, Kiaran McGee<sup>1</sup>, Armando Manduca<sup>3</sup>, Richard Ehman<sup>1</sup>, Richard Ehman<sup>1</sup>, and Philip Arazo<sup>1</sup>

<sup>1</sup>Radiology, Mayo Clinic, ROCHESTER, MN, United States,

<sup>2</sup>Cardiovascular Diseases, Mayo Clinic, ROCHESTER, MN, United States,

<sup>3</sup>Biomedical Engineering and Physiology, Mayo Clinic, ROCHESTER, MN, United States

Abnormal thickening of myocardium in patients with hypertrophic cardiomyopathy impairs the pump function, and in particular affects diastolic filling with a known increase in myocardial stiffness. The purpose of this work was to determine if 3D high frequency cardiac MR elastography (MRE) can quantitatively differentiate increased myocardial stiffness in HCM patients compared to healthy volunteers. 36 patients with clinical diagnosis for hypertrophic cardiomyopathy (HCM) and 47 healthy volunteers were studied. The myocardial stiffness of HCM patients (mean: 12.01 kPa) was found to be significantly stiffer ( $p < 0.01$ ) than healthy controls (mean: 7.79 kPa).

Study	Year	Sample Size	Population	Primary Outcome	Secondary Outcome
1	2015	50	Healthy	Normal	Normal
2	2016	100	Healthy	Normal	Normal
3	2017	150	Healthy	Normal	Normal
4	2018	200	Healthy	Normal	Normal
5	2019	250	Healthy	Normal	Normal
6	2020	300	Healthy	Normal	Normal
7	2021	350	Healthy	Normal	Normal
8	2022	400	Healthy	Normal	Normal
9	2023	450	Healthy	Normal	Normal
10	2024	500	Healthy	Normal	Normal

## CMR Demonstrates Structure-Function Relationship in Patients after Heart Transplantation

Ryan Dolan<sup>1</sup>, Amir Rahsepar<sup>1</sup>, Julie Blaisdell<sup>1</sup>, Kai Lin<sup>1</sup>, Kenichiro Suwa<sup>1</sup>, Allen Anderson<sup>2</sup>, Kambiz Ghafourian<sup>2</sup>, Esther Vorovich<sup>2</sup>, Jonathan Rich<sup>2</sup>, Jane Wilcox<sup>2</sup>, Clyde Yancy<sup>2</sup>, Jeremy Collins<sup>1</sup>, James Carr<sup>1</sup>, and Michael Markl<sup>1</sup>

<sup>1</sup>Radiology, Northwestern University, Chicago, IL, United States,

<sup>2</sup>Cardiology, Northwestern University, Chicago, IL, United States

Cardiac MRI demonstrates differences between heart transplant recipients and controls using tissue phase mapping (TPM), T2, and T1. Significant correlations between myocardial velocities and dyssynchrony obtained from TPM (myocardial function) and T2 and T1 (myocardial tissue structure) suggest a relationship between impaired structure and function among transplant recipients.

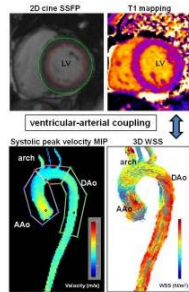


Fig. 1. Ventricular-arterial coupling in BAV. Top: Assessment of LV function, mass & aortic/aortic valve fraction (ECV) by 2D cine SSFP combined with pre- and post-contrast T1-mapping. Bottom: 4D flow MRI and 3D segmentation of the aorta for calculation of regional peak velocities along its maximum intensity projection (MIP) and 3D wall shear stress (WSS). AAO=ascending aorta, C=descending aorta.

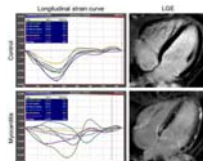
## 4D Flow MRI, Cardiac Function, and Myocardial T1-Mapping: Ventricular-arterial coupling in Patients with Bicuspid Aortic Valve (BAV)

Julia Geiger<sup>1</sup>, Amir Rahsepar<sup>1</sup>, Kenichiro Suwa<sup>1</sup>, Alex Powell<sup>1</sup>, Alex J Barker<sup>1</sup>, Jeremy D Collins<sup>1</sup>, James Carr<sup>1</sup>, and Michael Markl<sup>1,2</sup>

<sup>1</sup>Radiology, Northwestern University, Chicago, IL, United States,

<sup>2</sup>Biomedical Engineering, Northwestern University, Chicago, IL, United States

BAV is the most prevalent congenital cardiovascular malformation. Its association with progressive ascending aortic dilatation and concomitant aortic valve stenosis or regurgitation with increasing age has a critical impact on patients' morbidity. We applied a comprehensive CMR protocol in 50 BAV patients consisting of cine-imaging, T1-mapping and 4D flow MRI to simultaneously assess cardiac parameters and aortic hemodynamics. We observed significant relationships between LV mass and WSS as well as peak velocities in the AAO and arch, likewise in the sub-cohort with normal valve function, leading us to the hypothesis that there is proof for ventricular-aortic coupling in BAV patients.



## Feature tracking myocardial strain analysis in acute myocarditis:

Diagnostic value and association with myocardial inflammation and edema

Julian A. Luetkens<sup>1</sup>, Ulrike Schlesinger-Irsch<sup>1</sup>, Daniel L. Kütting<sup>1</sup>, Darius Dabir<sup>1</sup>, Rami Homsy<sup>1</sup>, Jonas Doerner<sup>1</sup>, Frederic C. Schmeel<sup>1</sup>, Alois M. Sprinkart<sup>1</sup>, Claas P. Naehle<sup>1</sup>, Hans H. Schild<sup>1</sup>, and Daniel K. Thomas<sup>1</sup>

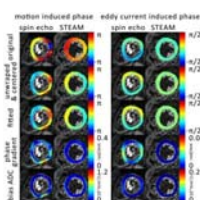


<sup>1</sup>Radiology, University of Bonn, Bonn, Germany

Cardiac magnetic resonance (CMR) can detect inflammatory myocardial alterations in patients with acute myocarditis. The addition of myocardial strain analysis might further broaden the diagnostic targets of CMR. We investigated myocarditis patients using multiparametric CMR including a feature-tracking analysis of myocardial strain parameters. We could demonstrate that myocardial strain measurements can reliably discriminate between diseased and healthy patients. Furthermore, strain measurements are associated with the extent of myocardial edema/inflammation. These findings indicate that CMR feature-tracking strain analysis adds important diagnostic information, and might serve as a new tool for the assessment of myocardial dysfunction in patients with acute myocarditis.

926

17:03



Impact of eddy-currents and cardiac motion in DTI of the in-vivo heart - a comparison of second-order motion compensated SE versus STEAM

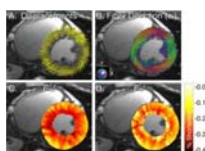
Christian Torben Stoeck<sup>1</sup>, Constantin von Deuster<sup>1</sup>, Robbert van Gorkum<sup>1</sup>, and Sebastian Kozerke<sup>1</sup>

<sup>1</sup>Institute for Biomedical Engineering / University and ETH Zurich, Zurich, Switzerland

Motion-compensated (M2) spin-echo (SE) and stimulated-echo acquisition mode (STEAM) sequences have been proposed to generate diffusion contrast in in-vivo cardiac imaging. When comparing measured fractional anisotropy and mean diffusivity of cardiac tissue, marked differences have been reported between SE and STEAM. Cardiac motion, perfusion, different mixing times and eddy-currents have been discussed as potential source of discrepancies. In this study it is shown that signal dephasing due to eddy-currents play a minor role. While SE is more prone to motion-induced dephasing compared to STEAM, reported differences in mean diffusivity can only marginally be explained by motion-induced signal loss in SE.

927

17:15



In Vivo Assessment of Cardiomyocyte Performance Using Combined Cardiac DENSE and cDTI

Patrick Magrath<sup>1,2</sup>, Luigi E. Perotti<sup>1,2</sup>, Eric Aliotta<sup>2,3</sup>, Ilya A. Verzhbinsky<sup>2</sup>, Kévin Moulin<sup>2</sup>, and Daniel B. Ennis<sup>1,2,3</sup>





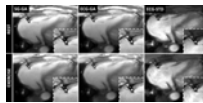
<sup>1</sup>Department of Bioengineering, University of California, Los Angeles, CA, United States, <sup>2</sup>Department of Radiological Sciences, University of California, Los Angeles, CA, United States, <sup>3</sup>Biomedical Physics IDP, University of California, Los Angeles, CA, United States

Circumferential strain ( $E_{cc}$ ) derived from cardiac DENSE 3D displacement maps is a promising biomarker for diagnosing early stages of cardiac disease.  $E_{cc}$  is commonly evaluated only in the mid-wall where it is expected to align with the local myofiber direction. Our aim was to combine cDTI and DENSE displacement data to directly characterize strain along the fiber direction ( $E_{ff}$ ) throughout the heart. Across all healthy subjects (N=9),  $E_{ff}$  had a smaller peak systolic transmural gradient than  $E_{cc}$  ( $-0.035 \pm 0.041$  vs.  $-0.097 \pm 0.030$  (unitless),  $p < 0.001$ ).  $E_{ff}$  is a more spatially uniform measure of regional LV function in healthy volunteers and provides a microstructurally anchored measure of cardiomyocyte performance.

---

928

17:27



### Self-Gated Golden Angle Spiral CINE MRI for Endothelial Function Assessment

Gabriele Bonanno<sup>1,2</sup>, Allison G Hays<sup>1</sup>, Robert G Weiss<sup>1,2</sup>, and Michael Schär<sup>2</sup>

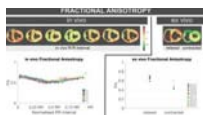
<sup>1</sup>Division of Cardiology, Department of Medicine, Johns Hopkins University School of Medicine, Baltimore, MD, United States, <sup>2</sup>Division of MR Research, Russel H. Morgan Department of Radiology and Radiological Science, Johns Hopkins University School of Medicine, Baltimore, MD, United States

A novel self-gated 2D spiral CINE MRI method is proposed to assess coronary endothelial function (CEF) and was tested in healthy volunteers. Cardiac self-gating data were extracted from the k-space center and showed high correlation with simultaneously-recorded ECG. High coronary image quality and CEF measures, in good agreement with a standard ECG-triggered method, can now be obtained without the need for ECG.

---

929

17:39



### Characterisation of in-vivo and ex-vivo cardiac Diffusion Tensor Imaging scalar measures of cardiac microstructure in healthy swine

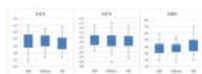
Sonia Nielles-Vallespin<sup>1,2</sup>, Pedro F Ferreira<sup>2</sup>, Andrew D Scott<sup>2</sup>, Ranil de Silva<sup>2</sup>, Philip Kilner<sup>2</sup>, Daniel B Ennis<sup>3</sup>, Dudley J Pennell<sup>2</sup>, David N Firmin<sup>2</sup>, and Andrew E Arai<sup>1</sup>

<sup>1</sup>NHLBI, NIH, Bethesda, MD, United States, <sup>2</sup>Royal Brompton Hospital, Imperial College of London, London, United Kingdom, <sup>3</sup>Department of Radiological Sciences, University of California Los Angeles, Los Angeles, CA, United States

In-vivo cDTI was performed at several cardiac phases in healthy swine (N=16), followed by ex-vivo cDTI in two contractile states. The three eigenvalues (L1, L2, L3), MD, FA and Mode were compared. All trends between in-vivo diastole and systole matched those between ex-vivo relaxed and contracted states, except for MD, which decreased ~10% in-vivo from diastole to systole, with no significant differences ex-vivo between relaxed and contracted states. These results provide a useful baseline for future preclinical studies with cardiac disease models, and might contribute towards formulating a strain correction model that accounts for the microstructural constraints and deformations of the myocardium.

930

17:51



Strain analysis methods from CMR more sensitive than echocardiographic methods to small differences in cardiotoxicity remodeling between risk groups of cancer survivors.

Delphine Perie<sup>1</sup>, Hadi Begdouri<sup>1</sup>, Mohamed Aissiou<sup>1</sup>, Farida Cheriet<sup>1</sup>, Tarik Hafyane<sup>2</sup>, Matthias Friedrich<sup>3</sup>, Caroline Laverdière<sup>4</sup>, Maja Krajinovic<sup>5</sup>, Daniel Sinnott<sup>5</sup>, Gregor Andelfinger<sup>6</sup>, and Daniel Curnier<sup>7</sup>

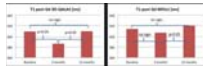
<sup>1</sup>Mechanical Engineering, Polytechnique Montreal, Montreal, QC, Canada, <sup>2</sup>Research Center, Montreal Heart Institute, Montreal, QC, Canada, <sup>3</sup>Health Center, McGill University, Montreal, QC, Canada, <sup>4</sup>Pediatric Oncology, CHU Sainte-Justine, Montreal, QC, Canada, <sup>5</sup>Research Center, CHU Sainte-Justine, Montreal, QC, Canada, <sup>6</sup>Pediatric Cardiology, CHU Sainte-Justine, Montreal, QC, Canada, <sup>7</sup>Kinesiology, Université de Montréal, Montreal, QC, Canada

The use of cardiac strain mapping may provide useful knowledge that may help in detecting doxorubicin-induced cardiotoxicity at a functional scale. Although the feasibility of CMR has been established, there are no standard acquisition protocols or processing pipelines to assess cardiac strain maps. Compared to echocardiography, strain analysis methods from CMR are more sensitive to small differences in cardiotoxicity between risk groups in cancer survivors. While strain mapping from echocardiography remains adequate to detect large differences between healthy volunteers and patients with diseases, our study highlighted the necessity to combine different strain mapping methods to fully describe small cardiac damages

---

931

18:03



Longitudinal study of myocardial T1 and T2 relaxation times in aortic stenosis patients: before, and 3- and 12 months after aortic valve replacement

Sofia Kvernby<sup>1,2</sup>, Mattias Rönnerfalk<sup>1</sup>, Marcel Warntjes<sup>2</sup>, Carl-Johan Carlhäll<sup>1,2</sup>, Eva Tamás<sup>1</sup>, Jan Engvall<sup>1,2</sup>, and Tino Ebbers<sup>1,2</sup>

<sup>1</sup>Institution for Medicine and Health, Linköping University, Linköping, Sweden, <sup>2</sup>Center for Medical Image Science and Visualization, Linköping, Sweden

The purpose of this pilot study is to investigate whether myocardial relaxation times (T1 and T2), alter over time in patients with severe aortic valve stenosis, from pre-surgery to 12 months after aortic valve replacement. Myocardial relaxation times were measured pre surgery, and 3 months and 12 months post surgery with 3D-QALAS, T1-MOLLI and T2-GraSE. The results demonstrated significant changes in myocardial relaxation times over time after surgery in this patient group.

---

## Oral

# Fingerprinting & Parameter Quantification

Room 313BC

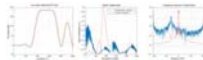
Wednesday 16:15 -  
18:15

Moderators: Dan Ma & Martin Uecker

---

932

16:15



Dictionary-free MR Fingerprinting with low-pass balanced-GRE sequences.

Alessandro Sbrizzi<sup>1</sup>, Tom Bruijnen<sup>1</sup>, Peter R. Luijten<sup>1</sup>, and Cornelis A.T. van den Berg<sup>1</sup>

<sup>1</sup>UMC Utrecht, Utrecht, Netherlands

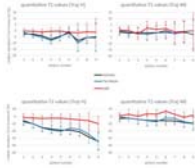
We reconsider balanced gradient-echo (GRE) sequence for MR fingerprinting and design an excitation scheme which is very robust to off-resonance. The corresponding data can be accurately reconstructed by standard least-squares fitting methods, a novelty for MRF. Construction of the pre-computed dictionary and exhaustive search are thus no longer needed.

---

933

16:27

Improved spiral trajectory correction using the gradient impulse response function (GIRF) with application to MR Fingerprinting



Martin Berzl<sup>1,2</sup>, Antoine Pfeil<sup>1</sup>, Craig Meyer<sup>3</sup>, Adrienne Campbell-Washburn<sup>4</sup>, Gregor Kördörfer<sup>1</sup>, Mathias Nittka<sup>1</sup>, Andreas Maier<sup>2</sup>, and Josef Pfeuffer<sup>1</sup>

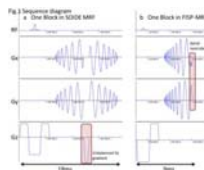
<sup>1</sup>Application Development, Siemens Healthcare, Erlangen, Germany, <sup>2</sup>Pattern Recognition Lab, Friedrich-Alexander University Erlangen-Nürnberg (FAU), Erlangen, Germany, <sup>3</sup>Biomedical Engineering, University of Virginia, Charlottesville, VA, United States, <sup>4</sup>Biochemistry and Biophysics Center, Division of Intramural Research, National Heart Lung and Blood Institute, National Institutes of Health, Bethesda, MD, United States

The purpose of this study is to evaluate different spiral trajectory prediction models - isotropic, Tan-Meyer and GIRF - to mitigate image artifacts for spiral MRI and improve accuracy of quantitative T1/T2 values for MR Fingerprinting. GIRF scan parameters were optimized to allow a total measurement time of only six minutes for a one-time calibration. GIRF similarly provided excellent results for vastly different trajectory types, varying in max. slew rate, gradient amplitude and number of interleaves, and showed some advantages against Tan-Meyer for trajectory designs with high k-space center slew rate, both for qualitative and quantitative results.

934



16:39



### Spiral-out and -in Double Echoes (SOIDE) Magnetic Resonance Fingerprinting with Improved T2 Mapping

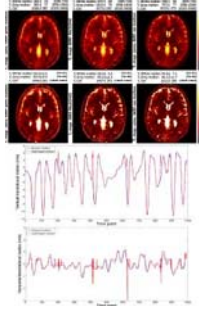
Huihui Ye<sup>1</sup>, Congyu Liao<sup>1</sup>, Qing Li<sup>1</sup>, Xiaozhi Cao<sup>1</sup>, Bo Zhao<sup>2</sup>, Berkin Bilgic<sup>2</sup>, Kawin Setsompop<sup>2</sup>, Hongjian He<sup>1</sup>, Huafeng Liu<sup>1</sup>, and Jianhui Zhong<sup>1</sup>

<sup>1</sup>Zhejiang University, Hangzhou, People's Republic of China, <sup>2</sup>Massachusetts General Hospital

Magnetic resonance fingerprinting (MRF) provides fast and simultaneous mapping of parameters including T1 and T2. However, T2 mapping in MRF has been less robust and accurate than T1 in its current form. In this work, we propose a new sequence with spiral-out and -in double echoes (SOIDE) for MRF in each TR block which provide double echo signal with better T2 contrast. The proposed SOIDE-MRF shows improved performance over FISP-MRF, as demonstrated in Monte Carlo simulation on a numerical brain phantom (at  $T_{acq}=6s/slice$ , NRMSE of T2 reduced to 9.41% in SOIDE-MRF, and FISP-MRF ~11% at  $T_{acq}=12s/slice$ ) and in vivo brain (less biased and more stable T2).

935

16:51



### Motion corrected Magnetic Resonance Fingerprinting using Soft-weighted key-Hole (MRF-McSOHO)

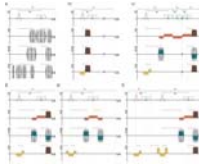
Gastao Cruz<sup>1</sup>, René Botnar<sup>1</sup>, and Claudia Prieto<sup>1</sup>

<sup>1</sup>Division of Imaging Sciences and Biomedical Engineering, King's College London, London, United Kingdom

Magnetic Resonance Fingerprinting (MRF) estimates multi-parametric maps from a large amount of highly undersampled time-point images. MRF has been shown to be robust to the presence of abrupt motion occurring towards the end of the acquisition. In this work we further study the effects of different types of motion on MRF, showing high sensitivity to periodic motion and motion occurring at the beginning of the MRF scan. A method for 2D translational motion correction in MRF is proposed and validated in vivo, showing significant improvements when compared with no motion correction.

936

17:03



### On optimizations of MRF patterns based on generalized MRI sequence schemes

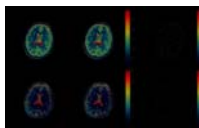
Mathies Breithaupt<sup>1,2</sup>, Sebastian Flassbeck<sup>1</sup>, and Mark E. Ladd<sup>1</sup>

<sup>1</sup>Medical Physics in Radiology, German Cancer Research Center (DKFZ), Heidelberg, Germany, <sup>2</sup>Institute for Forensic Medicine and Traffic Medicine, University Hospital Heidelberg, Heidelberg, Germany

Within this study, we introduce an MRF pattern generation by the incorporation of a generalized MRI sequence scheme. Optimizations of these patterns lead to a higher matching accuracy and a potential for higher efficiency.

937

17:15



### Calculation of Large MRF Dictionaries with Low Memory Overhead Using Randomized SVD

Mingrui Yang<sup>1</sup>, Dan Ma<sup>1</sup>, Yun Jiang<sup>2</sup>, Jesse Hamilton<sup>2</sup>, Nicole Seiberlich<sup>2</sup>, Mark Griswold<sup>1</sup>, and Debra McGivney<sup>1</sup>

<sup>1</sup>Department of Radiology, Case Western Reserve University, Cleveland, OH, United States, <sup>2</sup>Department of Biomedical Engineering, Case Western Reserve University, Cleveland, OH, United States

Direct calculation of MRF dictionaries can be prohibitive when high resolution or multi-component chemical exchange effects are taken into account. To address this problem, we propose a new approach based on the randomized SVD (rSVD) to generate a low rank approximation of the large sized dictionary without the need of pre-calculating, storing, or loading the dictionary. This in return saves significant amounts of memory, and speeds up the template matching process of MRF. In addition, when combined with polynomial fitting, one can generate MRF maps with arbitrary high resolution dictionaries.

---

938

17:27



### Off-Resonance Correction for MR Fingerprinting Using Multiple Frequency Interpolation

Jason Ostenson<sup>1,2</sup>, Ryan K. Robison<sup>3</sup>, Nicholas R. Zwart<sup>3</sup>, and E. Brian Welch<sup>1,4,5</sup>

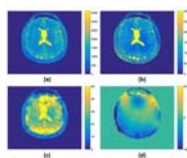
*<sup>1</sup>Vanderbilt University Institute of Imaging Science, Vanderbilt University, Nashville, TN, United States, <sup>2</sup>Program in Chemical and Physical Biology, Vanderbilt University, Nashville, TN, United States, <sup>3</sup>Neuroimaging Research, Barrow Neurological Institute, Phoenix, AZ, United States, <sup>4</sup>Department of Radiology and Radiological Sciences, Vanderbilt University, <sup>5</sup>Department of Biomedical Engineering, Vanderbilt University*

While T1 and T2 parameter mapping using fast imaging with steady-state precession (FISP) magnetic resonance fingerprinting (MRF) has shown consistency with classic relaxometry techniques under static field (B<sub>0</sub>) inhomogeneity, the use of spiral k-space trajectories blurs parameter map boundaries in regions of high B<sub>0</sub> variability. This work shows deblurring in phantom and *in vivo* relaxation maps generated using a published MRF sequence in conjunction with multi-frequency interpolation (MFI) acquired using undersampled and fully sampled spirals on a 3 Tesla human MR scanner.

---

939

17:39



### Multiparametric T2\* MR Fingerprinting

Cory Robert Wyatt<sup>1,2</sup>, Travis Smith<sup>3</sup>, Manoj K Sammi<sup>2</sup>, William Rooney<sup>2</sup>, and Alexander Guimaraes<sup>1</sup>

*<sup>1</sup>Radiology, Oregon Health and Science University, Portland, OR, United States, <sup>2</sup>Advanced Imaging Research Center, Oregon Health and Science University, Portland, OR, United States, <sup>3</sup>Casey Eye Institute, Oregon Health and Science University, Portland, OR, United States*

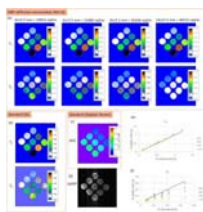
Previous magnetic resonance fingerprinting studies have focused on T1 and T2 relaxation times, relying solely on flip angle and repetition time changes, leaving the TE as short as possible for optimal SNR and phase. In this study, T1 and T2 MR fingerprinting is extended to include T2\* relaxation by varying echo times across acquisitions. The resulting T1, T2, T2\*, and B0 maps are then compared to maps obtained with conventional sequences, showing good spatial and quantitative agreement. A novel phase dictionary is used to before the full T1/T2/T2\* dictionary to produce B0 maps with fine resolution and reduce computational time.

---

940

17:51

Effect of diffusion weighting due to spoiler gradients in MR Fingerprinting  
Yasuhiko Terada<sup>1</sup> and Yuta Kobayashi<sup>1</sup>



<sup>1</sup>University of Tsukuba, Tsukuba, Japan

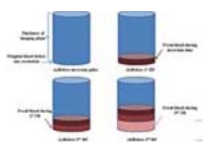
MR fingerprinting based on a fast imaging with steady-state precession (MRF-FISP) is immune to banding artifacts due to the inhomogeneous field, and thus has been widely used for rapid quantification of tissue parameters. However, the MRF-FISP could still be affected by banding artifacts for high-field-strengths, insufficient shimming, and wide field-of-view scanners. In such cases, use of much stronger spoiler gradients could alleviate the banding artifacts, but it would increase the diffusion weighting of the spoiler gradients and lead to the underestimation of T2 values. In this study, we examined the effect of the diffusion weighting and showed the correction methods.

---

941

18:03

A model-based velocity mapping of blood flow using MR fingerprinting  
Xiaozhi Cao<sup>1</sup>, Congyu Liao<sup>1</sup>, Zhixing Wang<sup>1</sup>, Qing Li<sup>1</sup>, Huihui Ye<sup>1</sup>, Ying Chen<sup>1</sup>, Hongjian He<sup>1</sup>, and Jianhui Zhong<sup>1</sup>



<sup>1</sup>Center for Brain Imaging Science and Technology, Department of Biomedical Engineering, Zhejiang University, Hangzhou, People's Republic of China

A hemodynamic mode was embedded into the extended phase graph algorithm for introducing the recognition ability of flow velocity into MR fingerprinting. The results of phantom and in-vivo experiments demonstrate that the proposed method can quantify the flow velocity, T<sub>1</sub>, T<sub>2</sub> and proton density simultaneously.

---



Oral

## Breast Imaging

Room 314

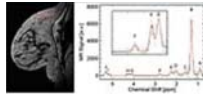
Wednesday 16:15 -  
18:15

Moderators: Christiane Kuhl & Elizabeth Morris

---

942

16:15



Saturated fatty acid fraction in breast adipose tissue is higher in patients with cancer than in those with benign lesions

Sungheon Gene Kim<sup>1</sup>, Neeti Bagadiya<sup>1</sup>, Pippa Storey<sup>1</sup>, Melanie Moccaldi<sup>1</sup>, and Linda Moy<sup>1</sup>

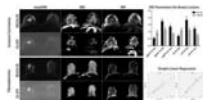
<sup>1</sup>Center for Advanced Imaging Innovation and Research, Radiology, New York University School of Medicine, New York, NY, United States

Gradient-echo Spectroscopic Imaging (GSI) was used to conduct voxel-wise analysis of fatty acid composition in breast adipose tissue in postmenopausal women. Parametric maps of fatty acid fractions show significantly higher saturated fatty acids in women with malignant tumors than in those with benign lesions. This result is consistent with a previous study based on manually selected regions of interest, and suggests that, for post-menopausal women, higher saturated fatty acids may be related to breast cancer development. Non-invasive evaluation of lipid composition using GSI may aid in breast cancer risk assessment and provide insight into physiological mechanisms that facilitate cancer development.

---

943

16:27



Diffusion Kurtosis Imaging with Readout-Segmented SE-EPI for Breast Lesions: Comparison with Single-shot SE-EPI at 3T

TAO AI<sup>1</sup>, Ya-guang Li<sup>1</sup>, and Li-ming Xia<sup>1</sup>

<sup>1</sup>Radiology, Tongji Hospital, Tongji Medical College, HUST, Wuhan, People's Republic of China

As an effective and sensitive diagnostic modality for tumor imaging, routine DWI and DKI based SS-EPI are limited by image distortion and poor spatial resolution at 3T, which can be significantly improved by RESOLVE technique.

---

944

16:39

Correlation between Breast Cancer Molecular Subtypes and Parameters of Dynamic Contrast Enhanced (DCE) MRI and Intravoxel Incoherent Motion (IVIM): Implication for Breast Cancer Anti-angiogenesis Treatment Guidance



WanChen Tsai<sup>1</sup>, KaiMing Chang<sup>2</sup>, and KuoJang Kao<sup>2</sup>

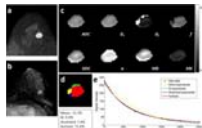
<sup>1</sup>Radiology, Koo Foundation Sun Yat-Sen Cancer Center, Taipei, Taiwan, <sup>2</sup>Research, Koo Foundation Sun Yat-Sen Cancer Center, Taipei, Taiwan

This prospective study correlates DCE MRI and IVIM with breast cancer molecular subtypes by examine the differences in vascular normalization signature genes. We found molecular subtype III and VI with higher pericyte gene scores to have significantly lower perfusion related parameters, higher extracellular extra-vascular space on DCE MRI and IVIM. These associations may be used to guide anti-angiogenesis treatment for breast cancer.

---

945

16:51



Multi-parametric Diffusion-weighted Imaging Models: Useful Tools for Diagnosis and Prognosis in Breast Cancer?

Shiteng Suo<sup>1</sup>, Fang Cheng<sup>1</sup>, Jia Hua<sup>1</sup>, Qing Lu<sup>1</sup>, Lyu Li<sup>2</sup>, and Jianrong Xu<sup>1</sup>

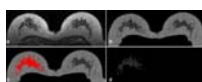
<sup>1</sup>Department of Radiology, Ren Ji Hospital, School of Medicine, Shanghai Jiao Tong University, Shanghai, People's Republic of China, <sup>2</sup>MR Clinical Science, Philips Healthcare, Greater China, Shanghai, People's Republic of China

Multi-parametric diffusion-weighted imaging (DWI) has shown potential in characterizing breast cancer. In this study, we for the first time evaluated the four common diffusion models in various breast lesions. Results showed that (1) optimal DWI signal attenuation behaviors differ between benign and malignant breast lesions (kurtosis model suited for benign and stretched-exponential model suited for malignant); (2) for predicting the malignancy of breast lesions, or the invasive nature of breast cancer, mono-exponential ADC is still the most preferred parameter; and (3) parameters based on non-mono-exponential DWI models may be more related with prognostic factors in invasive breast cancer.

---

946

17:03



Complementary value of contralateral parenchymal enhancement on DCE-MRI to conventional prognostic models and molecular assays of breast cancer

Bas H.M. van der Velden<sup>1</sup>, Tycho Bismeyer<sup>2</sup>, Claudette E. Loo<sup>3</sup>, Lodewyk F.A. Wessels<sup>2</sup>, Max A. Viergever<sup>1</sup>, and Kenneth G.A. Gilhuijs<sup>1</sup>

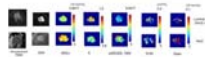
<sup>1</sup>Image Sciences Institute, University Medical Center Utrecht, Utrecht, Netherlands, <sup>2</sup>Division of Molecular Carcinogenesis, the Netherlands Cancer Institute–Antoni van Leeuwenhoek Hospital, Amsterdam, Netherlands, <sup>3</sup>Department of Radiology, the Netherlands Cancer Institute –Antoni van Leeuwenhoek Hospital, Amsterdam, Netherlands

The purpose of this study was to assess whether MR contrast-enhancement in healthy stromal tissue of the breast is able to further stratify survival of patients considered to be at high risk according to prognostic models derived from the tumor. In 415 patients with pathology proven unilateral invasive ER+HER2- breast cancer, the contralateral parenchymal enhancement was automatically extracted. Contralateral parenchymal enhancement appears to complement existing prognostic models derived from the tumor. In patients at high risk according to conventional prognostic models or molecular assays, contralateral parenchymal enhancement was able identify a subgroup with a relative good survival.

---

947

17:15



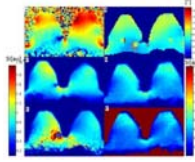
Quantitative non-Gaussian diffusion and IVIM MRI: Correlation between synthetic parameters and breast cancer biomarkers

Mami Ima<sup>1,2</sup>, Masako Kataoka<sup>1</sup>, Shotaro Kanao<sup>1</sup>, Natsuko Onishi<sup>1</sup>, Makiko Kawai<sup>1</sup>, Akane Ohashi<sup>1</sup>, Rena Sakaguchi<sup>1</sup>, Ayami Ohno Kishimoto<sup>1</sup>, Masakazu Toi<sup>3</sup>, and Kaori Togashi<sup>1</sup>

<sup>1</sup>Department of Diagnostic Imaging and Nuclear Medicine, Graduate School of Medicine, Kyoto University, Kyoto, Japan, <sup>2</sup>Hakubi Center for Advanced Research, Kyoto University, Kyoto, Japan, <sup>3</sup>Department of Breast Surgery, Graduate School of Medicine, Kyoto University, Kyoto, Japan

The association of IVIM/non-Gaussian diffusion MRI parameters with biological feature or subtypes in breast cancer was evaluated. For 144 malignant lesions, IVIM (fIVIM, D\*) and non-Gaussian diffusion (ADCo, K) parameters were estimated from DWI series with 16 b values (0-2500sec/mm<sup>2</sup>), as well as syntheticADC (sADC) (b=200, 1500sec/mm<sup>2</sup>) and ADC (b=0, 800sec/mm<sup>2</sup>). sADC and K values were significantly different between ER, PgR, and Her2 status (p<0.05, 0.01, 0.05 for sADC and p<0.05, 0.05, 0.05 for K). There was a significant difference of ADC values between PgR and Her2 status (p<0.05, 0.01). No significant difference of IVIM was found. ADCo, sADC, and ADC showed the statistical significance in differentiating subtypes of breast cancer (p<0.05, <0.01, <0.01).

---

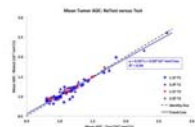


### B1 Mapping for Breast Sodium MRI at 7T- A Comparison between Double Angle and Phase-sensitive Method

Olgica Zanic<sup>1,2</sup>, Lenka Minarikova<sup>1</sup>, Sefan Zbyn<sup>1,3</sup>, Armin Nagel<sup>4,5</sup>, Lena Gast<sup>4</sup>, and Siegfried Trattnig<sup>1</sup>

<sup>1</sup>Department of Biomedical Imaging and Image-guided Therapy, Medical University of Vienna, Vienna, Austria, <sup>2</sup>Christian Doppler Laboratory for Clinical Molecular MRI, Christian Doppler Forschungsgesellschaft, Vienna, Austria, <sup>3</sup>Research Unit of Medical Imaging, Physics and Technology, University of Oulu, Oulu, Finland, <sup>4</sup>Institute of Radiology, University Hospital Erlangen, Erlangen, Germany, <sup>5</sup>Division of Medical Physics in Radiology, German Cancer Research Centre (DKFZ), Heidelberg, Germany

Absolute values of sodium content in tumors is one of the most important biomarkers for cancer diagnostics and therapy monitoring. An accurate quantitative values are influenced by B1 inhomogeneity that must be evaluated and corrected. In this work, we compared two mapping methods DAM and PS. On the basis of our results, we found that DAM gives overestimated flip angle values (approximately 30% higher than PS). Also, after correction is applied, DAM shows higher signal drop in comparison with PS. Accompanied with longer measurement time necessary for DAM, this findings give advantages to PS in clinical studies and routine implementation.



### Reproducibility of ADC measures by Breast DWI: Results of the ACRIN 6698 Trial

David C Newitt<sup>1</sup>, Zheng Zhang<sup>2</sup>, Jessica Gibbs<sup>1</sup>, Savannah C Partridge<sup>3</sup>, Thomas L Chenevert<sup>4</sup>, Patrick J Bolan<sup>5</sup>, Mark Rosen<sup>6</sup>, Helga Marques<sup>2</sup>, and Nola Hylton<sup>1</sup>

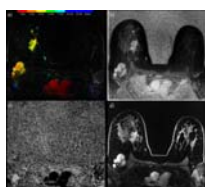
<sup>1</sup>Radiology and Biomedical Imaging, University of California, San Francisco, CA, United States, <sup>2</sup>Biostatistics, Brown University, Providence, RI, United States, <sup>3</sup>Radiology, University of Washington, Seattle, WA, United States, <sup>4</sup>Radiology, University of Michigan Health System, Ann Arbor, MI, United States, <sup>5</sup>Radiology, University of Minnesota, Minneapolis, MN, United States, <sup>6</sup>University of Pennsylvania, Philadelphia, PA, United States

The multi-institutional ACRIN 6698 trial investigates quantitative diffusion weighted imaging (DWI) for assessment of breast cancer response to treatment. A secondary aim is to perform a test/retest study to evaluate reproducibility of ADC measures. In a subset of 91 subjects, DWI was acquired twice in the same exam, before and after patient repositioning. Tumor ADC was measured separately for each acquisition. 80% of cases were found analyzable by a standardized quality-control procedure. Reproducibility of ADC was excellent, with intraclass correlation coefficient of 0.97 (95%CI 0.95, 0.98) and agreement index of 0.83 (95%CI 0.76,0.87). Results were similar for subgroups by field strength or study visit.

---

950

17:51



Earlier detection of breast cancer by abbreviated MRI screening using color intensity projections (CIP) applied to high spatiotemporal resolution imaging

Keith S Cover<sup>1</sup>, Katya M Duvivier<sup>2</sup>, Pim de Graaf<sup>2</sup>, Ben J Slotman<sup>3</sup>, Joost PA Kuijer<sup>1</sup>, Mark BM Hofman<sup>1</sup>, and Rudolf M Verdaasdonk<sup>1</sup>

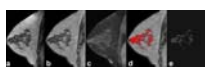
*<sup>1</sup>Physics and Medical Technology, VU University Medical Center, Amsterdam, Netherlands, <sup>2</sup>Radiology, VU University Medical Center, Amsterdam, Netherlands, <sup>3</sup>Radiotherapy, VU University Medical Center, Amsterdam, Netherlands*

Dynamic contrast enhancement (DCE) MRI is more sensitive than X-ray based mammography for detecting breast cancer especially for the 10% of women with extremely dense breasts. However, full diagnostic protocol (FDP) MR exams are too expensive for screening. Recent abbreviated MR protocols - which require only one quarter of the acquisition time - use high spatial temporal resolution (HSTR) sequences that generate thousands of images. We found color intensity projections (CIP) reduces radiologist reading time for detection of malignant tumours by visualizing their amount and time of enhancement (TOE) especially in combination with the value of the maximum slope (VMS).

---

951

18:03



Validation of contralateral parenchymal enhancement on DCE-MRI as a biomarker of survival in patients with ER-positive/HER2-negative breast cancer

Bas H.M. van der Velden<sup>1</sup>, Elizabeth J. Sutton<sup>2</sup>, Luca A. Carbonaro<sup>2,3</sup>, Ruud M. Pijnappel<sup>4</sup>, Elizabeth A. Morris<sup>2</sup>, and Kenneth G.A. Gilhuijs<sup>1</sup>

<sup>1</sup>Image Sciences Institute, University Medical Center Utrecht, Utrecht, Netherlands, <sup>2</sup>Department of Radiology, Memorial Sloan Kettering Cancer Center, New York, NY, United States, <sup>3</sup>Unità di Radiologia, IRCCS Policlinico San Donato, Milan, Italy, <sup>4</sup>Department of Radiology, University Medical Center Utrecht, Utrecht, Netherlands

This study was performed to validate whether MR contrast-enhancement in stromal tissue of the disease-free breast is related to the survival of patients with cancer in the other breast. A recent study in 398 patients with estrogen-receptor positive and human-epidermal-growth-factor-2 negative invasive breast cancer showed that more pronounced contralateral parenchymal enhancement (CPE) was associated with improved patient survival. In this study, we extracted CPE to re-test the finding in a comparable patient population from an independent cancer center. In 287 patients, CPE reproduces as a biomarker for long-term survival. This reproducible imaging finding has potential towards the personalization of care.

---

Oral

## fMRI Connectivity

Room 316BC

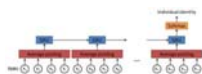
Wednesday 16:15 -  
18:15

Moderators: James Pekar & Stephen Smith

---

952

16:15



Individual identification using brain functional fingerprint detected by recurrent neural network

Shiyang Chen<sup>1</sup> and Xiaoping Hu<sup>2</sup>

<sup>1</sup>The Wallace H. Coulter Department of Biomedical Engineering, Georgia Institute of Technology, Atlanta, GA, United States, <sup>2</sup>Department of Bioengineering, University of California, Riverside, Riverside, CA, United States

We introduce a deep learning approach to derive functional fingerprint of the brain that can identify individuals. By investigating the features extracted by our model, we noticed that they mostly resemble the existing resting state networks, and three networks (default mode, attention, and frontoparietal control networks) contribute the most to individual discriminability.

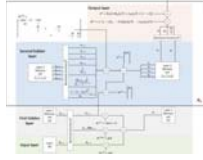
---

953

16:27

### Generalized Recurrent Neural Network accommodating Dynamic Causal Modelling for functional MRI analysis

Yuan Wang<sup>1</sup>, Yao Wang<sup>2</sup>, and Yvonne W Lui<sup>3</sup>



<sup>1</sup>Tandon School of Engineering, New York University, Brooklyn, NY, United States, <sup>2</sup>Tandon School of Engineering, New York University, <sup>3</sup>School of Medicine, New York University

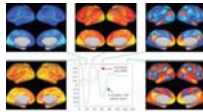
We propose DCM-RNN, a new model for effective connectivity estimation from fMRI signal that links the strengths of traditional Dynamic Causal Modelling (DCM) and deep learning. It casts DCM as a generalized Recurrent Neural Network (RNN) and estimates the effective connectivity using backpropagation. It extends DCM with a more flexible framework, unique estimation methods, and neural network compatibility. In simulated experiments, we demonstrate that DCM-RNN is feasible and can be used to estimate the effective connectivity.

954

16:39

### A simple data driven predictive dynamical model of whole brain resting state fMRI signal behavior

Eric Wong<sup>1</sup>



<sup>1</sup>Radiology/Psychiatry, UC San Diego, La Jolla, CA, United States

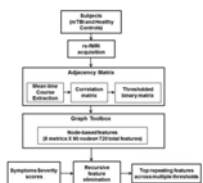
In this work we present a simple dynamical model that learns from resting state fMRI data to predict future brain states using information from one or more past brain states. We use a fully connected neural network model, and data from the Human Connectome Project. Our group model explains over 45% of the variance across 472 subjects, is very consistent when trained on subsets of the subjects, predicts realistic dynamics, gravitates towards the default mode when started in nearly any simulated brain state, and is complementary to correlation analysis.

955

16:51

### Selection of node-based graph metrics to predict symptom severity in mild traumatic brain injury (mTBI) using recursive feature elimination

Bharath Ram Sundar<sup>1</sup>, Hariharan Ravishankar<sup>1</sup>, Suresh E Joel<sup>1</sup>, Luca Marinelli<sup>2</sup>, Teena Shetty<sup>3</sup>, Pratik Mukherjee<sup>4</sup>, Joseph Masdeu<sup>5</sup>, Rakesh Mullick<sup>1</sup>, and Radhika Madhavan<sup>1</sup>



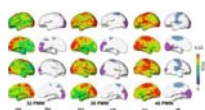
<sup>1</sup>GE Global Research, Bangalore, Karnataka, India, Bangalore, India, <sup>2</sup>GE Global Research, Niskayuna, NY, <sup>3</sup>Hospital for Special Surgery, New York City, NY, <sup>4</sup>University of California, San Francisco, CA, <sup>5</sup>Houston Methodist, Houston, TX



Recursive feature elimination (RFE), a machine learning technique, is used to sub-select node-based graph theoretical features that correlate with symptom severity in mTBI. Resting state functional connectivity was represented as a binary graph by thresholding correlation values computed between time courses of functional ROIs. Node-based graph theoretical metrics were computed and fed to the feature elimination model to regress on mTBI symptom scores. Using RFE we identified top features correlated to symptom severity in mTBI, which include eigen centrality and closeness of nodes within the salience and default-mode networks. Top features were analyzed for repeatability over multiple runs and multiple thresholds.

956

17:03



### Dynamic parcellation of cortical functional networks in developing preterm brains

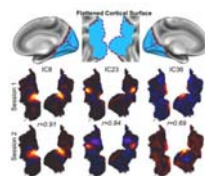
Qinmu Peng<sup>1,2</sup>, Risheng Liu<sup>3</sup>, Minhui Ouyang<sup>1</sup>, Chenying Zhao<sup>4</sup>, Xin Fan<sup>3</sup>, Bo Hong<sup>4</sup>, and Hao Huang<sup>1,2</sup>

<sup>1</sup>Department of Radiology, Children's Hospital of Philadelphia, Philadelphia, PA, United States, <sup>2</sup>Department of Radiology, Perelman School of Medicine, University of Pennsylvania, Philadelphia, PA, United States, <sup>3</sup>School of Software, Dalian University of Technology, People's Republic of China, <sup>4</sup>Biomedical Engineering, Tsinghua University, People's Republic of China

Connectivity is a major organizing principle of the central nervous system. However, little is known on how the cortical functional connectivity emerges in the network organization in the preterm brain. Here, we aimed to demonstrate emergence of primary functional regions using a parcellation method based on measurements from resting-state fMRI. Our results showed the clear emergence of primary sensorimotor and visual regions at 32, 36 and 40 postmenstrual weeks, while coherent parcellations of higher-order network regions are not apparent. The study demonstrated that dynamic parcellation based on resting-state fMRI can effectively delineate differentiated emergence of cortical networks during preterm development.

957

17:15



### Spontaneous Activity Patterns Reveal Non-Retinotopic Functional Parcellation and Organization of Human Visual Cortex

Kun-Han Lu<sup>1</sup>, Jun Young Jeong<sup>1</sup>, Haiguang Wen<sup>1</sup>, and Zhongming Liu<sup>1,2</sup>

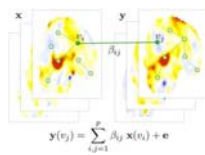


<sup>1</sup>Electrical and Computer Engineering, Purdue University, West Lafayette, IN, United States, <sup>2</sup>Biomedical Engineering, Purdue University, West Lafayette, IN, United States

We applied Independent Component Analysis (ICA) for mapping cortical visual areas and networks based on resting-state fMRI signals within the visual cortex. We found that spontaneous brain activity at rest exhibits reliable network patterns not only in the whole-brain scale but also in much finer scales. These networks show notable differences compared to the classical visual regions defined with retinotopic mapping or cytoarchitecture. In addition, these networks are anatomically segregated and functionally specialized into three modules: the dorsal pathway, the ventral pathway, and the early visual areas shared by these two pathways.

958

17:27



### Hyper Network Analysis on Paired Images

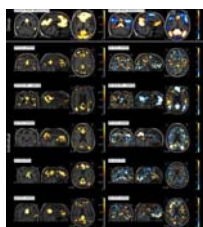
Moo K Chung<sup>1</sup>, Victoria Vilalta-Gil<sup>2</sup>, Paul J Rathouz<sup>1</sup>, Benjamin B Lahey<sup>3</sup>, and David H Zald<sup>2</sup>

<sup>1</sup>Department of Biostatistics and Medical Informatics, University of Wisconsin, Madison, WI, United States, <sup>2</sup>Department of Psychology, Vanderbilt University, Nashville, TN, United States, <sup>3</sup>Department of health Studies and Psychiatry and Behavioral Neuroscience, University of Chicago, Chicago, IL, United States

We present a new integrative framework for analyzing paired images using hyper-networks. The method is applied to twin fMRI study in characterizing the amount of heritability in the functional network.

959

17:39



### Sparse Network Analysis of Individual Resting-State BOLD-fMRI

Michael Hütel<sup>1</sup>, Andrew Melbourne<sup>1</sup>, David Thomas<sup>1</sup>, Jonathan Rohrer<sup>1</sup>, and Sebastien Ourselin<sup>1</sup>

<sup>1</sup>UCL, London, United Kingdom



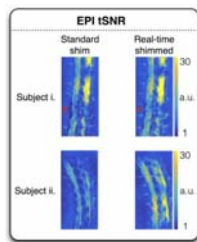


Spatial encoding and shimming in MRI commonly use dedicated coils that generate spherical harmonic fields. Recently introduced dynamic multi-coil technique (DYNAMITE) demonstrates that MRI-relevant magnetic fields can also be created by a generic set of coils that produce non-linear and non-orthogonal fields, through successful implementation of dynamic shimming, linear and non-linear encoding. Here, purely DYNAMITE-based, concurrent spatial encoding and B<sub>0</sub> shimming is demonstrated. The successful synthesis of all encoding and shimming fields with DYNAMITE encourages the simplification of MR scanner architecture by substitution of multi-layer spherical harmonic coil systems with a single-layer multi-coil array.

964



16:39



Real-time shimming of the human spinal cord using a 24-channel shim array coil

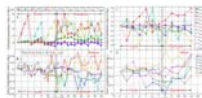
Ryan Topfer<sup>1</sup>, Alexandru Foias<sup>1</sup>, Nikola Stikov<sup>1,2</sup>, and Julien Cohen-Adad<sup>1,3</sup>

<sup>1</sup>NeuroPoly Lab, Institute of Biomedical Engineering, Polytechnique Montreal, Montreal, QC, Canada, <sup>2</sup>Montreal Heart Institute, Université de Montréal, Montreal, QC, Canada, <sup>3</sup>Functional Neuroimaging Unit, CRIUGM, Université de Montréal, Montreal, QC, Canada

Pathologies of the spinal cord are a primary cause of functional disability and chronic pain. Although MRI already plays a role in the evaluation of these pathologies, it continues to be hampered by artifacts due to magnetic field inhomogeneity. This study reports the first results from applying a specially designed 24-channel shim array to compensate respiration-induced magnetic field inhomogeneity in the human spinal cord in real-time. This approach has the potential to improve the quality of EPI and spectroscopy in the spinal cord.

965

16:51



Tracking head movement inside an MR scanner using voltages induced in coils by time-varying gradients

E. H. Bhuiyan<sup>1</sup>, G. S. Spencer<sup>1</sup>, P. M. Glover<sup>1</sup>, and R. Bowtell<sup>1</sup>

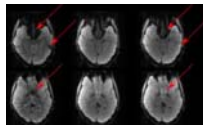
<sup>1</sup>Sir Peter Mansfield Imaging Centre, School of Physics and Astronomy, University of Nottingham, Nottingham, United Kingdom

We evaluate a new approach for monitoring head movement inside an MR scanner, which exploits the linear variation of the voltages induced in a set of coils by time-varying magnetic field gradients with respect to small changes in position/orientation. This approach was tested by attaching five coils to a structured agar phantom and a healthy volunteer's head. The results suggest that it is possible to estimate the position and orientation with 0.22mm and 0.24° root-mean-square error using this set-up. The new approach could be used for prospective or retrospective motion correction.

---

966

17:03



Combined multi-band z-shimming using a novel auto-calibration routine  
Michael Schwerter<sup>1</sup>, Seong Dae Yun<sup>1</sup>, and N. Jon Shah<sup>1,2</sup>

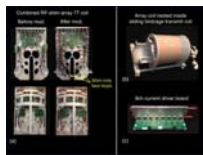
*<sup>1</sup>Institute of Neuroscience and Medicine, Medical Imaging Physics (INM-4), Forschungszentrum Juelich, Juelich, Germany, <sup>2</sup>Faculty of Medicine, Department of Neurology, JARA, RWTH Aachen University, Aachen, Germany*

EPI images suffer from signal dropouts and z-shimming is an effective technique to recover parts of the lost signal. Its inherent drawbacks are a scan time prolongation and the necessity to estimate subject-specific z-shim gradient moments. We introduce multi-band imaging to z-shimming to eliminate the scan time prolongation and propose a novel method to estimate optimal z-shim gradient moments. The results show less signal dropout in the z-shimmed images and prove our z-shim gradient moment estimation to be robust and efficient. Due to a reduced anatomical contrast, our multi-band z-shim approach might be most beneficial for BOLD-contrast based fMRI.

---

967

17:15



An integrated 32ch RF-shim array coil for improved B0 shimming of the brain at 7 Tesla

Jason Stockmann<sup>1,2</sup>, Thomas Witzel<sup>1,2</sup>, Nicolas Arango<sup>3</sup>, Azma Mareyam<sup>1</sup>, Charlotte Sappo<sup>1</sup>, Jiazheng Zhou<sup>4</sup>, Joshua Park<sup>1</sup>, Boris Keil<sup>1</sup>, Lucas Jenkins<sup>1</sup>, Markus May<sup>5</sup>, Jonathan R Polimeni<sup>1,6</sup>, Jacob White<sup>7</sup>, and Lawrence L Wald<sup>1,6</sup>

<sup>1</sup>A. A. Martinos Center for Biomedical Imaging, Massachusetts General Hospital, Charlestown, MA, United States, <sup>2</sup>Harvard Medical School, Boston, MA, United States, <sup>3</sup>Electrical Engineering and Computer Science, Massachusetts Institute of Technology, Cambridge, MA, <sup>4</sup>Institute of Biomedical Engineering, National Taiwan University, Taiwan, <sup>5</sup>Electronic and Mechatronic Systems, Technische Hochschule Nürnberg, Nürnberg, Germany, <sup>6</sup>Harvard Medical School, Boston, United States, <sup>7</sup>Electrical Engineering and Computer Science, Massachusetts Institute of Technology, Cambridge, MA, United States

Dual-purpose arrays of close-fitting coils, used to both receive RF and shim  $B_0$  to high spatial order, have recently been demonstrated in brain imaging at 3T. We extend this approach to 7T with an array comprised of: six RF coils, twenty-six RF/ $B_0$ -shim coils, and six shim-only coils. The shim coils are driven by an array of low-cost current-feedback amplifiers that can steer up to fifty amps of shimming currents rapidly and accurately enough to allow for slice-by-slice adjustments. The resulting slice-optimal high-order shim capability (wires and chokes) improves  $\sigma_{B_0}$  in brain slices by up to 60% (as compared to static 2nd-order global shimming), while worsening SNR by less than 10%, and increasing coil coupling by less than 3%.

968



17:27



### Monolithic Transmit Line Resonator as a Combined $B_1/B_0$ -shim Coil Element

Riccardo Stara<sup>1</sup>, Mihir Pendse<sup>2</sup>, Jason Stockmann<sup>3</sup>, and Brian K. Rutt<sup>1</sup>

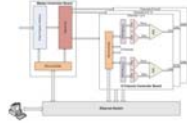
<sup>1</sup>The Richard M. Lucas Center for Imaging, Radiology Department, Stanford University, Stanford, CA, United States, <sup>2</sup>The Richard M. Lucas Center for Imaging, Electrical Engineering Department, Stanford University, Stanford, CA, United States, <sup>3</sup>A. A. Martinos Center for Biomedical Imaging, Massachusetts General Hospital, Charlestown, MA, United States

In this work we propose and evaluate, for the first time, the use of a single-turn-single-gap Transmit Line Resonator as a combined RF-transceive and  $B_0$ -shim element. We compare this design to a standard loop in terms of both RF and  $B_0$ -shimming performance. The benefits of our combined TLR/ $B_0$ -shim design are improved RF performance due to the fixed and smaller number of lumped elements, and the increase in  $B_0$ -shim efficiency. Our results show the TLR element design to be an ideal building block for high-channel-count integrated Parallel Reception, Excitation and Shimming (iPRES) arrays.



969

17:39



### The Design and Implementation of a 64 Channel Arbitrary Gradient Waveform Controller

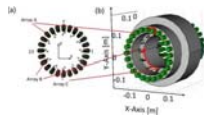
Terence W Nixon<sup>1</sup>, Scott McIntyre<sup>1</sup>, and Robin A de Graaf<sup>1</sup>

<sup>1</sup>MRRC Yale University, New Haven, CT, United States

Generating additional magnetic fields independently from the MR scanner's hardware requires additional controllers, current amplifiers and DC coils. Here we present the design and implementation of a 64 channel arbitrary gradient waveform controller that can be used to drive current amplifiers with analog inputs. We describe the controller's architecture and how sequences are developed. We will also discuss the important criteria needed to synchronize the waveforms with the MR scanner. Finally, we will show the completed controller and the first MR result.

970

17:51



### Dynamic permanent magnet array for ultra-low field magnetic resonance imaging

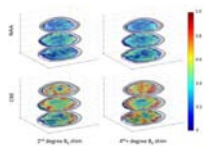
Michael W. Vogel<sup>1</sup>, Viktor Vegh<sup>1</sup>, Ruben Pellicer Guridi<sup>1</sup>, and David C. Reutens<sup>1</sup>

<sup>1</sup>University of Queensland, St Lucia, Australia

Conventional MRI scanners rely on superconducting magnets making them heavy and expensive and putting MRI beyond the reach of much of the world's population. Ultra-low field (ULF) MRI instruments offer the possibility of novel image contrast mechanisms, are less costly and are potentially portable, enabling use in unconventional situations. This project addresses ULF-MRI's biggest challenge, low signal-to-noise ratio, by using the novel approach of dynamic, mechanically-operated small permanent magnet arrays to generate the magnetic fields required for prepolarisation and spatial encoding.

971

18:03



### Multi-slice metabolite mapping with Very-High Degree Dynamic B0 Shim Updating at 9.4T using Accelerated 1H FID MRSI

Sahar Nassirpour<sup>1,2</sup>, Paul Chang<sup>1,2</sup>, and Anke Henning<sup>1,3</sup>

<sup>1</sup>MPI for Biological Cybernetics, Tuebingen, Germany, <sup>2</sup>IMPRS for Cognitive and Systems Neuroscience, Eberhard Karls University of Tuebingen, Tuebingen, Germany, <sup>3</sup>Institute of Physics, Ernst-Moritz-Arndt University Greifswald, Greifswald, Germany



In this work, we address the problem of  $B_0$  inhomogeneity in the human brain at 9.4T by using dynamic very high order  $B_0$  shimming. This enables multi-slice metabolite mapping in the human brain at this field strength. Furthermore, we investigate the advantage of low (2<sup>nd</sup>) versus very high (4<sup>th+</sup>) degree dynamic  $B_0$  shimming directly with respect to the quality of the metabolite maps.

---

## Combined Educational & Scientific Session

# Evaluation of Tissue Properties in Cancer: Heterogeneity and Structure

Room 315                      Wednesday 16:15 - 18:15                      *Moderators:* Arvind Pathak & Christopher Quarles

---

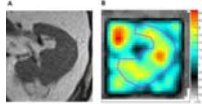
16:15                      [MR Elastography in Cancer](#)  
Ralph Sinkus<sup>1</sup>

*<sup>1</sup>Imaging Sciences & Biomedical Engineering Division, King's College London*

972



16:45                      [Characterization of Renal Tumors: Integrating Biomechanical, Functional and Morphological Assessment Using 3 Tesla Magnetic Resonance Elastography](#)



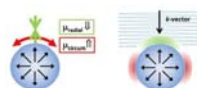
Davide Prezzi<sup>1</sup>, Radhouene Neji<sup>2,3</sup>, James J Stirling<sup>3</sup>, Sami Jeljeli<sup>3</sup>, Hema Verma<sup>4</sup>, Tim O'Brien<sup>5</sup>, Benjamin Challacombe<sup>5</sup>, Archana Fernando<sup>5</sup>, Ashish Chandra<sup>6</sup>, Vicky Goh<sup>1</sup>, and Ralph Sinkus<sup>7</sup>

*<sup>1</sup>Cancer Imaging, King's College London, London, United Kingdom, <sup>2</sup>MR Research Collaborations, Siemens Healthcare, Frimley, United Kingdom, <sup>3</sup>King's College London, London, United Kingdom, <sup>4</sup>Radiology, Guy's and St Thomas' NHS Foundation Trust, London, United Kingdom, <sup>5</sup>Urology, Guy's and St Thomas' NHS Foundation Trust, London, United Kingdom, <sup>6</sup>Pathology, Guy's and St Thomas' NHS Foundation Trust, London, United Kingdom, <sup>7</sup>Biomedical Engineering, King's College London, London, United Kingdom*

Incidentally detected renal tumors are overtreated surgically: up to 20% of them are benign, most frequently oncocytomas. We hypothesize that integrating biomechanical assessment with functional/morphological MRI can improve lesion characterization, precluding unnecessary surgery. Initial experience in 5 resected renal oncocytomas and 13 renal cell carcinomas (RCC) demonstrates that MR Elastography (MRE) at 30Hz with shear modulus parametric mapping is feasible and adds value within a multiparametric MRI assessment: oncocytoma displays higher median shear attenuation ( $\alpha$ ) and lower shear velocity (C) than RCC. MRE parameters appear to be stronger classifiers than quantitative DCE MRI parameters ( $K^{\text{trans}}$ ,  $k_{\text{ep}}$ ), ADC and T2 signal intensity.

973

16:57



Using non-linear tissue biomechanics to infer static forces within tissue: towards quantifying IFP

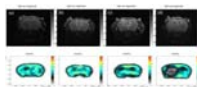
Daniel Fovargue<sup>1</sup>, Jack Lee<sup>1</sup>, Adela Capilnasiu<sup>1</sup>, Marco Fiorito<sup>1</sup>, David Nordsletten<sup>1</sup>, and Ralph Sinkus<sup>1</sup>

<sup>1</sup>*Division of Imaging Sciences and Biomedical Engineering, King's College London, London, United Kingdom*

Quantifying static forces in the context of oncology, such as interstitial fluid pressure, would represent a valuable biomarker in therapy monitoring. Nonlinear tissue mechanics leads to distinct signatures of apparent anisotropic changes in mechanical shear properties in the vicinity of an object that exerts pressure onto its surroundings. Tissue nonlinearity can be modelled for instance via hyper elasticity. We show that the apparent modulation in tissue stiffness can be accounted for when incorporating the nonlinear anisotropic model into the estimation of the biomechanics via MR-Elastography. Knowledge of the deformation tensor enables direct quantification of underlying static forces, hence pressure.

974

17:09



Monitoring Glioblastoma Progression in Mouse Brain with Magnetic Resonance Elastography

Navid Nazari<sup>1</sup>, Michal Nowicki<sup>2</sup>, Katharina Shregel<sup>2,3</sup>, Sean Lawler<sup>2,4</sup>, Ralph Sinkus<sup>5</sup>, Paul Barbone<sup>1</sup>, and Samuel Patz<sup>2,4</sup>

<sup>1</sup>*Boston University, Boston, MA, United States*, <sup>2</sup>*Brigham and Women's Hospital, Boston, MA, United States*, <sup>3</sup>*University Medicine Goettingen, Goettingen, Germany*, <sup>4</sup>*Harvard Medical School, Boston, MA, United States*, <sup>5</sup>*King's College, London, United Kingdom*



The longitudinal progression of glioblastoma was monitored in a cohort of mice with MRE and conventional RARE MRI. Increasing tumor size was easily seen with both modalities. In most cases, MRE maps showed a tumor margin that was sharper than RARE. Results were registered with histology, and variation of the shear modulus was compared with histology features. Both MRE and RARE demonstrated tumor regions with varying levels of heterogeneity, and in one animal, both homogeneous and heterogeneous parts were found to be growing separately as sub-populations of the same glioblastoma cell line within the brain.

---

17:21

### Addressing Tumor Heterogeneity by Multi-Parametric MRI

Richard Carano<sup>1</sup>

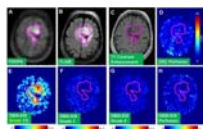
*<sup>1</sup>Biomedical Imaging, Genentech, CA, United States*

The presentation will focus on addressing tumor heterogeneity by a multi-parametric MRI approach.

---

975

17:51



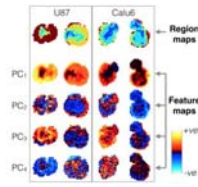
### Quantitative characterization of brain tumor heterogeneity using diffusion basis spectrum imaging with extended isotropic spectrum (DBSI\_EIS)

Qing Wang<sup>1</sup>, Gloria Guzman<sup>2</sup>, Yong Wang<sup>1</sup>, Maria R. Ponisio<sup>1</sup>, Yi Su<sup>1</sup>, Pamela LaMontagne<sup>1</sup>, Sheng-Kwei Song<sup>1</sup>, Keith M. Rich<sup>1</sup>, Sonika Dahiya<sup>1</sup>, Jon McConathy<sup>3</sup>, and Tammie Benzinger<sup>1</sup>

*<sup>1</sup>Washington University in St. Louis, St. Louis, MO, United States,*

*<sup>2</sup>University of Arizona, AZ, United States, <sup>3</sup>The university of Alabama at Birmingham, Birmingham, AL, United States*

Tumors are typically heterogeneous, and may contain different grades of tumor cells, different types of tumor cells, edema and/or abnormal vascular structures. A noninvasive, non-radioactive technique to provide multiple parametric and quantitative images for better profiling the heterogeneity of tumors is highly needed. We demonstrated that diffusion basis spectrum imaging with extended isotropic spectrum (DBSI-EIS) is capable to identify structural heterogeneity in brain tumor lesions, including various grades of tumor cells and perfusion, which make it a new and unique technique to clinically evaluate tumors for comprehensive diagnosis and accurate treatment evaluation.



## Automated identification of hypoxia-related regional variations in tumour microenvironment using dynamic contrast-enhanced MRI and oxygen-enhanced MRI

Adam K Featherstone<sup>1,2</sup>, James P B O'Connor<sup>2,3,4</sup>, Ross A Little<sup>1</sup>, Yvonne Watson<sup>1</sup>, Sue Cheung<sup>1</sup>, Muhammad Babur<sup>5</sup>, Victoria Tessyman<sup>2,5</sup>, Roben Gieling<sup>2,5</sup>, Kaye J Williams<sup>2,5</sup>, Julian C Matthews<sup>1,2</sup>, and Geoff J M Parker<sup>1,2,6</sup>

<sup>1</sup>Division of Informatics, Imaging and Data Sciences, The University of Manchester, Manchester, United Kingdom, <sup>2</sup>CRUK & EPSRC Cancer Imaging Centre in Cambridge and Manchester, Cambridge and Manchester, United Kingdom, <sup>3</sup>Division of Molecular and Clinical Cancer Studies, The University of Manchester, Manchester, United Kingdom, <sup>4</sup>Department of Radiology, The Christie NHS Foundation Trust, Manchester, United Kingdom, <sup>5</sup>Division of Pharmacy & Optometry, The University of Manchester, Manchester, United Kingdom, <sup>6</sup>Bioxydyn Ltd., Manchester, United Kingdom

Hypoxia is an important prognostic indicator in most solid tumours. We present here automated, data-driven methods, using principal component analysis (PCA) and Gaussian mixture modelling (GMM), that consistently locate functionally distinct sub-regions in preclinical tumours, some of which are postulated to be relevant to hypoxia. Methods are based on dynamic contrast-enhanced (DCE)-MRI (reflecting perfusion) and oxygen-enhanced (OE)-MRI (reflecting oxygen delivery). We demonstrate the utility and stability of our methods through a combination of evaluation metrics, which may be incorporated in similar studies elsewhere.

### Other

## Hands-On Workshop: GE Healthcare 2

Room 322AB

Wednesday 16:15 -  
18:15

(no CME credit)

### Other

## Hands-On Workshop: Philips Healthcare 2

Room 324                      Wednesday 16:15 -  
18:15                              *(no CME credit)*

---

**Other**

## ISMIRM Business Meeting

Room 314                      Wednesday 18:30 -  
19:30                              *(no CME credit)*

---

**Other**

## Women's Forum

Room 310                      Wednesday 19:30 -  
21:30                              *(no CME credit)*

---

## Thursday, 27 April 2017

[Go to top](#)

### **Sunrise Session**

## Cardiovascular MR: "More is Better": More Modalities

*Organizers:* Sonia Nilles-Vallespin, Ph.D., Daniel K. Sodickson, M.D., Ph.D., & Bernd J. Wintersperger, M.D.

Room 310                      Thursday 7:00 - 7:50                      *Moderators:* Claudia Calcagno & Rohan  
Dharmakumar

---

7:00                              [MR-PET](#)  
Georges El Fakhri

---

7:25                              [X-MR](#)  
Dara Kraitchman

---

7:50                              [Adjournment & Meet the Teachers](#)

---

## Sunrise Session

# Quantitative Susceptibility Mapping

*Organizers:* Herbert Köstler, Dipl.-Phys. & N. Jon Shah, Ph.D.

Room 311

Thursday 7:00 - 7:50

*Moderators:* Ute Goerke & Jürgen Reichenbach

---

7:00      [Susceptibility & Quantitative Mapping - Description, Overview & Method](#)  
Ferdinand Schweser

---

7:25      [Susceptibility & Quantitative Mapping - Clinical Potential & Relevance](#)  
Christian Ziener

---

7:50      [Adjournment & Meet the Teachers](#)

---

## Sunrise Session

# MR Imaging of Small Joints: Arthritis & Diabetic Arthropathy

*Organizers:* Jenny T. Bencardino, M.D., Eric Y. Chang, M.D., Christine Chung, M.D. & Philip Robinson, M.D.

Room 312

Thursday 7:00 - 7:50

*Moderators:* Kimberly Amrami & John Crues

---

7:00      [Inflammatory Arthritis](#)  
Leon Lenchik

---

7:25      [Diabetic Arthropathy](#)  
Parmanand Naidoo

---

7:50      [Adjournment & Meet the Teachers](#)

---

## Sunrise Session

# Magnetic Resonance Elastography: Abdominal & Cardiac

*Organizers:* Guoying Liu, Ph.D. & Joshua D. Trzasko, Ph.D.



Room 313A      Thursday 7:00 - 7:50      *Moderators: Curtis Johnson & Joshua Trzasko*

---

7:00      [Abdominal](#)  
Jin Wang

---

7:25      [Cardiac](#)  
Arunark Kolipaka

---

7:50      [Adjournment & Meet the Teachers](#)

---

### **Sunrise Session**

## **Individualized Brain MRI: Metabolic Imaging**

*Organizers: Christopher P. Hess, M.D., Ph.D.*

Room 313BC      Thursday 7:00 - 7:50      *Moderators: Yan Li & Eva-Maria Ratai*

---

7:00      [MR/PET – Clinical Applications](#)  
Timothy Shepherd

---

7:25      [MR Spectroscopy - New Metabolites](#)  
Dorothee Auer

---

7:50      [Adjournment & Meet the Teachers](#)

---

### **Sunrise Session**

## **Imaging Tumor Response to Therapy**

*Organizers: Linda Moy, M.D. & Valeria Panebianco, M.D.*

Room 314      Thursday 7:00 - 7:50      *Moderators: Linda Moy & Valeria Panebianco*

---

7:00      [Breast Imaging of Targeted Agents](#)  
Huong Le-Petross

---

7:25      [Gynecological Tumours - Imaging Therapy Response](#)

### Sunrise Session

## Local vs. Global Tractography

*Organizers:* Daniel C. Alexander, Ph.D. & Jennifer A. McNab, Ph.D.

Room 315

Thursday 7:00 - 7:50

*Moderators:* Fulvia Palesi & Jacques-Donald  
Tournier

---

7:00      [Local Tractography](#)  
Lauren O'Donnell

---

7:12      [Global Tractography](#)  
Marco Reisert

---

7:24      [Integration of Local & Global Tractography](#)  
Robert Smith

---

7:36      [Panel Discussion](#)

---

7:50      [Adjournment & Meet the Teachers](#)

---

---

### Sunrise Session

## The Consequence of Inter-Compartmental Water Exchange in the DCE-MRI Time-Course

*Organizers:* Linda Knutsson, Ph.D. & Steven P. Sourbron, Ph.D.

Room 316A

Thursday 7:00 - 7:50

*Moderators:* Joseph Ackerman & Kathleen  
Schminda

---

7:00      [DCE-MRI is Enriched by Water Exchange](#)  
Charles Springer, Jr.

---

7:15 Data Acquired Using DCE-MRI are Unsuitable for Measuring Water Exchange  
David Buckley

---

7:30 Debate

---

7:50 Adjournment & Meet the Teachers

---

## Sunrise Session

### Cases with the Aces: Female Pelvis

*Organizers:* Kathryn Fowler, M.D., Kartik Jhaveri, M.D., F.R.C.P.C., Lorenzo Mannelli, M.D., Ph.D. & Edwin J.R. van Beek, M.D., Ph.D., M.Ed., FRCR

Room 320 Thursday 7:00 - 7:50 *Moderators:* Gabriele Masselli & Iva Petkovska

---

7:00 Benign Diseases of the Uterus & Ovaries  
Akiko Takahata

---

7:25 Malignant Diseases of the Uterus & Ovaries  
Seung Hyup Kim

---

7:50 Adjournment & Meet the Teachers

---

## Traditional Poster: Cardiovascular

Exhibition Hall 2719-2767 Thursday 8:15 - 10:15 *(no CME credit)*

---

## Electronic Poster: fMRI

Exhibition Hall Thursday 8:15 - 9:15 *(no CME credit)*

---

## Study Groups

### Interventional MR Study Group

Room 323ABC Thursday 8:15 - 10:15 *(no CME credit)*

---

---

## Study Groups

### X-Nuclei Imaging Study Group

Room 317AB      Thursday 8:15 - 10:15    *(no CME credit)*

---

## Educational Course

### Clinical & Technical Perspectives on Trends in MR

*Organizers:* Sebastian Kozerke, Ph.D. & James G. Pipe, Ph.D.

Room 315      Thursday 8:15 - 10:15    *Moderators:* Sebastian Kozerke & James Pipe

---

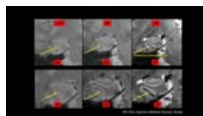
8:15      [The Ideal MR Scanner - a Clinician's Perspective](#)  
Daniel Sodickson

8:35      [The Ideal MR Scanner - an Engineer's Perspective](#)  
Cecilia Possanzini<sup>1</sup>

<sup>1</sup>*MRI Systems, Philips Healthcare*

In considering what an ideal MRI system might be, it is helpful to evaluate the user needs. No system is ideal for everything and most MRI system designs represent a balance of both requirements and constraints. This paper analyses the opportunities and the limitations offered by some selected recent technical trends in MRI systems and examines a strategy to reach the definition of what might be an optimal MRI system design.

8:55      [Future of MR Systems & Applications - Ultra High Field](#)  
Franz Schmitt<sup>1</sup>



<sup>1</sup>*Former Siemens Healthcare now Lakeside Imaging/e*

Ultra-High Field MRI has developed from a plain research instrument for mastering the required technology to a clinically recognised MR imaging field strength. Besides stronger magnets, the entire RF transmit and receive chain needed to be updated to the higher MR frequencies. The mitigation of the transmit B1+ inhomogeneity by means of parallel transmission is now fully understood and utilized in almost every UHF site in some sort or another. Beside the significantly higher resolution achieved with UHF, unique contrast and imaging possibilities opened up: better susceptibility weighting, quantitative susceptibility mapping, CEST imaging and sodium imaging, aiming for better diagnosis in neurodegenerative diseases, tumour imaging, musculoskeletal imaging and much more. All these aspects of UHF imaging will be considered in this educational talk.

---

9:15      **Future MR Magnets - Beyond NbTi**  
Mark D Bird<sup>1</sup>

*<sup>1</sup>National High Magnetic Field Lab, Florida State University, Tallahassee, FL, United States*

An overview of the challenges associated with development of higher field human MRI magnets is presented.

---

9:35      **All at Once - Finger- & Footprints**  
Mariya Doneva<sup>1</sup>

*<sup>1</sup>Philips Research, Hamburg, Germany*

In recent years, the field of quantitative MRI has been expanded by the introduction of MR Fingerprinting as well as several quantitative MRI methods applying extensive signal modeling. This lecture will give an overview of these recently introduced methods.

---

9:55      **Beyond Images - The Future of MR Diagnostics**  
Tim Leiner<sup>1</sup>

*<sup>1</sup>Utrecht University Medical Center, Utrecht, Netherlands*

---

10:15      **Adjournment & Meet the Teachers**

---

---

## Educational Course

# MR Physics & Techniques for Clinicians

Organizers: Marcus T. Alley, Ph.D. & Bernd Jung, Ph.D.

Room 316BC      Thursday 8:15 - 10:15      Moderators: Nicole Seiberlich & Matthias Weigel

---

8:15

[Artifacts to Artefacts: Causes & Cures from Clinical Perspective](#)

Vikas Gulani<sup>1</sup>

*<sup>1</sup>Radiology, Case Western Reserve University, Cleveland, United States*

---

8:55

[Contrast Agents](#)

Val M. Runge<sup>1</sup>

*<sup>1</sup>Universitätsinstitut für Diagnostische Radiologie, Inselspital, Bern, Switzerland*

“The gadolinium chelates (the GBCAs) are critical to disease diagnosis by MR, indeed to clinical medicine worldwide, and have proven to be overall a very safe class of contrast media.” This review focuses on the current knowledge regarding accumulation of gadolinium in the brain (dentate nucleus and other structures) and body, with clinical recommendations based on that and other safety data, including the recent European Agency recommendation.

---

9:35

[High Field Imaging](#)

Sebastian Schmitter<sup>1</sup>

*<sup>1</sup>Department of Biomedical Magnetic Resonance, Physikalisch-Technische Bundesanstalt, Berlin, Germany*

The MRI main field strength has been constantly increased over the past decades. Today, scanners with 3T, 7T and even beyond are in use, however ultra-high field ( $\geq 7T$ ) systems are mostly used in research centers although the transition into hospitals is expected. The reasons for using (ultra-)high fields are multifold and will be outlined in this presentation. Along with these benefits go a larger range of challenges, which are among the reasons for the rather slow transition of UHF into clinical applications. Solutions to most of these challenges will be presented and applications will be highlighted.

---

10:15

Adjournment & Meet the Teachers

---

## Power Pitch

# Pitch: Breakthrough Methods & Applications in Cancer Imaging

Power Pitch

Theater A -

Exhibition Hall

Thursday 8:15 - Moderators: Catalina Arteaga de

9:15

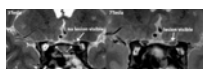
Castro & Joel Garbow

(no CME credit)

---

977

8:15



High resolution imaging of the optic chiasm at 7T MRI improves lesion detection and tumour delineation compared to 3T

Guido van Haren<sup>1</sup>, Lorna Grech-Fonk<sup>2,3</sup>, Marco Versteegen<sup>4</sup>, Wouter Teeuwisse<sup>2</sup>, Teresa Ferreira<sup>1</sup>, Irene Notting<sup>3</sup>, Wouter van Furth<sup>4</sup>, Alberto Pereira<sup>5</sup>, Gregorius Luyten<sup>3</sup>, Andrew Webb<sup>2</sup>, and Jan-Willem Beenakker<sup>2,3</sup>

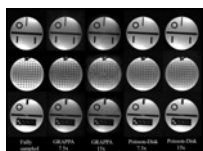
<sup>1</sup>Radiology, LUMC, Leiden, Netherlands, <sup>2</sup>Radiology, CJ Gorter center for high field MRI, LUMC, Leiden, Netherlands, <sup>3</sup>Ophthalmology, LUMC, Leiden, Netherlands, <sup>4</sup>Neurosurgery, LUMC, Leiden, Netherlands, <sup>5</sup>Endocrinology, LUMC, Leiden, Netherlands

---

978



8:15



Accelerated 3D bSSFP Imaging for Treatment Planning on an MRI-Guided Radiotherapy System

Yu Gao<sup>1,2</sup>, Ziwu Zhou<sup>1</sup>, Fei Han<sup>1</sup>, Percy Lee<sup>2,3</sup>, Daniel Low<sup>2,3</sup>, Peng Hu<sup>1,2</sup>, and Yingli Yang<sup>2,3</sup>

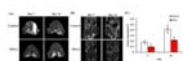


<sup>1</sup>Radiology, University of California, Los Angeles, Los Angeles, CA, United States, <sup>2</sup>Physics and Biology in Medicine IDP, University of California, Los Angeles, Los Angeles, CA, United States, <sup>3</sup>Radiation Oncology, University of California, Los Angeles, Los Angeles, CA, United States

979



8:15



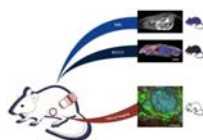
**Feasibility of magnetic resonance colonography for an immune checkpoint inhibitor in orthotopic colorectal rechallenge tumor models**

Jinil Kim<sup>1</sup>, Yoon Seok Choi<sup>2</sup>, Dong-Cheol Woo<sup>1</sup>, Chul-Woong Woo<sup>1</sup>, Sang Tae Kim<sup>1</sup>, Jae Im Kwon<sup>1</sup>, and Kyung Won Kim<sup>3</sup>

<sup>1</sup>Asan Institute for Life Sciences, ASAN Medical Center, Seoul, Korea, Republic of, <sup>2</sup>Medical research institute, Gangneung Asan Hospital, Gangneung, Korea, Republic of, <sup>3</sup>Department of Radiology, ASAN Medical Center, Seoul, Korea, Republic of

980

8:15



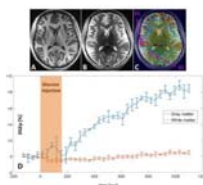
**Multi-modal and multi-scale measurement of metabolism in vivo in a breast cancer model**

Benjamin L Cox<sup>1,2,3</sup>, Joseph M Szulczewski<sup>3,4</sup>, David R Inman<sup>4</sup>, Erin B Adamson<sup>1</sup>, Kai D Ludwig<sup>1</sup>, Justin J Jeffery<sup>5</sup>, Stephen A Graves<sup>1</sup>, Alison B Roth<sup>1</sup>, David B Mummy<sup>1,6</sup>, Patricia J Keely<sup>4</sup>, Kevin W Eliceiri<sup>1,2,3,5,6</sup>, and Sean B Fain<sup>1,7</sup>

<sup>1</sup>Medical Physics, University of Wisconsin - Madison, Madison, WI, United States, <sup>2</sup>Medical Engineering, Morgridge Institute for Research, Madison, WI, United States, <sup>3</sup>Laboratory for Optical and Computational Instrumentation (LOCI), University of Wisconsin - Madison, Madison, WI, United States, <sup>4</sup>Cell and Regenerative Biology, University of Wisconsin - Madison, Madison, WI, United States, <sup>5</sup>UW Carbone Cancer Center, Madison, WI, United States, <sup>6</sup>Biomedical Engineering, University of Wisconsin - Madison, Madison, WI, United States, <sup>7</sup>Radiology, University of Wisconsin - Madison, Madison, WI, United States

981

8:15



**Dynamic Glucose Enhanced MRI - A prospective study in healthy volunteers and glioblastoma patients**

Daniel Paech<sup>1</sup>, Patrick Schuenke<sup>2</sup>, Christina Koehler<sup>1</sup>, Johannes Windschuh<sup>2</sup>, Siby Mundiyanapurath<sup>3</sup>, Sebastian Bickelhaupt<sup>1</sup>, Philipp Bäumer<sup>1</sup>, David Bonekamp<sup>1</sup>, Martin Bendszus<sup>4</sup>, Wolfgang Wick<sup>3</sup>, Peter Bachert<sup>2</sup>, Mark E. Ladd<sup>2</sup>, Heinz-Peter Schlemmer<sup>1</sup>, Moritz Zaiss<sup>5</sup>, and Alexander Radbruch<sup>1</sup>

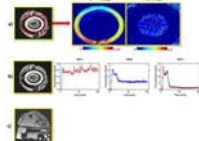
<sup>1</sup>Radiology, German Cancer Research Center, Heidelberg, Germany, <sup>2</sup>Medical Physics in Radiology, German Cancer Research Center, Heidelberg, Germany, <sup>3</sup>Neurology, University Hospital Heidelberg, Heidelberg, <sup>4</sup>Neuroradiology, University Hospital Heidelberg, Heidelberg, <sup>5</sup>Max-Planck-Institut Tübingen, Tübingen, Germany

---

982

8:15

[3D printed Breast DCE-MRI phantom to mimic structure and pharmacokinetics](#)



Nithin N Vajuvalli<sup>1</sup>, Chethan Kumar M<sup>1</sup>, Amaresha Shridhar Konar<sup>1,2</sup>, Shivaprasad Ashok Chikop<sup>1</sup>, Darshan Shivaramu Keelara<sup>1</sup>, Ashwini Kumnoor<sup>1</sup>, Ramesh Venkatesan<sup>2</sup>, and Sairam Geethanath<sup>1</sup>

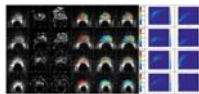
<sup>1</sup>Medical Imaging Research Centre, Dayananda Sagar Institution, Bangalore, India, <sup>2</sup>Wipro GE healthcare, Bangalore, India

---

983

8:15

[Recurrent Neural Network on DCE-MRI in Prostate Cancer](#)



Xia Li<sup>1</sup>, Vivek Vaidya<sup>2</sup>, Sandeep Gupta<sup>1</sup>, Rakesh Mullick<sup>2</sup>, Oguz Akin<sup>3</sup>, and Dattesh Shanbhag<sup>2</sup>

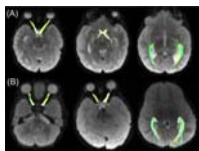
<sup>1</sup>GE Global Research Center, Niskayuna, NY, United States, <sup>2</sup>GE Global Research Center, Bengaluru, India, <sup>3</sup>Memorial Sloan-Kettering Cancer Center, NY, United States

---

984

8:15

[In vivo assessment of tumour invasion of the visual pathway in optic pathway glioma patients using multi-shell diffusion tensor MRI](#)



Patrick W Hales<sup>1</sup>, Victoria Smith<sup>2</sup>, Patricia O'Hare<sup>3</sup>, Kshitij Mankad<sup>4</sup>, Felice d'Arco<sup>4</sup>, Jessica Cooper<sup>4</sup>, Ramneek Kaur<sup>1</sup>, Kim Phipps<sup>3</sup>, Darren Hargrave<sup>3</sup>, and Christopher A Clark<sup>1</sup>

<sup>1</sup>Developmental Imaging & Biophysics Section, University College London, London, United Kingdom, <sup>2</sup>Ophthalmology Department, Great Ormond Street Children's Hospital, London, United Kingdom, <sup>3</sup>Haematology and Oncology Department, Great Ormond Street Children's Hospital, London, United Kingdom, <sup>4</sup>Radiology Department, Great Ormond Street Children's Hospital, London, United Kingdom

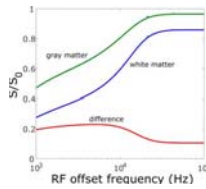
---

985

8:15

[Pipeline for longitudinal assessment of patient-derived mouse xenografts using 3D magnetization transfer-weighted MRI](#)

Kimberly L. Desmond<sup>1</sup>, David Bakhshinyan<sup>2</sup>, Maleeha Qazi<sup>2</sup>, Parvez Vora<sup>2</sup>, Chirayu Chokshi<sup>2</sup>, Sheila K. Singh<sup>2</sup>, and Nicholas A. Bock<sup>1</sup>

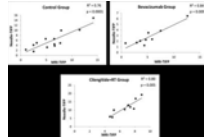


<sup>1</sup>Psychology, Neuroscience and Behaviour, McMaster University, Hamilton, ON, Canada, <sup>2</sup>McMaster Stem Cell and Cancer Research Institute, McMaster University, Hamilton, ON, Canada

986

8:15

**Tumor Interstitial Fluid Pressure and Hydraulic Conductivity Estimates by DCE-MRI in a Rat Model of Cerebral Tumor**



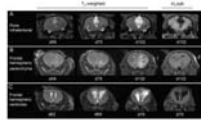
Rasha Elmghirbi<sup>1,2</sup>, Nagaraja N. Tavarekere<sup>3</sup>, Stephen L. Brown<sup>4</sup>, Swayamprava Panda<sup>1</sup>, Kelly A. Keenan<sup>3</sup>, Glauber Cabral<sup>1</sup>, Hassan Bagher-Ebadian<sup>2,4</sup>, and James R. Ewing<sup>1,2</sup>

<sup>1</sup>Neurology, Henry Ford Hospital, Detroit, MI, United States, <sup>2</sup>Physics, Oakland University, Rochester Hills, MI, United States, <sup>3</sup>Neurosurgery, Henry Ford Hospital, Detroit, MI, United States, <sup>4</sup>Radiation Oncology, Henry Ford Hospital, Detroit, MI, United States

987

8:15

**A preclinical MRI study investigating the impact of the local microenvironment on the progression of diffuse intrinsic pontine glioma in patient-derived xenografts**



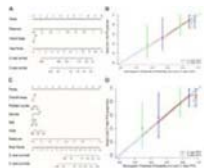
Mariama Fofana<sup>1</sup>, Jessica KR Boulton<sup>1</sup>, Maria Vinci<sup>1</sup>, Valeria Molinari<sup>1</sup>, Kathryn Taylor<sup>1</sup>, Sergey Popov<sup>1</sup>, Alan Mackay<sup>1</sup>, Chris Jones<sup>1</sup>, and Simon P Robinson<sup>1</sup>

<sup>1</sup>The Institute of Cancer Research, London, United Kingdom

988

8:15

**Multi-parametric MRI Radiomics for Pre-treatment Prediction of the Progression-Free Survival in Advanced Nasopharyngeal Carcinoma**



Bin Zhang<sup>1</sup>

<sup>1</sup>Guangdong General hospital, Guangzhou, People's Republic of China

989

8:15

**MR Elastography and Perfusion MRI for the Early Assessment of Treatment Response in Soft Tissue Sarcomas**

Tumor Location	Histology	Sex	Age (yrs)
<b>Patients Enrolled at a Single Time Point</b>			
1 Chest wall	Liposarcoma	M	37
2 Tricep	Pleomorphic sarcoma	F	55
3 Thigh	Pleomorphic sarcoma	M	64
4 Proximal Thigh	Fibrosarcoma	F	69
5 Ankle	Liposarcoma	M	52
6 Tricep	Ewing's sarcoma	M	55
<b>Patients Enrolled at Multiple Time Points and Pre-treatment</b>			
7 Paraspinal	Spindle cell sarcoma	M	43
8 Distal Thigh	Mixed liposarcoma	F	55
9 Calf	Mixed liposarcoma	F	62

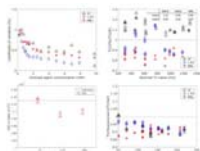
Kay Pepin<sup>1</sup>, Roger Grimm<sup>2</sup>, Soudabeh Kargar<sup>3</sup>, Sarah James<sup>1</sup>, Matthew Howe<sup>2</sup>, Karen Fritchie<sup>4</sup>, Matthew Frick<sup>2</sup>, Doris Wenger<sup>2</sup>, Richard Ehman<sup>2</sup>, Nadia Laack<sup>1</sup>, Michael Herman<sup>1</sup>, and Deanna Pafundi<sup>1</sup>

<sup>1</sup>Radiation Oncology, Mayo Clinic, Rochester, MN, United States, <sup>2</sup>Radiology, Mayo Clinic, Rochester, MN, United States, <sup>3</sup>Mayo Graduate School, Mayo Clinic, Rochester, MN, United States, <sup>4</sup>Pathology, Mayo Clinic, Rochester, MN, United States

990

8:15

### Quantitative Imaging for Radiotherapy on an MR-Linac Scanner



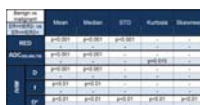
Folkert Koetsveld<sup>1</sup>, Leon C. ter Beek<sup>2</sup>, Petra J. van Houdt<sup>1</sup>, Laurens D. van Buuren<sup>1</sup>, and Uulke A. van der Heide<sup>1</sup>

<sup>1</sup>Radiotherapy, Netherlands Cancer Institute, Amsterdam, Netherlands, <sup>2</sup>Radiology, Netherlands Cancer Institute, Amsterdam, Netherlands

991

8:15

### Support vector machine for breast cancer classification using DWI histogram features: preliminary study



Igor Vidić<sup>1</sup>, Liv Egnell<sup>1</sup>, Jose R. Teruel<sup>2</sup>, Torill E. Sjøbakk<sup>3</sup>, Neil P. Jerome<sup>3</sup>, Agnes Østlie<sup>4</sup>, Hans E. Fjøsne<sup>5,6</sup>, Tone F. Bathen<sup>3</sup>, and Pål Erik Goa<sup>1</sup>

<sup>1</sup>Department of Physics, Norwegian University of Science and Technology (NTNU), Trondheim, Norway, <sup>2</sup>Department of Radiology, University of California, La Jolla, CA, United States, <sup>3</sup>Department of Circulation and Medical Imaging, Norwegian University of Science and Technology (NTNU), Trondheim, Norway, <sup>4</sup>Clinic of Radiology and Nuclear Medicine, St. Olavs University Hospital, Trondheim, Norway, <sup>5</sup>Department of Cancer Research and Molecular Medicine, Norwegian University of Science and Technology (NTNU), Trondheim, Norway, <sup>6</sup>Department of Surgery, St. Olavs University Hospital, Trondheim, Norway

## Power Pitch

## Pitch: Contrast Mechanisms: New Horizons

Power Pitch  
Theater B -  
Exhibition Hall

Thursday 8:15 - Moderators: Richard Dortch &  
9:15 Jongho Lee

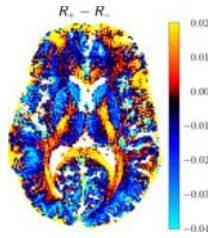
(no CME credit)

8:15

### On the decay of SSFP configurations

Damien Nguyen<sup>1,2</sup>, Rahel Heule<sup>1,2</sup>, Carl Ganter<sup>3</sup>, and Oliver Bieri<sup>1,2</sup>

992

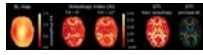


<sup>1</sup>Radiological Physics, University of Basel Hospital, Basel, Switzerland, <sup>2</sup>Department of Biomedical Engineering, University of Basel, Basel, Switzerland, <sup>3</sup>Department of Diagnostic Radiology, Klinikum rechts der Isar, Technical University Munich, Munich, Germany

993



8:15



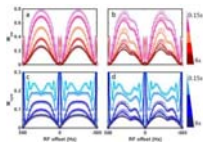
Asymmetries of the balanced SSFP profile allow to probe microstructure anisotropy at 9.4 Tesla

Philipp Ehses<sup>1,2</sup>, Mario Gilberto Báez-Yáñez<sup>2,3</sup>, Michael Erb<sup>1</sup>, and Klaus Scheffler<sup>1,2</sup>

<sup>1</sup>Biomedical Magnetic Resonance, University of Tübingen, Tübingen, Germany, <sup>2</sup>Dept. of High-Field Magnetic Resonance, Max Planck Institute for Biological Cybernetics, Tübingen, Germany, <sup>3</sup>Graduate Training Centre of Neuroscience, University of Tübingen, Tübingen, Germany

994

8:15



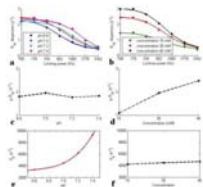
Quantitative modeling of exchange in bSSFPX

Shu Zhang<sup>1</sup>, Robert E Lenkinski<sup>1,2</sup>, and Elena Vinogradov<sup>1,2</sup>

<sup>1</sup>Department of Radiology, UT Southwestern Medical Center, Dallas, TX, United States, <sup>2</sup>Advanced Imaging Research Center, UT Southwestern Medical Center, Dallas, TX, United States

995

8:15



Spin-lock imaging of exogenous exchange-based contrast agents to assess tissue pH

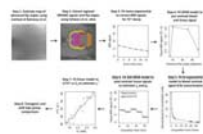
Zhongliang Zu<sup>1</sup>, Hua Li<sup>1</sup>, Xiaoyu Jiang<sup>1</sup>, and John C Gore<sup>1</sup>

<sup>1</sup>Vanderbilt University, Nashville, TN, United States

996



8:15



Quantification of trans-endothelial water exchange and vessel geometry using contrast-enhanced MRI and alterations in a transgenic rat model of Alzheimer's disease

Ben Dickie<sup>1</sup>, Hervé Boutin<sup>1,2</sup>, Jose Ulloa<sup>3,4</sup>, Laura M Parkes<sup>1</sup>, and Geoff JM Parker<sup>3</sup>

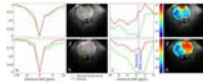
<sup>1</sup>Division of Neuroscience and Experimental Psychology, University of Manchester, Manchester, United Kingdom, <sup>2</sup>The Wolfson Molecular Imaging Centre, University of Manchester, Manchester, United Kingdom, <sup>3</sup>Division of Informatics, Imaging and Data Sciences, University of Manchester, Manchester, United Kingdom, <sup>4</sup>Bioxydyn, Manchester

---

997

8:15

[CEST-weighted MRI at 21.1 T: application to glioma and ischemic rat model](#)



Tangi Roussel<sup>1,2</sup>, Jens T. Rosenberg<sup>3</sup>, Samuel C. Grant<sup>3,4</sup>, and Lucio Frydman<sup>2</sup>

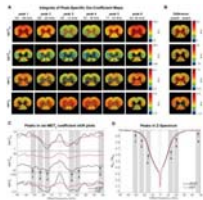
<sup>1</sup>NeuroSpin, Commissariat à l'Energie Atomique et aux Energies Alternatives, Gif-sur-Yvette, France, <sup>2</sup>Department of Chemical Physics, Weizmann Institute of Science, Rehovot, Israel, <sup>3</sup>National High Magnetic Field Laboratory, Florida State University, Tallahassee, FL, United States, <sup>4</sup>Department of Chemical & Biomedical Engineering, The Florida State University, Tallahassee, FL, United States

---

998

8:15

[Offset-Saturation-Induced \(osi-\) Variations in Multiexponential T2 at 16.4T: A New Dimension for Probing White Matter Contrast](#)



Teresa Serradas Duarte<sup>1</sup> and Noam Shemesh<sup>1</sup>

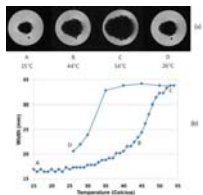
<sup>1</sup>Champlimaud Neuroscience Programme, Champlimaud Centre for the Unknown, Lisbon, Portugal

---

999

8:15

[Magneto-Caloric Materials as Tunable and Switchable Labels for MRI](#)



Mladen Barbic<sup>1</sup>, Tim D Harris<sup>1</sup>, Stephen Dodd<sup>2</sup>, H Douglas Morris<sup>3</sup>, Alan P Koretsky<sup>2</sup>, Barbara Marcheschi<sup>4</sup>, Alan Huston<sup>4</sup>, and Neil R Dilley<sup>5</sup>

<sup>1</sup>Applied Physics and Instrumentation Group, HHMI-Janelia Research Campus, Ashburn, VA, United States, <sup>2</sup>Laboratory of Functional and Molecular Imaging, NIH/NINDS, Bethesda, MD, United States, <sup>3</sup>NIH Mouse Imaging Facility, NIH/NINDS, Bethesda, MD, United States, <sup>4</sup>Code 5611, Optical Sciences Division, Naval Research Laboratory, Washington, DC, United States, <sup>5</sup>Quantum Design, Inc., San Diego, CA, United States

---

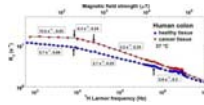
8:15

[The T1-Dispersion Curve as a Biomarker of Colorectal Cancer](#)

Vasileios Zampetoulas<sup>1</sup>, Lionel M. Broche<sup>1</sup>, Graeme I. Murray<sup>2</sup>, and David J. Lurie<sup>1</sup>



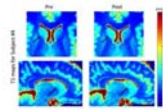
1000



<sup>1</sup>Aberdeen Biomedical Imaging Centre, School of Medicine, Medical Sciences & Nutrition, University of Aberdeen, AB25 2ZD, Scotland, United Kingdom, <sup>2</sup>Department of Pathology, University of Aberdeen, AB25 2ZD, Scotland, United Kingdom

1001

8:15



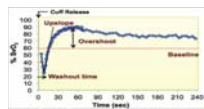
Detecting regional changes in brain tissue quantitative T1 values due to hydration status

Sofia Chavez<sup>1,2</sup>

<sup>1</sup>Centre for Addiction and Mental Health (CAMH), Toronto, ON, Canada, <sup>2</sup>Psychiatry, University of Toronto, Toronto, ON, Canada

1002

8:15



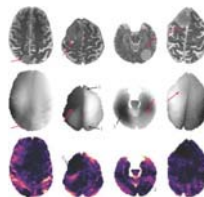
In vivo whole-blood  $T_2$  versus  $T_2^*$  calibration by modulating blood oxygenation level in the femoral vein through intermittent cuff occlusion

Michael C Langham<sup>1</sup>, Ana E Rodriguez-Soto<sup>1</sup>, Nadav Schwartz<sup>2</sup>, and Felix W Wehrli<sup>1</sup>

<sup>1</sup>Radiology, University of Pennsylvania, Philadelphia, PA, United States, <sup>2</sup>Obstetrics and Gynecology, University of Pennsylvania, Philadelphia, PA, United States

1003

8:15



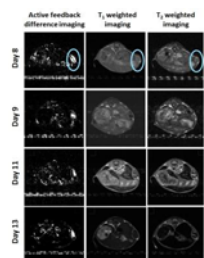
Visualizing local mechanical properties of agar phantoms and meningioma patients using magnetic resonance rheology

Sebastian Theilenberg<sup>1</sup>, Jakob Bindl<sup>1</sup>, Anna-Lisa Kofahl<sup>1</sup>, Carsten Urbach<sup>1</sup>, and Karl Maier<sup>1</sup>

<sup>1</sup>Helmholtz-Institut für Strahlen- und Kernphysik, University of Bonn, Bonn, Germany

1004

8:15



Early Cancer Detection Using Paramagnetic Liposome by a Novel Contrast Mechanism with Active-feedback Magnetic Resonance Imaging

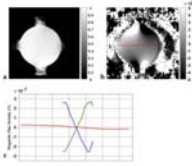
Sayoni Ray<sup>1</sup>, Chao-Hsiung Hsu<sup>2</sup>, Zhao Li<sup>1</sup>, Fang-Chu Lin<sup>1</sup>, Ying-Chih Lin<sup>2</sup>, and Yung-Ya Lin<sup>1</sup>

<sup>1</sup>DEPARTMENT OF CHEMISTRY AND BIOCHEMISTRY, University Of California, Los Angeles, Los Angeles, CA, United States, <sup>2</sup>Department of Chemistry, National Taiwan University, Taiwan



1005

8:15



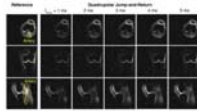
Analysis of magnetohydrodynamic effects in current injection induced magnetic flux density images at very high magnetic fields

Atul S Minhas<sup>1</sup>, Munish Chauhan<sup>2</sup>, and Rosalind J Sadleir<sup>2</sup>

<sup>1</sup>Centre for Pre-clinical Imaging, Department of Cellular and Molecular Physiology, University of Liverpool, Liverpool, United Kingdom, <sup>2</sup>School of Biological and Health Systems Engineering, Arizona State University, Tempe, AZ, United States

1006

8:15



Quadrupolar jump-and-return sequence for sodium knee MRI at 7 tesla

Jae Seung Lee<sup>1</sup>, Ding Xia<sup>1</sup>, and Ravinder Regatte<sup>1</sup>

<sup>1</sup>Radiology, New York University, New York, NY, United States

## Oral

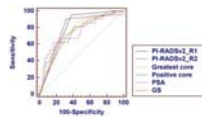
# Prostate Cancer

Room 310

Thursday 8:15 - 10:15 Moderators: Daniel Margolis

1007

8:15



PI-RADS Version 2: Preoperative Role in the Detection of Normal-sized Pelvic Lymph Node Metastasis in Prostate Cancer

Young Taik Oh<sup>1</sup>, Sung Yoon Park<sup>1</sup>, and Dae Chul Jung<sup>1</sup>

<sup>1</sup>Radiology, Yonsei University College of Medicine, Seoul, Korea, Republic of

Although the identification of pelvic lymph node metastasis (PLNM) is important in prostate cancer, sometimes PLNM are often not so enlarged on imaging. Therefore, we were trying to identify normal sized PLNM through PI-RADS v2 scores of 221 patients with prostate cancer. In our study, a threshold of PI-RADS v2 score of 5 seems to be associated with an increased risk of normal-sized PLNM, which may help identify the need for further node-specific imaging studies or pelvic lymph node dissection when a patient with prostate cancer has only normal-sized pelvic lymph nodes on preoperative imaging.

1008

8:27



Sparse Prostate Cancers on Whole-Mount Histopathology and Multiparametric MRI

Olga Starobinets<sup>1,2</sup>, Jeffrey P Simko<sup>3</sup>, Kyle Kuchinsky<sup>3</sup>, Peter R Carroll<sup>4</sup>, Kirsten L Greene<sup>4</sup>, John Kurhanewicz<sup>1,2</sup>, and Susan M Noworolski<sup>1,2</sup>

<sup>1</sup>Department of Radiology and Biomedical Imaging, University of California, San Francisco, San Francisco, CA, United States, <sup>2</sup>Graduate Group in Bioengineering, University of California, San Francisco and Berkeley, San Francisco, CA, United States, <sup>3</sup>Department of Pathology, University of California, San Francisco, San Francisco, CA, United States, <sup>4</sup>Department of Urology, University of California, San Francisco, San Francisco, CA, United States

The study purpose was to establish incidence and Gleason Score of sparse lesions on whole-mount histopathology in post-prostatectomy samples and to identify imaging characteristics associated with sparse cancers detected on multiparametric MRI (mpMRI). Based on histopathology, sparse lesions were smaller than dense lesions (0.065cc vs 0.916cc), with the majority (56/57 sparse) being low-grade (GS3+3). On imaging, we found statistically significant differences between sparse GS3+3 and benign tissues on apparent diffusion coefficient and peak enhancement maps. This combined with small-size and low-grade, and thus low clinical importance [1] of sparse lesions suggests that current mpMRI capabilities are sufficient to characterize these lesions.

1009



8:39

Characteristics	
Number of patients	76
Age	Median 67.8 IQR 63.8 - 71.3
Highest grade of histology	No histology
	Range
	Gleason 6
	Gleason 7
Gleason 8/9	
Highest mpMRI Likert score	2
	3
	4
	5

### Microstructural Diffusion-Weighted (VERDICT) MRI Metrics are Repeatable and Show Potential at Characterising Gleason 7 Prostate Cancer Non-Invasively

Edward William Johnston<sup>1</sup>, Elisenda Bonet-Carne<sup>2</sup>, Hayley Pye<sup>3</sup>, Joey Clemente<sup>1</sup>, Ben Yvernault<sup>2</sup>, Dominic Patel<sup>4</sup>, Susan Heavey<sup>3</sup>, Mrishta B Appayya<sup>1</sup>, Alexandra Saborowska<sup>5</sup>, Ashwin Sridhar<sup>6</sup>, Greg Shaw<sup>6</sup>, Sebastien Ourselin<sup>2</sup>, David Hawkes<sup>2</sup>, Caroline Moore<sup>6</sup>, Hayley Whitaker<sup>3</sup>, Manuel Rodriguez-Justo<sup>4</sup>, Alexander Freeman<sup>4</sup>, Eleftheria Panagiotaki<sup>2</sup>, Daniel Alexander<sup>2</sup>, and Shonit Punwani<sup>1</sup>

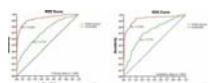
<sup>1</sup>Centre for Medical Imaging, University College London, London, United Kingdom, <sup>2</sup>Centre for Medical Image Computing, University College London, London, United Kingdom, <sup>3</sup>Research Department for Tissue & Energy, University College London, London, United Kingdom, <sup>4</sup>Department of Pathology, University College London Hospital, University Street, United Kingdom, <sup>5</sup>Radiology, University College London Hospitals, London, United Kingdom, <sup>6</sup>Department of Urology, University College London Hospital, London, United Kingdom

In this study we we assess the repeatability of VERDICT (Vascular, Extracellular, and Restricted Diffusion for Cytometry in Tumours) MRI parameters in prostate cancer consider their ability to distinguish between Gleason grades compared with the standard ADC model in 71 patients. Four of the parametric maps derived from the VERDICT technique were found to be satisfactorily repeatable for use as a clinical tool, and are capable of identifying a Gleason 7 component in prostate cancer where ADC failed to do so. VERDICT therefore holds great potential for use in clinical prostate cancer management pathways in the future.

---

1010

8:51



Machine learning analysis of multi-parametric MRI helps to improve the predictive performance in prostate cancer

Rui Wang<sup>1</sup> and Xiaoying Wang<sup>1</sup>

*<sup>1</sup>Peking University First Hospital, Beijing, People's Republic of China*

We first investigated the systemic outcome of a crowd underwent PSA-based screening and pre-biopsy mp-MRI, and demonstrated the predictive role of pre-biopsy mp-MRI for PCa by using an advanced machine learning-based approach. Here we answer one important question at the beginning of the paper: (1) mp-MRI coupled with PSA screening program can be used to detect PCa. By the constructed nomogram, the outcome of most patients could be accurately predicted in the first 1-yr follow-up period if they received a pre-biopsy mp-MRI examination, even without invasive TRUS biopsy.

---

1011

9:03



A comprehensive study of machine-assisted classifiers for predicting prostate cancer Gleason grade

Jing Wang<sup>1</sup>, Yang Fan<sup>2</sup>, and Yudong Zhang<sup>3</sup>

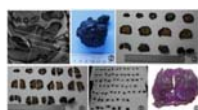
*<sup>1</sup>Center for Medical Device Evaluation, CFDA, Beijing, People's Republic of China, <sup>2</sup>MR Research China, GE Healthcare, Beijing, People's Republic of China, <sup>3</sup>Department of Radiology, the First Affiliated Hospital with Nanjing Medical University, Nanjing, People's Republic of China*

We performed comprehensive study of eight popularized classifiers for predicting prostate cancer (PCa) Gleason score (GS). The multi-parametric MRI data was obtained from 205 histopathology-confirmed PCa. The MR features were modeled using eight classifiers to predict high-GS (4+4) PCa, including Logistic Regression (LR), Artificial Neural Network (ANN), Support Vector Machine (SVM), Naive Bayes (NB), Relevance Vector Machine (RVM), Least Absolute Shrinkage and Selection operator (LASSO), Discriminant Analysis (DA) and Decision Tree (DT) analysis. Results showed that LASSO and DA had significantly higher area under curve than other classifiers, thus could be valuable for automatic prediction of PCa grade.

---

1012

9:15



The value of multiparametric MR Imaging in predicting the volume of clinically significant prostate cancer: a whole-mount step-section analysis

Jian Jiang<sup>1</sup>, Huihui Wang<sup>1</sup>, and Xiaoying Wang<sup>1</sup>

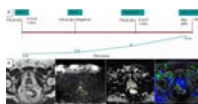
*<sup>1</sup>Peking University First Hospital, Beijing, People's Republic of China*

This study is to assess the factors influencing multiparametric (MP) MR Imaging accuracy in estimating the volume of clinically significant prostate cancer (Vh) by using whole-mount step-section slides as standard of reference.

---

1013

9:27



MRI guided biopsy in Patients with positive TRUS-biopsy: Necessity or Overkill?

Kareem K Elfatairy<sup>1</sup>, Christopher P Filson<sup>2</sup>, Adeboye O Osunkoya<sup>3</sup>, Rachel L Geller<sup>3</sup>, and Sherif G Nour<sup>1</sup>

*<sup>1</sup>Radiology, Emory University-School of Medicine, Atlanta, GA, United States, <sup>2</sup>Urology, Emory University-School of Medicine, Atlanta, GA, United States, <sup>3</sup>Pathology, Emory University-School of Medicine, Atlanta, GA, United States*

TRUS biopsy (TRUS-Bx) is the standard of care for prostate cancer diagnosis but has several limitations. Multiparametric MRI and MRI guided biopsy (MRGB) show considerable added benefits with better disease detection and stratification. The purpose of this study is to evaluate the role of in-bore MRI guided biopsy in patients with positive TRUS-Bx. 40 patients with 71 TRUS-Bx positive lesions were analyzed for cancer detection rate, false negative rate, and Gleason score upgrade by MRGB. MRGB showed 65% cancer detection rate, 35 % false negative rate, and upgraded disease status in 40% of the whole sample

1014

9:39



### Effects of 5 alpha-Reductase Inhibitors on Detection of Prostate Cancer on MRI

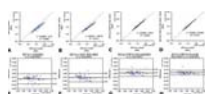
Lori Mankowski Gettle<sup>1</sup>, Shivashankar Damodaran<sup>2</sup>, David F. Jarrard<sup>2</sup>, and Frederick Kelcz<sup>1</sup>

*<sup>1</sup>Radiology, University of Wisconsin School of Medicine and Public Health, Madison, WI, United States, <sup>2</sup>Urology, University of Wisconsin School of Medicine and Public Health, Madison, WI, United States*

5 alpha reductase inhibitors have shown promise in increasing the detection of prostate cancer in prior ultrasound studies. No studies have been performed looking at the effect of 5 alpha reductase inhibitors on increasing the conspicuity of prostate cancer in MRI. The purpose of this study was to determine if treatment with a 5 alpha reductase inhibitor could increase sensitivity for the detection of prostate cancer in the background setting of benign prostatic hypertrophy.

1015

9:51



### Improved Accuracy of Apparent Diffusion Coefficient (ADC) Quantification: Evaluation in Prostate Diffusion Imaging without Using Endorectal Coils

Xiaodong Zhong<sup>1,2</sup>, Marcel D. Nickel<sup>3</sup>, Stephan A.R. Kannengiesser<sup>3</sup>, Alto Stemmer<sup>3</sup>, Brian M. Dale<sup>4</sup>, Berthold Kiefer<sup>3</sup>, and Mustafa R. Bashir<sup>5</sup>

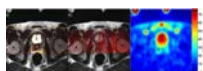
*<sup>1</sup>MR R&D Collaborations, Siemens Healthcare, Atlanta, GA, United States, <sup>2</sup>Department of Radiology and Imaging Sciences, Emory University, Atlanta, GA, United States, <sup>3</sup>MR Application Predevelopment, Siemens Healthcare, Erlangen, Germany, <sup>4</sup>MR R&D Collaborations, Siemens Healthcare, Cary, NC, United States, <sup>5</sup>Center for Advanced Magnetic Resonance Development, Duke University Medical Center, Durham, NC, United States*

In prostate DWI, low SNR often causes inaccuracy in ADC quantification if not compensated, especially when using surface array coils. Endorectal coils can be used, although associated with substantial setup time, patient discomfort and complications. In this work, a noise bias correction framework was developed and validated in a Monte Carlo simulation, a diffusion phantom, and 14 prostate imaging subjects. Using data acquired with an endorectal coil as a reference, this framework showed improved accuracy of ADC quantification in the prostate when only non-endorectal coils were used. This framework may allow quantitative prostate diffusion imaging without requiring endorectal coils.

1016



10:03



Multi-Parametric/-Nuclear  $1\text{H}/^{23}\text{Na}$  Clinical Protocol of the Prostate at 3T using a Double Resonant Coil

Nadia K Paschke<sup>1</sup>, Daniel Hausmann<sup>2</sup>, Lothar R Schad<sup>1</sup>, Stefan O Schönberg<sup>2</sup>, and Frank G Zöllner<sup>1</sup>

<sup>1</sup>Computer Assisted Clinical Medicine, Medical Faculty Mannheim, Heidelberg University, Mannheim, Germany, <sup>2</sup>Institute of Clinical Radiology and Nuclear Medicine, University Medical Center Mannheim, Medical Faculty Mannheim, Heidelberg University, Mannheim, Germany

Prostate cancer is the most common malignancy in men. T2-weighted magnetic resonance imaging (MRI) has been shown to provide detailed information about anatomical structures but suffers from low specificity of morphological abnormalities. To enhance identification of malignant lesions, we set up a multi-parametric and multi-nuclear clinical protocol, in which sodium ( $^{23}\text{Na}$ -) MRI and diffusion weighted imaging with standard and high b-values are added to the morphological T2-weighted sequences. Using a double resonant  $^{23}\text{Na}/^1\text{H}$  abdominal coil allows acquiring sodium images directly after high resolution clinical proton sequences. Coil changes become unnecessary, which improves clinical feasibility.

Oral

## Motion Correction: No Brainer

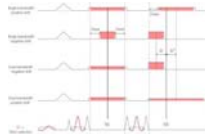
Room 311

Thursday 8:15 - 10:15

Moderators: Martina Callaghan & Daniel Gallichan

1017

8:15



T1-weighted two-point fat/water separated PROPELLER acquired with dual bandwidths

Henric Rydén<sup>1</sup>, Johan Berglund<sup>2,3</sup>, Enrico Avventi<sup>1,4</sup>, Ola Norbeck<sup>1,4</sup>, and Stefan Skare<sup>1,4</sup>

<sup>1</sup>Neuroradiology, Karolinska University Hospital, Stockholm, Sweden, <sup>2</sup>Department of Clinical Science, Intervention and Technology, Karolinska Institutet, Stockholm, Sweden, <sup>3</sup>Department of Medical Radiation Physics, Karolinska University Hospital, Stockholm, Sweden, <sup>4</sup>Department of Clinical Neuroscience, Karolinska Institutet, Stockholm, Sweden

A PROPELLER sequence with dual bandwidths was developed for T1-weighted fat/water separated imaging. The bandwidth of the second readout was adjusted to remove dead time related to shifted readouts in order to improve SNR efficiency. Before PROPELLER reconstruction, blade-wise fat/water separation was performed in k-space to remove chemical shift displacement artifacts. This enabled low bandwidth acquisitions without smearing of the fat signal, which further improved SNR efficiency. Strong fat suppression insensitive to B0 inhomogeneity was demonstrated in imaging of the neck and orbits.

1018

8:27



Fast, non-local temporally regularized elastic group-wise motion correction for improved fidelity of liver DCE-MRI

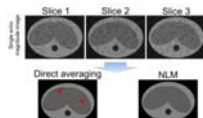
Ks Shriram<sup>1</sup>, Dattesh D Shanbhag<sup>1</sup>, Jeong Hee Yoon<sup>2</sup>, Uday Patil<sup>1</sup>, Moon Jung Hwang<sup>3</sup>, Jeong Min Lee<sup>2</sup>, Rakesh Mullick<sup>1</sup>, and Sheshadri Thiruvankadam<sup>1</sup>

<sup>1</sup>GE Global Research, Bangalore, India, <sup>2</sup>Seoul National University Hospital, Seoul, Korea, Republic of, <sup>3</sup>GE Healthcare, Seoul, Korea, Republic of

A novel group-wise registration methodology using non-local regularization is presented for liver DCE-MRI data that can provide robust motion correction even in cases of large deformations, restores DCE data characteristics, generates physiologically relevant PK maps and is feasible for clinical practice due to short computation time.

1019

8:39



A novel fat and iron quantification technique with non-rigid motion-corrected averaging based on non-local means

Huiwen Luo<sup>1,2</sup>, Curtis Wiens<sup>1</sup>, Ann Shimakawa<sup>3</sup>, Scott B. Reeder<sup>1,4,5,6,7</sup>, Kevin M. Johnson<sup>1,4</sup>, and Diego Hernando<sup>1,4</sup>

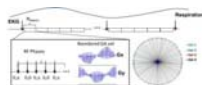


<sup>1</sup>Radiology, University of Wisconsin-Madison, Madison, WI, United States, <sup>2</sup>Electronic engineering, Tsinghua University, Beijing, People's Republic of China, <sup>3</sup>Global MR Applications and Workflow, GE Healthcare, Madison, WI, United States, <sup>4</sup>Medical Physics, University of Wisconsin-Madison, Madison, WI, United States, <sup>5</sup>Biomedical engineering, University of Wisconsin-Madison, Madison, WI, United States, <sup>6</sup>Medicine, University of Wisconsin-Madison, Madison, WI, United States, <sup>7</sup>Emergency Medicine, University of Wisconsin-Madison, Madison, WI, United States

In this study, we developed and validated a free-breathing fat and R2\* quantification technique using a multi-average 2D sequential acquisition with non-rigid motion-corrected averaging based on a non-local means (NLM) approach. The proposed technique was applied to simulated data as well as free-breathing liver acquisitions in volunteers. Both direct averaging and the proposed NLM technique were applied to the data to improve SNR. Compared to direct averaging, the proposed NLM technique resulted in improved image quality without motion artifacts, as well as accurate fat and R2\* measurements in both simulations and in vivo acquisitions.

1020

8:51



Investigation of Simultaneous Multi-slice Imaging Utilized for Respiratory Gating: A Golden Angle Radial CAIPI Free-Breathing Cine Method

Dana C Peters<sup>1</sup>, Chenxi Hu<sup>2</sup>, Yuqing Wan<sup>1</sup>, and Maolin Qiu<sup>1</sup>

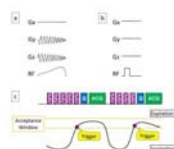
<sup>1</sup>Yale University, New Haven, CT, United States, <sup>2</sup>Yale University

<sup>1</sup>Yale University, New Haven, CT, United States, <sup>2</sup>Yale University

We investigated simultaneous multi-slice as a method for performing respiratory-gating. One slice is used to monitor respiration, while another slice is targeted for imaging. Radial CAIPI data was acquired using a golden angle ordering for free-breathing 2D cine. At each cardiac phase and at each heart-beat, images of the heart and the diaphragm were obtained. Finally, a composite image of the heart was reconstructed using data from all frames acquired at end-expiration, with more projections and higher quality than a single heart-beat image.

1021

9:03



Silent Navigator-Triggered Silent-MRI in Abdomen

Yuji Iwadate<sup>1</sup>, Atsushi Nozaki<sup>1</sup>, Yoshinobu Nunokawa<sup>2</sup>, Shigeo Okuda<sup>3</sup>, Masahiro Jinzaki<sup>3</sup>, and Hiroyuki Kabasawa<sup>1</sup>

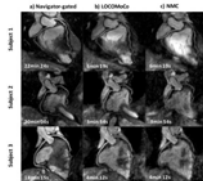
<sup>1</sup>Global MR Applications and Workflow, GE Healthcare Japan, Hino, Japan, <sup>2</sup>Office of Radiation Technology, Keio University Hospital, Tokyo, Japan, <sup>3</sup>Department of Radiology, Keio University School of Medicine, Tokyo, Japan

We incorporated a silent navigator (sNav) with the whole volume excitation into zero-TE pulse sequence for respiratory motion corrected silent abdominal imaging. The sNav signals showed an excellent correlation between the bellows signals, and resultant zero-TE images had better contrasts than those acquired without respiratory triggering. The sNav-triggered zero-TE technique is expected to be used in abdominal MRI where acoustic noise is problematic (e.g. pediatric patient imaging with anesthesia).

1022

9:15

Accelerated motion compensated 3D isotropic coronary MRA using variable density Cartesian sampling



Teresa M Correia<sup>1</sup>, Gastao Cruz<sup>1</sup>, Camila Munoz<sup>1</sup>, Rene Botnar<sup>1</sup>, and Claudia Prieto<sup>1</sup>

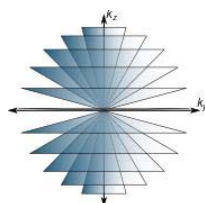
<sup>1</sup>Division of Imaging Sciences and Biomedical Engineering, King's College London, London, United Kingdom

Accelerated whole-heart 3D isotropic coronary MR angiography (CMRA) is achieved by undersampling the acquisition using a variable-density radial Cartesian (VDRC) trajectory and performing non-rigid respiratory motion correction directly in the low-dimensional-structure self-learning and thresholding (LOST) reconstruction. The proposed approach corrects for 2D beat-to-beat translational and 3D bin-to-bin non-rigid motion. The former is estimated from interleaved image navigators and the latter directly from the CMRA data. The VDRC trajectory provides improved respiratory bin reconstructions and initial image estimate for LOST. The proposed approach produces good quality images, comparable to those of a two-fold accelerated navigator-gated acquisition with ~4x longer scan time.

1023

9:27

Evaluation of Self-Navigated Golden-Angle Ordered Conical Ultrashort Echo Time (UTE) MRI of the Abdomen on Pediatric Patients in Multiple Sedation States



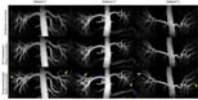
Anshul Haldipur<sup>1</sup>, Evan James Zucker<sup>1</sup>, Joseph Y. Cheng<sup>1</sup>, Michael Carl<sup>2</sup>, and Shreyas S. Vasanawala<sup>1</sup>

<sup>1</sup>Radiology, Stanford University, Stanford, CA, United States, <sup>2</sup>Applied Science Laboratory, GE Healthcare, San Diego, CA, United States

To assess the feasibility of conical k-space trajectory free-breathing UTE abdominal MRI and the effects on image quality of 50% data subsampling (thereby potentially shortening scans) and soft-gated motion correction reconstruction techniques, 42 consecutive pediatric patients were recruited and scanned. The images were scored in blinded fashion by two readers. Adequate delineation was obtained for all evaluated abdominal structures except the hepatic artery. 50% subsampling decreased image quality only slightly, favoring the implementation of a shorter scan time with negligible diagnostic compromise. Overall, motion correction mildly degraded image quality, possibly due to greater noise from data subsampling.

1024

9:39



Quantification, Analysis, and Correction of Nonrigid Motion in Free-Breathing, Non-Contrast-Enhanced Renal Angiography using 3D Image-Based Navigators

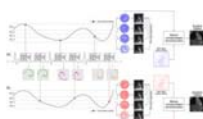
Srivathsan P. Koundinyan<sup>1</sup>, Corey A. Baron<sup>1</sup>, Mario O. Malavé<sup>1</sup>, Nii Okai Addy<sup>1</sup>, Jieying Luo<sup>1</sup>, R. Reeve Ingle<sup>1</sup>, and Dwight G. Nishimura<sup>1</sup>

<sup>1</sup>Electrical Engineering, Stanford University, Stanford, CA, United States

We present a method that leverages 3D image-based navigators (iNAVs) for nonrigid motion correction in free-breathing, non-contrast-enhanced renal angiography scans. We begin by performing an ROI-based analysis of 3D iNAV motion, with ROI selection based on published biomechanical simulations of the renal arteries during respiration. Then, we demonstrate that localized motion estimates derived from different ROIs agree with the findings of the simulations. Finally, we combine the extracted motion information with an autofocusing technique for respiratory motion compensation. Across all patient studies, the proposed method significantly improves the depiction of the renal arteries as compared to 3D translational motion correction.

1025

9:51



Highly efficient respiratory motion corrected dual-phase coronary MR angiography in a 3T PET-MR system

Camila Munoz<sup>1</sup>, Radhouene Neji<sup>1,2</sup>, Rene Botnar<sup>1</sup>, and Claudia Prieto<sup>1</sup>

<sup>1</sup>Division of Imaging Sciences and Biomedical Engineering, King's College London, London, United Kingdom, <sup>2</sup>MR Research Collaborations, Siemens Healthcare, Frimley, United Kingdom

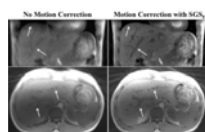


Respiratory motion remains a major challenge for dual-phase coronary MR angiography (CMRA). Here we propose an efficient acquisition and reconstruction scheme, that allows for inline 2D translational and offline 3D non-rigid motion-corrected systolic and diastolic CMRA using image-based navigators. Results from healthy volunteers show that motion correction improves visualization of the right and left coronary arteries in both cardiac phases. The proposed scheme potentially allows for comprehensive diagnosis of coronary artery disease using simultaneous PET-MR by acquiring coronary anatomy and left-ventricular function with the dual-phase CMRA and myocardial perfusion/viability with PET in an efficient cardiac and respiratory motion-compensated framework.

---

1026

10:03



### Respiratory Motion Compensation in the Liver using Fat-Only Self Gated Signal

Thomas Martin<sup>1,2</sup>, Tess Armstrong<sup>1,2</sup>, Ely Felker<sup>2</sup>, James Sayre<sup>2</sup>, Steve Raman<sup>2</sup>, Holden Wu<sup>2</sup>, and Kyunghyun Sung<sup>2</sup>

<sup>1</sup>Biomedical Physics, University of California, Los Angeles, Los Angeles, CA, United States, <sup>2</sup>Radiological Sciences, University of California, Los Angeles, Los Angeles, CA, United States

A multi-echo 3D golden angle radial gradient echo (GRE) sequence for fat-only respiratory motion extraction is a promising technique for liver dynamic contrast enhancement MRI (DCE-MRI), because it has inherent motion robustness, while providing other advantages, such as water-only images and  $R_2^*$  mapping. In this work we demonstrate that respiratory motion correction in the liver can be achieved using a fat-only self-navigated signal with minimal error in the fat-water separation (< 5%). Using this technique has implications of a more robust motion correction for liver DCE-MRI due to its inherent separation between respiratory motion signal and contrast uptake.

---

Oral

## Preclinical Molecular Imaging

Room 313A

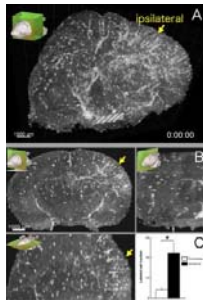
Thursday 8:15 - 10:15 Moderators: Xiaoping Hu & Paula Foster

---

1027

8:15

Quantitative four-dimensional motility tracking of individual immune cells in living mouse brain



Yuki Mori<sup>1,2</sup>, Daniela Martinez de la Mora<sup>1,2</sup>, Atsuki Tashita<sup>3</sup>, Syoji Kobashi<sup>3</sup>, Ikuhiro Kida<sup>2</sup>, Yutaka Hata<sup>4</sup>, and Yoshichika Yoshioka<sup>1,2</sup>

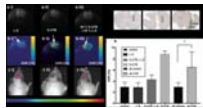
<sup>1</sup>Biofunctional Imaging, WPI Immunology Frontier Research Center, Osaka University, Suita, Osaka, Japan, <sup>2</sup>Center for Information and Neural Networks, National Institute of Information and Communications Technology and Osaka University, <sup>3</sup>Graduate School of Engineering, University of Hyogo, <sup>4</sup>Graduate School of Simulation Studies, University of Hyogo

Improved imaging techniques are being used to broaden the scope and better understanding of the complex cell behaviours in the body. Nonetheless, the migratory behavior of immune cells after CNS injury is still poorly understood. In this study, we employed four-dimensional (4D) MRI to monitor the dynamic migration of infiltrating monocytes/macrophages in the living mouse brain. Our results demonstrate the possibility of non-invasive long-term monitoring of individual live cells. Moreover, this innovative technique furthers our understanding of the cellular mechanisms occurring in the normal and injured brain tissues.

1028



8:27



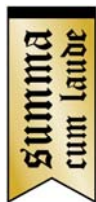
A gene reporter detected using MRI measurements of reporter-mediated increases in transmembrane water exchange

Franz Schilling<sup>1</sup>, Susana Ros<sup>1</sup>, De-En Hu<sup>1</sup>, Paula D'Santos<sup>1</sup>, Sarah McGuire<sup>1</sup>, Richard Mair<sup>1</sup>, Alan Wright<sup>1</sup>, Elizabeth Mannion<sup>1</sup>, Robin J.M. Franklin<sup>2</sup>, André A. Neves<sup>1</sup>, and Kevin M. Brindle<sup>1</sup>

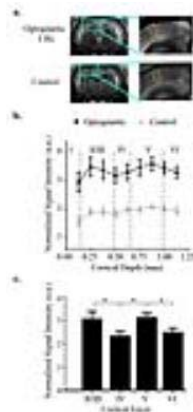
<sup>1</sup>Cancer Research UK Cambridge Institute, University of Cambridge, Cambridge, United Kingdom, <sup>2</sup>Wellcome Trust-Medical Research Council Stem Cell Institute and Department of Clinical Neurosciences, University of Cambridge

Non-invasive imaging of gene expression can be used to track cells in vivo but often requires the addition of an exogenous contrast agent that may have limited tissue access. We show that the urea transporter (UT-B) can be used as a gene reporter, where reporter expression was detected using <sup>1</sup>H MRI measurements of UT-B-mediated increases in plasma membrane water exchange. AXR values measured in UT-B-expressing HEK cell xenografts, were significantly higher compared with non-expressing controls. Transduction of rat brain cells with a lentiviral vector expressing UT-B resulted in a  $\approx$  2-fold increase in AXR at the site of virus injection.

1029



8:39



### Brain-wide Interaction of Low Frequency Hippocampal Activity with Layer-specific Cortical and Subcortical Regions: An Optogenetic Manganese-enhanced MRI Study

Yongrong Qiu<sup>1,2</sup>, Leon C. Ho<sup>1,2</sup>, Russell W. Chan<sup>1,2</sup>, Alex T.L. Leong<sup>1,2</sup>, Xunda Wang<sup>1,2</sup>, Celia M. Dong<sup>1,2</sup>, and Ed X. Wu<sup>1,2</sup>

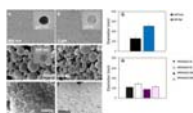
<sup>1</sup>Laboratory of Biomedical Imaging and Signal Processing, The University of Hong Kong, Hong Kong, SAR, People's Republic of China, <sup>2</sup>Department of Electrical and Electronic Engineering, The University of Hong Kong, Hong Kong, SAR, People's Republic of China

The hippocampus, including the dentate gyrus (DG), and the sensory cortices, which consist of six distinct layers, have reciprocal connections with the entorhinal cortex (EC). However, the low frequency hippocampal-cortical interactions and layer-specific cortical responses remains largely unknown. Combining the optogenetic stimulation and manganese-enhanced MRI, the present study revealed layer-specific responses of sensory cortices and EC involvement in hippocampal-cortical interactions during low frequency stimulation, but not high frequency, at dorsal DG. In summary, we demonstrated an effective combination of optogenetic stimulation and manganese-enhanced MRI to uncover the frequency-dependent and cortical layer-specific responses involved in brain-wide interactions.

1030



8:51



### Novel Polymer and Peptide REACTION-based Theranostics for MRI.

Laura Szkolar Sienkiewicz<sup>1</sup>, Dorela Shuboni-Mulligan<sup>1</sup>, Christiane Mallett<sup>1</sup>, and Erik Shapiro<sup>1</sup>

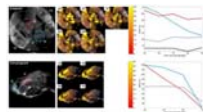
<sup>1</sup>Radiology, Michigan State University, East Lansing, MI, United States

MRI offers a unique opportunity for theranostic agent development. By engineering both polymer and peptide materials, we have scope to successfully target, image and treat a range of biological conditions. Here we successfully demonstrate the use of targeted and triggered nanoparticles, encapsulating imaging and chemotherapeutic agents, as theranostics for MRI.

1031



9:03



### Maternal and fetal glucose uptake followed by chemical exchange saturation transfer imaging (glucoCEST) on pregnant mice at 21.1T

Stefan Markovic<sup>1</sup>, Jens Rosenberg<sup>2</sup>, Shannon Helsper<sup>2</sup>, Tangi Roussel<sup>3</sup>, Michal Neeman<sup>4</sup>, Samuel Grant<sup>2,5</sup>, and Lucio Frydman<sup>1</sup>



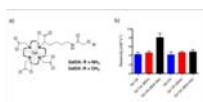
<sup>1</sup>Department of Chemical Physics, Weizmann Institute of Science, Rehovot, Israel, <sup>2</sup>National High Magnetic Field Laboratory, Florida State University, Tallahassee, FL, United States, <sup>3</sup>NeuroSpin Centre CEA Saclay, Gif-sur-Yvette, France, <sup>4</sup>Department of Biological Regulation, Weizmann Institute of Science, Rehovot, Israel, <sup>5</sup>Chemical & Biomedical Engineering Department, FAMU-FSU College of Engineering, Tallahassee, FL

GlucoCEST generates a contrast that is sensitive to glucose uptake and metabolism. While previously shown with tumor models, a distinct glucose metabolism is also characteristic of pregnancy. This study explores the potential of glucoCEST under this condition. Glucose was administered to pregnant mice by gavage in a manner akin to that used in human pregnancy-induced diabetes tests, and subsequently monitored *in-vivo* by glucoCEST at 21.1T. Distinct differences were apparent upon instituting glucose, with organ-specific glucoCEST contrast exceeding 50-70%. Notable imaging differences were noted between dams and fetuses upon glucose gavage, as well as between pregnant and non-pregnant animals.

1032



9:15



Molecular MR imaging of pulmonary fibrogenesis using the novel probe GdOA

Philip Alan Waghorn<sup>1</sup>, Chloe Jones<sup>1</sup>, Clemens Probst<sup>2</sup>, Diego Ferreira<sup>1</sup>, Nicholas Rotile<sup>1</sup>, Howard Chen<sup>1</sup>, Andrew Tager<sup>2</sup>, and Peter Caravan<sup>1</sup>

<sup>1</sup>A.A. Martinos Center for Biomedical Imaging, Charlestown, MA, United States, <sup>2</sup>Center for Immunology and Inflammatory Diseases, Massachusetts General Hospital, Charlestown, MA, United States

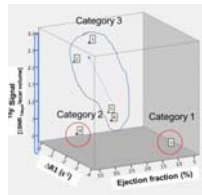
Fibrogenesis is a feature of idiopathic pulmonary fibrosis (IPF) that leads to the increased deposition and cross-linking of collagen. There remains a demand for non-invasive imaging of fibrogenesis in patients with suspected IPF to deliver earlier diagnoses and monitor treatment response. One universal feature of fibrogenesis is the oxidation of lysines on collagen to form allysine, which is a fundamental component for the cross-linking of collagen. We developed GdOA, a Gd-based MR probe that targets allysine as a marker for active fibrogenesis. We demonstrate that GdOA MR signal enhancement correlates with extent of disease and is sensitive to therapeutic response.

9:27

Molecular imaging of inflammation and extracellular matrix remodeling in a murine model of myocardial infarction



1033



Isabel Teixeira Ramos<sup>1,2</sup>, Markus Henningson<sup>1</sup>, Maryam Nezafat<sup>1</sup>, Begoña Lavin<sup>1</sup>, Silvia Lorrio<sup>1</sup>, Alkystis Phinikaridou<sup>1,2</sup>, Ulrich Flögel<sup>3</sup>, Ajay Shah<sup>2,4</sup>, and René Botnar<sup>1,2</sup>

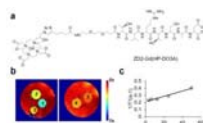
<sup>1</sup>Division of Imaging Sciences and Biomedical Engineering, King's College London, London, United Kingdom, <sup>2</sup>Cardiovascular Division, The British Heart Foundation Centre of Excellence, King's College London, London, United Kingdom, <sup>3</sup>Heinrich Heine University Düsseldorf, Düsseldorf, Germany, <sup>4</sup>Cardiovascular Division, James Black Centre, King's College London, London, United Kingdom

A suitable degree and timely resolution of inflammation and extracellular matrix (ECM) deposition are requirements for optimal healing and remodeling after myocardial infarction (MI). In this study, we explored the merits of multinuclear <sup>1</sup>H/<sup>19</sup>F MRI for the simultaneous assessment and quantification of cardiac inflammation and elastin deposition in a murine model of MI. <sup>19</sup>F containing particles, uptaken by macrophages, were used to investigate inflammatory cell recruitment into injured myocardium and an elastin-specific MR contrast agent was used to evaluate changes in elastin content in the ECM post-MI.

1034



9:39



MR molecular imaging of extradomain-B fibronectin for characterizing prostate cancer aggressiveness

Zheng Han<sup>1</sup>, Sarah Roelle<sup>1</sup>, Yuchi Liu<sup>1</sup>, Xin Yu<sup>1</sup>, and Zheng-Rong Lu<sup>1</sup>

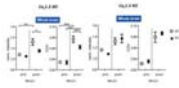
<sup>1</sup>Department of Biomedical Engineering, Case Western Reserve University, Cleveland, OH, United States

Accurate risk stratification is critical to the clinical management of prostate cancer. The objective of our study is to investigate the effectiveness of MR molecular imaging of EDB-FN for non-invasive localization and characterization of prostate cancer aggressiveness. An EDB-FN targeting Gd-based contrast, ZD2-Gd(HP-DO3A), was designed and synthesized. Molecular MRI of EDB-FN with ZD2-Gd(HP-DO3A) can specifically improve contrast enhancement in high-risk prostate tumors, not low-risk tumors, enabling accurate characterization of prostate cancer aggressiveness. Molecular MRI with the contrast agent has great promise for detection of high-risk prostate cancer, and non-invasive differential diagnosis and risk stratification of human prostate cancer.

1035

9:51

The Role of the L-type calcium channel Cav1.2 in MEMRI



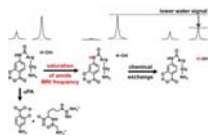
Benedikt Bedenk<sup>1</sup>, Suellen Almeida-Correa<sup>1</sup>, Carsten T Wotjak<sup>1</sup>, and Michael Czisch<sup>1</sup>

<sup>1</sup>Max Planck Institute of Psychiatry, Munich, Germany

L-type voltage-dependent  $\text{Ca}^{2+}$  channels of type  $\text{Ca}_v1.2$ , but not  $\text{Ca}_v1.3$ , are essential for  $\text{Mn}^{2+}$  accumulation in MEMRI.  $\text{Ca}_v1.2$  conditional knock-out animals were exploited to show that a bias exists towards  $\text{Mn}^{2+}$  accumulation in axon terminals and highly dense output structures. Our results have strong implications for the analysis of activity dependent  $\text{Mn}^{2+}$  accumulation.

1036

10:03



Detecting in vivo urokinase Plasminogen Activator activity with a catalyCEST MRI contrast agent

Sanhita Sinharay<sup>1</sup>, Christine M. Howison<sup>2</sup>, Amanda F. Baker<sup>3</sup>, and Mark D. Pagel<sup>2</sup>

<sup>1</sup>Chemistry and Biochemistry, University of Arizona, Tucson, AZ, United States, <sup>2</sup>Medical Imaging, University of Arizona, Tucson, AZ, United States, <sup>3</sup>University of Arizona Cancer Center, University of Arizona, Tucson, AZ, United States

**SYNOPSIS:** We have designed a nonmetallic contrast agent, GR-4Am-SA, that can detect the activity of urokinase Plasminogen Activator with CEST MRI. uPA cleaves a peptide of the agent which causes CEST at 5.0 ppm to decrease, but CEST at 9.5 ppm is unchanged. The two CEST signals were used to determine a reaction coordinate, representing the extent of enzyme-catalyzed cleavage of the GR-4Am-SA agent. GR-4Am-SA detected uPA activity in solution, and in a flank xenograft model of Capan-2 pancreatic cancer.

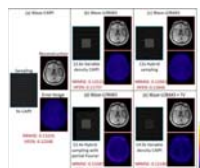
Oral

## All But Cartesian

Room 313BC

Thursday 8:15 - 10:15 Moderators: Pablo Irarrazaval & Craig Meyer

8:15



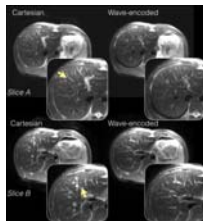
Wave-LORAKS for faster Wave-CAIPI MRI

Tae Hyung Kim<sup>1</sup>, Berkin Bilgic<sup>2,3</sup>, Daniel Polak<sup>4</sup>, Kawin Setsompop<sup>2,3</sup>, and Justin P. Haldar<sup>1</sup>



<sup>1</sup>Electrical Engineering, University of Southern California, Los Angeles, CA, United States, <sup>2</sup>A. A. Martinos Center for Biomedical Imaging, Charlestown, MA, United States, <sup>3</sup>Radiology, Harvard Medical School, Charlestown, MA, United States, <sup>4</sup>Medical Physics in Radiology, German Cancer Research Center (DKFZ), Heidelberg, Germany

Wave-CAIPI is a novel technique that enables accelerated acquisition with negligible g-factor penalty by using corkscrew readout trajectories, while LORAKS (LOW-RANK modeling of local K-Space neighborhoods) is a powerful approach to constrained reconstruction that integrates sparse support, phase, and parallel imaging constraints into a unified linear prediction framework. In this work, we propose a new fast imaging technique called Wave-LORAKS, which combines Wave-CAIPI acquisition with LORAKS-based reconstruction. Retrospective undersampling experiments with 3D T1-weighted data show that Wave-LORAKS enables higher acceleration and more flexible sampling compared to traditional Wave-CAIPI, allowing up to 15-fold acceleration with similar quality as 9-fold accelerated Wave-CAIPI.



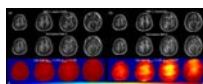
### Variable Density Single-Shot Fast Spin Echo with Auto-Calibrated Wave Encoding

Feiyu Chen<sup>1</sup>, Valentina Taviani<sup>2</sup>, Joseph Y Cheng<sup>3</sup>, Tao Zhang<sup>4</sup>, Brian A Hargreaves<sup>3</sup>, John M Pauly<sup>1</sup>, and Shreyas S Vasanawala<sup>3</sup>

<sup>1</sup>Electrical Engineering, Stanford University, Stanford, CA, United States, <sup>2</sup>Global MR Applications and Workflow, GE Healthcare, Menlo Park, CA, United States, <sup>3</sup>Radiology, Stanford University, Stanford, CA, United States, <sup>4</sup>Global MR Applications and Workflow, GE Healthcare, Houston, TX, United States

Wave encoding was implemented in a variable-density single-shot fast spin echo (VD-SSFSE) pulse sequence. Auto-calibrated estimation of the wave-encoding point-spread function (PSF) and coil sensitivity maps was used. Images were reconstructed with parallel imaging and compressed sensing reconstruction. Compared to non-wave-encoded Cartesian imaging, wave-encoded VD-SSFSE achieves improved image quality with reduced aliasing artifacts at higher acceleration factors and with full k-space coverage, providing fast acquisitions and clinically relevant echo times.

### Wave-CAIPI ViSta: Accelerated mapping for direct visualization of myelin water



Zhe Wu<sup>1</sup>, Berkin Bilgic<sup>2,3</sup>, Hongjian He<sup>1</sup>, Yi Sun<sup>4</sup>, Kawin Setsompop<sup>2,3</sup>, and Jianhui Zhong<sup>1</sup>

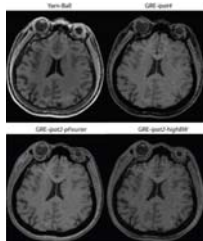
<sup>1</sup>Center for Brain Imaging Science and Technology, Department of Biomedical Engineering, Zhejiang University, Hangzhou, People's Republic of China, <sup>2</sup>Athinoula A. Martinos Center for Biomedical Imaging, Department of Radiology, Massachusetts General Hospital, Charlestown, MA, United States, <sup>3</sup>Department of Radiology, Harvard Medical School, Boston, MA, United States, <sup>4</sup>MR Collaboration NE Asia, Siemens Healthcare, Shanghai, People's Republic of China

Direct Visualization of Short Transverse relaxation time component (ViSTa) is a new myelin water imaging method, which directly extracts myelin water signal through double inversion RF pulses (DIR) to preserve signal from short  $T_1$  components. This method is robust and sensitive to demyelinated lesions, but suffers from extremely long scan time. Herein, we propose accelerated ViSTa acquisition through Simultaneous Multi-Slice (SMS) wave-CAIPI while keeping the high fidelity of ViSTa and MWF maps. As the average/maximum q-factor noise amplification is only 3/10% at MultiBand-4, further acceleration is likely to shorten whole brain MWF acquisition to within 5 minutes.

---

1040

8:51



Novel 3D Yarn-Ball k-space Acquisition for Fast High-Resolution T<sub>1</sub>-Weighted Brain Imaging

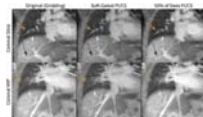
Robert W. Stobbe<sup>1</sup>, Peter Seres<sup>1</sup>, and Christian Beaulieu<sup>1</sup>

<sup>1</sup>Biomedical Engineering, University of Alberta, Edmonton, AB, Canada

Novel 3D Yarn-Ball k-space acquisition is applied for the first time in vivo with application to T<sub>1</sub>-weighted human brain imaging and a goal of 0.9x0.9x0.9 mm<sup>3</sup> voxels in ~2 minutes at 3T. This efficient, large-looping trajectory allows much more of k-space to be sampled following each excitation than the 1 line of 3D-Gradient-Echo (3D-GRE), facilitating longer repetition times (TR), greater acquisition duty cycle, and full sampling. We demonstrate that as a result images created with Yarn-Ball yield better resolution phantom element distinction, and considerably higher SNR (2x on average) in vivo than the three different 3D-GRE methods tested.

---

9:03



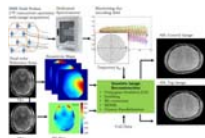
Flexibility and Robustness of Cones UTE for Pediatric Abdominal and Chest Imaging

Joseph Y. Cheng<sup>1</sup>, Wenwen Jiang<sup>2</sup>, Michael Carl<sup>3</sup>, Michael Lustig<sup>4</sup>, and Shreyas S. Vasanawala<sup>1</sup>



<sup>1</sup>Department of Radiology, Stanford University, Stanford, CA, United States, <sup>2</sup>Department of Bioengineering, University of California, Berkeley, CA, <sup>3</sup>Applied Science Laboratory, GE Healthcare, San Diego, CA, <sup>4</sup>Department of Electrical Engineering and Computer Sciences, University of California, Berkeley, CA, United States

Three-dimensional cones k-space sampling trajectory in UTE imaging is ideal for pediatric abdominal and chest MRI which are often hindered by patient motion and lengthy scan durations. The scan-time efficiency of the trajectory reduces scan durations with little to no subsampling. With the repeated sampling and oversampling of the k-space center, the acquisition is robust to motion and can flexibly retrospectively tradeoff spatial and temporal resolutions. Lastly, the method enables retrospective delineation of physiological dynamics. These features of cones UTE enable flexibility and robustness that is ideal for pediatric MRI.



### Single-Shot Spiral Arterial Spin Labeling MRI Enabled by Concurrent Field Monitoring

Mustafa Cavusoglu<sup>1</sup>, Lars Kasper<sup>1</sup>, and Klaas Paul Pruessmann<sup>1</sup>

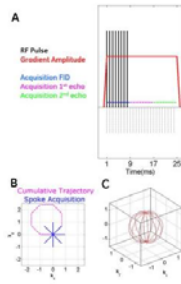
<sup>1</sup>Institute of Biomedical Engineering, ETH Zurich, Zurich, Switzerland

Spiral k-space sampling holds great potential for many MRI applications particularly for arterial spin labeling which has inherently very low SNR. Besides providing significant increase in SNR by reducing the echo time and readout durations, spiral trajectories with single shot acquisitions are highly robust against motion artifacts. However their sensitivity to encoding deficiencies such as B0 off-resonance, field drifts, eddy currents, gradient coupling, gradient delays and concomitant fields prevents their utilization effectively in practice. In this work, we provide ASL with single-shot spiral readouts that are robust against all those deficiencies by using dynamic field monitoring concurrent with image acquisition.

### Looping Star

Florian Wiesinger<sup>1</sup>, Anne Menini<sup>1</sup>, and Ana Beatriz Solana<sup>1</sup>

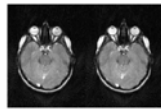
<sup>1</sup>GE Global Research, Munich, Germany



This abstract describes a novel imaging method called Looping Star. The unique imaging characteristics are 1) continuous 3D radial imaging with close to 100% sampling efficiency, 2) inaudible/silent scanning, and produces 3) multi-gradient echo images at equidistant echo times including an FID image at TE=0. Looping Star is demonstrated in phantom, and in-vivo experiments for T2\* weighted imaging and T2\* BOLD fMRI.

1044

9:39



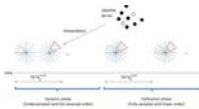
Dynamic imaging of eye and optic nerve with golden angle radial MRI. Saikat Sengupta<sup>1,2</sup>, David Smith<sup>1,2</sup>, Alex Smith<sup>2,3</sup>, E. Brian Welch<sup>1,2</sup>, and Seth Smith<sup>1,2</sup>

<sup>1</sup>Department of Radiology, Vanderbilt University Medical Center, Nashville, TN, United States, <sup>2</sup>Vanderbilt University Institute of Imaging Science, <sup>3</sup>Department of Biomedical Engineering, Vanderbilt University, Nashville, TN, United States

In this abstract we present dynamic imaging of the eyes and the optic nerves in humans using golden angle radial MRI. Continuous 15 s radial scans with azimuthal profile steps of 111.246 degrees are acquired under various eye motion states. Qualitative analyses of the images reveal features of basic eye and nerve mechanics. Image-based characterization of eye mechanics can improve understanding eye physiology and disease.

1045

9:51



A scalable composite through-time radial GRAPPA method. Seng-Wei Chieh<sup>1</sup>, Steen Moeller<sup>2</sup>, Mehmet Akcakaya<sup>1</sup>, and Mostafa Kaveh<sup>1</sup>

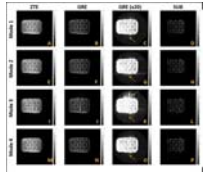
<sup>1</sup>Electrical and Computer Engineering, University of Minnesota, Minneapolis, MN, United States, <sup>2</sup>Center for Magnetic Resonance Research, University of Minnesota

Through-time radial GRAPPA showed promising reconstruction for cardiac imaging. However, it's challenging to extend 3D Kooshball trajectory because of long calibration scans. We propose a novel and flexible data-driven calibration method. The MRXCAT numerical phantom image results show image similarity with through-time radial GRAPPA.



1046

10:03



Exploring various radial trajectories for optimal relative phase correction in dual-echo subtraction ZTE MRI

Hyo Min Lee<sup>1</sup>, Markus Weiger<sup>1</sup>, and Klaas Paul Pruessmann<sup>1</sup>

<sup>1</sup>Institute for Biomedical Engineering, University and ETH Zürich, Zürich, Switzerland

In dual-echo subtraction ZTE MRI, it is crucial to correct for gradient delays and phase offsets induced by eddy currents for high image quality. Relative phase correction is a data-driven approach to correct for the gradient hardware imperfection, but it requires that phase offsets induced by eddy current in positive and negative projections to be exact opposite of each other. This work has explored various radial trajectories to satisfy this condition in order to achieve optimal correction for gradient hardware imperfection in dual-echo subtraction ZTE MRI.

---

Oral

## Novel Engineering & Technology

Room 314

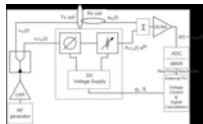
Thursday 8:15 - 10:15 Moderators: Gang Chen & Fraser Robb

---

1047



8:15



In vivo MRI with Concurrent Excitation and Acquisition using Dynamic Analog Cancellation with Real-time Feedback

Ali Caglar Özen<sup>1</sup>, Jan Korvink<sup>2</sup>, Ergin Atalar<sup>3</sup>, and Michael Bock<sup>1</sup>

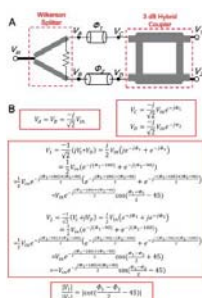
<sup>1</sup>Department of Radiology, Medical Physics, Medical Center – University of Freiburg, Freiburg, Germany, <sup>2</sup>Institute of Microstructure Technology, Karlsruhe Institute of Technology, Karlsruhe, Germany, <sup>3</sup>Department of Electrical and Electronics Engineering, Bilkent University, Ankara, Turkey

In this work concurrent excitation and acquisition (CEA) was realized in a clinical MRI system using a fully automated analog cancellation unit to suppress the unwanted transmit signal leakage during acquisition. The cancellation circuit is composed of a voltage-controlled phase shifter and attenuator, which changes phase and amplitude of a small copy of the transmit signal with a real-time feedback from MRI system. 90 dB on-resonant isolation was achieved within 2 s, where an isolation threshold was set to trigger re-adjustment of decoupling parameters when coil loading changes. To demonstrate feasibility, CEA MR data of a phantom and *in vivo* wrist were acquired.

---



8:27



### Ratio-adjustable power splitters for array-compressed parallel transmission and RF shimming

Xinqiang Yan<sup>1,2</sup>, Zhipeng Cao<sup>1,3</sup>, and William A. Grissom<sup>1,2,3</sup>

<sup>1</sup>Institute of Imaging Science, Vanderbilt University, Nashville, TN, United States, <sup>2</sup>Department of Radiology and Radiological Sciences, Vanderbilt University, Nashville, TN, United States, <sup>3</sup>Department of Biomedical Engineering, Vanderbilt University, Nashville, TN, United States

Array-compressed parallel transmission was recently proposed as a way to reduce the number of RF power amplifiers required for many-coil parallel transmission. This is achieved by connecting a large number of coils to a small number of channels via an array compression network that implements optimized coil-to-channel combinations using power splitters, attenuators and phase shifters. Previous array compression networks used tunable attenuators, but this resulted in significant power dissipation in the network. Here we propose novel ratio-adjustable power splitters (RAPS), which perform the combined duties of power splitting and attenuating, and will enable array compression networks with minimal power loss. The splitters could also be useful for RF shimming with a single amplifier, with the ability to tune the shims by adjusting transmission line lengths.

8:39



### Improved uniformity of the spatial PSF for portable MRI using an optimized rotating magnet

Clarissa Zimmerman Cooley<sup>1,2</sup>, Jason P Stockmann<sup>1,2</sup>, Patrick C. McDaniel<sup>3</sup>, Charlotte Sappo<sup>1</sup>, Christopher Ha<sup>1</sup>, Christopher E. Vaughn<sup>1</sup>, Matthew S. Rosen<sup>1,2</sup>, Thomas Witzel<sup>1,2</sup>, and Lawrence L. Wald<sup>1,2</sup>

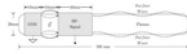
<sup>1</sup>A.A. Martinos Center for Biomedical Imaging, Massachusetts General Hospital, Charlestown, MA, United States, <sup>2</sup>Harvard Medical School, Boston, MA, United States, <sup>3</sup>EECS, Massachusetts Institute of Technology, Cambridge, MA, United States

The development of a low-cost portable MRI scanner for brain imaging could facilitate imaging in new sites with insufficient space, power, or funding for traditional scanners. To address this need, we previously established a 3D encoding method using a rotating inhomogeneous B0 field and RF phase gradients, but uncontrolled field patterns showed encoding problems near the object center. Here we show this problem can be fixed in an optimized 122 kg head-sized permanent magnet with a built-in approximately linear encoding field in 2D images with improved resolution homogeneity across the field of view.

---

1050

8:51



### Plasma antennas in MRI: A four-channel transmit-receive plasma array at 3T

Markus Düring<sup>1,2</sup>, Sebastian Außenhofer<sup>3,4</sup>, Daniel Gensler<sup>2,5</sup>, Cord Meyer<sup>1</sup>, Andrew G. Webb<sup>3</sup>, Peter Michael Jakob<sup>1,2</sup>, and Florian Fidler<sup>2</sup>

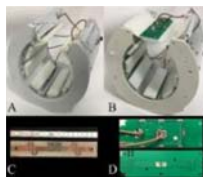
<sup>1</sup>Experimental Physics 5, University of Wuerzburg, Würzburg, Germany, <sup>2</sup>Magnetic Resonance and X-ray Imaging MRB, Development Center X-ray Technology EZRT Fraunhofer Institute for Integrated Circuits IIS, Würzburg, Germany, <sup>3</sup>C.J. Gorter Center for High Field MRI, Leiden University Medical Center, Leiden, Netherlands, <sup>4</sup>Noras MRI products GmbH, Höchberg, Germany, <sup>5</sup>Comprehensive Heart Failure Center (CHFC), University of Wuerzburg, Würzburg, Germany

In this work a new type of antenna array based on plasma columns was designed, and the feasibility of using such an array for both transmit and signal reception was investigated. A four-channel plasma antenna array for a 3T whole-body scanner was designed and constructed. Images were successfully acquired for the first time, and negligible mutual coupling of the individual array elements was observed. Both acquired signal-to-noise maps and the acquired images show a great potential, particularly due to the absence of mutual coupling of the individual array elements.

---

1051

9:03



### A Geometrically Adjustable Loop-Dipole (LD) Head Array for 10.5T

Myung Kyun Woo<sup>1</sup>, Russell L Lagore<sup>1</sup>, Lance DelaBarre<sup>1</sup>, Byeong-Yeul Lee<sup>2</sup>, Yigitcan Eryaman<sup>1</sup>, Jerahmie Radder<sup>1</sup>, Arcan Erturk<sup>1</sup>, Gregory Metzger<sup>1</sup>, Pierre- Francois van de Moortele<sup>1</sup>, Kamil Ugurbil<sup>1</sup>, and Gregor Adriany<sup>1</sup>

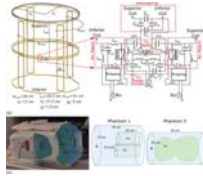
<sup>1</sup>University of Minnesota, Center for Magnetic Resonance Research (CMRR), Minneapolis, MN, United States, <sup>2</sup>University of Minnesota, Center for Magnetic Resonance Research (CMRR)

We designed a geometrically adjustable 16 channel transceiver head Loop-Dipole (LD) array which allowed for variation in element placement. Functionality was established without inter element decoupling circuitry. We simulated the resulting 16-channel LD array and compare to 8 channel dipole only and 8 channel loop only configurations. Finally we acquired in-vivo porcine images from a 10.5T whole-body imaging system to demonstrate principle functionality.

---

1052

9:15



### Combined Transmit Array and 8-channel Receive Coil Array for $^{19}\text{F}/^1\text{H}$ for Human Lung Imaging at 1.5 T Utilizing MEMS Transmit-Receive Detuning

Adam Maunder<sup>1</sup>, Madhwesha Rao<sup>1</sup>, Fraser J. L. Robb<sup>1,2</sup>, and Jim M Wild<sup>1</sup>

<sup>1</sup>Unit of Academic Radiology, University of Sheffield, Sheffield, United Kingdom, <sup>2</sup>GE Healthcare Inc., Aurora, OH, United States

MRI of inert fluorinated gases is a developing method for pulmonary ventilation imaging, but image quality is constrained by low spin density. Additionally, proton imaging is desirable for complementary structural information from the lungs. Here, an 8-element transmit/receive coil array for 1.5 T is presented, which is capable of imaging both  $^{19}\text{F}$  and  $^1\text{H}$  nuclei with higher SNR when compared to single-element alternatives. Microelectromechanical systems (MEMS) switches are utilized to provide broadband transmit-receive isolation over the frequency range of both nuclei. Coil channel isolation is demonstrated and MEMS switching performance with phantom imaging of both nuclei.

1053

9:27



### Size-adaptable 13-channel receive array for brain imaging in human neonates at 3 T

Nibardo Lopez Rios<sup>1,2</sup>, Alexandru Foias<sup>1</sup>, Gregory Lodygensky<sup>3,4,5</sup>, Nikola Stikov<sup>1,5</sup>, Mathieu Dehaes<sup>3,6,7</sup>, and Julien Cohen-Adad<sup>1,8</sup>

<sup>1</sup>NeuroPoly Lab, Institute of Biomedical Engineering, Polytechnique Montreal, Montreal, QC, Canada, <sup>2</sup>Medical Biophysics Center, University of Oriente, Santiago de Cuba, Cuba, <sup>3</sup>Sainte-Justine Hospital University Center, Montreal, QC, Canada, <sup>4</sup>Department of Pediatrics, Faculty of Medicine, University of Montreal, Montreal, QC, Canada, <sup>5</sup>Montreal Heart Institute, Montreal, QC, Canada, <sup>6</sup>Department of Radiology, Radio-oncology and Nuclear Medicine, University of Montreal, Montreal, QC, Canada, <sup>7</sup>Institute of Biomedical Engineering, University of Montreal, Montreal, QC, Canada, <sup>8</sup>Functional Neuroimaging Unit, CRIUGM, University of Montreal, Montreal, QC, Canada

A size-adaptable receive array that can accommodate a variety of heads in a pediatric population (27-week-premature to 1.5-month-old) is proposed. Thirteen spherically distributed loops can move in radial and axial directions to maximize their proximity to the subject. Decoupling between elements is ensured by strong preamplifier decoupling (-27 to -33 dB). Tests on a scanner with two phantoms (8 and 10 cm in diameter) resulted in higher SNR with the proposed coil compared to 8-Ch and 32-Ch commercial head coils. The method restricts head motion and could be of interest for other size-varying body parts, such as breast and limbs.

---

1054

9:39



A 16 channel head-only pTX array using high efficiency in-bore RFPAs at 3T

Michael Twieg<sup>1</sup>, Bhairav B Mehta<sup>1</sup>, Simone Coppo<sup>1</sup>, Jan Ruff<sup>2</sup>, Rene Gumbrecht<sup>2</sup>, and Mark A Griswold<sup>1</sup>

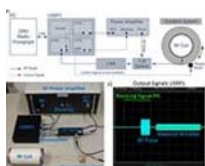
<sup>1</sup>Dept of Radiology, Case Western Reserve University, Cleveland, OH, United States, <sup>2</sup>Siemens Healthcare GmbH, Erlangen, Germany

Parallel transmit (pTX) has been proposed as a solution to flip angle inhomogeneity and SAR at ultrahigh fields, as well as safety hazards with implantable devices. However, pTX systems come at high cost, partially due to the use of remotely located linear RF power amplifiers (RFPAs), which have poor power efficiency and rely on costly RF power cables to couple power to the subject. Here we demonstrate a 16 channel transmit array utilizing high efficiency RFPA modules inside the scanner bore. They RFPAs can deliver a total of over 1kW to the array while only cooled by natural convection.

---

1055

9:51



COSI Transmit: Open Source Soft- and Hardware Transmission System for traditional and rotating MR

Christian Blücher<sup>1</sup>, Haopeng Han<sup>1</sup>, Werner Hoffmann<sup>2</sup>, Reiner Seemann<sup>2</sup>, Frank Seifert<sup>2</sup>, Thoralf Niendorf<sup>1,3,4</sup>, and Lukas Winter<sup>1</sup>

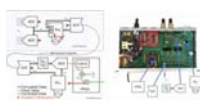
<sup>1</sup>Berlin Ultrahigh Field Facility (B.U.F.F.), Max Delbrück Center for Molecular Medicine in the Helmholtz Association, Berlin, Germany, <sup>2</sup>Physikalische Technische Bundesanstalt (PTB), Berlin, Germany, <sup>3</sup>Experimental and Clinical Research Center (ECRC), a joint cooperation between the Charité Medical Faculty and the Max Delbrück Center for Molecular Medicine, Berlin, Germany, <sup>4</sup>MRI.TOOLS GmbH, Berlin, Germany

As part of the open source imaging initiative ([www.opensourceimaging.org](http://www.opensourceimaging.org)), a collaborative effort to build an open source MRI, we proposed and built a transmission/reception RF system mostly consisting of open source components for traditional and rotating spatial encoding schemes. COSI Transmit is based on a GNU Radio compatible software defined radio (SDR) as a spectrometer, a 1kW RF-power amplifier, T/R switch, low noise preamplifier and a transmit/receive solenoid RF coil. The system operates in the frequency range from 1.8-30MHz ( $B_0=0.042-0.7T$ ) and can potentially be extended to  $B_0=1.27T$ . Material cost of the system is ~3000€.

---

1056

10:03



### Correction of Gradient Induced Clock Phase Modulation for In-Bore Sampling Receivers

Jonas Reber<sup>1</sup>, Josip Marjanovic<sup>1</sup>, Christoph Schildknecht<sup>1</sup>, David Otto Brunner<sup>1</sup>, and Klaas Paul Pruessmann<sup>1</sup>

*<sup>1</sup>ETH Zuerich and University of Zuerich, Institute for Biomedical Engineering, Zuerich, Switzerland*

With increasing receive channel counts, moving digitizer electronics close to the coil is desirable for reduced cabling and cable coupling and improved patient safety. However, gradient induction degrades in-bore operated circuit performance. Particularly vulnerable are high quality sampling or mixing clocks, required for digitization or demodulation. Gradient induced oscillator modulations add to the already stringent jitter requirements and therefore directly reduce SNR. We present a method which corrects large parts of clock modulations and therefore increases phase SNR of in-bore acquired data e.g. 18 dB for a sinewave corrupted by EPI gradients.

---

Oral

## Novel MRS Methods & Applications

Room 316A

Thursday 8:15 - 10:15

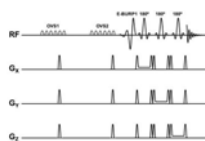
Moderators: Ovidiu Andronesi & Melissa Terpstra

---

8:15

A new pulse sequence for single-voxel <sup>1</sup>H MRS measurement of cerebral Nicotinamide adenine dinucleotide (NAD<sup>+</sup>) in humans at 7T using 32-channel volume coil

1057



Puneet Bagga<sup>1</sup>, Hari Hariharan<sup>1</sup>, Kevin D'Aquila<sup>1</sup>, Ravi Prakash Reddy Nanga<sup>1</sup>, Mohammad Haris<sup>2</sup>, and Ravinder Reddy<sup>1</sup>

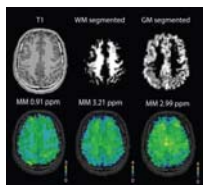
<sup>1</sup>Department of Radiology, University of Pennsylvania, Philadelphia, PA, United States, <sup>2</sup>Research Branch, Sidra Medical and Research Center, Doha, Qatar

Nicotinamide adenine dinucleotide (NAD<sup>+</sup>) is a ubiquitous molecule present in all cells and tissues of the body with an important role in the redox reactions and metabolism. Small changes in NAD<sup>+</sup> levels may lead to oxidative stress and may be a cause for various disorders. Currently, NAD<sup>+</sup> can be detected *in vivo* only by <sup>31</sup>P NMR spectroscopy. Recently, NAD<sup>+</sup> measurement with <sup>1</sup>H MRS in the human brain with a surface coil was demonstrated. In the present study, we show a novel MR pulse sequence for the *in vivo*, single voxel localized detection of NAD<sup>+</sup> from the human brain at 7T.

1058



8:27



Detection of MM using metabolite-nulled MEGA-LASER at 3T – A possible effect on GABA+ signal

Michal Považan<sup>1,2</sup>, Petra Hnilicová<sup>3</sup>, Gilbert Hangel<sup>1</sup>, Bernhard Strasser<sup>1</sup>, Ovidiu Andronesi<sup>4</sup>, Stephan Gruber<sup>1</sup>, Siegfried Trattnig<sup>1,2</sup>, and Wolfgang Bogner<sup>1,2</sup>

<sup>1</sup>Department of Biomedical Imaging and Image-guided Therapy, High Field MR Centre, Medical University Vienna, Vienna, Austria, <sup>2</sup>Christian Doppler Laboratory for Clinical Molecular MR Imaging, Vienna, Austria, <sup>3</sup>Jessenius Faculty of Medicine in Martin, Biomedical Center Martin, Division of Neurosciences, Comenius University in Bratislava, Martin, Slovakia, <sup>4</sup>Harvard Medical School, Martinos Center for Biomedical Imaging, Massachusetts General Hospital, Boston, MA, United States

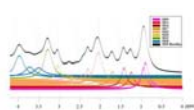
In GABA-edited spectroscopy signal of macromolecules overlaps the signal of GABA. This macromolecular contribution to GABA signal (GABA+) is variable throughout the brain and can bias the quantification. We aimed to map the signal of macromolecules at 2.99 ppm using metabolite-nulled 3D MEGA-LASER MRSI. We found the GABA+/total creatine to be higher in white matter (45%), which contradicts the literature. The MM<sub>2.99ppm</sub> was found higher in white matter as well (24%). The macromolecular tissue distribution is among other factors affecting the GABA+ signal, therefore the detection of GABA is preferable to GABA+ if the removal of macromolecules is possible.



1059



8:39



### High resolution maps of individual macromolecule components in the human brain at 9.4T

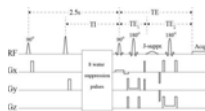
Sahar Nassirpour<sup>1,2</sup>, Paul Chang<sup>1,2</sup>, and Anke Henning<sup>1,3</sup>

<sup>1</sup>MPI for Biological Cybernetics, Tuebingen, Germany, <sup>2</sup>IMPRS for Cognitive and Systems Neuroscience, Eberhard Karls University of Tübingen, Tuebingen, Germany, <sup>3</sup>Institute of Physics, Ernst-Moritz-Arndt University Greifswald, Greifswald, Germany

Although ultra-short TE spectroscopy sequences enhance the information content of the spectrum, they are, in their nature, prone to quantification biases if the macromolecular (MM) components are not taken into account. The aim of this study, was to 1) perform macromolecule mapping at 9.4T using an ultra-short TE double-inversion recovery (DIR) MRSI sequence, 2) model and parametrize the individual MM components, and 3) extract high resolution maps of individual MM components using the modelled MM basis set.

1060

8:51



### Simultaneous Measurement of T1 and T2 Relaxation Times of Glutamate in the Frontal Cortex at 7T

Li An<sup>1</sup>, Shizhe Li<sup>1</sup>, and Jun Shen<sup>1</sup>

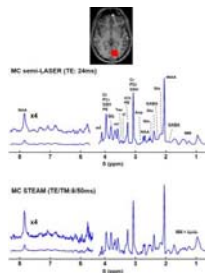
<sup>1</sup>National Institute of Mental Health, National Institutes of Health, Bethesda, MD, United States

Many central nervous system (CNS) abnormalities lead to significant changes in the microenvironment of glutamatergic neurons, which may alter relaxation times of glutamate. In this study, a method for simultaneously determining T1 and T2 of glutamate at 7T was presented. The method uses a point resolved spectroscopy (PRESS) sequence with multiple echo times, inversion-recovery times and RF suppression of aspartyl moiety of N-acetyl-aspartate (NAA).

1061



9:03



### Metabolite cycled semi-LASER and STEAM at 9.4T. Comparison and in vivo results.

Ioannis-Angelos Giapitzakis<sup>1,2</sup>, Tingting Shao<sup>1</sup>, Nikolai Avdievitch<sup>1</sup>, Nicole Fichtner<sup>3,4</sup>, Ralf Mekte<sup>5</sup>, Roland Kreis<sup>3</sup>, and Anke Henning<sup>1,6</sup>



<sup>1</sup>High Field Magnetic Resonance, Max Planck Institute for Biological Cybernetics, Tuebingen, Germany, <sup>2</sup>Graduate School of Neural and Behavioural Sciences, Tuebingen, Germany, <sup>3</sup>Departments of Radiology and Clinical Research, University Bern, Bern, Switzerland, <sup>4</sup>Institute for Biomedical Engineering, UZH and ETH Zurich, Zurich, Switzerland, <sup>5</sup>Center for Stroke Research Berlin (CSB), Charité Universitätsmedizin Berlin, Berlin, Germany, <sup>6</sup>Institute of Physics, Ernst-Moritz-Arndt University Greifswald, Greifswald, Germany

The purpose of this study was the development of two new localization schemes for ultra high field (UHF) spectroscopic applications while utilizing the advantages of the Metabolite Cycling (MC) technique. In particular, a semi-adiabatic asymmetric pulse optimized for MC at 9.4T was incorporated into STEAM and semi-LASER localization schemes. In this study, these two new sequences along with the appropriate hardware setup were used to acquire in vivo 1H MRS data from the occipital lobe of the human brain and compare the corresponding results. In addition, the effect of frequency and phase correction based on the MC water spectra on data quality was investigated.

1062



9:15

A small, low-resolution thumbnail image of a table with multiple columns and rows, likely containing data from a research paper.

Paediatric brain lesion classification using 3T MRS: Comparison of different pattern recognition techniques, A multi-centre study.

Niloufar Zarinabad<sup>1,2</sup>, Laurence J J Abernethy<sup>3</sup>, Dorothee P Auer<sup>4,5,6</sup>, Theodoros N Arvanitis<sup>2,7</sup>, Simon Bailey<sup>8</sup>, Nigel P Davies<sup>1,2,9</sup>, Daniel Rodriguez Gutierrez<sup>4,5</sup>, Richard G. Grundy<sup>4</sup>, Tim Jaspan<sup>4,6</sup>, Dipayan Mitra<sup>10</sup>, Paul S Morgan<sup>4,6,11</sup>, Barry Pizer<sup>12</sup>, Martin Wilson<sup>1</sup>, Lesley MacPherson<sup>2</sup>, and Andrew Peet<sup>1,2</sup>

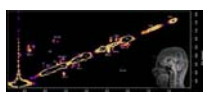
<sup>1</sup>University of Birmingham, Birmingham, United Kingdom, <sup>2</sup>Birmingham children hospital, Birmingham, United Kingdom, <sup>3</sup>Department of Radiology, Alder Hey Children's NHS Foundation Trust, <sup>4</sup>The Children's Brain Tumour Research Centre, University of Nottingham, Nottingham, United Kingdom, <sup>5</sup>Radiological Sciences, Department of Clinical Neuroscience, University of Nottingham, Nottingham, United Kingdom, <sup>6</sup>Neuroradiology, Nottingham University Hospital, Queen's Medical Centre, Nottingham, United Kingdom, <sup>7</sup>Institute of Digital Healthcare, WMG, University of Warwick, Coventry, United Kingdom, <sup>8</sup>Paediatric Oncology Department, Great North Children's Hospital, Newcastle upon Tyne, United Kingdom, <sup>9</sup>Department of Imaging and Medical Physics, University Hospitals Birmingham NHS Foundation Trust, Birmingham, United Kingdom, <sup>10</sup>Neuroradiology Department, Newcastle upon Tyne Hospitals, Newcastle upon Tyne, United Kingdom, <sup>11</sup>Medical Physics, Nottingham University Hospital, Queen's Medical Centre, Nottingham, United Kingdom, <sup>12</sup>Department of Paediatric Oncology, Alder Hey Children's NHS Foundation Trust, Liverpool, United Kingdom

The purpose of the study was to investigate the discriminative potential of metabolites obtained from 3T scanners in classifying paediatric posterior fossa brain tumours by comparing performance of three different pattern recognition techniques on a multicentre data set. A total of 52 paediatric patients with cerebellar tumours (16 Medulloblastomas, 31 Pilocytic Astrocytomas and 5 Ependymomas) were scanned using PRESS, TE 30-46 ms, across 4 different hospitals. Achieved balanced classification accuracy were 88% with random-forest, 84 % for the support-vector-machine and 81% for naïve-bays classifier. The achieved accuracy was better than the balanced accuracy previously reported for multi-centre datasets at 1.5T.

1063



9:27



### Diurnal variability of cerebral metabolites with 2D L-COSY

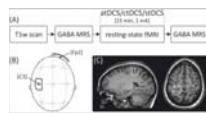
Jameen ARM<sup>1</sup>, Karen Ribbons<sup>2</sup>, Jeannette Lechner-Scott<sup>3</sup>, Kate Skehan<sup>3</sup>, Shiami Luchow<sup>3</sup>, and Saadallah Ramadan<sup>4</sup>

<sup>1</sup>University of Newcastle, Newcastle, Australia, <sup>2</sup>Neurology, John Hunter Hospital, Australia, <sup>3</sup>Hunter Medical Research Institute, Australia, <sup>4</sup>University of Newcastle, Australia

Diurnal factors such as brain temperature, hydration and osmotic regulation have the potential to change metabolic profiles in two dimensional localised correlation spectroscopy (2D L-COSY). Ten Healthy subjects underwent repeated 2D L-COSY on a 3T system over a 10hour period at three time points (0700, 1200 and 1700) to evaluate diurnal effects on brain neurometabolites. Results show significant diurnal effects between morning and evening scans. The present findings highlight the importance of maintaining a specific time when spectral data is acquired, especially in longitudinal studies where the dynamic nature of subject can present a confounding factor.

1064

9:39



Transcranial direct current-induced modulation of GABA levels and resting-state functional connectivity in older subjects

Florian Schubert<sup>1</sup>, Daria Antonenko<sup>2</sup>, Florian Bohm<sup>2</sup>, Semiha Aydin<sup>1</sup>, Dayana Hayek<sup>2</sup>, Ulrike Grittner<sup>3</sup>, Agnes Flöel<sup>2,3</sup>, and Bernd Ittermann<sup>1</sup>

<sup>1</sup>Physikalisch-Technische Bundesanstalt (PTB), Berlin, Germany, <sup>2</sup>Department of Neurology, NeuroCure Clinical Research Center, Charité, Berlin, Germany, <sup>3</sup>Center for Stroke Research, Charité, Berlin, Germany

Transcranial direct current stimulation (tDCS) modulates human behavior, neuronal patterns and metabolite concentrations. To unravel tDCS-induced alterations on the neuronal level we investigated tDCS-induced effects in older adults (50-79 years) using MRS to quantify GABA levels and resting-state fMRI to assess sensorimotor network strength and inter-hemispheric connectivity. Anodal, cathodal and sham tDCS were applied over the left sensorimotor region in a randomized, cross-over design. Compared to sham, anodal tDCS induced significantly reduced GABA levels, representing local plasticity, as well as lower large-scale network coupling and inter-hemispheric connectivity.

1065



9:51

	Baseline	Post-tDCS	Post-hypoglycemia
Age (years)	58.1 ± 1.2	58.1 ± 1.2	58.1 ± 1.2
Gender (M/F)	10/10	10/10	10/10
Diabetes type 1	10/10	10/10	10/10
Insulin (mU/L)	10.0 ± 2.0	10.0 ± 2.0	10.0 ± 2.0
Glucose (mmol/L)	5.0 ± 0.5	5.0 ± 0.5	5.0 ± 0.5
Lactate (mmol/L)	1.0 ± 0.2	1.0 ± 0.2	1.0 ± 0.2

The effect of high-intensity interval training on brain lactate levels during subsequent hypoglycemia in type 1 diabetes

Evita Wiegers<sup>1</sup>, Hanne Rooijackers<sup>2</sup>, Cees Tack<sup>2</sup>, Arend Heerschap<sup>1</sup>, Bastiaan de Galan<sup>2</sup>, and Marinette van der Graaf<sup>1,3</sup>

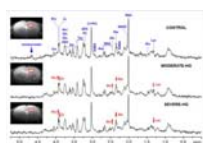
<sup>1</sup>Radiology and Nuclear Medicine, Radboud university medical center, Nijmegen, Netherlands, <sup>2</sup>Internal Medicine, Radboud university medical center, Nijmegen, Netherlands, <sup>3</sup>Pediatrics, Radboud university medical center, Nijmegen, Netherlands

Adaptations in brain lactate handling in response to hypoglycemia may play a role in the pathophysiology of impaired awareness of hypoglycemia (IAH). Therefore, we determined the effect of high-intensity interval training (HIIT)-induced hyperlactatemia on brain lactate during subsequent hypoglycemia in type 1 diabetic (T1DM) patients with IAH, in T1DM patients with normal awareness of hypoglycemia (NAH) and in healthy controls. Brain lactate concentration was determined using a J-difference editing semi-LASER  $^1\text{H}$ -MRS sequence. After HIIT, brain lactate concentration increased most in T1DM IAH, consistent with an enhanced lactate transport capacity, and also dropped most during subsequent hypoglycemia, suggestive for increased lactate oxidation.

---

1066

10:03



Long-term Effects of Recurrent Neonatal Hyperglycemia on the Hippocampal Neurochemical Profile of Rats.

Raghavendra Rao<sup>1</sup> and Ivan Tkac<sup>2</sup>

<sup>1</sup>Department of Pediatrics, University of Minnesota, Minneapolis, MN, United States, <sup>2</sup>Center for Magnetic Resonance Research, University of Minnesota, Minneapolis, MN, United States

Hyperglycemia is common in extremely low-gestational-age neonates (ELGAN) and increases the risk of serious health problems in the neonatal period. However, the long-term effects are not well understood. The purpose of this study was to assess long-term effects of the recurrent neonatal hyperglycemia on the hippocampal neurochemical profile. Metabolite changes were quantified by in vivo  $^1\text{H}$  MRS at 9.4T using a rat model of neonatal hyperglycemia. The results of this study indicate that the recurrent hyperglycemia during neonatal period may alter energy metabolism and glutamatergic neurotransmission, which can contribute to delayed hippocampal development and cognitive deficits in ELGANs.

---

Oral

## GI, Diabetes, & Metabolism

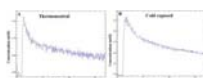
Room 320

Thursday 8:15 - 10:15 Moderators: Chris Flask & Houchun Hu

---

1067

8:15



Evaluation of the Vascular Perfusion in Activated Brown Adipose Tissue by Dynamic Contrast Enhanced MR Imaging

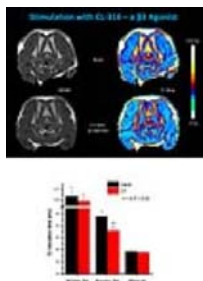
Jadegoud Yaligar<sup>1</sup>, Sanjay Kumar Verma<sup>1</sup>, Venkatesh Gopalan<sup>1</sup>, Anantharaj Rengaraj<sup>1</sup>, Tian Xianfeng<sup>1</sup>, and S. Sendhil Velan<sup>1</sup>

<sup>1</sup>Laboratory of Metabolic Imaging, Singapore Bioimaging Consortium, A\*STAR, Singapore

Vasculature plays an important role in white and brown adipose tissue (WAT and BAT) metabolism. In expanding WAT, abnormal vasculature may lead to energy (fat) deposition whereas in activated BAT it may potentially facilitate the energy consumption by oxidizing the fat. Understanding the vascular network and blood perfusion properties of the activated BAT is important for triglyceride clearance, increased blood flow and oxygen. In this feasibility study we have investigated the vascular properties and blood perfusion rate constant of the activated BAT by quantitative dynamic contrast enhanced MR imaging in a rodent model.

1068

8:27



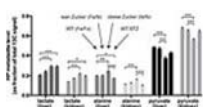
Functional Assessment of Brown Adipose Tissue by T2 Mapping  
Ulrich Flögel<sup>1</sup>, Christoph Jacoby<sup>1</sup>, Jens W. Fischer<sup>2</sup>, and Maria Grandoch<sup>2</sup>

<sup>1</sup>Experimental Cardiovascular Imaging, Heinrich Heine University, Düsseldorf, Germany, <sup>2</sup>Pharmacology and Clinical Pharmacology, Heinrich Heine University, Düsseldorf, Germany

Within the last decade, the scientific interest in brown adipose tissue (BAT) was greatly invigorated by the discovery of functional BAT in adult humans. Importantly, reduced BAT activity has recently been associated with predisposition to obesity and abnormal glucose homeostasis. The current gold standard for functional BAT imaging is CT-guided <sup>18</sup>F-FDG-PET. Here, we describe a robust T2 mapping method to assess the metabolic activity of BAT independent of substrate selection and without the need of harmful radiation or contrast agents. Compared to previous T2\*-based techniques the present approach is less prone to susceptibility and physiological artifacts especially at high fields.

1069

8:39



Hyperpolarized <sup>13</sup>C-pyruvate MRI of the liver and kidneys in rodent models of type 1 and type 2 diabetes

Cornelius von Morze<sup>1</sup>, Prasanna KR Allu<sup>2</sup>, Gene-Yuan Chang<sup>2</sup>, Irene Marco-Rius<sup>1</sup>, Eugene Milshteyn<sup>1</sup>, Catherine Gleason<sup>2</sup>, Daniel B Vigneron<sup>1</sup>, and David Pearce<sup>2</sup>

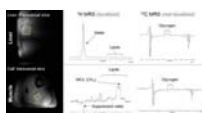
<sup>1</sup>Radiology & Biomedical Imaging, UCSF, San Francisco, CA, United States, <sup>2</sup>Nephrology, UCSF, San Francisco, CA, United States

The purpose of this study was to characterize changes in hyperpolarized <sup>13</sup>C-pyruvate spectra in the liver and kidneys of two contrasting models of diabetes, obese Zucker diabetic fatty (ZDF) rats and streptozotocin (STZ)-treated (insulin-deficient) wild type Zucker rats. The results were interpreted in combination with transcriptional analysis of freeze-clamped tissue samples from these animals. Hyperpolarized lactate levels were elevated in both models while hyperpolarized alanine signals clearly diverged, decreasing in the type 1 model but increasing in type 2. Overall, the results suggest a complex interplay of transcriptional and substrate-level effects in determining the metabolic phenotype in diabetes.

1070



8:51



Multinuclear in vivo MR spectroscopy at 7T reveals differences in liver and muscle metabolism in NAFLD patients and healthy controls

Martin Gajdošík<sup>1,2</sup>, Sabina Smajjš<sup>2</sup>, Christian Kienbacher<sup>3</sup>, Lorenz Pflieger<sup>1,2</sup>, Anton Luger<sup>2</sup>, Siegfried Trattnig<sup>1,4</sup>, Michael Trauner<sup>3</sup>, Michael Krebs<sup>2</sup>, and Martin Krššák<sup>1,2</sup>

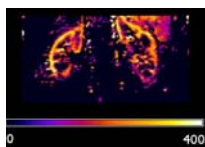
<sup>1</sup>High-field MR Centre, Department of Biomedical Imaging and Image-guided Therapy, Medical University of Vienna, Vienna, Austria, <sup>2</sup>Division of Endocrinology and Metabolism, Department of Internal Medicine III, Medical University of Vienna, Vienna, Austria, <sup>3</sup>Division of Gastroenterology and Hepatology, Department of Internal Medicine III, Medical University of Vienna, Vienna, Austria, <sup>4</sup>Christian Doppler Laboratory for Clinical Molecular MR Imaging, Vienna, Austria

Recent developments at 7T allowed for qualitative assessment of the hepatic lipids, faster measurement of glycogen and ATP turnover. Improved spectral resolution also enabled better separation and quantitation of hepatic metabolites. The aim of the study was to employ the advanced methods of multinuclear in vivo MR spectroscopy at 7T in the liver and muscles in non-alcoholic fatty liver disease (NAFLD) patients and healthy controls. Static and dynamic multinuclear MRS data, supported by mixed meal test and euglycemic-hyperinsulinemic clamp study, showed metabolic changes and disturbed interorgan crosstalk in NAFLD patients.

1071

9:03

Renal Arterial Spin Labeling in Diabetes Mellitus



José M. Mora-Gutierrez<sup>1</sup>, Nuria García-Fernández<sup>1</sup>, María F. Slon<sup>2</sup>, Danny JJ Wang<sup>3</sup>, Alberto Benito<sup>4</sup>, José Páramo<sup>5</sup>, and María Fernández-Seara<sup>4,6</sup>

<sup>1</sup>*Nephrology, University of Navarra Hospital, Pamplona, Spain,*

<sup>2</sup>*Nephrology, Navarra Hospital, Pamplona, Spain,* <sup>3</sup>*Laboratory of Functional MRI Technology, Stevens Neuroimaging and Informatics Institute, University of Southern California, Los Angeles, United States,*

<sup>4</sup>*Radiology, University of Navarra Hospital, Pamplona, Spain,*

<sup>5</sup>*Hematology, University of Navarra Hospital, Pamplona, Spain,*

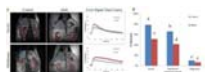
<sup>6</sup>*Biomedical Engineering, TECNUN, University of Navarra, San Sebastian, Spain*

Diabetic nephropathy (DN) is a microvascular complication of diabetes mellitus (DM) and a leading cause of chronic kidney disease (CKD). However evidence of renal damage is not detected until the advanced disease stages, using current clinical diagnostic tools. The goal of this study was to investigate renal hemodynamic changes in diabetic patients using ASL and evaluate whether the technique is sensitive enough to detect renal dysfunction early in the disease course, which could have relevant clinical and therapeutic implications. The results demonstrated detection of hemodynamic changes in kidney microvasculature in diabetic patients. Moreover, ASL was able to detect small changes in kidney perfusion across different stages of CKD in the diabetic population.

---

1072

9:15



Dynamic Contrast-Enhanced Magnetic Resonance Imaging: A Pre-Clinical Approach to Detect and Monitor Diabetes

Dorela Doris Shuboni-Mulligan<sup>1</sup>, Christiane L Mallett<sup>2</sup>, Maciek Parys<sup>3</sup>, Barbara Blanco-Fernandez<sup>4</sup>, and Erik M Shapiro<sup>1</sup>

<sup>1</sup>*Radiology, Michigan State University, East Lansing, MI, United States,*

<sup>2</sup>*Radiology, Michigan State University, East Lansing, MI,* <sup>3</sup>*Department of Comparative Medicine and Integrative Biology Program, Michigan State University, East Lansing, MI, United States,* <sup>4</sup>*Radiology, East Lansing, MI, United States*



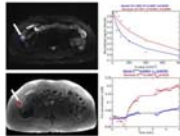


Parametric mapping may provide estimates of the degree and spatial distribution of fibrosis in Crohn's Disease (CD) patients but is subject to respiratory and peristaltic motion. Validation of out-of-the-box registration strategies and their impact on quality and robustness of parametric maps-delayed gain of enhancement (DGE) and magnetization transfer ratio (MTR) were evaluated.

1075



9:51



### Quantitative IVIM-DWI and DCE-MRI for assessment of bowel inflammation in Crohn's disease

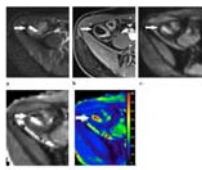
Stefanie Hectors<sup>1</sup>, Sonja Gordic<sup>1</sup>, Octavia Bane<sup>1</sup>, Joana Torres<sup>2</sup>, Judy Cho<sup>2,3</sup>, Jean-Frederic Colombel<sup>2</sup>, and Bachir Taouli<sup>1</sup>

<sup>1</sup>Translational and Molecular Imaging Institute, Icahn School of Medicine at Mount Sinai, New York, NY, United States, <sup>2</sup>Division of Gastroenterology, Icahn School of Medicine at Mount Sinai, New York, NY, United States, <sup>3</sup>Department of Genetics and Genomic Sciences, Icahn School of Medicine at Mount Sinai, New York, NY, United States

The aims of this study were to quantify intravoxel incoherent motion DWI (IVIM-DWI) and DCE-MRI metrics and to assess the correlation between IVIM-DWI and DCE-MRI metrics in abnormal and normal appearing bowel segments in Crohn's disease (CD) patients. ADC was significantly reduced in abnormal vs. normal bowel wall segments. A significant negative correlation between  $K^{\text{trans}}$  (measured with DCE-MRI) and perfusion fraction  $f$  (measured with IVIM-DWI) was observed. Our preliminary results suggest that IVIM-DWI could potentially be used for simultaneous assessment of perfusion and diffusion in the bowel wall of CD patients, which needs to be verified in a larger cohort of patients.

1076

10:03



### Inflammatory activity of Crohn's disease: Evaluation by MR T2\* mapping without intravenous enhancement

Si yun Huang<sup>1</sup>, Xue hua Li<sup>1</sup>, Zhong wei Zhang<sup>2</sup>, Jin jiang Lin<sup>1</sup>, Li Huang<sup>1</sup>, Zhuang nian Fang<sup>1</sup>, Meng chen Zhang<sup>1</sup>, Meng jie Jiang<sup>3</sup>, Hua song Cai<sup>1</sup>, Margaret H. Pui<sup>4</sup>, Shi ting Feng<sup>1</sup>, Can hui Sun<sup>3</sup>, and Zi ping Li<sup>3</sup>

<sup>1</sup>Department of Radiology, The First Affiliated Hospital of Sun Yat-Sen University, Guangzhou, China, Guangzhou, People's Republic of China, <sup>2</sup>Department of Biomedical Engineering, Cancer Biology and Radiology, Wake Forest School of Medicine, <sup>3</sup>Department of Radiology, Hospital of Stomatology, Guanghua School of Stomatology, Sun Yat-Sen University, Guangdong Provincial Key Laboratory of Stomatology, <sup>4</sup>Department of Radiology, Conde de S. Januario Central Hospital, Macau

Crohn's disease (CD) is a chronic relapsing inflammatory bowel disease leading to structurally irreversible bowel damage. The incidence of CD had been increasing in the past century epidemiologically . Accurate evaluation of CD activity is crucial for new therapeutic goals of mucosal healing, preventing bowel damage, limiting disability, and improving quality of life . Although colonoscopy remains the gold standard for assessing CD activity, it is invasive, limited to assessment of the small bowel, and not suitable for continuing monitoring of CD activity . Thus, seeking for alternative noninvasive and accurate approaches to assess CD activity is necessary.

---

---

## Combined Educational & Scientific Session

# Combining Structural and Functional Brain Connectivity

Organizers: Fernando E. Boada, Ph.D. & John D. Port, M.D., Ph.D.

Room 312

Thursday 8:15 - 10:15 Moderators: John Port & Michael Zeineh

---

8:15



DTI & rsfMR Imaging Acquisition Strategies for Connectivity Analysis  
An Vu<sup>1</sup>

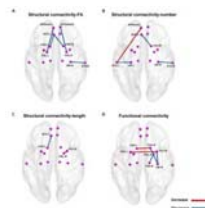
<sup>1</sup>San Francisco VA Health Care System

The Human Connectome Project (HCP) relies primarily on resting state functional MR imaging (rfMRI) and diffusion MR imaging (dMRI) to generate detailed maps of brain connectivity. Technical improvements and optimization of these methods have enabled significant increases in the spatial and temporal resolutions of fMRI and dMRI at both 3T and 7T. Ongoing technical developments for acquisition will be presented, targeting higher spatial resolution while maintaining adequate SNR and sensitivity to functional signals.

1077



8:45



Dissociation of structural and functional dysconnectivity in first-episode drug-naïve schizophrenia

Jieke Liu<sup>1</sup>, Li Yao<sup>1</sup>, Wenjing Zhang<sup>1</sup>, Su Lui<sup>1</sup>, and Qiyong Gong<sup>1</sup>

<sup>1</sup>Radiology, Huaxi MR Research Center, West China Hospital of Sichuan University, Chengdu, People's Republic of China

Combining DTI and fMRI data sets, the present study revealed the dissociation of structural and functional dysconnectivity in a large cohort of first-episode drug-naive schizophrenia patients.

1078

8:57

Altered effective connectivity of dorsolateral prefrontal cortex in obsessive-compulsive disorder: a Granger causality analysis with resting-state fMRI

Table 1 Demographic and clinical characteristics of participants

	Obsessive	Controls	Significance
Demographics	Mean (SD)	Mean (SD)	F-value
Age (years)	30.00 (7.1)	27.00 (6.0)	0.00
Education (years)	12.00 (2.0)	12.00 (2.0)	0.00
Duration of illness (years)	1.00 (1.0)	0.00 (0.0)	0.00
Y-BOCS total	20.70 (5.0)	0.00 (0.0)	0.00
Obsessions	12.00 (4.0)	0.00 (0.0)	0.00
Compulsions	8.70 (3.0)	0.00 (0.0)	0.00
HAM-D-21	6.70 (3.0)	0.00 (0.0)	0.00
HAM-A-19	6.70 (3.0)	0.00 (0.0)	0.00

Hailong Li<sup>1</sup>, Xinyu Hu<sup>1</sup>, Ming Zhou<sup>1</sup>, Lu Lu<sup>1</sup>, Lianqing Zhang<sup>1</sup>, Xiaoxiao Hu<sup>1</sup>, Xuan Bu<sup>1</sup>, Xiaoqi Huang<sup>1</sup>, and Qiyong Gong<sup>1</sup>

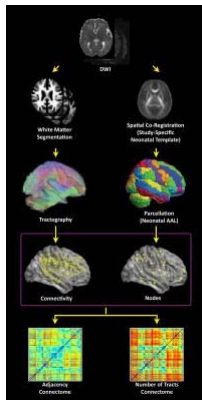
<sup>1</sup>Huaxi Magnetic Resonance Research Centre(HMRRC), West China Hospital of Sichuan University, Chengdu, People's Republic of China

In current study, we demonstrated the altered effective connectivity between bilateral dorsolateral prefrontal cortex(DLPFC) and other brain regions in obsessive compulsive disorder(OCD) using the Granger causality analysis of resting-state functional MRI. We found that the effective connectivity from the bilateral DLPFC to some brain regions are increased or decreased in OCD, and DLPFC is the important information flow center. We also observed positive correlations between the abnormal causal effect and clinical symptoms such as obsession. These findings provide insight into OCD-related neural network disorders and may potentially guide clinical diagnosis and treatment of OCD in the future.

1079

9:09

Reduced Functional Network Segregation is Associated with Reduced Structural Network Integration and Cost Pre-Operatively in Neonates with Complex Congenital Heart Disease (CHD)



Vincent Schmithorst<sup>1</sup>, Vince Lee<sup>1</sup>, Jodie K. Votava-Smith<sup>2</sup>, Richard Kim<sup>3</sup>, Rafael Ceschin<sup>4</sup>, Shahida Sulaiman<sup>1</sup>, Hollie Lai<sup>5</sup>, Jennifer Johnson<sup>6</sup>, Joan Sanchez De Toledo<sup>7</sup>, Stefan Bluml<sup>5</sup>, Lisa Paquette<sup>8</sup>, and Ashok Panigrahy<sup>1</sup>

<sup>1</sup>Radiology, Children's Hospital of Pittsburgh of UPMC, Pittsburgh, PA, United States, <sup>2</sup>Division of Cardiology, Children's Hospital Los Angeles, <sup>3</sup>Division of Pediatric Cardiothoracic Surgery, Children's Hospital Los Angeles, <sup>4</sup>Department of Biomedical Informatics, University of Pittsburgh, <sup>5</sup>Radiology, Children's Hospital Los Angeles, <sup>6</sup>Division of Pediatric Cardiology, University of Pittsburgh School of Medicine, <sup>7</sup>Department of Critical Care, University of Pittsburgh School of Medicine, <sup>8</sup>Division of Neonatology, Children's Hospital Los Angeles

Neonates with complex congenital heart disease (CHD) pre-operatively show alterations in both structural network topology (as assessed via DTI) and functional network topology (as assessed via rs-fcMRI). Structurally, decreases in global efficiency, transitivity, and nodal efficiency are driven by decreased network cost and reflect alterations in white matter microstructure such as reduced fiber density. Functionally, CHD neonates display decreased network segregation in the later-developing frontal and temporal lobes, independent of cost, which likely reflect alterations at a more hierarchical level of architecture. These results may stem from different etiologies of brain dysmaturation (hypoperfusion vs. genetic factors).

---

9:21

### Connectivity Analysis Methods Optimized to Identify Structural/Functional Brain Connectivity

R. Todd Constable<sup>1</sup>

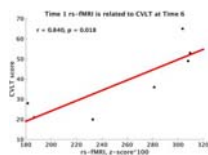
<sup>1</sup>*Yale University*

---

1080

9:51

### Functional and structural connectivity of the cingulate bundle related to future cognitive performance in MS



Katherine A Koenig<sup>1</sup>, Erik Beall<sup>2</sup>, Jian Lin<sup>1</sup>, Ken Sakaie<sup>1</sup>, Lael Stone<sup>3</sup>, Stephen Rao<sup>4</sup>, Micheal Phillips<sup>1</sup>, and Mark Lowe<sup>1</sup>

<sup>1</sup>*Imaging Institute, The Cleveland Clinic, Cleveland, OH, United States,*  
<sup>2</sup>*Hemalmaging,* <sup>3</sup>*Neurological Institute, The Cleveland Clinic, Cleveland, OH, United States,* <sup>4</sup>*Center for Brain Health, The Cleveland Clinic, Cleveland, OH, United States*

This work assesses the relationship of resting state fMRI (rs-fMRI) and DTI of the posterior cingulum bundle to future cognitive performance. We find that rs-fMRI is related to performance on measures related to episodic memory, and radial diffusivity is related to performance on a measure of speed of processing.

---

1081

10:03

### A multivariate machine learning framework for psychosis: integrating diffusion and structural MRI

Vasiliki Chatzi<sup>1</sup>, Rui Pedro A.G.Teixeira<sup>2</sup>, and Jacques Donald Tournier<sup>2</sup>



11:05      [Imaging at the Level of Neural Circuits](#)  
Anna Wang Roe<sup>1</sup>

*<sup>1</sup>Interdisciplinary Institute of Neuroscience & Technology, Zhejiang University, Hangzhou, People's Republic of China*

---

11:25      [Human Brain Mapping: Challenges & Opportunities](#)  
Heidi Johansen-Berg<sup>1</sup>

*<sup>1</sup>University of Oxford, United Kingdom*

---

11:45      [Adjournment & Meet the Teachers](#)

---

### **Traditional Poster: General Cancer Imaging**

Exhibition Hall 2888-2910      Thursday 13:00 - 15:00 *(no CME credit)*

---

### **Traditional Poster: MR Spectroscopy**

Exhibition Hall 2931-2965      Thursday 13:00 - 15:00 *(no CME credit)*

---

### **Traditional Poster: Molecular Imaging**

Exhibition Hall 3030-3046      Thursday 13:00 - 15:00 *(no CME credit)*

---

### **Electronic Poster: Interventional MRI**

Exhibition Hall      Thursday 13:00 - 14:00 *(no CME credit)*

---

### **Electronic Poster: MRI Safety**

Exhibition Hall      Thursday 13:00 - 14:00 *(no CME credit)*

---

### **Electronic Poster: MR Spectroscopy**

Exhibition Hall      Thursday 13:00 - 14:00 *(no CME credit)*

---

### **Study Groups**

Molecular & Cellular Imaging Study Group



Room 323ABC

Thursday 13:00 - 15:00 (no CME credit)

---

## Study Groups

### MR Flow & Motion Quantitation Study Group

Room 317AB

Thursday 13:00 - 15:00 (no CME credit)

---

## Educational Course

### Advanced Techniques in Pediatric Neuroimaging

Organizers: Christopher D. Smyser, M.D.

Room 316A

Thursday 13:00 - 15:00 Moderators: Silvina Ferradal & Chris Smyser

---

13:00

[Unique Methodological Challenges in Pediatric Neuroimaging](#)

Duan Xu<sup>1</sup>

<sup>1</sup>*Radiology and Biomedical Imaging, University of California San Francisco, San Francisco, CA, United States*

This educational session will introduce and discuss challenges for brain imaging of pediatric subjects. A brief overview of key differences between the developing brain and adult brain will be discussed. The presentation will address logistics of patient handling, image acquisition, post-processing techniques and analyses for improved characterization of the maturing brain. Translational studies will also be presented to highlight the importance of advancing pediatric brain imaging not only in research but also in clinical care, and further identify the area of needs to spur interests from the audience.

13:30

[Structural Insights Using Surface Based & Volumetric Analyses](#)

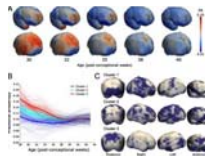
Patricia Ellen Grant<sup>1</sup>

<sup>1</sup>*Boston Children's Hospital, United States*

14:00

[Microstructural Investigation Using Diffusion Tensor Imaging](#)

Serena J Counsell<sup>1</sup>



<sup>1</sup>Centre for the Developing Brain, King's College London, London

14:30 [Functional Assessment Using Resting State Functional MRI](#)  
Damien Fair

15:00 [Adjournment & Meet the Teachers](#)

## Power Pitch

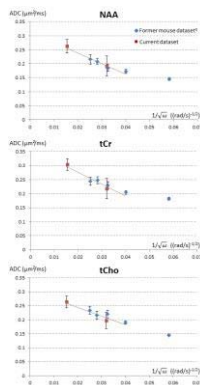
### Pitch: Cutting Edge Diffusion

Power Pitch  
Theater A - Thursday 13:00 - Moderators: Hua Guo & Markus Nilsson  
Exhibition Hall 14:00 (no CME credit)

1082

13:00

[Approaching free intracellular diffusion by diffusion-weighted MRS at ultra-short time scales: initial results in the rodent brain using a 1.5 T/m gradient](#)



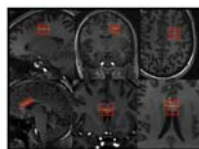
Clémence Ligneul<sup>1</sup>, Marco Palombo<sup>1</sup>, Julien Flament<sup>2</sup>, and Julien Valette<sup>1</sup>

<sup>1</sup>Molecular Imaging Research Center (MIR Cen), Commissariat à l'Energie Atomique, Fontenay-aux-Roses, France, <sup>2</sup>UMS 27, INSERM, Fontenay-aux-Roses, France

1083

13:00

[Accurate estimation of intra-axonal diffusivity and anisotropy of NAA in humans at 7T](#)

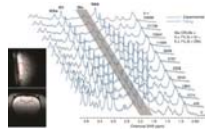


Henrik Lundell<sup>1</sup>, Carson Ingo<sup>2</sup>, Tim Bjørn Dyrby<sup>1,3</sup>, and Itamar Ronen<sup>4</sup>

*<sup>1</sup>Danish Research Centre for Magnetic Resonance, Centre for Functional and Diagnostic Imaging and Research, Copenhagen University Hospital Hvidovre, Copenhagen, Denmark, <sup>2</sup>Department of Physical Therapy and Human Movement Sciences, Northwestern University, Chicago, IL, United States, <sup>3</sup>Department of Applied Mathematics and Computer Science, Technical University of Denmark, Kongens Lyngby, Denmark, <sup>4</sup>C. J. Gorter Center for High Field MRI, Department of Radiology, Leiden University Medical Center, Leiden, Denmark*

1084

13:00



Glutamate diffusion at high b-values in the rat brain in vivo under light and deep anesthesia conditions

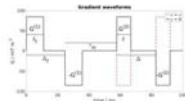
Xi Chen<sup>1</sup>, Siddartha Moktan Tamang<sup>1</sup>, Fei Du<sup>1</sup>, and Dost Ongur<sup>1</sup>

*<sup>1</sup>McLean Hospital, Belmont, MA, United States*

1085



13:00



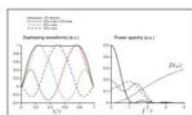
Bias in the apparent exchange rate measurements: insight from numerical simulations

Patricia Ulloa<sup>1</sup>, Vincent Methot<sup>1</sup>, and Martin A. Koch<sup>1</sup>

*<sup>1</sup>University of Lübeck, Lübeck, Germany*

1086

13:00



Microscopic anisotropy with spectrally modulated q-space trajectory encoding

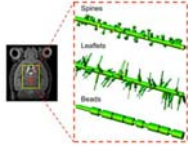
Henrik Lundell<sup>1</sup>, Markus Nilsson<sup>2</sup>, Tim Bjørn Dyrby<sup>1,3</sup>, Geoff JM Parker<sup>4,5</sup>, Penny L Hubbard Cristinacce<sup>4</sup>, Fenglei Zhou<sup>4</sup>, Daniel Topgaard<sup>6</sup>, and Samo Lasic<sup>1,7</sup>

*<sup>1</sup>Danish Research Centre for Magnetic Resonance, Centre for Functional and Diagnostic Imaging and Research, Copenhagen University Hospital Hvidovre, Hvidovre, Denmark, <sup>2</sup>Clinical Sciences Lund, Radiology, Lund University, Lund, Sweden, <sup>3</sup>4. Department of Applied Mathematics and Computer Science, Technical University of Denmark, Kongens Lyngby, Denmark, <sup>4</sup>Centre for Imaging Sciences, The University of Manchester, Manchester, United Kingdom, <sup>5</sup>Bioxydyn Limited, Manchester, United Kingdom, <sup>6</sup>Division of Physical Chemistry, Department of Chemistry, Lund University, Lund, Sweden, <sup>7</sup>CR Development AB, Lund, Sweden*

1087



13:00



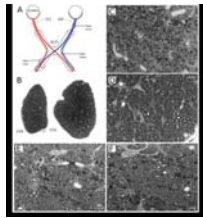
Can we detect the effect of spines, leaflets and beads on the diffusion of brain intracellular metabolites? A confrontation between high b-values and high-frequencies diffusion-weighted MRS in the mouse brain in vivo.

Marco Palombo<sup>1</sup>, Clemence Ligneul<sup>1</sup>, Edwin Hernandez-Garzon<sup>1</sup>, and Julien Valette<sup>1</sup>

<sup>1</sup>Molecular Imaging Research Center (MIRCen), Commissariat à l'Energie Atomique, Fontenay-aux-Roses, France

1088

13:00



Diffusion MRI of axonal degeneration in areas of fiber crossing: Histological correspondence.

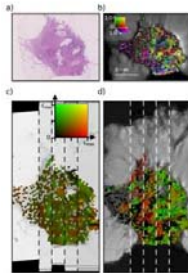
Luis Concha<sup>1</sup>, Jorge Larriva-Sahd<sup>1</sup>, Gilberto Rojas-Vite<sup>1</sup>, Ramsés Noguez-Imm<sup>1</sup>, Ricardo Coronado-Leija<sup>2</sup>, Alonso Ramírez-Manzanares<sup>2</sup>, and José Luis Marroquín<sup>2</sup>

<sup>1</sup>Institute of Neurobiology, Universidad Nacional Autonoma de Mexico, Queretaro, Mexico, <sup>2</sup>Computer Science, Centro de Investigación en Matemáticas, Guanajuato, Mexico

1089



13:00



Diffusion anisotropy in breast cancer tissue corresponds to spatial patterns of collagen alignment from structure tensor analysis of histology

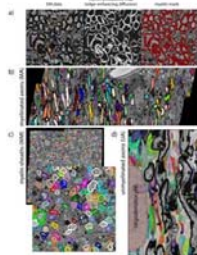
Colleen Bailey<sup>1</sup>, Francesco Grussu<sup>2</sup>, Bernard Siow<sup>3,4</sup>, Thomy Mertzani<sup>1</sup>, John H Hipwell<sup>1</sup>, Julie Owen<sup>5</sup>, Patrycja Gazinska<sup>5</sup>, Sarah E Pinder<sup>5</sup>, Daniel C Alexander<sup>1</sup>, David J Hawkes<sup>1</sup>, and Eleftheria Panagiotaki<sup>1</sup>

<sup>1</sup>Centre for Medical Image Computing, University College London, London, United Kingdom, <sup>2</sup>Institute of Neurology, University College London, London, United Kingdom, <sup>3</sup>Centre for Advanced Biomedical Imaging, University College London, London, United Kingdom, <sup>4</sup>Imaging, Francis Crick Institute, London, United Kingdom, <sup>5</sup>Breast Research Pathology, King's College London and Guy's Hospital, London, United Kingdom

1090



13:00



A 3D electron microscopy segmentation pipeline for hyper-realistic diffusion simulations

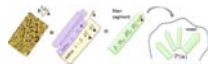
Michiel Kleinnijenhuis<sup>1</sup>, Errin Johnson<sup>2</sup>, Jeroen Mollink<sup>1,3</sup>, Saad Jbabdi<sup>1</sup>, and Karla Miller<sup>1</sup>

<sup>1</sup>Oxford Centre for Functional MRI of the Brain, University of Oxford, Oxford, United Kingdom, <sup>2</sup>Sir William Dunn School of Pathology, University of Oxford, Oxford, United Kingdom, <sup>3</sup>Department of Anatomy, Donders Institute for Brain, Cognition & Behaviour, Radboud University Medical Center, Nijmegen, Netherlands

---

1091

13:00



Rotationally invariant mapping of microstructural and orientational neuronal tissue parameters in human brain

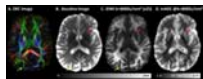
Dmitry S Novikov<sup>1</sup>, Jelle Veraart<sup>1</sup>, Ileana O Jelescu<sup>1</sup>, and Els Fieremans<sup>1</sup>

<sup>1</sup>Radiology, NYU School of Medicine, New York, NY, United States

---

1092

13:00



Isotropic Diffusion Weighted MRI (IDWI) – a novel, efficient clinical method for quantifying orientationally-averaged features of water diffusion in tissues

Alexandru Vlad Avram<sup>1</sup>, Joelle Sarlls<sup>2</sup>, Elizabeth Hutchinson<sup>3</sup>, and Peter Basser<sup>3</sup>

<sup>1</sup>NIBIB, National Institutes of Health, Bethesda, MD, United States,

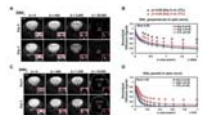
<sup>2</sup>NINDS, National Institutes of Health, Bethesda, MD, United States,

<sup>3</sup>NICHHD, National Institutes of Health, Bethesda, MD, United States

---

1093

13:00



Diffusion MRI differentiated acute inflammation from axonal injury but missed axonal loss

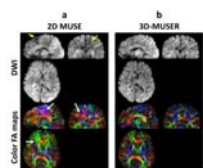
Tsen-Hsuan (Abby) Lin<sup>1</sup>, Michael Wallendorf<sup>2</sup>, Peng Sun<sup>1</sup>, and Sheng-Kwei Song<sup>1,3,4</sup>

<sup>1</sup>Radiology, Washington University School of Medicine, St. Louis, MO, United States, <sup>2</sup>Biostatistics, Washington University School of Medicine, St. Louis, MO, United States, <sup>3</sup>The Hope Center for Neurological Disorders, Washington University School of Medicine, St. Louis, MO, United States, <sup>4</sup>Biomedical Engineering, Washington University in St. Louis, St. Louis, MO

---

1094

13:00



Three-Dimensional Multiplexed Sensitivity Encoding and Reconstruction (3D-MUSER): 3D Phase Correction for 3D Multi-shot DWI

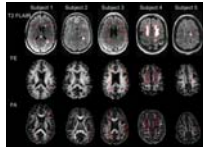
Hing-Chiu Chang<sup>1</sup>, Edward S. Hui<sup>1,2</sup>, Xiaoxi Liu<sup>1</sup>, Pui-Wai Chiu<sup>1</sup>, and Nan-kuei Chen<sup>3,4</sup>

<sup>1</sup>Department of Diagnostic Radiology, The University of Hong Kong, Hong Kong, Hong Kong, <sup>2</sup>The State Key Laboratory of Brain and Cognitive Sciences, The University of Hong Kong, Hong Kong, <sup>3</sup>Department of Biomedical Engineering, University of Arizona, Tucson, AZ, United States, <sup>4</sup>Brain Imaging and Analysis Center, Duke University Medical Center, Durham, NC, United States

1095



13:00



### Visualizing Axonal Damage in Multiple Sclerosis Using Double Diffusion Encoding MRI in a Clinical Setting

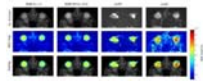
Grant Kaijun Yang<sup>1,2</sup>, Qiyuan Tian<sup>1,2</sup>, Christoph Leuze<sup>2</sup>, Max Wintermark<sup>2</sup>, and Jennifer McNab<sup>2</sup>

<sup>1</sup>Electrical Engineering, Stanford University, Stanford, CA, United States,

<sup>2</sup>Radiology, Stanford University, Stanford, CA, United States

1096

13:00



### Accelerated Diffusion-Sensitized MR Imaging of the Eye and Orbit at 3.0 T and 7.0 T free of Geometric Distortions Using a Combined RARE-EPI Acquisition Technique

Katharina Paul<sup>1</sup>, Helmar Waiczies<sup>2</sup>, André Kuehne<sup>2</sup>, Till Huelnhagen<sup>1</sup>, Eva Oberacker<sup>1</sup>, Oliver Stachs<sup>3</sup>, and Thoralf Niendorf<sup>1,2,4</sup>

<sup>1</sup>Berlin Ultrahigh Field Facility (B.U.F.F.), Max Delbrueck Center for Molecular Medicine in the Helmholtz Association, Berlin, Germany,

<sup>2</sup>MRI.TOOLS GmbH, Berlin, Germany, <sup>3</sup>Department of Ophthalmology, University of Rostock, Rostock, Germany, <sup>4</sup>Experimental and Clinical Research Center (ECRC), a joint cooperation between the Charité

Medical Faculty and the Max Delbrueck Center for Molecular Medicine in the Helmholtz Association, Berlin, Germany

## Power Pitch

## Pitch: Emerging Neuroimaging Techniques

Power Pitch

Theater B -

Exhibition Hall

Thursday 13:00 -Moderators: Peter Bandettini &

14:00

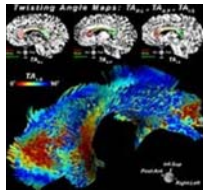
Jennifer McNab

(no CME credit)

1097

13:00

### Characterization of White Matter Tortuosity using High-Resolution gSlider-SMS Diffusion Imaging



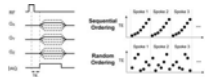
Choukri Mekkaoui<sup>1</sup>, Marcel P Jackowski<sup>2</sup>, Kawin Setsompop<sup>1</sup>, Qiuyun Fan<sup>1</sup>, Ned A Ohringer<sup>1</sup>, William J Kostis<sup>3</sup>, Timothy G Reese<sup>1</sup>, Alexandra J Golby<sup>4</sup>, and Susie Y Huang<sup>1</sup>

<sup>1</sup>Harvard Medical School - Massachusetts General Hospital, Boston, MA, United States, <sup>2</sup>University of São Paulo, São Paulo, Brazil, <sup>3</sup>Rutgers Robert Wood Johnson Medical School, New Brunswick, NJ, United States, <sup>4</sup>Brigham and Women's Hospital, Harvard Medical, Boston, MA, United States

1098

13:00

**In Vivo Characterization of an Ultrashort-T2 Component in the Brain Reveals a Chemical Shift**



Peder Eric Zufall Larson<sup>1</sup>, Tanguy Boucneau<sup>2</sup>, Shuyu Tang<sup>1</sup>, Misung Han<sup>1</sup>, Peng Cao<sup>1</sup>, and Roland G Henry<sup>3</sup>

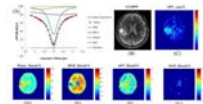
<sup>1</sup>Radiology and Biomedical Imaging, University of California - San Francisco, San Francisco, CA, United States, <sup>2</sup>Ecole normale supérieure de Cachan, Paris, France, <sup>3</sup>Neurology, University of California - San Francisco, San Francisco, CA, United States

1099



13:00

**Improved Differentiation of Low- and High-Grade Gliomas by APT Contrast Fitted from Z-Spectrum**



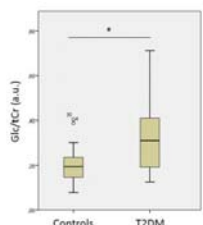
Jiaxuan Zhang<sup>1,2</sup>, Rongwen Tain<sup>1,3</sup>, Xiaohong Joe Zhou<sup>1,4</sup>, Wenzhen Zhu<sup>2</sup>, and Kejia Cai<sup>1,5</sup>

<sup>1</sup>Center for MR Research, University of Illinois at Chicago, Chicago, IL, United States, <sup>2</sup>Department of Radiology, Tongji Hospital, Huazhong University of Science and Technology, Wuhan, People's Republic of China, <sup>3</sup>Department of Radiology, University of Illinois at Chicago, Chicago, IL, United States, <sup>4</sup>Departments of Radiology, Neurosurgery, and Bioengineering, University of Illinois at Chicago, Chicago, IL, United States, <sup>5</sup>Departments of Radiology and Bioengineering, University of Illinois at Chicago, Chicago, IL, United States

1100

13:00

**3T 1H PRESS (TE 68 ms) reveals elevated cerebral glucose in patients with diabetes mellitus type 2, which is associated with fasting blood glucose**



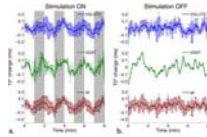
Frank C.G. van Bussel<sup>1</sup>, Tamar M van Veenendaal<sup>1</sup>, Miranda T Schram<sup>2</sup>, Coen D.A. Stehouwer<sup>2</sup>, Walter H Backes<sup>1</sup>, and Jacobus F.A. Jansen<sup>1</sup>



*<sup>1</sup>Radiology, Maastricht University Medical Center, Maastricht, Netherlands, <sup>2</sup>Internal Medicine, Maastricht University Medical Center, Maastricht, Netherlands*

1101

13:00



**Towards opto-fMRS: Ultra high field MRS measurement of T2\* changes due to optogenetic stimulation**

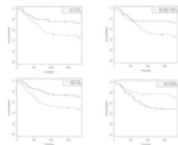
Jamie Near<sup>1,2</sup>, Dan Madularu<sup>1,2</sup>, Jennifer Robinson<sup>3</sup>, Chathura Kumaragamage<sup>4</sup>, Axel Mathieu<sup>2</sup>, Sylvain Williams<sup>1,2</sup>, M Natasha Rajah<sup>1,2</sup>, and Uzay Emir<sup>5</sup>

*<sup>1</sup>Department of Psychiatry, McGill University, Montreal, QC, Canada, <sup>2</sup>Centre d'Imagerie Cérébrale, Douglas Mental Health University Institute, Montreal, QC, Canada, <sup>3</sup>Integrated Program in Neuroscience, McGill University, Montreal, QC, Canada, <sup>4</sup>Biomedical Engineering, McGill University, Montreal, QC, Canada, <sup>5</sup>Nuffield Department of Clinical Neurosciences, University of Oxford, Oxford, United Kingdom*

1102



13:00



**Glycine, a marker of survival in paediatric brain tumours measured with non-invasive Magnetic Resonance Spectroscopy: A five-year survival analysis.**

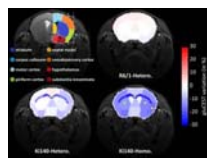
Ben Babourina-Brooks<sup>1</sup>, Sarah Kohe<sup>1</sup>, Simrandip K Gill<sup>1</sup>, Martin Wilson<sup>2</sup>, Lesley Macpherson<sup>3</sup>, Nigel P Davies<sup>4</sup>, and Andrew C Peet<sup>1,3</sup>

*<sup>1</sup>University of Birmingham, Birmingham, United Kingdom, <sup>2</sup>Birmingham University Imaging Centre, University of Birmingham, Birmingham, United Kingdom, <sup>3</sup>Birmingham Children's Hospital NHS Foundation Trust, Birmingham, United Kingdom, <sup>4</sup>Imaging & Medical Physics, University Hospitals Birmingham NHS Foundation Trust, Birmingham, United Kingdom*

1103



13:00



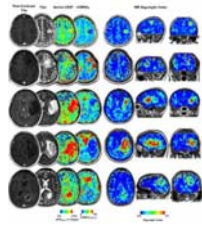
**About the complementarity of gluCEST and 1H-MRS for the study of neurodegenerative diseases using animal models**

Jérémy Pépin<sup>1</sup>, Clémence Ligneul<sup>1</sup>, Julien Valette<sup>1</sup>, Emmanuel Brouillet<sup>1</sup>, and Julien Flament<sup>1,2</sup>

*<sup>1</sup>Molecular Imaging Research Center (MIRCE), Commissariat à l'Energie Atomique (CEA), Fontenay-aux-Roses, France, <sup>2</sup>UMS27, INSERM, Fontenay-aux-Roses, France*

1104

13:00



A "Glycolytic Index" for quantifying abnormal metabolism in human gliomas using multi-echo amine chemical exchange saturation transfer spin-and-gradient echo echoplanar imaging (ME-aCEST-SAGE-EPI) at 3T

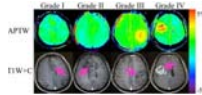
Robert J Harris<sup>1</sup>, Kevin Leu, Timothy F Cloughesy, Whitney B Pope, Phioanh L Nghiemphu, Albert Lai, Linda M Liau, and Benjamin M Ellingson<sup>2</sup>

<sup>1</sup>University of California Los Angeles, Los Angeles, CA, United States,

<sup>2</sup>Radiological Sciences, University of California Los Angeles, Los Angeles, CA, United States

1105

13:00



Qualitative and quantitative analysis of amide proton transfer-weighted MR images at 3 Tesla of adult gliomas

Xianlong Wang<sup>1</sup>, Hao Yu<sup>2</sup>, Shanshan Jiang<sup>2</sup>, Yu Wang<sup>3</sup>, Yanyu Wang<sup>2</sup>, Ge Zhang<sup>4</sup>, Chunxiu Jiang<sup>2</sup>, Guodong Song<sup>5</sup>, Yi Zhang<sup>6</sup>, Hye-Young Heo<sup>6</sup>, Jinyuan Zhou<sup>6</sup>, and Zhibo Wen<sup>2</sup>

<sup>1</sup>Radiology, Zhujiang Hospital of Southern Medical University,

Guangzhou, People's Republic of China, <sup>2</sup>Radiology, Zhujiang Hospital

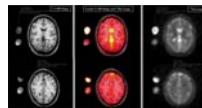
of Southern Medical University, <sup>3</sup>Pathology, Zhujiang Hospital of

Southern Medical University, <sup>4</sup>Radiology, Hainan General Hospital,

<sup>5</sup>Radiology, Beijing Hospital, <sup>6</sup>Radiology, Johns Hopkins University

1106

13:00



Cerebral Sodium (<sup>23</sup>Na) Magnetic Resonance Imaging in Patients with Migraine

Melissa M Ong<sup>1</sup>, Alexander Schmidt<sup>1</sup>, Simon Konstandin<sup>2</sup>, Justus Benrath<sup>3</sup>, Mathias Meyer<sup>1</sup>, Lothar R Schad<sup>4</sup>, Stefan O Schoenberg<sup>1</sup>, and Stefan Haneder<sup>1,5</sup>

<sup>1</sup>Institute of Clinical Radiology and Nuclear Medicine, University Medical Center Mannheim, University of Heidelberg, Mannheim, Germany,

<sup>2</sup>University of Bremen, MR-Imaging and Spectroscopy, Faculty 01

(Physics/Electrical Engineering), Bremen, Germany, <sup>3</sup>Clinic for

Anaesthesiology and Operative Intensive Care, University Medical

Center Mannheim, University of Heidelberg, Mannheim, Germany,

<sup>4</sup>Computer Assisted Clinical Medicine, University Medical Center

Mannheim, University of Heidelberg, Mannheim, Germany, <sup>5</sup>Institute of

Diagnostic and Interventional Radiology, University Hospital Cologne,

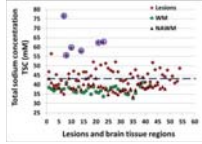
Cologne, Germany

1107

13:00

Differentiating subtypes of multiple sclerosis lesions using sodium MR imaging

Yulin Ge<sup>1</sup>, Yongxian Qian, Jean-Christophe Brisset, and Fernando E Boada



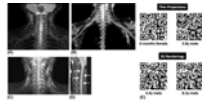
<sup>1</sup>New York University School of Medicine, New York, NY, United States

1108



13:00

Imaging of the Brachial Plexus using a 3D Dixon-TSE Pulse Sequence with Blood Vessel and CSF Signal Suppression: Preliminary Experience in Children



Barbara Cervantes<sup>1</sup>, Amber L. Pokorney<sup>2</sup>, Jan S. Kirschke<sup>3</sup>, Patricia Cornejo<sup>2</sup>, Jeffrey H. Miller<sup>2</sup>, Dimitrios C. Karampinos<sup>1</sup>, and Houchun Harry Hu<sup>2</sup>

<sup>1</sup>Department of Diagnostic and Interventional Radiology, Klinikum rechts der Isar, Technische Universität München, Munich, Germany,

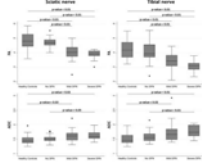
<sup>2</sup>Department of Radiology, Phoenix Children's Hospital, Phoenix, AZ, United States, <sup>3</sup>Department of Neuroradiology, Klinikum rechts der Isar, Technische Universität München, Munich, Germany

1109



13:00

Diffusion-Tensor-Imaging MR-Neurography for the detection of polyneuropathy in Type 1 diabetes



Michael Vaeggemose<sup>1</sup>, Mirko Pham<sup>2</sup>, Steffen Ringgaard<sup>3</sup>, Hatice Tankisi<sup>4</sup>, Niels Ejksjaer<sup>1</sup>, Sabine Heiland<sup>5</sup>, Per L. Poulsen<sup>6</sup>, and Henning Andersen<sup>1</sup>

<sup>1</sup>Dept. of Neurology, Aarhus University Hospital, Aarhus C, Denmark,

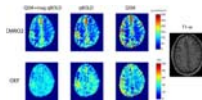
<sup>2</sup>Dept. of Neuroradiology, Würzburg University Hospital, Würzburg, Germany, <sup>3</sup>MR Research Centre, Aarhus University Hospital, Aarhus N, Denmark, <sup>4</sup>Dept. of Neurophysiology, Aarhus University Hospital, Aarhus C, Denmark, <sup>5</sup>Heidelberg University Hospital, Heidelberg, Germany,

<sup>6</sup>Dept. of Endocrinology, Aarhus University Hospital, Aarhus C, Denmark

1110

13:00

Optimal quantitative mapping of Cerebral Metabolic Rate of Oxygen (CMRO<sub>2</sub>) by combining quantitative susceptibility mapping (QSM)-based method and quantitative BOLD (qBOLD)

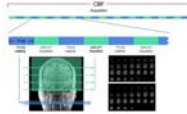


Junghun Cho<sup>1</sup>, Youngwook Kee<sup>2</sup>, Pascal Spincemaille<sup>2</sup>, Thanh Nguyen<sup>2</sup>, Jingwei Zhang<sup>1</sup>, and Yi Wang<sup>1,2</sup>

<sup>1</sup>Cornell University, Ithaca, NY, United States, <sup>2</sup>Weill Cornell Medical College, New York, NY, United States

1111

13:00



Asynchronous Local Analysis of simultaneous BOLD ASL Multislice Acquisition (ALABAMA): Toward Whole-Brain Noninvasive Estimation of Resting-State Neuronal-Vascular Coupling

Vincent Schmithorst<sup>1</sup>, Vince Lee<sup>1</sup>, and Ashok Panigrahy<sup>1</sup>

<sup>1</sup>Radiology, Children's Hospital of Pittsburgh of UPMC, Pittsburgh, PA, United States

Oral

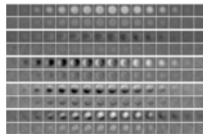
## Cancer Treatment Response

Room 310

Thursday 13:00 - 15:00 Moderators: Ferdia Gallagher & Jana Kim

1112

13:00



Eigentumors of dynamic contrast-enhanced MR images of the breast for prediction of treatment failure

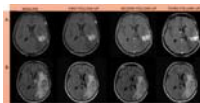
Hui Shan Chan<sup>1</sup>, Claudette Loo<sup>2</sup>, and Kenneth Gilhuijs<sup>1</sup>

<sup>1</sup>Image Sciences Institute, University Medical Center Utrecht, Utrecht, Netherlands, <sup>2</sup>Netherlands Cancer Institute - Antoni van Leeuwenhoek Hospital, Amsterdam, Netherlands

A method is proposed for predicting long-term treatment failure using “eigentumors”: principal components computed from volumes surrounding breast tumors in contrast-enhanced images. The dataset contains pre-treatment scans of 563 consecutively included patients with early-stage breast cancer with median follow-up of 86 months. Principal components of washin and washout in box-shaped regions surrounding the tumors were computed, and LASSO and logistic regression were used to construct a model for predicting the probability of treatment failure. ROC analysis yields a bootstrapped performance of 0.73, and bootstrapped Kaplan-Meier survival curves based on the model's outcome show significant separation ( $\chi=32.89$ ,  $P < 0.0001$ ).

1113

13:12



Radiomic Analysis Differentiates between True Progression and Pseudo-progression in Glioblastoma patients: A Large Scale Multi-institutional Study

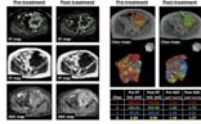
Aikaterini Kotrotsou<sup>1</sup>, Srishti Abrol<sup>1</sup>, Nabil A Elshafeey<sup>1</sup>, Islam Hassan<sup>1</sup>, Dunia Giniebra Camejo<sup>2</sup>, Ahmed Hassan<sup>1</sup>, Tagwa Idris<sup>1</sup>, Ahmed Salem<sup>1</sup>, Kamel El Salek<sup>1</sup>, Ahmed Elakkad<sup>1</sup>, Kristin D Alfaro-Munoz<sup>3</sup>, Shiao-Pei Weathers<sup>3</sup>, Fanny E Moron<sup>4</sup>, John F deGroot<sup>3</sup>, Meng Law<sup>5</sup>, Pascal O Zinn<sup>6</sup>, and Rivka R Colen<sup>1,2</sup>

<sup>1</sup>Diagnostic Radiology, MD Anderson Cancer Center, Houston, TX, United States, <sup>2</sup>Cancer Systems Imaging, MD Anderson Cancer Center, Houston, TX, United States, <sup>3</sup>Neuro-Oncology, MD Anderson Cancer Center, Houston, TX, United States, <sup>4</sup>Neuroradiology, Baylor College of Medicine, Houston, TX, United States, <sup>5</sup>Neuroradiology, University of Southern California Keck Medical Center, Los Angeles, CA, United States, <sup>6</sup>Neurosurgery, Baylor College of Medicine, Houston, TX, United States

The benign treatment-related imaging changes may pose a challenge in appropriate clinical decision making for the neuro-oncologists. The post-treatment changes are usually benign and differ largely in management approach from a progressive tumor. In this study, 304 glioblastoma patients were evaluated retrospectively to study the ability of radiomic analysis to distinguish the post-treatment changes from a truly progressive disease. 3D volumetrics using 3D Slicer 4.3.1 and texture analysis of the lesions were performed. On LOOCV, sensitivity and specificity of 97% and 72% were obtained respectively. We concluded that radiomics can differentiate between the progressive disease and pseudo-progression in glioblastoma patients.

1114

13:24



Supervised machine-learning enables segmentation and evaluation of heterogeneous post-treatment changes in multi-parametric MRI of soft-tissue sarcoma

Matthew David Blackledge<sup>1,2</sup>, Jessica M Winfield<sup>1,2</sup>, Aisha Miah<sup>3</sup>, Dirk Strauss<sup>4</sup>, Khin Thway<sup>5</sup>, Veronica A Morgan<sup>1,2</sup>, David J Collins<sup>1,2</sup>, Dow-Mu Koh<sup>1,2</sup>, Martin O Leach<sup>1,2</sup>, and Christina Messiou<sup>1,2</sup>

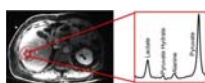
<sup>1</sup>Cancer Research UK Cancer Imaging Centre, The Institute of Cancer Research, London, United Kingdom, <sup>2</sup>MRI Unit, The Royal Marsden NHS Foundation Trust, Sutton, United Kingdom, <sup>3</sup>Department of Radiotherapy, The Royal Marsden NHS Foundation Trust, London, United Kingdom, <sup>4</sup>Department of Surgery, The Royal Marsden NHS Foundation Trust, London, United Kingdom, <sup>5</sup>Department of Histopathology, The Royal Marsden NHS Foundation Trust, London, United Kingdom

Multi-parametric MRI enables non-invasive response assessment in heterogeneous soft-tissue sarcomas, but evaluation of post-treatment changes in MRI parameters requires segmentation of cellular tumour-tissue, which might be expected to respond to treatment, from necrotic/cystic regions and fat. Six supervised Machine-Learning methods were explored using a randomized cross-validation approach, from which a candidate method (automatic Kernel Density Estimation) was selected owing to its high validation accuracy and automatic selection of hyper-parameters. The automatic-KDE method enabled evaluation of post-radiotherapy changes in volumes and ADCs of each tumour component, and provided visual depiction of heterogeneous changes in multi-parametric MR-images.

1115



13:36



### Hyperpolarized $^{13}\text{C}$ Dynamic Breath-held Molecular Imaging to Detect Targeted Therapy Response in Patients with Liver Metastases

Zihan Zhu<sup>1,2</sup>, Irene Marco-Rius<sup>3</sup>, Michael A Ohliger<sup>1</sup>, Lucas Carvajal<sup>1</sup>, Jeremy W Gordon<sup>1</sup>, Hsin-Yu Chen<sup>1,2</sup>, Ilwoo Park<sup>1</sup>, Peng Cao<sup>1</sup>, Peter J Shin<sup>1</sup>, Eugene Milshteyn<sup>1,2</sup>, Cornelius von Morze<sup>1</sup>, Marcus Ferrone<sup>4</sup>, James B Slater<sup>1</sup>, Zhen Wang<sup>1</sup>, Peder E.Z. Larson<sup>1</sup>, Rahul Aggarwal<sup>5</sup>, Robert Bok<sup>1</sup>, John Kurhanewicz<sup>1</sup>, Pamela Munster<sup>5</sup>, and Daniel B Vigneron<sup>1</sup>

<sup>1</sup>Department of Radiology and Biomedical Imaging, UCSF, San Francisco, CA, United States, <sup>2</sup>UC Berkeley-UCSF Graduate Program in Bioengineering, UC Berkeley and UCSF, San Francisco, CA, United States, <sup>3</sup>University of Cambridge, United Kingdom, <sup>4</sup>Department of Clinical Pharmacy, UCSF, San Francisco, CA, United States, <sup>5</sup>Department of Medicine, UCSF, San Francisco, CA, United States

New clinical trials are using hyperpolarized  $^{13}\text{C}$  molecular imaging technology to evaluate tumor metabolic activity and response to targeted drug therapies. The goal of this work was to develop and apply an experimental setup for HP  $^{13}\text{C}$  MR investigations of cancer metastases to liver. In this study, patients with liver metastases were imaged and the results demonstrated sufficient SNR and data quality for the quantification of the localized conversion rate of [1- $^{13}\text{C}$ ]pyruvate to [1- $^{13}\text{C}$ ]lactate through lactate dehydrogenase (LDH), which is a pathway targeted by numerous emerging pharmaceutical agents and currently prescribed Everolimus.

1116

13:48

Assessing Response Heterogeneity following Radium 223 administration using Whole Body Diffusion Weighted MRI



Time	ADC	ADC <sub>min</sub>	ADC <sub>max</sub>	ADC <sub>mean</sub>	ADC <sub>std</sub>	ADC <sub>var</sub>	ADC <sub>skew</sub>	ADC <sub>kurt</sub>	ADC <sub>entropy</sub>	ADC <sub>entropy</sub>
0:00	1.00	0.50	1.50	1.00	0.25	0.06	0.00	0.00	0.00	0.00
0:05	1.00	0.50	1.50	1.00	0.25	0.06	0.00	0.00	0.00	0.00
0:10	1.00	0.50	1.50	1.00	0.25	0.06	0.00	0.00	0.00	0.00
0:15	1.00	0.50	1.50	1.00	0.25	0.06	0.00	0.00	0.00	0.00
0:20	1.00	0.50	1.50	1.00	0.25	0.06	0.00	0.00	0.00	0.00
0:25	1.00	0.50	1.50	1.00	0.25	0.06	0.00	0.00	0.00	0.00
0:30	1.00	0.50	1.50	1.00	0.25	0.06	0.00	0.00	0.00	0.00
0:35	1.00	0.50	1.50	1.00	0.25	0.06	0.00	0.00	0.00	0.00
0:40	1.00	0.50	1.50	1.00	0.25	0.06	0.00	0.00	0.00	0.00
0:45	1.00	0.50	1.50	1.00	0.25	0.06	0.00	0.00	0.00	0.00
0:50	1.00	0.50	1.50	1.00	0.25	0.06	0.00	0.00	0.00	0.00
0:55	1.00	0.50	1.50	1.00	0.25	0.06	0.00	0.00	0.00	0.00
1:00	1.00	0.50	1.50	1.00	0.25	0.06	0.00	0.00	0.00	0.00

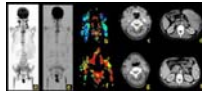
Matthew David Blackledge<sup>1,2</sup>, Dow Mu Koh<sup>1,2</sup>, David J Collins<sup>1,2</sup>, Erica Scurr<sup>2</sup>, Julie Hughes<sup>2</sup>, Martin O Leach<sup>1,2</sup>, Chris Parker<sup>1,3</sup>, and Nina Tunariu<sup>1,2</sup>

<sup>1</sup>Division of Radiotherapy and Imaging, The Institute of Cancer Research, London, United Kingdom, <sup>2</sup>MRI Unit, The Royal Marsden NHS Foundation Trust, Sutton, United Kingdom, <sup>3</sup>Urology Department, The Royal Marsden NHS Foundation Trust, Sutton, United Kingdom

Whole-Body Diffusion-Weighted-MRI is emerging as an imaging response biomarker in metastatic bone disease. Documentation of mixed therapeutic response is a key recommendation of the Prostate Cancer Working Group as recognition of coexistence of mixed response to therapy and clinical benefit. Radium-223 has shown efficacy in prostate cancer patients with symptomatic bone metastases. Monitoring Radium-223 therapy efficacy treatment is challenging, as Radium-223 administration can be associated with flare in pain, PSA and Bone Scan. These pilot data demonstrate that Radium-223 administration is associated with an increase in bone metastases ADC values together with a mixed response pattern.

1117

14:00



Whole-Body Diffusion-Weighted Imaging at 1.5T for assessment of treatment response in non-Hodgkin lymphoma

Xiaoyi Wang<sup>1</sup>, Yanfeng Zhao<sup>1</sup>, Ning Wu<sup>1</sup>, Han Ouyang<sup>1</sup>, and Lizhi Xie<sup>2</sup>

<sup>1</sup>National Cancer Center/Cancer Hospital, Chinese Academy of Medical Sciences and Peking Union Medical College, Beijing, People's Republic of China, <sup>2</sup>GE Healthcare, MR Research China, Beijing, People's Republic of China

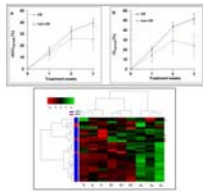
The diagnostic capability between WBDWI with contrast enhanced CT was compared in malignant lymphoma diagnosis. We found that WBDWI is a powerful tool on diagnosing non-Hodgkin(NHL) lymphoma by comparing with contrast enhanced CT. Chemotherapy causes rapid decrease of the restriction of water molecules diffusion movement, ADC-min could be valuable tools for treatment response evaluation of NHL. We recommended WBDWI examination for patients with NHL.

1118

14:12

Intravoxel incoherent motion diffusion-weighted MRI during chemoradiation therapy to monitor treatment response in human papillomavirus head and neck squamous cell carcinoma





Ramesh Paudyal<sup>1</sup>, Jung Hun Oh<sup>1</sup>, Nadeem Riaz<sup>2</sup>, Praveen Venigalla<sup>2</sup>, Jingao Li<sup>3</sup>, Vaios Hatzoglou<sup>4</sup>, Jonathan Leeman<sup>2</sup>, David Aramburu Nunez<sup>1</sup>, Yonggang Lu<sup>5</sup>, Joseph O. Deasy<sup>1</sup>, Nancy Lee<sup>2</sup>, and Amita Shukla-Dave<sup>1,4</sup>

<sup>1</sup>Medical Physics, Memorial Sloan Kettering Cancer Center, New York, NY, United States, <sup>2</sup>Radiation Oncology, Memorial Sloan Kettering Cancer Center, NY, United States, <sup>3</sup>Radiation Oncology, Jiangxi Cancer Hospital, Chile, <sup>4</sup>Radiology, Memorial Sloan Kettering Cancer Center, NY, United States, <sup>5</sup>Radiation Oncology, Washington University in St. Louis, MO, United States

This study aims to monitor treatment response in human papillomavirus (HPV) head and neck squamous cell carcinoma using pre- and intra-treatment (TX) week 1, 2 and 3 imaging metrics derived from intravoxel incoherent motion (IVIM) DW-MRI. An unsupervised hierarchical clustering with a distance based on the Pearson correlation coefficient was performed using the relative percentage changes in D, f and D\* to investigate similarities among features and samples. D showed a significant increase during treatment in complete response (CR) group. A heat map generated from the unsupervised hierarchical clustering identified subtypes in HPV positive [+] HNSCC patients.

1119



14:24



Multiparametric MRI with spatiotemporal evaluation reveals potential therapy response biomarkers for <sup>177</sup>Lu-octreotate therapy of mice with human neuroendocrine tumor

Mikael Montelius<sup>1</sup>, Johan Spetz<sup>1</sup>, Oscar Gustafsson<sup>1</sup>, Evelin Berger<sup>2</sup>, Ola Nilsson<sup>3</sup>, Maria Ljungberg<sup>1</sup>, and Eva Forssell-Aronsson<sup>1</sup>

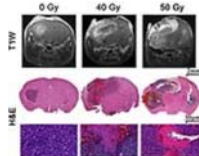
<sup>1</sup>Department of Radiation Physics, University of Gothenburg, Gothenburg, Sweden, <sup>2</sup>Proteomics Core Facility, University of Gothenburg, Gothenburg, Sweden, <sup>3</sup>Department of Pathology, University of Gothenburg, Gothenburg, Sweden

Tissue parameters derived from multiparametric MRI were evaluated as potential imaging biomarkers for therapy response assessment in mice with human neuroendocrine tumor treated with  $^{177}\text{Lu}$ -octreotate. Animals were imaged before and repeatedly after  $^{177}\text{Lu}$ -octreotate treatment, using T2w, IVIM-DWI, DCE-MRI, T1- and T2\*-mapping techniques. MR-parameters were evaluated regionally and longitudinally, and quantitative proteomics was used to evaluate underlying biological response in central and peripheral tumor separately. Several MR-parameters showed strong correlation with tumor response, as verified by MRI-based tumor volume measurements, but also with proteins associated with radiobiological effects on tumor tissue. Spatial and temporal evaluation increased sensitivity of the methods.

1120



14:36



### Irradiated Brain Parenchyma Promotes Virulent Proliferation of Naive Glioma Cells: Mouse Model of Recurrent Glioblastoma

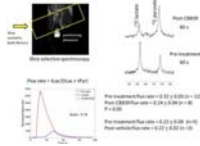
Chong Duan<sup>1</sup>, Ruimeng Yang<sup>2,3</sup>, Liya Yuan<sup>4</sup>, John A Engelbach<sup>2</sup>, Sonika Dahiya<sup>5</sup>, Christina I Tsien<sup>6</sup>, Keith Rich<sup>4</sup>, Joseph JH Ackerman<sup>1,2</sup>, and Joel R Garbow<sup>2,7</sup>

<sup>1</sup>Chemistry, Washington University in St. Louis, St. Louis, MO, United States, <sup>2</sup>Radiology, Washington University in St. Louis, St. Louis, MO, United States, <sup>3</sup>Radiology, Guangzhou First People's Hospital, Guangzhou, People's Republic of China, <sup>4</sup>Neurosurgery, Washington University in St. Louis, St. Louis, MO, United States, <sup>5</sup>Pathology and Immunology, Washington University in St. Louis, St. Louis, MO, United States, <sup>6</sup>Radiation Oncology, Washington University in St. Louis, St. Louis, MO, United States, <sup>7</sup>Alvin J Siteman Cancer Center, Washington University in St. Louis

For many years, research on recurrent glioblastoma has largely focused on therapy-induced cancer-cell changes. Herein, we show that gliomas resulting from naïve, non-irradiated DBT tumor cells implanted into irradiated mouse brains grow more rapidly than tumors resulting from naïve DBT cells implanted into non-irradiated mouse brains. Likewise, survival post-implantation is reduced, and MRI and histology document striking differences between naïve tumors implanted in irradiated vs. non-irradiated brain. Collectively, these data provide new insights into the enhanced invasiveness of recurrent gliomas and, importantly, demonstrate a novel recurrent glioblastoma model for further investigation of the long-term effects of radiotherapy on tumor microenvironment.

1121

14:48



### Assessing Metabolic Intervention in Acute Myeloid Leukemia with a Glutaminase Inhibitor by Hyperpolarized Magnetic Resonance

Niki Zacharias Millward<sup>1,2</sup>, Sriram Shanmugavelandy<sup>1</sup>, Jaehyuk Lee<sup>1</sup>, Natalia Baran<sup>3</sup>, Juliana Velez<sup>3</sup>, Prasanta Dutta<sup>1</sup>, Marina Konopleva<sup>3</sup>, and Pratip Bhattacharya<sup>1</sup>

<sup>1</sup>Cancer Systems Imaging, MD Anderson Cancer Center, Houston, TX, United States, <sup>2</sup>Bioengineering, Rice University, Houston, TX, <sup>3</sup>Leukemia, MD Anderson Cancer Center, Houston, TX, United States

Acute myeloid leukemia (AML) is glutamine addicted cancer. We determined if hyperpolarized pyruvate could be utilized to detect in vivo metabolic changes in AML (OCI-AML3 cell line) bearing mice after CB839 (glutaminase inhibitor) treatment. We found a reduction of pyruvate to lactate conversion after treatment. In vitro analysis of OCI-AML3 reveal that NADH/NAD<sup>+</sup> ratio, ATP, hydrogen peroxide levels and respiratory capacity reduce in CB839 treated cells compared to vehicle controls. Our data supports the hypothesis that in AML glutamine generates reducing equivalences by the citric acid cycle and inhibiting this process with CB839 reduces the rate of conversion of pyruvate to lactate.

## Oral

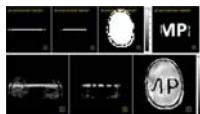
## UHF Applications & Technology

Room 311

Thursday 13:00 - 15:00 *Moderators:* Özlem Ipek & Benedikt Poser

1122

13:00



### Homogeneous high-flip-angle 3D localization by parallel transmission at 9.4T

Tingting Shao<sup>1</sup>, Yun Zhang<sup>2</sup>, Nikolai I. Avdievich<sup>1</sup>, Christian Mirkes<sup>1</sup>, Klaus Scheffler<sup>1</sup>, Steffen Glaser<sup>2</sup>, and Anke Henning<sup>1,3</sup>

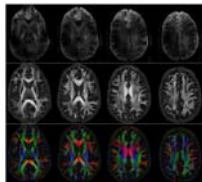
<sup>1</sup>Max Planck Institute for Biological Cybernetics, Tuebingen, Germany, <sup>2</sup>Department of Chemistry, Technical University of Munich, Garching, Germany, <sup>3</sup>Institute of Physics, Ernst-Moritz-Arndt University Greifswald, Greifswald, Germany

This work presents in vivo experimental result of high-flip-angle multi-dimensional parallel transmission at a 9.4T human whole-body MRI scanner. A 2D pTx saturation pulse (90°) and a slice selective 3D pTx excitation pulse (60°) were designed by using an algorithm that combines LSQR and optimal control (OC) methods and enables high-flip-angle pTx pulse design with a strict constraint of transmit power. An actual flip angle imaging (AFI) sequence was coded to measure the flip angle map of the pre-saturated slice excitation profile achieved by the sequentially implemented pTx pulses.

1123



13:12



### High Resolution Multi-shot Diffusion Imaging at 7T without Navigators

Merry Mani<sup>1</sup>, Mathews Jacob<sup>2</sup>, Baolian Yang<sup>3</sup>, and Vincent Magnotta<sup>2</sup>

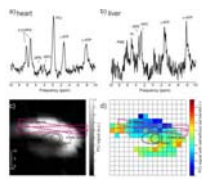
<sup>1</sup>Department of Radiology, University of Iowa, Iowa City, IA, United States, <sup>2</sup>University of Iowa, Iowa City, IA, United States, <sup>3</sup>GE Healthcare

The higher signal-to-noise ratio (SNR) offered by the ultra-high field (UHF) strengths are often exploited to improve the spatial resolution capabilities of several MR imaging modalities. However, SNR advantage of UHF scanners do not often translate to improved diffusion weighted images (DWIs), especially using conventional single-shot echo-planar imaging-based acquisitions. The presence of diffusion gradients limit the lowest echo-time (TE) achievable, while the shortened T2 and T2\* values lead to faster decay of the MRI signal, both of which are detrimental to the already signal-starved DWIs. We propose a short-TE acquisition based on multi-shot EPI and partial Fourier acquisition to enable high resolution diffusion imaging at 7T that does not need navigator scans or phase calibration.

1124



13:24



### Initial experiences with a fully-removable whole-body birdcage transmit coil and 16-element receive array for cardiac 31P-MRS at 7T

Ladislav Valkovic<sup>1</sup>, Iulius Dragonu<sup>2</sup>, Karsten Wicklow<sup>2</sup>, Ulrich Joerg Fontius<sup>2</sup>, Salam Almujaayaz<sup>3</sup>, Alex Batzakis<sup>3</sup>, Liam Young<sup>1</sup>, Lucian AB Purvis<sup>1</sup>, William T Clarke<sup>1</sup>, Tobias Wichmann<sup>4</sup>, Titus Lanz<sup>4</sup>, Stefan Neubauer<sup>1</sup>, Matthew D Robson<sup>1</sup>, Dennis WJ Klomp<sup>3,5</sup>, and Christopher T Rodgers<sup>1</sup>

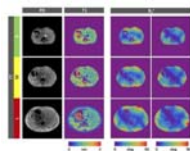
<sup>1</sup>Oxford Centre for Clinical MR Research (OCMR), RDM Cardiovascular Medicine, University of Oxford, Oxford, United Kingdom, <sup>2</sup>Siemens Healthcare GmbH, Erlangen, Germany, <sup>3</sup>MR Coils BV, Zaltbommel, Netherlands, <sup>4</sup>Rapid Biomedical GmbH, Rimpar, Germany, <sup>5</sup>Department of Radiology, University Medical Center Utrecht, Utrecht, Netherlands

This abstract describes our experiences implementing a volume transmit, local receive setup for cardiac  $^{31}\text{P}$ -MRS on a Siemens research 7T MRI scanner. Two strands of development work have been performed in tandem: (i) development of a fully removable whole-body transmit RF-coil and testing with the standard 8kW RFPA and SAR monitoring and combined with a 16ch receive array, and (ii) integration of a 35kW RF power amplifier, a new energy chain, and adapted SAR monitoring.

---

1125

13:36



### Abdominal Imaging with Heterogeneous Radiofrequency Fields at 7 Tesla

Martijn A Cloos<sup>1,2</sup>, Jan Paška<sup>1,2</sup>, Zidan Yu<sup>1,2,3</sup>, Jakob Assländer<sup>1,2</sup>, Tiejun Zhao<sup>1,2,4</sup>, Riccardo Lattanzi<sup>1,2,3</sup>, Graham C Wiggins<sup>1,2</sup>, and Daniel K Sodickson<sup>1,2,3</sup>

*<sup>1</sup>Bernard and Irene Schwartz Center for Biomedical Imaging, Department of Radiology, New York University School of Medicine, New York, NY, United States, <sup>2</sup>Center for Advanced Imaging Innovation and Research (CAI2R), Department of Radiology, New York University School of Medicine, New York, NY, United States, <sup>3</sup>The Sackler Institute of Graduate Biomedical Sciences, New York University School of Medicine, New York, NY, United States, <sup>4</sup>Siemens Medical Solutions USA, Inc., Siemens Healthineers, New York, NY, United States*

Body imaging using ultra-high field systems operating at 7T or more is extremely challenging due to the non-uniformities in the excitation field. Traditionally, these field variations are seen as a nuance that must be calibrated out, leading to a formidable engineering challenge. Recently, a new paradigm was proposed which deliberately interweaves multiple uncalibrated non-uniform RF fields into the scan. In this work we demonstrate these principles in-vivo and show that it is possible to obtain artifact free cross-sectional quantitative maps of the abdomen at 7T across a variety of different subject sizes without the need for any specific calibrations.

---

1126

13:48



### An 8/15-Channel Tx/Rx Head Neck RF Coil Combination with Semi-Dynamic B1 Shimming for Improved fMRI of the Cerebellum at 7 T

Viktor Pfaffenrot<sup>1,2</sup>, Sascha Brunheim<sup>1,2</sup>, Stefan H.G. Rietsch<sup>1,2</sup>, Thomas M. Ernst<sup>1,3</sup>, Oliver Kraff<sup>1</sup>, Stephan Orzada<sup>1</sup>, and Harald H. Quick<sup>1,2</sup>

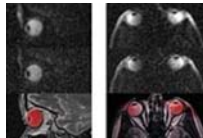
<sup>1</sup>Erwin L. Hahn Institute for Magnetic Resonance Imaging, University Duisburg-Essen, Essen, Germany, <sup>2</sup>High Field and Hybrid MR Imaging, University Hospital Essen, Essen, Germany, <sup>3</sup>Department of Neurology, University Hospital Essen, Essen, Germany

Functional MRI of the human cerebellum is challenging at ultrahigh fields, since conventional RF head coils hardly cover the cerebellum with sufficient signal-to-noise ratio and  $B_1^+$ -inhomogeneities introduce challenges. In order to overcome these problems, a coil combination consisting of an 8ch transceiver head coil and a 7ch receive only array are combined to improve imaging of the whole brain with special focus on the cerebellum. A 'semi-dynamic'  $B_1^+$ -shimming technique is introduced which provides a tSNR-gain of 29 % and voxels with higher significance in a finger tapping fMRI experiment when comparing the coil combination to a 32ch receive head coil.

1127



14:00



**Panning for Salt: One Millimeter Resolution In Vivo Sodium MRI of the Human Eye at 7.0 Tesla Using a Six Channel Transceiver Array**

Daniel Wenz<sup>1</sup>, Oliver Weinberger<sup>1</sup>, Andre Kuehne<sup>2</sup>, Helmar Waiczies<sup>2</sup>, Armin Nagel<sup>3,4</sup>, Celal Oezerdem<sup>1</sup>, Till Huelnhagen<sup>1</sup>, Dariusz Lysiak<sup>2</sup>, Lukas Winter<sup>1</sup>, Oliver Stachs<sup>5</sup>, Soenke Langner<sup>6</sup>, Erdmann Seeliger<sup>7</sup>, Bert Flemming<sup>7</sup>, and Thoralf Niendorf<sup>1,8</sup>

<sup>1</sup>Berlin Ultrahigh Field Facility (B.U.F.F.), Max Delbrück Center for Molecular Medicine in the Helmholtz Association (MDC), Berlin, Germany, <sup>2</sup>MRI.TOOLS GmbH, Berlin, Germany, <sup>3</sup>Institute of Radiology, University Hospital Erlangen, Erlangen, Germany, <sup>4</sup>Division of Medical Physics in Radiology, German Cancer Research Centre (DKFZ), Heidelberg, Germany, <sup>5</sup>Department of Ophthalmology, University of Rostock, Rostock, Germany, <sup>6</sup>Institute for Diagnostic Radiology and Neuroradiology, University Medicine Greifswald, Greifswald, Germany, <sup>7</sup>Institute for Physiology, Charité University Medicine, Berlin, Germany, <sup>8</sup>Experimental and Clinical Research Center, a joint cooperation between the Charité Medical Faculty and the Max Delbrück Center for Molecular Medicine in the Helmholtz Association



Sodium quantification in the eye may be a valuable aid not only in diagnosis of ocular diseases, but in follow-up after proton therapy of eye tumors. Recognizing this potential, this is the first report on high fidelity in vivo sodium ( $^{23}\text{Na}$ ) MRI of the human eye at 7.0 Tesla. To achieve this goal a six-channel  $^{23}\text{Na}$  transceiver array was designed, simulated, built and validated in phantoms. The in vivo studies demonstrated the feasibility of 1 mm isotropic spatial resolution  $^{23}\text{Na}$  MRI of the eye and provided encouragement for clinical studies.

---

1128

14:12



### High dielectric constant (HDC) disk dipoles for 10.5T imaging

Russell L Lagore<sup>1</sup>, Lance DelaBarre<sup>1</sup>, Qing X Yang<sup>2</sup>, Michael Lanagan<sup>3</sup>, Yigitcan Eryaman<sup>1</sup>, Sebastian Rupprecht<sup>2</sup>, Wei Luo<sup>3</sup>, Byeong-Yeul Lee<sup>1</sup>, Xiao-Hong Zhu<sup>1</sup>, Kamil Ugurbil<sup>1</sup>, Wei Chen<sup>1</sup>, and Gregor Adriany<sup>1</sup>

*<sup>1</sup>Center for Magnetic Resonance Research, University of Minnesota, Minneapolis, MN, United States, <sup>2</sup>Center of NMR Research, Department of Radiology and Neurosurgery, Penn State College of Medicine, University Park, PA, United States, <sup>3</sup>Materials Science and Engineering, Pennsylvania State University, University Park, PA, United States*

A small coil element is developed for 10.5T imaging by affixing an end-loaded 82mm long dipole to a high dielectric constant (HDC) flat disk. This coil element produces localized but very high  $B_1$  fields similar to a loop of a similar diameter without suffering from diverging  $B_{1+}$  and  $B_{1-}$  that loops experience at high field. Furthermore, these elements are inherently highly decoupled in all possible spatial configurations, making them well suited to use in large, densely packed transmit arrays.

---

1129

14:24



### Lighter is better: A Flexible Lightweight Eight Channel Slot Antenna Array for Cardiac MRI at 7.0 Tesla

Celal Oezerdem<sup>1</sup>, Till Huelnhagen<sup>1</sup>, Andre Kuehne<sup>2</sup>, Daniel Wenz<sup>1</sup>, Jason Millward<sup>1</sup>, Lukas Winter<sup>1</sup>, and Thoralf Niendorf<sup>1,3,4</sup>

*<sup>1</sup>Berlin Ultrahigh Field Facility (B.U.F.F.), Max Delbrück Center for Molecular Medicine in the Helmholtz Association, Berlin, Germany, <sup>2</sup>MRI.TOOLS GmbH, Berlin, Germany, <sup>3</sup>Experimental and Clinical Research Center (ECRC), a joint cooperation between the Charité Medical Faculty and the Max Delbrück Center for Molecular Medicine in the Helmholtz Association, Berlin, Germany, <sup>4</sup>DZHK (German Centre for Cardiovascular Research, partner site Berlin, Germany*



The wave length in tissue at ultrahigh fields allows for practical realization of RF antenna architectures such as dipole elements, high dielectric resonators and slot antennae. This work presents a novel flexible eight channel slot antenna array customized for cardiac MRI at 7.0 T. The proposed array is lightweight, easy to build, and affords a tight fit for a broad range of upper torso geometries while ensuring good matching and tuning. The in vivo study demonstrated the feasibility of the array for high fidelity, whole heart coverage MRI at 7.0 T and showed rather uniform signal intensity across the heart.

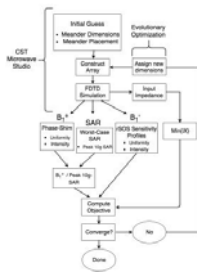
1130

14:36

### Shape-Optimization of Electric Dipoles for Human Head Imaging at 7 Tesla

Ian Robert Oliphant Connell<sup>1,2</sup> and Ravi S Menon<sup>1,2</sup>

<sup>1</sup>Centre for Functional and Metabolic Mapping, Robarts Research Institute, London, ON, Canada, <sup>2</sup>Medical Biophysics, University of Western Ontario, London, ON, Canada



Dipole antennae have been proposed as an alternative solution for RF transmission at ultra-high field (UHF) strengths. However, adapting dipoles to achieve self-resonance, while minimizing SAR for a given transmission field homogeneity, is challenging given the geometry of the human head. In this study, the design of dipole elements is performed via computer aided shape optimization and is demonstrated to meet several of these design parameters. The final design relies upon meandered-conductor paths to produce electromagnetic fields that minimize local SAR without the use of additional RF shimming or pulse design algorithms.

1131

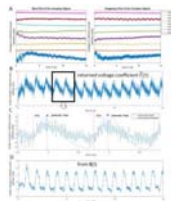


14:48

### Evaluating the Influence of B1-Shimming on Contact-free Cardiac Gating using Scatter of a Parallel Transmit Coil at 7T MRI

Sven H.F. Jaeschke<sup>1</sup>, Matthew D. Robson<sup>1</sup>, and Aaron T. Hess<sup>1</sup>

<sup>1</sup>Oxford Centre for Magnetic Resonance, University of Oxford, Oxford, United Kingdom



We propose a contact-free cardiac MRI triggering method based on reflected power measurements that requires no additional hardware other than that provided with a commercial parallel transmit (pTx) MRI scanner and evaluate the influence of B1+ shim on the cardiac information extracted. Time series of scattering matrices of the pTx monitoring system were used with random, uniformly distributed phases to simulate B1+ shims. Preliminary results in 7T MRI are shown with successfully, retrospectively gated 2D-CINE images using the proposed method.

---

Oral

## Elastography

Room 312

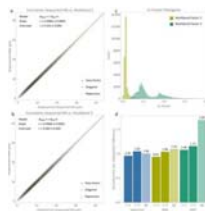
Thursday 13:00 - 15:00 *Moderators: Arvin Arani & Lynne Bilston*

---

1132



13:00



### Simultaneous Multislice Acquisition for Magnetic Resonance Elastography

Christian Guenther<sup>1</sup>, Jurgen H Runge<sup>2,3</sup>, Ralph Sinkus<sup>2</sup>, and Sebastian Kozerke<sup>1</sup>

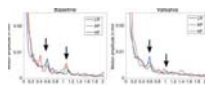
*<sup>1</sup>Institute for Biomedical Engineering, University and ETH Zurich, Zurich, Switzerland, <sup>2</sup>Division of Imaging Sciences and Biomedical Engineering, King's College London, London, United Kingdom, <sup>3</sup>Department of Radiology, Academic Medical Center, Amsterdam, Netherlands*

We propose the use of simultaneous multislice acquisition for Magnetic Resonance Elastography (MRE) of the full displacement vector field. To this end, multiband composite RF pulses are used for slice excitation in a fast, "eXpresso" type gradient echo based MRE acquisition. Slice and k-line dependent RF-phases are used to shift simultaneously acquired slices leading to improved unfolding performance (CAIPIRINHA). In this abstract, we demonstrate that multiband MRE with CAIPIRINHA can be used to acquire up to three slices simultaneously with only little SNR penalty in a gel phantom and show the feasibility to acquire full-brain images in-vivo.

---

1133

13:12



### Towards single-shot 3D MR elastography: Application to intrinsically activated motion fields in the human brain.

Sebastian Hirsch<sup>1</sup>, Rüdiger Stinberg<sup>2</sup>, Tony Stöcker<sup>2,3</sup>, Florian Dittmann<sup>4</sup>, Jing Guo<sup>4</sup>, Eric Barnhill<sup>1</sup>, Jürgen Braun<sup>1</sup>, and Ingolf Sack<sup>4</sup>

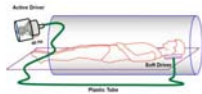
<sup>1</sup>Department of Medical Informatics, Charité - Universitätsmedizin Berlin, Berlin, Germany, <sup>2</sup>German Center for Neurodegenerative Diseases (DZNE), Bonn, Germany, <sup>3</sup>Department of Physics and Astronomy, University of Bonn, Germany, <sup>4</sup>Department of Radiology, Charité - Universitätsmedizin Berlin, Berlin, Germany

This study introduces a single-shot 3D EPI sequence for rapid motion field acquisition. The method can be applied for MRE under pulsatile motion or for directly analyzing intrinsic motion fields in pulsatile organs such as the brain. Through 3D k-space sampling, inter-slice phase offset artifacts, which essentially result from 2D k-space MRE, are most effectively avoided. In a first application we used the new method for the measurement of intrinsic brain pulsation in the human brain and analyzed the intensity of deflection field components by stochastic sampling at rest and during Valsalva maneuver.

---

1134

13:24



Preoperative assessment of tumor stiffness and tumor-brain adhesion in patients with vestibular schwannoma using MR elastography-based method

Prateek Kalra<sup>1</sup>, Arunark Kolipaka, PhD<sup>1</sup>, Brian Raterman<sup>1</sup>, Oliver Adunka, MD<sup>2</sup>, Michael Harris, MD<sup>2</sup>, and Daniel M. Prevedello, MD<sup>3</sup>

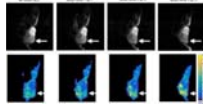
<sup>1</sup>Department of Radiology, Ohio State University Wexner Medical Center, Columbus, OH, United States, <sup>2</sup>Department of Otolaryngology, Ohio State University Wexner Medical Center, Columbus, OH, United States, <sup>3</sup>Department of Neurological Surgery, Ohio State University Wexner Medical Center, Columbus, OH, United States

Microsurgery in vestibular schwannoma patients aims to complete tumor resection without compromising any neurological functionality. Inadequate preoperative knowledge of tumor may prolong surgical time and increase risk of postoperative complications. Previous studies have used magnetic resonance elastography (MRE) based method to determine tumor stiffness and tumor-brain adhesion, separately. But none of the studies have investigated tumor stiffness and tumor-brain adhesion together. The aim of this study is to bring together the two MRE-based outcomes – tumor stiffness and tumor-brain adhesion – and correlate with surgical findings. Preliminary results show a good correlation between preoperative assessment of tumor and surgical findings.

---

1135

13:36



### Assessing tumor mechanical nonlinearity by MR elastography at different strain levels

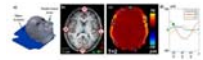
Marion Tardieu<sup>1</sup>, Laurent Besret<sup>2</sup>, Lydia Blot<sup>2</sup>, Joaquim Lopes<sup>2</sup>, Ralph Sinkus<sup>3</sup>, Bernard Van Beers<sup>1</sup>, and Philippe Garteiser<sup>1</sup>

*<sup>1</sup>Laboratory of Imaging Biomarkers CRI UMR1149, INSERM, Paris, France, <sup>2</sup>Sanofi oncology, Vitry-sur-Seine, France, <sup>3</sup>Imaging Sciences and Biomedical Engineering, King's College London, London, United Kingdom*

In this study we attempt to access nonlinear mechanical properties of tumors by applying external loads. Experiments were performed on subcutaneous tumors implanted in mice. MR elastography acquisitions were realized at 600 Hz while deformations were applied, in order to obtain apparent elasticity ( $G'$ ) values for each strain application. Results showed nonlinear  $G'$  values increasing with loads, when deformations were clearly observed. Some results showed a decrease of  $G'$  potentially due to wave displacement polarization. We showed the feasibility of assessing the nonlinear regime of tumor mechanical properties that may potentially be an indicator of internal tumor forces.

1136

13:48



### Measurement of Human Brain, Scalp, and Skull Motion in vivo using Magnetic Resonance Elastography and Triaxial Accelerometers

Andrew A Badachhape<sup>1</sup>, Ruth J Okamoto<sup>2</sup>, Curtis L Johnson<sup>3</sup>, and Philip V Bayly<sup>1,2</sup>

*<sup>1</sup>Biomedical Engineering, Washington University in St. Louis, St. Louis, MO, United States, <sup>2</sup>Mechanical Engineering and Materials Science, Washington University in St. Louis, St. Louis, MO, United States, <sup>3</sup>Biomedical Engineering, University of Delaware, Newark, DE, United States*

Characterizing motion transmission from the skull to the brain and from skull to external soft tissue would provide valuable insight into traumatic brain injury mechanics and injury assessment by external sensors. In this study, we estimated rigid-body displacement components of brain and scalp using magnetic resonance elastography for comparison with skull motion estimated from three triaxial accelerometers. Comparison of the relative amplitudes and phases of harmonic motion in the skull, scalp, and brain of five human subjects indicated differences between each region. These measured amplitude and phase relationships can improve both simulations and experimental characterization of head biomechanics.

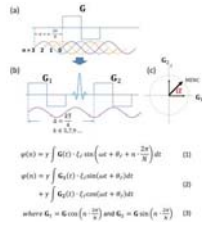
1137

14:00

### Quadrature Motion Encoding (QuME): A Novel Motion Encoding Scheme for MR Elastography

Yi Sui<sup>1</sup>, Kevin J. Glaser<sup>1</sup>, Ziyang Yin<sup>1</sup>, Joshua D. Trzasko<sup>1</sup>, Jun Chen<sup>1</sup>, Richard L. Ehman<sup>1</sup>, and John Huston III<sup>1</sup>

<sup>1</sup>Radiology, Mayo Clinic, Rochester, MN, United States



We propose a novel approach to motion encoding for spin-echo-based MR elastography called quadrature motion encoding (QuME) in which the second motion-encoding gradient (MEG) after the refocusing pulse is used to measure the quadrature component of the in vivo harmonic motion induced by an external mechanical vibration. Unlike the conventional encoding method that shifts the temporal relation between the motion and MEGs, QuME alters the amplitudes of MEGs from one time step to the next. This concept was implemented on a 3T GE scanner and demonstrated the ability to shorten the echo time of SLIM-MRE for human brain MRE.

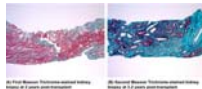
1138

14:12

### Fibrosis in a Renal Allograft: The Role of Magnetic Resonance Elastography as a Non-Invasive Measurement Tool

Jin Kyu Kim<sup>1,2</sup>, Darren Yuen<sup>3</sup>, General Leung<sup>1,2</sup>, Serge Jothy<sup>4</sup>, Jeffrey Zaltzman<sup>3</sup>, Ramesh Prasad<sup>3</sup>, and Anish Kirpalani<sup>1,2</sup>

<sup>1</sup>Medical Imaging, St. Michael's Hospital, Toronto, ON, Canada, <sup>2</sup>Li Ka Shing Knowledge Institute, St. Michael's Hospital, Toronto, ON, Canada, <sup>3</sup>Medicine – Division of Nephrology, St. Michael's Hospital, Toronto, ON, Canada, <sup>4</sup>Pathology, St. Michael's Hospital, Toronto, ON, Canada

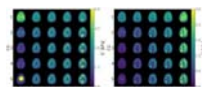


A major reason for poor long-term kidney transplant outcomes is interstitial fibrosis. Currently, percutaneous biopsy, an invasive procedure that samples <1% of the allograft, is the gold standard for detecting renal allograft fibrosis. As the allograft scars, it stiffens due to the deposition of stiff extracellular matrix. This stiffening can be imaged non-invasively using magnetic resonance elastography (MRE). We used serial renal stiffness MRE imaging and serial percutaneous biopsies to measure whole allograft fibrosis preprogression in a kidney transplant recipient. We show that renal allograft MRE can detect changes in overall fibrotic burden, as confirmed by biopsy.

1139

14:24

### Inversion Parameters based on Convergence and Error Metrics for Nonlinear Inversion MR Elastography



Aaron T Anderson<sup>1,2</sup>, Curtis L Johnson<sup>3</sup>, Matthew DJ McGarry<sup>4,5</sup>, Keith D Paulsen<sup>4,6</sup>, Bradley P Sutton<sup>2,7</sup>, Elijah EW Van Houten<sup>4,8</sup>, and John G Georgiadis<sup>9</sup>

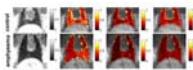
<sup>1</sup>Mechanical Science & Engineering, University of Illinois at Urbana-Champaign, Urbana, IL, United States, <sup>2</sup>Beckman Institute for Advanced Science and Technology, University of Illinois at Urbana-Champaign, Urbana, IL, United States, <sup>3</sup>Biomedical Engineering, University of Delaware, Newark, DE, United States, <sup>4</sup>Thayer School of Engineering, Dartmouth College, Hanover, NH, United States, <sup>5</sup>Biomedical Engineering, Columbia University, New York, NY, United States, <sup>6</sup>Radiology, Dartmouth-Hitchcock Medical Center, Lebanon, NH, United States, <sup>7</sup>Bioengineering, University of Illinois at Urbana-Champaign, Urbana, IL, United States, <sup>8</sup>Génie Mécanique, Université de Sherbrooke, Sherbrooke, QC, Canada, <sup>9</sup>Biomedical Engineering, Illinois Institute of Technology, Chicago, IL, United States

Nonlinear inversion (NLI) of brain MRE data has shown the promise in sensitive detection of complex neurodegenerative disease by showing repeatable and accurate assessments of both white matter and gray matter regions in healthy subjects. This study looks to further improve the accuracy of the NLI-MRE framework by characterizing two major inversion parameters: subzone size and conjugate gradient iterations. Additionally, two convergence criteria are proposed as means to quantify the confidence in final reported statistics while fully capturing the distribution of heterogeneity within white matter regions.

---

1140

14:36



### Magnetic Resonance Elastography of Emphysematous Rat Lung in vivo

Hongchen Wang<sup>1</sup>, Catherine Sebré<sup>1</sup>, Georges Willoquet<sup>1</sup>, Jinlong Yue<sup>1</sup>, Felicia Julea<sup>1</sup>, Rose-Marie Dubuisson<sup>1</sup>, Sébastien Judé<sup>2</sup>, Anne Maurin<sup>2</sup>, and Xavier Maître<sup>1</sup>

<sup>1</sup>Imagerie par Résonance Magnétique Médicale et Multi-Modalités (UMR8081) IR4M, CNRS, Univ. Paris-Sud, Université Paris-Saclay, Orsay, France, <sup>2</sup>Centre de Recherches Biologiques, CERB, Baugy, France

Emphysema is a chronic respiratory disease, which has become the fifth most common cause of death worldwide. Emphysema is characterized by alveolar wall destruction, leading to distal airspace enlargement and decreased elastic recoil. The altered structure and function of the lung is related to modified mechanical properties of pulmonary tissues, which are difficult to probe in vivo by standard techniques. Magnetic Resonance Elastography (MRE) allows to characterize the mechanical properties correlated with lung physiopathologies. Here, we implemented MRE lung imaging in vivo on emphysematous rat models.

---

1141

14:48



Multifrequency MR elastography of the human prostate by multiple surface-based compressed-air drivers: reproducibility and first patient results

Florian Dittmann<sup>1</sup>, Jing Guo<sup>1</sup>, Heiko Tzschätzsch<sup>1</sup>, Sebastian Hirsch<sup>2</sup>, Rolf Reiter<sup>1</sup>, Patrick Asbach<sup>1</sup>, Andreas Maxeiner<sup>3</sup>, Jürgen Braun<sup>2</sup>, and Ingolf Sack<sup>1</sup>

*<sup>1</sup>Institute of Radiology, Charité, Berlin, Germany, <sup>2</sup>Department of Medical Informatics, Charité, Berlin, Germany, <sup>3</sup>Department of Urology, Charité, Berlin, Germany*

A new setup for prostate MR Elastography is proposed that uses surface-based wave excitation by compressed-air drivers. The post-processing with tomoelastography combining wave fields at drive frequencies of 60, 70, and 80 Hz leads to highly resolved elasticity maps. A study in healthy volunteers demonstrates the good reproducibility of the method. Furthermore, the first patient results show excellent agreement with contrast-enhanced reference images, which motivates future patient studies.

---

Oral

## The Bee's Knees

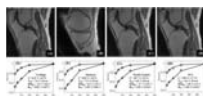
Room 313A

Thursday 13:00 - 15:00

Moderators: Elisabeth Garwood & Valentina Taviani

---

13:00



Three-dimensional Ultrashort Echo Time Cones Imaging with Magnetization Transfer Modeling (3D UTE-Cones-MT): Simulation, Specimen and Volunteer Studies of the Knee Joint

Yajun Ma<sup>1</sup>, Eric Y Chang<sup>1,2</sup>, Michael Carl<sup>3</sup>, and Jiang Du<sup>1</sup>





<sup>1</sup>Radiology, University of California, San Diego, San Diego, CA, United States, <sup>2</sup>Radiology Service, VA San Diego Healthcare System, San Diego, CA, United States, <sup>3</sup>GE Healthcare, San Diego, CA, United States

A major limitation associated with conventional clinical MRI sequences is the magic angle effect. The conventional T2 and T1rho measures may increase more than 100% when the fibers are oriented from 0° to the magic angle (~55°) relative to the B0 field, far more than that associated with osteoarthritis (OA). Magnetization transfer (MT) imaging has shown less sensitivity to the magic angle effect, and can indirectly evaluate macromolecules which have extremely short T2 (~10 us) and invisible with all MRI sequences. However, conventional MT techniques cannot be applied to short T2 tissues such as menisci, ligaments, tendons and bone. Ultrashort echo time (UTE) sequences with TEs 100-1000 times shorter than those of clinical sequences have been developed to image these short T2 tissues. In this study, we aimed to develop 3D UTE with Cones sampling and MT (3D UTE-Cones-MT) imaging and signal modeling to quantify water and macromolecules in both short and long T2 tissues in the knee joint at 3T.

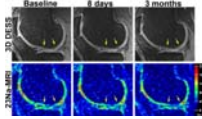
Group	Age	Sex	Age (SD)	Sex (SD)
1	20-30	M	25.0 ± 3.0	100%
2	30-40	M	35.0 ± 3.0	100%
3	40-50	M	45.0 ± 3.0	100%
4	50-60	M	55.0 ± 3.0	100%
5	60-70	M	65.0 ± 3.0	100%
6	70-80	M	75.0 ± 3.0	100%
7	80-90	M	85.0 ± 3.0	100%
8	90-100	M	95.0 ± 3.0	100%

Two compartmental diffusion model of skeletal muscle: application to aging and chronic limb suspension induced DTI changes in the medial gastrocnemius

Usha Sinha<sup>1</sup>, Vadim Malis<sup>2</sup>, and Shantanu Sinha<sup>3</sup>

<sup>1</sup>Physics, San Diego State University, San Diego, CA, United States, <sup>2</sup>Physics, UC San Diego, San Diego, CA, United States, <sup>3</sup>Radiology, UC San Diego, San Diego, CA, United States

Diffusion tensor imaging (DTI) is a powerful technique that allows one to probe tissue at the microstructural level. Though microarchitecture determines the DTI indices, a diffusion model is required to make inferences about the microstructure. We applied a two compartmental diffusion model for muscle to explain differences in the DTI indices with age and with atrophy induced by limb suspension. The model qualitatively explains the changes in DTI seen in limb suspension that is linked to decrease in muscle fiber diameter and in intracellular volume fraction. Extensions to the model are required to explain the age related changes in DTI.



### In Vivo Follow-up of Low-Grade Femoral Cartilage Defects using Sodium MRI at 7T

Stefan Zbyn<sup>1,2,3</sup>, Vladimir Mlynarik<sup>1</sup>, Vladimir Juras<sup>1</sup>, Markus Schreiner<sup>1,4</sup>, Pavol Szomolanyi<sup>1</sup>, Didier Laurent<sup>5</sup>, Celeste Scotti<sup>5</sup>, Harry Haber<sup>5</sup>, Joerg Goldhahn<sup>5</sup>, Ewa Kubiak<sup>5</sup>, Oliver Bieri<sup>6</sup>, Stefan Marlovits<sup>7</sup>, Miika T. Nieminen<sup>2,8,9</sup>, and Siegfried Trattnig<sup>1,3</sup>

<sup>1</sup>High Field MR Center, Department of Biomedical Imaging and Image-Guided Therapy, Medical University of Vienna, Vienna, Austria, <sup>2</sup>Research Unit of Medical Imaging, Physics and Technology, University of Oulu, Oulu, Finland, <sup>3</sup>CD Laboratory for Clinical Molecular MR Imaging, Vienna, Austria, <sup>4</sup>Department of Orthopaedics, Medical University of Vienna, Vienna, Austria, <sup>5</sup>Novartis Institutes for Biomedical Research, Basel, Switzerland, <sup>6</sup>Division of Radiological Physics, Department of Radiology, University of Basel Hospital, Basel, Switzerland, <sup>7</sup>Department of Traumatology, Medical University of Vienna, Vienna, Austria, <sup>8</sup>Department of Diagnostic Radiology, Oulu University Hospital, Oulu, Finland, <sup>9</sup>Medical Research Center, University of Oulu and Oulu University Hospital, Oulu, Finland

Sodium (<sup>23</sup>Na) MRI was employed for the evaluation of patients with ICRS Grade I-II cartilage defects at 7T. <sup>23</sup>Na data from defect, weight-bearing, and non-weight-bearing region of femoral cartilage were obtained at baseline, 8-days, 3-months and 6-months follow-up. Significantly lower <sup>23</sup>Na values were found in defect than in weight-bearing and non-weight-bearing regions at all time-points. While <sup>23</sup>Na values in weight-bearing and in non-weight-bearing regions were stable over time, a significant decrease was found in the defects. <sup>23</sup>Na-MRI allows noninvasive follow-up of changes in the cartilage GAG content and thus might be particularly useful for the evaluation of cartilage regenerating therapies.



Population	Timepoints			
	Baseline	8 Months	3 Months	1 Year
ACL-Injured Knee	✓	✓	✓	✓
Contralateral Knee	✓	✓	✓	✓
Healthy Knee	✓	✓	✓	✓

### Cluster Analysis of Cartilage T2 and T1rho Relaxation Times: Can the Contralateral Knee be used as a Control in the ACL-injured population?

Uchekukwuka Monu<sup>1,2</sup>, Emily McWalter<sup>3</sup>, Caroline Jordan<sup>4</sup>, Brian Hargreaves<sup>1,2,5</sup>, and Garry Gold<sup>2,5</sup>

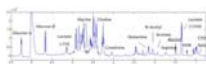
<sup>1</sup>Electrical Engineering, Stanford University, Stanford, CA, United States, <sup>2</sup>Radiology, Stanford University, Stanford, CA, United States, <sup>3</sup>Mechanical Engineering, University of Saskatchewan, SK, Canada, <sup>4</sup>Radiology and Biomedical Imaging, University of California San Francisco, CA, United States, <sup>5</sup>Bioengineering, Stanford University, Stanford, CA, United States

In an ACL-injured population, longitudinal studies that use advanced MRI techniques such as T2 and T1rho mapping to assess cartilage health, typically compare ACL-injured knees with a separate healthy group or the contralateral knees. It is still unclear whether the contralateral knees can be used as a control group. Using a cluster analysis-based technique, we identify in the contralateral knees, significant increase in T1rho relaxation times over 1-year that is comparable to the increase in the ACL-injured knees. These focal cluster areas may represent degenerative changes and demonstrate that the contralateral knees may not be good controls.

---

1146

13:48



Novel NMR biomarkers characterizing human knee synovial fluid after ACL-injuries: correlation with immunoassay and longitudinal cartilage MR T1 $\rho$  and T2 imaging

Kaipin Xu<sup>1</sup>, Keiko Amano<sup>1</sup>, Matthew Tanaka<sup>1</sup>, Subramaniam Sukumar<sup>1</sup>, John Kurhanewicz<sup>1</sup>, Virginia Kraus<sup>2</sup>, Benjamin Ma<sup>1</sup>, and Xiaojuan Li<sup>1</sup>

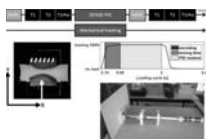
<sup>1</sup>University of California, San Francisco, San Francisco, CA, United States, <sup>2</sup>Duke University, Durham, NC, United States

Subjects with acute anterior cruciate ligament (ACL) injury have a high risk of developing post-traumatic osteoarthritis (PTOA) even after ACL reconstruction. To identify novel NMR biomarkers of synovial fluid that may predict cartilage degeneration after acute injury and to develop potential preventative strategies for PTOA, human knee synovial fluid harvested from 25 anterior cruciate ligament (ACL) injured subjects were studied using high resolution magic angle spinning (HR-MAS) NMR spectroscopy and correlated to immunoassay and longitudinal cartilage MR T1 $\rho$  and T2 imaging.

---

1147

14:00



Biomechanical properties of bovine knee cartilage under compressive loading: A study at high field MRI (9.4T) using T1, T2 and T1rho relaxometry combined with DENSE-FID.

Willy Gsell<sup>1</sup>, Willy Zevenbergen<sup>2</sup>, Tom Dresselaers<sup>1</sup>, Deva Chan<sup>3</sup>, Corey Neu<sup>4</sup>, Uwe Himmelreich<sup>1</sup>, and Ilse Jonkers<sup>5</sup>

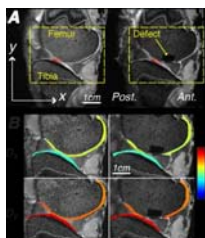
<sup>1</sup>Biomedical MRI group, KU Leuven, Leuven, Belgium, <sup>2</sup>Human Movement Biomechanics Research Group, KU Leuven, Leuven, <sup>3</sup>Rensselaer Polytechnic Institute, <sup>4</sup>Mechanical Engineering, University of Colorado Boulder, <sup>5</sup>Human Movement Biomechanics Research Group, KU Leuven

The aim of this study was to correlate the cartilage displacement pattern during cartilage on cartilage contact through displacement encoding imaging during compressive loading with the T1, T2 and T1rho changes, indices of changes in collagen matrix, water and proteoglycan contents. We demonstrated that local mechanical changes in the cartilage during loading were correlated to global molecular changes assessed through T1, T2 and T1rho. The localized cartilage deformation and strain fields suggest a differential response to loading of the different regions of the cartilage which could help in further optimizing cell based therapy for osteoarthritis.

1148

14:12

### Intratissue Strains Increase in a Full Thickness and Critical Sized Ovine Cartilage Defect Model



Deva Chan<sup>1</sup>, Luyao Cai<sup>2</sup>, Kent Butz<sup>2</sup>, Eric Nauman<sup>2</sup>, Darryl Dickerson<sup>2</sup>, Ilse Jonkers<sup>3</sup>, and Corey Neu<sup>4</sup>

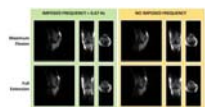
<sup>1</sup>Rensselaer Polytechnic Institute, Troy, NY, United States, <sup>2</sup>Purdue University, <sup>3</sup>KU Leuven, <sup>4</sup>University of Colorado Boulder, Boulder, CO, United States

Functional imaging of intratissue strain in articular cartilage provides an opportunity to probe the healthy or diseased state of the tissue. We utilized displacement encoded MRI to document the increase in deformation following creation of a critical sized femoral defect in a large animal model *ex vivo*. Strain heterogeneity indicated that the implant replacement is critical to long-term repair success and restoration of physiological cartilage strain and mechanical function. This study represents a crucial step toward the evaluation of biomechanical imaging biomarkers to evaluate tissue damage, repair, and regeneration in the intact joint of a clinically-relevant and translational animal model.

1149

14:24

### Dynamic knee imaging using 4D self-gated MRI with compressed sensing reconstruction



Valentina Mazzoli<sup>1,2,3</sup>, Jasper Schoormans<sup>4</sup>, Martijn Froeling<sup>5</sup>, Andre M Sprengers<sup>3</sup>, Klaas Nicolay<sup>2</sup>, Bram F Coolen<sup>4</sup>, Nico Verdonschot<sup>3</sup>, Aart J Nederveen<sup>1</sup>, and Gustav J Strijkers<sup>4</sup>

<sup>1</sup>Department of Radiology, Academic Medical Center, Amsterdam, Netherlands, <sup>2</sup>Biomedical NMR, Department of Biomedical Engineering, Eindhoven University of Technology, Eindhoven, Netherlands, <sup>3</sup>Orthopaedic Research Lab, Radboud UMC, Nijmegen, Netherlands, <sup>4</sup>Biomedical Engineering and Physics, Academic Medical Center, Amsterdam, Netherlands, <sup>5</sup>Department of Radiology, University Medical Center Utrecht, Utrecht, Netherlands

Knee abnormalities and pain are sometimes elucidated during motion, therefore the ability to obtain 4D images of the moving knee could add diagnostic value to the conventional static MRI scans. In this work we present a method to obtain 4D imaging of the human knee during motion, without the use of an external gating system.

---

1150

14:36



Rapid knee MRI using TSE sequences accelerated with a combination of simultaneous multislice, multicoil compressed sensing and elongated echo trains

Akio Yoshimoto<sup>1,2</sup>, Steven H Baete<sup>1,3</sup>, Mary Bruno<sup>4</sup>, Mitchell Kline<sup>4</sup>, Elisabeth Garwood<sup>4</sup>, Fernando Boada<sup>1,4</sup>, Ricardo Otazo<sup>1,4</sup>, and Michael Recht<sup>4</sup>

<sup>1</sup>Center for Advanced Imaging Innovation and Research (CAI2R), NYU School Of Medicine, New York, NY, United States, <sup>2</sup>Biomedical Engineering, School of Engineering, New York University, Brooklyn, NY, United States, <sup>3</sup>Center for Biomedical Imaging, Dept of Radiology, NYU School Of Medicine, New York, NY, United States, <sup>4</sup>Department of Radiology, NYU School Of Medicine, New York, NY, United States

Turbo spin echo imaging is accelerated with a novel combination of simultaneous multislice, multicoil compressed sensing and elongated echo times to reduce the scan time of routine knee examinations to 7 minutes. The accelerated protocol is validated against the conventional technique in a cohort of 10 patients based on the opinion of expert radiologists. Diagnostic accuracy was found to be similar despite the reduction in scan time. This might be useful to expand the utilization of MRI and to increase patient throughput.

---

1151

14:48

3D MRI of Knee in Pediatric Patients with CAIPIRINHA SPACE: Diagnostic Performance Assessment with Arthroscopic Correlation

Jan Fritz<sup>1</sup>, Shivani Ahlawat<sup>1</sup>, Gaurav K Thawait<sup>1</sup>, Esther Raithe<sup>2</sup>, Wesley Gilson<sup>3</sup>, and Rushyuan J Lee<sup>1</sup>

Parameters	Interpolation Magnitude of CAIPIRINHA SPACE	T2 STAR of CAIPIRINHA SPACE
Orientation	isotropic	isotropic
Resolution (mm)	1.000	1.000
Echo time (ms)	20	100
Echo train length	60	42
Receiver bandwidth (Hz)	400	400
Field of view (mm)	160 x 160	160 x 160
Matrix	160 x 160	256 x 256
Voxel dimensions (mm)	0.5 x 0.5 x 0.5	0.5 x 0.5 x 0.5
Number of slices	200	200
In-plane frequency encoding direction	anterior to posterior	anterior to posterior
Acquisition time	4 min 46 s	5 min 05 s

<sup>1</sup>The Johns Hopkins University School of Medicine, Baltimore, MD, United States, <sup>2</sup>Siemens Healthcare GmbH, <sup>3</sup>Siemens Healthcare USA

3D CAIPIRINHA SPACE permits the acquisition of 4-fold accelerated, high quality data sets and has been shown to be feasible for efficient 3D MRI of the knee; however, the clinical application has not been demonstrated. We report the performance of 3D CAIPIRINHA SPACE MRI for the diagnosis of internal derangement of the knee in children and adolescents using arthroscopy correlation as the standard of reference. 3D CAIPIRINHA SPACE enables clinically feasible isotropic 3D MRI of the knee in children and adolescents with an acquisition time of 10 min and high accuracy for the diagnosis of meniscal, ligamentous and cartilage abnormalities.

Oral

## fMRI: Multimodal & Neuromodulation

Room 313BC

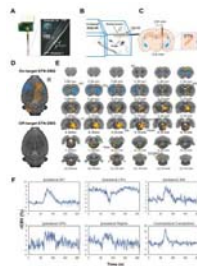
Thursday 13:00 - 15:00

Moderators: Kai-Hsiang Chuang & Shella Keilholz

1152



13:00



On- and off-target circuit effects of high frequency electrical deep brain stimulation at the subthalamic nucleus

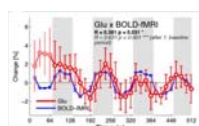
SungHo Lee<sup>1</sup>, Daniel L. Albaugh<sup>1</sup>, You-Yin Chen<sup>2</sup>, and Yen-Yu Ian Shih<sup>1,3</sup>

<sup>1</sup>Neurology, University of North Carolina at Chapel Hill, Chapel Hill, NC, United States, <sup>2</sup>National Chiao-Tung University, <sup>3</sup>Neurology, UNC at Chapel Hill, Chapel Hill, NC, United States

This study introduces a novel hybrid methodology for DBS-fMRI research. Our findings demonstrate robust stimulus evoked fMRI and fcMRI responses during STN-DBS, which should shed light on how DBS exerts its therapeutic effects on whole-brain functional networks and delineate a road-map for future optimization of DBS therapy to enhance outcomes and reduce side-effects.

1153

13:12



Combined fMRI-MRS measures simultaneous glutamate and BOLD-fMRI signals in the human brain at 7T

Betina Ip<sup>1,2</sup>, Adam Berrington<sup>2</sup>, Aaron T Hess<sup>3</sup>, Andrew Parker<sup>1</sup>, Holly Bridge<sup>2</sup>, and Uzay E Emir<sup>2</sup>



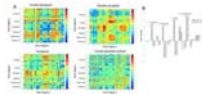
<sup>1</sup>Department of Physiology, Anatomy & Genetics, University of Oxford, Oxford, United Kingdom, <sup>2</sup>Oxford Centre for Functional MRI of the Brain (FMRIB), University of Oxford, Oxford, United Kingdom, <sup>3</sup>Centre for Clinical Magnetic Resonance Research (OCMR), University of Oxford, Oxford, United Kingdom

We quantified neural activity using a novel method for simultaneous acquisition of blood-oxygenation level dependent (BOLD)-fMRI signals and proton magnetic resonance spectroscopy (<sup>1</sup>H-MRS)-MRI at 7 Tesla. We have demonstrated the correlation of glutamate, the principal excitatory neurotransmitter in the nervous system, with BOLD-fMRI responses during brief (64 s) periods of visual stimulation. These results establish the feasibility of concurrent measurements of BOLD-fMRI and neurochemicals at a temporal resolution compatible with human fMRI studies.

1154



13:24



GABA promotes beta-Amyloid related changes in dynamic network expression of elderly subjects at risk for Alzheimer's disease

Frances-Catherine Quevenco<sup>1</sup>, Simon J. Schreiner<sup>2,3</sup>, Maria Giulia Preti<sup>4</sup>, Jiri van Bergen<sup>1</sup>, Thomas Kirchner<sup>5</sup>, Michael Wyss<sup>5</sup>, Stephanie C. Steininger<sup>1,3</sup>, Anton Gietl<sup>1</sup>, Sandra Leh<sup>1,3</sup>, Alfred Buck<sup>6</sup>, Klaas P. Pruessman<sup>5</sup>, Christoph Hock<sup>2,3</sup>, Roger M. Nitsch<sup>2</sup>, Anke Henning<sup>5,7</sup>, Dimitri Van de Ville<sup>4</sup>, and Paul Gerson Unschuld<sup>2,8</sup>

<sup>1</sup>Institute of Regenerative Medicine, University of Zurich, Zurich, Switzerland, <sup>2</sup>Institute for Regenerative Medicine, University of Zurich, Switzerland, <sup>3</sup>Hospital for Psychogeriatric Medicine, University of Zurich, Switzerland, <sup>4</sup>Institute of Bioengineering, École polytechnique fédérale de Lausanne, Switzerland, <sup>5</sup>Institute for Biomedical Engineering, ETH Zurich, Switzerland, <sup>6</sup>Division of Nuclear Medicine, University of Zurich, Switzerland, <sup>7</sup>Max Planck Institute for Biological Cybernetics, Tübingen, Germany, <sup>8</sup>Hospital for Psychogeriatric Medicine, University of Zurich, Zurich, Switzerland

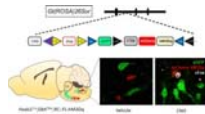
This study observes dynamic functional connectivity changes in an elderly AD-risk population mediated by both regional A $\beta$ -deposits and GABA levels, using PiB-PET and MRSI. The sample is grouped into subjects with high regional A $\beta$  and high GABA, and changes in dynamic network expression are compared between groups. Our preliminary findings show dynamic network changes specific to high A $\beta$ -deposits in the neocortex and the frontal and temporal lobe. This indicates region-specific network changes that may in part explain the weak correlation between global A $\beta$  and AD progression.



1155



13:36



### Chemogenetic fMRI and 18F-FDG PET Reveal Functional Projections of Hoxb1-Derived Noradrenergic Neurons

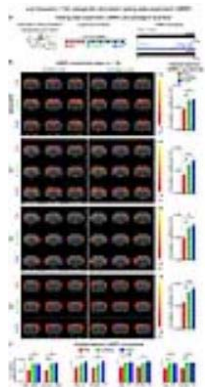
Manasmita Das<sup>1</sup>, Esteban Oyarzabal<sup>1</sup>, Yu-Wei Chen<sup>2</sup>, Sung Ho Lee<sup>1</sup>, Lars Chen<sup>1</sup>, Weiting Zhang<sup>1</sup>, Patricia Jensen<sup>2</sup>, and Yen-Yu Ian Shih<sup>1</sup>

<sup>1</sup>Biomedical Research Imaging Center, Department of Neurology, University of North Carolina Chapel Hill, Chapel Hill, NC, United States, <sup>2</sup>Developmental Neurobiology, NIEHS/NIH

In this study, we show that chemogenetic fMRI and 18 F FDG PET can sensitively dissect the functional neurocircuits of noradrenergic cells derived from rhombomere 4 expressing Hoxb1 during neurodevelopment. To address this, we used a novel genetically engineered mouse line expressing Designer Receptors Exclusively Activated for Designer Drugs (DREADD) in Hoxb1-derived noradrenergic neurons in several subpopulations throughout the pons and medulla. For the first time, we used ICA-based fMRI analysis to dissect the complex polysynaptic pathways associated with chemogenetic modulation of Hoxb-1 derived noradrenergic neurons.

1156

13:48



### Low frequency hippocampal-cortical activity contributes to brain-wide connectivity as measured by resting-state fMRI

Russell W. Chan<sup>1,2</sup>, Alex T. L. Leong<sup>1,2</sup>, Leon C. Ho<sup>1,2</sup>, Xunda Wang<sup>1,2</sup>, Anthea To<sup>1,2</sup>, and Ed X. Wu<sup>1,2</sup>

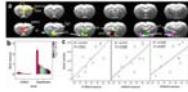
<sup>1</sup>Laboratory of Biomedical Imaging and Signal Processing, The University of Hong Kong, Hong Kong, Hong Kong, <sup>2</sup>Electrical and Electronic Engineering, The University of Hong Kong, Hong Kong, Hong Kong

The hippocampus, including dorsal dentate gyrus (dDG), and cortex engage in bidirectional communication. We propose that low frequency activities in hippocampal-cortical pathway underlie brain-wide resting-state fMRI (rsfMRI) connectivity to mediate distinct cognitive functions and integrate sensory information. Using optogenetics and fMRI, we determined large-scale spatiotemporal specific hippocampal-cortical activity. Low, but not high, frequency optogenetic stimulation of dDG excitatory neurons evoked robust cortical and subcortical responses, and enhanced interhemispheric hippocampal and cortical rsfMRI connectivity. In addition, pharmacological inactivation of dDG decreased rsfMRI connectivity. These findings directly indicate that low frequency activity propagates in hippocampal-cortical pathway and contributes to brain-wide rsfMRI connectivity.

---

1157

14:00



Brain regions associated with reward induced by optogenetic stimulation at the medial prefrontal cortex

Yuzheng Hu<sup>1</sup>, Aleksandr Talishinsky<sup>1</sup>, Hanbing Lu<sup>1</sup>, Satoshi Ikemoto<sup>1</sup>, and Yihong Yang<sup>1</sup>

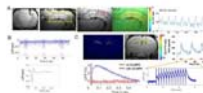
*<sup>1</sup>National Institute on Drug Abuse (NIDA-IRP), NIH, BALTIMORE, MD, United States*

Optogenetics and fMRI were combined to examine the neural activity underlying the rewarding behavior mediated by the medial prefrontal cortex (MPFC) in rats. Animals were trained to press lever for optogenetic self-administration in MPFC. FMRI showed that MPFC photostimulation activated many regions known to receive MPFC afferents. Notably, the activation of hypothalamus, agranular insula, and ventral striatum was positively correlated with the lever press. Our finding may shed light on brain circuits involved in therapeutic effects of recent deep brain stimulation studies in major depression, in which the MPFC plays an important role.

---

1158

14:12



Decipher the hippocampal neurovascular coupling with simultaneous fMRI and GCaMP-mediated calcium recording

XuMing Chen<sup>1,2</sup>, Yi Chen<sup>1</sup>, and Xin Yu<sup>1</sup>

*<sup>1</sup>High-Field Magnetic Resonance, Max Planck Institute for Biological Cybernetics, Tuebingen, Germany, <sup>2</sup>Neurology, Renmin Hospital of Wuhan University, Wuhan, People's Republic of China*

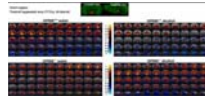
Decipher the hippocampal neurovascular coupling with simultaneous fMRI and GCaMP-mediated calcium recording

Previously, we have developed a single-vessel fMRI method to visualize the hemodynamic signal propagation from individual venules and arterioles in the deep layer cortex and hippocampus. Here, we combined the single-vessel SSFP-fMRI with the GCaMP-mediated calcium recording to decipher the hippocampal neurovascular coupling events. Optogenetic stimulation led to epileptic activity, which could be detected as the bursting calcium spikes coupled to elongated fMRI signal from individual hippocampal arterioles and venules up to 20-30s following the epileptic events. This work establishes a multi-modal fMRI platform to characterize the hippocampal vascular dynamics of both normal and optogenetically driven seizure-like states.

---

1159

14:24



### GPR88 signatures on the reward resting state brain networks after alcohol exposure in mice

Tanzil Mahmud Arefin<sup>1,2,3</sup>, Sami Ben Hamida<sup>3,4</sup>, Thomas Bienert<sup>1</sup>, Thiago Marques De Melo<sup>1,5</sup>, Hsu-Lei Lee<sup>1</sup>, Jürgen Hennig<sup>1</sup>, Dominik von Elverfeldt<sup>1</sup>, Brigitte Kieffer<sup>3,4</sup>, and Laura-Adela Harsan<sup>1,6,7</sup>

<sup>1</sup>Advanced Molecular Imaging Center, Medical Physics, Department of Radiology, University Medical Center Freiburg, Freiburg, Germany, <sup>2</sup>Faculty of Biology, University of Freiburg, Freiburg, Germany, <sup>3</sup>Department of Translational Medicine and Neurogenetics, Institute of Genetics and Molecular and Cellular Biology (IGBMC), Illkirch-Graffenstaden, Strasbourg, France, <sup>4</sup>Department of Psychiatry, Douglas Hospital Research Center, School of Medicine, McGill University, Montreal, QC, Canada, <sup>5</sup>Spemann Graduate School of Biology and Medicine, University of Freiburg, Germany, <sup>6</sup>Department of Biophysics and Nuclear Medicine, University Hospital Strasbourg, Strasbourg, France, <sup>7</sup>Laboratory of Engineering, Informatics and Imaging, University of Strasbourg, Strasbourg, France

Identifying the genetic and molecular factors regulating the development and the dynamics of brain functional connectivity (FC) networks in health and disease is important to develop novel therapeutic strategies. Resting state functional magnetic resonance imaging (rsfMRI) can reveal the FC remodeling in psychiatric disorders and drug addiction. Emerging studies suggest that neuronal responses to alcohol involve several G protein-coupled receptors (GPCR)-mediated signaling pathways, inducing short-term to long-term changes in behavioral and neuronal plasticity. This study investigates the role of GPR88 in the acquisition and development of alcohol dependence and unravels the rsFC modifications underpinning this processes in the mouse brain.

---

1160

14:36



### Systematically mapping anatomical connectivity in the macaque using combined electrical microstimulation and fMRI

Atsushi Mark Takahashi<sup>1</sup>, Rui Xu<sup>1</sup>, Narcisse P. Bichot<sup>1</sup>, Pauline K. Weigand<sup>1</sup>, and Robert Desimone<sup>1</sup>

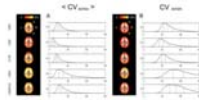
<sup>1</sup>McGovern Institute for Brain Research, Massachusetts Institute of Technology, Cambridge, MA, United States

Connectivity of prefrontal cortex was studied with electrical microstimulation and fMRI in the macaque.

---

1161

14:48



### Assessing the repeatability of absolute CMRO<sub>2</sub> measurements from calibrated fMRI

Alberto Merola<sup>1</sup>, Michael A Germuska<sup>1</sup>, Kevin Murphy<sup>1</sup>, and Richard G Wise<sup>1</sup>

<sup>1</sup>*CUBRIC, Cardiff University, Cardiff, United Kingdom*

O<sub>2</sub> metabolism is a crucial biomarker of brain physiology. We aim at measuring the repeatability of estimates of O<sub>2</sub> metabolism obtained with a dual calibrated fMRI experiment and a newly proposed parameter estimation approach based on a forward model. The analysis is carried out on two datasets from volunteers scanned at rest. The performances are shown to depend on the physiological parameter considered, resolution (bulk or voxel-wise level) and decreasing from within- to between-sessions repeatability. Overall the repeatability is demonstrated to be comparable with PET and a previous calibrated fMRI method, but supplying a more complete mapping of brain O<sub>2</sub> metabolism.

---

Oral

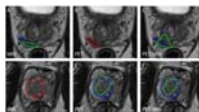
## Multimodal & Multiparametric

Room 314

Thursday 13:00 - 15:00 *Moderators: Dimitrios Karampinos & Christopher Roy*

1162

13:00



### Multimodal multiparametric 18F-Fluciclovine PET/MRI improves computer-assisted detection of primary prostate cancer

Mattijs Elschot<sup>1</sup>, Kirsten M Selnæs<sup>1,2</sup>, Elise Sandsmark<sup>1</sup>, Jose R Teruel<sup>3</sup>, Brage Krüger-Stokke<sup>1,4</sup>, Øystein Størkersen<sup>5</sup>, May-Britt Tessem<sup>1</sup>, Siver A Moestue<sup>1,6</sup>, Helena Bertilsson<sup>7,8</sup>, and Tone F Bathen<sup>1,2</sup>

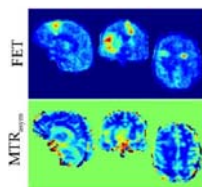
<sup>1</sup>Department of Circulation and Medical Imaging, NTNU, Norwegian University of Science and Technology, Trondheim, Norway, <sup>2</sup>St. Olavs Hospital, Trondheim University Hospital, Trondheim, Norway, <sup>3</sup>Department of Radiology, University of California San Diego, La Jolla, CA, United States, <sup>4</sup>Department of Radiology and Nuclear Medicine, St. Olavs Hospital, Trondheim University Hospital, Trondheim, Norway, <sup>5</sup>Department of Pathology, St. Olavs Hospital, Trondheim University Hospital, Trondheim, Norway, <sup>6</sup>Department of Laboratory Medicine, Children's and Women's Health, NTNU, Norwegian University of Science and Technology, Trondheim, Norway, <sup>7</sup>Department of Cancer Research and Molecular Medicine, NTNU, Norwegian University of Science and Technology, Trondheim, Norway, <sup>8</sup>Department of Urology, St. Olavs Hospital, Trondheim University Hospital, Trondheim, Norway

Computer-assisted algorithms have been proposed to support radiological reading of multiparametric MRI (mpMRI) images for the detection of primary prostate cancer, but have limited sensitivity. In this work, we investigated if standardized uptake values (SUV) from combined <sup>18</sup>F-Fluciclovine PET/mpMRI can improve automated tumor detection. We found that, at the same number of false positives, a model based on combined PET/mpMRI correctly detected more tumors than models based on mpMRI only or PET only. These findings suggest that there is a potential role for multimodal multiparametric <sup>18</sup>F-Fluciclovine PET/MRI for computer-assisted detection of primary prostate cancer.

1163



13:12



### Hybrid MR-PET of Brain Tumours with amino acid-PET and Amide Proton Transfer MRI

Nuno André da Silva<sup>1</sup>, Philipp Lohmann<sup>1</sup>, James Fairney<sup>2,3</sup>, Arthur W. Magill<sup>1</sup>, Ana-Maria Oros-Peusquens<sup>1</sup>, Chang-Hoon Choi<sup>1</sup>, Rüdiger Stirnberg<sup>1,4</sup>, Xavier Golay<sup>2,3</sup>, Karl-Josef Langen<sup>1,5,6</sup>, and N Jon Shah<sup>1,7,8</sup>







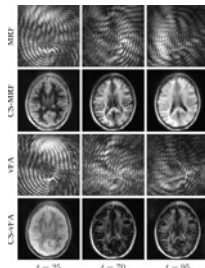
<sup>1</sup>MGH/MIT/HMS Athinoula A. Martinos Center for Biomedical Imaging, Massachusetts General Hospital, Harvard Medical School, Charlestown, MA, United States, <sup>2</sup>Siemens Healthcare AG, Advanced Clinical Imaging Technology, Lausanne, Switzerland, <sup>3</sup>Department of Radiology, University Hospital (CHUV), Lausanne, Switzerland, <sup>4</sup>LTS5, École Polytechnique Fédérale de Lausanne, Lausanne, Switzerland, <sup>5</sup>Neuroimmunology Unit, Neurology, Department of Clinical Neurosciences, Centre Hospitalier Universitaire Vaudois (CHUV) and University of Lausanne (UNIL), Lausanne, Switzerland

Radioligands used in PET imaging and binding to the translocator protein (TSPO) have proved to be useful to study inflammatory brain processes. Relatedly, quantitative Magnetic Resonance Imaging provides metrics of tissue-level microstructure, which permit to study the consequences of brain inflammation. In this work, we have investigated the relationship between PBR28 radioligand uptake and T1 and T2 metric of brain tissue microstructure based on analysis of PET images, T1 and T2 relaxometry images of 5 HIV subjects.

1167



14:00



### Accelerated parameter mapping with compressed sensing: an alternative to MR Fingerprinting

Pedro A. Gómez<sup>1,2</sup>, Guido Buonincontri<sup>3</sup>, Miguel Molina-Romero<sup>1,2</sup>, Jonathan I. Sperl<sup>2</sup>, Marion I. Menzel<sup>2</sup>, and Bjoern H. Menze<sup>1</sup>

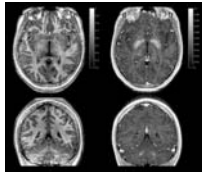
<sup>1</sup>Technical University of Munich, Munich, Germany, <sup>2</sup>GE Global Research, Munich, Germany, <sup>3</sup>Imago7 Foundation, Pisa, Italy

We introduce a method for MR parameter mapping based on three concepts: 1) an inversion recovery, variable flip angle acquisition strategy designed for speed, signal, and contrast; 2) a compressed sensing reconstruction which exploits spatiotemporal correlations through low rank regularization; and 3) a model-based optimization to simultaneously estimate proton density, T1, and T2 values from the acquired measurements. Compared to MR Fingerprinting, the proposed method achieves a five-fold acceleration in acquisition time, reconstructs an unaliased series of images, and does not rely on dictionary matching for parameter estimation.

1168

14:12

Ultra-high resolution in vivo multi-parameter mapping of the human brain  
Kerrin J Pine<sup>1</sup>, Luke J Edwards<sup>1</sup>, Martina F Callaghan<sup>2</sup>, Pierre-Louis Bazin<sup>1</sup>, and Nikolaus Weiskopf<sup>1</sup>

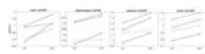


<sup>1</sup>Department of Neurophysics, Max Planck Institute for Human Cognitive and Brain Sciences, Leipzig, Germany, <sup>2</sup>Wellcome Trust Centre for Neuroimaging, UCL Institute of Neurology, London, United Kingdom

We present the first multi-parameter maps of R1, R2\* and effective proton-density (PD\*) acquired at 400  $\mu\text{m}$  isotropic resolution at 7T. Prospective motion correction (PMC) by external optical tracking was used to reduce motion artifacts, as well as to avoid a co-registration step during calculation of the maps. The maps allow for characterizing of subtle subcortical and cortical features such as the line of Gennari in the visual cortex.

1169

14:24



Changes in Hippocampal Subfield Volumes, Diffusivity and Brain Metabolism after Electroconvulsive Therapy: a Pilot PET/MR Study

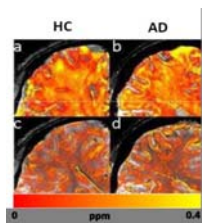
Chuan Huang<sup>1,2,3</sup>, Laura Kunkel<sup>1</sup>, Adeeb Yacoub<sup>1</sup>, Jie Ding<sup>3</sup>, Christine DeLorenzo<sup>1,3</sup>, and Ramin Parsey<sup>1</sup>

<sup>1</sup>Psychiatry, Stony Brook Medicine, Stony Brook, NY, United States, <sup>2</sup>Radiology, Stony Brook Medicine, Stony Brook, NY, United States, <sup>3</sup>Biomedical Engineering, Stony Brook University, Stony Brook, NY, United States

Major depression disorder is a highly prevalent illness with low treatment response rates. Fortunately, electroconvulsive therapy (ECT) is an effective treatment for patients with pharmacotherapy resistant depression, although its mechanism of action remains unclear. There is disagreement regarding the predictive value of amygdala and hippocampal volumes and whether ECT causes neuroplastic effects on these regions in patients with MDD. In this study, we used simultaneous PET/MR to look at structural, diffusion and metabolism changes in brain before and after ECT.

1170

14:36



In-vivo and ex-vivo R2\* and Quantitative Susceptibility Mapping in Alzheimer's Disease at Ultra-High Magnetic Field compared to Histology

Elisa Tuzzi<sup>1</sup>, Gisela Elisabeth Hagberg<sup>2</sup>, David Balla<sup>3</sup>, Joana Loureiro<sup>1</sup>, Manuela Neumann<sup>4</sup>, Christoph Laske<sup>5</sup>, Rolf Pohmann<sup>6</sup>, Matthias Valverde<sup>1</sup>, and Klaus Scheffler<sup>1</sup>

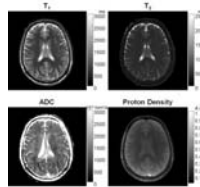
<sup>1</sup>High Field Magnetic Resonance, Max Planck Institute for Biological Cybernetics, Tuebingen, Germany, <sup>2</sup>High-field Magnetic Resonance, Max Planck Institute for Biological Cybernetics, Tuebingen, Germany, <sup>3</sup>Physiology of Cognitive Processes, Max Planck Institute for Biological Cybernetics, Tuebingen, Germany, <sup>4</sup>Division of Neuropathology, University Hospital Tuebingen, Tuebingen, Germany, <sup>5</sup>Section for Dementia Research, DE, Hertie-Institute for Clinical Brain Research, Tuebingen, Germany, <sup>6</sup>High Field Magnetic Resonance, Max Planck Institute for Biological Cybernetics, Tuebingen

Amyloid- $\beta$  plaques are classical hallmarks of the post-mortem Alzheimer's Disease (AD) brain. Ultra-High-Field (UHF) MRI provides a compelling means to investigate pathological processes at an unprecedented level of detail.  $\beta$ -amyloid plaques can be detected in T2\* weighted images at UHF, ex-vivo, due to the local iron content and to the plaque geometry per se. With this study we aim to explore the source of the observed MR signal changes in AD at UHF using quantitative MRI methods in-vivo and ex-vivo.

1171



14:48



### Simultaneous T<sub>1</sub>, T<sub>2</sub> and Diffusion Quantification using Multiple Contrast Prepared Magnetic Resonance Fingerprinting

Yun Jiang<sup>1</sup>, Jesse Ian Hamilton<sup>1</sup>, Wei-Ching Lo<sup>1</sup>, Katherine L. Wright<sup>2</sup>, Dan Ma<sup>2</sup>, Andrew J. Coristine<sup>1,3</sup>, Nicole Seiberlich<sup>1</sup>, Vikas Gulani<sup>1,2</sup>, and Mark A. Griswold<sup>1,2</sup>

<sup>1</sup>Department of Biomedical Engineering, Case Western Reserve University, Cleveland, OH, United States, <sup>2</sup>Department of Radiology, University Hospitals of Cleveland, Cleveland, OH, United States, <sup>3</sup>Department of Radiology, University Hospital (CHUV), Lausanne, Switzerland

A novel MRF sequence is designed for generating high quality, distortion-free T<sub>1</sub>, T<sub>2</sub> and apparent diffusion coefficient (ADC) maps simultaneously in less than 60 seconds per slice. The method inserts multiple magnetization preparation modules in a FISP-based MRF sequence. The use of magnetization preparation modules shortens the preparation time to achieve variable image contrast. Accurate T<sub>1</sub>, T<sub>2</sub> and ADC quantification is demonstrated in a phantom and *in vivo* in human brains. This method enables the simultaneous collection of T<sub>1</sub>, T<sub>2</sub> and diffusion maps for tissue characterization without the need to co-register separately acquired maps as in conventional MRI.

Oral

## Thermometry & Focused Ultrasound

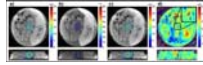
Room 315

Thursday 13:00 - 15:00 *Moderators: Clemens Bos & Christiaan Overduin*

1172



13:00



### Efficiency improvement in multi-point MR acoustic radiation force impulse imaging

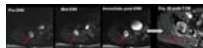
Henrik Odéen<sup>1</sup>, Joshua de Bever<sup>2</sup>, Lorne W Hofstetter<sup>3</sup>, and Dennis L Parker<sup>1</sup>

*<sup>1</sup>Department of Radiology and Imaging Sciences, University of Utah, Salt Lake City, UT, United States, <sup>2</sup>Department of Radiology, Stanford University, <sup>3</sup>Department of Radiology and Imaging Sciences, University of Utah*

Focused ultrasound (FUS) treatment endpoint can potentially be evaluated using MR acoustic radiation force impulse (MR-ARFI) imaging, which can non-invasively and with very low energies interrogate tissue mechanical properties. In this work we investigate two ways of improving the efficiency of a previously published multi-point (MP)-MR-ARFI pulse sequence which simultaneously measure ARFI displacement and PRFS temperature maps. We investigate view-sharing of higher k-space frequencies from FUS-OFF images to FUS-ON images, and focusing in multiple positions during a single motion encoding gradient lobe as ways to speed up acquisition. Combining these methods full 3D MP-displacement maps could be achieved in a clinically acceptable time of 30-60s.

1173

13:12



### MR guided High Intensity Focused Ultrasound for treating painful bone metastases: relating intra-procedural ADC changes and thermal dose to volume of ablated tissue

Sharon L Giles<sup>1,2</sup>, Matthew RD Brown<sup>3</sup>, Jessica Winfield<sup>1,2</sup>, David J Collins<sup>1</sup>, Ian Rivens<sup>4</sup>, John Civalè<sup>4</sup>, Gail R ter Haar<sup>4</sup>, and Nandita M deSouza<sup>1</sup>

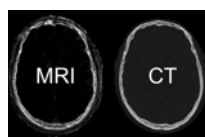
*<sup>1</sup>CRUK Cancer Imaging Centre, Institute of Cancer Research, London, United Kingdom, <sup>2</sup>CRUK Cancer Imaging Centre, Royal Marsden Hospital, London, United Kingdom, <sup>3</sup>Pain Management Team, Department of Anaesthetics, Royal Marsden Hospital, <sup>4</sup>Therapeutic Ultrasound, Institute of Cancer Research, London, United Kingdom*

Thermal dose estimates and apparent diffusion coefficient (ADC) changes during MR-guided High Intensity Focused Ultrasound of painful bone metastases (n=11) were correlated with ablated tissue volumes assessed on Gd-T1W imaging acquired immediately, and at 30 days post-treatment. Thermal dose volume and mean maximum temperature were estimated from proton resonance frequency shift thermometry. Ablated tissue volume did not change significantly over 30 days. Mean maximum temperature and thermal dose volume were significant indicators of ablated volume, and mean maximum temperature was significantly higher in those with enduring ADC changes at Day 30. Further work will relate imaging changes to pain outcomes.

---

1174

13:24



### Estimating Acoustic Velocity of Human Skull Bone with CT and MRI

Taylor D Webb<sup>1</sup>, Ethan M Johnson<sup>1</sup>, Steven Leung<sup>2</sup>, Jeremy Dahl<sup>3</sup>, Norbert Pelc<sup>3</sup>, John Pauly<sup>1</sup>, and Kim Butts Pauly<sup>1,2,3</sup>

<sup>1</sup>Electrical Engineering, Stanford University, Stanford, CA, United States,

<sup>2</sup>Bionengineering, Stanford University, Stanford, CA, United States,

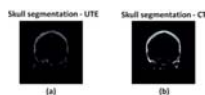
<sup>3</sup>Radiology, Stanford University, Stanford, CA, United States

Focusing of transcranial focused ultrasound requires knowledge of the speed of sound in the skull. Clinically, estimates of the speed of sound in the skull are obtained from a CT scan. We measure the acoustic velocity in several human skull fragments and correlate it to the average Hounsfield units, MR-Simulated-CT value (derived from an ultrashort echo time MR sequence), and R2\* value of each fragment. Results show that both CT and MR can be used to accurately estimate the acoustic velocity in human skull bone and that replacing CT with MR to plan transcranial FUS treatments is feasible.

---

1175

13:36



### Ultrashort Echo-Time Imaging based Skull Density Ratio Assessment for Transcranial MR guided Focused Ultrasound

Sijia Guo<sup>1</sup>, Jiachen Zhuo<sup>1</sup>, and Rao Gullapalli<sup>1</sup>

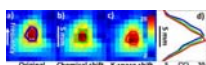
<sup>1</sup>Department of Diagnostic Radiology & Nuclear Medicine, University of Maryland School of Medicine, Baltimore, MD, United States

Transcranial MRI-guided focused ultrasound (tcMRgFUS) applications have been growing steadily on treatment of brain diseases. Typically a CT skull scan is used with the MR scan to perform treatment planning in tcMRgFUS procedures. In this study we examine the use of ultrashort echo time imaging to perform the skull imaging and assess the feasibility of using the information from MRI to perform treatment planning through acoustic and temperature modeling with skull characteristics generated from UTE imaging. We further compared the simulation results with existing data from tcMRgFUS treatment of essential tremor procedure that used CT images of the skull for treatment planning. We demonstrated that UTE based treatment planning is feasible and avoids the use of CT based images thus avoiding unnecessary radiation exposure.

---

1176

13:48



### Focus Correction in MR thermography for Precise Targeting in Focused Ultrasound Thalamotomy for Essential Tremor

Chang-Sheng Mei<sup>1</sup>, Bruno Madore<sup>2</sup>, Shenyang Zong<sup>3</sup>, Pei-Hsin Wu<sup>2</sup>, Garth Rees Cosgrove<sup>2</sup>, and Nathan J. McDannold<sup>2</sup>

*<sup>1</sup>Physics, Soochow University, Taipei, Taiwan, <sup>2</sup>Radiology, Harvard Medical School, Brigham and Women's Hospital, Boston, MA, United States, <sup>3</sup>Biomedical Engineering, Shanghai Jiao Tong University, Shanghai, People's Republic of China*

MRI-guided focused ultrasound thalamotomy has proved an effective method for the treatment of Essential Tremor. Precise alignment of the focus to the target in the thalamus is crucial. Proper targeting is complicated by artifactual shifts in hot spot location, with respect to anatomical images. We identified two sources of errors and proposed solutions to both; the correction scheme does not require any modification to the pulse sequence or imaging protocol. Shifts by  $1.0 \pm 0.1$  mm were detected and corrected, for three separate sonications in one given patient. The size of the shifts agreed with observations from the literature.

---

1177

14:00



### Image-registered whole mount histology technique for validation of MRgFUS therapies

Allison Payne<sup>1</sup>, Sara Johnson<sup>2</sup>, Robb Merrill<sup>1</sup>, Nicole Winkler<sup>1</sup>, Rachel Factor<sup>3</sup>, and Jill Shea<sup>4</sup>

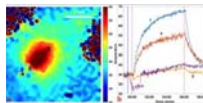


<sup>1</sup>Radiology and Imaging Sciences, University of Utah, Salt Lake City, UT, United States, <sup>2</sup>Bioengineering, University of Utah, Salt Lake City, UT, United States, <sup>3</sup>Pathology, University of Utah, Salt Lake City, UT, United States, <sup>4</sup>Surgery, University of Utah, Salt Lake City, UT, United States

Clinical pathological review of histological samples is the gold standard for identification of tissue damage. For the development of new magnetic resonance-guided focused ultrasound (MRgFUS) procedures, in vivo post-treatment imaging assessment techniques require correlation to histopathology. Our study presents methodology and preliminary preclinical results of a new MRI-registered whole mount histology technique for efficacy evaluation of MRgFUS therapies.

1178

14:12



A Combined Intravascular MRI Endoscope and Intravascular Ultrasound (IVUS) Transducer for High-Resolution Image-Guided Ablation

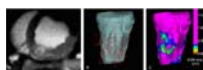
Xiaoyang Liu<sup>1,2</sup>, Nicholas Ellens<sup>1</sup>, Emery Williams<sup>3</sup>, Everette Clif Burdette<sup>3</sup>, Parag Karmarkar<sup>1</sup>, and Paul Bottomley<sup>1,2</sup>

<sup>1</sup>Russell H. Morgan Department of Radiology, Johns Hopkins University, Baltimore, MD, United States, <sup>2</sup>Electrical and Computer Engineering, Johns Hopkins University, Baltimore, MD, United States, <sup>3</sup>Acoustic MedSystems, Inc, Champaign, IL, United States

An intravascular MRI (IMRI) loopless antenna is combined for the first time with an intravascular water-cooled ultrasound ablation transducer as a possible tool for providing high-resolution MRI-guided ablations of pathological tissue via intravascular access. High resolution anatomical MRI, and real-time MRI thermometry were used to monitor ablation delivery in phantoms and tissue specimens. Results show that IMRI can guide IVUS-mediated directional ablation with minimal image artifacts. This permits the monitoring of thermal dose and therapy titration while minimizing potential thermal damage to the vessel wall.

1179

14:24



MRI-based myocardial ablation lesion extent relates to area of voltage reduction in MR-guided electroanatomical voltage maps

Philippa Krahn<sup>1,2</sup>, Venkat Ramanan<sup>2</sup>, Labonny Biswas<sup>2</sup>, Nicolas Yak<sup>2</sup>, Kevan Anderson<sup>2</sup>, Jennifer Barry<sup>2</sup>, Mihaela Pop<sup>1,2</sup>, and Graham A Wright<sup>1,2</sup>

<sup>1</sup>Medical Biophysics, University of Toronto, Toronto, ON, Canada, <sup>2</sup>Sunnybrook Research Institute, Toronto, ON, Canada

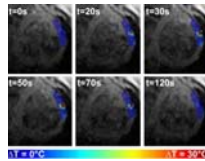




In this study we investigated subtle features of acute RF ablation lesions using co-registered MR images and electroanatomic voltage maps (EAVM) acquired under MR guidance. Of particular interest was the relationship between the extent of edema detected in T2 maps and altered electrical activity surrounding the ablation site. The results from this study aim to elucidate mechanisms of high ventricular arrhythmia recurrence rates after successful RF ablation therapy, which may be driven by transient conduction block produced acutely by edema.

1180

14:36



### In-vivo Imaging of Ablation Lesions during MRI-guided Epicardial Ventricular Ablation in Swine

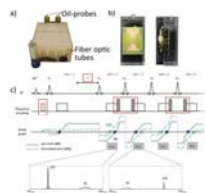
Sébastien Roujol<sup>1</sup>, Radhouene Neji<sup>1,2</sup>, Henry Chubb<sup>1</sup>, John Silberbauer<sup>1</sup>, Tom Lloyd<sup>3</sup>, Thomas Pohl<sup>4</sup>, Rainer Schneider<sup>4</sup>, Nick Kampa<sup>3</sup>, James Harrison<sup>1</sup>, Steven Williams<sup>1</sup>, Rahul Mukherjee<sup>1</sup>, Louisa O'Neill<sup>1</sup>, John Whitaker<sup>1</sup>, Matthew Wright<sup>1</sup>, Tobias Schaeffter<sup>1</sup>, Mark O'Neill<sup>1</sup>, and Reza Razavi<sup>1</sup>

<sup>1</sup>Division of Imaging Sciences and Biomedical Engineering, King's College London, London, United Kingdom, <sup>2</sup>MR Research Collaborations, Siemens Healthcare Limited, Frimley, United Kingdom, <sup>3</sup>Imricor Medical Systems, Burnsville, MN, United States, <sup>4</sup>Siemens Healthcare GmbH, Erlangen, Germany

Cardiac MR (CMR) shows promise for the guidance of ventricular tachycardia (VT) ablation procedures and imaging of ablation lesions. CMR-thermometry is a promising approach for real-time tissue temperature monitoring and tissue characterization for prediction of permanent ablation lesions. In this study, we sought to develop an integrated multi-parametric framework for real-time, hyper-acute and acute imaging of ablation lesions using CMR-thermometry, native T1 mapping and late gadolinium enhancement (LGE), respectively. This framework is evaluated during MR-guided epicardial ventricular ablation in swine.

1181

14:48



Toward hybrid MR thermometry in aqueous and adipose tissue using simultaneous dual contrast weighting with double echo RARE imaging  
Hendrik Paysen<sup>1</sup>, Katharina Paul<sup>1</sup>, Michal Pham<sup>1</sup>, Lukas Winter<sup>1</sup>, and Thoralf Niendorf<sup>1,2,3</sup>

<sup>1</sup>Berlin Ultrahigh Field Facility (B.U.F.F.), Max Delbrück Center for Molecular Medicine in the Helmholtz Association, Berlin, Germany, <sup>2</sup>Experimental and Clinical Research Center (ECRC), a joint cooperation between the Charité Medical Faculty and the Max Delbrück Center for Molecular Medicine, Berlin, Germany, <sup>3</sup>MRI.TOOLS GmbH, Berlin, Germany

Proton resonance frequency (PRF) shift is the most common MR thermometry (MRTh) technique for water based tissue. For adipose tissue MRTh exploits the temperature dependent relaxation times  $T_1$  and  $T_2$ . Hybrid methods that allow simultaneous acquisition of water and fat based thermometry are of great clinical need. Recognizing this need this work investigates a hybrid temperature mapping technique, designated as 2in1-Thermometry, which combines simultaneous PRF and  $T_2$ -based temperature mapping using simultaneous dual contrast weighting with double echo RARE imaging.

---

Oral

## Thoracic MRI: Lung & Mediastinum

Room 320

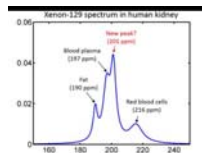
Thursday 13:00 - 15:00 Moderators: Scott Nagle & Edwin VanBeek

---

1182

13:00

### Dynamic Spectroscopy of Dissolved-Phase Xenon-129 in the Human Kidney



G. Wilson Miller<sup>1</sup>, Gordon D. Cates Jr.<sup>1,2</sup>, David Keder<sup>2</sup>, Talissa A. Altes<sup>3</sup>, Jaime F. Mata<sup>1</sup>, Kun Qing<sup>1</sup>, Iulian Ruset<sup>4</sup>, F. William Hersman<sup>4</sup>, and John P. Mugler III<sup>1</sup>

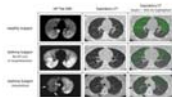
<sup>1</sup>Radiology & Medical Imaging, University of Virginia, Charlottesville, VA, United States, <sup>2</sup>Physics, University of Virginia, <sup>3</sup>Radiology, University of Missouri, <sup>4</sup>Xemed LLC

The increase in available dissolved-phase signal made possible by high-performing Xe-129 polarizers has led to renewed interest in dissolved-phase imaging of Xe-129 outside the lung. Here we examine the time course of the dissolved phase Xe-129 signal in the human kidney following gas inhalation, in order to optimize kidney image acquisition and explore the potential for studying kidney function using hyperpolarized Xe-129. In addition to spectral peaks commonly associated with Xe-129 dissolved in tissue/plasma, red blood cells, and fat, we have identified an additional peak at 201 ppm that lags the blood peaks by a few seconds.

1183



13:12



### Ventilation Defect Percent in Helium-3 MRI is Associated with Severe Outcomes in Asthma

David Mummy<sup>1</sup>, Stanley Kruger<sup>1</sup>, Michael Evans<sup>2</sup>, Wei Zha<sup>1</sup>, Ronald Sorkness<sup>3</sup>, Nizar Jarjour<sup>4</sup>, Mark Schiebler<sup>5</sup>, Loren Denlinger<sup>4</sup>, and Sean Fain<sup>1</sup>

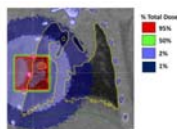
<sup>1</sup>Medical Physics, University of Wisconsin-Madison, Madison, WI, United States, <sup>2</sup>Biostatistics & Medical Informatics, University of Wisconsin-Madison, Madison, WI, United States, <sup>3</sup>School of Pharmacy, University of Wisconsin-Madison, Madison, WI, United States, <sup>4</sup>Medicine, University of Wisconsin-Madison, Madison, WI, United States, <sup>5</sup>Radiology, University of Wisconsin-Madison, Madison, WI, United States

We assessed the ventilation defect percent (VDP) on hyperpolarized helium-3 MRI as an indicator of severe clinical outcomes (emergency department [ED] visits and hospitalizations as surrogates for significant asthma exacerbations). We compared VDP with conventional biomarkers of lung function and inflammation and found VDP was more strongly associated with both ED and hospitalizations as outcomes. VDP was correlated with spirometry, air trapping measured on CT, and eosinophil levels in sputum and peripheral blood. These findings suggest that VDP is a candidate biomarker associated with clinical outcomes of asthma exacerbation and stability.

1184



13:24



### Regional Detection of Lung Injury using Hyperpolarized Xenon-129 Mapping of Blood Hematocrit in a Rat Model Involving Partial-Lung Irradiation

Brandon Zanette<sup>1,2</sup>, Elaine Stirrat<sup>1</sup>, Salomeh Jelveh<sup>3</sup>, Andrew Hope<sup>3,4</sup>, and Giles E. Santyr<sup>1,2</sup>

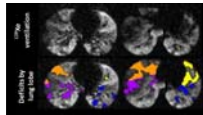
<sup>1</sup>Peter Gilgan Centre for Research and Learning, The Hospital for Sick Children, Toronto, ON, Canada, <sup>2</sup>Department of Medical Biophysics, University of Toronto, Toronto, ON, Canada, <sup>3</sup>Radiation Medicine Program, Princess Margaret Cancer Centre, Toronto, ON, Canada, <sup>4</sup>Department of Radiation Oncology, University of Toronto, Toronto, Canada

Dissolved <sup>129</sup>Xe imaging holds promise for the detection of early functional decline due to radiation-induced lung injury through the extraction of regional quantitative parameters relating to lung physiology and gas exchange. In this work a spiral-IDEAL imaging technique was used with a partial-lung irradiation rat model to investigate regional changes lung function associated with injury and compare to histology. A significant reduction in capillary hematocrit (HCT) was observed in the vicinity of irradiation. These results were in agreement with quantitative histology of red blood cells. Imaging results were more sensitive than whole-lung spectroscopy, which was performed simultaneously.

---

1185

13:36



Ventilation heterogeneity of pediatric cystic fibrosis accessed via lung clearance index and hyperpolarized <sup>129</sup>Xe MRI

Laura L Walkup<sup>1</sup>, Robert P Thomen<sup>1</sup>, Emily Bell<sup>2</sup>, Beth Decker<sup>2</sup>, Zackary I Cleveland<sup>1</sup>, John Paul Clancy<sup>2</sup>, and Jason C Woods<sup>1</sup>

<sup>1</sup>Center for Pulmonary Imaging Research, Division of Pulmonary Medicine and Department of Radiology, Cincinnati Children's Hospital Medical Center, Cincinnati, OH, United States, <sup>2</sup>Division of Pulmonary Medicine, Cincinnati Children's Hospital Medical Center, Cincinnati, OH, United States

Quantitative hyperpolarized <sup>129</sup>Xe ventilation MRI was compared to FEV<sub>1</sub>, the spirometric gold standard for assessing lung function, and lung clearance index (LCI), an emerging pulmonary function test to assess global ventilation heterogeneity, in 12 pediatric cystic fibrosis subjects. A range of severity and spatial distributions of <sup>129</sup>Xe ventilation deficits were observed, with a <sup>129</sup>Xe ventilation defect percentage (VDP) of 18.0% ± 8.1%. VDP did not correlate with FEV<sub>1</sub> (p=0.45) but correlated very strongly with LCI (p=0.0001), suggesting that the spatial distribution of defects in the <sup>129</sup>Xe images represents obstructed areas of the lung that give rise to elevated LCI.

---

13:48

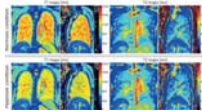
Quantitative ventilation-perfusion imaging using co-registered hyperpolarized gas and contrast enhanced <sup>1</sup>H perfusion MRI



Paul John Clifford Hughes<sup>1</sup>, Bilal Tahir<sup>1,2</sup>, Felix C. Horn<sup>1</sup>, Alberto Biancardi<sup>1</sup>, Rob Ireland<sup>2</sup>, Helen Marshall<sup>1</sup>, and Jim Wild<sup>1,3</sup>

<sup>1</sup>POLARIS, Academic Unit of Radiology, University of Sheffield, Sheffield, United Kingdom, <sup>2</sup>Academic Unit of Clinical Oncology, University of Sheffield, Sheffield, United Kingdom, <sup>3</sup>Insigneo Institute for in silico Medicine, Sheffield, United Kingdom

Analysis of the matching of ventilation and perfusion using MRI is an important area of research in the pulmonary MRI community. This work presents a quantitative method of voxelwise analysis of ventilation from hyperpolarized gas MRI and perfusion from dynamic contrast enhanced <sup>1</sup>H MRI. The method developed allows for direct comparison of ventilation and perfusion including global measurements of ventilated and perfused volume.

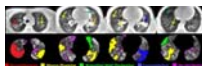


Oxygen-enhanced pulmonary relaxometry using ultra-fast steady-state free precession imaging

Grzegorz Bauman<sup>1,2</sup>, Orso Pusterla<sup>1,2</sup>, Francesco Santini<sup>1,2</sup>, and Oliver Bieri<sup>1,2</sup>

<sup>1</sup>Division of Radiological Physics, Department of Radiology, University of Basel Hospital, Basel, Switzerland, <sup>2</sup>Department of Biomedical Engineering, University of Basel, Basel, Switzerland

This study demonstrates the feasibility of fast and simultaneous T1 and T2 mapping of the lung parenchyma in oxygen-enhanced MRI. The data acquisition was performed using an adapted 2D inversion recovery ultra-fast steady-state free precession imaging in healthy human subjects. Relaxation time maps were generated for normoxic and hyperoxic acquisitions. Statistical analysis was performed to compare the relaxation times in the lung parenchyma for both gas conditions.



Investigating regional pulmonary structure-function relationships using hyperpolarized <sup>129</sup>Xe MRI and ultra-short echo-time MRI

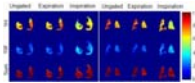
Robert P Thomen<sup>1</sup>, Laura L Walkup<sup>1</sup>, David J Roach<sup>1</sup>, Zackary I Cleveland<sup>1</sup>, John Paul Clancy<sup>2</sup>, and Jason C Woods<sup>1</sup>

<sup>1</sup>Center for Pulmonary Imaging Research, Cincinnati Children's Hospital Medical Center, Cincinnati, OH, United States, <sup>2</sup>Pulmonology, Cincinnati Children's Hospital Medical Center, Cincinnati, OH, United States

We have quantified the extent of ventilation impairment in lungs due to specific pathologies associated with cystic fibrosis (CF) lung disease using ultrashort echo-time (UTE) MRI to identify structural abnormalities and hyperpolarized (HP)  $^{129}\text{Xe}$  MRI to identify ventilation deficits. We found that bronchiectasis demonstrates the best correlation with lung function decline, as measured by the percent predicted forced expiratory volume in 1 second ( $\text{FEV}_{1\%}$  predicted) and demonstrated the greatest deficit in HP  $^{129}\text{Xe}$  signal within corresponding defective regions. However, the greatest volume-percentage of defects identified were due to mucus plugging.

1189

14:24



Respiratory self-gating and estimation of gas/proton fractions in SF6 and proton lung imaging in free-breathing mice

Marta Tibiletti<sup>1</sup> and Volker Rasche<sup>2</sup>

<sup>1</sup>Core Facility Small Animal MRI, Ulm University, Ulm, Germany,

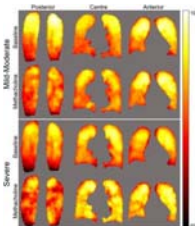
<sup>2</sup>Internal Medicine II, University Hospital of Ulm, Ulm, Germany

Fluorinated gases are a promising alternative to hyperpolarized gases to study ventilation in clinical and preclinical applications. 3D Ultra Short Echo Time (UTE) acquisitions can be employed to visualize inhaled SF6 and lung parenchyma. DC self-gating was applied to discriminate between inspiration and expiration in free-breathing acquisitions. Proton and gas density were estimated in inspiration, expiration and in ungated data. The information derived from tissue-density changes matched the changes observed in the gas density, thus indicating the ventilation information can be derived from tissue density mapping.

1190



14:36



Pulmonary MRI Ventilation Defects in Asthma: Stochastic or Deterministic?

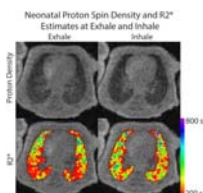
Rachel L Eddy<sup>1</sup>, Dante PI Capaldi<sup>1</sup>, Khadija Sheikh<sup>1</sup>, Sarah Svenningsen<sup>1</sup>, David G McCormack<sup>2</sup>, and Grace Parraga<sup>1</sup>

<sup>1</sup>Robarts Research Institute, London, ON, Canada, <sup>2</sup>Division of Respirology, The University of Western Ontario, London, ON, Canada

Pulmonary MRI provides strong evidence of ventilation abnormalities that are temporally and spatially persistent; this has generated a paradigm shift in our understanding of asthma as a spatially and temporally heterogeneous, non-stochastic disease. Based on these findings, here our objective was to develop image-processing methods to estimate and mathematically describe the spatial probability distribution of MRI-derived ventilation defects. To accomplish this, we generated functional lung MRI atlases based on asthmatics who were evaluated before and post-methacholine using hyperpolarized  $^3\text{He}$  static-ventilation MRI. This proof-of-concept evaluation showed that in asthmatics, ventilation abnormalities are not diffuse nor stochastic, but heterogeneous and deterministic.

1191

14:48



### Proton Density and $R_2^*$ Estimation of Neonatal Lung Parenchyma During Free Breathing with UTE MRI

Andrew Hahn<sup>1</sup>, Nara Higano<sup>2,3</sup>, Jean Tkach<sup>4</sup>, Laura Walkup<sup>2</sup>, Robert Thomen<sup>2</sup>, Xuefeng Cao<sup>2,5</sup>, Stephanie Merhar<sup>6</sup>, Jason Woods<sup>2,3</sup>, and Sean Fain<sup>1</sup>

<sup>1</sup>Medical Physics, University of Wisconsin - Madison, Madison, WI, United States, <sup>2</sup>Center for Pulmonary Imaging Research, Division of Pulmonary Medicine and Department of Radiology, Cincinnati Children's Hospital Medical Center, Cincinnati, OH, United States, <sup>3</sup>Department of Physics, Washington University in St. Louis, St. Louis, MO, United States, <sup>4</sup>Imaging Research Center, Department of Radiology, Cincinnati Children's Hospital Medical Center, Cincinnati, OH, <sup>5</sup>Department of Physics, University of Cincinnati, Cincinnati, OH, United States, <sup>6</sup>Perinatal Institute, Division of Neonatology, Cincinnati Children's Hospital Medical Center, Cincinnati, OH, United States

The majority of patients in the neonatal intensive care unit (NICU) have pulmonary morbidities, yet little is known about the underlying parenchymal structure. We quantify parenchymal proton density and  $R_2^*$  in the lungs of quiet breathing, non-sedated neonates in the NICU using a multi-echo 3D radial UTE MRI. Results indicate that lung proton density decreases as expected with lung inflation, while  $R_2^*$  increases. A positive relationship between gravitational dependence and tissue density is also apparent, while  $R_2^*$  decreases in more gravitationally dependent regions. Overall, our findings support a negative relationship between tissue density and  $R_2^*$  in the neonatal lung.



## Combined Educational & Scientific Session

# Body DWI

Organizers: Kathryn Fowler, M.D., Kartik Jhaveri, M.D., F.R.C.P.C. & Lorenzo Mannelli, M.D., Ph.D.

Room 316BC Thursday 13:00 - 15:00 Moderators: Hersh Chandarana & Giuseppe Palma

---

13:00

### Liver DWI

Satoshi Goshima<sup>1</sup>

<sup>1</sup>Radiology, Gifu University Hospital, Gifu City, Japan

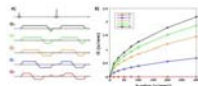
N.A.

---

1192



13:20



### Efficient IVIM of the Liver using Convex Optimized Diffusion Encoding Waveforms With Variable Flow Encoding Strengths

Kévin Moulin<sup>1</sup>, Eric Aliotta<sup>1,2</sup>, and Daniel B. Ennis<sup>1,2</sup>

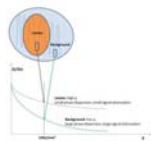
<sup>1</sup>Department of Radiological Sciences, University of California, Los Angeles, CA, United States, <sup>2</sup>Biomedical Physics IDP, University of California, Los Angeles, CA, United States

Accounting for the flow encoding strength  $\alpha$  in addition to the  $b$ -value in the Intra-Voxel Incoherent Motion (IVIM) technique enables robust perfusion estimation. However, this approach still requires long scan times and  $\alpha$  is dependent on both the diffusion encoding waveform and the  $b$ -value. In this study, waveforms were generated using the convex diffusion encoding (CODE) framework and led to a range of  $\alpha$  for a given  $b$ -value. By sampling of flow- and diffusion-encoding space, capillary blood velocity ( $V_b$ ), perfusion fraction ( $f$ ) and true diffusion ( $D$ ) was estimated with higher precision without any cost in time compared to conventional IVIM.

---

1193

13:32



### IVIM virtual MR elastography of the liver

Denis Le Bihan<sup>1</sup>, Shintaro Ichikawa<sup>2</sup>, and Utaroh Motosugi<sup>2</sup>

<sup>1</sup>NeuroSpin, <sup>2</sup>BM/CEA-Saclay, Gif-sur-Yvette, France, <sup>2</sup>Radiology Department, Yamanashi University, Kofu, Japan

We have investigated the potential of diffusion MRI to provide quantitative estimates of tissue stiffness and compared results with those obtained by standard MR elastography (MRE). We revealed that water diffusion, calculated from 2 key b values, can be directly and quantitatively converted into shear stiffness without using mechanical vibrations. Propagating shear waves can also be simulated leading to a new elasticity-driven IVIM attenuation contrast. Such virtual elastograms give a variety of contrasts by simulating various ranges of vibration frequencies and amplitudes or MRI gradient strengths not limited by MRE hardware capacities.

---

13:44

Prostate DWI  
Daniel Margolis<sup>1</sup>

*<sup>1</sup>Department of Radiology, Weill Cornell Medical College, New York, NY, United States*

Diffusion-weighted imaging has gone from being a research tool to a correlate of cancer aggressiveness to a mainstay in routine prostate magnetic resonance imaging. From the basic components required for clinically useful imaging, to esoteric and technically demanding pulse sequences that tantalize us with the potential of obviating tissue diagnosis, diffusion-weighted imaging of the prostate runs the gamut from the mundane to the sublime.

---

1194

14:04



Year	Volume	Page
2018	10	1194
2019	11	1194

Gaussian and non-Gaussian diffusion models for Differential Diagnosis of Prostate Cancer with in bore Transrectal MR-Guided Biopsy as a Pathological Reference

Chunmei Li<sup>1</sup>, Min Chen<sup>1</sup>, and Bing Wu<sup>2</sup>

*<sup>1</sup>Beijing Hospital, Beijing, People's Republic of China, <sup>2</sup>GE Healthcare, China*

This study is to compare the utility of various metrics derived from different models based DWI and DKI in the differential diagnosis of prostate cancer. ADC, ADCslow, DDC, and MD values were significantly lower while MK value was significantly higher in prostate cancer lesions than those of prostatitis and BPH. Parameters derived from both Gaussian and non-Gaussian models could characterize prostate cancer. Diagnosis performance benefit was observed for DKI model as compared to MEM.

1195

14:16

### In-vivo Reproducibility of Quantitative Diffusion MRI in the Prostate using Reduced Field-of-View and Multi-shot Acquisitions

Prostate Diffusion MRI Parameters									
Parameter	Sequence	FOV	Shot	Model	Mean	SD	CV	ICC	P-value
ADC	ssEPI	Full	1	1	1.15	0.15	0.13	0.98	<0.001
ADC	rFOV	Reduced	1	1	1.15	0.15	0.13	0.98	<0.001
ADC	msEPI	Reduced	4	1	1.15	0.15	0.13	0.98	<0.001
ADC	ssEPI	Full	1	2	1.15	0.15	0.13	0.98	<0.001
ADC	rFOV	Reduced	1	2	1.15	0.15	0.13	0.98	<0.001
ADC	msEPI	Reduced	4	2	1.15	0.15	0.13	0.98	<0.001

Yuxin Zhang<sup>1,2</sup>, James H. Holmes<sup>2</sup>, Arnaud Guidon<sup>3</sup>, Shane A Wells<sup>2</sup>, and Diego Hernando<sup>1,2</sup>

<sup>1</sup>Medical Physics, University of Wisconsin, Madison, Madison, WI, United States, <sup>2</sup>Radiology, University of Wisconsin, Madison, Madison, WI, United States, <sup>3</sup>MR Applications & Workflow, GE Healthcare, Boston, MA, United States

Novel diffusion weighted MRI pulse sequences based on reduced FOV (rFOV) and multi-shot echo-planar imaging (msEPI), respectively, have been proposed to reduce distortions present in standard single-shot EPI. In this study, the quantitative reproducibility of prostate diffusion measurements with rFOV and msEPI is investigated with healthy volunteers. Diffusion parameters were estimated from different sequences (ssEPI, rFOV, msEPI), b-value groups, and diffusion models (mono-exponential, stretched exponential and kurtosis). Measurements from rFOV and msEPI are in good agreement with the standard ssEPI, demonstrating reproducibility across pulse sequences.

14:28

### Renal DWI

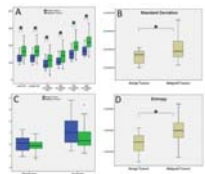
Harriet Thöny<sup>1</sup>

<sup>1</sup>University of Bern

1196

14:48

### Subtype Differentiation of Small (< 4 cm) Solid Renal Mass Using Histogram Analysis of Reduced Field-of-View Diffusion Weighted MRI at 3-T



Anqin Li<sup>1</sup>, Zhen Li<sup>1</sup>, Haojie Li<sup>1</sup>, and Daoyu Hu<sup>1</sup>

<sup>1</sup>Department of Radiology, Tongji Hospital, Tongji Medical College, Huazhong University of Science and Technology, Wuhan, People's Republic of China

To evaluate the utility of volumetric histogram analysis originated from reduced field-of-view (r-FOV) diffusion-weighted (DW) imaging for small (< 4cm) solid renal mass subtypes at 3-T MR. Differences of ADC histogram parameters among different subtypes of renal tumor were compared. Benign tumors had significantly lower mean ADC, median ADC, 10<sup>th</sup>, 25<sup>th</sup>, 75<sup>th</sup>, 90<sup>th</sup> percentiles ADC, SD and entropy values compared to malignant tumors. ADC histogram analysis of the entire lesion was complementary to the mean ADC measure and may have a certain value to help differentiate the majority of subtypes of small solid renal tumor.

---

---

## Study Groups

### PET-MRI Study Group

Room 323ABC      Thursday 15:30 - 17:30 *(no CME credit)*

---

## Study Groups

### Reproducible Research Study Group

Room 317AB      Thursday 15:30 - 17:30 *(no CME credit)*

---

## Educational Course

### Imaging in Joint Health & Disease

*Organizers:* Jenny T. Bencardino, M.D., Eric Y. Chang, M.D., Christine Chung, M.D. & Philip Robinson, M.D.

Room 314      Thursday 15:30 - 17:30 *Moderators:* Emad Almusa & Karen Chen

---

15:30      [Rotator Cuff Arthropathy](#)  
James Griffith

---

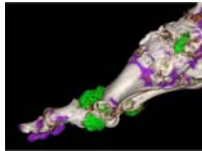
16:00      [Osteoarthritis](#)  
Sharmila Majumdar<sup>1</sup>

*<sup>1</sup>Radiology and Biomedical Imaging, University of California San Francisco, San Francisco, CA, United States*

This session will cover quantitative MR imaging methods applied in the assessment of knee and hip osteoarthritis. It will explore the connection between making metrics, gait, skeletal biomechanics and diseases severity and progression.

---

16:30



### Crystal Deposition Disease

Marcelo Abreu<sup>1</sup>

*<sup>1</sup>Hospital Mae de Deus*

Several crystals (urate, CPPD and hydroxyapatite) can deposit in tissues of the musculoskeletal system in asymptomatic individuals. In some cases, those deposits can be associated with diseases such as Gout, Pseudogout and Calcific Tendinitis. MRI examination can be very useful in the diagnosis of such entities, differential diagnosis and help treatment decisions.

---

17:00

### Sacroiliac Joint Disorders

Mary Jesse

---

17:30

### Adjournment & Meet the Teachers

---

## Educational Course

# Wait Wait... Don't Tell Me!: MRI Artifacts!

*Organizers:* Adrienne E. Campbell-Washburn, Ph.D., Michael S. Hansen, Ph.D., Eric G. Stinson, Ph.D., & Dominik Von Elverfeldt, Dr.Rer.Nat.

Room 316A

Thursday 15:30 - 17:30

*Moderators:* Adrienne Campbell-Washburn & Eric Stinson

---

15:30

### MRI Artifact Game Show

---

Oral

## Frontiers in Reconstruction

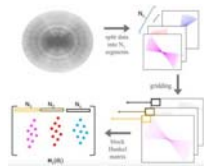
Room 310

Thursday 15:30 - 17:30 Moderators: Dong Liang & Claudia Prieto

---

1197

15:30



### Trajectory Correction of Radial Data Using MUSSELS

Merry Mani<sup>1</sup>, Sunrita Poddar<sup>2</sup>, Vincent Magnotta<sup>1</sup>, and Mathews Jacob<sup>2</sup>

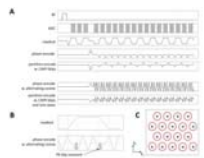
<sup>1</sup>Department of Radiology, University of Iowa, Iowa City, IA, United States, <sup>2</sup>Department of Electrical and Computer Engineering, University of Iowa, Iowa City, IA, United States

Radial acquisitions are time efficient and flexible and enable several MR imaging applications. However, the sensitivity of radial acquisitions to trajectory deviations can result in severe artifacts in the images. We propose a trajectory correction method that can reconstruct the images for the ideal trajectory without the need for trajectory estimation or calibration.

---

1198

15:42



### Echo-planar imaging with wave-CAIPI acquisition and reconstruction

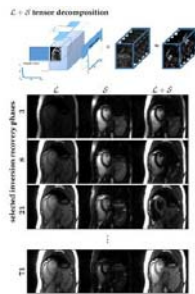
Benedikt A Poser<sup>1</sup>, Berkin Bilgic<sup>2</sup>, Borjan A. Gagoski<sup>3,4</sup>, Kâmil Uludağ<sup>1</sup>, V Andrew Stenger<sup>5</sup>, Lawrence L Wald<sup>2,6,7</sup>, and Kawin Setsompop<sup>2,6</sup>

<sup>1</sup>Faculty of Psychology and Neuroscience, Maastricht University, Maastricht, Netherlands, <sup>2</sup>Athinoula A. Martinos Center for Biomedical Imaging, Massachusetts General Hospital, Charlestown, MA, United States, <sup>3</sup>Department of Radiology, Harvard Medical School, Boston, MA, United States, <sup>4</sup>Fetal-Neonatal Neuroimaging & Developmental Science Center, Boston Children's Hospital, Boston, MA, United States, <sup>5</sup>Department of Medicine, John A. Burns School of Medicine, University of Hawaii, Honolulu, HI, United States, <sup>6</sup>Harvard Medical School, Boston, MA, United States, <sup>7</sup>Harvard-MIT Division of Health Sciences and Technology, Massachusetts Institute of Technology, Cambridge, MA, United States

wave-CAIPI allows for high undersampling factors and hence acquisition speed-up in anatomical images sequences including 3D GRE, 2D SMS-TSE and MP-RAGE (3D TFL). The coil array's full 3D sensitivity encoding is exploited, resulting in negligible g-factor penalties even in highly accelerated scans. Echo-planar imaging (EPI) sequences, both 2D and 3D EPI with Cartesian blipped-CAIPI have recently brought tremendous speed-up to BOLD and diffusion imaging in the neurosciences. We here explore the potential of going beyond blipped-CAIPI EPI by incorporating sinusoidal z- and y- gradient wave perturbations into the EPI readout. Initial results are shown for 3D wave-CAIPI EPI at 7T.

1199

15:54



Low-rank plus sparse tensor reconstruction for high-dimensional cardiac MRI

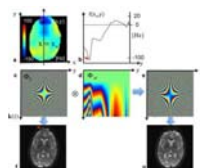
Rebecca Ramb<sup>1</sup>, Michael Zenge<sup>2</sup>, Li Feng<sup>1</sup>, Matthew Muckley<sup>1</sup>, Christoph Forman<sup>3</sup>, Leon Axel<sup>1</sup>, Dan Sodickson<sup>1</sup>, and Ricardo Otazo<sup>1</sup>

<sup>1</sup>Department of Radiology, New York University School of Medicine, New York, NY, United States, <sup>2</sup>Siemens Medical Solutions USA, Inc., Malvern, PA, United States, <sup>3</sup>Siemens Healthcare GmbH, Erlangen, Germany

The recently proposed general low rank tensor framework enabled a paradigm change, where data acquisition and image reconstruction are represented in a higher-dimensional space. The overall data space is sampled only as different states randomly coincide, which leads to data gaps. These gaps can introduce challenges in spatiotemporal fidelity for only low-rank- or only sparsity-based reconstructions. Here, a  $\mathcal{L} + \mathcal{S}$  tensor decomposition is investigated, which offers a more robust solution as the sparse component captures updates on top of the overall dynamics represented in the low-rank component. A free-breathing, T1-sensitive cardiac MRI with real-time Cartesian data acquisition over multiple cardiac and inversion recovery phases is employed to investigate potentials for comprehensive cardiac MRI, including for instance late gadolinium scar cine imaging.

1200

16:06



Extended Hybrid-SENSE: off-resonance and eddy corrected joint blip up/down reconstruction with reduced g-factor penalty

Benjamin Zahneisen<sup>1</sup>, Murat Aksoy<sup>1</sup>, Julian Maclaren<sup>1</sup>, Christian Wuerstin<sup>1</sup>, and Roland Bammer<sup>1</sup>

<sup>1</sup>Stanford University, Stanford, CA, United States

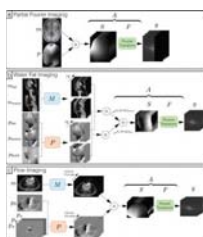


Geometric distortions caused by off-resonant spins are a major issue in EPI based functional and diffusion imaging. We present a novel approach to the problem of geometric distortions. An extension of the model-based, algebraic hybrid-SENSE reconstruction method in combination with a known fieldmap, calculated from blip up/down scans, allows for correction of off-resonance effects during the reconstruction. This enables a joint blip up/down reconstruction that significantly reduces g-factor penalty if the blip-down trajectory is chosen to fill in missing k-space samples from the blip-up scan. The resulting high SNR images are automatically eddy-current corrected and geometric distortions are minimized.

---

1201

16:18



General Phase Regularized Reconstruction with Phase Cycling  
Frank Ong<sup>1</sup>, Joseph Cheng<sup>2</sup>, and Michael Lustig<sup>1</sup>

<sup>1</sup>*Department of Electrical Engineering and Computer Sciences, University of California, Berkeley, Berkeley, CA, United States,*

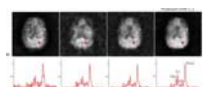
<sup>2</sup>*Department of Radiology, Stanford University, Stanford, CA*

We present a general phase regularized image reconstruction method that is robust to phase wraps in initial solutions, with application to partial Fourier imaging, chemical shift imaging and flow imaging. The problem of constraining phase structures in reconstruction was studied under a regularized inverse problem framework. Since phase regularized reconstruction is inherently non-convex and sensitive to phase wraps in the initial solution, a reconstruction technique, named phase cycling, was proposed. The proposed method was applied to in vivo datasets and compared with state of the art reconstruction methods. The proposed phase cycling reconstruction provides an alternative way to perform phase regularized reconstruction, without the need of performing phase unwrapping. It is robust to the choice of initial solutions and flexible to incorporate into different phase imaging applications.

---

1202

16:30



Accelerated J-Resolved MRSI Using Joint Subspace and Sparsity Constraints

Fan Lam<sup>1</sup>, Bowen Cheng<sup>2</sup>, and Zhi-Pei Liang<sup>1,2</sup>

<sup>1</sup>*Beckman Institute for Advanced Science and Technology, University of Illinois at Urbana-Champaign, Urbana, IL, United States,*

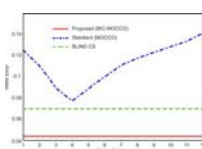
<sup>2</sup>*Department of Electrical and Computer Engineering, University of Illinois at Urbana-Champaign, Urbana, IL, United States*

A new reconstruction method for accelerated J-resolved MRSI acquisitions is proposed. The proposed method performs a joint reconstruction from the data acquired with multiple echo times (TEs), using a formulation that integrates a subspace representation of the entire J-resolved spatio-spectral function and a joint sparsity constraint exploiting the correlation across different TEs. Both simulation and in vivo experiments have been performed to evaluate the proposed method, demonstrating its superior performance over methods using joint sparsity or subspace constraint alone.

---

1203

16:42



Accurate, Rank-Adaptive Reconstruction of Undersampled Dynamic MRI Data Using Bayesian Information Criterion

Julia Velikina<sup>1</sup> and Alexey Samsonov<sup>2</sup>

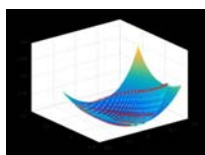
<sup>1</sup>Medical Physics, University of Wisconsin - Madison, Madison, WI, United States, <sup>2</sup>Radiology, University of Wisconsin - Madison, Madison, WI, United States

Dynamic MRI must contend with imaging time limits imposed by physiological and physical constraints. Methods promoting low-rank solutions have become increasingly popular for dynamic MRI acceleration due to their ability to reconstruct from limited data. In this work we present a novel model-based reconstruction approach exploiting statistical machinery to spatially adapt the model to underlying signal. It overcomes deficiencies of low-rank techniques to preserve complex temporal dynamics of physiological processes.

---

1204

16:54



Low Rank Approximation of High Resolution MRF through Dictionary Fitting

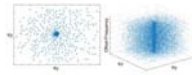
Mingrui Yang<sup>1</sup>, Yun Jiang<sup>2</sup>, Mark Griswold<sup>1</sup>, and Debra McGivney<sup>1</sup>

<sup>1</sup>Department of Radiology, Case Western Reserve University, Cleveland, OH, United States, <sup>2</sup>Department of Biomedical Engineering, Case Western Reserve University, Cleveland, OH, United States

One of the challenges MRF faces is the amount of data needed to be stored, loaded, and processed, especially when a high resolution dictionary is needed or large multi-dimensional analyses need to be taken into account. A low rank approximation to the high resolution MRF dictionary using a coarse dictionary is an effective remedy to this problem. Here we present one of many possible ways to implement low rank approximation to an arbitrary fine MRF dictionary by a coarse dictionary equipped with polynomial fitting, so as to avoid the need of pre-calculating, storing, and processing the large, finely-resolved MRF dictionary.

1205

17:06



### Accelerated z-Spectrum Imaging

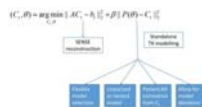
Melany Mclean<sup>1</sup>, Matthew Ethan MacDonald<sup>2</sup>, R. Marc Lebel<sup>1,2,3</sup>, Mathieu Boudreau<sup>4</sup>, and Bruce Pike<sup>2</sup>

<sup>1</sup>Biomedical Engineering, University of Calgary, Calgary, AB, Canada, <sup>2</sup>Radiology, University of Calgary, Calgary, AB, Canada, <sup>3</sup>GE Healthcare, Calgary, AB, Canada, <sup>4</sup>Montreal Neurological Institute, McGill University, Montreal, QC, Canada

Long acquisition times preclude many potential applications of z-spectrum based imaging techniques, and have hindered their widespread use. Using SparseSENSE, a combined parallel imaging and compressed sensing acceleration technique, we present a method to reduce the acquisition time of z-spectrum images by a factor of 16. Z-spectrum images have been retrospectively undersampled to simulate 2-20× acceleration factors. Sparsifying reconstruction algorithms enable high quality image reconstructions for ambitious acceleration factors and are shown to maintain z-spectrum accuracy.

1206

17:18



### Reconstruction of DCE tracer kinetic parameters from under-sampled data with a flexible model consistency constraint

Yi Guo<sup>1</sup>, Sajan Goud Lingala<sup>1</sup>, and Krishna S Nayak<sup>1</sup>

<sup>1</sup>Electrical Engineering, University of Southern California, Los Angeles, CA, United States

Recently, it has been shown that DCE-MRI tracker-kinetic (TK) parameter maps can be directly estimated from under-sampled (k,t)-space data. Two major limitations of this approach are that 1) the gradient of a complicated cost function with respect to each TK parameter needs to be computed, and 2) it does not allow for any TK model deviation in the data. In this work, we present an alternative formulation where instead of forcing every voxel to follow the selected TK model, the model consistency is used as a constraint with a weighting penalty. This method is uniquely compatible with the use of multiple or nested TK models, and we show that it provides more accurate TK parameter restoration.

---

Oral

## Susceptibility & QSM : Applications & Techniques

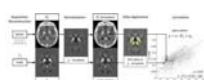
Room 311

Thursday 15:30 - 17:30 *Moderators:* Karin Shmueli & Hongfu Sun

---

1207

15:30



Assessing the cellular distribution of iron in deep gray matter based on  $R_2^*$  and Quantitative Susceptibility Mapping (QSM) - Application to healthy controls and patients with Multiple Sclerosis (MS)

Yanis Taege<sup>1</sup>, Robert Zivadinov<sup>1,2</sup>, Jannis Hanspach<sup>1</sup>, Jesper Hagemeyer<sup>1</sup>, Michael G Dwyer<sup>1</sup>, Balint P Sule<sup>1</sup>, Nicola Bertolino<sup>1</sup>, Dhaval Shah<sup>1</sup>, Dejan Jakimovski<sup>1</sup>, Niels P Bergsland<sup>1,3</sup>, Bianca Weinstock-Guttman<sup>4</sup>, and Ferdinand Schweser<sup>1,2</sup>

<sup>1</sup>Buffalo Neuroimaging Analysis Center, Department of Neurology, Jacobs School of Medicine and Biomedical Sciences, University at Buffalo, The State University of New York, Buffalo, NY, United States,

<sup>2</sup>MRI Clinical and Translational Research Center, Jacobs School of Medicine and Biomedical Sciences, University at Buffalo, The State University of New York, Buffalo, NY, United States, <sup>3</sup>MR Research Laboratory, IRCCS, Don Gnocchi Foundation ONLUS, Milan, Italy,

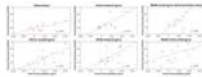
<sup>4</sup>BairdMS Center, Department of Neurology, Jacobs School of Medicine and Biomedical Sciences, The State University of New York at Buffalo, Buffalo, NY, United States

This work introduces a clinically applicable technique to assess the cellular distribution of iron based on  $R_2^*$  and Quantitative Susceptibility Mapping (QSM). The method was applied to 68 MS patients and 29 controls, showing significant differences in the cellular iron distribution with age and disability.

1208



15:42



### Correlations of beta-Amyloid and brain iron load (QSM): preliminary results of simultaneous assessment in a large sample

Jiri MG van Bergen<sup>1</sup>, Xu Li<sup>2</sup>, Frances-Catherine Quevenco<sup>1</sup>, Sandra Leh<sup>1</sup>, Anton F Gietl<sup>1</sup>, Valerie Treyer<sup>1,3</sup>, Rafeal Meyer<sup>1</sup>, Alfred Buck<sup>3</sup>, Roger M Nitsch<sup>1</sup>, Peter CM van Zijl<sup>2</sup>, Christoph Hock<sup>1</sup>, and Paul G Unschuld<sup>1</sup>

<sup>1</sup>Institute for Regenerative Medicine, University of Zurich, Zurich, Switzerland, <sup>2</sup>F.M. Kirby center for Functional Brain Imaging, Kennedy Krieger Institute and Johns Hopkins School of Medicine, MD, United States, <sup>3</sup>Department of Nuclear Medicine, University of Zurich, Switzerland

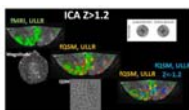
To extend findings on the use of QSM in Alzheimer's Disease and possible direct interactions with Amyloid- $\beta$ , this study is investigating a growing sample of elderly subjects using simultaneous assessment of Amyloid-PET for A $\beta$ -load and QSM for estimation of iron load (indicated by susceptibility) using a combined PET-MRI instrument.

Our preliminary data suggests a significant correlation between susceptibility and A $\beta$  in subjects with high brain A $\beta$  load or clinically diagnosed Mild Cognitive Impairment, in several cortical and sub-cortical regions. The sample is expected to grow considerably in the upcoming months.

1209



15:54



### Discrimination of volumes with positive and negative functional QSM activation within fMRI-positive volumes in high-resolution, high-field task-based and resting-state data

Pinar Senay Özbay<sup>1,2</sup>, Lars Kasper<sup>2</sup>, Klaas Paul Pruessmann<sup>2</sup>, and Daniel Nanz<sup>1</sup>

<sup>1</sup>Department of Radiology, University Hospital Zürich, Zurich, Switzerland, <sup>2</sup>Institute of Biomedical Engineering, ETH Zürich, Zurich, Switzerland

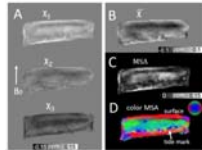
In this work, we wanted to explore the bidirectional activation in functional Quantitative Susceptibility Mapping (fQSM) via Independent Component Analysis (ICA) in various cases, hence we included i) visual paradigm, ii) motor task and iii) resting state experiments with high-resolution data acquired at 7-Tesla. We investigated the behavior in terms of activation patterns and temporal evaluations of functional-PHASE, fQSM and traditional fMRI. Furthermore, we compared regions of activation with phase-contrast-angiography data. In all scenarios, we have found out that the total (positive + negative) activated area in fQSM was well matching with positive activation in fMRI.

1210

16:06

### Magnetic Susceptibility Anisotropy of Collagen Fibrils in the Articular Cartilage

Hongjiang Wei<sup>1</sup>, Kyle Decker<sup>2</sup>, Yuyao Zhang<sup>1</sup>, and Chunlei Liu<sup>1</sup>



<sup>1</sup>Department of Electrical Engineering and Computer Sciences, University of California, Berkeley, Berkeley, CA, United States, <sup>2</sup>Center for In Vivo Microscopy, Duke University, Durham, NC, United States

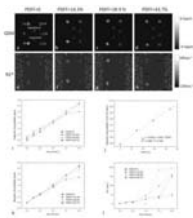
Articular cartilage with depth dependent ultra-layer structure is constructed by collagen fibrils, which is shown by histology having three distinct layers: the fibrils are mostly parallel to the surface, randomly distributed and mostly oriented perpendicular to the surface in superficial zone, middle zone and deep zone, respectively. Quantitative susceptibility mapping is particularly sensitive to molecular content and cellular arrangement, thus is suitable to probe such highly organized microstructure and evaluate its magnetic susceptibility. Our study shows a clear  $B_0$ -orientation-dependent susceptibility contrast in the articular cartilage and that the collagen fibril orientations can be well measured by susceptibility tensor imaging.

1211

16:18

### Quantitative Susceptibility Mapping (QSM) Overcomes $R2^*$ Confounding Factors for Measuring Liver Iron

Jianqi Li<sup>1</sup>, Qi Song<sup>2</sup>, Tian Liu<sup>3</sup>, Zhuwei Zhang<sup>4</sup>, Martin R Prince<sup>3</sup>, Kelly Gillen<sup>3</sup>, Xu Yan<sup>5</sup>, Shu Cheng<sup>6</sup>, Ting Hua<sup>4</sup>, Xiance Zhao<sup>1</sup>, Miao Zhang<sup>1</sup>, Yu Zhao<sup>1</sup>, Gaiying Li<sup>1</sup>, Guangyu Tang<sup>4</sup>, Guang Yang<sup>1</sup>, Gary M Brittenham<sup>7</sup>, and Yi Wang<sup>1,3,8</sup>



<sup>1</sup>Shanghai Key Laboratory of Magnetic Resonance and Department of Physics, East China Normal University, Shanghai, People's Republic of China, <sup>2</sup>Department of Radiology, Ruijin Hospital, Shanghai Jiao Tong University School of Medicine, Shanghai, People's Republic of China, <sup>3</sup>Department of Radiology, Weill Medical College of Cornell University, New York, New York, United States, <sup>4</sup>Department of Radiology, Shanghai Tenth People's Hospital Affiliated to Tongji University, School of Medicine, Shanghai, People's Republic of China, <sup>5</sup>MR Collaboration NE Asia, Siemens Healthcare, Shanghai, People's Republic of China, <sup>6</sup>Department of Hematology, Ruijin Hospital, Shanghai Jiao Tong University School of Medicine, Shanghai, People's Republic of China, <sup>7</sup>Department of Pediatrics, Columbia University, New York, New York, United States, <sup>8</sup>Department of Biomedical Engineering, Cornell University, Ithaca, New York, United States

A major challenge in the R2 and R2\* methods for mapping liver iron content is that they can be confounded by fat, fibrosis and other changes in cellularity that are known to contribute to R2 and R2\*. In this paper, the fat contribution to liver susceptibility was estimated and removed from the measured liver susceptibility with validation on a gadolinium-fat-water phantom. In patients, fat-corrected QSM was found to be insensitive to liver diseases including fat and tumor, which had extensive effects on R2\*. Therefore, QSM can overcome confounding factors in R2\* for mapping liver iron content.

1212

16:30

Method	Phase	R2	R2*	Mean	Standard deviation
QSM	0°	140.00	100.00	120.00	10.00
QSM	45°	140.00	100.00	120.00	10.00
QSM	90°	140.00	100.00	120.00	10.00
QSM	135°	140.00	100.00	120.00	10.00
QSM	180°	140.00	100.00	120.00	10.00
QSM	225°	140.00	100.00	120.00	10.00
QSM	270°	140.00	100.00	120.00	10.00
QSM	315°	140.00	100.00	120.00	10.00

### The effect of white matter fiber orientation in Quantitative Susceptibility Mapping at 7T

Marta Lancione<sup>1</sup>, Mauro Costagli<sup>2</sup>, Graziella Donatelli<sup>1</sup>, Mirco Cosottini<sup>1</sup>, and Michela Tosetti<sup>2,3</sup>

<sup>1</sup>University of Pisa, Pisa, Italy, <sup>2</sup>Imago7 Research Center, Pisa, Italy, <sup>3</sup>IRCCS Stella Maris, Pisa, Italy

The tensorial nature of magnetic susceptibility affects frequency-shift images and quantitative maps (QSM), whose reliability should be questioned. Three healthy volunteers underwent 7T MRI exams including diffusion tensor imaging (DTI) and three QSM acquisitions, each with different orientation of the head. In order to assess the effect of susceptibility anisotropy, we sorted brain voxels depending on their fractional anisotropy (FA) and, by plotting their QSM values against the angle between the static field and the eigenvector corresponding to the largest eigenvalue in DTI, we observed an empirical threshold of FA that reflects the reliability of susceptibility measures.



---

1213

16:42



Signal compartments modelled from 7T multi-echo GE data showed variation across the corpus callosum

Kiran Thapaliya<sup>1</sup>, Steffen Bollmann<sup>1</sup>, Viktor Vegh<sup>1</sup>, and Markus Barth<sup>1</sup>

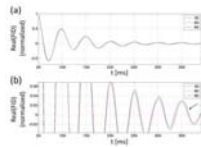
<sup>1</sup>University of Queensland, St. Lucia, Australia

Quantitative assessment of myelin water fraction using a multi-compartment model can be useful to improve our understanding of white matter diseases. Our work aims to explore tissue microstructure information contained in voxel signals by analysing voxel compartment volume fraction, frequency shift and  $T_2^*$  from data acquired at 7T. We performed our analysis across from the rostrum to the splenium of corpus callosum. Parameterisation of tissue characteristics can potentially delineate structural and chemical changes in tissue with biologically meaningful information. This in turn provides a framework for new imaging biomarker development in neurodegenerative diseases and disorders, such as multiple sclerosis

---

1214

16:54



Nuclear susceptibility shift

Seung-Kyun Lee<sup>1,2</sup>, Jinil Park<sup>1,2</sup>, Jeongtaek Lee<sup>1,2</sup>, and Jang-Yeon Park<sup>1,2</sup>

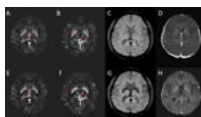
<sup>1</sup>Biomedical Engineering, Sungkyunkwan University, Suwon, Korea, Republic of, <sup>2</sup>Center for Neuroscience Imaging Research (CNIR), Institute for Basic Science, Suwon, Korea, Republic of

We have observed in a clinical scanner that the center frequency of water MRI changed with the <sup>1</sup>H spin flip angle. The amount of the change could be explained by the tip-angle dependent nuclear spin paramagnetic susceptibility, much the same way as the usual, tissue electronic para- and dia-magnetic susceptibility induces  $B_0$  shift in MRI. The observed shift, corresponding to nuclear susceptibility of +0.004 ppm in water, may affect the ultimate accuracy of MR-based tissue magnetic susceptibility measurements if not properly accounted for.

---

1215

17:06



An interleaved sequence for simultaneous MRA, SWI and QSM

Yongsheng Chen<sup>1,2</sup>, Saifeng Liu<sup>3</sup>, Yan kang<sup>1</sup>, and E. Mark Haacke<sup>1,2,3,4</sup>

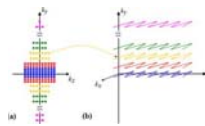
<sup>1</sup>Sino-Dutch Biomedical and Information Engineering School, Northeastern University, Shenyang, People's Republic of China, <sup>2</sup>Department of Radiology, Wayne State University, Detroit, MI, United States, <sup>3</sup>The MRI Institute for Biomedical Research, Waterloo, ON, Canada, <sup>4</sup>The MRI Institute for Biomedical Research, Detroit, United States

MRA, SWI and QSM are important for identifying thrombus, hemorrhage, CMBs and assessing oxygen saturation and iron deposition in diseases such as stroke and traumatic brain injury (TBI). Practically, it is important to acquire these data with sufficient resolution, good SNR, co-registered and rapidly. Therefore, we developed a 3D interleaved GRE sequence that produces MRA, SWI, R2\* and QSM for imaging arteries, veins and the basal ganglia in 4 minutes at 3T for the entire brain with a resolution of 0.67x1.33x2.0mm<sup>3</sup>. Five healthy volunteers' data were acquired approved by the local IRB to demonstrate the utility of this approach.

---

1216

17:18



### Quantitative Susceptibility Mapping from Unsuppressed Water Signals in 1H-MRSI Data

Xi Peng<sup>1,2</sup>, Fan Lam<sup>2</sup>, Bryan Clifford<sup>2,3</sup>, Yudu Li<sup>2,3</sup>, and Zhi-Pei Liang<sup>2</sup>

<sup>1</sup>Shenzhen Institutes of Advanced Technology, Shenzhen, People's Republic of China, <sup>2</sup>Beckman Institute for Advanced Science and Technology, University of Illinois Urbana-Champaign, Urbana, IL, United States, <sup>3</sup>Department of Electrical and Computer Engineering, University of Illinois Urbana-Champaign, Urbana, IL, United States

This work presents a new method to extract QSM from the unsuppressed water signals in 1H-MRSI data and enables simultaneous MRSI and QSM in a single acquisition. The proposed method builds on the recently proposed subspace imaging method called SPICE (SPectroscopicImaging by exploiting spatiospectral CorrElation), which allows MRSI acquisition without water suppression, thus encoding susceptibility induced phase variations in the water spectroscopic signals. Parallel imaging, subspace-based modeling and constrained reconstruction are integrated to generate QSM and high-resolution MRSI reconstruction from such data. In-vivo experiment results demonstrate the capability of proposed method in producing susceptibility map along with metabolite spatiospectral distributions from a single 6-minute scan.

---

Oral

# Highly Parallel RF Systems

Room 312

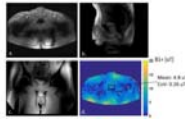
Thursday 15:30 - 17:30 *Moderators: Mary McDougall & Bei Zhang*

---

1217



15:30



## Towards massively parallel multi-transmit for body imaging at 7 T

Bart R. Steensma<sup>1</sup>, J. Nuno Teixeira<sup>1</sup>, Ingmar Voogt<sup>1</sup>, Lijten R. Peter<sup>1</sup>, Dennis W.J. Klomp<sup>1</sup>, van den Berg A.T. Nico<sup>2</sup>, and Alexander J.E. Raaijmakers<sup>1,3</sup>

<sup>1</sup>*Division Imaging, Department of Radiology, University Medical Center Utrecht, Utrecht, Netherlands,* <sup>2</sup>*Division Imaging, Department of Radiotherapy, University Medical Center Utrecht, Utrecht, Netherlands,* <sup>3</sup>*Biomedical Image Analysis, Eindhoven University of Technology, Eindhoven, Netherlands*

A simulation study was done to assess optimal transmit setups for massively parallel (up to 32 channels) transmit body imaging at 7 tesla. Moving from 8 to 24 and 32 dipole setups increases transmit efficiency on a pelvis-shaped phantom. Our current multitransmit system was adapted to obtain 24 semi-phase controlled channels. A 24 channel transmit setup consisting of small dipoles was constructed and tested on a male volunteer.

1218

15:42



## An integrated 32-channel transmit and 64-channel receive 7 tesla MRI system

Edward Auerbach<sup>1</sup>, Lance DelaBarre<sup>1</sup>, Pierre-Francois Van de Moortele<sup>1</sup>, John Strupp<sup>1</sup>, Rene Gumbrecht<sup>2</sup>, Andreas Potthast<sup>2</sup>, Georg Pirkl<sup>2</sup>, Steen Moeller<sup>1</sup>, Brian Hanna<sup>1</sup>, Andrea Grant<sup>1</sup>, Gregor Adriany<sup>1</sup>, and Kâmil Uğurbil<sup>1</sup>

<sup>1</sup>*Center for Magnetic Resonance Research, University of Minnesota, Minneapolis, MN, United States,* <sup>2</sup>*Siemens Healthcare, Erlangen, Germany*

At 7T, commercial MRI systems are currently available with a maximum of 8-16 transmit channels and 32 receive channels. To explore the potential benefits of increasing these numbers, which have been predicted by prior experimental and simulation work, we have developed and installed 32-channel RF transmitter and 64-channel receiver upgrades for a standard 7T commercial MRI system. These additions have been fully integrated into the system in a way that they can be reliably employed for routine studies without requiring significant workflow modifications or special user training.

---



### A 32-channel transmit system add-on for 7 Tesla body imaging

Stephan Orzada<sup>1</sup>, Andreas K. Bitz<sup>2</sup>, Marcel Gratz<sup>1,3</sup>, Sören Johst<sup>1</sup>, Samaneh Shoostary<sup>4</sup>, Maximilian N. Voelker<sup>1</sup>, Stefan H. G. Rietsch<sup>1,3</sup>, Martina Flöser<sup>2</sup>, Ashraf Abuelhaija<sup>4</sup>, Mark Oehmigen<sup>3</sup>, Sascha Brunheim<sup>1,3</sup>, Thomas M. Fiedler<sup>2</sup>, Oliver Kraff<sup>1</sup>, Harald H. Quick<sup>1,3</sup>, Klaus Solbach<sup>4</sup>, and Mark E. Ladd<sup>1,2</sup>

<sup>1</sup>Erwin L. Hahn Institute for MRI, University Duisburg-Essen, Essen, Germany, <sup>2</sup>Medical Physics in Radiology, German Cancer Research Center (DKFZ), Heidelberg, Germany, <sup>3</sup>High-Field and Hybrid MR Imaging, University Hospital Essen, Essen, Germany, <sup>4</sup>RF & Microwave Technology, University Duisburg-Essen, Duisburg, Germany

At ultra-high field, severe transmit field inhomogeneities affect the quality of imaging. To cope with this, multi-channel solutions are necessary. In this work we present an add-on 32-channel transmit system including an integrated transmit/receive body coil for large field of view imaging. First phantom and in-vivo results are shown. A 50 cm field of view can be achieved and the system is capable of 100 kHz sampling, allowing parallel spatially selective transmit pulses for in-vivo imaging.



### A 64 Channel 3T Array Coil for Highly Accelerated Fetal Imaging at 22 Weeks of Pregnancy

Mark Spatz<sup>1,2</sup>, Pablo García-Polo<sup>1,3</sup>, Boris Keil<sup>1</sup>, Christopher Ha<sup>4</sup>, and Lawrence L. Wald<sup>1,5</sup>

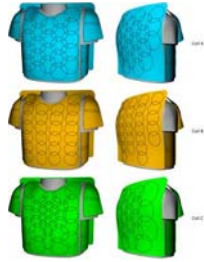
<sup>1</sup>A. A. Martinos Center for Biomedical Imaging, Massachusetts General Hospital, Charlestown, MA, United States, <sup>2</sup>Department of Electrical Engineering and Computer Science, Massachusetts Institute of Technology, Cambridge, MA, United States, <sup>3</sup>M+Visión Advanced Fellowship, Hospital Universitario de Fuenlabrada, Madrid, Spain, <sup>4</sup>Boston Children's Hospital, Boston, MA, United States, <sup>5</sup>Harvard Medical School, Boston, MA, United States

MRI is an attractive tool for fetal imaging due to its unique ability to provide detailed anatomical and physiological data in an inherently safe manner. In practice, fetal MRI is limited by fetal motion, inherently poor SNR in the maternal abdomen, and widely varying body shapes. A 64 channel receive array designed to conform to a range of body shapes at 22 weeks of pregnancy was built and tested. Compared to standard product arrays, the coil provides 5% better SNR in the fetal brain region of an anthropomorphic phantom and allows increasing SENSE acceleration factor from R=4 to R=5.

1221

16:18

### Receive Coil Array Considerations for Simultaneous Multislice Imaging in Cardiac MRI



Robin Etzel<sup>1</sup>, Laleh Golestanirad<sup>2</sup>, Choukri Mekkaoui<sup>2</sup>, Timothy G Reese<sup>2</sup>, David E Sosnovik<sup>2</sup>, Andreas H Mahnken<sup>3</sup>, and Boris Keil<sup>1</sup>

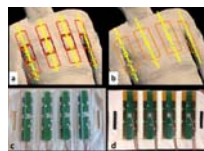
<sup>1</sup>Institute of Medical Physics and Radiation Protection, Department of Life Science Engineering, Mittelhessen University of Applied Sciences (THM), Giessen, Germany, <sup>2</sup>A.A. Martinos Center for Biomedical Imaging, Department of Radiology, Massachusetts General Hospital, Harvard Medical School, Boston, MA, United States, <sup>3</sup>Philipps University of Marburg, Department of Diagnostic and Interventional Radiology, Marburg, Germany

Receiver coil array simulation within realistic constrains are helpful for decision-making in coil design, especially when the array comprises many surface coil elements. Three coil array arrangements utilizing 64 loop elements were systematically evaluated regarding their encoding capabilities for accelerated simultaneous multi-slice cardiac acquisitions. Loop arrays consisting of small loop element near target region, but large once beyond the heart, seems to be best-suited for highly accelerated cardiac MRI.

1222

16:30

### A 32-channel loop-dipole transceiver array for body imaging at 7.0 Tesla



M. Arcan Erturk<sup>1</sup>, Xiaoping Wu<sup>1</sup>, Gregor Adriany<sup>1</sup>, Pierre-Francois Van de Moortele<sup>1</sup>, Edward J Auerbach<sup>1</sup>, Andrea Grant<sup>1</sup>, Kamil Ugurbil<sup>1</sup>, and Gregory J Metzger<sup>1</sup>

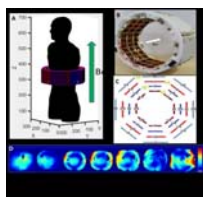
<sup>1</sup>Radiology, University of Minnesota, Minneapolis, MN, United States

A 32-channel transmit/receive (transceiver) body array (32LD) was developed by combining eight dipole elements with 24 loops, 3 each stacked lengthwise under each dipole. The transmit/receive performance was compared against a 16-channel loop-dipole (16LD) array in numerical simulations and phantom experiments. The 32LD had improved SNR near the surface and enabled accelerations in foot-head dimension as expected. Inside deeply situated organs, SNR of 32LD was comparable to 16LD. Furthermore, the 32LD had ~30% higher local SAR than the 16LD with single-spoke RF shimming inside the kidneys and torso. High channel count body imaging arrays can be developed by combining dipoles and loops with geometric decoupling.

1223

16:42

### In-vivo (8x4) 32-ch Tx-only Body Array for UHF MRI.



Shailesh B. Raval<sup>1,2</sup>, Tales Santini<sup>3</sup>, Sossena Wood<sup>3</sup>, Narayanan Krishnamurthy<sup>3</sup>, Tiejun Zhao<sup>4</sup>, and Tamer S. Ibrahim<sup>5,6</sup>

<sup>1</sup>Bioengineering, University of Pittsburgh, Pittsburgh, PA, United States, <sup>2</sup>Radiology, University of Pittsburgh, Pittsburgh, PA, United States, <sup>3</sup>Bioengineering, University of Pittsburgh, <sup>4</sup>MR Research & Collaboration, Siemens Healthineers, NY, <sup>5</sup>Bioengineering, University of Pittsburgh, PA, <sup>6</sup>Radiology, University of Pittsburgh

The Clinical and Research potential of MRI especially for Whole Body imaging is limitless. Body MR exams are growing part of total clinical MRI exams today. It however faces considerable challenges such as significant rise in RF power deposition in tissue and daunting high field inhomogeneities/signal voids across the anatomy of interest most especially at 7T and higher. This study aims at utilizing the intrinsic sensitivity advantage of 7T by exploring a 32-ch transmit coil design in order to generate a circularly polarized field with homogeneous and extended coverage in abdominal/body regions (liver, kidney, and abdomen in general) at 7T.

---

1224

16:54



Sub-Millimeter Cortical Imaging at 7T using a High-Density Motor-Cortex 32-Channel Array Coil

Boris Keil<sup>1</sup>, Charlotte Sappo<sup>2</sup>, Berkin Bilgic<sup>2</sup>, Jonathan R Polimeni<sup>2,3</sup>, Laleh Golestanirad<sup>2</sup>, Robin Etzel<sup>1</sup>, Lawrence L Wald<sup>2,3</sup>, David A Feinberg<sup>4,5</sup>, and Kawin Setsompop<sup>2,3</sup>

<sup>1</sup>Institute of Medical Physics and Radiation Protection, Department of Life Science Engineering, Mittelhessen University of Applied Sciences (THM), Giessen, Germany, <sup>2</sup>A.A. Martinos Center for Biomedical Imaging, Department of Radiology, Massachusetts General Hospital, Harvard Medical School, Boston, MA, United States, <sup>3</sup>Harvard-MIT Division of Health Sciences and Technology, Cambridge, MA, United States, <sup>4</sup>Helen Wills Neuroscience Institute, UC Berkeley, Berkeley, MA, United States, <sup>5</sup>Advanced MRI Technologies, Sebastopol, CA, United States

A densely packed 32-channel motor cortex array coil was designed, constructed and compared to a 32-channel whole-head coil at 7T. The developed design allows coil adaptability to a wide range of head sizes, thereby minimizing the distance of the brain to the individual small loop elements. Using the high SNR and parallelism afforded by this array, a substantial gain in sensitivity and performance for imaging the human motor cortex was achieved, enabling 0.15x0.15x0.65 mm<sup>3</sup> resolution SWI scans.



---

1225

17:06



### 31-Channel brain array for hyperpolarized $^{13}\text{C}$ imaging at 3T

Azma Mareyam<sup>1</sup>, Lucas Carvajal<sup>2</sup>, Duan Xu<sup>2</sup>, Jeremy Gordon<sup>2</sup>, Ilwoo Park<sup>2</sup>, Daniel B Vigneron<sup>2</sup>, Sarah J Nelson<sup>2</sup>, Jason P Stockmann<sup>1,3</sup>, Boris Keil<sup>1,3</sup>, and Lawrence L Wald<sup>1,3</sup>

<sup>1</sup>Massachusetts General Hospital, A.A Martinos Center for Biomedical Imaging, Dept. of Radiology, Charlestown, MA, United States, <sup>2</sup>Radiology and Biomedical Imaging, UCSF School of Medicine, San Francisco, CA, United States, <sup>3</sup>Harvard Medical school, Boston, MA, United States

We describe the design and the performance of an integrated RF Tx and Rx coil to enable highly accelerated  $^{13}\text{C}$  imaging of the human brain at 3T. This system combines a 31-channel receive array with integrated preamps and a high-power transmit coil in an improved mechanical design, overcoming several longstanding design challenges that previously limited hyperpolarized  $^{13}\text{C}$  imaging. The shorter imaging times and more uniform spatial coverage attainable with our design will lead to a substantially increase in the range of hyperpolarized imaging applications, and enable the transition to clinical use.

---

1226

17:18



### Universal Size-Optimized 48-Channel Phased-Array Receive Head Coil for 3T Clinical fMRI/Silent Imaging Application

Yun-Jeong Stickle<sup>1</sup>, Victor Taracila<sup>1</sup>, Sarah Tenley<sup>1</sup>, Clyve Follante<sup>1</sup>, Balint Franko<sup>1</sup>, Nabeel Malik<sup>1</sup>, Patrick Quarterman<sup>2</sup>, Fotis Vlachos<sup>2</sup>, and Peter Roemer<sup>2</sup>

<sup>1</sup>Engineering, GE Healthcare Coils, Aurora, OH, United States, <sup>2</sup>Engineering, GE Healthcare, Waukesha, WI, United States

Typical high density phased-array head coils are design to fit tightly around the head to achieve increasing SNR and improving acceleration limiting space and excluding its use for larger patients. This study shows the results for an optimized 48-Channel phased-array receive head coil design on a universally sized football helmet-shaped former (fitting to more than 99<sup>th</sup> - percentile US male) providing similar SNR and improved acceleration compared to a 32-Channel close-fitting design coil. The performance of this array is demonstrated in highly accelerated head images on variously sized human subjects. This coil is optimized for Hyperband, fMRI and Silent imaging.

---

---



Oral

## Novel Abdominal Applications & Developments

Room 313A

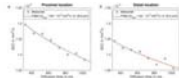
Thursday 15:30 - 17:30 Moderators: Houchun Hu & ChangHee Lee

---

1227



15:30



Probing bone marrow adipocyte cell size in vivo at a clinical 3 T scanner using high b-value DW-MRS at long diffusion times

Dominik J. Weidlich<sup>1</sup>, Andreas Hock<sup>2</sup>, Stefan Ruschke<sup>1</sup>, Daniela Franz<sup>1</sup>, Katja Steiger<sup>3</sup>, Thomas Skurk<sup>4</sup>, Hans Hauner<sup>4</sup>, Ernst J. Rummeny<sup>1</sup>, and Dimitrios C. Karampinos<sup>1</sup>

*<sup>1</sup>Department of Diagnostic and Interventional Radiology, Technical University Munich, Munich, Germany, <sup>2</sup>Philips Healthcare, Hamburg, Germany, <sup>3</sup>Department of Pathology, Technical University Munich, Munich, Germany, <sup>4</sup>Else Kröner Fresenius Center for Nutritional Medicine, Technical University Munich, Munich, Germany*

Despite its strong relevance in metabolism, non-invasive measurement of adipocyte size remains an unmet need. High b-value DW-MRS has been previously applied to probe diffusion restriction effects of intramyocellular lipids or brown adipocytes using preclinical systems with strong gradient systems. The present work proposes a methodology to in vivo probe diffusion restriction effects in bone marrow adipocytes with high b-value long diffusion time DW MRS in a clinical system and examines the feasibility of bone marrow adipocyte size estimation in the tibia of healthy subjects.

---

1228

15:42



Quantifying Fat Mass and Energy Content in Brown Adipose Tissue

Jedrzej Burakiewicz<sup>1</sup>, Gustavo de Abreu Vieira<sup>2</sup>, Laura G.M. Janssen<sup>2</sup>, Kimberly J. Nahon<sup>2</sup>, Mariëtte R. Boon<sup>2</sup>, Andrew G. Webb<sup>1</sup>, Hermien E. Kan<sup>1</sup>, and Patrick C.N. Rensen<sup>2</sup>

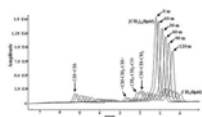
*<sup>1</sup>Gorter Center for High Field MRI, Radiology, Leiden University Medical Centre, Leiden, Netherlands, <sup>2</sup>Endocrinology, Leiden University Medical Centre, Leiden, Netherlands*

MRI of Brown Adipose Tissue (BAT) is gaining popularity as an alternative to PET-CT. Most commonly used marker in quantifying BAT is fat fraction, however there is no consensus to the range of fat fractions separating BAT and WAT. In this work we show how calculating energy content and total fat mass allows to avoid partial volume effect and provides more quantitative markers than fat fraction. We also argue that the fat fractions in the high end of the range (80% - 100%) contribute significantly to BAT activity.

---

1229

15:54



### Metabolic Imaging of Dynamic Fat Mobilization in Activated Brown Adipose Tissue

Jadegoud Yaligar<sup>1</sup>, Sanjay Kumar Verma<sup>1</sup>, Venkatesh Gopalan<sup>1</sup>, Tian Xianfeng<sup>1</sup>, Anantharaj Rengaraj<sup>1</sup>, and S. Sendhil Velan<sup>1</sup>

*<sup>1</sup>Laboratory of Metabolic Imaging, Singapore Bioimaging Consortium, A\*STAR, Singapore*

Brown adipose tissue (BAT) is a target fat compartment for treatment of metabolic diseases due to its high metabolic capacity. BAT is major site for adaptive thermogenesis involving uncoupling protein-1. We have studied the dynamic oxidative fat metabolism in interscapular brown adipose tissue by activation of  $\beta$ 3-adrenergic receptors. Progressive reduction of the lipids from iBAT region is indicative of oxidative metabolism by utilizing the lipids as fuel substrate. Evaluation of lipid mobilization in real time is important to assess the altered metabolic rate and mitochondrial biogenesis involving lipid oxidative metabolism.

---

1230

16:06



### Measurement of Brown Adipose Tissue Activity in Response to Thermal Challenges Using Dixon MRI

Jie Deng<sup>1,2</sup>, Nicholas Rubert<sup>1</sup>, Lisa M Neff<sup>3</sup>, Richard Shore<sup>1,2</sup>, Christina Sammet<sup>1,2</sup>, and Jonathan Samet<sup>1,2</sup>

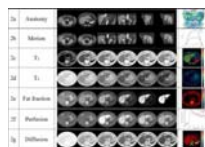
*<sup>1</sup>Medical Imaging, Ann & Robert H. Lurie Children's Hospital of Chicago, Chicago, IL, United States, <sup>2</sup>Radiology, Feinberg School of Medicine, Northwestern University, Chicago, IL, United States, <sup>3</sup>Division of Endocrinology, Metabolism and Molecular Medicine, Feinberg School of Medicine, Northwestern University, Chicago, IL, United States*

Brown adipose tissue (BAT) is the primary site of adaptive thermogenesis, which may play a potential role in the pathogenesis and treatment of obesity, and related metabolic disorders. The purpose of this study is to use Dixon MRI to measure BAT tissue properties under pre-cold, post-cold individualized non-shivering thermogenesis, and re-warm-up conditions, in order to evaluate BAT activity among normal-weight, over-weight and obese subjects.

1231



16:18



### Realistic 4D abdominal phantom for magnetic resonance imaging

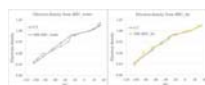
Wei-Ching Lo<sup>1</sup>, Yong Chen<sup>2</sup>, Yun Jiang<sup>1</sup>, Vikas Gulani<sup>1,2</sup>, and Nicole Seiberlich<sup>1,2</sup>

<sup>1</sup>Dept. of Biomedical Engineering, Case Western Reserve University, Cleveland, OH, United States, <sup>2</sup>Dept. of Radiology, University Hospitals of Cleveland, Cleveland, OH, United States

Validation and evaluation of novel data acquisition and reconstruction strategies are major challenges in abdominal magnetic resonance imaging, and particularly in quantitative imaging. Here, a new 4D numerical abdominal phantom combining anatomical morphology, respiratory motion, tissue properties, and physiological function is introduced to enable comparison of different data collection and reconstruction schemes for abdominal MRI.

1232

16:30



### Towards Addressing Unmet Needs in MR-only Radiotherapy Treatment Planning: The Feasibility of Estimating Electron Density from Quantitative Water/Fat Imaging

Abraam S Soliman<sup>1,2</sup>, Masoud Hashemi<sup>2</sup>, Alex Karotki<sup>2,3</sup>, and William Y Song<sup>1,2,3</sup>

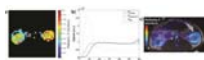
<sup>1</sup>Physical Sciences, Sunnybrook Research Institute, Toronto, ON, Canada, <sup>2</sup>Medical Physics, Sunnybrook Health Sciences Centre, Toronto, ON, Canada, <sup>3</sup>Radiation Oncology, University of Toronto, ON, Canada

MR-only treatment planning requires the knowledge of electron density to account for medium heterogeneities during dose calculation. This work introduces a novel perspective for electron density estimation by utilizing quantitative water/fat imaging. Water/fat phantoms with different percentages were scanned on MR and CT. Water/fat separation was performed while correcting (or minimizing) major sources of signal bias. A linear regression model between CT and corrected MR signals was calculated and used to derive MR-based electron density curve. This approach targets radiotherapy applications that require sensitive soft-tissue heterogeneity correction such as prostate and breast low-dose-rate (LDR) brachytherapy.

1233



16:42



### A Hyperpolarized $^{13}\text{C}$ MRI Approach for Calculating Glomerular Filtration Rate

Eugene Milshteyn<sup>1,2</sup>, Cornelius von Morze<sup>1</sup>, Jeremy W. Gordon<sup>1</sup>, Galen D. Reed<sup>3</sup>, Robert A. Bok<sup>1</sup>, and Daniel B. Vigneron<sup>1,2</sup>

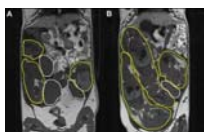
<sup>1</sup>Radiology and Biomedical Imaging, UCSF, San Francisco, CA, United States, <sup>2</sup>UC Berkeley-UCSF Graduate Program in Bioengineering, UCSF and University of California, Berkeley, San Francisco, CA, United States, <sup>3</sup>HeartVista Inc., Los Altos, CA, United States

The feasibility of calculating glomerular filtration rate (GFR) using hyperpolarized  $^{13}\text{C}$  MRI is demonstrated in this project. HP001 is exhibited as a potential probe for GFR calculation due to its long  $T_1$ , allowing for high spatiotemporal resolution, and favorable filtration properties. Multiple iterations of common clinical sequences, including EPI and bSSFP, were utilized, and each sequence yielded GFR values close to those found in literature. The results shown here indicate potential for a new noninvasive imaging measurement of GFR.

1234



16:54



### Measurement of placental oxygenation in a guinea pig model of intrauterine growth restriction

Kevin J Sinclair<sup>1</sup>, Lanette J Friesen-Waldner<sup>1</sup>, Trevor P Wade<sup>2</sup>, Cheryl Vander Tuin<sup>1</sup>, Barbra de Vrijer<sup>3,4</sup>, Timothy RH Regnault<sup>3,4,5</sup>, and Charles A McKenzie<sup>1,2,4</sup>

<sup>1</sup>Medical Biophysics, University of Western Ontario, London, ON, Canada, <sup>2</sup>Robarts Research Institute, London, ON, Canada, <sup>3</sup>Obstetrics and Gynaecology, University of Western Ontario, London, ON, Canada, <sup>4</sup>Division of Maternal, Fetal and Newborn Health, Children's Health Research Institute, London, ON, Canada, <sup>5</sup>Physiology and Pharmacology, University of Western Ontario, London, ON, Canada

We sought to examine the placental oxygenation status in a guinea pig model of intrauterine growth restriction (IUGR). We measured T2\* in placentae of IUGR and control fetuses during a maternal oxygen challenge, where imaging was performed at both 20% and 100% inhaled oxygen. IUGR was defined by an elevated brain to liver volume ratio, indicative of blood flow redistribution secondary to fetal hypoxia. No significant difference in  $\Delta T2^*$  was observed, indicating that the placentae of the IUGR fetuses were not hypoxic. Thus we concluded that placental hypoxia is not necessary to induce fetal hypoxia in the guinea pig.

1235



17:06

	2D-SWI		T2-TrueFISP		p-value	
	Mean	SD	Mean	SD	Mean	SD
Cervical region	1.14	1.01	1.04	1.13	0.0002	0.0001
Thoracic region	1.76	1.01	1.86	1.01	0.0002	0.0001
Lumbar region	1.12	1.01	1.04	1.13	0.0002	0.0001

Two-dimensional susceptibility-weighted MRI at 1.5T: preliminary utility in the assessment of the fetal osseous spine

Xin Chen<sup>1</sup>, Guangbin Wang<sup>1</sup>, Tianyi Qian<sup>2</sup>, Wen Liu<sup>1</sup>, Xinhong Wei<sup>1</sup>, and Fei Gao<sup>1</sup>

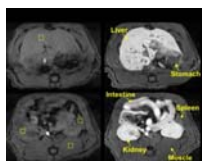
<sup>1</sup>Shandong Medical Imaging Research Institute, Shandong University, Jinan, People's Republic of China, <sup>2</sup>Siemens Healthcare, MR Collaborations NE Asia, Beijing, People's Republic of China

This study aimed to explore the utility of two-dimensional susceptibility-weighted imaging (2D-SWI) for assessing the fetal osseous spine. Whole-spine MRI was performed on fetuses, which included 2D-SWI and T2-weighted true fast imaging with steady-state precession (T2-TrueFISP) sequences. The image quality of the 2D-SWI was superior to the T2-TrueFISP, allowing for improved diagnostic accuracy in the diagnosis of spinal abnormalities. 2D-SWI was valuable in elucidating the structures of the fetal osseous spine allowing for better assessment of spinal deformity, especially in the cervical segment of the spine.

1236



17:18



Mapping Abdominal Inflammatory Response Using Manganese-Enhanced MRI (MEMRI)

Kun-Han Lu<sup>1</sup>, Jiayue Cao<sup>2</sup>, Lauren Kelly Marussich<sup>2</sup>, Tom C.-C. Hu<sup>3</sup>, and Zhongming Liu<sup>1,2</sup>

<sup>1</sup>Electrical and Computer Engineering, Purdue University, West Lafayette, IN, United States, <sup>2</sup>Biomedical Engineering, Purdue University, West Lafayette, IN, United States, <sup>3</sup>Division of CBRN Countermeasures, Biomedical Advanced Research and Development Authority, DC, United States

We used in vivo Manganese-Enhanced MRI (MEMRI) to image and assess the increase in calcium influx into immune cells so as to report the cellular responses to systemically LPS-induced inflammation throughout the abdomen. We found that: (1) The contrast enhancement was dose- and time-dependent with variation across organs. (2) An increase in Mn<sup>2+</sup> uptake was observed in the liver and the kidney, but not in the spleen or the muscle given inflammation. (3) The inflammation-induced enhancement was dependent on the time after the initial exposure to LPS.

---

Oral

## fMRI Clinical & Neuroscience Applications

Room 313BC

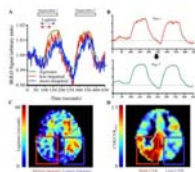
Thursday 15:30 - 17:30 Moderators: Victoria Morgan & Stefan Posse

---

1237



15:30



Time delay processing of BOLD cerebrovascular reactivity data in patients with moyamoya pre- and post-surgical revascularization reveals a potential new indicator of vascular compliance

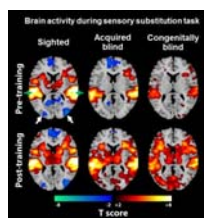
Jennifer M Watchmaker<sup>1</sup>, Blaise deB Frederick<sup>2,3</sup>, Meher R Juttukonda<sup>1</sup>, Sarah K Lants<sup>1</sup>, Larry T Davis<sup>1</sup>, Matthew R Fusco<sup>4</sup>, and Manus J Donahue<sup>1,5,6</sup>

<sup>1</sup>Radiology & Radiological Sciences, Vanderbilt University, Nashville, TN, United States, <sup>2</sup>Mclean Hospital, Brain Imaging Center, Belmont, MA, United States, <sup>3</sup>Department of Psychiatry, Harvard Medical School, Boston, MA, United States, <sup>4</sup>Department of Neurosurgery, Vanderbilt University Medical Center, Nashville, TN, United States, <sup>5</sup>Department of Psychiatry, Vanderbilt University Medical Center, Nashville, TN, United States, <sup>6</sup>Department of Neurology, Vanderbilt University Medical Center, Nashville, TN, United States

Structural and BOLD-weighted hemodynamic imaging was performed in patients with intracranial steno-occlusion due to moyamoya disease before and after surgical revascularization. A novel data-driven time-delay analysis was performed using cross-correlation of functional imaging data to find the time at which maximum correlation occurs between the BOLD signal from each voxel and a reference regressor. This provides a novel metric of hemodynamic impairment (lagtime) that may be indicative of vascular smooth muscle dysfunction and therefore delayed reactivity. We found that in patients with successful revascularization on angiography, lagtimes decreased, and in patients with unsuccessful revascularization and progressive disease, lagtimes increased.

1238

15:42



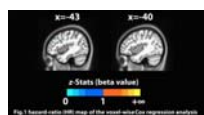
Top-down modulation in the visual cortex negatively correlates with duration of blindness and reaction time during sensory substitution  
Kevin C. Chan<sup>1,2,3</sup>, Matthew C. Murphy<sup>1,2</sup>, Jasmine Kashkoush<sup>1</sup>, and Amy C. Nau<sup>2</sup>

<sup>1</sup>Neuroimaging Laboratory, University of Pittsburgh, Pittsburgh, PA, United States, <sup>2</sup>Department of Ophthalmology, University of Pittsburgh, Pittsburgh, PA, United States, <sup>3</sup>Department of Bioengineering, University of Pittsburgh, Pittsburgh, PA, United States

Visual cortex functionality in the blind has been shown to shift away from sensory networks toward task-positive networks that are involved in top-down modulation. However, how such modulation is shaped by experience and reflected behaviorally remains unclear. Using blood-oxygenation-level-dependent functional MRI with a sensory substitution task, we found that top-down visual cortex activity negatively correlates with duration of blindness and reaction time. Our results suggest that alterations in top-down brain activity due to visual deprivation progress as a function of time. Furthermore, the degree of top-down activity in the visual cortex may reflect the speed of performance during sensory substitution.

1239

15:54



Functional connectivity of DLPFC circuits predicts cocaine relapse  
Tianye Zhai<sup>1</sup>, Hong Gu<sup>1</sup>, and Yihong Yang<sup>1</sup>

<sup>1</sup>Neuroimaging Research Branch, Intramural Research Program, National Institute on Drug Abuse, Baltimore, MD, United States

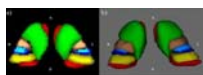


TMS targeting the DLPFC has been shown to effectively manipulate inter-temporal behaviors in healthy individuals and drug-using behaviors in cocaine users. However, the neural mechanism through which the DLPFC is involved in the alteration of these behaviors remains unclear. In the current study, we utilized resting-state fMRI to investigate the relationship between the DLPFC functional connectivity and relapse in cocaine addiction. Our voxel-wise Cox regression analyses revealed that two DLPFC circuits have protective effects against cocaine relapse.

---

1240

16:06



Thalamic functional connectivity in Multiple Sclerosis: the role of temporal thalamic sub-region in maladaptation

Paola Valsasina<sup>1</sup>, Alessandro D'Ambrosio<sup>1</sup>, Milagros Hidalgo<sup>1</sup>, Elisabetta Pagani<sup>1</sup>, Bruno Colombo<sup>2</sup>, Mariaemma Rodegher<sup>2</sup>, Andrea Falini<sup>3</sup>, Giancarlo Comi<sup>2</sup>, Massimo Filippi<sup>1</sup>, and Maria Assunta Rocca<sup>1</sup>

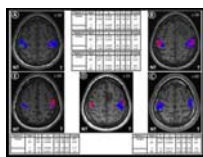
*<sup>1</sup>Neuroimaging Research Unit, San Raffaele Scientific Institute, Vita-Salute San Raffaele University, Milan, Italy, <sup>2</sup>Department of Neurology, San Raffaele Scientific Institute, Vita-Salute San Raffaele University, Milan, Italy, <sup>3</sup>Department of Neuroradiology, San Raffaele Scientific Institute, Vita-Salute San Raffaele University, Milan, Italy*

We compared resting state (RS) functional connectivity (FC) of five thalamic sub-regions (frontal, motor, post-central, occipital and temporal) between patients with multiple sclerosis (MS) and healthy controls. There was an overall increase of intra- and inter-thalamic RS FC for almost all thalamic sub-regions, apart from the temporal thalamic sub-region, which showed reduced intra-thalamic RS FC and higher RS FC with the fronto-parietal somatomotor cortex. Compared to cognitively preserved, cognitively impaired MS patients had lower RS FC between thalamic sub-regions and caudate nucleus, anterior cingulate cortex, as well as higher RS FC between thalamic sub-regions and several temporal areas.

---

1241

16:18



Acquisition of sensorimotor fMRI under general anaesthesia in neurosurgical patients: evaluation of the effect of anaesthesia on the BOLD response.

Adam Kenji Yamamoto<sup>1</sup>, Joerg Magerkurth<sup>2</sup>, Laura Mancini<sup>3</sup>, Mark J White<sup>4</sup>, Anna Miserocchi<sup>5</sup>, Andrew McEvoy<sup>5</sup>, Ian Appleby<sup>6</sup>, Martin Smith<sup>7</sup>, John Thornton<sup>3</sup>, Nikolaus Weiskopf<sup>8</sup>, and Tarek A Yousry<sup>1</sup>

<sup>1</sup>Department of Brain Repair and Rehabilitation, UCL Institute of Neurology, London, United Kingdom, <sup>2</sup>UCL Psychology and Language Sciences, Birkbeck-UCL Centre for Neuroimaging, London, United Kingdom, <sup>3</sup>Lysholm Department of Neuroradiology, National Hospital for Neurology and Neurosurgery, London, United Kingdom, <sup>4</sup>Medical Physics and Biomedical Engineering, University College London Hospital, London, United Kingdom, <sup>5</sup>Department of Neurosurgery, National Hospital for Neurology and Neurosurgery, London, United Kingdom, <sup>6</sup>Department of Neuroanaesthesia, National Hospital for Neurology and Neurosurgery, London, United Kingdom, <sup>7</sup>Department of Neuroanaesthesia and Neurocritical Care, National Hospital for Neurology and Neurosurgery, London, United Kingdom, <sup>8</sup>Department of Neurophysics, Max Planck Institute for Human Cognitive and Brain Sciences, Leipzig, Germany

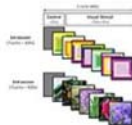
fMRI performed intra-operatively has the potential to significantly improve the outcomes from neurosurgery. The question remains however as to whether the BOLD signal can be detected in anaesthetised patients and what effect anaesthesia has on the response. In 5 patients with brain tumours anaesthetised for surgery we performed a passive sensorimotor fMRI paradigm. Anaesthesia resulted in a reduction in the BOLD response relative to the awake state, but also reduced the variance in the statistical model resulting in significant, accurate activation in all patients.

We conclude that the fMRI BOLD signal can be accurately detected in anaesthetised neurosurgical patients.

---

1242

16:42



### Olfactory suggestion capacity of colors: a functional MRI study

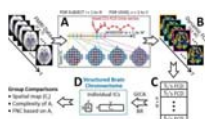
Céline Charroud<sup>1</sup>, Muriel Jacquot<sup>2,3</sup>, Romain Tonnelet<sup>4</sup>, Julie Boyer<sup>1</sup>, Léa Nehmé<sup>3</sup>, Faustine Noël<sup>2</sup>, Jacques Felblinger<sup>1,5</sup>, Marc Braun<sup>1,4</sup>, and Gabriela Hossu<sup>1,5</sup>

<sup>1</sup>IADI, INSERM U947, Université de Lorraine, CHRU Nancy, Nancy, France, <sup>2</sup>Myrissi, Nancy, France, <sup>3</sup>InnoCIM, ENSAIA, Université de Lorraine, Nancy, France, <sup>4</sup>Department of Diagnostic and Interventional Neuroradiology, CHRU Nancy, Nancy, France, <sup>5</sup>CIC 1433 Innovation Technologique, INSERM, Université de Lorraine, CHRU Nancy, Nancy, France

We know that colors modify odor's perception. It demonstrates that colors arrangement (chromatic cards) could evoke the appropriate odor, but we have not neural evidence of these chromatic cards olfactory suggestion capacity. Our goal is to compare the olfactory suggestion capacity of picture with that of chromatic arrangements using functional MRI paradigm. We show that chromatic card visualization could suggest an odor more efficiently than picture visualization. Our results support the involvement of multiple cognitive processes (olfactory, emotional, visuospatial, language, memory, taste) which interact to produce olfactory suggestion from colors visualization. Therefore, chromatic card application could be varied (health, marketing...).

1243

16:54



### Structured Brain “Chronnectome” Reveals New Brain Dynamic Patterns for Early Detection of Alzheimer’s Disease

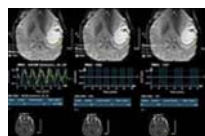
Han Zhang<sup>1</sup>, Xiaobo Chen<sup>1</sup>, Lichi Zhang<sup>1</sup>, and Dinggang Shen<sup>1,2</sup>

<sup>1</sup>Department of Radiology and BRIC, University of North Carolina at Chapel Hill, Chapel Hill, NC, United States, <sup>2</sup>Department of Brain and Cognitive Engineering, Korea University, Seoul, Korea, Republic of

To understand dynamics of human brain connectome, we introduce a novel method named “structured brain chronnectome (SBC)”, which measures spatiotemporal architecture of dynamic functional connectivities, a pivotal mechanism for human to adapt to the outside world. From dynamic view angle, with graph theoretic analysis and blind-source separation, we detect meaningful SBCs with typical and atypical configurations compared with traditional networks. They reflect high-order brain functional organization. By applying SBC to an Alzheimer’s disease progression data, we revealed pre-symptomatic brain high-level function alterations from early mild cognitive impairment subjects which are difficult to detect using traditional methods.

1244

17:06



### Silent Sentence Completion Paradigm Shows Superiority in Localization of Wernicke’s Area and Changes in Functional Activation in the Distinct Language Paradigms Correlate with Key Genomic Markers: A Prospective Study

Kamel El Salek<sup>1</sup>, Islam Hassan<sup>1</sup>, Scott H Faro<sup>2</sup>, Srishti Abrol<sup>1</sup>, Aikaterini Kotrotsou<sup>1</sup>, Feroze B Mohamed<sup>2</sup>, Pascal O Zinn<sup>3</sup>, Wei Wei<sup>4</sup>, Nan Li<sup>4</sup>, Ashok J Kumar<sup>1</sup>, Jeffrey S Weinberg<sup>5</sup>, Jeffrey S Wefel<sup>6</sup>, Shelli R Kesler<sup>6</sup>, Ho-Ling Anthony Liu<sup>7</sup>, Ping Hou<sup>7</sup>, Jason R Stafford<sup>7</sup>, Sujit Prabhu<sup>5</sup>, Raymond Sawaya<sup>5</sup>, and Rivka R Colen<sup>1,8</sup>

<sup>1</sup>Diagnostic Radiology, MD Anderson Cancer Center, Houston, TX, United States, <sup>2</sup>Radiology, Temple University, Philadelphia, PA, United States, <sup>3</sup>Neurosurgery, Baylor College of Medicine, Houston, TX, United States, <sup>4</sup>Biostatistics, MD Anderson Cancer Center, Houston, TX, United States, <sup>5</sup>Neurosurgery, MD Anderson Cancer Center, Houston, TX, United States, <sup>6</sup>Neuro-Oncology, MD Anderson Cancer Center, Houston, TX, United States, <sup>7</sup>Imaging Physics, MD Anderson Cancer Center, Houston, TX, United States, <sup>8</sup>Cancer Systems Imaging, MD Anderson Cancer Center, Houston, TX, United States

The reliability of fMRI for preoperative mapping of language areas depends on the paradigms used, as different tasks harness distinct capabilities to activate areas of speech processing. By comparing 3 language tasks [Silent Sentence Completion (SSC), Category Naming (CAT) and Word Generation (FAS)], we seek to determine the most robust and consistent task in localizing Wernicke's area. Further the association between genomic markers and functional activation was determined. We included 15 healthy volunteers and 35 patients with gliomas. Results demonstrated that SSC is superior compared to other language paradigms and a correlation exists between tumor genomics and functional activation signals.

1245

17:18

	HGG	LGG
<b>BOLD fluctuations</b>		
Temporal shift (sec)	-0.77s 0.22***	0.42s 0.31*
ALFF	1.074s 0.029**	0.977s 0.024*
ReHo	0.376s 0.022	0.393s 0.014*
<b>f1 contrast perfusion</b>		
CBV	2.37s 0.33***	1.36s 0.22
TTP	0.71s 0.31	0.89s 0.21

\*Statistical significance  
HGG: High grade glioma, LGG: Low grade glioma  
ALFF: Amplitude of low frequency fluctuations  
ReHo: Regional homogeneity  
CBV: Cerebral blood volume  
TTP: Time to peak  
\*\*p<0.01, compared to contralateral cortex (Student's t-test)  
\*\*\*p<0.001, HGG compared with LGG (Student's t-test)

### Altered BOLD fluctuations in gliomas and clinical possibilities

Lalit Gupta<sup>1</sup>, Rakesh K Gupta<sup>2</sup>, Prativa Sahoo<sup>2</sup>, Pradeep K Gupta<sup>2</sup>, Rana Patir<sup>2</sup>, Sunita Ahlawat<sup>2</sup>, Indrajit Saha<sup>3</sup>, and Walter H Backes<sup>1</sup>

<sup>1</sup>Departments of Radiology and Nuclear Medicine, Maastricht University Medical Center, Maastricht, Netherlands, <sup>2</sup>Fortis Memorial Research Institute, Gurgaon, India, <sup>3</sup>Philips India Ltd., Gurgaon, India

In this study, our primary objectives were to characterize the BOLD signal in gliomas using the temporal shift (TS), amplitude of low frequency fluctuations (ALFF) and regional homogeneity (ReHo) measures relative to the contralateral cortex, and to analyse the effectiveness of these measures in distinguishing high grade (HGG) from low grade glioma (LGG). Twenty-one patients with HGG and 13 patients with LGG were investigated. Abnormal hemodynamic fluctuations manifest in HGG, but not for LGG, and can be assessed using functional MRI. BOLD measures reflecting TS and ALFF show promise as an alternative to contrast-enhanced perfusion based techniques in future.

1246

17:30



Improved mapping of epileptic networks based on the correlation of BOLD-fMRI dynamic functional connectivity components with simultaneous EEG

Rodolfo Abreu<sup>1</sup>, Alberto Leal<sup>2</sup>, and Patrícia Figueiredo<sup>1</sup>

<sup>1</sup>ISR-Lisboa/LARSyS and Department of Bioengineering, Instituto Superior Técnico, Universidade de Lisboa, Lisbon, Portugal,

<sup>2</sup>Department of Neurophysiology, Centro Hospitalar Psiquiátrico de Lisboa, Lisboa, Portugal

We propose the use of BOLD dynamic functional connectivity (dFC) analyses to provide further insights into the dynamics of epileptic networks, in simultaneous EEG-fMRI studies. We performed brain parcellation using the AAL atlas and estimated dFC across brain regions using sliding-window correlation. We then tested different approaches for the extraction of functional networks related with the EEG epileptic activity. We found that PCA is a suitable tool to disentangle functional connectivity changes of different origins, and that epilepsy-related networks may be accurately identified based on the correlation of their weights time-courses with metrics of EEG epileptic activity in four patients.

---

Oral

## MRSI Acquisition & Reconstruction

Room 316BC

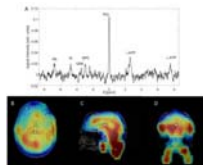
Thursday 15:30 - 17:30

Moderators: Wolfgang Bogner & Tom Scheenen

---

1247

15:30



Three-dimensional <sup>31</sup>P Radial Echo-Planar Spectroscopic Imaging In Vivo at 7T

Dominik Ludwig<sup>1</sup>, Andreas Korzowski<sup>1</sup>, Loreen Ruhm<sup>1</sup>, Mark E. Ladd<sup>1</sup>, and Peter Bachert<sup>1</sup>

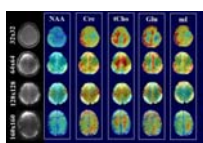
<sup>1</sup>Medical Physics in Radiology, German Cancer Research Center (DKFZ), Heidelberg, Germany

$^{31}\text{P}$  MR spectroscopic imaging ( $^{31}\text{P}$  MRSI) *in vivo* suffers from low spatial resolution and long measurement times. The purpose of this study was to prove feasibility of a three-dimensional  $^{31}\text{P}$  radial Echo-Planar Spectroscopic Imaging sequence (3D radial EPSI) for  $^{31}\text{P}$  MRSI *in vivo* at 7T. The presented data with an isotropic spatial resolution of  $(10\text{mm})^3$  in the human calf muscle and  $(18\text{mm})^3$  in the human brain show well-resolved localized spectra proving feasibility of the 3D  $^{31}\text{P}$  radial EPSI sequence with measurement times of about 35min at 7T.

1248



15:42



Pushing the limits of ultra-high field MRSI: benefits and limitations of 9.4T for metabolite mapping of the human brain

Sahar Nassirpour<sup>1,2</sup>, Paul Chang<sup>1,2</sup>, and Anke Henning<sup>1,3</sup>

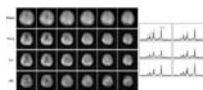
<sup>1</sup>MPI for Biological Cybernetics, Tuebingen, Germany, <sup>2</sup>IMPRS for Cognitive and Systems Neuroscience, Eberhard Karls University of Tuebingen, Tuebingen, Germany, <sup>3</sup>Institute of Physics, Ernst-Moritz-Arndt University Greifswald, Greifswald, Germany

MRSI can benefit greatly from ultra-high field strengths. Given the higher SNR and higher chemical shift dispersion, metabolite mapping can be done with higher quantification precision and at higher spatial resolution. The aim of this work was to study the competing effects of spatial resolution, SNR, linewidth and higher field strengths by pushing the spatial resolution limits of 3T and 9.4T for metabolite mapping of the human brain.

1249



15:54



Simultaneous Mapping of Brain Metabolites, Macromolecules and Tissue Susceptibility Using SPICE

Fan Lam<sup>1</sup>, Yudu Li<sup>1,2</sup>, Bryan Clifford<sup>1,2</sup>, Xi Peng<sup>1</sup>, and Zhi-Pei Liang<sup>1,2</sup>

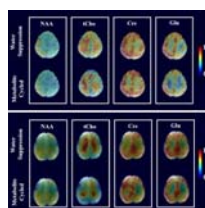
<sup>1</sup>Beckman Institute for Advanced Science and Technology, University of Illinois at Urbana-Champaign, Urbana, IL, United States, <sup>2</sup>Department of Electrical and Computer Engineering, University of Illinois at Urbana-Champaign, Urbana, IL, United States

In this work, we present a new imaging capability for simultaneous mapping of metabolites, macromolecules and tissue susceptibility in the brain, using a single scan for about 5 minutes. This new capability builds on the recently proposed subspace imaging framework SPICE (SPectroscopic Imaging by exploiting spatioSpectral CorrElation) and uses a union-of-subspaces based approach to extract tissue susceptibility, metabolite and macromolecule spatioSpectral distributions from an ultrashort-TE, short-TR, high-resolution MRSI scan without water suppression. In vivo results were used to demonstrate this exciting capability.

1250



16:06



Fast non-water suppressed metabolite cycled 1H FID MRSI at both 3T and 9.4T

Paul Chang<sup>1,2</sup>, Sahar Nassirpour<sup>1,2</sup>, and Anke Henning<sup>1,3</sup>

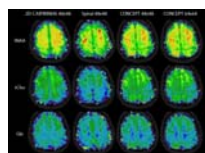
<sup>1</sup>MPI for Biological Cybernetics, Tuebingen, Germany, <sup>2</sup>IMPRS for Cognitive and Systems Neuroscience, Eberhard University of Tuebingen, Tuebingen, Germany, <sup>3</sup>Institute of Physics, Ernst-Moritz-Arndt University Greifswald, Greifswald, Germany

The purpose of this study is to use a metabolite cycling scheme combined with FID MRSI, acquire and compare spectra and metabolite maps from both water suppressed and non-water suppressed FID MRSI at 9.4T and 3T.

1251



16:18



Comparison of Acceleration Methods for Brain MRSI at 7T

Bernhard Strasser<sup>1</sup>, Lukas Hingerl<sup>1</sup>, Borjan A Gagoski<sup>2</sup>, Philipp Moser<sup>1</sup>, Gilbert Hangel<sup>1</sup>, Siegfried Trattning<sup>1,3</sup>, and Wolfgang Bogner<sup>1</sup>

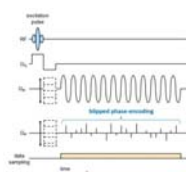
<sup>1</sup>Department of Biomedical Imaging and Image-guided Therapy, High Field MR Centre, Medical University of Vienna, Vienna, Austria, <sup>2</sup>Department of Electrical Engineering and Computer Science, MIT, Cambridge, MA, United States, <sup>3</sup>Christian Doppler Laboratory for Clinical Molecular MR Imaging, Medical University of Vienna, Vienna, Austria



In this work three different acceleration methods, 2D-CAIPIRINHA with phase-encoding, spiral encoding and concentric circles (CONCEPT) for brain MRSI at 7T were compared. The metabolic maps were compared qualitatively, and the CRLB and SNR values were compared quantitatively. The metabolic maps of 2D-CAIPIRINHA with phase-encoding provided the best data with respect to metabolic maps, CRLB and SNR values. Improving the PSF by increasing the matrix size from 48x48 to 64x64 enhanced the data quality again for CONCEPT. Spiral and CONCEPT encoding are prone to spectral baseline distortions. Nevertheless, CONCEPT has a high potential for high resolution brain MRSI at 7T.

1252

16:30



### Accelerated Magnetic Resonance Spectroscopic Imaging Using Readout Segmentation (ASPIRES)

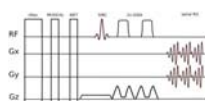
Marco Vicari<sup>1</sup> and David Andrew Porter<sup>1</sup>

<sup>1</sup>Fraunhofer MEVIS, Bremen, Germany

ASPIRES is a novel method for accelerated, high-resolution, large-bandwidth echo-planar spectroscopic imaging. It uses readout segmentation to decouple the echo spacing from the spatial resolution and gradient-system performance. Readout segmentation is combined with blipped phase encoding to accelerate scans by random undersampling along the readout-segment, phase-encoding and time directions. An elliptical acquisition window in the readout-phase encoding plane reduces scan time further. Distributed-multisensory compressed sensing reconstruction efficiently restores signal properties in both spatial and frequency domains. ASPIRES promises to enhance the diagnostic performance of MR spectroscopic imaging in clinical routine and improve the study of metabolites at high field strengths.

1253

16:42



### Spiral-accelerated short-TE MRSI with B1-insensitive 1D-semiLASER localization and real-time motion correction at 7T

Philipp Moser<sup>1</sup>, Bernhard Strasser<sup>1</sup>, Lukas Hingerl<sup>1</sup>, Michal Povazan<sup>1,2</sup>, Gilbert Hangel<sup>1</sup>, Ovidiu C. Andronesi<sup>3</sup>, Borjan Gagoski<sup>4</sup>, Aaron T. Hess<sup>5</sup>, Dylan M. Tisdall<sup>6</sup>, Andre van der Kouwe<sup>3</sup>, Siegfried Trattnig<sup>1,2</sup>, and Wolfgang Bogner<sup>1</sup>



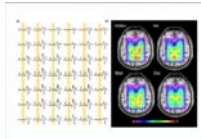
<sup>1</sup>High Field MR Centre, Department of Biomedical Imaging and Image-guided Therapy, Medical University of Vienna, Vienna, Austria, <sup>2</sup>Christian Doppler Laboratory for Clinical Molecular MR Imaging, Medical University of Vienna, Vienna, Austria, <sup>3</sup>Athinoula A. Martinos Center for Biomedical Imaging, Department of Radiology, Massachusetts General Hospital, Harvard Medical School, Charlestown, MA, United States, <sup>4</sup>Fetal-Neonatal Neuroimaging & Developmental Science Center, Boston Children's Hospital, Harvard Medical School, Boston, MA, United States, <sup>5</sup>Centre for Clinical Magnetic Resonance Research, Division of Cardiovascular Medicine, Radcliffe Department of Medicine, University of Oxford, Oxford, United Kingdom, <sup>6</sup>Perelman School of Medicine, Department of Radiology, University of Pennsylvania, Pennsylvania, PA, United States

*In vivo* MRSI at 7T offers advantages compared to lower field strengths, in particular higher SNR and improved spectral resolution. However, spectral quality is often limited by strong B1+ inhomogeneities, motion-related artifacts and scanner instability related B0 field drifts. To overcome these limitations, we have developed a 1D-semiLASER 2D-spiral-encoded MRSI sequence with real-time motion monitoring/correction using 3D EPI-based navigators (vNavs). Besides sequence stability we show that accurate B1-insensitive excitation can be achieved throughout the slice until the border of the brain. Using 7T-optimized motion correction, high spectral and metabolic map qualities are feasible even in the presence of motion.

1254



16:54



### Brain-Structure-Specific Metabolite Quantification of MEGA-LASER 3D MRSI data

Ruoyun Ma<sup>1,2</sup>, Wolfgang Bogner<sup>3</sup>, Ovidiu C. Andronesi<sup>4</sup>, and Ulrike Dydak<sup>1,2</sup>

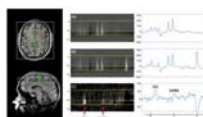
<sup>1</sup>School of Health Sciences, Purdue University, West Lafayette, IN, United States, <sup>2</sup>Department of Radiology and Imaging Sciences, Indiana University School of Medicine, Indianapolis, IN, United States, <sup>3</sup>Department of Biomedical Imaging and Image-guided Therapy, High Field MR Center, Medical University of Vienna, Vienna, Austria, <sup>4</sup>Martinos Center for Biomedical Imaging, Massachusetts General Hospital, Harvard Medical School, Boston, MA, United States

To overcome box-shaped ROIs and enable brain-structure-specific comparison of metabolite levels across patient groups, a fully-automated brain-structure-specific metabolite quantification approach was developed and applied to the analysis of MEGA-LASER 3D MRSI data. Structure-specific GABA, Glx, NAA and tCho levels and their hemispheric variation in healthy volunteers was studied. The four metabolite levels varied significantly across different brain regions, but did not differ between left and right hemispheres. Correlations between the left and right hemisphere metabolite levels were observed only for some structures.

---

1255

17:06



GABA-edited echo-planar spectroscopic imaging (EPSI) with MEGA-sLASER at 7T

Peter O Magnusson<sup>1</sup>, Vincent O Boer<sup>1</sup>, Anouk Marsman<sup>1</sup>, Henrik Lundell<sup>1</sup>, Lars G Hanson<sup>1,2</sup>, and Esben T Petersen<sup>1,2</sup>

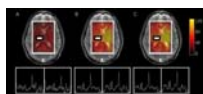
*<sup>1</sup>Danish Research Centre for Magnetic Resonance, Centre for Functional and Diagnostic Imaging and Research, Copenhagen University Hospital, Hvidovre, Denmark, <sup>2</sup>Center for Magnetic Resonance, DTU Elektro, Technical University of Denmark, Lyngby, Denmark*

Magnetic resonance spectroscopy (MRS) benefits from increased magnetic field-strength in terms of increased sensitivity and spectral separation and human cerebral concentrations of neurotransmitters have been measured with improved precision at 7T. We utilize the high sensitivity at 7T for accelerated magnetic resonance spectroscopic imaging (MRSI) of the gamma-aminobutyric acid (GABA) inhibitory neurotransmitter in the human brain at 7T using spectral editing (MEGA) and a semi-localized by adiabatic selective refocusing (sLASER) with echo-planar readout (EPSI). The proposed method is shown to allow for localized GABA detection and demonstrate potential for efficient imaging of GABA.

---

1256

17:18



High-Resolution Phase Correction in Overdiscrete Spectroscopic Imaging Reconstruction using Piecewise Polynomial Interpolation

Eduardo Coello<sup>1,2</sup>, Fatih Sueleyman Hafalir<sup>1,2</sup>, Bjoern Menze<sup>1</sup>, Axel Haase<sup>1</sup>, and Rolf Schulte<sup>2</sup>

*<sup>1</sup>Technische Universität München, Munich, Germany, <sup>2</sup>GE Global Research, Munich, Germany*

A full phase correction at high resolution is incorporated into the overdiscrete reconstruction for  $^1\text{H}$  MR Spectroscopic Imaging (MRSI). This allows to correct spectral artifacts generated by phase disturbances and increase SNR in one step, hence improving metabolite detection for fast MRSI acquisitions at short echo times. The phase correction term is approximated as a piecewise polynomial, fitted from a water reference scan that is acquired simultaneously with the metabolite signal. The method was applied to standard phase encoded MRSI and Echo-Planar Spectroscopic Imaging (EPSI) brain scans showing comparable improvements.

---

Oral

## Velocity & Flow Imaging: Novelty & Speed

Room 320

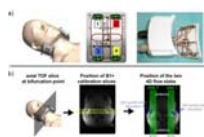
Thursday 15:30 - 17:30

Moderators: Alex Frydrychowicz & Susanne Schnell

---

1257

15:30



Simultaneous MultiSlab 4D Flow MRI for Quantification of Hemodynamics in the Carotid Bifurcation at 7 Tesla

Sebastian Schmitter<sup>1,2</sup>, Gregor Adriany<sup>1</sup>, Steen Moeller<sup>1</sup>, Edward Auerbach<sup>1</sup>, Pierre-Francois Van de Moortele<sup>1</sup>, Michael Markl<sup>3,4</sup>, Kamil Ugurbil<sup>1</sup>, and Susanne Schnell<sup>3</sup>

<sup>1</sup>University of Minnesota Medical School, Center for Magnetic Resonance Research, Minneapolis, MN, United States, <sup>2</sup>Physikalisch-Technische Bundesanstalt (PTB), Braunschweig and Berlin, Germany, <sup>3</sup>Department of Radiology, Northwestern University, Feinberg School of Medicine, Chicago, IL, United States, <sup>4</sup>Biomedical Engineering, Northwestern University, McCormick School of Engineering, Chicago, IL, United States

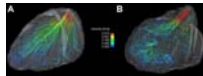
Simultaneous Multislice (SMS) imaging, also termed "Multiband" (MB), was integrated into slab-selective 4D flow MRI to quantify blood hemodynamics simultaneously in both carotid bifurcations at 7T. Therefore, sagittal oriented MB 4D flow acquisitions with 0.8mm isotropic resolution were performed in 4 volunteers using a dedicated carotid coil. The same protocol was then repeated twice, but only a single slab ("SingleBand" - SB) targeting the left or right carotid bifurcation was excited. Peak velocity and net flow quantification was performed for reconstructed MB and SB data on 3 planes each, one before and two after the bifurcation.

1258

15:42

### 4D Flow MRI in the Post-Myocardial Infarction Left Ventricle

Jacob Macdonald<sup>1</sup>, Jonathan Weinsaft<sup>2</sup>, Christopher J Francois<sup>3</sup>, and Oliver Wieben<sup>1,3</sup>



<sup>1</sup>Medical Physics, University of Wisconsin - Madison, Madison, WI, United States, <sup>2</sup>Medicine, Cornell University, New York, NY, United States, <sup>3</sup>Radiology, University of Wisconsin - Madison, Madison, WI, United States

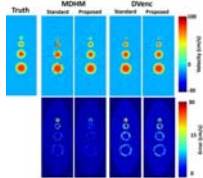
Left ventricular thrombus (LVT) formation is a serious complication of anterior ST segment elevation myocardial infarction (MI) that impacts prognosis. LVT has been linked to blood stasis in the LV apex, but conventional predictors of LVT formation are limited. This study employed 4D-flow MRI as a new means of quantifying MI induced alterations in LV flow physiology. Among a mixed cohort of post-MI subjects and controls, 4D-flow MRI demonstrated MI to be associated with increased flow stagnance in the LV apex. These findings will inform use of 4D-flow MRI in future studies to predict longitudinal risk for post-MI LVT.

1259

15:54

### Pushing the Boundaries of Low-Venc PC-MRI Acquisition Strategies with a Weighted, Regularized Optimization Reconstruction

Michael Loecher<sup>1</sup> and Daniel B. Ennis<sup>1</sup>



<sup>1</sup>Department of Radiological Sciences, University of California, Los Angeles, CA, United States

We propose a novel reconstruction method for low-Venc (high-moment) PC-MRI reconstructions to allow for significant VNR gains while being more robust to the errors associated with these methods. The reconstruction accounts for unequal signal variances due to intravoxel dephasing, and includes constraints to account for residual phase wrapping errors. The method is tested in simulations, phantoms, and volunteers.

1260

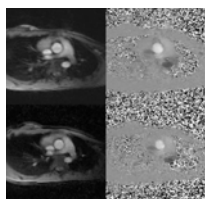
16:06

### Improving left ventricular 4D Flow MRI analysis using intensity based image registration with cine-bSSFP images

Vikas Gupta<sup>1,2</sup>, Mariana Bustamante<sup>1,2</sup>, Alexandru Fredriksson<sup>1</sup>, Carl-Johan Carlhäll<sup>1,2,3</sup>, and Tino Ebbers<sup>1,2</sup>







Grzegorz Tomasz Kowalik<sup>1</sup>, Adèle Courot<sup>1</sup>, Jennifer Anne Steeden<sup>1</sup>, and Vivek Muthurangu<sup>1,2</sup>

<sup>1</sup>Institute of Cardiovascular Science, University College London, London, United Kingdom, <sup>2</sup>Great Ormond Street Hospital for Children, London, United Kingdom

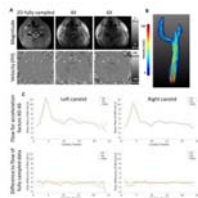
Compressed Sensing for 2D spiral PCMR with golden angle acquisition schema.

The work presents a significant improvement in spatial-temporal resolution of the real-time spiral PCMR data, which are comparable with the standard high resolution cardiac gated sequences. The technique proved to be suitable for clinical use with the benefits of short acquisition times and no breathing artefacts.

---

1263

16:42



Compressed Sensing accelerated 4D flow MRI using a pseudo spiral Cartesian sampling technique with random undersampling in time

Lukas M. Gottwald<sup>1</sup>, Eva S. Peper<sup>1</sup>, Qinwei Zhang<sup>1</sup>, Valentijn Q. Pronk<sup>1</sup>, Bram F. Coolen<sup>2</sup>, Pim van Ooij<sup>1</sup>, Gustav J. Strijkers<sup>2</sup>, and Aart J. Nederveen<sup>1</sup>

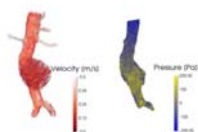
<sup>1</sup>Department of Radiology, Academic Medical Center, Amsterdam, Netherlands, <sup>2</sup>Department of Biomedical Engineering & Physics, Academic Medical Center, Amsterdam, Netherlands

Clinical applications of three-dimensional time-resolved (4D) flow MRI are still hindered by long acquisition times. Using compressed sensing image reconstruction, undersampled 4D flow data may be recovered without a notable loss of image quality. In this study pseudo-spiral sampling on a Cartesian grid was implemented on a Philips 3T Ingenia system to facilitate random undersampling in time. The technique was tested under controlled conditions in a pulsatile phantom for different acceleration factors. An additional in vivo volunteer data set confirmed the stability of this technique.

---

1264

16:54



Highly accelerated Multi-Directional Velocity Encoding 4D Flow MRI: feasibility and preliminary results

Henrik Haraldsson<sup>1</sup>, Evan Kao<sup>1</sup>, Yan Wang<sup>1</sup>, David Saloner<sup>1,2</sup>, and Jing Liu<sup>1</sup>



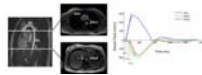
<sup>1</sup>Department of Radiology and Biomedical Imaging, University of California, San Francisco, San Francisco, CA, United States, <sup>2</sup>Veteran Affairs Medical Center, San Francisco, CA, United States

Velocity-to-noise ratio in 4D flow improves with low velocity encoding (VENC), but is usually compromised to prevent velocity aliasing. Dual-VENC and multi-directional velocity encoding schemes have been proposed to circumvent these issues, but result in an increased acquisition time. In this study, we developed a motion-robust highly accelerated 4D flow acquisition with multi-directional velocity encodings to target applications with a wide range of velocities in clinically acceptable acquisition times, for applications such as imaging of abdominal aneurysms, and simultaneous assessment of cardiac tissue phase mapping and intracardiac blood flow.

---

1265

17:06



### Simultaneous Multi-Slice Phase Contrast Imaging for Pulse Wave Velocity Measurement in the Vessel

Ning Jin<sup>1</sup>, Jianing Pang<sup>2</sup>, Shivraman Giri<sup>2</sup>, Peter Speier<sup>3</sup>, and Dingxin Wang<sup>4,5</sup>

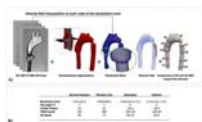
<sup>1</sup>Siemens Healthcare, Columbus, OH, United States, <sup>2</sup>Siemens Healthcare, Chicago, IL, United States, <sup>3</sup>Application Development, Siemens Healthcare, Erlangen, Germany, <sup>4</sup>Siemens Healthcare, Minneapolis, MN, United States, <sup>5</sup>Center for Magnetic Resonance Research-Radiology, University of Minnesota, Minneapolis, MN, United States

Pulse wave velocity can be derived from sequential 2D phase contrast measurements in multiple breath-holds, resulting in a long scan time and patient discomfort. Physiological conditions, may change during the measurement series, leading to flow waveform shifts and hence errors in PWV estimation. We developed a prototype SMS cine-PC sequence to measure blood flow in multiple slices simultaneously and applied it to measure PWV in the aorta.

---

1266

17:18



### Tridimensional Axial and Circumferential WSS from 4D flow data using a finite element method and a Laplacian approach

Julio Sotelo<sup>1,2</sup>, Jesús Urbina<sup>3</sup>, Bram Ruijsink<sup>4</sup>, David Nordsletten<sup>4</sup>, Joaquín Mura<sup>1</sup>, Reza Razavi<sup>4</sup>, Daniel Hurtado<sup>5</sup>, and Sergio Uribe<sup>1,3</sup>

<sup>1</sup>Biomedical Imaging Center, Pontificia Universidad Católica de Chile, Santiago, Chile, <sup>2</sup>Department of Electrical Engineering, Pontificia Universidad Católica de Chile, Santiago, Chile, <sup>3</sup>Department of Radiology, School of Medicine, Pontificia Universidad Católica de Chile, Santiago, Chile, <sup>4</sup>Department of Biomedical Engineering, King's College London, London, United Kingdom, <sup>5</sup>Department of Structural and Geotechnical Engineering, Pontificia Universidad Católica de Chile, Santiago, Chile

The WSS and OSI play a critical role in the progression of different vascular diseases, the multidirectional nature of WSS, can alter the balance of the endothelial cells. But the multidirectional nature of WSS only has been analyzed in 2D section. In this work, we propose a new method based on 3D finite-element and a Laplacian approach to decompose the WSS vector in an axial ( $WSS_A$ ) and circumferential ( $WSS_C$ ) component in a 3D domain. The 3D method provides an excellent agreement of the quantification of  $WSS_A$  and  $WSS_C$  in comparison with the actual 2D method.

---

## Combined Educational & Scientific Session

# Diffusion of the Changing Brain

Organizers: Stephan E. Maier, M.D., Ph.D & Jennifer A. McNab, Ph.D.

Room 315

Thursday 15:30 - 17:30

Moderators: Petra Huppi & Christopher Kroenke

---

15:30

Diffusion Imaging in Neurodevelopment  
C. Lebel<sup>1</sup>

<sup>1</sup>University of Calgary

Diffusion imaging has been used extensively over the last decade or so to study healthy brain maturation during childhood and adolescence. Methods vary greatly across studies, but studies consistently report nonlinear maturation that continues into young adulthood, with the most protracted development occurring in frontal-temporal connections. These diffusion changes suggest increasing myelination, axonal packing, and/or coherence with age. Less consistent findings have been reported for specific timing of development (e.g., age at peak), and sex differences. Emerging new methods and large longitudinal or multi-site studies will greatly add to our understanding of brain development over the next few years.

---

16:00

Diffusion Imaging in Aging  
Konstantinos Arfanakis<sup>1</sup>

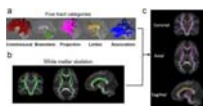
*<sup>1</sup>Illinois Institute of Technology, United States*

Diffusion MRI has an important role in research of the aging brain. Diffusion MRI can help elucidate the role of brain characteristics in the mechanisms supporting cognitive and motor health or leading to cognitive and motor decline in old age. Combining diffusion MRI with other imaging, clinical, neuropsychological, and most importantly neuropathologic information may provide invaluable insights towards the development of useful biomarkers of age-related diseases. To successfully accomplish the above, however, it is important to first realize the intricacies of conducting meaningful diffusion imaging investigations of the older adult brain.

---

1267

16:30



Differentiated maturation of white matter tracts in early developing brain aged 0-3 years

Qinlin Yu<sup>1,2,3,4</sup>, Huiying Kang<sup>1,5</sup>, Qinmu Peng<sup>1,2</sup>, Minhui Ouyang<sup>1,2</sup>, Michelle Slinger<sup>1,2</sup>, Yun Peng<sup>5</sup>, Fang Fang<sup>3,4</sup>, and Hao Huang<sup>1,2</sup>

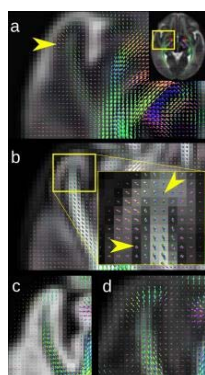
*<sup>1</sup>Department of Radiology, Children's Hospital of Philadelphia, Philadelphia, PA, United States, <sup>2</sup>Department of Radiology, Perelman School of Medicine, University of Pennsylvania, Philadelphia, PA, United States, <sup>3</sup>School of Psychological and Cognitive Sciences, Peking University, Beijing, People's Republic of China, <sup>4</sup>Peking-Tsinghua Center for Life Science, Peking University, Beijing, People's Republic of China, <sup>5</sup>Department of Radiology, Beijing Children's Hospital, Capital Medical University, Beijing, People's Republic of China*

The brain development in the first several years after birth is perhaps most dynamic. However, the studies on white matter maturation of infants and toddlers with relatively evenly distributed ages in 0-3 years are rare. Here, we charted white matter development in subjects 0-3 years-of-age through measurements of DTI-derived metrics at the tract level and tract-group level. A 3-stage maturational pattern was revealed for all white matter tracts. The differentiated maturation among the white matter tracts and tract groups was found using DTI measurements.

1268



16:42



### Multi-shell neonatal brain HARDI template

Maximilian Pietsch<sup>1</sup>, Jana Hutter<sup>1</sup>, Anthony Price<sup>1</sup>, Maria Kuklisova Murgasova<sup>1</sup>, Emer Hughes<sup>1</sup>, Johannes Steinweg<sup>2</sup>, Nora Tusor<sup>2</sup>, Jesper Andersson<sup>3</sup>, Matteo Bastiani<sup>4</sup>, Stamatios Sotiropoulos<sup>3</sup>, Joseph V Hajnal<sup>1</sup>, and J-Donald Tournier<sup>1</sup>

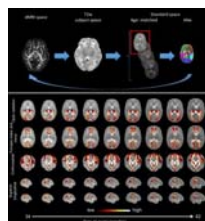
<sup>1</sup>Division of Imaging Sciences & Biomedical Engineering, King's College London, London, United Kingdom, <sup>2</sup>Department of Perinatal Imaging & Health, King's College London, London, United Kingdom, <sup>3</sup>FMRIB Centre, University of Oxford, Oxford, United Kingdom, <sup>4</sup>Nuffield Department of Clinical Neurosciences, University of Oxford, Oxford, United Kingdom

We describe a method for creating a group template of the developing brain using advanced multi-shell high angular resolution diffusion (HARDI) data. We decompose the signal into an anisotropic CSF-like and a white matter-like directional component and build an unbiased template of those tissue types from 27 healthy term control babies acquired as part of the Developing Human Connectome Project (gestational age: 40.2+/-1.4 weeks). This template will facilitate the analysis of microstructural features at a group level and allow longitudinal investigations into healthy and pathological brain maturation.

1269



16:54



### Automated pre-processing pipeline and quality control for neonatal diffusion MRI in the developing Human Connectome Project (dHCP)

Matteo Bastiani<sup>1</sup>, Jesper Andersson<sup>1</sup>, Lucilio Cordero-Grande<sup>2</sup>, Maria Murgasova<sup>2</sup>, Jana Hutter<sup>2</sup>, Anthony N. Price<sup>2</sup>, Antonios Makropoulos<sup>3</sup>, Emer Hughes<sup>2</sup>, Johannes Steinweg<sup>2</sup>, Nora Tusor<sup>2</sup>, Daniel Rueckert<sup>3</sup>, A. David Edwards<sup>2</sup>, Stephen Smith<sup>1</sup>, Jacques-Donald Tournier<sup>2</sup>, Joseph V. Hajnal<sup>2</sup>, Saad Jbabdi<sup>1</sup>, and Stamatios Sotiropoulos<sup>1</sup>

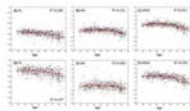
<sup>1</sup>Oxford Centre for Functional Magnetic Resonance Imaging of the Brain (FMRIB), Oxford University, Oxford, United Kingdom, <sup>2</sup>Centre for the Developing Brain, King's College London, London, United Kingdom, <sup>3</sup>Department of Computing, Imperial College London, London, United Kingdom

The developing Human Connectome Project (dHCP) is a collaborative 6-year project set to create a 4-dimensional map of structural and functional changes occurring throughout early development. Up to 1300 multi-modal MRI scans of fetuses and neonates (20 to 44 weeks gestational age) are currently being acquired. We present a fully automated pre-processing pipeline that allows us to efficiently analyse in-vivo diffusion MRI (dMRI) data despite the considerable technical challenges specific to neonatal imaging. We developed a quality control (QC) framework that allows us to identify issues or inconsistencies. This is especially useful when processing a very large number of subjects.

1270



17:06



Interpreting age-related changes based on the mean signal diffusion kurtosis

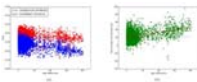
Rafael Neto Henriques<sup>1</sup> and Marta Morgado Correia<sup>1</sup>

<sup>1</sup>Cognition and Brain Sciences Unit, MRC, Cambridge, United Kingdom

Previous studies have shown that measures of non-Gaussian diffusion from diffusion kurtosis images (DKI) provide unique information on age-related tissue changes. In this study, a novel non-Gaussian diffusion index invariant to the distribution of fibres is proposed and applied to 650 datasets from the Cam-CAN ageing project. The results show that the proposed biomarker is not only applicable to any tissue configuration but also less sensitive to noise and artefacts when compared to traditional DKI measures. Moreover, for white matter regions, age-related changes measured by this index seem to reflect axonal alterations likely related to axonal loss mechanisms.

1271

17:18



Registration-free analysis of diffusion MRI tractography data across subjects through the human lifespan

Viviana Siless<sup>1</sup>, Juliet Y Davidow<sup>2</sup>, Jared Nielsen<sup>2</sup>, Qiuyun Fan<sup>1</sup>, Trey Hedden<sup>1</sup>, Marisa Hollinshead<sup>1</sup>, Constanza Vidal Bustamante<sup>2</sup>, Michelle K Drews<sup>1,2</sup>, Koene R.A. Van Dijk<sup>1</sup>, Margaret A Sheridan<sup>3</sup>, Randy L Buckner<sup>1,2</sup>, Bruce Fischl<sup>1,4</sup>, Leah Somerville<sup>2</sup>, and Anastasia Yendiki<sup>1</sup>



18:00

Mansfield Lecture

Penny Anne Gowland<sup>1</sup>

<sup>1</sup>University of Nottingham, SPMIC, Nottingham, United Kingdom

---

---

**Other**

## Closing Party

Convention Center

Rooftop

Thursday 19:00 - 21:00 (*no CME credit*)

---

---

---